CARBON-CARBON FRAGMENTATION: HISTORY AND NEW APPLICATIONS IN COMPLEX TERPENE SYNTHESIS

by

MICHAEL A. DRAHL

A dissertation submitted to the

Graduate School-New Brunswick

Rutgers, The State University of New Jersey

in partial fulfillment of the requirements

for the degree of

Doctor of Philosophy

Graduate Program in Chemistry and Chemical Biology

written under the direction of

Professor Lawrence J. Williams, Ph.D.

and approved by

_____

_____

_____

_____

New Brunswick, New Jersey

October, 2013

ABSTRACT OF THE DISSERTATION

Carbon-Carbon Fragmentation: History and New Applications

in Complex Terpene Synthesis

by MICHAEL A. DRAHL

Dissertation Director:

Professor Lawrence J. Williams, Ph.D.

C-C fragmentation is both powerful and elegant. Capable of stereospecifically introducing sp^1-sp^1, sp^2-sp^2, and sp^2-sp-sp^2 bond connectivity, it is the key transformation that allows all of the chemistry described herein. This dissertation begins with a comprehensive review of C-C fragmentation, which notably uncovers the lost origins of this transformation. Extensions of its utility in complex terpene synthesis are presented next. An integrated routing strategy was realized in the divergent enantioselective synthesis of the core ring systems of the xeniolide, xenibellol, and florlide natural products. A more general synthetic route was developed to gain direct access to the previously restricted, diverse, semi-validated structure space of the xenicane superfamily, and more than forty xenicane congeners were synthesized. These include xeniolides, blumiolides, florlides, bridgehead olefins and epoxides, keto-enol tautomeric mixtures, and the deshydroxymethyl xeniolide framework. Several other terpene motifs were also prepared, including functionalized cyclopentanones, CD ring systems of 18-methoxy-18-oxo-17-ketosteroids, and nine-membered ring-opening products. Seven of these novel

compounds were found to selectively induce Bak- and Bax-dependent apoptosis in precancerous immortalized baby mouse kidney epithelial cells.

Acknowledgements

Celgene Corporation: Celgene Drug Discovery Graduate Fellowship

Oak Ridge Associated Universities: travel/food/lodging for the 60th Lindau Meeting of Nobel Laureates

Rutgers, The State University of New Jersey: Louis Bevier Dissertation Fellowship

Da Xu: vernonia allene project

Dr. Robert V. Kolakowski, Dr. Yue Zhang, and Dr. Joseph R. Cusick: helpful discussions

Professor Madhuri Manpadi and Huan Wang: contributions to second-generation xenicane project

Alex J. Baranowski and Michael P. Olson: synthesis of starting materials

Seidel Group: chiral HPLC and microwave reactor

Dr. Novruz G. Akhmedov (West Virginia University): 2D NMR and HR-MS

Dr. Thomas J. Emge: X-ray crystallography

Dr. Eric H. Andrianasolo: natural product isolation and characterization

Liti Haramaty: Bak- and Bax-dependent apoptosis induction assays

Prof. Lawrence J. Williams: guidance and encouragement

Prof. Roger A. Jones, Prof. Ralf Warmuth, and Dr. James A. Johnson: serving on my dissertation committee

Dedication

To Mom, Dad, Carmen, and Uncle Antonio

Table of Contents

Abstract……ii

Acknowledgements……iv

Dedication……....v

List of Tables……...……...ix

List of Schemes…..……...……...x

List of Figures…….…..…xix

Chapter I: C-C Fragmentation: Origins and Recent Applications

1.1 Introduction...…….... 1

1.2 Origins..... 4

1.2.1 sp^1-sp^1 bond forming fragmentations..... 6

1.2.2 sp^2-sp^2 bond forming fragmentations..... 15

1.3 Progress and Applications..... 33

1.3.1 sp^1-sp^1 bond forming fragmentations..... 34

1.3.2 sp^2-sp^2 bond forming fragmentations..... 42

1.3.3 sp^2-sp^1 bond forming fragmentations..... 58

1.3.4 Complex Molecule Synthesis..... 64

1.4 Summary and Outlook..... 85

1.5 References and Notes..... 89

Chapter II: First Generation Studies: Selective Conversion of an Enantioenriched Cyclononadienone to the Xeniolide, Xenibellol, and Florlide Cores

2.1 Introduction..... 101

2.2 Xenicane Diterpenoids..... 103

2.3 First Generation Synthetic Studies Towards Xenicanes..... 107

2.4 Integrated Routing Strategy..... 109

2.5 Postulated Xenicane Biosynthesis..... 113

2.6 Extended Work..... 115

2.7 Summary..... 117

2.8 References and Notes..... 118

Chapter III: Accessing Anticancer Structure Space: Second Generation Studies Toward the Synthesis of Xenicane Diterpenoids

3.1 Introduction..... 122

3.2 Second Generation Design of the Key Intermediate..... 130

3.3 Racemic Synthesis of the Key Intermediate..... 132

3.4 Progress Towards an Asymmetric Route..... 145

3.5 Stability of the Key Intermediate..... 147

3.6 Racemization Kinetics of the Dissymmetric Platform..... 148

3.7 Enone Reactivity..... 150

3.8 Stereoselective Syntheses of Xeniolide and Blumiolide Congeners..... 152

3.9 Divergent Syntheses of Terpene Side Chains and Attempts at Use..... 161

3.10 Conjugate Additions of Active Methylene Compounds..... 170

3.11 Rearrangement to Second Generation Florlide Core and Synthesis of Bicyclic Congeners..... 178

3.12 Return to Xeniolide Targets: Conjugate Additions of sp-Hybridized Carbon Nucleophiles..... 185

3.13 Anticancer Evaluations of the Compound Library: Specific Apoptosis Induction Screen..... 195

3.14 Ongoing Studies..... 209

3.15 Integrated Route to Xenicanes and Diverse Motifs: Summary..... 210

3.16 References and Notes..... 212

Chapter IV: Experimental

4.1 Chapter II..... 217

4.2 Chapter III..... 262

Résumé..... 768

List of Tables

Table III.1 Broad spectrum biological potency: anticancer activities..... 124

Table III.2 Broad spectrum biological potency: antibiotic activities..... 126

Table III.3 Chemo- and diastereoselective reduction screening (*crude NMR yields).. 139

Table III.4 Change in relative W2 and D3 cell viability (**3.39**)..... 197

Table III.5 Change in relative W2 and D3 cell viability (**3.116**)..... 199

Table III.6 Change in relative W2 and D3 cell viability (**3.65**)..... 200

Table III.7 Change in relative W2 and D3 cell viability (**3.46**)..... 201

Table III.8 Change in relative W2 and D3 cell viability (**3.108**)..... 202

Table III.9 Change in relative W2 and D3 cell viability (**3.63**)..... 203

Table III.10 Change in relative W2 and D3 cell viability (**3.59**)..... 204

Table III.11 Change in relative W2 and D3 cell viability (**3.94-3.96**)..... 207

List of Schemes

Scheme I.1 The original designed C-C fragmentation, by Eschenmoser (1952)..... 2

Scheme I.2 The optimized Wallach nitrile synthesis (1911)..... 7

Scheme I.3 Morphine degradation studies by Schöpf (1927)..... 8

Scheme I.4 Grob's oxime fragmentation studies (1963)..... 9

Scheme I.5 Grob's ene-nitrile synthesis (1963)..... 10

Scheme I.6 Stork's ring expansion in the total synthesis of (±)-byssochlamic acid (**1.32**) (1972)..... 11

Scheme I.7 Colvin's heteroatom-assisted fragmentation in the total synthesis of (±)-trichodermine (**1.35**) (1973)..... 11

Scheme I.8 The original alkyne synthesis, by Bodendorf (1963), and Eschenmoser's and Tanabe's cyclic alkyne syntheses (1967)..... 12

Scheme I.9 Tanabe's secosteroid synthesis (1967)..... 13

Scheme I.10 Borrevang's A-nor steroid synthesis (1968)..... 13

Scheme I.11 Corey's acetylenic aldehyde synthesis (1975)..... 14

Scheme I.12 Coke (1977) and Kuwajima's (1981) acetylenic ketone syntheses..... 15

Scheme I.13 Eschenmoser's original alkene synthesis (1952)..... 17

Scheme I.14 Gibbs-Henry degradation of quinidine (**1.57**) (1939) and Mosher's mechanistic interpretation (1952)..... 17

Scheme I.15 Cationic fragmentations (1907-1952)..... 19

Scheme I.16 The original stereochemical investigation on concerted C-C fragmentation, by Henbest (1953)..... 20

Scheme I.17 English and Jefferies' cationic fragmentations (1956-1957)..... 21

Scheme I.18 The original C-C fragmentation mechanistic framework, by Eschenmoser (1952)..... 21

Scheme I.19 Grob's 1,4-eliminations and diene synthesis (1955)..... 22

Scheme I.20 The original C-C fragmentative ring expansion, by Stork (1956)..... 22

Scheme I.21 Wharton's convergent ring expansion (1961)..... 23

Scheme I.22 Wharton's cyclodecene syntheses (1965)..... 24

Scheme I.23 Wharton's cyclodecadiene synthesis (1965)..... 24

Scheme I.24 Grob's kinetic studies (1964)..... 26

Scheme I.25 The original total synthesis via C-C fragmentation, by Corey (1964)..... 27

Scheme I.26 Tanabe's cyclononene synthesis (1964)..... 27

Scheme I.27 Marshall's ring expansions (1965)..... 28

Scheme I.28 Marshall's divergent fragmentations (1967)..... 29

Scheme I.29 The original boronate electrofuge, by Marshall (1966)..... 30

Scheme I.30 The original dithianyl electrofuge and malonyl electrofuge, by Marshall (1971)..... 30

Scheme I.31 Mander's germacrane scaffold synthesis (1977)..... 31

Scheme I.32 The Syntex sequential fragmentation (1968)..... 32

Scheme I.33 Eschenmoser's extended decarboxylative elimination/C-C fragmentation (1979)..... 33

Scheme I.34 Kirihara's fluorinative ketoxime fragmentations (1997)..... 34

Scheme I.35 Subba Rao's [4.3.3]propellane scaffold synthesis (2000)..... 35

Scheme I.36 Čeković's nitrile synthesis (2001)..... 36

Scheme I.37 Maroto's ring opening (2004)..... 37

Scheme I.38 de Meijere's cyclic alkynone synthesis (2001)..... 37

Scheme I.39 Dudley's cascade synthesis of alkynes (2005-2010)..... 39

Scheme I.40 Dudley's homopropargyl amine syntheses (2011)..... 39

Scheme I.41 Dudley's *in situ* generation of alkynyl aldehydes (2006)..... 40

Scheme I.42 Brewer's ynoate and ynone syntheses (2008-2010)..... 41

Scheme I.43 Brewer's alkynone synthesis (2012)..... 41

Scheme I.44 The original C-C fragmentation of nitrones, by Murphy (2007)..... 42

Scheme I.45 Lupton's dendrimer core syntheses (2010)..... 43

Scheme I.46 Mehta's cyclopentitol scaffold synthesis (1999)..... 44

Scheme I.47 West's nine-membered oxacycle synthesis (1998)..... 45

Scheme I.48 Molander's cascade synthesis of medium-sized rings (2001)..... 45

Scheme I.49 Charette's γ-amino halide fragmentations (2008)..... 46

Scheme I.50 Risch's γ-amino halide fragmentations (1991)..... 47

Scheme I.51 Plumet's sulfonium-initiated fragmentation (2001)..... 47

Scheme I.52 Ochiai's oxidative fragmentation (2004)..... 48

Scheme I.53 Kabalka's cationic alkene synthesis (1998-1999)..... 49

Scheme I.54 Barluenga's terpene fragmentation (2003)..... 50

Scheme I.55 Zard's cyclononene synthesis (1999)..... 51

Scheme I.56 Kobayashi's *syn*-bicyclic pyroglutamic acid synthesis (2007)..... 51

Scheme I.57 Dowd's fluoride-induced ring expansion (1996)..... 52

Scheme I.58 Hesse's macrolactone synthesis (1995)..... 53

Scheme I.59 Jung's ozonide fragmentation (2001)..... 53

Scheme I.60 Adam's peroxide fragmentation (1995)..... 54

Scheme I.61 Sakai's *in situ* aldol product C-C fragmentation (1991)..... 55

Scheme I.62 Bettolo's angular acetate synthesis (1997)..... 55

Scheme I.63 Tamaru's nickel-mediated fragmentation (2006)..... 56

Scheme I.64 Michl's carba-*closo*-dodecaborate fragmentation (2004)..... 57

Scheme I.65 Liu's allene synthesis (2010)..... 58

Scheme I.66 The original allene synthesis via C-C fragmentation (Kuwajima, 1997).... 59

Scheme I.67 Fragmentations of vinyl triflates to allenes (2009)..... 61

Scheme I.68 Synthesis of an endocyclic allene related to the germacranolides (2011)... 62

Scheme I.69 Saget and Cramer's allene synthesis (2010)..... 63

Scheme I.70 Fragmentation favors the allene over the alkyne (2009)..... 64

Scheme I.71 Hu's ring opening fragmentation *en route* to elegansidiol (**1.292**) (2007)... 65

Scheme I.72 Mander's synthesis of (±)-GB-13 (**1.295**) used a late stage fragmentation (2003)..... 66

Scheme I.73 Dudley's synthesis of moth pheromone **1.296** (2006)..... 67

Scheme I.74 Dudley's synthesis of a palmerolide A segment (**1.298**) (2010)..... 67

Scheme I.75 Krief and Surleraux's *cis*- and *trans*-chrysanthemic carboxylate syntheses (**1.300** and **1.301**) (1991)..... 68

Scheme I.76 de Groot's divergent synthesis of insect pheromones (2003)..... 68

Scheme I.77 Nagaoka's zaragozic acid core synthesis (**1.309**) (1999)..... 69

Scheme I.78 C-C fragmentation in Peng and Wong's syntheses of (±)-pallavicinin (**1.312**) and (±)-neopallavicinin (**1.313**) (2006)..... 70

Scheme I.79 A C-C fragmentation in Kim and Cha's syntheses of (±)-cyathin B_2 (**1.316**) and (±)-cyathin A_3 (**1.317**) (2009)..... 71

Scheme I.80 The C-C fragmentations in Mulzer's formal syntheses of epothilone D, discodermolide, and peloruside A (2009-2010)..... 72

Scheme I.81 Key steps in Charette's enantioselective total syntheses of 209I (**1.326**) and 223J (**1.327**) (2010)..... 73

Scheme I.82 Key fragmentation of Joseph-Nathan's syntheses of (±)-parvifoline (**1.330**) and (±)-isoparvifolinone (**1.331**) (1995)..... 74

Scheme I.83 Nagaoka's approach to CP-263,114 (1999)..... 75

Scheme I.84 Wood's approach to CP-263,114 (2001)..... 75

Scheme I.85 The key fragmentation in Paquette's synthesis of (±)-jatrophatrione (**1.338**) (2002)..... 76

Scheme I.86 Thornton's approach to the aquariolide core (**1.340**) (2006)..... 76

Scheme I.87 Key fragmentation in Leumann's synthesis of coraxeniolide A (**1.343**) (2000)..... 77

Scheme I.88 Enantioenriched **1.344** gives enantioenriched **1.345** via fragmentation in Corey's syntheses of β-caryophyllene (**1.115**) and coraxeniolide A (**1.343**) (2008)..... 78

Scheme I.89 Saicic's key fragmentation *en route* to syntheses of (±)-periplanones **1.348-1.350** (2004)..... 79

Scheme I.90 Ley's approach towards the thapsigargins (2004)..... 80

Scheme I.91 Winkler's fragmentation cascade to the eleutherobin core (**1.357**) (2003).. 81

Scheme I.92 Holton's Lewis acid promoted epoxy-alcohol fragmentation in the synthesis of Taxol® (**1.360**) (1994)..... 82

Scheme I.93 Wender's base-promoted epoxy-alcohol fragmentation in the synthesis of Taxol® (1997)..... 83

Scheme I.94 The key fragmentation in Baran's synthesis of (±)-vinigrol (**1.365**) (2009) 84

Scheme I.95 *Arabidopsis* oxidosqualene cyclase fragmentation in the biosynthesis of marneral (**1.370**), identified by Matsuda (2006)..... 85

Scheme II.1 Integrated route to three xenicane diterpenoid cores..... 104

Scheme II.2 Danishefsky's xenibellol core synthesis..... 107

Scheme II.3 Enantioselective synthesis of the C-C fragmentation precursor..... 108

Scheme II.4 Retardation of racemization rates permits stereoselective synthesis..... 108

Scheme II.5 Epoxydiene **2.2**: a possible gateway to disparate targets..... 110

Scheme II.6 Preparation of racemic and enantioenriched epoxydiene **2.2**..... 110

Scheme II.7 Radical-induced transannulation to xenibellol core **2.3**..... 111

Scheme II.8 Carbocation-induced transannulation to florlide core **2.4**..... 112

Scheme II.9 Fenical-Faulkner xenicane biogenesis proposal..... 114

Scheme II.10 Kashman's proposal: mixed biogenesis via xeniaphyllanes..... 115

Scheme II.11 Biosynthesis of caryophyllene..... 115

Scheme II.12 Bridgehead olefin formation: facile in nature?..... 116

Scheme II.13 Attempted Burgess elimination to the umbellacin core..... 117

Scheme II.14 Selective benzylation of the florlide core..... 117

Scheme III.1 Low-energy conformations of cyclononadienone **3.5** (bird's-eye view) and revised carboxylate-substituted target **3.6**..... 131

Scheme III.2 Dr. Yue Zhang's failed fragmentation..... 133

Scheme III.3 Planned fragmentation..... 133

Scheme III.4 Nine-membered ring core synthesis..... 134

Scheme III.5 Presumed intramolecular NHK mechanism: olefin geometry inconsequential..... 136

Scheme III.6 Proposed mechanism of optimized cyclization reaction..... 137

Scheme III.7 Recycling of the overprotection product..... 138

Scheme III.8 Attempts to expedite the route with inversion chemistry..... 141

Scheme III.9 Fragmentation analysis: mechanism..... 143

Scheme III.10 Fragmentation analysis: computed ground state torsion angles..... 144

Scheme III.11 Unscalable enzymatic desymmetrization..... 146

Scheme III.12 Spontaneous epoxidation of strained olefins and proposed mechanism. 147

Scheme III.13 Conformational interconversion (racemization) possible?..... 149

Scheme III.14 Kinetic resolution of **3.6**..... 149

Scheme III.15 Lewis acid-mediated silylation-cuprate addition-decarboxylation..... 153

Scheme III.16 Setting two stereocenters via butyl cuprate addition..... 155

Scheme III.17 Optimized alkyl cuprate conjugate additions..... 157

Scheme III.18 Derivatization of cuprate addition products..... 157

Scheme III.19 Thermal and radical-induced *E* to *Z* isomerizations..... 158

Scheme III.20 Phenyl cuprate addition and trapping of the less stable enolate..... 159

Scheme III.21 Chemoselective Tebbe olefinations to *exo*-methylene analogues..... 159

Scheme III.22 Neat conjugate addition of heteroatom nucleophiles..... 161

Scheme III.23 Divergent syntheses of side chains and model iodo-ol..... 162

Scheme III.24 Intramolecular trapping of an *in situ* vinyl anion..... 164

Scheme III.25 Allene formation: presumed flaw of the vinyl anion conjugate addition strategy..... 165
Scheme III.26 Synthesis of an intramolecular conjugate addition substrate..... 166
Scheme III.27 Cope rearrangement revisited: temperature sensitivity..... 167
Scheme III.28 Conjugate addition-transannulation-dehalogenation radical chain reaction to the steroid CD ring core..... 168
Scheme III.29 Steroidal methyl ester synthesis and attempted proteodestannylations.. 169
Scheme III.30 Two steps from deoxyxeniolide B: dead-end intermediate..... 170
Scheme III.31 Active methylene conjugate addition strategy to xenicane natural products..... 171
Scheme III.32 Mild, catalytic, water-insensitive, solvent-free Michael addition: initial product structure assignment..... 171
Scheme III.33 Michael-retro-Michael-Michael-aldol-lactonization-decarboxylation cascade..... 173
Scheme III.34 Structural reassignment: interrupted Hagemann's ester synthesis..... 174
Scheme III.35 Prevention of the retro-Michael process: chloride protecting groups..... 176
Scheme III.36 Kashman's postulated biosynthetic intermediate: retro-Michael candidate?..... 176
Scheme III.37 Preparation and testing of a substrate less likely to undergo retro-Michael reaction..... 177
Scheme III.38 Delayed retro-Michael ring opening..... 177
Scheme III.39 Synthesis of second generation xeniolide epoxide and florlide cores..... 178
Scheme III.40 Optimization of florlide monomer yield..... 180

Scheme III.41 Postulated biosynthesis of dictyotadimer A: hydroxydictyodial dimerization..... 180

Scheme III.42 Unprecedented xenicane core synthesis via forceful ionizing conditions (compare **3.79** with **3.80**)..... 181

Scheme III.43 Doubled reaction time: improved yield and novel derivatization..... 182

Scheme III.44 Postulated bridgehead olefin biosynthesis..... 184

Scheme III.45 Bridgehead alkene epoxidation..... 185

Scheme III.46 Unhindered alkynylalane: access to a xeniolide side chain handle..... 186

Scheme III.47 Reprioritized targets for total synthesis..... 187

Scheme III.48 Enyne side chain synthesis..... 188

Scheme III.49 Enyne side chain installation..... 189

Scheme III.50 Lewis acid required for chemoselective alane addition..... 191

Scheme III.51 Synthesis of the deshydroxymethyl xeniolide framework..... 192

Scheme III.52 One-pot *syn*-hydrostannylation-iodination..... 193

Scheme III.53 Synthetic plan towards new xeniolide..... 193

Scheme III.54 Towards synthesis of terminal alkyne-diene..... 194

Scheme III.55 Terminal alkyne-diene synthesis..... 195

Scheme III.56 New target scaffolds for SAR development..... 210

Scheme III.57 Integrated route to xenicanes and diverse motifs..... 211

List of Figures

Figure I.1 Selected natural products synthesized in the 1950s..... 5

Figure I.2 Monoterpene fragmentation substrates from Forster (**1.53**) (1902), Czerny (**1.54**) (1900), and Wallach (**1.55**) (1896)..... 16

Figure I.3 Grob's γ-amino halide fragmentations (1962)..... 25

Figure II.1 Retrosynthetic analysis vs. integrated routing strategy..... 103

Figure II.2 Xenicanes from the soft coral *Xenia umbellata*..... 105

Figure II.3 Published xenicane total syntheses (excluding xeniaphyllanes)..... 106

Figure III.1 Global oncology market growth..... 123

Figure III.2 Xenicane superfamily: structural complexity, novelty, and homology..... 123

Figure III.3 Proapoptotic xenicane isolates..... 128

Figure III.4 Structure space targeting..... 130

Figure III.5 First-order racemization kinetics and computed half-life of **3.6**..... 150

Figure III.6 ^{13}C NMR analysis of enone electrophilicity and conj. addition precedent. 151

Figure III.7 NOE-derived structures of the major and minor conformers of **3.33**..... 156

Figure III.8 Carbanion intermediate to be avoided..... 175

Figure III.9 Danishefsky's synthetic xenicane cores..... 179

Figure III.10 Wiseman's method for comparing bridgehead olefin strain..... 183

Figure III.11 Unfunctionalized bridgehead olefin models..... 184

Figure III.12 Functionalized bridgehead olefin models..... 184

Figure III.13 2D NMR-derived structures of **3.107** and **3.108** with key NOEs..... 190

Figure III.14 Proposed model for *syn*-hydrostannylation regioselectivity..... 192

Figure III.15 Change in relative W2 and D3 cell viability (**3.39**)..... 197

Figure III.16 Change in relative W2 and D3 cell viability (**3.116**)..... 199

Figure III.17 Change in relative W2 and D3 cell viability (**3.65**)..... 200

Figure III.18 Change in relative W2 and D3 cell viability (**3.46**)..... 201

Figure III.19 Change in relative W2 and D3 cell viability (**3.108**)..... 202

Figure III.20 Change in relative W2 and D3 cell viability (**3.63**)..... 203

Figure III.21 Change in relative W2 and D3 cell viability (**3.59**)..... 204

Figure III.22 Lowest effective concentrations of pro-apoptotic synthetic compounds.. 205

Figure III.23 Xenicane congeners yielding inconsistent results..... 206

Figure III.24 Change in relative W2 and D3 cell viability (**3.94**-**3.96**)..... 206

Figure III.25 Nonspecifically toxic terpenoids..... 207

Figure III.26 Inactive compounds at 100-200 μM..... 208

Chapter I

C-C Fragmentation: Origins and Recent Applications

1.1 Introduction

It has been sixty years since Eschenmoser disclosed the archetypal C-C fragmentation reaction. New fragmentations and several variants of the original quickly followed. Many of these variations, which include the Beckmann, Grob, Wharton, Marshall, and Eschenmoser-Tanabe fragmentations, among others, have been reviewed on occasion over the intervening years. A close examination of the origins of fragmentation has not been described. Recently, useful new methods have flourished, particularly fragmentations that give alkynes and allenes, and fragmentation reactions have been applied to a range of complex motifs and natural products. This review traces the origins of fragmentation reactions and provides a summary of the methods, applications, and new insights of heterolytic C-C fragmentation reactions advanced over the last twenty years.

Reaction development is one of the primary vehicles of molecular science. Most synthetic methods focus on direct means by which to establish carbon-carbon (C-C), carbon-heteroatom (C-X), or heteroatom-heteroatom (X-Y) bond connectivity, to effect oxidation and reduction, or to achieve some combination of these. Direct chemical methods are powerful tools for synthesis. Yet the immense variety of invented and naturally occurring molecules includes many structural motifs and motif combinations that are difficult to access directly.

Fragmentation reactions constitute distinctly different sorts of transformations. They effect bond cleavage and require the recognition of indirect synthetic planning strategies. As shown in Scheme I.1, for example, in the archetypal C-C fragmentation several objectives are achieved (**1.1** → **1.4**): creation of two π bonds (one of them transient, see **1.3**), scission of one C-C σ bond, and expulsion of a leaving group. Addition of a nucleophile to establish new connectivity constitutes an elegant embellishment that renders the overall process a cascade sequence. However, C-C cleavage is the key feature of the transformation and the lynchpin that enables the nucleophilic addition to leverage site-selective introduction of the C-C double bond. This contribution emanated from the Eschenmoser laboratories and appeared in 1952.[1] The report, and its complement of 1953,[2] contains all the features most closely associated with C-C fragmentation reactions. These include a mechanistic framework, applications in the selective preparation of otherwise difficult to form alkenes, and a review of the scattered antecedent observations of the reactivity principle, which to that point had not been mechanistically rationalized but which, given the author's insight, were clearly best understood as fragmentations.

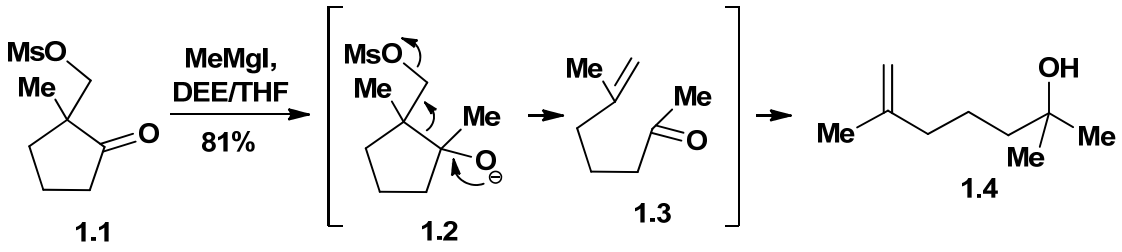

Scheme I.1 The original designed C-C fragmentation, by Eschenmoser (1952).[1]

Additional contributions that further established the Eschenmoser fragmentation as a general reaction paradigm were supplied by many. Strategically creative, mechanistically insightful, and otherwise useful developments were evident from the work of Henbest,

Grob, Stork, Wharton, and others within years of the landmark publication. Since most work in this field finds strong precedent in early reports, the review presents a chronological examination of the antecedents (*Origins*). Hence, we begin with the Beckmann fragmentation, which appeared in the German literature of the late nineteenth century but was not generally recognized as such until the mid-twentieth century, and proceed through the first designed anionic fragmentation, which was advanced by Eschenmoser. This is followed by a brief history of cationic fragmentations and a detailed discussion of the early studies. The majority of the review describes recent examples of C-C fragmentation from the past two decades (*Progress and Applications*). The organization of *Progress and Applications* parallels that of *Origins*, with the addition of sp^2-sp^1 bond forming fragmentations. We conclude with a reflection on remaining challenges in the field (*Summary and Outlook*).

The present review does not essay to cover the entire field of fragmentations, or even the entirety of C-C fragmentations, but only its most elementary and recent divisions. There are a number of reactions that share the general features of heterolytic C-C fragmentation; nevertheless, they are more appropriately discussed elsewhere. For the purposes of this review, therefore, the following reaction classes will not be covered: free radical homolytic C-C fragmentation,[3] carbon-heteroatom (C-X) fragmentations,[4] decarboxylative eliminations,[5] eliminations in general,[6] retro-Michael,[2] retro-aldol,[2] retro-Mannich,[7] and related processes.

Most schemes in this review are accompanied by a framed rendition of the reactive intermediate in a conformation that approximates the presumed transition structure. The

bonds directly involved in fragmentation are rendered in bold. These figures are intended to facilitate an understanding of these transformations.

Several fragmentation reviews have appeared over the years.[8] In most cases these emphasize one aspect of the reaction class. For example, the first and most important review of the field, by Grob,[8a] emphasized cationic pathways, nitrogen heterocycle substrates, and the mechanistic framework, and did not describe Eschenmoser's contributions,[9] whereas the most recent review by Mulzer[8i] emphasized carbonyl-forming fragmentations that generated C-C double bonds. The most recent comprehensive review appeared in 1991.[8g]

1.2 Origins

In the 1950s organic chemistry went through a period of explosive growth in understanding molecular structure and reactivity as well as in demonstrating this understanding in complex settings. A short, and only partial, list of fundamentally important findings with broad implications reported in – or directly traceable to – that decade includes such iconic achievements as ground and transition state conformational analysis of cyclic systems,[10] models for stereoinduction in acyclic systems,[11,12] recognition of rate accelerating anchimeric effects,[13] mechanistic and stereochemical models for polyene cyclizations,[14] the discovery of important natural substances such as erythromycin,[15] formulation of the double helical structure of DNA,[16] the application of nuclear magnetic resonance spectroscopy to the study of organic compounds,[17] and an organon for designing syntheses of complex target molecules.[18]

Natural product synthesis, ever at the forefront of organic chemistry, took on an entirely new level of sophistication in this decade (Figure I.1). Ground breaking syntheses

were reported across structural classes, such as those for ATP (triacridinium salt **1.5**),[19] sucrose (**1.6**),[20] penicillin V (**1.7**),[21] oxytocin (**1.8**),[22] morphine (**1.9**),[23] strychnine (**1.10**),[24] reserpine (**1.11**),[25] pentacyclosqualene (**1.12**),[26] cedrol (**1.13**),[27] cantharadin (**1.14**),[28] and cortisone (**1.15**).[29]

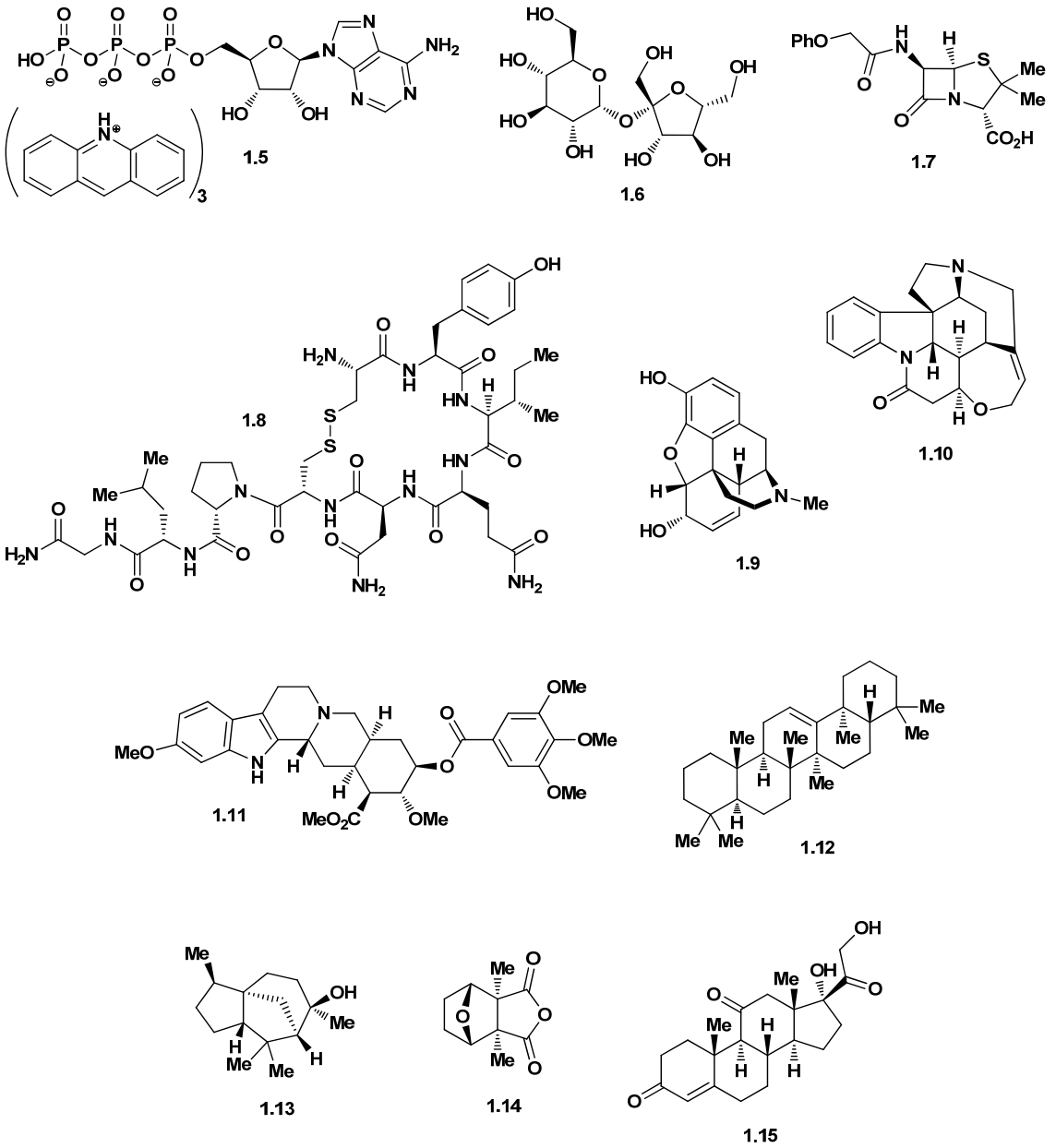

Figure I.1 Selected natural products synthesized in the 1950s.[19-29]

This was the exciting timeframe in which Eschenmoser put forth his fragmentation. The broad development of C-C fragmentation included reactions that produce sp^1-sp^1 connectivity as well as sp^2-sp^2 connectivity but did not extend to producing the sp^2-sp^1 connectivity present in cumulenes until much later. Although they were originally misinterpreted, the earliest recorded fragmentations fall in the sp^1-sp^1 category. Accordingly, we describe these developments first and then return to the early work of sp^2-sp^2 bond forming fragmentations.

1.2.1 sp^1-sp^1 bond forming fragmentations

The first C-C fragmentation reaction, the Beckmann fragmentation, was conducted unknowingly by Wallach at the end of the nineteenth century and gives a nitrile as the signature product (Scheme I.2).[30] This cleavage process is often encountered as an undesired side reaction of Beckmann rearrangement, which had been discovered by Beckmann in 1886.[31] Wallach's 1890 observation[30a] was optimized, though still not interpreted correctly, by Schroeter in 1911.[32] It was not until 1955, when Brown and co-workers repeated Schroeter's work, that a correct mechanistic formulation of the Wallach transformation was recorded in the literature.[33] In this optimization the competing Beckmann pathways are controlled by activating reagent. Thus, treatment of pivalophenoxime (**1.16**) with phosphorous pentachloride under mild conditions gives a quantitative yield of benzonitrile (see also **I**, inset).

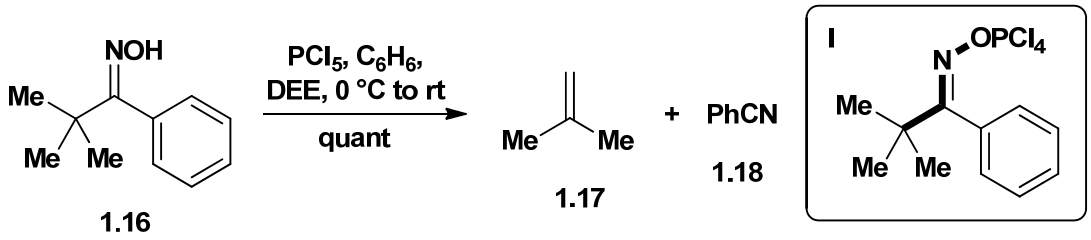

Scheme I.2 The optimized Wallach nitrile synthesis (1911).[30a,32,33]

The Beckmann fragmentation was recognized as a useful transformation long before 1955. Perhaps the most astute early use of the reaction was in the context of the morphine structure determination. For more than a century, chemists aimed to elucidate the structure of morphine and related opium alkaloids. The Gulland-Robinson proposals of the early 1920s,[34] which contradicted the long-accepted Knorr-Hörlein formula,[35] were strongly supported by Schöpf's degradation studies of 1927 (Scheme I.3).[36] Schöpf sought to determine whether the C-terminus of the ethylamine bridge was located at C-13 or C-5 by subjecting dihydrocodeinone oxime (**1.19a**/**b**) to Beckmann conditions. After further degradation, the Beckmann fragmentation product was assigned as aldehyde nitrile **1.20**, not ketonitrile **1.21**. The 1952 synthesis of morphine by Gates proved these assignments to be correct.[23]

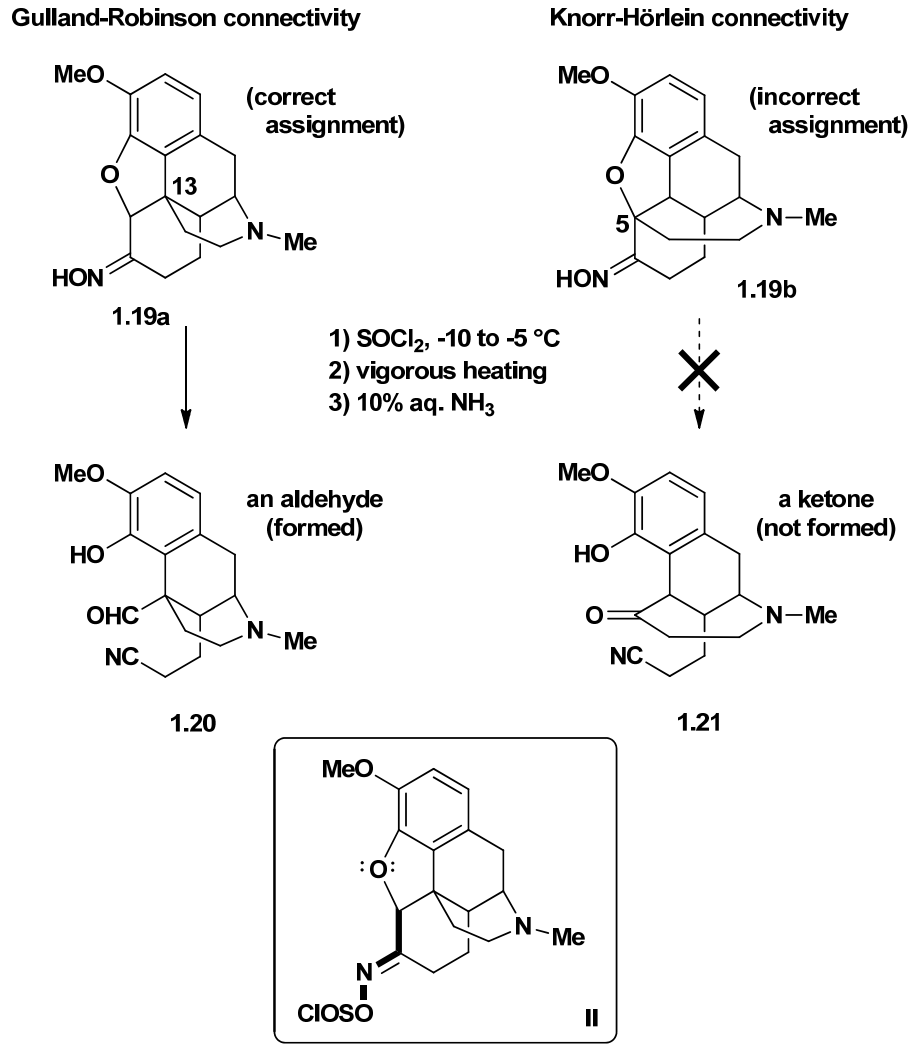

Scheme I.3 Morphine degradation studies by Schöpf (1927).[34-36]

For most of its history, this reaction had been referred to by various names, including "Beckmann fission," "abnormal Beckmann rearrangement," and "second-order Beckmann rearrangement."[8c] It was not until the 1960s, after the mechanistic studies of Grob and Fischer,[37] that the synthetic community adopted the term Beckmann fragmentation.

Although Grob was not the first to deliberately design substrates to undergo useful C-C fragmentation or to recognize the reactivity principle, he was the greatest protagonist

and made manifold contributions to the field. He was instrumental in advancing the generality of fragmentation for sp^1-sp^1 and sp^2-sp^2 systems, C-C and C-X linkages, homolytic and heterolytic reactions, and cationic, anionic, and neutral pathways. Grob also advocated that fragmentations be considered distinct from other reactions, e.g. eliminations. His 1967 review is especially noteworthy in this regard.[8a,9] Grob's first work on the Beckmann fragmentation appeared in 1963 in which he reported the fragmentation kinetics of α-amino-acetophenone oxime derivatives (e.g. **1.22** and **1.23**, Scheme I.4).[37b] Throughout his work, he favored the term nucleofuge, which refers to the leaving group of a fragmentation (e.g. **X** in Scheme I.4), and the term electrofuge, which refers to the group that donates electrons in the fragmentation (e.g. the amine nitrogen).

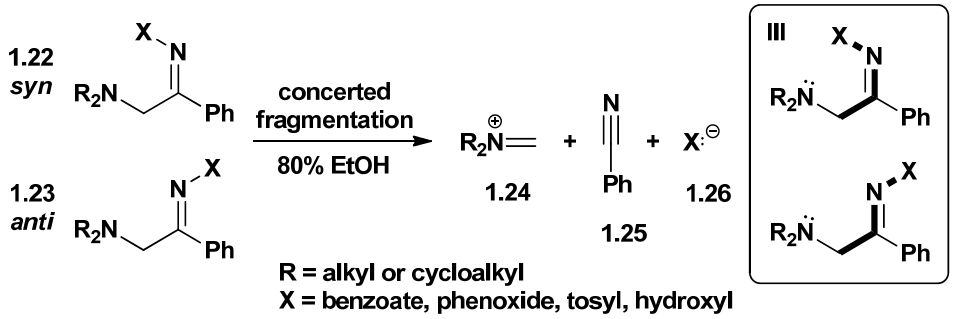

Scheme I.4 Grob's oxime fragmentation studies (1963).[37b]

Also in 1963, Grob extended the Beckmann fragmentation to include the formation of ene-nitriles (Scheme I.5).[37c] Ketotosylate **1.27** was shown to give **1.28** or **1.29** depending on the reaction conditions. Nitrile **1.28** was formed cleanly upon treatment with bulky base, whereas **1.29** was formed, albeit inefficiently, upon treatment with hydroxide. By this time the use of hydroxide to promote fragmentation had clear precedent.[1] It should be noted that the reactive intermediates were not characterized, as is often the case, and the structure shown (**IV**) is meant as a qualitative guide only.

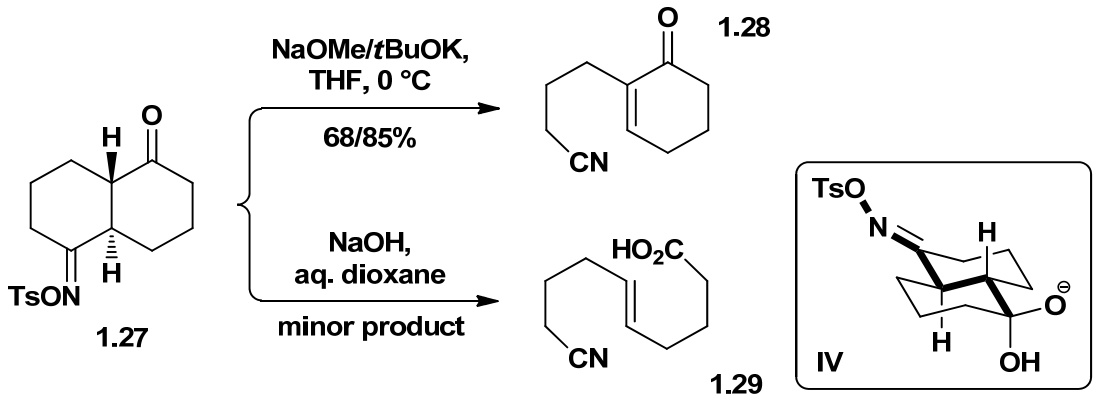

Scheme I.5 Grob's ene-nitrile synthesis (1963).[37c]

The first applications of the Beckmann fragmentation to complex molecule synthesis continue to stand as the central paradigm for its strategic use. In 1972 Stork reported the first total synthesis of byssochlamic acid (**1.32**, Scheme I.6), a nonadride mold metabolite.[38] The nine-membered ring was constructed via fragmentation of oxime **1.30**. Acid-induced isomerization of the exocyclic olefin intermediate gave endocyclic olefin **1.31** in good yield. In 1973 Colvin and co-workers utilized a heteroatom-assisted Beckmann fragmentation that is reminiscent of Schöpf's work on opium alkaloids (cf. **II** and **VI**).[39] Under ionizing conditions, the oxime tosylate derived from **1.33** fragmented to furnish derivative **1.34**, an early stage intermediate in their synthesis of the sesquiterpene antibiotic trichodermine (**1.35**).[40]

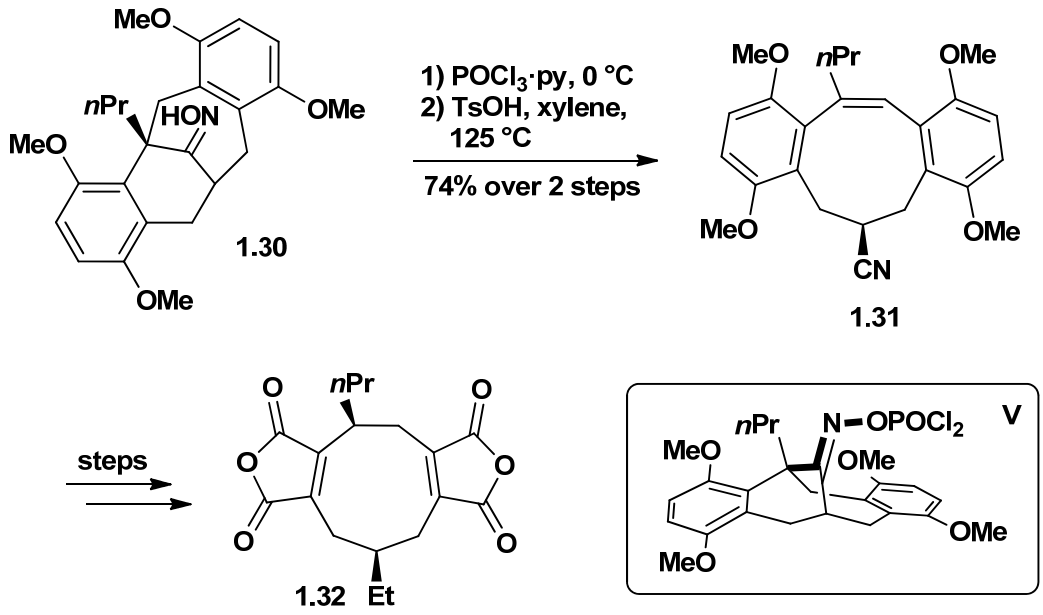

Scheme I.6 Stork's ring expansion in the total synthesis of (±)-byssochlamic acid (1.32) (1972).[38]

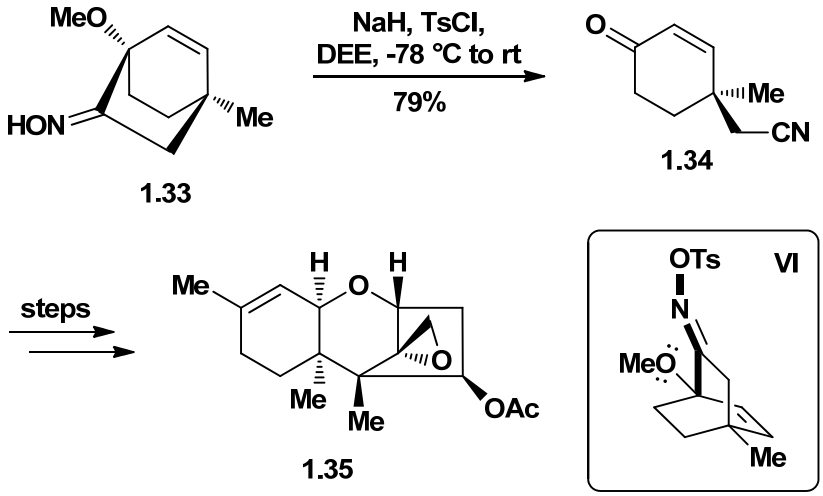

Scheme I.7 Colvin's heteroatom-assisted fragmentation in the total synthesis of (±)-trichodermine (1.35) (1973).[39]

The earliest sp^1-sp^1 bond forming fragmentation reactions that did not give nitrile products were reported by Bodendorf in the early 1960s.[41] In the presence of aqueous

sodium hydroxide, substituted β-chloroacroleins were shown to fragment to acetylenes and formic acid (e.g. **1.36** → **1.37**, Scheme I.8). In 1967 Eschenmoser disclosed an α,β-epoxyketone fragmentation that gave cyclic alkynes (**1.38** → **1.39**).[42,43] Shortly after Eschenmoser's first paper on this transformation appeared, Tanabe disclosed essentially the same reaction[44] and followed the work with a study on its application to secosteroids from testosterone (**1.40**, Scheme I.9).[45] To circumvent the problem of epoxidation of α,β-unsaturated ketones, the ketone was activated first to the *p*-toluenesulfonylhydrazone, then treated with *m*-CPBA to effect fragmentation.

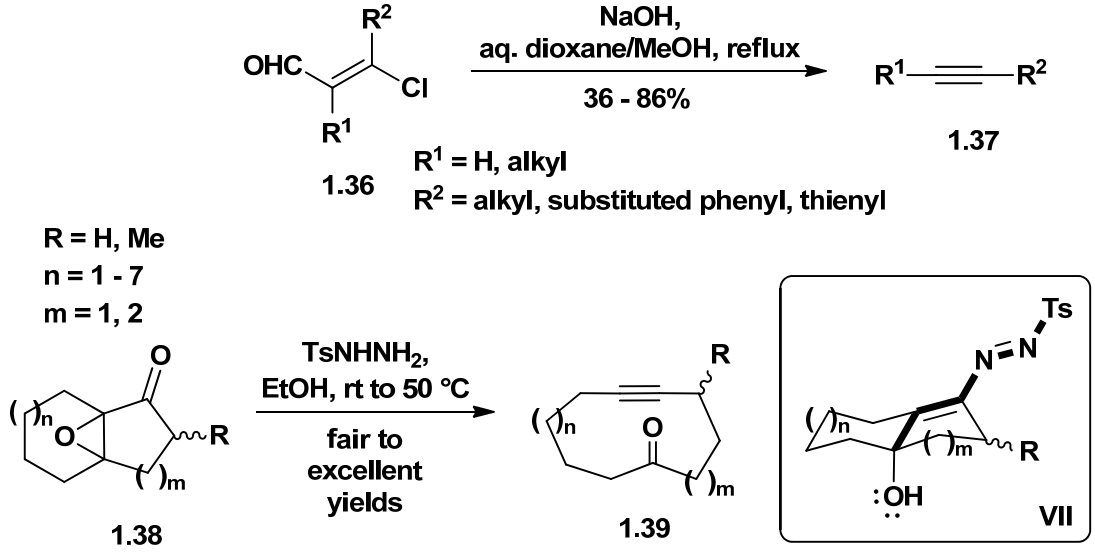

Scheme I.8 The original alkyne synthesis, by Bodendorf (1963),[41] and Eschenmoser's and Tanabe's cyclic alkyne syntheses (1967).[42,44]

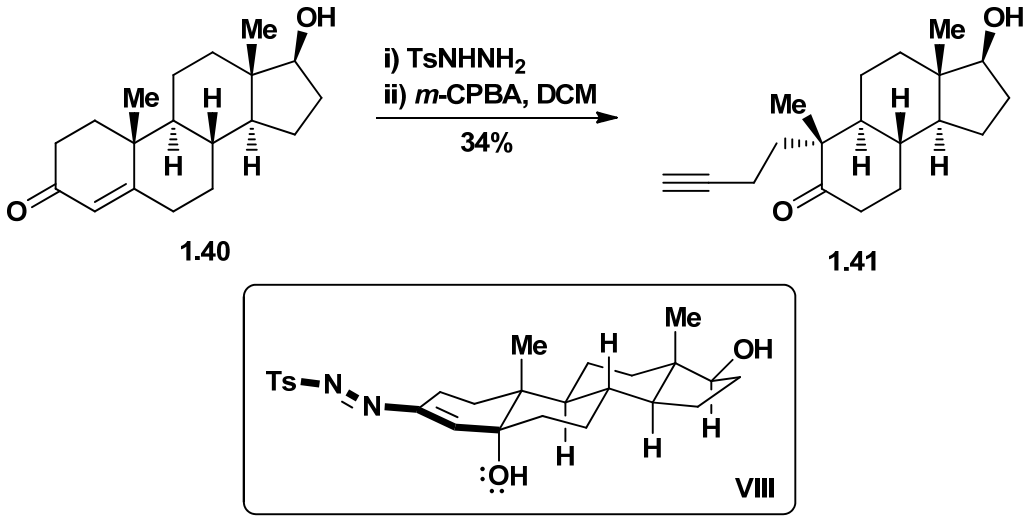

Scheme I.9 Tanabe's secosteroid synthesis (1967).[45]

Creative extensions and important improvements followed shortly after the original findings. In 1968 Borrevang and co-workers extended the mechanistic framework to include epoxy-diazirines to give acetylenic aldehydes (e.g. **1.42** → **1.43**, Scheme I.10).[46]

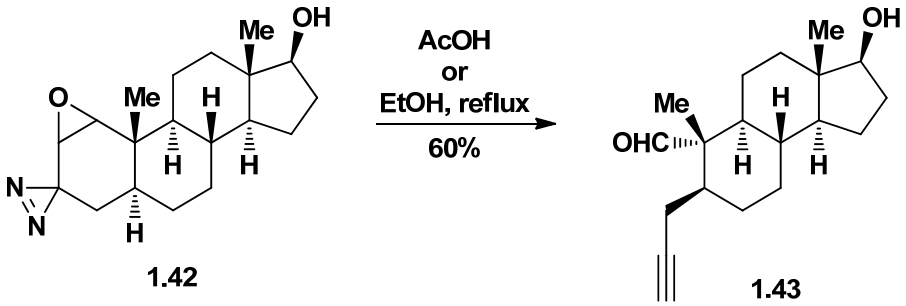

Scheme I.10 Borrevang's A-nor steroid synthesis (1968).[46]

In 1975 Corey showed that 2,4-dinitrobenzenesulfonylhydrazine is superior to *p*-toluenesulfonylhydrazine in the synthesis of acetylenic aldehydes (Scheme I.11).[47] The increased electron withdrawing nature of this reagent renders the corresponding sulfinate a better leaving group, and thereby enables fragmentation to occur under conditions more

compatible with the product (e.g. **1.45**). This early modification of the Eschenmoser-Tanabe fragmentation remains in use.

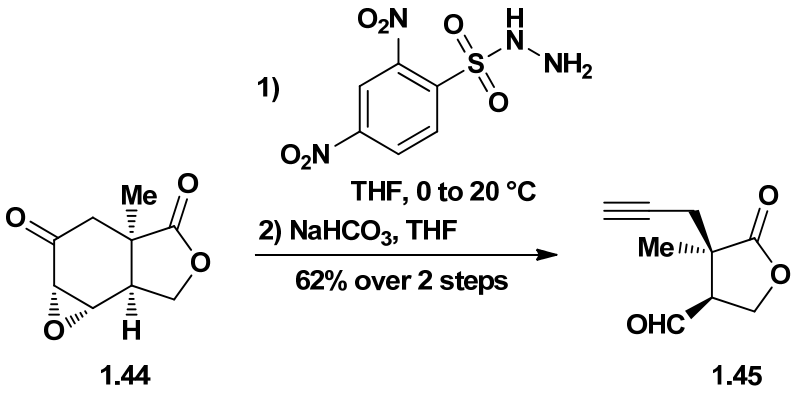

1.44 1.45

Scheme I.11 Corey's acetylenic aldehyde synthesis (1975).[47]

The 1977 report by Coke and co-workers is particularly relevant to much of the alkyne forming fragmentations reported in recent years (**1.46** → **1.47**, Scheme I.12).[48] The method was applied to the synthesis of *exo*-brevicomin (**1.48**), a pheromone produced by the western pine beetle. Addition of alkyllithium reagents to β-halo-α,β-unsaturated ketones followed by warming promotes fragmentation (see **IX**). This advance can be viewed as the fusion of the Bodendorf[41] and Eschenmoser[1] studies. This reaction modality was also demonstrated to include selenones as the leaving group.[49] Treatment of cyclic 3-hydroxyvinyl phenyl selenones (**1.49** and **1.51**) with base at room temperature leads to fragmentation. Bases of low nucleophilicity (NaH, *t*BuOK, LDA) promote direct fragmentation. Alkoxides, however, add to the vinyl selenone, which is followed by proton transfer and then fragmentation. Although the formation of **1.52** formally belongs to the sp^2-sp^2 category, the finding is relevant here, since selection of base determines the product distribution.

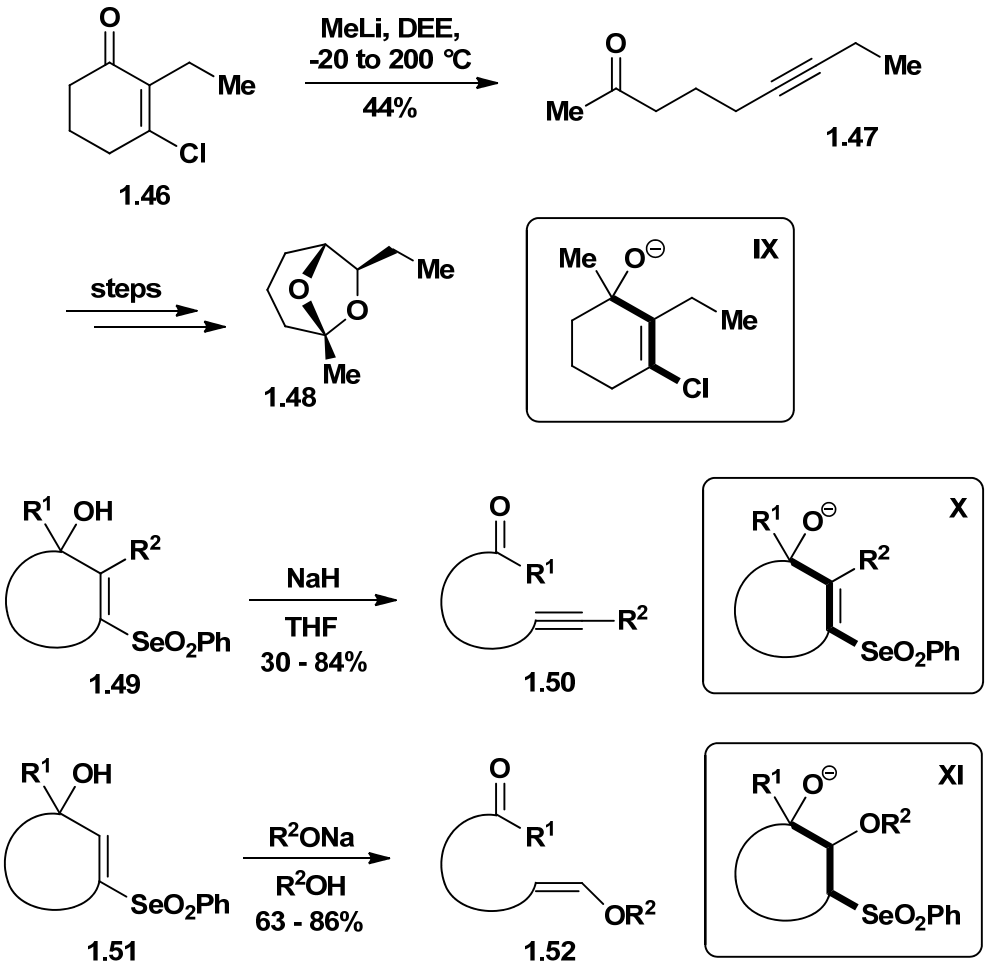

Scheme I.12 Coke (1977)[48] and Kuwajima's (1981)[49] acetylenic ketone syntheses.

1.2.2 sp^2-sp^2 bond forming fragmentations

The 1952 Eschenmoser disclosure described alkene synthesis via fragmentation under basic conditions so as to ensure proper placement of the resultant C-C double bond.[1] The report included a comprehensive collection of the relevant anionic observations that had been recorded as otherwise isolated and unrelated. These observations were summarized together in the context of a unified mechanistic framework, which provided insight as to likely product structures. Hence, certain reactions of halide-substituted monoterpenes with alkali reportedly produced ene-acids, such as β-bromocamphor (**1.53**,

Figure I.2),[50] monobromofenchone (**1.54**, the constitutional structure of which had not yet been fully assigned),[51] and a pulegone dibromide (**1.55**).[52] In light of the suggested mechanism the product structures could then be readily formulated. Certain β-bromo-acids and α-tosyloxy-β,β-dimethyl-butyrolactone were noted to undergo base-promoted decarboxylative or decarbonylative elimination (not shown).[53,54] The final observation cited was a 1951 report on the reaction of β-chloroketones with Grignard reagents (not shown).[55]

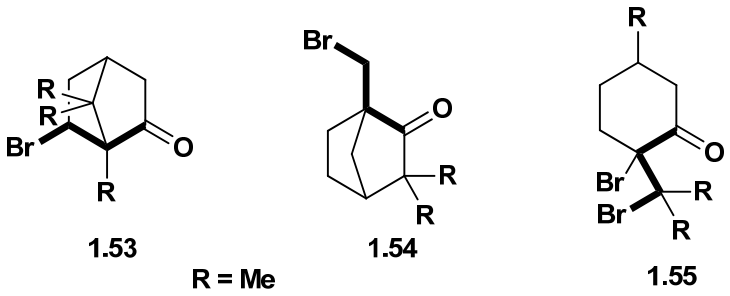

Figure I.2 Monoterpene fragmentation substrates from Forster (1.53) (1902), Czerny (1.54) (1900), and Wallach (1.55) (1896).[50-52]

To illustrate the potential of the revealed reactivity, Eschenmoser designed substrate **1.1** (Scheme I.13) for the selective preparation of a 1,1-disubstituted alkene (**1.56**).[1] The C-C cleavage (*spaltung*, viz. Wallach) offered an improvement over existing methods of alkene synthesis,[56] which often required vigorous conditions and resulted in mixtures of products usually favoring the more substituted double bond. Base-induced C-C cleavage and loss of the properly positioned leaving group guaranteed site-selective introduction of the alkene.

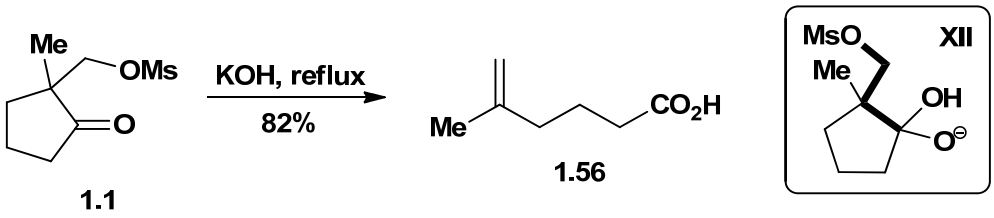

Scheme I.13 Eschenmoser's original alkene synthesis (1952).[1]

One antecedent not mentioned in Eschenmoser's original report was the degradation reactions of cinchona alkaloids under neutral conditions. Although initially interpreted incorrectly, the fragmentation of a quinine derivative was first reported by Skraup in 1892.[57-59] In the late 1930s, Gibbs and Henry confirmed the loss of formaldehyde in the degradation of quinidine (**1.57**) to niquidine (**1.62**) and provided constitutional formulae of the isomeric products and the subsequent single hydrogenation product, dihydroniquidine (**1.63**, Scheme I.14).[60] In a 1952 synthetic study, Mosher offered a sound mechanism to explain the conversion of **1.57** to **1.62**.[61] However, this appeared in the same timeframe as the Eschenmoser report and could not have been included as a citation.

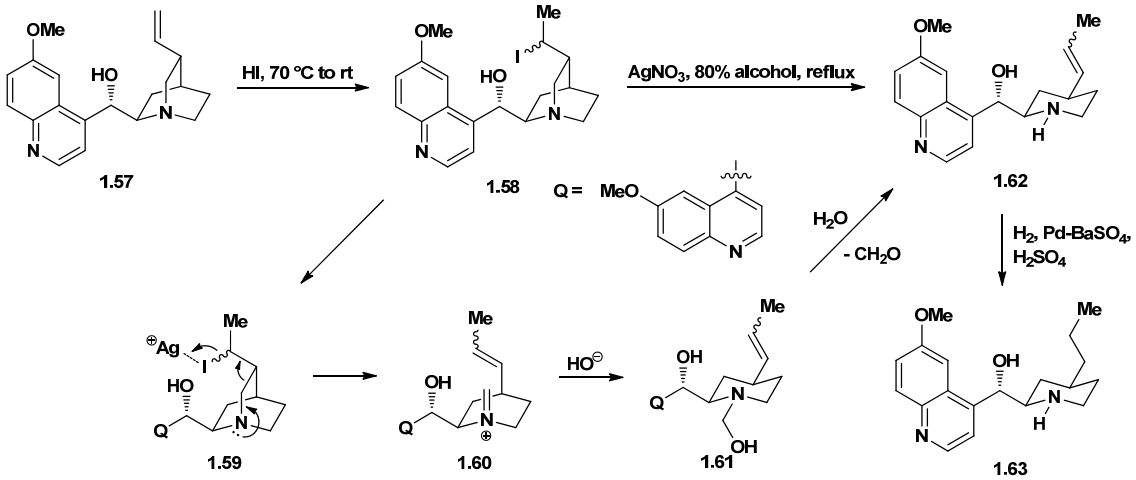

Scheme I.14 Gibbs-Henry degradation of quinidine (1.57) (1939)[60] and Mosher's mechanistic interpretation (1952).[61]

Perhaps understandably, Beckmann and cationic pathways that led to overall fragmentation were not mentioned. Controlled alkene formation, germane to the Eschenmoser fragmentation, is compromised in cationic pathways. The discovery and study of what we now call cationic fragmentations began in the early twentieth century and nearly coincided with the discovery of the reverse transformation: the Prins reaction (where the resultant cation is captured by nucleophile).[62] The first Prins-type report was published in 1899. Indeed, many cationic fragmentations could well be described as retro-Prins type reactions. Still, such transformations are now considered fragmentations. The etiology of this type of reaction is traceable to Slawjanov[63a] and Kalishev[63b] who independently reported the acid-induced conversion of hexamethyl-1,3-propanediol to isobutylene and acetone (**1.64** → **1.67** and **1.68**, R^1, R^2, and R^3 = CH_3, Scheme I.15). In 1933 Whitmore and Stahly demonstrated a similar process in the dehydration of di-*tert*-butylcarbinol (**1.69**).[64] Loss of water and formation of the secondary carbocation is followed by 1,2-methyl shift and then C-C fragmentation to produce trimethylethylene (**1.73**) and isobutylene (**1.67b**).[65]

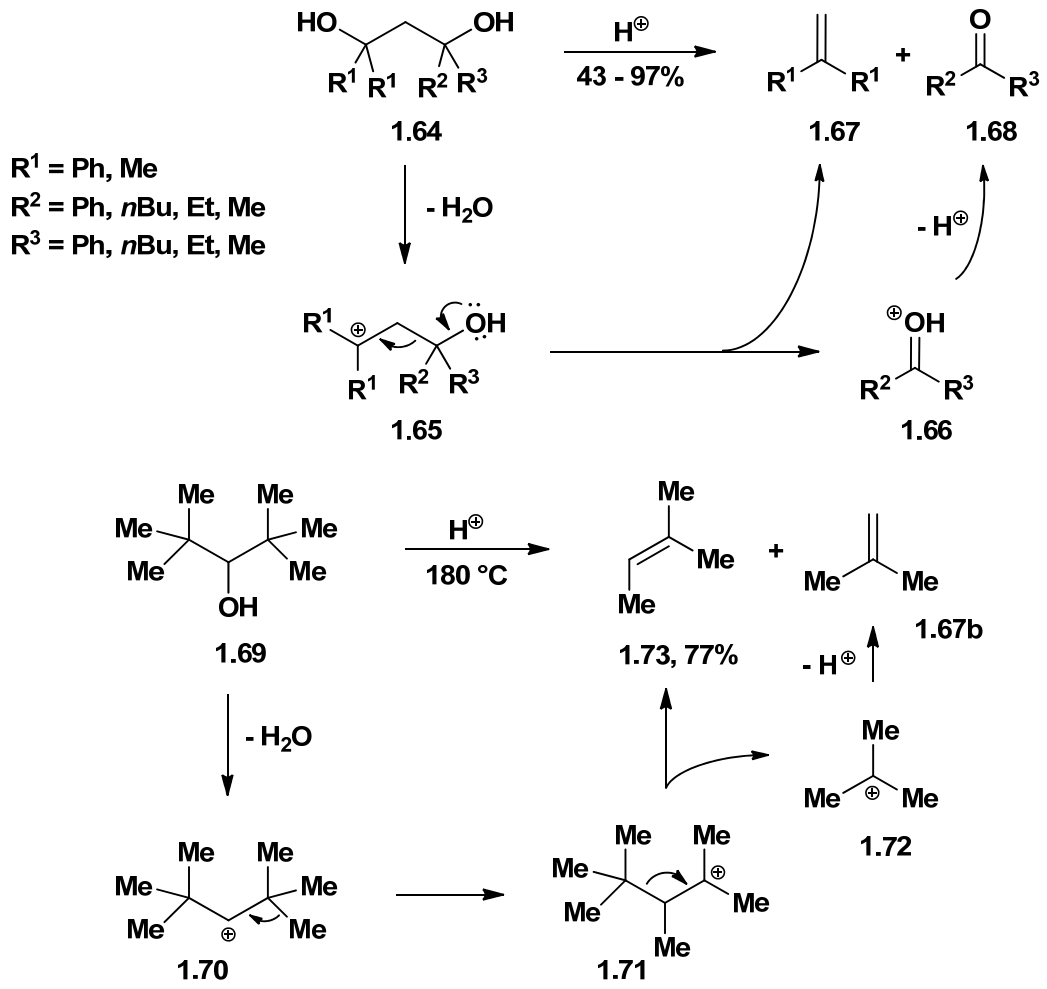

Scheme I.15 Cationic fragmentations (1907-1952).[63,64,66]

After 1952 a treasure trove of discoveries and reactivity insights were published. The first such study emanated from the Henbest laboratories in 1953 (Scheme I.16).[67] This group explored the competing reaction pathways of 3-chloro-1-ols in basic solution.[67,68] Using monocyclic and steroidal substrates, they demonstrated that fragmentation depends on the relative stereochemical arrangement of the reaction centers. Treatment of *trans*-chlorocholestanol **1.74** with potassium *tert*-butoxide afforded significant quantities of the *seco*-ketone **1.75**; exposure of epimeric chlorocholestanol **1.77** to the same

conditions predominantly gave the elimination product **1.78**. Henbest was the first to assert that fragmentation is possible only when the bonds to be severed are in an antiparallel arrangement (see **XIII**).[67,68]

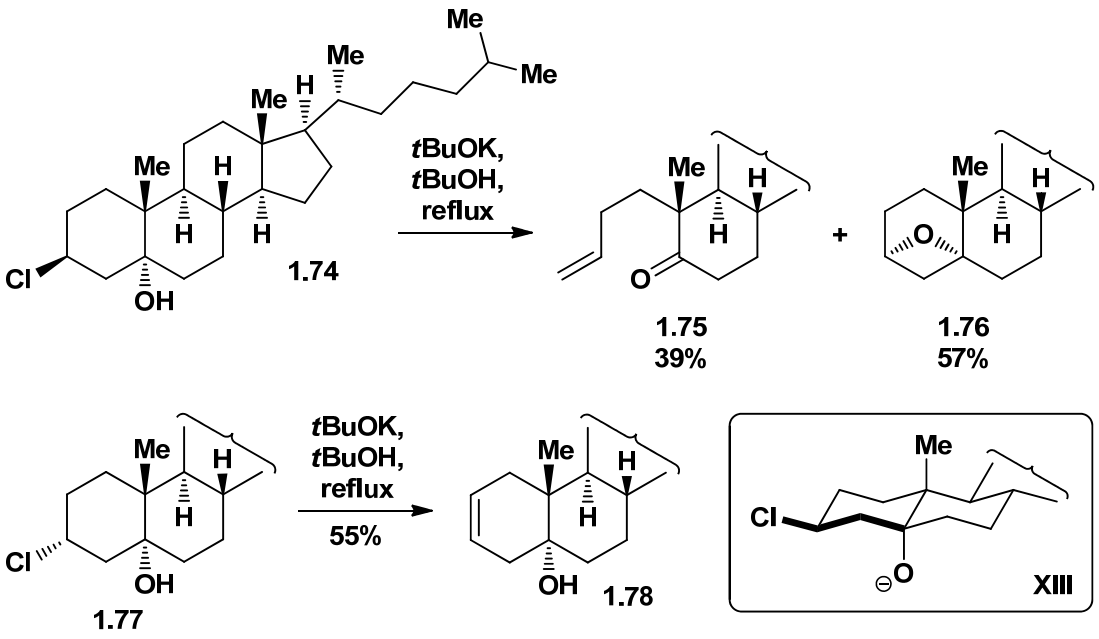

Scheme I.16 The original stereochemical investigation on concerted C-C fragmentation, by Henbest (1953).[67,68]

In the early 1950s, English and co-workers expanded the scope of acid-catalyzed cleavage reactions of 1,3-diols and singled out the importance of cationic intermediate **1.65** (Scheme I.15).[66] In 1956 English and Bliss rationalized that other compounds capable of generating β-hydroxycarbocations should also undergo fragmentation.[69] Accordingly, they studied the nitrous acid-catalyzed deamination of 1,3-amino alcohols (e.g. **1.79**, Scheme I.17). Shortly after this disclosure, Jefferies and co-workers reported the rupture of *cis*- and *trans*-3-aminocyclohexanol (**1.82**) under similar conditions.[70]

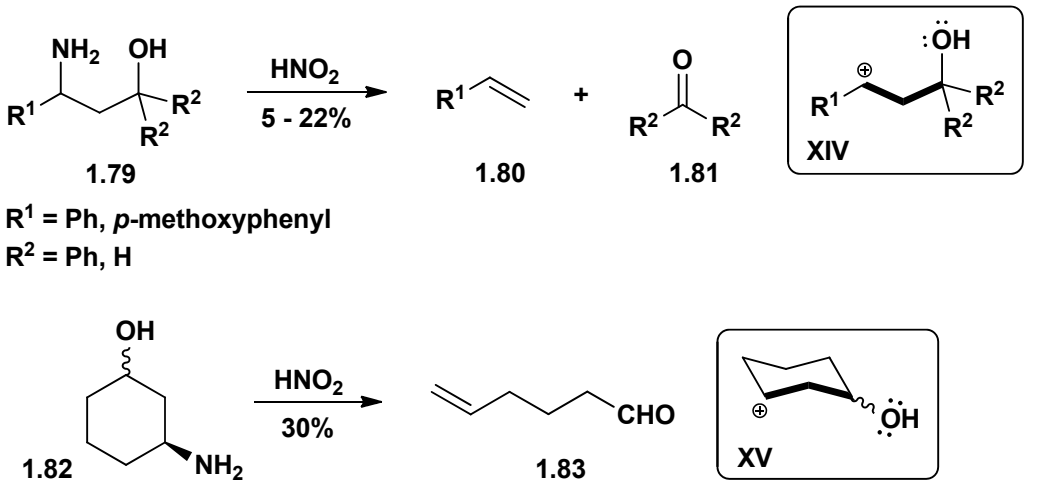

Scheme I.17 English and Jefferies' cationic fragmentations (1956-1957).[69,70]

Grob's first contribution to C-C fragmentation appeared in 1955.[71] In this paper he introduced the term fragmentation (*fragmentierung*), presented the Eschenmoser mechanistic framework (Scheme I.18) in a generalized form,[72,73] reviewed a series of 1,4-elimination reactions, including the zinc mediated elimination of 1,4-dihalides (e.g. **1.89**), and converted 1,4-dihalocyclohexane to hexa-1,5-diene in high yield (**1.91**, Scheme I.19).

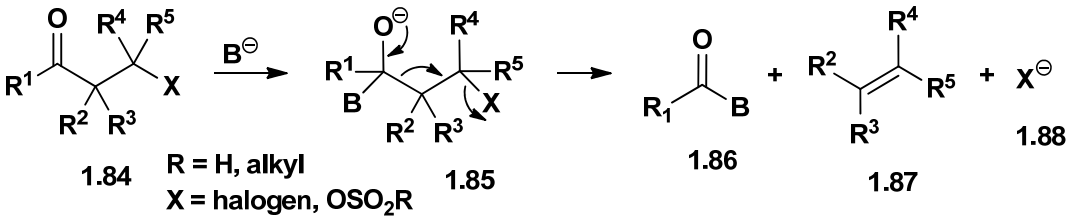

Scheme I.18 The original C-C fragmentation mechanistic framework, by Eschenmoser (1952).[1]

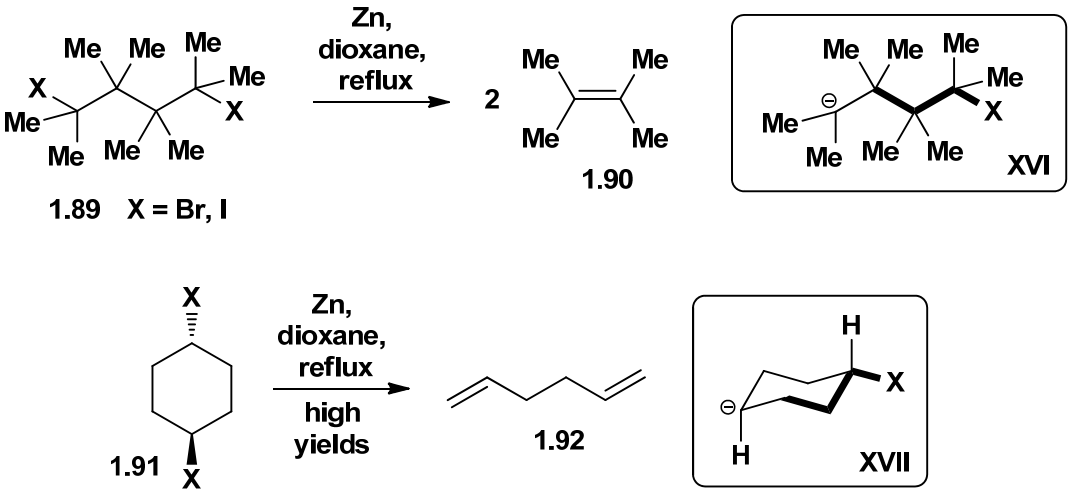

Scheme I.19 Grob's 1,4-eliminations and diene synthesis (1955).[71]

Stork reported the first ring-expansion by fragmentation in 1956 (**1.93** → **1.94**, Scheme I.20).[74] However, beginning in 1961 Wharton demonstrated that site-selective olefin formation via C-C fragmentation could be stereospecific and could be used to generate medium-sized rings from bicyclic precursors (e.g. **1.95** → **1.96**, Scheme I.21).[75] This strategic insight has been immensely useful for preparing cyclic alkenes of defined geometry.

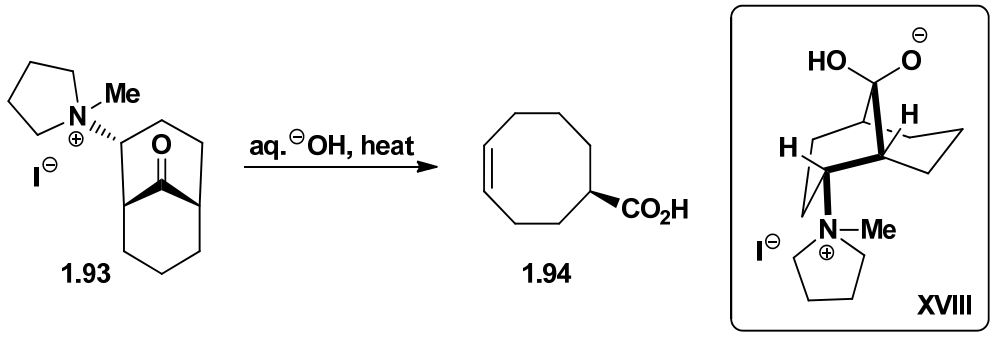

Scheme I.20 The original C-C fragmentative ring expansion, by Stork (1956).[74]

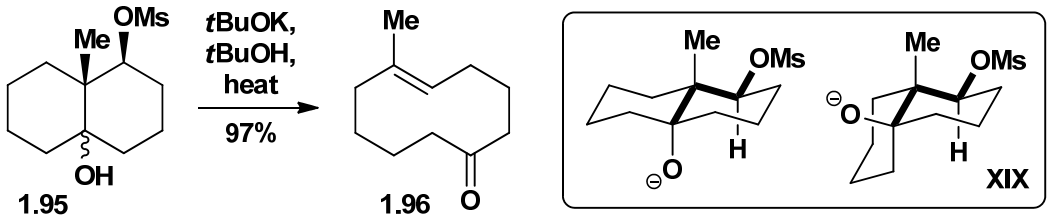

Scheme I.21 Wharton's convergent ring expansion (1961).[75]

In 1965 Wharton reported numerous other examples of fragmentation in the decalindiol series, which are now considered classic studies. Importantly, these findings emphasize the efficiency of the method when the bonds to be broken are antiperiplanar.[76,77] Moreover, epimeric monotosylates **1.97** and **1.98** fragment under identical conditions to yield the same product, *trans*-5-cyclodecenone (**1.99**), in excellent yields (Scheme I.22).[75] Thus, the stereochemistry of the procarbonyl carbon was suggested to be irrelevant in a fragmentation process (*cf.* **XIX**). The complementary *cis* isomer was obtained from the epimeric monotosylate **1.100**. Wharton also executed the stereospecific fragmentation of dibromoperhydroanthracene **1.102** to bicyclo[8.4.0]tetradecadiene **1.103** (Scheme I.23).[78,79]

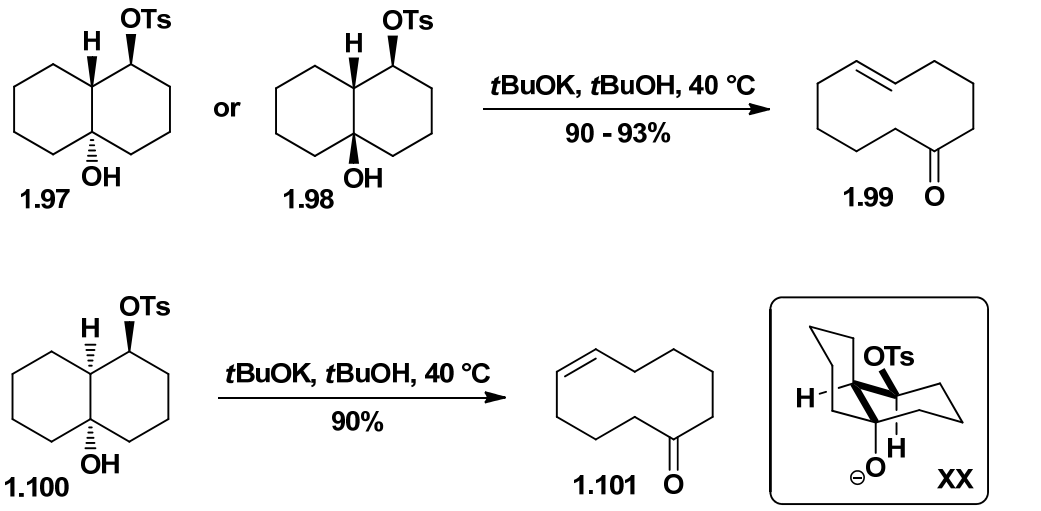

Scheme I.22 Wharton's cyclodecene syntheses (1965).[76]

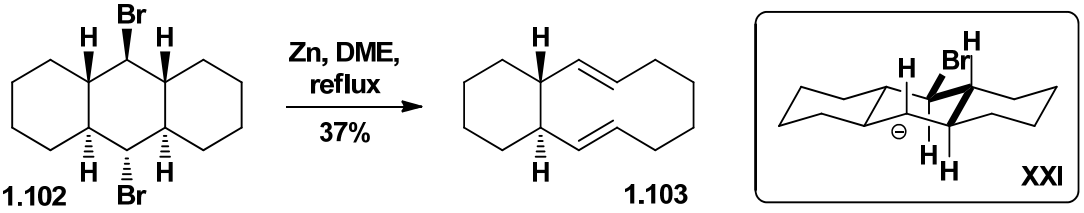

Scheme I.23 Wharton's cyclodecadiene synthesis (1965).[78]

Grob reported in 1962 the solvolysis of acyclic, monocyclic, and bicyclic γ-amino halides **1.104-1.106** (Figure I.3),[80] and thereby demonstrated that the degradative fragmentations of the cinchona alkaloids are general.[57,58,60] He showed that fragmentation predominates over substitution and elimination in these systems. A series of *N*-methyl decahydroquinoline tosylates were also investigated (**1.107**, **1.109**, and **1.111**, Scheme I.24).[81] In accordance with Henbest,[67,68] Grob confirmed that a concerted pathway is favored over a two-step mechanism provided both the C-OTs bond and nitrogen lone pair are antiperiplanar to the scissile C-C bond (see **XXV**-**XXVII**). Solvolysis of **1.107**, **1.109**,

and **1.111** afforded products of stereospecific fragmentation exclusively, whereas the corresponding epimeric tosylates (not shown), which could not adopt an antiperiplanar arrangement, were much slower to solvolyze and yielded mixtures of fragmentation, substitution, and elimination products. Grob argued that, although the *N*-methyl groups are predominantly in the equatorial position, concerted fragmentation occurs most readily when they are axial, placing the nitrogen lone pair antiperiplanar to the rupturing bonds.[82-84]

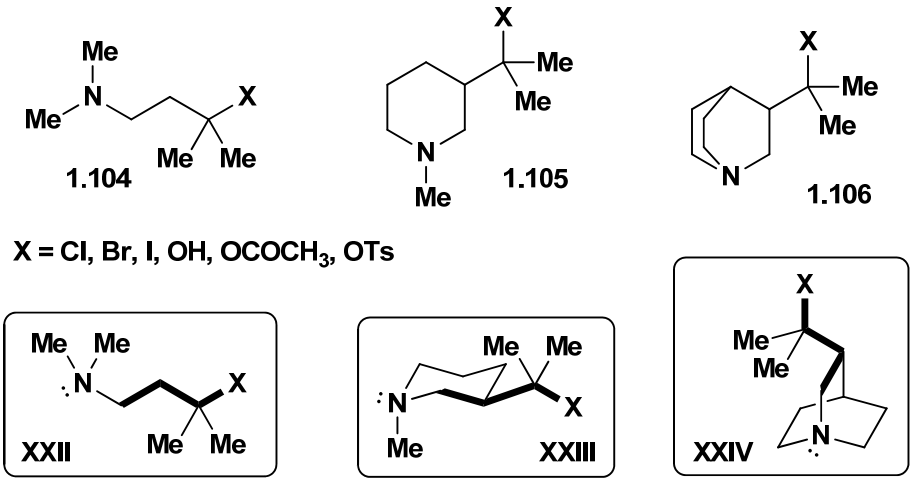

Figure I.3 Grob's γ-amino halide fragmentations (1962).[80]

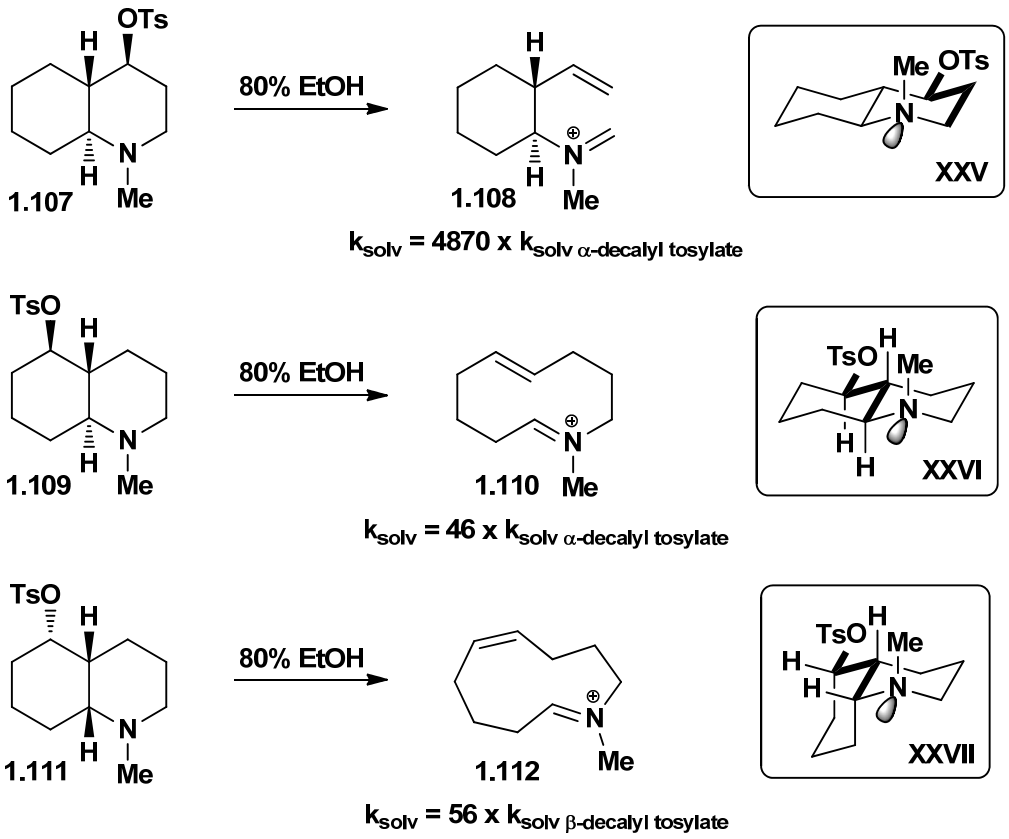

Scheme I.24 Grob's kinetic studies (1964).[8b,81]

Corey's 1963 and 1964 work on caryophyllene stands as a classic in chemical synthesis (**1.115**, Scheme I.25).[85] Corey noted that the contributions of Eschenmoser, Henbest, Jefferies, and Wharton provided the strategic foundation upon which this natural product and its isomers were prepared.[86] Indeed, the trisubstituted alkene was installed stereospecifically within this challenging context (**1.113** → **1.114**).

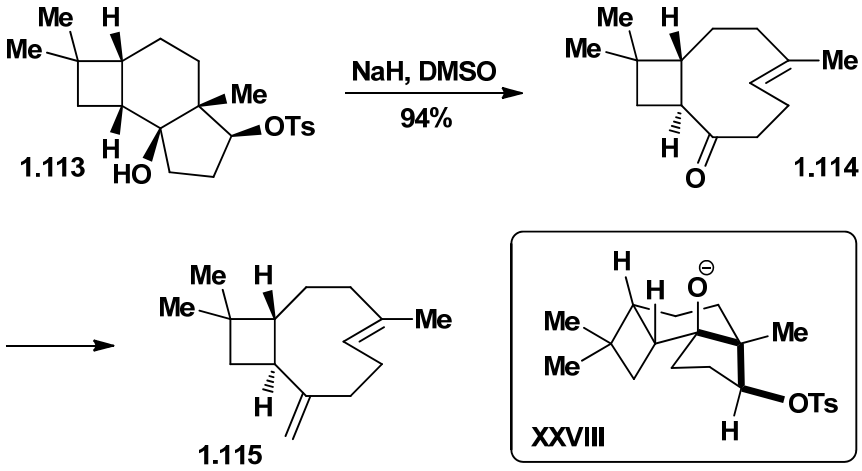

Scheme I.25 The original total synthesis via C-C fragmentation, by Corey (1963-1964).[85]

Concurrent with Corey's syntheses of nine-membered rings, Tanabe constructed the cyclononenone-containing 13,14-secosteroid **1.117** from hydroxytosylate **1.116** (Scheme I.26).[87] Presumably, the *cis* relationship between the C-17 hydrogen and C-18 methyl group was retained (**XXIX**). The C-8 stereochemistry was not assigned due to the enolizability of this α-proton under the reaction conditions.

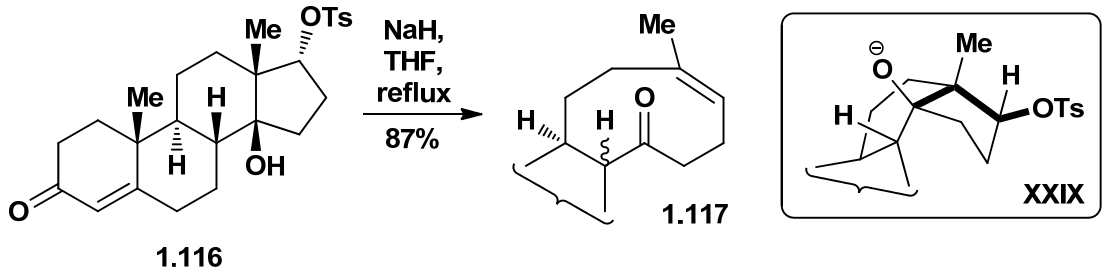

Scheme I.26 Tanabe's cyclononene synthesis (1964).[87]

In a 1965 study reminiscent of Stork's ring expansion,[74] Marshall prepared substituted *cis*-cyclodecenes from activated [5.3.1] bicycles (e.g. **1.118 → 1.119**, Scheme

I.27).[88] Similarly, the reactivity of hydroxytosylate **1.120** was studied (Scheme I.28).[89] Under nucleophilic basic conditions, compound **1.120** fragmented and the *Z* olefin (not shown) rearranged to the thermodynamic *E* olefin **1.121**. In the presence of hydride, **1.120** formed alcohol **1.122**. Under solvolytic conditions, however, the rearrangement product **1.125** was isolated. This product was rationalized in terms of cationic ring expansion and then fragmentation (shown as **1.123** → **1.124** → **1.125**).

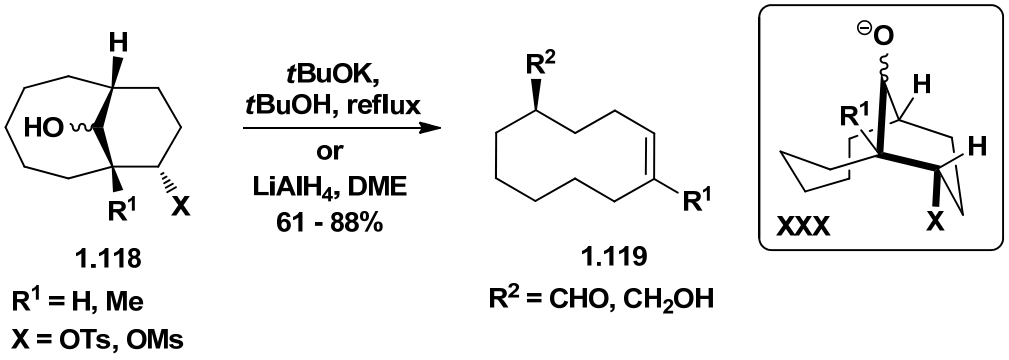

1.118
R^1 = H, Me
X = OTs, OMs

1.119
R^2 = CHO, CH_2OH

Scheme I.27 Marshall's ring expansions (1965).[88]

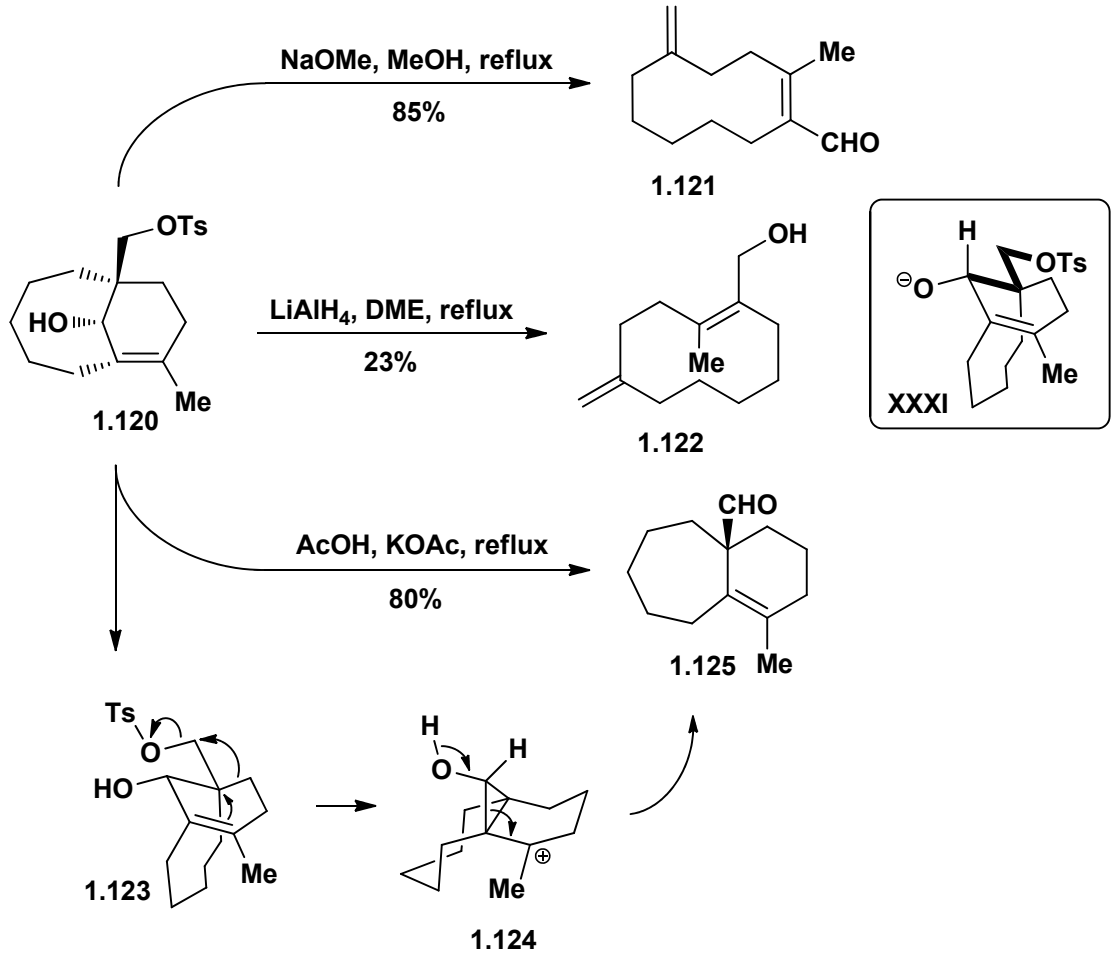

Scheme I.28 Marshall's divergent fragmentations (1967).[89]

Marshall ingeniously expanded the scope of the electrofuge. The first of these contributions appeared in 1966.[90] In it he showed that an *in situ*-generated boronate, probably as a mixture of diastereomers, could serve as the electron source in a fragmentation through the stereospecific formation of **1.127** from **1.126** (Scheme I.29).[91] The Marshall group also introduced the use of stabilized dithianyl[92] and malonyl[93] anions, reminiscent of Grob's ene-nitrile work (*cf.* Scheme I.5). For example, **1.128** and **1.130** led to the corresponding products **1.129** and, after base-induced olefin migration, **1.131** (Scheme I.30).

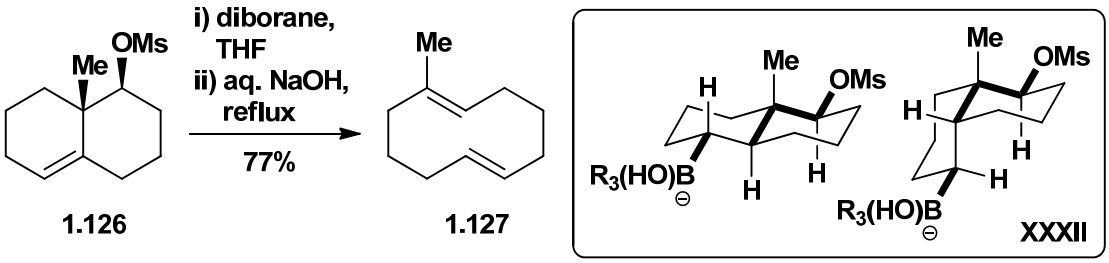

Scheme I.29 The original boronate electrofuge, by Marshall (1966).[90]

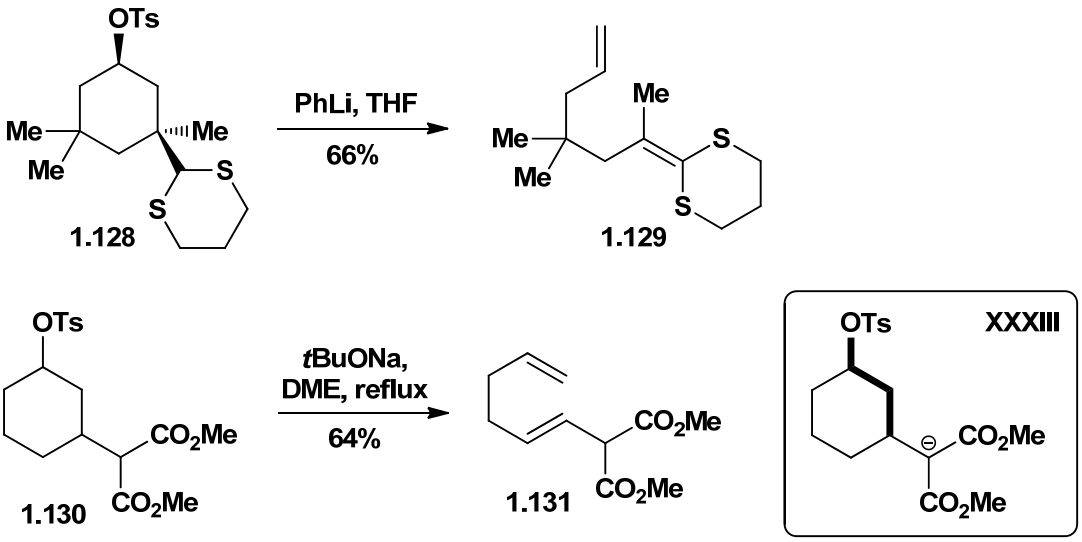

Scheme I.30 The original dithianyl electrofuge and malonyl electrofuge, by Marshall (1971).[92,93]

The Grob/Marshall-type electrofuge was used by Mander to access complex germacranes and related sesquiterpenes.[94] The enolate of *trans*-decalin **1.132** underwent clean conversion to diene **1.133** (Scheme I.31). Production of this single geometric isomer under non-isomerizing conditions implies that fragmentation occurred predominantly with the methyl ester in a pseudo-axial position.

Scheme I.31 Mander's germacrane scaffold synthesis (1977).[94]

Four years after the synthesis of caryophyllene (**1.115**),[85] the Syntex group reported the synthesis of a polyunsaturated acyclic system (**1.137**, Scheme I.32).[95] In this classic synthesis two challenging trisubstituted alkenes were generated by way of a sequential fragmentation of a cyclic precursor. Bicycle **1.134** was designed to stereospecifically transform into **1.135** then **1.137**. This work constituted a formal synthesis of juvenile hormone I (**1.138**).

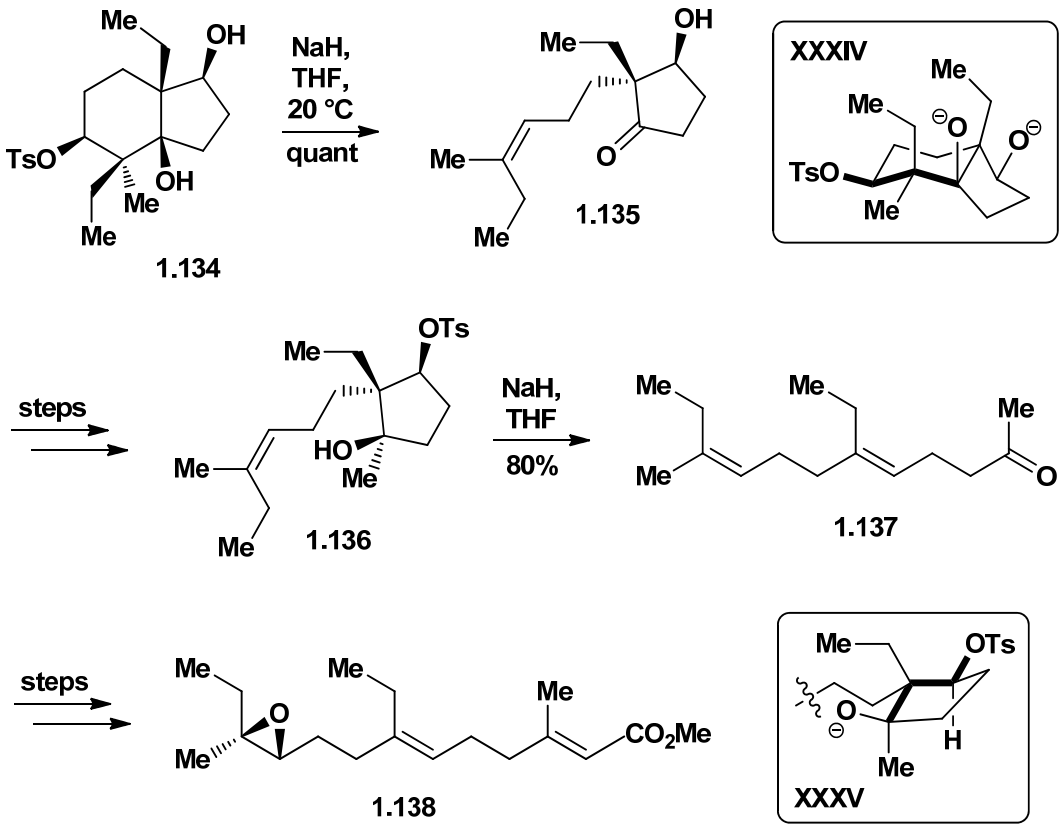

Scheme I.32 The Syntex sequential fragmentation (1968).[95]

In this section we summarized the foundational studies of C-C fragmentation and focused on the applications that presage much of the work in the field. We close with a final classic study and one of the boldest transformations of this sort. It appeared in 1979.[96] In an approach towards macrolides, Eschenmoser designed diastereomeric amidinium carboxylates **1.139** and **1.140** to undergo extended fragmentation to produce macrolactone **1.141** (Scheme I.33). Although the mechanisms of these transformations were not studied, both were designed to effect tandem decarboxylative elimination and heterolytic C-C fragmentation processes that alter the connectivity of nine atoms of the substrate. Another pair of tricyclic substrates was also examined (not shown).[97]

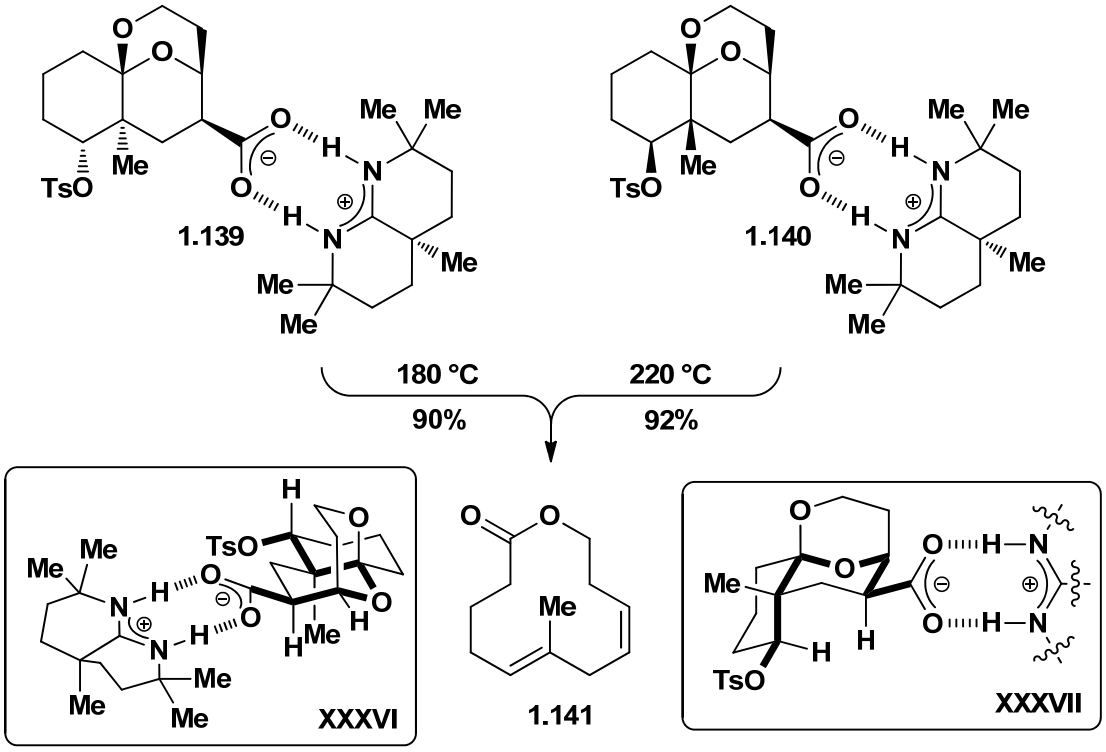

Scheme I.33 Eschenmoser's extended decarboxylative elimination/C-C fragmentation (1979).[96]

1.3 Progress and Applications

The key findings described above have enabled many innovative advances in chemical synthesis. This section highlights recent examples of the reactions and novel fragmentation methodologies used to prepare sp^1-sp^1, sp^2-sp^2, and sp^2-sp^1 connectivity, presented in an order that parallels the preceding historical discussion. Examples that generate sp^2-sp^1 bonds are comparitively rare. The possible use of a fragmentation may be difficult to discern in the planning stages of a synthesis owing to the subtleties associated with retron[18] and pattern recognition.[98] Successful implementation of a C-C fragmentation in a complex setting is often perceived as elegant. Therefore, the final section summarizes the application of C-C fragmentation in complex molecule synthesis. Examples that

generate sp^1-sp^1 bonds are discussed first. The more common sp^2-sp^2 examples are described next, beginning with ring openings and concluding with ring expansions.

1.3.1 sp^1-sp^1 bond forming fragmentations

Several useful modifications and applications of the Beckmann fragmentation have appeared over the past several years. In 1997 Kirihara reported that diethylaminosulfur trifluoride (DAST) effects Beckmann fragmentation of cyclic ketoximes (e.g. **1.142** and **1.144**) and is accompanied by capture of the cationic intermediate with fluoride (Scheme I.34).[99] This significant contribution is favored in substrates that possess electron-donating substituents α to the oximino carbon. The substrates evaluated were relatively complex, including both terpenes and steroids.

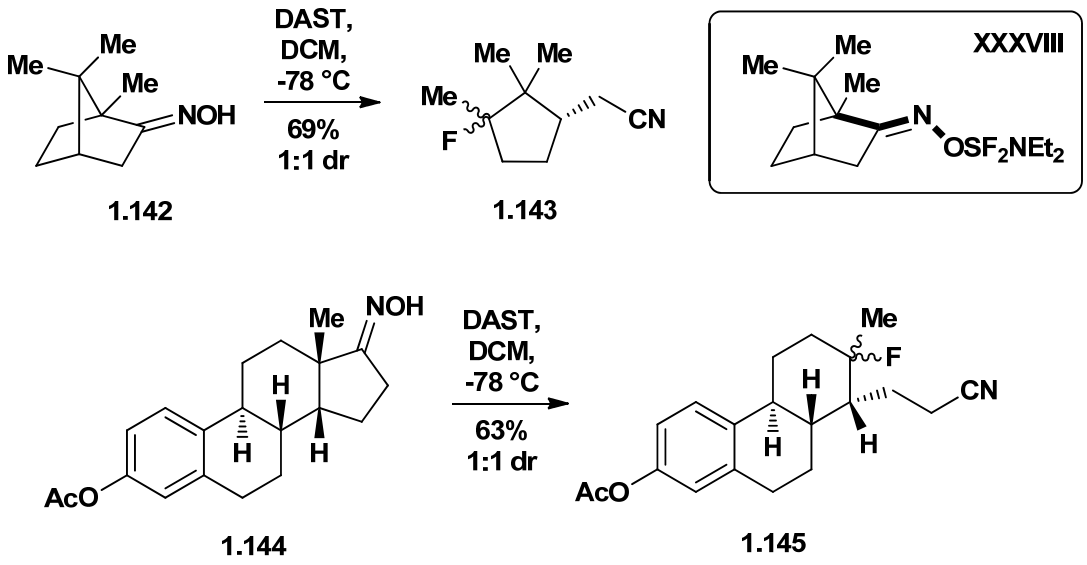

Scheme I.34 Kirihara's fluorinative ketoxime fragmentations (1997).[99]

Reminiscent of the original morphine work,[36] Subba Rao described an efficient heteroatom-assisted Beckmann fragmentation of **1.146**, which furnished the [4.3.3]propellane derivative **1.147** (Scheme I.35).[100] This product is a potential

intermediate *en route* to natural [3.3.3]propellanes such as modhephene (**1.148**). In related studies, Čeković and co-workers describe what they call Beckmann rearrangements on diastereomeric oximes **1.149** and **1.154** (Scheme I.36).[101] They rationalize that the activated oxime, formulated as **1.150**, undergoes 1,2-migration to give a cation (e.g. **1.151**), which undergoes C-N bond cleavage instead of trapping with hydroxide. Of course, direct Beckmann fragmentation of the activated oxime in the usual way, **1.150** → **1.152**, *cf.* **XL**, may be the operative pathway.

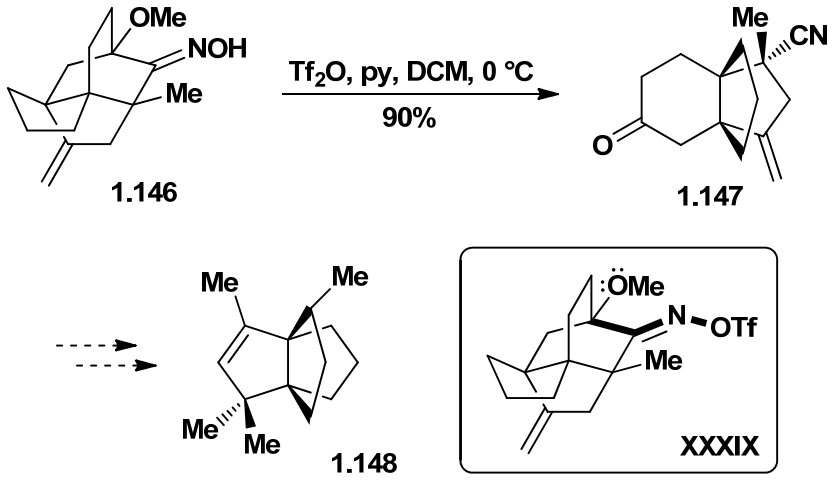

Scheme I.35 Subba Rao's [4.3.3]propellane scaffold synthesis (2000).[100]

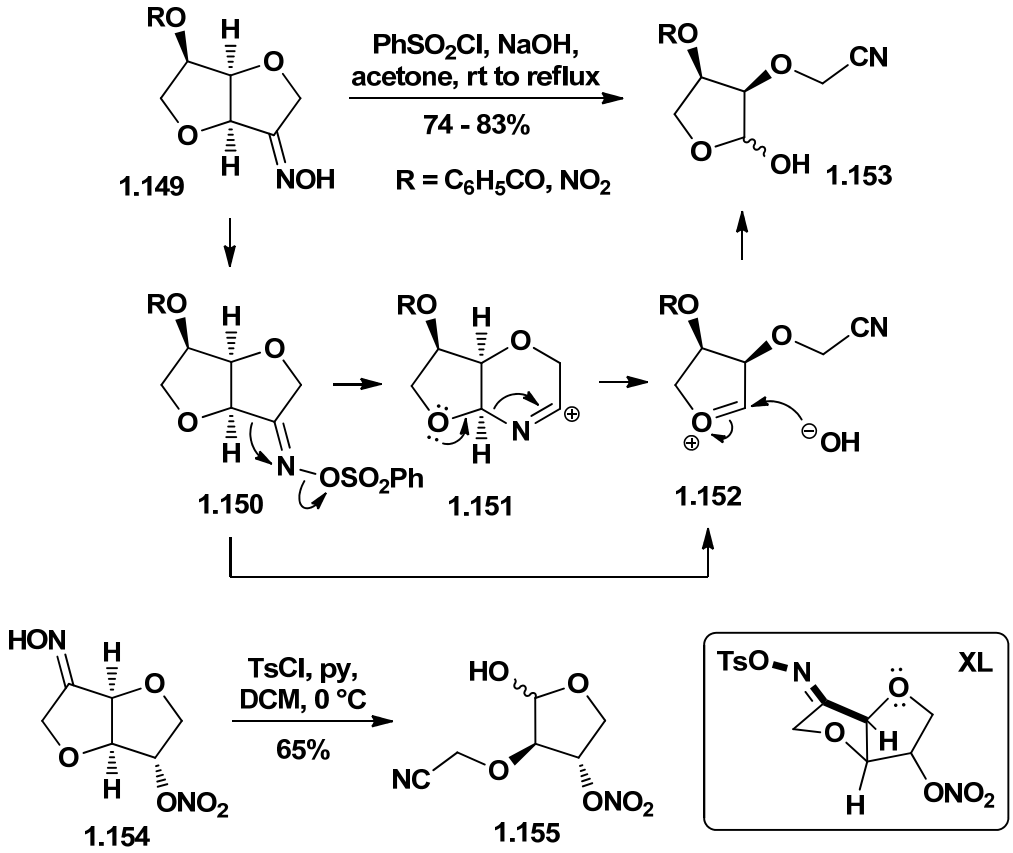

Scheme I.36 Čeković's nitrile synthesis (2001).[101]

An unexpected Beckmann fragmentation product of a C(1)-substituted-7-bromonorbornane-2-one was observed by Maroto upon hydroxylamine treatment of **1.156** (Scheme I.37).[102] Further studies on this highly efficient transformation led to the suggestion that this process is driven by intramolecular activation of the bromo group by the amide nitrogen. Fragmentation did not take place when the amide was replaced with a methyl group. The reaction pathway appears to be oxime formation, fragmentation, and then amide hydrolysis. The fate of the bromo group and the role of the amide are intriguing.[103]

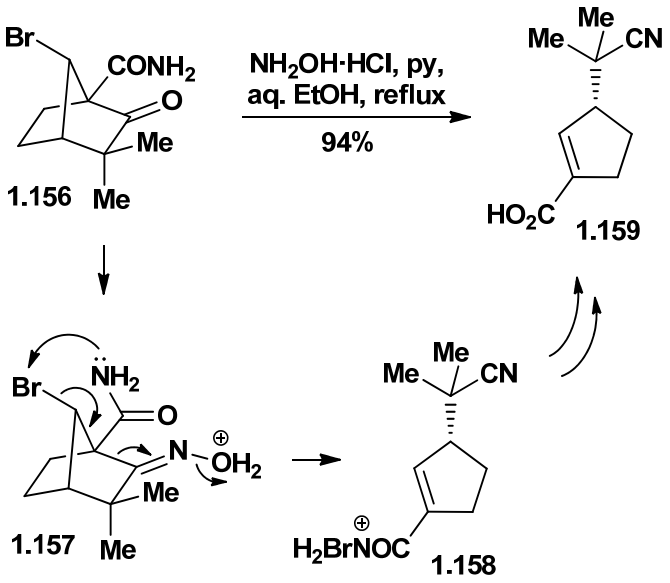

Scheme I.37 Maroto's ring opening (2004).[102]

Fragmentations that give alkynes have been an area of much activity. In close analogy to the original Eschenmoser-Tanabe studies,[42,44] bicyclic epoxyketone **1.160** fragmented as expected to give cyclodecynone **1.161** in good yield (Scheme I.38).[104] This was part of a study that demonstrated the utility of various 1,3,5-hexatrienes produced from a one-pot sequence of Stille and Heck couplings.

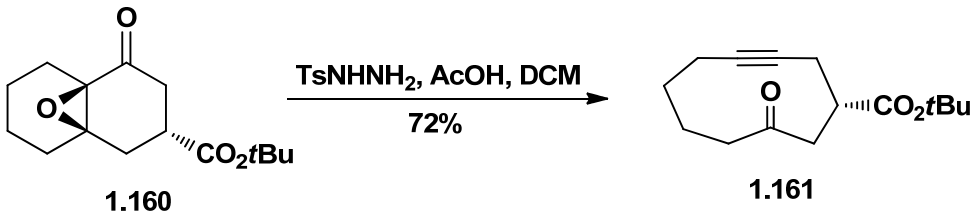

Scheme I.38 de Meijere's cyclic alkynone synthesis (2001).[104]

The most extensive and generally useful advance in this area has been registered by Dudley. He and his co-workers have thoroughly demonstrated the synthetic versatility of

cyclic vinylogous acyl triflates in mild nucleophilic addition/fragmentative ring opening cascades (Scheme I.39).[105] The use of triflates is a simplifying and efficiency-enhancing extension of the early work on halides[48] and selenones.[49] Additionally, the cascade sequences, reminiscent as they are of the original fragmentation reaction,[1] are both elegant and useful. A wide array of nucleophiles, such as Grignard and organolithium reagents, stabilized lithium enolates, strong hydride donors, and primary lithium amides, reliably participate in the reaction and provide efficient and inexpensive access to acyclic acetylenic ketones (e.g. **1.163**), 1,3-diketones (**1.164**), tertiary alcohols (**1.165**), and amides (**1.166**). Deuterium-labeling experiments are consistent with their proposed mechanism: fast 1,2-addition of the nucleophile to the carbonyl forms a tetrahedral alkoxide (e.g. **XLI**), and then slow, irreversible fragmentation. Mild heating is required for certain substrates and/or nucleophiles. The scope of this methodology was further expanded with the conversion of dihydropyridone triflates (e.g. **1.167**) to homopropargyl amines (**1.168**) with retention of stereochemistry (Scheme I.40).[106]

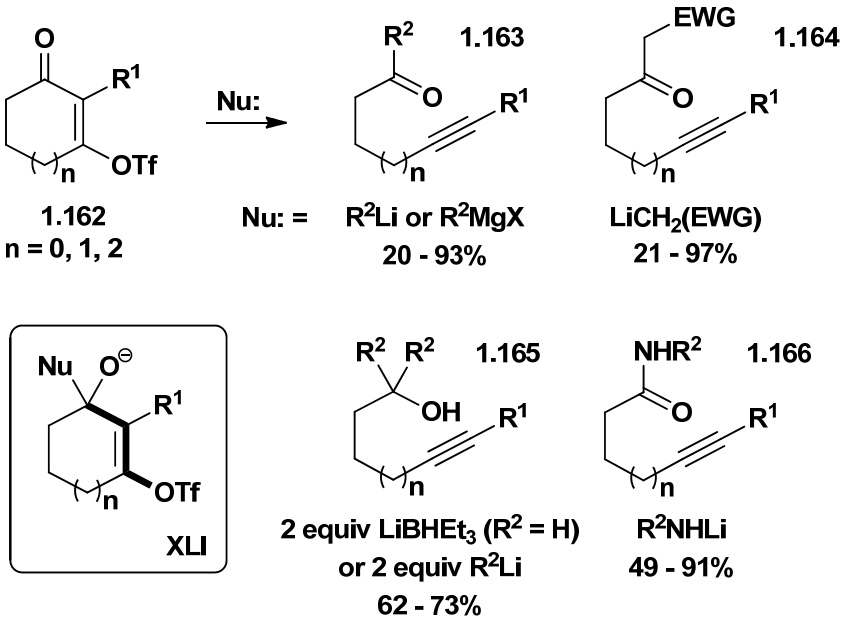

Scheme I.39 Dudley's cascade synthesis of alkynes (2005-2010).[105]

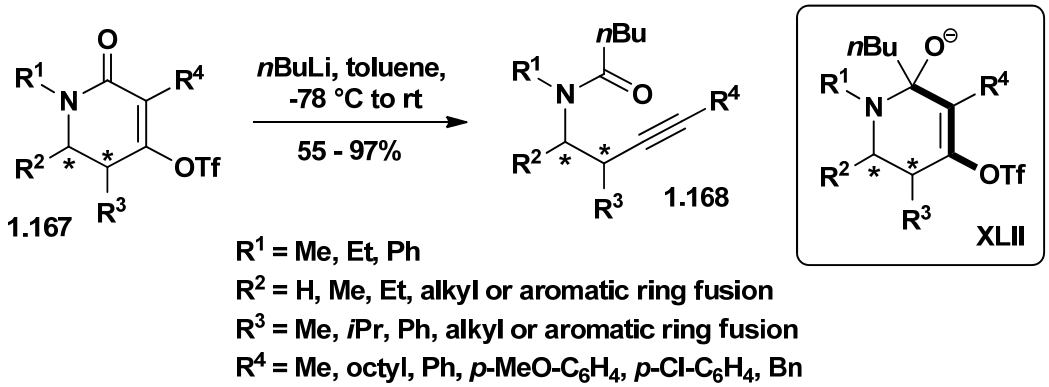

Scheme I.40 Dudley's homopropargyl amine syntheses (2011).[106]

Dudley also reported that cyclic vinylogous triflate hemiacetals can serve as stable synthetic equivalents for alkynyl aldehydes (e.g. **1.169** → **1.171**, Scheme I.41).[107] The first equivalent of Grignard reagent deprotonates the alcohol, inducing fragmentation to an aldehyde, which undergoes nucleophilic attack from a second equivalent of Grignard to

produce a secondary alkynol (e.g. **1.170**). This process is high-yielding for a variety of Grignard reagents, including aryl, vinyl, alkyl, allyl, and alkynyl variants.

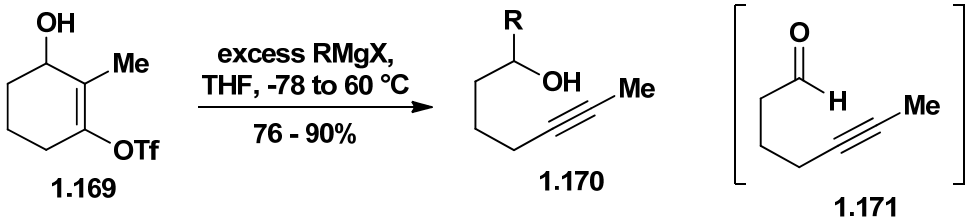

Scheme I.41 Dudley's *in situ* generation of alkynyl aldehydes (2006).[107]

As shown in Scheme I.42, Brewer and co-workers advanced an insightful C-C fragmentation of cyclic γ-oxo-β-hydroxy-α-diazo carbonyl derivatives (e.g. **1.172**) in the presence of stoichiometric tin tetrachloride. The fragmentation products are either ynoates or ynones (**1.174**).[108] The ring size, γ-oxy group, and diazo portion of the starting material can each be varied. Thus, access to a wide range of functional group-rich products should be possible. They hypothesize that the reaction proceeds via a vinyl diazonium species (e.g. **XLIII**) in which the C_β-C_γ and C-N bonds are antiperiplanar. Loss of nitrogen and C-C bond cleavage gives the corresponding oxocarbenium ion (not shown). Subsequent loss of the silyl, benzyl, or methyl R^4 substituent gives the observed product. This method was extended to the ring expansion of bicyclic γ-silyloxy-β-hydroxy-α-diazoketones to medium-sized cyclic 2-alkynones (e.g. **1.175** → **1.176**, Scheme I.43).[109]

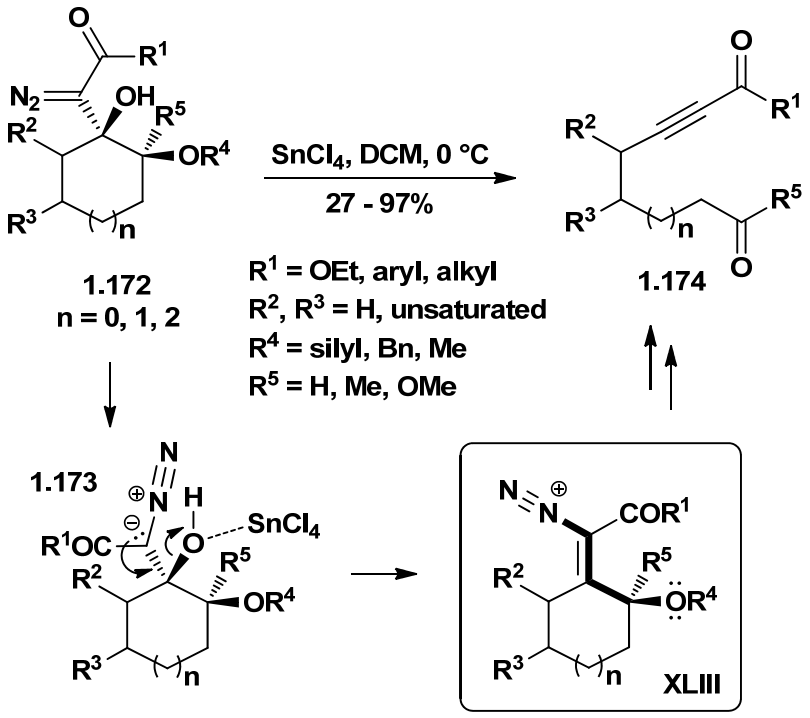

Scheme I.42 Brewer's ynoate and ynone syntheses (2008-2010).[108]

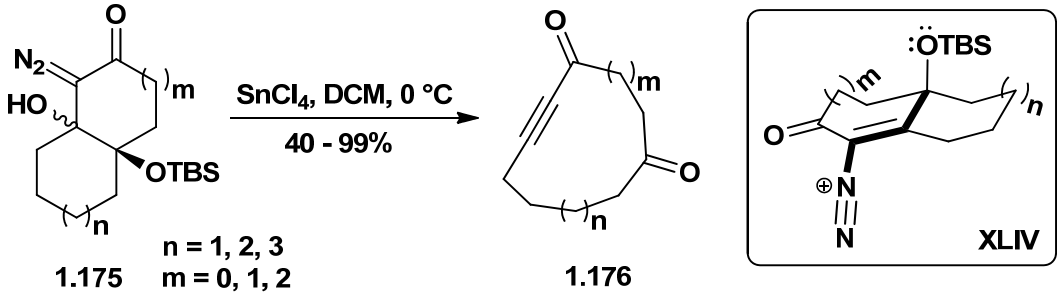

Scheme I.43 Brewer's alkynone synthesis (2012).[109]

Murphy and co-workers designed a series of innovative fragmentation reactions of polycyclic nitrones (e.g. **1.177**, **1.179**, and **1.181**, Scheme I.44).[110] The transformation is induced by exposure of the nitrone to triflic anhydride. The nitrone triflate then undergoes spontaneous C-C and N-O bond cleavage. In one study an enolate equivalent trapped the intermediate nitrilium species in a transannular fashion, and tautomerization gave the

observed product (**1.186**). Hence, similar to oximes, nitrones can be induced to rearrange (Barton rearrangement)[111] or to fragment.

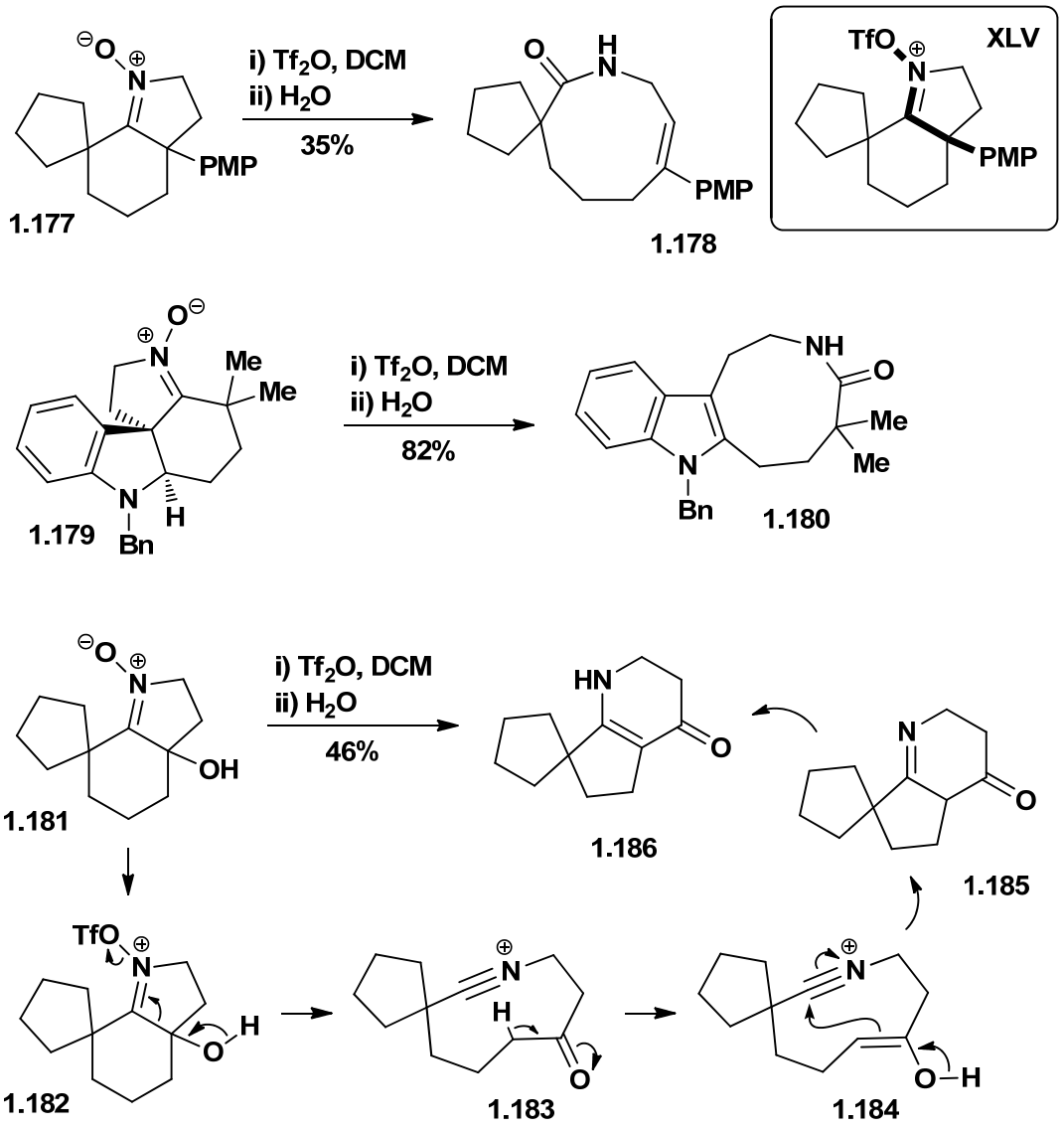

Scheme I.44 The original C-C fragmentation of nitrones, by Murphy (2007).[110]

1.3.2 sp^2-sp^2 bond forming fragmentations

The bulk of the work in the C-C fragmentation field has focused on sp^2-sp^2 bond forming transformations. Although these often closely follow the original precedent, many

useful extensions of the method and instructive applications in motif building have been reported over the last twenty years.

Lupton and co-workers optimized the fragmentation of systems of type **1.187** (Scheme I.45, *cf.* Scheme I.1), analogs of the original Eschenmoser substrate, and applied these to the divergent synthesis of modular dendrimers.[112] Six 1st-generation dendrimers were thus prepared (e.g. **1.188**). Kinetic studies supported a concerted fragmentation over a retro-Dieckmann/elimination pathway. The presence of the electron withdrawing ester appears to promote the fragmentation pathway. This method was reliable for five-, six-, and seven-membered rings with various electron withdrawing groups and nitrogen- and oxygen-containing nucleophiles.[113]

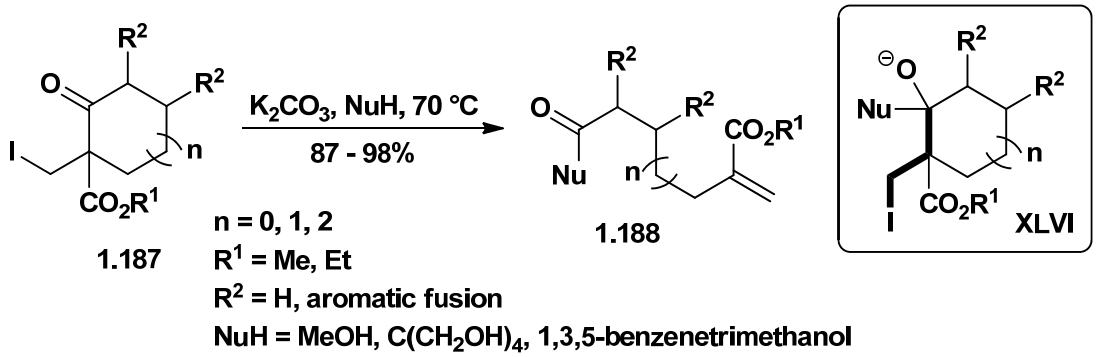

Scheme I.45 Lupton's dendrimer core syntheses (2010).[112]

Similarly, the bridged norbornane **1.189** gave the versatile, stereochemically defined, cyclopentane scaffold **1.190**, from which a range of biologically active cyclopentitols are accessible (Scheme I.46).[114] In this study, it was noted that displacement of the mesylate by methoxide (~20% yield) competes with fragmentation. The most obvious approaches to **1.190** include the sequential functionalization of cyclopentene, 1,3-cyclopentadiene, and fulvene; however, these routes are prone to poor stereo- and

regiocontrol. The fragmentation approach harnesses the intrinsic reactivity of the norbomyl system, granting access to **1.189** in eight high-yielding steps (>70% each) from commercially available materials.

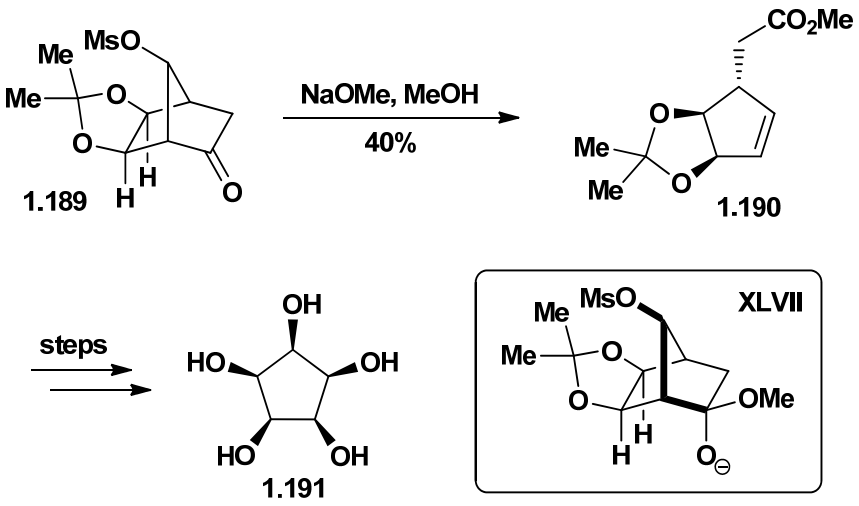

Scheme I.46 Mehta's cyclopentitol scaffold synthesis (1999).[114]

Medium-sized carbocycles and heterocycles are often difficult to access by direct ring closure.[115] Building on the studies of Wharton,[75,76,78] West has shown that an appropriately functionalized bicyclic ether is suitable for the preparation of delicate medium sized oxacycles.[116] Subjection of the monotosylate of **1.192** to strongly basic conditions gave nine-membered ether **1.193** (Scheme I.47). However, this product was accompanied by a similar amount of the elimination product. Elimination was not observed for **1.194**, which has a methyl group in place of the angular hydrogen, and consequently product **1.195** was obtained in excellent yield.

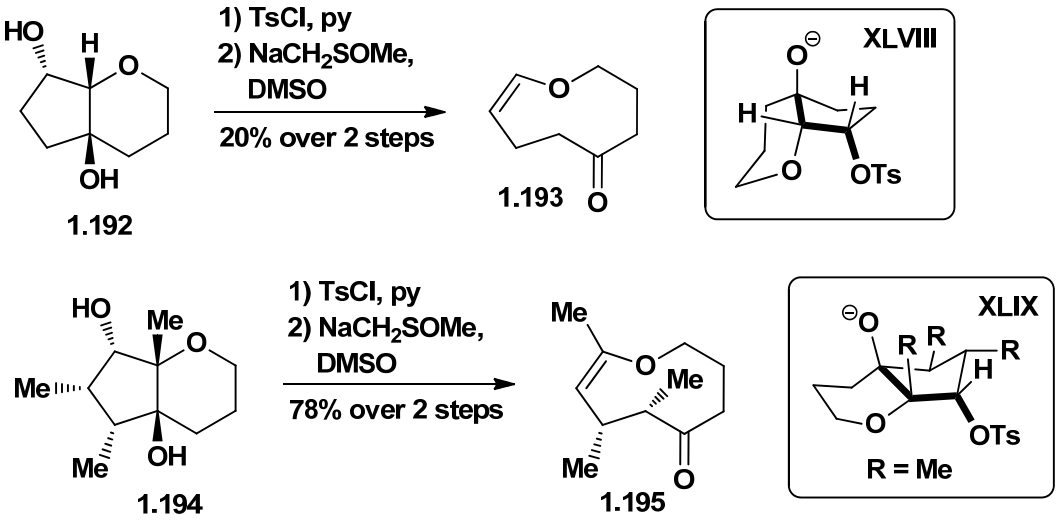

Scheme I.47 West's nine-membered oxacycle synthesis (1998).[116]

One of the most useful advances in fragmentation reaction methodology was reported by Molander and co-workers.[117] They developed a conceptually simple and synthetically concise intramolecular Barbier-type cyclization/fragmentation cascade (e.g. **1.196**, Scheme I.48). The method appears to be an excellent means by which to prepare functionalized and stereodefined eight-, nine-, and ten-membered carbocyclic *Z*-alkenes (e.g. **1.197**).

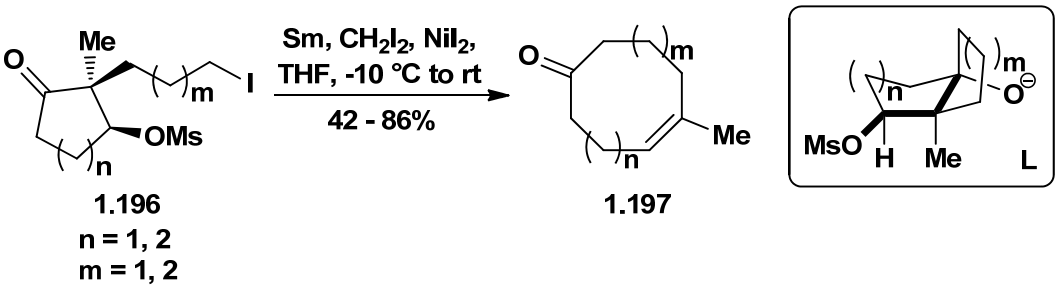

Scheme I.48 Molander's cascade synthesis of medium-sized rings (2001).[117]

Charette and co-workers optimized the silver ion-induced fragmentation of γ-amino halides (e.g. **1.198**, Scheme I.49),[118] thereby extending and generalizing the early cinchona alkaloid fragmentation (*cf.* Scheme I.14). Additionally, this group showed that 1,2-dihydropyridinium ion intermediates (e.g. **1.199**) can be trapped *in situ* with Grignard reagents in a highly regio- and diastereoselective fashion. The polysubstituted piperidine products (e.g. **1.200**) are of considerable interest in drug discovery and alkaloid synthesis. To avoid the use of expensive silver salts, they showed that triflates are excellent alternatives to the corresponding iodo derivatives.[119]

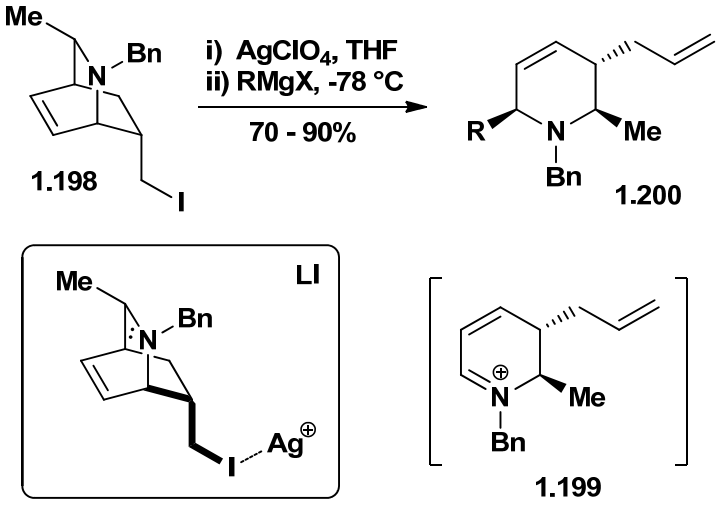

Scheme I.49 Charette's γ-amino halide fragmentations (2008).[118]

Functionalized 3-azabicyclo[3.3.1]nonane derivatives are readily accessible from azaadamantanones of type **1.201** via regioselective fragmentation (Scheme I.50).[120] Exposure of the dichloride **1.201** to aqueous ammonia gives **1.203** (via **1.202**). The reaction mechanism is not altogether unambiguous. Nevertheless, the chloride axial to the carbocyclic ring is the presumed leaving group. Interestingly, the alternative fragmentation

pathway, which would give the less thermodynamically stable β,γ-unsaturated product, was not observed.

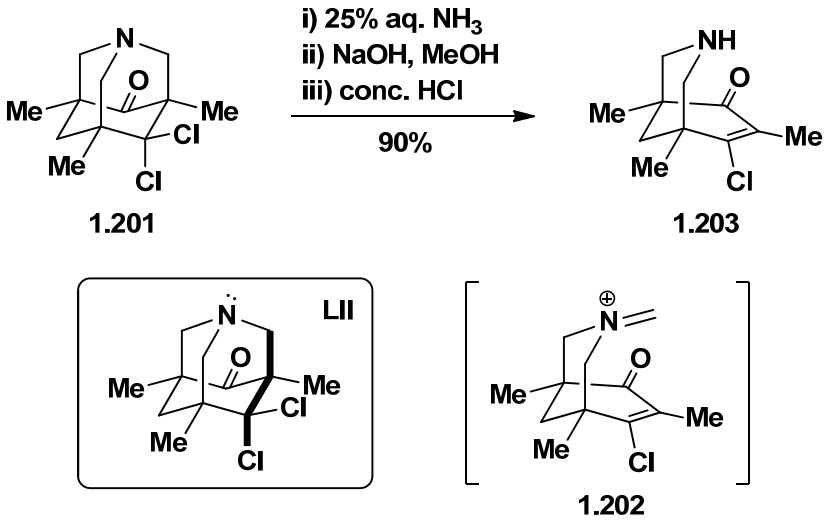

Scheme I.50 Risch's γ-amino halide fragmentations (1991).[120]

Phenylsulfenyl chloride was used by Plumet and co-workers to effect fragmentation of imines of type **1.204** to amides of type **1.205** (Scheme I.51).[121] This insight anticipates sulfonium-initiated fragmentation, nitrilium ion formation, and capture by chloride, which upon aromatization and hydrolysis gives the amide product.

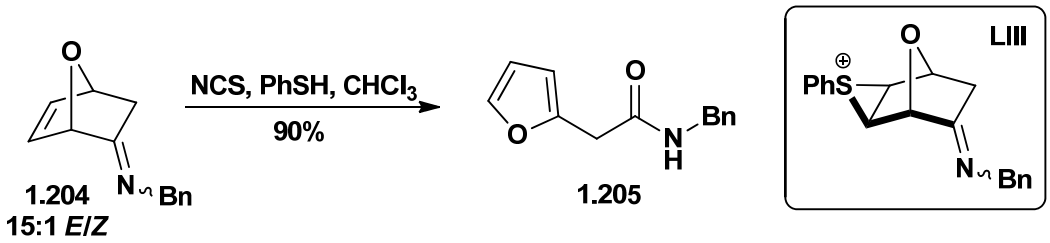

Scheme I.51 Plumet's sulfonium-initiated fragmentation (2001).[121]

Oxidation of 3-hydroxypiperidine (**1.206**) with iodosylbenzene in water affords 2-pyrrolidinone (**1.210**, Scheme I.52).[122] Ochiai and co-workers propose an initial ligand

exchange on iodine(III) of iodosylbenzene, producing the labile aminoiodane and/or the cyclic iodane (not shown). Alternative mechanisms with *O*- rather than *N*-activation are also plausible (see **LV**). Rapid oxidative fragmentation to iminoaldehyde **1.207** is followed by hydrolysis, cyclization, and then oxidation to give **1.210**.

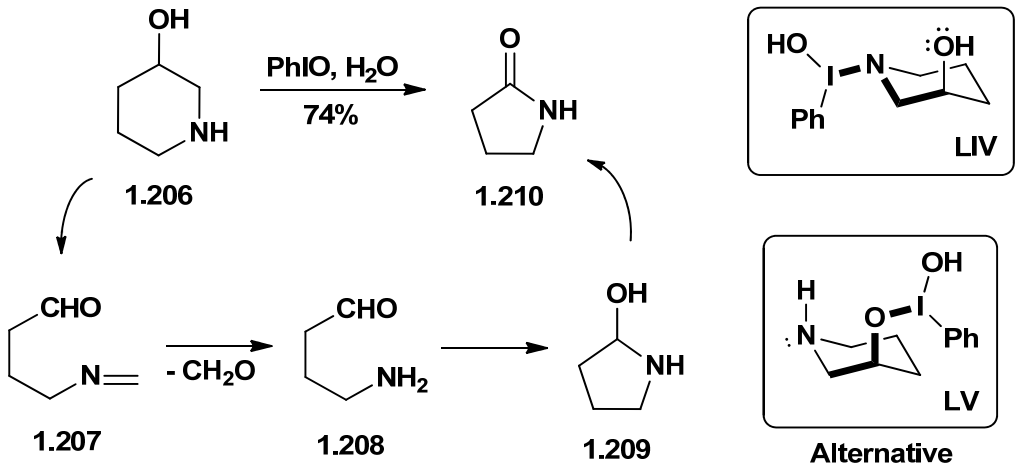

Scheme I.52 Ochiai's oxidative fragmentation (2004).[122]

Kabalka and co-workers developed an interesting tandem aldol/fragmentation sequence.[123] As shown in Scheme I.53, aromatic aldehydes (e.g. **1.211**) and ketones (e.g. **1.212**) react in the presence of boron trifluoride to provide (*E*)-arylalkenes (e.g. **1.213**) with high stereoselectivity. This versatile one-pot alkene synthesis requires the combination of a strong Lewis acid and very low polarity solvent to prevent formation of the aldol condensation products.

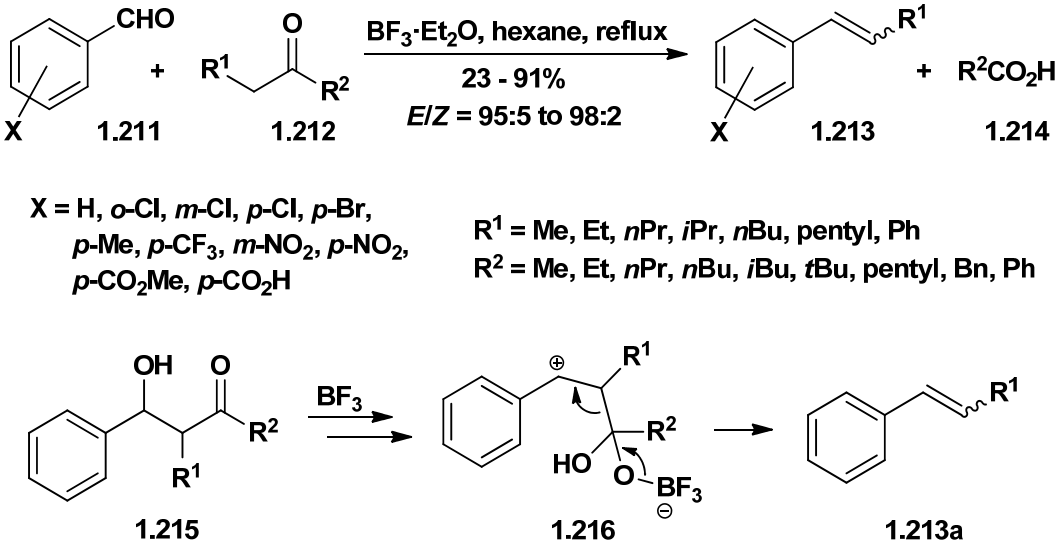

Scheme I.53 Kabalka's cationic alkene synthesis (1998-1999).[123]

Several other fragmentations are summarized in Schemes I.54-I.56. Suitably functionalized acetonides (e.g. **1.217**) undergo C-C fragmentation upon treatment with catalytic Brønsted or Lewis acid.[124] The terpene-derived substrates yield enantiopure aldehydes (e.g. **1.220**) that contain a cyclopropane or cyclobutane ring and an alkene or diene moiety. Barluenga and co-workers conducted several experiments that support a stepwise mechanism. The anticipated structure of oxonium ion **1.218** was suggested to lack the necessary orbital overlap for concerted fragmentation. Instead, the acetonide appears to open selectively to give the stabilized carbocation **1.219** in accord with early cationic fragmentations/retro-Prins reactions (*cf.* Schemes I.15 and I.17). Loss of acetone, C-C bond cleavage, and stereoselective alkene generation gives the observed product. Zard and co-workers have synthesized a series of strained nine-membered rings via fragmentation (e.g. **1.222**, Scheme I.55).[125] Although Molander has provided a general method for direct entry into *Z* alkene-containing nine-membered rings by fragmentation (Scheme I.48),

indirect multistep routes are still required in many cases. The Zard approach expands upon earlier ring expansion work and demonstrates the effectiveness of alternatives to the sulfonate nucleofuge. Hence, bicyclic xanthates (e.g. **1.221**) were selectively cleaved. The crude thiols were converted to the sulfonium products, which fragmented *in situ*. Bromide was also shown to be an effective leaving group. The reaction of *N*-acylindole **1.223** gave *syn*-bicyclic pyroglutamic acid **1.227** (Scheme I.56).[126] The authors suggest that this transformation follows a pathway wherein a ketene is formed in a fragmentative ring expansion. The ketene intermediate is then suggested to undergo cycloaddition to give the β-lactone followed by hydrolysis to the observed product. The non-fragmentation pathway, by way of retro-aldol/aldol isomerization followed by hydrolysis (not shown), was not discussed but may also be relevant.

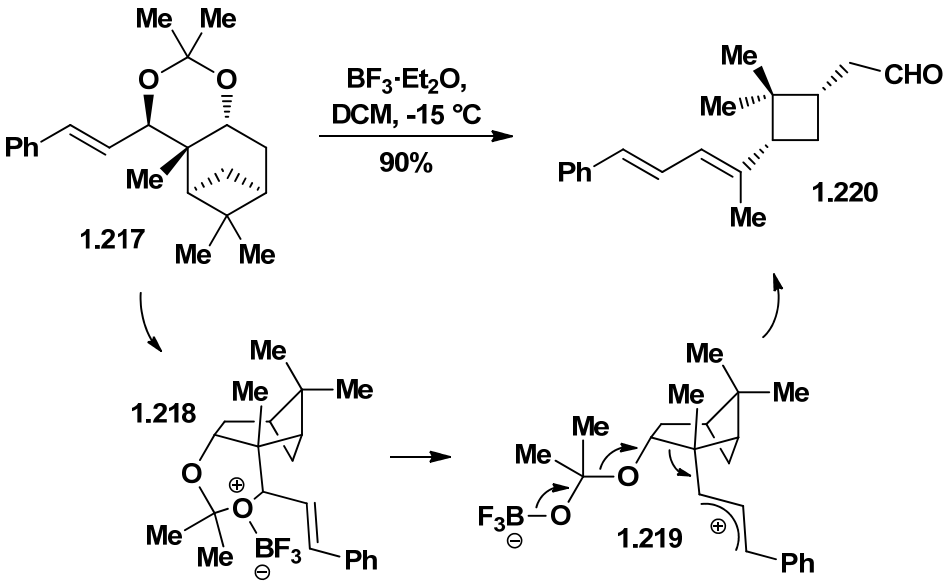

Scheme I.54 Barluenga's terpene fragmentation (2003).[124]

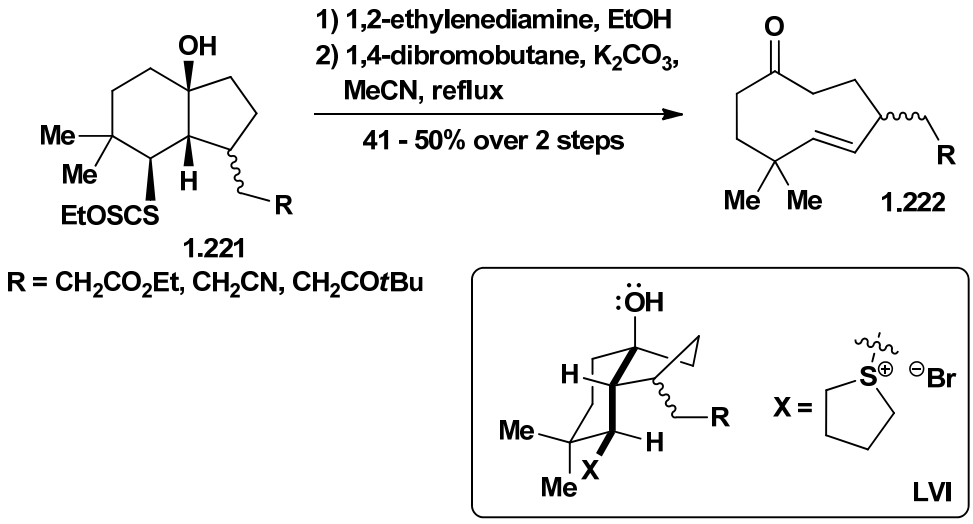

Scheme I.55 Zard's cyclononene synthesis (1999).[125]

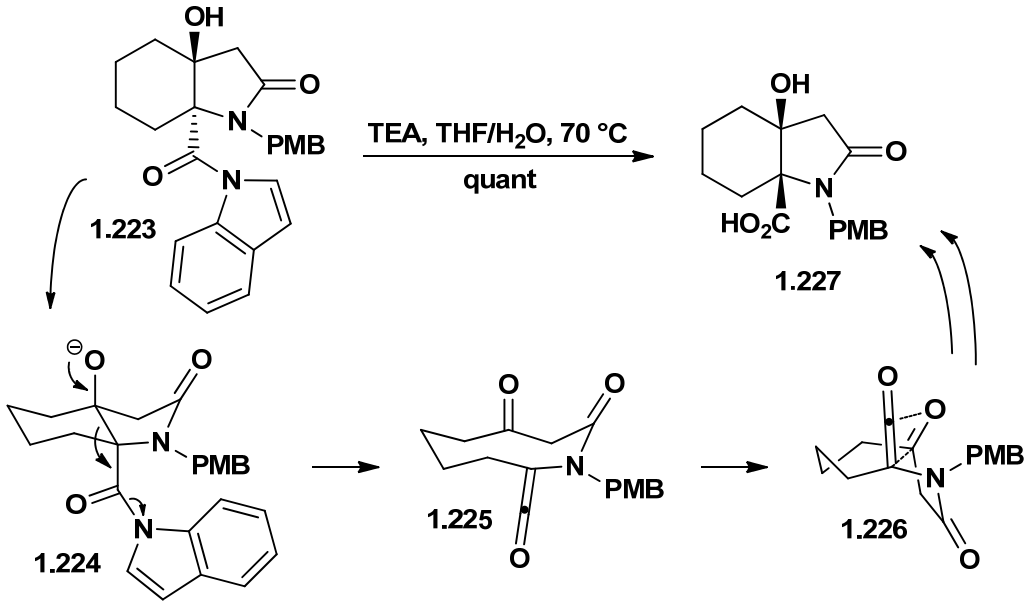

Scheme I.56 Kobayashi's *syn*-bicyclic pyroglutamic acid synthesis (2007).[126]

Fluoride-induced fragmentation of silyl-protected 1,3-hydroxysulfonates was shown be an excellent alternative to exposure of a 1,3-hydroxysulfonate to strong base. Hence, treatment of **1.228** with tetrabutylammonium fluoride gave the

cis-cyclododecenone **1.229** as a single isomer (Scheme I.57).[127] Unexpectedly, the silyl ether **1.230** afforded a mixture of *cis* and *trans* isomers (**1.231** and **1.232**). Dowd pointed out the possibility of ionization of the sulfonate to account for the *trans* product.

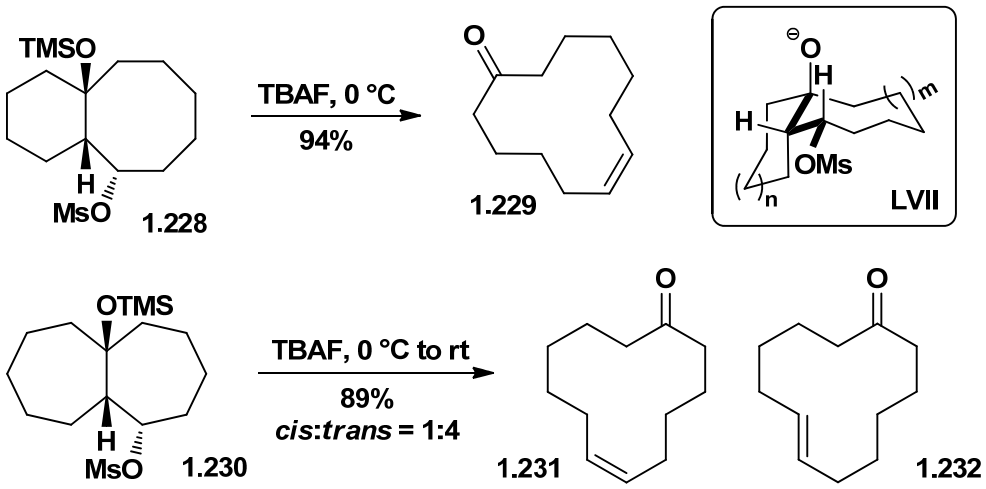

Scheme I.57 Dowd's fluoride-induced ring expansion (1996).[127]

In contrast to the Eschenmoser-Tanabe fragmentation of α,β-unsaturated epoxyketones,[42,44] Hesse showed that appropriately functionalized cyclic β,γ-epoxyketones undergo fragmentation to give macrocyclic lactones (e.g. **1.233** → **1.234**, Scheme I.58).[128] The product necessarily contains an allylic alcohol, present as a consequence of the fragmentative epoxide opening.

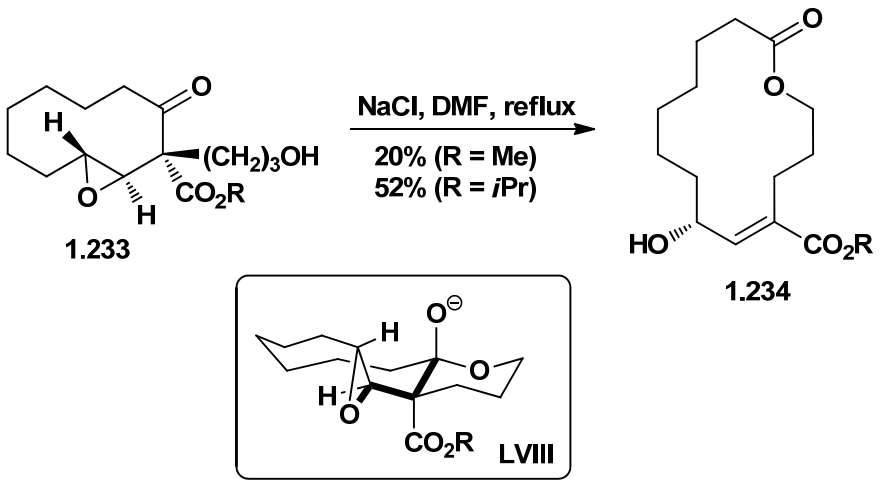

Scheme I.58 Hesse's macrolactone synthesis (1995).[128]

The vast majority of fragmentations reported to date involve common functional groups, as shown throughout this review. In 2001, Jung and Davidov reported a remarkable fragmentation under ozonolysis conditions (**1.235** → **1.238**, Scheme I.59).[129] The aesthetic of their mechanistic rationale is pleasing. They suggest that formation of the primary ozonide derived from the strained allylic alcohol provides a facile pathway for fragmentation. The release of angle strain in the cyclobutane ring combined with the weakness of the O-O bond facilitates the fragmentation.

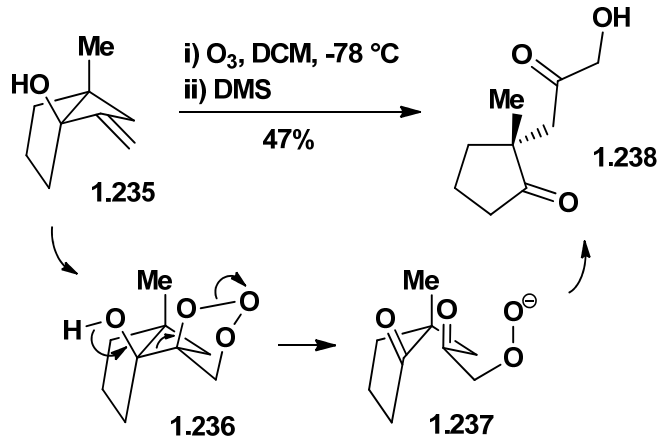

Scheme I.59 Jung's ozonide fragmentation (2001).[129]

Morpholine was shown to induce fragmentation of 3,3-disubstituted-1,2-dioxetanes to afford the corresponding ketones (e.g. **1.239** → **1.240**, Scheme I.60).[130] The presence of *N*-oxide **1.241** was also noted. The reaction was rationalized as proceeding through the deprotonated form of **1.241**. Electron-withdrawing groups on the aryl ring appear to decrease the basicity of the intermediate alkoxide and to thereby promote fragmentation.

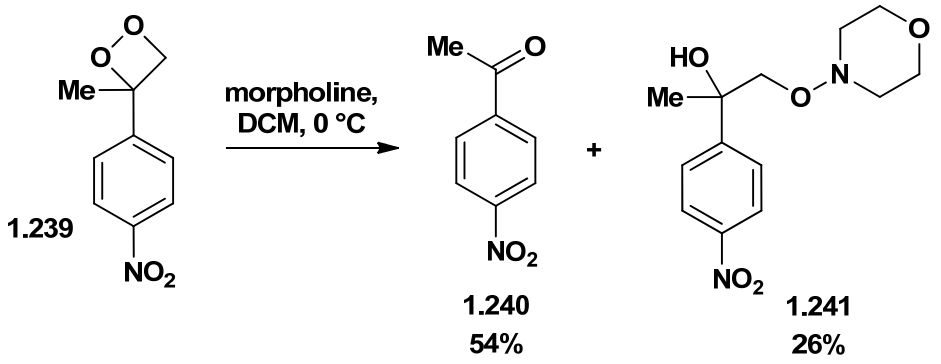

Scheme I.60 Adam's peroxide fragmentation (1995).[130]

Sakai and co-workers showed that aldol products can be induced to fragment in the presence of Lewis acid and a diol (Scheme I.61).[131] Moreover, they effected the aldol reaction *in situ*. Hence, 1,6-diones (e.g. **1.242**) undergo a cascade reaction consisting of aldol addition, ketalization, C-C fragmentation, and then collapse of the resultant tetrahedral intermediate to give functionalized cyclopentenes (e.g. **1.247**). Mechanistic studies revealed that the sequence follows mainly the ketal pathway but may partially proceed via the hemiketal.

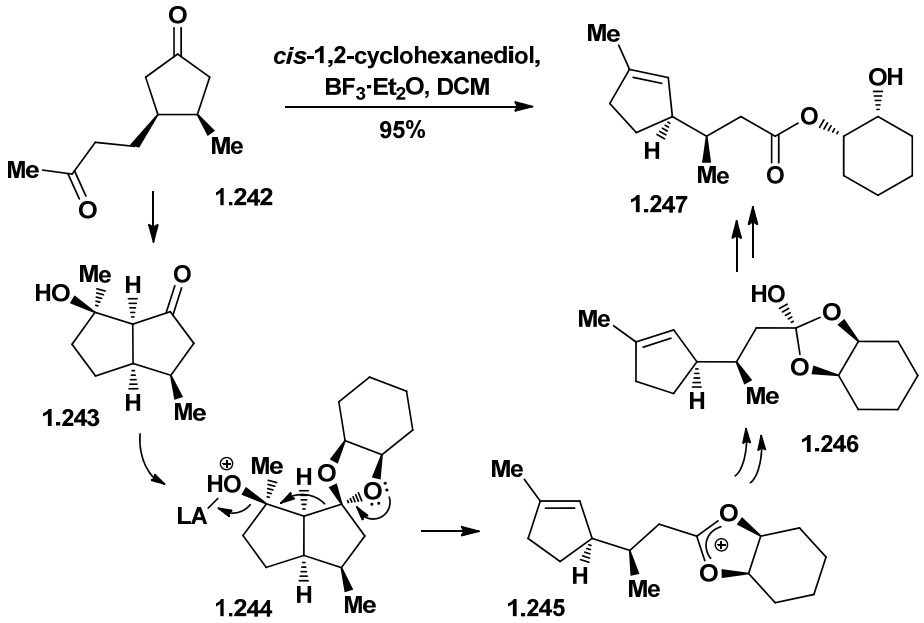

Scheme I.61 Sakai's *in situ* aldol product C-C fragmentation (1991).[131]

Bettolo and co-workers reported an analogous fragmentation (Scheme I.62).[132] Upon acid exposure, 5-dioxolan-bicyclo[4.2.0]-octan-2-one **1.248** yields 3-(methoxycarbonylmethyl)cyclohexanone **1.249**. Although the experimental data do not preclude a stepwise mechanism, the authors propose that the cyclobutane and protonated dioxolane rings open simultaneously. This method represents a strategy to introduce angular acetate to functionalized decalin systems.

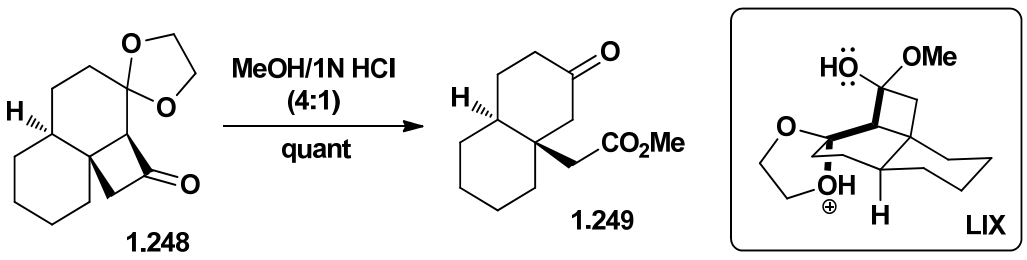

Scheme I.62 Bettolo's angular acetate synthesis (1997).[132]

Nickel and palladium catalysts have been used in the double ring opening of cyclic carbonates (e.g. **1.250**) to give ω-dienyl aldehydes (e.g. **1.251**, Scheme I.63).[133] Carbonates possessing ring and/or torsional strain smoothly undergo fragmentation with use of monodentate phosphane ligands and $Ni(cod)_2$. The strain-free carbonates studied required the addition of bidentate phosphanes with bite angles of at least 95˚. The synperiplanar arrangement of scissile bonds of the organometallic intermediate and the isolation of *E*/*Z* product mixtures suggest a stepwise cationic mechanism (see inset).

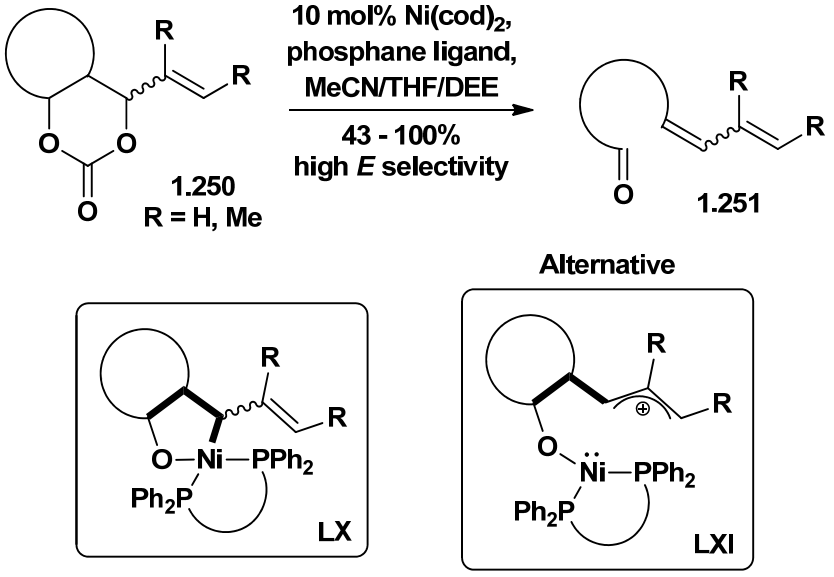

Scheme I.63 Tamaru's nickel-mediated fragmentation (2006).[133]

The most exotic C-C fragmentations reported to date are shown in Scheme I.64. In this case, substituted icosahedral carba-*closo*-dodecaborate anions undergo C-C bond cleavage (e.g. **1.252** and **1.255** → **1.253**).[134] Moreover, the C-C cleavage of alkyl halide-substituted derivative **1.255** apparently involves intramolecular hydride transfer via a five- or six-membered transition state (*cf.* **LXIII**). Isotopic labeling experiments demonstrated that the double bond in the sideproducts is located at the terminus originally

attached to the carborane cage. Although the likelihood of this reaction becoming a useful synthetic method seems remote at present, it remains a fascinating example of what technically can be classified as a C-C fragmentation.

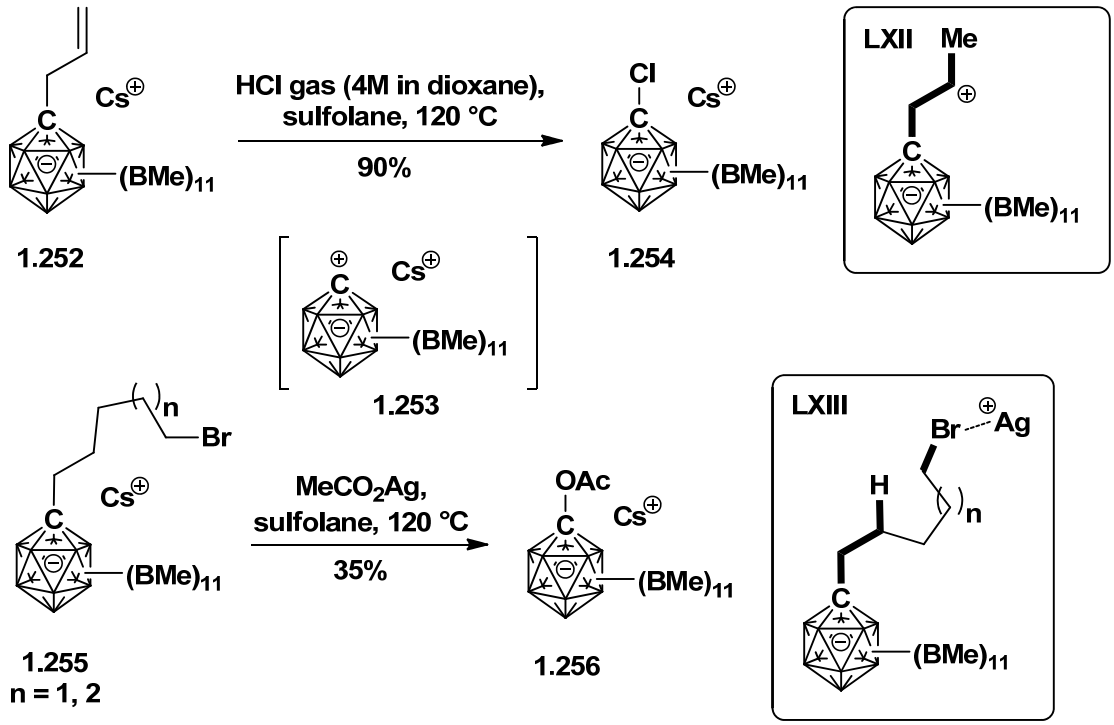

Scheme I.64 Michl's carba-*closo*-dodecaborate fragmentation (2004).[134]

In closing this section we note that fragmentation may be buried within more complex rearrangements. This is especially true of certain organometallic transformations. We deliberately have not delved into such areas. The mechanisms are obscured by lack of relevant data and are nuanced and layered with speculation. This notwithstanding, the reactions are not fundamentally fragmentations. For example, Liu and co-workers optimized a gold-catalyzed reaction of 3-alkynyl-indolediols (e.g. **1.257** → **1.261**, Scheme I.65).[135] The reaction has good substrate scope. It was rationalized as proceeding via cationic gold activation of the alkyne followed by intramolecular nucleophilic attack by the

indole. Fragmentation of the spirocyclic iminium cation regenerates the indole. Elimination of the Au(I) catalyst and water gives the allene. Buried within the Liu speculation are the recognizable fragmentation elements: an electron source, an electron sink, and a cleaved C-C bond (**1.259**). This step can be considered the reverse of electrophilic aromatic substitution as well. We suggest that the Liu transformation be considered a gold(I) catalyzed rearrangement.[136]

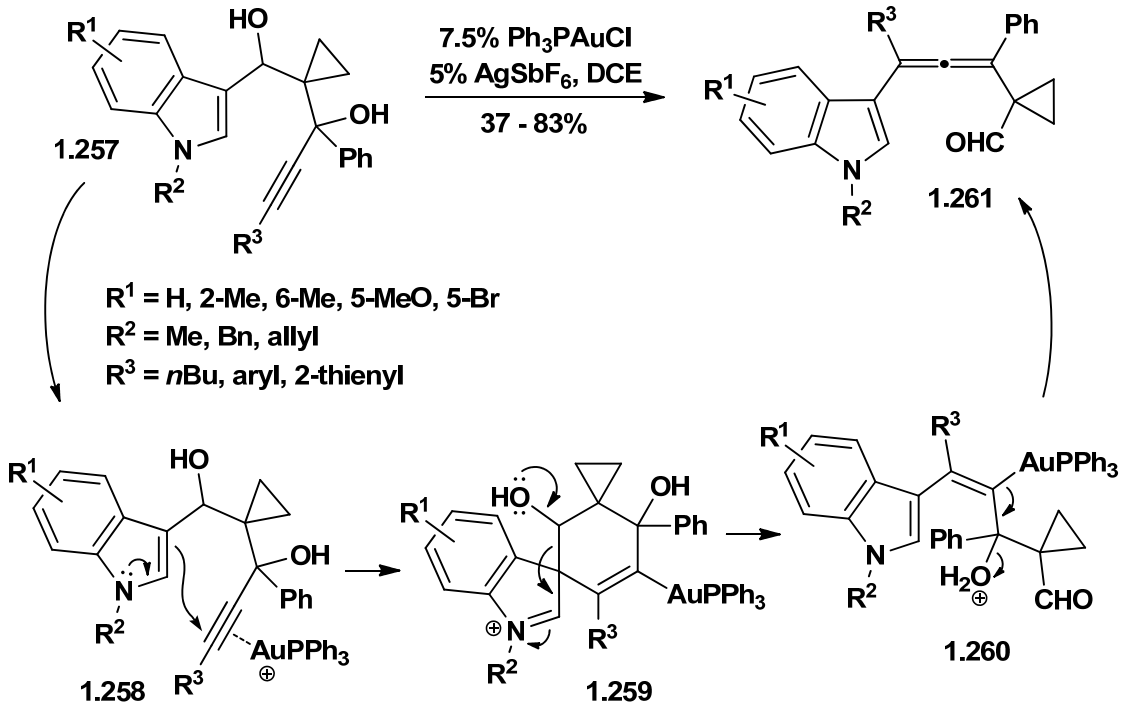

Scheme I.65 Liu's allene synthesis (2010).[135]

1.3.3 sp^2-sp^1 bond forming fragmentations

The structural and reactive properties of allenes complement the chemistry of alkynes and alkenes,[137] and the synthesis of allenes by way of fragmentation is an exciting area of recent development. Importantly, however, this transformation is not altogether new. Three key antecedents presage much of the work in this area: Kuwajima's thermolysis

studies on vinyl triflates (see below), Dudley's demonstration of the general utility of vinyl triflates for anionic fragmentations (see above), and the cumulative studies – first demonstrated by Eschenmoser – that fragmentations can be initiated by nucleophiles.

Numerous elimination processes are known to give allenes;[4b,138] however, Kuwajima and co-workers reported the first fragmentation to give allenes.[139] Thermolytic ring expansion of enol triflates **1.262** and **1.264** gave medium-sized cyclic allenes **1.263** and **1.265** (Scheme I.66). Since high temperature and high polarity were required, it was reasoned that the rate-determining step is ionization of the triflate and that the fragmentation is cationic. These original experiments provided difficult-to-form cyclic allenes from bicyclic precursors.

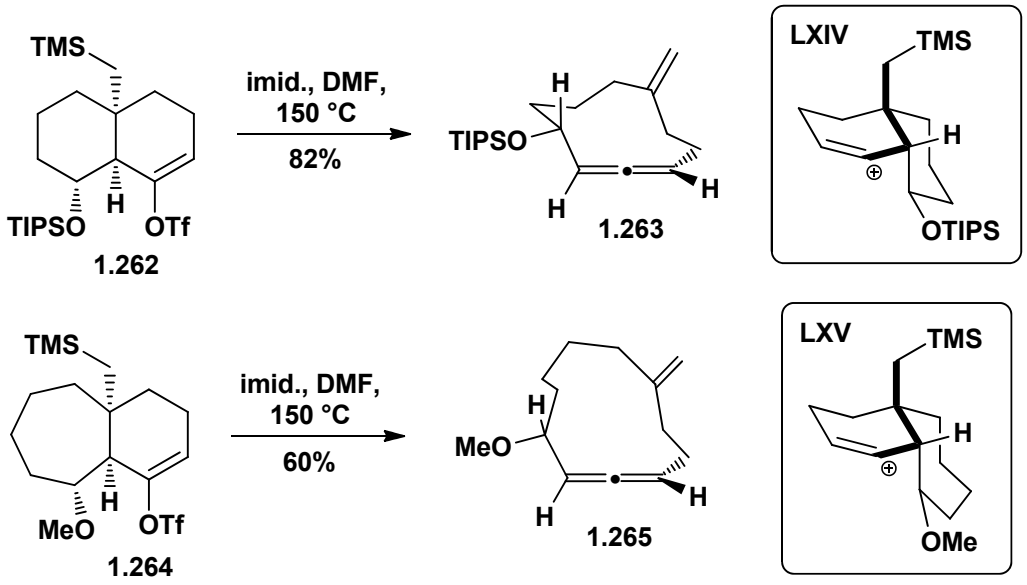

Scheme I.66 The original allene synthesis via C-C fragmentation, by Kuwajima (1997).[139]

Our group realized a new synthesis of allenes based on the concerted fragmentation of functionalized vinyl triflates.[140] Nucleophilic addition to a ketone of type **1.266**

generates allenic ketones by way of fragmentation of the *in situ* generated alkoxide (e.g. **1.267**, Scheme I.67). Use of excess nucleophile gave the corresponding tertiary alcohols (e.g. **1.268**). Fragmentation appears rate limiting and was shown to be stereospecific (*cf.* **1.269** → **1.270** and **1.271** → **1.272**).[141] Consistent with earlier studies,[127] fluoride was shown to promote fragmentation. Hence, upon exposure to fluoride bicyclic silyl ether **1.273** fragments to ten-membered endocyclic allene **1.274**, presumably via the dianion.

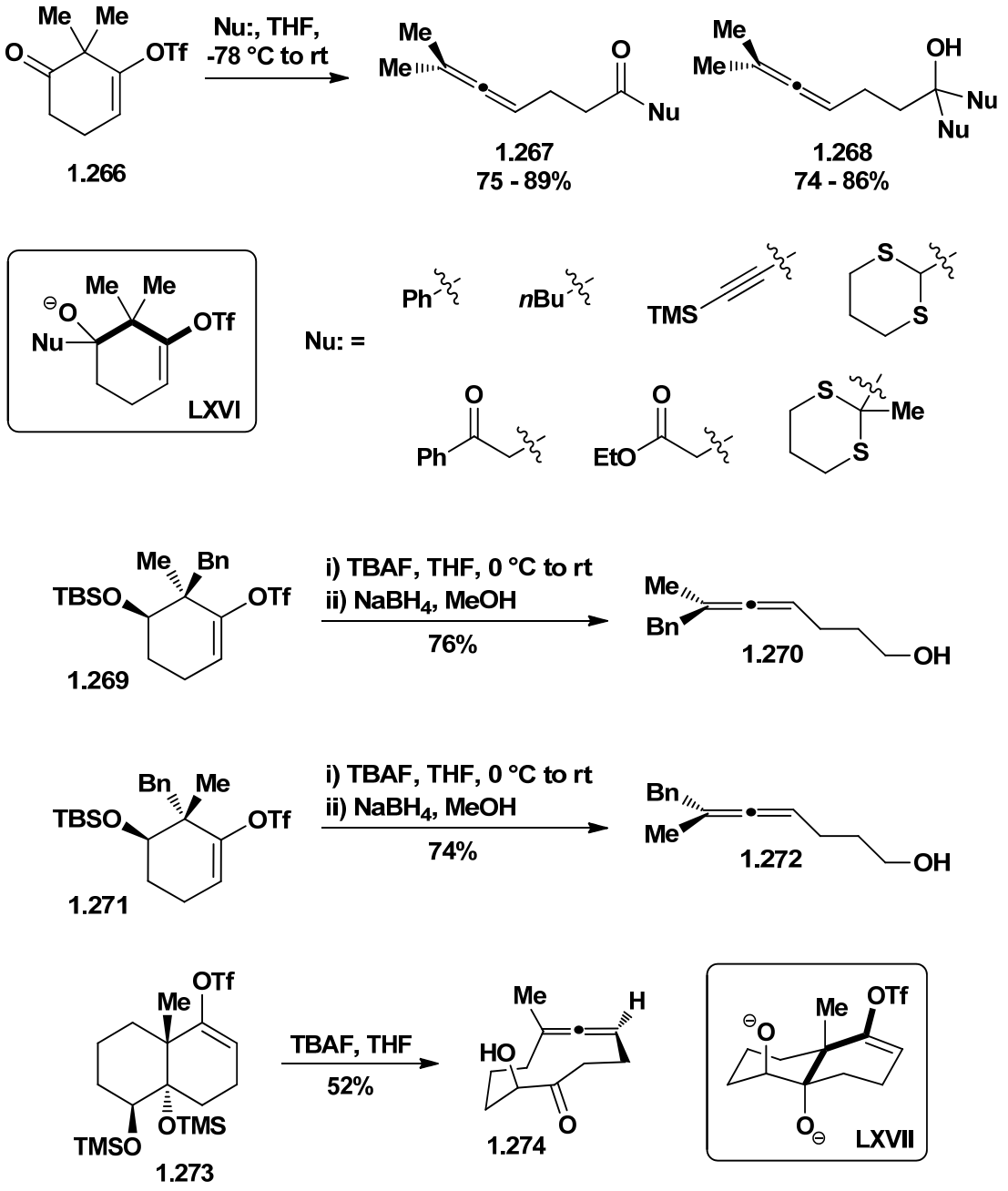

Scheme I.67 Fragmentations of vinyl triflates to allenes (2009).[140]

My colleague Da Xu and I extended this mild methodology to *cis*-decalin-derived substrates.[142] Treatment of bicyclic vinyl triflate **1.275** with TBAF afforded the ten-membered endocyclic allenone **1.276** (Scheme I.68). This simplified scaffold is related

to the germacrane terpenes, especially the vernonia allenes (**1.277**-**1.279**), the only known endocyclic allene-containing natural products.

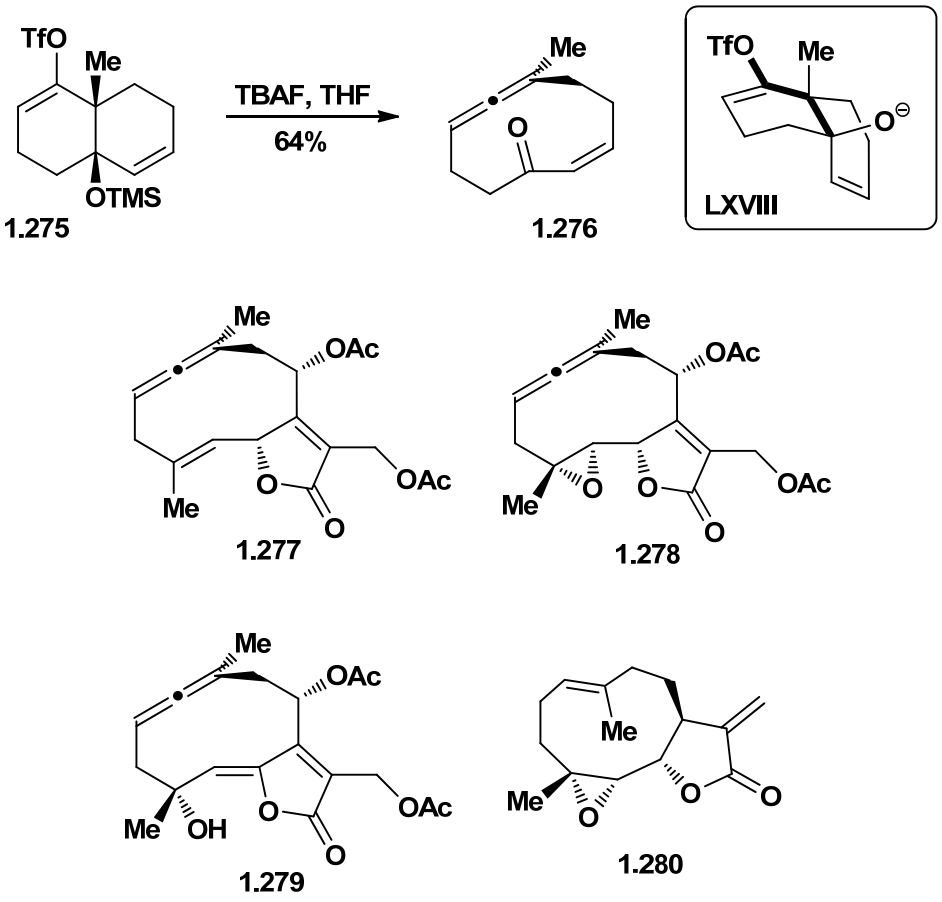

Scheme I.68 Synthesis of an endocyclic allene related to the germacranolides (2011).[142]

Saget and Cramer reported a series of complementary fragmentations.[143] They used heteroatom nucleophiles to access trisubstituted allenes (e.g. **1.282**, Scheme I.69). Fragmentation of vinyl triflates (**1.281**) is highly favored in polar aprotic solvents with an excess of base and, in some cases, mild heating. Some of the substrates were designed to undergo domino reactions to form even more structurally diverse motifs. For example, vigorous heating of the vinyl triflate in the presence of sodium azide generated a carbamate

1.285 through a designed *in situ* Curtius rearrangement of the acyl azide fragmentation product **1.283**.

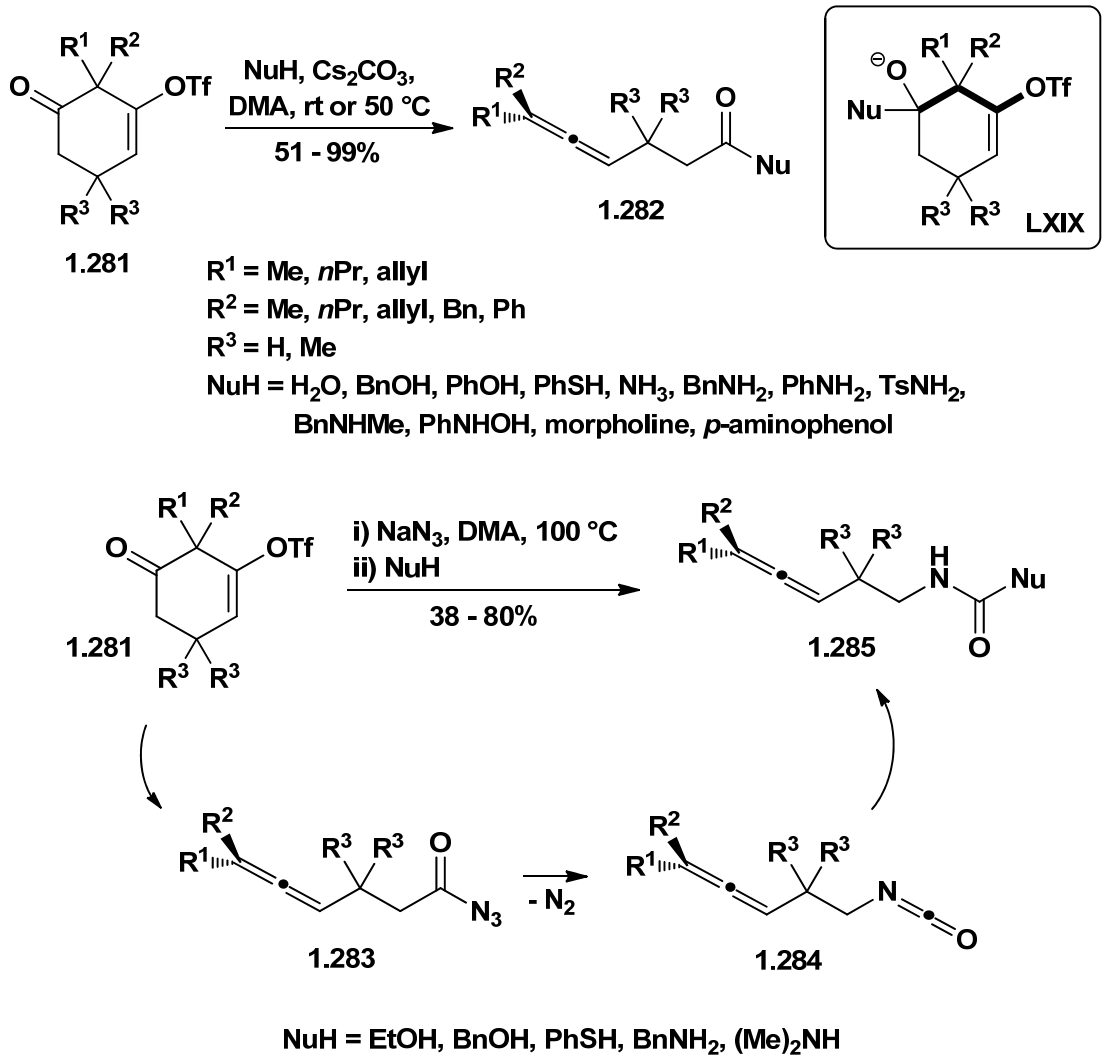

Scheme I.69 Saget and Cramer's allene synthesis (2010).[143]

There is only one study where divergent fragmentation pathways are compared in a single substrate. Triflate **1.286** was designed to be able to fragment to give an alkyne or an allene (Scheme I.70).[140] Remarkably, base promotes **1.286** to undergo C-C fragmentation to give allene **1.287** significantly faster than to give alkyne **1.288**. Computational modeling of bromide **1.289** reveals a greater positive charge on C-5 than on C-1, indicating that the

sp^3 network of the substrate is more polarized by the triflyl group than the sp^2 network. The greater positive charge leads to a stronger interaction with the anionic nitrogen and a lower barrier to the allene product, despite proper stereoelectronic alignment for both pathways.

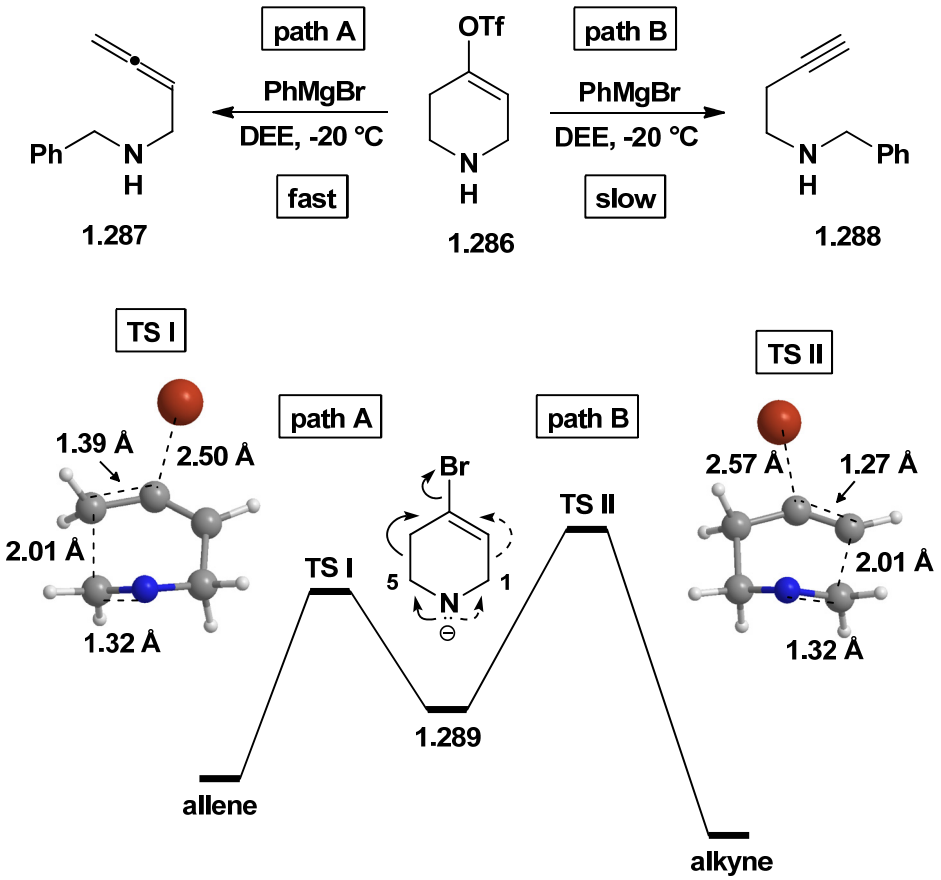

Scheme I.70 Fragmentation favors the allene over the alkyne (2009).[140]

1.3.4 Complex Molecule Synthesis

The synthesis of natural products is a test sui generis for the utility of a synthetic method or strategy. Consequently, the synthesis of natural products and natural product core structures that have appeared over the last twenty years and that rely upon the use of a fragmentation are described here as distinct from motif-building studies described in the previous sections. The strategic application of C-C fragmentation has found the widest use

in terpene natural products and has been used to effect ring openings and ring expansions. Fragmentation reactions of complex substrates that give sp^1-sp^1 connectivity are rare (Schemes I.71-I.74), whereas those that give sp^2-sp^2 connectivity are common (Schemes I.75-I.95). Fragmentations leading to sp^2-sp^1 connectivity have not been applied to complex targets other than those mentioned above.

Ring opening reactions achieved by C-C fragmentation that give sp^1-sp^1 products are shown below. Beckmann fragmentation of oxime **1.290** provided *exo*-olefin **1.291** regioselectively *en route* to (−)-elegansidiol (**1.292**), a mono-carbocyclic sesquiterpene (Scheme I.71).[144] The fragmentation is especially interesting because the least substituted alkene was formed. Hu and co-workers note that a bulky, non-nucleophilic base at reduced temperature was required for this product to be obtained in high yield.

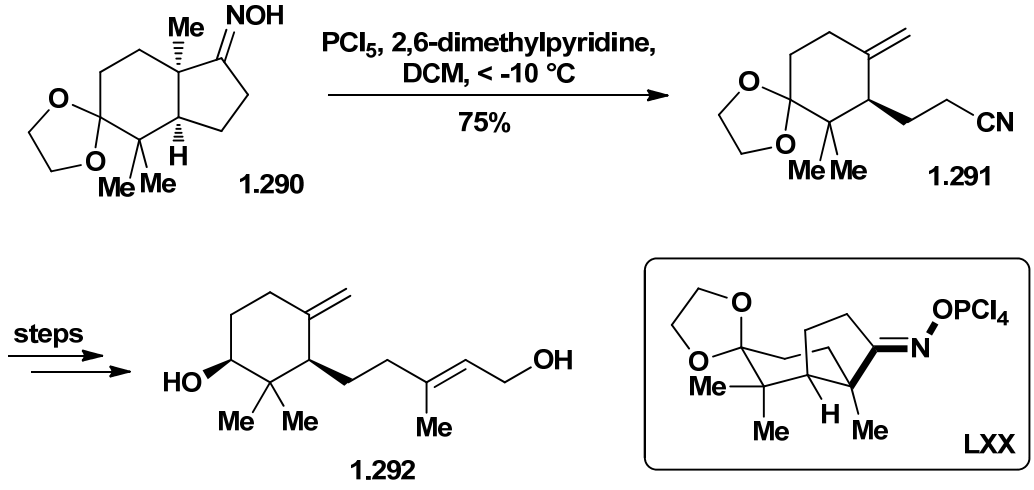

Scheme I.71 Hu's ring opening fragmentation *en route* to elegansidiol (1.292) (2007).[144]

A modified Eschenmoser-Tanabe fragmentation was utilized in the racemic total synthesis of GB-13 (**1.295**), a complex polycyclic alkaloid isolated from the rainforest tree

Galbulimima belgraveana (Scheme I.72).[145] In this synthesis by Mander, epoxyketone **1.293** was converted to alkynone **1.294**, a late stage intermediate.

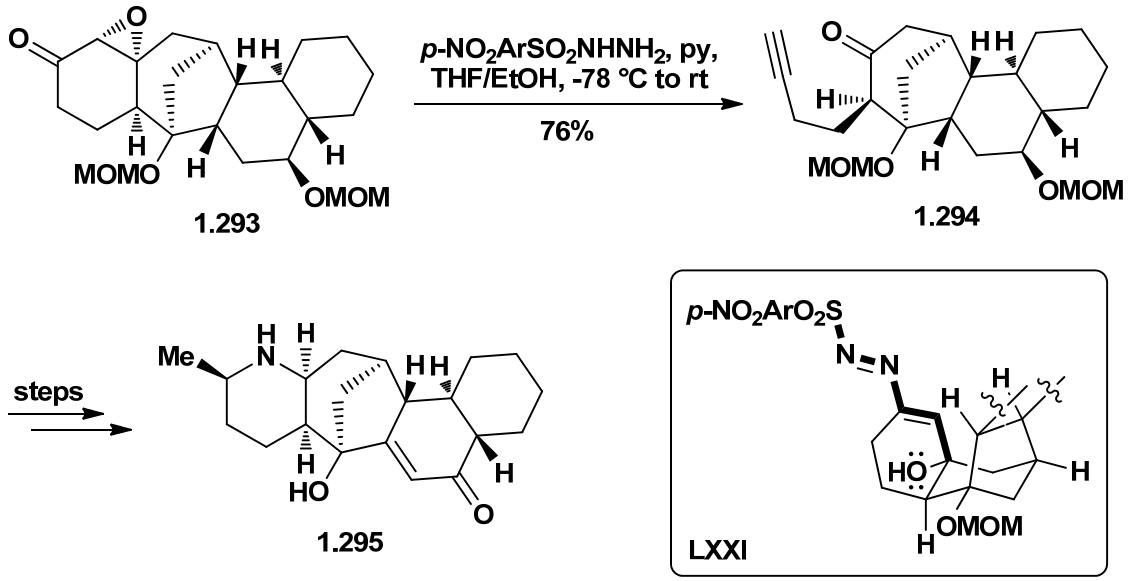

Scheme I.72 Mander's synthesis of (±)-GB-13 (1.295) used a late stage fragmentation (2003).[145]

Dudley and co-workers extended their ring opening cascade to target several natural products. The reaction of vinylogous acyl triflate **1.162a** with *n*-decylmagnesium bromide afforded the keto alkyne (not shown), which upon semi-reduction gave the sex attractant of the Douglas fir tussock moth (**1.296**, Scheme I.73).[146] More recently they used fragmentation to expedite the synthesis of the eastern hemisphere of the macrolide palmerolide A (not shown), a potent inhibitor of vacuolar ATPase and a selective anti-skin cancer agent.[147] Treatment of **1.162b** with a lithiated phosphine oxide provided β-keto phosphine oxide **1.297** and subsequently **1.298** (Scheme I.74).

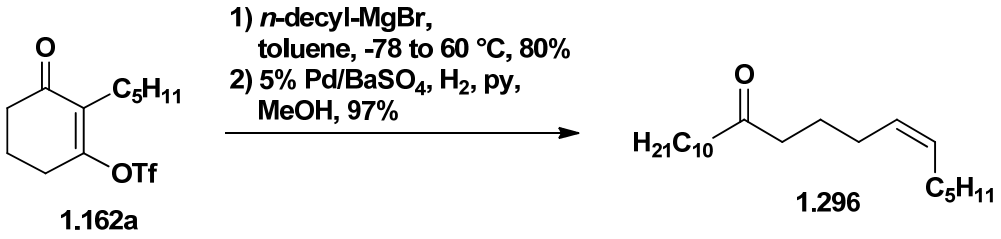

Scheme I.73 Dudley's synthesis of moth pheromone 1.296 (2006).[146]

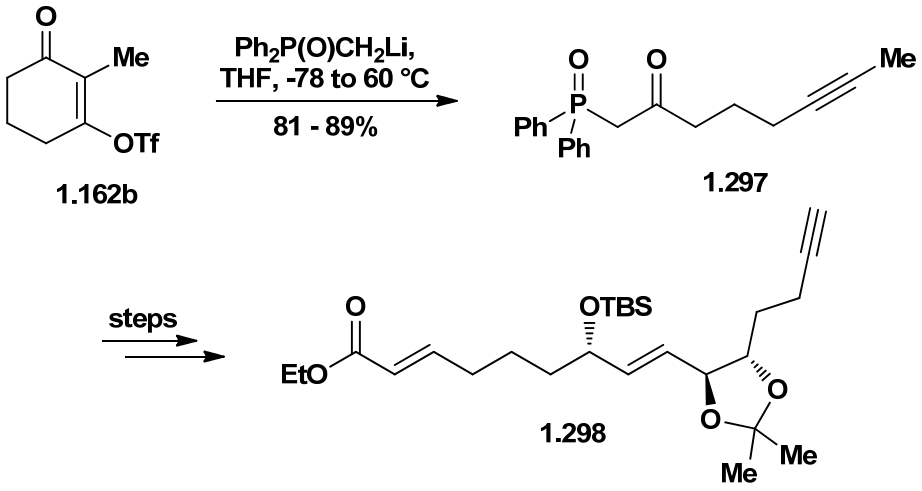

Scheme I.74 Dudley's synthesis of a palmerolide A segment (1.298) (2010).[147]

Ring opening fragmentations that give acyclic alkene (sp^2-sp^2) motifs have been used to generate a diverse range of natural product-related compounds. Among the many creative approaches to the iconic chrysanthamates, Krief and Surleraux demonstrated that functionalized cyclopentanone **1.299** is a suitable substrate for fragmentation that grants access to both *cis*- and *trans*-chrysanthemic acids (Scheme I.75).[148] These are common intermediates in the production of pyrethroid insecticides. The action of potassium hydroxide gives retention of stereochemistry, whereas lithium methoxide induces epimerization to the thermodynamic *trans* carboxylate. A related and mechanistically complementary fragmentation of hydroxybromide **1.302** gave, after reduction of the

unstable aldehyde, *Z* olefin **1.303** in good yield (Scheme I.76).[149] From this intermediate, de Groot and co-workers completed the synthesis of three related insect pheromones: (*R*)-10-methyl-2-tridecanone (**1.304**), (*S*)-9-methylnonadecane (**1.305**), and (*meso*)-13,23-dimethylpentatriacontane (**1.306**).

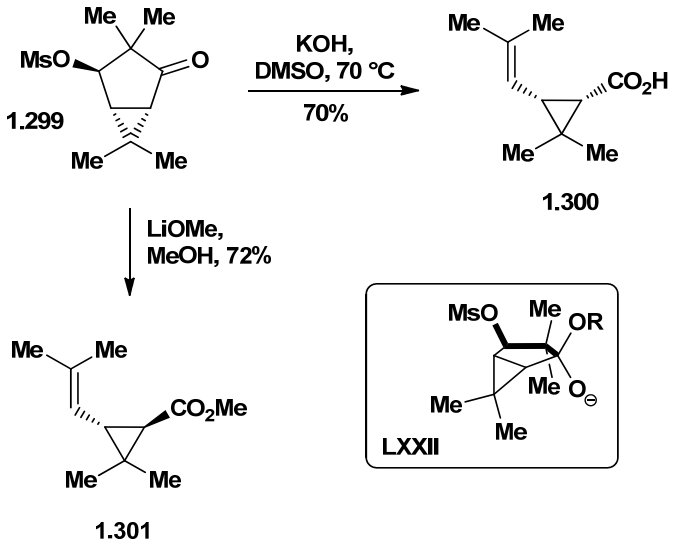

Scheme I.75 Krief and Surleraux's *cis*- and *trans*-chrysanthemic carboxylate syntheses (1.300 and 1.301) (1991).[148]

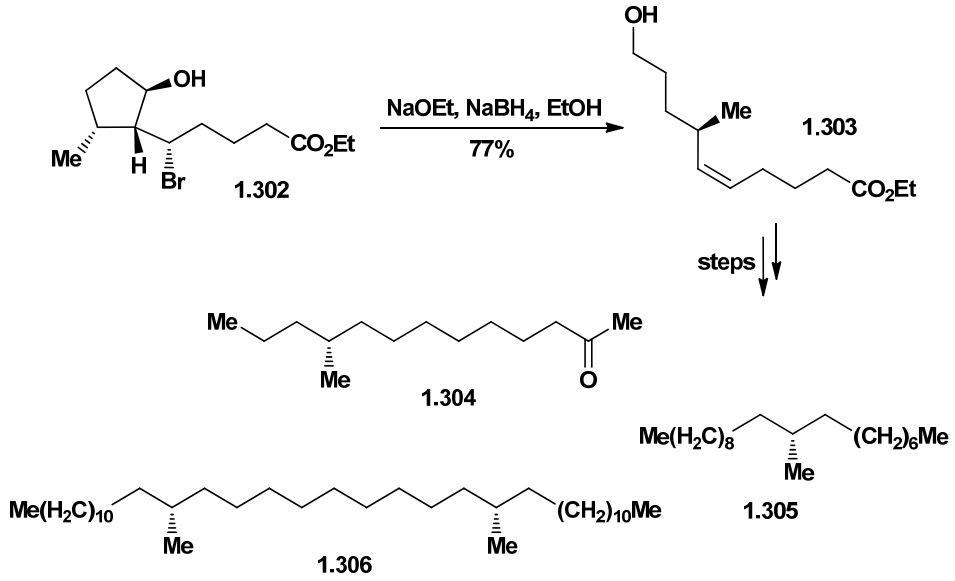

Scheme I.76 de Groot's divergent synthesis of insect pheromones (2003).[149]

The zaragozic acids (squalestatins, not shown) are fungal metabolites that inhibit squalene synthase and farnesyl-protein transferase.[150] These complex natural products challenge the art and science of synthesis and continue to inspire new synthetic studies. The 2,8-dioxabicyclo[3.2.1]octane core (**1.309**) of this family was constructed by Nagaoka and co-workers through the strategic use of fragmentation (**1.307** → **1.308**), followed by reduction/iodo acetalization (Scheme I.77).

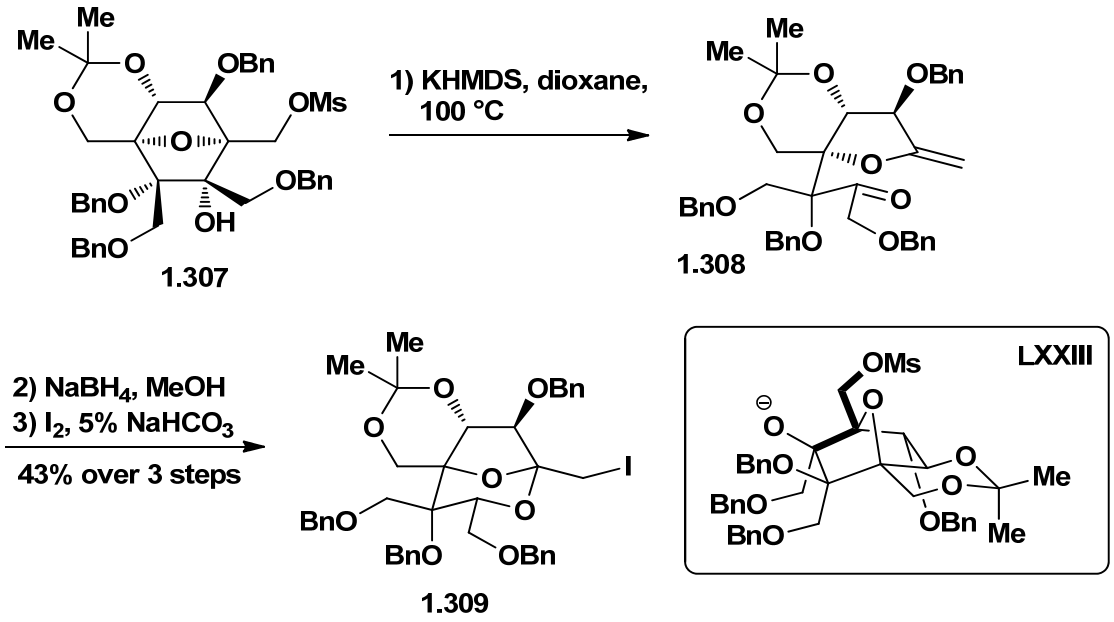

Scheme I.77 Nagaoka's zaragozic acid core synthesis (1.309) (1999).[150]

Recently, a C-C fragmentation strategy was applied to the racemic total syntheses of pallavicinin (**1.312**) and neopallavicinin (**1.313**) by Peng and Wong (Scheme I.78).[151] These modified labdane diterpenoids exhibit bioactivities ranging from fever reduction to muscle regeneration and detoxification. Heating the free secondary alcohol derived from **1.310** with strong base produced **1.311**, the key intermediate for a planned biomimetic intramolecular aldol sequence.

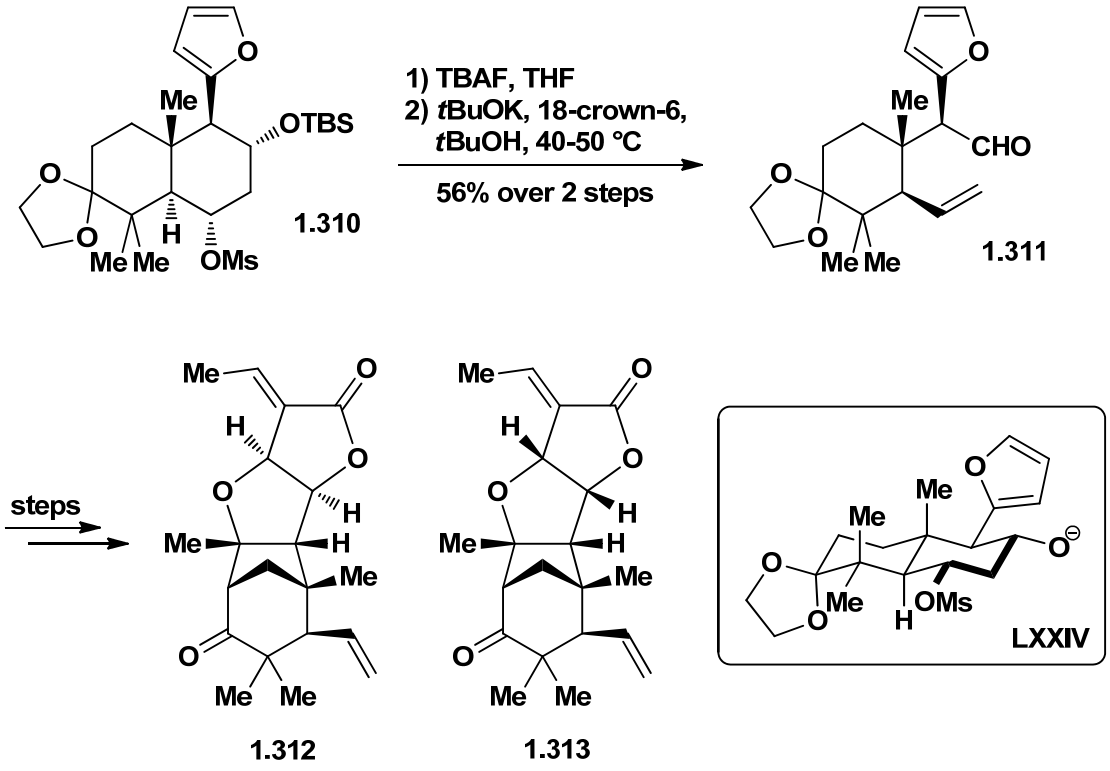

Scheme I.78 C-C fragmentation in Peng and Wong's syntheses of (±)-pallavicinin (1.312) and (±)-neopallavicinin (1.313) (2006).[151]

Release of ring strain was used to leverage fragmentation in Kim and Cha's recent racemic synthesis of cyathin B_2 (**1.316**) and cyathin A_3 (**1.317**, Scheme I.79).[152] Several members of this tricyclic diterpene family of natural products exhibit antimicrobial and anticancer properties.

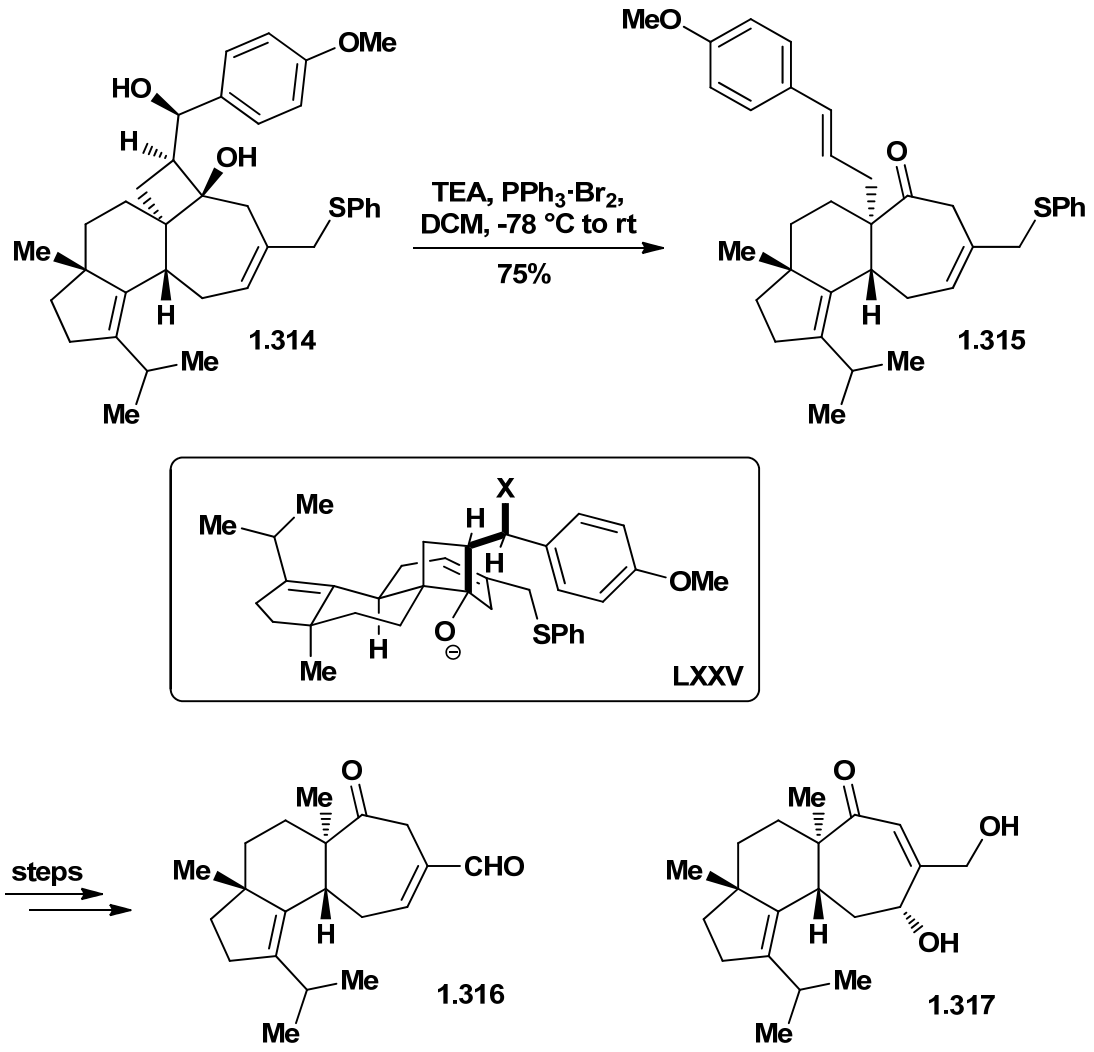

Scheme I.79 A C-C fragmentation in Kim and Cha's syntheses of (±)-cyathin B_2 (1.316) and (±)-cyathin A_3 (1.317) (2009).[152]

In a series of studies, Prantz and Mulzer developed stereocontrolled syntheses of methyl-branched trisubstituted *Z* olefins (**1.319**, **1.321**, and **1.323**) via hydroxide mediated fragmentation of mesyloxylactones (**1.318**, **1.320**, and **1.322**, Scheme I.80).[153] This was applied to formal syntheses of anticancer polyketides epothilone D, discodermolide, and peloruside A (not shown). Sodium, potassium, and lithium hydroxides were equally effective in the conversion of **1.318** to **1.319** in tetrahydrofuran. When the stereoelectronic

requirements for fragmentation are satisfied (e.g. see inset), fragmentation appears to precede hydrolysis. These reactions may follow a decarboxylative pathway. Both pathways would give the observed product.

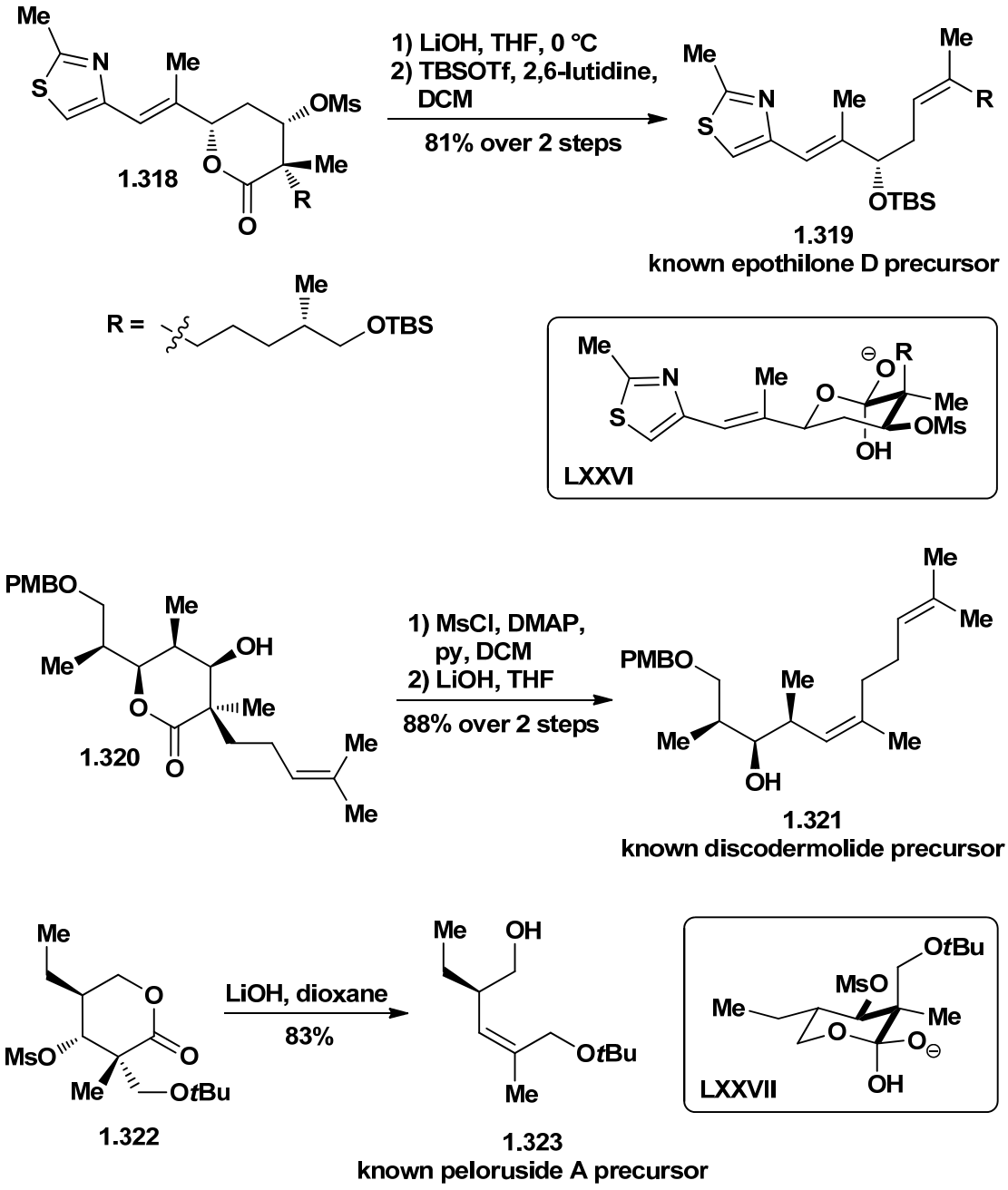

Scheme I.80 The C-C fragmentations in Mulzer's formal syntheses of epothilone D, discodermolide, and peloruside A (2009-2010).[153]

Charette's triflic anhydride-mediated methodology (*cf.* Scheme I.49) was applied in a ring opening fragmentation of γ-amino hydroxide **1.324** (Scheme I.81). This intermediate was used to advance the stereoselective total syntheses of frog skin indolizidine alkaloids 209I (**1.326**) and 223J (**1.327**).[154]

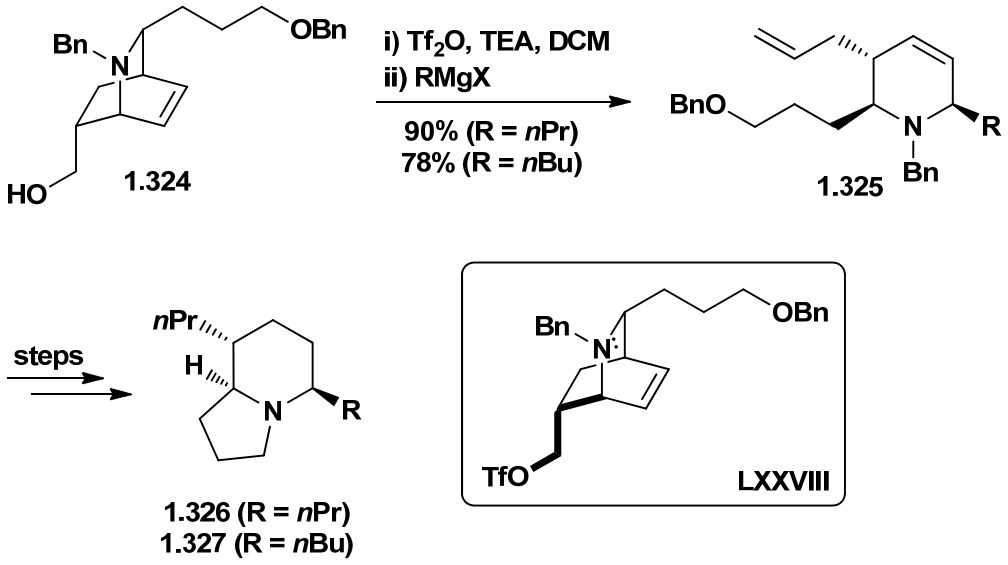

Scheme I.81 Key steps in Charette's enantioselective total syntheses of 209I (1.326) and 223J (1.327) (2010).[154]

The power of C-C fragmentation is especially evident in ring expansion strategies. Direct methods for the preparation of functionalized, or otherwise complex, eight-, nine-, and ten-membered rings can be particularly challenging. In these contexts, C-C fragmentation has found its most important application. The functionalized eight-membered ring skeleton of parvifoline (**1.330**) and isoparvifolinone (**1.331**) was constructed via fragmentative ring expansion from the racemic *trans*-hydroxymesylate **1.328** (Scheme I.82).[155] The *Z* olefin **1.329** was then advanced to access both sesquiterpenes.

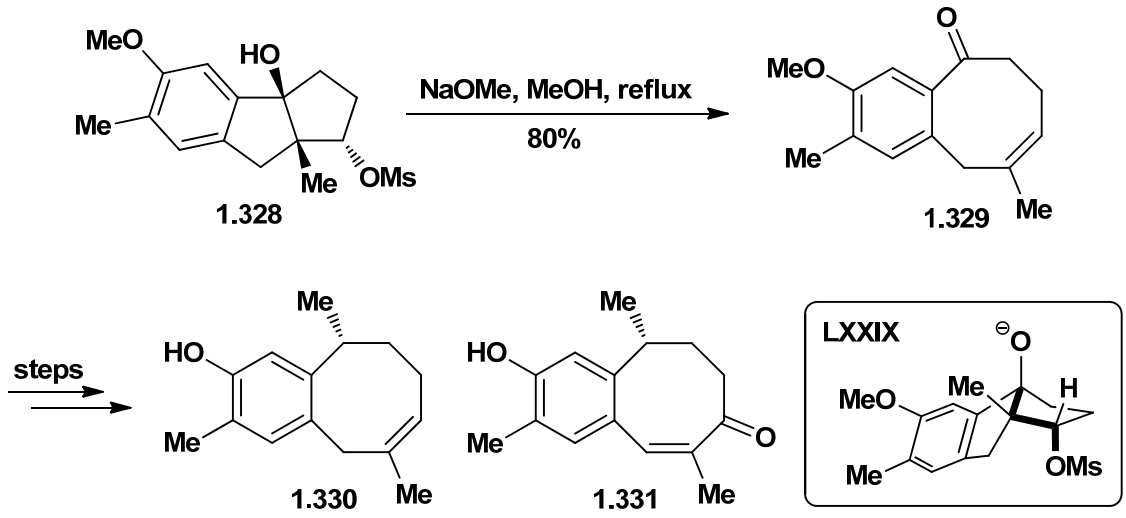

Scheme I.82 Key fragmentation of Joseph-Nathan's syntheses of (±)-parvifoline (1.330) and (±)-isoparvifolinone (1.331) (1995).[155]

The bridgehead olefin **1.333**, which includes a nine-membered ring and constitutes the core of the novel *ras* farnesyl transferase and squalene synthase inhibitor CP-263,114 (not shown), was accessed via fragmentation of tricycle **1.332** (Scheme I.83).[156] Nagaoka and co-workers suggested that sequestration of the sodium cation from the alkoxide electrofuge drives this transformation. In an alternative approach towards the natural product, Wood and co-workers designed a mesylate derived from isotwistane **1.334** that underwent ring expansion upon mild methanolysis to give the related bicycle **1.335** (Scheme I.84).[157]

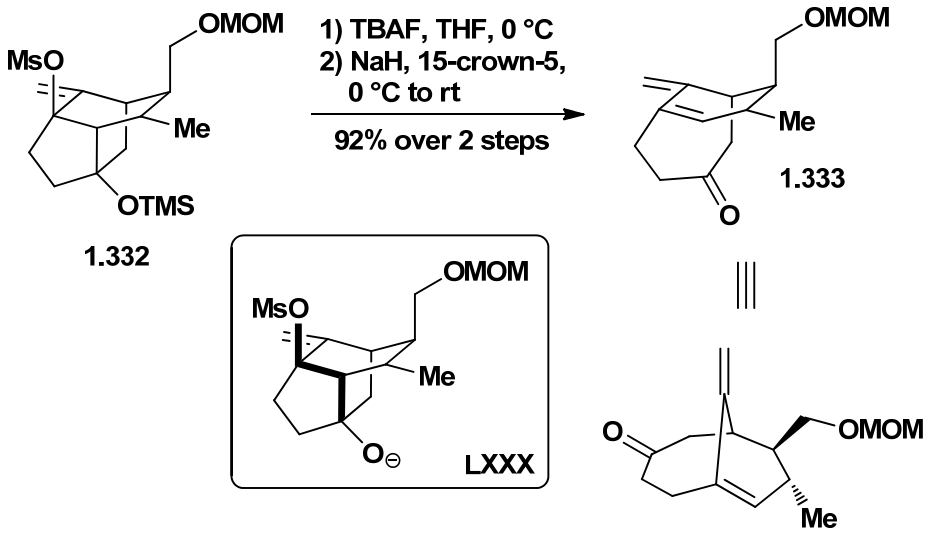

Scheme I.83 Nagaoka's approach to CP-263,114 (1999).[156]

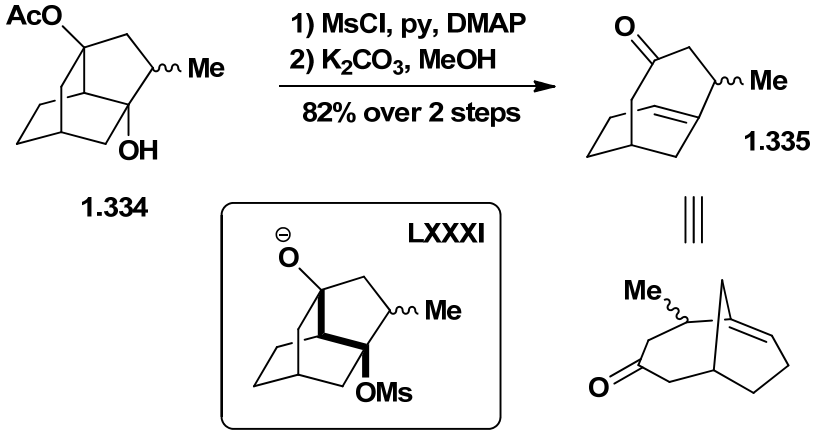

Scheme I.84 Wood's approach to CP-263,114 (2001).[157]

Following detailed preliminary studies,[158] Paquette and co-workers achieved the first total synthesis of the antileukemic agent jatrophatrione (**1.338**, Scheme I.85).[159] The unique nine-membered ring-containing diterpene framework of this natural product was revealed upon fragmentation of the complex monomesylate derived from tetracycle **1.336** (see **LXXXII**).

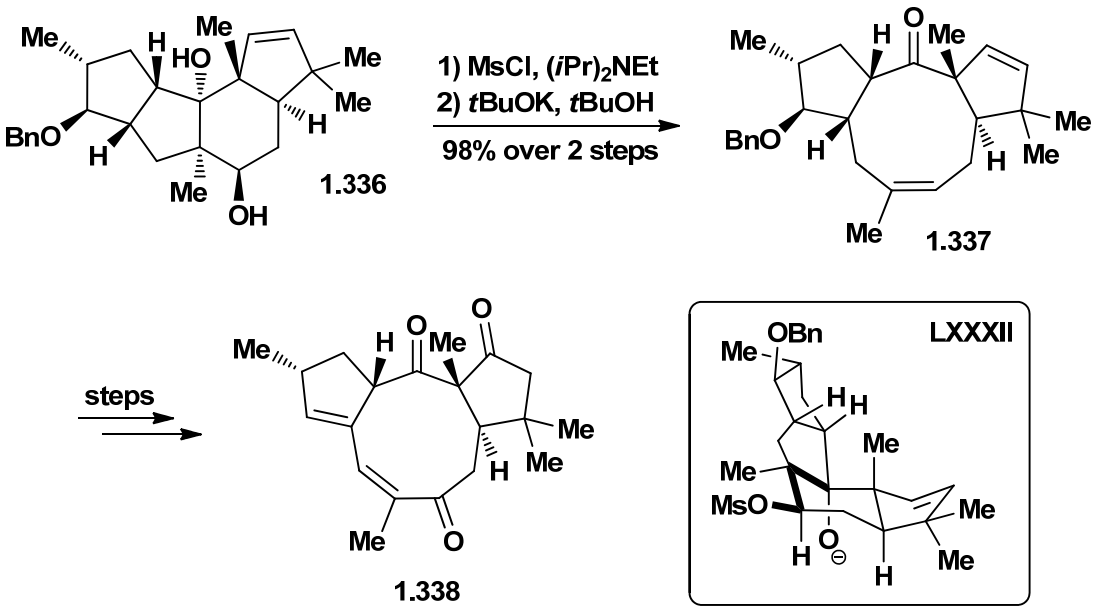

Scheme I.85 The key fragmentation in Paquette's synthesis of (±)-jatrophatrione (1.338) (2002).[159]

The aquariane carbocyclic ring system (**1.340**) was also successfully synthesized through ring expansion (Scheme I.86).[160] The gorgonian diterpene natural product targets (not shown) exhibit cytotoxicity against human breast cancer cells. Thornton and Burnell prepared this scaffold from tetracycle **1.339**. Base-induced C-C fragmentation gave the nine-membered ring fused to the diquinane core.

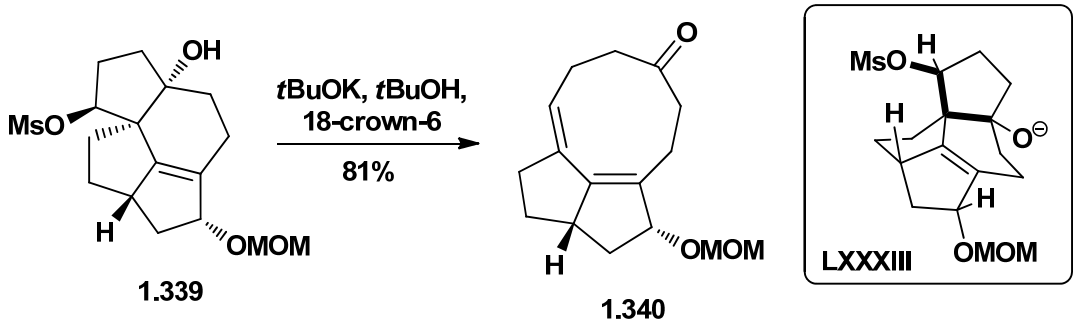

Scheme I.86 Thornton's approach to the aquariolide core (1.340) (2006).[160]

Many members of the xenicane diterpene superfamily have been described and the majority have been found to be bioactive. These compounds have captured the attention of several research groups. Studies that utilize C-C fragmentation reactions have appeared over the past decade from the groups of Leumann and Corey, as well as our group. Leumann and co-workers successfully completed the first total synthesis of optically active coraxeniolide A (**1.343**, Scheme I.87), one of many challenging targets in this class.[161] The strategy was related to Corey's original synthesis of caryophyllene.[85] Fragmentation of hydroxytosylate **1.341** was pivotal for the stereospecific elaboration of the strained cyclononene **1.342**. Corey revisited the caryophyllene problem with a new approach.[162] He and Larionov reported the synthesis of enantioenriched cyclononadienone **1.345** (Scheme I.88). This versatile atropisomeric intermediate granted access to β-caryophyllene (**1.115**), and the enantiomer of **1.345** was used to access coraxeniolide A (**1.343**).

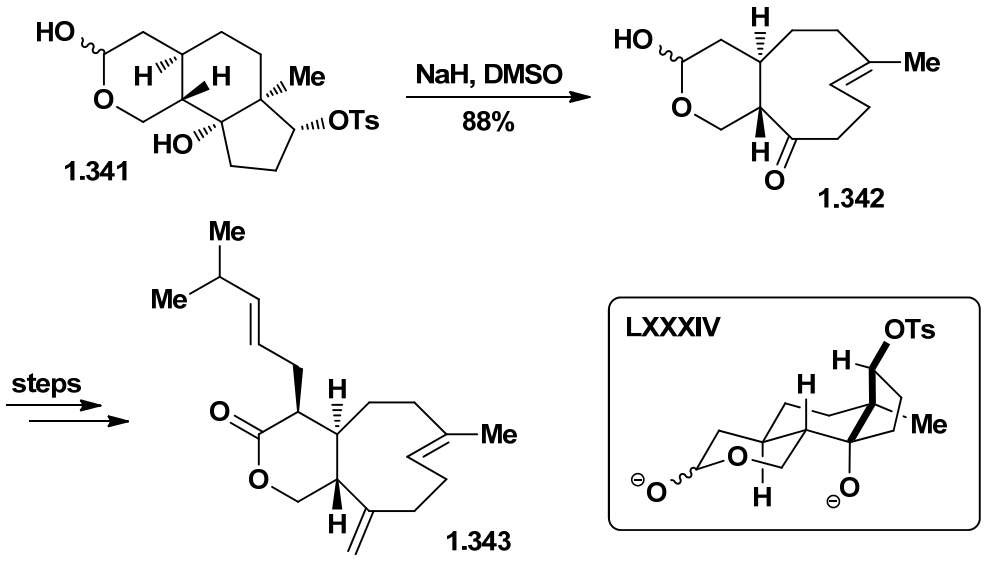

Scheme I.87 Key fragmentation in Leumann's synthesis of coraxeniolide A (1.343) (2000).[161]

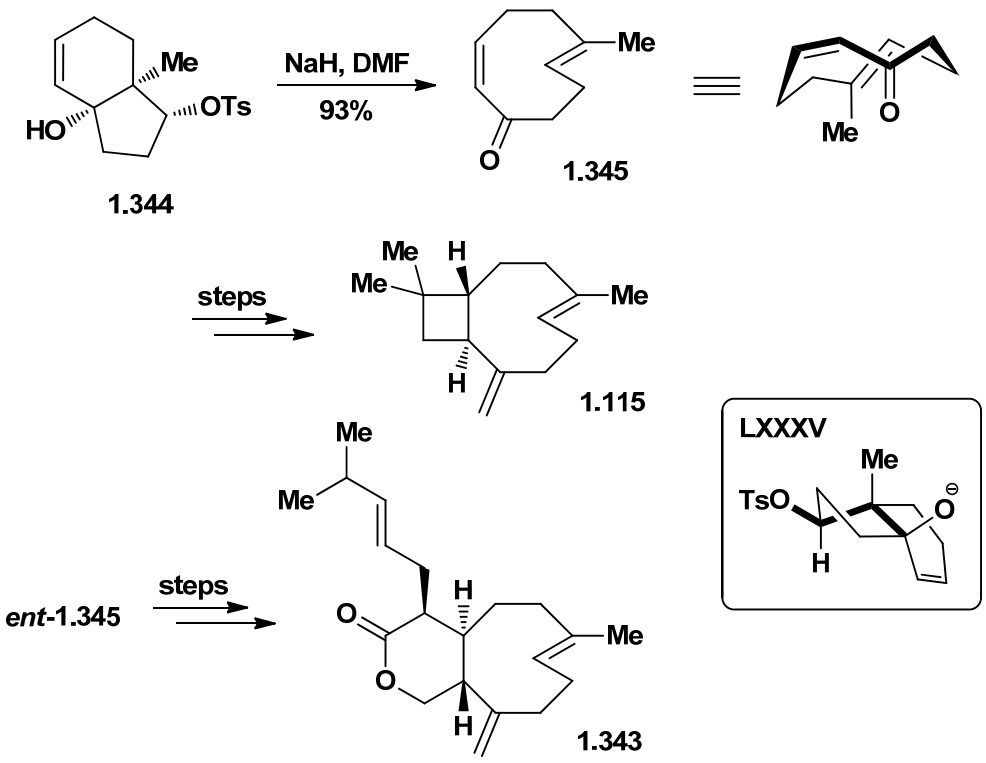

Scheme I.88 Enantioenriched 1.344 gives enantioenriched 1.345 via fragmentation in Corey's syntheses of β-caryophyllene (1.115) and coraxeniolide A (1.343) (2008).[162]

The classic periplanone targets, highly unsaturated sesquiterpenes and sex pheromones of the American cockroach, were also prepared by C-C fragmentation (Scheme I.89).[163] The key reaction gave an *exo*-olefin and the desired ten-membered ring. Saicic and co-workers designed the primary mesylate derived from **1.346** to undergo hydroxide-promoted fragmentation late in the synthesis. Subsequent arrival at periplanone C (**1.348**) also constituted formal syntheses of periplanones A (**1.349**) and D (**1.350**).

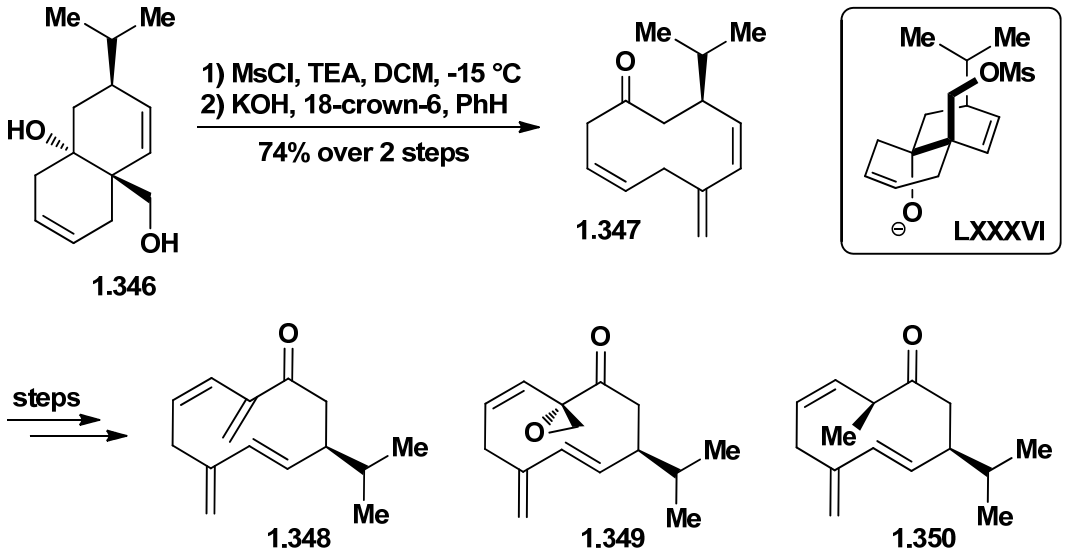

Scheme I.89 Saicic's key fragmentation *en route* to syntheses of (±)-periplanones 1.348-1.350 (2004).[163]

Ley and co-workers used a variation of the Marshall embodiment of C-C fragmentation in an exploratory route towards thapsigargins such as nortrilobolide (**1.353**, Scheme I.90).[164] This family of complex guaianolide terpenes exhibits a range of biological activities, including potent and selective Ca^{2+} modulation and apoptosis induction in prostate cancer cells. Face-selective hydroboration of **1.351** gave the α-alkylborane intermediate. Ring expansion, via fragmentation of the boronate promoted by methoxide (see inset), proceeded smoothly to yield cyclodecadiene **1.352**.

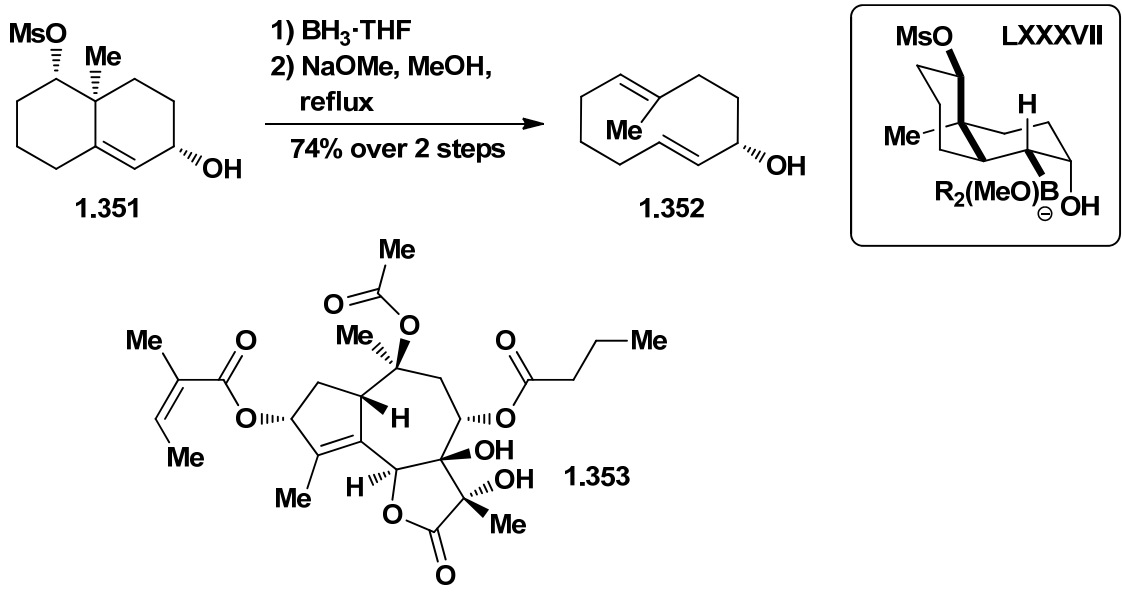

Scheme I.90 Ley's approach towards the thapsigargins (2004).[164]

Winkler and co-workers reported the synthesis of the core carbon framework of eleutherobin (not shown), a diterpene glycoside with robust antitumor activity, by way of a regioselective fragmentation-decarboxylation-double hemiketal formation process (Scheme I.91).[165] Heating **1.354** in the presence of potassium carbonate in DMF furnished **1.357** as the only product. The authors did not comment on the possibility of a stepwise process, i.e. retro-aldol/β-elimination. Lupton's findings (Scheme I.45) may be relevant to the selective cleavage of the primary carbonate C-O bond over the secondary carbonate C-O (**1.355**). Regardless, this selectivity and the elegant strategy are especially noteworthy.

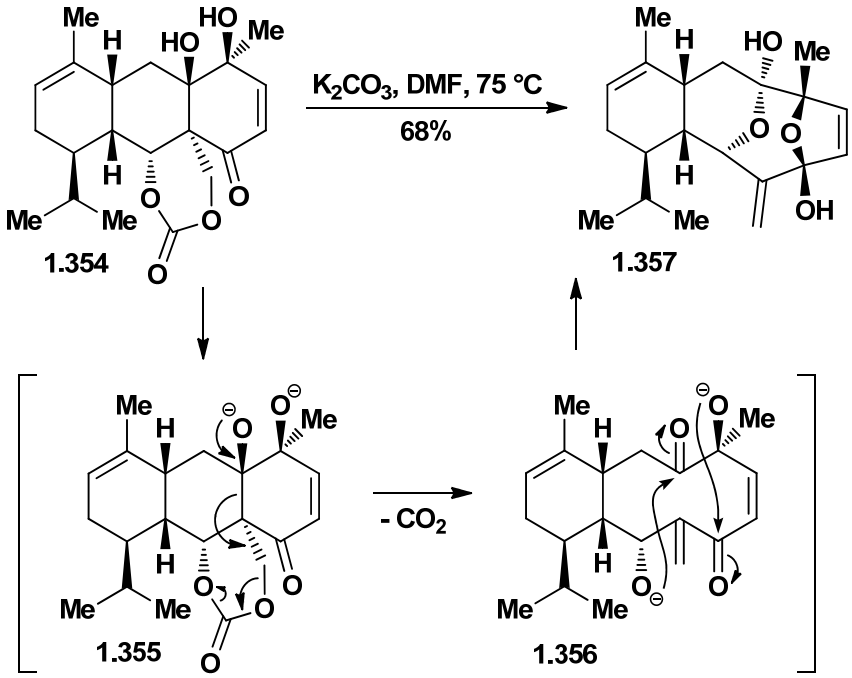

Scheme I.91 Winkler's fragmentation cascade to the eleutherobin core (1.357) (2003).[165]

Perhaps the most complex natural products prepared to date using fragmentation as the key step are those housing highly functionalized ten-membered rings in a challenging context. For example, Holton and co-workers achieved the total synthesis of the potent anticancer drug Taxol® (**1.360**) using this transformation (Scheme I.92).[166] A Lewis acid promoted epoxy-alcohol fragmentation of bicyclo[3.2.1]octane **1.358** unveiled the AB ring system **1.359**. The apparent synperiplanar orientation of the fragmentation is noteworthy (see inset). This reaction was planned based on model studies that confirmed that this stereochemical arrangement accommodates facile fragmentation. The corresponding *exo* epoxides in the model study did not give clean conversion to the target alkenes.[167]

This phenomenon might be best understood through a stepwise mechanism in which the epoxide ionizes first to reveal a tertiary carbocation. In another classic synthesis

of this target, Wender and co-workers realized an even more concise route via the related epoxide derived from bicyclo[3.1.1]heptane **1.361** (Scheme I.93).[168] Interestingly, this fragmentation (**LXXXIX**), which was the subject of several model studies,[169] was performed under mild basic conditions.

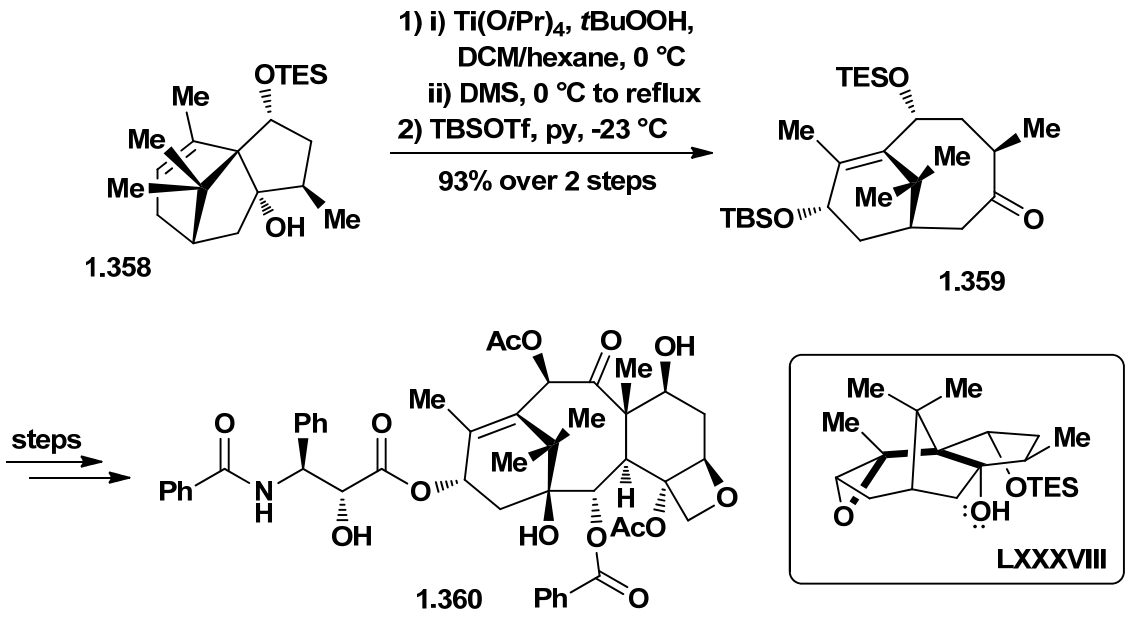

Scheme I.92 Holton's Lewis acid promoted epoxy-alcohol fragmentation in the synthesis of Taxol® (1.360) (1994).[166]

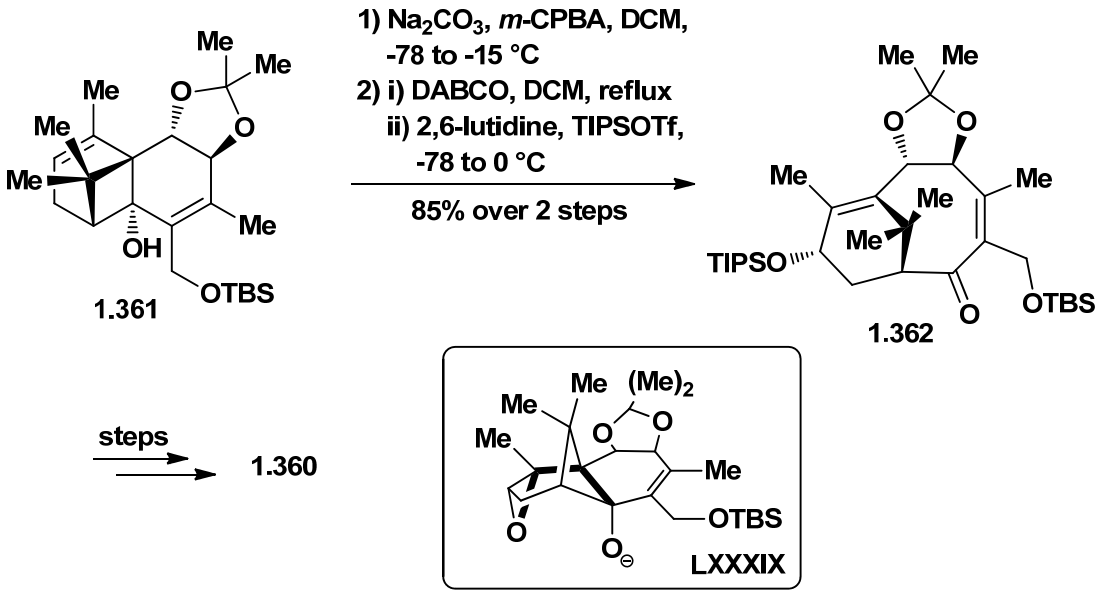

Scheme I.93 Wender's base-promoted epoxy-alcohol fragmentation in the synthesis of Taxol® (1997).[168]

The structurally intricate diterpene vinigrol (**1.365**, Scheme I.94) is an antihypertensive, a tumor necrosis factor antagonist, and an inhibitor of platelet activating factor-induced platelet aggregation. Baran and co-workers developed a concise approach to the challenging core structure via base-induced fragmentation.[170] They also applied this maneuver to the total synthesis of vinigrol.[171] In this ring expansion, deprotonation of the tertiary alcohol of the monomesylate derived from tetracycle **1.363** was accompanied by clean fragmentation to tricycle **1.364**, which was properly functionalized for completion of the synthesis.

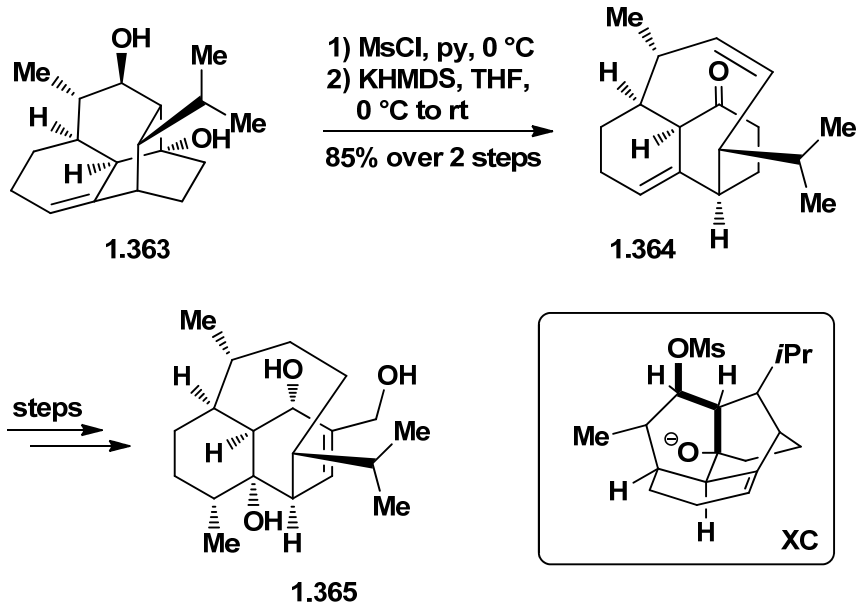

Scheme I.94 The key fragmentation in Baran's synthesis of (±)-vinigrol (1.365) (2009).[171]

The final entry in this section is the C-C fragmentation recently discovered in triterpene biosynthesis.[172] Synthase At5g42600, from the small flowering plant *Arabidopsis thaliana*, was shown to catalyze the conversion of oxidosqualene (**1.366**) to marneral (**1.370**), a carbocyclic precursor to more complex triterpenes (Scheme I.95). Oxidosqualene appears first to be protonated by aspartate 487 and then to undergo carbocationic cyclizations (**1.366** → **1.368**). Following a series of 1,2-hydride and methyl shifts (**1.368** → **1.369**), fragmentation of tertiary carbocation **1.369**, facilitated in part by aspartate 487, produces *seco* aldehyde **1.370**.

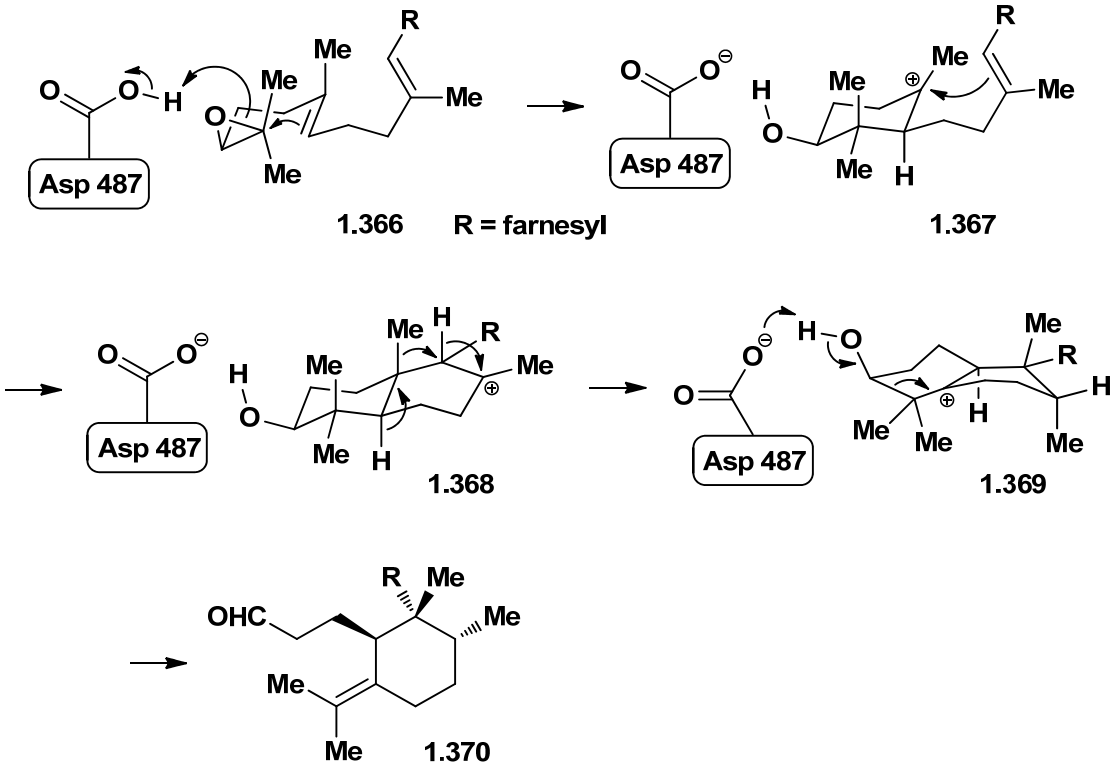

Scheme I.95 ***Arabidopsis*** **oxidosqualene cyclase fragmentation in the biosynthesis of marneral (1.370), identified by Matsuda (2006).**[172]

1.4 Summary and Outlook

In a decade of iconic achievements in the field of organic chemistry, Eschenmoser advanced a reaction that simultaneously accomplished the cleavage of a carbon-carbon single bond and the site specific formation of a carbon-carbon double bond.[1] In this parvum opus the relevant antecedent data from the previous fifty years were collected and rationalized under a new, single mechanistic umbrella, and the new transformation manifold was used in a ring opening cascade sequence that illustrated the effectiveness of the advance. The scope and limitations of the reaction manifold were evaluated by many. Early key contributors included Henbest,[67,68] Grob,[71,80,81] Stork,[74] and especially Marshall,[90,92,93] who demonstrated that many synthetically useful anion equivalents will

participate in the reaction manifold, Wharton, who significantly extended the strategy to include ring expansion,[75,76,78] and Corey, who first demonstrated that this transformation can be powerfully simplifying in natural product total synthesis.[85] Other extensions and clarifications were advanced as well. Grob's contributions were instrumental to developing a clear understanding of the reaction. He coined the terms electrofuge, nucleofuge, and fragmentation, and categorized the transformation-type as distinct from additions, eliminations, substitutions, and rearrangements.[8a,b] He also studied the cinchona alkaloid-type C-C fragmentations, and others not reviewed here, and showed that the mechanistic underpinning for the formation of nitriles under Beckmann conditions fell within this framework.[37a-d] Fragmentation methods that resulted in the formation of alkynes were advanced by Bodendorf,[41] Eschenmoser,[42,43] and Tanabe.[44,45] Practical refinements were advanced by Corey[47] and others. Hence, heterolytic C-C fragmentation emerged as a powerful indirect ring opening and ring expansion method for the selective preparation of functionalized nitriles, alkynes, and especially alkenes.

Many new and modified methods of C-C fragmentation have been advanced over the past twenty years. Many reports serve to broaden the substrate scope through motif-building and operate within the original reaction paradigm. Several expand the paradigm of alkene, alkyne, or allene synthesis. For example, Molander developed an approach to medium-sized alkene-containing rings with a single-flask cyclization/fragmentation cascade,[117] Charette applied new insights to gain rapid entry to alkaloid natural products,[118,119] Dudley[105-107] demonstrated that a vinyl-positioned triflate is an excellent leaving group for alkyne synthesis via fragmentation,[48] and our work,[140,142]

along with that of Cramer,[143] established anionic (concerted) fragmentations as a means to access allenic products.[139]

Numerous creative applications of C-C fragmentation have been catalogued as well. A broad range of natural products and natural product motifs have been prepared through ring opening or ring expansion fragmentations. The list of recent natural product syntheses that use C-C fragmentations is extensive: caryophyllene,[162] coraxeniolide A,[161,162] (*Z*)-6-heneicosen-11-one,[146] chrysanthamates,[148] cyathin B2 and A3,[152] discodermolide, epothilone D, and peloruside A,[153] elegansidiol,[144] GB-13,[145] insect pheromones,[149] isoparvifoline and parvifolinone,[155] jatrophatrione,[159] pallavicinin and neopallavicinin,[151] periplanone A, C, and D,[163] taxol,[166,168] vinigrol,[171] and 209I and 223J,[154] among others. Moreover, virtually every report on C-C fragmentation advances a synthesis of a natural product-related intermediate or motif.

There have been few quantitative mechanistic studies of C-C fragmentation. Henbest reported the first experimental test of the mechanism and stereoelectronic requirements.[67,68] Subsequent numerous detailed studies by Grob constitute the bulk of the quantitative work in this field.[8b] Mechanistic insight over the past twenty years has been gleaned primarily through qualitative examination of specific systems, especially by Barluenga,[124] Dudley,[105c,d] Lupton,[112] Maroto,[102] Sakai,[131] and our group.[140,142] Fragmentation reactions have strict limitations. At a minimum, five substrate atoms are involved in this transformation, which is high compared to most methods. Probably the most restrictive aspect of concerted C-C fragmentation is the minimum torsion angle required for reaction. The ideal angle is 180°.[67,68,76] For sp^1-sp^1 bond generating substrates the torsion angles are necessarily near 180° or 0°.[8e] The minimum angle has not been

established for concerted sp^2-sp^2 and sp^2-sp^1 bond forming fragmentations, and few failed fragmentation attempts have been described in detail. Still, substrates with angles that deviate significantly from 180° appear to fail.[67,68] Ground state structural analysis of substituted bicycles indicates that electronic effects alter the torsion angle of activated substrates and can therefore enhance or attenuate fragmentation.[142] Although computational studies have been limited in scope thus far, electronic structure calculations appear to be useful in predicting the feasibility of fragmentation.

There is still much to be learned and discovered about C-C fragmentations. Additional mechanistic studies would provide useful insight into the stereoelectronic requirements of these reactions and would improve the predictability of planned fragmentations. In principle, the transformation can be expanded by inclusion of new electron sources (electrofuges) and new electron sinks (nucleofuges). Perhaps most notable is that fragmentations are used primarily in their most elementary form. The designed synthesis of multiple carbon-carbon double bonds via fragmentation has rarely been explored over the past thirty years. Ley's work towards the thapsigargins is one such example,[164] and yet, concerted C-C fragmentation as a means to generate multiple olefinic sites within a molecule has the potential to further expedite organic synthesis. Pleasingly, C-C fragmentation remains indispensably useful, and the possibilities are far from exhausted.

1.5 References and Notes

1. A. Eschenmoser, A. Frey, *Helv. Chim. Acta* **1952**, *35*, 1660-1666.

2. S. A. Julia, A. Eschenmoser, H. Heusser, N. Tarköy, *Helv. Chim. Acta* **1953**, *36*, 1885-1891.

3. a) D. M. Oldroyd, G. S. Fisher, L. A. Goldblatt, *J. Am. Chem. Soc.* **1950**, *72*, 2407-2410; b) G. Dupont, R. Dulou, G. Clément, *Bull. Soc. Chim. Fr.* **1950**, 1056-1057; c) G. Dupont, R. Dulou, G. Clément, *Bull. Soc. Chim. Fr.* **1950**, 1115-1120.

4. a) J. Schreiber, H. Maag, N. Hashimoto, A. Eschenmoser, *Angew. Chem. Int. Ed. Engl.* **1971**, *10*, 330-331; b) W. C. Agosta, A. M. Foster, *J. Org. Chem.* **1972**, *37*, 61-63; c) J. J. C. Grové, C. W. Holzapfel, D. B. G. Williams, *Tetrahedron Lett.* **1996**, *37*, 1305-1308; d) J. J. C. Grové, C. W. Holzapfel, D. B. G. Williams, *Tetrahedron Lett.* **1996**, *37*, 5817-5820; e) J.-J. Wang, W.-P. Hu, H.-W. Chung, L.-F. Wang, M.-H. Hsu, *Tetrahedron* **1998**, *54*, 13149-13154; f) W.-P. Hu, J.-J. Wang, P.-C. Tsai, *J. Org. Chem.* **2000**, *65*, 4208-4209; g) E. R. Alonso, K. A. Tehrani, M. Beolens, D. W. Knight, V. Yu, N. De Kimpe, *Tetrahedron Lett.* **2001**, *42*, 3921-3923.

5. These transformations are very old (reference 53, below) and were first described as decarboxylative eliminations by Corey (E. J. Corey, *J. Am. Chem. Soc.* **1952**, *74*, 5897-5905). The stereochemical requirements were first described by Cristol and Norris (S. J. Cristol , W. P. Norris, *J. Am. Chem. Soc.* **1953**, *75*, 632-636).

6. M. B. Smith, J. March, *March's Advanced Organic Chemistry: Reactions, Mechanisms, and Structure*, Fifth ed., Wiley-Interscience, New York, **2001**.

7. a) N. Risch, M. Langhals, T. Hohberg, *Tetrahedron Lett.* **1991**, *32*, 4465-4468; b) N. Cramer, J. Juretschke, S. Laschat, A. Baro, W. Frey, *Eur. J. Org. Chem.* **2004**, 1397-1400.

8. a) C. A. Grob, P. W. Schiess, *Angew. Chem. Int. Ed.* **1967**, *6*, 1-15; b) C. A. Grob, *Angew. Chem. Int. Ed.* **1969**, *8*, 535-622; c) R. T. Conley, S. Ghosh, in *Mechanisms of Molecular Migrations*, Vol. 4 (Ed: B. S. Thyagarajan), Wiley-Interscience, New York, **1971**, pp. 197-308; d) J. A. Marshall, *Synthesis* **1971**, *5*, 229-235; e) R. E. Gawley, *Org. React.* **1988**, *35*, 1-420; f) D. Caine, *Org. Prep. Proc. Int.* **1988**, *20*, 1-51; g) P. Weyerstahl, H. Marschall, in *Comprehensive Organic Synthesis*, Vol. 6 (Eds: B. M. Trost, I. Fleming, E. Winterfeldt), Pergamon Press, Oxford, **1991**, pp. 1041-1070; h) Z. Wang, *Comprehensive Organic Name Reactions and Reagents*, Wiley-Interscience, Chicester, **2009**, pp. 288-295; i) K. Prantz, J. Mulzer, *Chem. Rev.* **2010**, *110*, 3741-3766; j) T.-L. Ho, *Heterolytic Fragmentation of Organic Molecules*, Wiley, New York, **1993**; k) C. J. M. Stirling, *Chem. Rev.* **1978**, *78*, 517-567; l) J. Reucroft, P. G. Sammes, *Q. Rev. Chem. Soc.***1971**, *25*, 135-169. For an excellent discussion of the

stereoelectronics of fragmentation, see P. Deslongchamps, *Stereoelectronic Effects in Organic Chemistry*, Pergamon Press, Oxford, **1983**, pp. 209-290.

9. Grob cited Eschenmoser's contributions twice: in his first report (reference 71 below) and in his second review (reference 8b, above). Grob did not credit Eschenmoser for being the first to collect the relevant anionic antecedents, for being the first to formulate the correct mechanism, for recognizing the utility of the transformation, or for being the first to design a fragmentation reaction that selectively gave an otherwise difficult to form product. Taken together, this may have served to promulgate the notion that Grob invented this reaction.

10. a) D. H. R. Barton, *Experientia* **1950**, *6*, 316-320; b) D. H. R. Barton, E. Miller, *J. Am. Chem. Soc.* **1950**, *72*, 1066-1070; c) D. H. R. Barton, *Science* **1970**, *169*, 539-544.

11. D. J. Cram, F. A. A. Elhafez, *J. Am. Chem. Soc.* **1952**, *74*, 5828-5835.

12. H. E. Zimmerman, M. D. Traxler, *J. Am. Chem. Soc.* **1957**, *79*, 1920-1923.

13. S. Winstein, M. Shatavsky, C. Norton, R. B. Woodward, *J. Am. Chem. Soc.* **1955**, *77*, 4183-4184.

14. a) G. Stork, A. W. Burgstahler, *J. Am. Chem. Soc.* **1955**, *77*, 5068-5077; b) A. Eschenmoser, L. Ruzicka, O. Jeger, D. Arigoni, *Helv. Chim. Acta* **1955**, *38*, 1890-1904.

15. J. M. McGuire, R. L. Bunch, R. C. Anderson, H. E. Boaz, E. H. Flynn, H. M. Powell, J. W. Smith, *Antibiot. Chemother.* **1952**, *2*, 281-283.

16. J. D. Watson, F. H. C. Crick, *Nature* **1953**, *171*, 737-738.

17. J. T. Arnold, S. S. Dharmatti, M. E. Packard, *J. Chem. Phys.* **1951**, *19*, 507.

18. E. J. Corey, *Angew. Chem. Int. Ed. Engl.* **1991**, *30*, 455-465. In this Nobel Lecture, Corey discusses retrosynthetic analysis, which he traces to 1957.

19. J. Baddiley, A. M. Michelson, A. R. Todd, *Nature* **1948**, *161*, 761-762.

20. R. U. Lemieux, G. Huber, *J. Am. Chem. Soc.* **1953**, *75*, 4118.

21. J. C. Sheehan, K. R. Henery-Logan, *J. Am. Chem. Soc.* **1959**, *81*, 3089-3094.

22. V. du Vigneaud, C. Ressler, J. M. Swan, C. W. Roberts, P. G. Katsoyannis, S. Gordon, *J. Am. Chem. Soc.* **1953**, *75*, 4879-4880.

23. M. Gates, G. Tschudi, *J. Am. Chem. Soc.* **1952**, *74*, 1109-1110.

24. R. B. Woodward, M. P. Cava, W. D. Ollis, A. Hunger, H. U. Daeniker, K. Schenker, *J. Am. Chem. Soc.* **1954**, *76*, 4749-4751.

25. R. B. Woodward, F. E. Bader, H. Bickel, A. J. Frey, R. W. Kierstead, *J. Am. Chem. Soc.***1956**, *78*, 2023-2025.

26. E. J. Corey, R. R. Sauers, *J. Am. Chem. Soc.* **1959**, *81*, 1739-1743.

27. G. Stork, F. H. Clarke, Jr., *J. Am. Chem. Soc.* **1955**, *77*, 1072-1073.

28. G. Stork, E. E. van Tamelen, L. J. Friedman, A. W. Burgstahler, *J. Am. Chem. Soc.* **1953**, *75*, 384-392.

29. R. B. Woodward, F. Sondheimer, D. Taub, *J. Am. Chem. Soc.* **1951**, *73*, 4057.

30. a) O. Wallach, *Justus Liebigs Ann. Chem.* **1890**, *259*, 309-331; b) O. Wallach, *Justus Liebigs Ann. Chem.* **1899**, *309*, 1-31.

31. E. Beckmann, *Ber. Dtsch. Chem. Ges.* **1886**, *19*, 988-993.

32. G. Schroeter, *Ber. Dtsch. Chem. Ges.* **1911**, *44*, 1201-1209.

33. R. F. Brown, N. M. van Gulick, G. H. Schmid, *J. Am. Chem. Soc.* **1955**, *77*, 1094-1097.

34. a) J. M. Gulland, R. Robinson, *J. Chem. Soc.* **1923**, 980-998; b) J. M. Gulland, R. Robinson, *Mem. Proc. Manch. Lit. Phil. Soc.* **1925**, *69*, 79-86.

35. L. Knorr, H. Hörlein, *Ber. Dtsch. Chem. Ges.* **1907**, *40*, 3341-3355.

36. C. Schöpf, *Justus Liebigs Ann. Chem.* **1927**, *452*, 211-267.

37. a) H. P. Fischer, C. A. Grob, E. Renk, *Helv. Chim. Acta* **1962**, *45*, 2539-2553; b) H. P. Fischer, C. A. Grob, *Helv. Chim. Acta* **1963**, *46*, 936-943; c) W. Eisele, C. A. Grob, E. Renk, *Tetrahedron Lett.* **1963**, *4*, 75-76; d) C. A. Grob, H. P. Fischer, W. Raudenbusch, J. Zergenyi, *Helv. Chim. Acta* **1964**, *47*, 1003-1021; e) H. P. Fischer, *Helv. Chim. Acta* **1965**, *48*, 1279-1288.

38. G. Stork, J. M. Tabak, J. F. Blount, *J. Am. Chem. Soc.* **1972**, *94*, 4735-4737.

39. E. W. Colvin, S. Malchenko, R. A. Raphael, J. S. Roberts, *J. Chem. Soc., Perkin Trans. 1* **1973**, 1989-1997.

40. For other early examples of Beckmann fragmentation, refer to the reviews of Conley (reference 8c, above) and Gawley (reference 8e, above).

41. a) K. Bodendorf, P. Kloss, *Angew. Chem.* **1963**, *75*, 139; b) K. Bodendorf, P. Kloss,

Angew. Chem. Int. Ed. Engl. **1963**, *2*, 98-99; c) K. Bodendorf, R. Mayer, *Chem. Ber.* **1965**, *98*, 3554-3560.

42. A. Eschenmoser, D. Felix, G. Ohloff, *Helv. Chim. Acta* **1967**, *50*, 708-713.

43. a) J. Schreiber, D. Felix, A. Eschenmoser, M. Winter, F. Gautschi, K. H. Schulte-Elte, E. Sundt, G. Ohloff, J. Kalovoda, H. Kaufmann, P. Wieland, G. Anner, *Helv. Chim. Acta* **1967**, *50*, 2101-2108; b) D. Felix, J. Schreiber, K. Piers, U. Horn, A. Eschenmoser, *Helv. Chim. Acta* **1968**, *51*, 1461-1465; c) R. K. Müller, D. Felix, J. Schreiber, A. Eschenmoser, *Helv. Chim. Acta* **1970**, *53*, 1479-1484; d) D. Felix, J. Schreiber, G. Ohloff, A. Eschenmoser, *Helv. Chim. Acta* **1971**, *54*, 2896-2912; e) D. Felix, R. K. Müller, U. Horn, R. Joos, J. Schreiber, A. Eschenmoser, *Helv. Chim. Acta* **1972**, *55*, 1276-1319.

44. M. Tanabe, D. F. Crowe, R. L. Dehn, *Tetrahedron Lett.* **1967**, *8*, 3943-3946.

45. M. Tanabe, D. F. Crowe, R. L. Dehn, G. Detre, *Tetrahedron Lett.* **1967**, *8*, 3739-3743.

46. P. Borrevang, J. Hüort, R. T. Rapala, R. Edie, *Tetrahedron Lett.* **1968**, *9*, 4905-4907.

47. E. J. Corey, H. S. Sachdev, *J. Org. Chem.* **1975**, *40*, 579-581.

48. J. L. Coke, H. J. Williams, S. Natarajan, *J. Org. Chem.* **1977**, *42*, 2380-2382.

49. a) M. Shimizu, R. Ando, I. Kuwajima, *J. Org. Chem.* **1981**, *46*, 5246-5248; b) M. Shimizu, R. Ando, I. Kuwajima, *J. Org. Chem.* **1984**, *49*, 1230-1238.

50. M. O. Forster, *J. Chem. Soc., Trans.* **1902**, *81*, 264-274.

51. H. Czerny, *Ber. Dtsch. Chem. Ges.* **1900**, *33*, 2287-2294.

52. a) O. Wallach, *Justus Liebigs Ann. Chem.* **1896**, *289*, 337-361; b) O. Wallach, J. Meyer, F. Collmann, *Justus Liebigs Ann. Chem.* **1903**, *327*, 125-157.

53. R. Fittig, *Justus Liebigs Ann. Chem.* **1877**, *188*, 42-104.

54. H. Bretschneider, H. Haas, *Monatsh. Chem.* **1950**, *81*, 945-951.

55. G. Richard, *Bull. Soc. Chim. Fr.* **1951**, 61C.

56. a) O. Wallach, *Justus Liebigs Ann. Chem.* **1908**, *359*, 265-286; b) O. Wallach, *Justus Liebigs Ann. Chem.* **1908**, *359*, 287-316; c) O. Wallach, *Justus Liebigs Ann. Chem.* **1908**, *360*, 26-81.

57. Zd. H. Skraup, *Ber. Dtsch. Chem. Ges.* **1892**, *25*, 2909-2912.

58. Similar observations were also reported by Rosenmund (K. W. Rosenmund, C. Kittler, *Arch. Pharm. Pharm. Med. Chem.* **1924**, *262*, 18-24) and Podlewski (J. K. Podlewski, J. Suszko, *Recl. Trav. Chim. Pays-Bas* **1936**, *55*, 392-400).

59. Hoffmann (W. Braje, J. Frackenpohl, P. Langer, H. M. R. Hoffmann, *Tetrahedron* **1998**, *54*, 3495-3512), Smith (M. B. Smith, *Organic Synthesis*, McGraw Hill, New York, **2002**), and Williams (reference 140, below) have mistakenly cited Prelog for work in this area: a) V. Prelog, E. Zalán, *Helv. Chim. Acta* **1944**, *27*, 535-545; b) V. Prelog, O. Häflinger, *Helv. Chim. Acta* **1950**, *33*, 2021-2029. Although Prelog may indeed have used this reaction, to our knowledge these reports do not include fragmentations.

60. E. M. Gibbs, T. A. Henry, *J. Chem. Soc.* **1939**, 240-246.

61. H. S. Mosher, R. Forker, H. R. Williams, T. S. Oakwood, *J. Am. Chem. Soc.* **1952**, *74*, 4627-4629. In this report, Mosher offers the mechanism in footnote #4 on p. 4627. It is notable that he does not suggest it as a general reactivity principle.

62. a) O. Kriewitz, *Ber. Dtsch. Chem. Ges.* **1899**, *32*, 57-60; b) O. Kriewitz, *J. Chem. Soc., Abstr.* **1899**, *76*, 298; c) H. J. Prins, *Chem. Weekblad* **1919**, *16*, 1072-1073; d) H. J. Prins, *Chem. Weekblad* **1917**, *14*, 627-630. For lead references see I. M. Pastor, M. Yus, *Curr. Org. Chem.* **2007**, *11*, 925-957.

63. a) A. Slawjanov, *Chem. Zenir.* **1907**, *78*, 134-135; b) A. Kalishev, *Zh. Russ. Fiz.-Khim. O-va.* **1914**, *46*, 427-453.

64. F. C. Whitmore, E. E. Stahly, *J. Am. Chem. Soc.* **1933**, *55*, 4153-4157.

65. There is also the curious 1950 observation of Witkop, where smooth oxidative cleavage of hydroxyindole **A** (below) with perbenzoic acid yielded cyclic lactam **B** (B. Witkop, *J. Am. Chem. Soc.* **1950**, *72*, 1428-1429). The same product was obtained from the corresponding peroxyindole **C** under neutral or slightly acidic conditions. Although not described as such, both of these transformations appear to be C-C fragmentations.

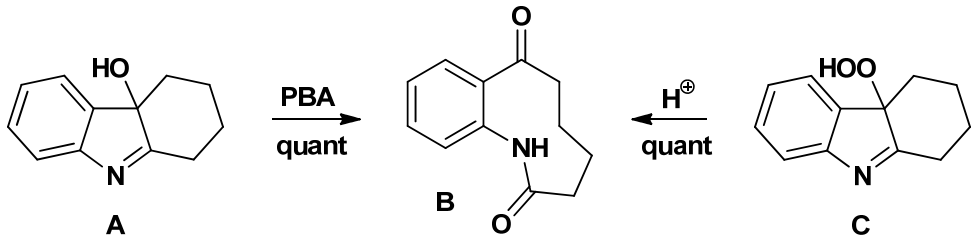

66. a) J. English, Jr., F. W. Brutcher, Jr., *J. Am. Chem. Soc.* **1952**, *74*, 4279-4282; b) H. E. Zimmerman, J. English, Jr., *J. Am. Chem. Soc.* **1954**, *76*, 2285-2290; c) H. E. Zimmerman, J. English, Jr., *J. Am. Chem. Soc.* **1954**, *76*, 2291-2294; d) H. E. Zimmerman, J. English, Jr., *J. Am. Chem. Soc.* **1954**, *76*, 2294-2300.

67. R. B. Clayton, H. B. Henbest, *Chem. and Ind.* **1953**, 1315-1316.

68. R. B. Clayton, H. B. Henbest, M. Smith, *J. Chem. Soc.* **1957**, 1982-1993.

69. J. English, Jr., A. D. Bliss, *J. Am. Chem. Soc.* **1956**, *78*, 4057-4060.

70. R. R. Burford, F. R. Hewgill, P. R. Jefferies, *J. Chem. Soc.* **1957**, 2937-2942.

71. C. A. Grob, W. Baumann, *Helv. Chim. Acta* **1955**, *38*, 594-610.

72. Eschenmoser's work (references 1 and 2) seems to have been overlooked by many in the early days of fragmenation.

73. Grob's definition of heterolytic fragmentation (below) was broadly interpreted. In later work Grob did not refer to it (e.g. reference 8a). Decarboxylative eliminations, retro-Michael, retro-aldol, and retro-Mannich processes are sometimes described as fragmentations.

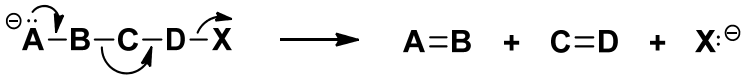

74. G. Stork, H. K. Landesman, *J. Am. Chem. Soc.* **1956**, *78*, 5129-5130.

75. P. S. Wharton, *J. Org. Chem.* **1961**, *26*, 4781-4782.

76. P. S. Wharton, G. A. Hiegel, *J. Org. Chem.* **1965**, *30*, 3254-3257.

77. This nomenclature was originally proposed by Klyne and Prelog, see: W. Klyne, V. Prelog, *Experientia* **1960**, *16*, 521-523.

78. P. S. Wharton, Y. Sumi, R. A. Kretchmer, *J. Org. Chem.* **1965**, *30*, 234-237.

79. For other early examples of Wharton fragmentation, refer to Caine's review (reference 8f , above).

80. C. A. Grob, F. Ostermayer, *Helv. Chim. Acta* **1962**, *45*, 1119-1132.

81. C. A. Grob, H. R. Kiefer, H. Lutz, H. Wilkens, *Tetrahedron Lett.* **1964**, *5*, 2901-2904.

82. W. J. le Noble, H. Guggisberg, T. Asano, L. Cho, C. A. Grob, *J. Am. Chem. Soc.* **1976**, *98*, 920-924.

83. For more discussions by Grob, refer to: a) C. A. Grob, *Experientia* **1957**, *13*, 126-129; b) C. A. Grob, in *Theoretical Organic Chemistry* (Kekulé Symposium, London, 1958), Butterworths, London, **1959**, pp. 114-126; c) C. A. Grob, *Bull. Soc. Chim. Fr.* **1960**, *27*, 1360-1365; d) C. A. Grob, *Gazz. Chim. Ital.* **1962**, *92*, 902-915.

84. As early as 1968, the term "Grob-type" fragmentation appeared in the literature (L. I. Peterson, R. B. Hager, A. F. Vellturo, G. W. Griffin, *J. Org. Chem.* **1968**, *33*, 1018-1021) and eventually came into common usage. Grob's obituary article (P. Schiess, *Angew. Chem. Int. Ed.* **2004**, *43*, 4392) errantly states that C-C fragmentation "entered textbooks under the name of its discoverer."

85. a) E. J. Corey, R. B. Mitra, H. Uda, *J. Am. Chem. Soc.* **1963**, *85*, 362-363; b) E. J. Corey, R. B. Mitra, H. Uda, *J. Am. Chem. Soc.* **1964**, *86*, 485-492.

86. Described in a footnote (#22) on p. 487 of reference 85b.

87. a) M. Tanabe, D. F. Crowe, *Tetrahedron Lett.* **1964**, *5*, 2955-2958; b) M. Tanabe, D. F. Crowe, *J. Org. Chem.* **1965**, *30*, 2776-2779.

88. J. A. Marshall, C. J. V. Scanio, *J. Org. Chem.* **1965**, *30*, 3019-3023.

89. J. A. Marshall, C. J. V. Scanio, W. J. Iburg, *J. Org. Chem.* **1967**, *32*, 3750-3754.

90. J. A. Marshall, G. L. Bundy, *J. Am. Chem. Soc.* **1966**, *88*, 4291-4292.

91. For a detailed account of the early development of this reaction, refer to Marshall's review (reference 8d, above).

92. J. A. Marshall, J. L. Belletire, *Tetrahedron Lett.* **1971**, *13*, 871-874.

93. J. A. Marshall, J. L. Belletire, *Synth. Comm.* **1971**, *1*, 93-97.

94. J. M. Brown, T. M. Cresp, L. N. Mander, *J. Org. Chem.* **1977**, *42*, 3984-3986.

95. R. Zurflüh, E. N. Wall, J. B. Siddall, J. A. Edwards, *J. Am. Chem. Soc.* **1968**, *90*, 6224-6225.

96. D. Sternbach, M. Shibuya, F. Jaisli, M. Bonetti, A. Eschenmoser, *Angew. Chem. Int. Ed. Engl.* **1979**, *18*, 634-635.

97. M. Shibuya, F. Jaisli, A. Eschenmoser, *Angew. Chem. Int. Ed. Engl.* **1979**, *18*, 636-637.

98. R. M. Wilson, S. J. Danishefsky, *J. Org. Chem.* **2007**, *72*, 4293-4305.

99. M. Kirihara, K. Niimi, T. Momose, *Chem. Commun.* **1997**, 599-600.

100. M. S. Laxmisha, G. S. R. Subba Rao, *Tetrahedron Lett.* **2000**, *41*, 3759-3761.

101. Z. Tokić-Vujošević, Ž. Čeković, *Synthesis* **2001**, *13*, 2028-2034.

102. A. G. Martínez, E. T. Vilar, A. G. Fraile, S. M. Cerero, B. L. Maroto, *Tetrahedron*

2004, *60*, 9447-9451.

103. For other recent examples of Beckmann fragmentation, see reference 8h (above).

104. P. von Zezschwitz, F. Petry, A. de Meijere, *Chem. Eur. J.* **2001**, *7*, 4035-4046.

105. a) S. Kamijo, G. B. Dudley, *J. Am. Chem. Soc.* **2005**, *127*, 5028-5029; b) S. Kamijo, G. B. Dudley, *J. Am. Chem. Soc.* **2006**, *128*, 6499-6507; c) S. Kamijo, G. B. Dudley, *Org. Lett.* **2006**, *8*, 175-177; d) D. M. Jones, M. P. Lisboa, S. Kamijo, G. B. Dudley, *J. Org. Chem.* **2010**, *75*, 3260-3267.

106. J. Tummatorn, G. B. Dudley, *Org. Lett.* **2011**, *13*, 158-160.

107. S. Kamijo, G. B. Dudley, *Tetrahedron Lett.* **2006**, *47*, 5629-5632.

108. a) C. Draghici, M. Brewer, *J. Am. Chem. Soc.* **2008**, *130*, 3766-3767; b) A. Bayir, C. Draghici, M. Brewer, *J. Org. Chem.* **2010**, *75*, 296-302.

109. N. P. Tsvetkov, A. Bayir, S. Schneider, M. Brewer, *Org. Lett.* **2012**, *14*, 264-267.

110. J. A. Murphy, M. Mahesh, G. McPheators, R. V. Anand, T. M. McGuire, R. Carling, A. R. Kennedy, *Org. Lett.* **2007**, *9*, 3233-3236.

111. a) D. H. R. Barton, M. J. Day, R. H. Hesse, M. M. Pechet, *J. Chem. Soc. D* **1971**, 945-946; b) Y. Zeng, B. T. Smith, J. Hershberger, J. Aubé, *J. Org. Chem.* **2003**, *68*, 8065-8067.

112. J. Hierold, A. Gray-Weale, D. W. Lupton, *Chem. Commun.* **2010**, *46*, 6789-6791.

113. J. Hierold, T. Hsia, D. W. Lupton, *Org. Biomol. Chem.* **2011**, *9*, 783-792.

114. G. Mehta, N. Mohal, *Tetrahedron Lett.* **1999**, *40*, 5791-5794.

115. a) V. Prelog, K. Schenker, *Helv. Chim. Acta* **1952**, *35*, 2044-2053; b) M. A. Casadei, C. Galli, L. Mandolini, *J. Am. Chem. Soc.* **1984**, *106*, 1051-1056.

116. C. M. Amann, P. V. Fisher, M. L. Pugh, F. G. West, *J. Org. Chem.* **1998**, *63*, 2806-2807.

117. G. A. Molander, Y. Le Huérou, G. A. Brown, *J. Org. Chem.* **2001**, *66*, 4511-4516.

118. G. Barbe, M. St-Onge, A. B. Charette, *Org. Lett.* **2008**, *10*, 5497-5499.

119. G. Lemonnier, A. B. Charette, *J. Org. Chem.* **2012**, *77*, 5832-5837.

120. N. Risch, M. Langhals, W. Mikosch, H. Bögge, A. Müller, *J. Am. Chem. Soc.* **1991**,

113, 9411-9412.

121. O. Arjona, A. G. Csákÿ, M. C. Murcia, J. Plumet, *Helv. Chim. Acta* **2001**, *84*, 3667-3672.

122. N. Tada, K. Miyamoto, M. Ochiai, *Chem. Pharm. Bull.* **2004**, *52*, 1143-1144.

123. a) G. W. Kabalka, D. Tejedor, N.-S. Li, R. R. Malladi, S. Trotman, *J. Org. Chem.* **1998**, *63*, 6438-6439; b) G. W. Kabalka, N.-S. Li, D. Tejedor, R. R. Malladi, S. Trotman, *J. Org. Chem.* **1999**, *64*, 3157-3161.

124. J. Barluenga, M. Álvarez-Pérez, K. Wuerth, F. Rodríguez, F. J. Fañanás, *Org. Lett.* **2003**, *5*, 905-908.

125. J. Boivin, J. Pothier, L. Ramos, S. Z. Zard, *Tetrahedron Lett.* **1999**, *40*, 9239-9241.

126. M. Vamos, K. Ozboya, Y. Kobayashi, *Synlett* **2007**, 1595-1599.

127. W. Zhang, P. Dowd, *Tetrahedron Lett.* **1996**, *37*, 957-960.

128. D. S. Stojanova, M. Hesse, *Helv. Chim. Acta* **1995**, *78*, 925-934.

129. M. E. Jung, P. Davidov, *Org. Lett.* **2001**, *3*, 627-629.

130. W. Adam, R. Stössel, A. Treiber, *J. Org. Chem.* **1995**, *60*, 2879-2884.

131. T. Yamamoto, H. Suemune, K. Sakai, *Tetrahedron* **1991**, *47*, 8523-8528.

132. M. D. Giacomo, R. M. Bettolo, R. Scarpelli, *Tetrahedron Lett.* **1997**, *38*, 3469-3470.

133. M. Mori, M. Kimura, Y. Takahashi, Y. Tamaru, *Chem. Commun.* **2006**, 4303-4305.

134. K. Vyakaranam, S. Körbe, H. Divišová, J. Michl, *J. Am. Chem. Soc.* **2004**, *126*, 15795-15801.

135. G. Li, Y. Liu, *J. Org. Chem.* **2010**, *75*, 3526-3528.

136. The systems that were used to model these complex fragmentations are described in the cited references and are not summarized here.

137. a) A. S. K. Hashmi, in *Modern Allene Chemistry*, Vol. 1 (Eds: N. Krause, A. S. K. Hashmi), Wiley-VCH Verlag, Weinheim, **2004**, pp. 3-36; b) S. Ma, in *Modern Allene Chemistry*, Vol. 2 (Eds: N. Krause, A. S. K. Hashmi), Wiley-VCH Verlag, Weinheim, **2004**, pp. 595-684; c) H. Kim, L. J. Williams, *Curr. Opin. Drug Discovery Dev.* **2008**, *11*, 870-894.

138. a) E.-i. Negishi, A. O. King, W. L. Klima, W. Patterson, A. Silveira, Jr., *J. Org. Chem.* **1980**, *45*, 2526-2528; b) E.-i. Negishi, A. O. King, J. M. Tour, *Org. Synth.* **1986**, *64*, 44-47; c) E. Torres, G. L. Larson, G. J. McGarvey, *Tetrahedron Lett.* **1988**, *29*, 1355-1358; d) K. M. Brummond, E. A. Dingess, J. L. Kent, *J. Org. Chem.* **1996**, *61*, 6096-6097; e) K. M. Brummond, H. Wan, J. L. Kent, *J. Org. Chem.* **1998**, *63*, 6535-6545; f) X. Pu, J. M. Ready, *J. Am. Chem. Soc.* **2008**, *130*, 10874-10875; g) P. Maity, S. D. Lepore, *J. Org. Chem.* **2009**, *74*, 158-162.

139. M. Sugai, K. Tanino, I. Kuwajima, *Synlett* **1997**, 461-462.

140. R. V. Kolakowski, M. Manpadi, Y. Zhang, T. J. Emge, L. J. Williams, *J. Am. Chem. Soc.* **2009**, *131*, 12910-12911.

141. In the original publication the stereospecifically generated allenes are rendered incorrectly.

142. D. Xu, M. A. Drahl, L. J. Williams, *Beilstein J. Org. Chem.* **2011**, *7*, 937-943.

143. T. Saget, N. Cramer, *Angew. Chem. Int. Ed.* **2010**, *49*, 8962-8965.

144. L. Cao, J. Sun, X. Wang, R. Zhu, H. Shi, Y. Hu, *Tetrahedron* **2007**, *63*, 5036-5041.

145. L. N. Mander, M. M. McLachlan, *J. Am. Chem. Soc.* **2003**, *125*, 2400-2401.

146. D. M. Jones, S. Kamijo, G. B. Dudley, *Synlett* **2006**, 936.

147. D. M. Jones, G. B. Dudley, *Synlett* **2010**, 223.

148. a) A. Krief, D. Surleraux, H. Frauenrath, *Tetrahedron Lett.* **1988**, *29*, 6157-6160; b) A. Krief, D. Surleraux, *Synlett* **1991**, 273-275; c) A. Krief, D. Surleraux, N. Ropson, *Tetrahedron: Asymm.* **1993**, *4*, 289-292.

149. Y. M. A. W. Lamers, G. Rusu, J. B. P. A. Wijnberg, A. de Groot, *Tetrahedron* **2003**, *59*, 9361-9369.

150. H. Koshimizu, T. Baba, T. Yoshimitsu, H. Nagaoka, *Tetrahedron Lett.* **1999**, *40*, 2777-2780.

151. X.-S. Peng, H. N. C. Wong, *Chem. Asian. J.* **2006**, *1*, 111-120.

152. K. Kim, J. K. Cha, *Angew. Chem. Int. Ed.* **2009**, *48*, 5334-5336.

153. a) K. Prantz, J. Mulzer, *Angew. Chem. Int. Ed.* **2009**, *48*, 5030-5033; b) K. Prantz, J. Mulzer, *Chem. Eur. J.* **2010**, *16*, 485-506.

154. G. Lemonnier, A. B. Charette, *J. Org. Chem.* **2010**, *75*, 7465-7467.

155. R. Villagómez-Ibarra, C. Alvarez-Cisneros, P. Joseph-Nathan, *Tetrahedron* **1995**, *51*, 9285-9300.

156. T. Yoshimitsu, M. Yanagiya, H. Nagaoka, *Tetrahedron Lett.* **1999**, *40*, 5215-5218.

157. J. T. Njardarson, J. L. Wood, *Org. Lett.* **2001**, *3*, 2431-2434.

158. a) L. A. Paquette, S. Nakatani, T. M. Zydowsky, S. D. Edmondson, L.-Q. Sun, R. Skerlj, *J. Org. Chem.* **1999**, *64*, 3244-3254; b) L. A. Paquette, S. D. Edmondson, N. Monck, R. D. Rogers, *J. Org. Chem.* **1999**, *64*, 3255-3265.

159. L. A. Paquette, J. Yang, Y. O. Long, *J. Am. Chem. Soc.* **2002**, *124*, 6542-6543.

160. P. D. Thornton, D. J. Burnell, *Org. Lett.* **2006**, *8*, 3195-3198.

161. D. Renneberg, H. Pfander, C. J. Leumann, *J. Org. Chem.* **2000**, *65*, 9069-9079.

162. O. L. Larionov, E. J. Corey, *J. Am. Chem. Soc.* **2008**, *130*, 2954-2955.

163. A. Ivkovic, R. Matovic, R. N. Saicic, *Org. Lett.* **2004**, *6*, 1221-1224.

164. S. V. Ley, A. Antonello, E. P. Balskus, D. T. Booth, S. B. Christensen, E. Cleator, H. Gold, K. Högenauer, U. Hünger, R. M. Myers, S. F. Oliver, O. Simic, M. D. Smith, H. Søhoel, A. J. A. Woolford, *Proc. Natl. Acad. Sci. USA* **2004**, *101*, 12073-12078.

165. J. D. Winkler, K. J. Quinn, C. H. MacKinnon, S. D. Hiscock, E. C. McLaughlin, *Org. Lett.* **2003**, *5*, 1805-1808.

166. R. A. Holton, C. Somoza, H.-B. Kim, F. Liang, R. J. Biediger, P. D. Boatman, M. Shindo, C. C. Smith, S. Kim, H. Nadizadeh, Y. Suzuki, C. Tao, P. Vu, S. Tang, P. Zhang, K. K. Murthi, L. N. Gentile, J. H. Liu, *J. Am. Chem. Soc.* **1994**, *116*, 1597-1598.

167. R. A. Holton, R. M. Kennedy, *Tetrahedron Lett.* **1984**, *25*, 4455-4458.

168. a) P. A. Wender, N. F. Badham, S. P. Conway, P. E. Floreancig, T. E. Glass, C. Gränicher, J. B. Houze, J. Jänichen, D. Lee, D. G. Marquess, P. L. McGrane, W. Meng, T. P. Mucciaro, M. Mühlebach, M. G. Natchus, H. Paulsen, D. B. Rawlins, J. Satkofsky, A. J. Shuker, J. C. Sutton, R. E. Taylor, K. Tomooka, *J. Am. Chem. Soc.* **1997**, *119*, 2755-2756; b) P. A. Wender, N. F. Badham, S. P. Conway, P. E. Floreancig, T. E. Glass, J. B. Houze, N. E. Krauss, D. Lee, D. G. Marquess, P. L. McGrane, W. Meng, M. G. Natchus, A. J. Shuker, J. C. Sutton, R. E. Taylor, *J. Am. Chem. Soc.* **1997**, *119*, 2757-2758.

169. a) P. A. Wender, T. P. Mucciaro, *J. Am. Chem. Soc.* **1992**, *114*, 5878-5879; b) B. Kerkar, D. D. Khac, M. Fétizon, F. Guir, *Tetrahedron Lett.* **1997**, *38*, 3223-3226.

170. T. J. Maimone, A.-F. Voica, P. S. Baran, *Angew. Chem. Int. Ed.* **2008**, *47*, 3054-3056.

171. T. J. Maimone, J. Shi, S. Ashida, P. S. Baran, *J. Am. Chem. Soc.* **2009**, *131*, 17066-17067.

172. Q. Xiong, W. K. Wilson, S. P. T. Matsuda, *Angew. Chem. Int. Ed.* **2006**, *45*, 1285-1288.

Chapter II

First Generation Studies: Selective Conversion of an Enantioenriched Cyclononadienone to the Xeniolide, Xenibellol, and Florlide Cores

2.1 Introduction

Complex molecule synthesis remains the foremost challenge for synthetic organic chemists. As the targets, technologies, and societal demands have evolved over the past century, so too have synthetic strategies, each with its own benefits and drawbacks. Biomimetic synthesis began with Robinson's one-step synthesis of tropinone in 1917.[1] While it is elegant chemistry, biomimetic synthesis can be unselective and low-yielding. Woodward ushered in the modern era of total synthesis in 1944 with the formal synthesis of quinine.[2] Throughout the 1940s and 1950s, the father of natural product synthesis placed a great emphasis on understanding the reactivity of each intermediate. Since the 1960s, Corey's principles of retrosynthetic analysis have guided the field in the synthesis of individual targets.[3] This strategy is still the standard, but how much new chemical knowledge can be gained from it? During his prostaglandin work in 1969, Corey also anticipated the idea of diverted total synthesis (DTS).[4] This strategy may suffer from long routes and limited flexibility. Since the beginning of this millennium, Schreiber has advocated for diversity-oriented synthesis (DOS) to find bioactive molecules faster.[5] The randomness of this method, however, limits the ability to identify bioactive structure space.

Natural product-inspired diversity-oriented synthesis (NPI-DOS) also emerged in the 2000s and remains a popular strategy.[6]

In 2009 our lab introduced the concept of integrated routing. The strategy is to access multiple related sectors of complex semi-validated structure space (i.e. different core structures within a superfamily of bioactive natural products) through selective reaction pathways from a single common intermediate accessible via a concise route. It can be thought of as a combination of DTS and NPI-DOS. The origins of the integrated routing concept are traceable in Fieser's bile acid series.[7] In this study, Fieser obtained several minor products from divergent reactions of a common steroid intermediate. He then optimized the reaction conditions to each product.

Figure II.1 illustrates the conceptual differences between retrosynthetic analysis and the integrated routing strategy. Conventional retrosynthetic analysis generates designed routes that are usually reliable in the final stages of the synthesis. Since the speculative reactions are conducted on simpler starting materials, the opportunities to learn new chemical reactivity are limited. Conversely, the integrated routing strategy invokes high-risk proposals in the latter stages of total synthesis. Even if a natural product is unattainable via this strategy, the creative reaction conditions will likely lead to new discoveries and analogues valuable in their own right.

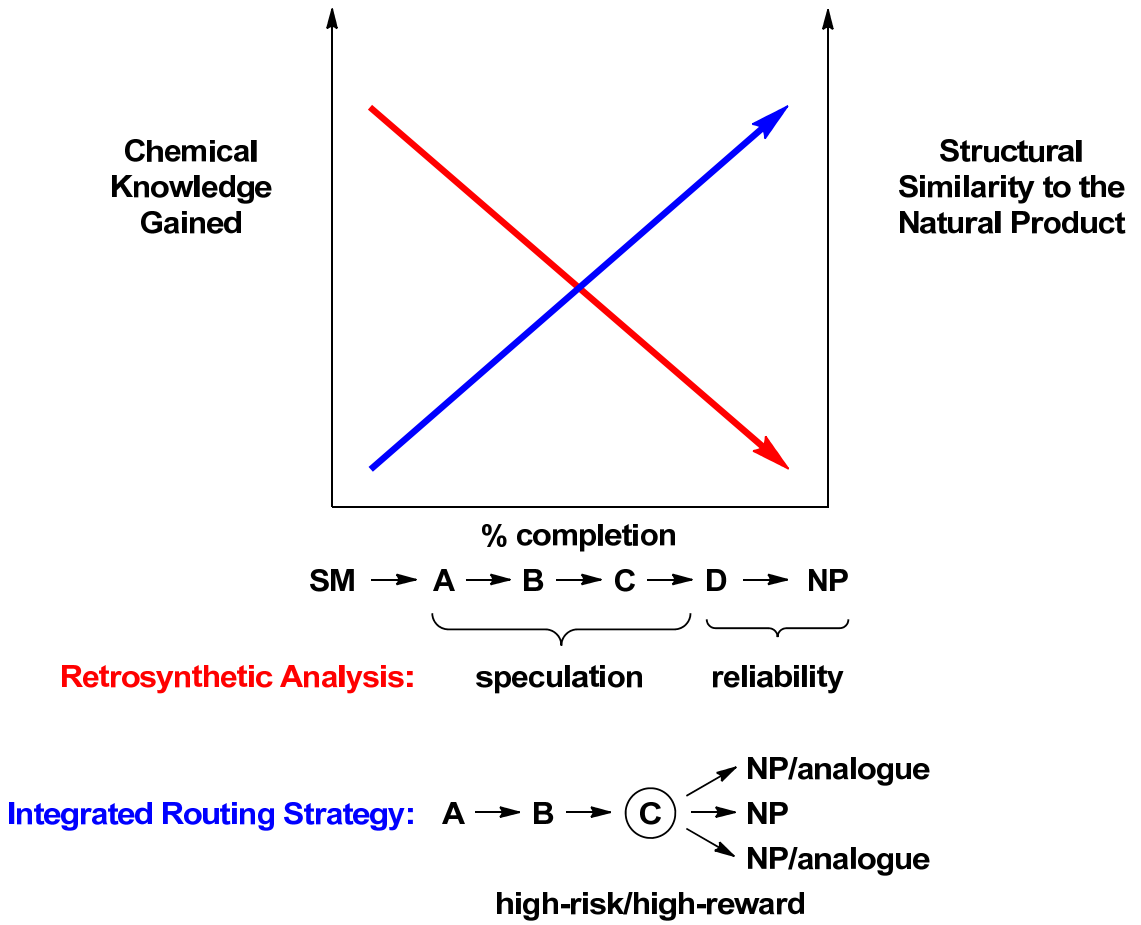

Figure II.1 Retrosynthetic analysis vs. integrated routing strategy.

2.2 Xenicane Diterpenoids

Diterpenes of the extended xenicane family represent a combination of structural complexity, structural novelty, and biological potency that warrants closer scrutiny. However, these marine natural products are not readily available in sufficient quantities to allow detailed analysis. Our strategy is to develop a short chemical synthesis to a molecule-type that contains functionality that can be called upon to react along disparate pathways. Such a strategy integrates the routes to multiple targets and thereby allows efficient access – especially in terms of step economy – to large, varied sets of bioactive compounds, including natural products and molecularly edited

congeners. Here we report the conversion of an enantioenriched cyclononadienone (**2.1**, Scheme II.1) to a simplified model xeniolide epoxide (**2.2**) and its subsequent selective conversion to the core frameworks of the xenibellols (**2.3**) and florlides (**2.4**).

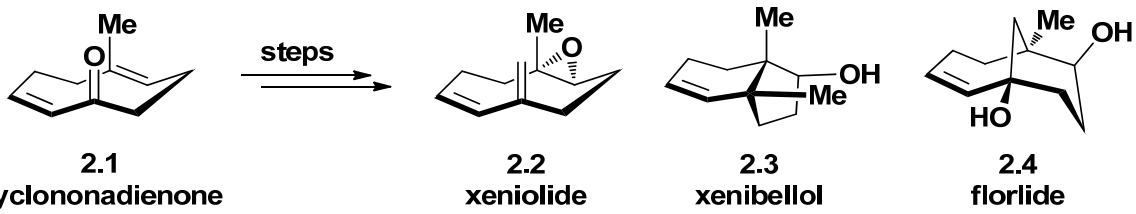

2.1 cyclononadienone **2.2** xeniolide **2.3** xenibellol **2.4** florlide

Scheme II.1 Integrated route to three xenicane diterpenoid cores.

Xenicane metabolites closely related to these families have been identified by bioassay-guided isolation,[8,9] and little is known of their biological properties other than the insight provided by the initial isolation screen. The heterogeneity of the assays prevents meaningful functional comparisons to be made between xenicane family members, despite elements of high structural homology within and among certain families (e.g. **2.5**-**2.7**, Figure II.2). Many of the discovery assays were designed to screen for anticancer,[8a-h] antibiotic,[8i] antifungal,[8j] or anti-HIV[8k] activity, and some screened for ichthyotoxicity,[8l] elastase release,[8m] or superoxide release.[8n] Our attention, however, was captivated by reports of Bak- and Bax-dependent induction of apoptosis in epithelial cancer cells by new isolates of the xeniolide class.[8h]

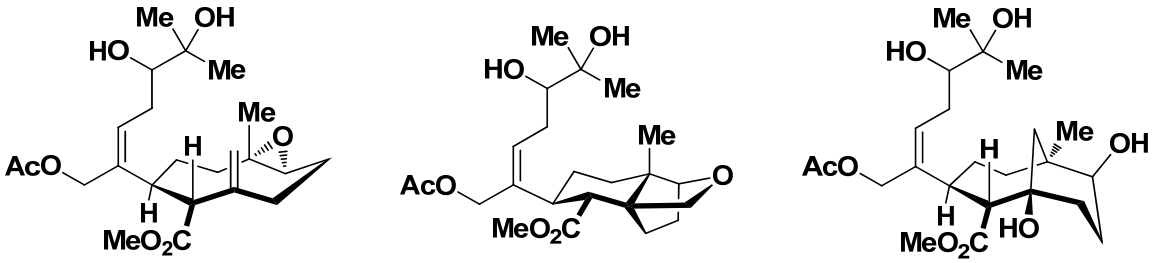

Figure II.2 Xenicanes from the soft coral *Xenia umbellata*.[8g]

The xenicanes vary in oxidation state and connectivity of their core structures, as well as their side chains and fused ring appendages. The distinguishing structural features of the xeniolides (e.g. **2.5**) are a nine membered ring, a *trans*-trisubstituted olefin or the corresponding epoxide, and a vicinal triad composed of two side chains and an *exo*-methylene. The xenibellols (carbon core featured in **2.6**) lack the *exo*-methylene and the *trans*-trisubstituted olefin. Instead, these are replaced by a 6-5 ring fusion that houses a vicinal quaternary moiety. The florlides (e.g. **2.7**) contain connectivity isomeric to the xenibellols. The methylene serves to bridge the nine membered ring and thereby establishes a [4.3.1]-bicycle. These core differences aside, there is considerable homology in the structure of the xeniolides, xenibellols, and florlides, especially in the side chains.[10]

Excluding xeniaphyllanes,[11] there appear to be only five total syntheses of xenicane diterpenes (Figure II.3),[12] even though over one hundred natural products in this superfamily have been reported to date. Nevertheless, these and related synthetic studies[13] provide much-needed insight into the complex structure and reactivity of these compounds and indicate that such targets pose substantive synthetic challenges. For

example, a xenibellol model was recently prepared by Danishefsky and co-workers (Scheme II.2).[14] In that study, the stepwise installation of the vicinal quaternary motif of the target proved troublesome.

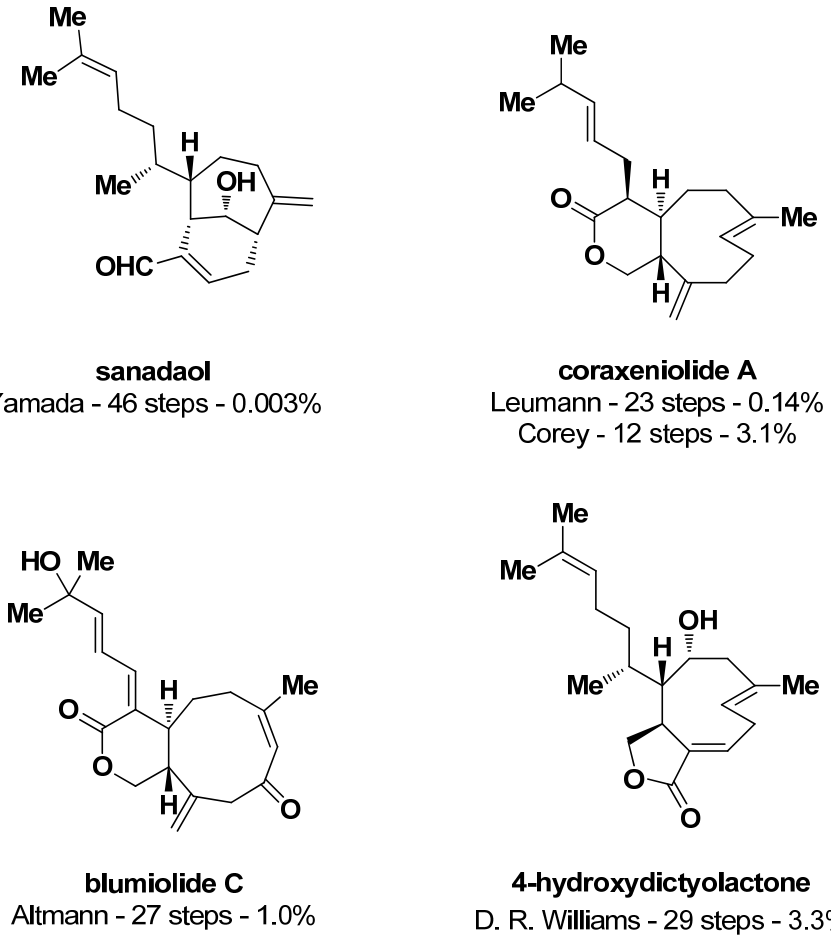

Figure II.3 Published xenicane total syntheses (excluding xeniaphyllanes).[12]

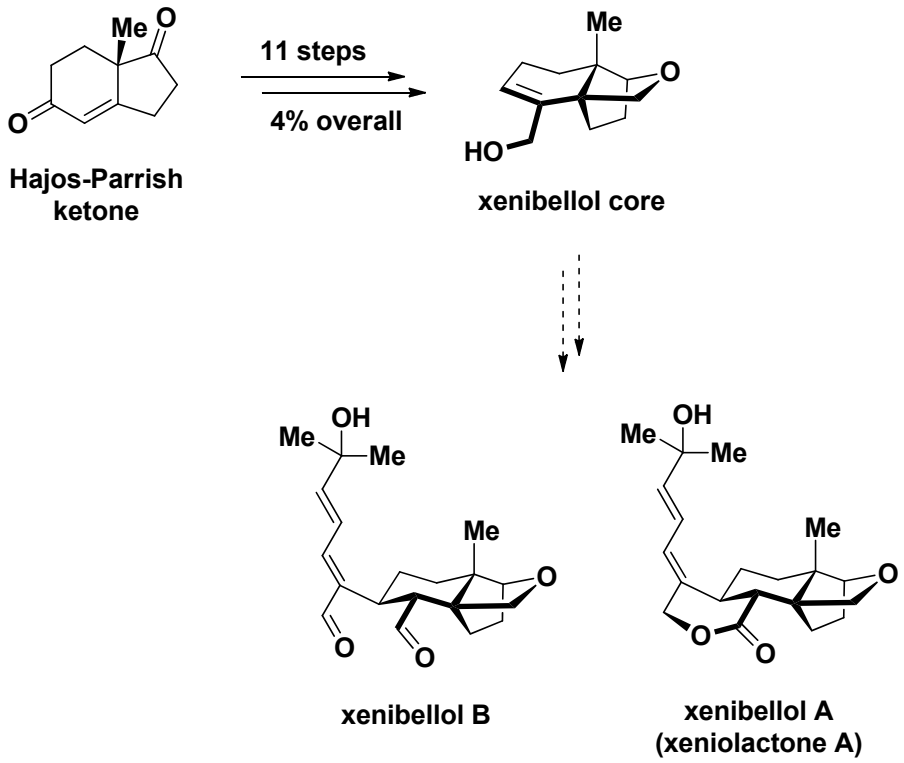

Scheme II.2 Danishefsky's xenibellol core synthesis.[14]

2.3 First Generation Synthetic Studies Towards Xenicanes

We have focused on dissymmetric scaffolds as potential platforms for an integrated routing strategy to access these terpene natural products. Recently, my colleague Dr. Yue Zhang reported the synthesis, reactivity, and racemization kinetics of dissymmetric cyclononadienone **2.1**.[15] In contrast to *trans*-cyclononene (**2.8**, $t_{1/2}$ = 6 s, 25 °C),[16] cyclononadienone **2.1** undergoes slow racemization by conformational interconversion (**2.1** → ***ent*-2.1**, $t_{1/2}$ = 32 h, 23 °C). The precursor **2.9** was prepared in highly enantioenriched form from the Hajos-Parrish ketone (Scheme II.3).[12c,15] C-C fragmentation of **2.9** provided **2.1** in 87% *ee* after column chromatography, as determined by chiral HPLC, whereas epoxidation of crude **2.1** gave **2.10** in 90% *ee* (Scheme II.4). Thus, **2.9** was converted to predominantly a single atropisomer of **2.1**,

which was subsequently converted to highly enantioenriched nine-membered ring derivatives.[15] The substantially lower rate of racemization of **2.1** compared to **2.8** is presumably due to increased Prelog (transannular) strain in the transition structures required for conformational interconversion.

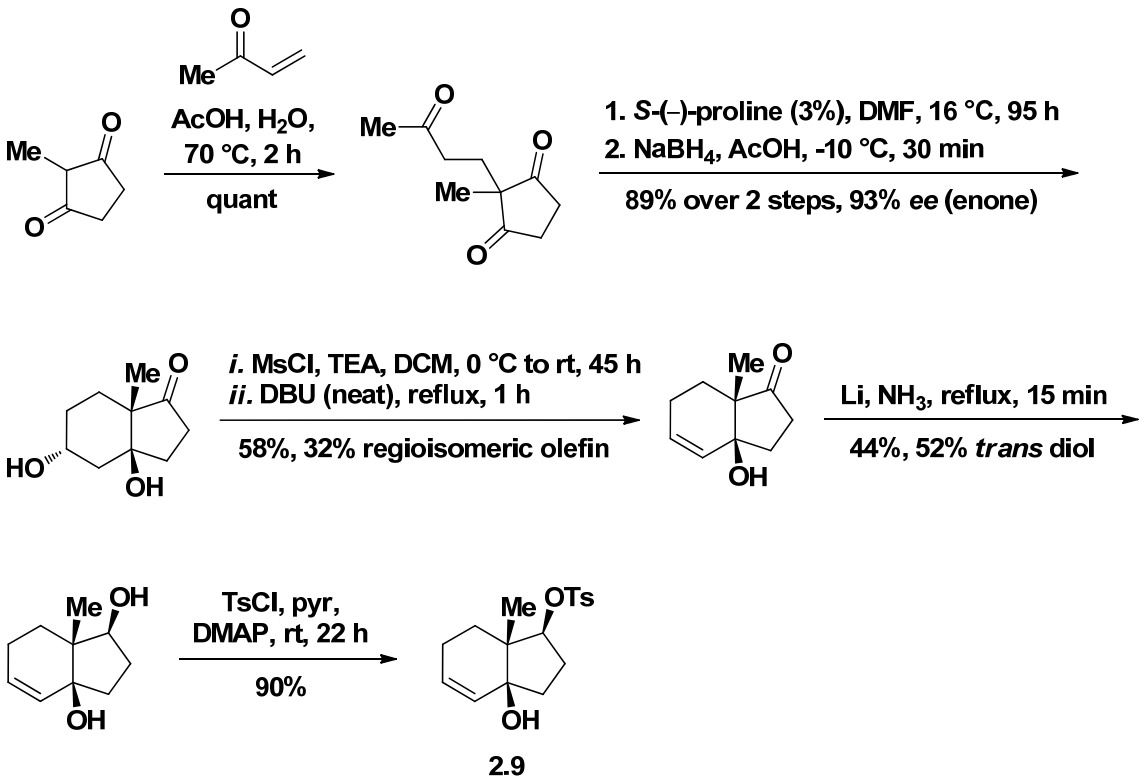

Scheme II.3 Enantioselective synthesis of the C-C fragmentation precursor.[15]

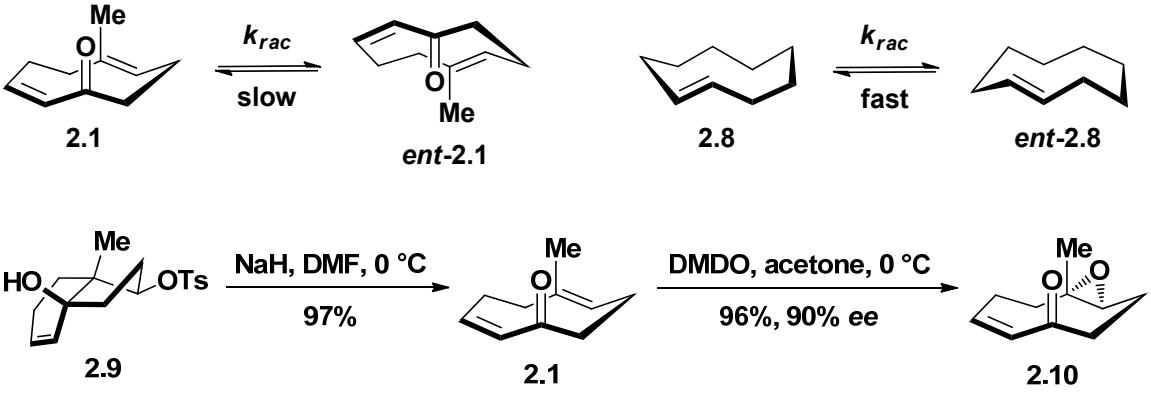

Scheme II.4 Retardation of racemization rates permits stereoselective synthesis.[15]

2.4 Integrated Routing Strategy

To develop an integrated route, we aimed to prepare epoxide **2.2** from **2.1**, and to explore the conversion of **2.2** to the xenibellol and florlide cores (**2.2** → **2.3**/**2.4**, Scheme II.5). The conversion of epoxide **2.10** to **2.2** by direct olefination proved problematic. Attempted Wittig and Tebbe olefination reactions gave complex product mixtures that did not include the desired *exo*-olefin. The alternative sequence, olefination of **2.1** followed by epoxidation, proved successful (Scheme II.6). Surprisingly, application of standard conditions for workup and purification, as well as storage of **2.11** at room temperature, produced near-racemic **2.2**. Moreover, cyclononatriene **2.11** was found to be volatile. This hydrocarbon was expected to racemize more slowly than the parent enone, since the steric bulk of the *exo*-methylene substituent in **2.11**, relative to the carbonyl of **2.1**, was expected to increase the barriers associated with conformational interconversion. Computational modeling[17] suggests that the carbon framework of **2.11** is less rigid than **2.1**. The ground state torsion angle of the bond that connects the two π systems (-C=CH-C(=X)-) increases from 53° in **2.1** (X = O) to 65° in **2.11** (X = CH_2). This is not attributable to steric congestion caused by the *exo*-methylene. Instead, loss of carbonyl-induced polarization appears to relax the geometric constraints. The loss of rigidity in the cyclic framework of **2.11** may translate to a lower barrier for conformational interconversion/racemization as compared to **2.1**. Additionally, the reaction conditions, and perhaps transient species formed in the reaction of **2.1** to **2.11**, may be responsible for acceleration of racemization and deterioration of enantiomeric homogeneity.[18]

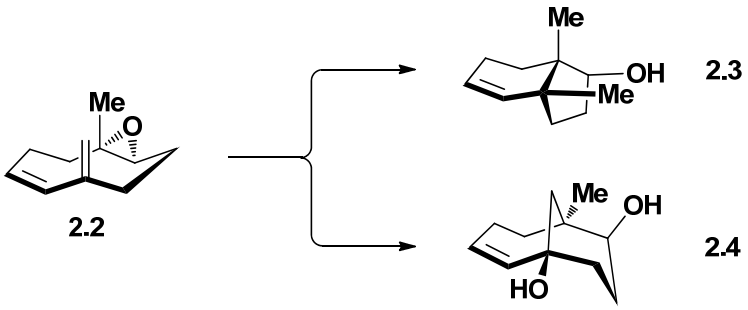

Scheme II.5 Epoxydiene 2.2: a possible gateway to disparate targets.

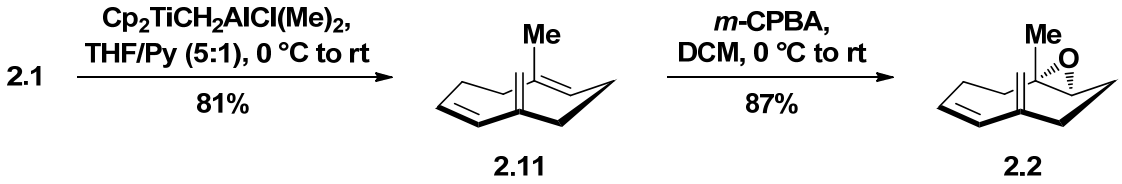

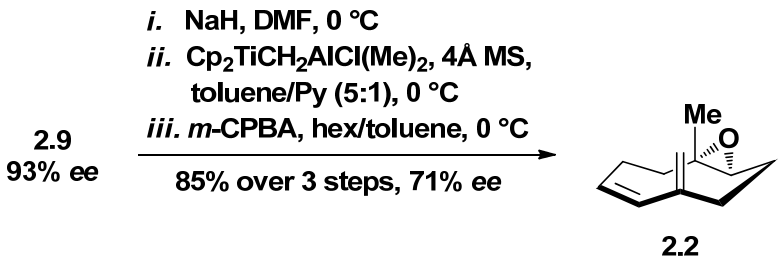

Scheme II.6 Preparation of racemic and enantioenriched epoxydiene 2.2.

In order to minimize racemization, the nine-membered ring was kept at or below 0 °C throughout processing from **2.9** to **2.2**. Under these conditions, smooth olefination of **2.1** was achieved, loss of volatile cyclononatriene **2.11** was minimized, and face-selective oxidative trapping of the trisubstituted olefin with *m*-CPBA furnished the model xeniolide epoxide **2.2** in 85% overall yield and 71% *ee*.[19]

Exposure of **2.2** to mild Ti(III) conditions,[20] using strictly dry and degassed solvent, smoothly established the vicinal all-carbon quaternary pattern characteristic of the xenibellol core (**2.3**, Scheme II.7). Routine NMR analysis of **2.3** established the

structure as shown. Thus, the desired *cis*-hydrindene was obtained in 46% yield as a single isomer. Presumably, single-electron reductive epoxide opening gives the tertiary radical, which initiates transannular cyclization, and this occurs preferentially in an *exo*-fashion. Subsequent radical trapping gives the observed product, e.g. by a second equivalent of Ti(III) followed by proteodemetalation. Trapping the primary radical with freshly sublimed iodine was attempted but not observed.[21] It is known that such radicals are highly reactive and are readily reduced by solvent.[22]

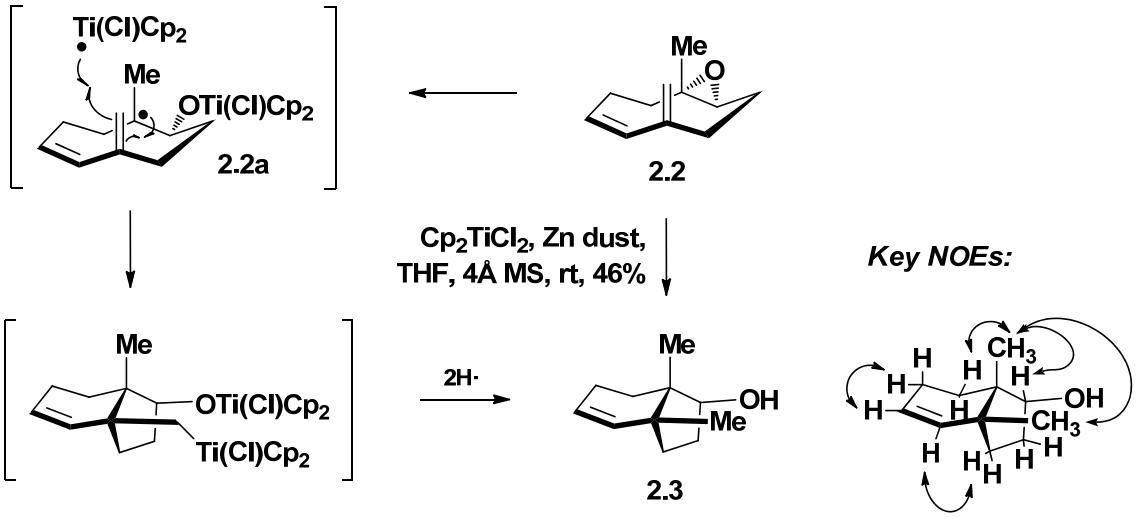

Scheme II.7 Radical-induced transannulation to xenibellol core 2.3.

In contrast to titanium (III)-induced conversion of **2.2** to xenibellol **2.3**, reaction of **2.2** with the Lewis acid $BF_3 \cdot Et_2O$ afforded the isomeric florlide core as a single isomer (→ **2.4**, 73% yield, Scheme II.8). Extensive NMR studies confirm the structural assignment of **2.4**. This transannular cyclization appears to favor an *endo*-type process (compare with **2.2** → **2.3**), and proceeds by way of the bridgehead carbocation.[23] Trapping with water then gives the desired **2.4**. Molecular modeling[17] suggests that the bridgehead carbocation is further stabilized by significant orbital overlap with the

adjacent olefin.

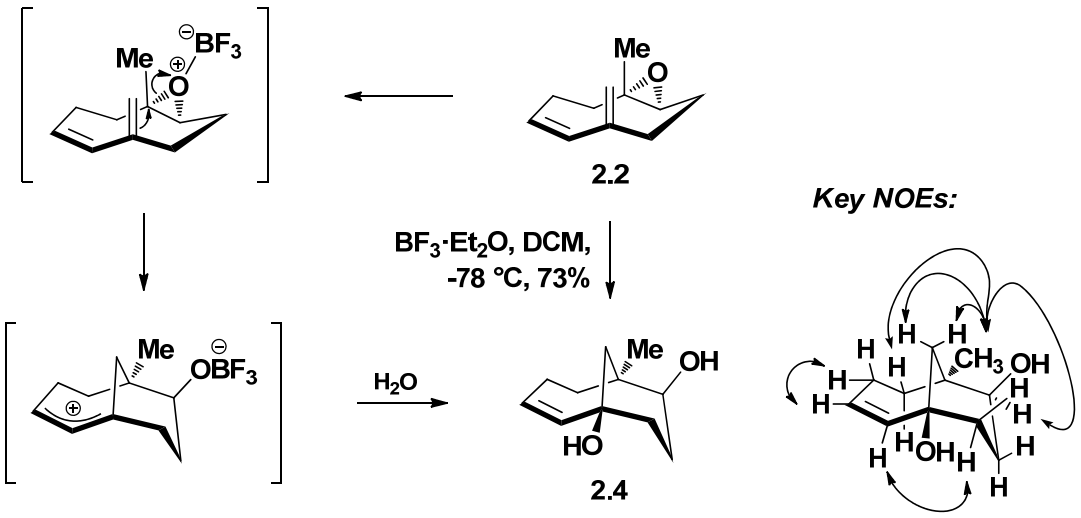

Scheme II.8 Carbocation-induced transannulation to florlide core 2.4.

These complementary transannular conversions differ significantly from earlier reports. Primary radicals produced by epoxyolefin cyclizations have been shown to lead to mixtures of *cis*- and *trans*-fused hydrindanes in related systems. For example, Cuerva and co-workers[24] recently reported the use of Cp_2TiCl on caryophyllene β-oxide under a variety of conditions. In contrast, the geometric constraints imposed by the C2-C3 double bond (xeniolide numbering) of putative intermediate **2.2a** (Scheme II.7) appear to selectively favor the formation of the *cis*-hydrindene. This mode – addition to the internal carbon of the butadiene moiety – is contrary to normal modes of radical addition that form allyl radical intermediates.[25] Barton and co-workers[26] were the first to describe carbocation-induced transannular reactions in the caryophyllene series. Other elegant transannular cationic sequences on related caryophyllene substrates are also known.[27]

2.5 Postulated Xenicane Biosynthesis

Xeniolide precursors are thought to give rise to at least eleven other distinct polycarbocyclic arrangements, including the xenibellol and florlide skeletons.[28] The biosyntheses still require clarification. Over thirty years ago, Fenical[28a] posited a provocative proposal that xenicane metabolites arise from an intramolecular anti-Markovnikoff electrophilic carbocyclization of geranylgeraniol pyrophosphate (GGPP, Scheme II.9). Faulkner[28b] later suggested that more complex marine natural products could be derived from xeniolide precursors via transannular carbocation cyclizations. Kashman[29] has proposed a mixed biogenesis via xeniaphyllanes (Scheme II.10). Although no biosynthetic studies have been reported for the xenicanes, the biosynthesis of caryophyllene is supported by Croteau and Gundy.[30] They demonstrated that an enzyme preparation obtained from leaves harvested from *Salvia officinalis* (sage) catalyzes the divalent metal-ion dependent cyclization of *trans*, *trans*-farnesyl pyrophosphate (FPP, Scheme II.11) to produce the sesquiterpene. Rationales that involve cationic intermediates have been put forth to account for the xenibellols.[8d,8e] Although these biosyntheses do not involve radicals, the transannular reactions of **2.2** → **2.3**/**2.4** may parallel the general features of the biosyntheses of these natural products.

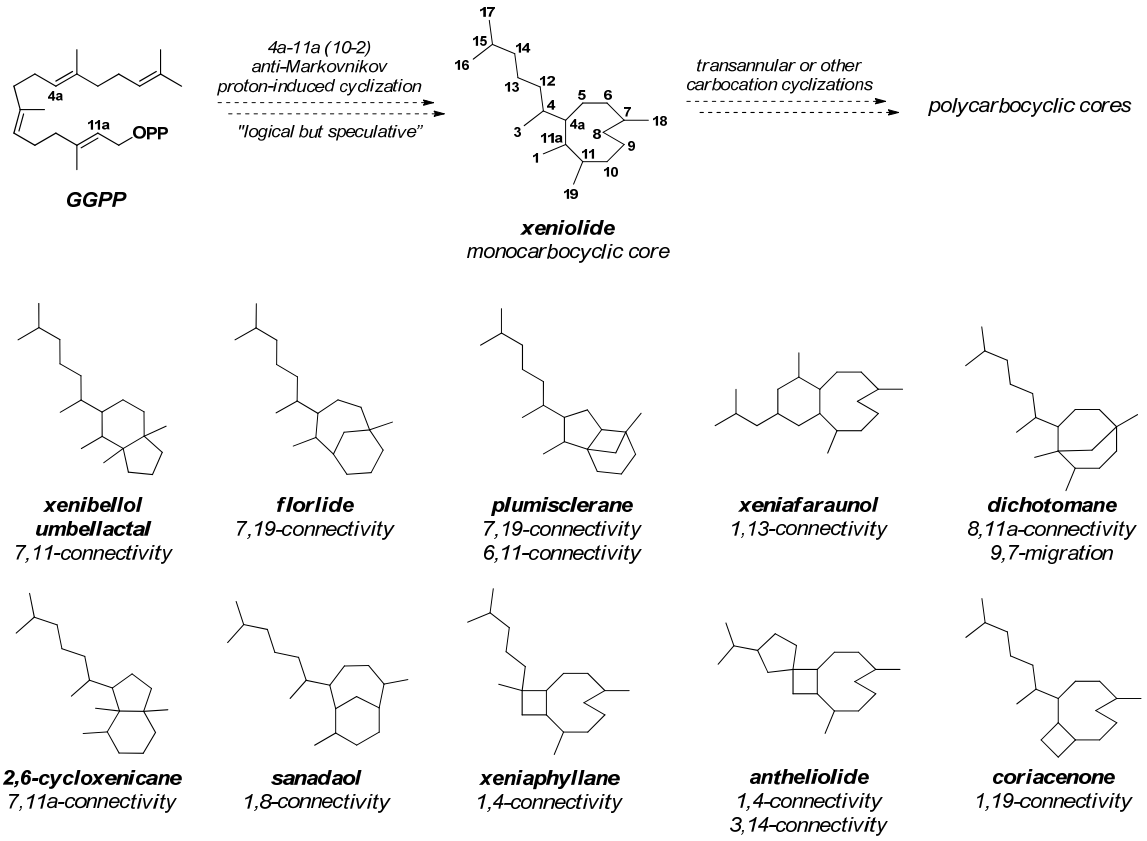

Scheme II.9 Fenical-Faulkner xenicane biogenesis proposal (skeletons shown, GGPP numbering in parentheses).[28]

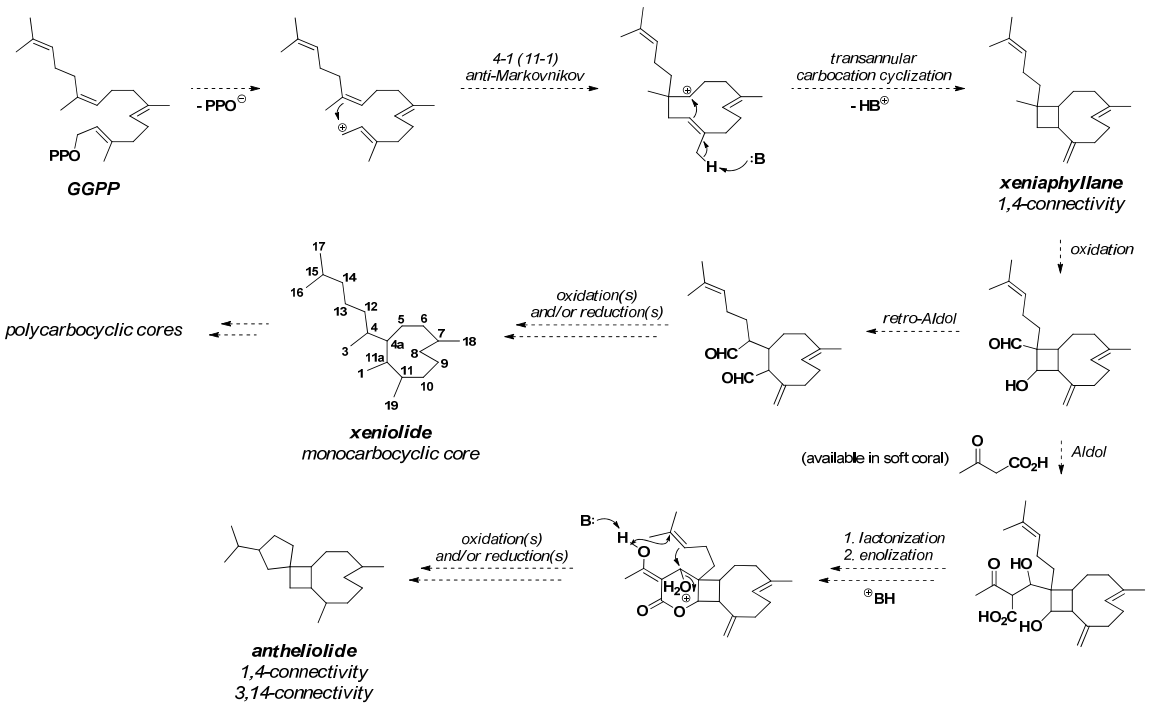

Scheme II.10 Kashman's proposal: mixed biogenesis via xeniaphyllanes (GGPP numbering in parentheses).[29]

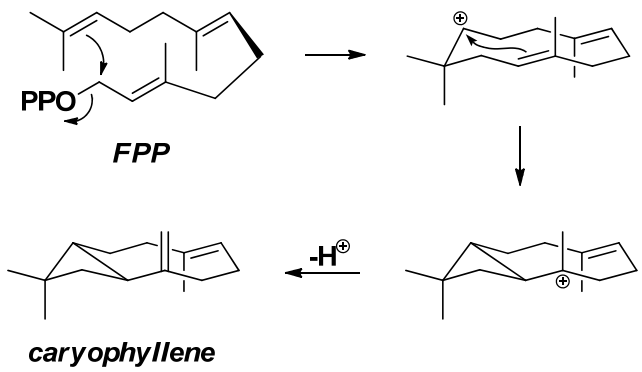

Scheme II.11 Biosynthesis of caryophyllene.[30]

2.6 Extended Work

Bredt's rule[31] does not forbid formation of a bridgehead olefin in bicyclo[4.3.1]decane systems (Scheme II.12); nevertheless, the synthesis of such alkenes is

often challenging.[32] Molecular dynamics calculations[17] on **2.4** (Scheme II.13) suggest that the bridgehead hydroxyl can achieve a 0˚ torsion angle with the vicinal β-proton, permitting a *syn* elimination to the umbellacin core though modeling suggests that the desired diene is very strained. To evaluate this hypothesis experimentally, **2.4** was differentially protected then treated with Burgess reagent under vigorous conditions. No reaction was observed. The sp^2-hybridized bridgehead carbon of a hypothetical saturated analogue, which more closely resembles the natural products, is closer to planarity and significantly less strained, so an elimination to such a product may be more facile.

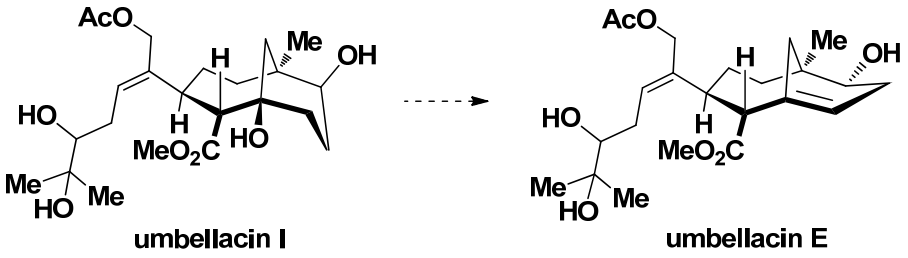

Scheme II.12 Bridgehead olefin formation: facile in nature?

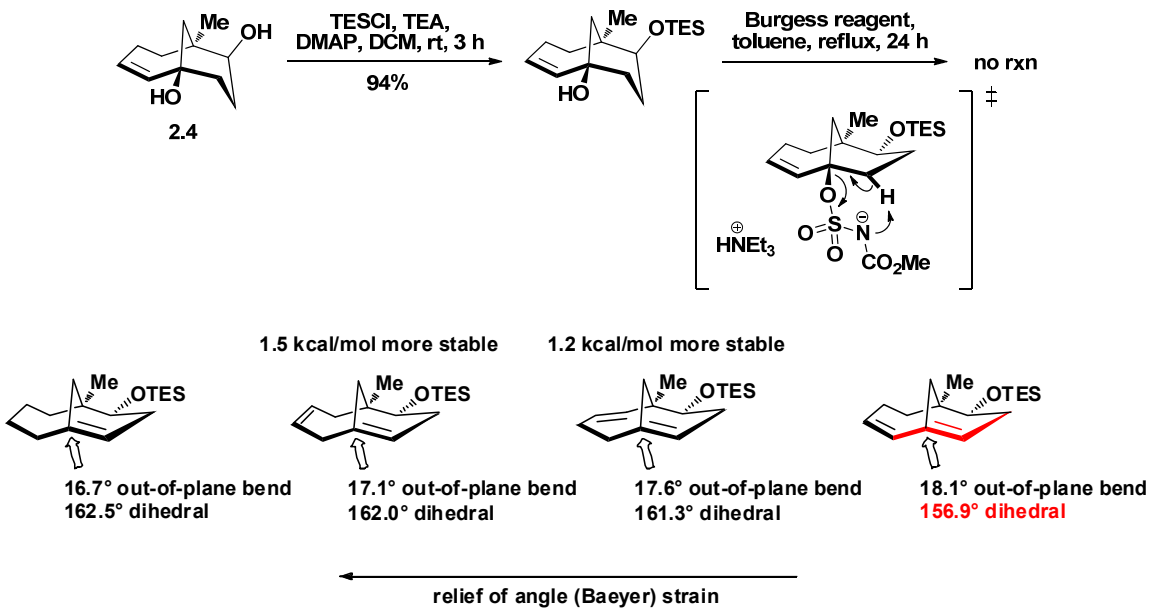

Scheme II.13 Attempted Burgess elimination to the umbellacin core.

The secondary alcohol of florlide core **2.4** was also benzylated (→ **2.12**, Scheme II.14). The product is an example of many potentially useful xenicane congeners that are accessible from this scaffold.

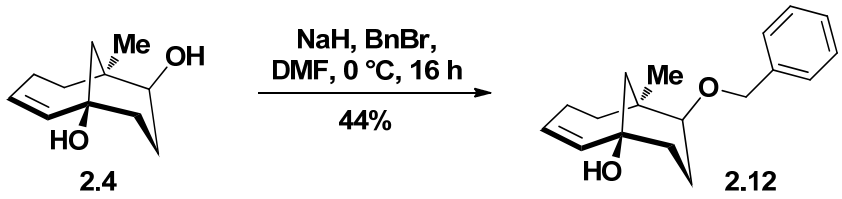

Scheme II.14 Selective benzylation of the florlide core.

2.7 Summary

In summary, we have realized a route to the core structures of three distinct diterpene natural product classes. This integrated strategy aims to realize concise routes to molecule-types that can react along disparate pathways to give rise to diverse bioactive molecules. In the present study, a chiral cyclononadienone (**2.1**, available in

eight steps from commercial reagents) was used to prepare the xeniolide core (**2.11**) and the corresponding epoxide (**2.2**, two steps from **2.1**). One additional step – with the appropriate reagent – enabled the conversion of **2.2** to a xenibellol *cis*-hydrindene (**2.3**) and separately to a florlide [4.3.1]-bicycle (**2.4**). This integrated routing strategy complements other approaches to gain access to bioactive compounds of significant complexity.[33-35]

2.8 References and Notes

1. R. Robinson, *J. Chem. Soc., Trans.* **1917**, *111*, 762-768.
2. R. B. Woodward, W. E. Doering, *J. Am. Chem. Soc.* **1944**, *66*, 849-849.
3. E. J. Corey, *Angew. Chem. Int. Ed. Engl.* **1991**, *30*, 455-465.
4. E. J. Corey, N. M. Weinshenker, T. K. Schaaf, W. Huber, *J. Am. Chem. Soc.* **1969**, *91*, 5675-5677.
5. M. D. Burke, S. L. Schreiber, *Angew. Chem. Int. Ed.* **2003**, *43*, 46-58.
6. L. A. Marcaurelle, C. W. Johannes, *Prog. Drug Res.* **2008**, *66*, 189-216.
7. L. F. Fieser, S. Rajagopalan, *J. Am. Chem. Soc.* **1950**, *72*, 5530-5536.
8. For bioassay-guided isolation papers, see: a) Y. Kashman, M. Saltoun, A. Rudi, Y. Benayahu, *Tetrahedron Lett.* **1994**, *35*, 8855-8858; b) C. Anta, N. González, G. Santafé, J. Rodríguez, C. Jiménez, *J. Nat. Prod.* **2002**, *65*, 766-768; c) C.-Y. Duh, A. A. H. El-Gamal, C.-Y. Chiang, C.-J. Chu, S.-K. Wang, C.-F. Dai, *J. Nat. Prod.* **2002**, *65*, 1882-1885; d) A. A. H. El-Gamal, S.-K. Wang, C.-Y. Duh, *Org. Lett.* **2005**, *7*, 2023-2025; e) Y.-C. Shen, Y.-C. Lin, A. F. Ahmed, Y.-H. Kuo, *Tetrahedron Lett.* **2005**, *46*, 4793-4796; f) A. A. H. El-Gamal, C.-Y. Chiang, S.-H. Huang, S.-K. Wang, C.-Y. Duh, *J. Nat. Prod.* **2005**, *68*, 1336-1340; g) A. A. H. El-Gamal, S.-K. Wang, C.-Y. Duh, *J. Nat. Prod.* **2006**, *69*, 338-341; h) E. H. Andrianasolo, L. Haramaty, K. Degenhardt, R. Mathew, E. White, R. Lutz, P. Falkowski, *J. Nat. Prod.* **2007**, *70*, 1551-1557; P. Falkowski, E. H. Andrianasolo, L. Haramaty, E. White, R. Lutz, U.S. Patent No. 8,183,395, issued May 22, 2012; i) T. Iwagawa, J.-i. Kawasaki, T. Hase, *J. Nat. Prod.* **1998**, *61*, 1513-1515; j) J. Tanaka, T. Higa, *Chemistry Lett.* **1984**, 231-232; k) M. Ninomya, S. Matsuka, A. Kawakubo, N. Bito, Jpn. Kokai Tokkyo Koho 07-285877, 1995; l) T. Miyamoto, Y. Takenaka, K. Yamada, R. Higuchi, *J. Nat. Prod.* **1995**, *58*, 924-928; m) Y.-C. Lin, M. H. Abd El-Razek, T.-L. Hwang, M. Y. Chiang,

Y.-H. Kuo, C.-F. Dai, Y.-C. Shen, *J. Nat. Prod.* **2009**, *72*, 1911-1916; n) G. J. Hooper, M. T. Davies-Coleman, M. Schleyer, *J. Nat. Prod.* **1997**, *60*, 889-893.

9. See also: a) D. J. Vanderah, P. A. Steudler, L. S. Ciereszko, F. J. Schmitz, J. D. Ekstrand, D. Van der Helm, *J. Am. Chem. Soc.* **1977**, *99*, 5780-5784; b) A. Groweiss, Y. Kashman, *Tetrahedron Lett.* **1978**, *19*, 2205-2208; c) A. Groweiss, Y. Kashman, *Tetrahedron Lett.* **1978**, *19*, 4833-4836; d) J. Finer, J. Clardy, W. Fenical, L. Minale, R. Riccio, J. Battaile, M. Kirkup, R. E. Moore, *J. Org. Chem.* **1979**, *44*, 2044-2047; e) R. E. Schwartz, P. J. Scheuer, V. Zabel, W. H. Watson, *Tetrahedron* **1981**, *37*, 2725-2733; f) A. Groweiss, Y. Kashman, *Tetrahedron* **1983**, *39*, 3385-3396; g) G. Guella, I. N'Diaye, G. Chiasera, F. Pietra, *J. Chem. Soc., Perkin Trans. 1* **1993**, *14*, 1545-1546; h) T. Iwagawa, J.-i. Kawasaki, T. Hase, C.-M. Yu, J. A. Walter, J. L. C. Wright, *J. Chem. Soc., Chem. Commun.* **1994**, 2073-2074; i) T. Iwagawa, Y. Amano, T. Hase, M. Shiro, *Tetrahedron* **1995**, *51*, 11111-11118; j) T. Iwagawa, J.-i. Kawasaki, T. Hase, J. L. C. Wright, *Tetrahedron* **1997**, *53*, 6809-6816; k) H. Miyaoka, M. Nakano, K. Iguchi, Y. Yamada, *Tetrahedron* **1999**, *53*, 12977-12982; l) H. Miyaoka, H. Mitome, M. Nakano, Y. Yamada, *Tetrahedron* **2000**, *56*, 7737-7740; m) T. Iwagawa, K. Nakamura, T. Hirose, H. Okamura, M. Nakatani, *J. Nat. Prod.* **2000**, *63*, 468-472; n) M. Hiroaki, N. Masakazu, I. Kazuo, Y. Yasuji, *Heterocycles* **2003**, *61*, 189-196; o) E. Fattorusso, A. Romano, O. Taglialatela-Scafati, M. J. Achmad, G. Bavestrello, C. Cerrano, *Tetrahedron* **2008**, *64*, 3141-3146; p) Y. Viano, D. Bonhomme, M. Camps, J.-F. Briand, A. Ortalo-Magné, Y. Blache, L. Piovetti, G. Culioli, *J. Nat. Prod.* **2009**, *72*, 1299-1304.

10. Although the absolute and relative stereochemistries of many xenicane compounds are unknown, for some isolates the configuration appears to vary with the producing organism (e.g. soft corals, sea fans, or brown algae).

11. a) E. J. Corey, R. B. Mitra, H. Uda, *J. Am. Chem. Soc.* **1964**, *86,* 485-492; b) Y. Ohtsuka, S. Niitsuma, H. Tadokoro, T. Hayashi, T. Oishi, *J. Org. Chem.* **1984**, *49*, 2326-2332; c) C. S. Mushti, J.-H. Kim, E. J. Corey, *J. Am. Chem. Soc.* **2006**, *128*, 14050-14052.

12. a) H. Nagaoka, K. Kobayashi, T. Matsui, Y. Yamada, *Tetrahedron Lett.* **1987**, *28*, 2021-2024; b) D. Renneberg, H. Pfander, C. J. Leumann, *J. Org. Chem.* **2000**, *65*, 9069-9079; c) O. V. Larionov, E. J. Corey, *J. Am. Chem. Soc.* **2008**, *130*, 2954-2955; d) C. Hamel, E. V. Prusov, J. Gertsch, W. B. Schweizer, K.-H. Altmann, *Angew. Chem. Int. Ed.* **2008**, *47*, 10081-10085; e) D. R. Williams, M. J. Walsh, N. A. Miller, *J. Am. Chem. Soc.* **2009**, *131*, 9038-9045.

13. a) V. Prelog, K. Schenker, *Helv. Chim. Acta* **1952**, *35*, 2044-2053; b) J. D. Dunitz, V. Prelog, *Angew. Chem.* **1960**, *72*, 896-902; c) W. C. Still, I. Galynker, *Tetrahedron* **1981**, *37*, 3981-3996; d) T. Ohnung, N. Hata, N. Miyachi, T. Wakamatsu, Y. Ban, *Tetrahedron Lett.* **1986**, *27,* 219-222; e) B. M. Trost, P. R. Seoane, *J. Am. Chem. Soc.* **1987**, *109,* 615-617; f) V. Enen, E. Tsankova, B. Mikhova, *Tetrahedron* **1989**, *45*, 3879-3888; g) J. H. Rigby, *Acc. Chem. Res.* **1993**, *26,* 579-585; h) G. Liu, T. C. Smith,

H. Pfander, *Tetrahedron Lett.* **1995**, *36*, 4979-4982; i) J. H. Rigby, K. R. Fales, *Tetrahedron Lett.* **1998**, *35*, 1525-1528; j) J. S. Clark, F. Marlin, B. Nay, C. Wilson, *Org. Lett.* **2003**, *5*, 89-92; k) A. Pollex, M. Hiersemann, *Org. Lett*. **2005**, *7*, 5705-5708.

14. W. H. Kim, A. R. Angeles, J. H. Lee, S. J. Danishefsky, *Tetrahedron Lett.* **2009**, *50*, 6440-6441.

15. Y. Zhang, S. D. Lotesta, T. J. Emge, L. J. Williams, *Tetrahedron Lett.* **2009**, *50*, 1882-1885.

16. A. C. Cope, K. Banholzer, H. Keller, B. A. Pawson, J. J. Whang, H. J. S. Winkler, *J. Am. Chem. Soc.* **1965**, *87*, 3644-3649.

17. a) Computational analyses used (DFT-B3LYP 6-31G(d, p)), including diffuse functions and charges where appropriate; b) All structures were fully optimized by analytical gradient methods using the GAUSSIAN 03 suites: M. J. Frisch, G. W. Trucks, H. B. Schlege, G. E. Scuseria, M. A. Robb, J. R. Cheeseman, J. A. Montgomery, Jr., T. Vreven, K. N. Kudin, J. C. Burant, *GAUSSIAN 03, Revision E.01*, Gaussian: Wallingford, CT, 2004; c) Density functional theory (DFT) calculations used the exchange potentials of: A. D. Becke, *J. Chem. Phys.* **1993**, *98*, 5648-5652; the correlation functional of: C. Lee, W. Yang, R. G. Parr, *Phys. Rev. B* **1988**, *37*, 785-789.

18. The racemization kinetics of **2.11** could not be studied directly by chiral HPLC due to lack of an appropriate separation method for this nonpolar hydrocarbon.

19. Intermediates **2.11** and **2.2** are prone to further oxidation in air and solution.

20. For selected reviews on Ti(III)-mediated radical epoxide opening, see: a) T. V. Rajanbabu, W. A. Nugent, *J. Am. Chem. Soc.* **1994**, *116*, 986-997; b) A. Gansäuer, B. Rinker, N. Ndene-Schiffer, M. Pierobon, S. Grimme, M. Gerenkamp, C. Mück-Lichtenfeld, *Eur. J. Org. Chem.* **2004**, 2337-2351; c) J. M. Cuerva, J. Justicia, J. L. Oller-López, B. Bazdi, J. E. Oltra, *Mini-Rev. Org. Chem.* **2006**, *3*, 23-35.

21. L. J. Williams, M. A. Drahl, M. Manpadi, U.S. Patent Appl. No. 13/215931, 2011.

22. A. Gansäuer, B. Rinker, M. Pierobon, S. Grimme, M. Gerenkamp, C. Mück-Lichtenfeld, *Angew. Chem. Int. Ed.* **2003**, *42*, 3687-3690.

23. G. A. Kraus, Y.-S. Hon, P. J. Thomas, S. Laramay, S. Liras, J. Hanson, *Chem. Rev.* **1989**, *89*, 1591-1598.

24. J. M. Cuerva, A. G. Campaña, J. Justicia, A. Rosales, J. L. Oller-López, R. Robles, D. J. Cárdenas, E. Buñuel, J. E. Oltra, *Angew. Chem. Int. Ed.* **2006**, *45*, 5522-5526.

25. I. B. Afanas'ev, G. I. Samokhvalov, *Russ. Chem. Rev.* **1969**, *38*, 318-329.

26. a) A. Aebi, D. H. R. Barton, A. S. Lindsey, *J. Chem. Soc.* **1953**, 3124-3129; b) A. Aebi, D. H. R. Barton, A. W. Burgstahler, A. S. Lindsey, *J. Chem. Soc*. **1954**, 4659-4665.

27. a) U. Vogt, U. Eggert, A. M. Z. Slawin, D. J. Williams, H. M. R. Hoffmann, *Angew. Chem. Int. Ed.* **1990**, *29*, 1456-1457; b) X. Cheng, N. L. Harzdorf, T. Shaw, D. Siegel, *Org. Lett.* **2010**, *12*, 1304-1307.

28. a) W. Fenical, in *Marine Natural Products: Chemical and Biological Perspectives, Vol. II*, P. J. Scheuer, Ed.; Academic Press: New York, 1978; Vol. 2, pp 173-245; b) D. J. Faulkner, *J. Nat. Prod. Rep.* **1984**, *1*, 251-280.

29. a) D. Green, S. Carmely, Y. Benayahu, Y. Kashman, *Tetrahedron Lett.* **1988**, *29*, 1605-1608; b) Y. Kashman, A. Rudi, *Phytochem. Rev.* **2004**, *3*, 309-323.

30. R. Croteau, A. Gundy, *Arch. Biochem. Biophys.* **1984**, *233*, 838-841.

31. J. Bredt, *Liebigs Ann. Chem.* **1924**, *12*, 1-9.

32. a) J. Sicher, *Angew. Chem. Int. Ed.* **1972**, *11*, 200-214; b) R. Keese, *Angew. Chem. Int. Ed.* **1975**, *14*, 528-538; c) K. J. Shea, *Tetrahedron* **1980**, *36*, 1683-1715; d) S. G. Levine, R. L. McDaniel, *J. Org. Chem.* **1981**, *46*, 2199-2200; e) Y. Sakai, S. Toyotani, M. Ohtani, M. Matsumoto, Y. Tobe, Y. Odaira, *Bull. Chem. Soc. Jpn.* **1981**, *54*, 1474-1480; f) K. B. Becker, M. P. Labhart, *Helv. Chim. Acta* **1983**, *66*, 1090-1100; g) J. B. Bremner, R. J. Smith, G. J. Tarrant, *Tetrahedron Lett.* **1996**, *37*, 97-100; h) H. Yoon, W. Chae, *Tetrahedron Lett.* **1997**, *38*, 5169-5172; i) D. L. J. Clive, S. Sun, X. He, J. Zhang, V. Gagliardini, *Tetrahedron Lett.* **1999**, *40*, 4605-4609; j) A. Armstrong, T. J. Critchley, M.-E. Gourdel-Martin, R. D. Kelsey, A. A. Mortlock, *Tetrahedron Lett.* **2002**, *43*, 6027-6030; k) S. E. Lewis, *Tetrahedron* **2006**, *62*, 8655-8681.

33. Diverted total synthesis, see: R. M. Wilson, S. J. Danishefsky, *Angew. Chem. Int. Ed.* **2010**, *49*, 6032-6056.

34. Natural product-inspired synthesis, see: K. Kumar, H. Waldmann, *Angew. Chem. Int. Ed.* **2009**, *48*, 3224-3242.

35. Diversity-oriented synthesis, see: S. L. Schreiber, *Nature* **2009**, *457*, 153-154.

Chapter III

Accessing Anticancer Structure Space: Second Generation Studies Toward the Synthesis of Xenicane Diterpenoids

3.1 Introduction

The global oncology market continues to grow faster than the pharmaceutical industry as a whole (Figure III.1), with forecasted revenues for 2013 exceeding $100 billion.[1] The xenicane superfamily (examples of which are shown in Figure III.2) comprises at least thirteen classes of natural products. Approximately one-third of the known compounds are reportedly active against cancer cell lines in the high nanomolar to low micromolar range; hence, the natural products are an untapped resource for cancer drug discovery. Many of these complex terpenes have provocative activity in various assays, but this evaluation has been ad hoc (Table III.1). For example, researchers have experimented with P-388, A-549, HT-29, MEL-28, WiDr, Daoy, Hep-G2, HCT-116, and MDA-MB-231 cancer cells, but no one assay has been used to evaluate all of the xenicanes (though P-388 is the most common), nor has any one compound been evaluated with more than two or three assays. Many xenicanes, including the first reported isolate named xenicin, have not been assessed for biological activity.

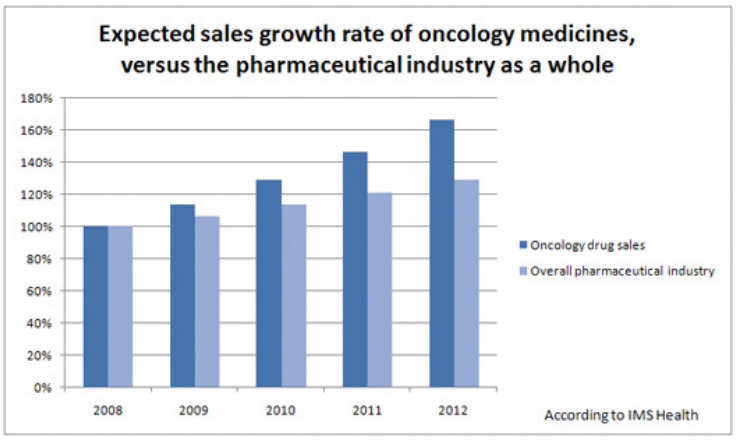

Figure III.1 Global oncology market growth.[1]

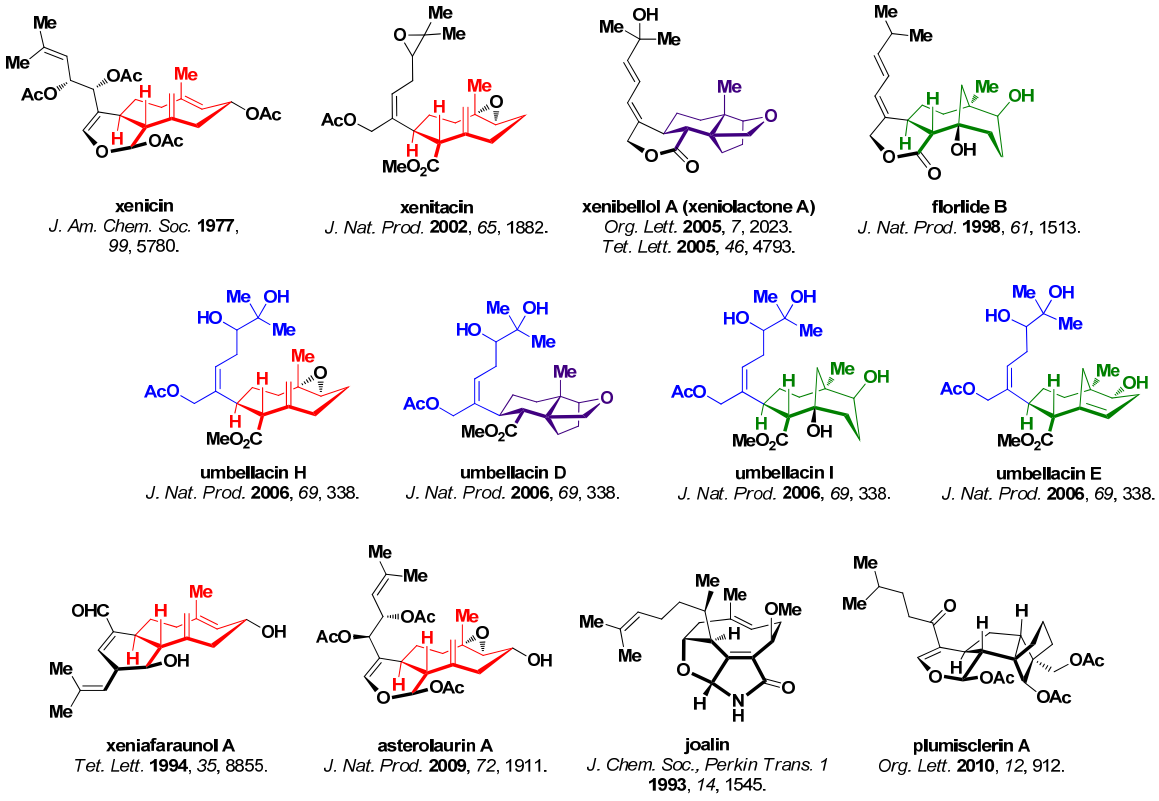

Figure III.2 Xenicane superfamily: structural complexity, novelty, and homology (shared structural motifs are in the same color).

MIC50, ED50, LC50, and GI50 values											
Xenicane	**Year Isolated**	**P-388**	**A-549**	**HT-29**	**HCT-116**	**WiDr**	**MEL-28**	**Daoy**	**Hep-G2**	**MDA-MB-231**	**W2**
xeniafaraunol A	1994	1.2 µg/mL									
xeniafaraunol B	2000	1.2 µg/mL									
xeniolide F	2002	> 1 µg/mL	> 1 µg/mL	> 1 µg/mL			> 1 µg/mL				
9-hydroxyxeniolide F	2002	> 1 µg/mL	> 1 µg/mL	> 1 µg/mL			> 1 µg/mL				
isoxeniolide A	2002	> 1 µg/mL	> 1 µg/mL	> 1 µg/mL			> 1 µg/mL				
7,8-oxido-isoxeniolide A	2002	> 1 µg/mL	> 1 µg/mL	> 1 µg/mL			> 1 µg/mL				
9-deoxyxeniloide E	2002	2.87 µg/mL	11.2 µg/mL	21.1 µg/mL							
9-deoxy-7,8-epoxyxeniloide E	2002	3.35 µg/mL	11.6 µg/mL	7.77 µg/mL							
xeniolide G	2002	0.04 µg/mL	4.77 µg/mL	8.31 µg/mL							
9-deoxyxenialactol C	2002	3.45 µg/mL	4.85 µg/mL	12.9 µg/mL							
xenibecin	2002	3.96 µg/mL	13.4 µg/mL	12.5 µg/mL							
xeniolide H	2002	3.66 µg/mL	18.8 µg/mL	5.33 µg/mL							
xenitacin	2002	1.09 µg/mL	3.26 µg/mL	1.12 µg/mL							
blumiolide A	2005	3.3 µg/mL		4.6 µg/mL							
blumiolide B	2005	3.7 µg/mL		4.9 µg/mL							
9-deoxyisoxeniolide A	2005	> 20 µg/mL		8.7 µg/mL							
9-deoxy-7,8-epoxy-isoxeniolide A	2005	4.7 µg/mL		5.6 µg/mL							
9-deacetoxy-7,8-epoxy-13-epi-xenicin	2005	> 20 µg/mL		> 20 µg/mL							
9-deoxy-7,8-epoxy-xeniolide A	2005	6.9 µg/mL		8.6 µg/mL							
blumiolide C	2005	0.2 µg/mL	10 µM (33% growth inhibition)	0.5 µg/mL	13.8 µM						
blumicin A	2005	> 20 µg/mL		> 20 µg/mL							
xenibellol A (xeniolactone A)	2005	3.6 µg/mL				13.6 µg/mL		15.3 µg/mL			
xenibellol B	2005	2.8 µg/mL									
umbellactal	2005	3.6 µg/mL									
umbellacin B	2006	1.6 µg/mL									
umbellacin D	2006	4.2 µg/mL									
umbellacin E	2006	3.8 µg/mL									
umbellacin F	2006	3.7 µg/mL									
umbellacin H	2006	3.4 µg/mL									
umbellacin I	2006	3.6 µg/mL									
unnamed isolate 1	2007										12 µM
unnamed isolate 2	2007										29 µM
unnamed isolate 3	2007										12 µM
unnamed isolate 4	2007										11 µM
asterolaurin A	2009								8.9 µM		
plumisclerin A	2010		4.7 µM	2.1 µM						6.1 µM	

Table III.1 Broad spectrum biological potency: anticancer activities. P-388 = lymphocytic leukemia, A-549 = lung, HT-29 = colon, HCT-116 = colon, WiDr = colon, MEL-28 = melanoma, Daoy = medulloblastoma, HepG2 = liver, MDA-MB-231 = breast, W2 = apoptosis-competent baby mouse kidney epithelial cells.

MIC50, ED50, LC50, and GI50 values						
Xenicane	**Year Isolated**	***Staphylococcus aureus***	***Aeromonas salmonisida***	***Bacillus subtilis***	***Orizias latipa***	***Curassius auratus***
dilophic acid	1987			inhibition at 100 µg/mL		toxicity at 50 µg/mL
deoxyxeniolide B	1995				15 ppm	
florlide B	1998	activity at 100 µg/disk	activity at 100 µg/disk			
florlide D	1998	activity at 100 µg/disk	activity at 100 µg/disk			
				human neutrophils		
		fertilized *Styela partita* eggs	**brine shrimp**	**superoxide anion release**	**superoxide inhibition**	**elastase release**
acalycigorgin A	1993	10 µg/mL				
acalycigorgin B	1993	5 µg/mL				
acalycigorgin C	1993		7.6 µg/mL			
acalycigorgin D	1994	8 µg/mL	20 µg/mL			
acalycigorgin E	1994	8 µg/mL	1.5 µg/mL			
tsitsixenicin A	1995				68% at 1.25 ug/mL	
tsitsixenicin B	1995				21% at 1.25 ug/mL	
zahavin A	1997			> 90% at 20 µg/mL		
9-deacetoxy-14,15-deepoxyxenicul	1997			> 90% at 20 µg/mL		
7,8-epoxyzahavin A	1997			> 90% at 20 µg/mL		
asterolaurin D	2009			23.6 µM		18.7 µM

Table III.2 Broad spectrum biological potency: antibiotic activities. *Staphylococcus aureus* = staph infection-causing gram positive bacteria, *Aeromonas salmonisida* = fish skin infection-causing gram negative bacteria, *Bacillus subtilis* = probiotic gram positive bacteria, *Orizias latipa* = mosquitofish, *Carassius auratus* = goldfish, *Styela partita* = rough sea tunicate.

Cancer can be viewed as a failure of apoptosis, the process of programmed cell death (PCD) that occurs in multicellular organisms, and uncontrolled cell growth. Two proapoptotic Bcl-2 multidomain proteins, Bax and Bak, are the functionally redundant, essential downstream regulators of most apoptosis signaling pathways. Apoptosis may therefore be functional only when a cascade signal passes through Bax and Bak. Our group is particularly interested in the ongoing collaborative studies by White and co-workers. In order to identify potential anticancer agents, they developed a specific apoptosis induction assay that probes the Bax- and Bak-dependent pathway.[2] A group of xenicane isolates (**3.1**-**3.4**, Figure III.3) was found to selectively induce apoptosis upstream of Bax and Bak in precancerous immortalized baby mouse kidney epithelial cells (iBMKECs).[3] At a concentration of 12 μM, compound **3.1** was the most selective. This work is suggestive of a new method of identifying potential anticancer agents. Our investigations into the chemical similarity within the xenicane superfamily suggest that these apparently structurally diverse compounds share many topographical features and therefore many of the compounds warrant closer scrutiny as potential inducers of apoptosis.

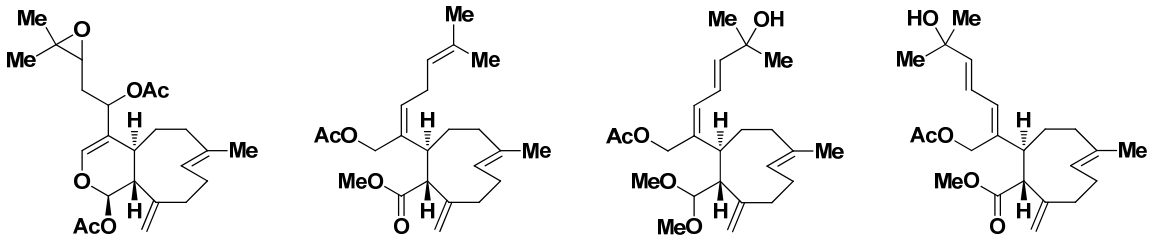

Figure III.3 Proapoptotic xenicane isolates.[3]

Since these complex terpenes are not readily available in sufficient quantities to allow detailed analysis, there is a need for a general synthetic route to the natural products and, perhaps more importantly, their unnatural congeners. Practical organic syntheses will enable the structure-activity relationship (SAR) studies necessary for thorough medicinal evaluation. It is likely that the apoptosis activity noted for the Falkowski isolates is shared by many of these compounds and their congeners. The natural products themselves are not useful as drugs since they would be expected to have poor bioavailability and be easily metabolized in the body. We therefore targeted the diverse, semi-validated structure space (Figure III.4) that these compounds populate. Before embarking on this project, we demonstrated the feasibility of the synthetic approach on a model system (see Chapter II). This research is aimed at providing a wide range of tools for the study of disease, which will in turn lay a foundation for investigating potential modes for disease management. Conventional drug discovery strategies rely on single-target or stochastic search strategies. Our multi-target approach can accelerate the search for new substances with desirable properties. As with conventional studies in total synthesis, we also expected to learn much about the structure and reactivity of new organic molecules.

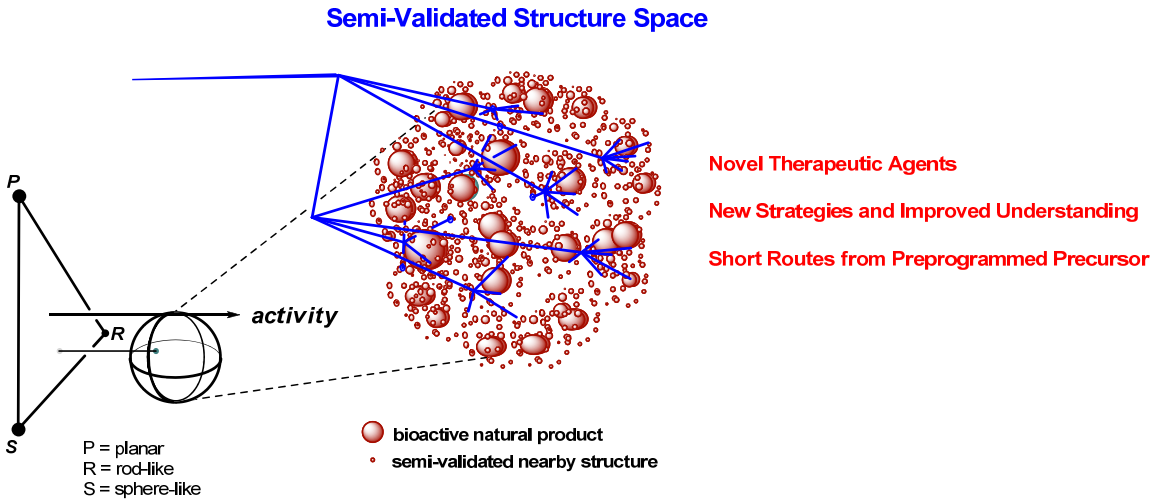

Figure III.4 Structure space targeting.

3.2 Second Generation Design of the Key Intermediate

Our laboratory has evaluated several approaches towards the synthesis of xenicanes.[4] We envisaged the construction of these diterpenoids via stereoselective conjugate addition of strategically-functionalized carbon nucleophiles to a sufficiently reactive nine-membered enone. My former colleague Dr. Yue Zhang accessed chiral cyclononadienone **3.5** (Scheme III.1), but many facile cuprate additions failed to add to this enone even in the presence of Lewis acid activators such as TMSCl, BF_3, Me_2AlCl, Et_2AlCl, and $AlCl_3$.[4a] The trityl cation was sufficiently Lewis acidic to promote Mukaiyama-type conjugate additions to this scaffold in Corey's elegant total syntheses of coraxeniolide A and β-caryophyllene.[5] The IR signature of **3.5** suggests that the ketone is in conjugation with the disubstituted olefin (1687 cm^{-1}). However, the ^{13}C NMR chemical shift of the β-carbon (136.8 ppm, $CDCl_3$) indicates that it is fairly electron rich. Additionally, computational analysis shows that the enone is far from conjugated in the

ground state (C=C-C=O dihedral angle of 53°).[6] Taken together, the data suggested that this intermediate is not ideal for accessing xenicane structure space.

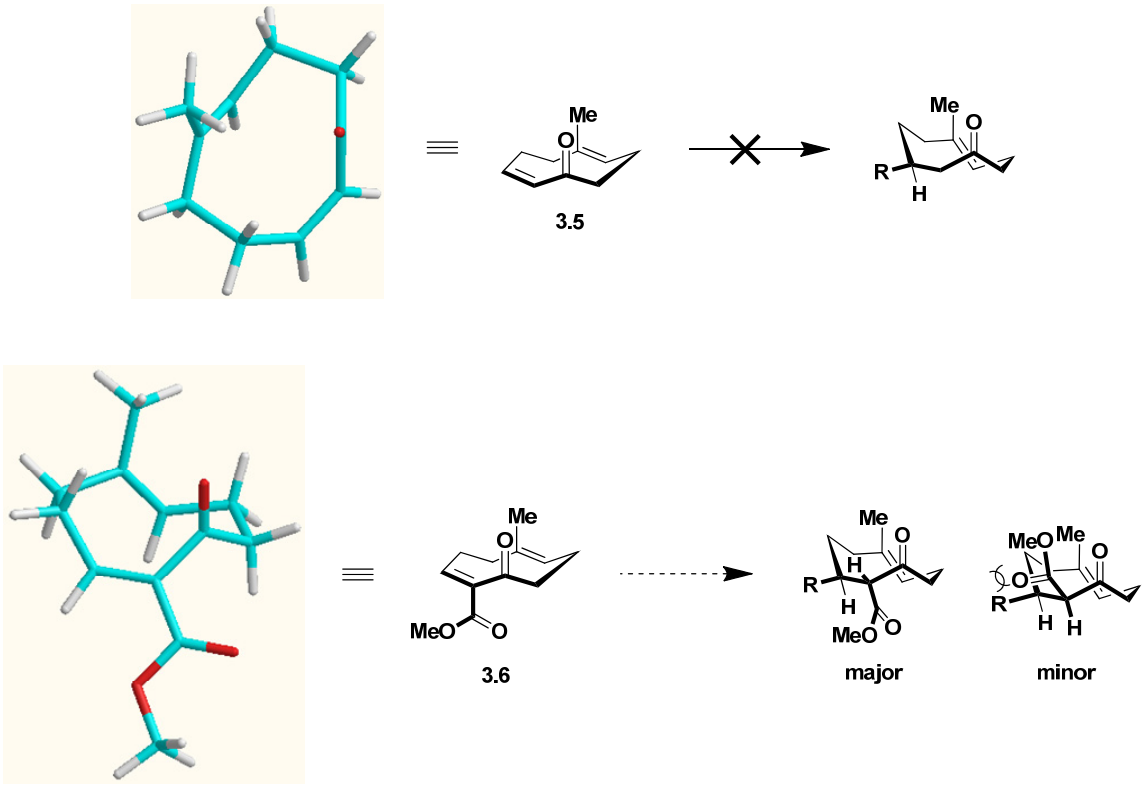

Scheme III.1 Low-energy conformations of cyclononadienone 3.5 (bird's-eye view) and revised carboxylate-substituted target 3.6.[6]

In order to enhance the reactivity of the enone and to increase the tempo of the general synthetic route, we targeted a new nine-membered platform (**3.6**) with a carboxylate group incorporated in the α-vinyl position. This electron-withdrawing moiety would force the olefin into conjugation, thereby rendering the β-vinyl carbon more electrophilic. Based on steric and torsional grounds, we expected conjugate additions to this enone to proceed with high stereoselectivity, with both nucleophilic addition and

protonation occurring on the less hindered face of the ring. Thus, the two stereocenters common to the majority of xenicanes would be set in a single step.

3.3 Racemic Synthesis of the Key Intermediate

Nine-membered cycloalkanes have the most repulsive transannular strain.[7] One of the difficulties of xenicane total synthesis lies in the construction and preservation of the strained electron-rich *E* olefin. Furthermore, the complex arrangement of olefins of different oxidation state requires meticulous synthetic planning, which will vary depending on the specific target.

Given the lack of applicable enantioselective methods at our disposable, we focused our initial efforts on a racemic route to **3.6**. Dr. Yue Zhang was unable to access **3.5** via intramolecular cyclizations.[4a] Indeed, C-C fragmentation was the only approach to this architecture that proved effective. The initial fragmentation target, silyl-protected cyclononenone **3.8**, was inaccessible from hydroxytosylate **3.7**, since this precursor failed to fragment (Scheme III.2). Computational modeling suggested that the reactive centers of **3.7** were not suitably aligned for fragmentation. It was reasoned that, in analogy to Corey's cyclobutane ring,[8] a double bond in that position would prevent conformational twisting in the *cis*-hydrindane and thus retain an adequate C-C-C-OTs torsion angle for fragmentation. Installation of the olefin indeed improved this geometry, and the near-antiperiplanar arrangement (165˚) appeared to facilitate the reaction.

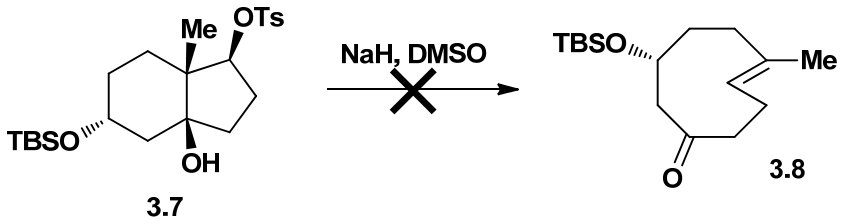

Scheme III.2 Dr. Yue Zhang's failed fragmentation.[4a]

Accordingly, we pursued the new core structure using the same powerful approach, and the critical double bond was incorporated into the design of the new route. To confirm this logic, several saturated fragmentation precursors were modeled,[6] and in each case the torsion angle was less favorable (< 165˚). We determined with confidence at the outset, therefore, that fragmentation would have to precede conjugate addition. We initially aimed to fragment ester-tosylate **3.9** (Scheme III.3), which shares the same torsion angle (165˚) as the precursor to **3.5**.

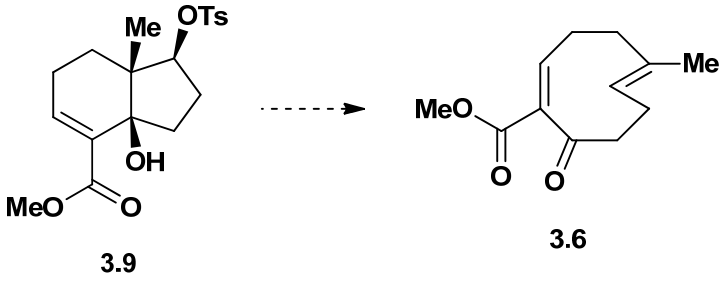

Scheme III.3 Planned fragmentation.

Several generations of experiments evolved into the linear route depicted in Scheme III.4. Acetic acid-catalyzed Michael addition of commercially available 2-methyl-1,3-cyclopentanedione (**3.10**) to acrolein gave a quantitative yield of pure crude aldehyde-dione **3.11**.[9] This was run quite concentrated in deionized water (1.75 M) to

facilitate extraction of the water-soluble product from the aqueous layer. Modified bromo-Wittig olefination of the aldehyde gave vinyl bromide **3.12** as a mixture of *Z*/*E* alkenes (6:1 *Z*:*E* ratio).[10] Since we were unable to isolate the bromo-Wittig reagent, it was prepared and used *in situ*. At least 2 hours were required for complete formation of the bromo-Wittig reagent. The best yields were obtained with anhydrous DCM and azeotropically-dried aldehyde. We were unable to monitor consumption of the starting material by TLC (a polar smear always remained), so the reaction was stirred for at least 20 hours to ensure high conversion.

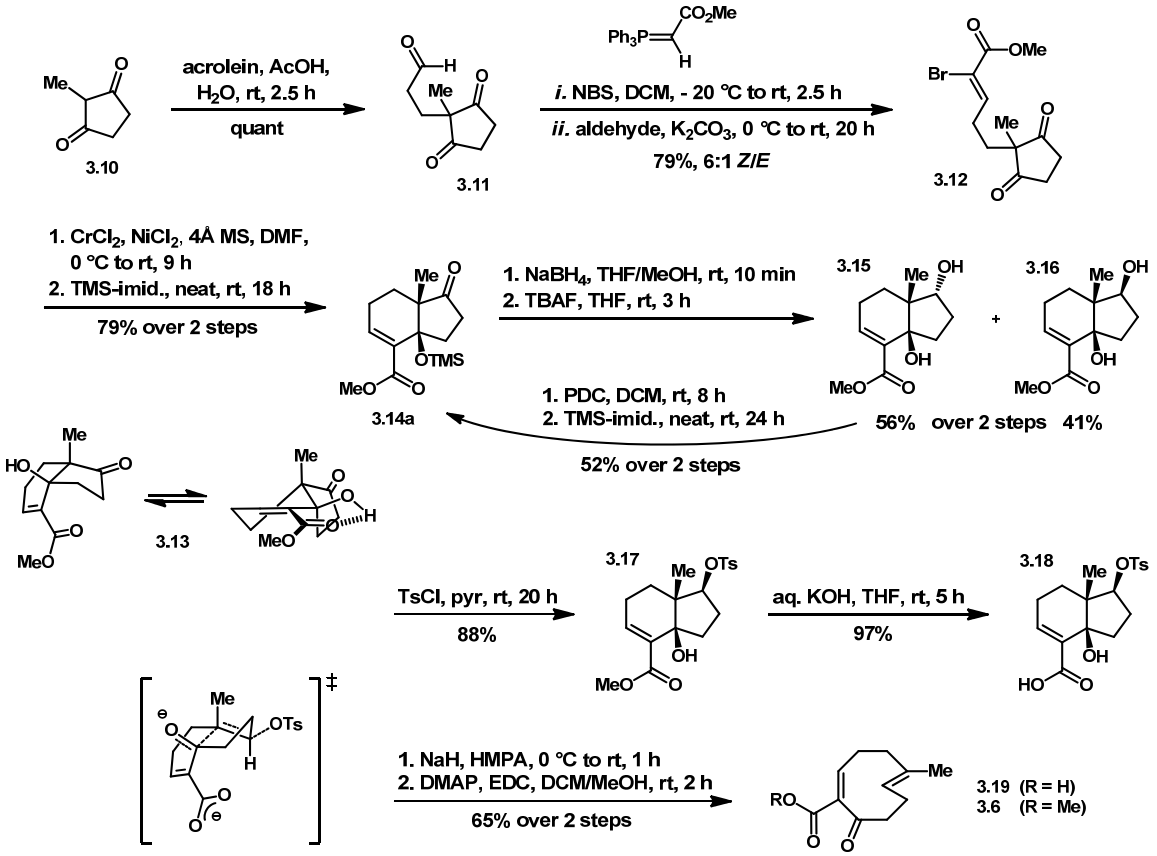

Scheme III.4 Nine-membered ring core synthesis.

Intramolecular Barbier-type addition of the vinyl anion derived from **3.12** to either ketone was initially problematic. Attempted lithium-halogen exchange (*t*-BuLi, THF, -78

°C), Grignard (*i*PrMgCl, THF, -78 °C to rt), and radical (SmI_2, THF, rt) reactions led to complex product mixtures. Transmetallation conditions used for activated (allylic/benzylic) alkyl halides (excess Zn dust, sat. aq. NH_4Cl/THF, 5:1 v/v, 0 °C to reflux) did not affect **3.12**.

The desired cyclization to ketol **3.13** was efficiently promoted under mild Nozaki-Hiyama-Kishi (NHK) conditions.[11] This coupling reaction is especially useful for joining vinyl halides and aldehydes intermolecularly. There is little precedent for intramolecular NHK reactions with ketones,[12] which are essentially unreactive in intermolecular cases. The *E/Z* ratio of **3.12** is inconsequential since both isomers are consumed according to TLC, a phenomenon that can be attributed to a reversible allenoate intermediate (Scheme III.5). The presence of the double bond in the alkyl chain of **3.12** ensures complete *cis*-selectivity in the cyclization. Bond rotations in the alkyl chain are restricted, so the vinyl anion can only approach a ketone *anti* to the methyl group. Saturated analogues of **3.12** have reportedly undergone cyclization under various conditions to give the *trans*-bicycle as a minor product: in this case the extra degrees of freedom for rotation allow for some approach *syn* to the methyl.[13] Excess $CrCl_2$ (5 equiv) was required to push the reaction to completion. Use of Aldrich 95% $CrCl_2$ was critical for reproducibility of the very good yield. The optimized procedure includes measures to exclude trace moisture from the reaction. Special workup conditions were developed to maximize extraction of the product and minimize extraction of DMF from the aqueous layer (see Experimental).

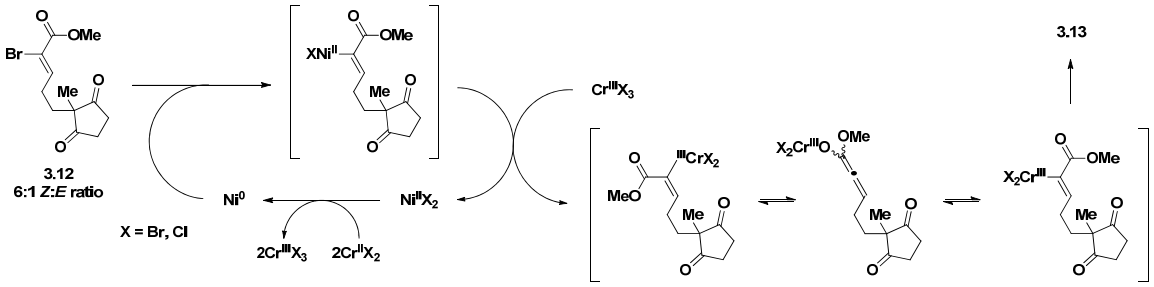

Scheme III.5 Presumed intramolecular NHK mechanism: olefin geometry inconsequential.[11]

Although high yielding, the NHK reaction was not scalable due to the large relative volume of DMF required to effect clean intramolecular coupling (< 0.05 M). The largest scale ever run was 2.5 g of starting material. The workup procedure took a long time. Significant material mass was lost with the bromine atom. Multiple batches were required to push material forward on multi-gram scale. Efforts were made towards an environmentally friendly NHK reaction (though it was already green-colored from toxic $CrCl_2$). Slow syringe pump addition of starting material to a concentrated suspension of metal salts (0.2 M in DMF overall) did not give clean conversion to the product on large scale (33% yield at best). No reaction was observed using catalytic Cr(III) and excess Mn (reducing agent) in THF/DMF,[14] so the use of excess Cr(II) could not be avoided.

After many experiments, my colleague Huan Wang developed a scalable cyclization (up to 10 g scale thus far) that circumvents the use of DMF. The optimized procedure employs activated Mg turnings (50 equiv), PBu_3 (2 equiv), and Et_2O (0.05 M). After 20 h at rt, yields of 65-75% of **3.13** are obtained. Both reagents are required for the transformation to proceed. The mechanism is not yet clear, but it may be as simple as a $MgCl_2$ catalyzed Morita-Baylis-Hillman reaction (Scheme III.6).

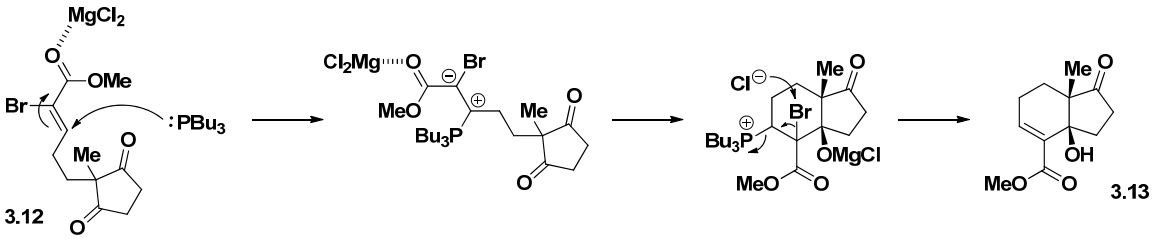

Scheme III.6 Proposed mechanism of optimized cyclization reaction.

The next goal was to selectively reduce the ketone to the β-alcohol. Under various reduction conditions, the tertiary alcohol of **3.13** appeared to direct hydride delivery to both the ketone and enone from two different conformations of the bicycle, producing mixtures of undesired α-alcohol (**3.15**) and 1,4-reduction product (not shown). Protection of the tertiary alcohol was required to effect clean reduction of the ketone and limit hydride delivery from the convex face. This alcohol was a poor nucleophile, likely due to hydrogen bonding with the carboxylate (see X-ray crystallography in Experimental). Silylation of the alcohol was slow under standard conditions (TMSCl, TEA, DMAP, DCM, rt). Neat addition of TMS-imidazole to crude **3.13** gave near quantitative conversion to TMS ether **3.14a** in a reasonable time. On large scaleup, however, homogenous stirring of the neat mixture was difficult and overprotection to TMS enol ether **3.20** (Scheme III.7) became problematic, necessitating a selective deprotection step with one equivalent of fluoride to recycle the byproduct.[15] *In situ* TMS protection of the dilute tertiary alkoxide formed during the NHK reaction was far too slow: only 14% conversion to **3.14a** was observed after 18 h using TMS-imidazole.

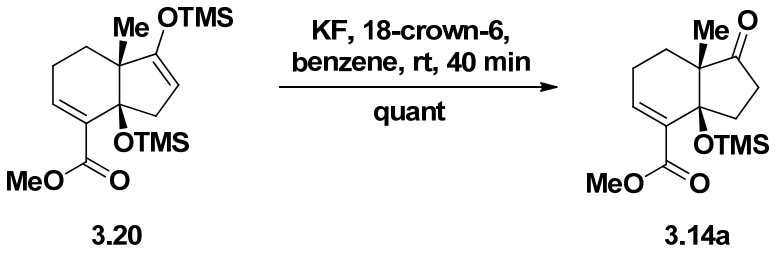

3.20 3.14a

Scheme III.7 Recycling of the overprotection product.

The *cis*-6,5 keto system is intrinsically favored to be reduced from the less hindered convex face. TMS ether **3.14a** was subjected to many different reduction conditions to maximize the yield of the β-alcohol. We varied both the steric bulk and hydride donating strength of the reducing agent, as well as temperature (Table III.3). The lower the temperature, the more α-alcohol was produced. Surprisingly, Luche reductions produced the α-alcohol with greater selectivity than $NaBH_4$ alone. The best *dr* (1.1:1 β/α) was obtained using $LiAl(O\textit{t}Bu)_3H$ in refluxing THF, but a byproduct formed that decreased the overall yield of the desired product. Standard $NaBH_4$ (5 equiv) reduction at room temperature gave the best combination of chemo- and diastereoselectivity. Minimal MeOH as co-solvent was required to solubilize $NaBH_4$. Thus, TMS ether-alcohols **3.14b** were synthesized in quantitative crude yield (1:1.4 β/α). No flash column chromatography was required at this stage.

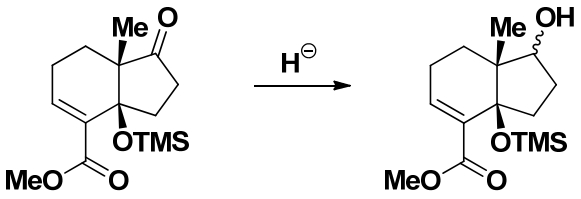

3.14a 3.14b

Reduction Conditions	Overall Yield(s)	α:β Ratio	*Yield of β-OH
$NaBH_4$, THF/MeOH (9:1 v/v), -78 °C, 24 h	quant	2.2:1	31%
$NaBH_4$, THF/MeOH (9:1 v/v), rt, 10 min	quant	1.4:1	42%
$NaBH_4$, MeOH, rt, 10 min	quant	1.4:1	42%
$NaBH_4$, THF/MeOH (9:1 v/v), reflux, 10 min	70%+ 1,2-ester reduction	1.1:1	33%
$NaBH_4$, $CeCl_3$, MeOH, 0 °C, 10 min	quant	3.3:1	23%
$NaBH_4$, $CeCl_3$, MeOH, rt, 10 min	quant	2.5:1	29%
$NaBH(Et)_3$, THF, -78 °C, 5 min	10%+ 60% byproducts + 20% recovered SM	-	-
$NaBH(Et)_3$, THF, rt, 5 min	65%+ other reduction byproducts	1:1	33%
$N(Me)_4BH(OAc)_3$, CH_3CN/H_2O (9:1 v/v), reflux, 72 h	loss of TMS group	-	-
$LiAl(O\text{-}tBu)_3H$, Et_2O, rt, 24 h	quant conversion, 84% after purification	1.2:1	38%
$LiAl(O\text{-}tBu)_3H$, THF, reflux, 1.5 h	81%+ unknown byproduct	1:1.1	39%
L-selectride, THF, 0 °C to rt, 2 h	complex mixture: 1,2- and 1,4-ester reduction	-	-
KS-selectride, THF, -78 °C to rt, 4 h	complex mixture/decomposition	-	-
(*S*)-Bu-CBS, $BH_3{\cdot}SMe_2$, toluene, 0 °C, 4 h	>100% crude, 2 byproducts	1.2:1	35%

Table III.3 Chemo- and diastereoselective reduction screening (*crude NMR yields).

Larger protecting groups were also explored in an effort to better shield the convex face. The TES-protected bicycle (TESOTf, 2,6-lutidine, DCM, rt, quant) was reduced with $NaEt_3BH$ in THF at rt, giving a 1.1:1 β/α ratio and a major byproduct. The TBDPS-protected bicycle (TBDPSOTf, 2,6-lutidine, DCM, 4Å MS, rt) was unstable on silica gel, and pushing the crude product through $NaBH_4$ reduction yielded a mixture of products, including the 1,2-ester reduction product. We also proposed a carboxylate-directed triacetoxyborohydride reduction from the concave face, but the desired substrate (free carboxylic acid with protected tertiary alcohol, not shown) was inaccessible to us via several attempted protection-saponification sequences.

Deprotection of the crude TMS ether-alcohols **3.14b** gave a partially separable mixture of diols **3.15** and **3.16**. This was the easiest pair of diastereomers to separate by flash column chromatography, though multiple slow columns and large volumes of solvent were required nonetheless. The corresponding tosylates were more nonpolar and even more difficult to separate. Separating at the diol stage also allowed for recycling of the undesired diastereomer **3.15** back to TMS ether **3.14a** by PDC oxidation and reprotection. This reduction-deprotection/separation-recycling sequence remains the bottleneck of the route.

Attempts were made with inversion chemistry to expedite the route to a *cis*-diol (Scheme III.8). The α-alcohol **3.15** was made stereospecifically via a tertiary alcohol-directed triacetoxyborohydride reduction of ketol **3.13**. Mitsunobu reaction using freshly prepared zinc ditosylate, the best source of soft nucleophilic tosylate,[16] gave mostly the elimination product **3.21** and unacceptable amounts of the desired inversion product **3.17**. Use of *p*-nitrobenzoic acid as the nucleophile gave a complex mixture of products and a poor yield of **3.22**. Sterically hindered alcohols in the steroid/prostaglandin fields have reportedly been inverted by treatment with excess KNO_2. Under the requisite vigorous conditions,[17] **3.23** was transformed into the same alkene product **3.21**, with no detectable amounts of inverted alcohol **3.16**. Since this neopentyl center was prone to elimination, we pressed forward with the recycling route.

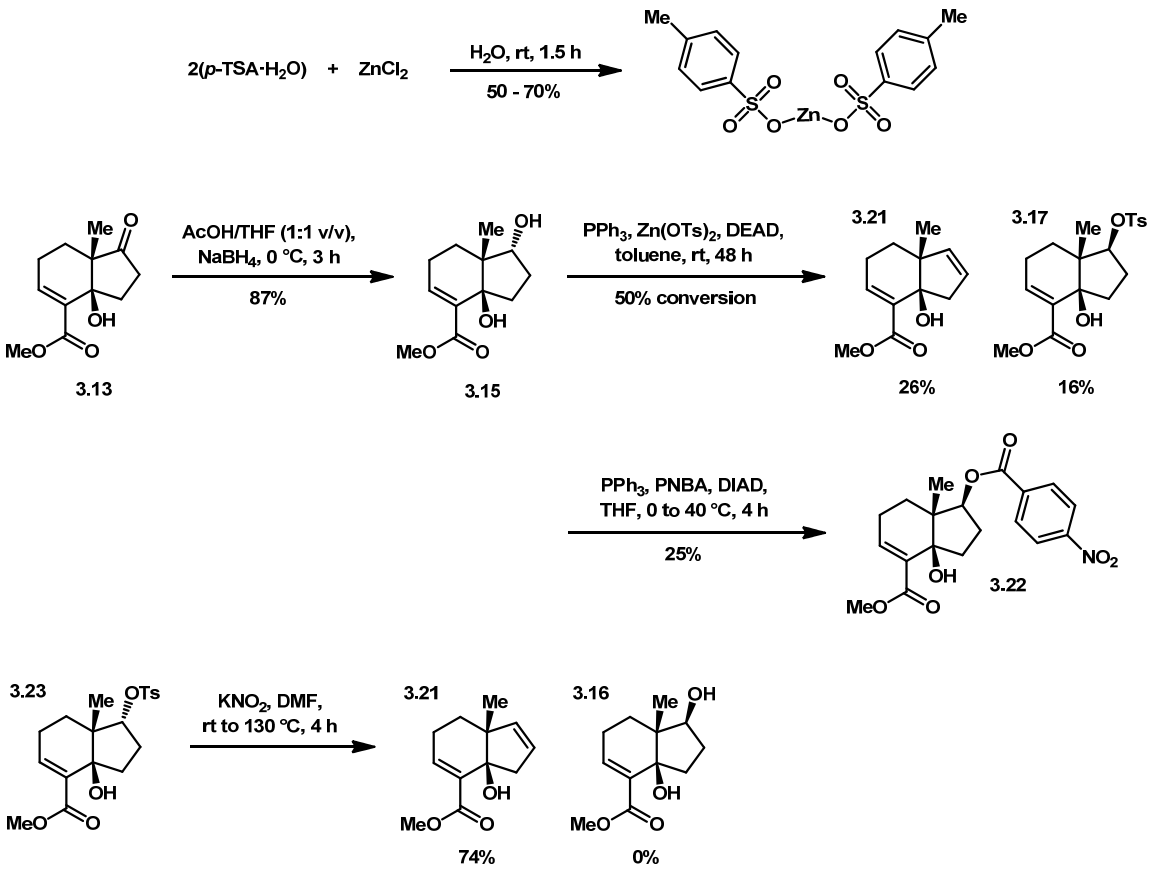

Scheme III.8 Attempts to expedite the route with inversion chemistry.

Monotosylation of diol **3.16** provided our targeted fragmentation substrate, ester-tosylate **3.17**, in very good yield. All efforts to fragment this bicycle were met with failure. Exposure to strong non-nucleophilic bases in anhydrous solvents (NaH, THF/DMF/HMPA, 0 to 60 °C; *t*-BuOK, *t*-BuOH/DMF, 0 °C to reflux) led to decomposition. Treatment of the corresponding TMS-ether (not shown) with TBAF (dried over 4Å MS, THF, rt to reflux) led only to deprotection.

We reasoned that the dianion derived from the corresponding carboxylic acid **3.18** should be more likely to fragment, so we sought to saponify the ester. Nicolaou's mild trimethyltin hydroxide method (DCE, 80 °C)[18] required a large excess of the reagent (>20 equiv.) and a long reaction time (48 h), resulting in a 62% yield of the elimination product

3.21. NaOH (1 M in H_2O, MeOH, rt) was not strong enough to saponify the conjugated ester, which is less electrophilic than a nonconjugated ester. A biphasic reaction consisting of aq. KOH and THF was found to be optimal. Employing no more than 2 equiv. of base, the ester was saponified in the presence of the tosylate, furnishing acid-tosylate **3.18**, whose structure was confirmed by X-ray crystallography (see Experimental), in near quantitative yield. While primary and secondary tosylates are unstable to such conditions, this neopentyl tosylate eliminates slowly relative to saponification. This is presumably due to the hindered nature of the α-proton that must be deprotonated to effect the E2 elimination. The neopentyl center that complicated the installation of the leaving group ironically allowed saponification at the most convenient point in the route. Saponification prior to activation of the hydroxyl would have introduced additional protecting group manipulations and solubility issues.

No appreciable fragmentation of **3.18** was observed upon treatment with NaH in THF or DMF, and heating the reactions resulted in elimination of the tosylate. A very large excess of NaH (up to 200 equiv.) in anhydrous HMPA promoted clean fragmentation of the dianion to the nine-membered carboxylate **3.19**. HMPA was apparently necessary to solvate the sodium cations. The required amount of NaH was found to vary from reaction to reaction, but it was clear that the ionic strength of the suspension needed to be very high. Given the excessive amount of NaH required and the large volume of foam produced during quenching, this reaction was usually run on 200-300 mg scale. Almost half of the mass of the material was lost with the tosylate. Trace HMPA in the crude product was removed by silica gel column chromatography in the next step.

Why is such a large concentration of strong base required to drive this reaction to completion? Consider the mechanism depicted in Scheme III.9. The intramolecular hydrogen bond in acid-tosylate **3.18** is strengthened after deprotonation of the carboxylic acid. This proton sharing/delocalization of negative charge between the carboxylate and alkoxide renders the pKa of this proton very high. Additionally, the electrostatic repulsion between the anionic oxygens in the dianion is relieved in the monoanion.[19]

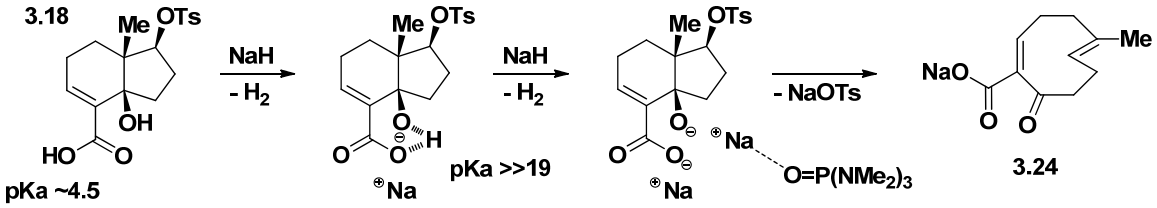

Scheme III.9 Fragmentation analysis: mechanism.

Why does ester-tosylate **3.17** fail to fragment? Computational modeling indicates that, although the parent alcohols **3.17** and **3.18** exhibit similar ground state torsion angles (165˚ and 164˚ respectively), significant deviation arises in the activated alkoxide intermediates (Scheme III.10).[6] For neutral **3.17**, the ester is coplanar with the double bond. For the alkoxide, however, the ester is twisted out of planarity. This appears to be a through-space electrostatic influence. As a consequence of this conformational twisting, the adequate torsion angle in the parent alcohol is reduced to 161˚, which is apparently enough to disfavor the fragmentation pathway. While the same electrostatic effect is observed in acid-tosylate **3.18**, the dianion does not represent a stable structure, and instead undergoes fragmentation during Gaussian step optimization (depicted here as the step after the C-OTs bond disappears). Thus, the intramolecular stereoelectronic effect disfavoring

fragmentation was overcome by generation of the unstable dianion, as demonstrated experimentally.

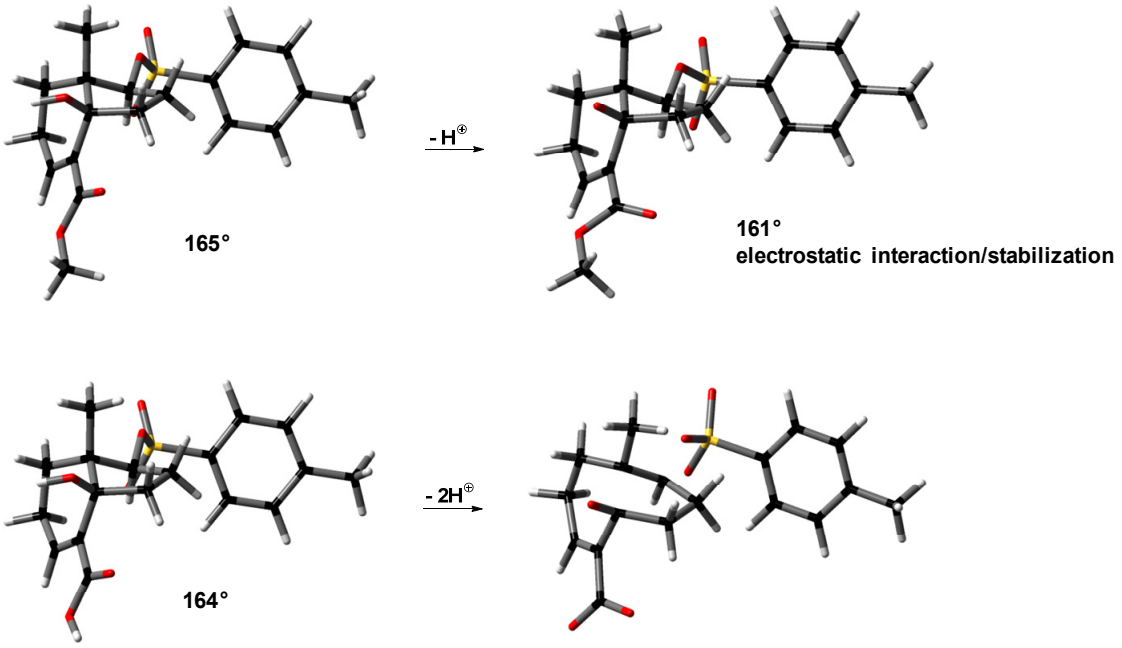

Scheme III.10 Fragmentation analysis: computed ground state torsion angles.[6]

Portionwise addition of water-sensitive TMS-diazomethane (2.0 M in DEE) to the crude carboxylic acid **3.19** in MeOH at 0 °C generated our targeted key intermediate **3.6**, but this product was unstable under the esterification conditions, reacting further to undesired byproducts lacking the enone and methyl ester. Clean generation of the methyl ester was accomplished via carbodiimide-mediated esterification. The best yield to date of cyclononadienone-carboxylate-methyl ester **3.6** is 65% over 2 steps. Surprisingly, this compound survived in dry silica gel overnight.

In order to understand the intrinsic reactivity of **3.6**, we studied its structure extensively. The IR frequency of the ester carbonyl (1731 cm^{-1}) was consistent with that of methyl acrylate, suggesting that the ester is in conjugation with the adjacent olefin.

VT-NMR experiments from -50 to 75 °C showed only a single conformer with very minor ^{1}H and ^{13}C chemical shift changes (< 0.05 ppm) due to partial ring flexibility. NOEs, coupling constants, and X-ray crystallographic analysis are consistent with a low energy conformation in which the ketone and methyl groups are on the same side of the ring (*cis*, see Experimental). The stereochemical relationship between the alcohol and methyl groups in the bicyclic precursors appears retained.

Thus, we realized a concise racemic route to the structurally processable intermediate. Under optimal experimental conditions and without recycling of byproducts, **3.6** is accessible in 10 linear steps and 14% overall yield. The protection-reduction-deprotection/separation sequence remains the major bottleneck of the route, requiring diol **3.16** to be made in several batches then combining before pushing forward on greater than 1 gram scale. It is not clear whether this can be improved.

3.4 Progress Towards an Asymmetric Route

Development of an enantioselective route to **3.6** may not be worthwhile given its racemization kinetics (see *Racemization Kinetics of the Dissymmetric Platform*). Before the kinetics were understood, an asymmetric route was pursued. Enantioselective intermolecular NHK couplings between vinyl iodides/triflates and aldehydes have been reported using a DIANANE salen catalyst (*ee*'s of 60-75%).[20] Exposure of vinyl bromide **3.12** to modified conditions (5 eq $CrCl_2$, 0.05 eq $NiCl_2$, 0.1 eq ligand, 0.2 eq TEA, 4Å MS, DMF, 0 °C to rt) gave a 75% yield of ketol **3.13**, but no enantioselectivity was observed.

Practical desymmetrization of 2,2-disubstitutedcycloalkane-1,3-diones remains a largely unsolved problem in chemical synthesis. Chiral amino acid-derived oxazaborolidines have been used in stoichiometric quantities, yielding monoreduction

products in moderate yields and enantioselectivities.[21] Environmentally friendly microbial-mediated reductions have been highly chemo- and stereoselective for a wider range of substrates.[22] Under carefully controlled conditions, slow aerobic enzymatic reduction of vinyl bromide **3.12** granted access to highly enantioenriched ketol **3.25** as the major diastereomer (Scheme III.11). New baker's yeast (*Saccharomyces cerevisiae*) was required for reproducibility. According to chiral HPLC, each isomer was produced in >99% *ee*. Both *Z* and *E* olefin-containing substrates were reduced with analogous selectivity. The diastereoselectivity of the reduction was dependent on substrate concentration, consistent with the findings of Node and co-workers. This extremely low concentration (8 mM), combined with a yield limited by reversibility and autolysis, rendered this reaction unsuitable for the third step of total synthesis. Tosylation of the hindered alcohol proceeded very slowly, furnishing **3.27** as the only detectable diastereomer, and it failed to cyclize cleanly under NHK conditions.

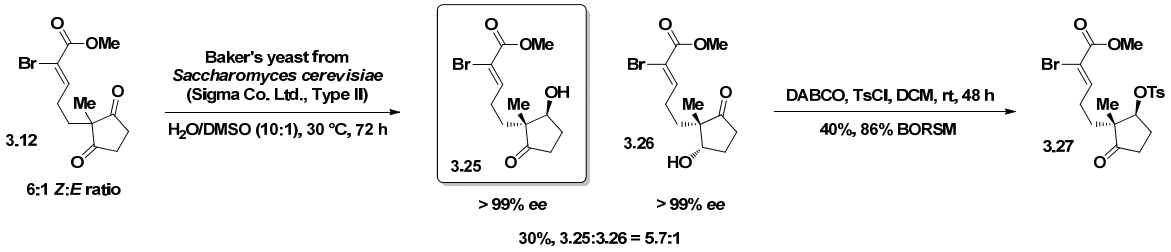

Scheme III.11 Unscalable enzymatic desymmetrization.

Snowden and co-workers conducted a methodical investigation on the achiral monoreduction of 2,2-disubstitutedcyclopentane-1,3-diones in studies toward the xenicane family.[23] Their best conditions ($NaBH_4$, DME, -60 °C) applied to similar substrates gave poor yields of the desired diastereomer, suggesting that steric hindrance and diastereoselectivity are intimately related in these systems.

3.5 Stability of the Key Intermediate

A TLC sample of **3.6** in $CDCl_3$ in a capped NMR tube was left standing on a laboratory bench at room temperature. Under these acidic and aerobic conditions, the strained *E* olefin underwent slow spontaneous epoxidation to *trans*-epoxide **3.28** (Scheme III.12). This type of process has precedent in a xenicane natural product isolation report.[24] Upon stirring open to air in chloroform, deoxyxeniolide B (**3.29**) was gradually oxidized to **3.30** and **3.31**.

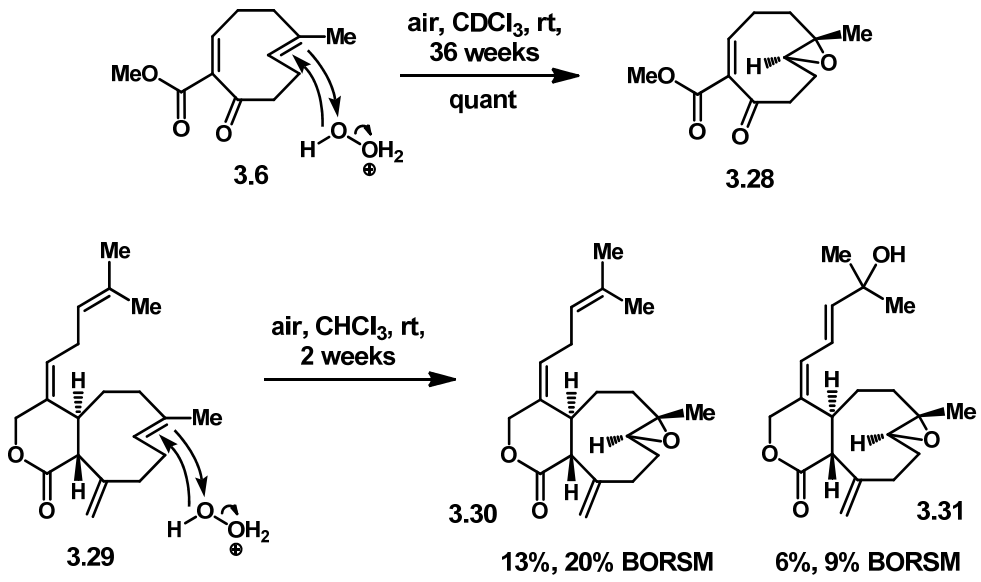

Scheme III.12 Spontaneous epoxidation of strained *E* olefins and proposed mechanism.[24]

Mechanistically, we propose that this is a concerted epoxidation process since any stepwise mechanism involving radicals, for example triplet oxygen, would lead to the unobserved thermodynamic *cis*-epoxide (2 kcal/mol more stable).[6] Hydrogen peroxide is produced in the atmosphere when UV light reacts with oxygen in the presence of moisture, and is present in the air at low levels (ppb to ppm). It is a poor oxidant in the absence of

activation. Mild base (aq. sodium bicarbonate)-activated H_2O_2 is used to epoxidize electron-deficient alkenes such as acrylic acid,[25] so it is plausible that mild acid-activated H_2O_2 epoxidizes electron-rich alkenes such as these. To our knowledge there is no available data on the reactivity of protonated hydrogen peroxide, but it is known to be a highly active oxidant in the gas phase.[26]

These data implicitly question the authenticity of many reported xenicane natural products that contain the *trans* epoxide – these may not be natural in the sense that the parent organism did not install the epoxide. Due to this intrinsic reactivity, prolonged storage of **3.6** and subsequent nine-membered compounds was avoided.

3.6 Racemization Kinetics of the Dissymmetric Platform

The fragmentation approach to xenicane synthesis converts point chirality to conformational chirality. Interestingly, nine-membered rings may undergo conformational ring flipping. Complete ring flipping of cyclononadienone-carboxylate-methyl ester **3.6** effects racemization of this atropisomeric intermediate (Scheme III.13). Cyclononenes are thought to racemize via a two-step mechanism.[4a] The prototype descarboxymethyl compound **3.5** was previously found to racemize with a half-life of 31.9 h. Based on MM2 molecular dynamics simulations, we suspected that methyl ester **3.6** may not undergo complete ring flip. If the mechanism for racemization requires the enone double bond substituents to flip inside the ring, the carboxylate moiety would be too bulky to fit and any enantiopurity in **3.6** would be preserved indefinitely.

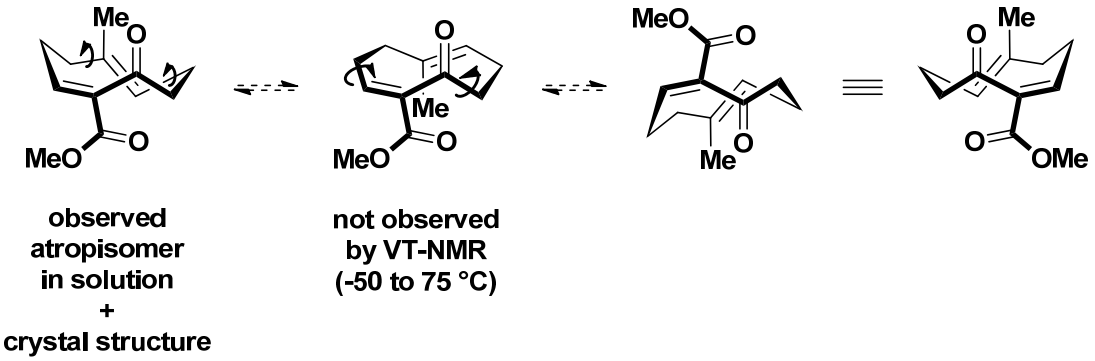

Scheme III.13 Conformational interconversion (racemization) possible?

My colleague Huan Wang obtained enantioenriched **3.6** via kinetic resolution of the racemic material (Scheme III.14). Unexpectedly, the data indicate that **3.6** racemizes much faster than **3.5** (~4 h vs. ~32 h, Figure III.5). The ester group appears to destabilize the ground state of **3.6** relative to the descarboxymethyl compound.[27] The energy barrier of the rate-determining step of racemization of **3.6** appears to be lower, assuming that the racemization mechanisms are the same. Unfortunately, the rapid deterioration of *ee* limits the direct use of this intermediate as an enantiopure scaffold.

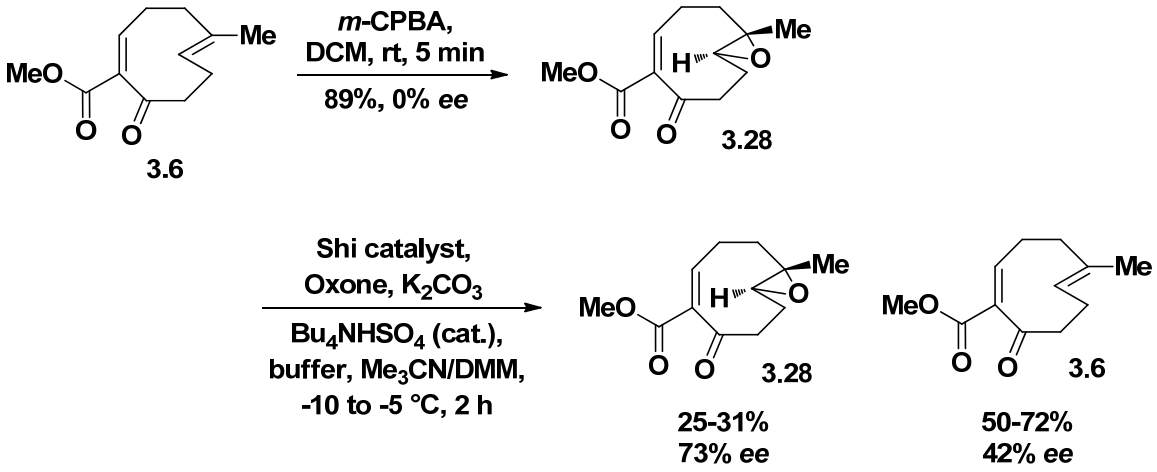

Scheme III.14 Kinetic resolution of 3.6.

time (h)	ee (%)
1	41.6
2	34.0
3	29.6
4	23.7
5	19.9
6	16.6
7	13.8
8	11.6

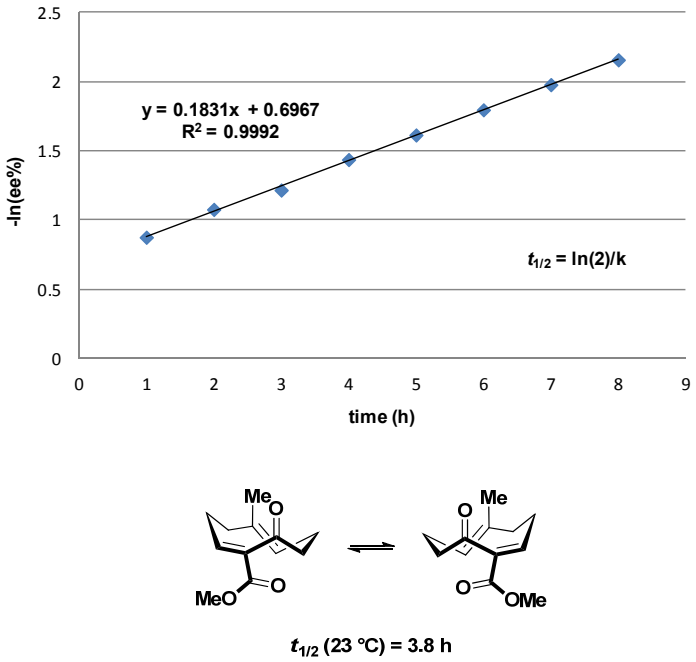

Figure III.5 First-order racemization kinetics and computed half-life of 3.6.[28]

3.7 Enone Reactivity

The reactivity of enones in conjugate addition reactions depends on both electrophilicity and sterics. α,β-unsaturated esters by themselves are generally poor electrophiles. For example, acrylic ester derivatives do not react with standard organocuprates,[29] and use of Lewis acids or high temperatures improves yields on a substrate-dependent basis.[30] Analysis of the ^{13}C NMR chemical shifts of β-carbons of similar enones provides a reasonable comparison of their relative electrophilicity (Figure III.6). According to this data, our enone **3.6** is not nearly as electrophilic as the corresponding cyclohexenone, in which the olefin is also in conjugation with the ketone. Indeed, ^{13}C NMRs predict that **3.6** is only slightly more reactive than methyl tiglate. The ketone in **3.6** provides a relatively small inductive effect which we found to be critical, as described below. Conjugate additions also become increasingly disfavored as substitution

around the olefin increases.[31] The sterics of trisubstituted α,β-unsaturated esters are therefore another obstacle.

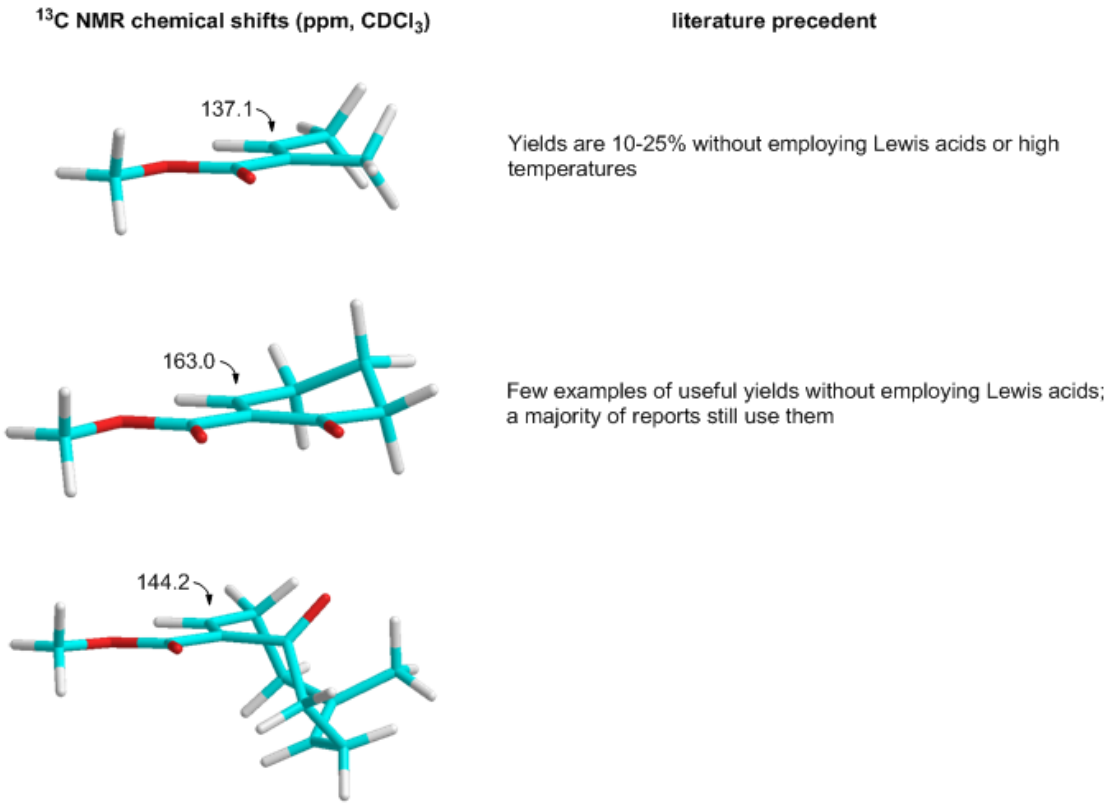

Figure III.6 ^{13}C NMR analysis of enone electrophilicity and conjugate addition precedent.[32]

Despite these challenges, we maintained that the methyl ester was a simple, relevant, and effective activating group for total synthesis. The reactivity of the bicyclic precursor limited the types of functional groups that could occupy the vinyl position during fragmentation. Conversion of **3.6** to a diketone would have certainly increased enone reactivity, but would lead to other problems such as functional group differentiation. Although sulfones are also better electrophiles, the resulting products are not immediately useful intermediates, and esters are better conjugate acceptors than nitriles.

3.8 Stereoselective Syntheses of Xeniolide and Blumiolide Congeners

Key intermediate **3.6** initially appeared resistant to conjugate addition. Preliminary studies gave either no reaction or decomposition. These included sodium methanethiolate (20% aq., THF/MeOH, -78 °C to rt), dimethyl malonate (NaH, THF, 0 °C to rt), higher order butyl cuprate ($Bu_2Cu(CN)Li_2$, THF, -78 to 0 °C), and $BF_3{\cdot}OEt_2$ activated butyl cuprate ($Bu_2Cu(CN)Li_2{\cdot}BF_3$, THF, -78 to 0 °C). Lower order cuprates are known to be unreactive, and simple cuprates add preferentially in the undesired 1,2-fashion.

After a successful model conjugate addition of the higher order butyl cuprate to *in situ* TMS-protected tiglic acid (*i.* *n*-BuLi, TMSCl, THF, 0 °C, 30 min; *ii.* TMSCl, -78 to 10 °C, 30 min; *iii.* $Bu_2Cu(CN)Li_2$, THF, -78 °C to rt, 1 h, quant crude yield, 1.9:1 *dr*), we applied these conditions to carboxylic acid **3.19** (Scheme III.15).[33] With great care working on small scale, stoichiometric redistilled TMSCl effectively activated both the cuprate and nine-membered enoate,[34] and the product of cuprate addition-decarboxylation, **3.32**, was isolated after FCC. Unreacted starting material and silylated starting material decomposed on the column. Serendipitously, **3.32** was one of our original targets from the descarboxymethyl scaffold **3.5**.

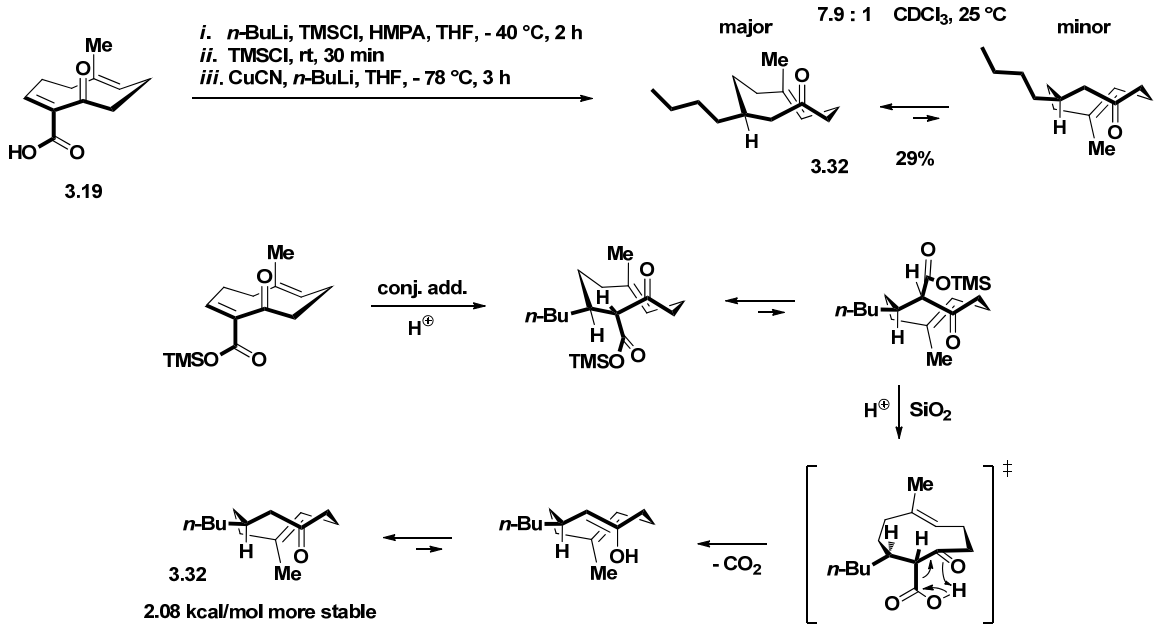

Scheme III.15 Lewis acid-mediated silylation-cuprate addition-decarboxylation.[6]

It appeared that the product of conjugate addition was acid sensitive, and it decarboxylated on TLC and silica gel. The TMS group was presumably labile. β-keto acids are well known to undergo spontaneous decarboxylation under basic conditions. However, TMS-protected β-keto acids often require vigorous conditions (HCl, MeOH, 100 °C) to convert to the ketone.[35] Only the proposed minor conformer of the conjugate addition product can adopt the six-membered transition state required for concerted decarboxylation.

Ketone **3.32** was our first nine-membered product with saturation in the enone position. We were delighted to find that slow ring flipping occurs in compounds with this hybridization pattern, and that the major and minor conformers are observable by NMR. The slow exchange rates (a few seconds up to a minute) between conformers give two sharp, distinctly separated NMR resonances for most protons and carbons. Indeed, many of

the natural products exist in more than one stable conformation, further complicating their structure determination and synthesis. These equilibria appear to depend on the balance between torsional and transannular strain. Approximately 2 kcal/mol is the maximum energy difference that can exist between conformers in solution in order to observe the minor one by NMR. Although we do not know the mechanisms of conformational inversion, we believe they are stepwise processes since some natural products exist in a half-flipped form.[36]

VT-NMR experiments (8 to 48 °C) on **3.32** revealed peak shifting but no broadening or significant change in conformational equilibrium. While the yield of this reaction was low, it was deemed unnecessary to optimize. This was a breakthrough reaction: we had found conditions suitable for adding carbon nucleophiles. We proceeded working with methyl ester **3.6** to avoid decarboxylation.

The TMSCl-mediated higher order cuprate procedure granted access to several xeniolide congeners. 5 equivalents of cuprate were found to be optimal on small scale. Larger excess of cuprate resulted in complex mixtures of products. Butyl cuprate addition to methyl ester **3.6** proceeded cleanly to afford **3.33** in good yield (Scheme III.16). At -78 °C, the desired *trans* stereochemistry of the α and β protons was set. This configuration was exclusive in both conformations of the product (see Experimental). The two conformers appear as overlapping interconverting spots on 2D TLC. The α-carbon is epimerizable under basic conditions above 0 °C.

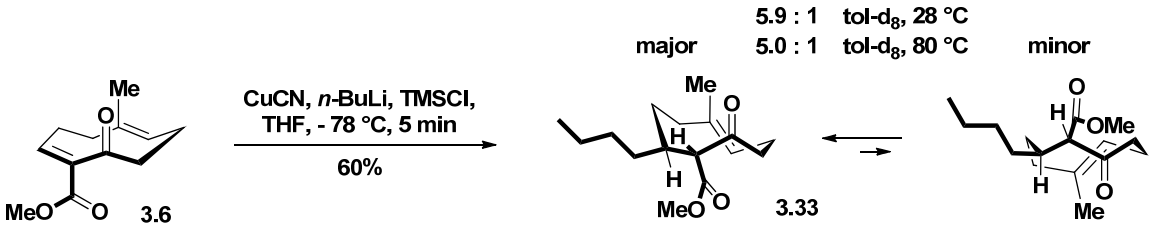

Scheme III.16 Setting two stereocenters via butyl cuprate addition.

Extensive NMR analysis of this complex product was required to confirm its structure unambiguously and to use it as a model for characterization of future compounds. Many of the products from this point forward were characterized in C_6D_6, which gave improved resolution of proton signals compared to $CDCl_3$. The two species of **3.33** in solution were differentiated by 1D TOCSY spectra. The coupling constants of the α-protons (10.0 Hz) suggested the *trans* stereochemistry, but the absolute configuration of the stereocenters was proven by intramolecular and transannular NOEs. The existence of two conformers of a single diastereomer was proven by DPFGSE-NOEs, which revealed an exchange between conformers. In other words, selective irradiation of a proton from one conformer gave rise to an inverted signal from the same proton in the other conformer. Additionally, a change in conformational equilibrium was observed when analyzing the sample in different deuterated solvents. The upfield shift of the α-proton of the major conformer indicated it was *syn* to the ketone, while the downfield shift of this proton in the minor conformer indicated it was *anti* to the ketone. This is the anistropy effect of the ketone. Comparison of the NOE-derived proton space proximities with ground state computational modeling[6] established the 3D structures as shown (Figure III.7).

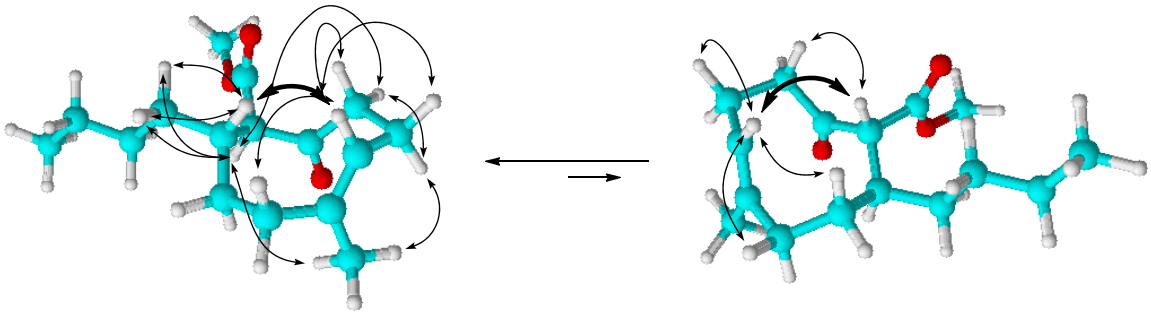

Figure III.7 NOE-derived structures of the major and minor conformers of 3.33.[6]

VT-NMR experiments up to 90 °C revealed more about conformer dynamics. Proton chemical shift changes and broadening at higher temperatures were consistent with a faster exchange of conformers. For example, both trisubstituted olefin and methyl signals merged. Upon heating, the α-proton signal of the major conformer moved farther upfield (more *syn*), while this proton signal of the minor conformer moved farther downfield (more *anti*), suggesting that in both conformers these protons moved to positions that are more parallel to the ketone.

The yield of this product was improved to 72% by employing CuI and tributylphosphine additive (Scheme III.17). With this cuprate procedure, the corresponding methyl addition product **3.34** was synthesized in 82% yield. Both conformers of these products were reactive in subsequent derivatization reactions (Scheme III.18). Sodium borohydride reduction of ketone **3.33** gave alcohol **3.35** as the major diastereomer. The major conformer of **3.33** is apparently reduced faster. Epoxidation of **3.34** with *m*-CPBA gave a 1:1 mixture of diastereomers (**3.37** + **3.38**). Reagent delivery appears to occur exclusively from the outside of the ring, and the minor conformer of **3.34** is apparently epoxidized faster.

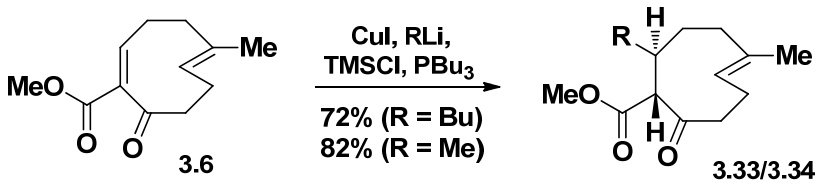

Scheme III.17 Optimized alkyl cuprate conjugate additions.

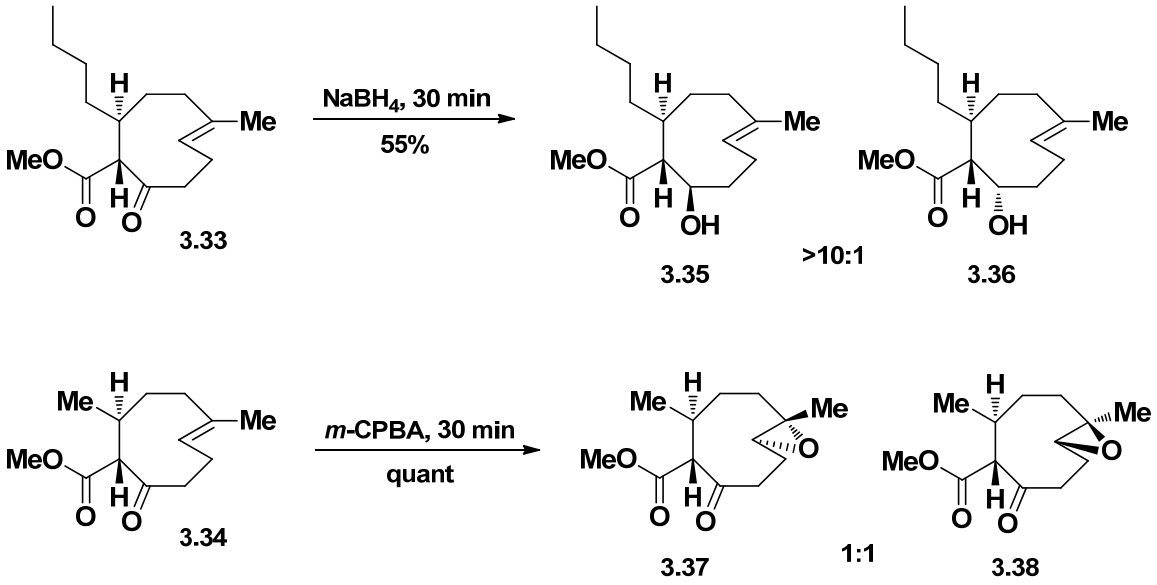

Scheme III.18 Derivatization of cuprate addition products.

Exposure of **3.33** to high temperature microwave irradiation induced isomerization of the endocyclic *E* olefin to the thermodynamic *Z* olefin (**3.39**, Scheme III.19), relieving the distortion from planarity of the *E* system. No change in the ^{1}H NMR of **3.33** was observed until heating the DMSO-d_6 solution to 150 °C. Amongst other changes to the spectrum, the olefinic proton signal transformed from a doublet of doublets to a triplet characteristic of the *Z* olefins in the xenicane family. This reaction therefore represents an entry to blumiolide congeners such as **3.39**. *Z* olefin-containing nine-membered rings are also known to exist in multiple stable conformations.[37] This isomerization was observed

during structural studies of xenicane isolates, where the temperature required for isomerization was substrate-dependent.[38]

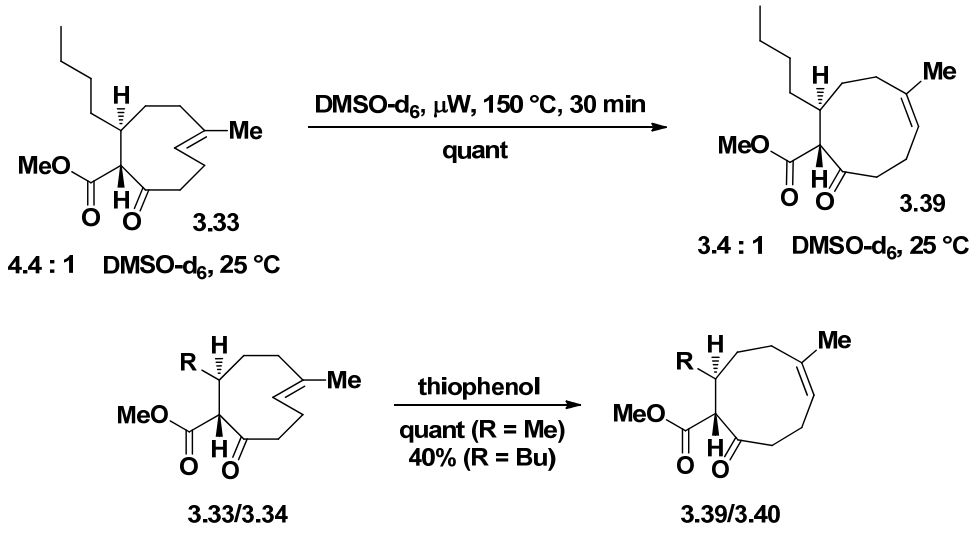

Scheme III.19 Thermal and radical-induced *E* to *Z* isomerizations.

Thermal isomerization of the *E* olefins was difficult to reproduce (100-150 °C for 30-60 min), leading to incomplete conversion and/or degradation of starting materials. The transformations were effected more cleanly by the use of thiophenol, which presumably induces isomerization via reversible addition of the corresponding thiyl radical.

Higher order phenyl cuprate addition to **3.6** also proceeded smoothly (Scheme III.20). Extended reaction time gave the TMS enol-ether **3.42**, which exists as a single conformer. This substance was slowly hydrolyzed back to **3.41** on 2D-TLC and silica gel. Curiously, the *E*-enol ether was isolated. A number of xenicane natural products have an alkene in the same position as this enol with an exocyclic functionalized carbon.

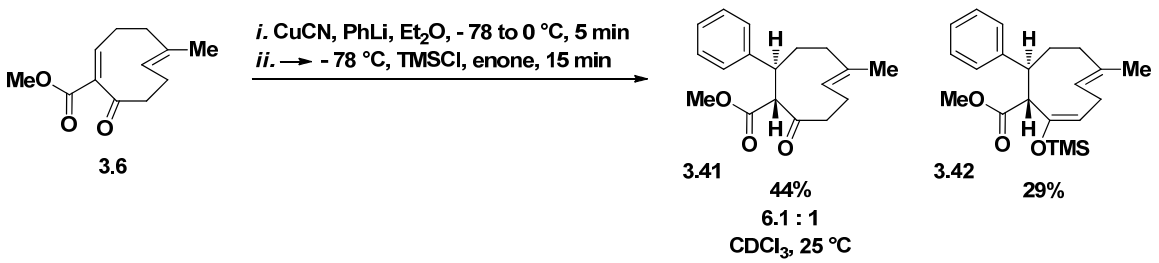

Scheme III.20 Phenyl cuprate addition and trapping of the less stable enolate.

With one equivalent of Tebbe reagent, the sterically unhindered ketones of **3.33** and **3.41** were selectively olefinated in the presence of the methyl esters, furnishing *exo*-methylene xenicane analogues **3.43** and **3.44** in very good yields (Scheme III.21). The conformational equilibria for these homologues were very similar. Wittig reagents were deemed inappropriate for these transformations due to their basicity. The Tebbe reagent, in contrast, does not epimerize α-carbons.

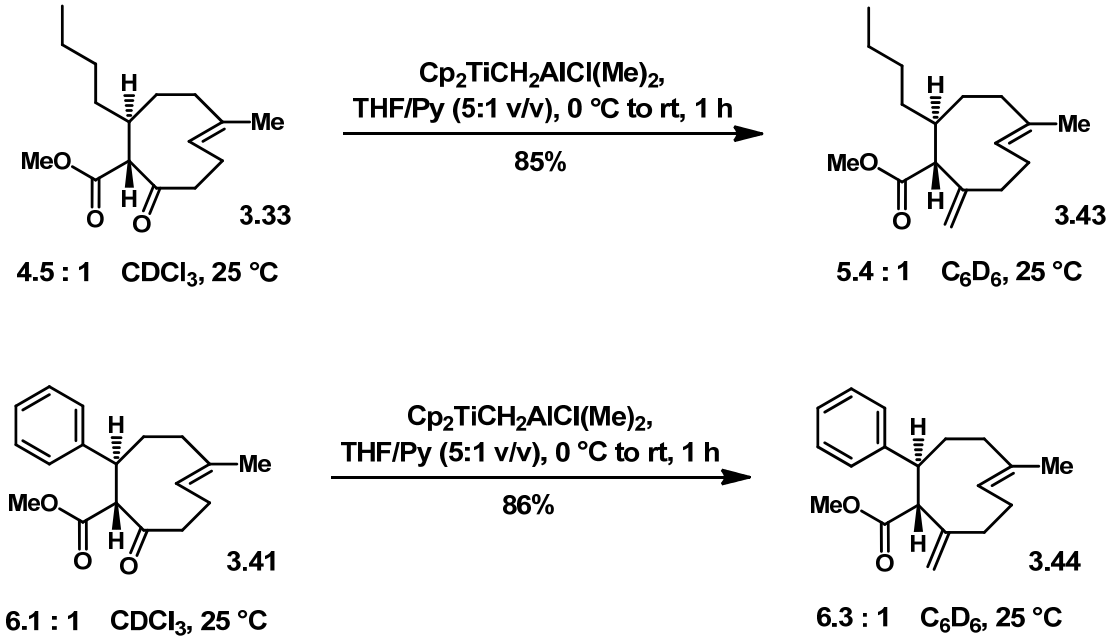

Scheme III.21 Chemoselective Tebbe olefinations to *exo*-methylene xeniolide analogues.

Having incorporated the phenyl substituent into our scaffold, we wondered if an *ortho*-substituted aromatic group could be added as well. This goal served two purposes: 1) to determine the feasibility of adding a nucleophile with sterics of the most challenging side chain targets in the xenicane structure space (see next section) and 2) to access more analogues of potential use in medicinal chemistry. Attempted addition of 2-iodotoluene under reductive Heck conditions ($Pd(OAc)_2$, AcOH, TEA, 65 °C) resulted in a complex mixture of products. Attempted addition of the unprecedented higher order cuprate derived from lithiated 2-iodotoluene to methyl acrylate gave no reaction. Similar reactions with methyl tiglate have been reported to give poor yields (< 20%) due to sterics of the nucleophile.[39] Higher order alkyl cuprate reactions with epoxide **3.28** gave low yields of epoxide-opened products ($LiCuMe_2$, THF, TMSCl, -78 °C, 30 min; $LiCuBu_2$, THF, TMSCl, -78 °C, 30 min).

In the interest of medicinal chemistry, heteroatom nucleophiles were also incorporated into the nine-membered scaffolds (Scheme III.22). Under neat conditions, both pyrrolidine and thiophenol added in a conjugate fashion to enone **3.6**, albeit in low yields. In the former reaction, excess base induced epimerization of the α carbon *in situ*, producing a mixture of two diastereomers and four conformers. In the latter reaction, isomerization to the *Z* olefin also occurred. Addition of thiophenol to epoxide **3.28** proceeded in quantitative yield.

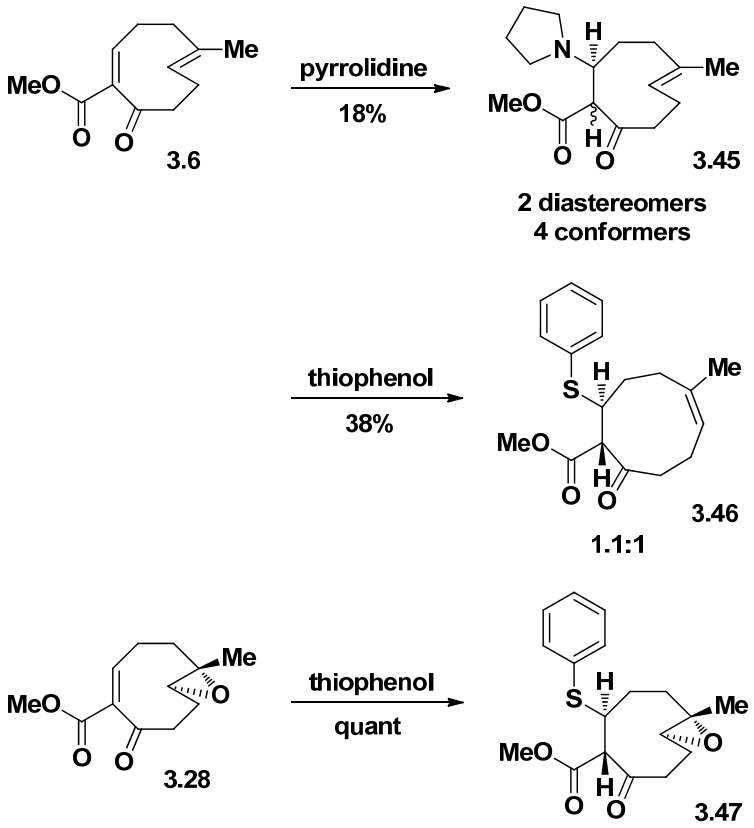

Scheme III.22 Neat conjugate addition of heteroatom nucleophiles.

3.9 Divergent Syntheses of Terpene Side Chains and Attempts at Use

Once we demonstrated conjugate addition of an sp^2-hybridized carbon nucleophile to **3.6**, we were poised to target several natural products of the xeniolide class (Scheme III.23). These and the lactone equivalent, deoxyxeniolide B (**3.29**), appear to be biosynthetic precursors to many xenicanes of higher oxidation state (mono and diepoxides, diols, and products of transannular chemistry), so we anticipated accessing the entire suite of natural products via this integrated route.

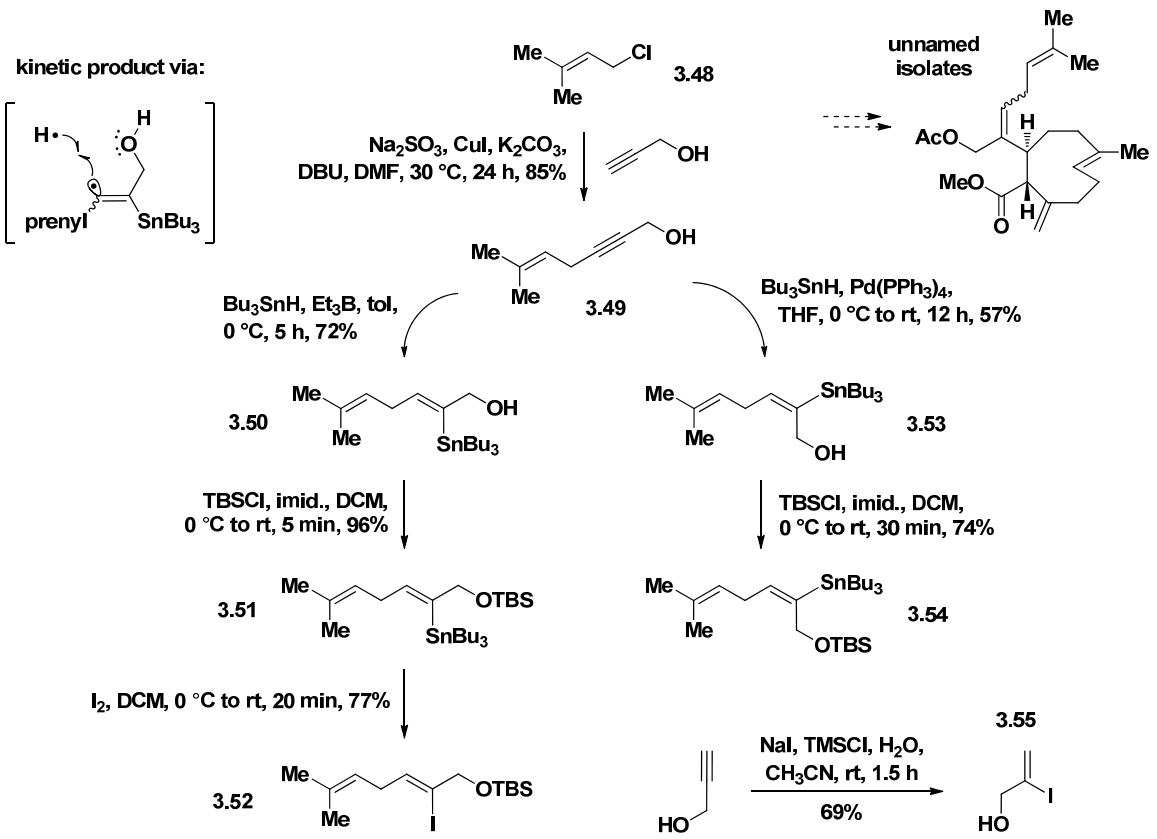

Scheme III.23 Divergent syntheses of side chains and model iodo-ol.

We designed two isomeric terpene side chains to be added 1,4- to **3.6** as vinyl cuprates. They were prepared in no more than four steps each. Alkynol **3.49** was obtained from the mild Cu(I)-catalyzed regioselective coupling of prenyl chloride (**3.48**) and propargyl alcohol promoted by weak inorganic base.[40] The yield of **3.49** was optimized by increasing the reported CuI catalyst loading to 10 mol%, sodium sulfite to 1 equiv. for suppression of oxidative dimerization, DBU to 1 drop per mmol of propargyl alcohol, and reaction time to 24 h. Attempted stereospecific hydroxyl-directed *trans*-hydroalumination-iodinations, pioneered by Corey,[41] gave complex mixtures of products under a variety of conditions. The intramolecular reduction was too slow: after 48

h only 64% conversion to the vinylic aluminum intermediate was observed. Unable to make vinyl iodides directly, we turned to the corresponding vinyl stannanes.

Radical-mediated hydroxyl-directed hydrostannylation of **3.49** using AIBN as the radical initiator produced *Z* vinyl stannanol **3.50** stereoselectively.[42] The structure of **3.50** was confirmed by the large ^{119}Sn-^{1}H coupling constant (124 Hz)[43] and key NOE experiments (see Experimental). Though this kinetic product was the major product (62% yield), it was very difficult to separate from the byproducts. We thought that by substituting AIBN with triethylborane, we could generate radicals at a much lower temperature and increase selectivity.[44] Indeed, the conditions shown here produced **3.50** in a better yield. TBS protection and iodination provided two possible precursors of vinyl anions. Pd(0)-catalyzed *syn* hydrostannylation of **3.49** led to the *E* vinyl stannanol variants.[45] Lower yields were obtained using $Pd(PPh_3)_2Cl_2$ as the Pd(0) source. Certain stannanes underwent proteodestannylation on silica gel, so column chromatography was carried out using neutral alumina. The vinyl iodides decomposed within hours after isolation, so they were freshly prepared before use.

We were unable to generate synthetically useful vinyl anions from these intermediates. TMSCl-mediated conjugate additions were attempted with nine-membered platform **3.6** as well as methyl acrylate, methyl tiglate, and cyclohexenone as model enones. TBS-protected *Z* vinyl stannane **3.51** appeared inert to Li-Sn exchange (excess MeLi or *n*-BuLi, THF or Et_2O, -78 °C to rt). Transmetallation processes with similar sterically hindered stannanes have been found to be thermodynamically disfavored.[46] Li-Sn exchange was accomplished in the presence of HMPA, but was accompanied by

silyl migration (Scheme III.24). Direct transmetallation with CuCN (4Å MS, DMF, 60 °C) was achieved but gave only proteodestannylated product.

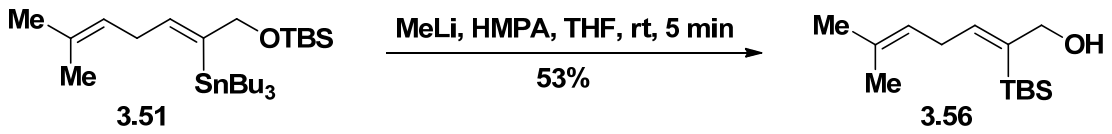

Scheme III.24 Intramolecular trapping of an *in situ* vinyl anion.

TBS-protected *Z* vinyl iodide **3.52** underwent facile Li-I exchange (excess *t*-BuLi, Et_2O, -78 °C). However, conversion to the cuprate followed by exposure to the conjugate addition substrate failed to give the desired product. Trapping experiments with CD_3OD indicated that the vinyl anion was quenched prior to addition of the deuterated solvent. Cooled cannula techniques were used but did not improve the outcome.

We switched our focus to the *E* vinyl stannanes in order to eliminate the issue of sterics in the nucleophile. TBS-protected *E* vinyl stannane **3.54** was very sluggish to Li-Sn exchange, suggesting the bulk of the silyl group was also problematic. Treatment of the free alcohol **3.53** with excess *n*-BuLi between -78 and -35 °C gave complete conversion to the dianion, but quenching with CD_3OD resulted in only 15% deuterium incorporation in the vinyl position. Trapping the vinyl anion with redistilled benzaldehyde was also ineffective. When the exchange reaction was in THF-d_8, 39% deuterium incorporation in the vinyl position was observed. Evidently, the dianion was abstracting deuterium from the solvent.

Before abandoning this approach, we conducted a model study with readily available iodoalcohol **3.55**, the simplest moiety that we aimed to add as a dianion. Application of Overman's optimized procedure[47] using 2-thienyl(cyano)copper lithium[48]

gave no conjugate addition product. Overman reported poor yields (< 40%) of the cuprate addition of similar iodoalcohols to cyclopentenone, an enone that is more electrophilic and less sterically hindered than **3.6**. Overman et al. suggested that allene generation from the vinyl anion intermediate (Scheme III.25) is the major problem.

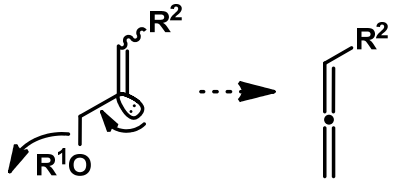

Scheme III.25 Allene formation: presumed flaw of the vinyl anion conjugate addition strategy.[48]

Refocusing our efforts on deoxyxeniolide B (**3.29**), we reasoned that the carboxylate handle of the nine-membered ring could facilitate an intramolecular conjugate addition and circumvent the problems associated with the intermolecular approach. *Z* vinyl iodoalcohol **3.57** was synthesized and coupled to crude carboxylic acid **3.19** (Scheme III.26). Baldwin's rules indicate that 6-*endo-trig* cyclizations are favorable,[49] and computational modeling demonstrated that this vinyl anion should be able to approach the convex face of the β-carbon with an angle of 109°. Iodoester **3.58** is two theoretical steps away from deoxyxeniolide B.

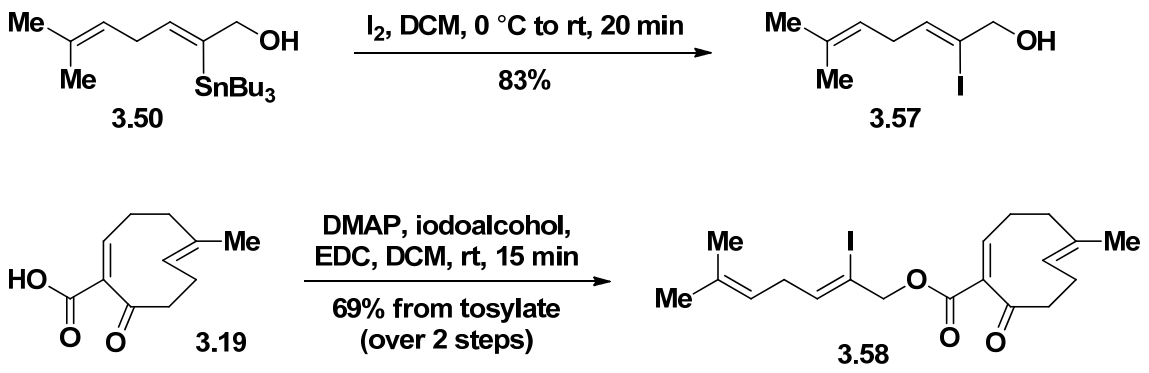

Scheme III.26 Synthesis of an intramolecular conjugate addition substrate.

Lithium-halogen exchange conditions (*t*-BuLi, TMSCl, HMPA, THF, -78 °C to rt) led to decomposition of **3.58**. Attempted anionic reductive Heck reactions ($Pd(OAc)_2$, Ph_3P, TEA, 0 to 65 °C) produced an unknown product which appeared polymeric by ^1H NMR. Our optimized NHK protocol had no detectable effect on the substrate. Subsequent heating to 100 °C effected Cope rearrangement of the 1,5-diene, yielding functionalized cyclopentanone **3.59** as the thermodynamic product (Scheme III.27). The most surprising feature of this transformation was the robustness of the iodide moiety. Even at elevated temperature, the trisubstituted alkenylhalide failed to undergo Ni(0) insertion. The Cope rearrangement is consistent with Dr. Yue Zhang's observations with **3.5**.[4a] Most recently, we effected Cope rearrangement of methyl ester **3.6** by heating it to 150 °C with microwave irradiation (not shown).

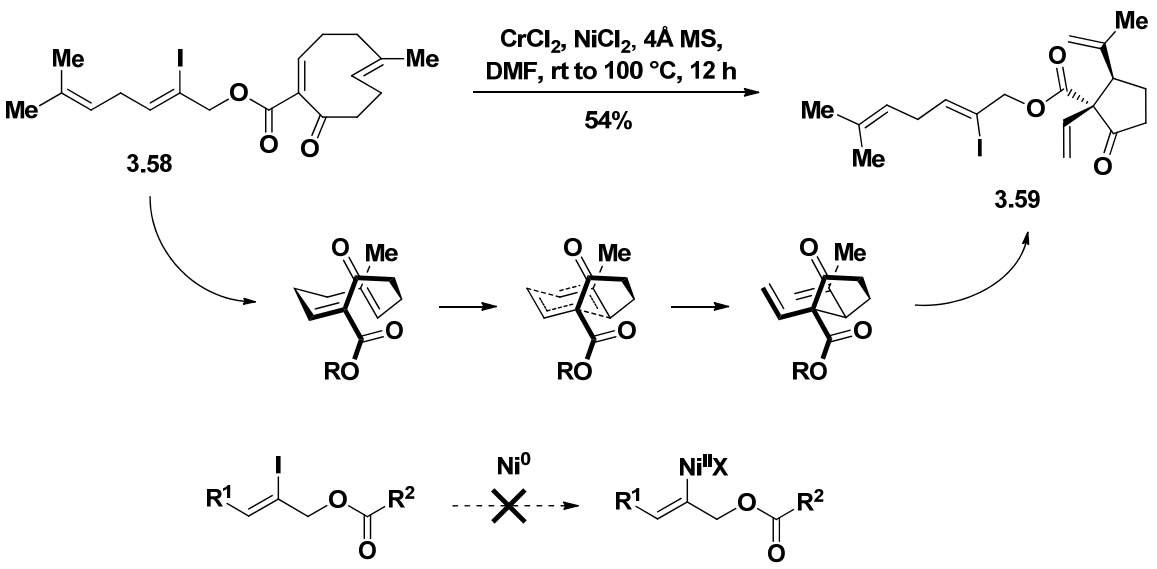

Scheme III.27 Cope rearrangement revisited: temperature sensitivity.

We turned to a mild radical conjugate addition approach,[50] which has been used to make 6-membered rings intramolecularly.[51] In our attempt to effect the vinyl radical cyclization with Bu_3SnH/Et_3B at high dilution and low temperature, we serendipitously constructed the *trans* hydrindanone system **3.60** in excellent yield (Scheme III.28). This corresponds to the CD ring system of 18-methoxy-18-oxo-17-ketosteroids. The structures of the bicyclic allylic esters were determined unambiguously by gHMBC and NOE correlations (see Experimental). Thus, we converted the conformational chirality of the nine-membered ring back to point chirality, generating four stereocenters with complete selectivity.

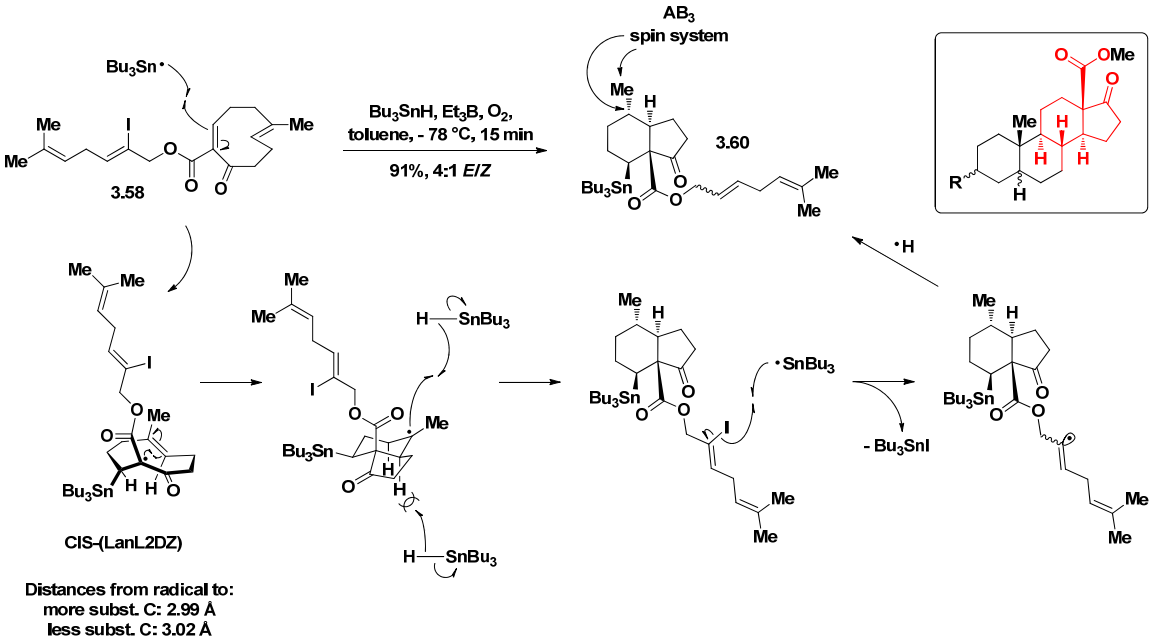

Scheme III.28 Conjugate addition-transannulation-dehalogenation radical chain reaction to the steroid CD ring core.

One plausible mechanism begins with the strongly nucleophilic tributyltin radical adding 1,4- to the enone from the top face. This generates a stabilized electron-deficient radical intermediate with the computed conformation shown. The radical, equidistant from both carbons of the electron-rich olefin across the ring, regioselectively adds to the less substituted carbon to give the *trans* ring junction and the more stable tertiary radical. The stereocenter at C-8 is set in a manner consistent with the known preference for axial attack in conformationally-stabilized cyclohexyl radicals (a torsional and kinetic effect).[52] Deiodination, vinyl radical isomerization, and reduction leads to the final product mixture. Kinetic conditions appear to give rise to a thermodynamic product. This is a new, indirect, and unconventional approach to steroid CD ring synthesis. Unfortunately, such radicals are strategically problematic for xenicane total synthesis.

Methyl ester **3.6** was subjected to the radical chain reaction conditions, and steroidal methyl ester **3.61** was obtained in a similarly impressive yield (Scheme III.29). We attempted to cleave the tin moiety from the six-membered ring under requisite acidic conditions, but no proteodestannylation was achieved. Stannanes bonded to sp^3-hybridized carbons are much more stable to acid than those attached to sp^2 carbons. Furthermore, this neopentyl stannane is sterically hindered.

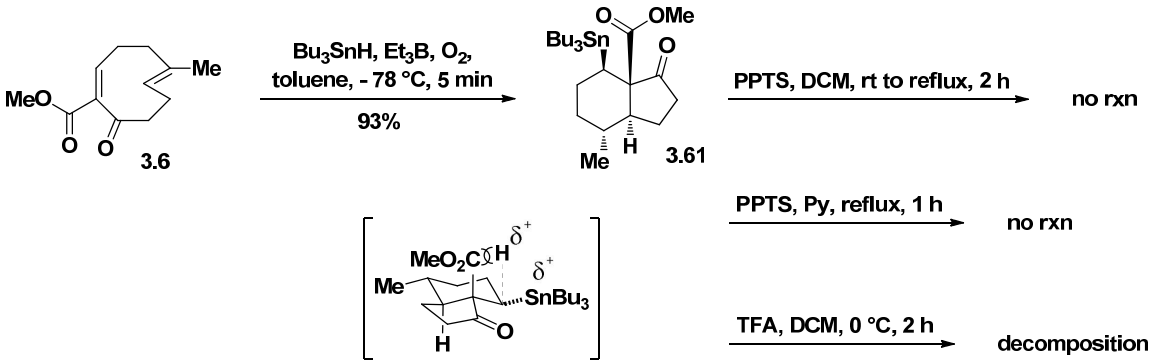

Scheme III.29 Steroidal methyl ester synthesis and attempted proteodestannylations.

In an effort to access 2,6-cycloxenicane structure space (Scheme II.9),[53] the radical chemistry was also applied to *trans*-epoxide **3.28**. This yielded a mixture of products with the enone intact. Nucleophilic radicals apparently open the epoxide before adding 1,4- to the enone.

No reaction conditions were found to effect the desired 6-*endo*-*trig* cyclization of **3.58**. There are no previously reported examples of such lactone formations, probably due to the energy barrier to rotation of the ester C-O single bond (10-15 kcal/mol, Scheme III.30).[54] Resonance delocalization gives it partial double bond character. Since the thermal energy available at room temperature is only 6 kcal/mol, much more energy must be

supplied to such a substrate. In the case of **3.58**, the Cope rearrangement competes at high temperature. Also, we identified $A_{1,3}$-strain in the transition state leading to the desired product. Alternative synthetic routes to enable cyclization were considered, but no gratifying end to a natural product was foreseen. We therefore proceeded to a new intermolecular conjugate addition approach.

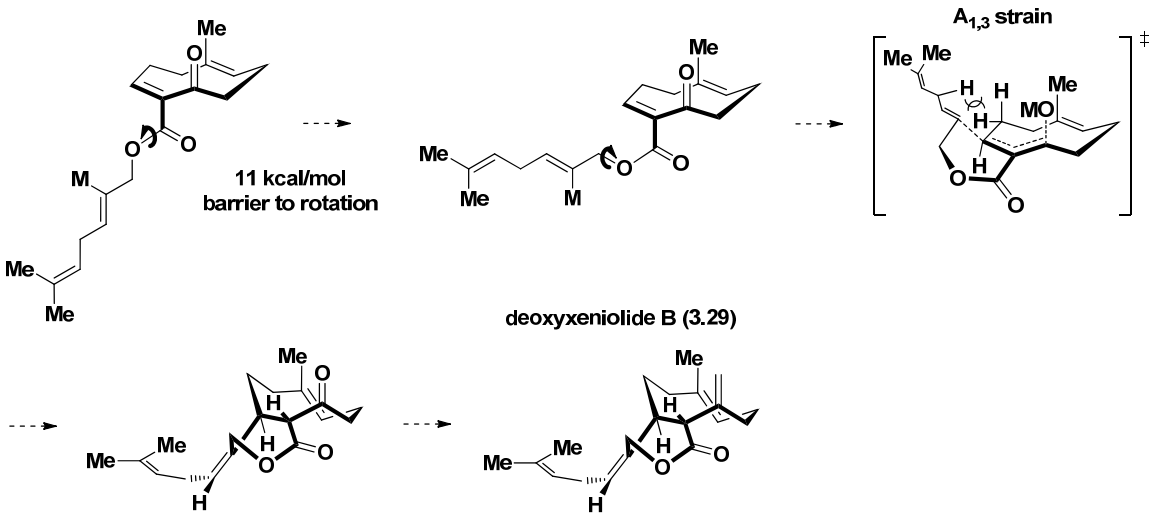

Scheme III.30 Two steps from deoxyxeniolide B: dead-end intermediate (M = metal).[6]

3.10 Conjugate Additions of Active Methylene Compounds

We envisaged adding a terpene side chain as a 1,3-dicarbonyl compound, which would then be manipulated further en route to a natural product (Scheme III.31). Previous attempts to add dimethyl malonate under standard basic conditions were met with failure (see section 3.8), but we were now determined to add this model nucleophile. A comprehensive literature search led us to an unusual procedure that reportedly effected otherwise sluggish Michael additions to disubstituted enones.[55] This simple, mild, water-insensitive, solvent-free method employed catalytic $LiClO_4$/TEA. Pleasingly, these

conditions overcame the disfavored combination of a bulky nucleophile and hindered electrophile, and dimethyl malonate was added to **3.6** (Scheme III.32). The product was initially assigned as **3.62**. This is the first example of addition to a trisubstituted enone with this methodology.

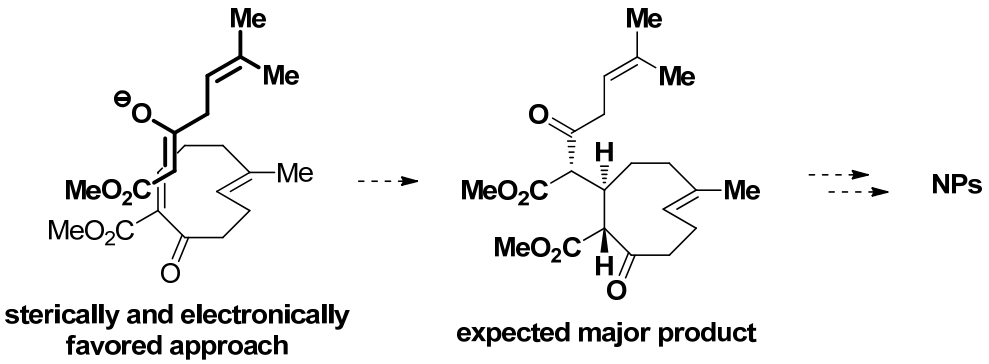

Scheme III.31 Active methylene conjugate addition strategy to xenicane natural products.

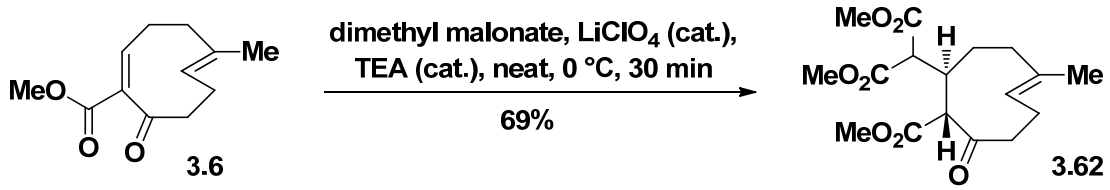

Scheme III.32 Mild, catalytic, water-insensitive, solvent-free Michael addition: initial product structure assignment.

How does this Michael addition work? The source of nucleophile, in this case dimethyl malonate, is the solvent. $LiClO_4$, although apparently insoluble, seems to serve to activate the enone. This may occur on the surface of the lithium salt. Saidi and co-workers noted that coordinating solvents, such as Et_2O, which are known to moderate the Lewis acidity of $LiClO_4$, drastically reduce reactivity of these conditions.

Having added an achiral nucleophile, the next goal was to add methyl acetoacetate and study the diastereoselectivity at the new chiral center. Based on sterics and electronics, we expected the asymmetric enolate to approach principally in the manner depicted in Scheme III.31. No reaction with methyl acetoacetate was observed at 0 °C, the standard temperature reported for the methodology. Indeed, no examples of this weaker carbon nucleophile had been published as part of this methodology.

Initially, we were pleased. Stirring the neat mixture at room temperature (Scheme III.33) resulted in the formation of several products. As the starting material was further consumed, both the major and minor products continued to react. No further reaction progress was noted after 36 h. Disappointingly, the structures of the major inseparable products, *trans*- and *cis*-substituted cyclohexenones **3.63**, were deduced from gHMBC and NOE correlations (see Experimental). ^{1}H NMR chemical shifts of both diastereomers were established on the basis of a series of 1D TOCSY spectra in conjunction with long-range HMBC correlations.

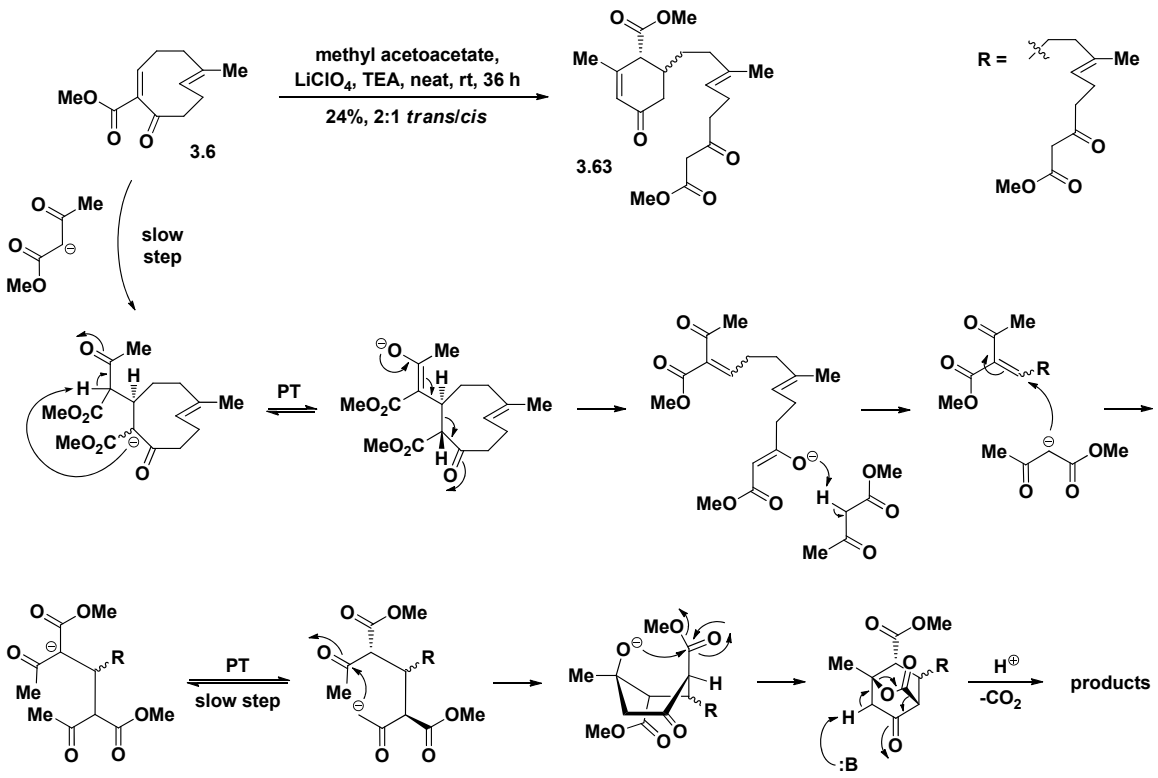

Scheme III.33 Michael-retro-Michael-Michael-aldol-lactonization-decarboxylation cascade.

How do these cyclohexene derivatives form? We reason that conjugate addition of the enolate of methyl acetoacetate is relatively slow. Under basic conditions, the enolate of the desired product is in equilibrium with the enolate of the side chain. Proton transfer is followed by irreversible strain-releasing retro-Michael ring opening. A second equivalent of the enolate of methyl acetoacetate adds to the new doubly activated enone, a better electrophile than **3.6**. The resulting symmetrical thermodynamic enolate undergoes slow proton transfer to a kinetic enolate. The two stereocenters in the products are set during an intramolecular aldol addition, which is followed by lactonization and decarboxylation. In an effort to improve the reaction rate and yield, the temperature was increased to 65 °C.

This did not appear to increase the rate, though it did decrease stereoselectivity of the aldol addition (65 °C, 14 h, 10%, 1.2:1 *trans*/*cis*).

The latter portion of this cascade reaction is a modification of the Hagemann's ester synthesis. Hagemann's ester was first prepared and described in 1893 by Carl Hagemann.[56] The motif has been used as a starting material in the synthesis of sterols, trisporic acids, and other terpenes.[57]

With complete spectral data and a sound mechanistic framework in hand, we began to doubt our structure assignment for **3.62**. Analysis of long-range HMBC correlations in C_6D_6 confirmed our suspicions, and the product was reassigned as pentaester **3.62** (Scheme III.34). This reaction can be regarded as an interrupted Hagemann's ester synthesis.

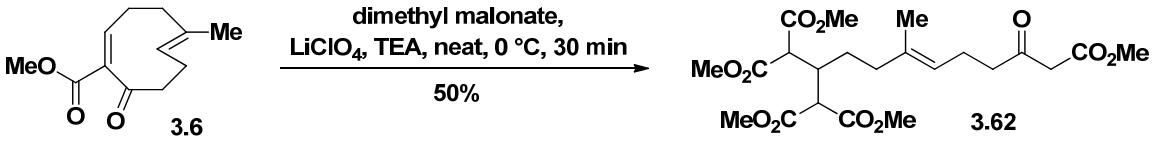

Scheme III.34 Structural reassignment: interrupted Hagemann's ester synthesis.

The retro-Michael pathway further limited our options for installation of the gamma-delta olefin of the natural products. Generation of a carbanion in the gamma position was avoided in subsequent synthetic plans (Figure III.8). Although not explicitly mentioned in his paper, Corey may have encountered a similar retro-Michael process during studies towards coraxeniolide A.[5] The regioselective deprotonation of a retro-Michael candidate required "carefully chosen conditions."

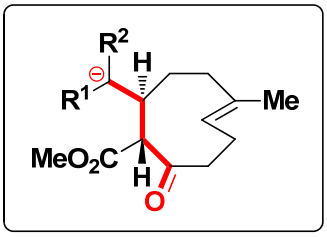

Figure III.8 Carbanion intermediate to be avoided.

We modified the structures of the nucleophiles in an effort to prevent the proton transfer step and hence the retro-Michael ring opening. Methyl acetoacetate was methylated (MeI, K_2CO_3, MeOH, reflux, 3 h, 88%), but the corresponding enolate did not add to **3.6**. Our modified method ($LiClO_4$, TEA, neat, rt) produced no addition product, and heating gave decomposition. Methylated Meldrum's acid also failed to add under two sets of conditions ($LiClO_4$, TEA/DCM, 0 °C to rt; $LiClO_4$, K_2CO_3, CH_3CN, rt). In all cases it seems as though the steric bulk introduced by the methyl group shut down reactivity.

Preliminary studies by my colleague Huan Wang showed that the retro-Michael process is prevented with the conjugate addition of chlorinated methylene compounds (Scheme III.35). The acetoacetate dimerized slowly under these conditions, so a minimum amount was employed in the optimized procedure. The desired conjugate addition reaction was very slow and produced the undesired stereochemistry at the α carbon (see gCOSY, Experimental) presumably to minimize *syn*-pentane interactions. Nonetheless, this approach provides access to functionalized side chains. Chlorinated dimethyl malonate was also added to epoxide **3.28** (not shown).

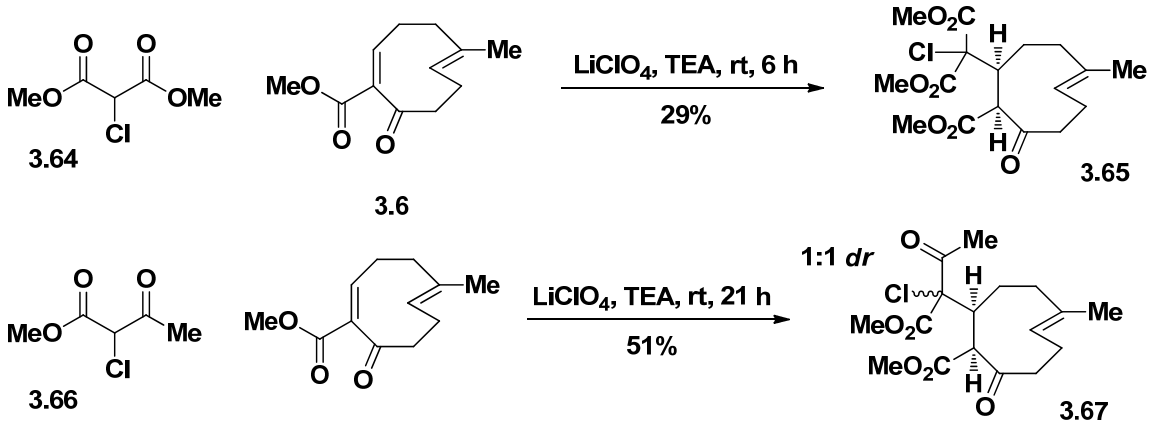

Scheme III.35 Prevention of the retro-Michael process: chloride protecting groups.

It is interesting to note that no reported xenicane natural products have an acidic proton in the gamma position. We wondered if the retro-Michael reaction was relevant to xenicane biosynthesis. In particular, Kashman's postulated biosynthetic intermediate, dialdehyde **3.68** (Scheme III.36),[58] may suffer this sort of ring opening instead of giving the natural products.

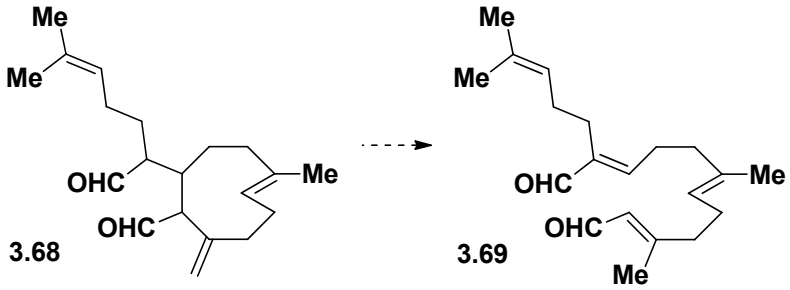

Scheme III.36 Kashman's postulated biosynthetic intermediate: retro-Michael candidate?[58]

We turned our attention to the *exo*-methylene group of the natural products. Is the retro-Michael reaction possible (or preventable) with this moiety in place? Compared to the β-ketoester, the β-olefinic ester is an inferior leaving group. We recognized that

rearrangement of the allylic enolate was a potential side reaction; nevertheless, we pressed forward and made triene **3.70** in 90% yield (Scheme III.37). Dimethyl malonate would not add to this inferior conjugate acceptor, even with an excess of $LiClO_4$ and heating. The slight inductive and/or conformational effect of the ketone is apparently critical for these conjugate additions.

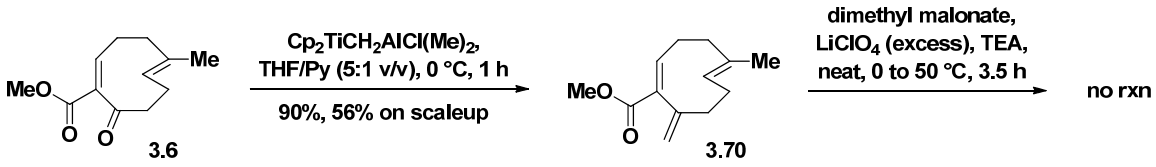

Scheme III.37 Preparation and testing of a substrate less likely to undergo retro-Michael reaction.

Dimethyl malonate was also added to the enone of *trans*-epoxide **3.28** (Scheme III.38). We obtained a 30% yield of triester **3.71**. While isolable via column chromatography, this product decomposed within 3 hours, probably via the retro-Michael pathway. A slower retro-Michael ring opening is consistent with the decreased transannular strain in the nine-membered epoxide relative to the parent alkene.

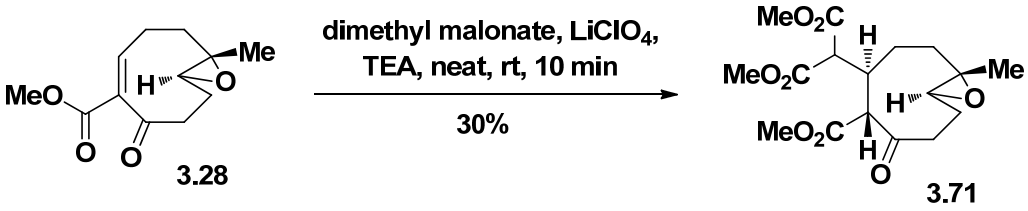

Scheme III.38 Delayed retro-Michael ring opening.

3.11 Rearrangement to Second Generation Florlide Core and Synthesis of Bicyclic Congeners

It appeared that the strained *E* olefin was impeding our progress towards the xeniolide natural products. With triene **3.70** in hand and the carbocationic *endo*-transannulation method previously developed in our lab (see Chapter II), we pursued the bicyclic florlide natural products. Regio- and diastereoselective epoxidation of **3.70** with no more than 1 equiv. of *m*-CPBA gave **3.72** in nearly quantitative yield (Scheme III.39). The diastereoselectivity of nine-membered ring epoxidation is largely dependent on the conformational equilibrium of the starting material. For example, the two stable conformations of β-caryophyllene are oxidized from the exterior, yielding a mixture of two epoxides.[59] The enone double bond in **3.70** locks the ring into a single conformation, which leads to a single epoxide.

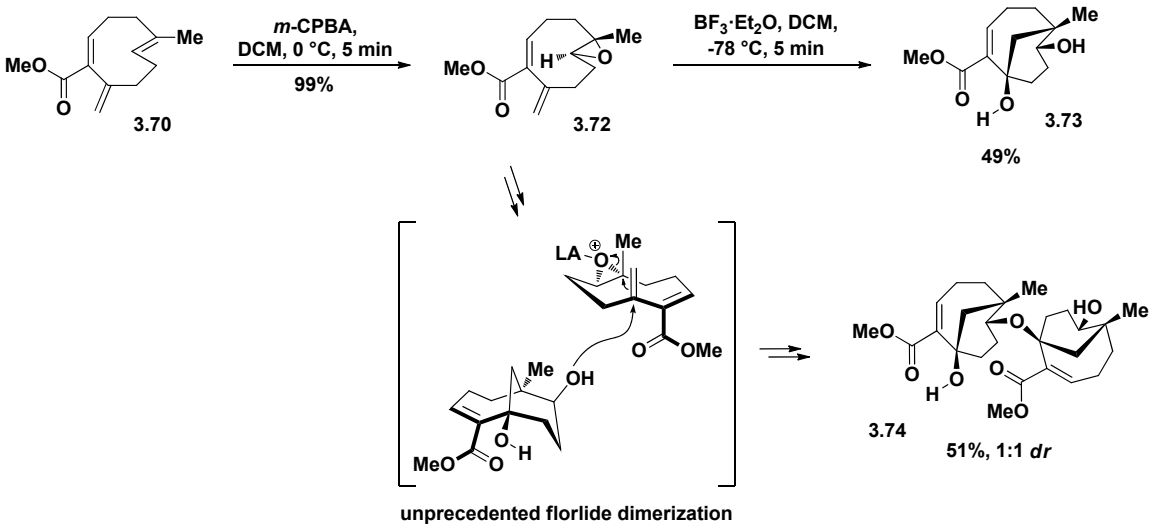

Scheme III.39 Synthesis of second generation xeniolide epoxide and florlide cores.

Treatment of xeniolide epoxide **3.72** with $BF_3{\cdot}Et_2O$ in anhydrous DCM led to a mixture of products. The desired florlide core, **3.73**, was isolated in 49% yield. ^{13}C NMR indicated that the β-carbon of the enone was more deshielded than in β-ketoester **3.6** (see Experimental). The tertiary hydroxyl proton signal was unusually far downfield as well. Our chemical intuition was validated by the X-ray crystal structure of **3.73**, which showed a hydrogen bond between the hydroxyl and carboxylate groups. Intramolecular Brønsted acid activation thus rendered this enone more electrophilic than expected. This intermediate, along with its nine-membered precursors, complements Danishefsky's xenibellol and umbellactal cores (**3.75** and **3.76**, Figure III.9).[60]

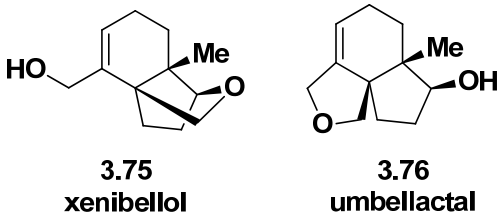

3.75
xenibellol

3.76
umbellactal

Figure III.9 Danishefsky's synthetic xenicane cores.[60]

The structures of the two apparent side products, inseparable by FCC, could not be determined by our 2D NMR techniques. Amidst the complexity of the aliphatic region, however, the bridging methylene ^1H signal characteristic of the florlides was observed. X-ray crystallographic analysis of this substance identified the products as diastereomeric florlide dimers (**3.74**). This dimerization is unprecedented in the xenicane literature, and a mechanistic framework for the transformation is presented in Scheme III.39. No such dimer was detected in the original model reaction (see Chapter II), which was run under the same conditions. The *exo*-olefin in **3.72** is more electron rich than in the descarboxymethyl substrate **2.2**. Depending on the concertedness of the transannulation-dimerization process,

this may explain why the starting material here is sufficiently nucleophilic to compete with trace amounts of water.

The yield of the desired monomer was improved by adding 3 equiv. of water to the epoxide solution (Scheme III.40). Curiously, the *dr* of the dimer increased to 3.1:1 under these conditions. The major diastereomer resulted from the coupling of opposite enantiomers (Scheme III.39). The mass balance of each reaction was excellent.

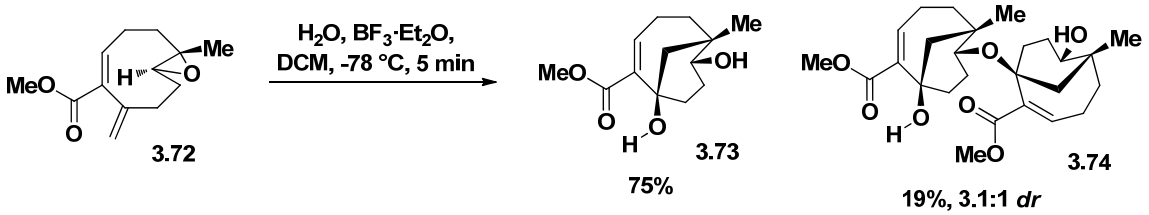

Scheme III.40 Optimization of florlide monomer yield.

The only xenicane dimerization described to date is part of a proposed biosynthesis of the *bis*-diterpene dictyotadimer A (**3.78**, Scheme III.41).[61] This is thought to arise from an extended intermolecular aldol reaction between hydroxydictyodial (**3.77**) and a rearranged hydroxydictyodial.

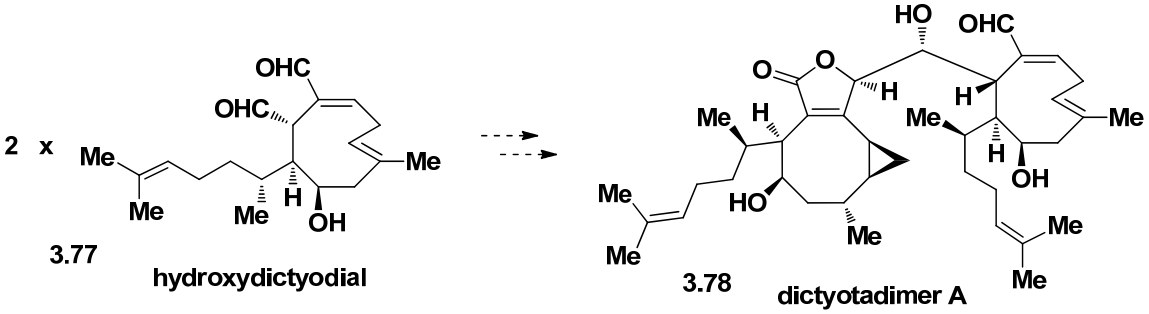

Scheme III.41 Postulated biosynthesis of dictyotadimer A: hydroxydictyodial dimerization.[61]

Trisubsituted enone **3.73** proved to be a poor Michael acceptor. TMSCl-mediated cuprate additions to the bis(TMS)-protected bicycle failed. The steric bulk of protecting groups on the tertiary alcohol appears to obstruct the Lewis acid from coordinating to the carbonyl. Undeterred by this, we thought it might be possible to add dimethyl malonate to the free diol **3.73** under our neat conjugate addition conditions. Intramolecular hydrogen-bonding activation alone was insufficient to promote the malonate addition (Scheme III.42). Neither catalytic nor stoichiometric amounts of $LiClO_4$ produced any noticeable reaction. Slow conjugate addition was achieved with a forceful ionizing medium (40 equiv. $LiClO_4$), and this was accompanied by elimination of the tertiary alcohol to yield strained bridgehead enone **3.79**. All observed homonuclear and heteronuclear NMR correlations confirmed this structure.

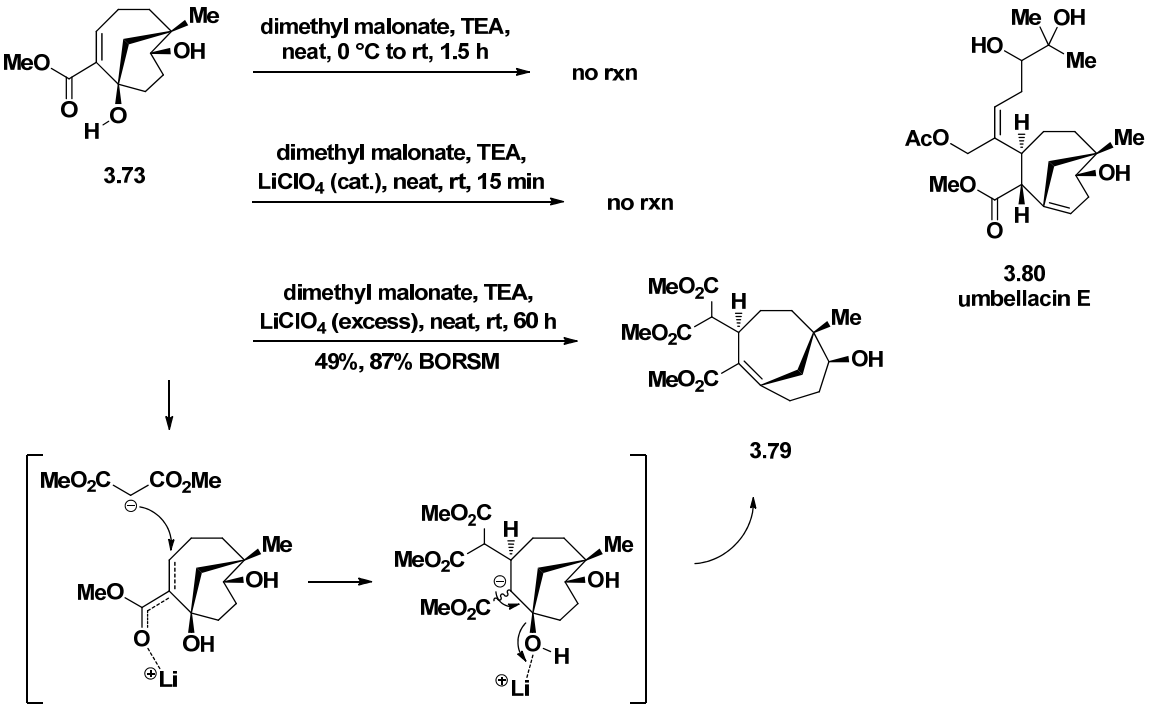

Scheme III.42 Unprecedented xenicane core synthesis via forceful ionizing conditions (compare 3.79 with 3.80).

The hydrogen bond must "break" for Li^+ to activate the ester. The retro-Michael pathway is not favored here since there is no ketone and the seven-membered ring is relatively strain-free. The elimination step is Lewis acid-assisted and is apparently favored under basic conditions. According to handheld molecular models, elimination cannot occur from a low-energy conformation of the α-hydroxy enolate intermediate, since this would be a gauche-like elimination. The enolate can adopt higher energy conformations whereby the anion is either *syn* or *anti* to the alcohol. Both elimination pathways produce the same alkene geometry, so it is unclear which pathway(s) are operative. Catalytic HCl was added to the reaction in an attempt to prevent the elimination step, but this inadvertently thwarted the already slow conjugate addition.

The reaction time was doubled from 60 to 120 h to maximize conversion (Scheme III.43). The yield of **3.79** improved to 69%, and the neopentyl alcohol underwent partial transesterification to **3.81**, another potentially useful congener.

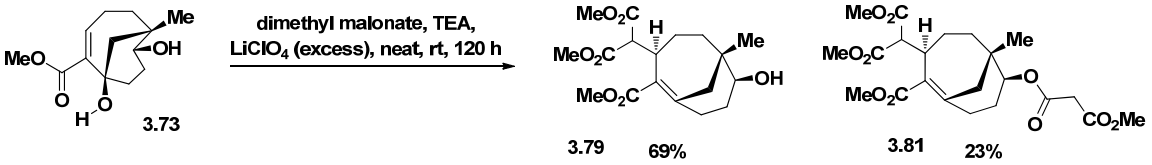

Scheme III.43 Doubled reaction time: improved yield and novel derivatization.

This unsaturated bicyclo[4.3.1] system is novel to the xenicane family and is a regioisomer of the umbellacin core (**3.80**, Scheme III.42), one of the most interesting targets within the xenicane structure space.[62] The umbellacins are rare (only three reported natural products) and the characteristic bridgehead olefin poses a challenge to synthesis.

Which bridgehead olefin is less stable? According to Wiseman, the relative strain of two bridgehead alkenes can be approximated by comparing the energies of the encompassing *trans*-cycloalkenes (Figure III.10).[63] While both **3.82** and **3.83** are certainly more stable than **3.84**, the relative stabilities of **3.82** and **3.83** are not clear and generally depend on the specific ring substituents.

Figure III.10 Wiseman's method for comparing bridgehead olefin strain.[63]

Ground state computational modeling of the unfunctionalized carbon frameworks indicates that the umbellacin isomer (**3.86**, Figure III.11) is 2.4 kcal/mol more stable.[6] This arrangement has fewer eclipsing substituents (4 versus 5) in the ring constrained by the alkene. The relative energies of the functionalized bicycles are switched, however (Figure III.12). Bridgehead enone **3.87** is 4.5 kcal/mol more stable than the umbellacin isomer **3.88**. This energy difference is independent of the malonate group. Vinyl-substituted models **3.89** and **3.90** are better approximations of the natural product geometry. The trend is consistent here, as bridgehead enone **3.89** is 6.7 kcal/mol more stable than **3.90**. Although the alkene is distorted more in the seven-membered ring (28.6° bent out of planarity) than in the six-membered ring (19.7° bent out of planarity), conjugation with the ester results in a lower overall energy. The umbellacins therefore appear to be the less thermodynamically stable regioisomers, making their biosynthesis that much more intriguing (Scheme III.44).

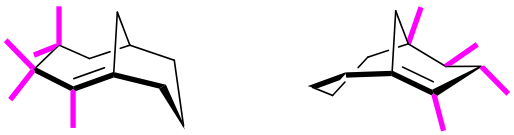

3.85 3.86

Figure III.11 Unfunctionalized bridgehead olefin models: eclipsing substituents highlighted.[6]

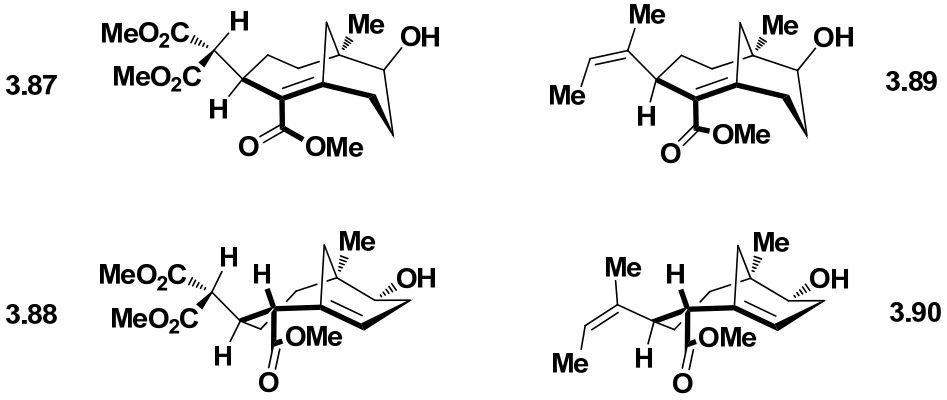

3.87 3.89

3.88 3.90

Figure III.12 Functionalized bridgehead olefin models.[6]

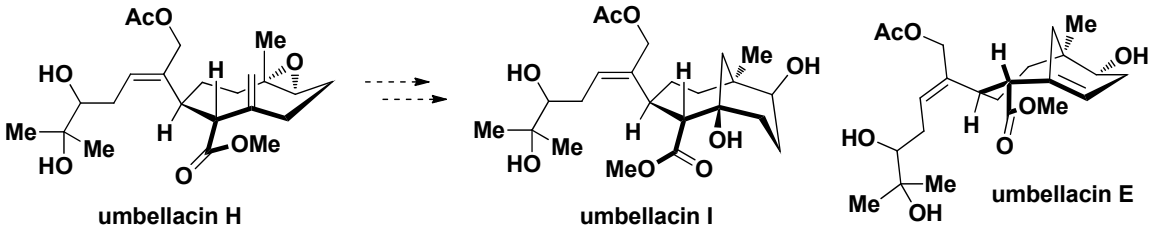

umbellacin H umbellacin I umbellacin E

Scheme III.44 Postulated bridgehead olefin biosynthesis.[62]

The novel structure of bridgehead enone **3.79** beckoned us to explore its reactivity and possible rearrangement to the umbellacin core. The olefinic bridgehead carbon ^{13}C shift of 155.1 ppm suggested that this was the most deshielded β-carbon of any enone we

had synthesized. Attempted acid-catalyzed hydration of the alkene to the tertiary alcohol gave decomposition [$HClO_4$, acetone/H_2O (80:20 v/v), reflux]. Thermal deconjugation could not be achieved with microwave irradiation (toluene-d_8, uW, 250 °C), which instead destroyed the material. Not surprisingly, this tetrasubstituted enone was inert to conjugate addition (PhSeH, excess $LiClO_4$, neat, rt to 60 °C). The alkene was sufficiently electron rich to react with *m*-CPBA at room temperature, furnishing bridgehead epoxide **3.91** in good yield (longest linear sequence of 15 steps, Scheme III.45).

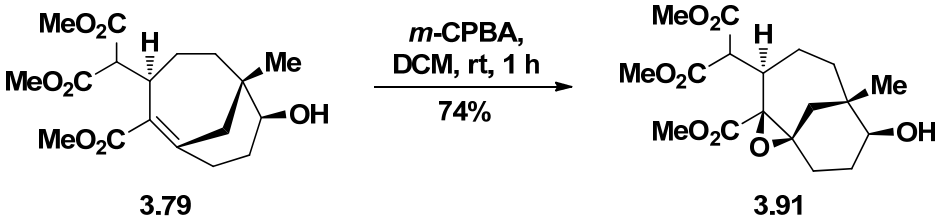

3.79 3.91

Scheme III.45 Bridgehead alkene epoxidation.

3.12 Return to Xeniolide Targets: Conjugate Additions of sp-Hybridized Carbon Nucleophiles

We refocused our efforts towards the xeniolide family. Both sp^3- and sp^2-hybridized carbon nucleophiles had been added to β-ketoester **3.6**, but alkynylides had yet to be utilized. We viewed an alkyne in the gamma-delta position as a precursor to a stereodefined alkene. Alkynylalanes add preferentially in a 1,4- fashion when the enone is capable of adopting a cisoid conformation (see transition state, Scheme III.46).[64]

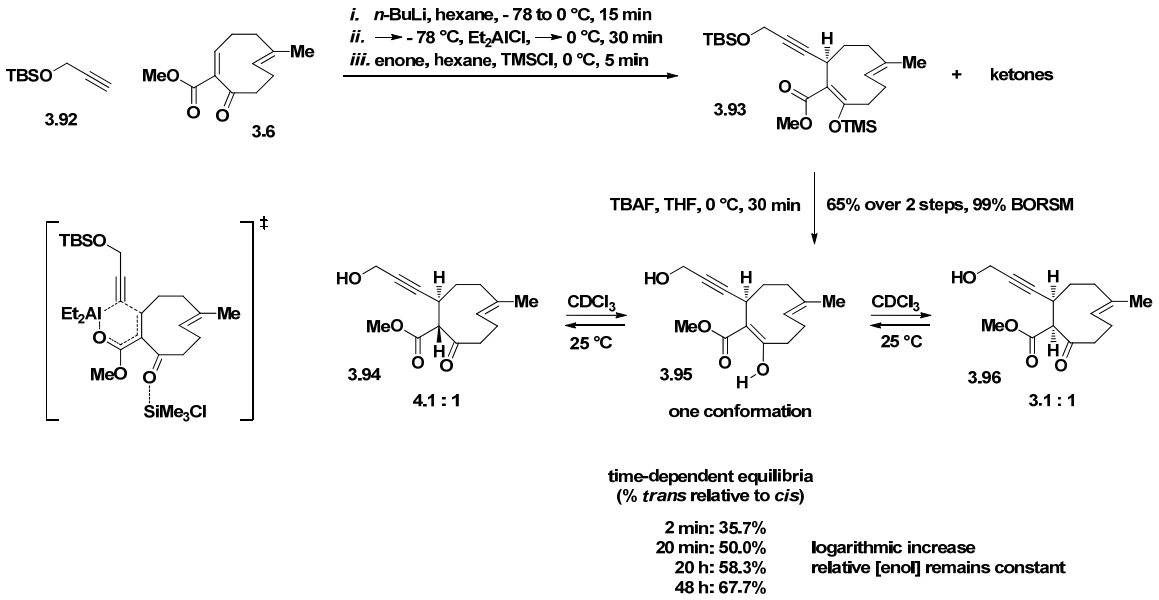

Scheme III.46 Unhindered alkynylalane: access to a xeniolide side chain handle.

TMSCl-mediated conjugate addition of the alane derived from protected propargyl alcohol **3.92** produced a complex mixture. A TMS-enol ether intermediate (possibly **3.93**) was observed by TLC, and the crude product mixture was globally deprotected at 0 °C. The resulting alcohols were difficult to completely separate by FCC, and the mass balance was very encouraging, but a pure sample of the presumed ketoester product had much more complex NMR spectra than expected. TLC monitoring of the separated products showed slow interconversion between product spots. 1D TOCSY and HMBC correlations revealed that this was a mixture of epimers and the corresponding enol. A total of five equilibrating species were identified in $CDCl_3$: two conformations of the *trans* ketoester (**3.94**), two conformations of the *cis* ketoester (**3.96**), and one conformation of the enol (**3.95**). The enol configuration was assigned as *Z* on the basis of the chemical shift of the enol proton (13.2 ppm), which is consistent with an intramolecular hydrogen bond. The sharpness of

the enol proton signal indicated a slow exchange between keto and enol forms. The *cis-trans* equilibrium shifted towards the thermodynamic *trans* epimer in $CDCl_3$.

Keto-enol tautomerism was found to be unique to the alkyne-substituted nine-membered ring compounds in this series. We hypothesize that alkynes are small such that the barriers to rotation of bonds are small enough to accommodate the structural details of both ketone and enol (e.g. C-H σ bond interacting with C=O π*, etc.).

With this methodology in hand, we targeted a series of related xenicanes: conjugated *E* dienes **3.99-3.101** (Scheme III.47).[65] Our approach was to install the common side chain via a selective reaction with a terminal alkyne.

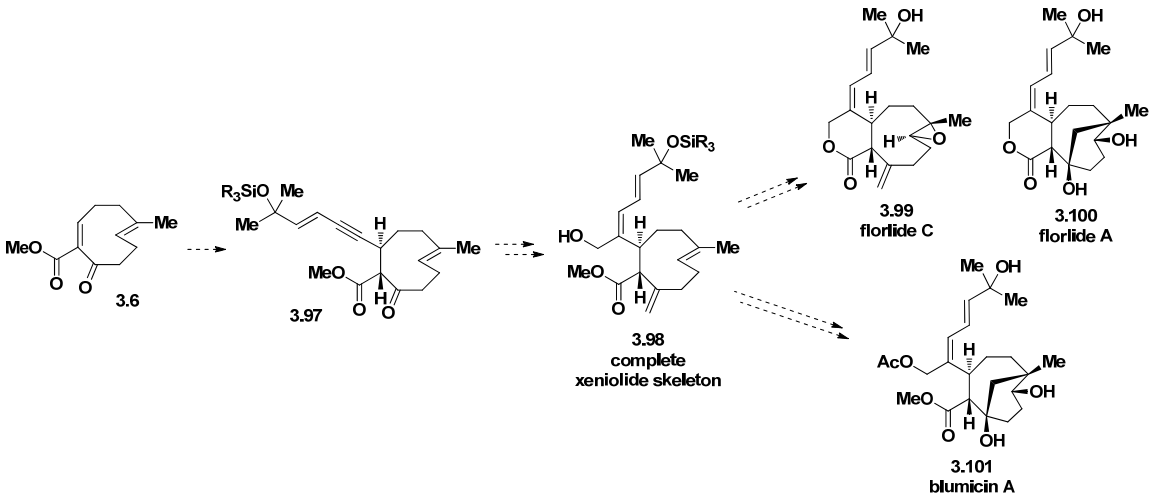

Scheme III.47 Reprioritized targets for total synthesis.[65]

The side chain synthesis commenced with 1,2-addition of ethynylmagnesium bromide to enal **3.102** (Scheme III.48), providing allylic alcohol **3.103** in quantitative yield.[66] Mild $MoO_2(AcAc)_2$-catalyzed [3,3]-sigmatropic rearrangement of the secondary alcohol gave tertiary alcohol **3.104**.[67] This volatile intermediate was protected *in situ* to

TBS ether **3.105**, which was also somewhat volatile. Azeotropic drying of the enyne was carried out carefully prior to conjugate addition.

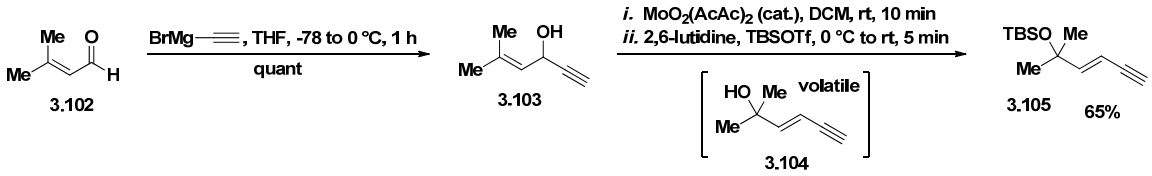

Scheme III.48 Enyne side chain synthesis.[66,67]

Alkynylation at 0 °C gave a 1:1 mixture of epimers **3.107** and **3.108** in very good combined yield (81%, Scheme III.49). The intermediate TMS enol ether **3.106** was hydrolyzed on silica gel. The minor conformer of **3.108** appeared strikingly different in structure from the conformers that we had observed routinely up to this point. Pure byproduct **3.108** was therefore studied extensively via NOE, long-range HMBC, and one-bond gHMQC correlations (see Experimental). Changes in deuterated solvent and/or temperature afforded the expected shifts in conformational equilibria. Low temperature experiments revealed chemical shift changes for several signals of each conformer.

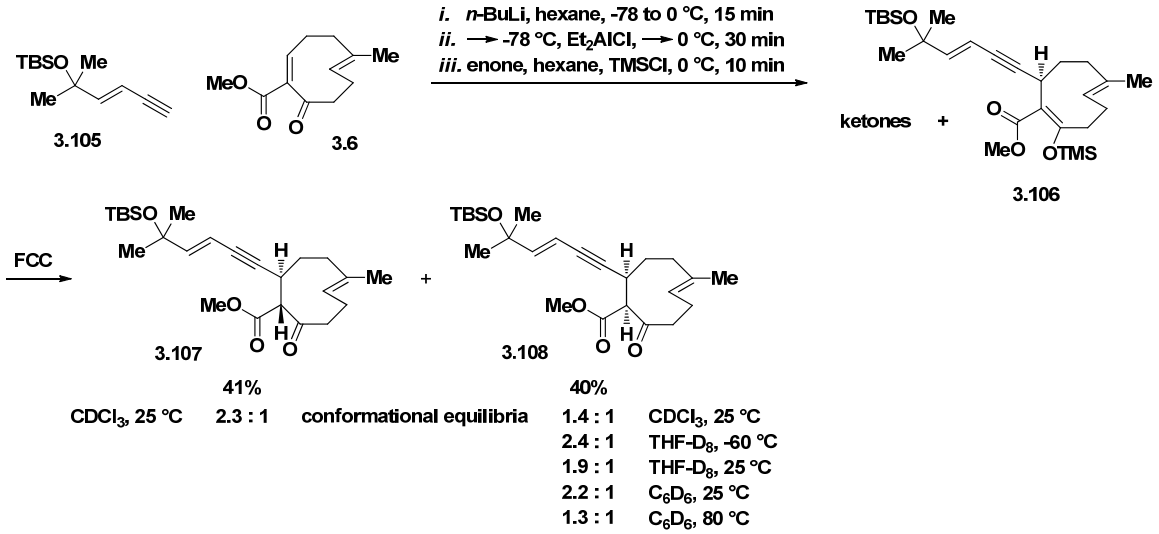

Scheme III.49 Enyne side chain installation.

Figure III.13 depicts the 3D structures of the four stable conformers identified in this reaction. The structures of **3.107** are consistent with the *trans*-fused conformers of other compounds in the series. The minor conformer of **3.108** appears to have half the ring flipped relative to the major conformer. Complete ring-flip presumably does not occur to avoid repulsive transannular interactions between the ester and strained olefinic proton.

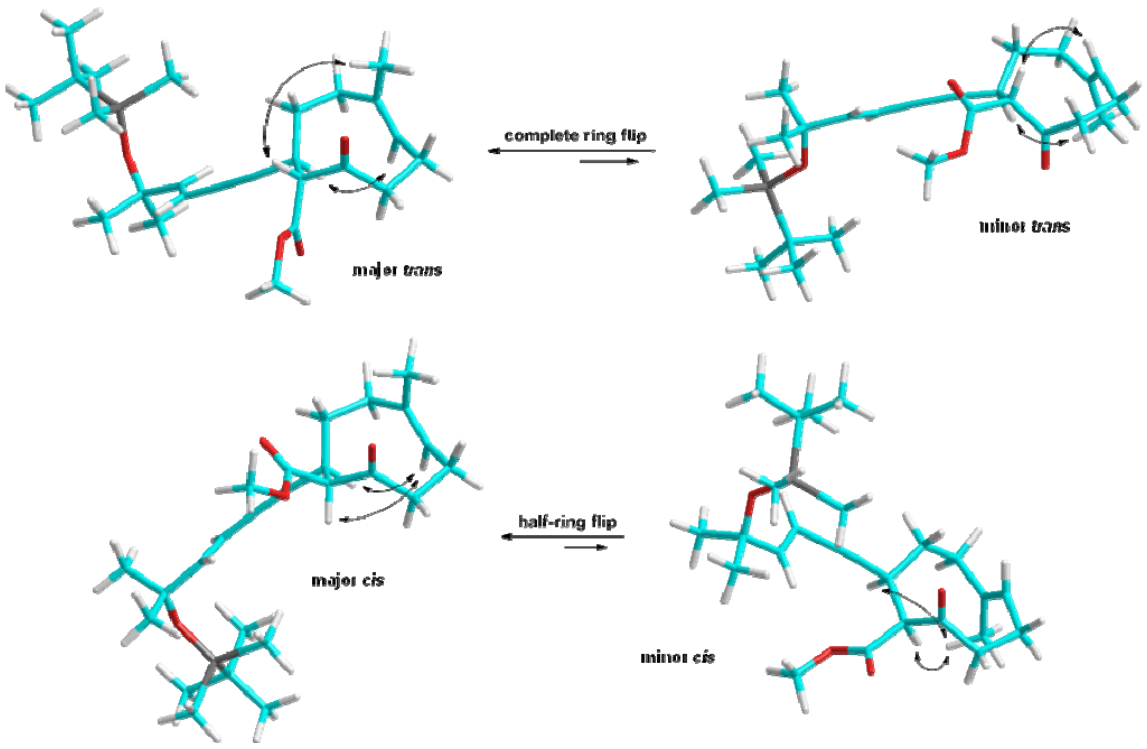

Figure III.13 2D NMR-derived structures of 3.107 and 3.108 with key NOEs.

The conformational equilibria observed by NMR are also consistent with the trend of relative ground state energies (ΔH) of terminal alkyne models (enyne replaced with acetylene): major *trans* = 0 kcal/mol; minor *trans* = 0.4 kcal/mol; major *cis* = 0.8 kcal/mol; minor *cis* = 1.8 kcal/mol.[6]

TMSCl was required for chemoselective addition of the enynylalane (Scheme III.50). Without the Lewis acid present, the alane partially added to the ketone, forming tertiary alcohol **3.109**. The alkynylalane methodology reportedly gave the best yields at 0 °C,[64] but protonation of the nine-membered enolate was not selective at this temperature. Addition of the enone solution to the alane solution at -78 °C followed by quenching at this reduced temperature generated the *trans* product **3.107** exclusively but in poor yield (< 20%, quant BORSM).

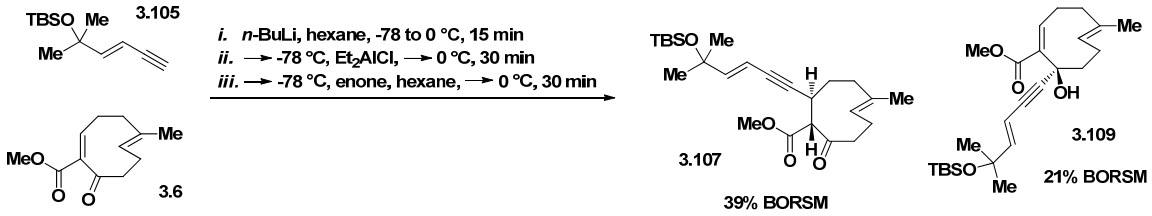

Scheme III.50 Lewis acid required for chemoselective alane addition.

Several mild reactions with the intricate and sensitive intermediate **3.107** were investigated for selective functionalization of the alkyne. Nickel-catalyzed alkene-directed *syn*-hydroxymethylation has weak precedent and yielded a product that was unrelated and not fully characterized ($Ni(COD)_2$, $PCyp_3$, Et_3B, 1,3,5-trioxane, EtOAc, 0 °C to rt). Buchwald hydroformylation gave poor conversion to a complex mixture of products including allenes [$Rh(CO)_2(AcAc)$, BiPhePhos, DCM, CO/H_2 (1:1, 1 atm), rt]. *Syn*-hydrostannylation of alkyne **3.107** proceeded cleanly.[68] After neutral alumina FCC, *E* vinylstannane **3.110** was isolated as the minor product in 12% yield (Scheme III.51). The starting material was polarized such that this regioisomer was electronically favored, but regioselectivity was clearly governed by sterics about the alkyne (Figure III.14). **3.110** exists as a single conformer and readily decomposes upon exposure to air. Thus, the deshydroxymethyl xeniolide framework was accessed in 0.4% overall yield (longest linear sequence of 12 steps).

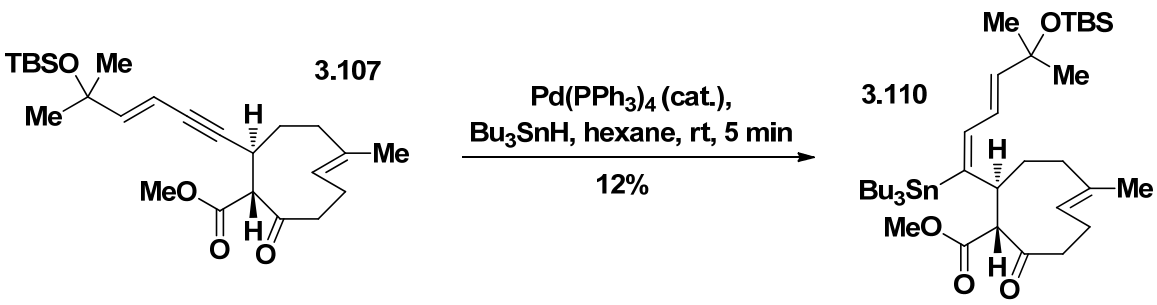

Scheme III.51 Synthesis of the deshydroxymethyl xeniolide framework.

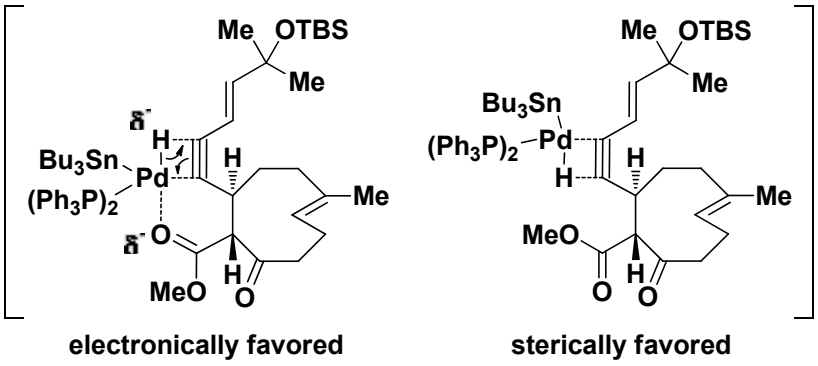

Figure III.14 Proposed model for *syn*-hydrostannylation regioselectivity.

The mixture of vinyl stannanes was also iodinated in the same pot (Scheme III.52). The vinyl iodide products were largely inseparable and also prone to decomposition. The structure of the major product **3.111** was confirmed by 1D TOCSY, gCOSY, and HRMS experiments. In an effort to utilize the intrinsic steric bias of alkyne **3.107**, it was lastly subjected to an iodoboration protocol (*i.* B-iodo-9-BBN, pentane, -78 °C; *ii.* AcOH, -78 °C to rt), but this produced a complex mixture of products and was not pursued.

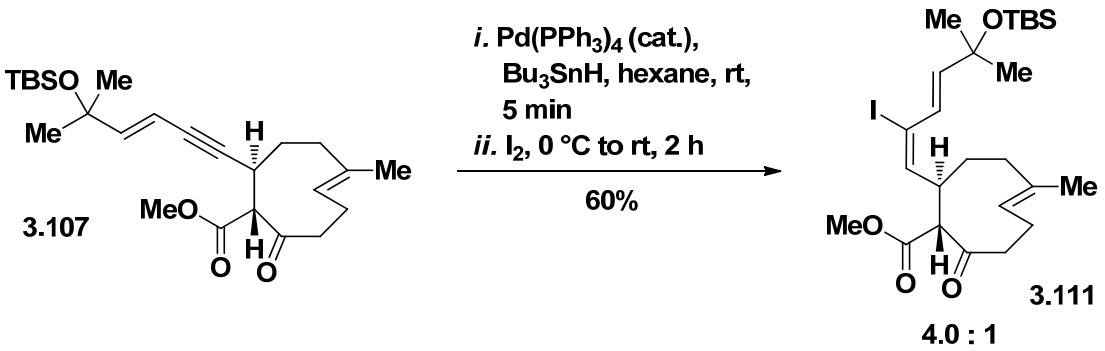

Scheme III.52 One-pot *syn*-hydrostannylation-iodination.

Generally, addition reactions to internal alkynes give mixtures of difficult-to-separate compounds with low selectivity. The low yields and instabilities of the *E* hydrostannylation/iodination products prompted us to examine related xenicanes. We turned our attention to an unpublished xeniolide diepoxide (**3.114**, Scheme III.53) that has the isomeric *Z* olefin geometry in the side chain. This diterpenoid was recently isolated by our collaborators Prof. Paul Falkowski and his co-worker Dr. Eric Andrianasolo. This substance is the most potent xenicane evaluated to date in the Bax- and Bak-dependent apoptosis induction assay.[2]

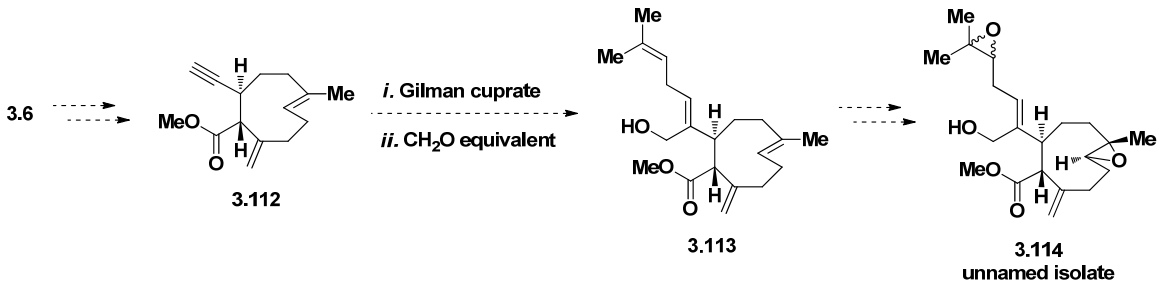

Scheme III.53 Synthetic plan towards new xeniolide.

We planned to effect a stereoselective carbocupration-hydroxymethylation across terminal alkyne-diene **3.112**. The pKa of the α proton was approximated at 24.9 (similar to

an alkyne).[69] Gilman cuprates are not basic enough to deprotonate alkynes,[70] so a proposed intermediate vinyl cuprate (not shown) was expected to be stable in the presence of the α proton for subsequent trapping with a formaldehyde equivalent.

Attempted direct conjugate addition of acetylide to **3.6** (*i.* homogenous sodium acetylide, Et_2AlCl, hexane, 0 °C to rt; *ii.* -78 °C, TMSCl, hexane) resulted in reduction of the ketone (24%, 59% BORSM). Et_2AlCl is known to reduce ketones, releasing ethylene gas as a byproduct.[71]

Portionwise addition of the alane derived from TMS-acetylene proceeded more smoothly, generating **3.115** in 66% yield (Scheme III.54). Deprotection with excess TBAF produced a seemingly complex mixture of products; however, after FCC only two products were isolated: the desired product **3.116** and the corresponding enol **3.117**, which appears as many spots on TLC and is a surprisingly stable species in $CDCl_3$. Attempted protection (TBSOTf, TEA, DCM, -78 °C) and Tebbe olefination of the combined ketone and enol gave complex mixtures of products. The Schrock carbene is known to react competitively with terminal alkynes.[72]

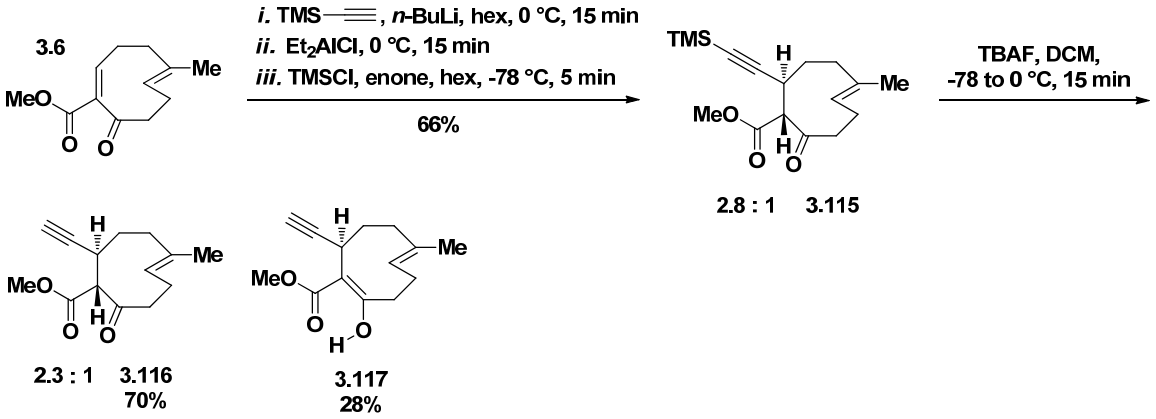

Scheme III.54 Towards synthesis of terminal alkyne-diene.

Tebbe olefination of internal alkyne **3.115** was a cleaner reaction, though it could not be pushed to completion (Scheme III.55). TMS deprotection of **3.118** with *in situ* methoxide gave the desired intermediate **3.112** without observed intramolecular proton transfer. No cuprate addition to this alkyne was noted, and large scale model studies on a simple terminal alkyne (not shown) yielded poor *cis*/*trans* selectivity (2.3:1) with only proton trapping (*i.* *n*-BuLi, CuI, Et_2O, -78 °C; *ii.* alkyne, Et_2O; *iii.* $(CH_2O)_n$, -78 °C to rt).

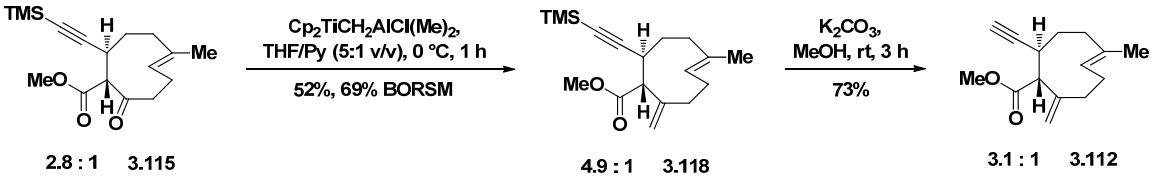

Scheme III.55 Terminal alkyne-diene synthesis.

3.13 Anticancer Evaluations of the Compound Library: Specific Apoptosis Induction Screen

With the bottleneck of availability to this semi-validated structure space significantly relieved, we were in position to evaluate the collection of terpenes for anticancer activity. In collaboration with Prof. Eileen White of the Cancer Institute of New Jersey, we subjected the compounds to the Bak- and Bax-dependent apoptosis induction assay.[2]

This MTT double knockout assay compares the activity of a compound at various concentrations in DMSO against two iBMKE cell lines. D3 cells are genetically engineered without the Bak and Bax proteins, thus the functional apoptosis pathway has been disabled and the cells are apoptosis-deficient. Wild-type W2 cells are unmodified,

thus the functional apoptosis pathway is intact and the cells are apoptosis-competent. A compound that selectively kills W2, but not D3 cells, is promoting cell death via the apoptosis pathway. Such a compound is presumably interacting with a protein upstream of Bak and Bax or with these proteins directly. Apoptosis induction is defined as at least 20% death of W2 cells and at least 10% growth of D3 cells relative to t_0 values after 48 h of cell culture incubation. Compounds that induce apoptosis are potential anticancer agents. Compounds that kill both W2 and D3 cells are promoting cell death via a non-apoptosis pathway. These compounds are considered nonspecifically toxic. Staurosporine, a known apoptosis inducer, and untreated cells (DMSO only) were used as positive and negative controls.

Thirty-six novel terpenoids were subjected to the bioassay, and sixteen of these compounds exhibited activity in micromolar concentrations. Seven were found to selectively induce apoptosis. Another four compounds gave inconsistent results, some of which were induction of apoptosis. Five compounds were nonspecifically toxic.

Z olefin **3.39** exhibited the best activity, inducing apoptosis at the lowest concentration (25 μM, Figure III.15, orange bar).[73] At concentrations of 50 μM and above, **3.39** was nonspecifically toxic. At concentrations less than 25 μM, selectivity for killing W2 cells was observed but not enough of a difference to be defined as apoptosis induction. Blumiolide C, one of the few xenicane natural products with an endocyclic *Z* olefin, is also active against several cancer cell lines (Table III.1). This promising hit prompted us to target more congeners with this olefin geometry.

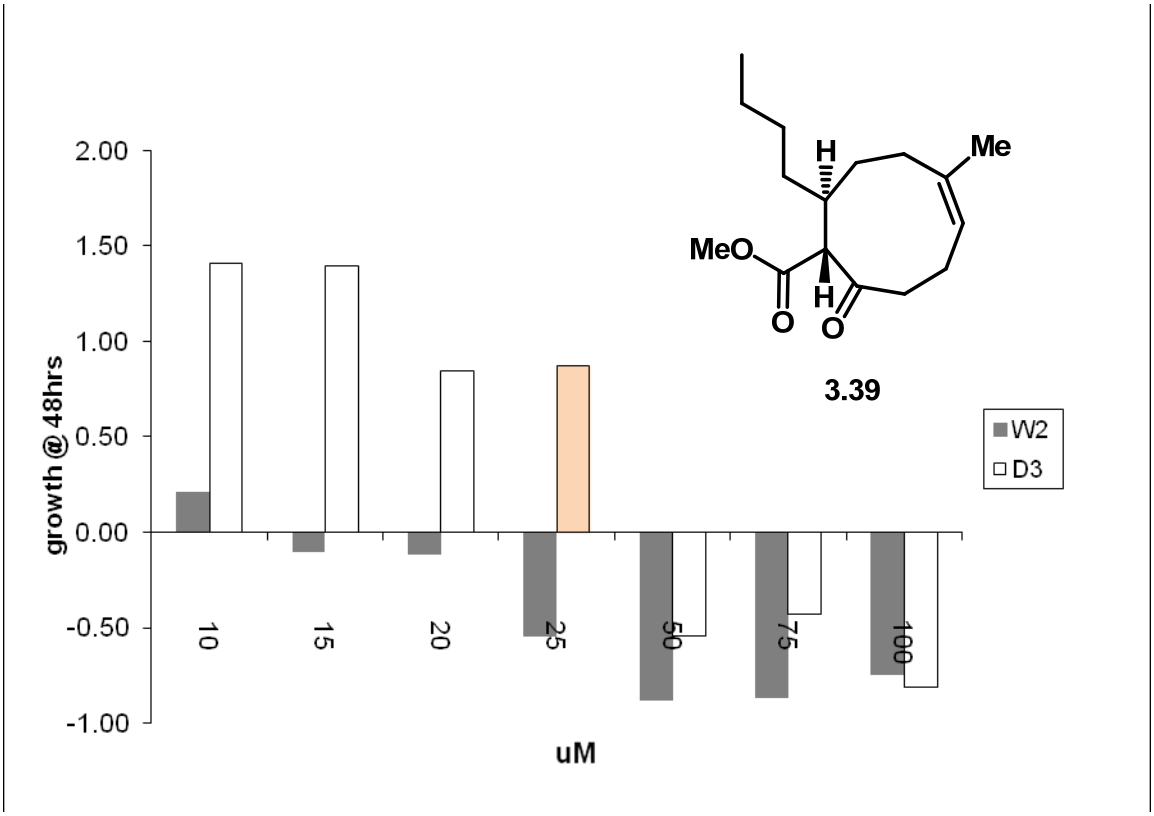

Figure III.15 Change in relative W2 and D3 cell viability (3.39).[73]

concentration (μM)	avg W2	avg D3	sd W2	sd D3
10	0.21	1.41	0.50	0.45
15	-0.10	1.40		
20	-0.12	0.84		
25	**-0.55**	**0.87**		
50	-0.88	-0.54	0.07	0.16
75	-0.87	-0.43		
100	-0.75	-0.81	0.21	0.15
DMSO	0.79	3.08		
staurosporine (0.1 μM)	-0.65	0.31		

Table III.4 Change in relative W2 and D3 cell viability (3.39).[73]

Six terpenoids exhibited smooth trends of activity (Figures III.16-III.21). As the concentrations increased, the compounds promoted growth arrest of both cell lines, and in all cases W2 was affected more than D3. At the key concentrations, the compounds induced apoptosis. At higher concentrations, both cell lines were killed via a non-apoptosis pathway. Apoptosis was induced by terminal alkyne **3.116** at 40-60 μM (Figure III.16), by chloride **3.65** in the same range with greater selectivity (Figure III.17), by *Z* olefin **3.46** at 60-90 μM (Figure III.18), by enyne **3.108** at 85 μM (Figure III.19), by Hagemann's esters **3.63** at 125-175 μM (Figure III.20), and by cyclopentanone **3.59** at 175 μM (Figure III.21). Figure III.22 is a summary of the lowest effective concentrations of these compounds.

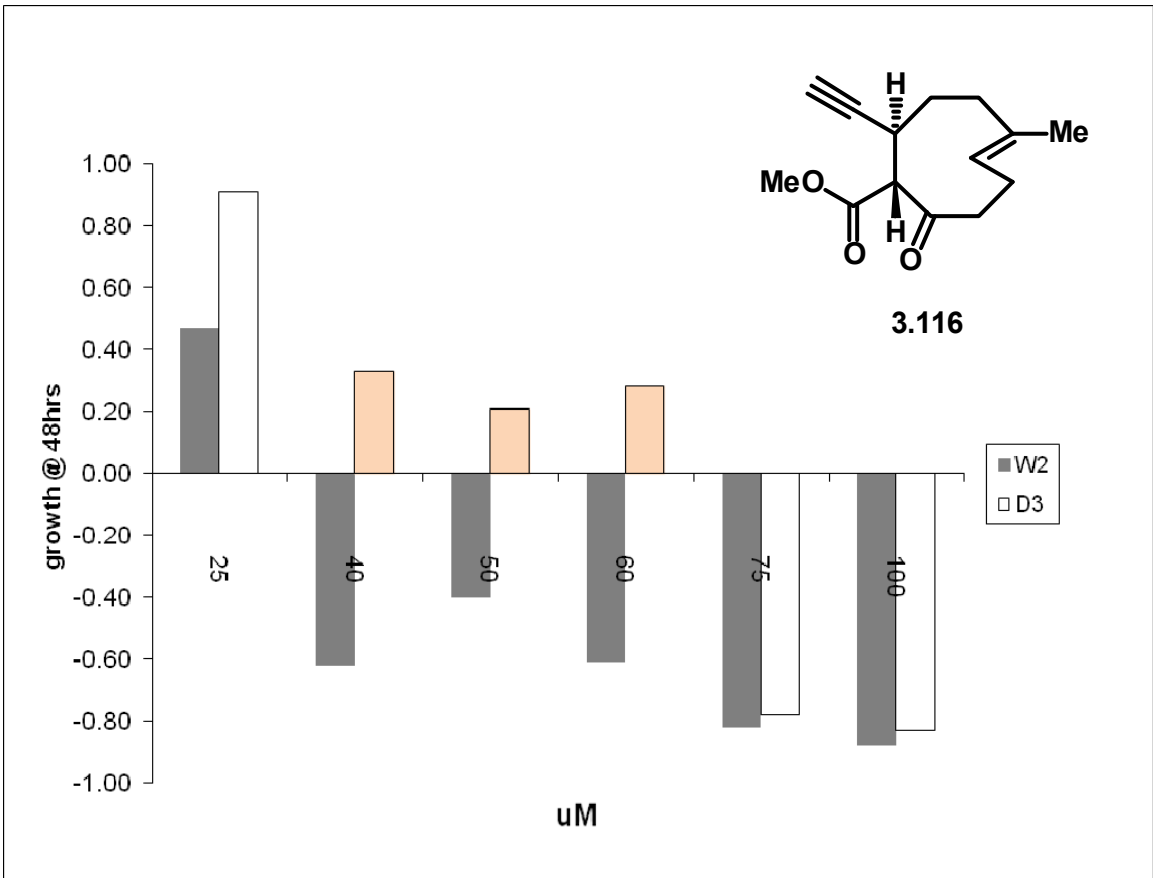

Figure III.16 Change in relative W2 and D3 cell viability (3.116).

concentration (μM)	avg W2	avg D3
25	0.47	0.91
40	**-0.62**	**0.33**
50	**-0.40**	**0.21**
60	**-0.61**	**0.28**
75	-0.82	-0.78
100	-0.88	-0.83
DMSO	2.39	2.60
staurosporine (0.1 μM)	-0.49	0.18

Table III.5 Change in relative W2 and D3 cell viability (3.116).

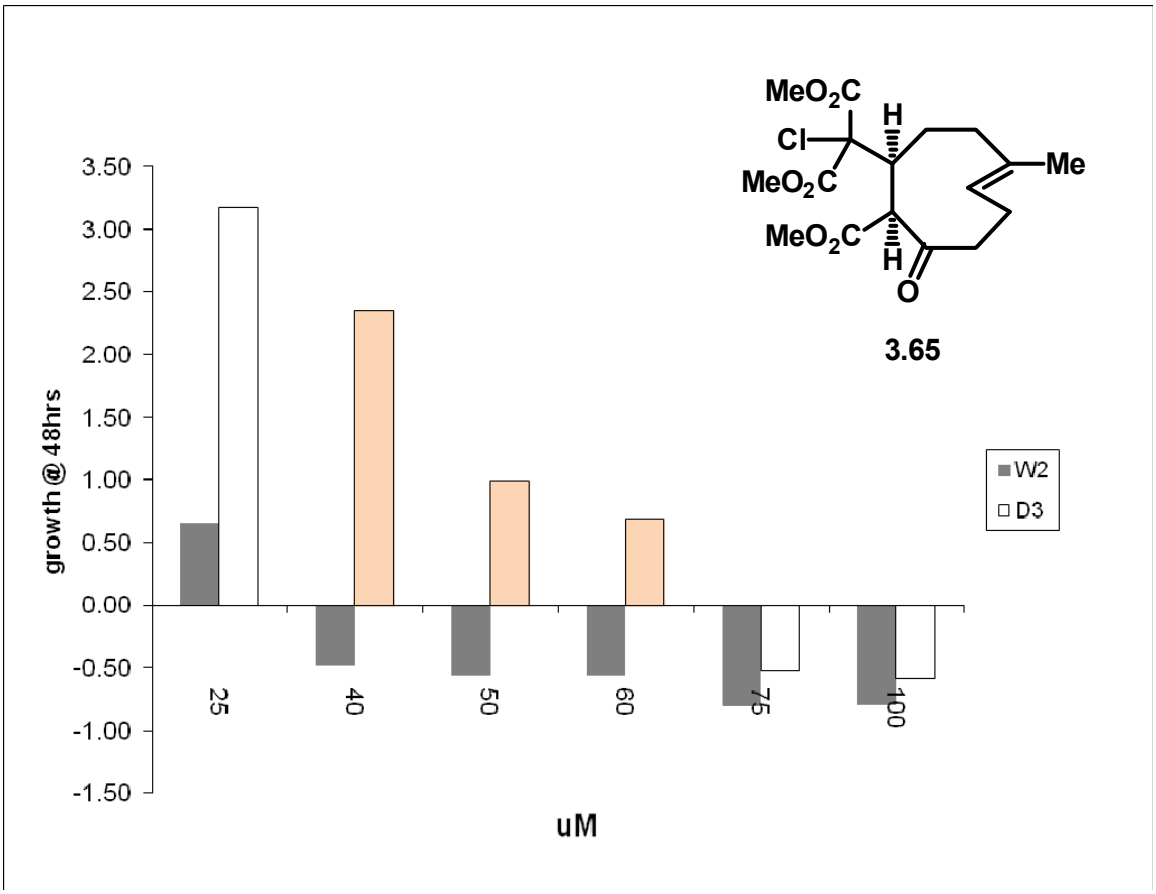

Figure III.17 Change in relative W2 and D3 cell viability (3.65).

concentration (μM)	avg W2	avg D3
25	0.66	3.17
40	**-0.48**	**2.35**
50	**-0.56**	**0.99**
60	**-0.56**	**0.69**
75	-0.81	-0.53
100	-0.80	-0.58
DMSO	2.39	2.60
staurosporine (0.1 μM)	-0.49	0.18

Table III.6 Change in relative W2 and D3 cell viability (3.65).

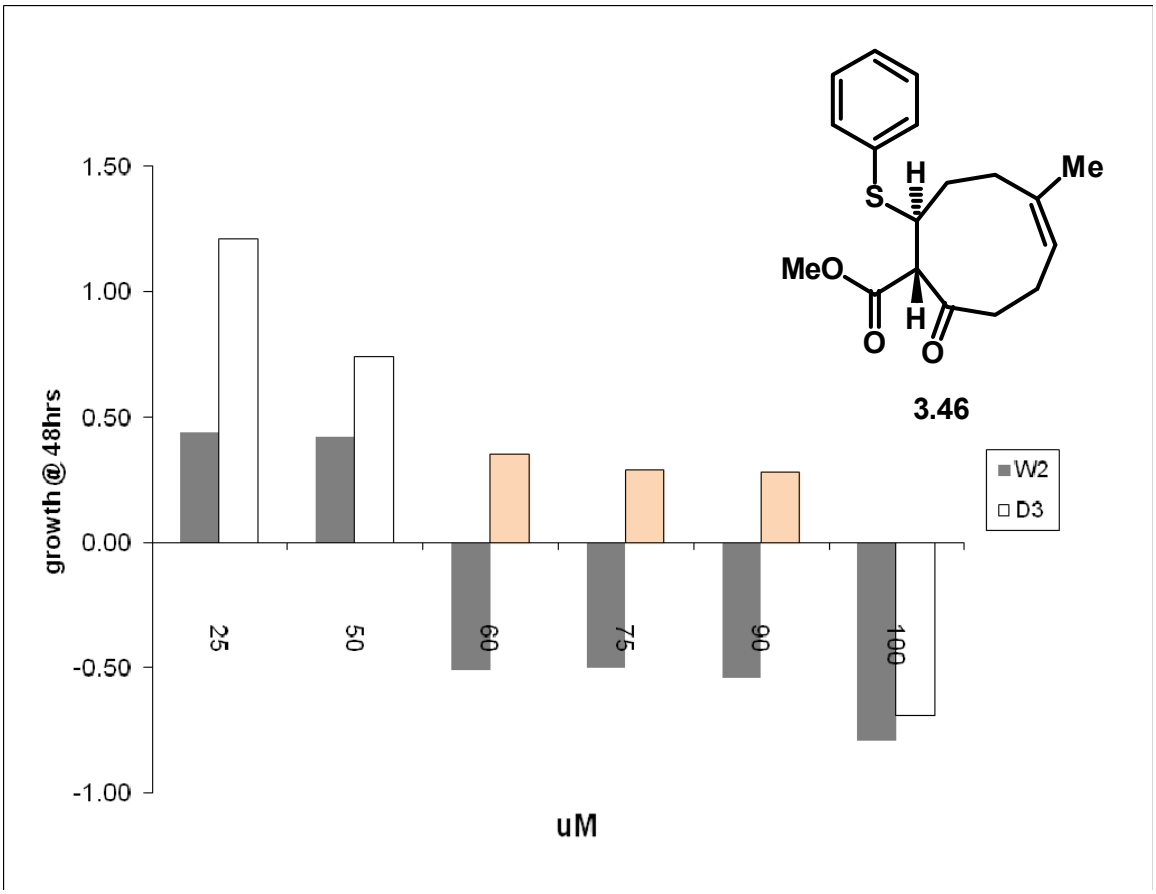

Figure III.18 Change in relative W2 and D3 cell viability (3.46).

concentration (μM)	avg W2	avg D3
25	0.44	1.21
50	0.42	0.74
60	**-0.51**	**0.35**
75	**-0.50**	**0.29**
90	**-0.54**	**0.28**
100	-0.79	-0.69
DMSO	2.39	2.60
staurosporine (0.1 μM)	-0.49	0.18

Table III.7 Change in relative W2 and D3 cell viability (3.46).

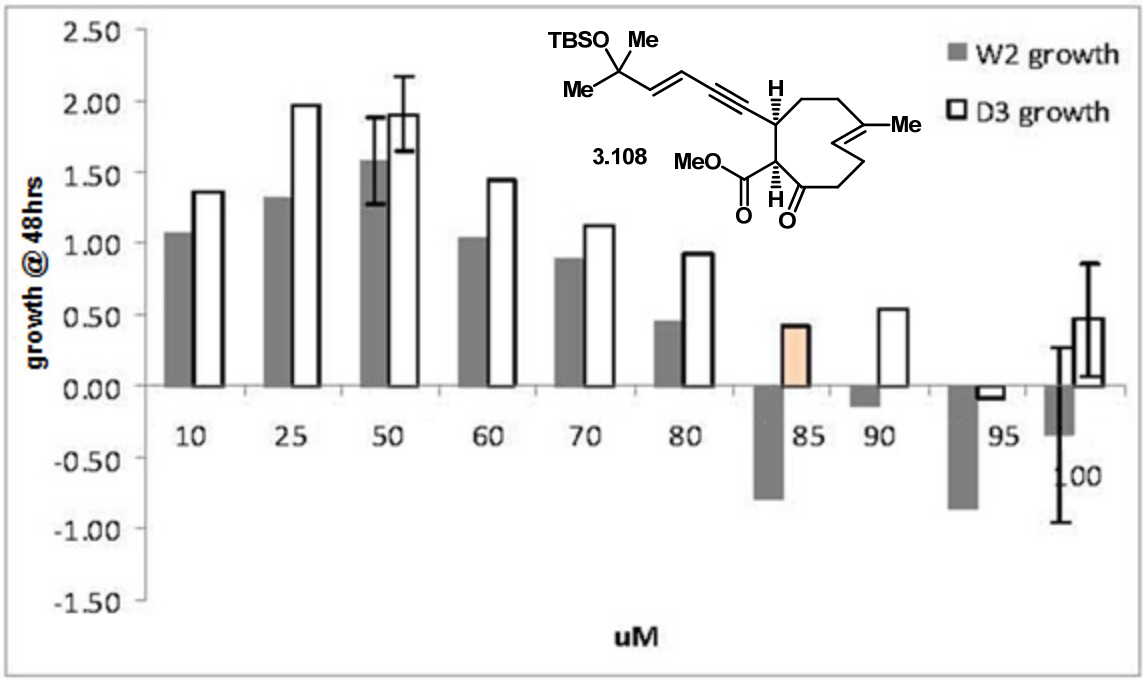

Figure III.19 Change in relative W2 and D3 cell viability (3.108).

concentration (μM)	avg W2	avg D3	sd W2	sd D3
10	1.06	1.36		
25	1.32	1.96		
50	1.57	1.90	0.30	0.26
60	1.04	1.45		
70	0.88	1.12		
80	0.46	0.92		
85	**-0.80**	**0.41**		
90	-0.14	0.54		
95	-0.86	-0.09		
100	-0.35	0.46	0.62	0.40
DMSO	1.26	1.60	0.79	0.58
staurosporine (0.1 μM)	-0.58	0.11	0.10	0.13

Table III.8 Change in relative W2 and D3 cell viability (3.108).

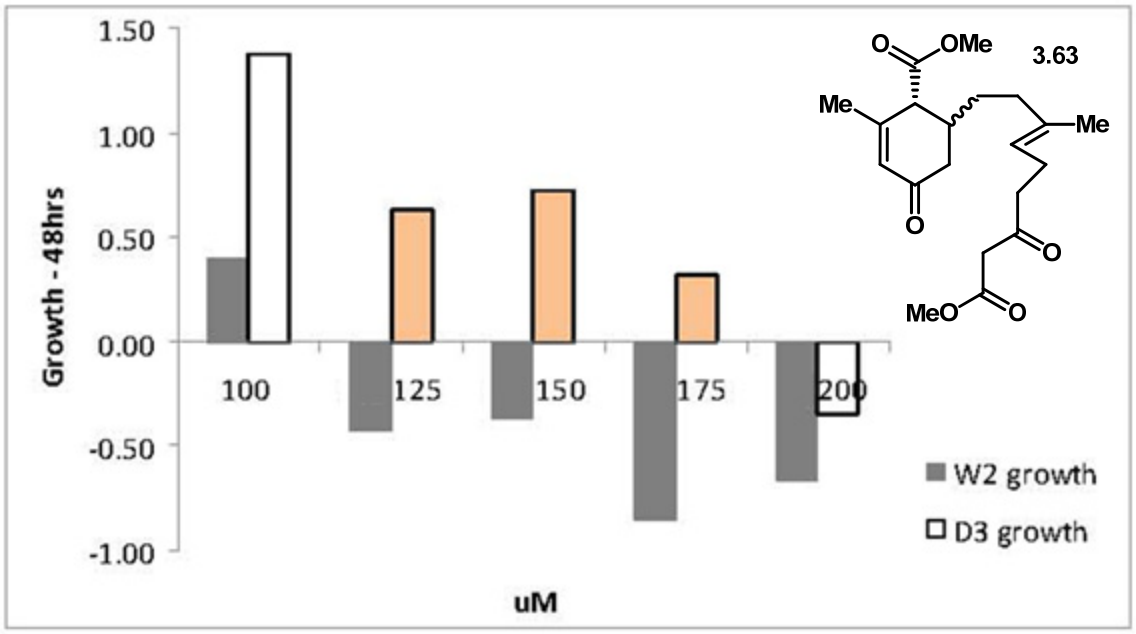

Figure III.20 Change in relative W2 and D3 cell viability (3.63).

concentration (μM)	avg W2	avg D3	sd W2	sd D3
100	0.40	1.37		
125	**-0.42**	**0.62**		
150	**-0.37**	**0.72**		
175	**-0.85**	**0.32**		
200	-0.67	0.35		
DMSO	1.26	1.60	0.79	0.58
staurosporine (0.1 μM)	-0.58	0.11	0.10	0.13

Table III.9 Change in relative W2 and D3 cell viability (3.63).

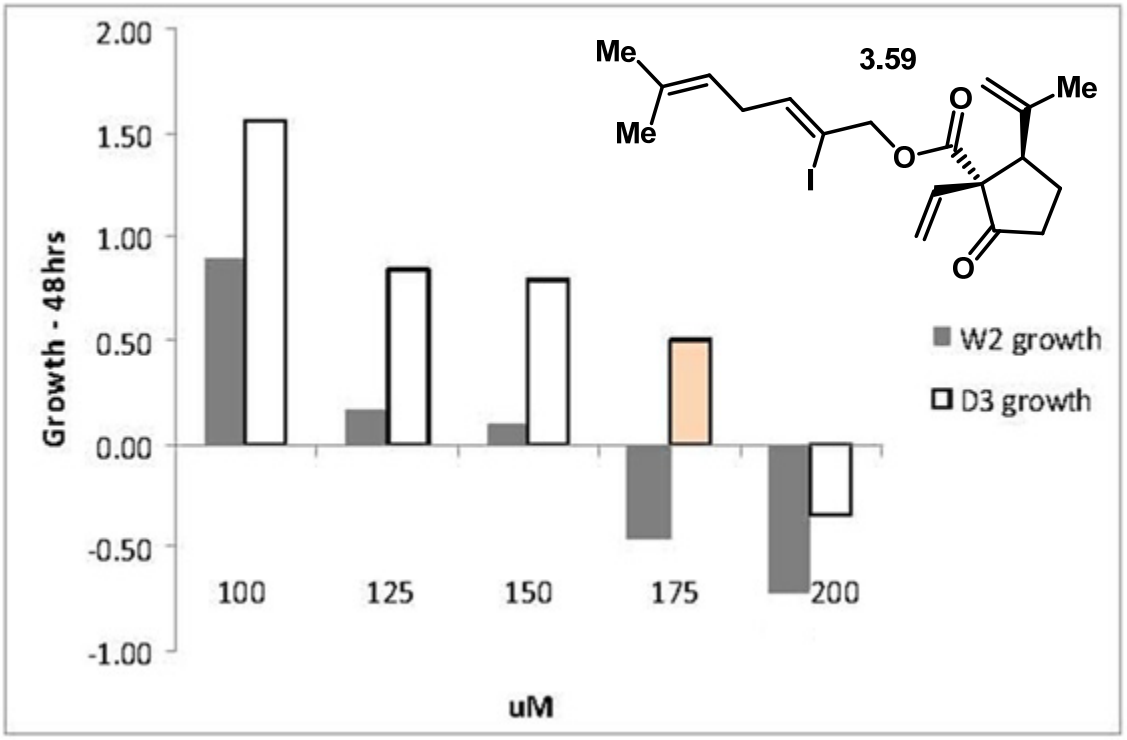

Figure III.21 Change in relative W2 and D3 cell viability (3.59).

concentration (μM)	avg W2	avg D3	sd W2	sd D3
100	0.89	1.56		
125	0.16	0.85		
150	0.09	0.79		
175	**-0.45**	**0.50**		
200	-0.70	-0.35		
DMSO	1.26	1.60	0.79	0.58
staurosporine (0.1 μM)	-0.58	0.11	0.10	0.13

Table III.10 Change in relative W2 and D3 cell viability (3.59).

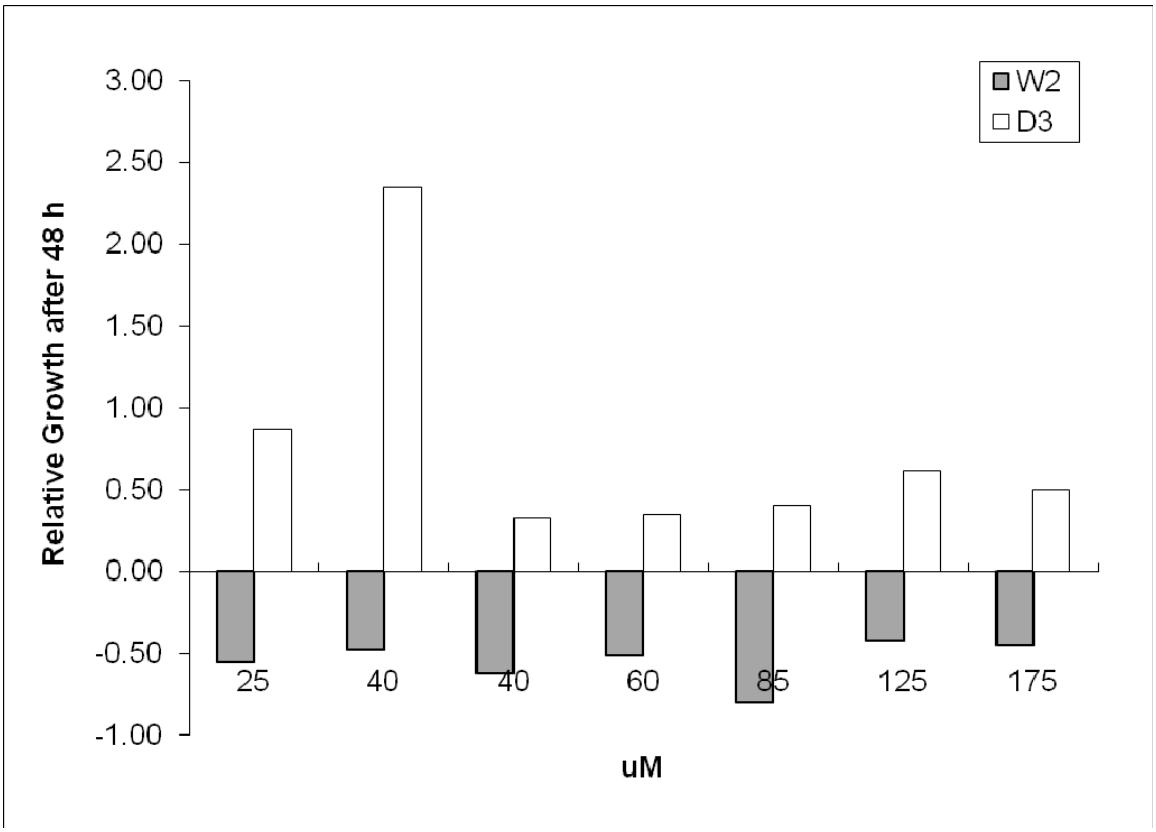

Figure III.22 Lowest effective concentrations of pro-apoptotic synthetic compounds.

Four xenicane congeners gave inconsistent results (Figure III.23). Des-carboxy ketone **3.32** induced apoptosis in one out of four assays at 100 μM (W2: -0.4, D3: +1.4). *n*-Butyl ketoester **3.33** induced apoptosis in one out of four assays at 9 μM (W2: -0.6, D3: +1.4). At 100 μM, phenyl *exo*-olefin **3.44** affected growth of W2 cells more than D3 cells, but this was not enough of a difference to be defined as apoptosis induction. One assay with epoxide **3.28** at 200 μM resulted in 38% death of W2 and 6% growth of D3, again not enough to be defined as apoptosis induction.

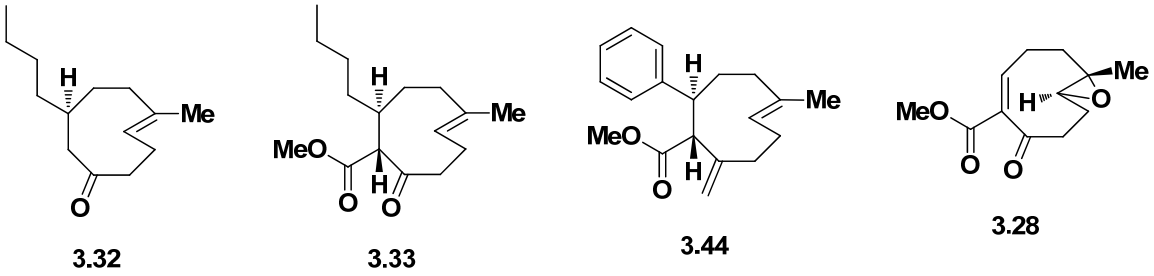

Figure III.23 Xenicane congeners yielding inconsistent results.

Five terpenoids were nonspecifically toxic. In some assays with keto-enol mixture **3.94-3.96**, growth of D3 cells was more affected than growth of W2 cells (Figure III.24). These strange results may be the consequence of cellular interactions with the five equilibrating species of **3.94-3.96** in solution. As low as 5 μM, steroidal allylic esters **3.60** were toxic to both cell lines (Figure III.25). The toxicity threshold for tertiary alcohol **3.109** was 50 μM. TMS-alkyne **3.118** was toxic as low as 100 μM. Pentaester **3.62** was the least toxic with a threshold of 200 μM. Figure III.26 contains all of the assayed compounds that were inactive between 100-200 μM.

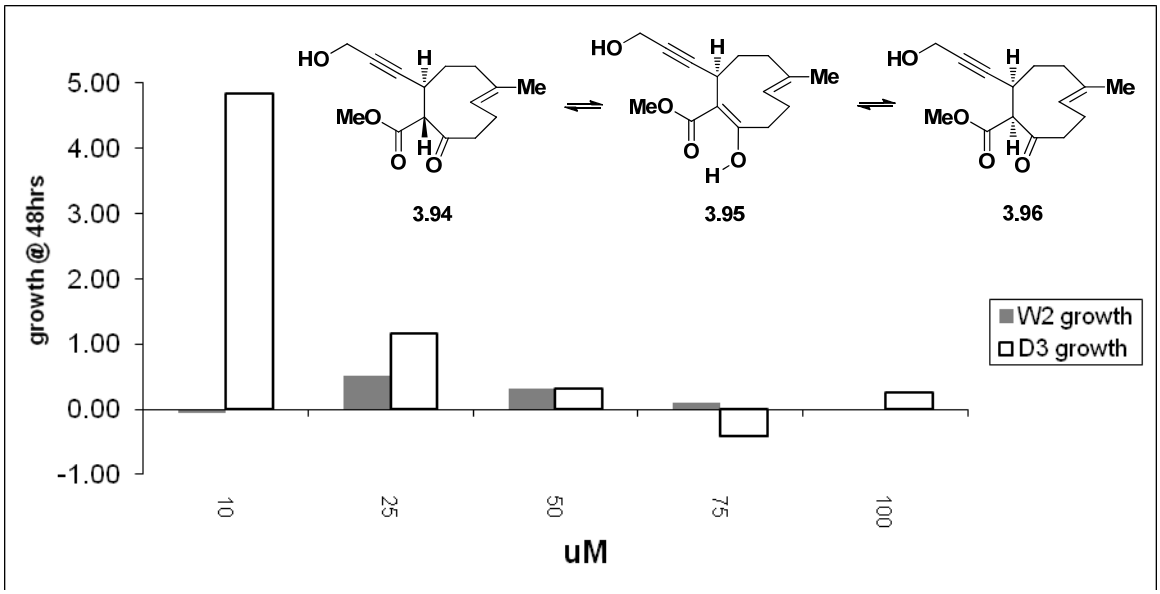

Figure III.24 Change in relative W2 and D3 cell viability (3.94-3.96).

concentration (uM)	avg W2	avg D3	sd W2	sd D3
10	-0.06	4.82		
25	0.52	1.16	0.73	1.97
50	0.32	0.31	0.50	0.82
75	0.09	-0.41	0.42	0.02
100	-0.02	0.25	0.56	1.38
DMSO	0.94	2.98		
staurosporine (0.1 uM)	-0.75	0.56		

Table III.11 Change in relative W2 and D3 cell viability (3.94-3.96).

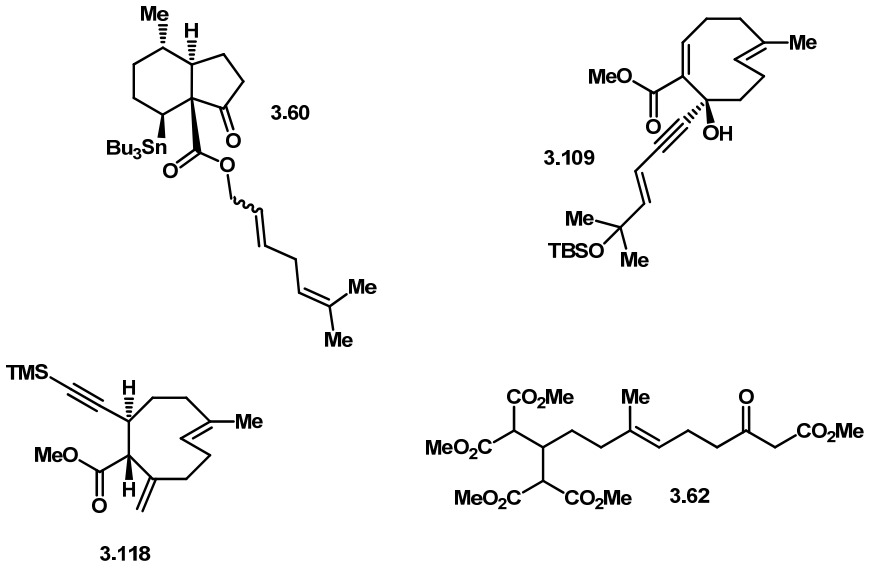

Figure III.25 Nonspecifically toxic terpenoids.

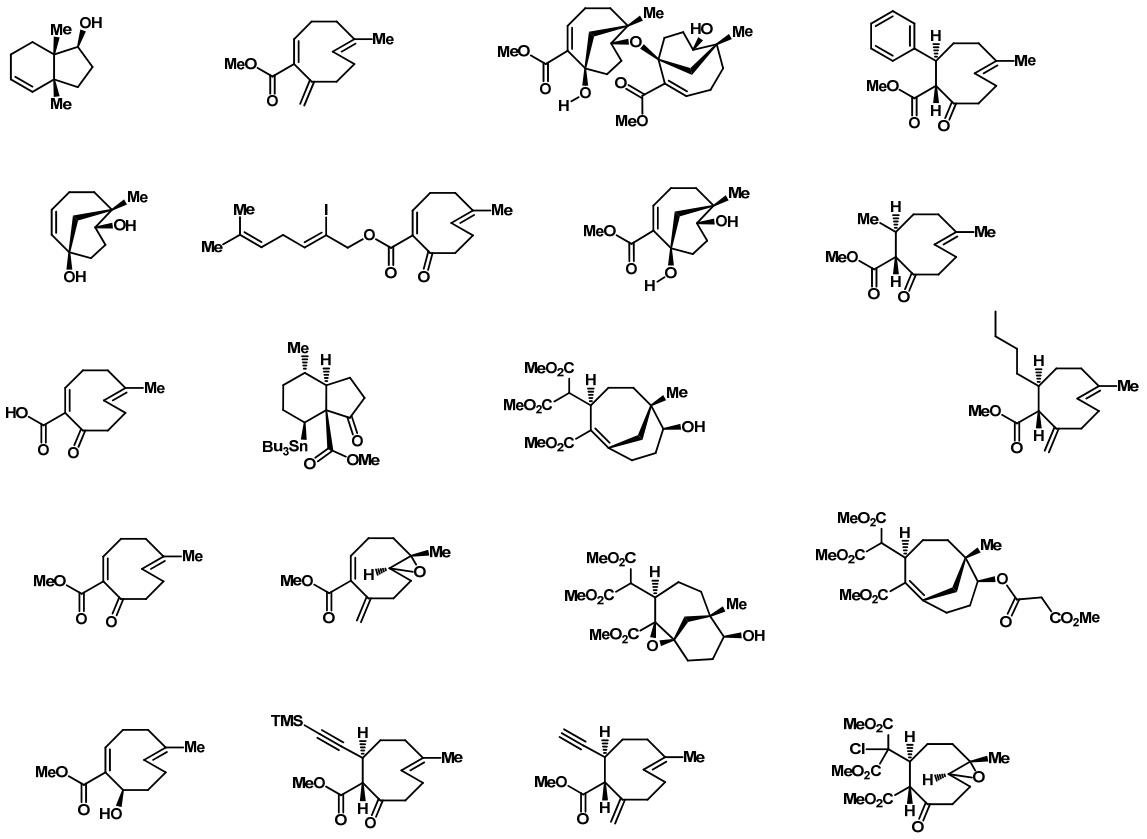

Figure III.26 Inactive compounds at 100-200 μM.

We thus demonstrated that structure space-targeting is an effective means by which to gain access to bioactive compounds of significant complexity. The natural products **3.1**-**3.4** were enantiopure and active between 11 and 29 μM.[3] All of our synthetic products are racemic. Assuming that only one enantiomer of each compound is active in the assay, the effective concentrations of our compounds can be cut in half, so their potency rivals that of the natural products. The synthetic compounds kill nonspecifically at high concentration; only at lower concentration is selectivity realized.

General structure-activity-relationships (SARs) were deduced from the apoptosis induction screen. The *Z* olefins appear more potent than the *E* olefins. The fact that steroidal allylic ester **3.60** was toxic and steroidal methyl ester **3.61** exhibited no activity

suggests that a greasy terpene chain is relevant in promoting cell death. Conversely, the tin moiety is not relevant to activity. The fact that the *n*-butyl addition product **3.33** was active, while the methyl addition product **3.34** was not, also points to the same suggestion. In general, the active compounds had greasy terpene chains and/or conformational equilibria analogous to the natural products. These structural characteristics may be critical to the pharmacophore for target binding in apoptosis-competent cells.

Collectively, the data are interesting and it is surprising as to why some congeners are active while others are not. More studies are needed to clarify this. SARs and structure optimization are ongoing, and an important future goal is to identify the target protein and mechanism of apoptosis induction. We speculate that these hydrophobic molecules may be binding to Bak and Bax directly or to the mitochondria.

3.14 Ongoing Studies

We are targeting new xenicane scaffolds (**3.121**-**3.124**, Scheme III.56). These molecules will provide the foundation for developing a complete SAR across all of the xenicane structure space. Many promising side chain variants will be accessible from these compounds. The effects of this important structural region on apoptosis induction will subsequently be examined.

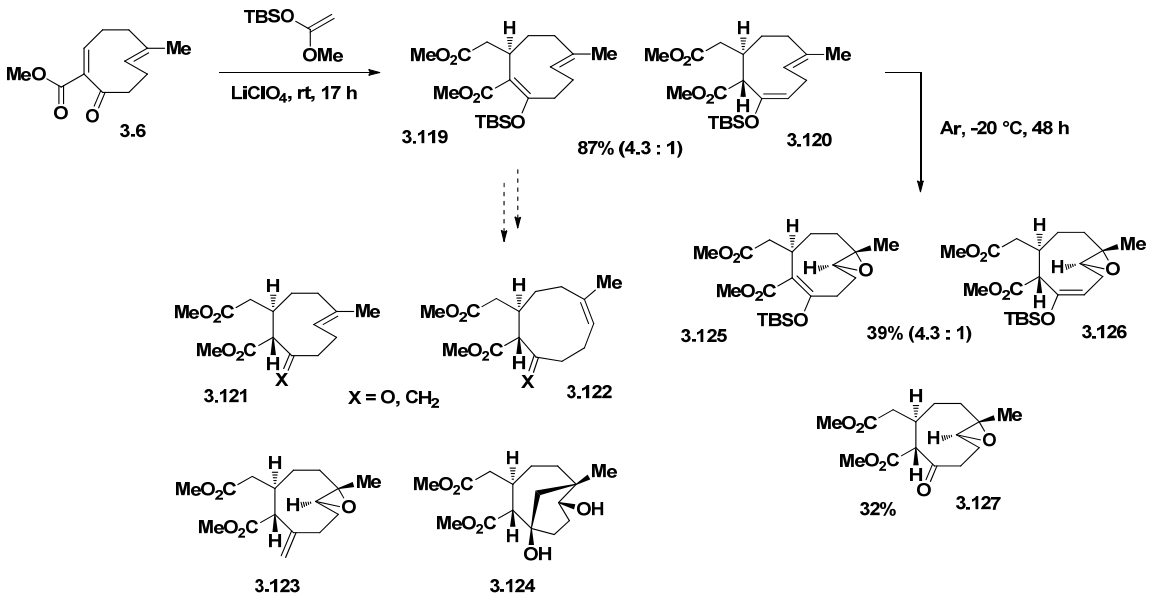

Scheme III.56 New target scaffolds for SAR development.

A mixture of TBS enol ethers **3.119** and **3.120** was prepared via $LiClO_4$-mediated neat Mukaiyama-Michael addition. Both acidic and basic deprotecting conditions destroyed this material. We are developing a slow, mild deprotection using $AcOH/H_2O/THF$. **3.119** and **3.120** must be used immediately since spontaneous epoxidation of the strained alkenes occurs very fast (→ **3.125** + **3.126**). Keto epoxide **3.127** was also isolated as a degradation product of **3.125** and **3.126**.

3.15 Integrated Route to Xenicanes and Diverse Motifs: Summary

Scheme III.57 provides an overview of our integrated route to the previously restricted, semi-validated xenicane structure space. The preceding work demonstrates the utility of the key nine-membered platform and structure space targeting in general to access diverse and complex structures. We have prepared over forty xenicane congeners. The intrinsic structure and reactivity of each product has been carefully studied. In particular,

enone resistance to conjugate addition has been overcome with the judicious use of Lewis acids and neat reaction conditions. Sixteen products exhibited anticancer activity, and seven were shown to selectively induce apoptosis in immortalized baby mouse kidney epithelial cells.

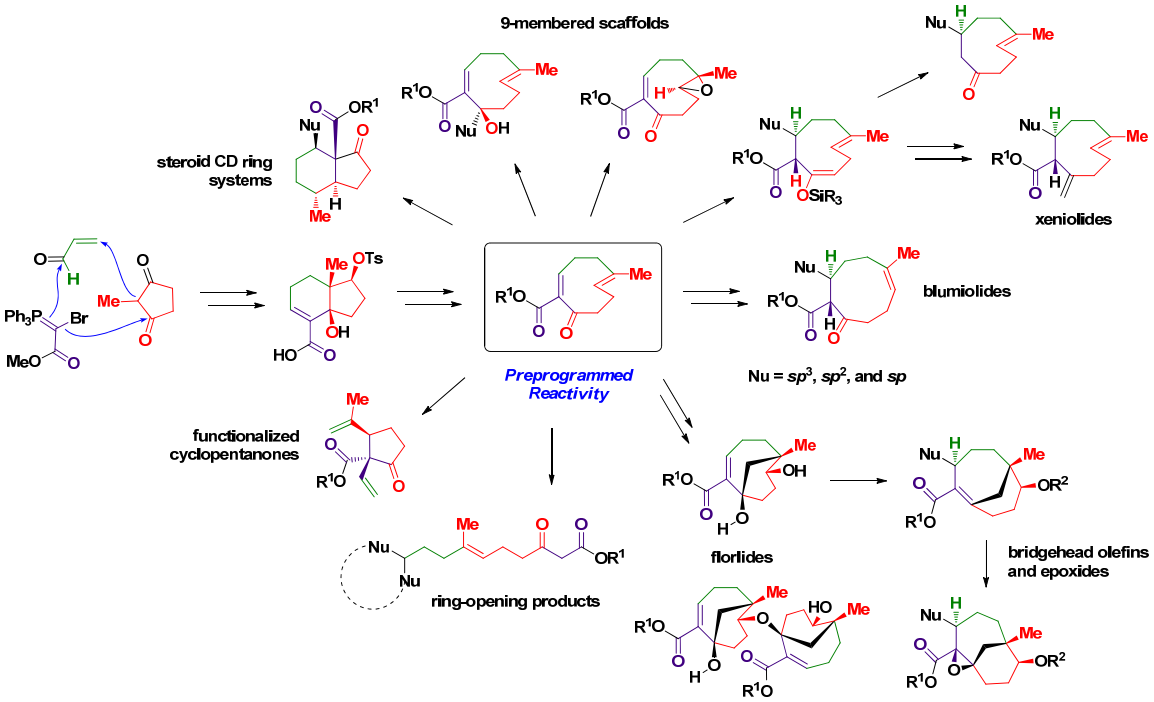

Scheme III.57 Integrated route to xenicanes and diverse motifs.

3.16 References and Notes

1. a) Oncology Market Leaders – Analyses and Outlook – 2010-2025. Visiongain. **January 2010**; b) Up or Out in Oncology? Bionest Partners. **November 2007**.

2. R. Mathew, K. Degenhart, L. Haramaty, C. M. Karp, E. White, *Methods Enzymol.* **2008**, *446*, 77-106.

3. a) P. Falkowski, U.S. Patent Appl. No. 12/530,415, Pub. No. 2010/0113585, 2010; b) E. H. Andrianasolo et al., *J. Nat. Prod.* **2007**, *70*, 1551-1557.

4. a) Y. Zhang, S. D. Lotesta, T. J. Emge, L. J. Williams, *Tetrahedron Lett.* **2009**, *50*, 1882-1885; b) Joseph Ryan Cusick, (2011). Doctoral dissertation, Rutgers, The State University of New Jersey, New Brunswick, New Jersey.

5. O. V. Larionov, E. J. Corey, *J. Am. Chem. Soc.* **2008**, *130*, 2954-2955.

6. a) Computational analyses used (DFT-B3LYP 6-31G(d, p)), including diffuse functions and charges where appropriate; b) All structures were fully optimized by analytical gradient methods using the GAUSSIAN 03 suites: M. J. Frisch, G. W. Trucks, H. B. Schlege, G. E. Scuseria, M. A. Robb, J. R. Cheeseman, J. A. Montgomery, Jr., T. Vreven, K. N. Kudin, J. C. Burant, *GAUSSIAN 03, Revision E.01*, Gaussian: Wallingford, CT, 2004; c) Density functional theory (DFT) calculations used the exchange potentials of: A. D. Becke, *J. Chem. Phys.* **1993**, *98*, 5648-5652; the correlation functional of: C. Lee, W. Yang, R. G. Parr, *Phys. Rev. B* **1988**, *37*, 785-789.

7. V. Prelog, K. Schenker, *Helv. Chim. Acta* **1952**, *35*, 2044-2053.

8. E. J. Corey, R. B. Mitra, H. Uda, *J. Am. Chem. Soc.* **1964**, *86,* 485-492.

9. R. R. Huddleston, M. J. Krische, *Org. Lett.* **2003**, *5*, 1143-1146.

10. D. Chapdelaine, J. Belzile, P. Deslongchamps, *J. Org. Chem.* **2002**, *67*, 5669-5672.

11. K. Takai, M. Tagashira, T. Kuroda, K. Oshima, K. Utimoto, H. Nozaki, *J. Am. Chem. Soc.* **1986**, *108*, 6048-6050.

12. a) B. M. Trost, A. B. Pinkerton, *Org. Lett.* **2000**, *2*, 1601-1603; b) B. M. Trost, A. B. Pinkerton, *J. Org. Chem.* **2001**, *66*, 7714-7722; c) K. Suzuki, H. Takayama, *Org. Lett.* **2006**, *8*, 4605-4608.

13. J. Deschamp, O. Riant, *Org. Lett.* **2009**, *11*, 1217-1220.

14. A. Fürstner, N. Shi, *J. Am. Chem. Soc.* **1996**, *118*, 12349-12357.

15. L. Wang, S. K. Meegalla, C.-L. Fang, N. Taylor, R. Rodrigo, *Can. J. Chem.* **2002**, *80*, 728-738.

16. I. Galynker, W. C. Still, *Tetrahedron Lett.* **1982**, *23*, 4461-4464.

17. B. Radüchel, *Synthesis* **1980**, 292-295.

18. K. C. Nicolaou, A. A. Estrada, M. Zak, S. H. Lee, B. S. Safina, *Angew. Chem. Int. Ed.* **2005**, *44*, 1378-1382.

19. C. L. Perrin, J. S. Lau, Y.-J. Kim, P. Karri, C. Moore, A. L. Rheingold, *J. Am. Chem. Soc.* **2009**, *131,* 13548-13554.

20. a) M. Bandini, P. G. Cozzi, A. Umani-Ronchi, *Polyhedron* **2000**, *19*, 537-539; b) A. Berkessel, D. Menche, C. A. Sklorz, M. Schröder, I. Paterson, *Angew. Chem. Int. Ed.* **2003**, *42*, 1032-1035.

21. M. Shimizu, S. Yamada, Y. Fujita, F. Kobayashi, *Tetrahedron: Asymmetry* **2000**, *11*, 3883-3886.

22. T. Katoh, S. Mizumoto, M. Fudesaka, Y. Nakashima, T. Kajimoto, M. Node, *Synlett* **2006**, *14*, 2176-2182.

23. a) Jeremy Matthew Carr, (2009). Doctoral dissertation, The University of Alabama, Tuscaloosa, Alabama; b) J. M. Carr, T. S. Snowden, *Tetrahedron* **2008**, *64*, 2897-2905.

24. T. Miyamoto, Y. Takenaka, K. Yamada, R. Higuchi, *J. Nat. Prod.* **1995**, *58*, 924-928.

25. H. Yao, D. E. Richardson, *J. Am. Chem. Soc.* **2000**, *122*, 3220-3221.

26. Å. M. L. Øiestad, A. C. Petersen, V. Bakken, J. Vedde, E. Uggerud, *Angew. Chem. Int. Ed.* **2001**, *40*, 1305-1309.

27. Comparable ground state energies were calculated in Gaussian.

28. J. L. Bada, R. Protsch, *Proc. Nat. Acad. Sci.* **1973**, *70*, 1331-1334.

29. Y. Yamamoto, *Angew. Chem. Int. Ed.* **1986**, *25*, 947-959.

30. H. Sakata, I. Kuwajima, *Tetrahedron Lett.* **1987**, *28*, 5719-5722.

31. S. Oi et al., *Tetrahedron* **2002**, *58*, 91-97.

32. SDBSWeb: http://riodb01.ibase.aist.go.jp/sdbs/ (National Institute of Advanced Industrial Science and Technology)

33. J. A. Vroman, H. N. ElSohly, M. A. Avery, *Synth. Comm.* **1998**, *28*, 1555-1562.

34. a) E. J. Corey, N. W. Boaz, *Tetrahedron Lett.* **1985**, *26*, 6019-6022; b) A. Alexakis, J. Berlan, Y. Besace, *Tetrahedron Lett.* **1986**, *27*, 1047-1050; c) S. H. Bertz, G. Miao, B. E. Rossiter, J. P. Snyder, *J. Am. Chem. Soc.* **1995**, *117*, 11023-11024.

35. Y.-N. Kuo, J. A. Yahner, C. Ainsworth, *J. Am. Chem. Soc.* **1971**, *93*, 6321-6323.

36. Y.-C. Lin, M. H. Abd El-Razek, T.-L. Hwang, M. Y. Chiang, Y.-H. Kuo, C.-F. Dai, Y.-C. Shen, *J. Nat. Prod.* **2009**, *72*, 1911-1916.

37. Comprehensive Heterocyclic Chemistry III: A Review of the Literature (1995-2007). Volume 12: Seven-Membered and Larger Heterocyclic Rings Including All Fused Derivatives, "Nine-Membered Rings." D. O. Tymoshenko, AMRI, Albany, NY. 2008 Elsevier Ltd.

38. G. Guella, G. Chiasera, I. N'Diaye, F. Pietra, *Helv. Chim. Acta.* **1994**, *77*, 1203-1221.

39. A. C. Spivey, L. Shukla, J. F. Hayler, *Org. Lett.* **2007**, *9*, 891-894.

40. L. W. Bieber, M. F. da Silva, *Tetrahedron Lett.* **2007**, *48*, 7088-7090.

41. a) E. J. Corey, J. A. Katzenellenbogen, G. H. Posner, *J. Am. Chem. Soc.* **1967**, *89*, 4245-4247; b) E. Corey, H. Kirst, J. Katzenellenbogen, *J. Am. Chem. Soc.* **1970**, *92*, 6314-6320.

42. C. Nativi, M. Taddei, *J. Org. Chem.* **1988**, *53*, 820-826.

43. H. E. Ensley, R. R. Buescher, K. Lee, *J. Org. Chem.* **1982**, *47*, 404-408.

44. C. Ollivier, P. Renaud, *Chem. Rev.* **2001**, *101*, 3415-3434.

45. J. A. Marshall, M. P. Bourbeau, *Tetrahedron Lett.* **2003**, *44*, 1087-1089.

46. a) D. Seyferth, L. G. Vaughan, *J. Am. Chem. Soc.* **1964**, *86*, 883-890; b) P. W. Collins, C. J. Jung, A. Gasiecki, R. Pappo, *Tetrahedron Lett.* **1978**, *19*, 3187-3190; c) K. H. Chu, K. K. Wang, *J. Org. Chem.* **1986**, *51*, 767-768.

47. S. D. Knight, L. E. Overman, G. Pairaudeau, *J. Am. Chem. Soc.* **1995**, *117*, 5776-5788.

48. B. H. Lipshutz, M. Koerner, D. A. Parker, *Tetrahedron Lett.* **1987**, *28*, 945-948.

49. J. E. Baldwin, *J. Chem. Soc., Chem. Commun.* **1976**, *18*, 734-736.

50. K. Miura, D. Itoh, T. Hondo, A. Hosomi, *Tetrahedron Lett.* **1994**, *35*, 9605-9608.

51. H. Takayama, F. Watanabe, M. Kitajima, N. Aimi, *Tetrahedron Lett.* **1997**, *38*, 5307-5310.

52. Stereochemistry of Radical Reactions: Concepts, Guidelines, and Synthetic Applications. D. P. Curran, N. A. Porter, B. Giese, 2008 John Wiley & Sons.

53. a) J. F. Blount, R. W. Dunlop, K. L. Erickson, R. J. Wells, *Aust. J. Chem.* **1982**, *35*, 145-163; b) E. Ioannou et al., *Tetrahedron* **2009**, *65*, 10565-10572.

54. K. B. Wiberg, K. E. Laidig, *J. Am. Chem. Soc.* **1987**, *109*, 5935-5943.

55. M. R. Saidi, N. Azizib, E. Akbaria, F. Ebrahimia, *J. Mol. Cat. A: Chemical* **2008**, *292*, 44-48.

56. C. Hagemann, *Th. L. Ber. Dtsch. Chem. Ges.* **1893**, *26*, 876-890.

57. G. P. Pollini, S. Benetti, C. De Risi, V. Zanirato, *Tetrahedron* **2010**, *66*, 2775-2802.

58. Y. Kashman, A. Rudi, *Phytochem. Rev.* **2004**, *3*, 309-323.

59. X. Cheng, N. L. Harzdorf, T. Shaw, D. Siegel, *Org. Lett.* **2010**, *12*, 1304-1307.

60. W. H. Kim, A. R. Angeles, J. H. Lee, S. J. Danishefsky, *Tetrahedron Lett*. **2009**, *50*, 6440-6441.

61. a) J. Tanaka, T. Higa, *Chem. Lett.* **1984**, 231-232; b) Y. Viano et al., *Tetrahedron Lett.* **2011**, *52*, 1031-1035.

62. A. A. H. El-Gamal, S.-K. Wang, C.-Y. Duh, *J. Nat. Prod.* **2006**, *69*, 338-341.

63. J. R. Wiseman, W. A. Pletcher, *J. Am. Chem. Soc.* **1970**, *92*, 956-962.

64. M. J. Campbell, P. D. Pohlhaus, G. Min, K. Ohmatsu, J. S. Johnson, *J. Am. Chem. Soc.* **2008**, *130*, 9180-9181.

65. a) T. Iwagawa, J. Kawasaki, T. Hase, *J. Nat. Prod.* **1998**, *61,* 1513-1515; b) A. A. H. El-Gamal, C.-Y. Chiang, S.-H. Huang, S.-K. Wang, C.-Y. Duh, *J. Nat. Prod.* **2005**, *68,* 1336-1340.

66. N. Majumdar, K. A. Korthals, W. D. Wulff, *J. Am. Chem. Soc.* **2012**, *134*, 1357-1362.

67. S. Matsubara, T. Okazoe, K. Oshima, K. Takai, H. Nozaki, *Bull. Chem. Soc. Jpn.* **1985**, *58*, 844-849.

68. M. F. Semmelhack, R. J. Hooley, *Tetrahedron Lett.* **2003**, *44*, 5737-5739.

69. ACE Organic acidity and basicity calculator: http://aceorganic.pearsoncmg.com/epoch-plugin/public/pKa.jsp

70. The Chemistry of Organocopper Compounds. Eds. Z. Rappoport, I. Marek, 2009 Wiley-Interscience: New York.

71. S. Pasynkiewicz, E. Sliwa, *J. Organomet. Chem.* **1965**, *3*, 121-128.

72. N. A. Petasis, D. K. Fu, *Organometallics* **1993**, *12*, 3776-3780.

73. These data have not been reproduced.

Chapter IV

Experimental

4.1 Chapter II

General Information: Starting materials, reagents, and solvents were purchased from commercial suppliers (Aldrich, Acros, Lancaster, and Fischer) and used as received unless otherwise noted. Water-sensitive reactions were conducted using anhydrous solvents in flame-dried glassware with magnetic stirring under an inert atmosphere of dry argon. Oven-dried syringes were used to transfer water-sensitive materials. Reaction progress was monitored by analytical thin layer chromatography (TLC), using 250 μm silica gel plates (Dynamic Absorbents F-254). Reactions in DMF, pyridine, and HMPA were monitored by drying spotted TLC plates under high vacuum for 5 min prior to running the TLCs. Visualization was accomplished with UV light and anisaldehyde stain, followed by heating on a hot plate. Flash column chromatography (FCC) was conducted using 230-400 mesh, pore size 60Å, Silicycle ultra pure silica gel unless otherwise noted. Optical rotations were recorded on a Perkin-Elmer 343 polarimeter at 589 nm and 298 K. Infrared (IR) spectra were recorded on an ATI Mattson Genesis Series FT-Infrared spectrophotometer. Proton nuclear magnetic resonance (^{1}H NMR) spectra were recorded on either a Varian-300 instrument (300 MHz), Varian-400 instrument (400 MHz), Varian-500 instrument (500 MHz), or a Varian-600 instrument (600 MHz). Chemical shifts are reported in ppm relative to chloroform or benzene as the internal standard. Data are reported as follows: chemical shift, integration, multiplicity (s = singlet, d = doublet, t = triplet, q = quartet, br = broad, m

= multiplet), and coupling constants (Hz). Carbon nuclear magnetic resonance (^{13}C NMR) spectra were recorded on either a Varian-300 instrument (75 MHz), Varian-400 instrument (100 MHz), Varian-500 instrument (125 MHz), or Varian-600 instrument (150 MHz). Chemical shifts are reported in ppm relative to chloroform or benzene as the internal standard. Mass spectra were recorded on a Finnigan LCQ-DUO mass spectrometer. The enantioenriched starting material (a*R*)-6-methylcyclonona-(2*Z*,6*E*)-dienone (**2.1**) was prepared according to published procedures.

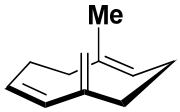

2.11

Cyclononatriene (2.11): To a solution of cyclononadienone **2.1** (R_f 0.45 in 5:1 hex/EtOAc, 0.2453 g, 1.633 mmol, azeotropically dried with toluene x 3) in THF/pyridine (5:1, 63 mL) at 0 °C was added Tebbe reagent (0.5 M in toluene, 13.1 mL, 6.55 mmol) dropwise. The solution gradually turned from orange to maroon as the reaction was gradually warmed to room temperature. The starting material was completely consumed after 2 h. The reaction mixture was diluted with 50 mL of diethyl ether and cooled to 0 °C. 1 M aqueous NaOH was added dropwise until the evolution of gas ceased, giving a creamy orange/red suspension. The quenched mixture was vacuum filtered through Celite and rinsed through with liberal amounts of diethyl ether. The orange filtrate was washed with brine (20 mL). The organic layer was dried over Na_2SO_4, filtered, and concentrated gently (rotovapped at no less than 50 torr at rt) to an oily orange residue. The crude material was purified by FCC (100% hex). Leftover toluene was gently rotovapped off (no less than 50

torr at rt), furnishing cyclononatriene **2.11** (R_f 0.5 in 100% hex, 0.195 g, 1.315 mmol, 81%) as a volatile, colorless oil with a distinct terpene scent. Blowing a gentle stream of argon over a solution of the triene in toluene at -78 °C effects evaporation of this product. IR ν_{max} (neat)/cm^{-1} 3073, 3046, 2994, 2926, 2854, 1453, 895, 759, 665. ^{1}H NMR ($CDCl_3$, 500 MHz) δ 5.81 (1H, d, J = 12.0 Hz), 5.24 (1H, ddd, J = 12.0, 8.5, 7.5 Hz), 5.14 (1H, dd, J = 10.5, 0.5 Hz), 4.62 (1H, br s), 4.58 (1H, br s), 2.42 – 2.27 (2H, m), 2.23 (1H, qt, J = 11.0, 1.5 Hz), 2.10 – 1.97 (3H, m), 1.96 – 1.88 (2H, m), 1.53 (3H, s) ppm. ^{13}C NMR ($CDCl_3$, 75 MHz) δ 146.9, 138.1, 133.9, 127.5, 126.0, 112.4, 39.8, 37.9, 28.4, 26.0, 17.6 ppm. ESI-MS $[M+H]^+$ *m/z* calcd 149.1, observed 149.2.

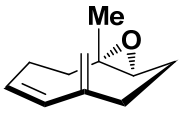

2.2

Racemic cyclononaepoxydiene (2.2): To a solution of **2.11** (R_f 0.5 in 100% hex, 0.0975 g, 0.658 mmol) in DCM (24 mL) at 0 °C was added *m*-CPBA (77%, 0.147 g, 0.658 mmol). The colorless solution was gradually warmed to room temperature over 2 h, quenched by the dropwise addition of saturated aq. Na_2SO_3 (5 mL), and extracted with DCM (3 x 10 mL). The combined organic layers were washed with brine (10 mL), dried over Na_2SO_4, filtered, and concentrated under reduced pressure to give an oily yellow residue. The crude product was purified by FCC (0 to 10% EtOAc/hex), furnishing cyclononaepoxydiene **2.2** (R_f 0.55 in 5:1 hex/EtOAc, 0.0941 g, 0.573 mmol, 87%) as a colorless amorphous solid with a distinct terpene scent. IR ν_{max} (thin film)/cm^{-1} 3074, 2956, 2918, 2849, 1726, 1463, 1379, 1262, 1073. ^{1}H NMR ($CDCl_3$, 400 MHz) δ 5.89 (1H, d, J = 11.5 Hz), 5.50 (1H, ddd,

J = 11.5, 9.0, 7.5 Hz), 4.99 (1H, br s), 4.95 (1H, br s), 3.13 (1H, dd, J = 12.0 Hz, 2.0 Hz), 2.66 – 2.57 (1H, m), 2.47 – 2.39 (1H, m), 2.14 – 2.06 (2H, m), 2.05 – 1.94 (2H, m), 1.45 (1H, qd, J = 11.5, 3.5 Hz), 1.29 (3H, s), 0.97 – 0.81 (1H, m) ppm. ^{13}C NMR ($CDCl_3$, 75 MHz) δ 145.9, 137.3, 127.5, 114.1, 62.1, 60.0, 36.2, 31.7, 27.2, 21.6, 18.5 ppm. ESI-MS $[M+H]^+$ *m/z* calcd 165.1, observed 165.1.

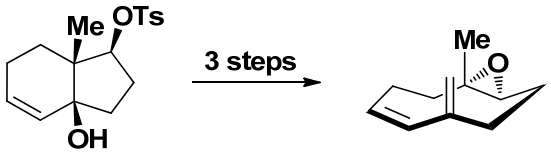

2.2

Enantioenriched cyclononaepoxydiene (2.2): For this three-pot procedure, all solvents were cooled to 0 °C or below in an explosion-proof freezer prior to usage. Ice cubes were added to the biphasic workup mixtures to maintain low temperature. To a solution of enantioenriched tosyl alcohol **2.9** (93% *ee*, R_f 0.1 in 5:1 hex/EtOAc, 0.153 g, 0.475 mmol, azeotropically dried with toluene x 3) in DMF (15 mL) at 0 °C was added a suspension of sodium hydride (60% in mineral oil, rinsed with hexane x 4, 0.0244 g, 0.638 mmol) in DMF (5 mL). The pale yellow suspension turned dark brown within 5 min. After 2 h at 0 °C, cold brine (13 mL) was added dropwise, and the quenched mixture was extracted with cold Et_2O (3 x 50 mL). The combined organic layers were washed with cold brine (2 x 25 mL), dried over Na_2SO_4 in an ice-water bath, filtered, and concentrated gently under reduced pressure at 0 °C (no less than 50 torr). To a solution of the crude enantioenriched cyclononadienone **2.1** in cold toluene/pyridine (5:1, 15 mL) was added freshly activated (and cooled under argon) 4Å molecular sieve beads. To this mixture at 0 °C was added Tebbe reagent (0.5M in toluene, 3.796 mL, 1.898 mmol) dropwise, turning the mixture

orange then dark brown. After 2 h, the reaction was diluted with 40 mL of cold Et_2O. Cold 1M aq NaOH was added dropwise until the evolution of gas ceased. The resulting creamy orange/red suspension was vacuum filtered through Celite into a filter flask in an ice-water bath and rinsed through with liberal amounts of cold Et_2O. The orange filtrate was washed with cold brine (50 mL). The organic layer was concentrated gently under reduced pressure at 0 °C (no less than 30 torr) to an oily orange residue. The crude material was quickly flushed through a silica gel plug with cold hexane and collected in a roundbottom flask in an ice-water bath. The purified solution of enantioenriched cyclononatriene **2.11** was concentrated at 0 °C to a volume of ~25 mL. To this solution at 0 °C was added *m*-CPBA (77%, 0.0954 g in 0.010 mg portions, 0.428 mmol). After 10 minutes, saturated aq Na_2SO_3 (5 mL) was added dropwise, and the quenched mixture was warmed to rt. After extraction with DCM (3 x 20 mL), the combined organic layers were washed with brine (10 mL), dried over Na_2SO_4, filtered, and concentrated under reduced pressure to an oily yellow residue. The crude material was purified by FCC (0 to 10% EtOAc/hexane), furnishing enantioenriched cyclononaepoxydiene **2.2** (0.0663 g, 0.404 mmol, 85%) as a colorless amorphous solid with a distinct terpene scent. $[\alpha]_D^{25}$ +3.2 (*c* 0.13, $CHCl_3$). HPLC: Daicel Chiralpak AS-H, *n*-hex/*i*-PrOH = 95/5, Flow rate = 1 mL/min, UV = 230 nm, t_R = 5.8 min and t_R = 13.6 min (major, 71% *ee*).

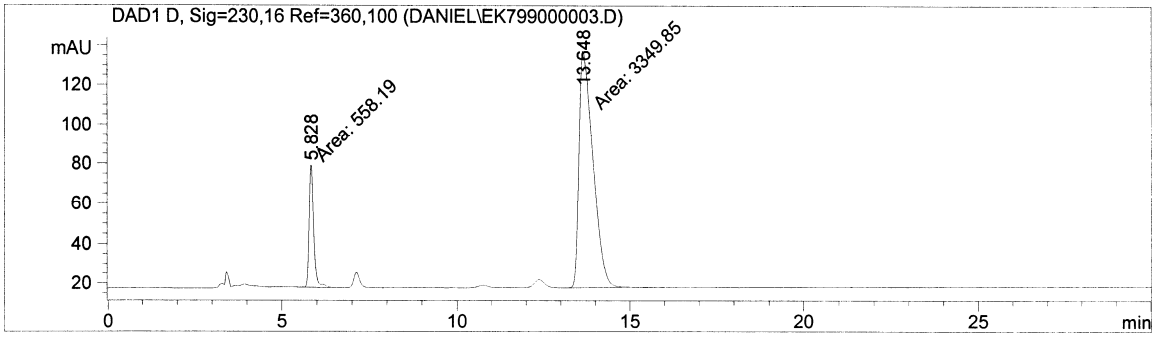

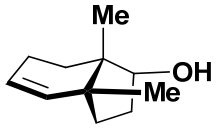

2.3

Xenibellol core (2.3): To freshly activated 4Å powdered molecular sieves was added zinc dust (0.0254 g, 0.390 mmol) and bright red bis(cyclopentadienyl)titanium dichloride (0.050 g, 0.195 mmol) under an inert atmosphere of dry argon. The flask was covered in aluminum foil, then charged with degassed THF (2.4 mL), producing a red solution upon stirring. After 25 minutes at rt, the red solution had turned lime green, indicating complete reduction to Ti(III). To this was added a solution of enantioenriched cyclononaepoxydiene **2.2** (0.008 g, 0.0488 mmol) in degassed THF (1.2 mL). Within a few seconds the reaction solution turned dark orange. Complete consumption of starting material was observed after 10 minutes, then the suspension was vacuum filtered, rinsing through with liberal amounts of Et_2O. The filtrate was partitioned between THF/Et_2O and brine (5 mL). The organic layer was separated, and the aqueous layer was extracted with Et_2O (2 x 2 mL). The combined organic layers were washed with brine (2 mL), dried over Na_2SO_4, filtered, and concentrated under reduced pressure to an oily orange residue. The crude material was purified by FCC (0 to 20% Et_2O/pentane), furnishing enantioenriched xenibellol core **2.3** (R_f 0.25 in 17% EtOAc/hex, 0.0037 g, 46%) as a colorless solid with a distinct terpene scent. $[\alpha]_D^{25}$ +2.4 (*c* 0.13, $CHCl_3$). IR ν_{max} (thin film)/cm^{-1} 3449, 2955, 2919, 2850, 1655, 1561, 1459, 1364. ^1H NMR (C_6D_6, 500 MHz) δ 5.39 (1H, dt, J = 7.0, 3.5 Hz), 5.30 (1H, dt, J = 4.0, 2.0 Hz), 3.91 (1H, t, 8.0 Hz), 1.94 – 1.82 (3H, m), 1.57 – 1.49 (1H, m), 1.46 – 1.30 (3H, m), 1.25 – 1.17 (1H, m), 0.93 (3H, s), 0.77 (3H, s), 0.45 (1H, br s) ppm. ^{13}C NMR

(C_6D_6, 125 MHz) δ 139.1, 123.7, 76.1, 45.3, 43.9, 36.7, 31.1, 28.4, 25.0, 22.7, 17.1 ppm. ESI-MS $[M+Na]^+$ *m/z* calcd 189.1, observed 188.5, 190.6.

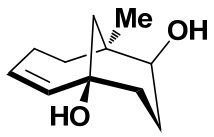

2.4

Florlide core (2.4): To a solution of enantioenriched cyclononaepoxydiene **2.2** (0.020 g, 0.122 mmol) in DCM (18 mL) at -78 ºC was added $BF_3{\cdot}Et_2O$ (purified, redistilled, 0.0306 mL, 0.244 mmol) dropwise. After 15 min, the colorless reaction was quenched by the addition of saturated aq. $NaHCO_3$ (1 mL). The resulting quenched mixture was allowed to warm to room temperature. After extracting with DCM (3 x 15 mL), the combined organic layers were washed with brine (8 mL), dried over Na_2SO_4, filtered, and concentrated under reduced pressure to give a colorless oily residue. The crude product was purified by FCC (0 to 75% EtOAc/hex), affording enantioenriched florlide core **2.4** (R_f 0.15 in 1:1 EtOAc/hex, 0.0161 g, 0.089 mmol, 73%) as a colorless solid. $[\alpha]_D^{25}$ -3.6 (*c* 0.13, $CHCl_3$). IR ν_{max} (thin film)/cm^{-1} 3318, 3014, 2918, 2850, 1457, 1385, 1031, 1018. ^1H NMR (C_6D_6, 600 MHz) δ 5.61 (1H, ddd, J = 11.5, 8.5, 3.5 Hz), 5.31 (1H, dt, J = 11.5, 2.5 Hz), 2.99 (1H, dd, J = 2.9, 2.6 Hz), 2.07 (1H, ddddd, J = 16.5, 12.7, 8.5, 2.6, 2.5 Hz), 1.80 (1H, ddd, J = 14.5, 4.3, -13.0 Hz), 1.72 (1H, ddd, J = 4.3, 2.6, -14.8 Hz), 1.65 (1H, dd, J = 13.4, 2.3 Hz), 1.63 (1H, d, 13.4 Hz), 1.63 (1H, ddddd, J = 16.5, 5.9, 3.5, 3.0, 0.5 Hz), 1.40 (1H, dd, J = 4.4, -13.0 Hz), 1.37 (1H, dddd, J = 14.5, 4.4, 2.9, -14.8 Hz), 1.16 (1H, ddd, J = 12.7, 3.0, -14.5 Hz), 1.11 (1H, ddd, J = 5.9, 2.6, -14.5 Hz), 1.03 (1H, br s), 0.86 (3H, s), 0.73 (1H, br s) ppm. ^{13}C NMR (C_6D_6, 150 MHz) δ 137.2, 129.8, 73.3, 73.0, 42.2, 38.1, 37.4, 32.8, 28.6, 27.7, 23.2

ppm. ESI-MS $[M\text{-}H_2O+H]^+$ *m/z* calcd 165.1, observed 165.0; $[M+2Na]^+$ *m/z* calcd 228.1, observed 228.5.

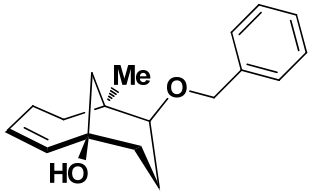

2.12

Benzylated florlide core (2.12): To a solution of florlide core **2.4** (0.004 g, 0.022 mmol, azeotropically dried with toluene x 3) in DMF (54.9 uL) was added NaH (60% in mineral oil, 0.0011 g, 0.0264 mmol) and benzyl bromide (5.32 uL, 0.044 mmol). The brown reaction mixture was stirred at rt for 16 h, then it was quenched with water (1 mL). The organics were extracted with EtOAc (3 x 1 mL), dried over anhydrous $MgSO_4$, filtered, and concentrated in vacuo. The crude yellow residue was purified by FCC (0 to 50% EtOAc/hex), providing **2.12** (R_f 0.7 in 1:1 EtOAc/hex, 0.0026 g, 0.0096 mmol, 44%) as a yellow oil. IR ν_{max} (thin film)/cm^{-1} 3423, 2926, 2851, 1717, 1648, 1467, 1108, 1067, 1027. ^1H NMR ($CDCl_3$, 500 MHz) δ 7.47 – 7.28 (5H, m), 5.85 (1H, ddd, J = 12.0, 9.0, 3.5 Hz), 5.37 (1H, td, J = 11.5, 2.5 Hz), 4.65 (1H, d, J = 12.0 Hz), 4.42 (1H, d, J = 12.0 Hz), 3.04 (1H, s), 2.42 – 2.28 (1H, m), 2.02 – 1.95 (1H, m), 1.94 – 1.86 (2H, m), 1.82 – 1.70 (3H, m), 1.65 – 1.36 (4H, m), 1.07 (3H, s). ^{13}C NMR ($CDCl_3$, 125 MHz) δ 137.9, 136.2, 131.1, 128.5, 127.6, 127.5, 80.7, 71.3, 42.9, 38.2, 33.0, 30.0, 29.0, 23.1, 22.6 ppm. ESI-MS $[M+Na]^+$ *m/z* calcd 295.2, observed 295.2.

*NOESY analysis of **2.3** was straightforward.

The complex structure of **2.4 required more rigorous 2D NMR characterization.

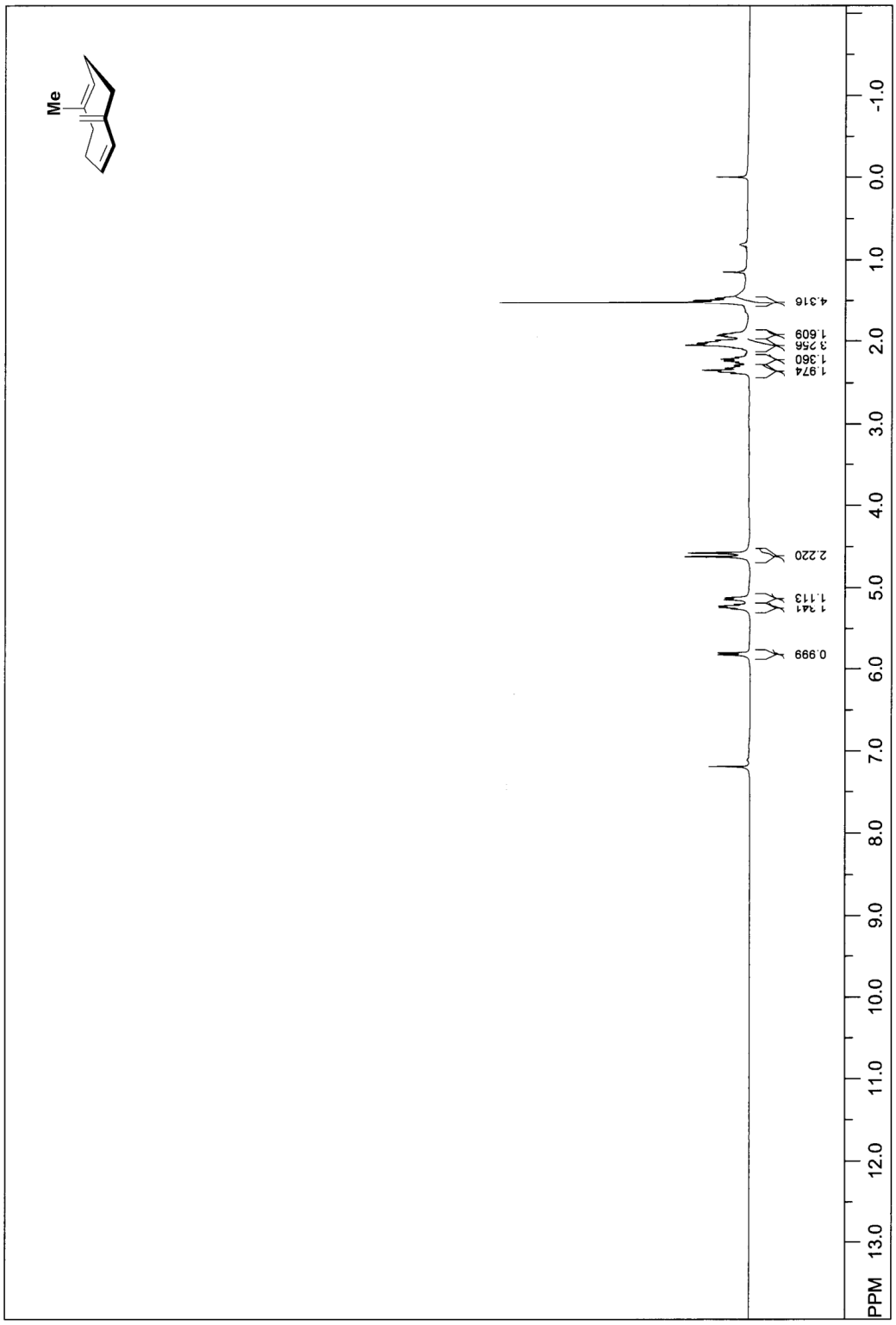
Me
4.316
1.974
1.360
3.256
1.609
2.220
1.341
1.113
0.999
PPM
13.0
12.0
11.0
10.0
9.0
8.0
7.0
6.0
5.0
4.0
3.0
2.0
1.0
0.0
-1.0

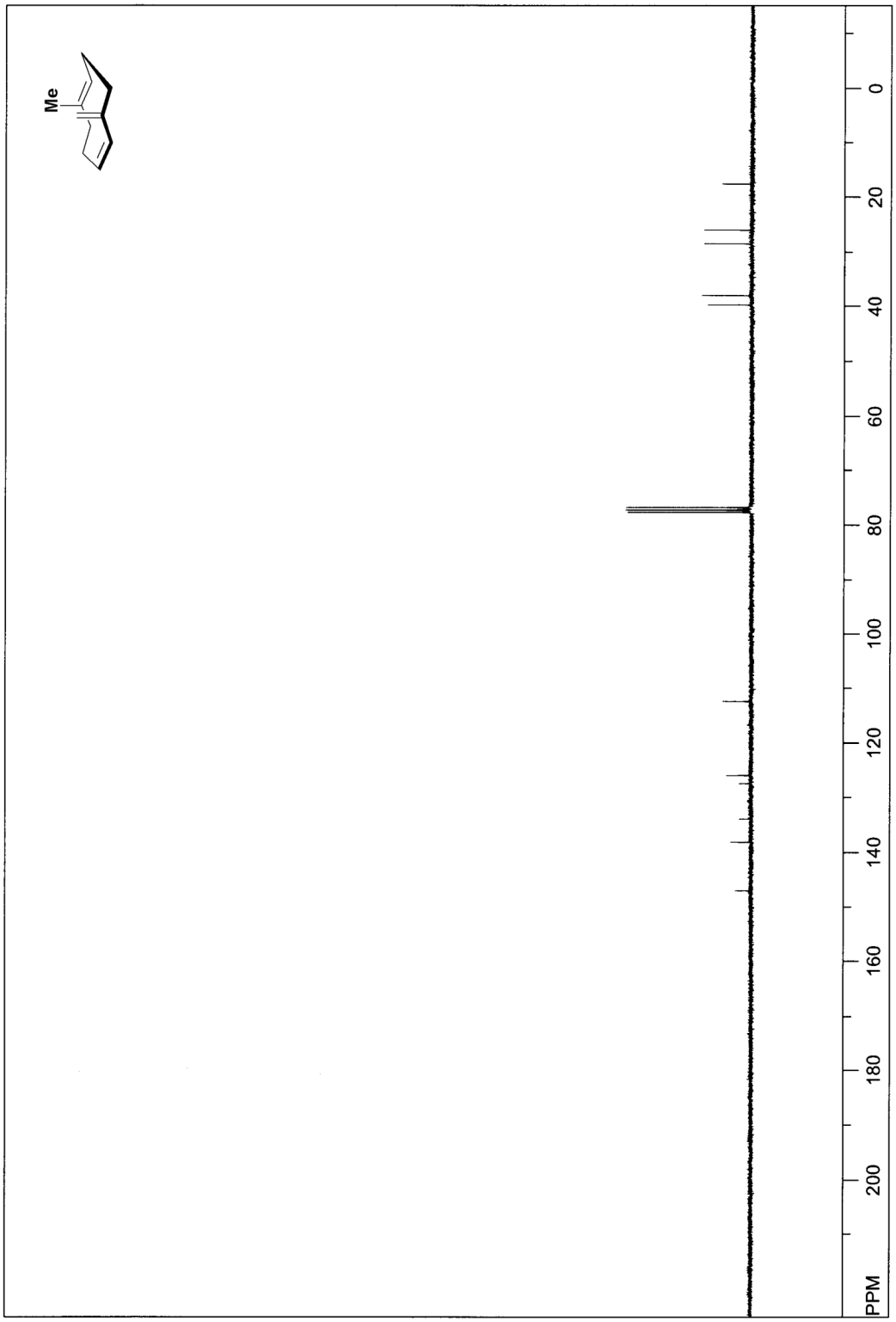
Me
PPM
200
180
160
140
120
100
80
60
40
20
0

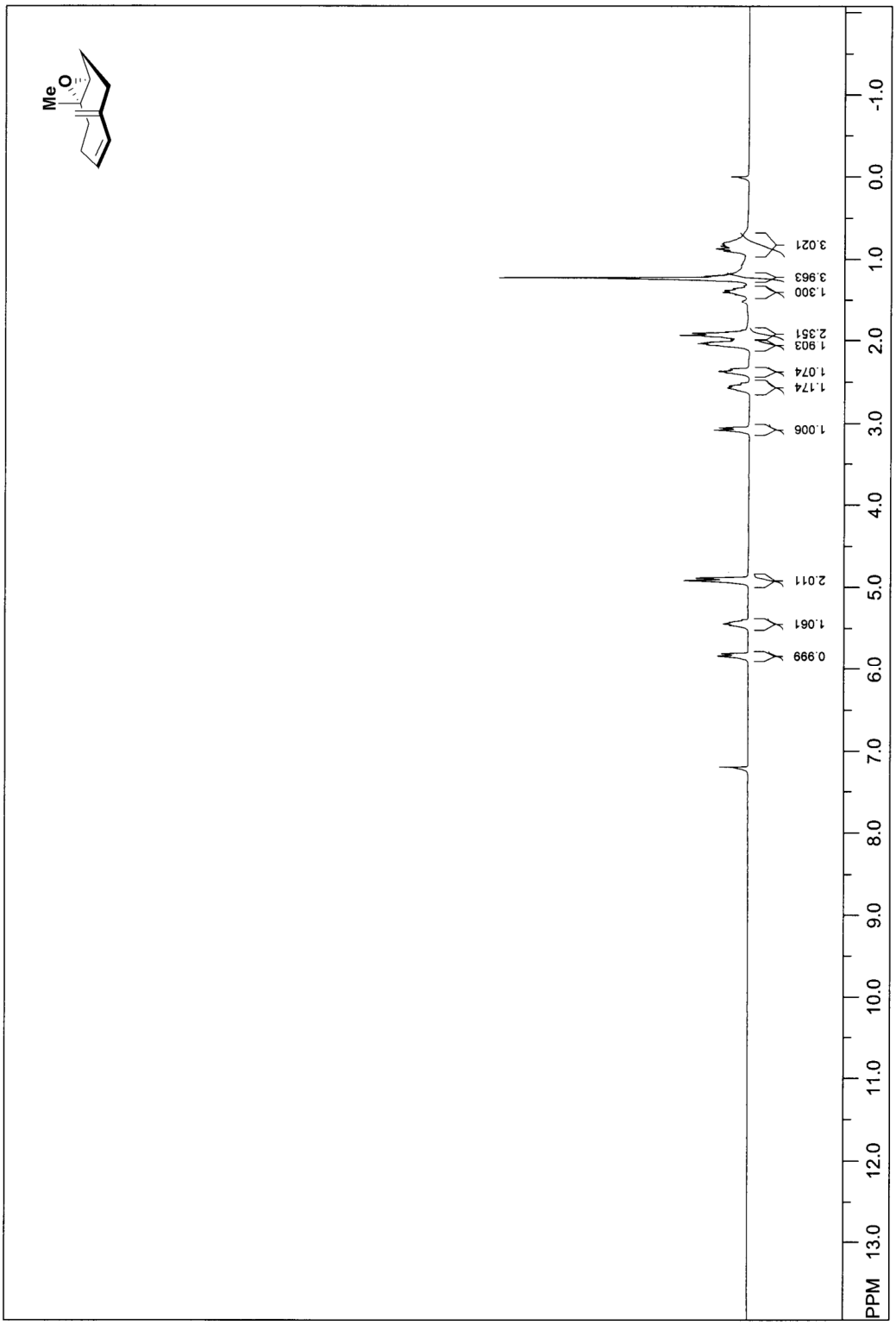
Me
O
3.021
3.963
1.300
1.903
2.351
1.074
1.174
1.006
2.011
1.061
0.999
PPM
13.0
12.0
11.0
10.0
9.0
8.0
7.0
6.0
5.0
4.0
3.0
2.0
1.0
0.0
-1.0

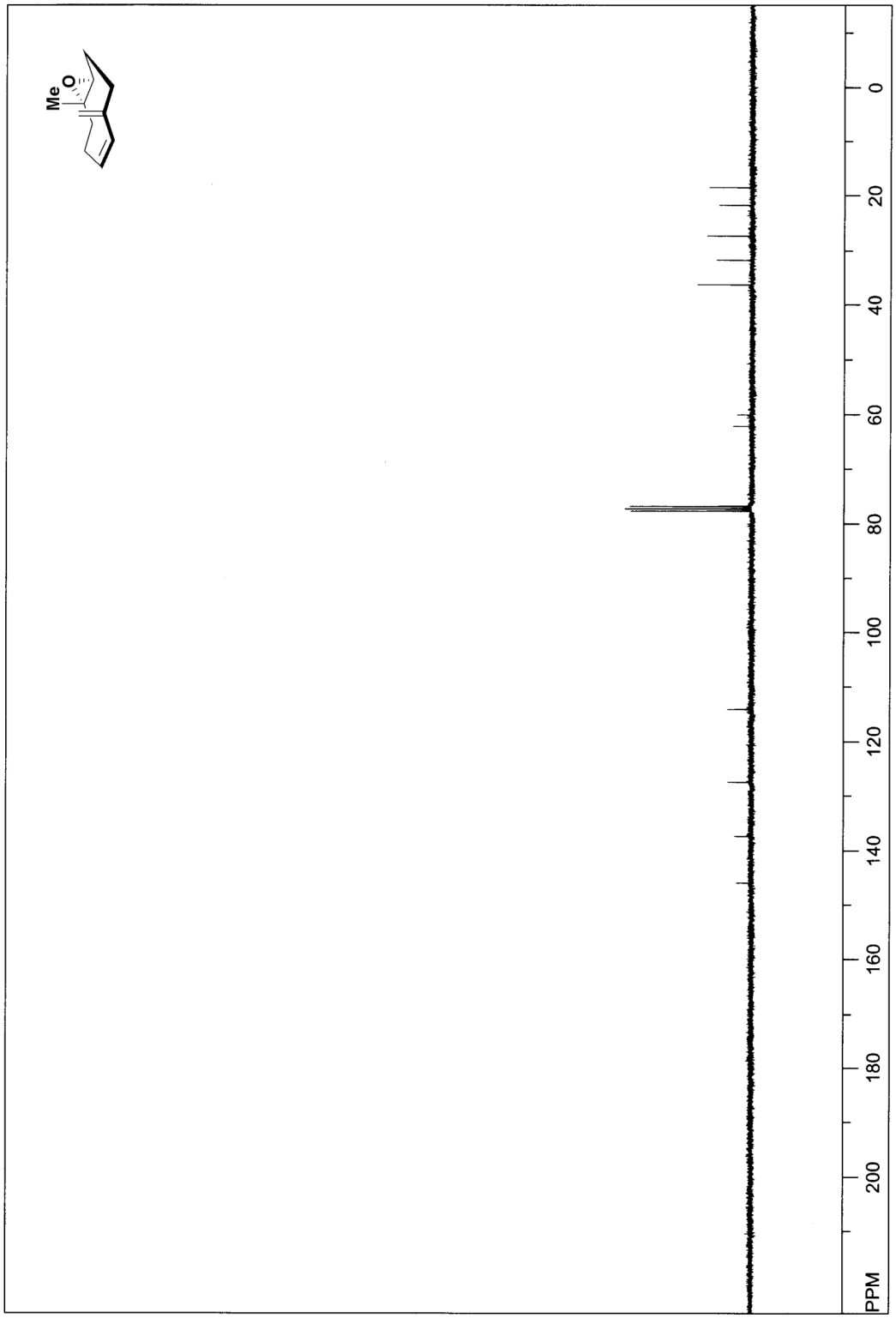
Me
O
PPM
0
20
40
60
80
100
120
140
160
180
200

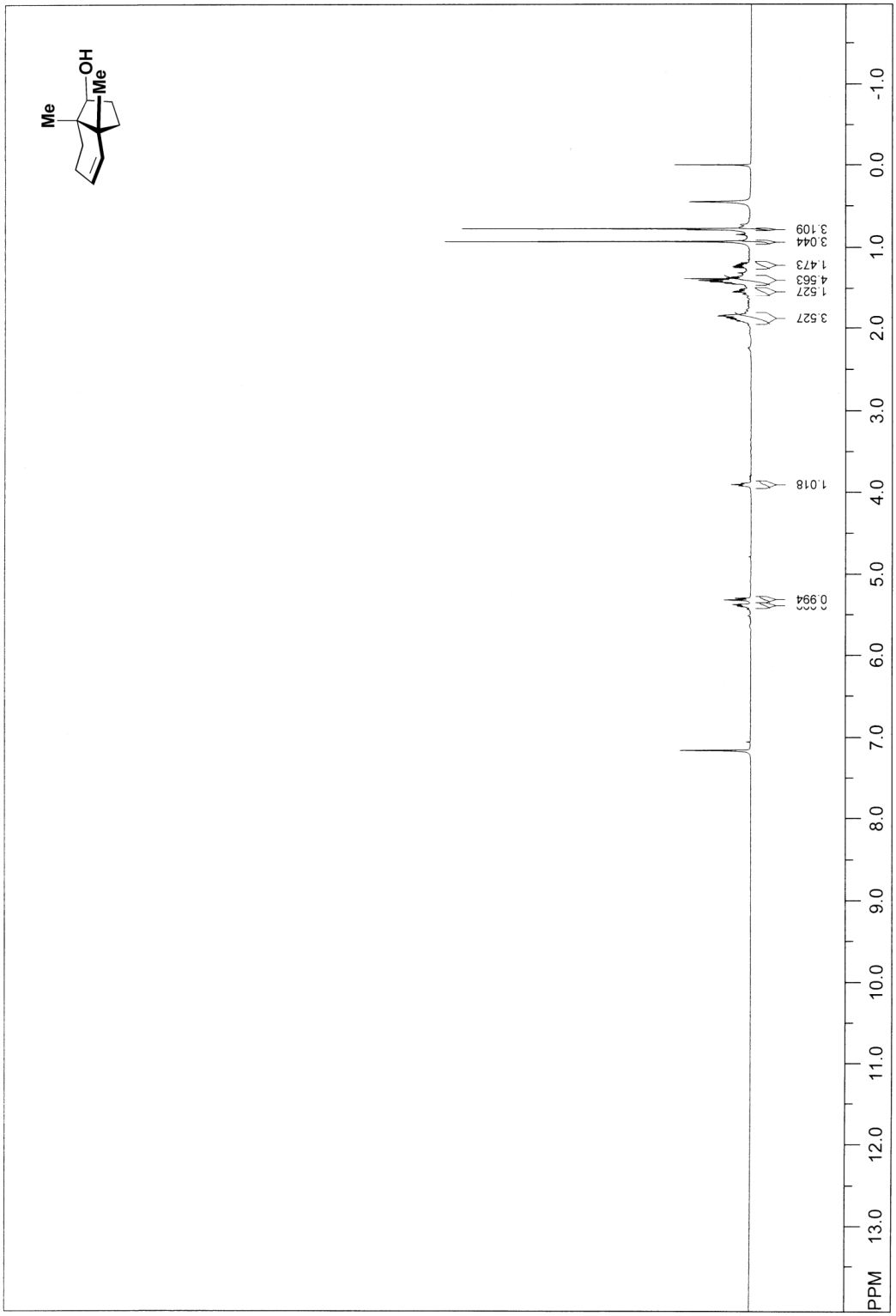
Me
OH
Me
3.109
3.044
1.473
4.563
1.527
3.527
1.018
0.994
PPM
13.0
12.0
11.0
10.0
9.0
8.0
7.0
6.0
5.0
4.0
3.0
2.0
1.0
0.0
-1.0

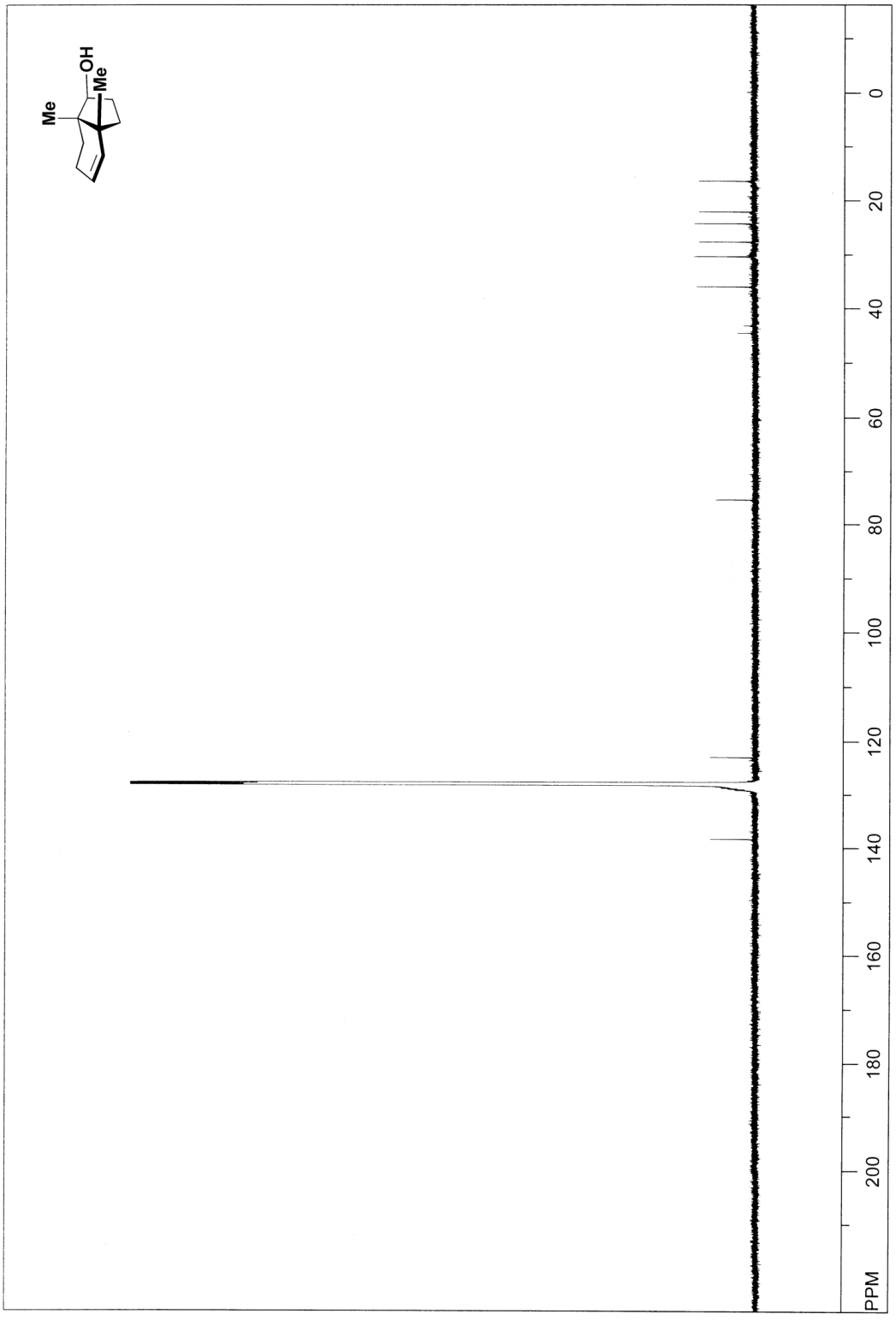
OH
Me
Me
PPM
0
20
40
60
80
100
120
140
160
180
200

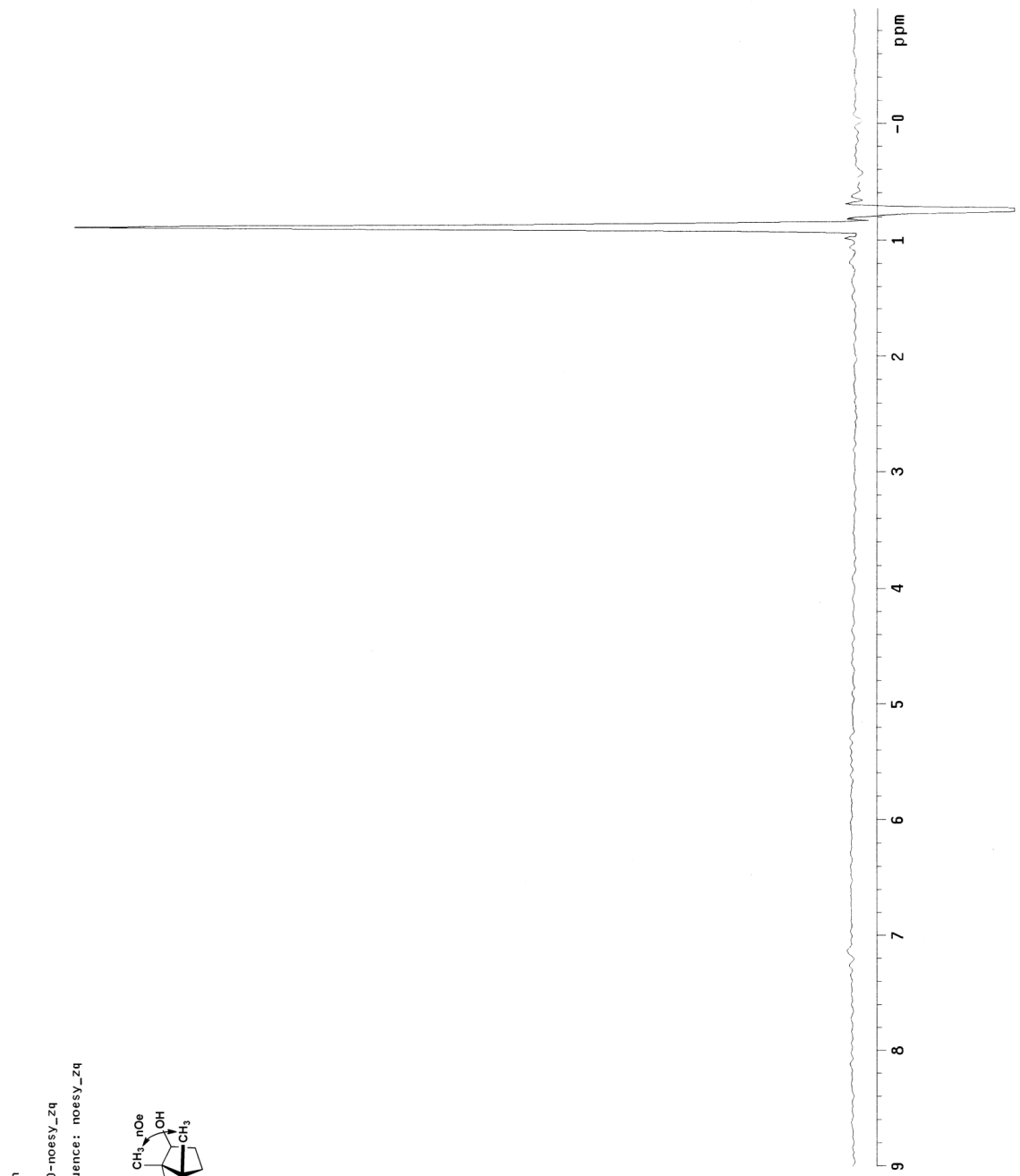
Std proton
File: 230-noesy_zq
Pulse Sequence: noesy_zq
CH3
nOe
OH
CH3
ppm
9
8
7
6
5
4
3
2
1
-0

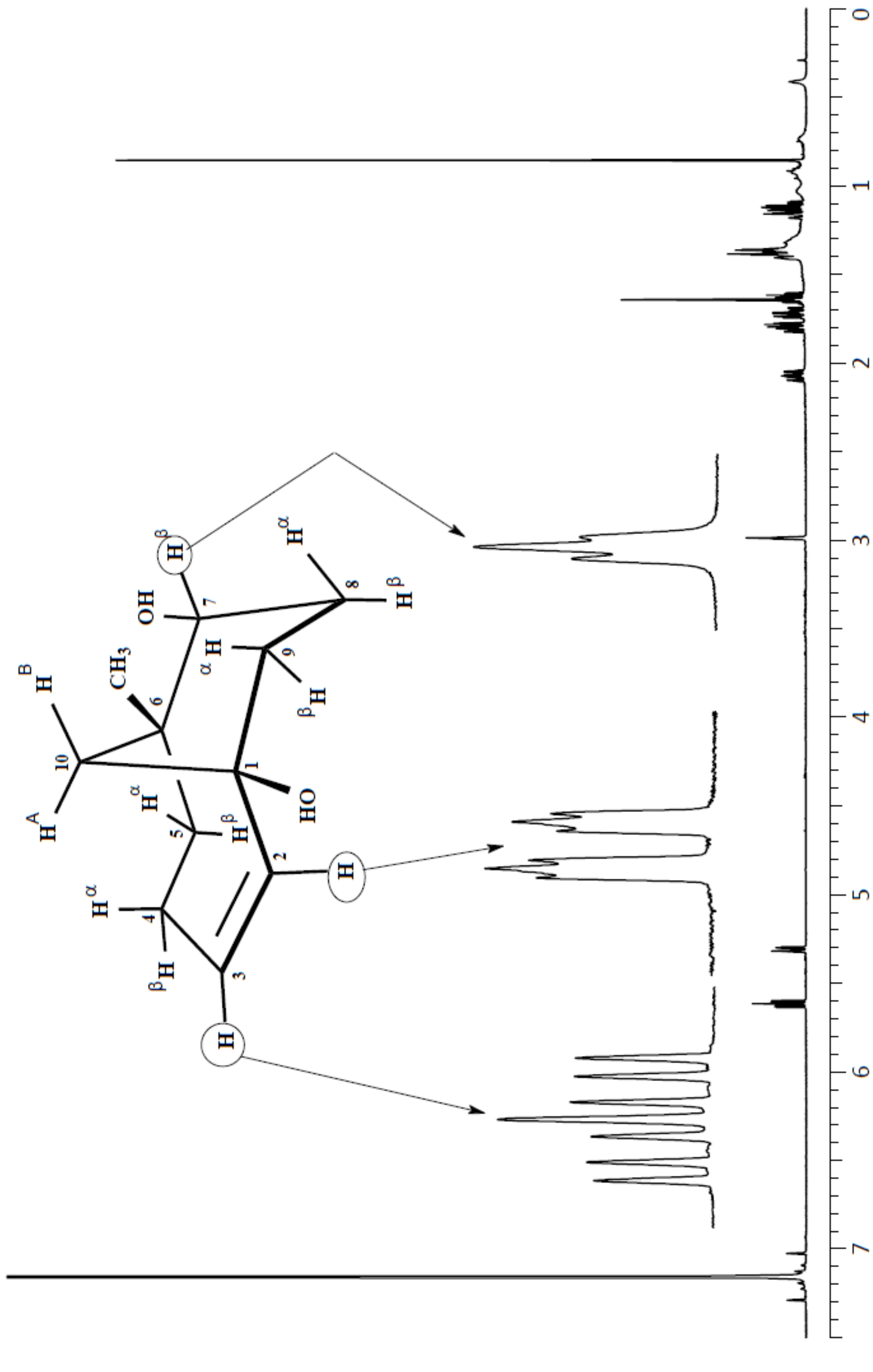
OH
HO
CH3
0
1
2
3
4
5
6
7

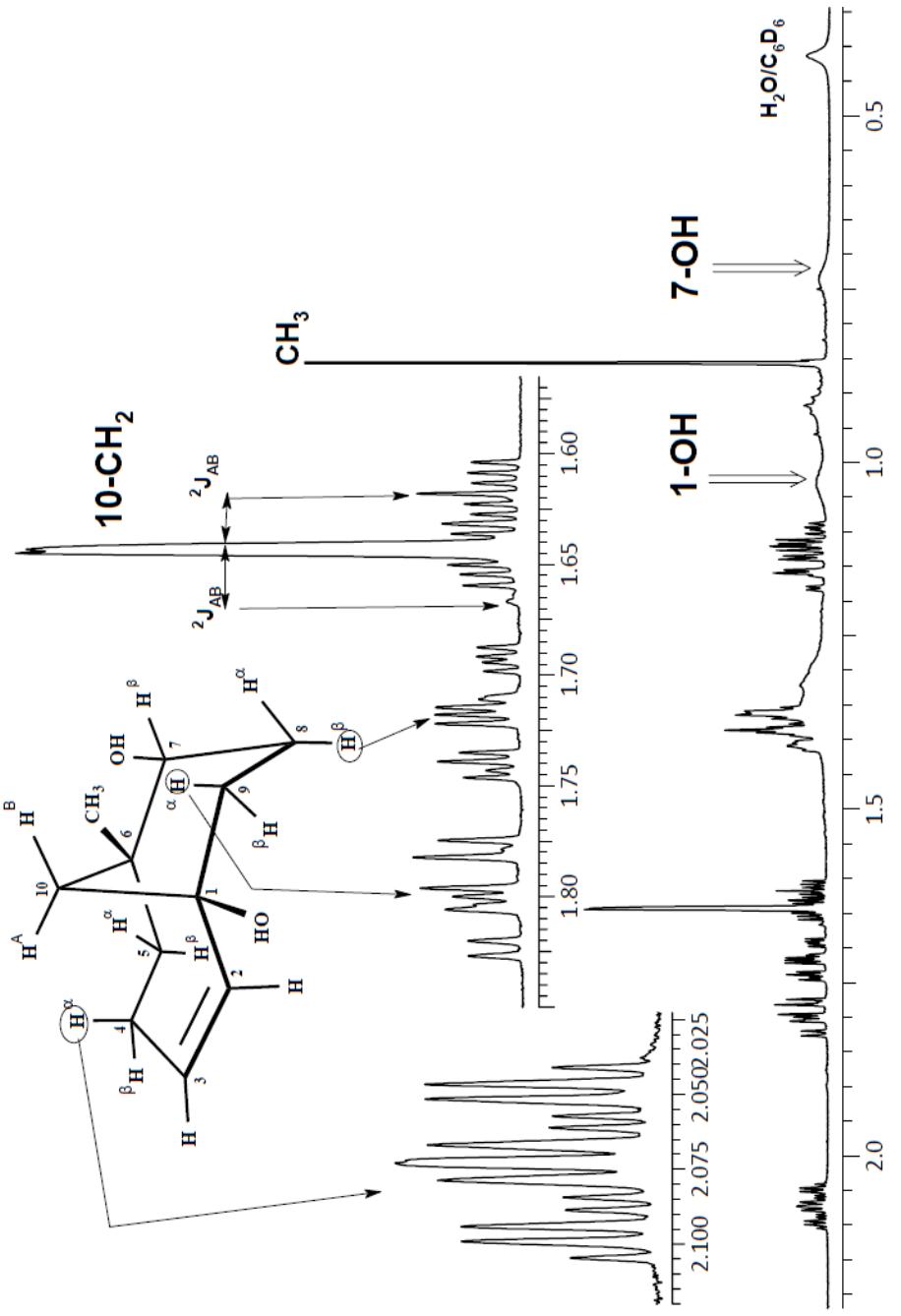
10-CH2
2JAB
2JAB
CH3
7-OH
1-OH
H2O/C6D6
2.100
2.075
2.050
2.025
1.80
1.75
1.70
1.65
1.60
2.0
1.5
1.0
0.5

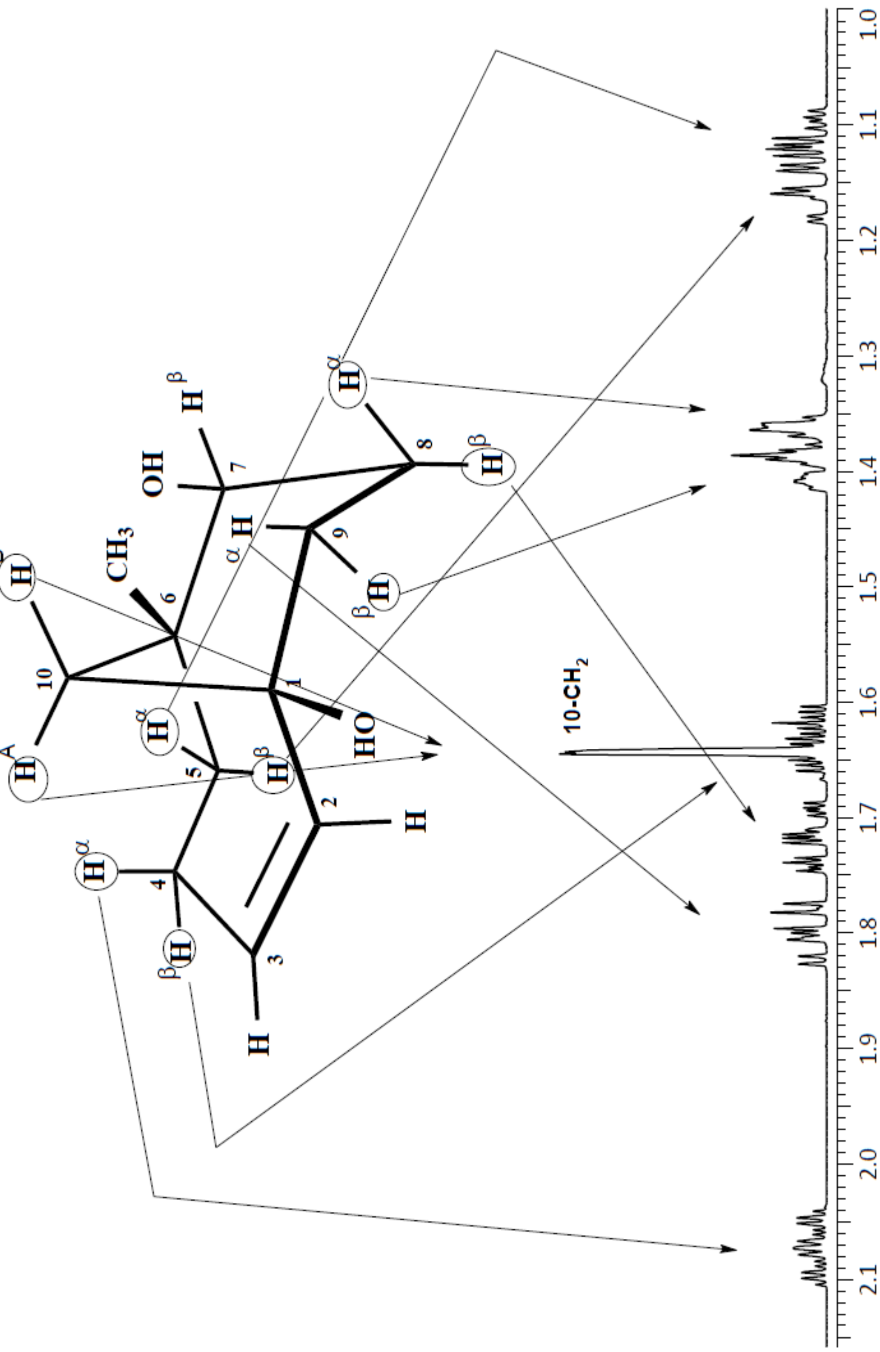

10-CH$_2$
CH$_3$
OH
HO
1.0
1.1
1.2
1.3
1.4
1.5
1.6
1.7
1.8
1.9
2.0
2.1

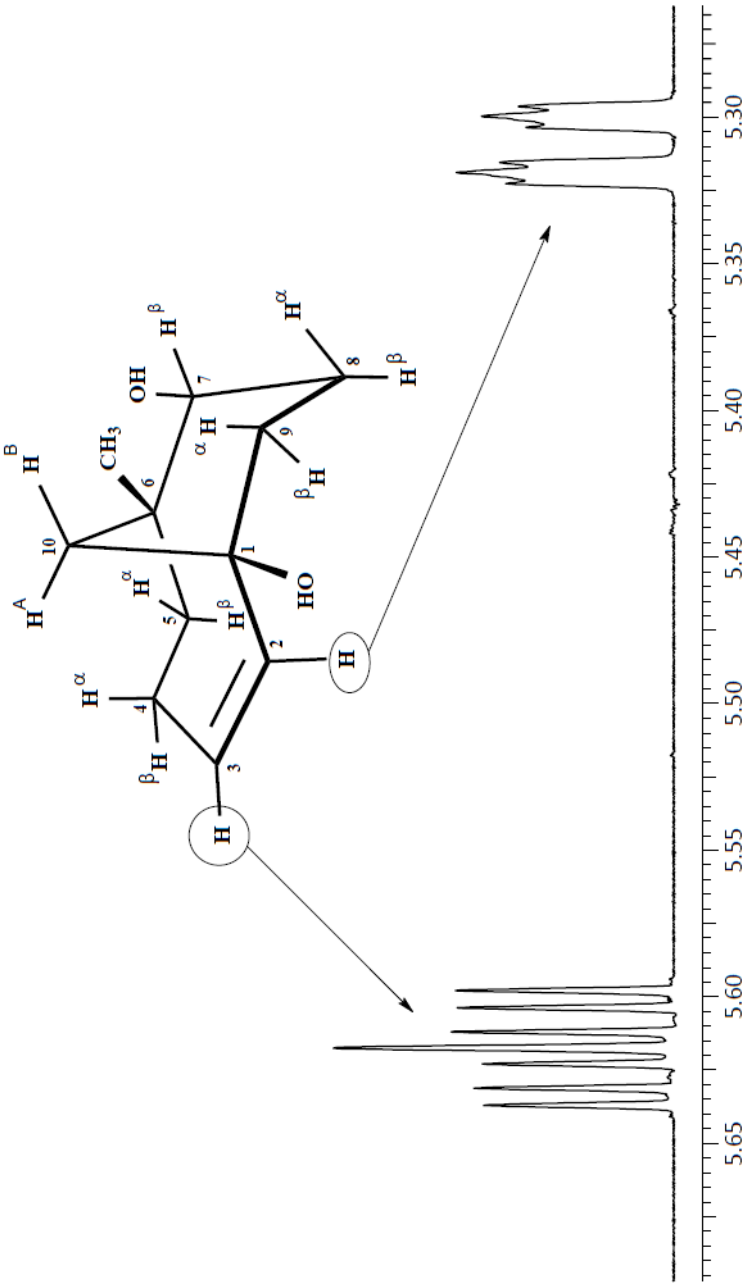
5.65
5.60
5.55
5.50
5.45
5.40
5.35
5.30

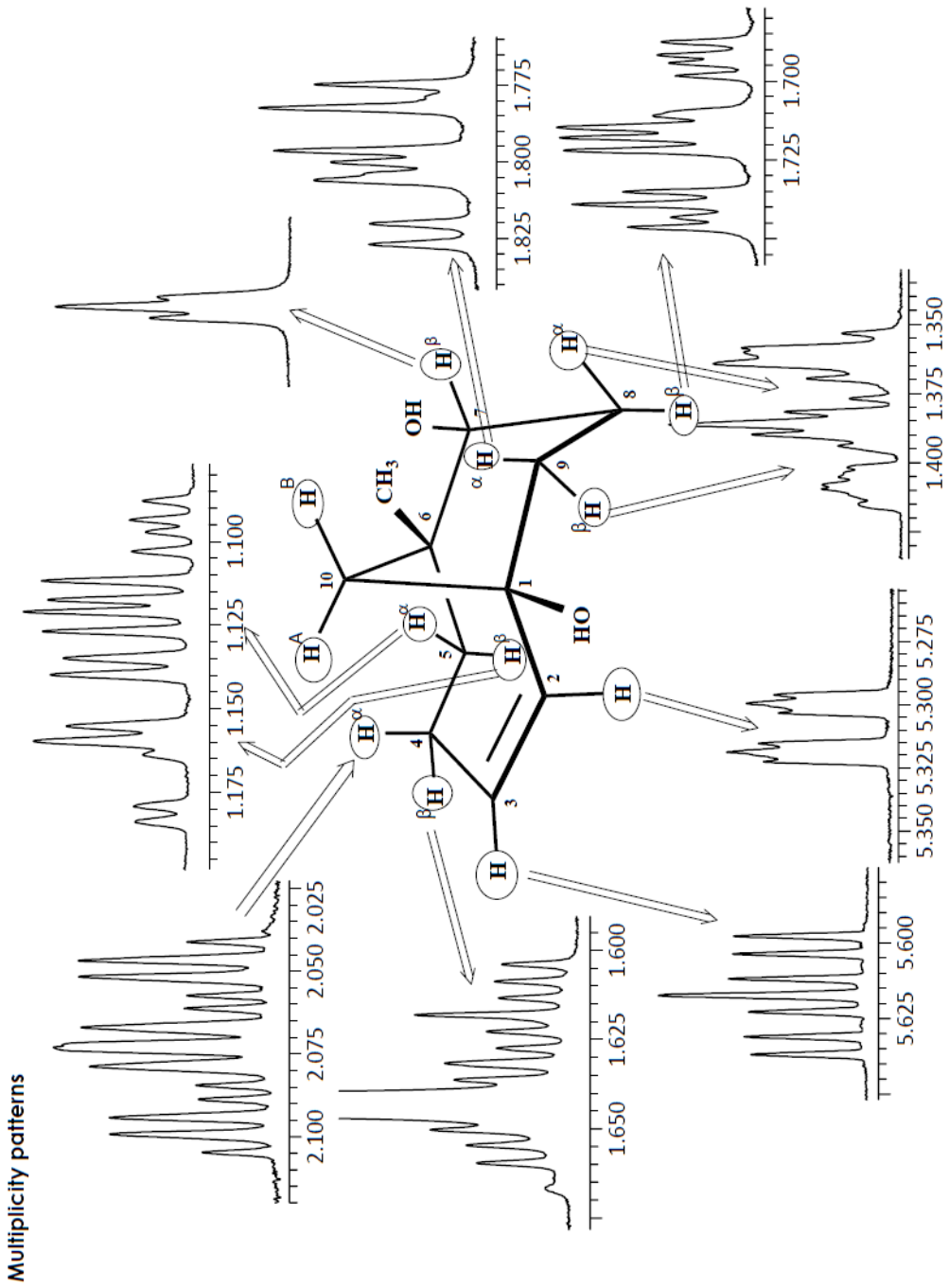
Multiplicity patterns
HO
OH
CH3
1
2
3
4
5
6
7
8
9
10
A
B
α
β

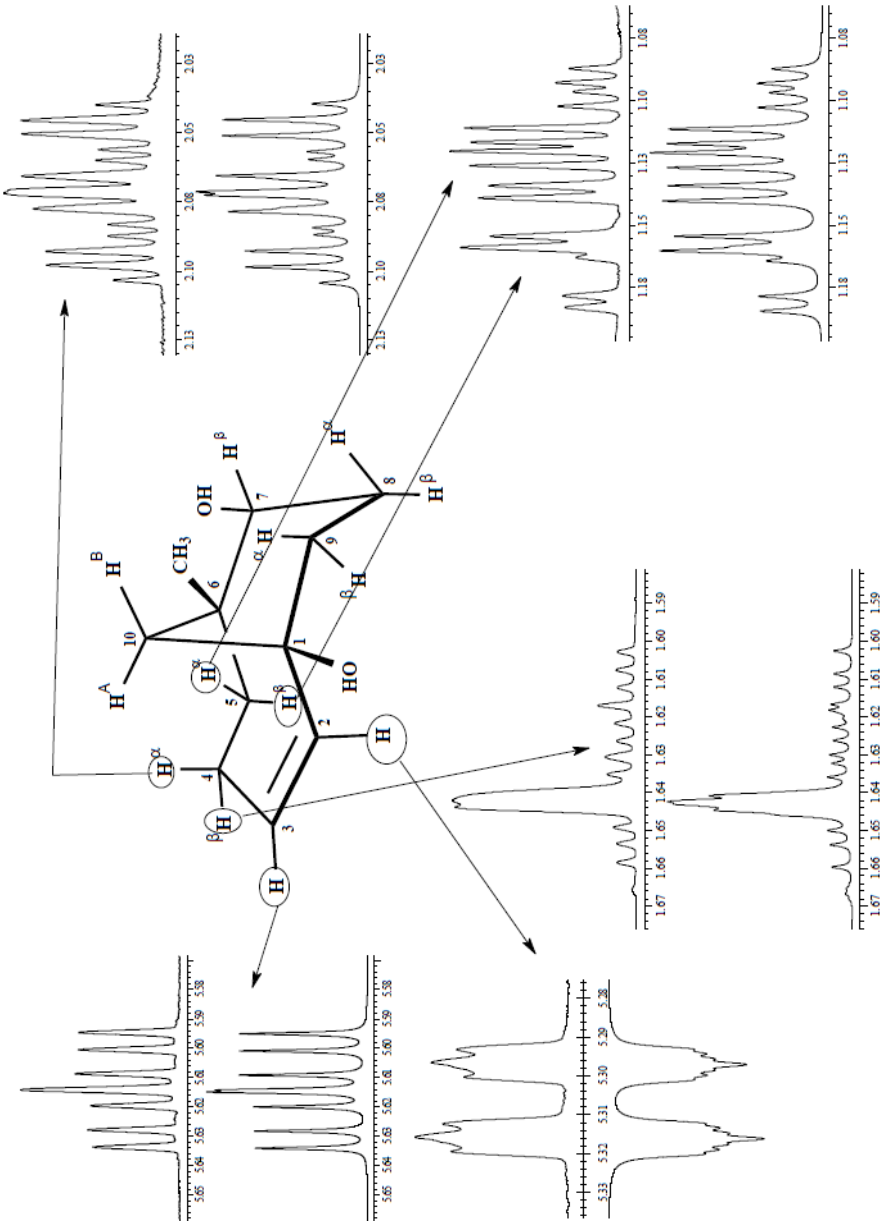

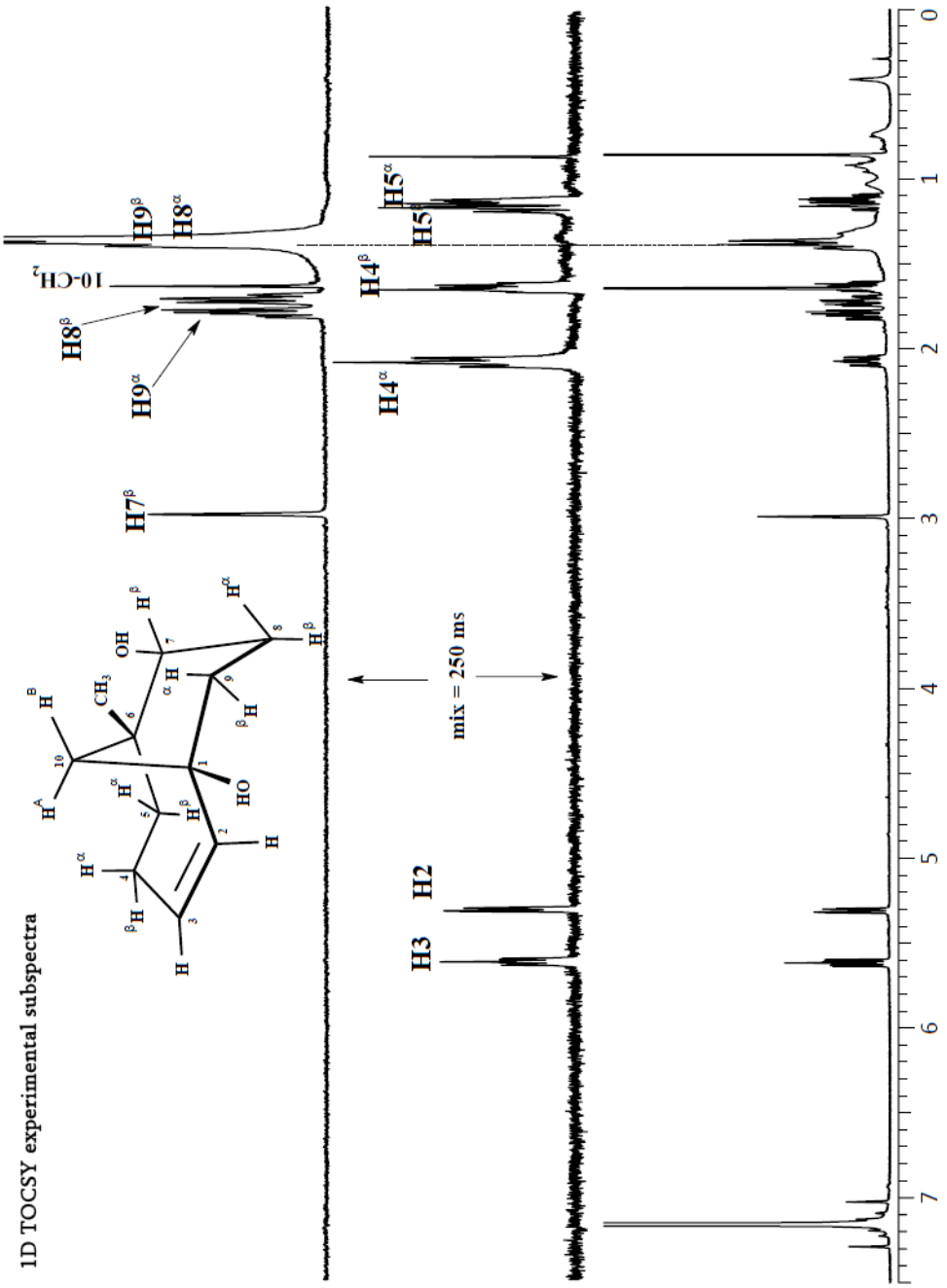
1D TOCSY experimental subspectra
mix = 250 ms
H3
H2
H4α
H4β
H5
H5α
H7β
H9α
H8β
10-CH2
H9β
H8α
0
1
2
3
4
5
6
7

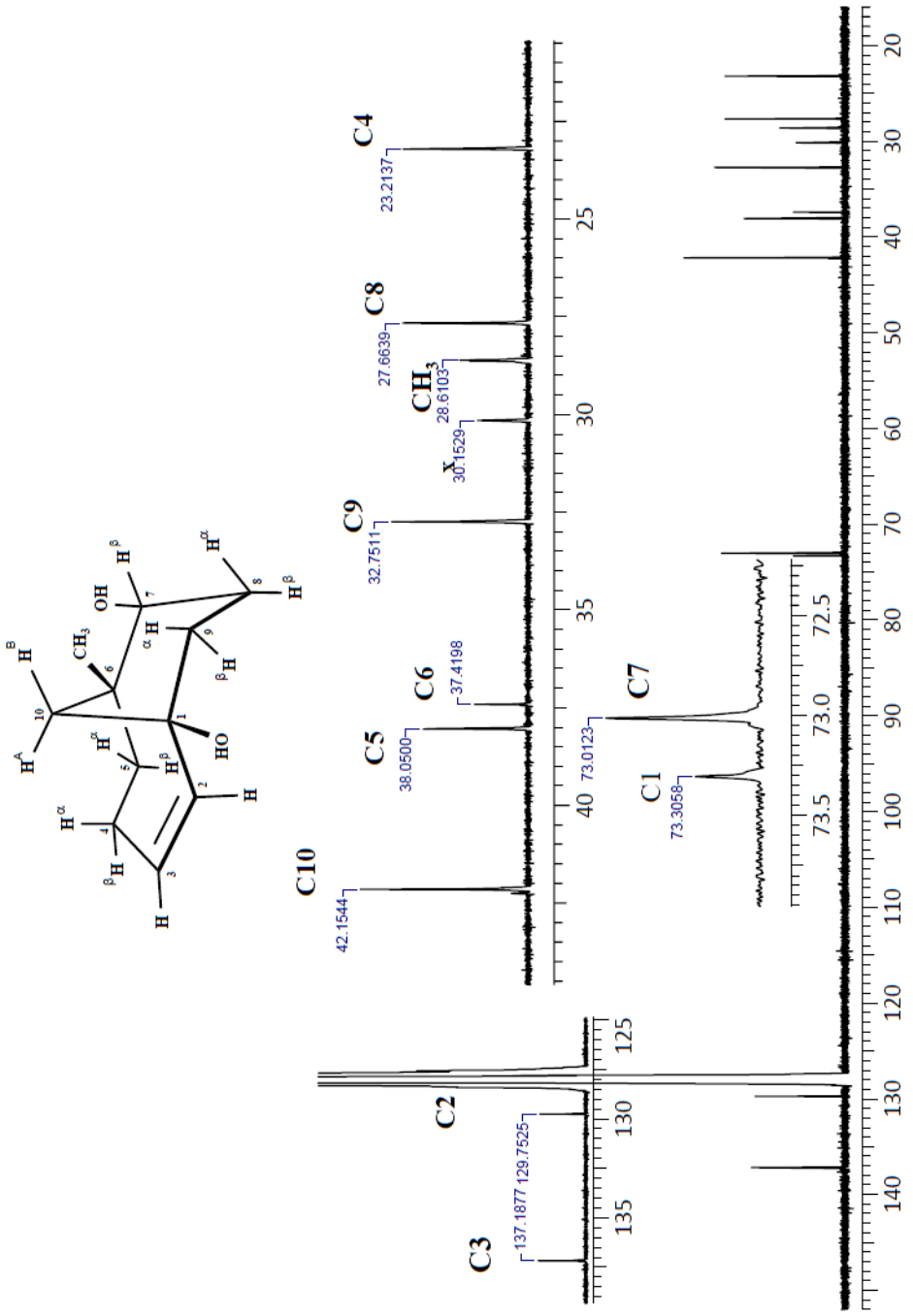
C10
42.1544
C5
38.0500
C6
37.4198
C9
32.7511
C4
23.2137
C8
27.6639
CH3
28.6103
30.1529
C7
73.0123
C1
73.3058
C2
129.7525
C3
137.1877

Experimental and calculated ^1H NMR spectrum

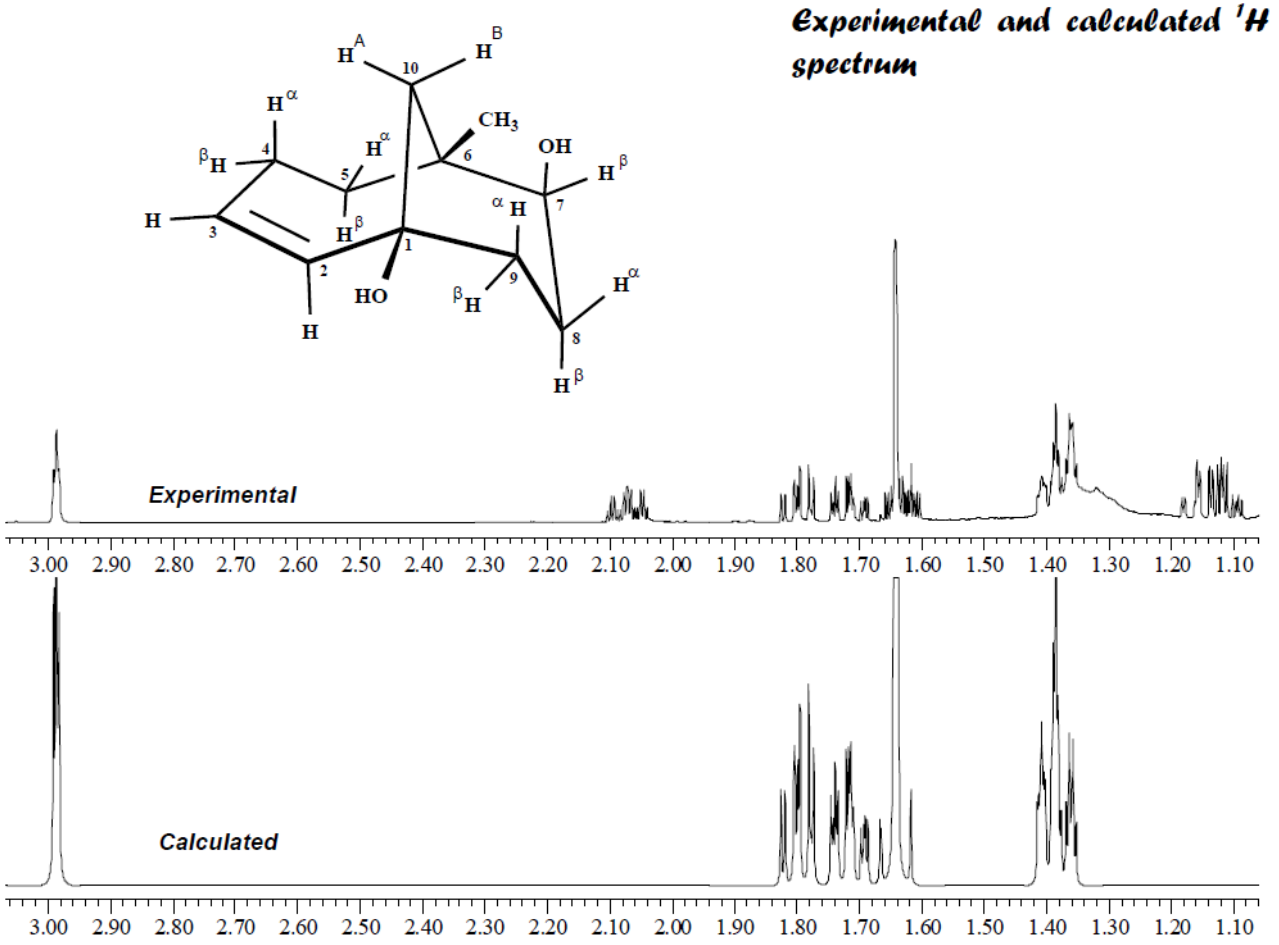

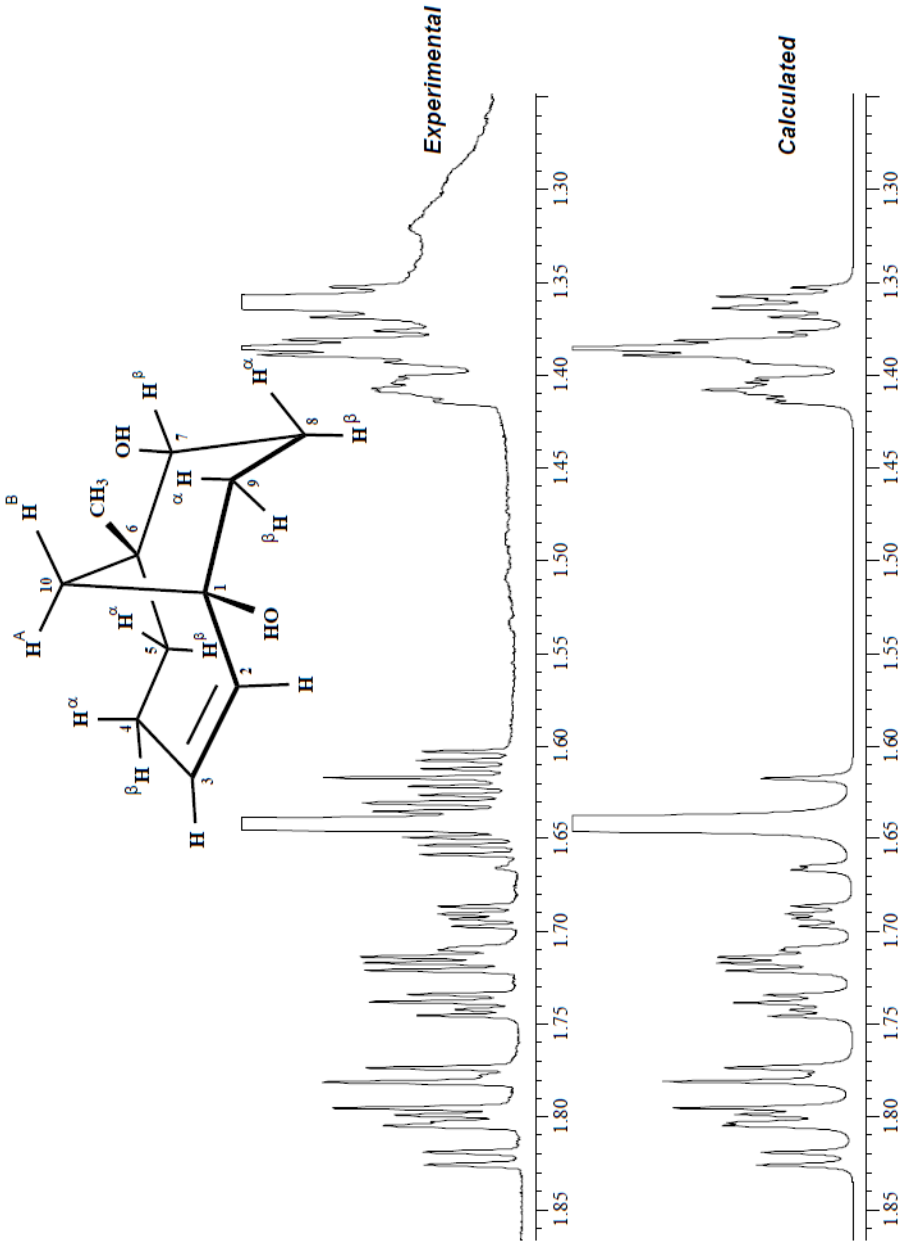
Experimental
Calculated
1.85
1.80
1.75
1.70
1.65
1.60
1.55
1.50
1.45
1.40
1.35
1.30
HO
OH
CH3

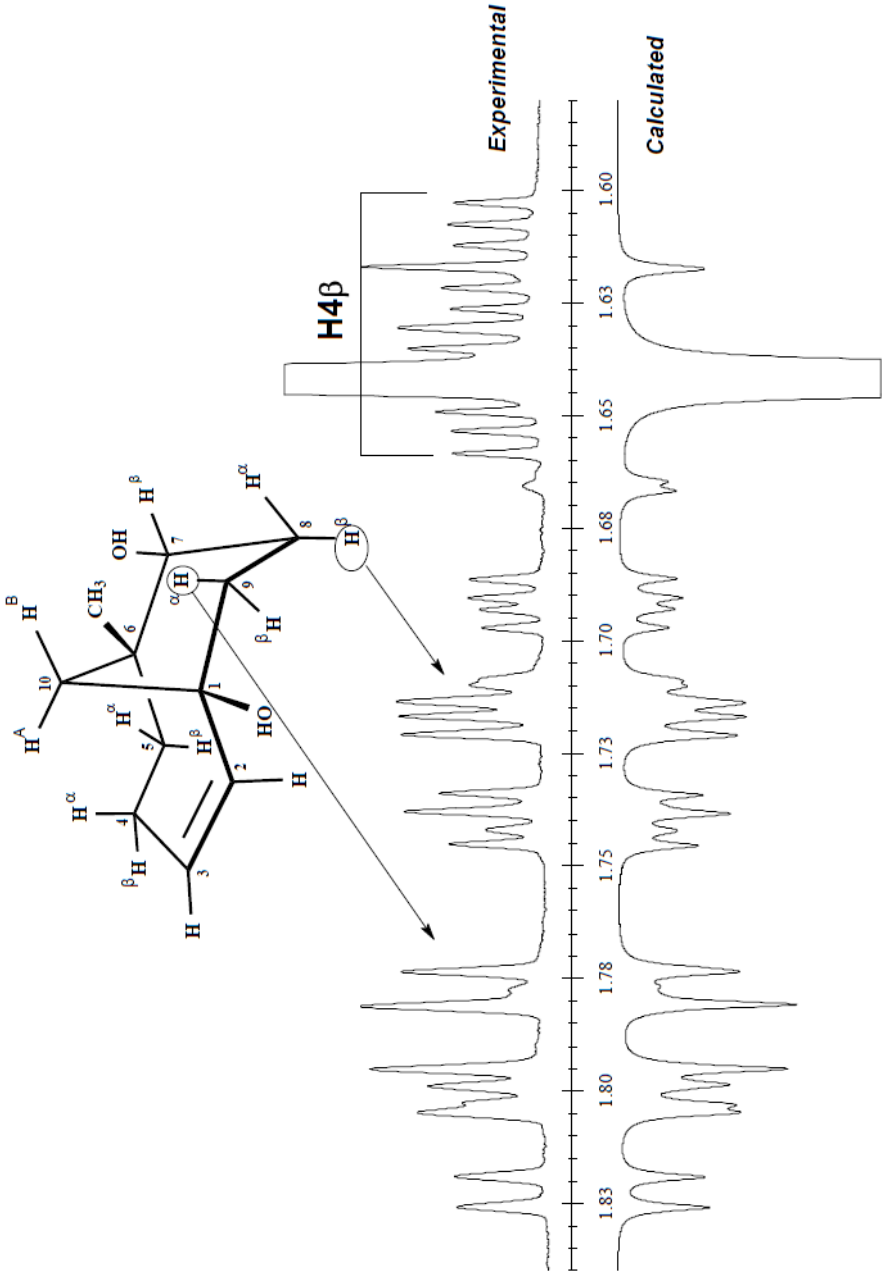
H4β
Experimental
Calculated
1.60
1.63
1.65
1.68
1.70
1.73
1.75
1.78
1.80
1.83
HO
OH
CH3

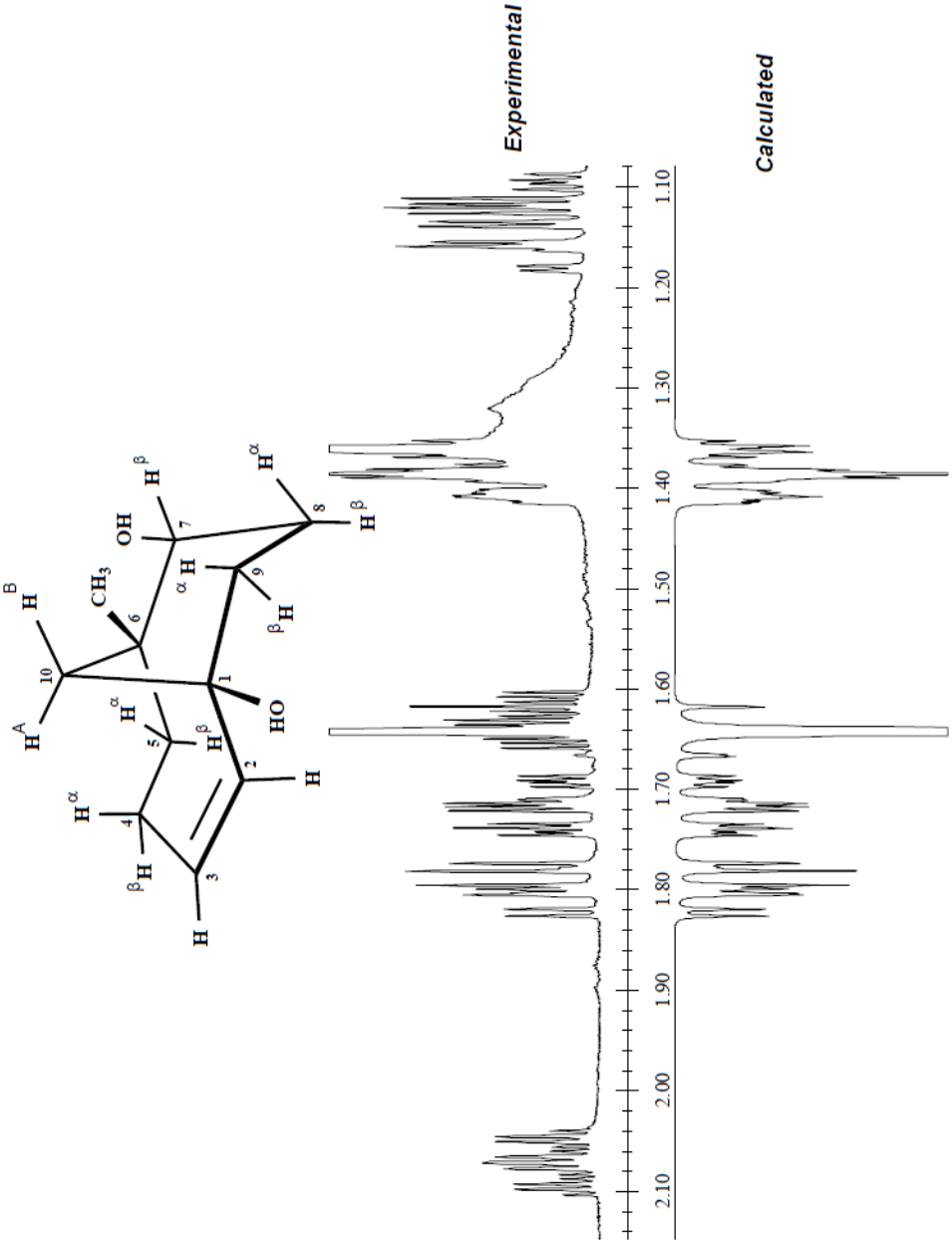
Experimental
Calculated
1.10
1.20
1.30
1.40
1.50
1.60
1.70
1.80
1.90
2.00
2.10

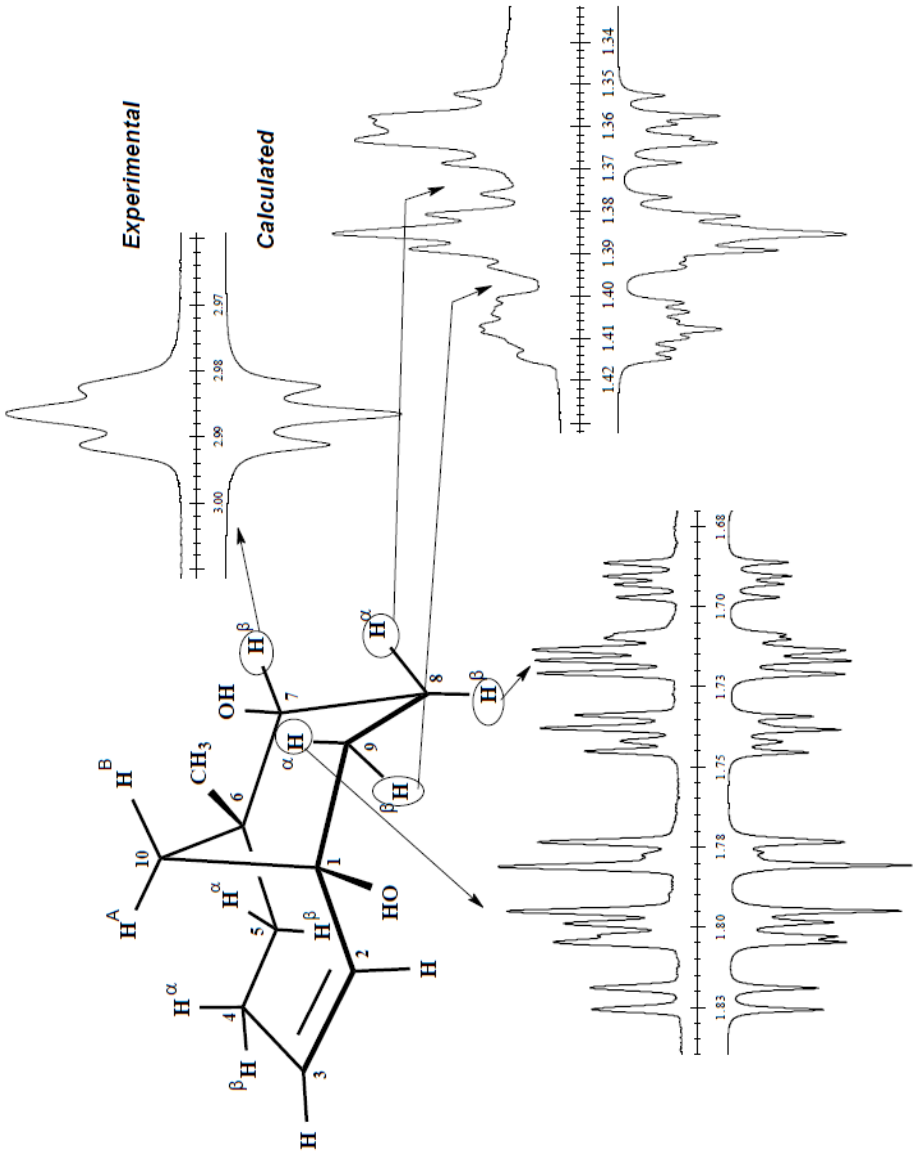
Experimental
Calculated
3.00
2.99
2.98
2.97
1.42
1.41
1.40
1.39
1.38
1.37
1.36
1.35
1.34
1.83
1.80
1.78
1.75
1.73
1.70
1.68
OH
CH3
HO
H
10
1
2
3
4
5
6
7
8
9

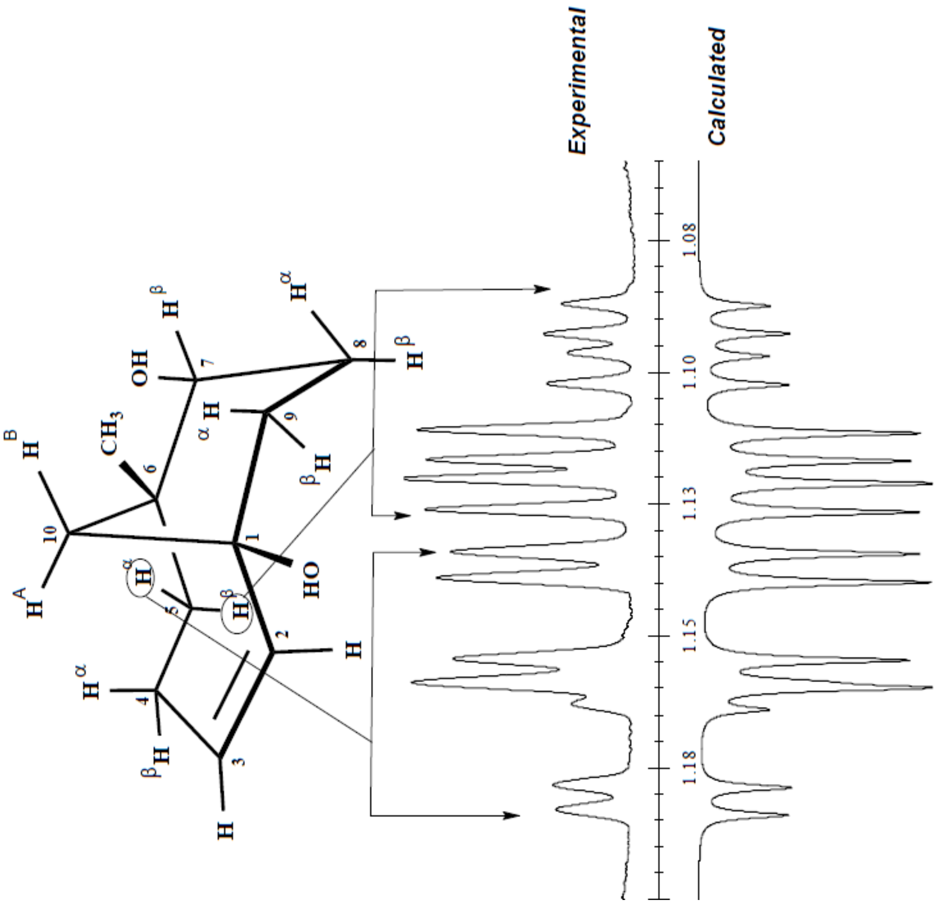
Experimental
Calculated
1.08
1.10
1.13
1.15
1.18
OH
CH3
HO

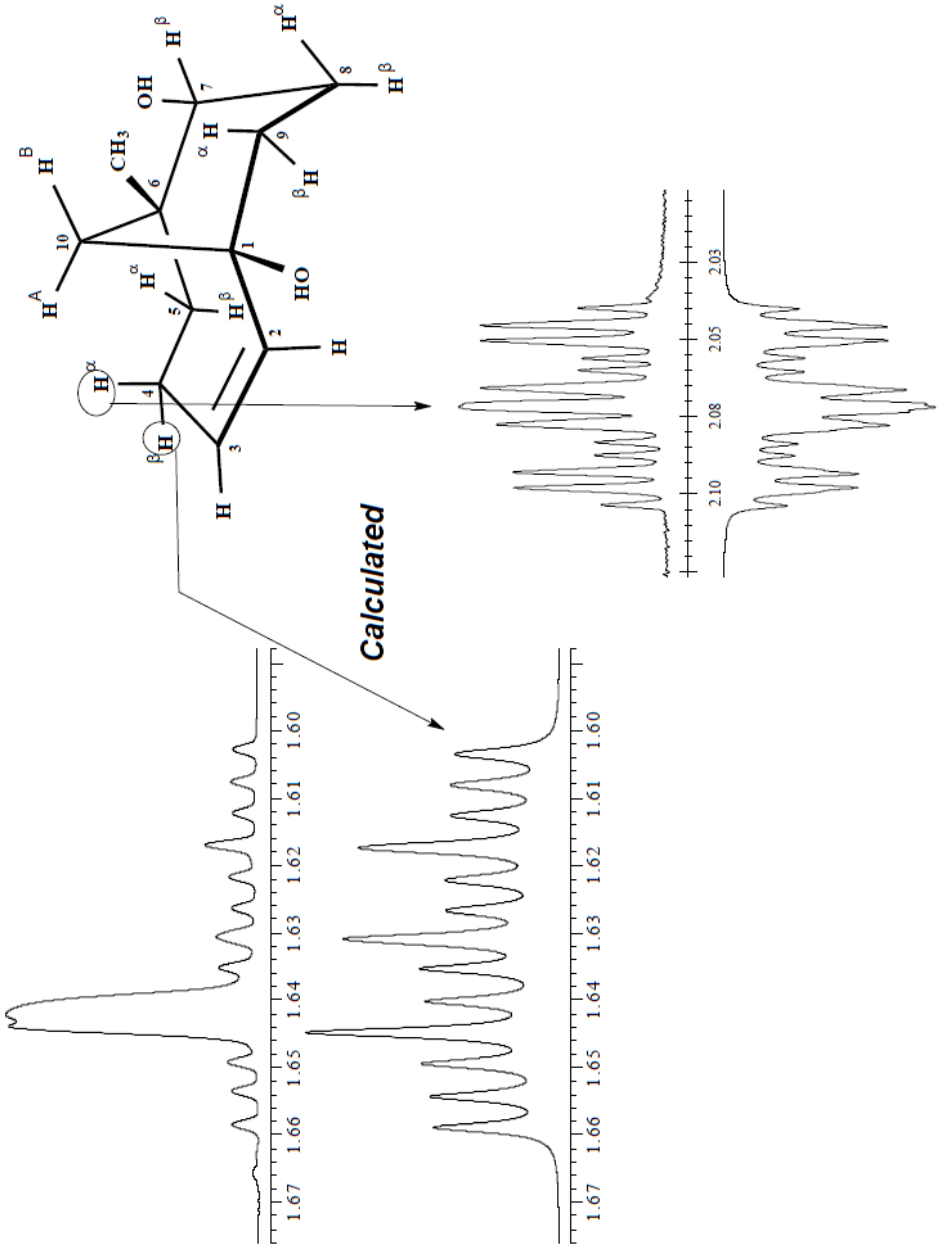
Calculated
1.67
1.66
1.65
1.64
1.63
1.62
1.61
1.60
2.10
2.08
2.05
2.03

Selected nOe correlations

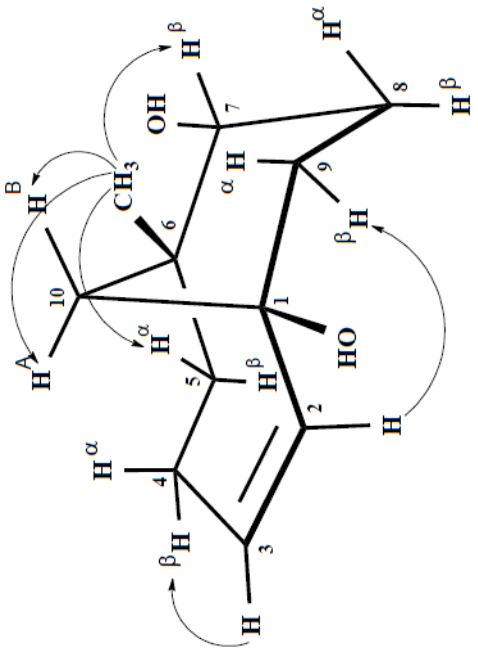

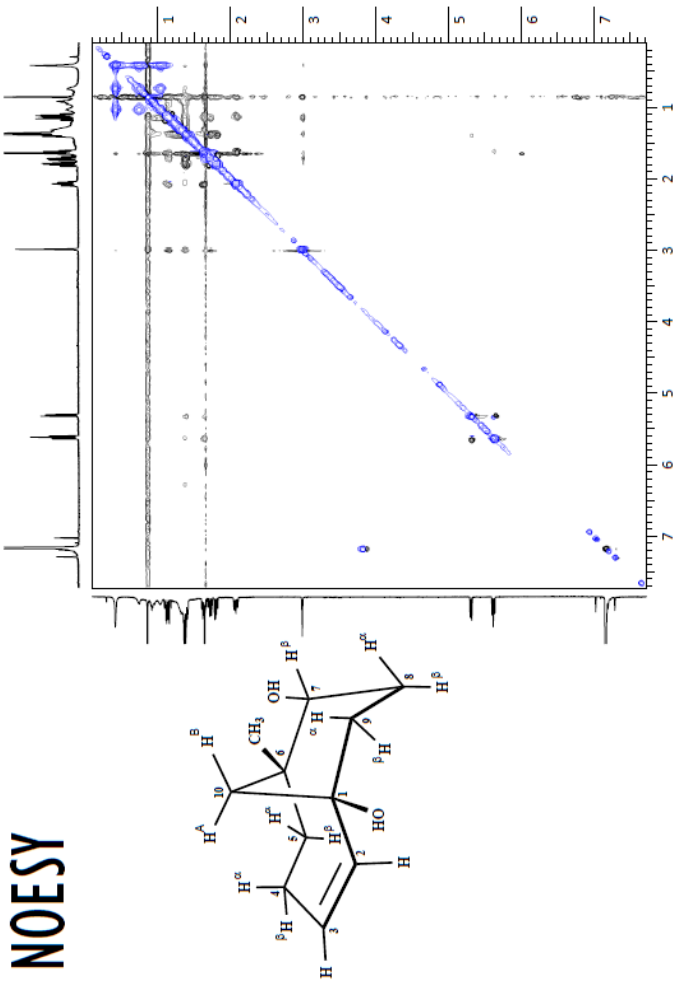
NOESY
1
2
3
4
5
6
7
OH
CH3
HO
H

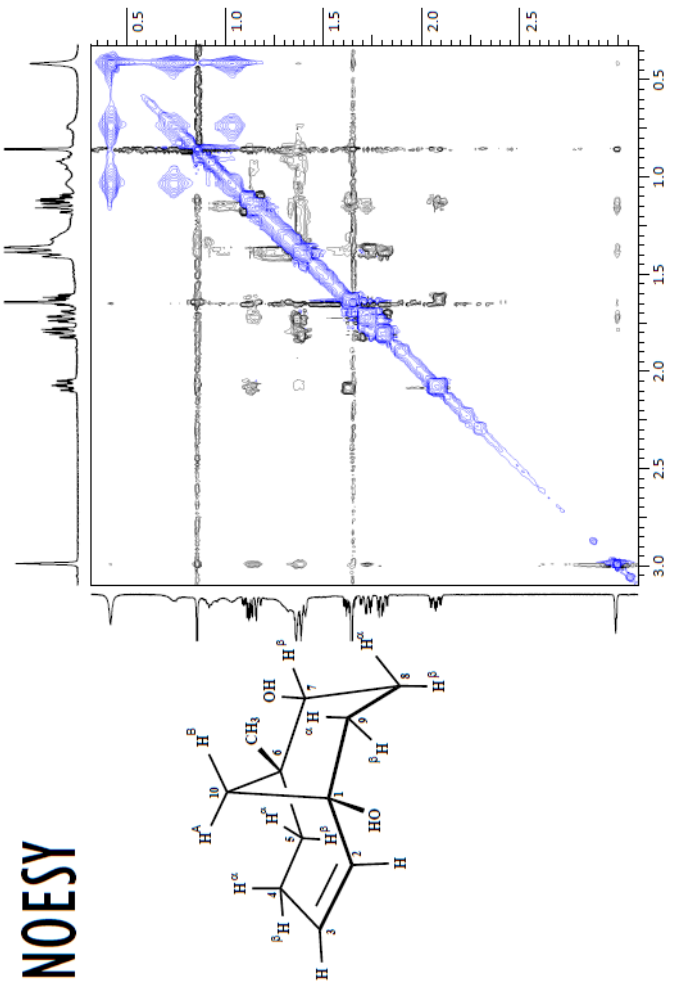
NOESY
0.5
1.0
1.5
2.0
2.5
3.0
OH
CH3
HO
H

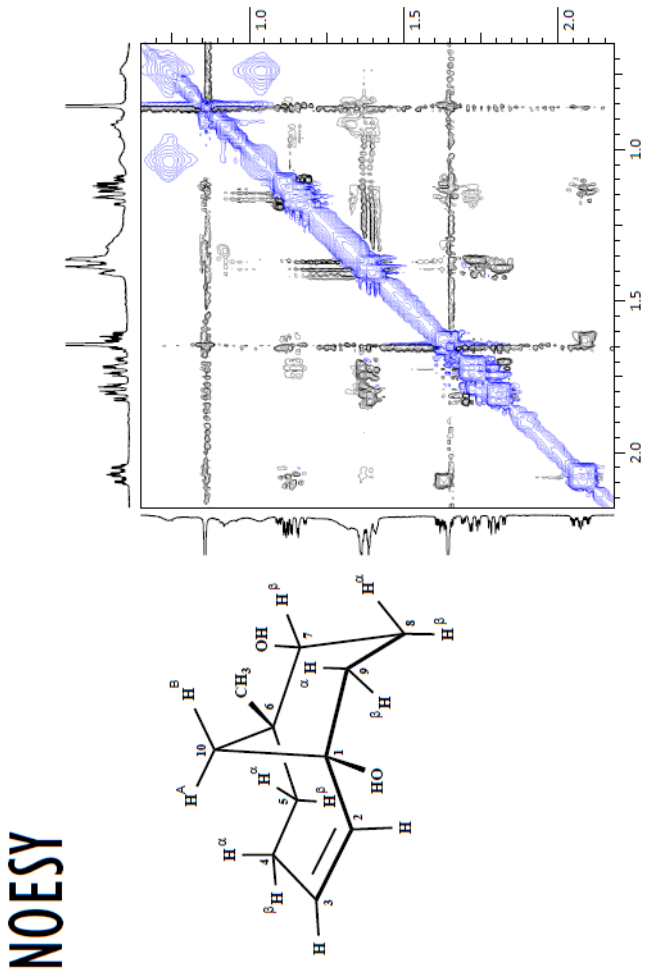

NOESY

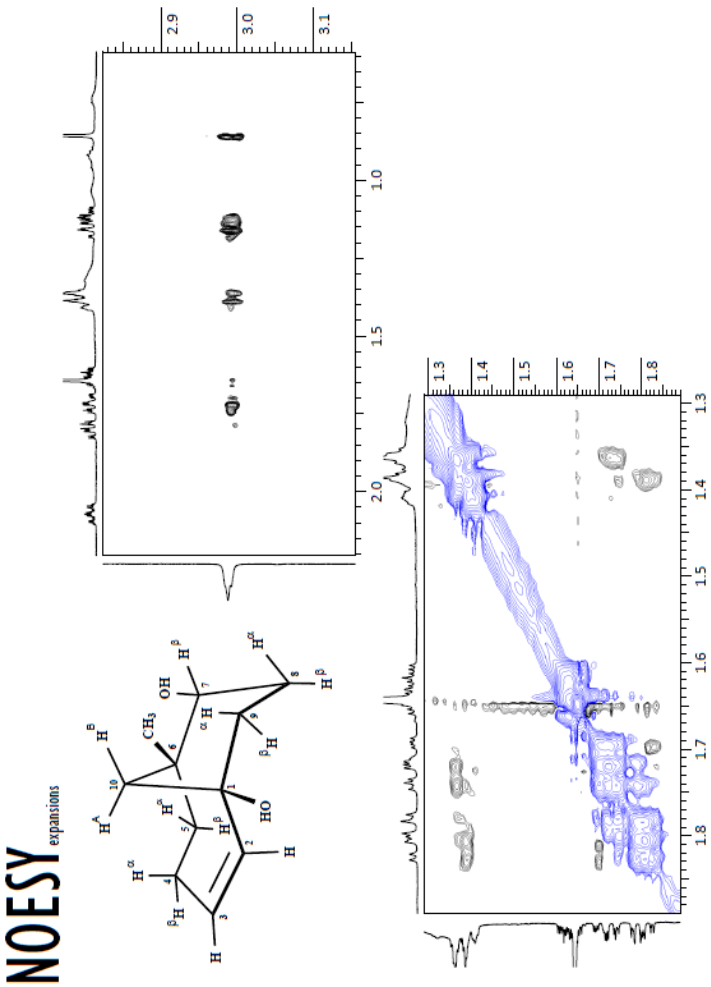
NOESY expansions
2.9
3.0
3.1
1.0
1.5
2.0
1.3
1.4
1.5
1.6
1.7
1.8
1.3
1.4
1.5
1.6
1.7
1.8
CH3
OH
HO
H

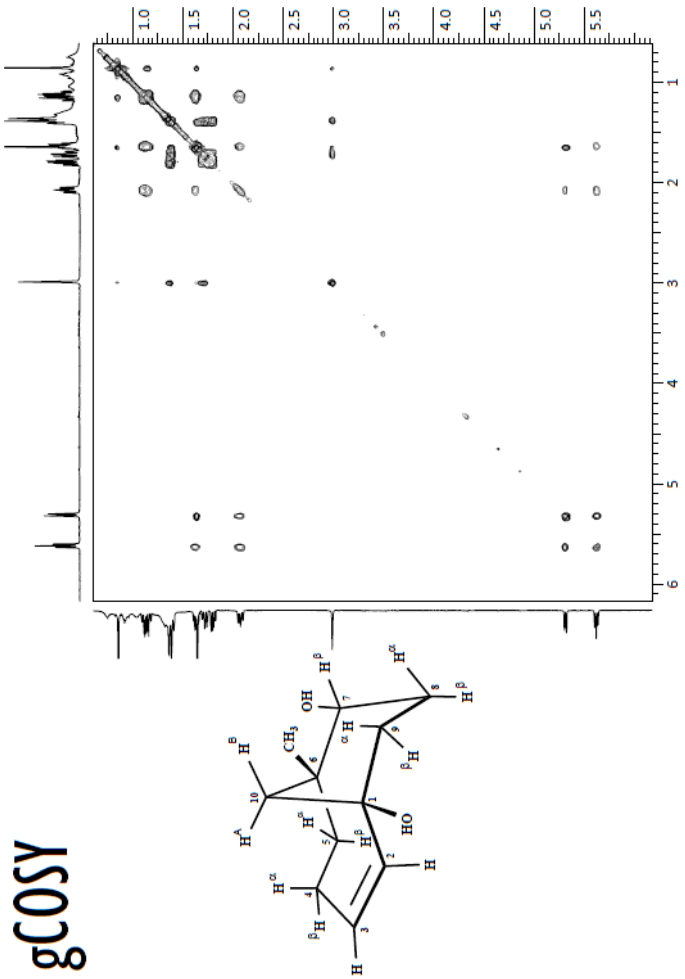
gCOSY
1.0
1.5
2.0
2.5
3.0
3.5
4.0
4.5
5.0
5.5
1
2
3
4
5
6

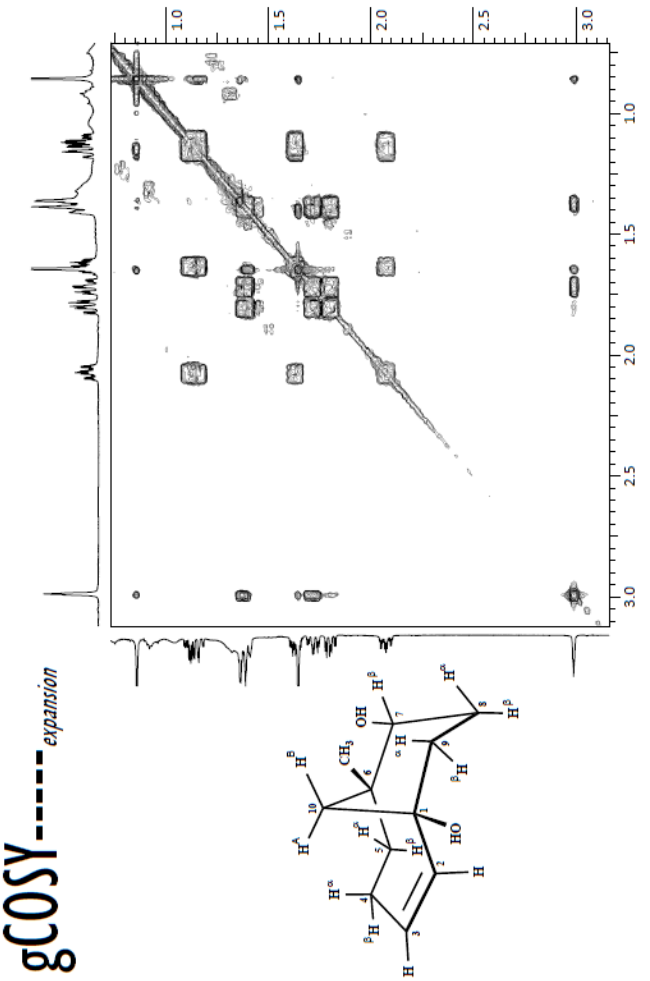
gCOSY-----expansion
1.0
1.5
2.0
2.5
3.0
OH
CH3
HO
H

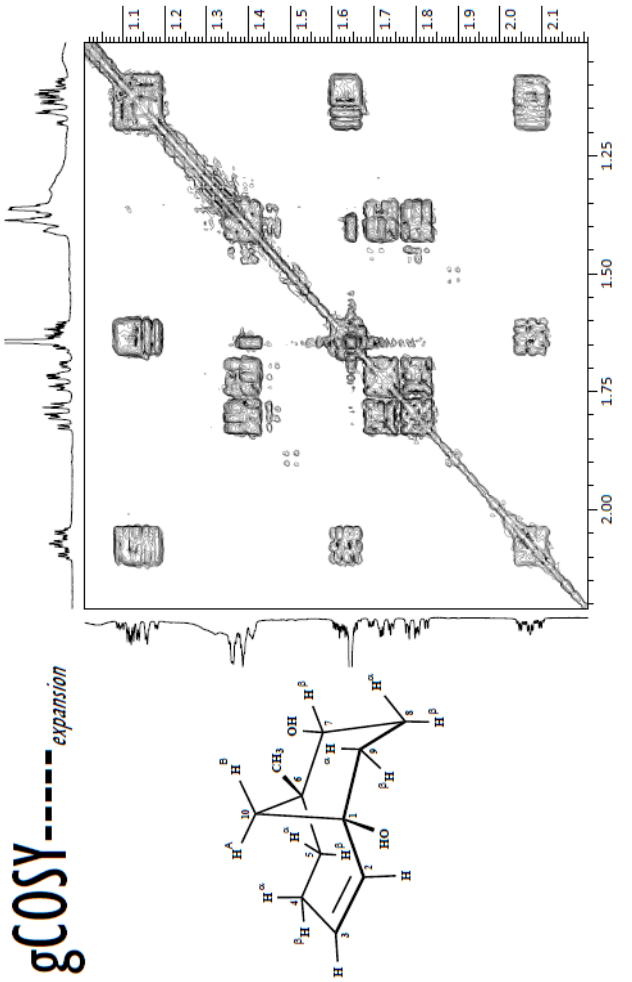
gCOSY----- expansion
1.1
1.2
1.3
1.4
1.5
1.6
1.7
1.8
1.9
2.0
2.1
2.00
1.75
1.50
1.25
CH3
OH
HO

Selected gHMBC correlations

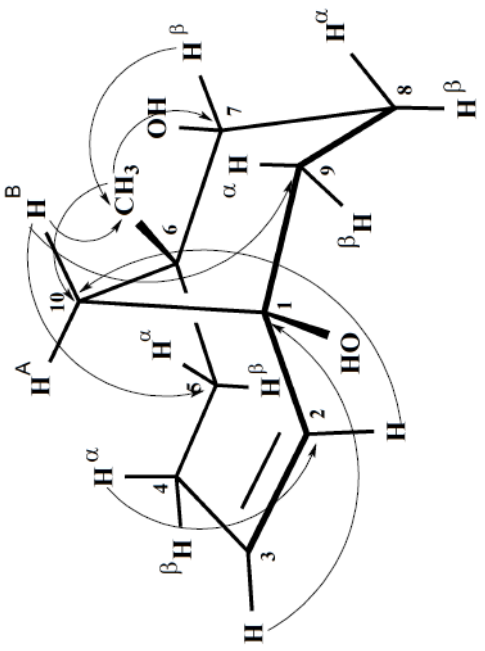

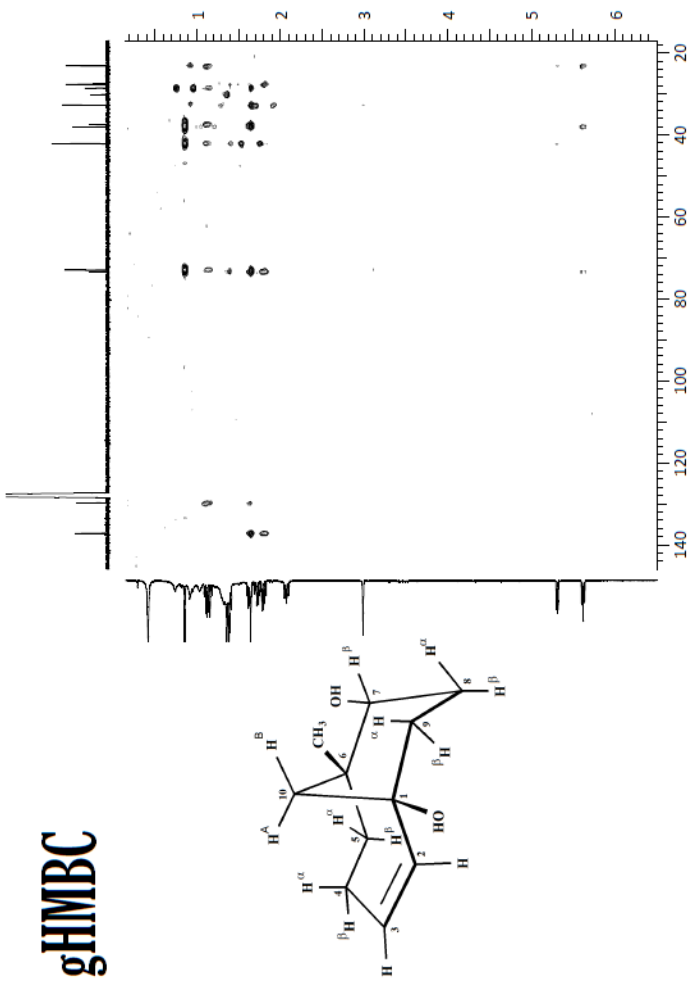
gHMBC
1
2
3
4
5
6
20
40
60
80
100
120
140
OH
CH3
HO

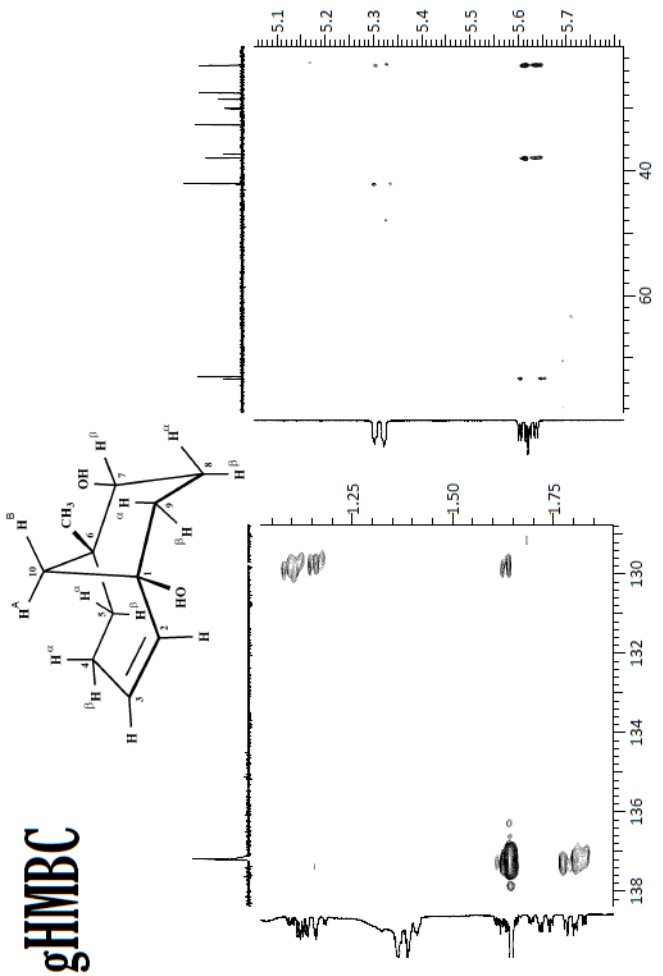
gHMBC
5.1
5.2
5.3
5.4
5.5
5.6
5.7
40
60
1.25
1.50
1.75
130
132
134
136
138
OH
CH3
HO

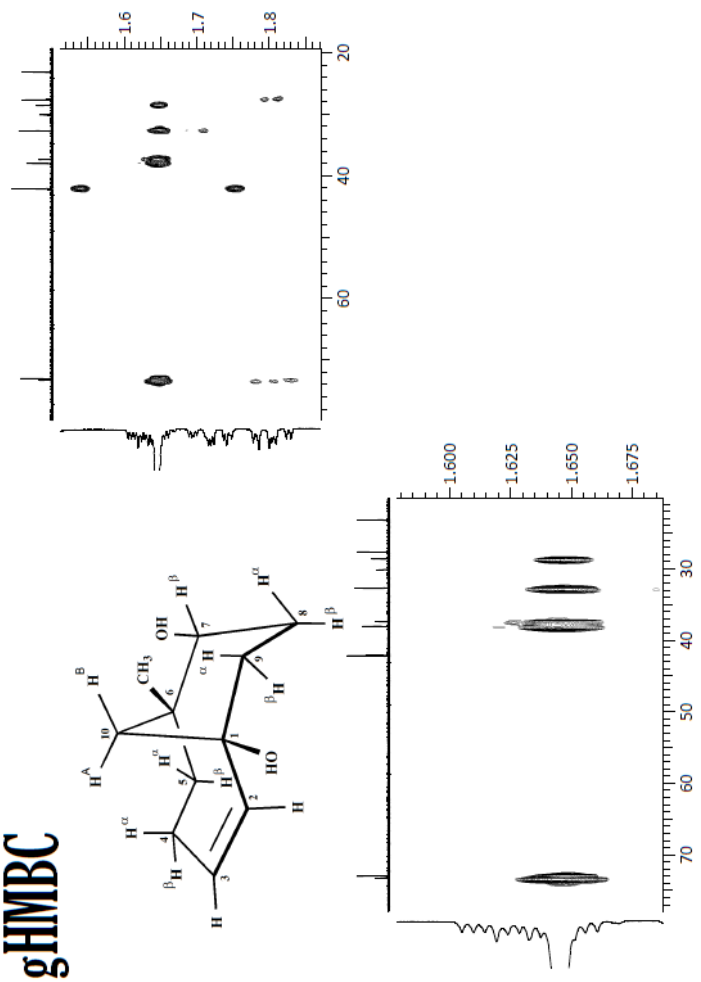
gHMBC
1.6
1.7
1.8
20
40
60
1.600
1.625
1.650
1.675
30
40
50
60
70
OH
CH3
HO

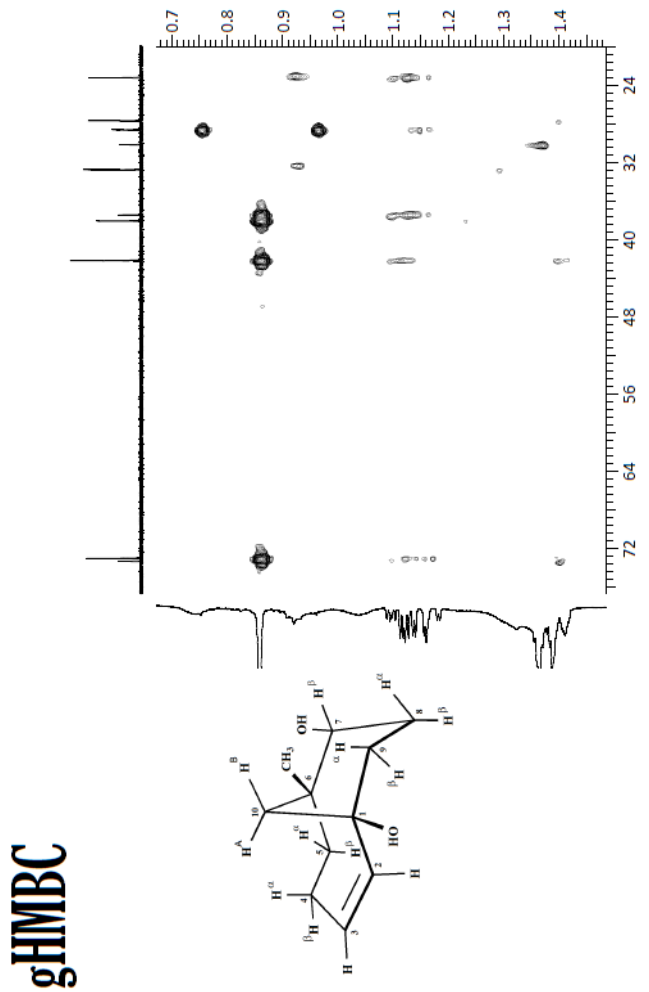
gHMBC
0.7
0.8
0.9
1.0
1.1
1.2
1.3
1.4
24
32
40
48
56
64
72
OH
CH3
HO

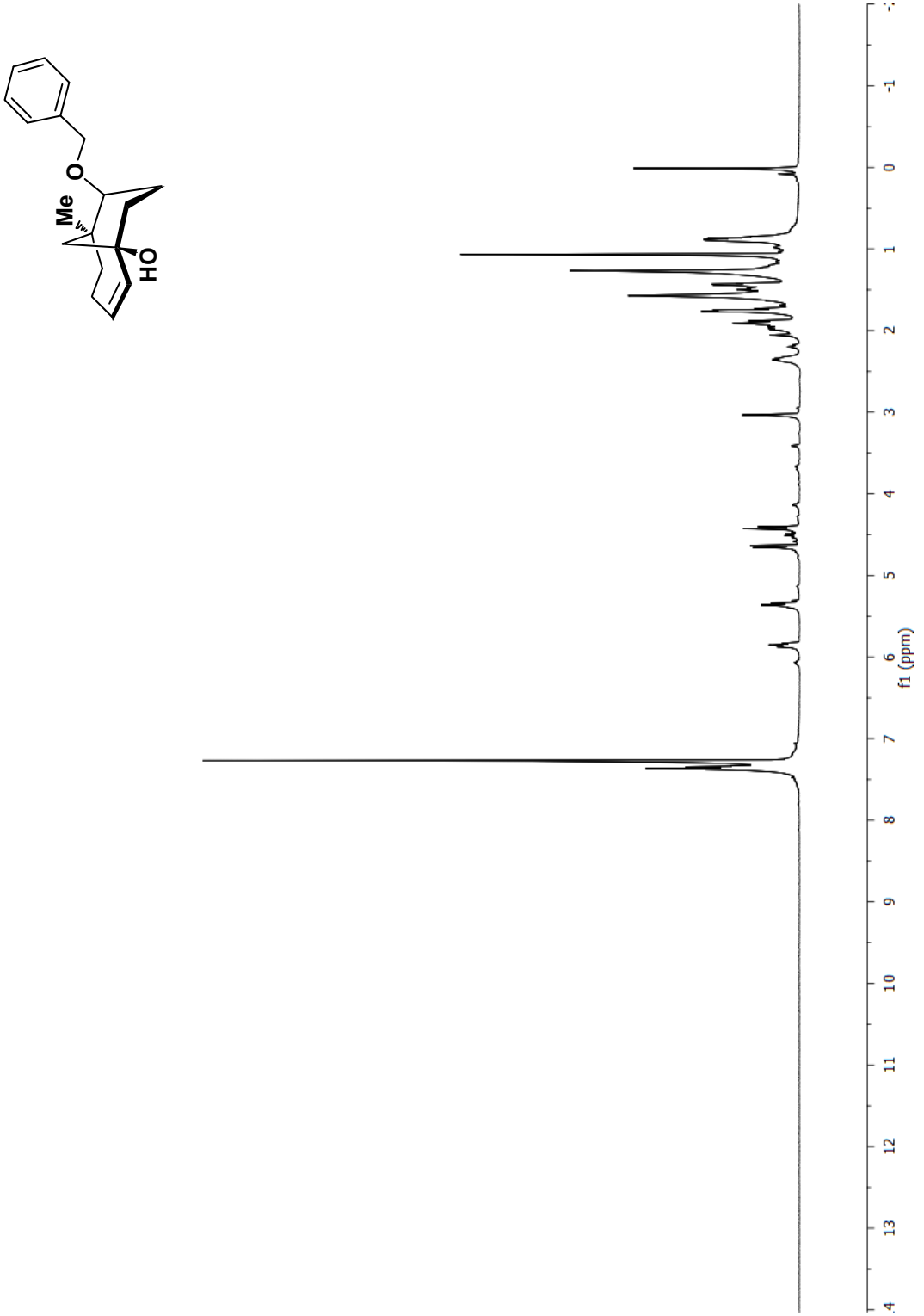
Me
O
HO
f1 (ppm)

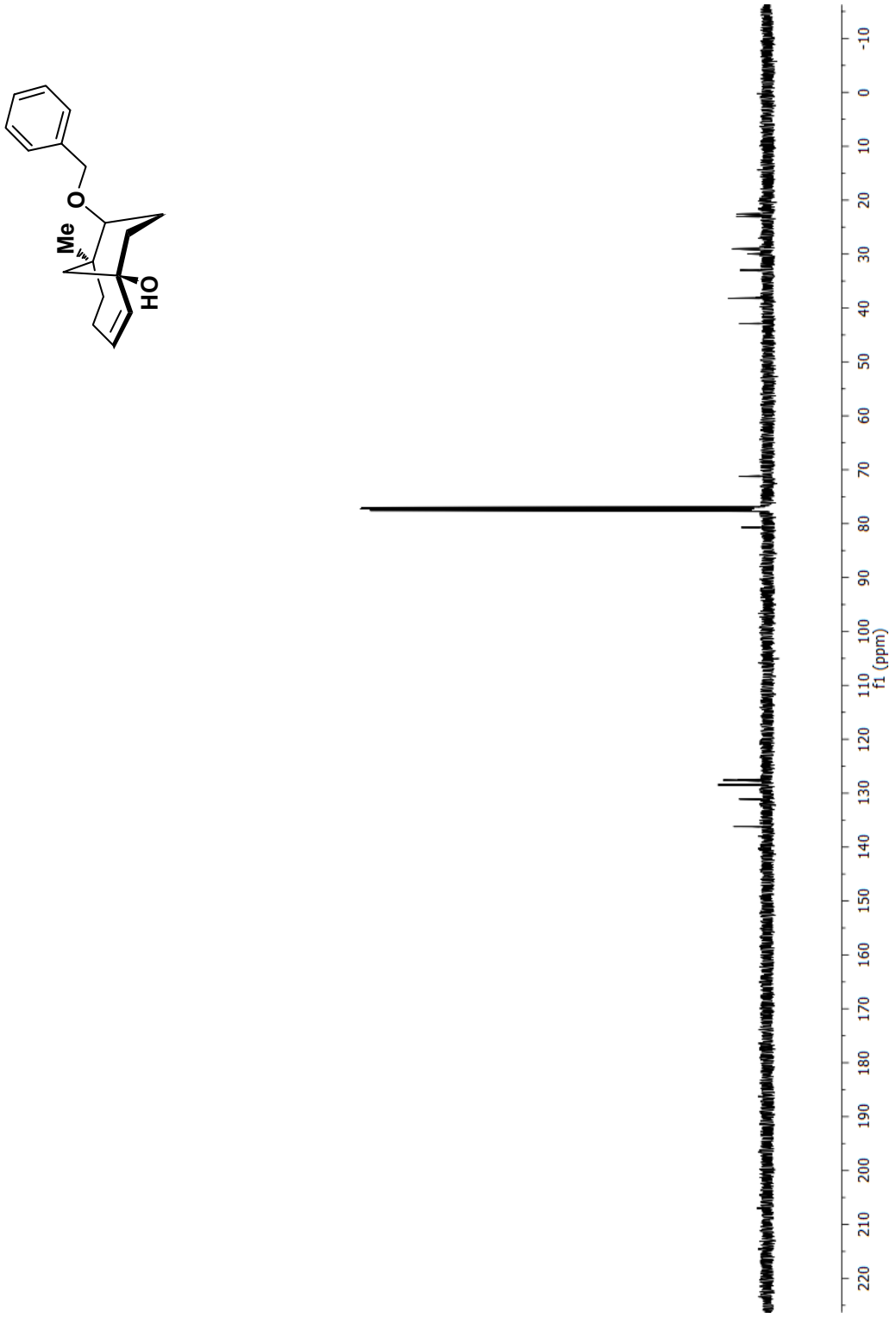
Me
O
HO
f1 (ppm)

4.2 Chapter III

General Information: Starting materials, reagents, and solvents were purchased from commercial suppliers (Aldrich, Acros, Lancaster, and Fischer) and used as received unless otherwise noted. Water-sensitive reactions were conducted using anhydrous solvents in flame-dried glassware with magnetic stirring under an inert atmosphere of dry argon. Microwave reactions were carried out in a CEM Discover reactor. Oven-dried syringes were used to transfer water-sensitive materials. Reaction progress was monitored by analytical thin layer chromatography (TLC) using 250 μm silica gel plates (Dynamic Absorbents F-254). Reactions in DMF, pyridine, triethylamine, and HMPA were monitored by drying spotted TLC plates under high vacuum for 5 min prior to running the TLCs. Visualization was accomplished with UV light and *p*-anisaldehyde, potassium permanganate, or vanillin stain, followed by heating on a hot plate. Flash column chromatography (FCC) was conducted using 230-400 mesh, pore size 60Å, Silicycle ultra pure silica gel unless otherwise noted. Optical rotations were recorded on a Perkin-Elmer 343 polarimeter at 589 nm and 298 K. X-ray crystallographic data were recorded on a Bruker-AXS Smart APEX CCD diffractometer. Infrared (IR) spectra were recorded on an ATI Mattson Genesis Series FT-Infrared spectrophotometer. Proton nuclear magnetic resonance (^{1}H NMR) spectra were recorded on either a Varian-300 instrument (300 MHz), Varian-400 instrument (400 MHz), Varian-500 instrument (500 MHz), or a Varian-600 instrument (600 MHz). Chemical shifts are reported in ppm relative to chloroform or benzene as the internal standard. Data are reported as follows: chemical shift, multiplicity (s = singlet, d = doublet, t = triplet, q = quartet, p = pentet, sext = sextet, sept = septet, m = multiplet, br = broad, app = apparent), coupling constants (Hz), and integration. Carbon

nuclear magnetic resonance (^{13}C NMR) spectra were recorded on either a Varian-300 instrument (75 MHz), Varian-400 instrument (100 MHz), Varian-500 instrument (125 MHz), or Varian-600 instrument (150 MHz). Chemical shifts are reported in ppm relative to chloroform or benzene as the internal standard. Mass spectra were recorded on either a Finnigan LCQ-DUO (ESI) system or a Finnigan LTQ-FT (HRMS-ESI) system.

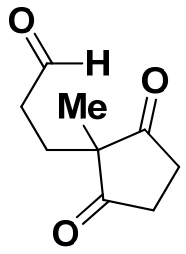

3.11

Aldehyde-dione (3.11): To a vigorously stirred suspension of 2-methyl-1,3-cyclopentanedione (20.0 g, 175 mmol) in deionized water (100 mL) at rt was added acetic acid (0.520 mL, 9.09 mmol) and acrolein (19.5 mL, 262 mmol). After 2.5 h, the suspension had turned into a clear yellow solution. The mixture was concentrated under reduced pressure, beginning at rt then heating gradually to 50 °C to distill off most of the water. The mixture was extracted with excess ethyl acetate (3 x 50 mL). The combined organic layers were dried over Na_2SO_4, filtered, and concentrated under reduced pressure, furnishing aldehyde-dione **3.11** (29.4 g, quant yield) as a viscous yellow oil. This product was partially characterized in a European patent application.[1] IR (neat) 3463, 2967, 2933, 2872, 2735, 1735, 1719, 1638, 1454, 1419, 1375, 1306, 1268, 1193, 1158, 1083, 1030, 1007, 954 cm^{-1}; ^1H NMR (300 MHz, $CDCl_3$) δ 9.64 (t, J = 1.1 Hz, 1H), 2.78 (s, 4H), 2.45

(td, J = 7.4, 1.0 Hz, 2H), 1.90 (t, J = 7.1 Hz, 2H), 1.10 (s, 3H) ppm; ^{13}C NMR (75 MHz, $CDCl_3$) δ 215.7, 200.9, 55.2, 38.4, 34.9, 26.1, 19.4 ppm; ESIMS *m/z* 169.3 ($M+H^+$).

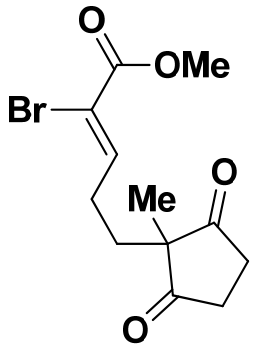

3.12

Vinyl bromide (3.12): To a suspension of *N*-bromosuccinimide (12.8 g, 71.3 mmol) in DCM (previously dried over 4Å molecular sieves, 110 mL) at −20 °C was added methyl (triphenylphosphoranylidene)acetate (12.2 g, 35.7 mmol) in one portion. As it was gradually warmed to rt, the yellow solution turned into an orange suspension. After 2.5 h, the mixture was cooled to 0 °C, then a solution of aldehyde-dione **3.11** (5.00 g, 29.7 mmol, azeotropically dried with toluene x 3) in DCM (40 mL) was added dropwise, followed by the addition of anhydrous potassium carbonate (10.4 g, 74.3 mmol). The mixture was gradually warmed to rt. After 20 h, the brown suspension was vacuum filtered through Celite and rinsed through with liberal amounts of DCM. The filtrate was concentrated under reduced pressure, and the dark brown residue was purified by FCC (thin layer of Florisil above silica gel, 0 to 35% EtOAc/hexane), furnishing vinyl bromide **3.12** (7.15 g, 79%, 6.25:1 *Z*/*E* ratio) as a pale yellow oil. Pure *Z* olefin can be obtained by very slowly increasing the solvent gradient polarity (*E* olefin elutes out first), but both olefins are useful

in the next step. All characterization data of both isomers were in accordance with a previous report.[2]

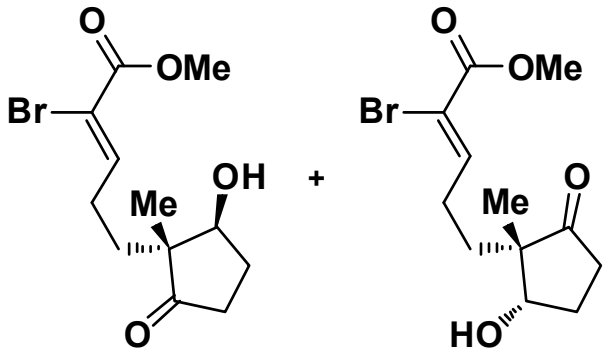

3.25 **3.26**

Ketols (3.25 and 3.26): A stirring solution of deionized water (350 mL) and DMSO (35 mL) was warmed to 30 °C open to air. Dry active baker's yeast (Sigma Type II, 30.8 g) was added and the tan slurry was stirred for 30 min. A solution of vinyl bromide **3.12** (6:1 *Z*/*E* ratio, 0.933 g, 3.08 mmol) in DMSO (2 mL) was then added dropwise, followed by rinsing portions of DMSO (3 x 0.5 mL) to ensure complete transfer. After stirring for 72 h at 30 °C, the suspension was diluted with DCM (50 mL) and sonicated for 20 min, then vacuum filtered through Celite, rinsing through with liberal amounts of DCM. Excess NaCl was added to the partitioned mixture, and the aqueous layer was extracted with DCM (3 x 25 mL). The combined organic layers were washed with brine (25 mL), dried over Na_2SO_4, filtered, and concentrated to a yellow oil. Residual DMSO was distilled off at 60 ˚C on a rotovap. The crude mixture was purified by FCC (0 to 50% EtOAc/hexane, very slow increase in solvent gradient), yielding recovered starting material (0.300 g, 32%) as a colorless oil and ketols **3.25** and **3.26** (0.280 g, 30%, 5.7:1 *dr*) as a colorless foam with a sweet/foul scent. Trace diol formation was observed. Reproducibility is dependent upon

substrate concentration (8.0 mM) and the quality of baker's yeast (<6 months old). These diastereomers were assigned by analogy to reported compounds.[3] Racemic **3.25** and **3.26** (for HPLC assay) were synthesized via the following procedure: To a solution of vinyl bromide **3.12** (pure *Z* olefin, 55 mg, 0.181 mmol) in THF (0.907 mL) in a septum-covered flask at 0 °C was added sodium borohydride (7.35 mg, 0.191 mmol). After 10 min, the reaction was quenched with 1M aq HCl (0.5 mL). The organics were extracted with diethyl ether (3 x 0.25 mL), washed with brine (0.25 mL), dried over Na_2SO_4, filtered, and concentrated. The crude material was purified by FCC (0 to 50% EtOAc/hex), yielding recovered starting material (19.3 mg, 35%) as a colorless oil and ketols **3.25** and **3.26** (33.6 mg, 61%, 1:1.4 *dr*) as a colorless amorphous solid. HPLC: Daicel Chiralpak AS-H, *n*-hexane/*i*-PrOH = 95/5, Flow rate = 1 mL/min, UV = 254 nm, t_R = 38.5 min and t_R = 41.5 min (major, >99% *ee*), t_R = 50.3 min (major, >99% *ee*), and t_R = 62.9 min. IR (thin film) 3444, 2954, 1728, 1622, 1455, 1435, 1265, 1075, 1048, 750, 665 cm^{-1}; **3.25** (major *Z* isomer): ^1H NMR (500 MHz, $CDCl_3$) δ 7.33 (t, J = 7.5 Hz, 1H), 4.20 – 4.17 (m, 1H), 3.82 (s, 3H), 2.54 – 2.44 (m, 1H), 2.43 – 2.14 (m, 4H), 2.05 (br s, 1H), 1.98 – 1.91 (m, 1H), 1.81 – 1.64 (m, 2H), 1.04 (s, 3H) ppm; ^{13}C NMR (125 MHz, $CDCl_3$) δ 220.2, 163.2, 146.5, 116.3, 77.4, 53.5, 53.1, 34.0, 28.5, 28.0, 27.3, 19.4 ppm; ESIMS *m/z* 327.2 ($M+Na^+$).

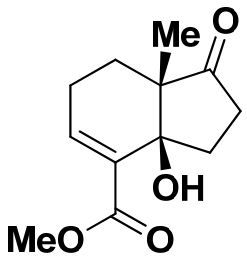

3.13

Ketol (3.13): To freshly activated 4Å powdered molecular sieves was added DMF (165 mL). The solvent was gently swirled and degassed with dry argon for 30 min. After the sieves fully settled to the bottom of the flask, 30 mL of DMF was syringed out and stored under dry argon for future transfer of starting material. To the bulk solvent was added chromium dichloride (Aldrich 95%, 4.27 g, 33.0 mmol) and nickel dichloride (Aldrich 98%, 0.044 g, 0.330 mmol) under an inert atmosphere of dry argon. To this light green suspension at 0 °C was added dropwise a solution of vinyl bromide **3.12** (6.25:1 *Z*/*E* ratio, 2.00 g, 6.60 mmol, azeotropically dried with toluene x 3) in DMF (10 mL). Rinses of starting material in DMF (2 x 10 mL) were subsequently added to ensure complete transfer. The suspension was gradually warmed to rt, changing from light green to dark green. After 9 h, the suspension was vacuum filtered through Celite and rinsed through with liberal amounts of 20% EtOAc/hexane. The green filtrate was partitioned between brine (200 mL) and excess 20% EtOAc/hexane. The organic layer was separated, and the aqueous layer was extracted with 20% EtOAc/hexane (3 x 100 mL). The combined organic layers were washed with brine (25 mL), dried over Na_2SO_4, filtered, and concentrated under reduced pressure. Residual DMF was distilled off at 50 ˚C on a rotovap. The colorless oily residue was purified by FCC (0 to 17% EtOAc/hexane), furnishing ketol **3.13** (1.20 g, 81%) as a colorless oil. This compound can be purified by FCC, but for practical purposes the crude

product should be used directly in the next step. IR (neat) 3508, 2952, 1739, 1716, 1698, 1694, 1440, 1286, 1251, 1056 cm^{-1}; ^1H NMR (500 MHz, $CDCl_3$) δ 6.99 (dd, J = 4.3, 3.6 Hz, 1H), 3.98 (s, 1H), 3.75 (s, 3H), 2.57 − 2.43 (m, 1H), 2.36 (ddd, J = 13.2, 9.3, 3.7 Hz, 1H), 2.32 − 2.22 (m, 2H), 2.21 − 2.06 (m, 2H), 1.64 (ddd, J = 15.2, 9.2, 6.0 Hz, 1H), 1.41 (dt, J = 9.5, 4.0 Hz, 1H), 1.03 (s, 3H) ppm; ^{13}C NMR (125 MHz, $CDCl_3$) δ 220.3, 167.5, 141.0, 132.8, 77.5, 52.1, 52.0, 34.7, 34.4, 27.6, 22.7, 14.5 ppm; ESIMS *m/z* 247.1 ($M+Na^+$); HPLC: Daicel Chiralpak AS-H, *n*-hexane/*i*-PrOH = 95/5, Flow rate = 1 mL/min, UV = 254 nm, t_R = 12.3 min and t_R = 16.7 min (racemic assay).

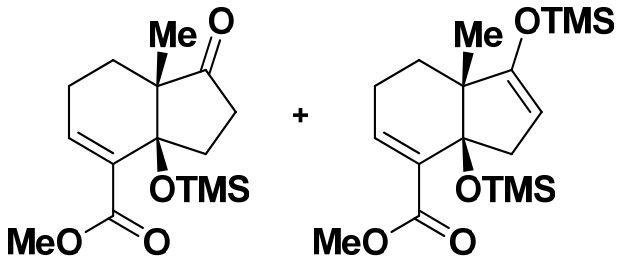

3.14a **3.20**

TMS ether (3.14a) and TMS enol ether (3.20): *N*-(Trimethylsilyl)imidazole (0.876 mL, 5.79 mmol) was added dropwise to ketol **3.13** (0.433 g, 1.93 mmol) at rt. After stirring the yellow solution neat for 18 hours, it was cooled to 0 °C. Saturated aq NH_4Cl (10 mL) was added dropwise, and the quenched mixture was extracted with 10% EtOAc/hexane (3 x 10 mL). The combined organic layers were dried over Na_2SO_4, filtered, and concentrated under reduced pressure. Purification of the crude orange residue by FCC (0 to 17% EtOAc/hexane) furnished TMS ether **3.14a** (0.559 g, 98%) as a colorless oil. **3.14a** undergoes slow overprotection to TMS enol ether **3.20** under these conditions, so the reaction must be quenched promptly after the starting material is consumed. Pushing crude

3.13 through this protection step gave **3.14a** in 79% yield over two steps. TMS ether **3.14a**: IR (neat) 2953, 2925, 2846, 1738, 1732, 1715, 1634, 1471, 1435, 1409, 1367, 1249, 1152, 1039 cm^{-1}; ^{1}H NMR (500 MHz, $CDCl_3$) δ 7.01 (t, J = 4.0 Hz, 1H), 3.75 (d, J = 0.7 Hz, 3H), 2.71 (dd, J = 11.1, 7.3 Hz, 1H), 2.45 − 2.32 (m, 2H), 2.29 − 1.95 (m, 3H), 1.79 (dt, J = 8.0, 5.5 Hz, 1H), 1.54 − 1.43 (m, 1H), 1.03 (s, 3H), 0.11 (s, 9H) ppm; ^{13}C NMR (125 MHz, $CDCl_3$) δ 220.1, 166.8, 143.0, 133.9, 80.0, 54.6, 51.6, 35.0, 32.3, 26.1, 22.9, 18.6, 2.5 ppm; ESIMS *m/z* 319.2 ($M+Na^+$). TMS enol ether **3.20**: IR (neat) 3068, 2955, 2934, 2862, 1720, 1647, 1451, 1435, 1364, 1342, 1318, 1248, 1219, 1190, 1138, 1106, 1093, 976, 931, 883, 840, 754 cm^{-1}; ^{1}H NMR (500 MHz, $CDCl_3$) δ 6.95 (s, 1H), 4.33 (s, 1H), 3.72 (s, 3H), 2.74 (q, J = 35.5, 15.5 Hz, 2H), 2.08 (q, J = 41.0, 19.0 Hz, 2H), 1.61 − 1.51 (m, 1H), 1.50 − 1.40 (m, 1H), 0.97 (s, 3H), 0.20 (s, 9H), 0.08 (s, 9H) ppm; ^{13}C NMR (125 MHz, $CDCl_3$) δ 167.8, 158.2, 140.7, 135.7, 96.0, 81.1, 51.4, 50.6, 40.4, 28.6, 23.3, 18.6, 2.8, 0.3 ppm; ESIMS *m/z* 369.8 ($M+H^+$).

TMS enol ether **3.20** is readily recycled back to TMS ether **3.14a** via the following procedure: To a solution of **3.20** (0.146 g, 0.396 mmol) in benzene (19.8 mL) at rt was added KF (0.0232 g, 0.396 mmol) and 18-crown-6 (85 uL, 0.396 mmol). Within 10 min the colorless suspension had turned into a pale yellow solution. After 40 min, saturated aq NH_4Cl (5 mL) was added, the organic layer was separated, and the aqueous layer was extracted with diethyl ether (3 x 1 mL). The combined organics were dried over Na_2SO_4, filtered, and concentrated to a pale yellow oil. FCC (0 to 10% EtOAc/hexane) of the crude product provided **3.14a** (0.117 g, quant) as a colorless oil.

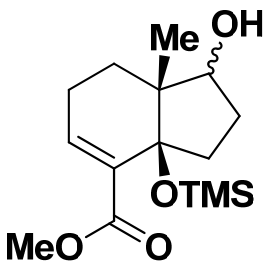

3.14b

TMS ether-alcohols (3.14b): To a solution of TMS ether **3.14a** (0.640 g, 2.16 mmol) in THF/MeOH (19:1, 43 mL) in an open flask at rt was added sodium borohydride (0.408 g, 10.8 mmol). Vigorous bubbling was observed from the colorless suspension. After 10 min, the exothermic reaction was cooled to 0 °C and diluted with Et_2O (50 mL). Saturated aq NH_4Cl (10 mL) was added dropwise, and the quenched mixture was vigorously stirred until bubbling ceased. The mixture was poured into brine (30 mL). The organic layer was separated, and the aqueous layer was extracted with Et_2O (2 x 20 mL). The combined organic layers were washed with brine (10 mL), dried over Na_2SO_4, vacuum filtered, and concentrated under reduced pressure. Residual water was removed by leaving the wet product on high vacuum for 10 min, then diluting with Et_2O (20 mL), washing with brine (3 x 2 mL), and drying over Na_2SO_4. Repeated filtration and concentration under reduced pressure furnished TMS ether-alcohols **3.14b** (0.644 g, quant yield, 1:1.4 β/α ratio) as a colorless oil. The diastereomers are inseparable by FCC at this stage. IR (neat) 3500, 2952, 2874, 1698, 1694, 1639, 1455, 1439, 1280, 1248, 1110, 1013, 842, 742, 668 cm^{-1}; Minor β diastereomer: ^1H NMR (500 MHz, $CDCl_3$) δ 6.81 (t, J = 4.0 Hz, 1H), 3.74 (s, 3H), 1.03 (s, 3H), 0.08 (s, 9H) ppm; Major α diastereomer: ^1H NMR (500 MHz, $CDCl_3$) δ 6.61 (t, J = 2.3 Hz, 1H), 4.20 (t, J = 8.3 Hz, 1H), 3.72 (s, 3H), 0.98 (s, 3H), 0.09 (s, 9H) ppm; ^{13}C NMR, mixture (100 MHz, $CDCl_3$) δ 167.9, 139.6, 137.6, 136.3, 105.0, 84.2, 80.6, 78.6, 51.7,

49.6, 48.5, 38.2, 37.1, 31.7, 29.9, 29.6, 25.1, 23.1, 22.6, 17.9, 15.5, 2.6, 2.6 ppm; ESIMS *m/z* 279.3 ($M-H_2O^+$).

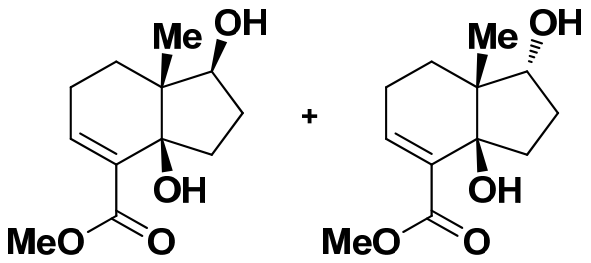

3.16 **3.15**

Diol (3.16) and diol (3.15): To a solution of TMS ether-alcohols **3.14b** (3.29 g, 11.0 mmol) in THF (110 mL) at rt was added tetrabutylammonium fluoride (1M in THF, 14.32 mL, 14.3 mmol), producing an orange solution. After 3 h, saturated aq NH_4Cl (20 mL) was added dropwise, and the quenched mixture was poured into water (80 mL). The organic layer was separated, and the aqueous layer was extracted with Et_2O (3 x 20 mL). The combined organic layers were washed with brine (15 mL), dried over Na_2SO_4, filtered, and concentrated under reduced pressure to a yellow oily residue. The crude material was purified by FCC (17% EtOAc/hexane), furnishing diol **3.16** (1.029 g, 41%) and diol **3.15** (1.396 g, 56%) as colorless oils. Complete separation is difficult to achieve, so a second or third column is usually required to obtain these yields. Diol **3.16**: IR (neat) 3500, 2950, 2877, 2243, 1723, 1714, 1694, 1682, 1651, 1644, 1435, 1278, 1011 cm^{-1}; ^1H NMR (500 MHz, $CDCl_3$) δ 6.90 (t, J = 2.0 Hz, 1H), 4.18 (s, 1H), 3.75 (s, 3H), 3.68 (dd, J = 11.0, 6.5 Hz, 1H), 3.05 (d, J = 11.3 Hz, 1H), 2.42 − 2.29 (m, 2H), 2.28 − 2.12 (m, 2H), 1.99 − 1.84 (m, 2H), 1.47 − 1.29 (m, 2H), 1.08 (s, 3H) ppm; ^{13}C NMR (125 MHz, $CDCl_3$) δ 167.7, 139.3, 133.4, 81.6, 81.4, 51.9, 48.3, 40.3, 32.1, 30.1, 23.5, 13.1 ppm; ESIMS *m/z* 249.9

($M+Na^+$). Diol **3.15**: IR (neat) 3454, 2952, 2876, 1693, 1639, 1439, 1376, 1363, 1283, 1248, 1135, 1109, 1062, 1019 cm^{-1}; ^1H NMR (400 MHz, $CDCl_3$) δ 6.99 − 6.91 (m, 1H), 4.37 (t, J = 8.5 Hz, 1H), 3.84 (s, 1H), 3.74 (s, 3H), 2.35 − 2.17 (m, 3H), 2.12 − 1.96 (m, 2H), 1.72 − 1.55 (m, 3H), 1.51 − 1.38 (m, 1H), 1.03 (s, 3H) ppm; ^{13}C NMR (75 MHz, $CDCl_3$) δ 167.8, 139.7, 134.0, 80.3, 79.8, 51.9, 46.6, 38.9, 29.4, 24.6, 23.0, 16.4 ppm; ESIMS *m/z* 249.8 ($M+Na^+$).

Diol **3.15** is readily recycled back to TMS ether **3.14a** via the following sequence: To a solution of diol **3.15** (1.17 g, 5.19 mmol) in DCM (77 mL) at rt was added pyridinium dichromate (2.19 g, 5.71 mmol). The orange suspension turned dark brown within 1 h. After 8 h, Celite (2.60 g) was added to sequester the black tar byproduct. After 15 min, the suspension was vacuum filtered through Celite and rinsed through with liberal amounts of DCM. The filtrate was concentrated under reduced pressure to a dark brown oil (1.20 g, essentially pure ketol **3.13** by crude NMR). *N*-(Trimethylsilyl)imidazole (2.38 mL, 15.6 mmol) was added dropwise to crude ketol **3.13** at rt. After stirring the brown solution neat for 24 hours, it was cooled to 0 °C. Saturated aq NH_4Cl (10 mL) was added dropwise, and the quenched mixture was extracted with DCM (3 x 10 mL). The combined organic layers were dried over Na_2SO_4, filtered, and concentrated under reduced pressure. Purification of the crude orange residue by FCC (0 to 17% EtOAc/hexane) furnished TMS ether **3.14a** (0.800 g, 52% over 2 steps) as a colorless oil.

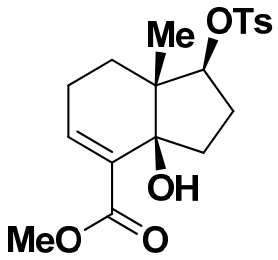

3.17

Ester-tosylate (3.17): To a solution of diol **3.16** (0.919 g, 4.06 mmol) in pyridine (5.28 mL) in an oversized flask at rt was added *p*-toluenesulfonyl chloride (0.939 g, 4.88 mmol). After 20 h, the beige suspension had turned orange. Pyridine was carefully removed under reduced pressure without bumping, leaving a pale orange residue that precipitated out colorless crystals upon standing. Purification of the crude material by FCC (0 to 30% EtOAc/hexane, pure product appeared as two spots on TLC, staining blue and green in anisaldehyde) furnished ester-tosylate **3.17** (1.364 g, 88%) as a colorless oil. IR (neat) 3521, 2951, 2928, 1693, 1438, 1357, 1282, 1247, 1188, 1175, 1100, 971, 667, 556 cm^{-1}; ^{1}H NMR (500 MHz, $CDCl_3$) δ 7.79 (d, J = 8.2 Hz, 2H), 7.32 (d, J = 8.5 Hz, 2H), 6.90 (t, J = 3.9 Hz, 1H), 4.53 (t, J = 6.8 Hz, 1H), 3.74 (s, 3H), 3.73 (s, 1H), 2.44 (s, 3H), 2.32 − 2.04 (m, 3H), 2.02 − 1.93 (m, 2H), 1.87 − 1.76 (m, 1H), 1.51 − 1.36 (m, 2H), 1.02 (s, 3H) ppm; ^{13}C NMR (125 MHz, $CDCl_3$) δ 167.8, 144.6, 139.7, 134.5, 133.9, 129.9, 127.9, 86.8, 78.1, 52.0, 47.6, 37.8, 29.9, 28.7, 22.9, 21.8, 14.6 ppm; ESIMS *m/z* 403.1 ($M+Na^+$).

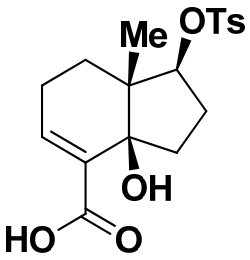

3.18

Acid-tosylate (3.18): To a vigorously stirred solution of ester-tosylate **3.17** (0.192 g, 0.505 mmol) in THF (4 mL) at rt was added 1M aq KOH (1.01 mL, 1.01 mmol). After 5 h under a positive pressure of argon, the biphasic mixture was partitioned between water (5 mL) and Et_2O (5 mL). The basic aqueous layer was separated and washed with Et_2O (2 x 1 mL). The organic layer was back-extracted with water (2 x 1 mL). The combined aqueous layers were carefully acidified to pH 1 with 1N HCl. The product was extracted from the acidic aqueous phase with Et_2O (3 x 2 mL). The combined organic layers were washed with brine (0.5 mL), dried over Na_2SO_4, filtered, and concentrated under reduced pressure, furnishing acid-tosylate **3.18** (0.180 g, 97%) as a colorless foam. The tosylate of **3.18** undergoes slow elimination under these basic conditions, so this reaction must be worked up promptly after the starting material is consumed. A 10 mg sample of **3.18** was recrystallized from 33% DCM/hexane. X-ray quality crystals were obtained via slow evaporation at rt in a parafilmed vial with small poked hole. See p. 326 for X-ray crystallography data. IR (thin film) 3479, 3065, 2929, 1703, 1698, 1693, 1682, 1355, 1189, 1175, 971, 668, 557 cm^{-1}; ^1H NMR (400 MHz, $CDCl_3$) δ 7.79 (d, J = 8.2 Hz, 2H), 7.33 (d, J = 8.1 Hz, 2H), 7.03 (t, J = 3.8 Hz, 1H), 4.53 (t, J = 6.5 Hz, 1H), 3.76 (br s, 1H), 2.44 (s, 3H), 2.37 − 2.09 (m, 3H), 2.06 − 1.94 (m, 2H), 1.93 − 1.80 (m, 1H), 1.51 − 1.39 (m, 2H), 1.02 (s, 3H) ppm; ^{13}C NMR (100

MHz, $CDCl_3$) δ 170.9, 144.8, 142.5, 134.4, 133.0, 129.9, 127.9, 87.2, 78.6, 47.9, 37.8, 30.0, 28.8, 23.1, 21.8, 14.5 ppm; ESIMS *m/z* 365.1 ($M-H^-$).

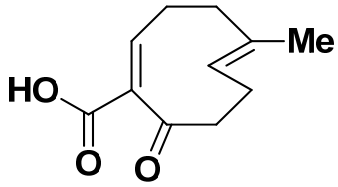

3.19

Cyclononadienone-carboxylic acid (3.19): To a solution of acid-tosylate **3.18** (0.546 g, 1.49 mmol) in HMPA (previously dried over 4Å molecular sieves, 9.93 mL) in an oversized flask at 0 °C was added excess sodium hydride (60% in mineral oil, portions of 0.300 g, 7.50 mmol, up to 200 equiv sometimes required, or 1 g/mL HMPA), producing a brown suspension. The mixture was warmed to rt after addition of the first batch of sodium hydride. To monitor this reaction, an acid-base workup was applied to each pipetted aliquot to remove as much HMPA as possible prior to spotting the TLC plate (45:45:10 EtOAc/hexane/AcOH solvent system). To prevent foaming over during the quench, the slurry was cooled to 0 °C, diluted with hexane, and a larger stirbar was added to ensure homogenous stirring. After 1 h, deionized water was added dropwise very slowly until the evolution of H_2 gas ceased. The basic aqueous layer was separated and washed with hexane (removing mineral oil, 1 x 3 mL). The combined organic layers were back-extracted with water (2 mL). The combined aqueous layers were stirred and carefully acidified to pH 1 with 1N HCl, turning the dark yellow solution to a cloudy light yellow suspension. The product was extracted from the acidic aqueous phase with small volumes of 20% EtOAc/hexane until no product was observed by TLC in the last extract. The combined

organic layers were washed with a small portion of brine, dried over Na_2SO_4, filtered, and concentrated under reduced pressure, furnishing crude cyclononadienone-carboxylic acid **3.19** in trace HMPA as a pale yellow liquid. HMPA is difficult to remove completely from this polar product. For practical purposes the crude product should be used directly in the next step. **3.19** is unstable on silica gel. By repeated brine washes and back-extractions, an analytical sample of **3.19** (8 mg) was secured as a colorless oil. IR (neat) 3126, 2937, 2861, 1698, 1682, 1384, 1278, 1161 cm^{-1}; ^1H NMR (300 MHz, $CDCl_3$) δ 7.04 (t, J = 8.7 Hz, 1H), 5.42 (dd, J = 12.0, 2.1 Hz, 1H), 3.18 (td, J = 11.5, 7.9 Hz, 1H), 2.70 (qd, J = 11.9, 7.2 Hz, 1H), 2.46 − 2.25 (m, 3H), 2.24 − 2.12 (m, 2H), 1.83 (t, J = 12.0 Hz, 1H), 1.60 (s, 3H) ppm; ^{13}C NMR (75 MHz, $CDCl_3$) δ 203.9, 169.9, 147.1, 139.8, 134.9, 127.6, 44.1, 36.1, 26.1, 25.3, 16.7 ppm; ESIMS *m/z* 193.3 ($M-H^-$).

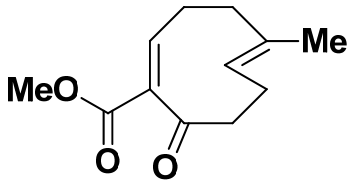

3.6

Cyclononadienone-carboxylate-methyl ester (3.6): To a yellow solution of crude cyclononadienone-carboxylic acid **3.19** (theoretical 0.117 g, 0.602 mmol) in DCM (6.02 mL) at rt under argon was added MeOH (0.122 mL, 3.01 mmol), 4-dimethylaminopyridine (7.4 mg, 0.060 mmol), and 1-ethyl-3-(3-dimethylaminopropyl)carbodiimide (0.110 mL, 0.602 mmol). Addition of another 0.25 equiv of EDC and 0.1 equiv of DMAP was required to push the reaction to completion. After 2 h, deionized water (6 mL) was added, and the organic layer was separated. The aqueous layer was extracted with DCM (3 x 2 mL). The

combined organic layers were washed with minimal brine (0.5 mL), dried over Na_2SO_4, filtered, and concentrated under reduced pressure to a dark yellow oil. Purification of the crude material by FCC (0 to 10% EtOAc/hexane) furnished cyclononadienone-carboxylate-methyl ester **3.6** (0.081 g, 65% over 2 steps) as a colorless oil. Upon storage in a freezer, pure **3.6** gradually crystallizes out. See p. 338 for X-ray crystallography data. IR (neat) 2983, 2936, 2860, 1731, 1699, 1456, 1435, 1277, 1245, 1050, 666 cm^{-1}; ^1H NMR (300 MHz, $CDCl_3$) δ 6.91 (t, J = 8.7 Hz, 1H), 5.41 (dd, J = 12.1, 2.2 Hz, 1H), 3.78 (s, 3H), 3.08 (td, J = 11.6, 7.7 Hz, 1H), 2.79 − 2.59 (m, 1H), 2.53 − 2.23 (m, 3H), 2.22 − 2.11 (m, 2H), 1.80 (dd, J = 17.5, 6.9 Hz, 1H), 1.59 (s, 3H) ppm; ^{13}C NMR (125 MHz, $CDCl_3$) δ 204.2, 165.4, 144.2, 140.4, 134.9, 127.4, 52.3, 44.0, 36.1, 25.9, 25.3, 16.7 ppm; ESIMS *m/z* 209.1 ($M+H^+$), 226.0 ($M+H_2O^+$), 231.0 ($M+Na^+$).

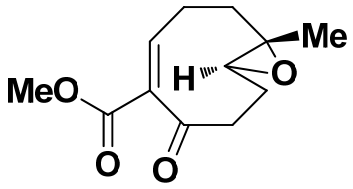

3.28

Epoxide (3.28): Racemic epoxide (for HPLC assay) was synthesized from **3.6** via an *m*-CPBA protocol (section 4.1 Chapter II). Kinetic resolution of **3.6** was achieved via a Shi epoxidation procedure[4]: To a vigorously stirred solution of **3.6** (0.022 g, 0.105 mmol), Shi dioxirane catalyst (0.0136 g, 0.053 mmol), and tetrabutylammonium hydrogen sulfate (0.0036 g, 0.011 mmol) in dimethoxymethane (2.1 mL), acetonitrile (1.1 mL), and buffer (0.05M $Na_2B_4O_7 \cdot 10H_2O$ in 4 x 10^{-4} M, 2.0 mL) was added a solution of Oxone (0.016 g, 0.026 mmol) in aq. Na_2EDTA (4 x 10^{-4} M, 0.21 mL) and a solution of K_2CO_3 (0.016 g,

0.116 mmol) in water (0.21 mL) separately at a rate of 0.1 mL per hour via syringe pump at 0 °C over 2 h. The reaction mixture was quenched with water, extracted with dichloromethane, washed with brine, dried over Na_2SO_4, filtered, concentrated, and purified by FCC (0 to 17% EtOAc/hexane), furnishing epoxide **3.28** (0.006 g, 25%) as a colorless solid [HPLC: Daicel Chiralpak AD-H, *n*-hexane/*i*-PrOH = 90/10, Flow rate = 1 mL/min, UV = 230 nm, t_R = 9.3 min and t_R = 10.3 min (major, 73% *ee*)] and resolved starting material **3.6** (0.011 g, 50%) as a colorless oil [HPLC: Daicel Chiralpak AS-H, *n*-hexane/*i*-PrOH = 90/10, Flow rate = 1 mL/min, UV = 230 nm, t_R = 5.1 min and t_R = 6.0 min (major, 42% *ee*)]. The *ee* of **3.6** was measured once per hour for 8 hours at rt. From these data, the half-life of racemization was calculated.

Spontaneous epoxidation: A solution of **3.6** (0.008 g) in $CDCl_3$ (0.75 mL) under air in a capped NMR tube was left standing on a laboratory bench at rt. Evaporated $CDCl_3$ was replenished periodically. After 36 weeks, TLC and crude NMR analysis of the solution indicated quantitative conversion to **3.28**. The solution was diluted with DCM, dried over Na_2SO_4, filtered, and concentrated in vacuo, furnishing **3.28** (0.008 g, quant) as a colorless amorphous solid.

IR (thin film) 2927, 1731, 1703, 1698, 1454, 1434, 1282, 1249, 1221, 1048 cm^{-1}; ^1H NMR (500 MHz, $CDCl_3$) δ 7.04 (t, J = 9.0 Hz, 1H), 3.82 (s, 3H), 3.00 (sext, J = 7.5 Hz, 1H), 2.92 (dd, J = 11.5, 2.0 Hz, 1H), 2.72 − 2.56 (m, 2H), 2.39 − 2.29 (m, 1H), 2.27 − 2.13 (m, 2H), 1.71 (sept, J = 7.0 Hz, 1H), 1.23 (s, 3H), 1.10 (t, J = 12.5 Hz, 1H) ppm; ^{13}C NMR (125

MHz, $CDCl_3$) δ 205.0, 165.0, 145.4, 140.6, 61.0, 59.4, 52.6, 38.5, 35.4, 25.0, 22.7, 17.4 ppm; ESIMS *m/z* 224.9 ($M+H^+$), 242.3 ($M+H_2O^+$).

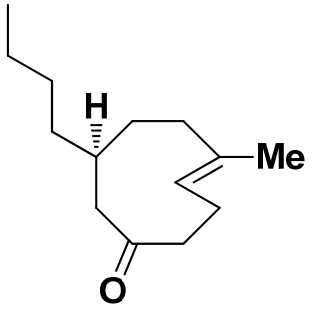

3.32

Des-carboxy ketone (3.32): To a degassed solution of cyclononadienone-carboxylic acid **3.19** (0.029 g, 0.149 mmol, azeotropically dried with toluene x 3) in THF (1 mL, trace HMPA present) at −40 °C was added *n*-BuLi (2.5M in hexanes, 0.19 mL, 0.475 mmol) and TMSCl (redistilled, 0.030 mL, 0.243 mmol). After 2 h, the pale yellow solution was warmed to rt and more TMSCl (redistilled, 0.059 mL, 0.464 mmol) was added. After 30 min, the solution was cooled to −78 °C. $Bu_2Cu(CN)Li_2$ was simultaneously prepared by adding *n*-BuLi (2.5M in hexanes, 0.41 mL, 1.03 mmol) to a degassed suspension of activated CuCN (0.0457 g, 0.510 mmol) in THF (5.1 mL) at −78 °C, generating a pale yellow solution within 5 min. After stirring the cuprate for 1 h, the solution of *in situ* silyl ester was added dropwise via cannula to the cuprate solution at −78 °C. After 3 h, saturated aq 20% NH_4OH/NH_4Cl (5 mL) was added dropwise, and the mixture was vigorously stirred while warming to rt. The blue aqueous layer was extracted with Et_2O (3 x 5 mL). The combined organic layers were washed with brine (3 mL), dried over Na_2SO_4, filtered, and concentrated under reduced pressure to an oily yellow residue. Purification of the crude material by FCC (0 to 17% EtOAc/hexane) furnished des-carboxy ketone **3.32**

(0.009 g, 29%) as a colorless oil. Decarboxylation of the crude product was presumably acid-catalyzed on TLC and silica gel. IR (neat) 2956, 2926, 2870, 2856, 1810, 1702, 1456, 1384, 1169, 1101 cm^{-1}; 7.9:1 conformational equilibrium ($CDCl_3$, 25 °C); ^1H NMR, major conformer (500 MHz, $CDCl_3$) δ 5.34 (dd, J = 10.5, 5.5 Hz, 1H), 2.66 − 2.56 (m, 1H), 2.53 − 2.46 (m, 1H), 2.45 − 2.38 (m, 1H), 2.16 − 2.05 (m, 4H), 1.92 (td, J = 12.5, 4.0 Hz, 1H), 1.79 (br s, 1H), 1.64 (d, J = 1.5 Hz, 3H), 1.59 − 1.54 (m, 1H), 1.31 (br s, 7H), 0.89 (br s, 3H) ppm; ^{13}C NMR, major conformer (125 MHz, $CDCl_3$) δ 215.0, 137.5, 123.6, 54.5, 41.0, 40.5, 39.5, 37.2, 35.2, 29.3, 23.2, 23.0, 16.9, 14.3 ppm; ESIMS *m/z* 209.1 ($M+H^+$), 226.0 ($M+H_2O^+$).

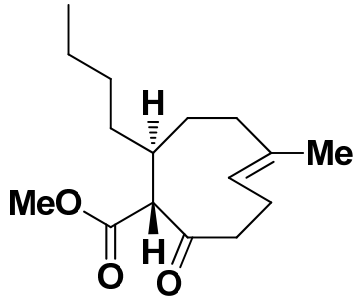

3.33

***n*-Butyl ketoester (3.33):** To a degassed suspension of activated CuCN (0.0434 g, 0.480 mmol) in THF (4.8 mL) at −78 °C was added *n*-BuLi (2.5M in hexanes, 0.384 mL, 0.960 mmol), generating a pale yellow/light brown solution within 5 min. After 15 min at −78 °C, TMSCl (redistilled, 0.062 mL, 0.480 mmol) was added followed immediately by a degassed solution of cyclononadienone-carboxylate-methyl ester **3.6** (0.017 g, 0.082 mmol, azeotropically dried with toluene x 3) in THF (1 mL), producing a dark yellow solution. After 5 min, saturated aq 20% NH_4OH/NH_4Cl (3 mL) was added dropwise, and the mixture was vigorously stirred while warming to rt. The blue aqueous layer was extracted with Et_2O (3 x 5 mL). The combined organic layers were washed with brine (2

mL), dried over Na_2SO_4, filtered, and concentrated under reduced pressure to an oily yellow residue. Purification of the crude material by FCC (0 to 5% EtOAc/hexane) furnished *n*-butyl ketoester **3.33** (0.013 g, 60%) as a colorless oil. Extensive 2D NMR analysis and comparisons with computational modeling[5] confirmed the structures of both conformers. Variable temperature ^{1}H NMR (up to 90 °C in tol-d_8) did not show a significant shift in conformational equilibrium. IR (neat) 2952, 2932, 2859, 1737, 1705, 1454, 1434, 1193, 1148 cm^{-1}; 4.5:1 conformational equilibrium ($CDCl_3$, 25 °C); ^{1}H NMR, major conformer (400 MHz, $CDCl_3$) δ 5.41 (dd, J = 11.6, 3.2 Hz, 1H), 3.67 (s, 3H), 3.12 (d, J = 10.0 Hz, 1H), 3.02 − 2.92 (m, 1H), 2.75 − 2.61 (m, 1H), 2.24 − 2.12 (m, 2H), 2.11 − 1.97 (m, 2H), 1.90 (td, J = 12.0, 3.2 Hz, 1H), 1.56 (s, 3H), 1.45 − 1.15 (m, 8H), 0.95 − 0.83 (m, 3H) ppm; ^{13}C NMR, major conformer (100 MHz, $CDCl_3$) δ 207.5, 170.8, 137.0, 123.8, 70.1, 52.1, 40.1, 39.6, 38.9, 35.0, 31.7, 28.8, 24.6, 23.0, 17.6, 14.2 ppm; ESIMS *m/z* 266.9 ($M+H^+$), 283.9 ($M+H_2O^+$).

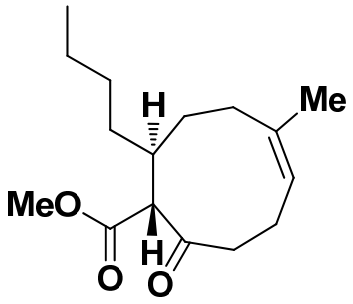

3.39

***Z* olefin (3.39):** A 10 mL microwave reaction tube was charged with **3.33** (0.001 g, 0.00375 mmol), DMSO-d_6 (0.75 mL), and a Teflon stir bar. The reaction tube was sealed with a Teflon-lined snap cap, and heated in a microwave reactor at 150 °C (250 W, 25 – 50 psi) for 30 min under efficient stirring (setting = "HIGH"). After cooling with compressed

air flow, crude NMR indicated quantitative conversion to the product. The crude pale yellow solution was poured into brine (7.5 mL) and extracted with Et_2O (3 x 1.5 mL). The combined organic layers were washed with brine (0.25 mL), dried over Na_2SO_4, filtered, and concentrated under reduced pressure, furnishing *Z* olefin **3.39** (0.001 g, quant yield) as a colorless solid. 3.4:1 conformational equilibrium (DMSO-d_6, 25 °C); ^{1}H NMR, major conformer (500 MHz, DMSO-d_6) δ 5.44 (t, J = 8.0 Hz, 1H), 3.62 (d, J = 2.0 Hz, 3H), 3.43 (d, J = 11.0 Hz, 1H), 2.63 (t, J = 11.5 Hz, 1H), 2.54 − 2.38 (m, 1H), 2.24 (td, J = 7.8, 2.0 Hz, 1H), 2.16 − 2.01 (m, 2H), 1.69 − 1.61 (m, 1H), 1.60 (s, 3H), 1.59 − 1.51 (m, 1H), 1.50 (s, 1H), 1.43 − 1.34 (m, 1H), 1.33 − 1.10 (m, 6H), 0.85 (m, 3H) ppm; ^{13}C NMR, major conformer (125 MHz, $CDCl_3$) δ 210.7, 170.0, 138.3, 124.7, 66.1, 52.4, 40.3, 34.9, 33.8, 30.5, 28.9, 24.8, 22.9, 22.4, 15.4, 14.2 ppm. ESIMS *m/z* 266.8 ($M+H^+$).

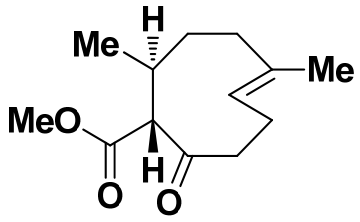

3.34

Methyl ketoester (3.34): To oven-dried CuI (0.086 g, 0.454 mmol) was added anhydrous diethyl ether (2 mL). To the vigorously stirring suspension at rt was added PBu_3 (0.196 mL, 0.908 mmol). After 10 min, the suspension became a clear solution, and the flask was cooled to -78 °C. To this was added MeLi (1.6M in diethyl ether, 0.57 mL, 0.908 mmol), generating a pale yellow solution. After 15 min, the temperature was raised to 0 °C. After 5 min, it was cooled back to -78 °C. TMSCl (redistilled, 0.058 mL, 0.454 mmol) was then added followed immediately by a solution of cyclononadienone-carboxylate-methyl ester

3.6 (0.0189 g, 0.0908 mmol) in diethyl ether (1 mL), producing a light yellow solution. After 15 min, the reaction was quenched with sat aq NH_4Cl (3 mL) and aq ammonia (1 mL). After warming to rt, the organic layer was separated, and the blue aqueous layer was extracted with diethyl ether (3 x 5 mL). The combined organic layers were washed with brine (5 mL), dried over Na_2SO_4, filtered, and concentrated under reduced pressure. Purification of the crude oil by FCC (0 to 10% EtOAc/hexane) furnished methyl ketoester **3.34** (0.0167 g, 82%) as a colorless oil. IR (neat) 2922, 2852, 1660, 1633, 1468, 1410, 1092 cm^{-1}; 3.9:1 conformational equilibrium ($CDCl_3$, 25 °C); ^1H NMR, major conformer (500 MHz, $CDCl_3$) δ 5.42 (dd, J = 11.5, 3.0 Hz, 1H), 3.69 (s, 3H), 3.10 (d, J = 9.0 Hz, 1H), 2.99 − 2.89 (m, 1H), 2.75 − 2.65 (m, 1H), 2.40 − 2.32 (m, 1H), 2.29 − 2.21 (m, 1H), 2.15 − 2.07 (m, 1H), 2.01 (app p, J = 2.5 Hz, 2H), 1.59 (s, 3H), 1.54 − 1.46 (m, 2H), 1.00 (d, J = 7.0 Hz, 3H) ppm; ^{13}C NMR, major conformer (125 MHz, $CDCl_3$) δ 207.8, 170.6, 137.2, 124.1, 71.0, 52.3, 39.6, 39.1, 35.1, 35.0, 24.6, 22.2, 17.7 ppm; ESIMS *m/z* 224.9 ($M+H^+$), 241.9 ($M+H_2O^+$).

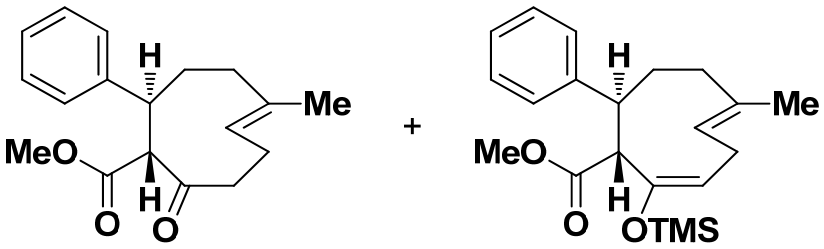

3.41 **3.42**

Phenyl ketoester (3.41) and TMS enol ether (3.42): To a degassed suspension of activated CuCN (0.0543 g, 0.600 mmol) in Et_2O (6.0 mL) at −78 °C was added PhLi (1.8M in *n*-Bu_2O, 0.667 mL, 1.20 mmol), generating a dark yellow color within 5 min. The cuprate was warmed to 0 °C, turning into a bright yellow solution. After cooling back to

−78 °C and stirring for 15 min, TMSCl (redistilled, 0.077 mL, 0.600 mmol) was added followed immediately by a degassed solution of cyclononadienone-carboxylate-methyl ester **3.6** (0.020 g, 0.096 mmol, azeotropically dried with toluene x 3) in Et_2O (1 mL), producing a dark olive green/light brown solution. After 15 min, saturated aq 20% NH_4OH/NH_4Cl (3 mL) was added dropwise, and the mixture was vigorously stirred while warming to rt. The blue aqueous layer was extracted with Et_2O (3 x 6 mL). The combined organic layers were washed with brine (3 mL), dried over Na_2SO_4, filtered, and concentrated under reduced pressure to a pale yellow oil in *n*-Bu_2O. Purification of the crude material by FCC (0 to 10% Et_2O/pentane) furnished phenyl ketoester **3.41** (0.012 g, 44%) and TMS enol ether **3.42** (0.010 g, 29%) as colorless oils. The relative stereochemistry of **3.41** was assigned by analogy to **3.33**. **3.42** was slowly hydrolyzed back to **3.41** on TLC and silica gel. **3.41**: IR (neat) 3084, 3060, 3028, 2933, 2856, 1737, 1703, 1452, 1434, 1201, 1163, 1147, 701 cm^{-1}; 6.1:1 conformational equilibrium ($CDCl_3$, 25 °C); ^1H NMR, major conformer (400 MHz, $CDCl_3$) δ 7.29 − 7.23 (m, 3H), 7.21 − 7.15 (br d, J = 7.2 Hz, 2H), 5.61 (dd, J = 11.6, 4.0 Hz, 1H), 3.61 (d, J = 10.4 Hz, 1H), 3.47 − 3.38 (m, 1H), 3.26 (s, 3H), 3.20 − 3.08 (m, 1H), 2.76 (ddd, J = 16.8, 11.2, 5.6 Hz, 1H), 2.26 − 2.18 (m, 1H), 2.17 − 2.10 (m, 1H), 2.09 − 2.02 (m, 2H), 1.94 − 1.81 (m, 2H), 1.62 (s, 3H) ppm; ^{13}C NMR, major conformer (100 MHz, $CDCl_3$) δ 207.0, 169.4, 145.5, 136.6, 128.5, 127.9, 126.6, 124.5, 71.6, 51.9, 46.5, 40.1, 38.8, 35.2, 24.8, 17.4 ppm; ESIMS *m/z* 287.0 ($M+H^+$), 304.0 ($M+H_2O^+$). **3.42**: IR (neat) 3085, 3057, 3023, 2949, 2936, 2864, 2848, 1698, 1598, 1444, 1433, 1280.2, 1252, 1236, 1213, 1156, 1139, 1100, 1076, 1054, 890, 859, 846 cm^{-1}; ^1H NMR (300 MHz, $CDCl_3$) δ 7.34 − 7.27 (m, 4H), 7.22 − 7.14 (m, 1H), 4.88 (d, J = 10.5 Hz, 1H), 4.42 (dd, J = 10.5, 6.3 Hz, 1H), 3.82 (d, J = 0.6 Hz, 3H), 3.67 − 3.62 (m, 1H), 3.61

− 3.52 (m, 1H), 2.51 − 2.26 (m, 3H), 2.25 − 2.01 (m, 3H), 1.74 (s, 3H), -0.03 (d, J = 0.9 Hz, 9H) ppm; ^{13}C NMR (75 MHz, $CDCl_3$) δ 171.9, 166.8, 146.0, 137.9, 128.0, 126.9, 125.6, 125.3, 120.5, 51.7, 43.8, 39.3, 32.3, 28.2, 22.7, 17.1, 0.7 ppm; ESIMS *m/z* 287.1 ($M-TMS+H^+$), 358.9 ($M+H^+$).

General Procedure for Tebbe Olefination of β-Keto Esters:

To a degassed solution of β-keto ester (azeotropically dried with toluene x 3) in THF/pyridine (5:1, 0.02 M) at 0 °C was added Tebbe reagent (Aldrich, 0.5M in toluene, 1 eq). The deep orange solution was warmed to rt. If the reaction was incomplete by TLC, the solution was cooled back to 0 °C and more Tebbe reagent (0.5M in toluene, 1 eq) was added. This cooling-adding-warming process was repeated until the starting material was completely consumed, generally within 1 h. The brown solution was diluted with Et_2O to a volume of ~5 mL and cooled to 0 °C. MeOH (1 mL) was added dropwise, generating a creamy orange/red suspension. The quenched mixture was vacuum filtered through Celite and rinsed through with liberal amounts of Et_2O. The orange filtrate was washed with brine (5 mL). The organic layer was dried over Na_2SO_4, filtered, and concentrated under reduced pressure to an oily orange residue. Pure *exo*-olefin ester was secured by FCC (Et_2O/pentane gradual solvent gradient).

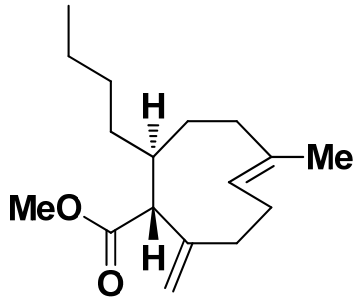

3.43

***n*-Butyl *exo*-olefin (3.43):** Following the general Tebbe olefination procedure, compound **3.43** was obtained as a colorless amorphous solid in 85% yield (0.0037 g). IR (thin film) 2954, 2922, 2852, 1737, 1659, 1631, 1552, 1451, 1384, 1148 cm^{-1}; 5.4:1 conformational equilibrium (C_6D_6, 25 °C); ^1H NMR, major conformer (500 MHz, C_6D_6) δ 5.38 (dd, J = 11.7, 3.3 Hz, 1H), 4.98 (s, 1H), 4.84 (s, 1H), 3.32 (s, 3H), 2.89 (d, J = 10.5 Hz, 1H), 2.48 (tdd, J = 7.0, 5.3, 1.8 Hz, 1H), 2.32 − 2.21 (m, 2H), 2.19 (br d, J = 12.5 Hz, 1H), 2.15 − 2.08 (m, 1H), 1.99 − 1.92 (m, 2H), 1.53 (s, 3H), 1.49 − 1.15 (m, 8H), 0.95 − 0.86 (m, 3H) ppm; ^{13}C NMR, major conformer (125 MHz, C_6D_6) δ 173.8, 146.3, 135.5, 124.9, 118.6, 63.4, 53.3, 51.0, 39.2, 35.7, 32.5, 32.0, 29.7, 29.3, 23.4, 18.6, 14.3 ppm; ESIMS *m/z* 265.1 ($M+H^+$).

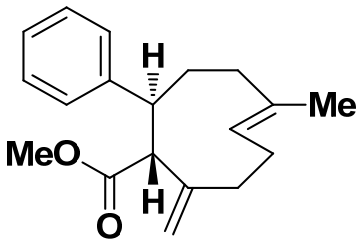

3.44

Phenyl *exo*-olefin (3.44): Following the general Tebbe olefination procedure, compound **3.44** was obtained as a colorless oil in 86% yield (0.0102 g). IR (neat) 3062, 3027, 2975,

2928, 2857, 1734, 1449, 1433, 1324, 1199, 1163, 1145, 892, 757, 701 cm^{-1}; 6.3:1 conformational equilibrium (C_6D_6, 25 °C); ^1H NMR, major conformer (300 MHz, C_6D_6) δ 7.21 − 7.10 (m, 4H), 7.08 − 6.98 (m, 1H), 5.47 (dd, J = 12.0, 3.6 Hz, 1H), 5.03 (s, 1H), 4.84 (s, 1H), 3.37 (d, J = 11.4 Hz, 1H), 3.29 − 3.19 (m, 1H), 2.94 (s, 3H), 2.62 − 2.49 (m, 1H), 2.28 (td, J = 12.0, 4.8 Hz, 1H), 2.17 (br d, J = 14.4 Hz, 1H), 1.95 (td, J = 12.3, 3.0 Hz, 1H), 1.85 − 1.76 (m, 1H), 1.72 − 1.61 (m, 1H), 1.49 (s, 3H), 1.26 (dd, J = 5.3, 2.5 Hz, 1H), 1.09 (t, J = 7.1 Hz, 1H) ppm; ^{13}C NMR, major conformer (125 MHz, $CDCl_3$) δ 172.9, 147.4, 145.2, 135.6, 128.4, 128.0, 126.1, 124.9, 119.8, 64.9, 51.3, 45.9, 40.0, 36.0, 31.5, 29.0, 18.6 ppm; ESIMS *m/z* 285.0 ($M+H^+$).

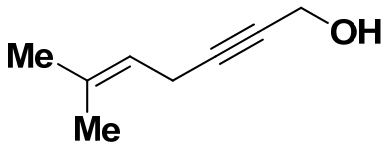

3.49

Propargyl alcohol (3.49): To a vigorously stirring solution of prenyl chloride (5.26 mL, 44.4 mmol) in bulk DMF (29.6 mL) was added propargyl alcohol (1.77 mL, 29.6 mmol), Na_2SO_3 (3.80 g, 29.6 mmol), CuI (Riedel-de Haën, 0.563 g, 2.96 mmol), and K_2CO_3 (4.09 g, 29.6 mmol). DBU (30 drops from a pipette) was then added, turning the light yellow suspension orange. The mixture was warmed to 30 °C, at which point it reverted back to a yellow color. Within 24 h it had turned into a green suspension. The reaction mixture was poured into water (150 mL) and extracted with 10% DCM/hexane (4 x 25 mL). The combined yellow organic extracts were washed with brine (5 mL), dried over Na_2SO_4, vacuum filtered, and concentrated under reduced pressure. Residual DMF was distilled off at 75 ˚C on a rotovap. The brown oily residue was purified by FCC (0 to 17%

EtOAc/hexane), furnishing propargyl alcohol **3.49** (3.13 g, 85%) as a colorless oil. This product was partially characterized in a monoterpene total synthesis.[6] IR (neat) 3338, 3036, 2971, 2929, 2871, 1448, 1377, 1288, 1227, 1136, 1094, 1012, 669 cm^{-1}; ^{1}H NMR (500 MHz, $CDCl_3$) δ 5.23 − 5.15 (m, 1H), 4.29 − 4.24 (m, 2H), 2.93 (d, J = 5.5 Hz, 2H), 1.72 (s, 3H), 1.64 (s, 3H), 1.63 − 1.54 (m, 1H) ppm; ^{13}C NMR (125 MHz, $CDCl_3$) δ 134.3, 118.9, 85.5, 78.1, 51.7, 25.8, 18.1, 17.9 ppm; ESIMS *m/z* 271.0 (dimer $M+Na^+$).

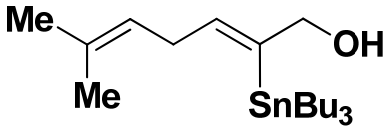

3.50

***Z* vinyl stannanol (3.50):** Bu_3SnH (0.444 mL, 1.61 mmol) and Et_3B (2.0 M in Et_2O, 0.840 mL, 1.70 mmol) were added in succession to a solution of propargyl alcohol **3.49** (0.100 g, 0.805 mmol) in toluene (16.1 mL) at 0 °C. After 5 h, the colorless solution was concentrated under reduced pressure. The crude colorless residue was purified by FCC (150 mesh, pore size 58Å, standard grade Brockmann I activated neutral aluminum oxide, 0 to 10% EtOAc/hexane), furnishing *Z* vinyl stannanol **3.50** (0.239 g, 72%) as a colorless oil. This product was stored as a frozen solution in benzene to prevent proteodestannylation. IR (neat) 3318, 2957, 2925, 2854, 1619, 1463, 1376, 1063, 994, 666 cm^{-1}; ^{1}H NMR (600 MHz, $CDCl_3$) δ 6.16 (tt, J = 124.3 (^{119}Sn), 7.1, 1.4 Hz, 1H), 5.07 (tp, J = 6.6, 1.2 Hz, 1H), 4.18 (dd, J = 39.2 (^{119}Sn), 6.0, 1.4 Hz, 2H), 2.74 (dd, J = 7.1, 7.1 Hz, 2H), 1.70 (d, J = 0.8 Hz, 3H), 1.64 (d, J = 0.8 Hz, 3H), 1.54 − 1.47 (m, 6H), 1.32 (sext, J = 7.4 Hz, 6H), 1.18 (t, J = 6.0 Hz, 1H), 0.99 − 0.95 (m, 6H), 0.89 (t, J = 7.4 Hz, 9H) ppm; ^{13}C

NMR (150 MHz, $CDCl_3$) δ 143.3, 140.3, 132.4, 122.3, 70.5, 33.3, 29.2, 27.4, 25.7, 17.9, 13.7, 10.2 ppm; ESIMS *m/z* 416.9 ($M+H^+$).

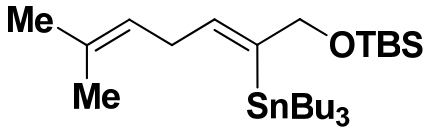

3.51

***Z* vinyl stannane (3.51):** To a solution of *Z* vinyl stannanol **3.50** (1.490 g, 3.59 mmol) in DCM (35.9 mL) at 0 °C was added imidazole (0.370 g, 5.38 mmol) and TBSCl (0.602 g, 3.91 mmol). The colorless suspension was gradually warmed to rt. After 5 min, deionized water (5 mL) was added dropwise. The organic layer was separated, and the aqueous layer was extracted with DCM (3 x 2 mL). The combined organics were dried over Na_2SO_4, filtered, and concentrated under reduced pressure. FCC (0 to 2% EtOAc/hexane) of the crude product provided *Z* vinyl stannane **3.51** (1.820 g, 96%) as a colorless oil. IR (neat) 2956, 2927, 2855, 1619, 1463, 1376, 1255, 1100, 1074, 1039, 836, 775, 667 cm^{-1}; ^1H NMR (300 MHz, $CDCl_3$) δ 6.13 (tt, J = 125.7 (^{119}Sn), 7.2, 1.5 Hz, 1H), 5.08 (tp, J = 6.9, 1.5 Hz, 1H), 4.20 (s, J = 33.3 (^{119}Sn) Hz, 2H), 2.73 (t, J = 6.3 Hz, 2H), 1.71 (s, 3H), 1.64 (s, 3H), 1.56 − 1.43 (m, 6H), 1.32 (sext, J = 7.5 Hz, 6H), 0.99 − 0.91 (m, 6H), 0.90 (s, 9H), 0.89 (t, J = 7.5 Hz, 9H), 0.05 (s, 6H) ppm; ^{13}C NMR (75 MHz, $CDCl_3$) δ 143.4, 138.1, 132.2, 123.0, 70.7, 33.5, 29.5, 27.7, 26.3, 25.9, 18.7, 18.2, 14.0, 10.6, 4.9 ppm; ESIMS *m/z* 531.1 ($M+H^+$).

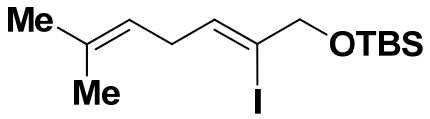

3.52

***Z* vinyl iodide (3.52):** To a solution of *Z* vinyl stannane **3.51** (azeotropically dried with toluene x 3, 0.484 g, 0.914 mmol) in DCM (18.3 mL) at 0 °C was added iodine chips (0.234 g, 0.914 mmol). The ice-water bath was removed and the solution was warmed to rt. After 20 min, the colorless reaction was quenched with 10% $Na_2S_2O_3$/sat. aq. $NaHCO_3$ (18.3 mL). The organic layer was separated, and the aqueous layer was extracted with DCM (3 x 5 mL). The combined organic layers were dried over Na_2SO_4, filtered, and concentrated under reduced pressure to a pale yellow oily residue. The crude product was purified by FCC (0 to 2% EtOAc/hexane), furnishing *Z* vinyl iodide **3.52** (0.257 g, 77%) as a colorless oil. This product undergoes gradual proteodehalogenation even when stored as a frozen solution in benzene. IR (neat) 2955, 2928, 2885, 2856, 1648, 1471, 1462, 1255, 1119, 1046, 838, 814, 777 cm^{-1}; ^1H NMR (300 MHz, $CDCl_3$) δ 5.88 (tt, J = 6.6, 1.5 Hz, 1H), 5.14 (tp, J = 7.2, 1.2 Hz, 1H), 4.26 (q, J = 1.2 Hz, 2H), 2.88 (t, J = 7.2 Hz, 2H), 1.71 (d, J = 0.9 Hz, 3H), 1.67 (s, 3H), 0.93 (s, 9H), 0.10 (s, 6H) ppm; ^{13}C NMR (100 MHz, $CDCl_3$) δ 133.6, 133.1, 120.5, 107.3, 71.8, 35.1, 26.2, 25.9, 18.7, 18.4, -4.9 ppm; ESIMS *m/z* 366.9 ($M+H^+$), 383.8 ($M+H_2O^+$).

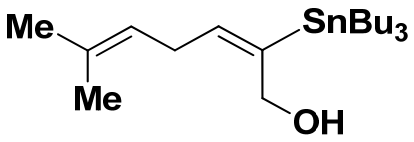

3.53

***E* vinyl stannanol (3.53):** To a degassed solution of propargyl alcohol **3.49** (1.000 g, 8.05 mmol) and Bu_3SnH (3.33 mL, 12.2 mmol) in bulk THF (81 mL) at 0 °C was added bright yellow $Pd(PPh_3)_4$ (Strem, 0.940 g, 0.805 mmol, weighed out under an inert atmosphere of argon and transferred with minimal exposure to air). The yellow solution was gradually warmed to rt, turning black. After 12 h, the solution was concentrated under reduced pressure to a dark brown oily residue. Purification by FCC (150 mesh, pore size 58Å, standard grade Brockmann I activated neutral aluminum oxide, 0 to 17% EtOAc/hexane, slow increase in solvent gradient) furnished *E* vinyl stannanol **3.53** (1.900 g, 57%) as a pale yellow oil. IR (neat) 3425, 2956, 2924, 2854, 1607, 1463, 1456, 1376, 1024, 665 cm^{-1}; ^1H NMR (400 MHz, C_6D_6) δ 5.72 (tt, J = 70.0 (^{119}Sn), 6.8, 2.0 Hz, 1H), 5.27 − 5.19 (m, 1H), 4.25 − 4.20 (m, J = 37.2 (^{119}Sn) Hz, 2H), 2.75 (t, J = 6.4 Hz, 2H), 1.72 − 1.63 (m, 6H), 1.62 (s, 3H), 1.53 (s, 3H), 1.42 (sext, J = 7.6 Hz, 6H), 1.30 (br d, J = 2.4 Hz, 1H), 1.10 − 1.03 (m, 6H), 0.96 (t, J = 7.2 Hz, 9H) ppm; ^{13}C NMR (75 MHz, C_6D_6) δ 147.0, 137.3, 131.9, 123.1, 63.8, 29.8, 29.4, 27.9, 25.8, 17.8, 14.1, 10.7 ppm; ESIMS *m/z* 416.9 ($M+H^+$).

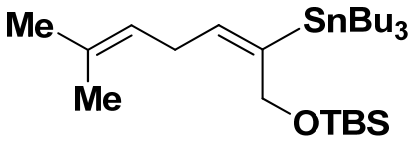

3.54

***E* vinyl stannane (3.54):** To a solution of *E* vinyl stannanol **3.53** (0.511 g, 1.23 mmol) in DCM (12.3 mL) at 0 °C was added imidazole (0.127 g, 1.85 mmol) and TBSCl (0.246 g, 1.60 mmol). The yellow suspension was gradually warmed to rt. After 30 min, deionized water (5 mL) was added dropwise. The organic layer was separated, and the aqueous layer was extracted with DCM (3 x 2 mL). The combined organics were dried over Na_2SO_4, filtered, and concentrated under reduced pressure to a crude yellow liquid. Purification by FCC (150 mesh, pore size 58Å, standard grade Brockmann I activated neutral aluminum oxide, 100% hexane) provided *E* vinyl stannane **3.54** (0.480 g, 74%) as a colorless oil. IR (neat) 2956, 2927, 2856, 1609, 1463, 1456, 1376, 1257, 1091, 1068, 855, 836, 780, 668 cm^{-1}; ^1H NMR (500 MHz, C_6D_6) δ 5.77 (tt, J = 70.0 (^{119}Sn), 6.5, 2.0 Hz, 1H), 5.30 − 5.23 (m, 1H), 4.58 − 4.55 (m, J = 35.5 (^{119}Sn) Hz, 2H), 2.83 (t, J = 7.0 Hz, 2H), 1.76 − 1.64 (m, 6H), 1.63 (s, 3H), 1.55 (s, 3H), 1.46 (sext, J = 7.5 Hz, 6H), 1.19 − 1.06 (m, 6H), 1.01 (s, 9H), 0.98 (t, J = 7.0 Hz, 9H), 0.14 (s, 6H) ppm; ^{13}C NMR (125 MHz, C_6D_6) δ 147.0, 136.8, 132.0, 123.1, 65.3, 29.9, 29.4, 28.0, 26.4, 25.8, 18.9, 17.8, 14.1, 10.8, -5.1 ppm; ESIMS *m/z* 531.1 ($M+H^+$).

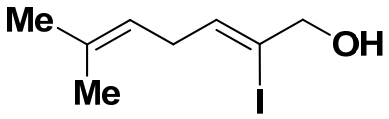

3.57

***Z* vinyl iodo-ol (3.57):** To a solution of *Z* vinyl stannanol **3.50** (azeotropically dried with toluene x 3, 0.800 g, 1.93 mmol) in DCM (18.3 mL) at 0 °C was added iodine chips (0.494 g, 1.93 mmol). The ice-water bath was removed and the solution was warmed to rt. After 20 min, another 0.1 equiv of iodine was added to drive the reaction to completion, turning the colorless solution dark purple. The reaction was quenched with 10% $Na_2S_2O_3$/sat. aq. $NaHCO_3$ (18.3 mL). The organic layer was separated, and the aqueous layer was extracted with DCM (3 x 5 mL). The combined organic layers were dried over Na_2SO_4, filtered, and concentrated under reduced pressure to a pale yellow oil. The crude product was purified by FCC (0 to 17% EtOAc/hexane), furnishing *Z* vinyl iodo-ol **3.57** (0.403 g, 83%) as a yellow oil. This product undergoes gradual proteodehalogenation even when stored as a frozen solution in benzene. IR (neat) 3333, 2969, 2913, 2856, 1636, 1446, 1376, 1079, 1003, 824, 668 cm^{-1}; ^1H NMR (500 MHz, $CDCl_3$) δ 5.87 (tt, J = 7.0, 1.0 Hz, 1H), 5.14 (tp, J = 7.0, 1.0 Hz, 1H), 4.25 (d, J = 5.5 Hz, 2H), 2.87 (t, J = 7.0 Hz, 2H), 2.03 (t, J = 6.0 Hz, 1H), 1.71 (d, J = 0.5 Hz, 3H), 1.67 (s, 3H) ppm; ^{13}C NMR (125 MHz, $CDCl_3$) δ 135.5, 134.1, 120.0, 107.9, 71.9, 35.3, 25.9, 18.4 ppm; ESIMS *m/z* 253.0 ($M+H^+$).

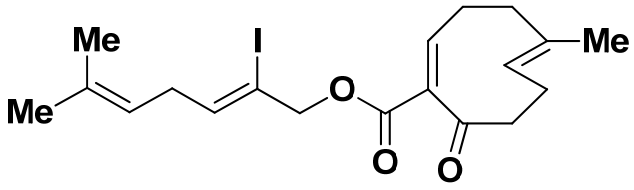

3.58

***Z* vinyl iodoester (3.58):** To a yellow solution of crude cyclononadienone-carboxylic acid **3.19** (theoretical 0.025 g, 0.129 mmol) in DCM (1.29 mL) at rt was added a pink solution of *Z* vinyl iodo-ol **3.57** (0.0324 g, 0.129 mmol) in DCM (2 mL), 4-dimethylaminopyridine (1.6 mg, 0.013 mmol), and 1-ethyl-3-(3-dimethylaminopropyl)carbodiimide (25.8 uL, 0.142 mmol). Addition of another 0.5 equiv of **3.57** and 1.0 equiv of EDC was required to push the reaction to completion. After 15 min, deionized water (3 mL) was added, and the organic layer was separated. The aqueous layer was extracted with DCM (3 x 1 mL). The combined organic layers were washed with minimal brine (0.5 mL), dried over Na_2SO_4, filtered, and concentrated under reduced pressure. Purification of the crude residue by FCC (0 to 17% Et_2O/pentane) furnished *Z* vinyl iodoester **3.58** (0.038 g, 69% over 2 steps) as a colorless oil. IR (neat) 2931, 2858, 1727, 1700, 1451, 1375, 1264, 1235, 1223, 1200, 1176, 1160, 1030, 1011 cm^{-1}; ^1H NMR (500 MHz, $CDCl_3$) δ 6.97 (t, J = 9.0 Hz, 1H), 5.92 (t, J = 6.5 Hz, 1H), 5.44 (dd, J = 12.5, 2.0 Hz, 1H), 5.13 (tp, J = 7.0, 1.5 Hz, 1H), 4.98 (d, J = 13.0 Hz, 1H), 4.80 (d, J = 12.5 Hz, 1H), 3.19 (q, J = 8.5 Hz, 1H), 2.87 (t, J = 7.0 Hz, 2H), 2.71 (dq, J = 12.0, 7.0 Hz, 1H), 2.52 (t, J = 9.0 Hz, 1H), 2.47 − 2.38 (m, 1H), 2.37 − 2.27 (m, 1H), 2.23 − 2.14 (m, 2H), 1.84 (t, J = 11.5 Hz, 1H), 1.72 (s, 3H), 1.67 (s, 3H), 1.61 (s, 3H) ppm; ^{13}C NMR (125 MHz, $CDCl_3$) δ 204.1, 164.2, 145.1, 140.4, 140.0, 135.0, 134.5, 127.7, 119.5, 98.6, 72.9, 44.6, 36.2, 35.6, 26.1, 25.9, 25.5, 18.4, 16.8 ppm; ESIMS *m/z* 451.0 ($M+Na^+$).

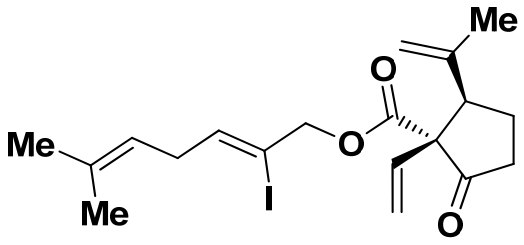

3.59

Cyclopentanone (3.59): To freshly activated 4Å powdered molecular sieves was added DMF (2.8 mL). The solvent was gently swirled and degassed with dry argon for 30 min. After the sieves fully settled to the bottom of the flask, 1 mL of DMF was syringed out and stored under dry argon for future transfer of starting material. To the 1.8 mL of DMF was added chromium dichloride (Aldrich 95%, 0.0181 g, 0.140 mmol) and nickel dichloride (Aldrich 98%, 0.2 mg, 1.40 umol) under an inert atmosphere of dry argon. To this light green suspension at rt was added dropwise a solution of *Z* vinyl iodoester **3.58** (0.012 g, 0.028 mmol, azeotropically dried with toluene x 3) in DMF (1 mL). The suspension was heated to 100 °C, changing from light green to dark green. After 12 h, the mixture was cooled to 0 °C, then to it was added sat. aq. NH_4Cl (3 mL). The suspension was vacuum filtered through Celite and rinsed through with liberal amounts of Et_2O. The organic layer was separated, and the aqueous layer was extracted with Et_2O (3 x 2 mL). The combined organic layers were washed with brine (2 mL), dried over Na_2SO_4, filtered, and concentrated under reduced pressure to a crude yellow oil in trace DMF. Purification by FCC (0 to 10% Et_2O/pentane) furnished cyclopentanone **3.59** (0.0065 g, 54%) as a colorless oil. This structure was assigned by analogy to a reported product.[7] IR (neat) 3087, 2968, 2917, 1754, 1732, 1644, 1446, 1383, 1232, 1207, 1142, 1095, 1005 cm^{-1}; ^1H NMR (500 MHz, $CDCl_3$) δ 5.94 (t, J = 7.0 Hz, 1H), 5.78 (dd, J = 11.0, 7.0 Hz, 1H), 5.38 (d, J = 11.0 Hz, 1H), 5.13 (d, J = 17.5 Hz, 1H), 5.12 (tp, J = 6.0, 1.5 Hz, 1H), 4.99 (t, J = 1.0 Hz,

1H), 4.91 (d, J = 12.5 Hz, 1H), 4.80 (d, J = 13.0 Hz, 2H), 3.49 (dd, J = 12.0, 5.5 Hz, 1H), 2.86 (t, J = 6.5 Hz, 2H), 2.47 (dd, J = 10.0, 4.5 Hz, 2H), 2.17 − 2.08 (m, 1H), 1.99 − 1.88 (m, 1H), 1.73 (s, 3H), 1.71 (s, 3H), 1.67 (s, 3H) ppm; ^{13}C NMR (125 MHz, $CDCl_3$) δ 212.2, 170.8, 142.6, 140.2, 134.4, 130.1, 120.4, 119.5, 113.6, 98.4, 73.3, 66.4, 52.1, 37.8, 35.6, 25.9, 23.8, 23.4, 18.4 ppm; ESIMS *m/z* 428.6 ($M+H^+$), 445.8 ($M+H_2O^+$).

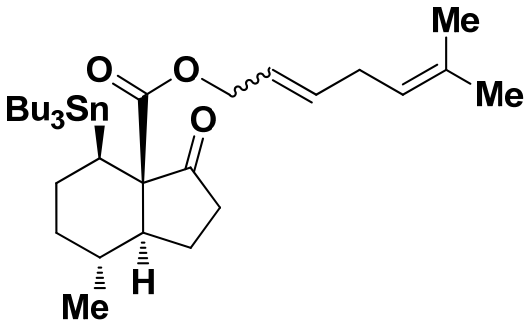

3.60

Steroidal allylic esters (3.60): Bu_3SnH (11.6 uL, 0.042 mmol) and Et_3B (2.0 M in Et_2O, 1.0 uL, 2.01 umol) were added in succession to a solution of *Z* vinyl iodoester **3.58** (0.0086 g, 0.020 mmol, azeotropically dried with toluene x 3) in toluene (3 mL) at -78 °C. After 15 min, the colorless suspension was warmed to rt, then the resulting solution was concentrated under reduced pressure. The crude product was purified by FCC (loaded with pentane, 0 to 2% Et_2O/pentane), furnishing steroidal allylic esters **3.60** (0.0108 g, 91%, 4.0:1 *E*/*Z* ratio) as a colorless oil. These structures were determined by extensive 2D NMR analysis. IR (neat) 2955, 2918, 2871, 2852, 1749, 1727, 1463, 1456, 1376, 1240, 1208, 1155, 668 cm^{-1}; Major *E* isomer: ^{1}H NMR (600 MHz, C_6D_6) δ 5.61 (dtt, J = 15.3, 6.4, 1.0 Hz, 1H), 5.54 (dtt, J = 15.3, 6.4, 1.3 Hz, 1H), 5.13 (tsept, J = 7.2, 1.4 Hz, 1H), 4.61 (ddq, J = 12.4, 6.4, 1.0 Hz, 1H), 4.41 (ddq, J = 12.4, 6.4, 1.0 Hz, 1H), 2.62 (t, J = 6.2 Hz, 2H), 2.40

(dd, J = 19.0, 9.2 Hz, 1H), 2.06 (dd, J = 49.5 (^{119}Sn), 14.1, 4.0 Hz, 1H), 1.95 − 1.91 (m, 1H), 1.90 (d, J = 19.0 Hz, 1H), 1.84 − 1.79 (m, 1H), 1.82 − 1.75 (m, 6H), 1.76 − 1.70 (m, 1H), 1.62 (d, J = 1.4 Hz, 3H), 1.51 (sext, J = 7.5 Hz, 6H), 1.50 − 1.45 (m, 1H), 1.46 (d, J = 1.4 Hz, 3H), 1.44 − 1.39 (m, 1H), 1.23 (qdd, J = 14.1, 12.8, 2.8 Hz, 1H), 1.18 − 1.14 (m, J = 52.5 (^{119}Sn) Hz, 6H), 1.03 (t, J = 7.4 Hz, 9H), 0.85 (qd, J = 12.8, 2.9 Hz, 1H), 0.70 (d, J = 6.0 Hz, 3H), 0.70 − 0.63 (m, 1H) ppm; ^{13}C NMR (150 MHz, C_6D_6) δ 214.7, 172.8, 135.7, 133.1, 123.4, 121.4, 66.0, 65.2, 50.1, 35.5, 34.7, 33.2, 31.2, 29.9, 28.2, 27.9, 25.8, 25.6, 22.0, 21.1, 17.5, 14.0, 10.5 ppm; ESIMS *m/z* 617.1 ($M+Na^+$).

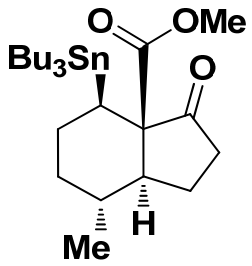

3.61

Steroidal methyl ester (3.61): Bu_3SnH (9.9 uL, 0.036 mmol) and Et_3B (2.0 M in Et_2O, 1.6 uL, 3.27 umol) were added in succession to a solution of cyclononadienone-carboxylate-methyl ester **3.6** (0.0068 g, 0.033 mmol, azeotropically dried with toluene x 3) in toluene (5.4 mL) at -78 °C. Addition of another 0.5 equiv of Bu_3SnH and 0.1 equiv of Et_3B was required to push the reaction to completion. After 5 min, the colorless suspension was warmed to rt, then the resulting solution was concentrated under reduced pressure. The crude product was purified by FCC (loaded with pentane, 0 to 2% Et_2O/pentane), furnishing steroidal methyl ester **3.61** (0.0152 g, 93%) as a colorless oil. The relative stereochemistry of this product was assigned by analogy to **3.60**.

IR (neat) 2954, 2919, 2871, 2851, 1750, 1730, 1463, 1243, 1225, 1214, 1158, 668 cm^{-1}; ^{1}H NMR (500 MHz, C_6D_6) δ 3.31 (s, 3H), 2.31 (dd, J = 19.5, 9.5 Hz, 1H), 2.00 (dd, J = 50.0 (^{119}Sn), 14.0, 4.0 Hz, 1H), 1.88 (q, J = 9.5 Hz, 1H), 1.86 − 1.82 (m, 1H), 1.81 − 1.77 (m, 1H), 1.78 − 1.71 (m, 6H), 1.72 − 1.66 (m, 1H), 1.69 − 1.61 (m, 1H), 1.48 (sext, J = 7.5 Hz, 6H), 1.44 − 1.37 (m, 1H), 1.20 (qd, J = 13.5, 2.5 Hz, 1H), 1.14 − 1.09 (m, J = 51.0 (^{119}Sn) Hz, 6H), 1.01 (t, J = 7.0 Hz, 9H), 0.84 (qd, J = 12.0, 2.5 Hz, 1H), 0.71 (d, J = 6.0 Hz, 3H), 0.70 − 0.59 (m, 1H) ppm; ^{13}C NMR (125 MHz, C_6D_6) δ 214.8, 173.6, 65.1, 51.8, 50.1, 35.6, 34.8, 33.2, 29.9, 28.2, 27.9, 26.1, 22.1, 21.2, 14.1, 10.4 ppm; ESIMS *m/z* 523.2 ($M+Na^+$).

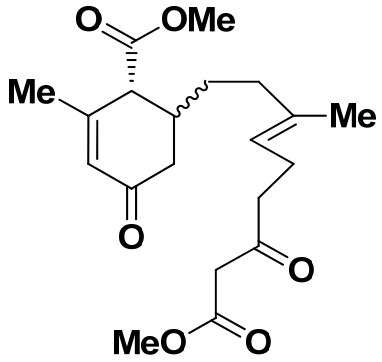

3.63

Hagemann's esters (3.63): To a solution of cyclononadienone-carboxylate-methyl ester **3.6** (0.017 g, 0.082 mmol) in methyl acetoacetate (0.41 mL, 3.80 mmol) at rt was added triethylamine (11.5 uL, 0.082 mmol) and $LiClO_4$ (0.0101 g, 0.090 mmol). After 36 h, the pale yellow suspension was diluted with Et_2O (4 mL) and washed with deionized water (0.5 mL). The organic layer was dried over Na_2SO_4, filtered, and concentrated under reduced pressure to a crude pale yellow oil. Purification by FCC (0 to 60% Et_2O/pentane) provided Hagemann's esters **3.63** (0.007 g, 24%, 2:1 *trans*/*cis* ratio) as a colorless oil. These structures were determined by extensive 2D NMR analysis. IR (neat) 2953, 2918,

2850, 1737, 1732, 1716, 1668, 1435, 1383, 1315, 1248, 1198, 1168 cm^{-1}; Major *trans* isomer: ^{1}H NMR (600 MHz, C_6D_6) δ 5.92 (app p, J = 1.5, 1.3 Hz, 1H), 4.95 (tq, J = 7.1, 1.4 Hz, 1H), 3.29 (s, 3H), 3.27 (s, 3H), 2.97 (d, J = 3.2 Hz, 2H), 2.76 (app d, J = 6.9, 1.3, 1.0 Hz, 1H), 2.60 (dd, J = 16.3, 4.5 Hz, 1H), 2.31 − 2.26 (m, 1H), 2.15 (app q, J = 8.0, 7.1, 6.8 Hz, 2H), 2.11 − 2.07 (m, 2H), 1.89 (dd, J = 16.3, 8.9 Hz, 1H), 1.86 − 1.77 (m, 1H), 1.73 − 1.66 (m, 1H), 1.51 (dd, J = 1.5, 1.0 Hz, 3H), 1.40 (d, J = 1.4 Hz, 3H), 1.40 − 1.29 (m, 1H), 1.20 − 1.12 (m, 1H) ppm; ^{13}C NMR (150 MHz, C_6D_6) δ 201.0, 196.0, 172.1, 167.4, 154.1, 135.3, 128.6, 123.7, 52.6, 51.6, 51.6, 48.9, 42.5, 40.4, 37.2, 36.5, 31.8, 22.4, 22.3, 15.6 ppm; Minor *cis* isomer: ^{1}H NMR (600 MHz, C_6D_6) δ 5.97 (s, 1H), 5.05 − 5.01 (m, 1H), 3.28 (s, 3H), 3.27 (s, 3H), 2.95 (s, 2H), 2.93 (d, J = 4.9 Hz, 1H), 2.67 (dd, J = 16.7, 13.8 Hz, 1H), 2.33 (dd, J = 16.7, 4.4 Hz, 1H), 2.16 − 2.12 (m, 2H), 2.11 − 2.07 (m, 2H), 1.87 − 1.83 (m, 1H), 1.85 − 1.80 (m, 1H), 1.83 − 1.78 (m, 1H), 1.49 (s, 3H), 1.44 (s, 3H), 1.40 − 1.31 (m, 1H), 1.27 − 1.18 (m, 1H) ppm; ^{13}C NMR (150 MHz, C_6D_6) δ 201.0, 197.1, 172.1, 167.4, 154.2, 135.6, 129.0, 123.7, 51.6, 51.3, 50.8, 48.9, 42.5, 39.3, 36.8, 36.8, 31.7, 22.8, 22.3, 15.7 ppm; HRMS-ESI *m/z* 365.19562 ($M+H^+$), 387.17760 ($M+Na^+$).

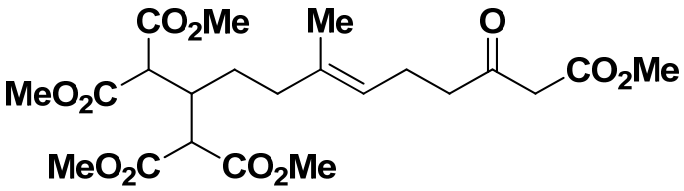

3.62

Pentaester (3.62): To a solution of cyclononadienone-carboxylate-methyl ester **3.6** (0.020 g, 0.096 mmol) in dimethyl malonate (0.48 mL, 4.19 mmol) at 0 °C was added triethylamine (1.4 uL, 9.60 umol) and $LiClO_4$ (0.0011 g, 9.60 umol). After 30 min, the

colorless suspension was diluted with Et_2O (4 mL) and washed with deionized water (0.5 mL). The organic layer was dried over Na_2SO_4, filtered, and concentrated under reduced pressure to a crude pale yellow oil. Purification by FCC (0 to 60% Et_2O/pentane) provided pentaester **3.62** (0.0225 g, 50%) as a colorless oil. This structure was determined by extensive 2D NMR analysis. IR (neat) 3000, 2955, 2850, 1755, 1738, 1732, 1715, 1435, 1409, 1312, 1247, 1155, 1025 cm^{-1}; ^1H NMR (600 MHz, C_6D_6) δ 5.09 (td, J = 6.5, 2.4 Hz, 1H), 4.15 (d, J = 5.5 Hz, 2H), 3.34 (s, 6H), 3.31 (s, 6H), 3.29 (s, 3H), 3.26 (p, J = 6.0 Hz, 1H), 2.99 (s, 2H), 2.16 (p, J = 6.5 Hz, 2H), 2.09 (t, J = 6.0 Hz, 4H), 2.02 − 1.96 (m, 2H), 1.52 (s, 3H) ppm; ^{13}C NMR (150 MHz, C_6D_6) δ 201.1, 169.1, 169.0, 167.4, 135.6, 124.1, 53.1, 52.0, 52.0, 51.6, 48.9, 42.6, 38.1, 37.8, 28.5, 22.3, 15.6 ppm; HRMS-ESI *m/z* 473.20164 ($M+H^+$).

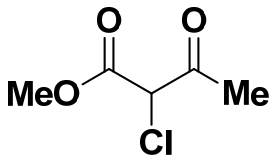

3.66

Methyl 2-chloro-3-oxobutanoate (3.66): Following a reported procedure,[8] this product was obtained as a colorless free-flowing liquid (1.48 g, quant). All characterization data were in accordance with the report. The corresponding enol was also observed by ^1H and ^{13}C NMR in $CDCl_3$.

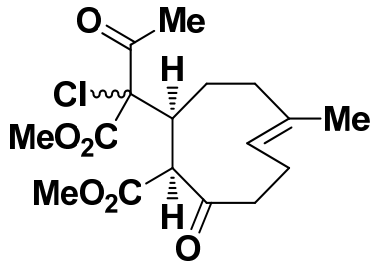

3.67

Diketone diester (3.67): To a solution of cyclononadienone-carboxylate-methyl ester **3.6** (52.0 mg, 0.250 mmol) in triethylamine (0.250 mL) in a vial at rt under argon was added methyl 2-chloro-3-oxobutanoate (**3.66**, 30.3 μL, 0.250 mmol) and $LiClO_4$ (8.4 mg, 0.075 mmol). The vial was sealed, and thorough stirring of the pale yellow suspension was maintained. An additional 40 μL of the chloride was added portionwise to the resulting orange suspension over the course of 21 h. The resulting dark green mixture was transferred to a small flask with EtOAc, then concentrated under reduced pressure to a crude dark green solid/oil. Purification by FCC (loaded with minimal MeOH, 0 to 17% EtOAc/hexane) provided diketone diester **3.67** (45.3 mg, 51%, 1:1 *dr*) as a colorless oil. The diastereomers are slightly separable by FCC. IR (neat) 2985, 2951, 2928, 2860, 1747, 1732, 1721, 1698, 1436, 1357, 1334, 1319, 1239, 1210, 1166, 1093, 1063 cm^{-1}; ^1H NMR, mixture (400 MHz, C_6D_6) δ 5.90 − 5.84 (m, 1H), 5.85 − 5.79 (m, 1H), 3.46 (s, 6H), 3.45 (s, 3H), 3.09 (s, 3H), 2.78 − 2.72 (m, 1H), 2.73 − 2.67 (m, 1H), 2.55 (d, J = 4.4 Hz, 1H), 2.52 (d, J = 4.0 Hz, 1H), 2.47 − 2.35 (m, 4H), 2.34 (s, 3H), 2.19 − 2.03 (m, 4H), 2.00 (s, 3H), 2.01 − 1.90 (m, 4H), 1.89 − 1.68 (m, 4H), 1.41 (s, 3H), 1.36 (s, 3H) ppm; ^{13}C NMR, mixture (125 MHz, C_6D_6) δ 200.6, 199.9, 199.8, 196.8, 169.5, 169.2, 169.2, 167.3, 136.9, 136.6, 123.3, 122.8, 54.5, 54.3, 52.6, 52.5, 52.5, 51.9, 49.6, 47.5, 41.1, 40.4, 39.2, 39.1, 38.6, 38.5, 30.9, 28.7, 23.1, 23.0, 22.4, 22.2, 17.1, 17.1 ppm; ESIMS *m/z* 322.8 ($M-Cl^-$).

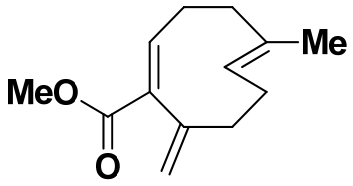

3.70

Triene (3.70): To a degassed solution of cyclononadienone-carboxylate-methyl ester **3.6** (0.0250 g, 0.120 mmol) in THF/pyridine (5:1, 4.80 mL) at 0 °C was added Tebbe reagent (Aldrich, 0.5M in toluene, 0.240 mL, 0.120 mmol). Portionwise addition of another 3.7 equiv of Tebbe reagent to the orange solution was required for complete consumption of starting material at 0 °C. After 1 h, the brown mixture was diluted with Et_2O (5 mL) and maintained at 0 °C. MeOH (1 mL) was added dropwise, generating a creamy orange/red suspension that solidified. After warming to rt, the liquified suspension was vacuum filtered through Celite and rinsed through with liberal amounts of Et_2O. The orange filtrate was concentrated under reduced pressure to an oily orange residue. Purification by FCC (0 to 8% Et_2O/pentane) provided triene **3.70** (0.0223 g, 90%) as a colorless oil with a distinct terpene scent. IR (neat) 3074, 3045, 2947, 2930, 2863, 1720, 1714, 1619, 1453, 1445, 1434, 1264, 1238, 1202, 1189, 1164, 1064, 1042, 905, 877, 772 cm^{-1}; ^1H NMR (300 MHz, $CDCl_3$) δ 6.82 (t, J = 8.5 Hz, 1H), 5.17 (d, J = 11.1 Hz, 1H), 4.98 (d, J = 2.1 Hz, 1H), 4.78 (d, J = 2.1 Hz, 1H), 3.74 (s, 3H), 2.66 − 2.53 (m, 1H), 2.49 − 2.26 (m, 3H), 2.28 − 2.19 (m, 1H), 2.16 − 2.02 (m, 2H), 1.76 (t, J = 11.5 Hz, 1H), 1.62 (s, 3H) ppm; ^{13}C NMR (75 MHz, $CDCl_3$) δ 168.0, 144.9, 140.4, 139.8, 134.0, 127.7, 116.2, 52.1, 39.7, 36.5, 28.8, 26.7, 17.5 ppm; ESIMS *m/z* 207.1 ($M+H^+$), 223.9 ($M+H_2O^+$).

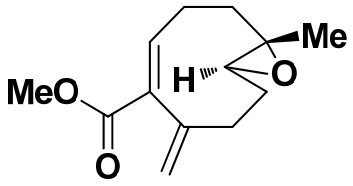

3.72

Epoxydiene (3.72): To a solution of triene **3.70** (0.0440 g, 0.213 mmol) in DCM (8.53 mL) at 0 °C was added *m*-CPBA (77%, 0.0478 g, 0.213 mmol) portionwise until complete conversion of starting material was observed by TLC. After 5 min, the colorless reaction was quenched by the dropwise addition of sat aq Na_2SO_3 (5 mL). The organic layer was separated, and the aqueous layer was extracted with DCM (3 x 5 mL). Deionized water (1 mL) was added to the biphasic mixtures to remove emulsions. The combined organic layers were washed sequentially with sat aq $NaHCO_3$ (3 mL) and brine (3 mL), dried over Na_2SO_4, filtered, and concentrated under reduced pressure, furnishing epoxydiene **3.72** (0.0470 g, 99% yield) as a colorless oil. IR (neat) 3075, 2948, 2933, 2866, 2850, 1716, 1625, 1454, 1435, 1268, 1244, 1217, 1064, 1043, 913, 774 cm^{-1}; ^1H NMR (500 MHz, C_6D_6) δ 6.83 (td, J = 8.5, 3.0 Hz, 1H), 4.87 (s, 1H), 4.78 (s, 1H), 3.41 − 3.39 (m, 3H), 2.75 (dt, J = 11.5, 2.0 Hz, 1H), 2.36 − 2.26 (m, 1H), 2.25 − 2.14 (m, 1H), 1.84 − 1.77 (m, 1H), 1.69 (br d, J = 9.5 Hz, 1H), 1.42 − 1.29 (m, 1H), 1.28 − 1.17 (m, 2H), 1.08 (d, J = 2.0 Hz, 3H), 0.96 − 0.75 (m, 1H) ppm; ^{13}C NMR (125 MHz, C_6D_6) δ 166.7, 144.3, 140.4, 130.9, 117.3, 60.9, 58.5, 51.5, 35.3, 31.4, 27.3, 22.8, 18.5 ppm; ESIMS *m/z* 223.0 ($M+H^+$).

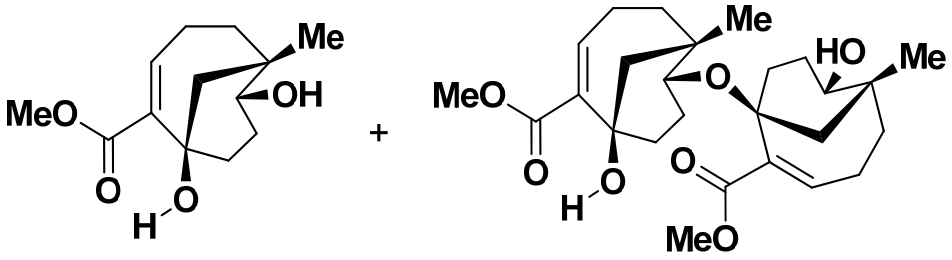

3.73 **3.74**

Florlide (3.73) and florlide dimer (3.74): To a solution of epoxydiene **3.72** (0.0200 g, 0.090 mmol) in DCM (13.2 mL) at rt was added deionized water (4.86 uL, 0.270 mmol). After stirring vigorously for 10 min, the solution was cooled to -78 ºC, then $BF_3{\cdot}Et_2O$ (purified, redistilled, 22.21 uL, 0.180 mmol) was added dropwise. After 5 min, sat aq $NaHCO_3$ (3 mL) was added to the colorless solution, and the resulting frozen mixture was melted upon warming to rt. The organic layer was separated, and the aqueous layer was extracted with DCM (3 x 10 mL). The combined organic layers were washed with brine (5 mL), dried over Na_2SO_4, filtered, and concentrated under reduced pressure to a colorless amorphous solid. The crude product was purified by FCC (50% EtOAc/benzene), furnishing florlide **3.73** (0.0162 g, 75%) and florlide dimer **3.74** (0.0040 g, 19%, 3.1:1 *dr*) as colorless solids. Florlide **3.73**: X-ray quality crystals were obtained via slow evaporation in $CDCl_3$ in a capped NMR tube at rt. See p. 347 for X-ray crystallography data. IR (thin film) 3411, 2970, 2946, 2862, 1681, 1409, 1384, 1270, 1251, 1233, 1207, 1103, 1065, 1027, 1016, 985, 955 cm^{-1}; ^1H NMR (300 MHz, $CDCl_3$) δ 7.29 (dd, J = 9.6, 3.6 Hz, 1H), 4.70 (br s, 1H), 3.75 (s, 3H), 3.37 (s, 1H), 2.53 (qt, J = 12.3, 4.5 Hz, 1H), 2.27 − 2.12 (m, 1H), 2.08 − 1.91 (m, 2H), 1.89 − 1.76 (m, 2H), 1.75 − 1.62 (m, 2H), 1.56 (br s, 1H), 1.50 − 1.35 (m, 2H), 1.06 (s, 3H) ppm; ^{13}C NMR (75 MHz, $CDCl_3$) δ 169.1, 145.3, 135.5, 74.0, 73.1, 52.2, 40.2, 37.2, 36.5, 31.8, 28.4, 27.1, 23.5 ppm; ESIMS *m/z* 240.9 ($M+H^+$), 258.1

($M+H_2O^+$). Florlide dimer **3.74**: X-ray quality crystals were obtained via slow evaporation in C_6D_6 in a loosely stoppered roundbottom flask at rt. See p. 370 for X-ray crystallography data. The structure of the major diastereomer was determined by comparing the ^1H NMR spectra of the diastereomeric mixture and the single X-ray crystal. IR (thin film) 3479, 2948, 2867, 1722, 1716, 1693, 1447, 1435, 1299, 1273, 1257, 1235, 1099, 1060, 1035, 998, 913, 732 cm^{-1}; Major diastereomer: ^1H NMR (600 MHz, $CDCl_3$) δ 7.25 (dd, J = 9.3, 3.3 Hz, 1H), 6.70 (dd, J = 9.0, 3.0 Hz, 1H), 4.50 (s, 1H), 3.74 (s, 3H), 3.73 (s, 3H), 3.38 (s, 1H), 3.26 (s, 1H), 1.05 (s, 3H), 0.94 (s, 3H) ppm; ^{13}C NMR (150 MHz, $CDCl_3$) δ 170.0, 169.1, 145.0, 138.6, 80.7, 74.0, 73.3, 71.4, 52.1, 51.9, 41.0, 38.6, 37.8, 37.4, 37.0, 36.8, 32.3, 29.5, 28.6, 27.4, 26.6, 26.0, 23.5, 23.3 ppm; ESIMS *m/z* 947.0 (dimer $M+Na^+$).

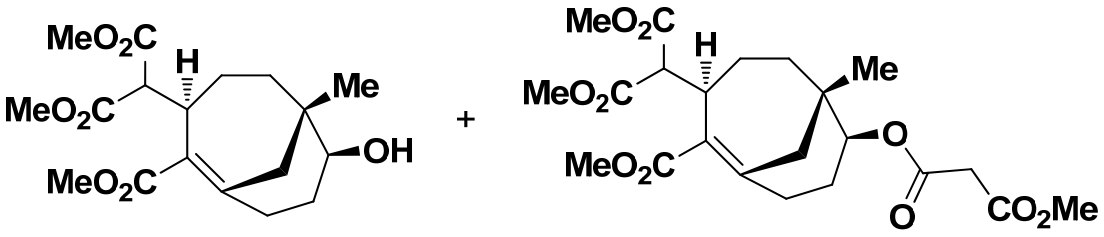

3.79 **3.81**

Bridgehead enone (3.79) and transesterificated bridgehead enone (3.81): To a suspension of florlide **3.73** (0.0184 g, 0.077 mmol) in dimethyl malonate (0.5 mL, 4.27 mmol) in an oversized septum-covered flask at rt was added triethylamine (0.108 mL, 0.766 mmol) and $LiClO_4$ (0.350 g, 3.13 mmol). The reaction slowly turned from a colorless free-flowing liquid to a cloudy viscous pale yellow gel with scattered bubbling. Evaporated triethylamine was replenished periodically (10 equiv portions). After 120 h, the mixture was diluted with DCM (10 mL) and washed with deionized water (3 x 1 mL). The organic

layer was dried over Na_2SO_4, filtered, and concentrated under reduced pressure to a crude pale yellow liquid. Purification by FCC (0 to 40% EtOAc/benzene) provided bridgehead enone **3.79** (0.0187 g, 69%) and transesterificated bridgehead enone **3.81** (0.0081 g, 23%) as colorless oils. The key to reproducibility of this reaction is effective homogenous stirring of the neat mixture and use of excess $LiClO_4$ (40 equiv optimal). Larger amounts of $LiClO_4$ were found to hinder stirring. These structures were confirmed by extensive 2D NMR analysis. Bridgehead enone **3.79**: IR (neat) 3543, 2952, 2927, 2868, 2850, 1755, 1738, 1733, 1712, 1699, 1634, 1435, 1302, 1248, 1216, 1152, 1014, 955 cm^{-1}; ^1H NMR (600 MHz, C_6D_6) δ 4.30 − 4.22 (m, 1H), 3.89 (d, J = 11.4 Hz, 1H), 3.52 (s, 3H), 3.32 (s, 3H), 3.30 (s, 3H), 3.06 (dp, J = 11.7, 2.7 Hz, 1H), 2.96 (app s, J = 3.3, 2.2, 1.0 Hz, 1H), 2.21 (dddd, J = 12.9, 11.7, 4.8, 2.8 Hz, 1H), 2.09 − 2.02 (m, 1H), 2.00 (d, J = 11.6 Hz, 1H), 1.76 (ddd, J = 11.6, 2.8, 1.0 Hz, 1H), 1.76 − 1.69 (m, 1H), 1.49 (ddt, J = 11.6, 4.8, 2.2 Hz, 1H), 1.22 − 1.14 (m, 2H), 0.90 − 0.84 (m, 1H), 0.69 (s, 3H), 0.67 (br s, 1H) ppm; ^{13}C NMR (150 MHz, C_6D_6) δ 169.9, 168.6, 168.4, 155.1, 123.9, 73.1, 57.6, 51.9, 51.9, 51.2, 42.4, 37.8, 37.6, 37.5, 32.5, 31.3, 24.2, 23.3 ppm; HRMS-ESI *m/z* 377.15707 ($M+Na^+$). Transesterificated bridgehead enone **3.81**: IR (neat) 2954, 2875, 2849, 1755, 1738, 1732, 1714, 1634, 1462, 1455, 1435, 1344, 1326, 1305, 1269, 1248, 1215, 1152, 1007 cm^{-1}; ^1H NMR (600 MHz, C_6D_6) δ 4.70 (app s, J = 3.3, 2.4 Hz, 1H), 4.25 − 4.18 (m, 1H), 3.85 (d, J = 11.3 Hz, 1H), 3.48 (s, 3H), 3.32 (s, 3H), 3.29 (s, 3H), 3.25 (s, 3H), 3.13 − 3.07 (m, 1H), 2.99 (d, J = 1.0 Hz, 2H), 2.10 (app td, J = 12.9, 12.5, 4.8 Hz, 1H), 1.98 − 1.92 (m, 1H), 1.86 − 1.82 (m, 1H), 1.85 (s, 2H), 1.74 − 1.67 (m, 1H), 1.16 − 1.08 (m, 1H), 1.12 − 1.05 (m, 1H), 0.87 − 0.82 (m, 1H), 0.66 (s, 3H) ppm; ^{13}C NMR (150 MHz, C_6D_6) δ 169.6, 168.5, 168.3,

166.6, 165.4, 153.4, 124.7, 76.5, 57.5, 52.0, 52.0, 51.7, 51.3, 41.4, 41.2, 38.4, 37.7, 34.2, 31.8, 31.7, 23.8, 23.0 ppm; HRMS-ESI *m/z* 455.19160 ($M+H^+$), 477.17354 ($M+Na^+$).

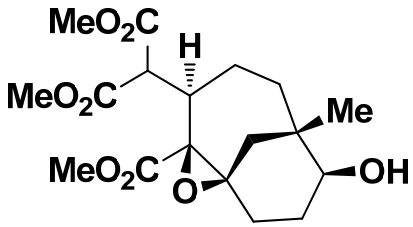

3.91

Bridgehead epoxide (3.91): To a solution of bridgehead enone **3.79** (0.0090 g, 0.025 mmol) in DCM (2.54 mL) at rt was added *m*-CPBA (77%, 0.0085 g, 0.038 mmol). After 1 h, the colorless reaction was quenched by the addition of sat aq Na_2SO_3 (1 mL). The organic layer was separated and the aqueous layer was extracted with DCM (3 x 1 mL). The combined organic layers were washed sequentially with sat aq $NaHCO_3$ (0.5 mL) and brine (0.5 mL), dried over Na_2SO_4, filtered, and concentrated under reduced pressure, furnishing bridgehead epoxide **3.91** (0.0070 g, 74% yield) as a colorless oil. IR (neat) 3542, 2955, 2920, 2872, 2851, 1755, 1747, 1738, 1732, 1716, 1673, 1463, 1440, 1384, 1259, 1151, 1088, 1035, 1016, 957, 796, 554, 501 cm^{-1}; ^1H NMR (500 MHz, C_6D_6) δ 4.07 − 3.98 (m, 1H), 3.73 (d, J = 12.0 Hz, 1H), 3.43 (s, 3H), 3.34 (s, 3H), 3.26 (s, 3H), 3.04 (s, 1H), 2.02 (qd, J = 12.5, 4.5 Hz, 1H), 2.00 − 1.92 (m, 1H), 1.91 − 1.83 (m, 1H), 1.47 − 1.26 (m, 4H), 1.27 − 1.15 (m, 1H), 0.97 (dd, J = 14.5, 6.5 Hz, 1H), 0.95 − 0.88 (m, 1H), 0.83 (app d, J = 13.0 Hz, 1H), 0.62 (s, 3H) ppm; ^{13}C NMR (125 MHz, C_6D_6) δ 172.8, 168.6, 168.4, 72.5, 68.1, 63.1, 55.8, 52.3, 52.1, 51.9, 42.2, 37.4, 35.6, 31.6, 29.8, 25.8, 24.0, 22.7 ppm; ESIMS *m/z* 388.0 ($M+H_2O^+$).

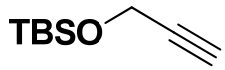

3.92

***Tert*-butyldimethyl(prop-2-yn-1-yloxy)silane (3.92):** Following a reported procedure,[9] this product was obtained as a pale yellow free-flowing liquid (13.75 g, 96%). All characterization data were in accordance with the report.

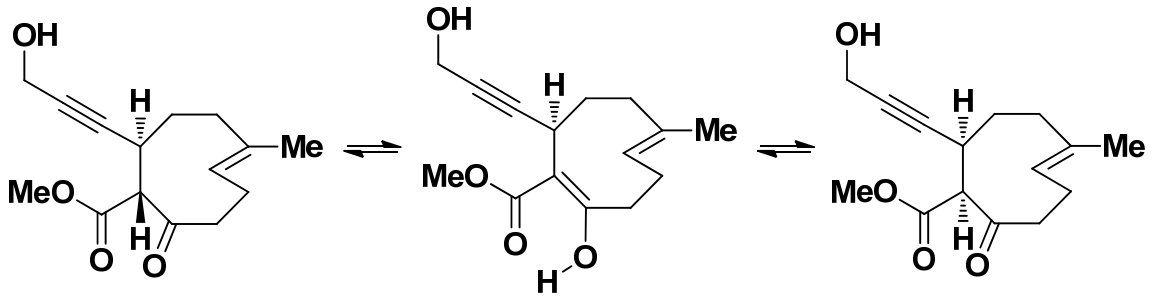

3.94 **3.95** **3.96**

Keto-enol propargyl alcohol (3.94, 3.95, and 3.96): A flame-dried roundbottom flask equipped with a magnetic stirbar was cooled under argon then charged with **3.92** (0.0282 g, 0.166 mmol, azeotropically dried with toluene x 3) and anhydrous hexane (0.5 mL). The solution was cooled to -78 °C, then *n*-BuLi (2.5M in hexanes, 61.8 uL, 0.155 mmol) was added dropwise, keeping the internal temperature less than 0 °C, and the colorless solution was stirred at 0 °C for 15 minutes. The solution was cooled back to -78 °C, then diethylaluminum chloride (1.0M in hexanes, 155 uL, 0.155 mmol) was added dropwise, keeping the internal temperature less than 0 °C, and the resulting pale yellow solution was stirred at 0 °C for 30 minutes. A solution of cyclononadienone-carboxylate-methyl ester **3.6** (0.0230 g, 0.110 mmol, azeotropically dried with toluene x 3) in hexane (1 mL) was added followed immediately by TMSCl (redistilled, 0.020 mL, 0.155 mmol). After 5 min,

the reaction was quenched at 0 °C with sat aq $NaHCO_3$ (1.1 mL). The mixture was warmed to rt and diluted with hexane (5 mL). The organic layer was separated, and the aqueous layer was extracted with hexane (2 x 1 mL). The combined organics were washed with brine (1 mL), dried over Na_2SO_4, filtered, and concentrated under reduced pressure to a colorless oil. The crude product mixture was dissolved in bulk THF (4.42 mL). To this solution at 0 °C was added TBAF (1M in THF, 0.331 mL, 0.331 mmol), and the resulting pale yellow solution was maintained at 0 °C for 30 min. Sat aq NH_4Cl (2 mL) was added, and the mixture was warmed to rt. The organic layer was separated, and the aqueous layer was extracted with Et_2O (3 x 2 mL). The combined organics were washed with brine (1 mL), dried over Na_2SO_4, filtered, and concentrated under reduced pressure to a colorless oil/solid. Purification by FCC (0 to 60% Et_2O/pentane) yielded keto-enol propargyl alcohol **3.94-3.96** (0.0190 g, 65% over 2 steps, 99% BORSM) as a colorless oil and recovered starting material **3.6** (0.0079 g, 34%). Keto-enol tautomerism and epimerization were observed by ^{1}H NMR. The enol form was present in the crude intermediate product before global deprotection. The *trans* epimer was assigned by analogy to **3.33**, and the concentration of this thermodynamic epimer increased logarithmically over time while the enol concentration remained constant. IR (neat) 3412, 2917, 2871, 2849, 1740, 1713, 1632, 1461, 1450, 1436, 1384, 1241, 1191, 1153, 1020, 730 cm^{-1}; *trans* epimer **3.94**: 4.1:1 conformational equilibrium ($CDCl_3$, 25 °C); ^{1}H NMR, major conformer (600 MHz, $CDCl_3$) δ 5.31 (dd, J = 9.0, 2.5 Hz, 1H), 4.20 (dd, J = 2.0, 0.5 Hz, 2H), 3.69 (s, 3H), 3.48 (d, J = 10.0 Hz, 1H), 1.37 (s, 3H), 1.55 (br s, 1H) ppm; *cis* epimer **3.96**: 3.1:1 conformational equilibrium ($CDCl_3$, 25 °C); ^{1}H NMR, major conformer (600 MHz, $CDCl_3$) δ 5.67 (dd, J = 9.0, 7.0 Hz, 1H), 4.24 (dd, J = 5.5, 1.8 Hz, 2H), 3.84 (s, 3H), 3.83 (d, J = 3.0 Hz, 1H), 3.38

− 3.34 (m, 1H), 1.78 (s, 3H), 1.40 (br s, 1H) ppm; enol **3.95**: 1 conformer: ^{1}H NMR (600 MHz, $CDCl_3$) δ 13.17 (s, 1H), 5.47 − 5.42 (m, 1H), 4.32 (dd, J = 2.0, 1.0 Hz, 2H), 3.72 (s, 3H), 3.40 (d, J = 9.0 Hz, 1H), 1.52 (s, 3H) ppm; ^{13}C NMR, mixture (150 MHz, $CDCl_3$): 205.2, 174.9, 173.8, 170.2, 169.0, 138.4, 137.1, 136.7, 127.0, 126.1, 124.9, 124.6, 105.0, 89.8, 89.7, 80.1, 74.3, 51.7, 51.5, 50.6, 39.4, 39.3, 37.3, 36.7, 35.2, 33.0, 28.6, 28.0, 26.1, 25.3, 23.1, 16.4 ppm; HRMS-ESI *m/z* 265.14351 ($M+H^+$), 287.12550 ($M+Na^+$).

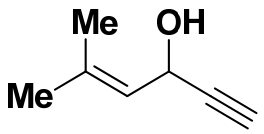

3.103

Allylic alcohol (3.103): This procedure was modified from the literature.[10] To a solution of 3-methylbut-2-enal (10.90 g, 125.7 mmol) in THF (251 mL) at -78 °C was added ethynylmagnesium bromide (0.5 M in THF, 277 mL, 138 mmol). The cream-colored suspension was warmed to 0 °C and became a light yellow solution. After 1 h, the reaction was quenched at 0 °C by dropwise addition of sat aq NH_4Cl (150 mL). The mixture was warmed to rt, then the organic layer was separated and the aqueous layer was extracted with EtOAc (3 x 50 mL). The combined organic layers were dried over Na_2SO_4, filtered, and concentrated under reduced pressure, furnishing allylic alcohol **3.103** (14.10 g, quant yield) as a dark yellow liquid. All characterization data were in accordance with the report.

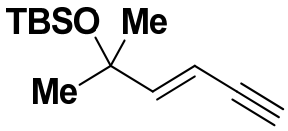

3.105

Enyne (3.105): To a light yellow solution of allylic alcohol **3.103** (1.000 g, 9.08 mmol, azeotropically dried with toluene x 3) in anhydrous DCM (49.9 mL) at rt was added $MoO_2(AcAc)_2$ (0.148 g, 0.454 mmol), generating an olive green then black solution. After 10 min, the solution of volatile tertiary alcohol was cooled to 0 °C. 2,6-lutidine (4.23 mL, 36.3 mmol) and TBSOTf (4.25 mL, 18.16 mmol) were added in succession with minimal gas evolution, and the black solution was warmed to rt. After 5 min, the reaction was quenched with sat aq $NaHCO_3$ (20 mL). The organic layer was separated and the aqueous layer was extracted with DCM (3 x 5 mL). The combined organic layers were washed with brine (10 mL) and dried over Na_2SO_4, turning from a brown to orange solution within 1 h. Filtration and concentration under reduced pressure (no high vacuum since the final product is somewhat volatile) gave a crude orange suspension. Purification by FCC (wide column, loaded with hexane, 100% hexane) furnished enyne **3.105** (1.332 g, 65%) as a colorless oil. The first reaction was monitored by taking an aliquot and co-spotting it on a TLC plate. The aliquot was then concentrated under high vacuum for 5 min, diluted back with DCM to the original volume, and co-spotted on the same TLC plate. Since the R_f values of the starting material and volatile intermediate are the same (R_f 0.4 in 17% EtOAc/hexane), the disappearance of this spot after high vacuum indicated complete conversion of starting material. IR (neat) 3316, 2976, 2958, 2930, 2888, 2858, 2105, 1472, 1463, 1379, 1361, 1255, 1235, 1167, 1152, 1044, 1006, 957, 891, 836, 806, 774, 640 cm^{-1}; ^1H NMR (300 MHz, $CDCl_3$) δ 6.29 (d, J = 15.6 Hz, 1H), 5.69 (dd, J = 15.6, 2.1 Hz, 1H),

2.86 (d, J = 2.1 Hz, 1H), 1.31 (s, 6H), 0.89 (s, 9H), 0.10 (s, 6H) ppm; ^{13}C NMR (125 MHz, $CDCl_3$) δ 154.0, 105.4, 82.6, 77.4, 73.4, 30.3, 26.1, 18.4, -1.9 ppm; ESIMS *m/z* 246.8 ($M+Na^+$).

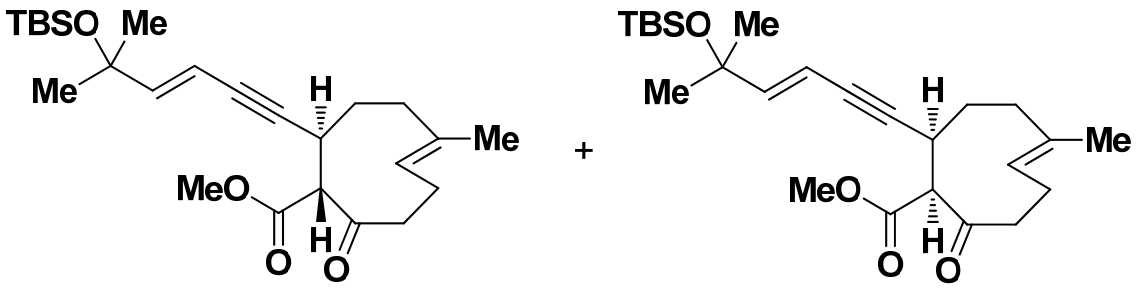

3.107 **3.108**

Enynyl *trans*-ketoester (3.107) and enynyl *cis*-ketoester (3.108): A flame-dried roundbottom flask equipped with a magnetic stirbar was cooled under argon then charged with enyne **3.105** (0.0548 g, 0.244 mmol, azeotropically dried with toluene x 3) and anhydrous hexane (0.69 mL). The solution was cooled to -78 °C, then *n*-BuLi (2.5M in hexanes, 92.0 uL, 0.229 mmol) was added dropwise, keeping the internal temperature less than 0 °C. To facilitate stirring, the viscous solution was then warmed to 0 °C. After 15 min, the colorless solution was cooled back to -78 °C, then diethylaluminum chloride (1.0M in hexanes, 229 uL, 0.229 mmol) was added dropwise, keeping the internal temperature less than 0 °C, and the resulting pale yellow solution was then stirred at 0 °C for 30 minutes. A solution of cyclononadienone-carboxylate-methyl ester **3.6** (0.0318 g, 0.153 mmol, azeotropically dried with toluene x 3) in hexane (1 mL) was added followed immediately by TMSCl (redistilled, 29.6 uL, 0.229 mmol). After 10 min, the reaction was quenched at 0 °C with sat aq $NaHCO_3$ (1.5 mL). The mixture was warmed to rt and diluted with hexane (5 mL). The organic layer was separated, and the aqueous layer was extracted

with hexane (2 x 1 mL). The combined organics were washed with brine (1 mL), dried over Na_2SO_4, filtered, and concentrated under reduced pressure to a colorless oil. Purification by FCC (0 to 10% EtOAc/hexane) furnished enynyl *trans*-ketoester **3.107** (0.0273 g, 41%) and enynyl *cis*-ketoester **3.108** (0.0266 g, 40%) as colorless oils. The TMS-enol ether byproduct hydrolyzed on the column. No epimerization of these products was observed by ^{1}H NMR ($CDCl_3$, 25 °C). **3.107** was obtained selectively by adding the enone solution to the alkynylalane solution at -78 °C, but no synthetically useful yields were achieved (< 20% with quant recovery of starting material). Enynyl *trans*-ketoester **3.107**: IR (neat) 2955, 2930, 2897, 2857, 1754, 1750, 1709, 1472, 1462, 1455, 1451, 1435, 1360, 1254, 1236, 1190, 1166, 1042, 836, 774 cm^{-1}; 2.3:1 conformational equilibrium ($CDCl_3$, 25 °C); ^{1}H NMR, major conformer (600 MHz, $CDCl_3$) δ 6.06 (d, J = 15.7 Hz, 1H), 5.62 (td, J = 15.7, 2.1 Hz, 1H), 5.37 (dd, J = 11.6, 4.6 Hz, 1H), 3.71 (d, J = 4.0 Hz, 3H), 3.48 (d, J = 10.0 Hz, 1H), 3.40 − 3.35 (m, 1H), 2.90 − 2.81 (m, 1H), 2.79 − 2.66 (m, 1H), 2.39 − 2.30 (m, 1H), 2.21 − 2.16 (m, 1H), 2.18 − 2.10 (m, 1H), 2.08 − 2.03 (m, 1H), 2.04 − 1.97 (m, 1H), 1.76 − 1.71 (m, 1H), 1.65 (s, 3H), 1.27 (d, J = 1.0 Hz, 6H), 0.87 (s, 9H), 0.07 (s, 6H) ppm; ^{13}C NMR, major conformer (150 MHz, $CDCl_3$) δ 205.5, 168.8, 151.1, 136.9, 124.3, 106.0, 90.5, 81.4, 73.1, 65.8, 52.4, 39.3, 37.5, 34.1, 32.4, 30.1, 25.8, 23.6, 18.1, 18.0, -2.1 ppm; ESIMS *m/z* 450.1 ($M+H_2O^+$), 455.3 ($M+Na^+$). Enynyl *cis*-ketoester **3.108**: IR (neat) 2953, 2930, 2897, 2857, 1755, 1751, 1733, 1712, 1699, 1472, 1462, 1455, 1435, 1384, 1379, 1360, 1253, 1237, 1201, 1169, 1041, 836, 774 cm^{-1}; 1.4:1 conformational equilibrium ($CDCl_3$, 25 °C); ^{1}H NMR, major conformer (600 MHz, THF-d_8) δ 6.06 (d, J = 15.8 Hz, 1H), 5.64 (dd, J = 15.8, 2.2 Hz, 1H), 5.50 (dd, J = 11.8, 3.9 Hz, 1H), 3.86 (d, J = 3.1 Hz, 1H), 3.59 (d, J = 8.5 Hz, 3H), 3.47 − 3.42 (m, 1H), 2.83 − 2.72 (m, 1H), 2.72 − 2.59 (m,

1H), 2.46 − 2.37 (m, 1H), 2.26 − 2.21 (m, 1H), 2.05 − 1.97 (m, 1H), 2.01 − 1.97 (m, 1H), 2.00 − 1.95 (m, 1H), 1.91 − 1.86 (m, 1H), 1.45 (s, 3H), 1.29 (d, J = 11.0 Hz, 6H), 0.89 (d, J = 1.5 Hz, 9H), 0.10 (d, J = 4.5 Hz, 6H) ppm; ^{13}C NMR (150 MHz, THF-d_8) δ 205.2, 169.3, 150.9, 137.0, 125.6, 107.8, 93.1, 80.4, 74.1, 65.9, 51.6, 42.8, 40.0, 32.4, 31.5, 30.5, 26.3, 25.4, 18.8, 17.7, -1.9 ppm; ESIMS *m/z* 449.8 ($M+H_2O^+$), 455.3 ($M+Na^+$).

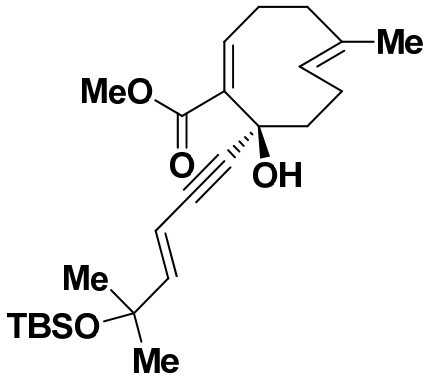

3.109

Enynyl alcohol (3.109): The preceding reaction was repeated on the same scale with the following modifications: the enone solution was added to the alkynylalane solution at -78 °C, TMSCl was not added, and the reaction was quenched at -78 °C. Purification of the crude product mixture by FCC (0 to 17% EtOAc/hexane) furnished enynyl *trans*-ketoester **3.107** (8.5 mg, 13%, 39% BORSM), recovered **3.6** (21.6 mg, 67%), and enynyl alcohol **3.109** (5.0 mg, 7%, 21% BORSM) as colorless oils. IR (neat) 3459, 2954, 2929, 2857, 1722, 1716, 1694, 1463, 1435, 1384, 1361, 1255, 1235, 1198, 1166, 1040, 996, 956, 836, 774 cm^{-1}; ^{1}H NMR (500 MHz, $CDCl_3$) δ 6.82 (dd, J = 10.5, 8.5 Hz, 1H), 6.23 (d, J = 16.0 Hz, 1H), 5.79 (d, J = 16.0 Hz, 1H), 5.06 (app d, J = 12.0 Hz, 1H), 4.58 (s, 1H), 3.79 (s, 3H), 3.05 (qd, J = 11.5, 1.5 Hz, 1H), 2.99 (sept, J = 6.5 Hz, 1H), 2.68 − 2.56 (m, 1H), 2.38 − 2.18

(m, 2H), 2.18 − 2.07 (m, 2H), 1.77 (d, J = 1.0 Hz, 3H), 1.73 − 1.64 (m, 1H), 1.30 (s, 6H), 0.89 (s, 9H), 0.09 (s, 6H) ppm; ^{13}C NMR (125 MHz, $CDCl_3$) δ 169.6, 152.5, 142.3, 137.6, 134.0, 127.6, 106.3, 90.2, 86.0, 73.5, 72.6, 52.5, 47.8, 34.5, 30.4, 28.0, 26.1, 25.7, 19.3, 18.4, -1.8 ppm; ESIMS *m/z* 455.2 ($M+Na^+$).

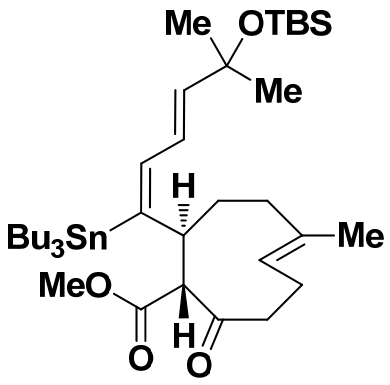

3.110

***E* vinylstannyl xeniolide (3.110):** To a degassed solution of enynyl *trans*-ketoester **3.107** (27.6 mg, 0.064 mmol) in hexane (1.5 mL) was added $Pd(PPh_3)_4$ (7.5 mg, 6.38 umol) under an inert atmosphere of argon. To the resulting yellow suspension at rt was added Bu_3SnH (34.9 uL, 0.128 mmol) dropwise. Upon vigorous stirring, the suspension became orange then dark brown. After 5 min, the reaction mixture was concentrated under reduced pressure. The crude brown oil was purified by FCC (150 mesh, pore size 58Å, standard grade Brockmann I activated neutral aluminum oxide, long plug, loaded with pentane, 0 to 1% EtOAc/pentane), furnishing *E* vinylstannyl xeniolide **3.110** (5.5 mg, 12%) as a colorless oil. This product undergoes proteodestannylation upon exposure to air. The undesired regioisomeric stannane (not shown) was the major product. IR (neat) 2955, 2926, 2870, 2855, 1738, 1733, 1704, 1699, 1463, 1455, 1435, 1384, 1360, 1251, 1165, 1146, 1040, 836, 774 cm^{-1}; ^{1}H NMR (300 MHz, $CDCl_3$) δ 6.79 (dd, J = 15.0, 10.8 Hz, 1H),

5.99 (d, J = 63.3 (^{119}Sn), 10.5 Hz, 1H), 5.72 (d, J = 14.7 Hz, 1H), 5.60 (app d, J = 11.4 Hz, 1H), 3.87 − 3.76 (m, 1H), 3.55 (s, 3H), 3.25 (td, J = 12.6, 3.9 Hz, 1H), 3.16 (d, J = 11.1 Hz, 1H), 2.74 (qd, J = 12.0, 4.8 Hz, 1H), 2.10 − 1.96 (m, 4H), 1.55 (s, 6H), 1.54 − 1.42 (m, 6H), 1.52 (s, 3H), 1.42 − 1.24 (m, 14H), 0.96 (s, 9H), 0.91 (t, J = 6.9 Hz, 9H), 0.08 (s, 6H) ppm; ^{13}C NMR (125 MHz, $CDCl_3$) δ 207.2, 169.3, 151.1, 143.8, 137.8, 136.8, 124.6, 121.9, 73.5, 72.1, 52.0, 43.7, 40.5, 38.3, 34.4, 31.0, 29.3, 27.7, 26.2, 25.6, 18.4, 17.5, 13.9, 11.4, -1.8 ppm; ESIMS *m/z* 747.3 ($M+Na^+$).

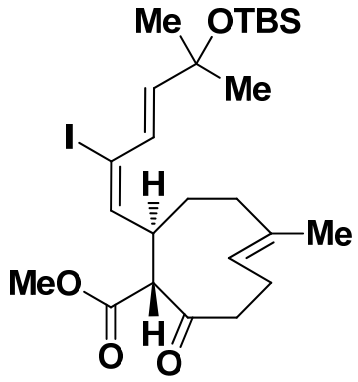

3.111

***E* vinyliodo xeniolide (3.111):** To a degassed solution of enynyl *trans*-ketoester **3.107** (15.0 mg, 0.035 mmol) in hexane (1.0 mL) was added $Pd(PPh_3)_4$ (4.1 mg, 3.47 umol) under an inert atmosphere of argon. To the resulting yellow suspension at rt was added Bu_3SnH (18.9 uL, 0.070 mmol) dropwise. Upon vigorous stirring, the suspension became orange then dark brown. After 5 min, the reaction mixture was diluted with hexane (1.0 mL) and cooled to 0 °C. Iodine chips (9.8 mg, 0.039 mmol) were added, and the suspension was warmed to rt. After 2 h, a purple solution had formed. The reaction was quenched with sat aq $Na_2S_2O_3$ (2 mL). The organic layer was separated, and the aqueous layer was extracted

with hexane (3 x 1 mL). The combined organic layers were dried over Na_2SO_4, filtered, and concentrated under reduced pressure to a crude colorless oil. Purification by FCC (long plug, loaded with pentane, 0 to 2% EtOAc/pentane) furnished *E* vinyliodo xeniolide **3.111** (11.7 mg, 60%) and the regioisomeric vinyl iodide (not shown, 4.4 mg, 23%) as colorless oils. Complete separation of the regioisomers is difficult to achieve. Both products undergo proteodehalogenation upon exposure to air. This structure was confirmed by extensive 2D NMR analysis. IR (neat) 2956, 2926, 2871, 2854, 1739, 1706, 1463, 1435, 1384, 1251, 1164, 1149, 1039, 836, 774, 668 cm^{-1}; 4.0:1 conformational equilibrium ($CDCl_3$, 25 °C); ^1H and ^{13}C NMR: see p. 746; HRMS-ESI *m/z* 583.17179 ($M+Na^+$).

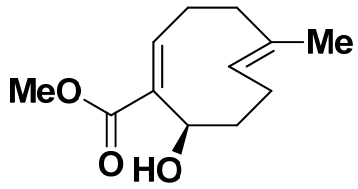

Ester-ol: A flame-dried roundbottom flask equipped with a magnetic stirbar was cooled under argon then charged with diethylaluminum chloride (1.0M in hexanes, 2.01 mL, 2.01 mmol) and cooled to 0 °C. Homogenous sodium acetylide (18% in xylene, 0.428 mL, 1.93 mmol) was added dropwise, and the resulting orange mixture was warmed to rt. After 2 h, it was cooled to -78 °C. To a separate solution of cyclononadienone-carboxylate-methyl ester **3.6** (0.0167 g, 0.080 mmol) in anhydrous hexane (0.80 mL) at -78 °C was added TMSCl (redistilled, 10.4 uL, 0.080 mmol). The alane solution was added portionwise (4 x 0.12 mL) to the enone solution, and reaction progress was monitored after each addition. When deemed complete as judged by TLC, the reaction was quenched at -78 °C with sat aq NH_4Cl (1 mL). After warming to rt, the organic layer was separated, and the aqueous layer

was extracted with EtOAc (3 x 1 mL). The combined organic layers were washed with brine (0.5 mL), dried over Na_2SO_4, filtered, and concentrated to a colorless oil. The crude product mixture was purified by FCC (17% EtOAc/pentane), furnishing the ester-ol (4.0 mg, 24%, 59% BORSM) and recovered **3.6** (10.0 mg, 60%) as colorless oils. IR (neat) 3523, 2934, 2866, 1692, 1457, 1436, 1384, 1294, 1274, 1256, 1218, 1195, 1169, 1103, 1028, 1014, 772 cm^{-1}; ^1H NMR (300 MHz, $CDCl_3$) δ 6.79 (t, J = 9.0 Hz, 1H), 5.07 (dd, J = 12.0, 2.4 Hz, 1H), 3.88 (t, J = 10.2 Hz, 1H), 3.79 (d, J = 0.9 Hz, 3H), 2.53 − 2.39 (m, 2H), 2.38 − 2.29 (m, 2H), 2.25 − 2.08 (m, 4H), 2.06 − 1.96 (m, 1H), 1.77 (s, 3H) ppm; ^{13}C NMR (125 MHz, $CDCl_3$) δ 168.7, 140.5, 138.2, 132.9, 129.6, 68.9, 52.1, 41.9, 35.5, 27.9, 25.4, 17.3 ppm; ESIMS *m/z* 228.1 ($M+H_2O^+$), 233.1 ($M+Na^+$).

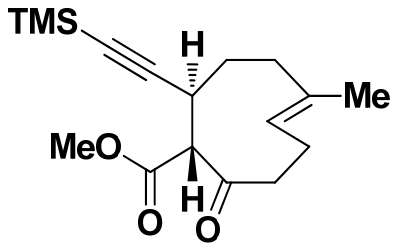

3.115

Silylalkynyl ketoester (3.115): A flame-dried 50 mL roundbottom flask equipped with a magnetic stirbar was cooled under argon. To it was added TMS-acetylene (1.95 mL, 13.78 mmol) and anhydrous hexane (10 mL). The stirring solution was cooled to 0 °C. A solution of *n*-butyllithium (2.5 M in hexanes, 5.51 mL, 13.78 mmol) was added dropwise, and the resulting white suspension was warmed to rt, stirred for 15 min, then cooled back to 0 °C. A solution of diethylaluminum chloride (1.0 M in heptane, 13.78 mL, 13.78 mmol) was added, precipitating out LiCl. The suspension was stirred for 15 min, then cooled to -78 °C.

The total volume of alane solution was 31.3 mL. Portions no more than 1.5 mL (1/20 of the total volume) would be transferred later via syringe. In a separate 50 mL roundbottom flask, enone **3.6** (143.5 mg, 0.689 mmol) and a stirbar were azeotropically dried with toluene (3 x 2 mL). Anhydrous hexane (6 mL) was added, and the solution was cooled to -78 °C. TMSCl (redistilled, 133 μL, 1.03 mmol) was added, followed by a portion of the alane solution. Additional portions of alane solution were added to the pale yellow suspension until complete consumption of starting material was observed by TLC. The reaction was quenched at -78 °C by the addition of sat aq NH_4Cl (10 mL). After warming to rt with vigorous stirring, the mixture was diluted with EtOAc (7 mL), and the organic layer was separated. Colorless gel byproduct was transferred into the separatory funnel with distilled water. The aqueous layer was extracted with EtOAc (3 x 3 mL). The combined organics were washed with brine (3 mL), dried over Na_2SO_4, filtered, and concentrated to a crude yellow oil. Purification by FCC (0 to 6% EtOAc/pentane) furnished silylalkynyl ketoester **3.115** (139 mg, 66%) as a colorless oil. Trace amounts of the 1,2-addition product (not shown) were also observed. IR (neat) 2955, 2938, 2857, 2170, 1748, 1707, 1449, 1435, 1250, 1194, 1166, 1150, 844 cm^{-1}; 2.8:1 conformational equilibrium ($CDCl_3$, 25 °C); ^1H NMR, major conformer (300 MHz, $CDCl_3$) δ 5.35 (dd, J = 11.7, 3.3 Hz, 1H), 3.71 (s, 3H), 3.47 (d, J = 10.2 Hz, 1H), 3.29 (ddd, J = 9.9, 6.0, 1.5 Hz, 1H), 3.04 − 2.63 (m, 2H), 2.55 − 2.28 (m, 2H), 2.24 − 1.90 (m, 4H), 1.64 (s, 3H), 0.13 (s, 9H) ppm; ^{13}C NMR, major conformer (75 MHz, $CDCl_3$) δ 205.6, 168.9, 137.1, 124.6, 107.8, 87.3, 66.4, 52.6, 39.5, 34.2, 32.9, 32.1, 24.0, 18.2, 0.3 ppm; ESIMS *m/z* 307.1 ($M+H^+$).

3.116 **3.117**

Alkynyl ketoester (3.116) and alkynyl enol (3.117): To a solution of silylalkynyl ketoester **3.115** (0.0108 g, 0.035 mmol) in DCM (1.0 mL) at -78 °C was added TBAF (1M in THF, 0.212 mL, 0.212 mmol). The pale yellow solution was warmed to 0 °C. After 15 min, the solution was cooled back to -78 °C and quenched with sat aq NH_4Cl (1 mL). After warming to rt, the mixture was diluted with DCM (5 mL), and the organic layer was separated. The aqueous layer was extracted with DCM (3 x 0.5 mL). The combined organics were washed with brine (0.5 mL), dried over Na_2SO_4, filtered, and concentrated to a crude pale yellow oil. Purification by FCC (0 to 10% EtOAc/petroleum ether) furnished alkynyl ketoester **3.116** (5.8 mg, 70%) and alkynyl enol **3.117** (2.3 mg, 28%) as colorless oils. The enol eluted first as several separated spots. Alkynyl ketoester **3.116**: IR (neat) 3284, 2936, 2857, 1749, 1707, 1436, 1273, 1239, 1227, 1194, 1166, 1151, 668, 642 cm^{-1}; 2.3:1 conformational equilibrium ($CDCl_3$, 25 °C); ^1H NMR, major conformer (500 MHz, $CDCl_3$) δ 5.35 (dd, J = 11.5, 4.0 Hz, 1H), 3.85 (s, 1H), 3.73 (s, 3H), 3.51 (d, J = 10.0 Hz, 1H), 3.34 − 3.27 (m, 1H), 2.86 − 2.68 (m, 2H), 2.55 − 2.44 (m, 2H), 2.24 − 2.12 (m, 4H), 1.68 (s, 3H) ppm; ^{13}C NMR, major conformer (125 MHz, $CDCl_3$) δ 205.2, 168.9, 137.3, 124.5, 85.6, 70.9, 65.6, 52.7, 39.7, 36.0, 33.9, 31.6, 23.7, 18.5 ppm; ESIMS *m/z* 235.1 ($M+H^+$). Alkynyl enol **3.117**: IR (neat) 3288, 2928, 2855, 1750, 1731, 1714, 1635, 1596, 1439, 1372, 1274, 1238, 1210, 1189, 1038, 871, 633 cm^{-1}; ^1H NMR (300 MHz, $CDCl_3$) δ

13.20 (s, 1H), 5.36 − 5.27 (m, 1H), 3.85 (s, 3H), 3.72 (s, 1H), 3.38 (dd, J = 8.7, 2.7 Hz, 1H), 2.51 − 2.32 (m, 4H), 2.25 − 2.09 (m, 4H), 1.39 (s, 3H) ppm; ^{13}C NMR (75 MHz, $CDCl_3$) δ 175.1, 173.8, 138.4, 127.1, 104.9, 88.0, 67.4, 51.7, 39.4, 37.4, 36.7, 27.8, 26.2, 16.5 ppm; ESIMS *m/z* 235.2 ($M+H^+$), 252.1 ($M+H_2O^+$).

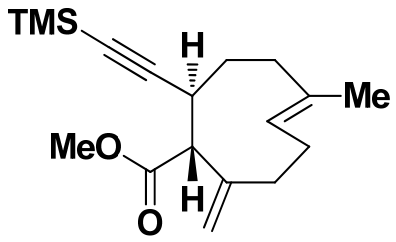

3.118

Silylalkynyl *exo*-olefin (3.118): To a degassed solution of silylalkynyl ketoester **3.115** (29 mg, 0.095 mmol) in THF/pyridine (5:1, 1.89 mL) at 0 °C was added Tebbe reagent (Aldrich, 0.5M in toluene, 0.189 mL, 0.095 mmol). Portionwise addition of more equivalents of Tebbe reagent to the orange solution was required to maximize conversion at 0 °C. After 1 h, the brown mixture was diluted with Et_2O (4 mL) and maintained at 0 °C. MeOH (1 mL) was added dropwise, generating a creamy orange/red suspension that solidified. After warming to rt, the liquified suspension was vacuum filtered through Celite and rinsed through with liberal amounts of Et_2O. The orange filtrate was concentrated under reduced pressure to a crude dark red oil. Purification by FCC (0 to 7% EtOAc/hexane) provided silylalkynyl *exo*-olefin **3.118** (15 mg, 52%, 69% BORSM) as a pale yellow oil and recovered **3.115** (7.1 mg, 24%) as a colorless oil. IR (neat) 3073, 3051, 2955, 2933, 2868, 2170, 1740, 1668, 1647, 1448, 1434, 1364, 1249, 1192, 1170, 1147, 843, 760 cm^{-1}; 4.9:1 conformational equilibrium (C_6D_6, 25 °C); ^{1}H NMR, major conformer

(500 MHz, C_6D_6) δ 5.08 (dd, J = 11.5, 3.0 Hz, 1H), 4.92 (s, 1H), 4.76 (s, 1H), 3.47 (s, 3H), 3.15 (s, 1H), 2.40 − 2.29 (m, 1H), 2.19 − 2.10 (m, 2H), 2.10 − 2.02 (m, 2H), 1.92 − 1.78 (m, 4H), 1.35 (s, 3H), 0.21 (s, 9H) ppm; ^{13}C NMR, major conformer (125 MHz, C_6D_6) δ 172.5, 144.6, 141.6, 135.1, 125.3, 104.4, 86.0, 64.2, 51.3, 34.3, 33.5, 29.7, 24.3, 18.6, 18.5, 0.3 ppm; ESIMS *m/z* 327.2 ($M+Na^+$).

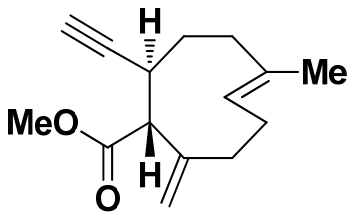

3.112

Alkynyl *exo*-olefin (3.112): To a vigorously stirred solution of silylalkynyl *exo*-olefin **3.118** (14.5 mg, 0.048 mmol) in MeOH (0.5 mL) in a septum-covered flask at rt was added finely powdered anhydrous K_2CO_3 (65.8 mg, 0.476 mmol). The resulting yellow slurry was stirred for 3 h, then sat aq NH_4Cl (1 mL) was added. The mixture was diluted with Et_2O (3 mL). The organic layer was separated, and the aqueous layer was extracted with Et_2O (3 x 1 mL). The combined organics were washed with brine (0.5 mL), dried over Na_2SO_4, filtered, and concentrated to a crude pale yellow oil. Purification by FCC (0 to 5% EtOAc/hexane) provided alkynyl *exo*-olefin **3.112** (8.1 mg, 73%) as a colorless oil. IR (neat) 3291, 3073, 2949, 2931, 2861, 2113, 1733, 1447, 1435, 1272, 1193, 1172, 1148, 1011, 897, 668, 637 cm^{-1}; 3.1:1 conformational equilibrium (C_6D_6, 25 °C); ^{1}H NMR, major conformer (300 MHz, C_6D_6) δ 5.14 − 5.01 (m, 1H), 4.91 (s, 1H), 4.77 (s, 1H), 3.59 (s, 1H), 3.41 (s, 3H), 3.13 (s, 1H), 2.58 (td, J = 11.4, 1.8 Hz, 1H), 2.38 − 2.22 (m, 2H), 2.21 − 2.08 (m, 2H), 2.01 − 1.75 (m, 4H), 1.42 (s, 3H) ppm; ^{13}C NMR, major conformer (125 MHz,

C_6D_6) δ 172.5, 144.5, 135.1, 125.2, 119.2, 87.9, 70.2, 61.7, 51.4, 38.2, 36.0, 34.2, 32.2, 27.5, 18.5 ppm; ESIMS *m/z* 255.2 ($M+Na^+$).

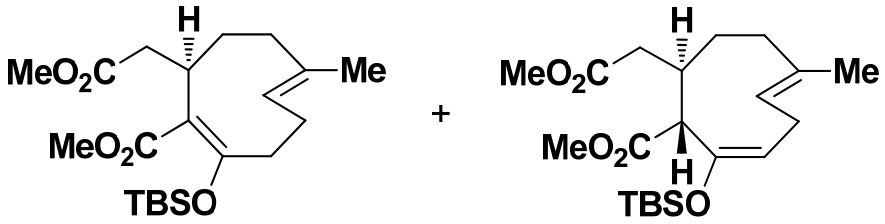

3.119 **3.120**

TBS enol ethers (3.119 and 3.120): To a solution of enone **3.6** (0.0504 g, 0.242 mmol) in 1-(*tert*-butyldimethylsilyloxy)-1-methoxyethene (436 μL, 1.936 mmol) at rt in a vial under argon was added $LiClO_4$ (0.0271 g, 0.242 mmol). The colorless suspension gradually turned into a white slurry. After 17 h, the completed reaction mixture was diluted with EtOAc and transferred to a small roundbottom flask. The crude solution was concentrated under reduced pressure, then excess silyl ketene acetal was removed under high vacuum. The crude pale yellow oil was purified by FCC (loaded with minimal MeOH, 0 to 3% EtOAc/hexane), furnishing an inseparable mixture of TBS enol ethers **3.119** and **3.120** (83.1 mg, 87%, 4.3:1) as a colorless oil. IR (neat) 2951, 2931, 2858, 1739, 1725, 1463, 1435, 1334, 1285, 1259, 1202, 1179, 1133, 1016, 839, 780 cm^{-1}; Major TBS enol ether **3.119**: ^1H NMR (300 MHz, $CDCl_3$) δ 5.25 (dd, J = 12.0, 3.0 Hz, 1H), 3.66 (s, 3H), 3.65 (s, 3H), 2.86 − 2.73 (m, 1H), 2.53 (d, J = 8.4 Hz, 1H), 2.38 (d, J = 7.5 Hz, 1H), 2.26 − 2.02 (m, 6H), 1.63 (s, 3H), 1.59 − 1.47 (m, 2H), 0.89 (s, 9H), 0.14 (s, 6H) ppm; ^{13}C NMR (75 MHz, $CDCl_3$) δ 173.4, 170.1, 150.9, 140.1, 126.1, 118.9, 51.6, 51.2, 40.3, 39.9, 35.9, 35.5, 34.8, 25.9, 25.4, 18.4, 16.4, -3.4 ppm; ESIMS *m/z* 397.2 ($M+H^+$).

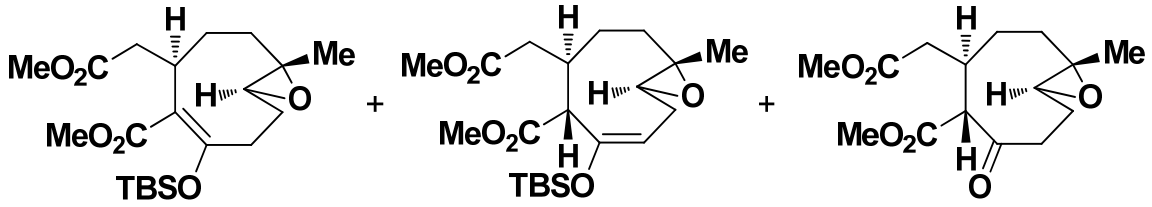

3.125 **3.126** **3.127**

TBS enol ether epoxides (3.125 and 3.126) and keto epoxide (3.127): A mixture of TBS enol ethers **3.119** and **3.120** (77.6 mg, 0.196 mmol) was stored under argon in a sealed roundbottom flask at -20 °C. After 48 h, ^{1}H NMR and TLC analysis indicated that the material had transformed completely into other products. Purification of the mixture by FCC (17 to 50% EtOAc/hexane) provided an inseparable mixture of TBS enol ether epoxides **3.125** and **3.126** (31.5 mg, 39%, 4.3:1) as a colorless oil and keto epoxide **3.127** (18.5 mg, 32%) as a colorless oil. TBS enol ether epoxides **3.125** and **3.126**: IR (neat) 2952, 2931, 2899, 2885, 2857, 1728, 1664, 1464, 1436, 1384, 1251, 1236, 1201, 1174, 1011, 839, 780 cm^{-1}; Major epoxide **3.125**: ^{1}H NMR (300 MHz, $CDCl_3$) δ 3.64 (s, 6H), 3.05 − 2.89 (m, 1H), 2.75 (d, J = 9.6 Hz, 2H), 2.36 − 2.20 (m, 2H), 2.19 − 2.03 (m, 2H), 2.02 − 1.87 (m, 1H), 1.86 − 1.63 (m, 2H), 1.62 − 1.45 (m, 2H), 0.92 (s, 3H), 0.87 (s, 9H), 0.19 (s, 3H), 0.15 (s, 3H) ppm; ^{13}C NMR (75 MHz, $CDCl_3$) δ 174.5, 172.8, 152.3, 97.9, 69.9, 51.6, 51.2, 51.1, 46.4, 37.7, 34.5, 29.7, 29.4, 26.1, 25.9, 18.3, 17.6, -3.9, -5.2 ppm; ESIMS *m/z* 413.3 ($M+H^+$). Keto epoxide **3.127**: IR (neat) 2954, 2881, 1732, 1437, 1384, 1228, 1198, 1174, 1047, 1007 cm^{-1}; ^{1}H NMR (300 MHz, $CDCl_3$) δ 3.70 (s, 3H), 3.65 (s, 3H), 2.94 (qd, J = 9.3, 3.9 Hz, 1H), 2.82 − 2.41 (m, 4H), 2.15 − 2.00 (m, 3H), 1.95 − 1.67 (m, 3H), 1.65 − 1.53 (m, 1H), 1.18 (s, 3H), 0.99 − 0.82 (m, 1H) ppm; ^{13}C NMR (75 MHz, $CDCl_3$) δ 207.5, 173.5, 171.0, 71.6, 71.4, 53.1, 52.0, 51.9, 42.1, 36.7, 36.5, 35.5, 29.0, 28.3, 18.7 ppm; ESIMS *m/z* 321.0 ($M+Na^+$).

References and Notes

1. H. Schick, H. Schwarz, S. Schwarz, U. Eberhardt, European Patent Appl. No. DD19760195469 19761027, Pub. No. DD128374 (A1), 1977.

2. D. Chapdelaine, J. Belzile, P. Deslongchamps, *J. Org. Chem.* **2002**, *67*, 5669-5672.

3. T. Katoh, S. Mizumoto, M. Fudesaka, Y. Nakashima, T. Kajimoto, M. Node, *Synlett* **2006**, *14*, 2176-2182.

4. M. Frohn, X. Zhou, J.-R. Zhang, Y. Tang, Y. Shi, *J. Am. Chem. Soc.* **1999**, *121*, 7718-7719.

5. a) Computational analyses used (DFT-B3LYP 6-31G(d, p)); b) All structures were fully optimized by analytical gradient methods using the GAUSSIAN 03 suites: M. J. Frisch, G. W. Trucks, H. B. Schlege, G. E. Scuseria, M. A. Robb, J. R. Cheeseman, J. A. Montgomery, Jr., T. Vreven, K. N. Kudin, J. C. Burant, *GAUSSIAN 03, Revision E.01*, Gaussian: Wallingford, CT, 2004; c) Density functional theory (DFT) calculations used the exchange potentials of: A. D. Becke, *J. Chem. Phys.* **1993**, *98*, 5648-5652; the correlation functional of: C. Lee, W. Yang, R. G. Parr, *Phys. Rev. B* **1988**, *37*, 785-789.

6. L. Kong, Z. Zhuang, Q. Chen, H. Deng, Z. Tang, X. Jia, Y. Li, H. Zhai, *Tetrahedron: Asymm.* **2007**, *18,* 451-454.

7. Y. Zhang, S. D. Lotesta, T. J. Emge, L. J. Williams, *Tetrahedron Lett.* **2009**, *50*, 1882-1885.

8. Z. Li, M. Khaliq, Z. Zhou, C. B. Post, R. J. Kuhn, M. Cushman, *J. Med. Chem.* **2008**, *51*, 4660-4671.

9. M. Higashino, N. Ikeda, T. Shinada, K. Sakaguchi, Y. Ohfune, *Tetrahedron Lett.* **2011**, *52*, 422-425.

10. N. Majumdar, K. A. Korthals, W. D. Wulff, *J. Am. Chem. Soc.* **2012**, *134*, 1357-1362.

X-Ray Crystallography Data

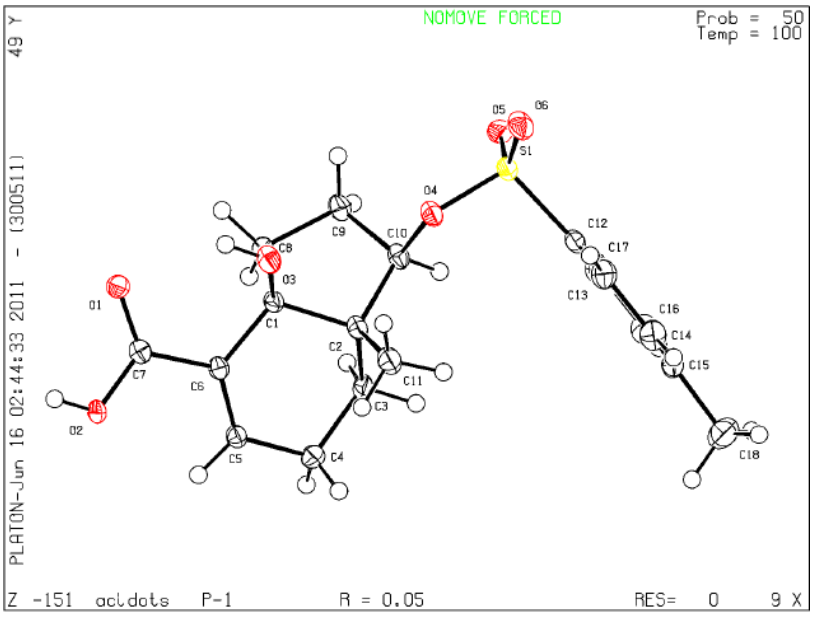

X-ray crystal structure of **3.18** (racemic).

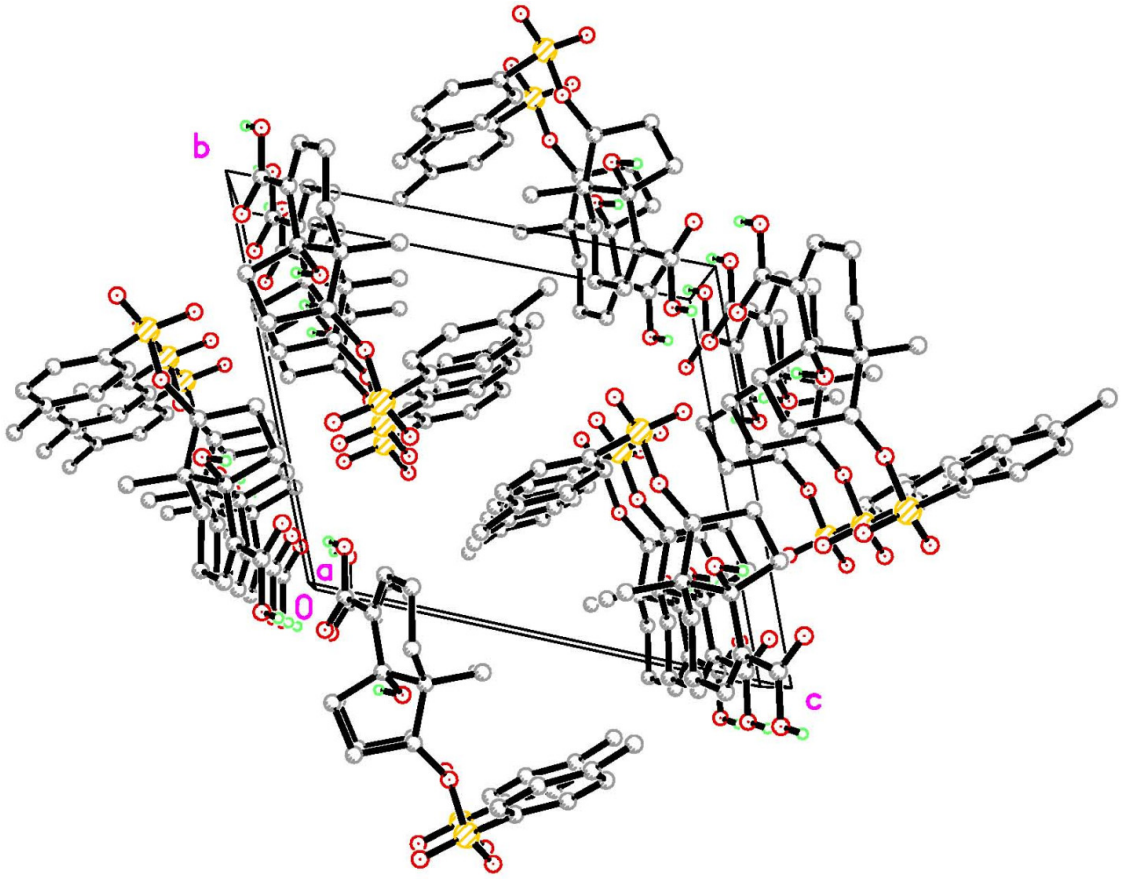

Crystal packing of **3.18** (note the H-bonds: one inter- and one intramolecular).

Table 1. Crystal data and structure refinement for acidOTs.

Identification code	acidOTs	
Empirical formula	C18 H22 O6 S	
Formula weight	366.42	
Temperature	100(2) K	
Wavelength	0.71073 Å	
Crystal system	Triclinic	
Space group	P-1	
Unit cell dimensions	a = 7.0253(9) Å	α= 110.657(2)°.
	b = 10.8709(14) Å	β= 100.814(3)°.
	c = 12.8285(16) Å	γ = 101.143(3)°.
Volume	863.84(19) $Å^3$	
Z	2	
Density (calculated)	1.409 Mg/m^3	
Absorption coefficient	0.219 mm^{-1}	
F(000)	388	
Crystal size	0.10 x 0.03 x 0.02 mm^3	
Theta range for data collection	2.12 to 26.73°.	
Index ranges	-8<=h<=8, -13<=k<=13, -14<=l<=16	
Reflections collected	6957	
Independent reflections	3600 [R(int) = 0.0367]	
Completeness to theta = 26.73°	98.3 %	
Absorption correction	Semi-empirical from equivalents	
Max. and min. transmission	0.9956 and 0.9784	
Refinement method	Full-matrix least-squares on F^2	
Data / restraints / parameters	3600 / 0 / 234	
Goodness-of-fit on F^2	1.011	
Final R indices [I>2sigma(I)]	R1 = 0.0493, wR2 = 0.1046	
R indices (all data)	R1 = 0.0791, wR2 = 0.1169	
Largest diff. peak and hole	0.381 and -0.341 $e.Å^{-3}$	

Table 2. Atomic coordinates (x 10^4) and equivalent isotropic displacement parameters ($Å^2$x 10^3) for acidOTs. U(eq) is defined as one third of the trace of the orthogonalized U^{ij} tensor.

	x	y	z	U(eq)
S(1)	2788(1)	-5418(1)	2356(1)	18(1)
O(1)	8467(2)	-1144(2)	177(2)	23(1)
O(2)	8688(2)	1086(2)	963(2)	19(1)
O(3)	7250(2)	-2360(2)	1595(2)	21(1)
O(4)	4159(2)	-4180(2)	2227(1)	19(1)
O(5)	1241(2)	-6216(2)	1290(2)	22(1)
O(6)	4177(3)	-6027(2)	2804(2)	26(1)
C(1)	5552(3)	-1885(2)	1266(2)	16(1)
C(2)	4281(3)	-1937(2)	2120(2)	17(1)
C(3)	2696(3)	-1160(2)	1981(2)	18(1)
C(4)	3640(4)	342(2)	2232(2)	20(1)
C(5)	5370(3)	526(2)	1726(2)	16(1)
C(6)	6246(3)	-451(2)	1305(2)	15(1)
C(7)	7895(3)	-204(2)	766(2)	16(1)
C(8)	4163(3)	-2931(2)	79(2)	16(1)
C(9)	2936(4)	-4074(2)	333(2)	19(1)
C(10)	3096(3)	-3463(2)	1631(2)	17(1)
C(11)	5531(4)	-1350(2)	3379(2)	23(1)
C(12)	1666(3)	-4603(2)	3420(2)	18(1)
C(13)	2779(4)	-4017(3)	4575(2)	23(1)
C(14)	1955(4)	-3290(3)	5402(2)	25(1)
C(15)	52(4)	-3112(2)	5097(2)	23(1)
C(16)	-1043(4)	-3740(3)	3940(2)	24(1)
C(17)	-263(3)	-4491(2)	3093(2)	20(1)
C(18)	-809(4)	-2261(3)	5994(3)	35(1)

Table 3. Bond lengths [Å] and angles [°] for acidOTs.

_____

S(1)-O(6)	1.4246(18)	C(12)-C(13)	1.386(3)
S(1)-O(5)	1.4295(18)	C(13)-C(14)	1.379(3)
S(1)-O(4)	1.5751(16)	C(13)-H(13)	0.9500
S(1)-C(12)	1.757(2)	C(14)-C(15)	1.391(4)
O(1)-C(7)	1.227(3)	C(14)-H(14)	0.9500
O(2)-C(7)	1.317(3)	C(15)-C(16)	1.384(4)
O(2)-H(2O)	0.81(3)	C(15)-C(18)	1.507(3)
O(3)-C(1)	1.439(3)	C(16)-C(17)	1.384(3)
O(3)-H(3O)	0.81(3)	C(16)-H(16)	0.9500
O(4)-C(10)	1.477(3)	C(17)-H(17)	0.9500
C(1)-C(6)	1.521(3)	C(18)-H(18A)	0.9800
C(1)-C(8)	1.535(3)	C(18)-H(18B)	0.9800
C(1)-C(2)	1.547(3)	C(18)-H(18C)	0.9800
C(2)-C(11)	1.521(3)		
C(2)-C(10)	1.540(3)		
C(2)-C(3)	1.543(3)		
C(3)-C(4)	1.529(3)		
C(3)-H(3A)	0.9900		
C(3)-H(3B)	0.9900		
C(4)-C(5)	1.495(3)		
C(4)-H(4A)	0.9900		
C(4)-H(4B)	0.9900		
C(5)-C(6)	1.331(3)		
C(5)-H(5)	0.9500		
C(6)-C(7)	1.484(3)		
C(8)-C(9)	1.539(3)		
C(8)-H(8A)	0.9900		
C(8)-H(8B)	0.9900		
C(9)-C(10)	1.532(3)		
C(9)-H(9A)	0.9900		
C(9)-H(9B)	0.9900		
C(10)-H(10)	1.0000		
C(11)-H(11A)	0.9800		
C(11)-H(11B)	0.9800		
C(11)-H(11C)	0.9800		
C(12)-C(17)	1.384(3)		

O(6)-S(1)-O(5)	120.16(11)	C(5)-C(6)-C(7)	120.3(2)
O(6)-S(1)-O(4)	104.50(9)	C(5)-C(6)-C(1)	123.2(2)
O(5)-S(1)-O(4)	108.96(10)	C(7)-C(6)-C(1)	116.35(19)
O(6)-S(1)-C(12)	110.19(11)	O(1)-C(7)-O(2)	122.8(2)
O(5)-S(1)-C(12)	108.65(11)	O(1)-C(7)-C(6)	121.8(2)
O(4)-S(1)-C(12)	102.96(10)	O(2)-C(7)-C(6)	115.4(2)
C(7)-O(2)-H(2O)	110.8(19)	C(1)-C(8)-C(9)	104.97(18)
C(1)-O(3)-H(3O)	103(2)	C(1)-C(8)-H(8A)	110.8
C(10)-O(4)-S(1)	116.25(13)	C(9)-C(8)-H(8A)	110.8
O(3)-C(1)-C(6)	111.07(17)	C(1)-C(8)-H(8B)	110.8
O(3)-C(1)-C(8)	109.72(18)	C(9)-C(8)-H(8B)	110.8
C(6)-C(1)-C(8)	113.13(19)	H(8A)-C(8)-H(8B)	108.8
O(3)-C(1)-C(2)	106.06(18)	C(10)-C(9)-C(8)	106.60(18)
C(6)-C(1)-C(2)	112.16(18)	C(10)-C(9)-H(9A)	110.4
C(8)-C(1)-C(2)	104.27(17)	C(8)-C(9)-H(9A)	110.4
C(11)-C(2)-C(10)	114.65(19)	C(10)-C(9)-H(9B)	110.4
C(11)-C(2)-C(3)	110.1(2)	C(8)-C(9)-H(9B)	110.4
C(10)-C(2)-C(3)	106.11(18)	H(9A)-C(9)-H(9B)	108.6
C(11)-C(2)-C(1)	113.70(19)	O(4)-C(10)-C(9)	110.39(19)
C(10)-C(2)-C(1)	103.33(18)	O(4)-C(10)-C(2)	110.25(18)
C(3)-C(2)-C(1)	108.41(19)	C(9)-C(10)-C(2)	107.31(18)
C(4)-C(3)-C(2)	113.04(18)	O(4)-C(10)-H(10)	109.6
C(4)-C(3)-H(3A)	109.0	C(9)-C(10)-H(10)	109.6
C(2)-C(3)-H(3A)	109.0	C(2)-C(10)-H(10)	109.6
C(4)-C(3)-H(3B)	109.0	C(2)-C(11)-H(11A)	109.5
C(2)-C(3)-H(3B)	109.0	C(2)-C(11)-H(11B)	109.5
H(3A)-C(3)-H(3B)	107.8	H(11A)-C(11)-H(11B)	109.5
C(5)-C(4)-C(3)	112.46(19)	C(2)-C(11)-H(11C)	109.5
C(5)-C(4)-H(4A)	109.1	H(11A)-C(11)-H(11C)	109.5
C(3)-C(4)-H(4A)	109.1	H(11B)-C(11)-H(11C)	109.5
C(5)-C(4)-H(4B)	109.1	C(17)-C(12)-C(13)	121.0(2)
C(3)-C(4)-H(4B)	109.1	C(17)-C(12)-S(1)	119.89(19)
H(4A)-C(4)-H(4B)	107.8	C(13)-C(12)-S(1)	119.07(18)
C(6)-C(5)-C(4)	123.7(2)	C(14)-C(13)-C(12)	119.1(2)
C(6)-C(5)-H(5)	118.1	C(14)-C(13)-H(13)	120.5
C(4)-C(5)-H(5)	118.1	C(12)-C(13)-H(13)	120.5

C(13)-C(14)-C(15)	121.4(2)
C(13)-C(14)-H(14)	119.3
C(15)-C(14)-H(14)	119.3
C(16)-C(15)-C(14)	118.1(2)
C(16)-C(15)-C(18)	120.4(2)
C(14)-C(15)-C(18)	121.5(2)
C(15)-C(16)-C(17)	121.7(2)
C(15)-C(16)-H(16)	119.1
C(17)-C(16)-H(16)	119.1
C(12)-C(17)-C(16)	118.7(2)
C(12)-C(17)-H(17)	120.7
C(16)-C(17)-H(17)	120.7
C(15)-C(18)-H(18A)	109.5
C(15)-C(18)-H(18B)	109.5
H(18A)-C(18)-H(18B)	109.5
C(15)-C(18)-H(18C)	109.5
H(18A)-C(18)-H(18C)	109.5
H(18B)-C(18)-H(18C)	109.5

Table 4. Anisotropic displacement parameters ($Å^2 x\ 10^3$) for acidOTs. The anisotropic displacement factor exponent takes the form: $-2\pi^2[\ h^2\ a^{*2}U^{11} + ...\ + 2\ h\ k\ a^*\ b^*\ U^{12}\ ]$

	U^{11}	U^{22}	U^{33}	U^{23}	U^{13}	U^{12}
S(1)	20(1)	16(1)	23(1)	11(1)	10(1)	6(1)
O(1)	22(1)	17(1)	34(1)	10(1)	18(1)	7(1)
O(2)	18(1)	16(1)	26(1)	10(1)	14(1)	3(1)
O(3)	14(1)	24(1)	34(1)	17(1)	10(1)	9(1)
O(4)	16(1)	19(1)	25(1)	13(1)	8(1)	5(1)
O(5)	23(1)	16(1)	24(1)	5(1)	10(1)	2(1)
O(6)	28(1)	27(1)	39(1)	22(1)	16(1)	15(1)
C(1)	14(1)	15(1)	21(1)	9(1)	8(1)	5(1)
C(2)	17(1)	16(1)	20(1)	10(1)	6(1)	3(1)
C(3)	18(1)	21(1)	20(1)	10(1)	11(1)	7(1)
C(4)	20(1)	19(1)	24(1)	9(1)	11(1)	8(1)
C(5)	16(1)	15(1)	16(1)	7(1)	4(1)	2(1)
C(6)	12(1)	16(1)	16(1)	7(1)	4(1)	2(1)
C(7)	12(1)	17(1)	18(1)	8(1)	3(1)	3(1)
C(8)	17(1)	16(1)	18(1)	7(1)	7(1)	6(1)
C(9)	17(1)	19(1)	22(1)	9(1)	4(1)	1(1)
C(10)	12(1)	19(1)	22(1)	12(1)	5(1)	4(1)
C(11)	26(1)	21(1)	22(1)	9(1)	7(1)	2(1)
C(12)	18(1)	16(1)	24(1)	12(1)	9(1)	6(1)
C(13)	19(1)	26(1)	25(2)	12(1)	6(1)	5(1)
C(14)	23(1)	26(1)	19(1)	8(1)	3(1)	0(1)
C(15)	26(1)	20(1)	22(1)	7(1)	12(1)	2(1)
C(16)	18(1)	28(1)	31(2)	15(1)	8(1)	9(1)
C(17)	19(1)	26(1)	15(1)	10(1)	4(1)	4(1)
C(18)	34(2)	33(2)	32(2)	6(1)	16(1)	7(1)

Table 5. Hydrogen coordinates (x 10^4) and isotropic displacement parameters ($Å^2$x 10^3) for acidOTs.

	x	y	z	U(eq)
H(2O)	9550(40)	1150(30)	630(20)	28
H(3O)	7820(40)	-2370(30)	1100(30)	31
H(3A)	1796	-1622	1179	21
H(3B)	1858	-1202	2514	21
H(4A)	2595	706	1910	24
H(4B)	4118	878	3082	24
H(5)	5873	1390	1703	19
H(8A)	4965	-3298	-452	19
H(8B)	3258	-2506	-278	19
H(9A)	1508	-4382	-132	23
H(9B)	3495	-4870	138	23
H(10)	1712	-3547	1741	20
H(11A)	4652	-1484	3863	35
H(11B)	6169	-368	3635	35
H(11C)	6577	-1818	3452	35
H(13)	4092	-4115	4795	28
H(14)	2703	-2902	6196	30
H(16)	-2363	-3654	3721	29
H(17)	-1038	-4920	2303	24
H(18A)	-405	-1305	6088	52
H(18B)	-296	-2318	6735	52
H(18C)	-2286	-2608	5740	52

Table 6. Torsion angles [°] for acidOTs.

O(6)-S(1)-O(4)-C(10)	172.30(15)
O(5)-S(1)-O(4)-C(10)	42.69(17)
C(12)-S(1)-O(4)-C(10)	-72.52(17)
O(3)-C(1)-C(2)-C(11)	45.4(2)
C(6)-C(1)-C(2)-C(11)	-76.0(2)
C(8)-C(1)-C(2)-C(11)	161.23(19)
O(3)-C(1)-C(2)-C(10)	-79.5(2)
C(6)-C(1)-C(2)-C(10)	159.09(18)
C(8)-C(1)-C(2)-C(10)	36.3(2)
O(3)-C(1)-C(2)-C(3)	168.20(17)
C(6)-C(1)-C(2)-C(3)	46.8(2)
C(8)-C(1)-C(2)-C(3)	-76.0(2)
C(11)-C(2)-C(3)-C(4)	65.2(2)
C(10)-C(2)-C(3)-C(4)	-170.2(2)
C(1)-C(2)-C(3)-C(4)	-59.7(2)
C(2)-C(3)-C(4)-C(5)	42.0(3)
C(3)-C(4)-C(5)-C(6)	-12.3(3)
C(4)-C(5)-C(6)-C(7)	177.1(2)
C(4)-C(5)-C(6)-C(1)	1.4(4)
O(3)-C(1)-C(6)-C(5)	-138.3(2)
C(8)-C(1)-C(6)-C(5)	97.8(3)
C(2)-C(1)-C(6)-C(5)	-19.8(3)
O(3)-C(1)-C(6)-C(7)	45.9(3)
C(8)-C(1)-C(6)-C(7)	-78.0(2)
C(2)-C(1)-C(6)-C(7)	164.40(19)
C(5)-C(6)-C(7)-O(1)	-165.7(2)
C(1)-C(6)-C(7)-O(1)	10.2(3)
C(5)-C(6)-C(7)-O(2)	14.1(3)
C(1)-C(6)-C(7)-O(2)	-169.90(19)
O(3)-C(1)-C(8)-C(9)	79.0(2)
C(6)-C(1)-C(8)-C(9)	-156.38(18)
C(2)-C(1)-C(8)-C(9)	-34.2(2)
C(1)-C(8)-C(9)-C(10)	18.7(2)
S(1)-O(4)-C(10)-C(9)	-92.93(18)
S(1)-O(4)-C(10)-C(2)	148.67(15)
C(8)-C(9)-C(10)-O(4)	-116.16(19)
C(8)-C(9)-C(10)-C(2)	4.0(2)
C(11)-C(2)-C(10)-O(4)	-28.9(3)
C(3)-C(2)-C(10)-O(4)	-150.60(18)
C(1)-C(2)-C(10)-O(4)	95.4(2)
C(11)-C(2)-C(10)-C(9)	-149.1(2)
C(3)-C(2)-C(10)-C(9)	89.1(2)
C(1)-C(2)-C(10)-C(9)	-24.8(2)
O(6)-S(1)-C(12)-C(17)	-150.91(18)
O(5)-S(1)-C(12)-C(17)	-17.4(2)
O(4)-S(1)-C(12)-C(17)	98.1(2)
O(6)-S(1)-C(12)-C(13)	32.5(2)
O(5)-S(1)-C(12)-C(13)	166.05(18)
O(4)-S(1)-C(12)-C(13)	-78.5(2)
C(17)-C(12)-C(13)-C(14)	-1.4(4)
S(1)-C(12)-C(13)-C(14)	175.19(18)
C(12)-C(13)-C(14)-C(15)	-1.2(4)
C(13)-C(14)-C(15)-C(16)	2.9(4)
C(13)-C(14)-C(15)-C(18)	-177.0(2)
C(14)-C(15)-C(16)-C(17)	-2.0(4)
C(18)-C(15)-C(16)-C(17)	177.9(2)
C(13)-C(12)-C(17)-C(16)	2.2(4)
S(1)-C(12)-C(17)-C(16)	-174.38(18)
C(15)-C(16)-C(17)-C(12)	-0.4(4)

Table 7. Hydrogen bonds for acidOTs [Å and °].

D-H...A	d(D-H)	d(H...A)	d(D...A)	<(DHA)
O(2)-H(2O)...O(1)#1	0.81(3)	1.89(3)	2.693(2)	175(3)
O(3)-H(3O)...O(1)	0.81(3)	2.11(3)	2.763(2)	137(3)

Symmetry transformations used to generate equivalent atoms:

#1 -x+2,-y,-z

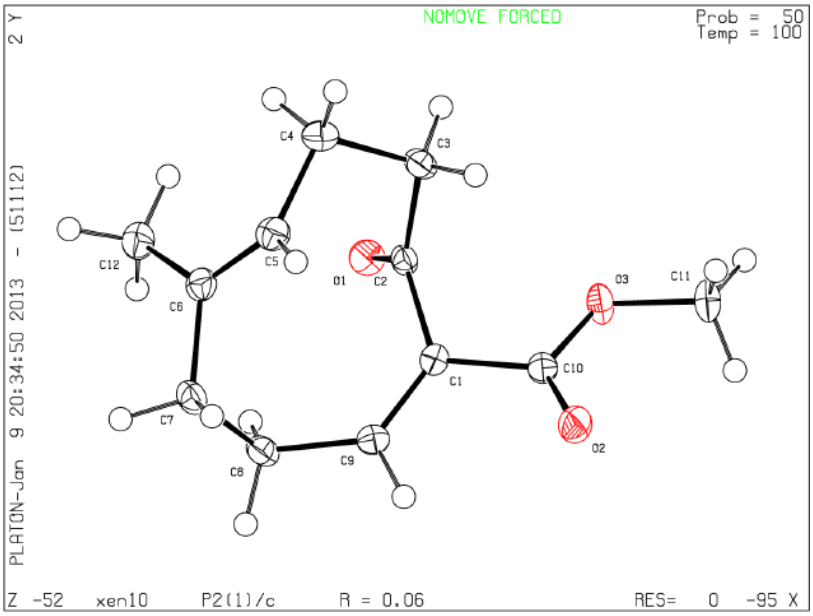

X-ray crystal structure of **3.6** (racemic).

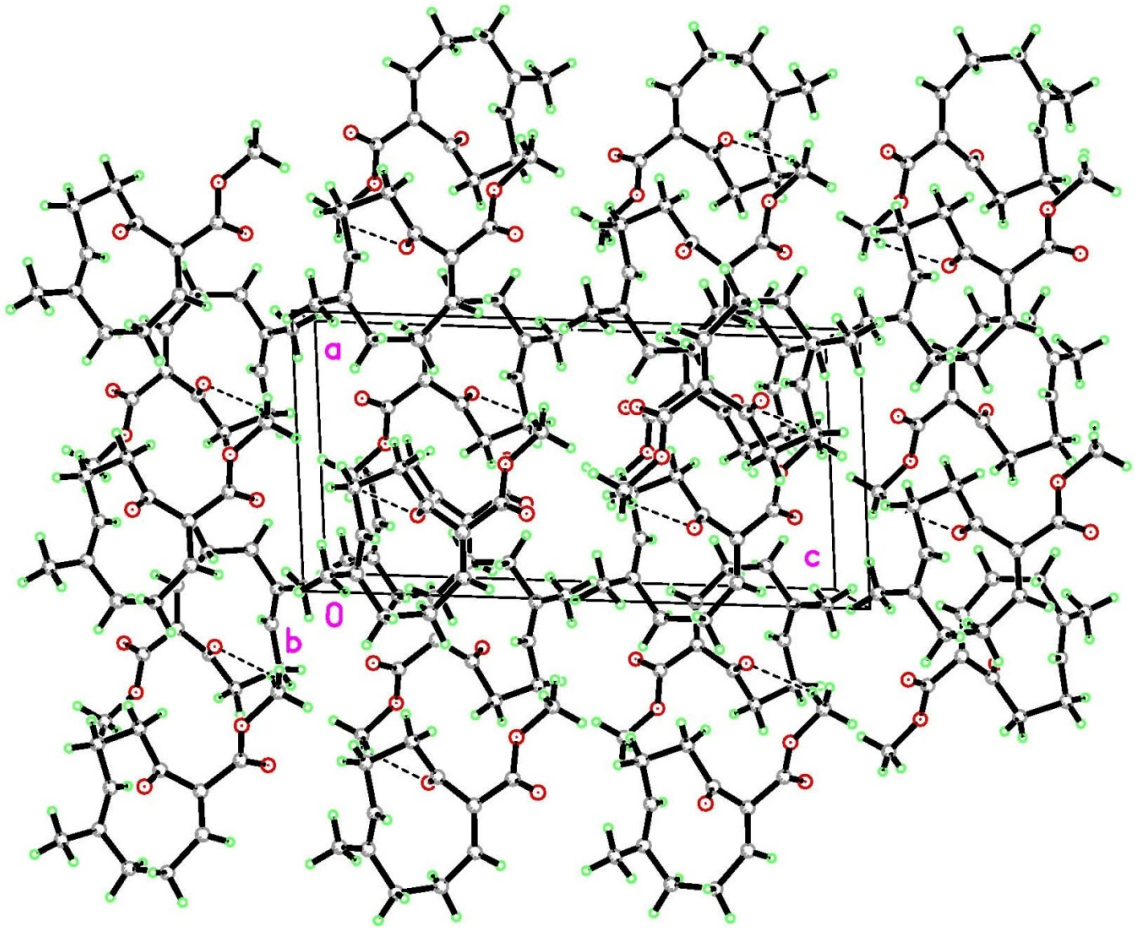

Crystal packing of **3.6**.

Table 1. Crystal data and structure refinement for xen10.

Identification code	xen10	
Empirical formula	C12 H16 O3	
Formula weight	208.25	
Temperature	100(2) K	
Wavelength	0.71073 Å	
Crystal system	Monoclinic	
Space group	P2(1)/c	
Unit cell dimensions	a = 7.9468(10) Å	α= 90°.
	b = 8.5993(10) Å	β= 94.226(2)°.
	c = 16.0932(19) Å	γ = 90°.
Volume	1096.8(2) $Å^3$	
Z	4	
Density (calculated)	1.261 Mg/m^3	
Absorption coefficient	0.090 mm^{-1}	
F(000)	448	
Crystal size	0.44 x 0.22 x 0.05 mm^3	
Theta range for data collection	2.54 to 30.51°.	
Index ranges	-11<=h<=11, -12<=k<=12, -22<=l<=22	
Reflections collected	12649	
Independent reflections	3336 [R(int) = 0.0401]	
Completeness to theta = 30.51°	99.5 %	
Absorption correction	Semi-empirical from equivalents	
Max. and min. transmission	0.9955 and 0.9617	
Refinement method	Full-matrix least-squares on F^2	
Data / restraints / parameters	3336 / 0 / 138	
Goodness-of-fit on F^2	1.007	
Final R indices [I>2sigma(I)]	R1 = 0.0608, wR2 = 0.1301	
R indices (all data)	R1 = 0.0801, wR2 = 0.1400	
Largest diff. peak and hole	0.440 and -0.274 $e.Å^{-3}$	

Table 2. Atomic coordinates (x 10^4) and equivalent isotropic displacement parameters ($Å^2$x 10^3) for xen10. U(eq) is defined as one third of the trace of the orthogonalized U^{ij} tensor.

	x	y	z	U(eq)
O(1)	2673(1)	5999(1)	1979(1)	21(1)
O(2)	3020(1)	9870(1)	3988(1)	24(1)
O(3)	4737(1)	7932(1)	3643(1)	22(1)
C(1)	2220(2)	8205(2)	2824(1)	15(1)
C(2)	3094(2)	7313(2)	2172(1)	16(1)
C(3)	4494(2)	8159(2)	1755(1)	20(1)
C(4)	3762(2)	8904(2)	925(1)	24(1)
C(5)	2043(2)	9518(2)	1076(1)	21(1)
C(6)	599(2)	8756(2)	898(1)	19(1)
C(7)	-898(2)	9121(2)	1384(1)	20(1)
C(8)	-810(2)	8049(2)	2167(1)	19(1)
C(9)	561(2)	8508(2)	2810(1)	17(1)
C(10)	3329(2)	8798(2)	3544(1)	17(1)
C(11)	5969(2)	8415(2)	4306(1)	24(1)
C(12)	401(2)	7358(2)	337(1)	25(1)

Table 3. Bond lengths [Å] and angles [°] for xen10.

_____

O(1)-C(2)	1.2123(18)	C(10)-O(3)-C(11)	116.01(12)
O(2)-C(10)	1.2028(18)	C(9)-C(1)-C(10)	118.00(13)
O(3)-C(10)	1.3435(18)	C(9)-C(1)-C(2)	126.05(13)
O(3)-C(11)	1.4541(18)	C(10)-C(1)-C(2)	115.94(12)
C(1)-C(9)	1.342(2)	O(1)-C(2)-C(1)	121.30(13)
C(1)-C(10)	1.493(2)	O(1)-C(2)-C(3)	121.88(13)
C(1)-C(2)	1.509(2)	C(1)-C(2)-C(3)	116.80(12)
C(2)-C(3)	1.526(2)	C(2)-C(3)-C(4)	109.65(12)
C(3)-C(4)	1.555(2)	C(2)-C(3)-H(3A)	109.7
C(3)-H(3A)	0.9900	C(4)-C(3)-H(3A)	109.7
C(3)-H(3B)	0.9900	C(2)-C(3)-H(3B)	109.7
C(4)-C(5)	1.502(2)	C(4)-C(3)-H(3B)	109.7
C(4)-H(4A)	0.9900	H(3A)-C(3)-H(3B)	108.2
C(4)-H(4B)	0.9900	C(5)-C(4)-C(3)	107.01(12)
C(5)-C(6)	1.334(2)	C(5)-C(4)-H(4A)	110.3
C(5)-H(5)	0.9500	C(3)-C(4)-H(4A)	110.3
C(6)-C(7)	1.503(2)	C(5)-C(4)-H(4B)	110.3
C(6)-C(12)	1.505(2)	C(3)-C(4)-H(4B)	110.3
C(7)-C(8)	1.559(2)	H(4A)-C(4)-H(4B)	108.6
C(7)-H(7A)	0.9900	C(6)-C(5)-C(4)	124.79(15)
C(7)-H(7B)	0.9900	C(6)-C(5)-H(5)	117.6
C(8)-C(9)	1.499(2)	C(4)-C(5)-H(5)	117.6
C(8)-H(8A)	0.9900	C(5)-C(6)-C(7)	119.12(14)
C(8)-H(8B)	0.9900	C(5)-C(6)-C(12)	124.87(15)
C(9)-H(9)	0.9500	C(7)-C(6)-C(12)	115.27(14)
C(11)-H(11A)	0.9800	C(6)-C(7)-C(8)	107.88(12)
C(11)-H(11B)	0.9800	C(6)-C(7)-H(7A)	110.1
C(11)-H(11C)	0.9800	C(8)-C(7)-H(7A)	110.1
C(12)-H(12A)	0.9800	C(6)-C(7)-H(7B)	110.1
C(12)-H(12B)	0.9800	C(8)-C(7)-H(7B)	110.1
C(12)-H(12C)	0.9800	H(7A)-C(7)-H(7B)	108.4
		C(9)-C(8)-C(7)	112.88(12)
		C(9)-C(8)-H(8A)	109.0
		C(7)-C(8)-H(8A)	109.0
		C(9)-C(8)-H(8B)	109.0
		C(7)-C(8)-H(8B)	109.0

H(8A)-C(8)-H(8B)	107.8
C(1)-C(9)-C(8)	128.61(14)
C(1)-C(9)-H(9)	115.7
C(8)-C(9)-H(9)	115.7
O(2)-C(10)-O(3)	123.99(13)
O(2)-C(10)-C(1)	126.04(14)
O(3)-C(10)-C(1)	109.96(12)
O(3)-C(11)-H(11A)	109.5
O(3)-C(11)-H(11B)	109.5
H(11A)-C(11)-H(11B)	109.5
O(3)-C(11)-H(11C)	109.5
H(11A)-C(11)-H(11C)	109.5
H(11B)-C(11)-H(11C)	109.5
C(6)-C(12)-H(12A)	109.5
C(6)-C(12)-H(12B)	109.5
H(12A)-C(12)-H(12B)	109.5
C(6)-C(12)-H(12C)	109.5
H(12A)-C(12)-H(12C)	109.5
H(12B)-C(12)-H(12C)	109.5

Table 4. Anisotropic displacement parameters ($Å^2 x\ 10^3$) for xen10. The anisotropic displacement factor exponent takes the form: $-2\pi^2[\ h^2\ a^{*2}U^{11} + ...\ + 2\ h\ k\ a^*\ b^*\ U^{12}\ ]$

	U^{11}	U^{22}	U^{33}	U^{23}	U^{13}	U^{12}
O(1)	23(1)	17(1)	24(1)	-4(1)	2(1)	0(1)
O(2)	24(1)	26(1)	22(1)	-8(1)	-1(1)	1(1)
O(3)	20(1)	22(1)	23(1)	-4(1)	-8(1)	4(1)
C(1)	18(1)	13(1)	15(1)	0(1)	0(1)	-1(1)
C(2)	13(1)	17(1)	16(1)	0(1)	-1(1)	2(1)
C(3)	13(1)	22(1)	23(1)	-2(1)	2(1)	-1(1)
C(4)	20(1)	30(1)	22(1)	2(1)	6(1)	-2(1)
C(5)	22(1)	21(1)	19(1)	4(1)	2(1)	1(1)
C(6)	20(1)	20(1)	17(1)	2(1)	0(1)	3(1)
C(7)	15(1)	23(1)	22(1)	0(1)	-2(1)	4(1)
C(8)	14(1)	21(1)	23(1)	-1(1)	2(1)	-1(1)
C(9)	18(1)	15(1)	18(1)	0(1)	3(1)	-1(1)
C(10)	17(1)	17(1)	16(1)	1(1)	1(1)	-1(1)
C(11)	22(1)	26(1)	21(1)	0(1)	-8(1)	-2(1)
C(12)	23(1)	31(1)	21(1)	-4(1)	-2(1)	1(1)

Table 5. Hydrogen coordinates (x 10^4) and isotropic displacement parameters ($Å^2$x 10^3) for xen10.

	x	y	z	U(eq)
H(3A)	5400	7417	1641	23
H(3B)	4985	8978	2131	23
H(4A)	4501	9759	759	29
H(4B)	3680	8117	475	29
H(5)	1978	10524	1317	25
H(7A)	-1957	8929	1036	24
H(7B)	-872	10227	1555	24
H(8A)	-1908	8086	2420	23
H(8B)	-619	6964	1992	23
H(9)	210	9092	3267	20
H(11A)	6465	9411	4159	36
H(11B)	6859	7628	4380	36
H(11C)	5411	8530	4826	36
H(12A)	-207	7658	-191	38
H(12B)	-237	6551	607	38
H(12C)	1517	6955	228	38

Table 6. Torsion angles [°] for xen10.

C(9)-C(1)-C(2)-O(1)	-56.5(2)
C(10)-C(1)-C(2)-O(1)	123.67(15)
C(9)-C(1)-C(2)-C(3)	121.87(16)
C(10)-C(1)-C(2)-C(3)	-57.94(17)
O(1)-C(2)-C(3)-C(4)	83.34(17)
C(1)-C(2)-C(3)-C(4)	-95.04(15)
C(2)-C(3)-C(4)-C(5)	38.65(17)
C(3)-C(4)-C(5)-C(6)	-95.57(18)
C(4)-C(5)-C(6)-C(7)	153.90(15)
C(4)-C(5)-C(6)-C(12)	-15.7(2)
C(5)-C(6)-C(7)-C(8)	-88.70(17)
C(12)-C(6)-C(7)-C(8)	81.92(16)
C(6)-C(7)-C(8)-C(9)	72.13(16)
C(10)-C(1)-C(9)-C(8)	-179.84(14)
C(2)-C(1)-C(9)-C(8)	0.4(3)
C(7)-C(8)-C(9)-C(1)	-79.7(2)
C(11)-O(3)-C(10)-O(2)	-3.4(2)
C(11)-O(3)-C(10)-C(1)	177.79(12)
C(9)-C(1)-C(10)-O(2)	-22.8(2)
C(2)-C(1)-C(10)-O(2)	156.98(15)
C(9)-C(1)-C(10)-O(3)	155.96(13)
C(2)-C(1)-C(10)-O(3)	-24.22(17)

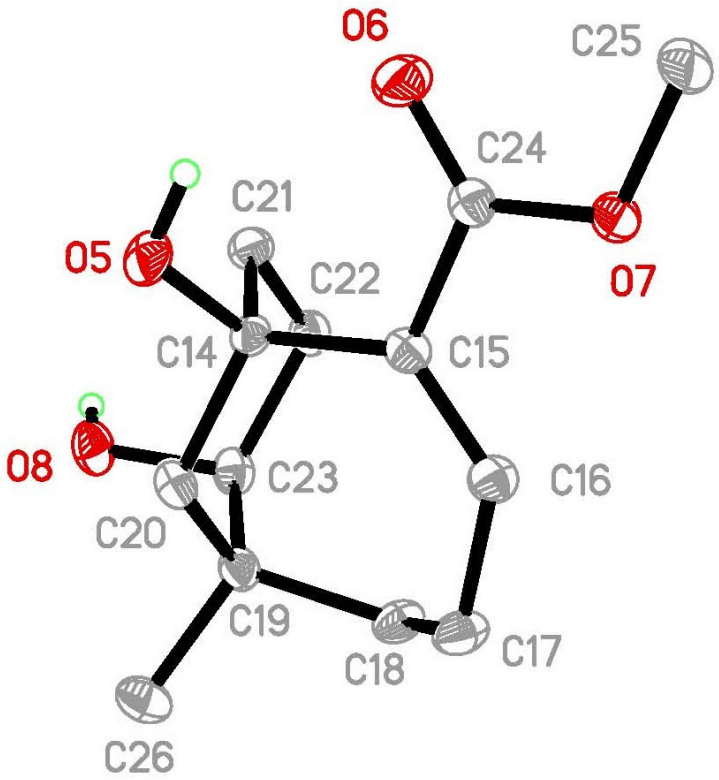

X-ray crystal structure of **3.73** (racemic, note the intramolecular H-bond).

Table 1. Crystal data and structure refinement for md401unk_sub.

Identification code	md401unk_sub	
Empirical formula	C13 H20 O4	
Formula weight	240.29	
Temperature	100(2) K	
Wavelength	0.71073 Å	
Crystal system	Triclinic	
Space group	P-1	
Unit cell dimensions	a = 10.0327(12) Å	α= 93.387(2)°.
	b = 14.8625(18) Å	β= 105.966(2)°.
	c = 8.4668(10) Å	γ = 91.067(2)°.
Volume	1210.9(3) $Å^3$	
Z	4	
Density (calculated)	1.318 Mg/m^3	
Absorption coefficient	0.096 mm^{-1}	
F(000)	520	
Crystal size	0.31 x 0.25 x 0.13 mm^3	
Theta range for data collection	2.11 to 29.57°.	
Index ranges	-13<=h<=13, -20<=k<=20, -11<=l<=11	
Reflections collected	13398	
Independent reflections	6701 [R(int) = 0.0363]	
Completeness to theta = 29.57°	98.5 %	
Absorption correction	Semi-empirical from equivalents	
Max. and min. transmission	0.746 and 0.648	
Refinement method	Full-matrix least-squares on F^2	
Data / restraints / parameters	6701 / 1680 / 622	
Goodness-of-fit on F^2	1.003	
Final R indices [I>2sigma(I)]	R1 = 0.0669, wR2 = 0.1541	
R indices (all data)	R1 = 0.0922, wR2 = 0.1626	
Largest diff. peak and hole	0.348 and -0.243 $e.Å^{-3}$	

Table 2. Atomic coordinates (x 10^4) and equivalent isotropic displacement parameters ($Å^2$x 10^3) for md401unk_sub. U(eq) is defined as one third of the trace of the orthogonalized U^{ij} tensor.

	x	y	z	U(eq)
O(1)	2904(2)	-1739(1)	-1898(2)	23(1)
O(2)	1584(8)	-400(3)	-3597(6)	27(1)
O(3)	2256(2)	979(1)	-2408(2)	24(1)
O(4)	1332(2)	-2617(1)	2190(2)	25(1)
C(1)	2479(3)	-1263(2)	-584(4)	17(1)
C(2)	2717(2)	-254(2)	-687(3)	17(1)
C(3)	3435(2)	335(2)	523(3)	22(1)
C(4)	4105(2)	180(2)	2308(3)	24(1)
C(5)	3169(5)	-362(2)	3103(6)	22(1)
C(6)	2979(4)	-1379(2)	2578(4)	19(1)
C(7)	3379(2)	-1636(2)	979(3)	20(1)
C(8)	950(2)	-1524(1)	-759(3)	19(1)
C(9)	506(2)	-1260(1)	790(3)	18(1)
C(10)	1451(2)	-1654(1)	2324(3)	18(1)
C(11)	2131(4)	86(2)	-2364(4)	20(1)
C(12)	1762(4)	1321(2)	-4030(4)	28(1)
C(13)	3909(3)	-1905(2)	3943(3)	27(1)
O(5)	1264(2)	3359(1)	-2103(2)	22(1)
O(6)	1874(9)	4775(4)	-3608(6)	29(1)
O(7)	1461(2)	6071(1)	-2432(2)	20(1)
O(8)	4528(2)	2386(1)	1941(2)	22(1)
C(14)	2279(3)	3820(2)	-717(3)	14(1)
C(15)	1994(2)	4825(1)	-746(2)	15(1)
C(16)	1830(2)	5372(1)	498(2)	18(1)
C(17)	2002(2)	5180(2)	2270(3)	21(1)
C(18)	3266(4)	4632(2)	3030(5)	18(1)
C(19)	3150(4)	3621(2)	2420(4)	17(1)
C(20)	2033(2)	3401(1)	788(2)	17(1)
C(21)	3732(2)	3578(1)	-850(3)	17(1)
C(22)	4877(2)	3790(1)	753(3)	18(1)
C(23)	4559(2)	3342(1)	2200(3)	18(1)

C(24)	1802(3)	5208(2)	-2392(4)	16(1)
C(25)	1245(3)	6444(2)	-4027(3)	22(1)
C(26)	2771(2)	3066(2)	3727(3)	24(1)
O(101)	1148(9)	-1650(6)	-1991(9)	30(2)
O(102)	1840(40)	-302(15)	-3620(30)	20(4)
O(103)	1572(11)	1048(6)	-2430(11)	25(2)
O(104)	4571(8)	-2570(5)	2061(11)	28(2)
C(101)	2183(14)	-1197(9)	-664(15)	19(3)
C(102)	1992(14)	-186(6)	-735(12)	22(2)
C(103)	1846(13)	382(7)	470(11)	25(2)
C(104)	2038(13)	230(8)	2264(12)	28(2)
C(105)	3360(20)	-303(10)	3000(30)	23(4)
C(106)	3182(17)	-1329(10)	2457(17)	22(3)
C(107)	2011(11)	-1578(7)	898(11)	23(2)
C(108)	3637(10)	-1448(7)	-858(12)	24(2)
C(109)	4844(11)	-1203(7)	715(12)	26(2)
C(110)	4577(10)	-1617(6)	2208(13)	23(2)
C(111)	1780(20)	167(10)	-2412(18)	21(3)
C(112)	1355(18)	1435(13)	-4010(20)	27(4)
C(113)	2868(13)	-1869(7)	3835(13)	26(2)
O(105)	3028(9)	3392(5)	-1843(10)	25(2)
O(106)	1990(40)	4710(18)	-3570(30)	21(5)
O(107)	2239(10)	6096(5)	-2338(10)	22(2)
O(108)	1379(9)	2450(5)	2076(11)	29(2)
C(114)	2569(16)	3839(9)	-553(16)	25(3)
C(115)	2756(13)	4858(6)	-650(11)	18(2)
C(116)	3428(12)	5462(7)	575(11)	24(2)
C(117)	4023(12)	5306(7)	2370(12)	23(2)
C(118)	3000(20)	4773(9)	3050(30)	23(4)
C(119)	2958(17)	3756(10)	2574(17)	26(3)
C(120)	3448(11)	3505(7)	1058(12)	24(2)
C(121)	1012(11)	3562(7)	-871(13)	25(2)
C(122)	470(10)	3777(7)	648(12)	22(2)
C(123)	1433(10)	3417(6)	2210(13)	24(2)
C(124)	2207(18)	5196(9)	-2330(17)	20(3)
C(125)	1869(18)	6479(11)	-3928(17)	32(3)

C(126)	3863(12)	3252(8)	3989(15)	30(2)

Table 3. Bond lengths [Å] and angles [°] for md401unk_sub.

_____

O(1)-C(1)	1.449(3)	C(13)-H(13B)	0.9600
O(1)-H(1)	0.8200	C(13)-H(13C)	0.9600
O(2)-C(11)	1.222(5)	O(5)-C(14)	1.451(3)
O(3)-C(11)	1.334(4)	O(5)-H(5)	0.8200
O(3)-C(12)	1.452(3)	O(6)-C(24)	1.201(4)
O(4)-C(10)	1.429(2)	O(7)-C(24)	1.334(3)
O(4)-H(4)	0.8200	O(7)-C(25)	1.453(3)
C(1)-C(7)	1.523(3)	O(8)-C(23)	1.423(2)
C(1)-C(2)	1.525(3)	O(8)-H(8)	0.8200
C(1)-C(8)	1.540(4)	C(14)-C(15)	1.526(3)
C(2)-C(3)	1.342(3)	C(14)-C(20)	1.528(3)
C(2)-C(11)	1.502(4)	C(14)-C(21)	1.540(4)
C(3)-C(4)	1.509(3)	C(15)-C(16)	1.340(3)
C(3)-H(3)	0.9300	C(15)-C(24)	1.501(3)
C(4)-C(5)	1.539(5)	C(16)-C(17)	1.507(3)
C(4)-H(4A)	0.9700	C(16)-H(16)	0.9300
C(4)-H(4B)	0.9700	C(17)-C(18)	1.530(4)
C(5)-C(6)	1.544(4)	C(17)-H(17A)	0.9700
C(5)-H(5A)	0.9700	C(17)-H(17B)	0.9700
C(5)-H(5B)	0.9700	C(18)-C(19)	1.551(4)
C(6)-C(10)	1.533(4)	C(18)-H(18A)	0.9700
C(6)-C(13)	1.535(4)	C(18)-H(18B)	0.9700
C(6)-C(7)	1.543(4)	C(19)-C(20)	1.534(4)
C(7)-H(7A)	0.9700	C(19)-C(23)	1.537(4)
C(7)-H(7B)	0.9700	C(19)-C(26)	1.541(4)
C(8)-C(9)	1.530(3)	C(20)-H(20A)	0.9700
C(8)-H(8A)	0.9700	C(20)-H(20B)	0.9700
C(8)-H(8B)	0.9700	C(21)-C(22)	1.529(3)
C(9)-C(10)	1.536(3)	C(21)-H(21A)	0.9700
C(9)-H(9A)	0.9700	C(21)-H(21B)	0.9700
C(9)-H(9B)	0.9700	C(22)-C(23)	1.532(3)
C(10)-H(10)	0.9800	C(22)-H(22A)	0.9700
C(12)-H(12A)	0.9600	C(22)-H(22B)	0.9700
C(12)-H(12B)	0.9600	C(23)-H(23)	0.9800
C(12)-H(12C)	0.9600	C(25)-H(25A)	0.9600
C(13)-H(13A)	0.9600	C(25)-H(25B)	0.9600

C(25)-H(25C)	0.9600	C(112)-H(11A)	0.9600
C(26)-H(26A)	0.9600	C(112)-H(11B)	0.9600
C(26)-H(26B)	0.9600	C(112)-H(11C)	0.9600
C(26)-H(26C)	0.9600	C(113)-H(11D)	0.9600
O(101)-C(101)	1.427(13)	C(113)-H(11E)	0.9600
O(101)-H(101)	0.8200	C(113)-H(11F)	0.9600
O(102)-C(111)	1.217(14)	O(105)-C(114)	1.431(14)
O(103)-C(111)	1.331(13)	O(105)-H(105)	0.8200
O(103)-C(112)	1.451(13)	O(106)-C(124)	1.205(14)
O(104)-C(110)	1.413(10)	O(107)-C(124)	1.337(12)
O(104)-H(104)	0.8200	O(107)-C(125)	1.449(12)
C(101)-C(107)	1.519(13)	O(108)-C(123)	1.433(11)
C(101)-C(102)	1.521(13)	O(108)-H(108)	0.8200
C(101)-C(108)	1.563(14)	C(114)-C(120)	1.524(13)
C(102)-C(103)	1.326(11)	C(114)-C(115)	1.531(13)
C(102)-C(111)	1.504(13)	C(114)-C(121)	1.554(15)
C(103)-C(104)	1.509(11)	C(115)-C(116)	1.349(11)
C(103)-H(103)	0.9300	C(115)-C(124)	1.498(12)
C(104)-C(105)	1.553(16)	C(116)-C(117)	1.506(11)
C(104)-H(10A)	0.9700	C(116)-H(116)	0.9300
C(104)-H(10B)	0.9700	C(117)-C(118)	1.538(15)
C(105)-C(106)	1.558(14)	C(117)-H(11G)	0.9700
C(105)-H(10C)	0.9700	C(117)-H(11H)	0.9700
C(105)-H(10D)	0.9700	C(118)-C(119)	1.538(14)
C(106)-C(107)	1.527(14)	C(118)-H(11I)	0.9700
C(106)-C(110)	1.537(15)	C(118)-H(11J)	0.9700
C(106)-C(113)	1.551(14)	C(119)-C(120)	1.524(14)
C(107)-H(10E)	0.9700	C(119)-C(126)	1.534(14)
C(107)-H(10F)	0.9700	C(119)-C(123)	1.544(16)
C(108)-C(109)	1.553(12)	C(120)-H(12D)	0.9700
C(108)-H(10G)	0.9700	C(120)-H(12E)	0.9700
C(108)-H(10H)	0.9700	C(121)-C(122)	1.547(12)
C(109)-C(110)	1.523(12)	C(121)-H(12F)	0.9700
C(109)-H(10I)	0.9700	C(121)-H(12G)	0.9700
C(109)-H(10J)	0.9700	C(122)-C(123)	1.540(11)
C(110)-H(110)	0.9800	C(122)-H(12H)	0.9700

C(122)-H(12I)	0.9700
C(123)-H(123)	0.9800
C(125)-H(12J)	0.9600
C(125)-H(12K)	0.9600
C(125)-H(12L)	0.9600
C(126)-H(12M)	0.9600
C(126)-H(12N)	0.9600
C(126)-H(12O)	0.9600

C(11)-O(3)-C(12)	115.3(2)
O(1)-C(1)-C(7)	104.1(2)
O(1)-C(1)-C(2)	108.2(2)
C(7)-C(1)-C(2)	113.8(2)
O(1)-C(1)-C(8)	108.7(2)
C(7)-C(1)-C(8)	108.8(2)
C(2)-C(1)-C(8)	112.7(2)
C(3)-C(2)-C(11)	117.9(2)
C(3)-C(2)-C(1)	127.2(2)
C(11)-C(2)-C(1)	114.9(2)
C(2)-C(3)-C(4)	128.8(2)
C(2)-C(3)-H(3)	115.6
C(4)-C(3)-H(3)	115.6
C(3)-C(4)-C(5)	113.5(2)
C(3)-C(4)-H(4A)	108.9
C(5)-C(4)-H(4A)	108.9
C(3)-C(4)-H(4B)	108.9
C(5)-C(4)-H(4B)	108.9
H(4A)-C(4)-H(4B)	107.7
C(4)-C(5)-C(6)	115.6(3)
C(4)-C(5)-H(5A)	108.4
C(6)-C(5)-H(5A)	108.4
C(4)-C(5)-H(5B)	108.4
C(6)-C(5)-H(5B)	108.4
H(5A)-C(5)-H(5B)	107.4
C(10)-C(6)-C(13)	110.2(2)
C(10)-C(6)-C(7)	108.8(2)
C(13)-C(6)-C(7)	107.1(2)
C(10)-C(6)-C(5)	108.0(3)
C(13)-C(6)-C(5)	108.9(3)
C(7)-C(6)-C(5)	113.7(3)
C(1)-C(7)-C(6)	116.0(2)
C(1)-C(7)-H(7A)	108.3
C(6)-C(7)-H(7A)	108.3
C(1)-C(7)-H(7B)	108.3
C(6)-C(7)-H(7B)	108.3

H(7A)-C(7)-H(7B)	107.4	O(5)-C(14)-C(20)	104.3(2)
C(9)-C(8)-C(1)	112.80(19)	C(15)-C(14)-C(20)	112.8(2)
C(9)-C(8)-H(8A)	109.0	O(5)-C(14)-C(21)	107.9(2)
C(1)-C(8)-H(8A)	109.0	C(15)-C(14)-C(21)	114.7(2)
C(9)-C(8)-H(8B)	109.0	C(20)-C(14)-C(21)	108.9(2)
C(1)-C(8)-H(8B)	109.0	C(16)-C(15)-C(24)	118.0(2)
H(8A)-C(8)-H(8B)	107.8	C(16)-C(15)-C(14)	127.1(2)
C(8)-C(9)-C(10)	111.82(17)	C(24)-C(15)-C(14)	114.8(2)
C(8)-C(9)-H(9A)	109.3	C(15)-C(16)-C(17)	129.34(19)
C(10)-C(9)-H(9A)	109.3	C(15)-C(16)-H(16)	115.3
C(8)-C(9)-H(9B)	109.3	C(17)-C(16)-H(16)	115.3
C(10)-C(9)-H(9B)	109.3	C(16)-C(17)-C(18)	114.5(2)
H(9A)-C(9)-H(9B)	107.9	C(16)-C(17)-H(17A)	108.6
O(4)-C(10)-C(6)	107.93(19)	C(18)-C(17)-H(17A)	108.6
O(4)-C(10)-C(9)	110.79(17)	C(16)-C(17)-H(17B)	108.6
C(6)-C(10)-C(9)	111.78(19)	C(18)-C(17)-H(17B)	108.6
O(4)-C(10)-H(10)	108.8	H(17A)-C(17)-H(17B)	107.6
C(6)-C(10)-H(10)	108.8	C(17)-C(18)-C(19)	115.2(3)
C(9)-C(10)-H(10)	108.8	C(17)-C(18)-H(18A)	108.5
O(2)-C(11)-O(3)	121.9(4)	C(19)-C(18)-H(18A)	108.5
O(2)-C(11)-C(2)	124.0(4)	C(17)-C(18)-H(18B)	108.5
O(3)-C(11)-C(2)	114.1(3)	C(19)-C(18)-H(18B)	108.5
O(3)-C(12)-H(12A)	109.5	H(18A)-C(18)-H(18B)	107.5
O(3)-C(12)-H(12B)	109.5	C(20)-C(19)-C(23)	108.5(2)
H(12A)-C(12)-H(12B)	109.5	C(20)-C(19)-C(26)	107.3(2)
O(3)-C(12)-H(12C)	109.5	C(23)-C(19)-C(26)	110.2(2)
H(12A)-C(12)-H(12C)	109.5	C(20)-C(19)-C(18)	114.0(2)
H(12B)-C(12)-H(12C)	109.5	C(23)-C(19)-C(18)	108.5(2)
C(6)-C(13)-H(13A)	109.5	C(26)-C(19)-C(18)	108.4(3)
C(6)-C(13)-H(13B)	109.5	C(14)-C(20)-C(19)	115.9(2)
H(13A)-C(13)-H(13B)	109.5	C(14)-C(20)-H(20A)	108.3
C(6)-C(13)-H(13C)	109.5	C(19)-C(20)-H(20A)	108.3
H(13A)-C(13)-H(13C)	109.5	C(14)-C(20)-H(20B)	108.3
H(13B)-C(13)-H(13C)	109.5	C(19)-C(20)-H(20B)	108.3
C(24)-O(7)-C(25)	114.8(2)	H(20A)-C(20)-H(20B)	107.4
O(5)-C(14)-C(15)	107.8(2)	C(22)-C(21)-C(14)	113.26(18)

C(22)-C(21)-H(21A)	108.9	O(101)-C(101)-C(102)	108.8(9)
C(14)-C(21)-H(21A)	108.9	C(107)-C(101)-C(102)	114.2(10)
C(22)-C(21)-H(21B)	108.9	O(101)-C(101)-C(108)	108.1(10)
C(14)-C(21)-H(21B)	108.9	C(107)-C(101)-C(108)	108.6(9)
H(21A)-C(21)-H(21B)	107.7	C(102)-C(101)-C(108)	110.8(11)
C(21)-C(22)-C(23)	111.70(17)	C(103)-C(102)-C(111)	117.8(9)
C(21)-C(22)-H(22A)	109.3	C(103)-C(102)-C(101)	126.7(9)
C(23)-C(22)-H(22A)	109.3	C(111)-C(102)-C(101)	115.1(9)
C(21)-C(22)-H(22B)	109.3	C(102)-C(103)-C(104)	129.5(9)
C(23)-C(22)-H(22B)	109.3	C(102)-C(103)-H(103)	115.3
H(22A)-C(22)-H(22B)	107.9	C(104)-C(103)-H(103)	115.3
O(8)-C(23)-C(22)	110.53(17)	C(103)-C(104)-C(105)	112.0(12)
O(8)-C(23)-C(19)	108.22(18)	C(103)-C(104)-H(10A)	109.2
C(22)-C(23)-C(19)	111.37(18)	C(105)-C(104)-H(10A)	109.2
O(8)-C(23)-H(23)	108.9	C(103)-C(104)-H(10B)	109.2
C(22)-C(23)-H(23)	108.9	C(105)-C(104)-H(10B)	109.2
C(19)-C(23)-H(23)	108.9	H(10A)-C(104)-H(10B)	107.9
O(6)-C(24)-O(7)	121.7(4)	C(104)-C(105)-C(106)	113.3(13)
O(6)-C(24)-C(15)	123.9(4)	C(104)-C(105)-H(10C)	108.9
O(7)-C(24)-C(15)	114.3(2)	C(106)-C(105)-H(10C)	108.9
O(7)-C(25)-H(25A)	109.5	C(104)-C(105)-H(10D)	108.9
O(7)-C(25)-H(25B)	109.5	C(106)-C(105)-H(10D)	108.9
H(25A)-C(25)-H(25B)	109.5	H(10C)-C(105)-H(10D)	107.7
O(7)-C(25)-H(25C)	109.5	C(107)-C(106)-C(110)	110.1(10)
H(25A)-C(25)-H(25C)	109.5	C(107)-C(106)-C(113)	106.4(11)
H(25B)-C(25)-H(25C)	109.5	C(110)-C(106)-C(113)	108.9(10)
C(19)-C(26)-H(26A)	109.5	C(107)-C(106)-C(105)	114.8(11)
C(19)-C(26)-H(26B)	109.5	C(110)-C(106)-C(105)	106.4(13)
H(26A)-C(26)-H(26B)	109.5	C(113)-C(106)-C(105)	110.2(13)
C(19)-C(26)-H(26C)	109.5	C(101)-C(107)-C(106)	115.5(9)
H(26A)-C(26)-H(26C)	109.5	C(101)-C(107)-H(10E)	108.4
H(26B)-C(26)-H(26C)	109.5	C(106)-C(107)-H(10E)	108.4
C(101)-O(101)-H(101)	109.5	C(101)-C(107)-H(10F)	108.4
C(111)-O(103)-C(112)	116.2(11)	C(106)-C(107)-H(10F)	108.4
C(110)-O(104)-H(104)	109.5	H(10E)-C(107)-H(10F)	107.5
O(101)-C(101)-C(107)	106.0(10)	C(109)-C(108)-C(101)	113.4(8)

C(109)-C(108)-H(10G)	108.9	O(105)-C(114)-C(115)	108.0(10)
C(101)-C(108)-H(10G)	108.9	C(120)-C(114)-C(115)	112.6(10)
C(109)-C(108)-H(10H)	108.9	O(105)-C(114)-C(121)	106.7(10)
C(101)-C(108)-H(10H)	108.9	C(120)-C(114)-C(121)	111.5(10)
H(10G)-C(108)-H(10H)	107.7	C(115)-C(114)-C(121)	110.9(11)
C(110)-C(109)-C(108)	111.0(8)	C(116)-C(115)-C(124)	117.3(9)
C(110)-C(109)-H(10I)	109.4	C(116)-C(115)-C(114)	127.3(9)
C(108)-C(109)-H(10I)	109.4	C(124)-C(115)-C(114)	115.3(9)
C(110)-C(109)-H(10J)	109.4	C(115)-C(116)-C(117)	127.8(9)
C(108)-C(109)-H(10J)	109.4	C(115)-C(116)-H(116)	116.1
H(10I)-C(109)-H(10J)	108.0	C(117)-C(116)-H(116)	116.1
O(104)-C(110)-C(109)	111.9(8)	C(116)-C(117)-C(118)	112.0(11)
O(104)-C(110)-C(106)	108.4(9)	C(116)-C(117)-H(11G)	109.2
C(109)-C(110)-C(106)	111.1(9)	C(118)-C(117)-H(11G)	109.2
O(104)-C(110)-H(110)	108.4	C(116)-C(117)-H(11H)	109.2
C(109)-C(110)-H(110)	108.4	C(118)-C(117)-H(11H)	109.2
C(106)-C(110)-H(110)	108.4	H(11G)-C(117)-H(11H)	107.9
O(102)-C(111)-O(103)	123.5(16)	C(117)-C(118)-C(119)	112.4(12)
O(102)-C(111)-C(102)	123.3(16)	C(117)-C(118)-H(11I)	109.1
O(103)-C(111)-C(102)	113.1(11)	C(119)-C(118)-H(11I)	109.1
O(103)-C(112)-H(11A)	109.5	C(117)-C(118)-H(11J)	109.1
O(103)-C(112)-H(11B)	109.5	C(119)-C(118)-H(11J)	109.1
H(11A)-C(112)-H(11B)	109.5	H(11I)-C(118)-H(11J)	107.9
O(103)-C(112)-H(11C)	109.5	C(120)-C(119)-C(126)	106.7(11)
H(11A)-C(112)-H(11C)	109.5	C(120)-C(119)-C(118)	115.1(12)
H(11B)-C(112)-H(11C)	109.5	C(126)-C(119)-C(118)	110.8(12)
C(106)-C(113)-H(11D)	109.5	C(120)-C(119)-C(123)	107.7(10)
C(106)-C(113)-H(11E)	109.5	C(126)-C(119)-C(123)	109.4(11)
H(11D)-C(113)-H(11E)	109.5	C(118)-C(119)-C(123)	107.0(12)
C(106)-C(113)-H(11F)	109.5	C(114)-C(120)-C(119)	115.6(10)
H(11D)-C(113)-H(11F)	109.5	C(114)-C(120)-H(12D)	108.4
H(11E)-C(113)-H(11F)	109.5	C(119)-C(120)-H(12D)	108.4
C(114)-O(105)-H(105)	109.5	C(114)-C(120)-H(12E)	108.4
C(124)-O(107)-C(125)	117.2(10)	C(119)-C(120)-H(12E)	108.4
C(123)-O(108)-H(108)	109.5	H(12D)-C(120)-H(12E)	107.5
O(105)-C(114)-C(120)	106.7(10)	C(122)-C(121)-C(114)	112.6(9)

C(122)-C(121)-H(12F)	109.1
C(114)-C(121)-H(12F)	109.1
C(122)-C(121)-H(12G)	109.1
C(114)-C(121)-H(12G)	109.1
H(12F)-C(121)-H(12G)	107.8
C(123)-C(122)-C(121)	111.3(8)
C(123)-C(122)-H(12H)	109.4
C(121)-C(122)-H(12H)	109.4
C(123)-C(122)-H(12I)	109.4
C(121)-C(122)-H(12I)	109.4
H(12H)-C(122)-H(12I)	108.0
O(108)-C(123)-C(122)	109.9(8)
O(108)-C(123)-C(119)	109.0(9)
C(122)-C(123)-C(119)	113.6(8)
O(108)-C(123)-H(123)	108.1
C(122)-C(123)-H(123)	108.1
C(119)-C(123)-H(123)	108.1
O(106)-C(124)-O(107)	122.6(17)
O(106)-C(124)-C(115)	122.6(17)
O(107)-C(124)-C(115)	113.6(11)
O(107)-C(125)-H(12J)	109.5
O(107)-C(125)-H(12K)	109.5
H(12J)-C(125)-H(12K)	109.5
O(107)-C(125)-H(12L)	109.5
H(12J)-C(125)-H(12L)	109.5
H(12K)-C(125)-H(12L)	109.5
C(119)-C(126)-H(12M)	109.5
C(119)-C(126)-H(12N)	109.5
H(12M)-C(126)-H(12N)	109.5
C(119)-C(126)-H(12O)	109.5
H(12M)-C(126)-H(12O)	109.5
H(12N)-C(126)-H(12O)	109.5

Table 4. Anisotropic displacement parameters ($Å^2 x\ 10^3$) for md401unk_sub. The anisotropic displacement factor exponent takes the form: $-2\pi^2[\ h^2\ a^{*2}U^{11} + ...\ + 2\ h\ k\ a^*\ b^*\ U^{12}\ ]$

	U^{11}	U^{22}	U^{33}	U^{23}	U^{13}	U^{12}
O(1)	29(1)	27(1)	15(1)	2(1)	8(1)	10(1)
O(2)	31(3)	30(2)	16(1)	0(1)	0(1)	0(1)
O(3)	33(1)	21(1)	16(1)	5(1)	6(1)	2(1)
O(4)	24(1)	17(1)	33(1)	3(1)	8(1)	0(1)
C(1)	16(1)	19(1)	15(1)	-1(1)	4(1)	2(1)
C(2)	15(1)	22(1)	15(1)	2(1)	5(1)	3(1)
C(3)	22(1)	26(1)	17(1)	4(1)	5(1)	-2(1)
C(4)	26(1)	27(1)	15(1)	2(1)	1(1)	-8(1)
C(5)	24(2)	28(2)	14(1)	-1(1)	7(1)	-10(1)
C(6)	20(1)	24(1)	14(1)	0(1)	6(1)	-2(1)
C(7)	17(1)	27(1)	16(1)	4(1)	4(1)	3(1)
C(8)	18(1)	18(1)	18(1)	-2(1)	1(1)	-1(1)
C(9)	16(1)	16(1)	23(1)	0(1)	6(1)	0(1)
C(10)	19(1)	17(1)	20(1)	0(1)	9(1)	-1(1)
C(11)	18(2)	23(1)	18(1)	4(1)	6(1)	4(1)
C(12)	38(2)	27(2)	19(1)	9(1)	8(1)	9(1)
C(13)	23(1)	38(1)	19(1)	7(1)	2(1)	-1(1)
O(5)	25(1)	20(1)	15(1)	-2(1)	-2(1)	-5(1)
O(6)	49(4)	21(2)	17(2)	4(1)	8(2)	10(2)
O(7)	30(1)	16(1)	14(1)	4(1)	3(1)	2(1)
O(8)	23(1)	15(1)	30(1)	6(1)	7(1)	3(1)
C(14)	17(1)	13(1)	11(1)	0(1)	1(1)	0(1)
C(15)	14(1)	18(1)	13(1)	2(1)	2(1)	0(1)
C(16)	19(1)	18(1)	16(1)	3(1)	4(1)	4(1)
C(17)	28(1)	23(1)	15(1)	2(1)	7(1)	8(1)
C(18)	20(2)	21(1)	13(1)	1(1)	3(1)	6(1)
C(19)	19(1)	15(1)	15(1)	3(1)	3(1)	-1(1)
C(20)	17(1)	16(1)	18(1)	4(1)	4(1)	-1(1)
C(21)	20(1)	17(1)	16(1)	1(1)	6(1)	2(1)
C(22)	17(1)	16(1)	20(1)	1(1)	6(1)	0(1)
C(23)	17(1)	16(1)	19(1)	3(1)	2(1)	0(1)
C(24)	14(1)	17(1)	17(1)	1(1)	3(1)	-1(1)

C(25)	30(2)	20(1)	14(1)	6(1)	0(1)	1(1)
C(26)	26(1)	27(1)	19(1)	9(1)	8(1)	3(1)
O(101)	38(4)	31(4)	20(4)	-7(3)	11(3)	-8(4)
O(102)	23(9)	21(6)	17(5)	0(4)	8(5)	0(5)
O(103)	33(5)	16(4)	28(4)	8(3)	8(4)	8(4)
O(104)	30(4)	18(4)	35(5)	4(3)	8(4)	-2(3)
C(101)	25(4)	22(4)	11(4)	-4(3)	8(3)	6(3)
C(102)	29(5)	18(4)	18(4)	1(3)	4(4)	3(4)
C(103)	41(5)	15(4)	19(4)	5(3)	6(4)	3(4)
C(104)	38(5)	27(5)	20(4)	5(4)	7(4)	12(4)
C(105)	26(6)	24(6)	14(6)	-2(5)	-1(5)	13(5)
C(106)	18(4)	21(4)	23(4)	8(3)	-1(3)	3(3)
C(107)	32(4)	17(4)	20(4)	6(3)	7(3)	-4(3)
C(108)	30(5)	21(4)	23(4)	-1(4)	10(4)	2(4)
C(109)	25(5)	22(5)	32(5)	-1(4)	13(4)	1(4)
C(110)	23(4)	16(4)	31(5)	3(4)	10(4)	2(4)
C(111)	27(7)	22(5)	18(5)	7(4)	10(4)	4(5)
C(112)	30(6)	29(5)	23(5)	9(4)	5(4)	2(4)
C(113)	35(6)	19(5)	24(5)	1(4)	10(4)	0(4)
O(105)	32(4)	10(3)	34(4)	4(3)	11(4)	3(3)
O(106)	13(6)	36(9)	14(7)	-5(7)	5(5)	6(6)
O(107)	28(3)	14(3)	25(3)	4(2)	7(3)	5(3)
O(108)	32(3)	20(3)	37(3)	10(3)	11(3)	-2(3)
C(114)	30(6)	16(5)	22(5)	0(4)	-5(4)	-4(4)
C(115)	25(4)	10(4)	22(4)	2(3)	9(4)	3(4)
C(116)	36(5)	14(4)	23(4)	2(4)	9(4)	1(4)
C(117)	34(5)	13(4)	21(4)	-4(3)	9(4)	-3(4)
C(118)	29(7)	15(5)	26(6)	5(5)	12(5)	-6(5)
C(119)	25(5)	29(5)	27(5)	8(5)	9(4)	6(4)
C(120)	33(4)	10(4)	27(4)	3(3)	5(4)	4(3)
C(121)	34(5)	9(4)	33(5)	7(4)	10(4)	-1(4)
C(122)	25(4)	16(4)	26(5)	5(4)	8(4)	-5(4)
C(123)	26(3)	18(3)	29(3)	10(3)	8(3)	0(3)
C(124)	27(7)	10(4)	23(5)	1(4)	4(5)	4(5)
C(125)	42(8)	28(6)	21(6)	-3(5)	2(7)	13(7)
C(126)	31(6)	23(5)	39(6)	10(5)	13(5)	6(4)

Table 5. Hydrogen coordinates (x 10^4) and isotropic displacement parameters ($Å^2$x 10^3) for md401unk_sub.

	x	y	z	U(eq)
H(1)	2505	-1539	-2780	35
H(4)	524	-2779	2081	37
H(3)	3532	919	220	26
H(4A)	4354	760	2920	29
H(4B)	4953	-139	2390	29
H(5A)	2262	-100	2841	26
H(5B)	3554	-293	4289	26
H(7A)	4331	-1428	1128	24
H(7B)	3350	-2288	821	24
H(8A)	366	-1231	-1681	23
H(8B)	808	-2170	-1002	23
H(9A)	-442	-1476	639	22
H(9B)	534	-608	956	22
H(10)	1168	-1432	3292	22
H(12A)	1891	1966	-3942	41
H(12B)	795	1161	-4481	41
H(12C)	2275	1064	-4738	41
H(13A)	4862	-1728	4089	41
H(13B)	3775	-2539	3641	41
H(13C)	3670	-1775	4954	41
H(5)	1304	3576	-2958	33
H(8)	5297	2222	1909	34
H(16)	1573	5953	229	22
H(17A)	1175	4856	2343	26
H(17B)	2074	5749	2915	26
H(18A)	3427	4672	4216	22
H(18B)	4071	4905	2798	22
H(20A)	1952	2751	573	21
H(20B)	1151	3600	918	21
H(21A)	3726	2940	-1168	21

H(21B)	3940	3909	-1712	21
H(22A)	4974	4438	995	21
H(22B)	5750	3580	616	21
H(23)	5288	3526	3209	21
H(25A)	1007	7065	-3948	33
H(25B)	505	6110	-4821	33
H(25C)	2080	6405	-4368	33
H(26A)	3452	3188	4768	36
H(26B)	2749	2435	3400	36
H(26C)	1875	3230	3827	36
H(101)	1151	-1431	-2856	44
H(104)	5356	-2735	2107	42
H(103)	1587	958	164	30
H(10A)	1231	-100	2381	34
H(10B)	2107	809	2880	34
H(10C)	3594	-230	4188	27
H(10D)	4124	-49	2655	27
H(10E)	1927	-2230	729	28
H(10F)	1149	-1370	1074	28
H(10G)	3629	-2091	-1137	29
H(10H)	3804	-1138	-1765	29
H(10I)	5704	-1421	549	31
H(10J)	4943	-553	913	31
H(110)	5318	-1404	3186	27
H(11A)	1210	2069	-3889	41
H(11B)	556	1146	-4784	41
H(11C)	2156	1346	-4406	41
H(11D)	2000	-1691	4003	38
H(11E)	3595	-1749	4837	38
H(11F)	2815	-2502	3516	38
H(105)	3238	3768	-2412	37
H(108)	570	2265	1862	44
H(116)	3537	6045	275	29
H(11G)	4259	5883	2993	27
H(11H)	4870	4977	2510	27
H(11I)	2080	5002	2639	27

H(11J)	3269	4867	4244	27
H(12D)	4390	3742	1252	29
H(12E)	3472	2853	933	29
H(12F)	468	3876	-1790	30
H(12G)	885	2920	-1173	30
H(12H)	409	4425	812	26
H(12I)	-453	3507	450	26
H(123)	1092	3616	3147	29
H(12J)	1928	7125	-3775	48
H(12K)	939	6286	-4522	48
H(12L)	2496	6281	-4542	48
H(12M)	3575	3381	4967	45
H(12N)	4816	3444	4184	45
H(12O)	3763	2615	3701	45

Table 6. Torsion angles [°] for md401unk_sub.

_____

O(1)-C(1)-C(2)-C(3)	-126.8(3)	C(1)-C(2)-C(11)-O(3)	175.2(3)
C(7)-C(1)-C(2)-C(3)	-11.5(4)	O(5)-C(14)-C(15)-C(16)	128.2(2)
C(8)-C(1)-C(2)-C(3)	113.0(3)	C(20)-C(14)-C(15)-C(16)	13.7(4)
O(1)-C(1)-C(2)-C(11)	49.9(3)	C(21)-C(14)-C(15)-C(16)	-111.7(3)
C(7)-C(1)-C(2)-C(11)	165.1(2)	O(5)-C(14)-C(15)-C(24)	-48.1(3)
C(8)-C(1)-C(2)-C(11)	-70.4(3)	C(20)-C(14)-C(15)-C(24)	-162.6(2)
C(11)-C(2)-C(3)-C(4)	178.8(2)	C(21)-C(14)-C(15)-C(24)	72.1(3)
C(1)-C(2)-C(3)-C(4)	-4.6(4)	C(24)-C(15)-C(16)-C(17)	-177.9(2)
C(2)-C(3)-C(4)-C(5)	-45.4(4)	C(14)-C(15)-C(16)-C(17)	6.0(4)
C(3)-C(4)-C(5)-C(6)	73.6(4)	C(15)-C(16)-C(17)-C(18)	42.0(4)
C(4)-C(5)-C(6)-C(10)	-138.4(3)	C(16)-C(17)-C(18)-C(19)	-72.5(3)
C(4)-C(5)-C(6)-C(13)	101.8(3)	C(17)-C(18)-C(19)-C(20)	19.0(4)
C(4)-C(5)-C(6)-C(7)	-17.5(4)	C(17)-C(18)-C(19)-C(23)	140.0(3)
O(1)-C(1)-C(7)-C(6)	-169.4(2)	C(17)-C(18)-C(19)-C(26)	-100.4(3)
C(2)-C(1)-C(7)-C(6)	73.0(3)	O(5)-C(14)-C(20)-C(19)	168.1(2)
C(8)-C(1)-C(7)-C(6)	-53.6(3)	C(15)-C(14)-C(20)-C(19)	-75.3(3)
C(10)-C(6)-C(7)-C(1)	54.8(3)	C(21)-C(14)-C(20)-C(19)	53.2(3)
C(13)-C(6)-C(7)-C(1)	173.9(2)	C(23)-C(19)-C(20)-C(14)	-55.9(3)
C(5)-C(6)-C(7)-C(1)	-65.7(4)	C(26)-C(19)-C(20)-C(14)	-174.9(2)
O(1)-C(1)-C(8)-C(9)	165.05(18)	C(18)-C(19)-C(20)-C(14)	65.2(3)
C(7)-C(1)-C(8)-C(9)	52.2(3)	O(5)-C(14)-C(21)-C(22)	-163.52(18)
C(2)-C(1)-C(8)-C(9)	-75.0(3)	C(15)-C(14)-C(21)-C(22)	76.4(2)
C(1)-C(8)-C(9)-C(10)	-55.1(2)	C(20)-C(14)-C(21)-C(22)	-51.0(3)
C(13)-C(6)-C(10)-O(4)	-48.8(3)	C(14)-C(21)-C(22)-C(23)	54.5(2)
C(7)-C(6)-C(10)-O(4)	68.4(3)	C(21)-C(22)-C(23)-O(8)	63.9(2)
C(5)-C(6)-C(10)-O(4)	-167.7(2)	C(21)-C(22)-C(23)-C(19)	-56.4(2)
C(13)-C(6)-C(10)-C(9)	-170.8(2)	C(20)-C(19)-C(23)-O(8)	-66.4(2)
C(7)-C(6)-C(10)-C(9)	-53.7(3)	C(26)-C(19)-C(23)-O(8)	50.8(3)
C(5)-C(6)-C(10)-C(9)	70.2(3)	C(18)-C(19)-C(23)-O(8)	169.3(2)
C(8)-C(9)-C(10)-O(4)	-64.6(2)	C(20)-C(19)-C(23)-C(22)	55.3(2)
C(8)-C(9)-C(10)-C(6)	55.8(2)	C(26)-C(19)-C(23)-C(22)	172.50(19)
C(12)-O(3)-C(11)-O(2)	-3.0(6)	C(18)-C(19)-C(23)-C(22)	-69.0(3)
C(12)-O(3)-C(11)-C(2)	177.0(3)	C(25)-O(7)-C(24)-O(6)	-2.4(6)
C(3)-C(2)-C(11)-O(2)	172.2(5)	C(25)-O(7)-C(24)-C(15)	-178.8(2)
C(1)-C(2)-C(11)-O(2)	-4.8(6)	C(16)-C(15)-C(24)-O(6)	-177.3(5)
C(3)-C(2)-C(11)-O(3)	-7.8(4)	C(14)-C(15)-C(24)-O(6)	-0.7(6)

C(16)-C(15)-C(24)-O(7)	-0.9(3)	C(101)-C(102)-C(111)-O(102)	-4(3)
C(14)-C(15)-C(24)-O(7)	175.7(2)	C(103)-C(102)-C(111)-O(103)	5(2)
O(101)-C(101)-C(102)-C(103)	125.8(14)	C(101)-C(102)-C(111)-O(103)	177.8(14)
C(107)-C(101)-C(102)-C(103)	7.6(19)	O(105)-C(114)-C(115)-C(116)	-127.4(13)
C(108)-C(101)-C(102)-C(103)	-115.4(15)	C(120)-C(114)-C(115)-C(116)	-9.8(19)
O(101)-C(101)-C(102)-C(111)	-46.4(17)	C(121)-C(114)-C(115)-C(116)	116.0(14)
C(107)-C(101)-C(102)-C(111)	-164.6(13)	O(105)-C(114)-C(115)-C(124)	48.2(15)
C(108)-C(101)-C(102)-C(111)	72.4(15)	C(120)-C(114)-C(115)-C(124)	165.8(12)
C(111)-C(102)-C(103)-C(104)	-177.7(14)	C(121)-C(114)-C(115)-C(124)	-68.4(15)
C(101)-C(102)-C(103)-C(104)	10(2)	C(124)-C(115)-C(116)-C(117)	177.3(12)
C(102)-C(103)-C(104)-C(105)	43.2(19)	C(114)-C(115)-C(116)-C(117)	-7(2)
C(103)-C(104)-C(105)-C(106)	-75.6(19)	C(115)-C(116)-C(117)-C(118)	-46.4(17)
C(104)-C(105)-C(106)-C(107)	21(2)	C(116)-C(117)-C(118)-C(119)	78.6(16)
C(104)-C(105)-C(106)-C(110)	142.6(15)	C(117)-C(118)-C(119)-C(120)	-22(2)
C(104)-C(105)-C(106)-C(113)	-99.4(17)	C(117)-C(118)-C(119)-C(126)	98.8(16)
O(101)-C(101)-C(107)-C(106)	168.5(10)	C(117)-C(118)-C(119)-C(123)	-142.0(13)
C(102)-C(101)-C(107)-C(106)	-71.7(14)	O(105)-C(114)-C(120)-C(119)	-168.9(10)
C(108)-C(101)-C(107)-C(106)	52.6(13)	C(115)-C(114)-C(120)-C(119)	72.7(14)
C(110)-C(106)-C(107)-C(101)	-56.2(13)	C(121)-C(114)-C(120)-C(119)	-52.8(14)
C(113)-C(106)-C(107)-C(101)	-174.0(10)	C(126)-C(119)-C(120)-C(114)	172.7(10)
C(105)-C(106)-C(107)-C(101)	63.8(17)	C(118)-C(119)-C(120)-C(114)	-64.1(17)
O(101)-C(101)-C(108)-C(109)	-165.4(9)	C(123)-C(119)-C(120)-C(114)	55.2(13)
C(107)-C(101)-C(108)-C(109)	-50.8(12)	O(105)-C(114)-C(121)-C(122)	164.6(8)
C(102)-C(101)-C(108)-C(109)	75.4(12)	C(120)-C(114)-C(121)-C(122)	48.4(12)
C(101)-C(108)-C(109)-C(110)	54.3(12)	C(115)-C(114)-C(121)-C(122)	-78.0(11)
C(108)-C(109)-C(110)-O(104)	65.4(11)	C(114)-C(121)-C(122)-C(123)	-50.0(11)
C(108)-C(109)-C(110)-C(106)	-56.0(12)	C(121)-C(122)-C(123)-O(108)	-67.2(10)
C(107)-C(106)-C(110)-O(104)	-67.3(12)	C(121)-C(122)-C(123)-C(119)	55.2(12)
C(113)-C(106)-C(110)-O(104)	49.0(13)	C(120)-C(119)-C(123)-O(108)	67.0(11)
C(105)-C(106)-C(110)-O(104)	167.7(11)	C(126)-C(119)-C(123)-O(108)	-48.6(13)
C(107)-C(106)-C(110)-C(109)	56.0(12)	C(118)-C(119)-C(123)-O(108)	-168.7(11)
C(113)-C(106)-C(110)-C(109)	172.3(10)	C(120)-C(119)-C(123)-C(122)	-56.0(12)
C(105)-C(106)-C(110)-C(109)	-68.9(13)	C(126)-C(119)-C(123)-C(122)	-171.6(10)
C(112)-O(103)-C(111)-O(102)	2(3)	C(118)-C(119)-C(123)-C(122)	68.3(13)
C(112)-O(103)-C(111)-C(102)	-179.8(14)	C(125)-O(107)-C(124)-O(106)	6(3)
C(103)-C(102)-C(111)-O(102)	-177(3)	C(125)-O(107)-C(124)-C(115)	173.4(12)

C(116)-C(115)-C(124)-O(106)	156(2)
C(114)-C(115)-C(124)-O(106)	-20(3)
C(116)-C(115)-C(124)-O(107)	-11.4(19)
C(114)-C(115)-C(124)-O(107)	172.6(13)

Table 7. Hydrogen bonds for md401unk_sub [Å and °].

D-H...A	d(D-H)	d(H...A)	d(D...A)	<(DHA)
O(1)-H(1)...O(2)	0.82	2.01	2.678(7)	138.2
O(101)-H(101)...O(102)	0.82	2.01	2.68(2)	138.9
O(5)-H(5)...O(6)	0.82	2.01	2.670(7)	136.5
O(105)-H(105)...O(106)	0.82	2.01	2.58(3)	125.6
O(4)-H(4)...O(5)#1	0.82	1.98	2.789(2)	168.7
O(8)-H(8)...O(1)#2	0.82	1.96	2.776(2)	175.4
O(104)-H(104)...O(105)#2	0.82	1.97	2.767(10)	165.2
O(108)-H(108)...O(101)#1	0.82	1.97	2.761(11)	162.4

Symmetry transformations used to generate equivalent atoms:

#1 -x,-y,-z #2 -x+1,-y,-z

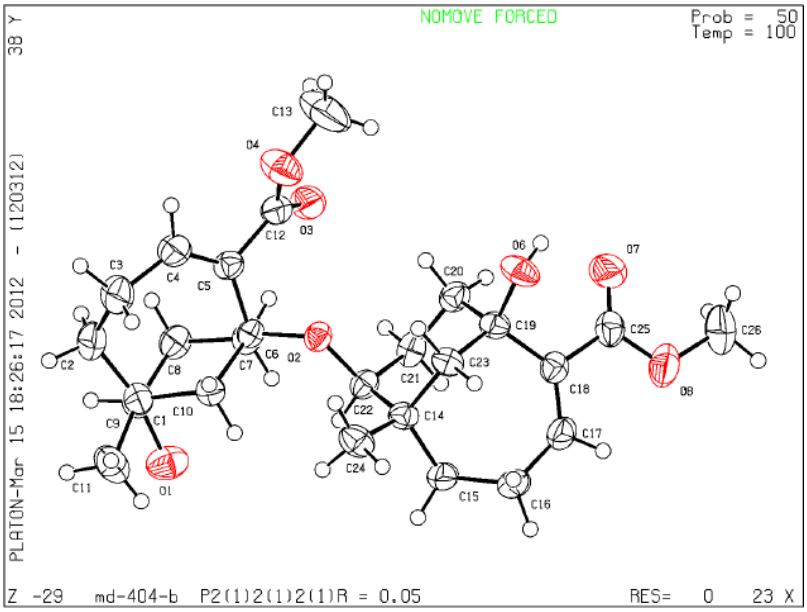

X-ray crystal structure of **3.74** (racemic, major diastereomer).

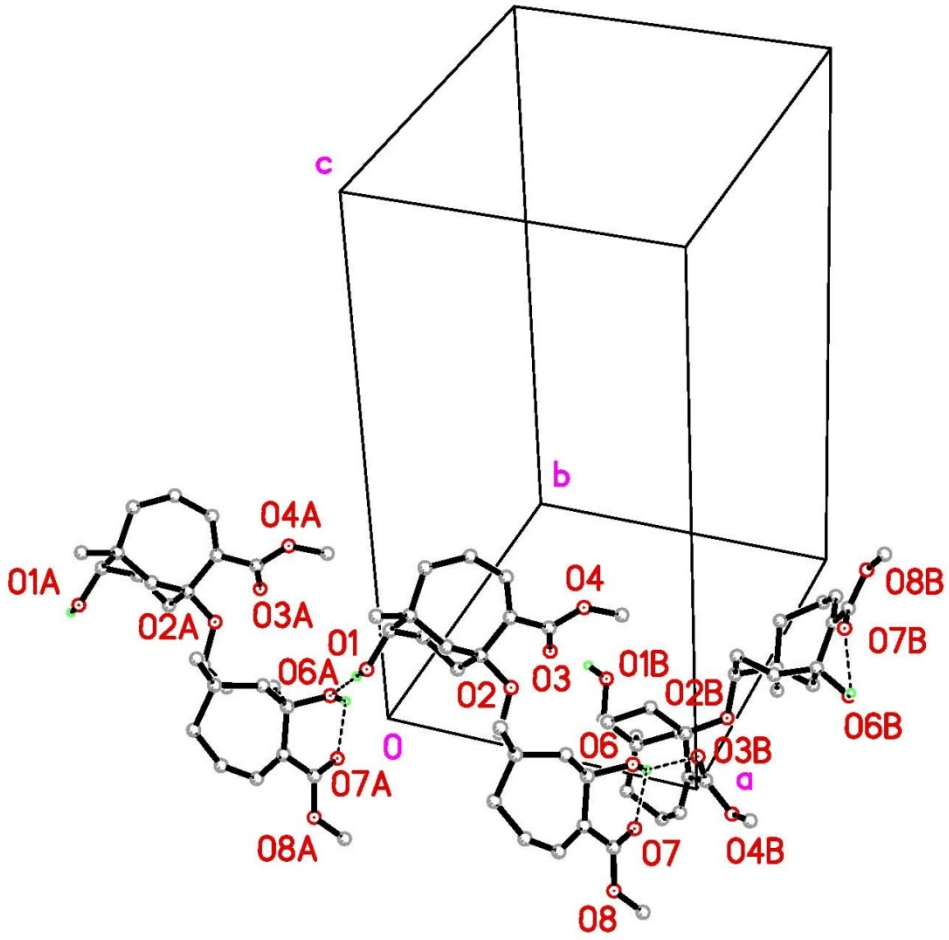

Crystal packing of **3.74** (note the H-bonds: one inter- and one intramolecular).

Table 1. Crystal data and structure refinement for md-404-b.

Identification code	md-404-b	
Empirical formula	C26 H38 O7	
Formula weight	462.56	
Temperature	100(2) K	
Wavelength	0.71073 Å	
Crystal system	Orthorhombic	
Space group	P2(1)2(1)2(1)	
Unit cell dimensions	a = 10.3318(6) Å	α= 90°.
	b = 12.6645(8) Å	β= 90°.
	c = 18.8450(11) Å	γ = 90°.
Volume	2465.8(3) $Å^3$	
Z	4	
Density (calculated)	1.246 Mg/m^3	
Absorption coefficient	0.089 mm^{-1}	
F(000)	1000	
Crystal size	0.46 x 0.38 x 0.13 mm^3	
Theta range for data collection	1.94 to 32.03°.	
Index ranges	-15<=h<=15, -18<=k<=18, -27<=l<=28	
Reflections collected	32033	
Independent reflections	8533 [R(int) = 0.0277]	
Completeness to theta = 32.03°	99.8 %	
Absorption correction	Semi-empirical from equivalents	
Max. and min. transmission	0.9885 and 0.9601	
Refinement method	Full-matrix least-squares on F^2	
Data / restraints / parameters	8533 / 2 / 311	
Goodness-of-fit on F^2	1.006	
Final R indices [I>2sigma(I)]	R1 = 0.0533, wR2 = 0.1257	
R indices (all data)	R1 = 0.0694, wR2 = 0.1365	
Absolute structure parameter	racemic twinning	
Largest diff. peak and hole	0.317 and -0.147 $e.Å^{-3}$	

Table 2. Atomic coordinates (x 10^4) and equivalent isotropic displacement parameters ($Å^2$x 10^3) for md-404-b. U(eq) is defined as one third of the trace of the orthogonalized U^{ij} tensor.

	x	y	z	U(eq)
O(1)	-418(1)	-238(1)	1090(1)	58(1)
O(2)	3952(1)	443(1)	990(1)	35(1)
O(3)	4027(1)	2756(1)	632(1)	53(1)
O(4)	5153(2)	2875(1)	1637(1)	65(1)
O(6)	7843(1)	331(1)	13(1)	50(1)
O(7)	7740(2)	505(1)	-1459(1)	66(1)
O(8)	7806(2)	-1095(1)	-1915(1)	73(1)
C(1)	824(2)	339(1)	2093(1)	42(1)
C(2)	894(2)	1259(2)	2639(1)	54(1)
C(3)	2226(2)	1575(2)	2897(1)	57(1)
C(4)	3074(2)	2094(1)	2348(1)	49(1)
C(5)	3278(2)	1834(1)	1674(1)	36(1)
C(6)	2757(1)	881(1)	1276(1)	32(1)
C(7)	1761(2)	1195(1)	704(1)	37(1)
C(8)	473(2)	1535(1)	1032(1)	43(1)
C(9)	-106(2)	671(1)	1500(1)	45(1)
C(10)	2147(1)	59(1)	1766(1)	36(1)
C(11)	335(2)	-650(2)	2474(1)	59(1)
C(12)	4157(2)	2524(1)	1248(1)	42(1)
C(13)	6031(3)	3574(3)	1270(2)	100(1)
C(14)	4893(1)	-1196(1)	571(1)	34(1)
C(15)	4635(2)	-2099(1)	31(1)	44(1)
C(16)	5845(2)	-2611(1)	-286(1)	52(1)
C(17)	6526(2)	-1927(1)	-820(1)	45(1)
C(18)	6835(1)	-906(1)	-781(1)	36(1)
C(19)	6618(1)	-164(1)	-152(1)	35(1)
C(20)	5595(2)	687(1)	-295(1)	40(1)
C(21)	4218(2)	254(1)	-280(1)	40(1)
C(22)	3905(1)	-306(1)	420(1)	34(1)
C(23)	6266(1)	-740(1)	530(1)	36(1)
C(24)	4724(2)	-1645(1)	1318(1)	46(1)

C(25)	7499(2)	-411(1)	-1405(1)	44(1)
C(26)	8502(3)	-664(3)	-2514(1)	85(1)

Table 3. Bond lengths [Å] and angles [°] for md-404-b.

_____

O(1)-C(9)	1.424(2)	C(10)-H(10B)	0.9900
O(1)-H(1)	0.837(10)	C(11)-H(11A)	0.9800
O(2)-C(22)	1.4333(16)	C(11)-H(11B)	0.9800
O(2)-C(6)	1.4561(16)	C(11)-H(11C)	0.9800
O(3)-C(12)	1.204(2)	C(13)-H(13A)	0.9800
O(4)-C(12)	1.339(2)	C(13)-H(13B)	0.9800
O(4)-C(13)	1.443(3)	C(13)-H(13C)	0.9800
O(6)-C(19)	1.4468(17)	C(14)-C(24)	1.529(2)
O(6)-H(6)	0.825(9)	C(14)-C(23)	1.5336(19)
O(7)-C(25)	1.191(2)	C(14)-C(22)	1.5467(19)
O(8)-C(25)	1.333(2)	C(14)-C(15)	1.553(2)
O(8)-C(26)	1.445(3)	C(15)-C(16)	1.530(2)
C(1)-C(11)	1.529(2)	C(15)-H(15A)	0.9900
C(1)-C(9)	1.532(2)	C(15)-H(15B)	0.9900
C(1)-C(10)	1.541(2)	C(16)-C(17)	1.503(3)
C(1)-C(2)	1.557(2)	C(16)-H(16A)	0.9900
C(2)-C(3)	1.513(3)	C(16)-H(16B)	0.9900
C(2)-H(2A)	0.9900	C(17)-C(18)	1.334(2)
C(2)-H(2B)	0.9900	C(17)-H(17)	0.9500
C(3)-C(4)	1.506(3)	C(18)-C(25)	1.498(2)
C(3)-H(3A)	0.9900	C(18)-C(19)	1.530(2)
C(3)-H(3B)	0.9900	C(19)-C(23)	1.522(2)
C(4)-C(5)	1.330(2)	C(19)-C(20)	1.533(2)
C(4)-H(4)	0.9500	C(20)-C(21)	1.526(2)
C(5)-C(12)	1.495(2)	C(20)-H(20A)	0.9900
C(5)-C(6)	1.5194(19)	C(20)-H(20B)	0.9900
C(6)-C(10)	1.528(2)	C(21)-C(22)	1.533(2)
C(6)-C(7)	1.5427(19)	C(21)-H(21A)	0.9900
C(7)-C(8)	1.529(2)	C(21)-H(21B)	0.9900
C(7)-H(7A)	0.9900	C(22)-H(22)	1.0000
C(7)-H(7B)	0.9900	C(23)-H(23A)	0.9900
C(8)-C(9)	1.527(2)	C(23)-H(23B)	0.9900
C(8)-H(8A)	0.9900	C(24)-H(24A)	0.9800
C(8)-H(8B)	0.9900	C(24)-H(24B)	0.9800
C(9)-H(9)	1.0000	C(24)-H(24C)	0.9800
C(10)-H(10A)	0.9900	C(26)-H(26A)	0.9800

C(26)-H(26B)	0.9800	C(9)-O(1)-H(1)	106.3(19)
C(26)-H(26C)	0.9800	C(22)-O(2)-C(6)	120.02(10)
		C(12)-O(4)-C(13)	115.10(18)
		C(19)-O(6)-H(6)	113.0(17)
		C(25)-O(8)-C(26)	115.95(19)
		C(11)-C(1)-C(9)	111.14(15)
		C(11)-C(1)-C(10)	106.98(14)
		C(9)-C(1)-C(10)	109.17(12)
		C(11)-C(1)-C(2)	108.52(14)
		C(9)-C(1)-C(2)	107.78(14)
		C(10)-C(1)-C(2)	113.29(13)
		C(3)-C(2)-C(1)	116.92(15)
		C(3)-C(2)-H(2A)	108.1
		C(1)-C(2)-H(2A)	108.1
		C(3)-C(2)-H(2B)	108.1
		C(1)-C(2)-H(2B)	108.1
		H(2A)-C(2)-H(2B)	107.3
		C(4)-C(3)-C(2)	115.10(15)
		C(4)-C(3)-H(3A)	108.5
		C(2)-C(3)-H(3A)	108.5
		C(4)-C(3)-H(3B)	108.5
		C(2)-C(3)-H(3B)	108.5
		H(3A)-C(3)-H(3B)	107.5
		C(5)-C(4)-C(3)	129.80(15)
		C(5)-C(4)-H(4)	115.1
		C(3)-C(4)-H(4)	115.1
		C(4)-C(5)-C(12)	117.72(14)
		C(4)-C(5)-C(6)	127.78(14)
		C(12)-C(5)-C(6)	114.46(12)
		O(2)-C(6)-C(5)	100.68(11)
		O(2)-C(6)-C(10)	108.25(11)
		C(5)-C(6)-C(10)	112.88(11)
		O(2)-C(6)-C(7)	113.92(11)
		C(5)-C(6)-C(7)	112.13(11)
		C(10)-C(6)-C(7)	108.82(12)
		C(8)-C(7)-C(6)	111.75(12)

C(8)-C(7)-H(7A)	109.3	H(13A)-C(13)-H(13C)	109.5
C(6)-C(7)-H(7A)	109.3	H(13B)-C(13)-H(13C)	109.5
C(8)-C(7)-H(7B)	109.3	C(24)-C(14)-C(23)	106.92(12)
C(6)-C(7)-H(7B)	109.3	C(24)-C(14)-C(22)	111.37(12)
H(7A)-C(7)-H(7B)	107.9	C(23)-C(14)-C(22)	109.08(11)
C(9)-C(8)-C(7)	111.91(13)	C(24)-C(14)-C(15)	108.04(12)
C(9)-C(8)-H(8A)	109.2	C(23)-C(14)-C(15)	113.80(12)
C(7)-C(8)-H(8A)	109.2	C(22)-C(14)-C(15)	107.68(11)
C(9)-C(8)-H(8B)	109.2	C(16)-C(15)-C(14)	115.32(13)
C(7)-C(8)-H(8B)	109.2	C(16)-C(15)-H(15A)	108.4
H(8A)-C(8)-H(8B)	107.9	C(14)-C(15)-H(15A)	108.4
O(1)-C(9)-C(8)	110.72(14)	C(16)-C(15)-H(15B)	108.4
O(1)-C(9)-C(1)	108.37(13)	C(14)-C(15)-H(15B)	108.4
C(8)-C(9)-C(1)	111.86(13)	H(15A)-C(15)-H(15B)	107.5
O(1)-C(9)-H(9)	108.6	C(17)-C(16)-C(15)	113.56(14)
C(8)-C(9)-H(9)	108.6	C(17)-C(16)-H(16A)	108.9
C(1)-C(9)-H(9)	108.6	C(15)-C(16)-H(16A)	108.9
C(6)-C(10)-C(1)	116.78(12)	C(17)-C(16)-H(16B)	108.9
C(6)-C(10)-H(10A)	108.1	C(15)-C(16)-H(16B)	108.9
C(1)-C(10)-H(10A)	108.1	H(16A)-C(16)-H(16B)	107.7
C(6)-C(10)-H(10B)	108.1	C(18)-C(17)-C(16)	129.36(15)
C(1)-C(10)-H(10B)	108.1	C(18)-C(17)-H(17)	115.3
H(10A)-C(10)-H(10B)	107.3	C(16)-C(17)-H(17)	115.3
C(1)-C(11)-H(11A)	109.5	C(17)-C(18)-C(25)	118.16(14)
C(1)-C(11)-H(11B)	109.5	C(17)-C(18)-C(19)	127.08(14)
H(11A)-C(11)-H(11B)	109.5	C(25)-C(18)-C(19)	114.74(12)
C(1)-C(11)-H(11C)	109.5	O(6)-C(19)-C(23)	103.64(11)
H(11A)-C(11)-H(11C)	109.5	O(6)-C(19)-C(18)	107.70(12)
H(11B)-C(11)-H(11C)	109.5	C(23)-C(19)-C(18)	113.30(11)
O(3)-C(12)-O(4)	122.14(16)	O(6)-C(19)-C(20)	109.63(12)
O(3)-C(12)-C(5)	126.33(15)	C(23)-C(19)-C(20)	108.75(12)
O(4)-C(12)-C(5)	111.53(14)	C(18)-C(19)-C(20)	113.33(11)
O(4)-C(13)-H(13A)	109.5	C(21)-C(20)-C(19)	112.75(12)
O(4)-C(13)-H(13B)	109.5	C(21)-C(20)-H(20A)	109.0
H(13A)-C(13)-H(13B)	109.5	C(19)-C(20)-H(20A)	109.0
O(4)-C(13)-H(13C)	109.5	C(21)-C(20)-H(20B)	109.0

C(19)-C(20)-H(20B)	109.0
H(20A)-C(20)-H(20B)	107.8
C(20)-C(21)-C(22)	112.25(12)
C(20)-C(21)-H(21A)	109.2
C(22)-C(21)-H(21A)	109.2
C(20)-C(21)-H(21B)	109.2
C(22)-C(21)-H(21B)	109.2
H(21A)-C(21)-H(21B)	107.9
O(2)-C(22)-C(21)	109.33(11)
O(2)-C(22)-C(14)	108.86(10)
C(21)-C(22)-C(14)	110.85(11)
O(2)-C(22)-H(22)	109.3
C(21)-C(22)-H(22)	109.3
C(14)-C(22)-H(22)	109.3
C(19)-C(23)-C(14)	116.30(11)
C(19)-C(23)-H(23A)	108.2
C(14)-C(23)-H(23A)	108.2
C(19)-C(23)-H(23B)	108.2
C(14)-C(23)-H(23B)	108.2
H(23A)-C(23)-H(23B)	107.4
C(14)-C(24)-H(24A)	109.5
C(14)-C(24)-H(24B)	109.5
H(24A)-C(24)-H(24B)	109.5
C(14)-C(24)-H(24C)	109.5
H(24A)-C(24)-H(24C)	109.5
H(24B)-C(24)-H(24C)	109.5
O(7)-C(25)-O(8)	121.35(16)
O(7)-C(25)-C(18)	124.81(15)
O(8)-C(25)-C(18)	113.83(15)
O(8)-C(26)-H(26A)	109.5
O(8)-C(26)-H(26B)	109.5
H(26A)-C(26)-H(26B)	109.5
O(8)-C(26)-H(26C)	109.5
H(26A)-C(26)-H(26C)	109.5
H(26B)-C(26)-H(26C)	109.5

Table 4. Anisotropic displacement parameters ($Å^2 x\ 10^3$) for md-404-b. The anisotropic displacement factor exponent takes the form: $-2\pi^2[\ h^2\ a^{*2}U^{11} + ...\ + 2\ h\ k\ a^*\ b^*\ U^{12}\ ]$

	U^{11}	U^{22}	U^{33}	U^{23}	U^{13}	U^{12}
O(1)	50(1)	49(1)	74(1)	-6(1)	-18(1)	0(1)
O(2)	33(1)	38(1)	33(1)	-7(1)	-1(1)	1(1)
O(3)	72(1)	45(1)	41(1)	5(1)	6(1)	-6(1)
O(4)	60(1)	76(1)	58(1)	6(1)	-4(1)	-26(1)
O(6)	46(1)	59(1)	43(1)	6(1)	-9(1)	-24(1)
O(7)	89(1)	58(1)	51(1)	-2(1)	17(1)	-20(1)
O(8)	88(1)	68(1)	62(1)	-7(1)	32(1)	11(1)
C(1)	39(1)	44(1)	42(1)	1(1)	6(1)	-1(1)
C(2)	57(1)	62(1)	44(1)	-8(1)	12(1)	3(1)
C(3)	70(1)	70(1)	31(1)	-8(1)	7(1)	-10(1)
C(4)	59(1)	52(1)	37(1)	-10(1)	1(1)	-13(1)
C(5)	42(1)	35(1)	31(1)	-2(1)	-2(1)	-1(1)
C(6)	34(1)	33(1)	29(1)	-2(1)	0(1)	2(1)
C(7)	40(1)	42(1)	30(1)	0(1)	-4(1)	4(1)
C(8)	41(1)	42(1)	45(1)	-1(1)	-4(1)	8(1)
C(9)	36(1)	44(1)	55(1)	-2(1)	1(1)	4(1)
C(10)	36(1)	37(1)	35(1)	2(1)	0(1)	1(1)
C(11)	51(1)	61(1)	65(1)	16(1)	13(1)	-4(1)
C(12)	50(1)	34(1)	43(1)	-2(1)	4(1)	-2(1)
C(13)	90(2)	118(2)	90(2)	9(2)	6(2)	-62(2)
C(14)	31(1)	31(1)	40(1)	2(1)	-3(1)	-1(1)
C(15)	36(1)	37(1)	60(1)	-10(1)	4(1)	-5(1)
C(16)	49(1)	31(1)	75(1)	-8(1)	10(1)	1(1)
C(17)	37(1)	42(1)	56(1)	-11(1)	4(1)	6(1)
C(18)	29(1)	40(1)	40(1)	-2(1)	-2(1)	4(1)
C(19)	34(1)	35(1)	36(1)	-1(1)	-4(1)	-6(1)
C(20)	52(1)	32(1)	36(1)	2(1)	3(1)	4(1)
C(21)	44(1)	45(1)	31(1)	-1(1)	-2(1)	12(1)
C(22)	34(1)	34(1)	32(1)	-4(1)	-4(1)	2(1)
C(23)	32(1)	38(1)	37(1)	4(1)	-6(1)	-4(1)
C(24)	45(1)	44(1)	50(1)	14(1)	0(1)	-2(1)

C(25)	36(1)	55(1)	41(1)	-4(1)	1(1)	3(1)
C(26)	87(2)	104(2)	62(1)	-10(1)	36(1)	1(2)

Table 5. Hydrogen coordinates (x 10^4) and isotropic displacement parameters ($Å^2$x 10^3) for md-404-b.

	x	y	z	U(eq)
H(1)	-920(20)	-30(20)	772(10)	75(8)
H(6)	8070(20)	763(15)	-290(10)	64(6)
H(2A)	482	1888	2423	65
H(2B)	369	1060	3058	65
H(3A)	2124	2066	3302	69
H(3B)	2673	937	3075	69
H(4)	3533	2699	2509	59
H(7A)	2114	1783	416	45
H(7B)	1612	588	383	45
H(8A)	610	2179	1320	51
H(8B)	-146	1710	648	51
H(9)	-918	947	1721	54
H(10A)	2760	-83	2158	43
H(10B)	2049	-606	1495	43
H(11A)	294	-1239	2137	89
H(11B)	-529	-516	2667	89
H(11C)	929	-829	2861	89
H(13A)	6425	3200	869	149
H(13B)	6710	3807	1597	149
H(13C)	5554	4189	1094	149
H(15A)	4120	-2654	270	53
H(15B)	4103	-1814	-362	53
H(16A)	6455	-2781	103	62
H(16B)	5595	-3283	-517	62
H(17)	6773	-2271	-1247	54
H(20A)	5677	1251	67	48
H(20B)	5762	1008	-765	48
H(21A)	4104	-249	-677	48
H(21B)	3600	843	-350	48
H(22)	3016	-616	393	40

H(23A)	6381	-244	932	43
H(23B)	6888	-1326	598	43
H(24A)	4986	-1114	1668	70
H(24B)	5264	-2276	1372	70
H(24C)	3814	-1832	1394	70
H(26A)	7959	-141	-2756	127
H(26B)	8720	-1234	-2845	127
H(26C)	9299	-325	-2348	127

Table 6. Torsion angles [°] for md-404-b.

_____

C(11)-C(1)-C(2)-C(3)	105.22(19)	C(4)-C(5)-C(12)-O(3)	-142.75(19)
C(9)-C(1)-C(2)-C(3)	-134.33(17)	C(6)-C(5)-C(12)-O(3)	39.3(2)
C(10)-C(1)-C(2)-C(3)	-13.4(2)	C(4)-C(5)-C(12)-O(4)	37.4(2)
C(1)-C(2)-C(3)-C(4)	68.8(2)	C(6)-C(5)-C(12)-O(4)	-140.53(14)
C(2)-C(3)-C(4)-C(5)	-44.1(3)	C(24)-C(14)-C(15)-C(16)	-100.92(17)
C(3)-C(4)-C(5)-C(12)	178.35(19)	C(23)-C(14)-C(15)-C(16)	17.6(2)
C(3)-C(4)-C(5)-C(6)	-4.0(3)	C(22)-C(14)-C(15)-C(16)	138.68(15)
C(22)-O(2)-C(6)-C(5)	-163.29(11)	C(14)-C(15)-C(16)-C(17)	-73.3(2)
C(22)-O(2)-C(6)-C(10)	78.10(14)	C(15)-C(16)-C(17)-C(18)	46.2(3)
C(22)-O(2)-C(6)-C(7)	-43.10(16)	C(16)-C(17)-C(18)-C(25)	-178.83(16)
C(4)-C(5)-C(6)-O(2)	-127.09(18)	C(16)-C(17)-C(18)-C(19)	3.0(3)
C(12)-C(5)-C(6)-O(2)	50.62(15)	C(17)-C(18)-C(19)-O(6)	127.02(16)
C(4)-C(5)-C(6)-C(10)	-11.9(2)	C(25)-C(18)-C(19)-O(6)	-51.25(15)
C(12)-C(5)-C(6)-C(10)	165.80(13)	C(17)-C(18)-C(19)-C(23)	13.0(2)
C(4)-C(5)-C(6)-C(7)	111.43(19)	C(25)-C(18)-C(19)-C(23)	-165.27(12)
C(12)-C(5)-C(6)-C(7)	-70.86(16)	C(17)-C(18)-C(19)-C(20)	-111.53(17)
O(2)-C(6)-C(7)-C(8)	173.71(11)	C(25)-C(18)-C(19)-C(20)	70.20(15)
C(5)-C(6)-C(7)-C(8)	-72.76(16)	O(6)-C(19)-C(20)-C(21)	-164.90(12)
C(10)-C(6)-C(7)-C(8)	52.84(15)	C(23)-C(19)-C(20)-C(21)	-52.23(15)
C(6)-C(7)-C(8)-C(9)	-57.34(17)	C(18)-C(19)-C(20)-C(21)	74.74(15)
C(7)-C(8)-C(9)-O(1)	-63.84(17)	C(19)-C(20)-C(21)-C(22)	55.88(16)
C(7)-C(8)-C(9)-C(1)	57.14(17)	C(6)-O(2)-C(22)-C(21)	100.92(13)
C(11)-C(1)-C(9)-O(1)	-47.74(18)	C(6)-O(2)-C(22)-C(14)	-137.85(11)
C(10)-C(1)-C(9)-O(1)	70.03(16)	C(20)-C(21)-C(22)-O(2)	64.14(14)
C(2)-C(1)-C(9)-O(1)	-166.53(14)	C(20)-C(21)-C(22)-C(14)	-55.88(15)
C(11)-C(1)-C(9)-C(8)	-170.08(14)	C(24)-C(14)-C(22)-O(2)	50.77(15)
C(10)-C(1)-C(9)-C(8)	-52.31(17)	C(23)-C(14)-C(22)-O(2)	-67.01(14)
C(2)-C(1)-C(9)-C(8)	71.13(16)	C(15)-C(14)-C(22)-O(2)	169.04(11)
O(2)-C(6)-C(10)-C(1)	-176.54(12)	C(24)-C(14)-C(22)-C(21)	171.06(12)
C(5)-C(6)-C(10)-C(1)	72.92(16)	C(23)-C(14)-C(22)-C(21)	53.29(15)
C(7)-C(6)-C(10)-C(1)	-52.24(16)	C(15)-C(14)-C(22)-C(21)	-70.66(14)
C(11)-C(1)-C(10)-C(6)	172.52(14)	O(6)-C(19)-C(23)-C(14)	169.98(12)
C(9)-C(1)-C(10)-C(6)	52.17(17)	C(18)-C(19)-C(23)-C(14)	-73.58(16)
C(2)-C(1)-C(10)-C(6)	-67.93(17)	C(20)-C(19)-C(23)-C(14)	53.40(16)
C(13)-O(4)-C(12)-O(3)	1.9(3)	C(24)-C(14)-C(23)-C(19)	-175.12(13)
C(13)-O(4)-C(12)-C(5)	-178.3(2)	C(22)-C(14)-C(23)-C(19)	-54.57(16)

C(15)-C(14)-C(23)-C(19)	65.68(16)
C(26)-O(8)-C(25)-O(7)	3.1(3)
C(26)-O(8)-C(25)-C(18)	-177.28(19)
C(17)-C(18)-C(25)-O(7)	174.21(18)
C(19)-C(18)-C(25)-O(7)	-7.4(2)
C(17)-C(18)-C(25)-O(8)	-5.4(2)
C(19)-C(18)-C(25)-O(8)	173.05(14)

Table 7. Hydrogen bonds for md-404-b [Å and °].

D-H...A	d(D-H)	d(H...A)	d(D...A)	<(DHA)
O(1)-H(1)...O(6)#1	0.837(10)	1.970(10)	2.8047(18)	176(3)
O(6)-H(6)...O(3)#2	0.825(9)	2.215(14)	2.9739(17)	153(2)
O(6)-H(6)...O(7)	0.825(9)	2.25(2)	2.7850(18)	122(2)

Symmetry transformations used to generate equivalent atoms:

#1 x-1,y,z #2 x+1/2,-y+1/2,-z

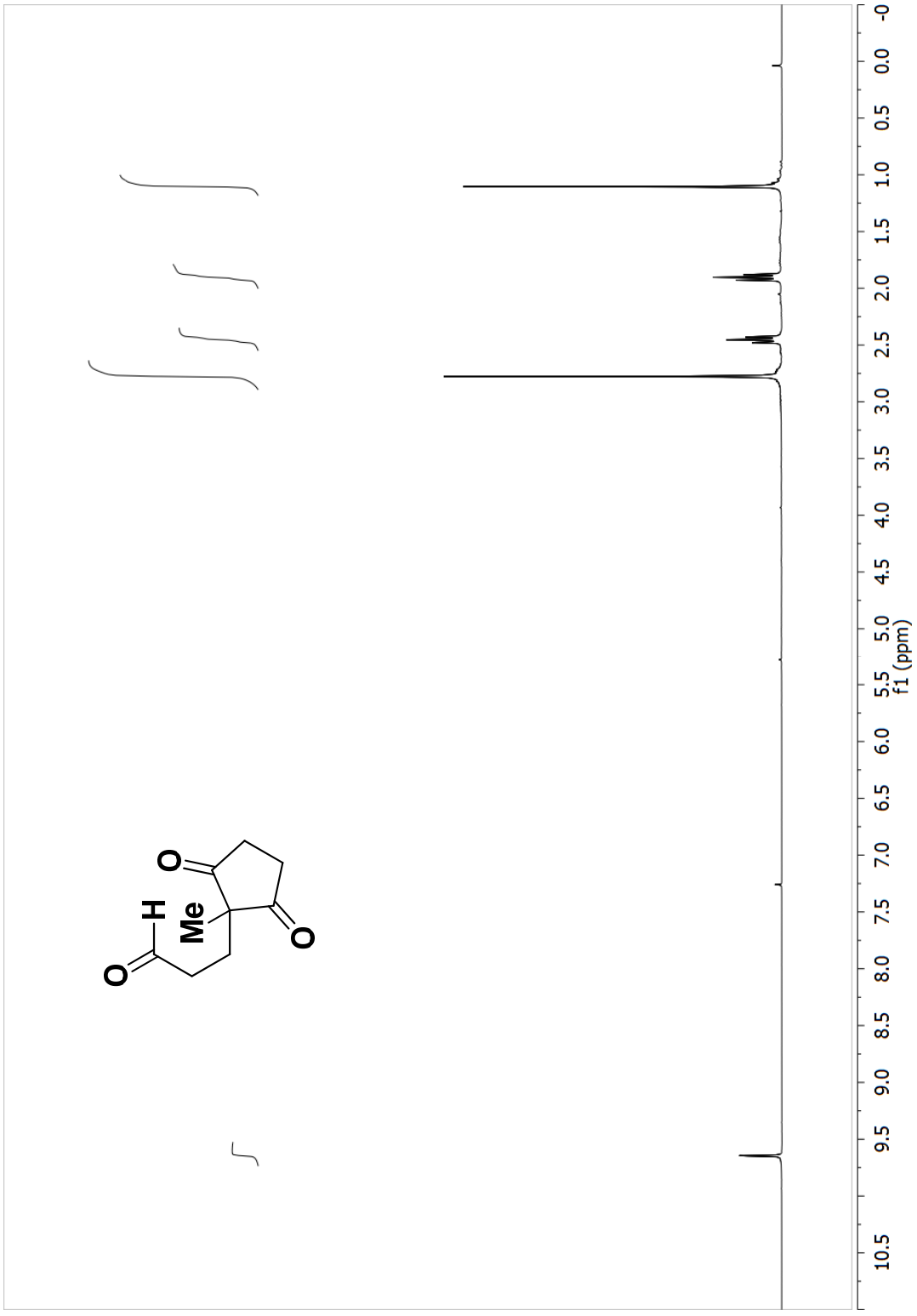
O
O
H
Me
O
O
10.5
9.5
9.0
8.5
8.0
7.5
7.0
6.5
6.0
5.5
5.0
4.5
4.0
3.5
3.0
2.5
2.0
1.5
1.0
0.5
0.0
-0
f1 (ppm)

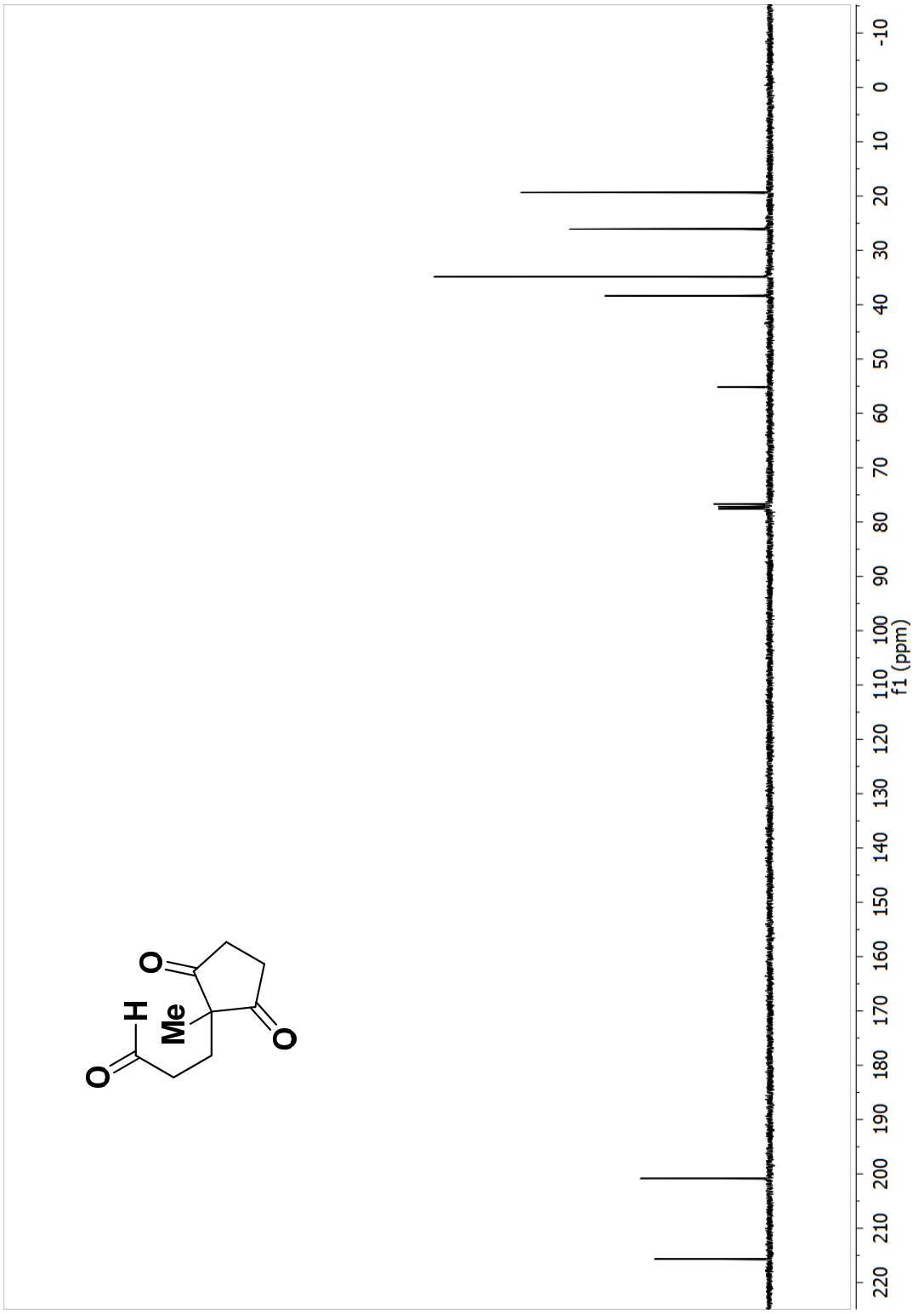
O
H
Me
O
O
-10
0
10
20
30
40
50
60
70
80
90
100
110
120
130
140
150
160
170
180
190
200
210
220
f1 (ppm)

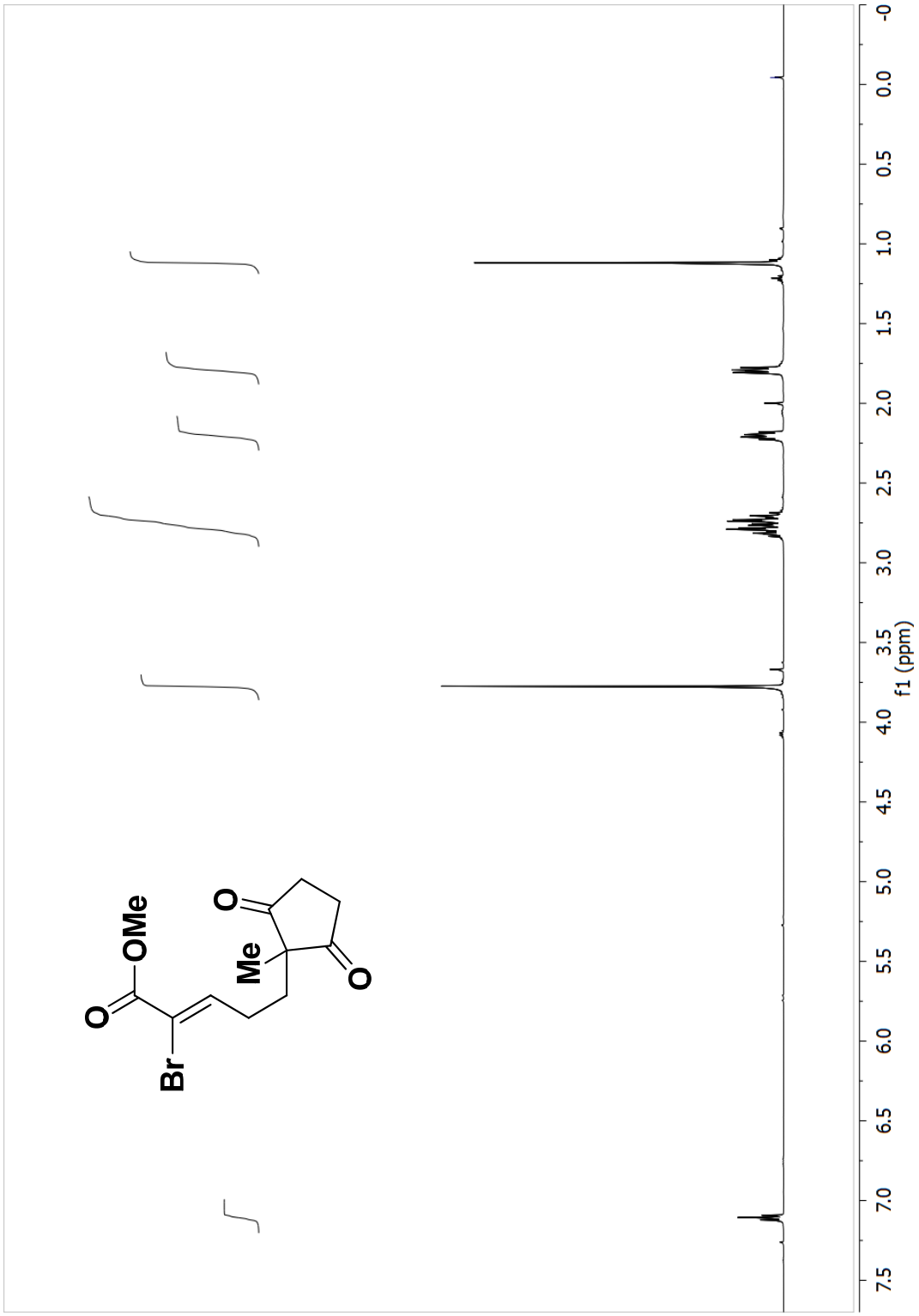
O
OMe
Br
Me
O
O
7.5
7.0
6.5
6.0
5.5
5.0
4.5
4.0
3.5
3.0
2.5
2.0
1.5
1.0
0.5
0.0
-0
f1 (ppm)

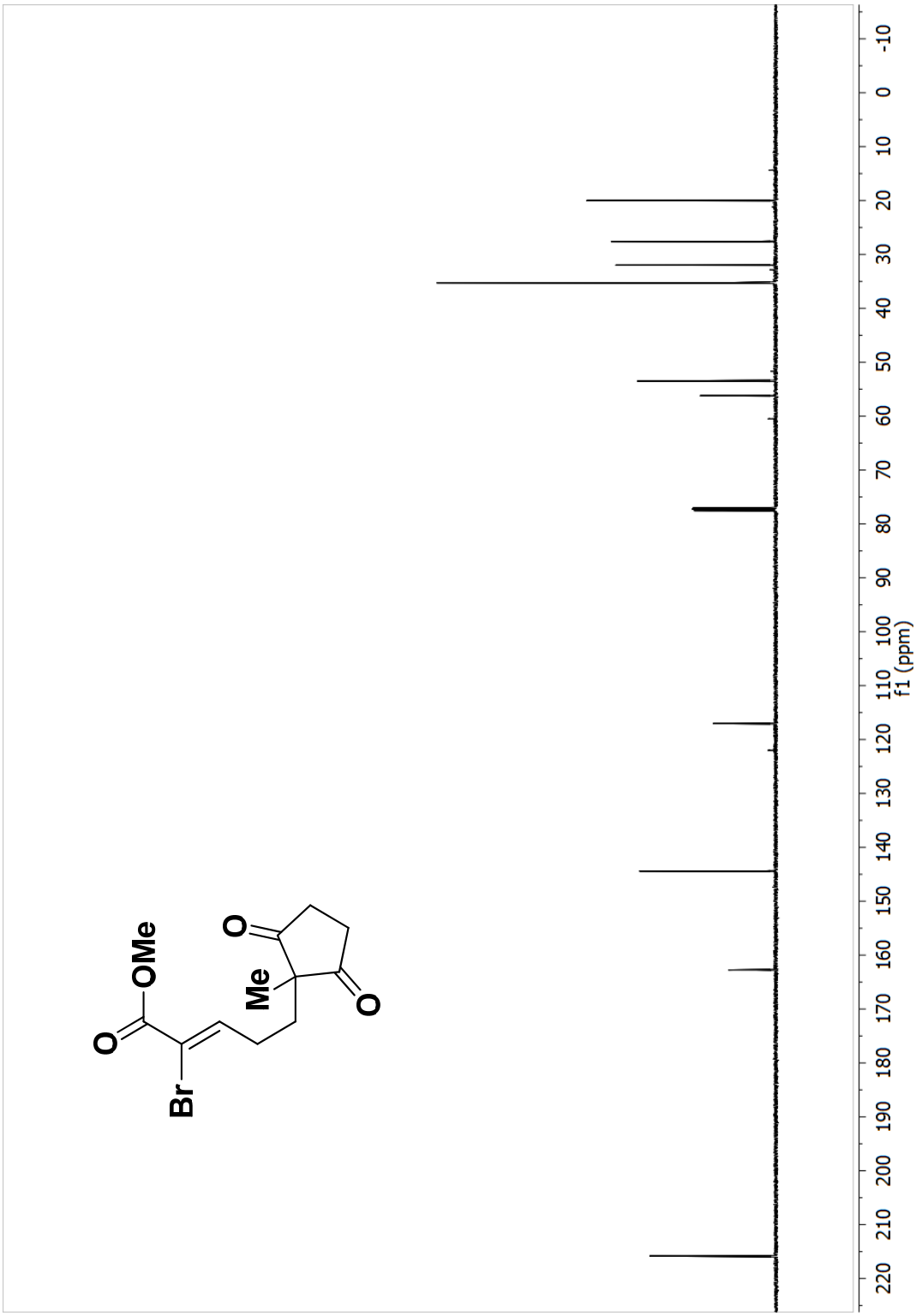
OMe
O
Br
Me
O
O
-10
0
10
20
30
40
50
60
70
80
90
100
110
120
130
140
150
160
170
180
190
200
210
220
f1 (ppm)

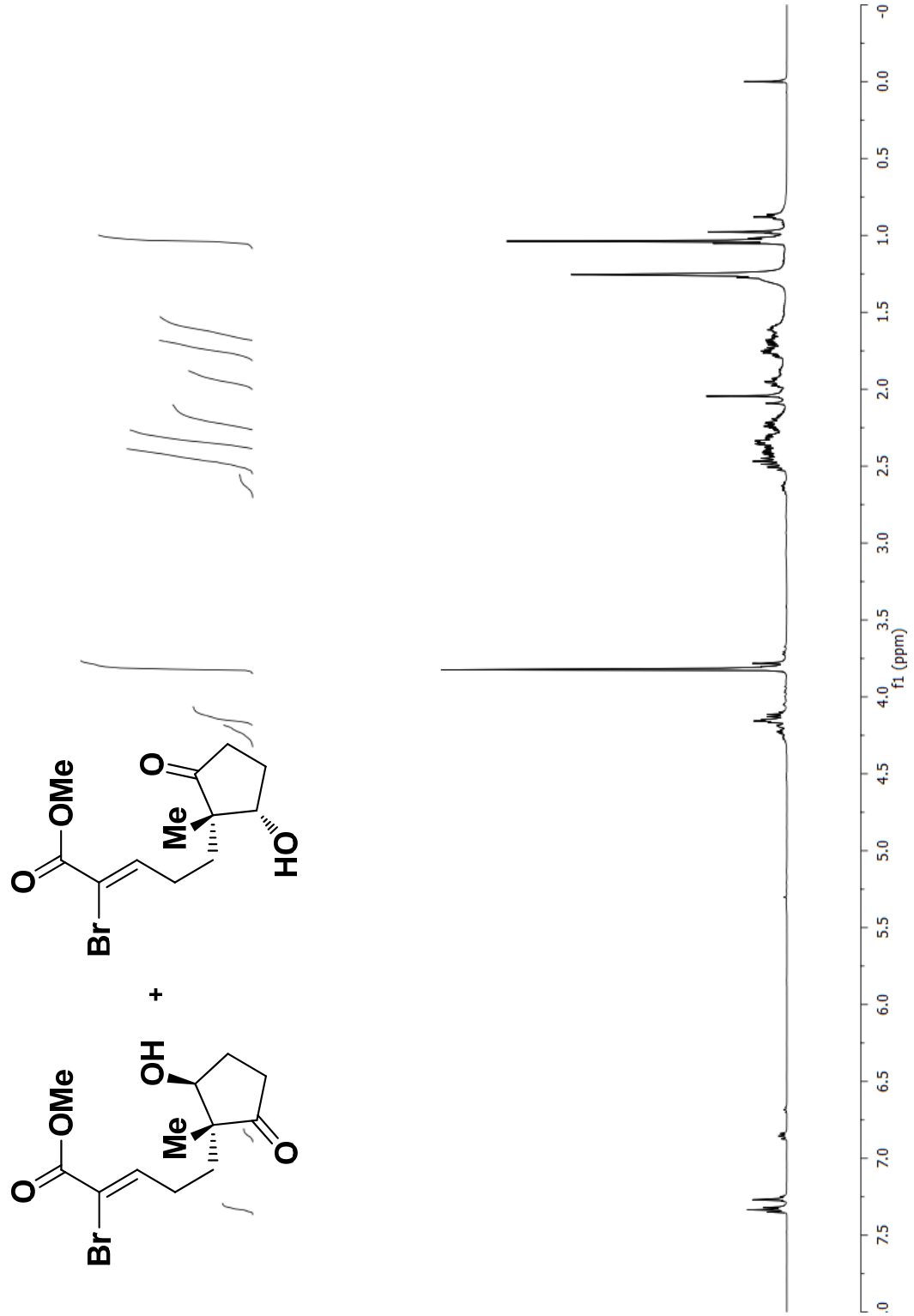
O
OMe
Br
Me
HO
+
OH
Me
O
f1 (ppm)

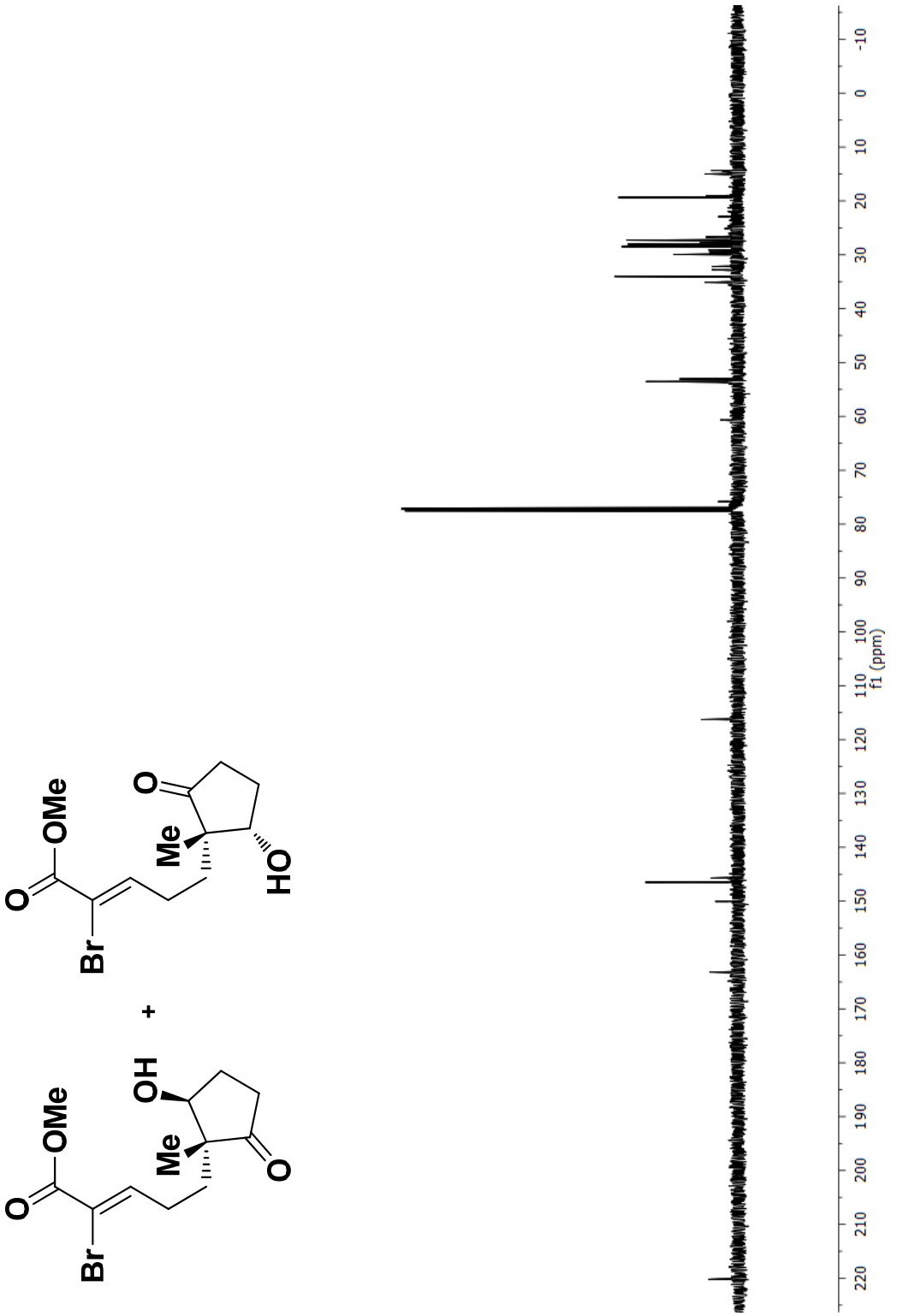
O
OMe
Br
Me
O
HO
+
O
OMe
Br
Me
OH
O
f1 (ppm)

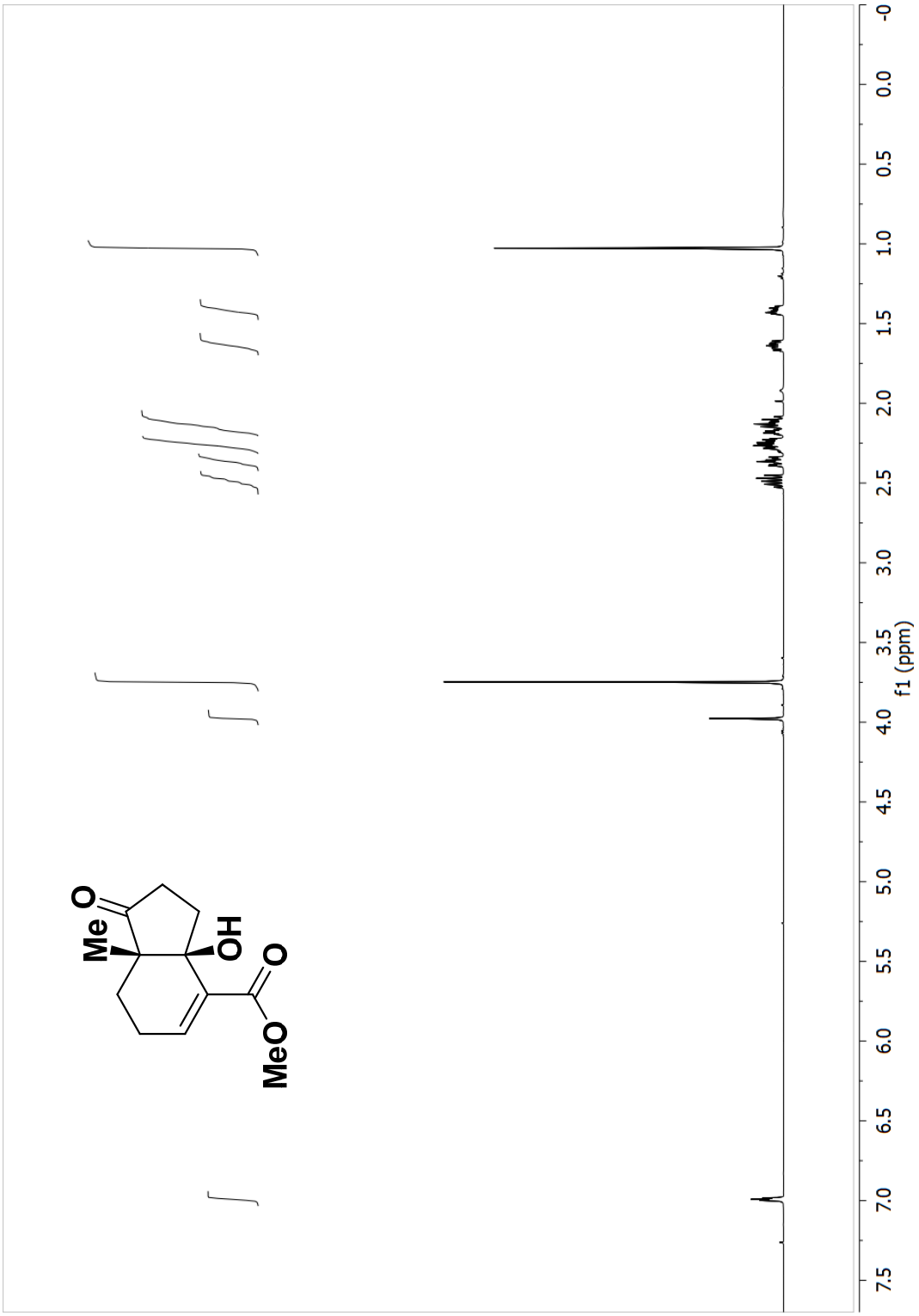
O
Me
OH
O
MeO
7.5
7.0
6.5
6.0
5.5
5.0
4.5
4.0
3.5
3.0
2.5
2.0
1.5
1.0
0.5
0.0
-0
f1 (ppm)

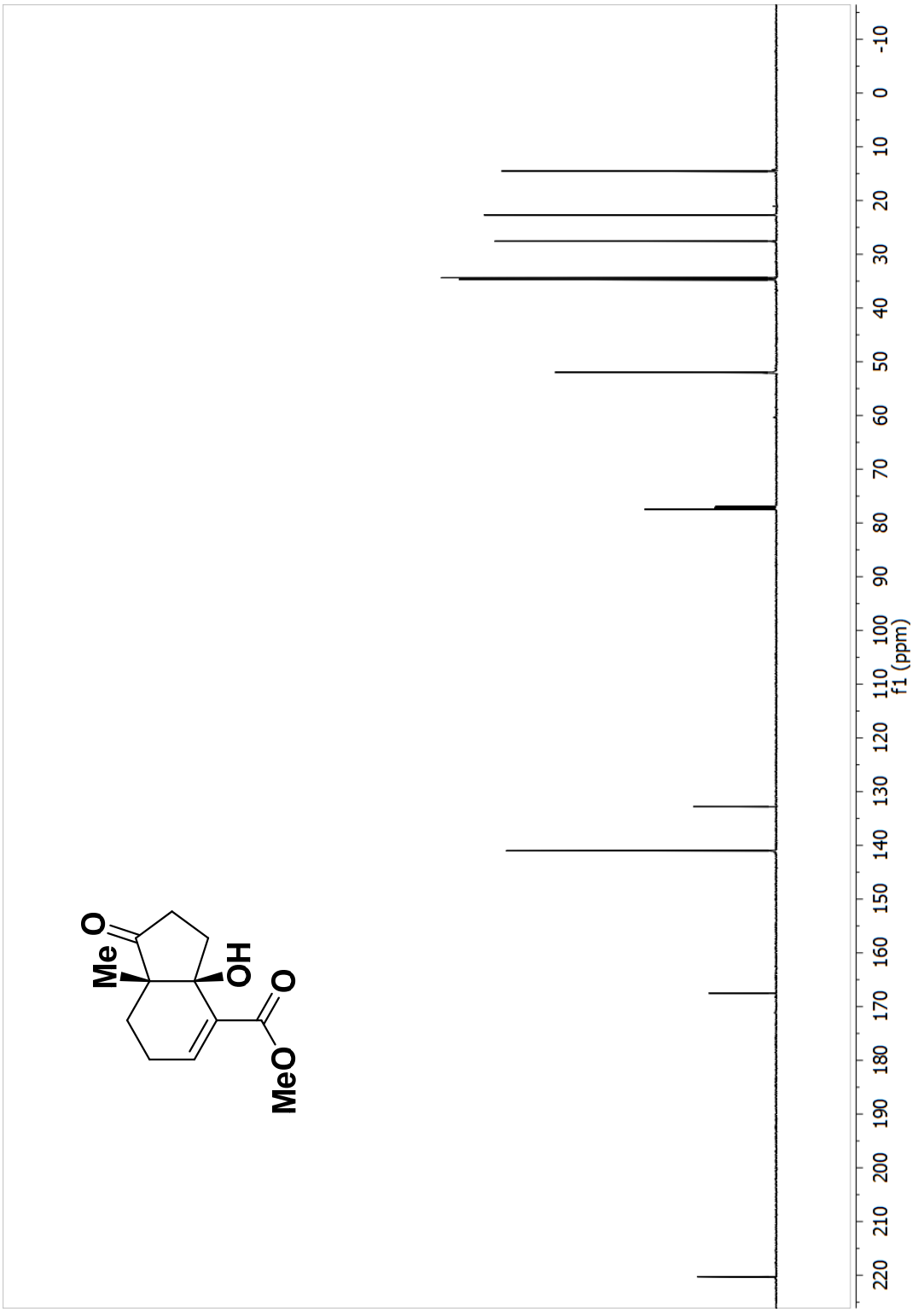
O
Me
OH
O
MeO
-10
0
10
20
30
40
50
60
70
80
90
100
110
120
130
140
150
160
170
180
190
200
210
220
f1 (ppm)

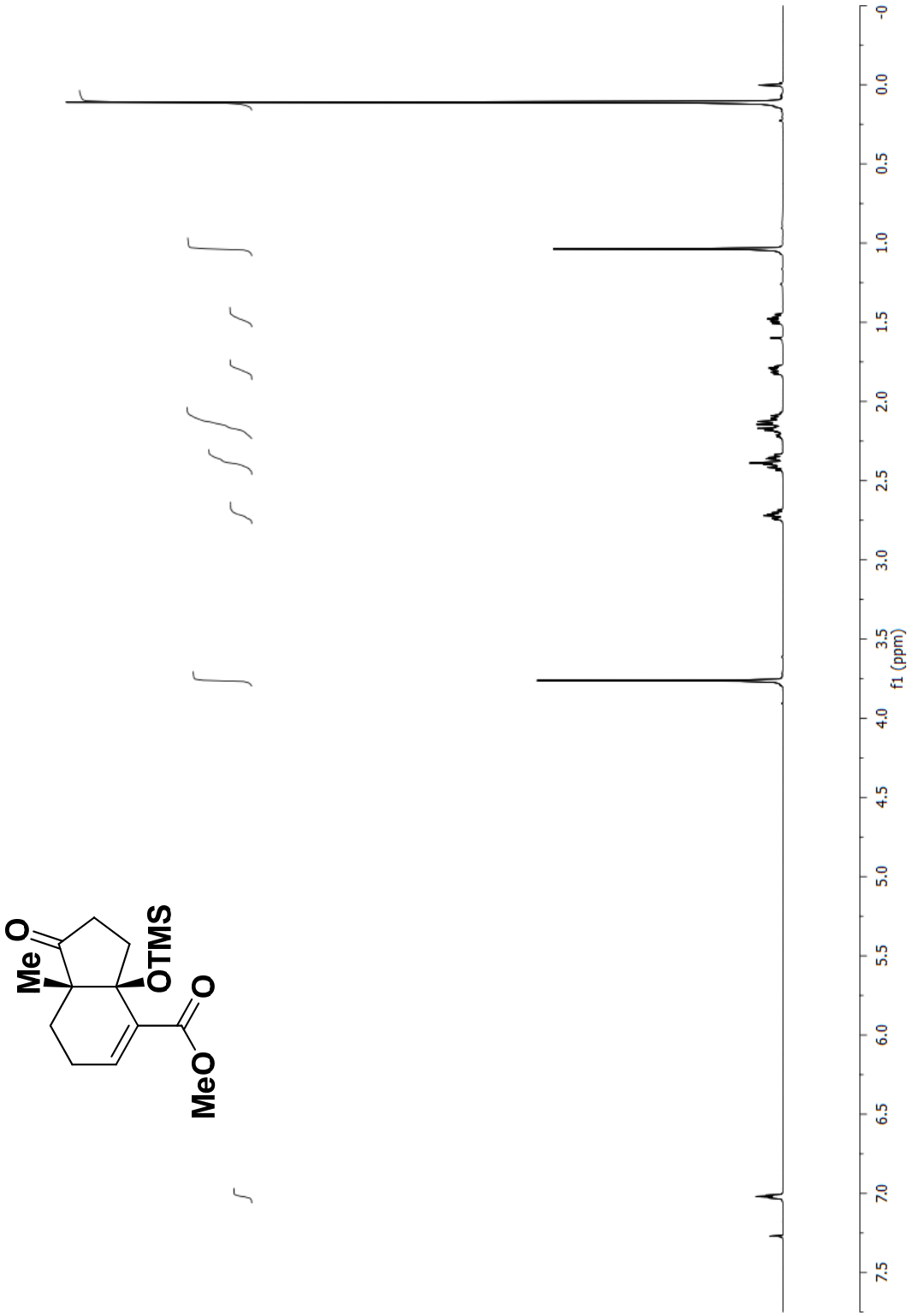
Me
O
OTMS
O
MeO
f1 (ppm)

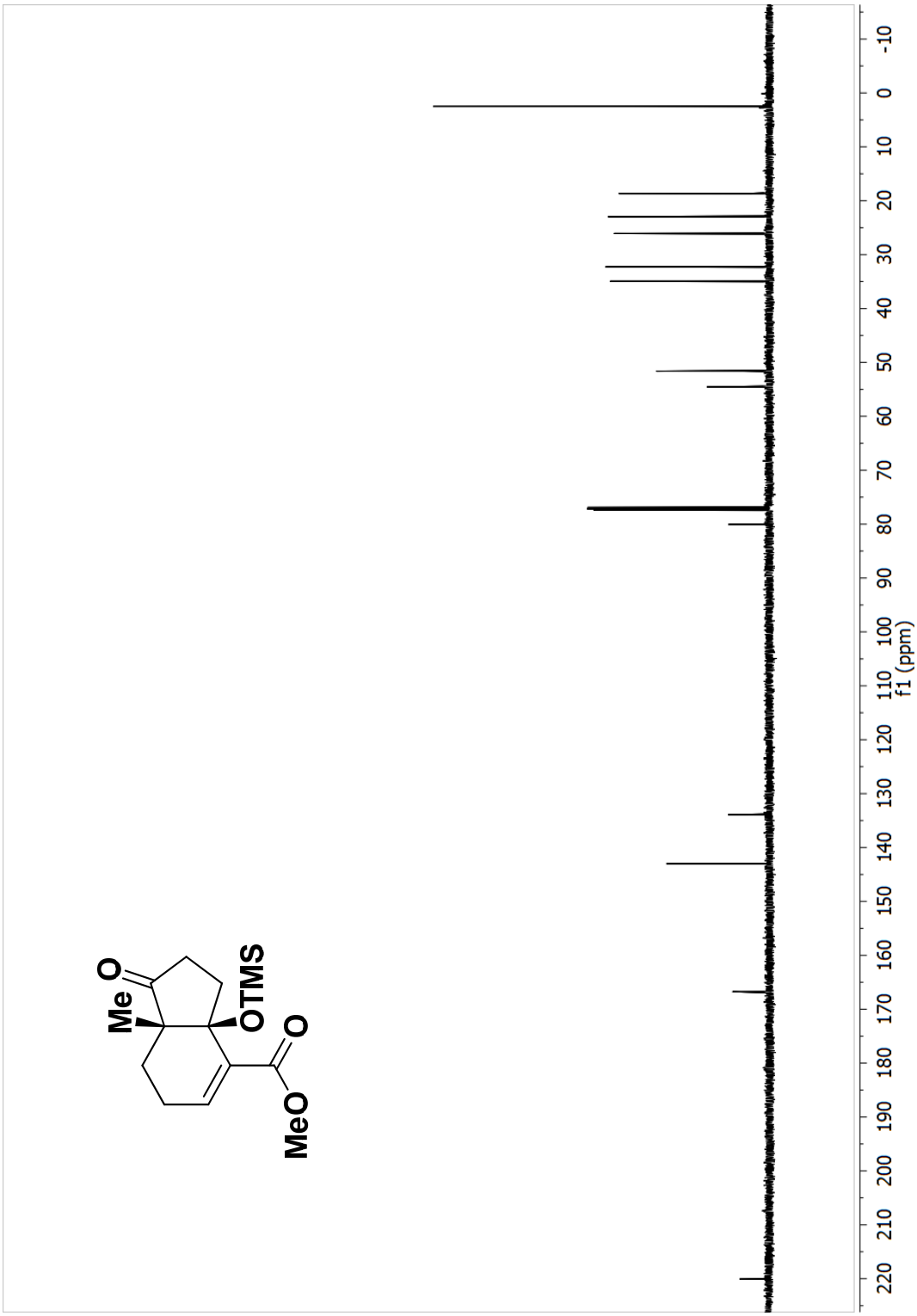
Me
O
OTMS
O
MeO
220
210
200
190
180
170
160
150
140
130
120
110
100
90
80
70
60
50
40
30
20
10
0
-10
f1 (ppm)

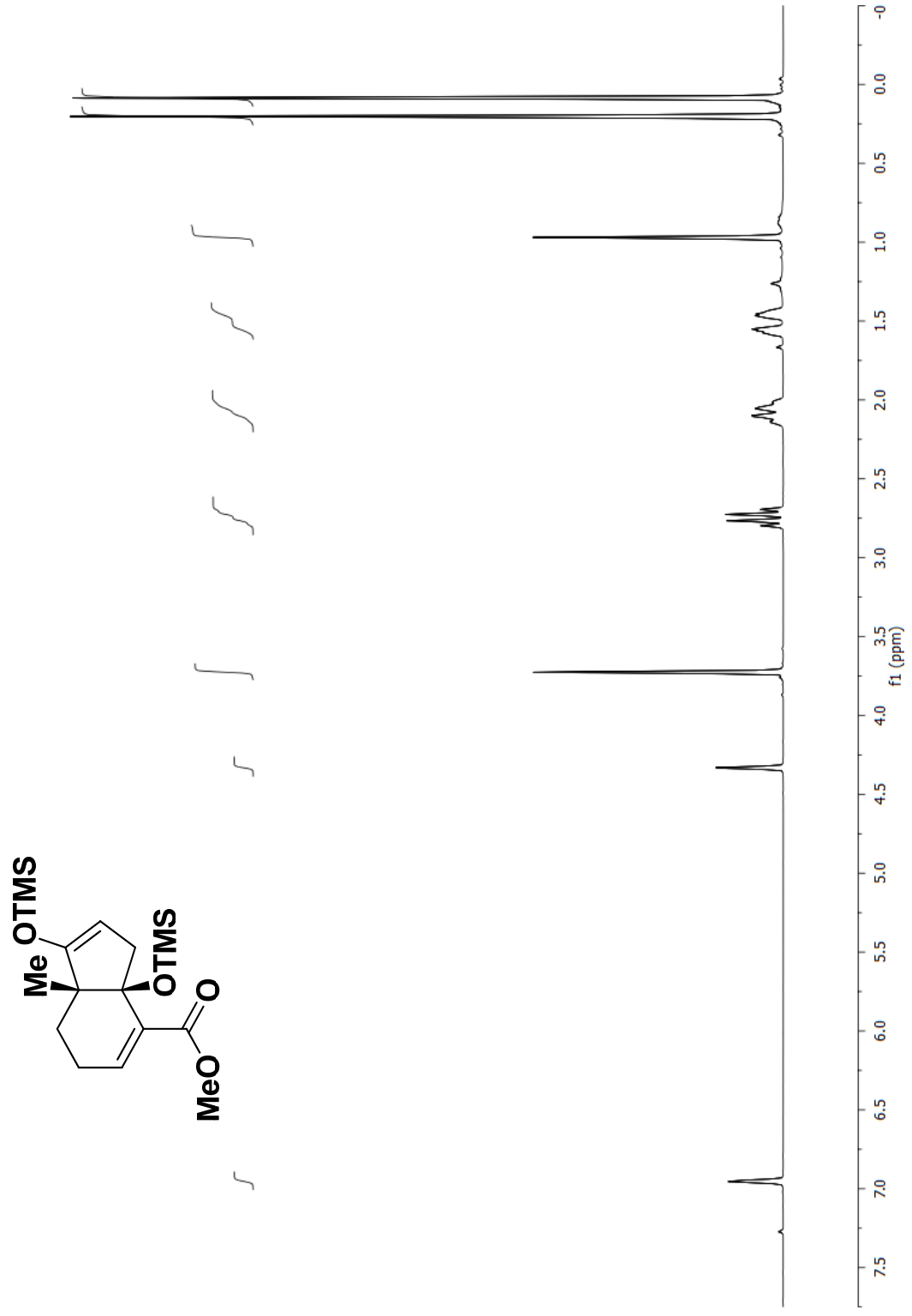
Me
OTMS
OTMS
O
MeO
f1 (ppm)

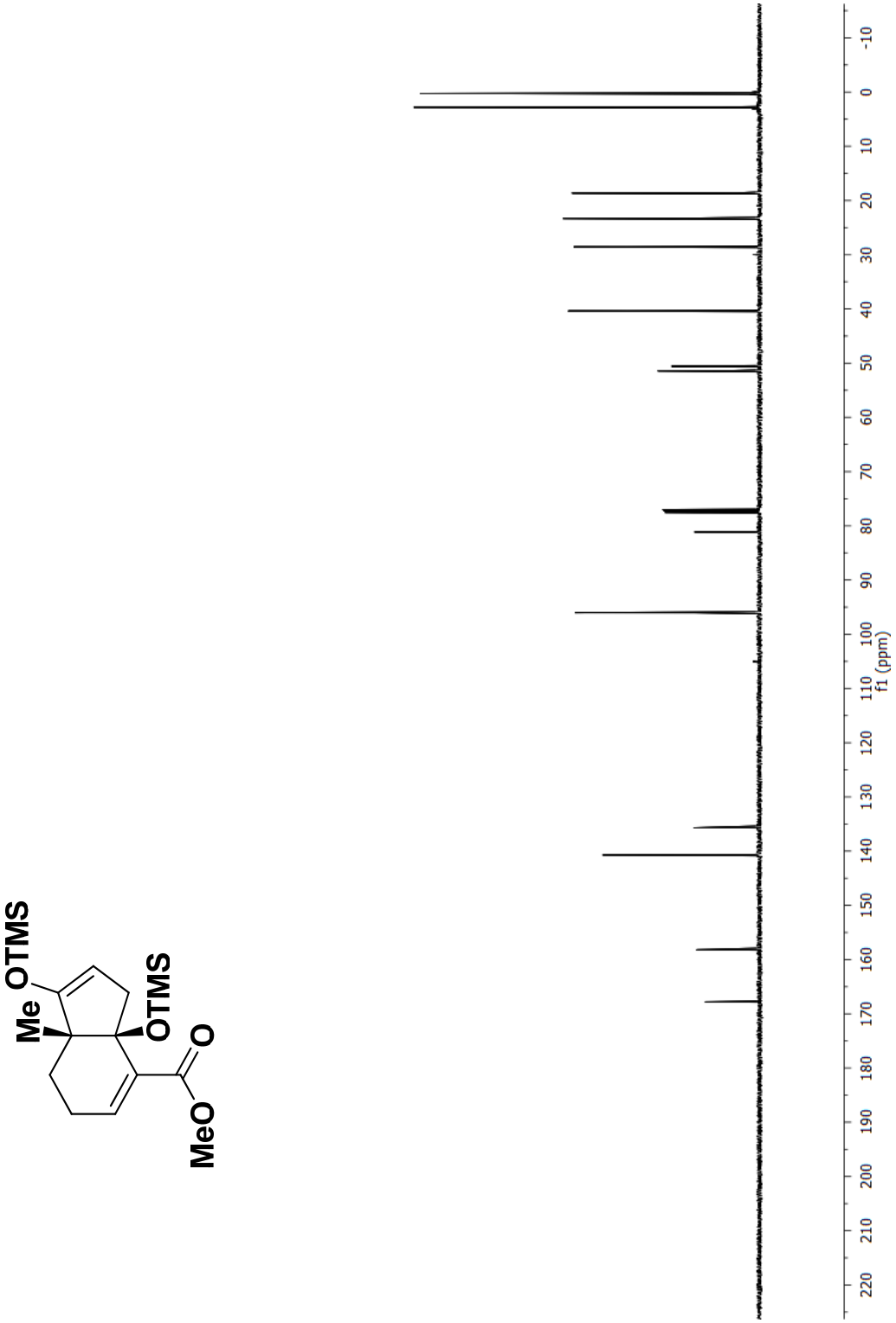
Me
OTMS
OTMS
O
MeO
f1 (ppm)

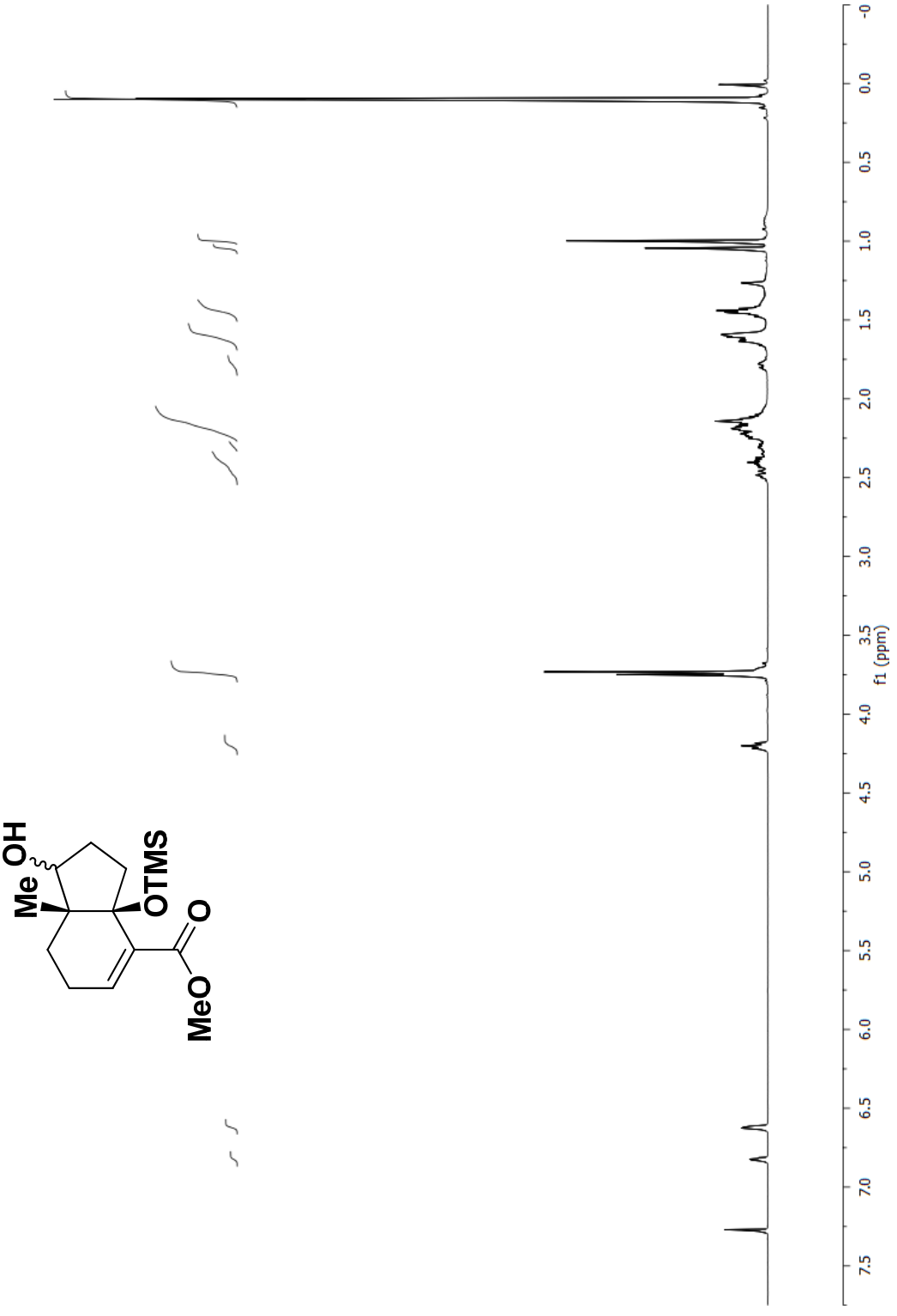
Me
OH
OTMS
O
MeO
f1 (ppm)

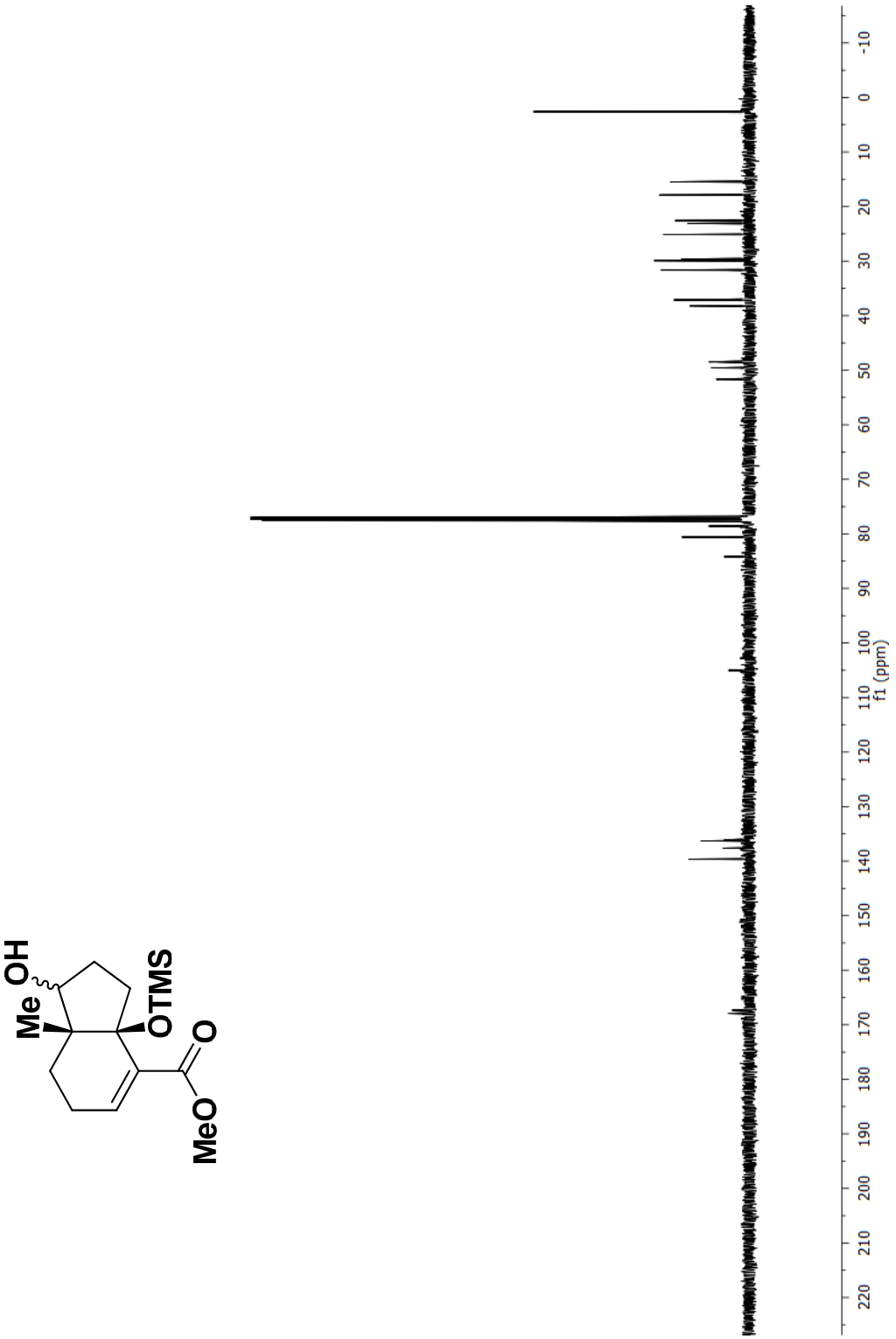
Me
OH
OTMS
O
MeO
f1 (ppm)

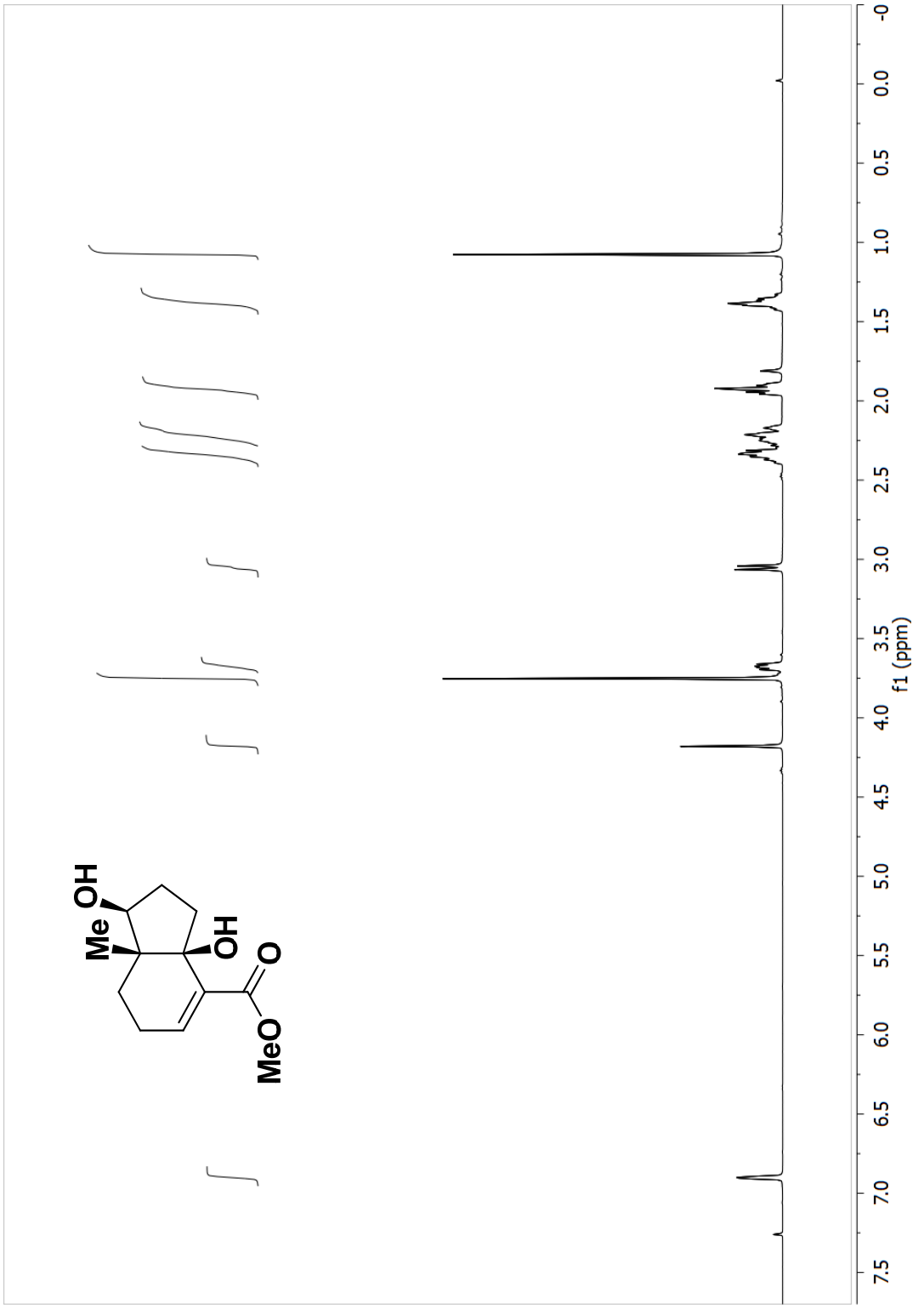
OH
Me
OH
O
MeO
7.5
7.0
6.5
6.0
5.5
5.0
4.5
4.0
3.5
3.0
2.5
2.0
1.5
1.0
0.5
0.0
-0
f1 (ppm)

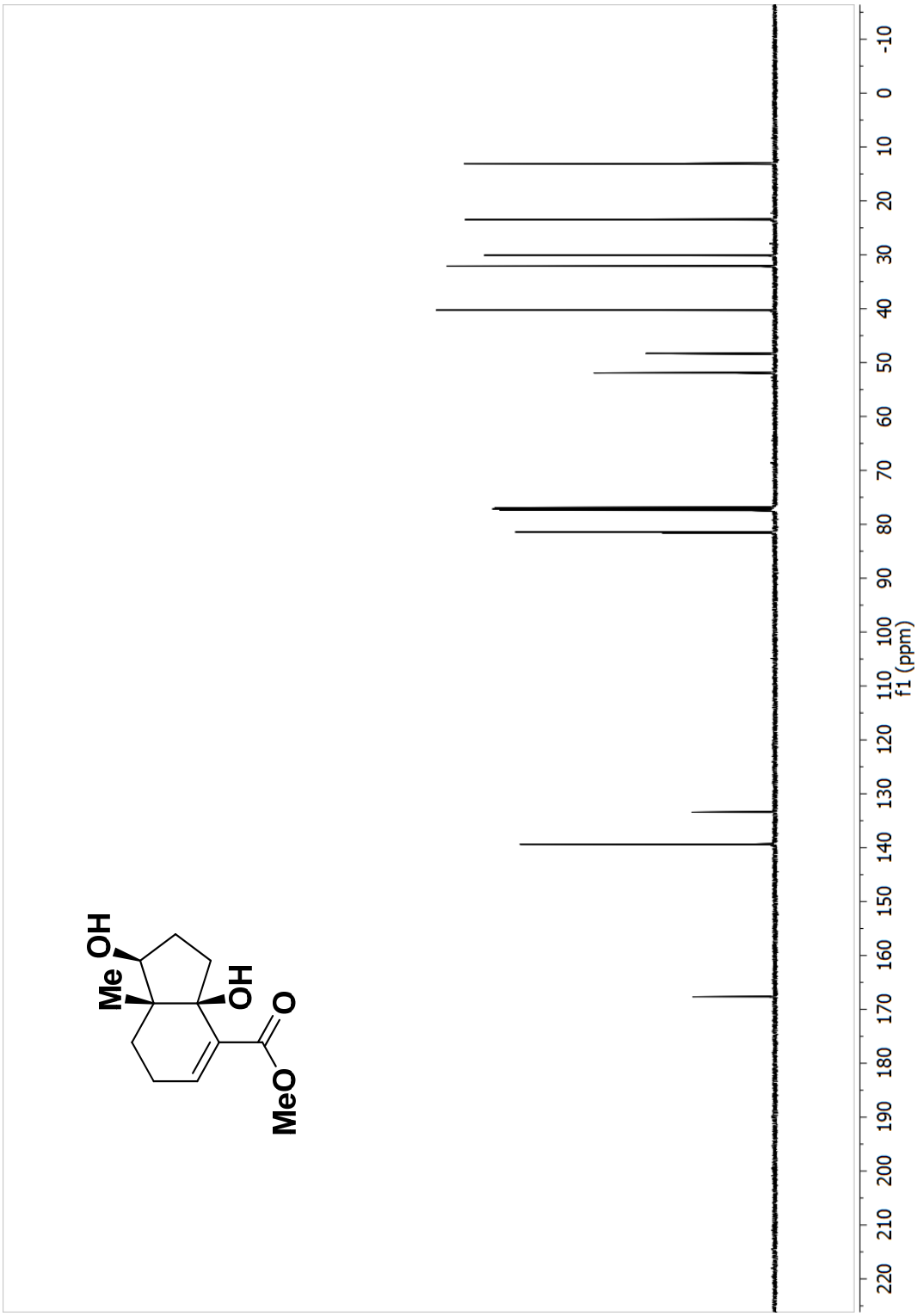
Me
OH
OH
O
MeO
-10
0
10
20
30
40
50
60
70
80
90
100
110
120
130
140
150
160
170
180
190
200
210
220
f1 (ppm)

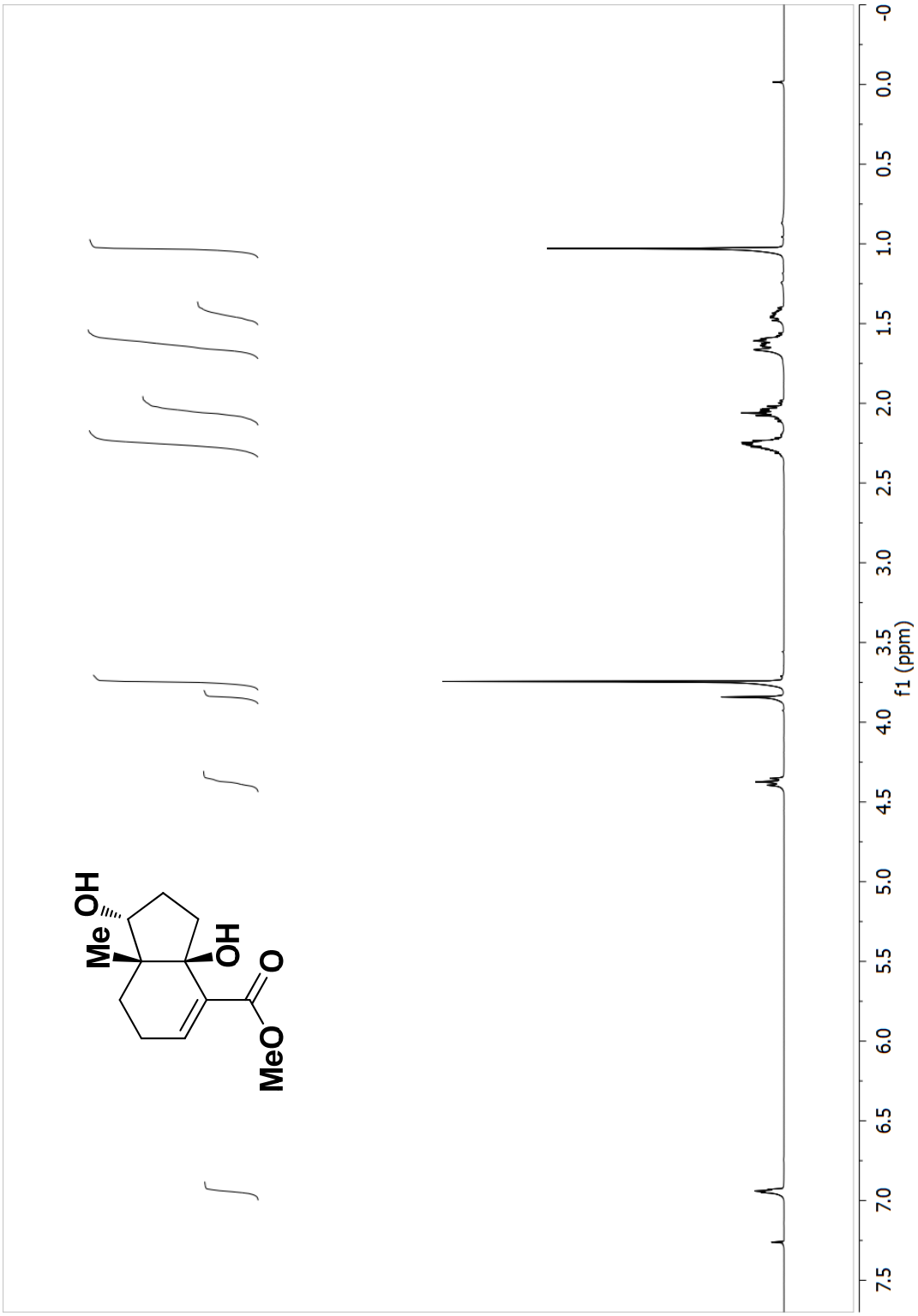
OH
Me
OH
O
MeO
7.5
7.0
6.5
6.0
5.5
5.0
4.5
4.0
3.5
3.0
2.5
2.0
1.5
1.0
0.5
0.0
-0
f1 (ppm)

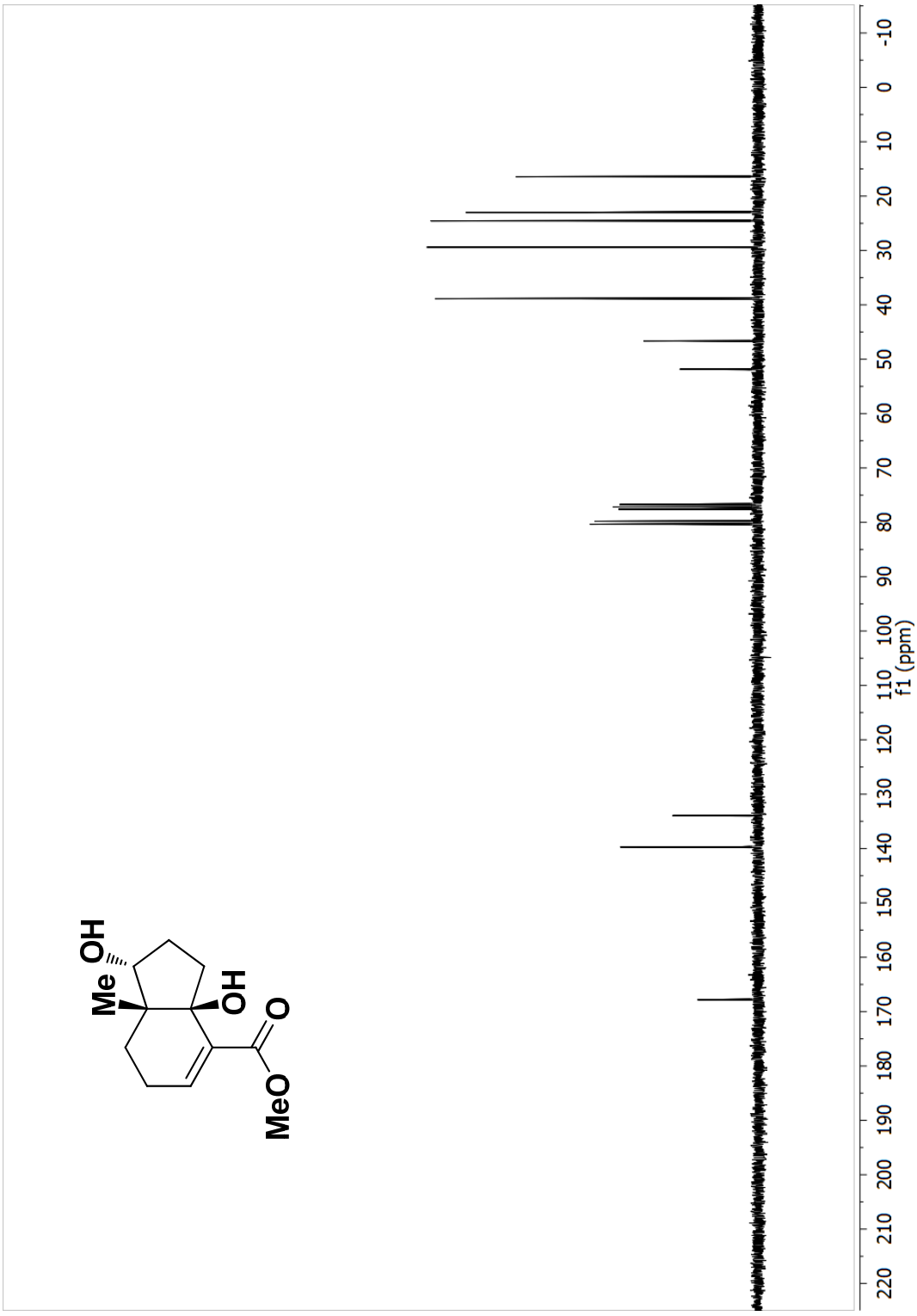
Me
OH
OH
O
MeO
f1 (ppm)
-10
0
10
20
30
40
50
60
70
80
90
100
110
120
130
140
150
160
170
180
190
200
210
220

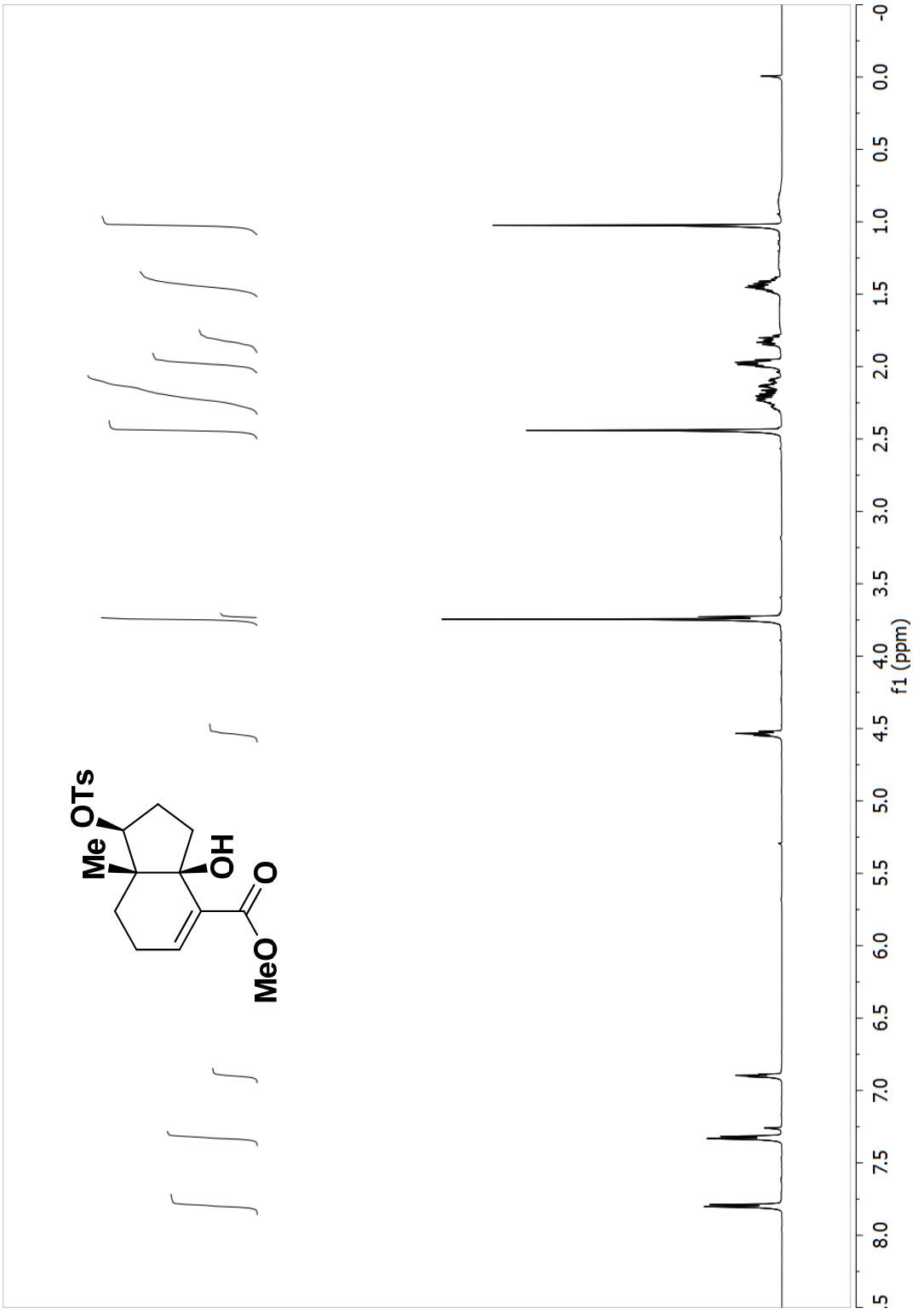
Me
OTs
OH
O
MeO
f1 (ppm)

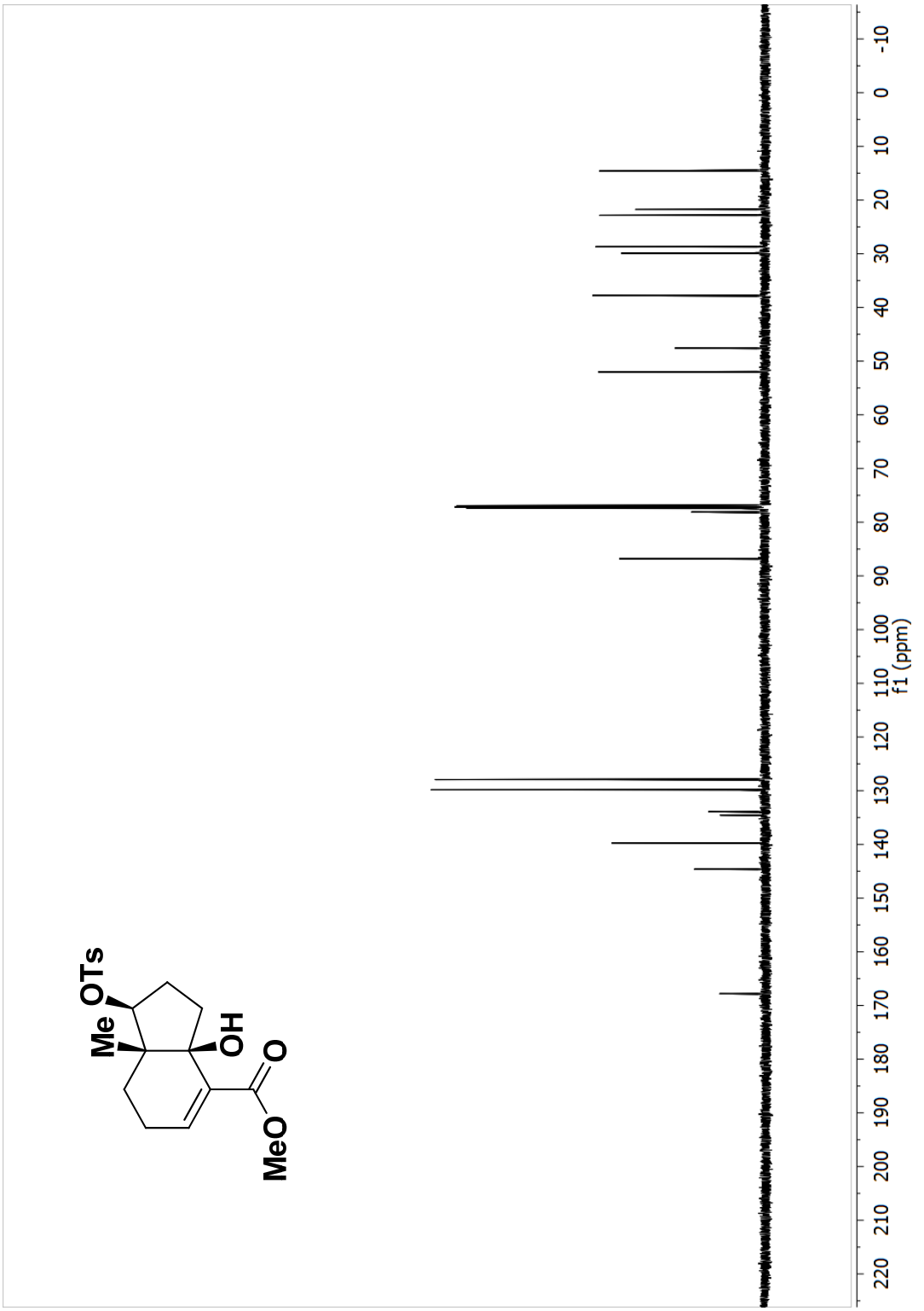
Me
OTs
OH
O
MeO
-10
0
10
20
30
40
50
60
70
80
90
100
110
120
130
140
150
160
170
180
190
200
210
220
f1 (ppm)

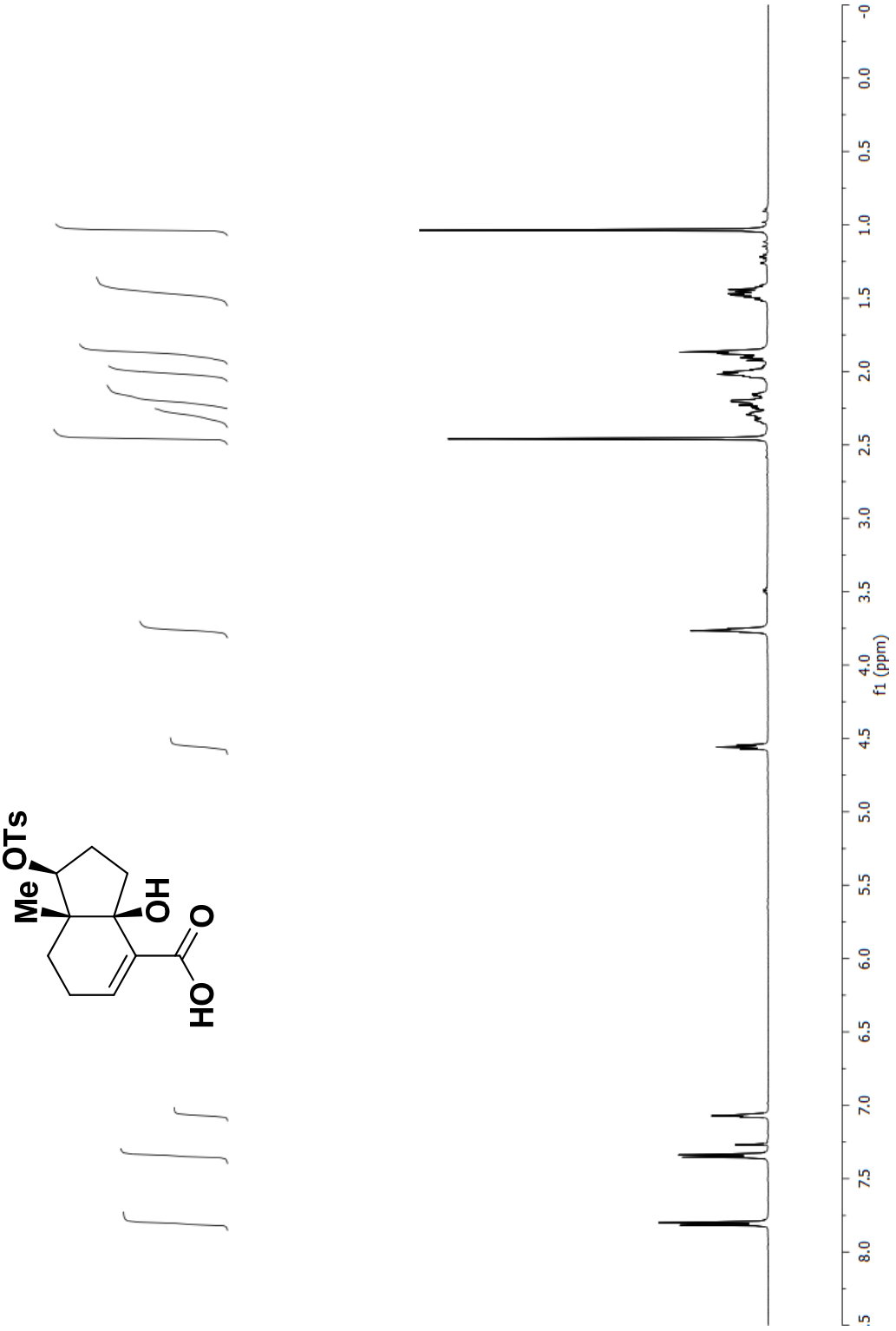
Me
OTs
OH
O
HO
f1 (ppm)

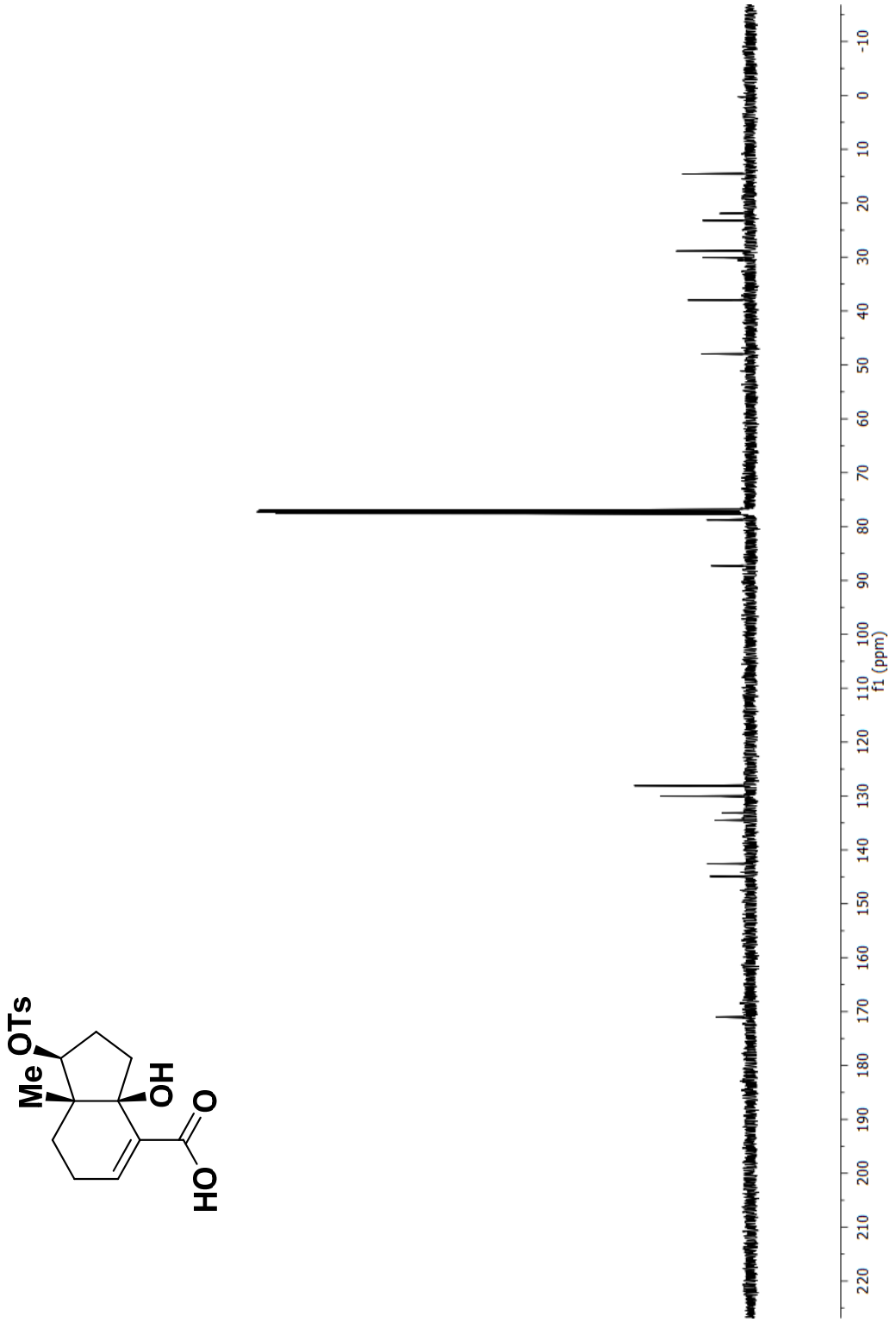
Me
OTs
OH
O
HO
f1 (ppm)

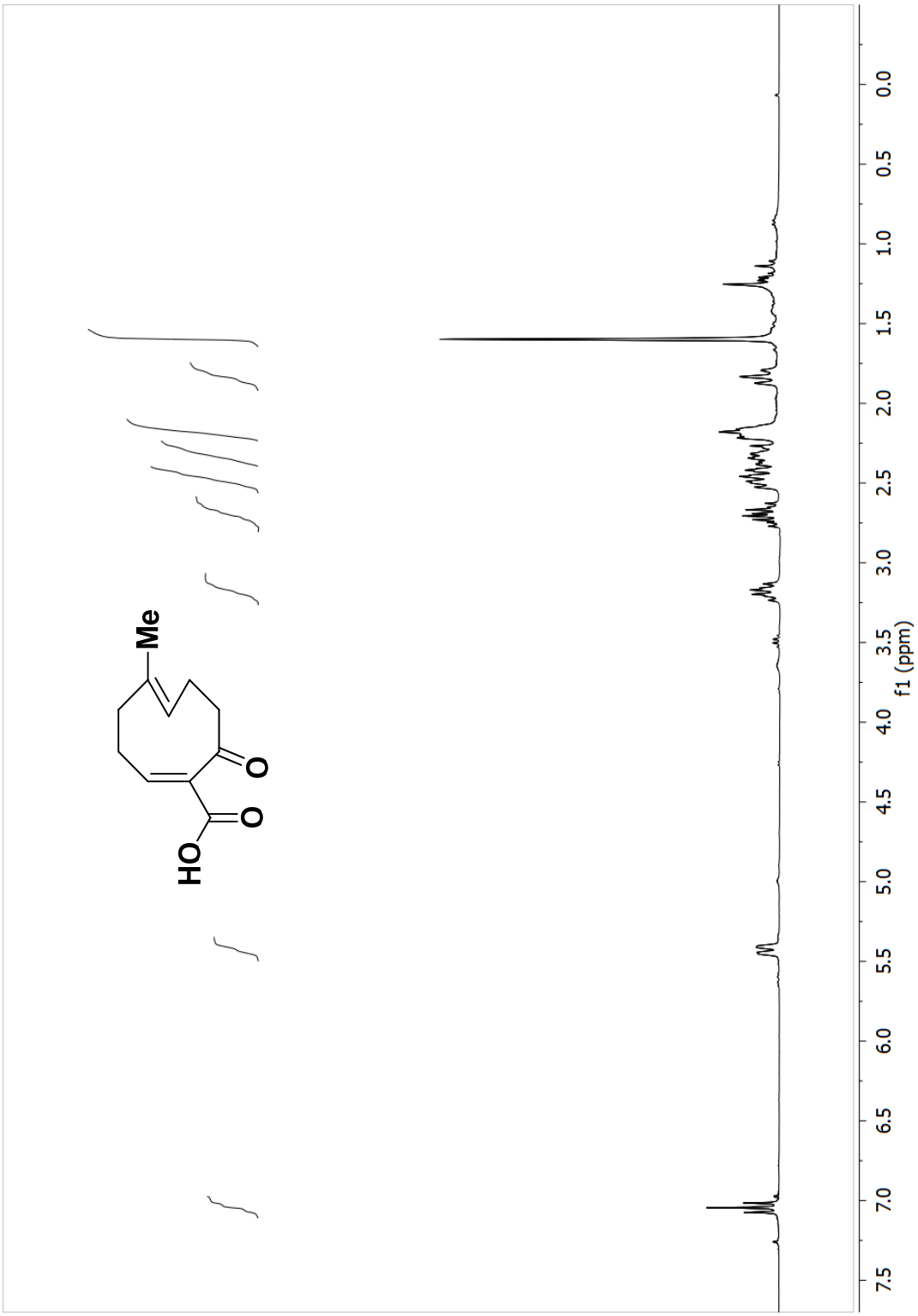
Me
O
O
HO
7.5
7.0
6.5
6.0
5.5
5.0
4.5
4.0
3.5
3.0
2.5
2.0
1.5
1.0
0.5
0.0
f1 (ppm)

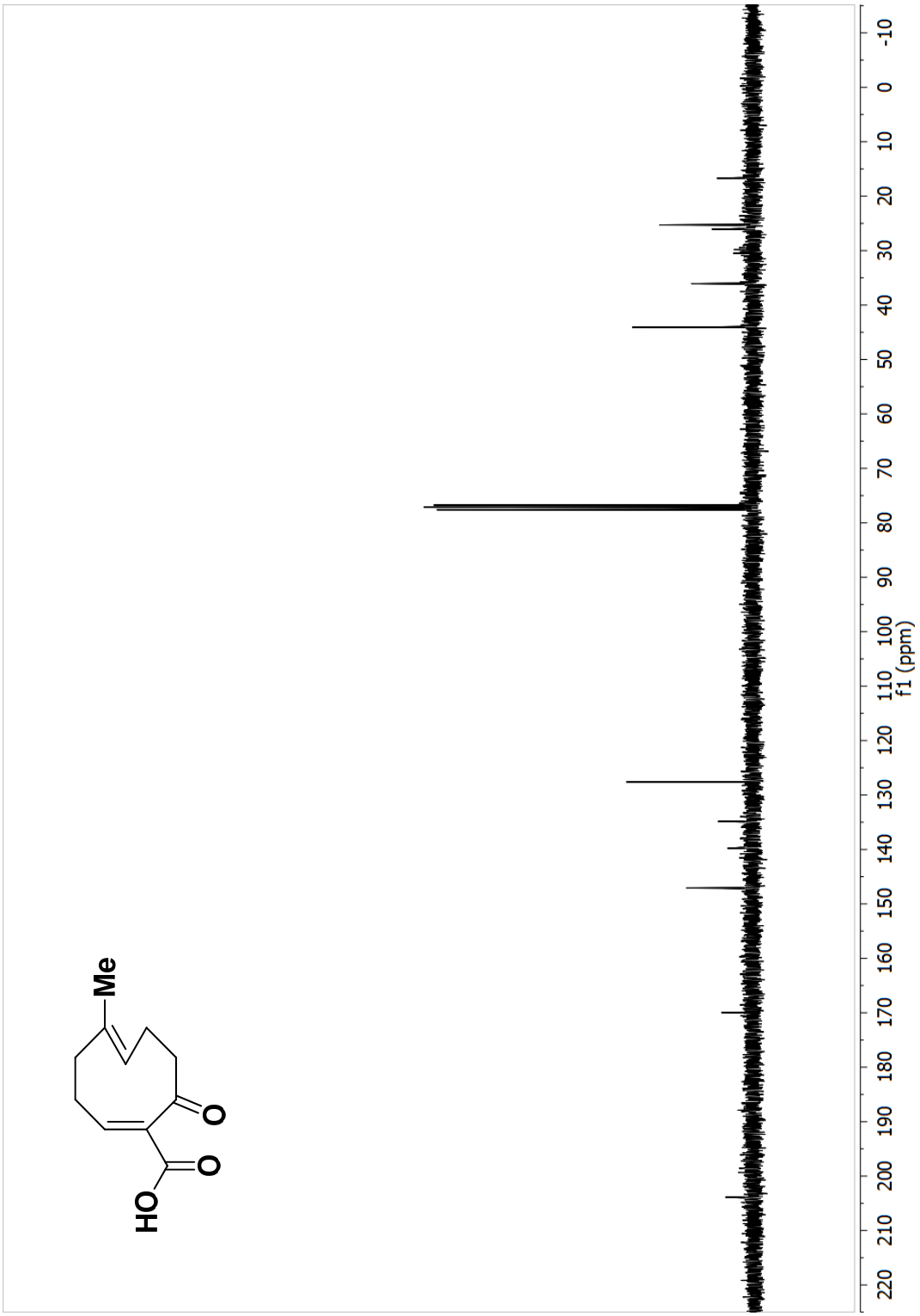
Me
O
O
HO
-10
0
10
20
30
40
50
60
70
80
90
100
110
120
130
140
150
160
170
180
190
200
210
220
f1 (ppm)

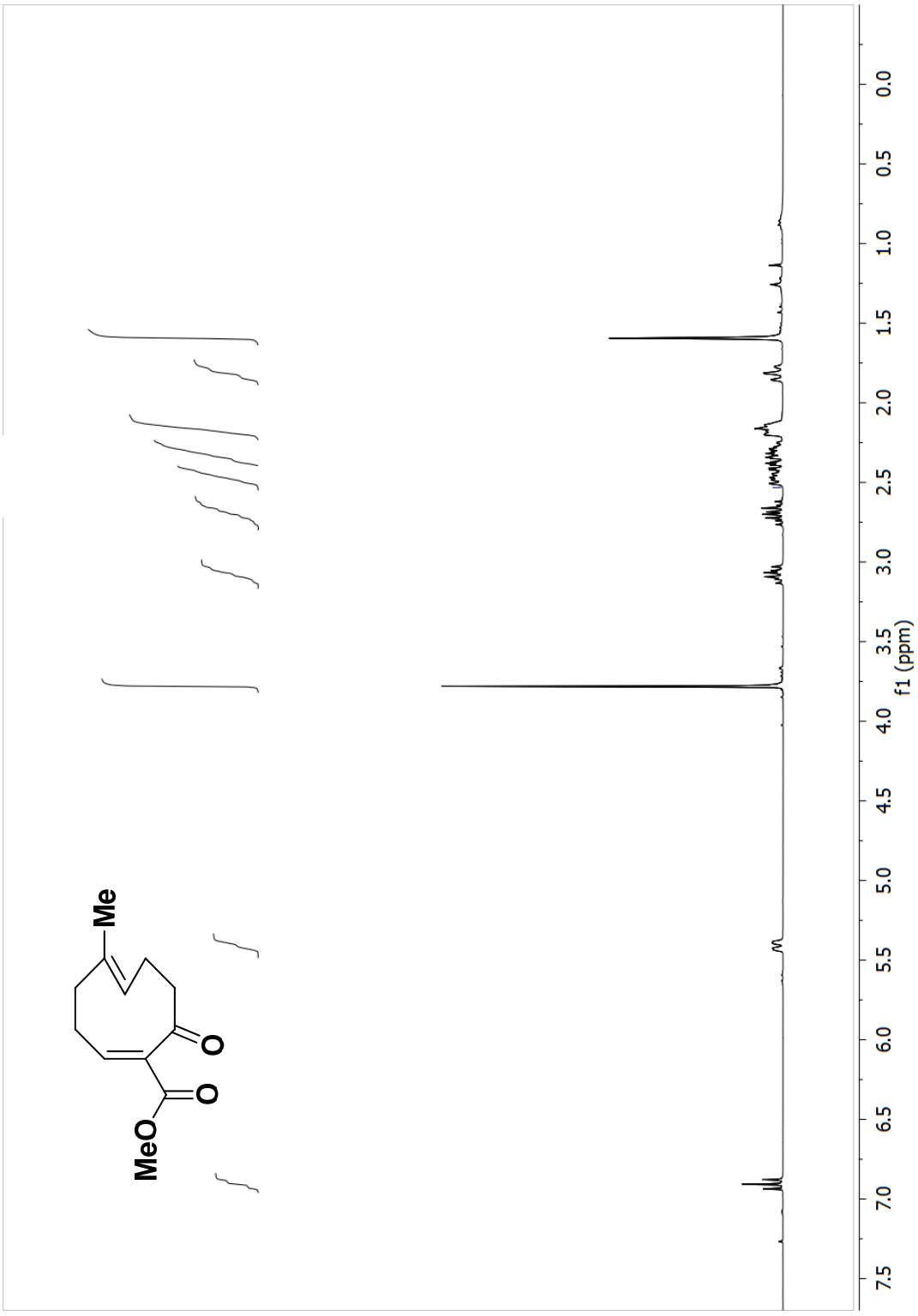
Me
O
O
MeO
7.5
7.0
6.5
6.0
5.5
5.0
4.5
4.0
3.5
3.0
2.5
2.0
1.5
1.0
0.5
0.0
f1 (ppm)

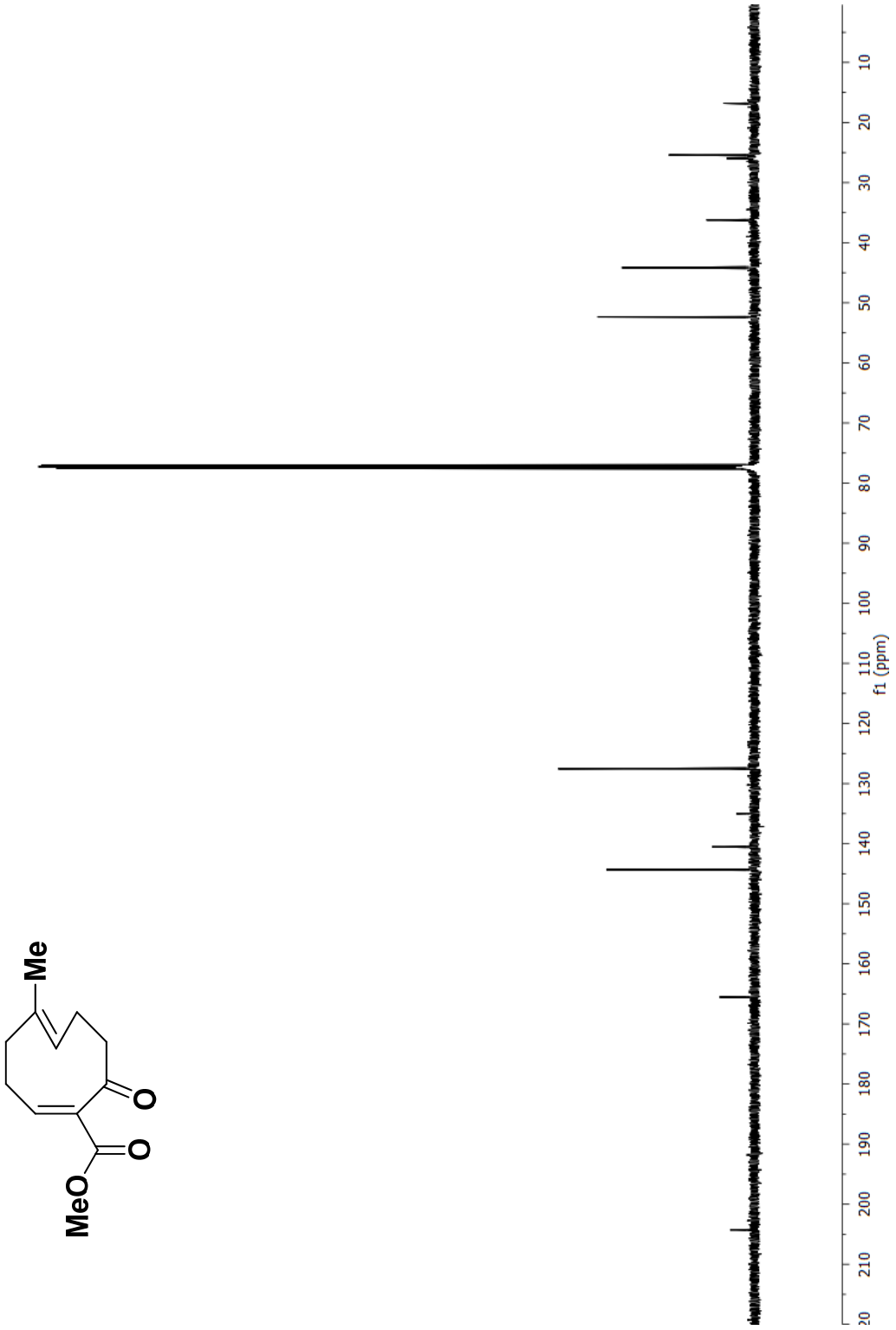
Me
O
O
MeO
f1 (ppm)

^{1}H and ^{13}C NMR chemical shifts and coupling constsnts of (1E,5E)-methyl 5-methyl-9-oxocyclonona-1,5-dienecarboxylate

δ_H/ppm		J/Hz	
H2a	2.8926	H2a - H2b	11.64
H2b	2.3880	H2a - H3a	7.15
H3a	2.5378	H2a - H3b	1.27
H3b	1.7909	H2b - H3a	12.03
H4	5.1596	H2b - H3b	7.61
5-CH_3	1.5009	H3a - H4	12.23
H6a	1.7115	H3b - H4	3.71
H6b	1.4232	H4 - 5-CH_3	1.45
H7a	2.3124	H6a - H6b	-11.95
H7b	1.7314	H6a - H7a	2.01
H8	6.7706	H6a - H7b	6.35
10-OCH_3	3.310	H6b - H7a	12.48
		H6b - H7b	2.28
		H7a - H7b	-11.92
		H7a - H8	8.58
		H7b - H8	8.58

δ_C/ppm	
C1	202.32
C2	43.99
C3	25.38
C4	127.47
C5	134.62
5-CH_3	16.52
C6	36.17
C7	25.61
C8	143.41
C9	141.05
C10	165.11
10-OCH_3	51.33

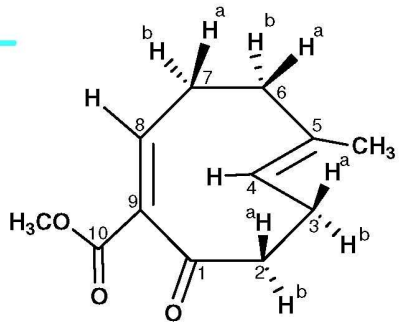

in C_6D_6

^{1}H NMR spectrum in C_6D_6

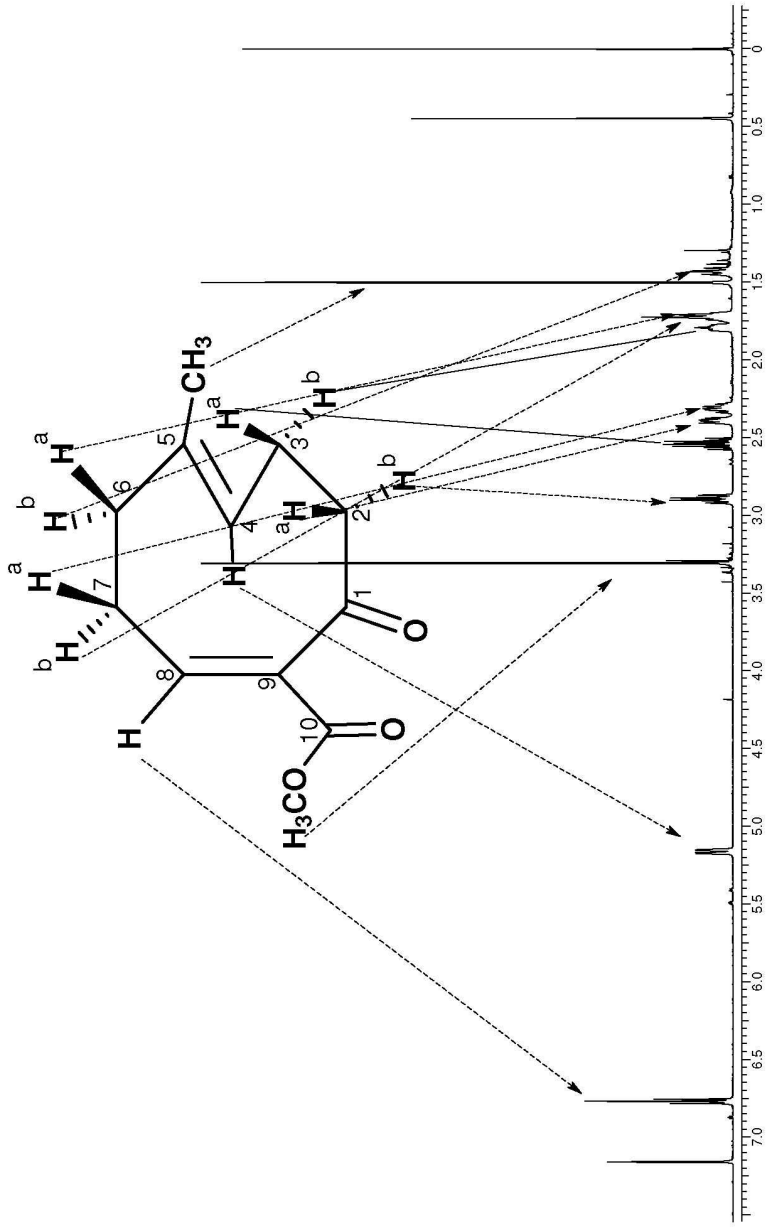

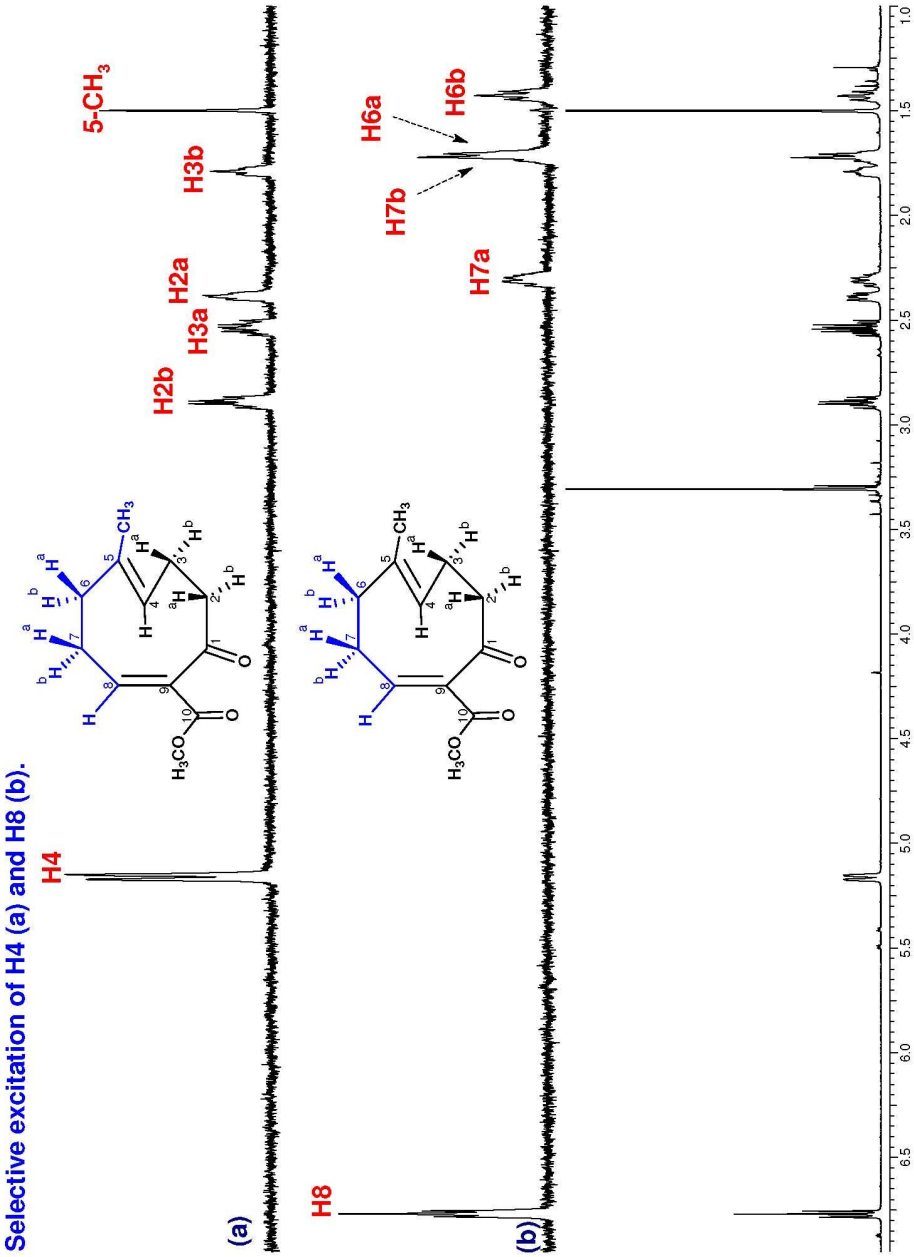
Selective excitation of H4 (a) and H8 (b).
H4
H8
5-CH3
H3b
H2a
H3a
H2b
H6a
H6b
H7b
H7a
(a)
(b)
H3CO
O
O
1.0
1.5
2.0
2.5
3.0
3.5
4.0
4.5
5.0
5.5
6.0
6.5

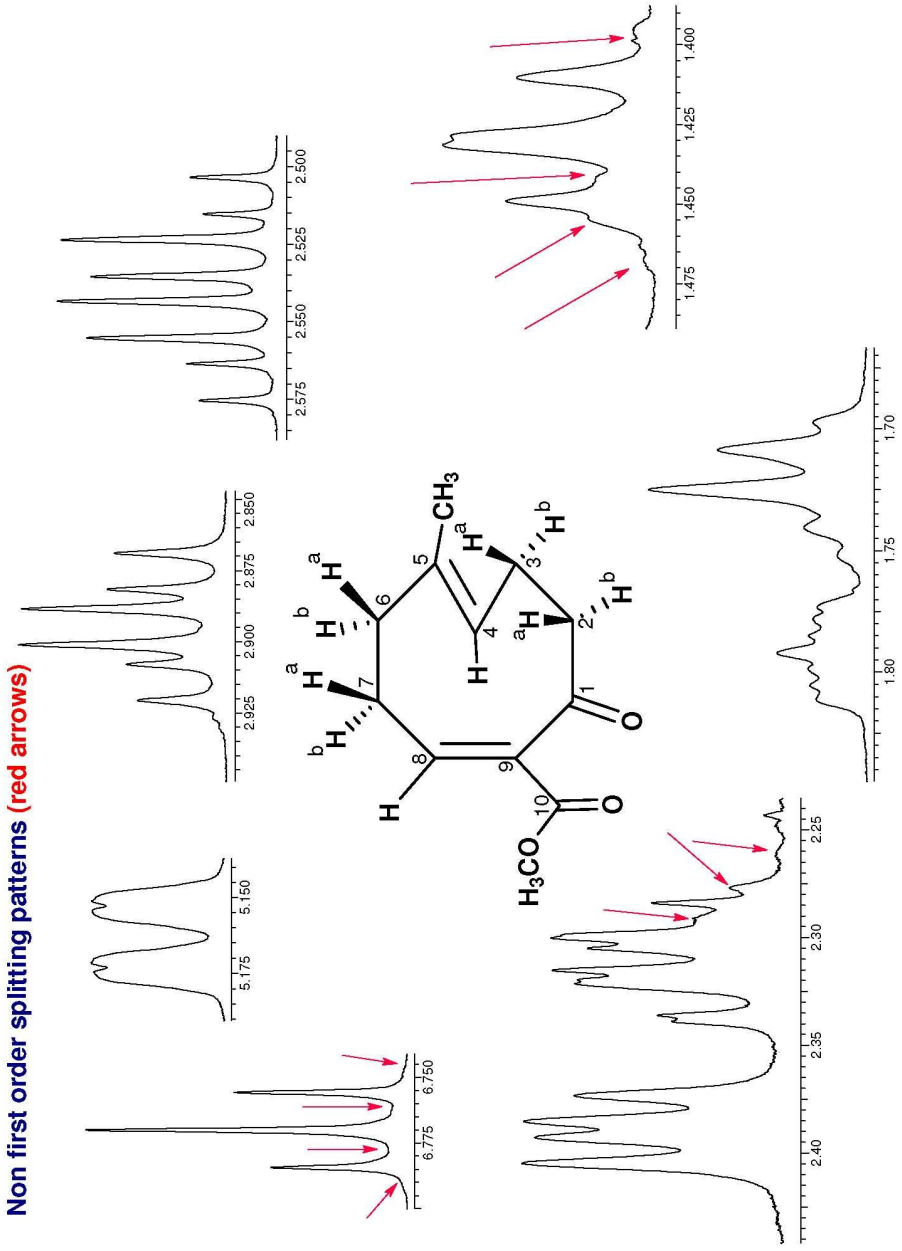
Non first order splitting patterns (red arrows)
H3CO
CH3
O
O
H
Ha
Hb
Ha
Hb
Ha
Hb
Ha
Hb
1
4
5
6
7
8
9
10
1'
2'
3'

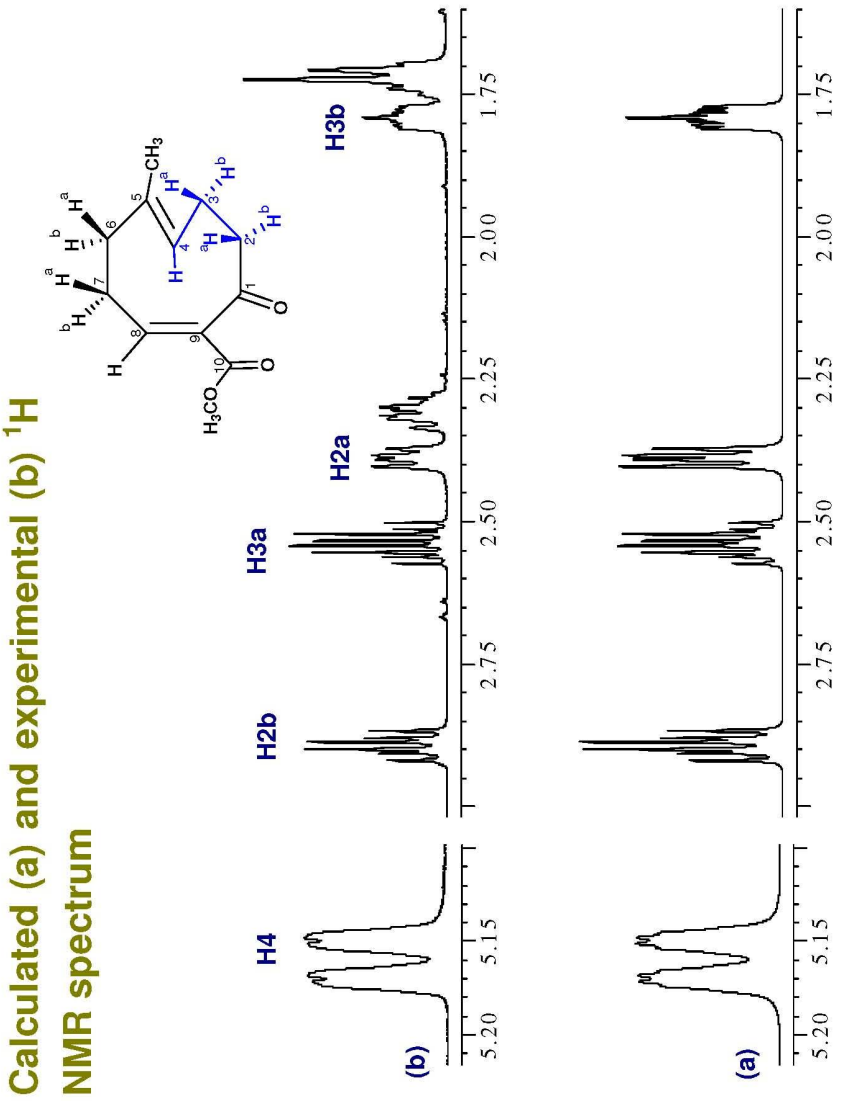
Calculated (a) and experimental (b) ^{1}H
NMR spectrum
H4
H2b
H3a
H2a
H3b
(b)
(a)
5.20
5.15
2.75
2.50
2.25
2.00
1.75
H_3CO
CH_3

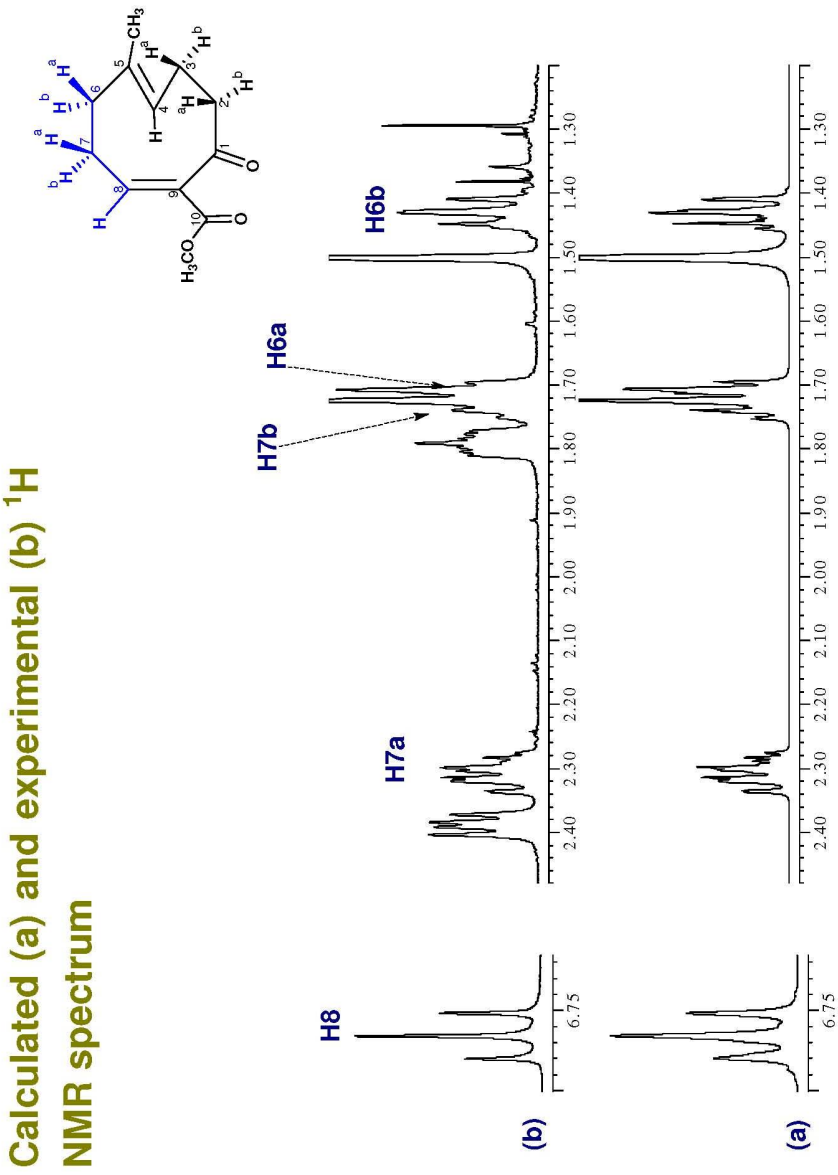
Calculated (a) and experimental (b) ^{1}H
NMR spectrum
H8
H7a
H7b
H6a
H6b
(b)
(a)
6.75
2.40
2.30
2.20
2.10
2.00
1.90
1.80
1.70
1.60
1.50
1.40
1.30

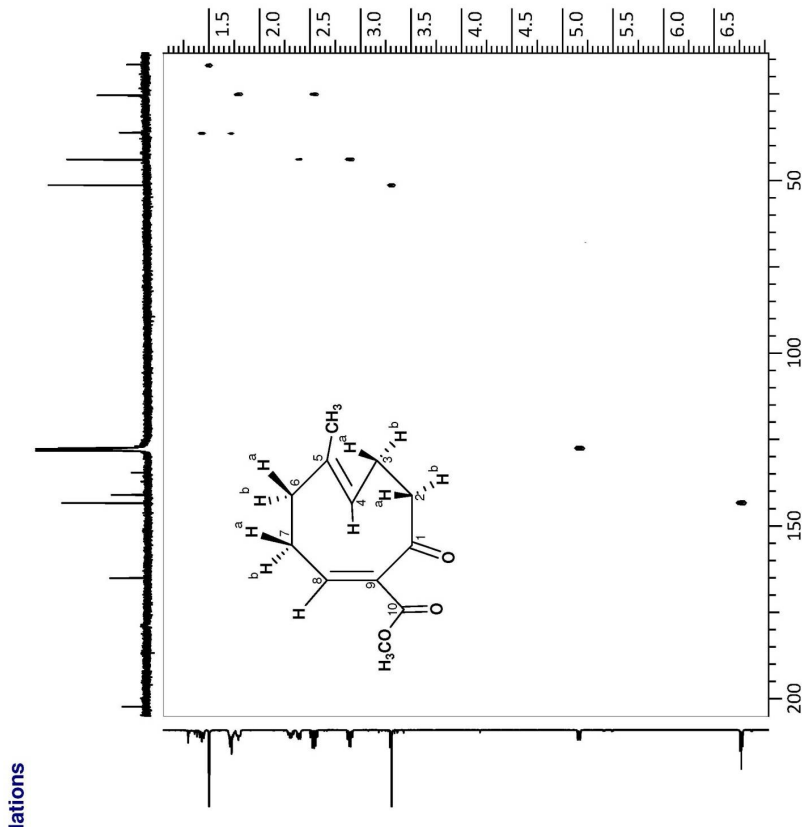
One-bond coorelations
HETCOR
1.5
2.0
2.5
3.0
3.5
4.0
4.5
5.0
5.5
6.0
6.5
50
100
150
200
CH3
H3CO
O
O

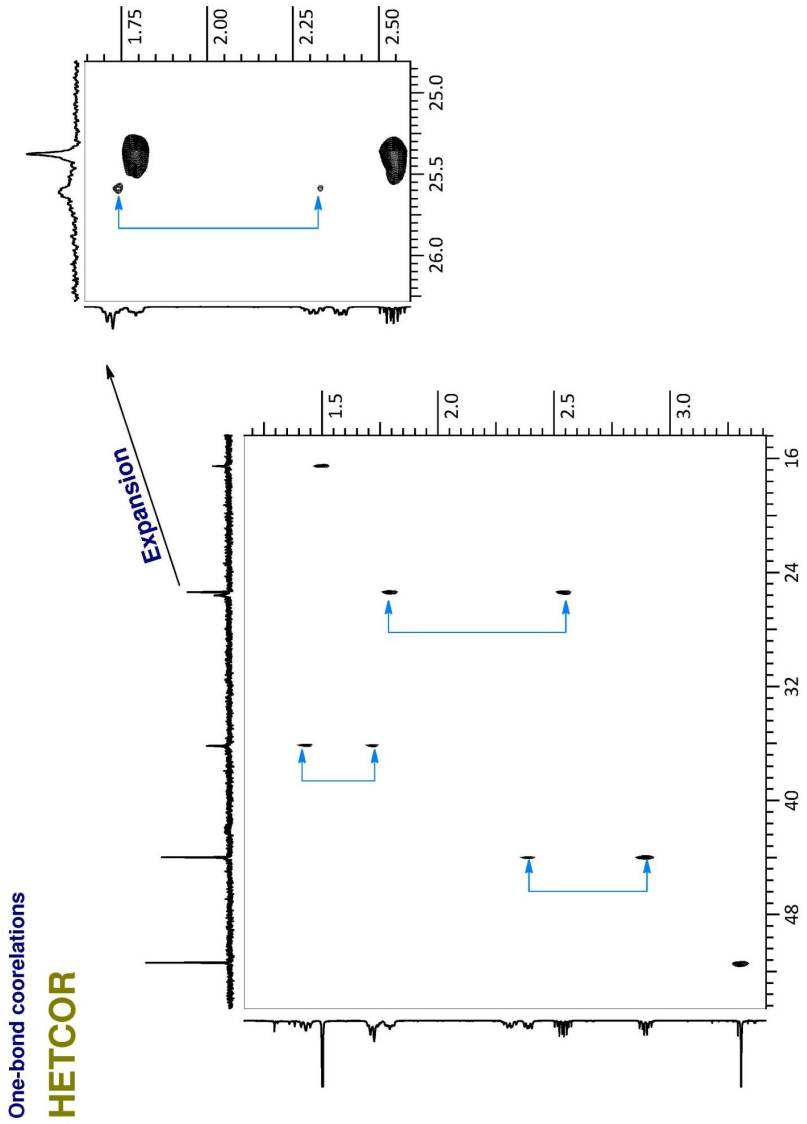
One-bond coorelations
HETCOR
Expansion
1.75
2.00
2.25
2.50
25.0
25.5
26.0
1.5
2.0
2.5
3.0
16
24
32
40
48

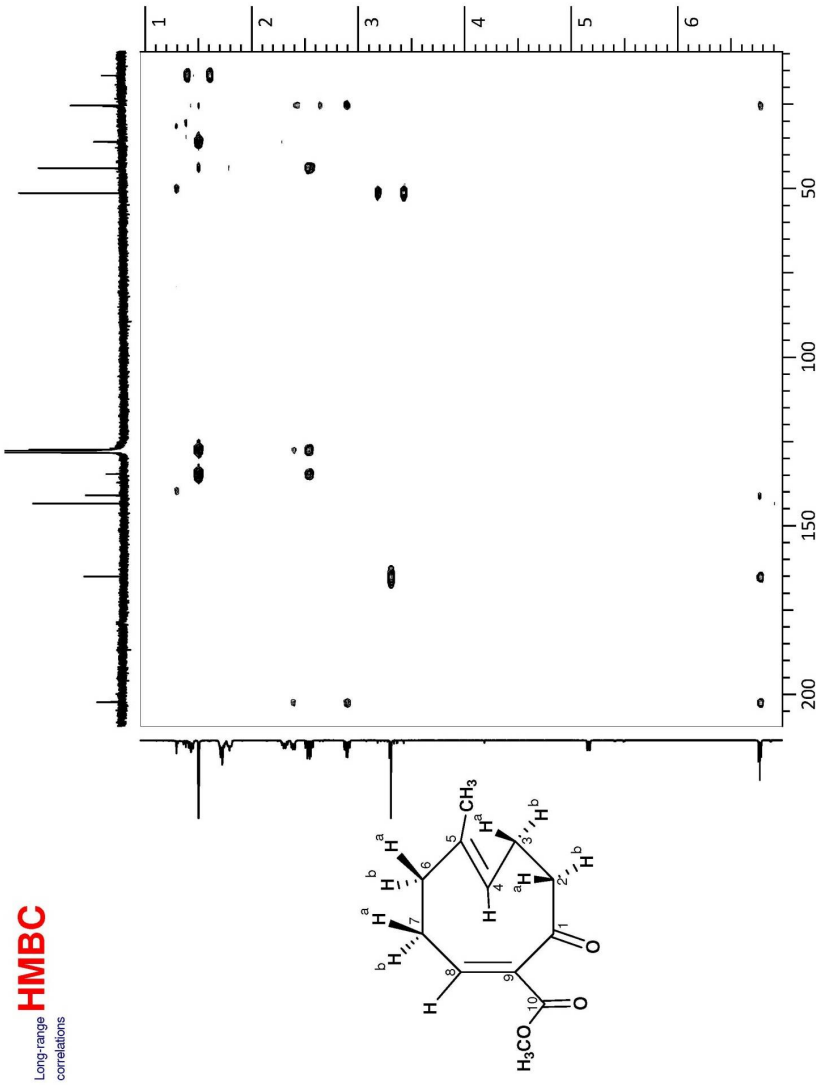
HMBC
Long-range correlations
1
2
3
4
5
6
50
100
150
200
CH3
H3CO
O
O
H

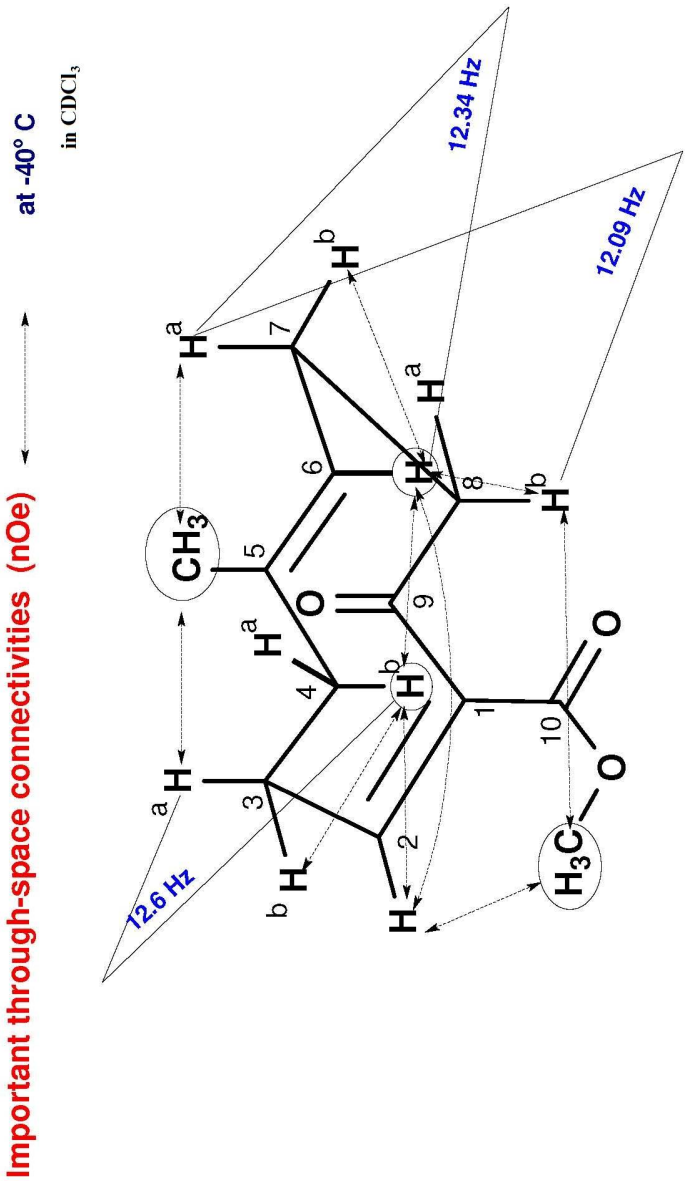
Important through-space connectivities (nOe)
at -40° C
in $CDCl_3$
12.6 Hz
12.34 Hz
12.09 Hz
CH_3
H_3C
O
O
O
1
2
3
4
5
6
7
8
9
10

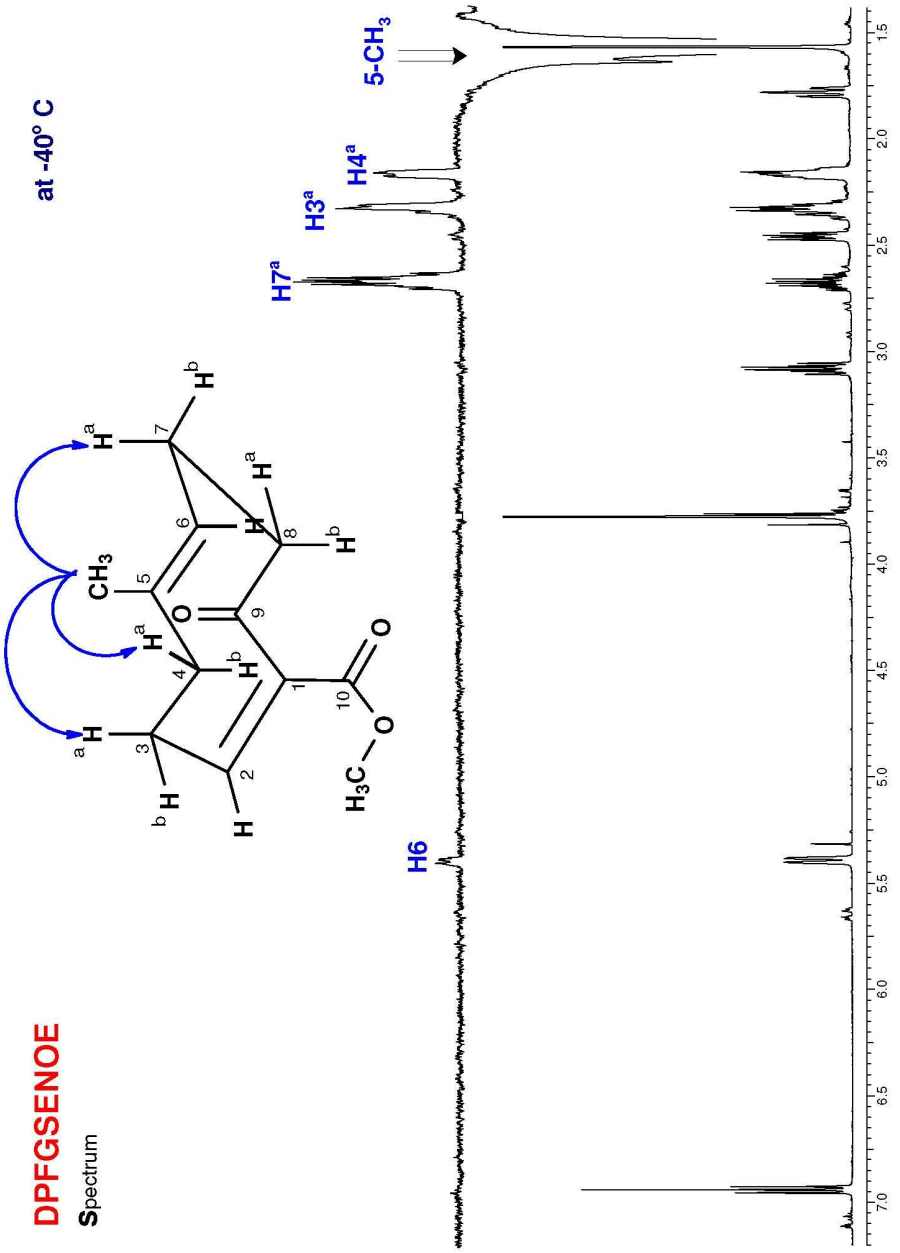
DPFGSENOE
Spectrum
at -40° C
H6
H7a
H3a
H4a
5-CH3
CH3
H3C
O
O
O
1.5
2.0
2.5
3.0
3.5
4.0
4.5
5.0
5.5
6.0
6.5
7.0

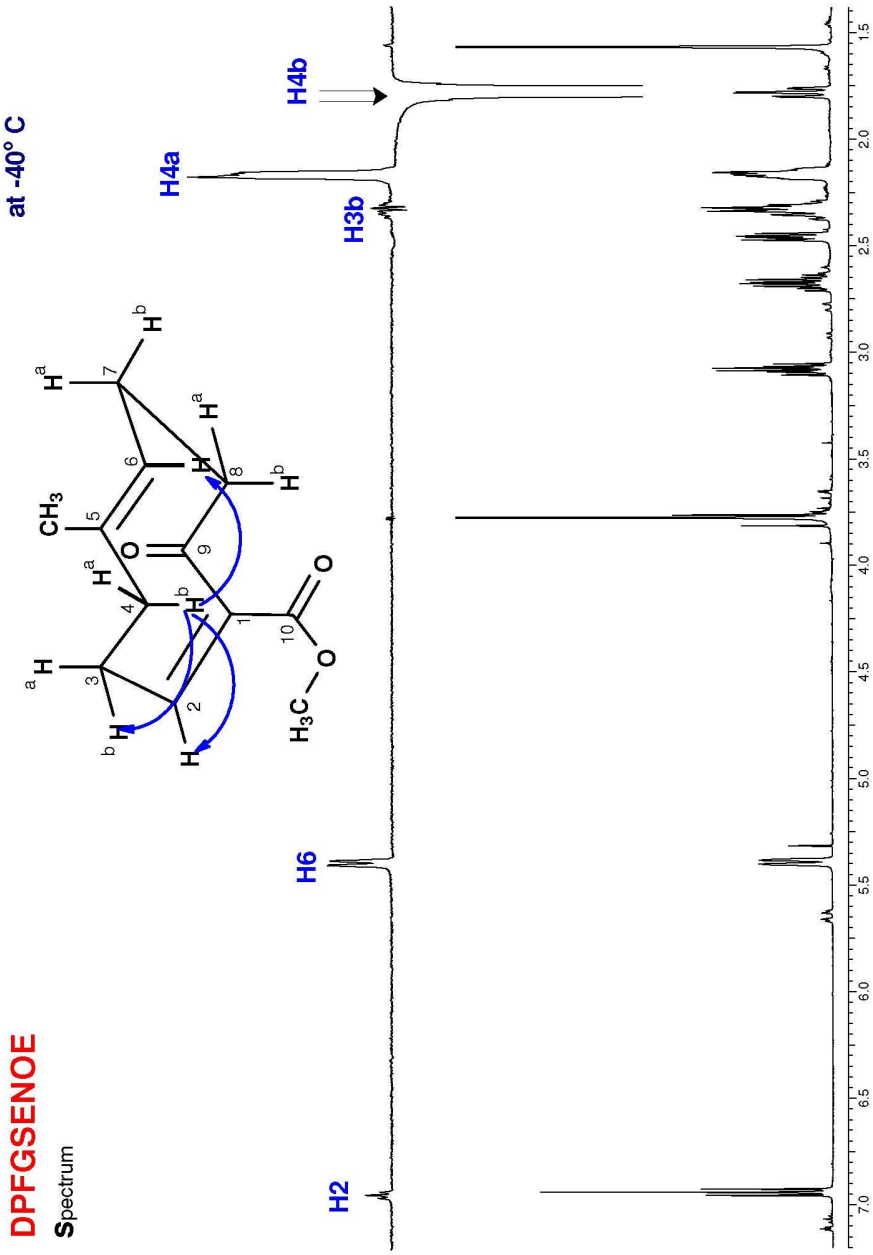
DPFGSENOE
Spectrum
at -40° C
H2
H6
H3b
H4a
H4b
CH3
O
H3C
O
O
1.5
2.0
2.5
3.0
3.5
4.0
4.5
5.0
5.5
6.0
6.5
7.0

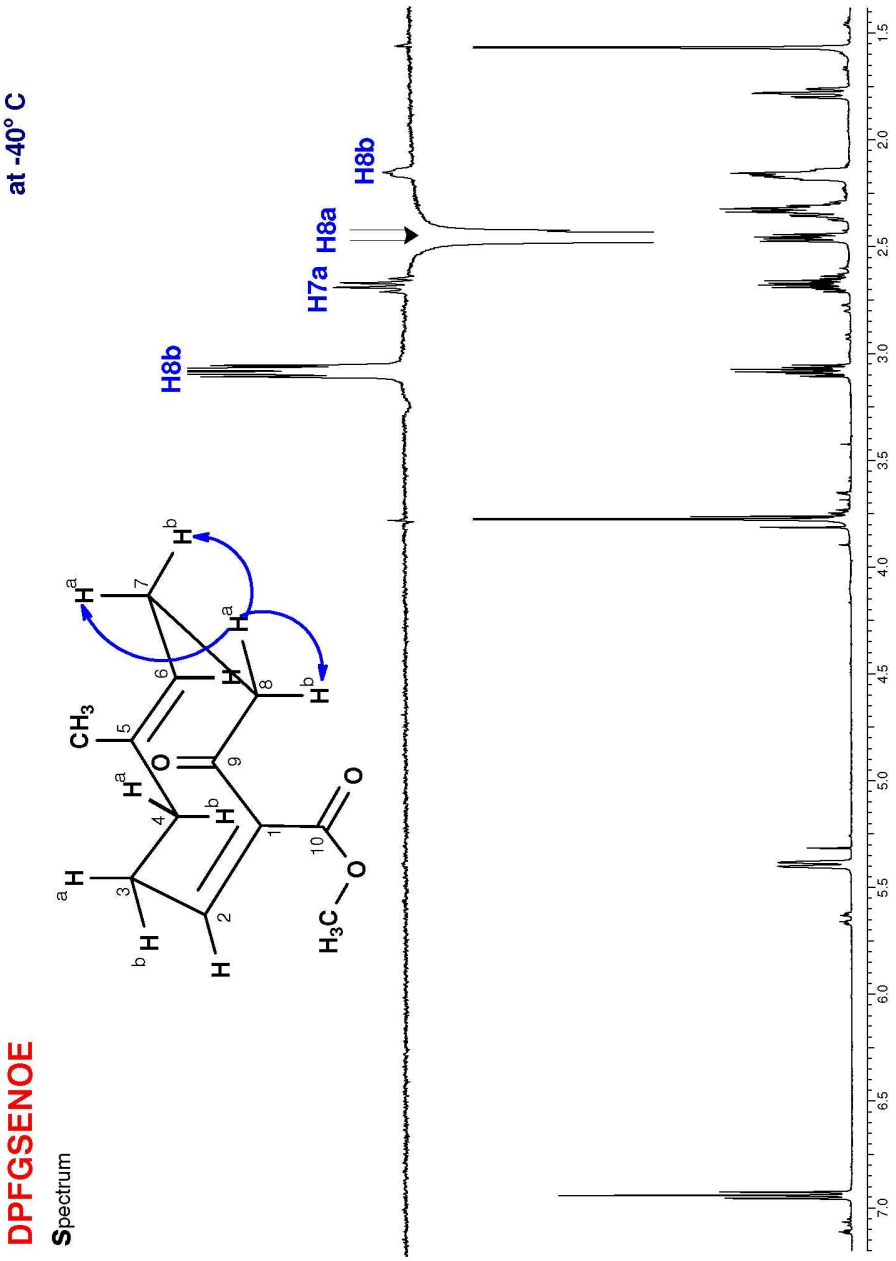
DPFGSENOE
Spectrum
at -40° C
H8b
H7a
H8a
H8b
CH3
H3C
O
O
O

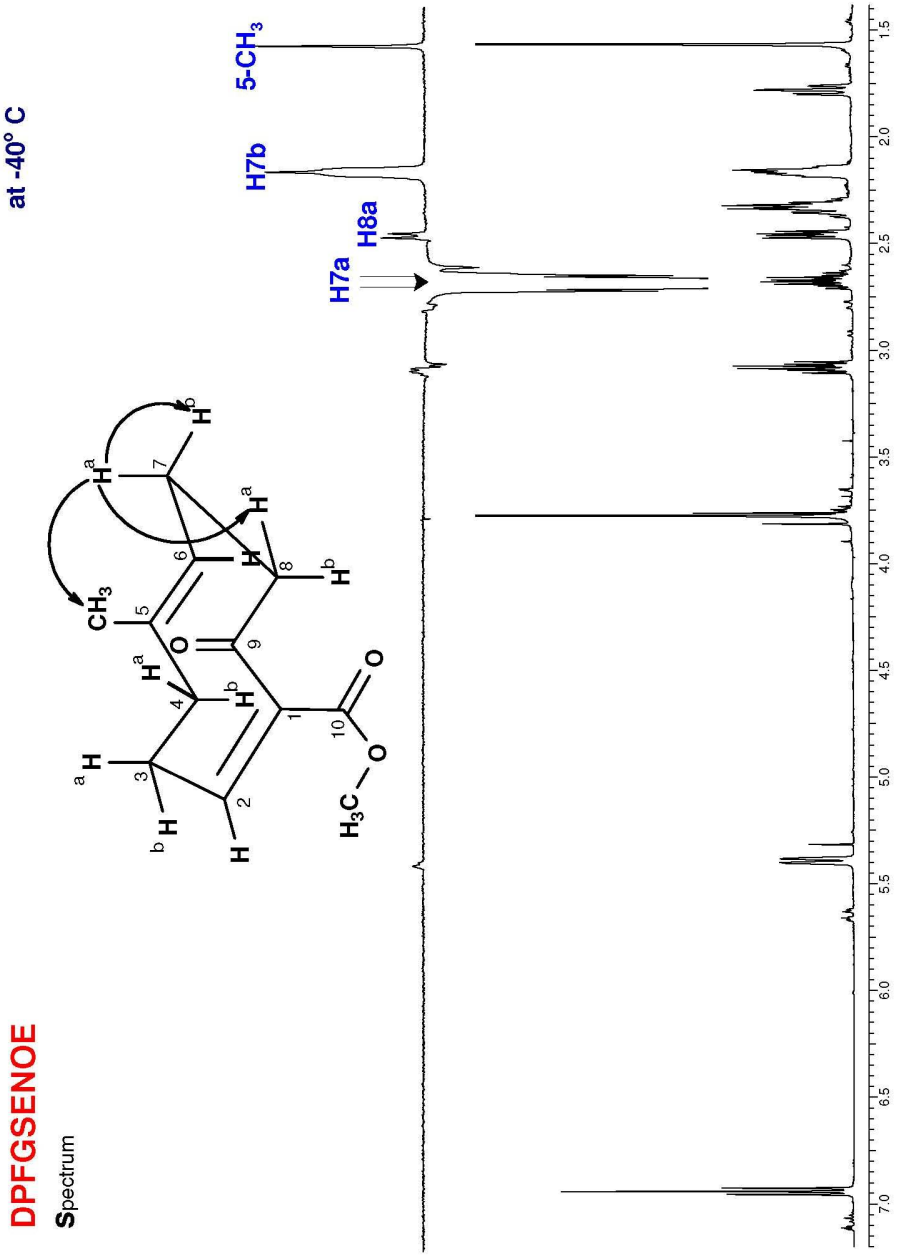
DPFGSENOE
Spectrum
at -40° C
5-CH3
H7b
H8a
H7a
CH3
H3C
O
O
O
1.5
2.0
2.5
3.0
3.5
4.0
4.5
5.0
5.5
6.0
6.5
7.0

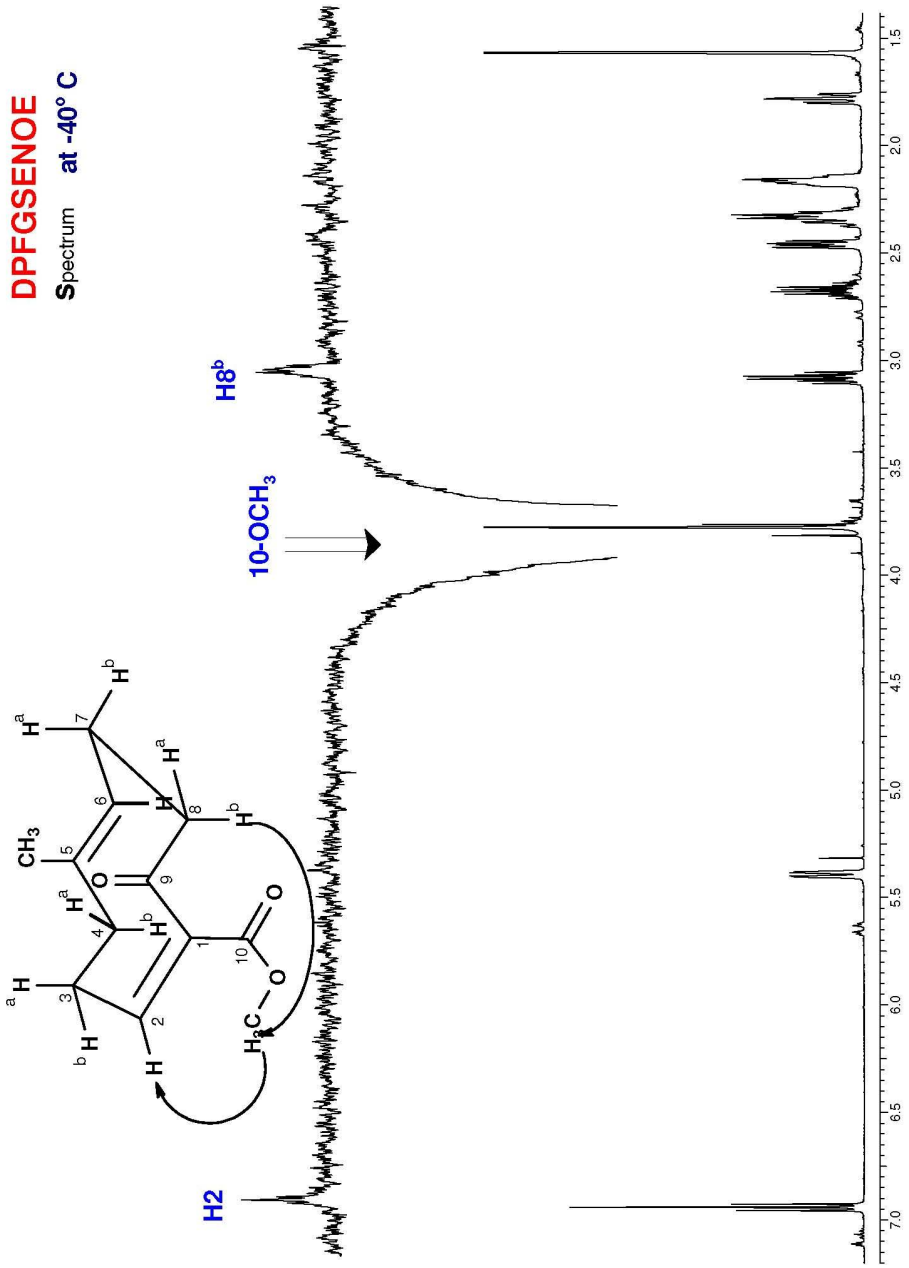
DPFGSENOE
Spectrum at -40° C
H8b
10-OCH3
H2
CH3
7.0
6.5
6.0
5.5
5.0
4.5
4.0
3.5
3.0
2.5
2.0
1.5

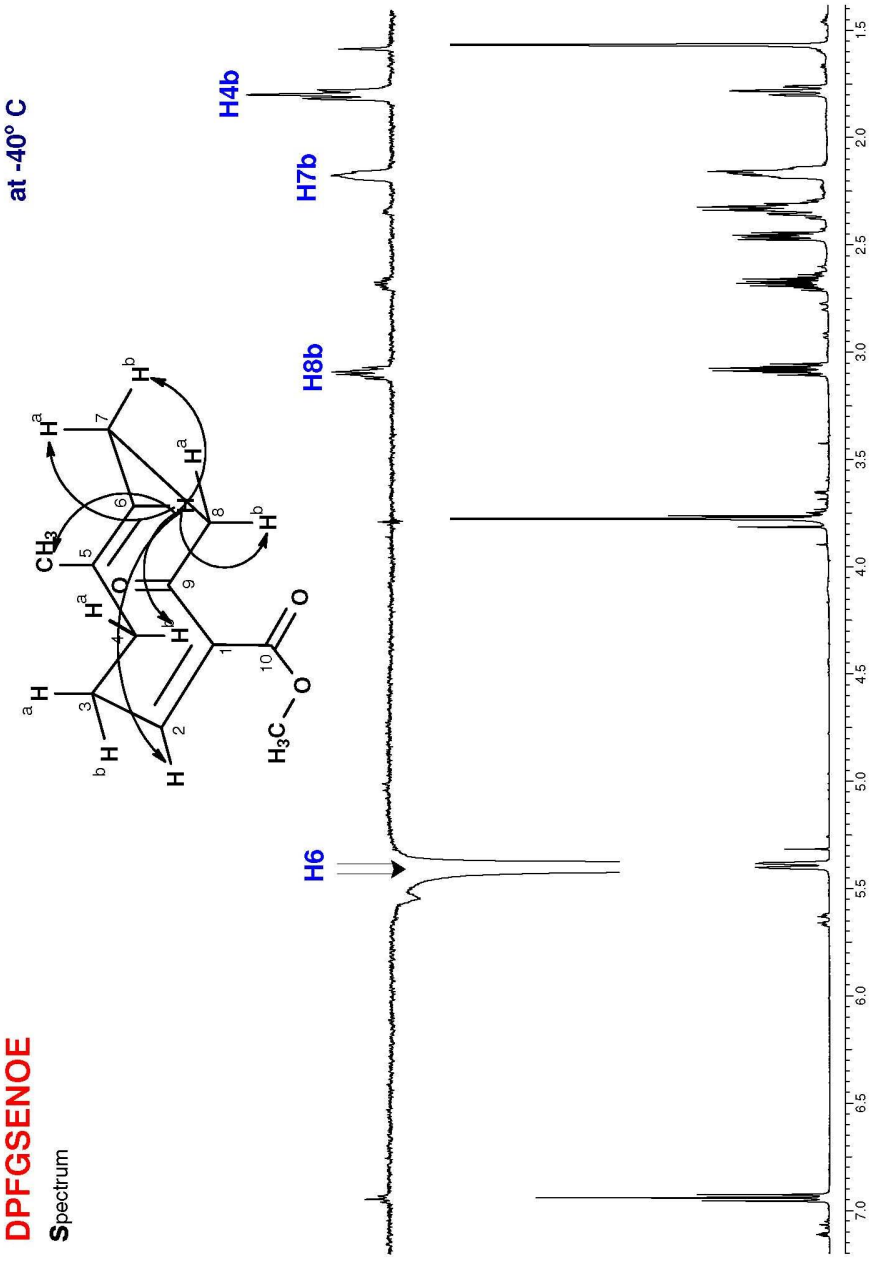
DPFGSENOE
Spectrum
at -40° C
H4b
H7b
H8b
H6
7.0
6.5
6.0
5.5
5.0
4.5
4.0
3.5
3.0
2.5
2.0
1.5

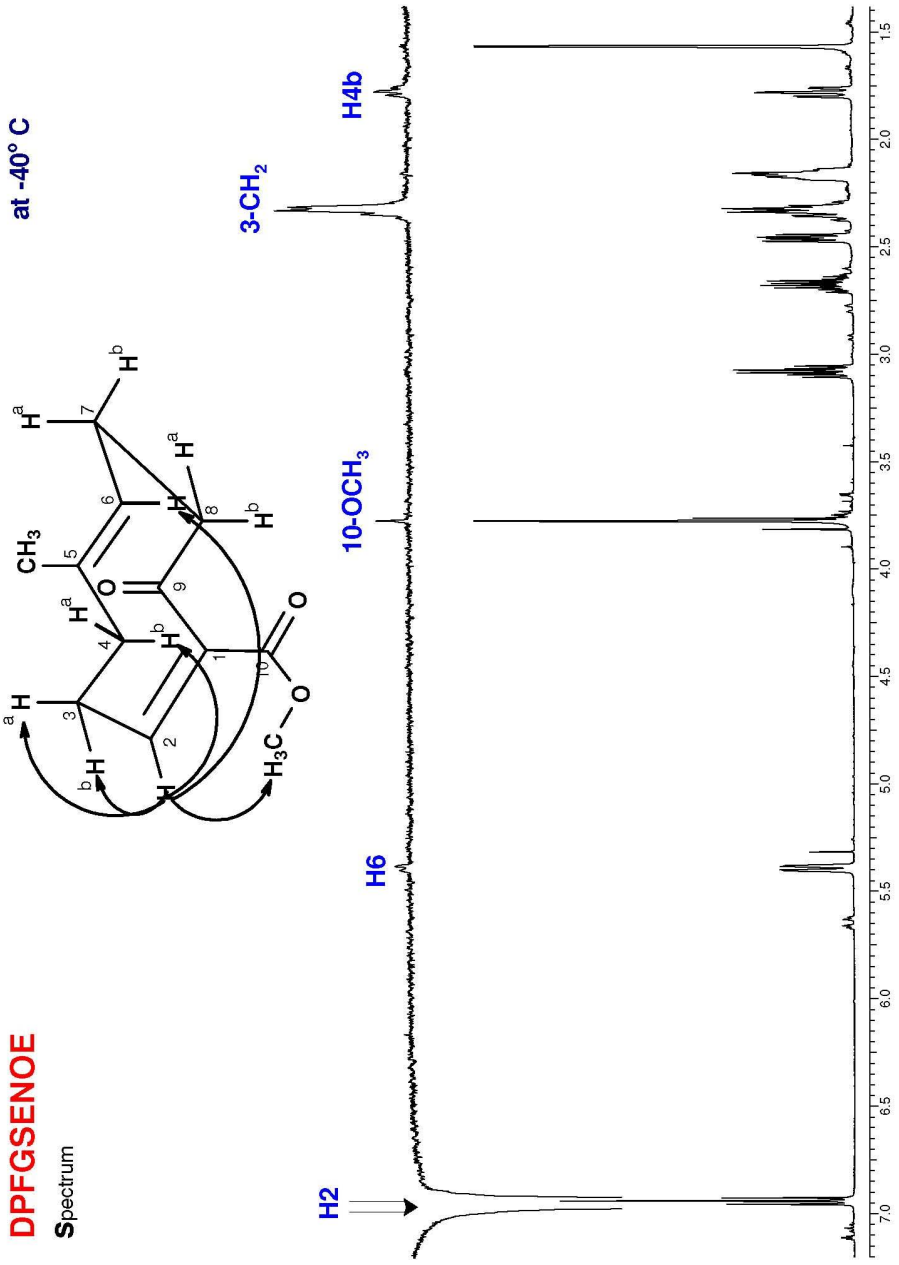
DPFGSENOE
Spectrum
at -40° C
H2
H6
10-OCH3
3-CH2
H4b
CH3
H3C
O
O
O
7.0
6.5
6.0
5.5
5.0
4.5
4.0
3.5
3.0
2.5
2.0
1.5

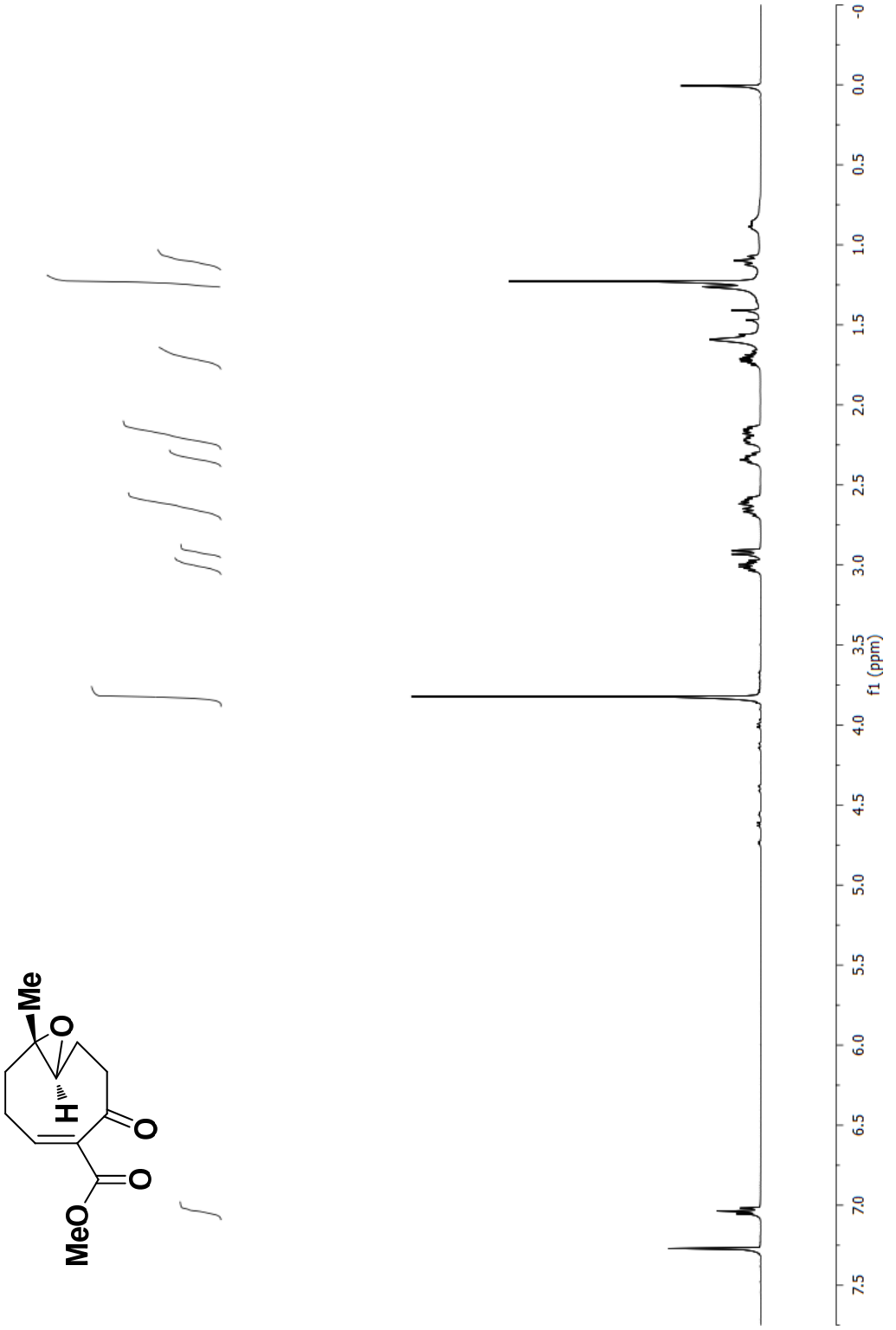
Me
O
H
O
O
MeO
f1 (ppm)

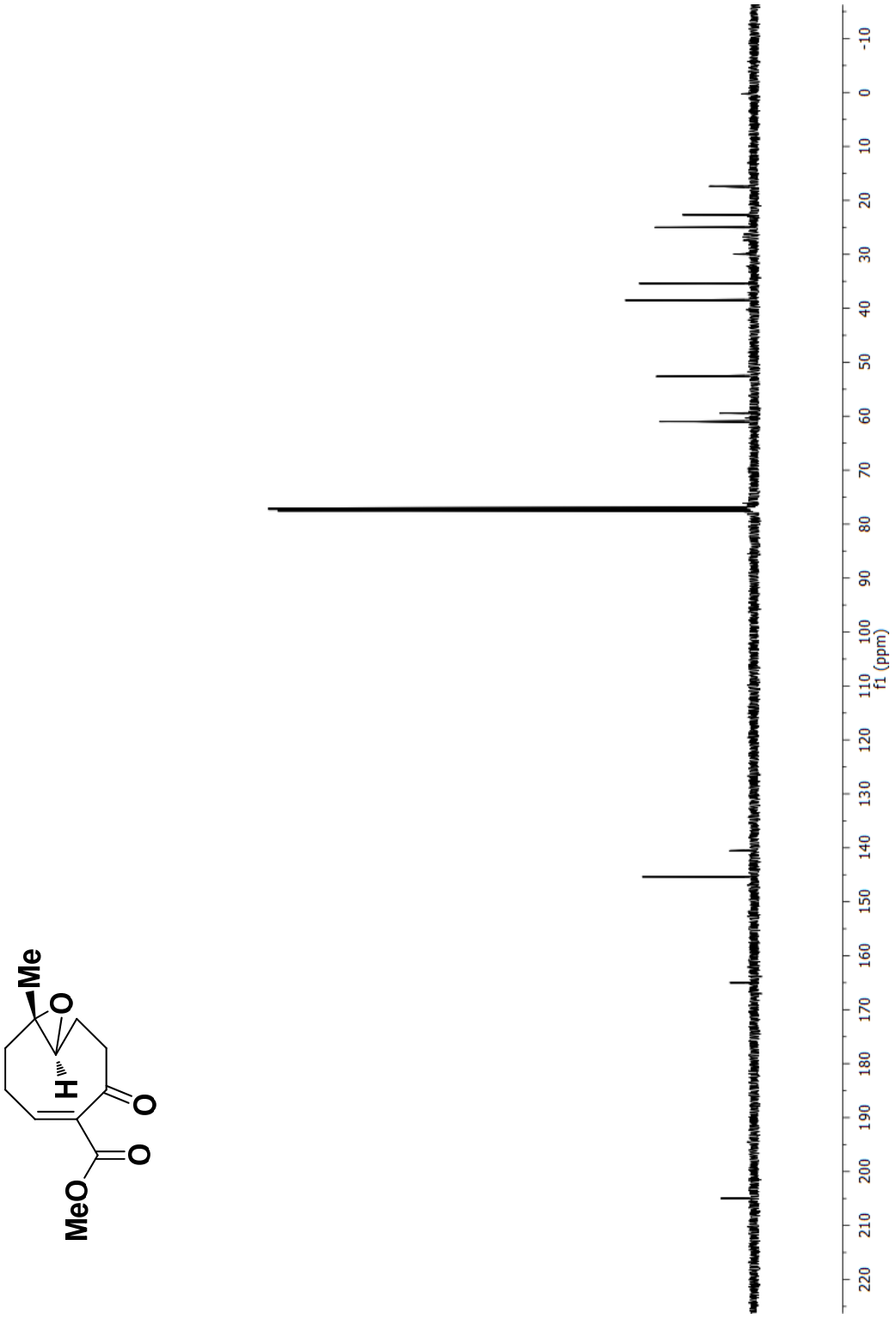
Me
O
H
O
O
MeO
f1 (ppm)

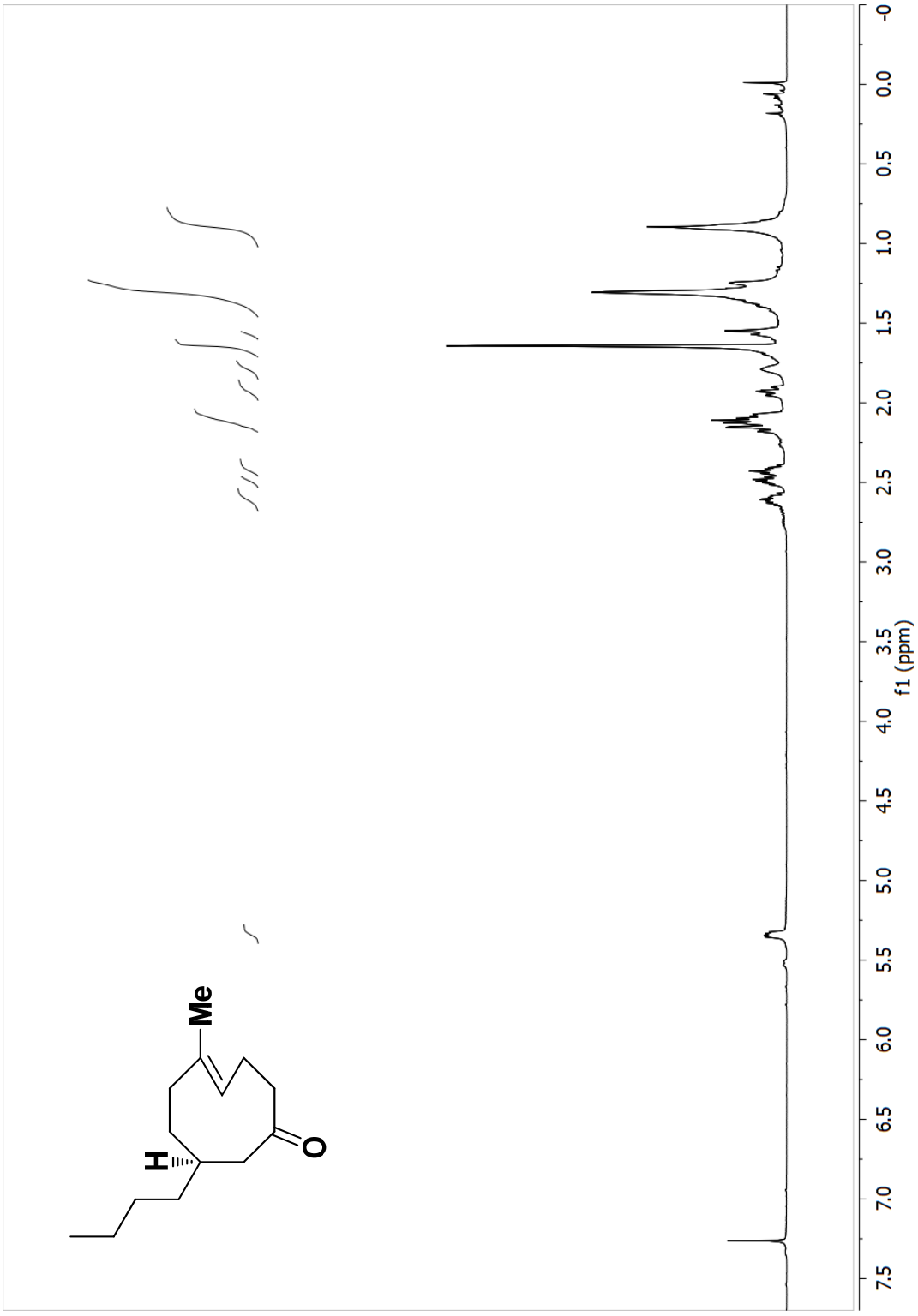
Me
H
O
7.5
7.0
6.5
6.0
5.5
5.0
4.5
4.0
3.5
3.0
2.5
2.0
1.5
1.0
0.5
0.0
-0
f1 (ppm)

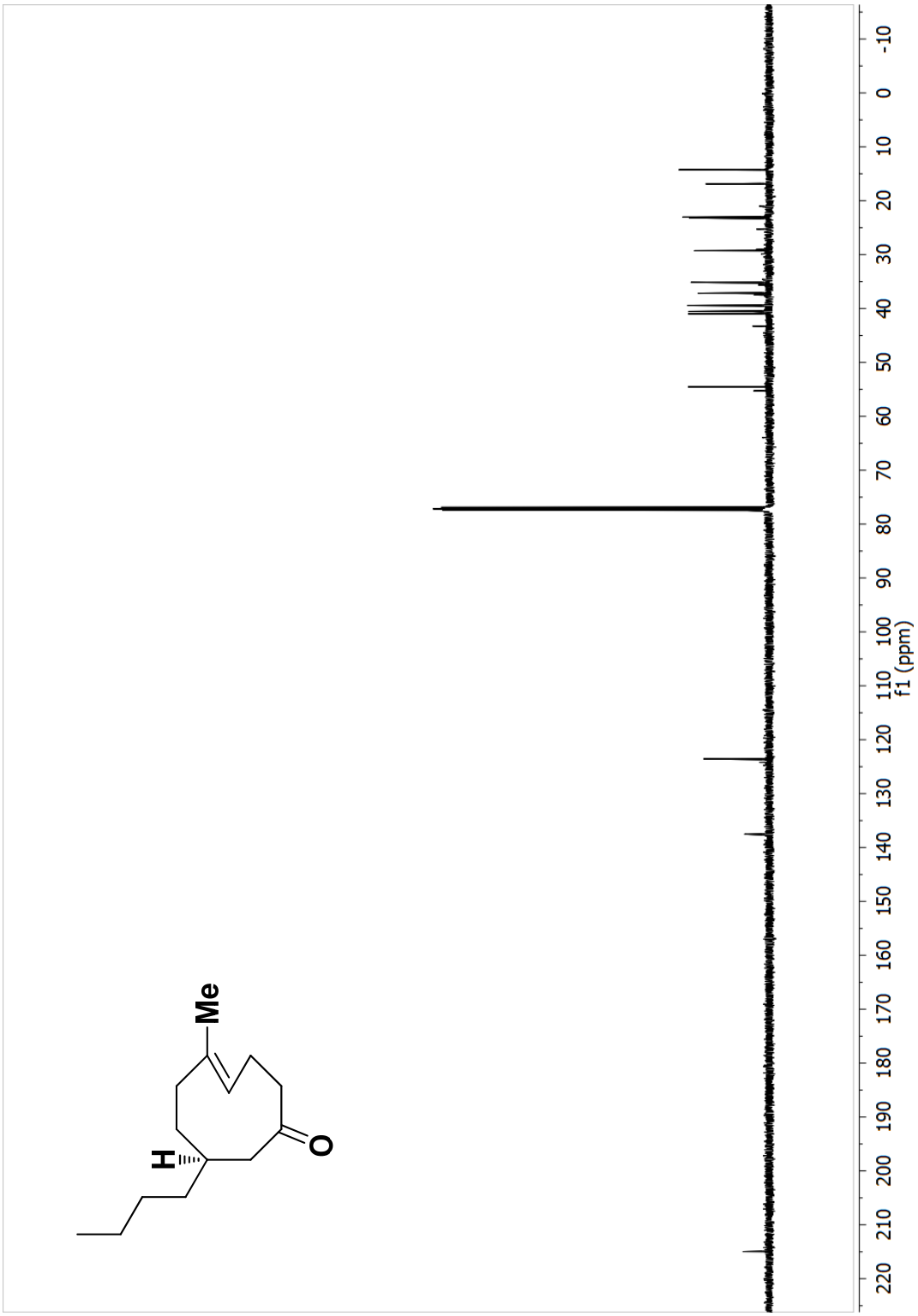
Me
H
O
-10
0
10
20
30
40
50
60
70
80
90
100
110
120
130
140
150
160
170
180
190
200
210
220
f1 (ppm)

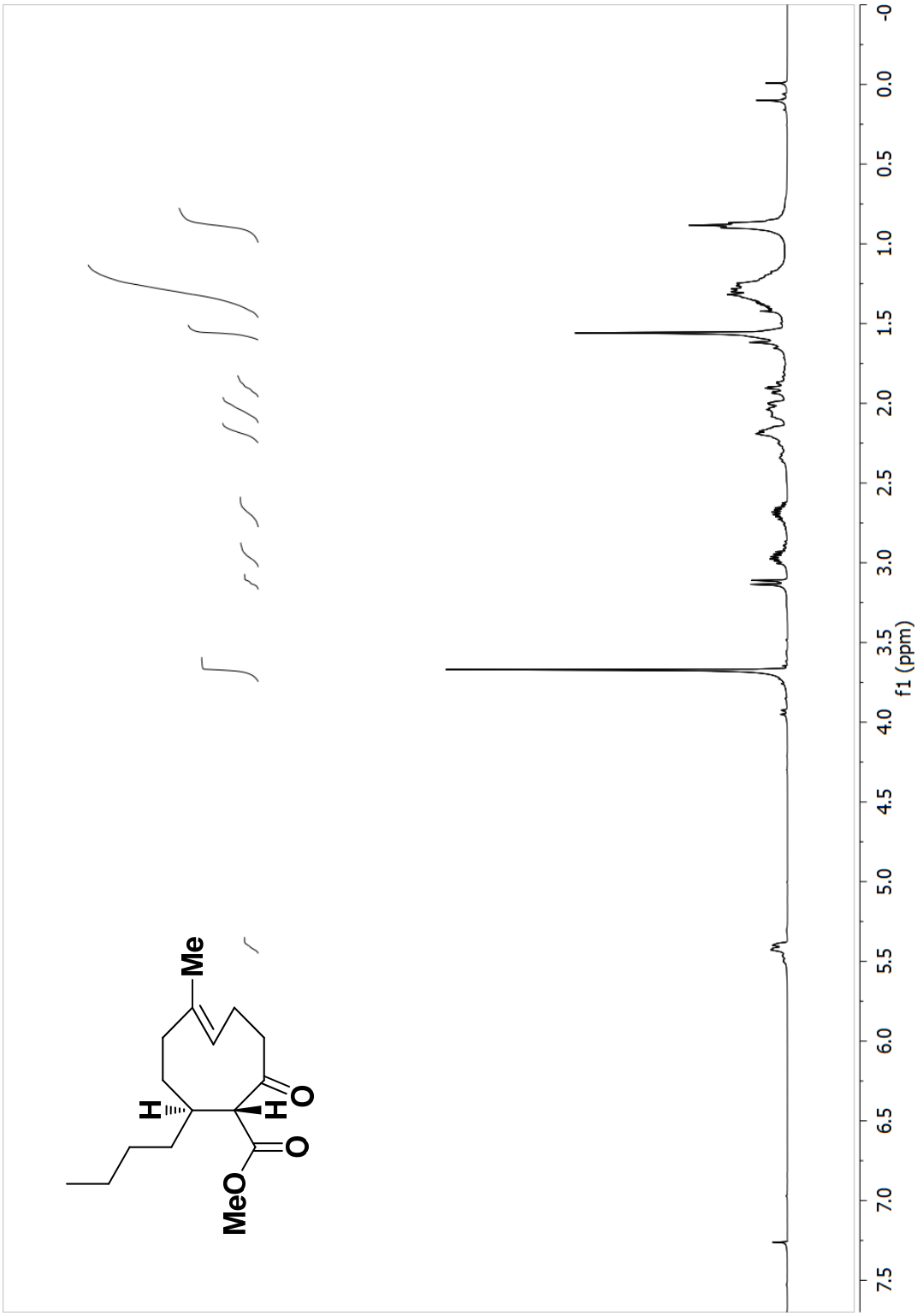
Me
H
H
O
O
MeO
7.5
7.0
6.5
6.0
5.5
5.0
4.5
4.0
3.5
3.0
2.5
2.0
1.5
1.0
0.5
0.0
-0
f1 (ppm)

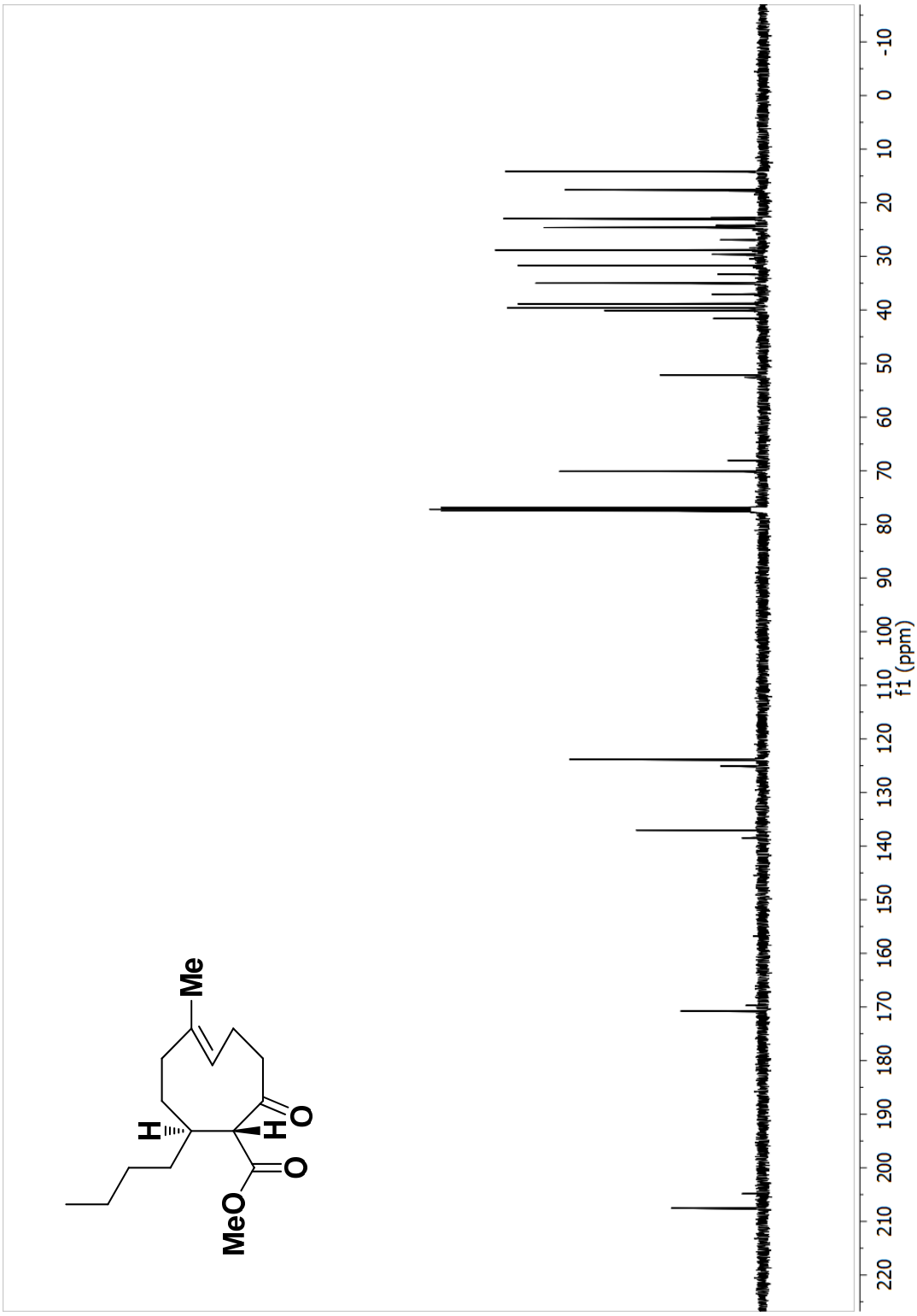
Me
H
H
O
O
MeO
-10
0
10
20
30
40
50
60
70
80
90
100
110
120
130
140
150
160
170
180
190
200
210
220
f1 (ppm)

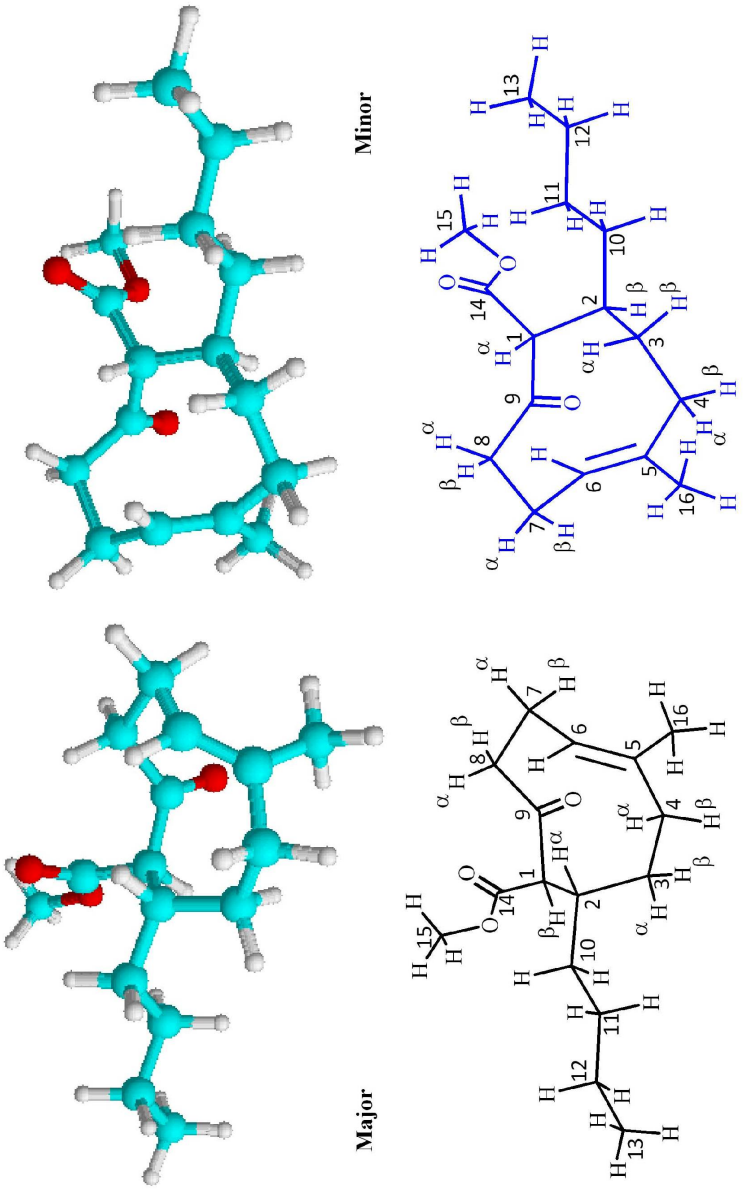
Minor
Major

^{1}H NMR chemical shifts (δ/ppm)

Protons	Major[a]	Minor[b]
H1α	3.27	3.81
H2β	2.28	2.64
H3α	1.35	1.46
H3β	1.40	1.89
H4α	1.79	1.71
H4β	1.85	2.11
H6	5.30	5.19
H7α	2.65	1.87
H7β	1.78	2.56
H8α	2.99	2.71
H8β	1.99	2.22

a: 0.87 (H13); 1.15-1.36 (m, H10,H11,H12); 1.58 (H16)
b: 0.87 (H13); 1.15-1.36 (m, H10,H11,H12) 1.56 (H16)

in C_6D_6

Determined vicinal (^3J) and geminal (^2J) coupling constants (in Hz)

Proton-proton	^nJ	Major	Minor
H1β–H2α	^3J	10.4	10.5
H2α–H3α	^3J	4.0	3.8
H2α–H3β	^3J	10.4	10.7
H3α–H3β	^2J	11.0	15.1
H3α–H4α	^3J	3.0	2.2
H3α–H4β	^3J	3.0	7.8
H3β–H4α	^3J	3.0	10.7
H3β–H4β	^3J	4.0	2.1
H4α–H4β	^2J	11.0	13.8
H7α–H6	^3J	11.8	4.8
H7β–H6	^3J	3.7	11.9
H7α–H7β	^2J	11.8	12.6
H7α–H8β	^3J	5.4	2.2
H7α–H8α	^3J	11.6	8.2
H7β–H8α	^3J	5.9	10.6
H7β–H8β	^3J	3.1	8.2
H8α–H8β	^2J	12.1	11.4

Carbons	Major isomer	Minor isomer
C1	70.59	67.64
C2	39.54	36.88
C3	31.69	26.66
C4	40.52	41.39
C5	136.57	138.19
C6	124.24	125.25
C7	25.03	24.26
C8	38.58	35.16
C9	205.47	203.01
C10	35.42	33.55
C11	28.83	29.87
C12	23.18	23.02
C13	14.15	14.15
C14	170.69	169.37
C15	51.35	51.71
C16	17.59	17.59

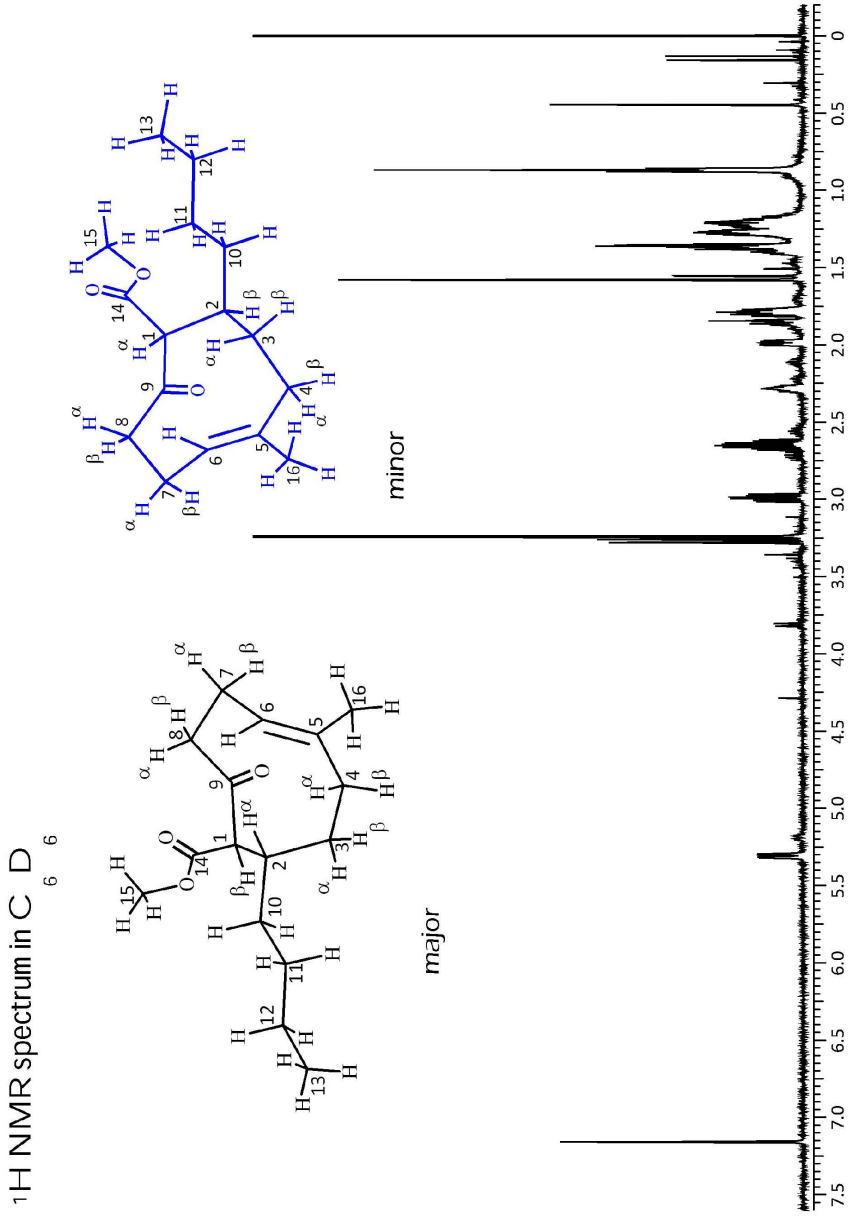
^{1}H NMR spectrum in C_6D_6
major
minor
0
0.5
1.0
1.5
2.0
2.5
3.0
3.5
4.0
4.5
5.0
5.5
6.0
6.5
7.0
7.5

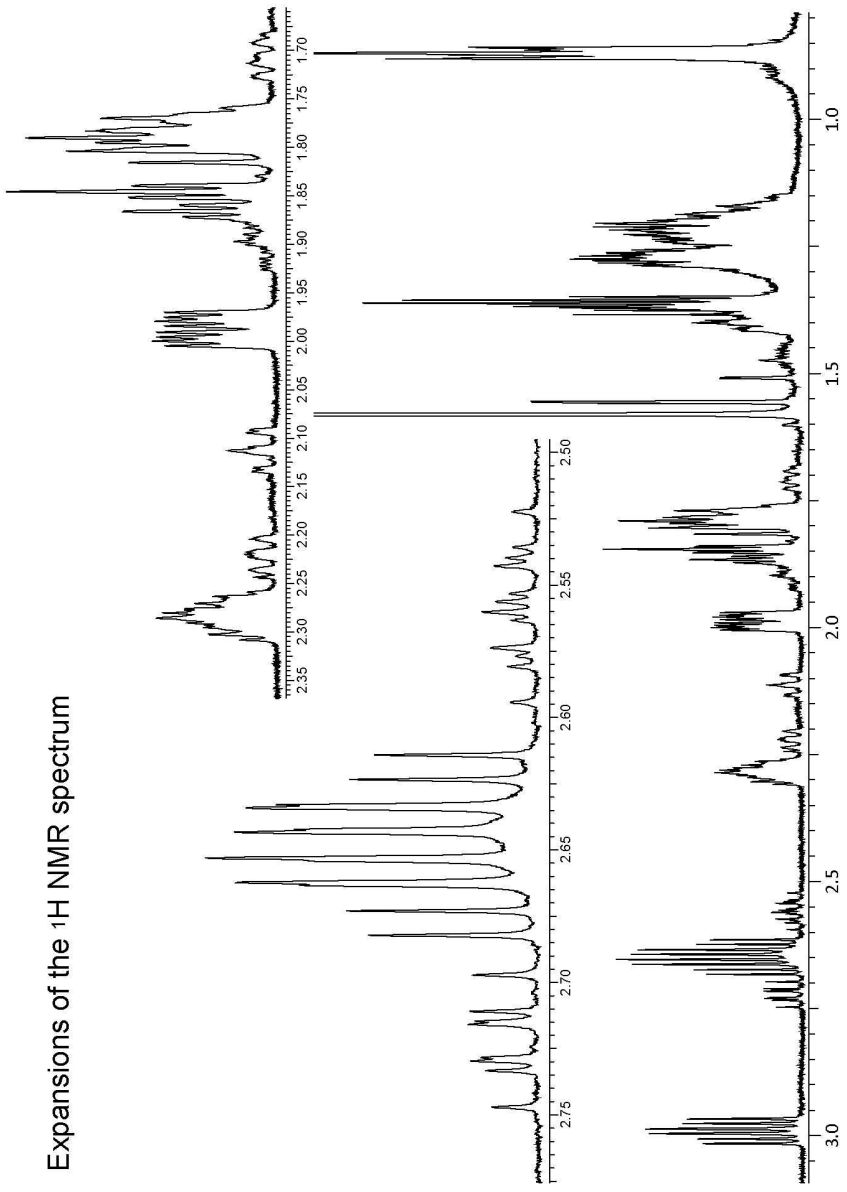
Expansions of the 1H NMR spectrum
3.0
2.5
2.0
1.5
1.0
2.75
2.70
2.65
2.60
2.55
2.50
2.35
2.30
2.25
2.20
2.15
2.10
2.05
2.00
1.95
1.90
1.85
1.80
1.75
1.70

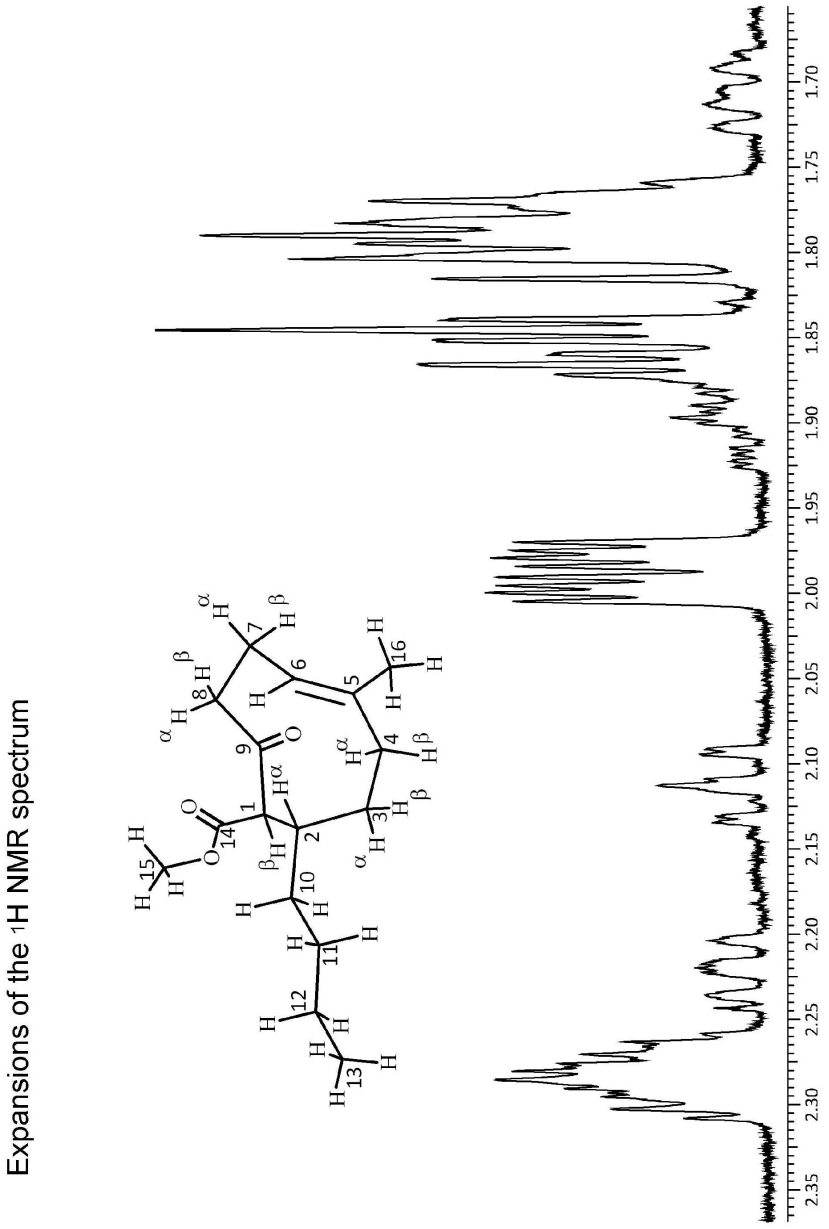
Expansions of the 1H NMR spectrum
2.35
2.30
2.25
2.20
2.15
2.10
2.05
2.00
1.95
1.90
1.85
1.80
1.75
1.70

Expansions of the ^{1}H NMR spectrum

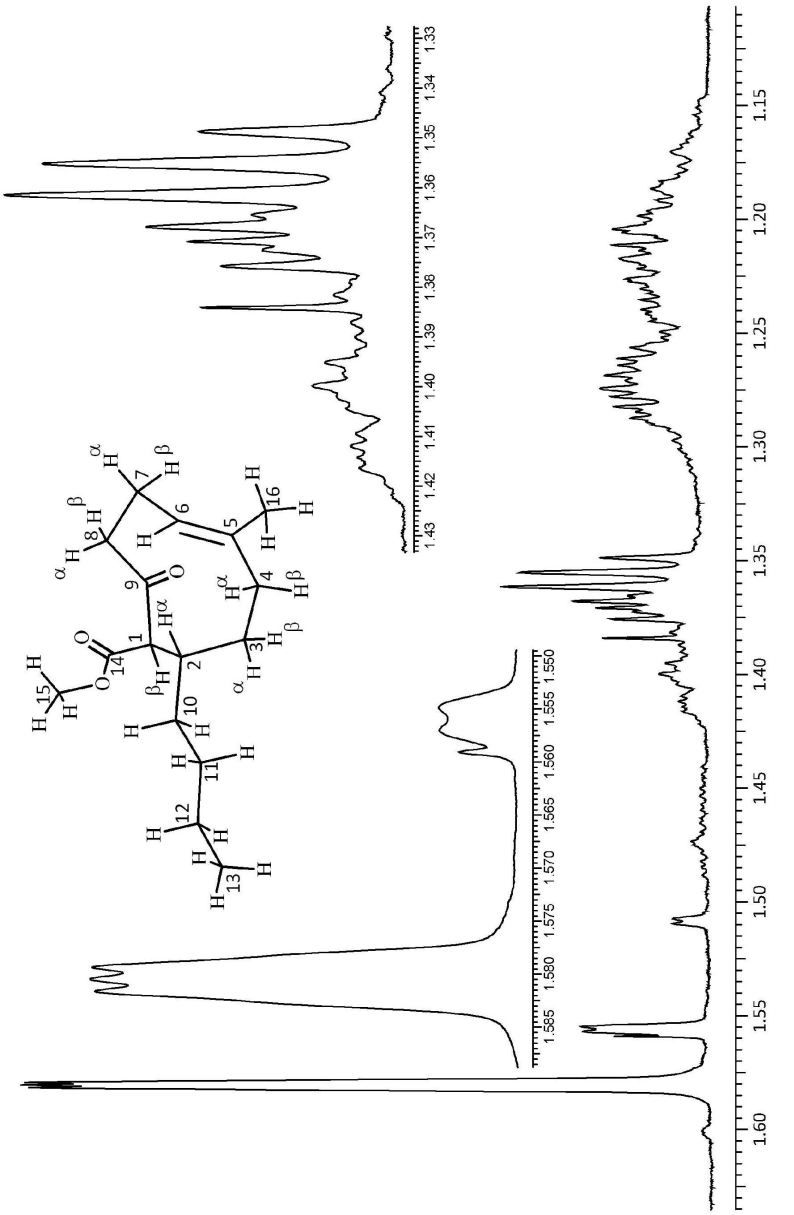

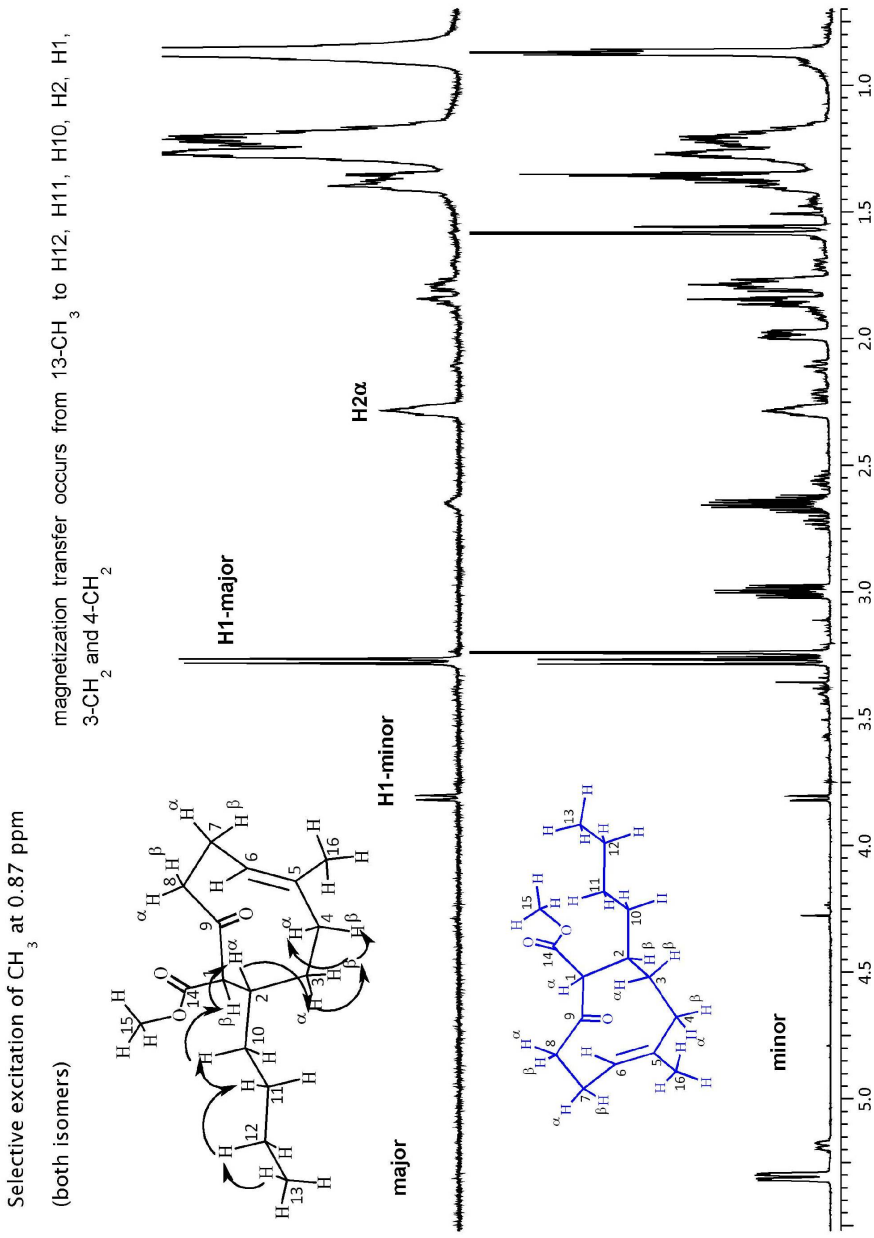
Selective excitation of CH3 at 0.87 ppm
(both isomers)
magnetization transfer occurs from 13-CH3 to H12, H11, H10, H2, H1, 3-CH2 and 4-CH2
H1-major
H2α
H1-minor
major
minor
5.0
4.5
4.0
3.5
3.0
2.5
2.0
1.5
1.0

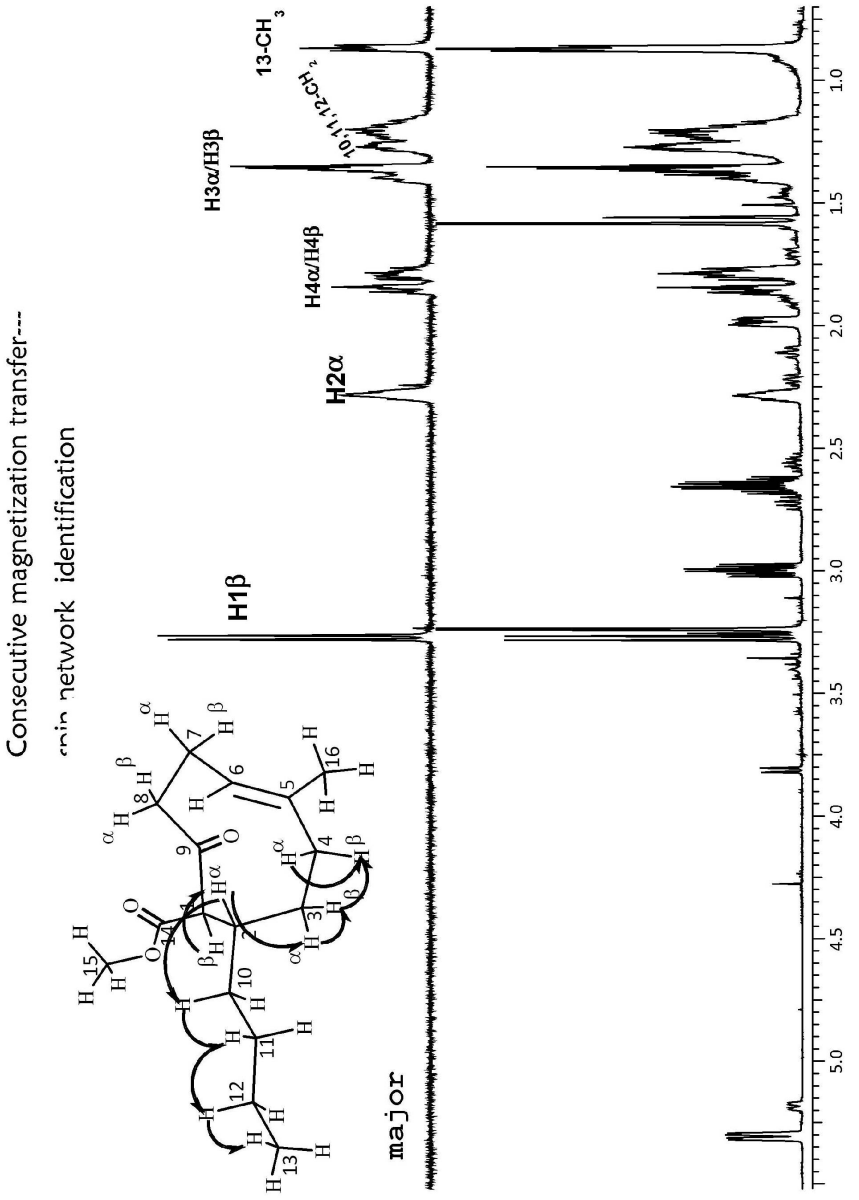
Consecutive magnetization transfer---
H1β
H2α
H4α/H4β
H3α/H3β
13-CH3
major
5.0
4.5
4.0
3.5
3.0
2.5
2.0
1.5
1.0

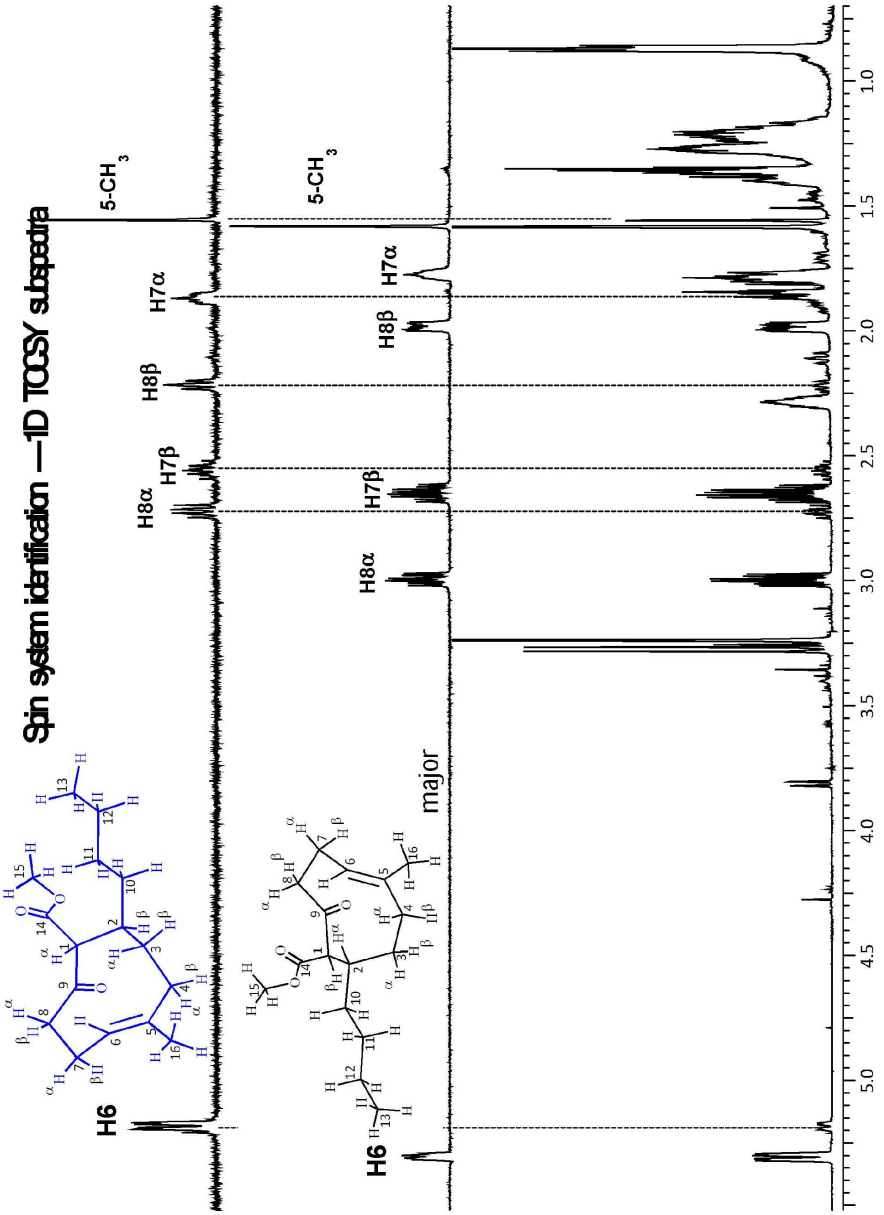
Spin system identification —1D TOCSY subspectra
5-CH3
H7α
H8β
H7β
H8α
H6
major
5.0
4.5
4.0
3.5
3.0
2.5
2.0
1.5
1.0

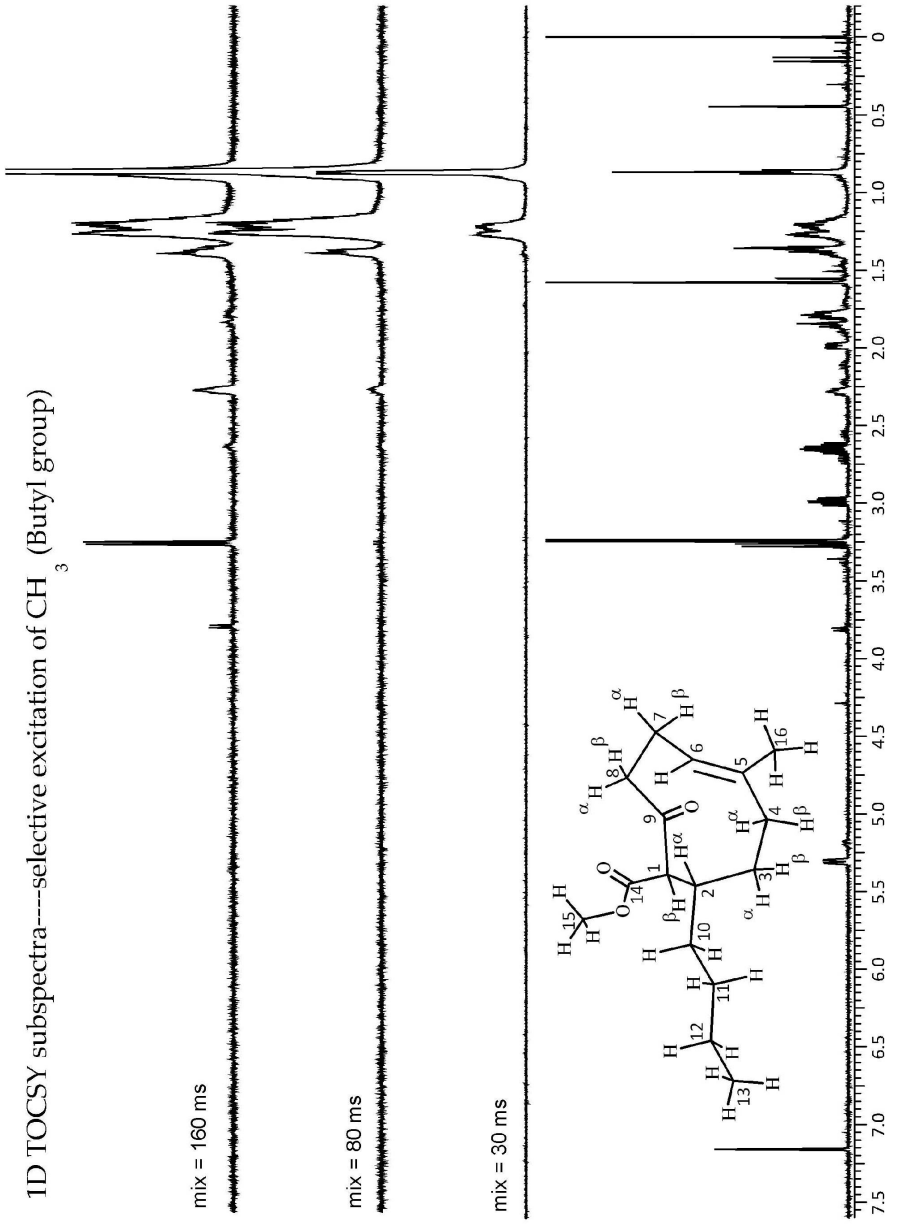
1D TOCSY subspectra---selective excitation of CH3 (Butyl group)
mix = 160 ms
mix = 80 ms
mix = 30 ms
7.5
7.0
6.5
6.0
5.5
5.0
4.5
4.0
3.5
3.0
2.5
2.0
1.5
1.0
0.5
0

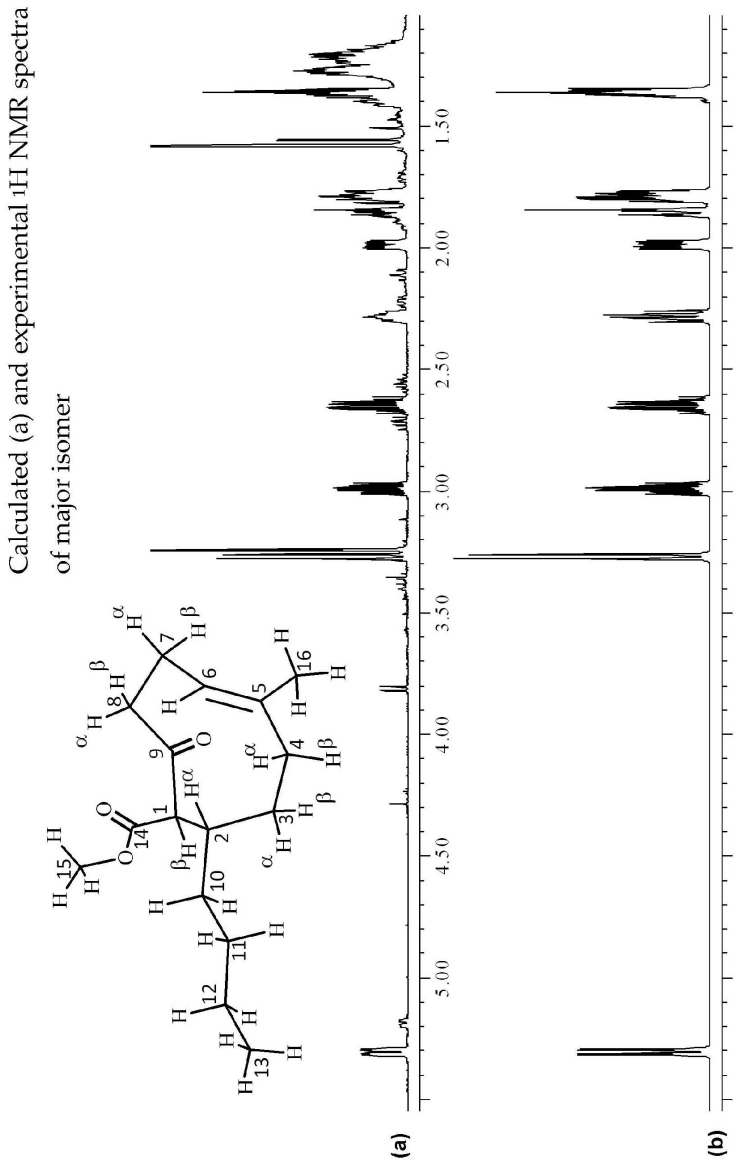
Calculated (a) and experimental 1H NMR spectra
of major isomer
(a)
(b)
5.00
4.50
4.00
3.50
3.00
2.50
2.00
1.50

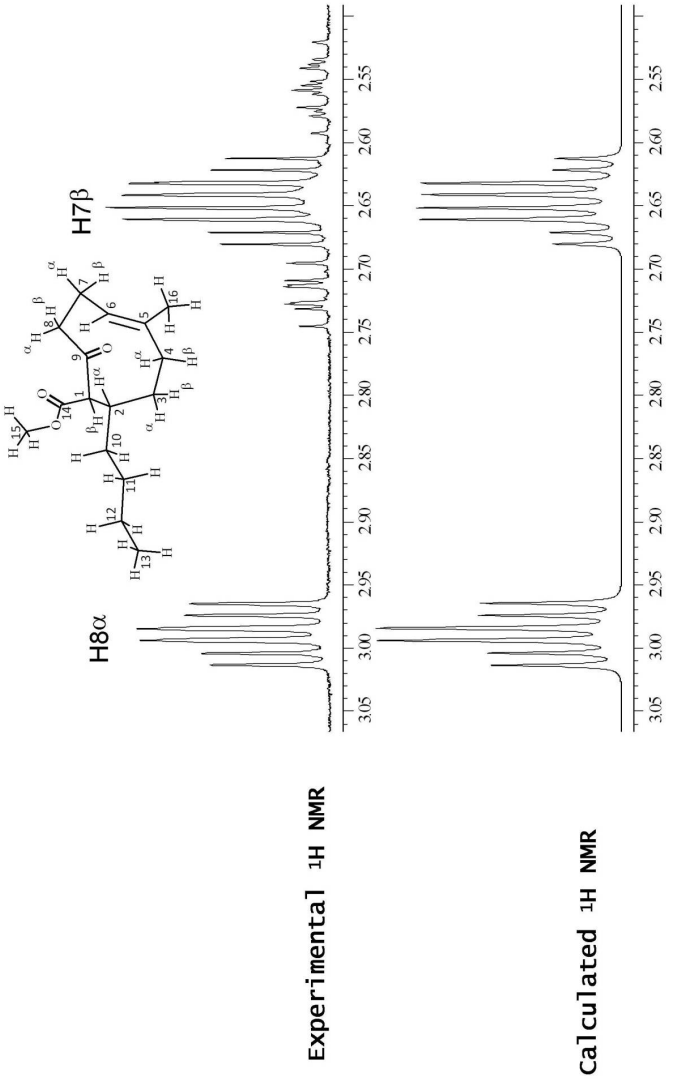
H8α
H7β
Experimental 1H NMR
Calculated 1H NMR
3.05
3.00
2.95
2.90
2.85
2.80
2.75
2.70
2.65
2.60
2.55

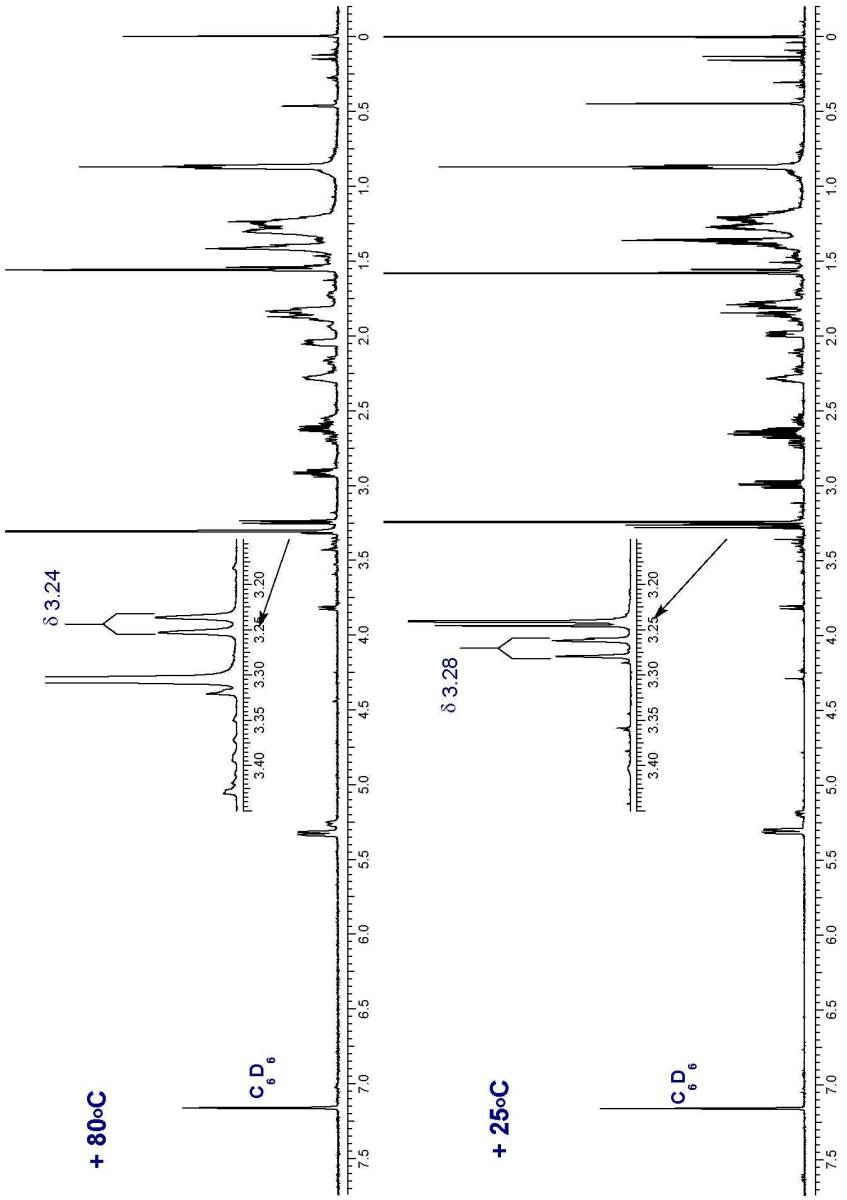
+ 80oC
δ 3.24
C6D6
+ 25oC
δ 3.28
C6D6

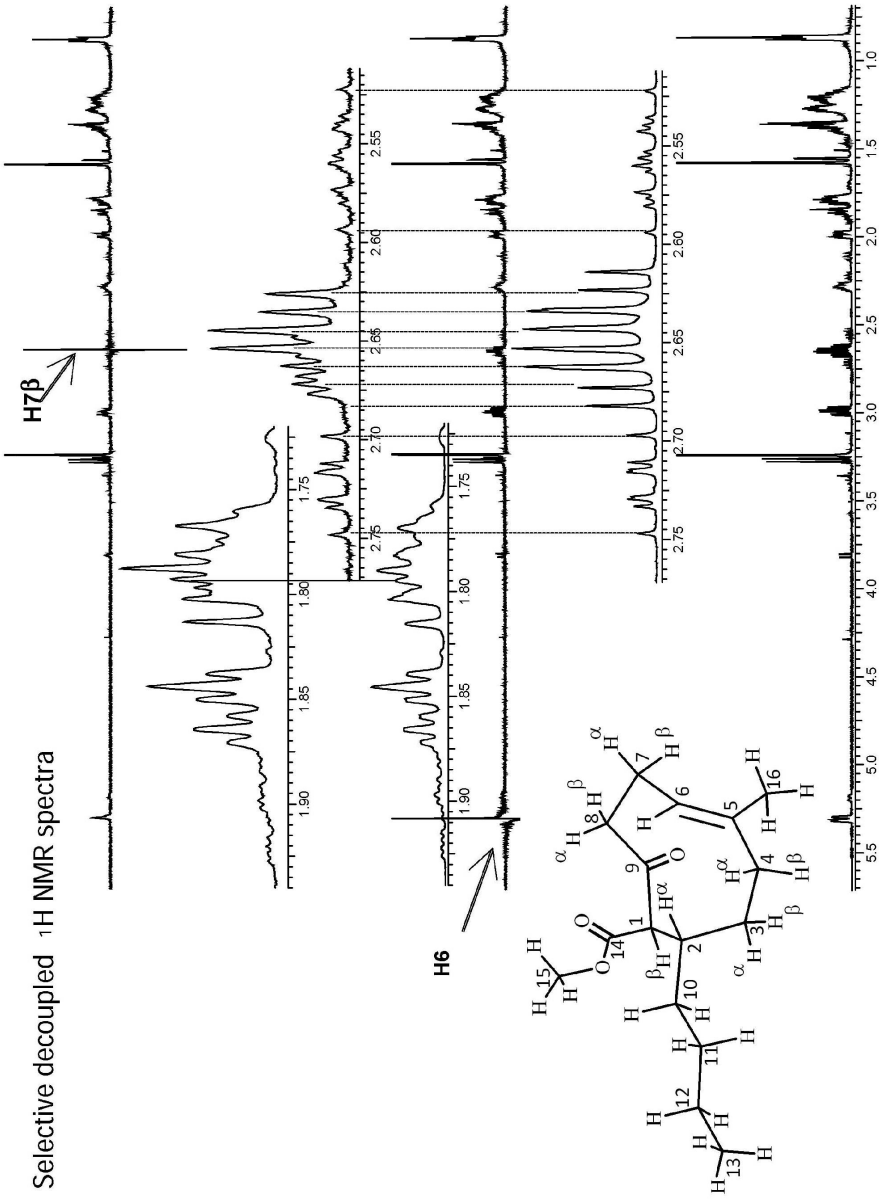
Selective decoupled 1H NMR spectra
H7β
H6

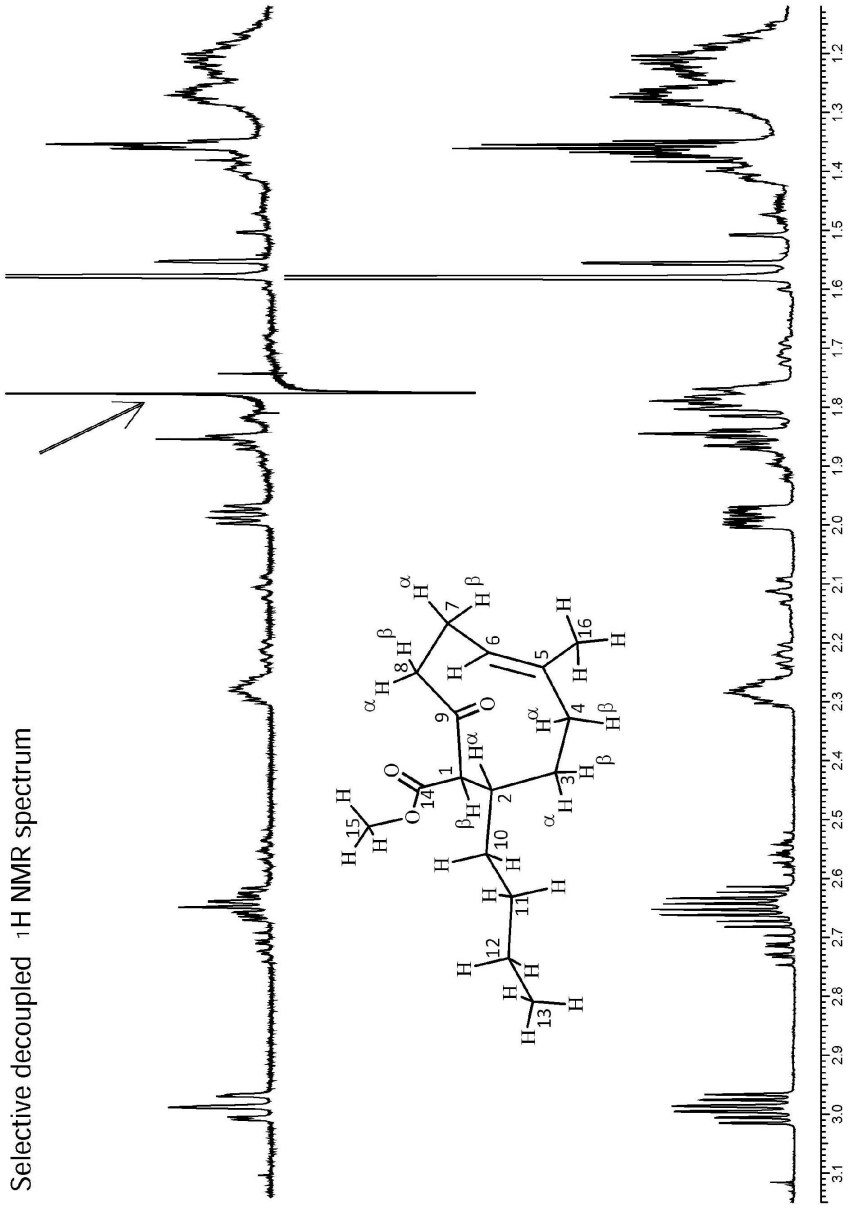
Selective decoupled 1H NMR spectrum
3.1
3.0
2.9
2.8
2.7
2.6
2.5
2.4
2.3
2.2
2.1
2.0
1.9
1.8
1.7
1.6
1.5
1.4
1.3
1.2

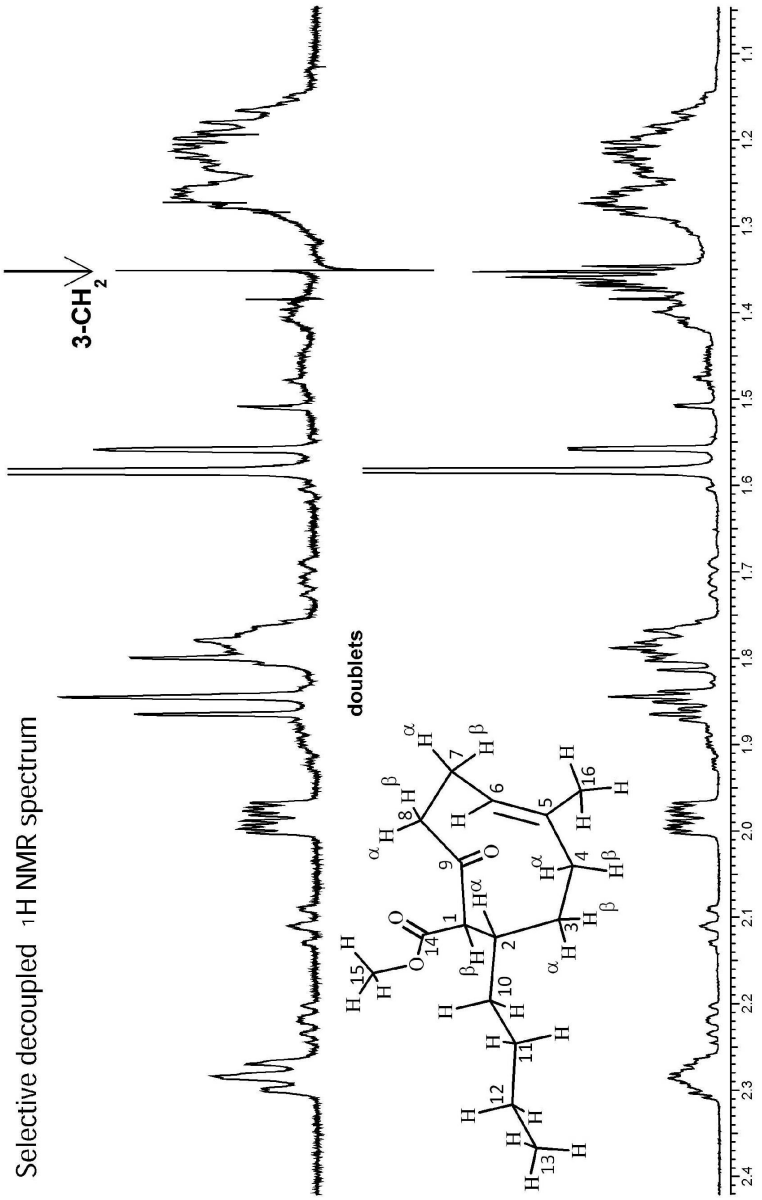
Selective decoupled ₁H NMR spectrum
3-CH2
doublets
2.4
2.3
2.2
2.1
2.0
1.9
1.8
1.7
1.6
1.5
1.4
1.3
1.2
1.1

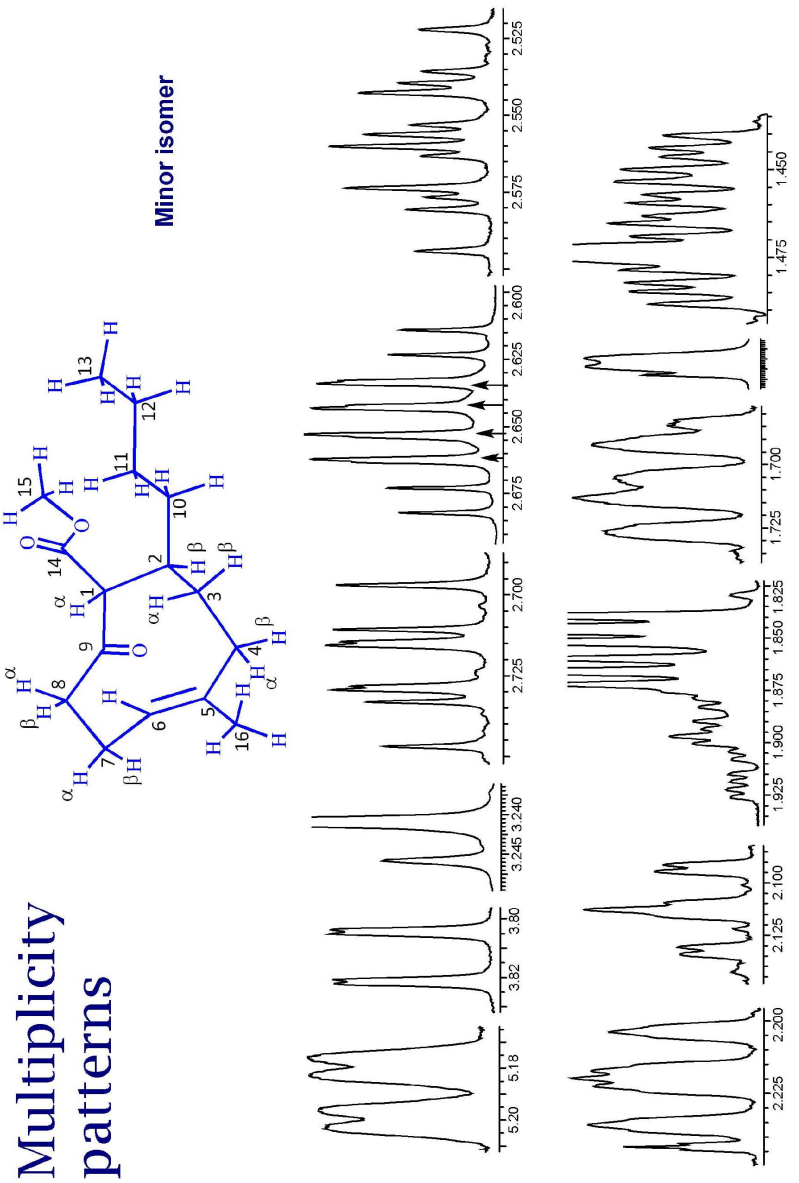
Multiplicity patterns
Minor isomer

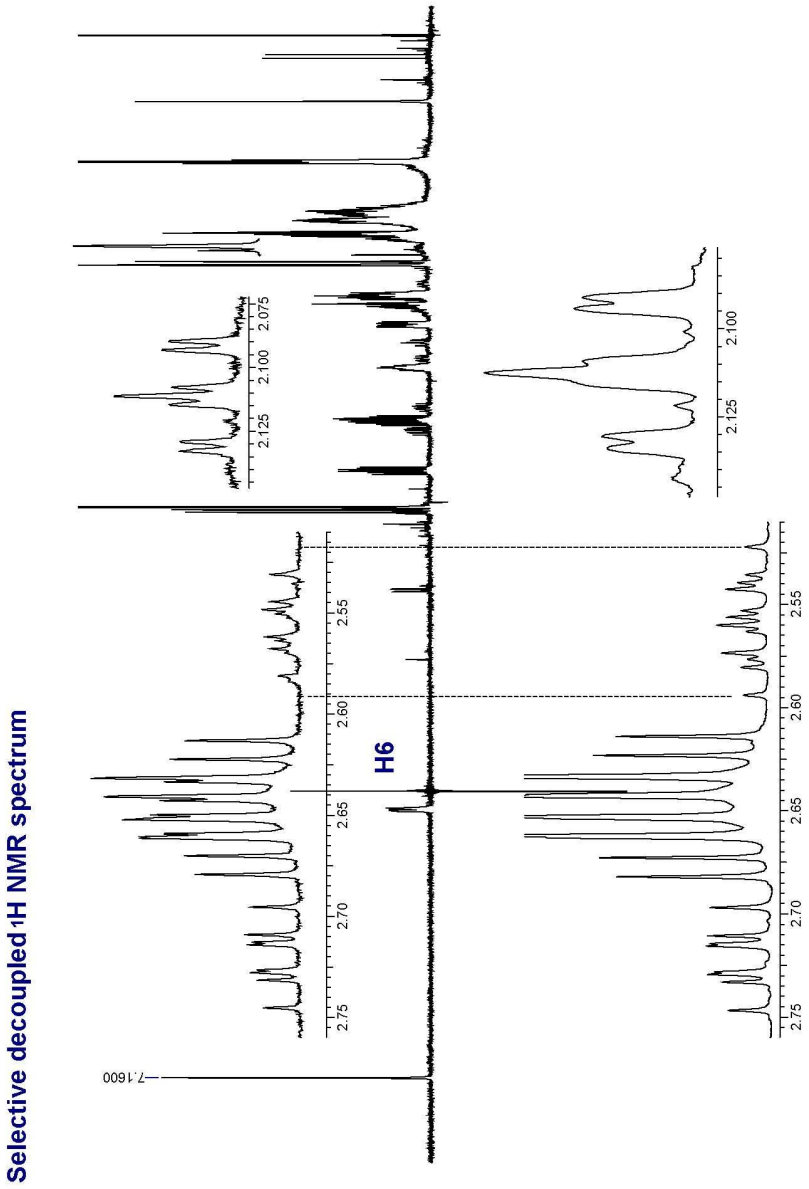
Selective decoupled 1H NMR spectrum
7.1600
H6
2.75
2.70
2.65
2.60
2.55
2.125
2.100
2.075

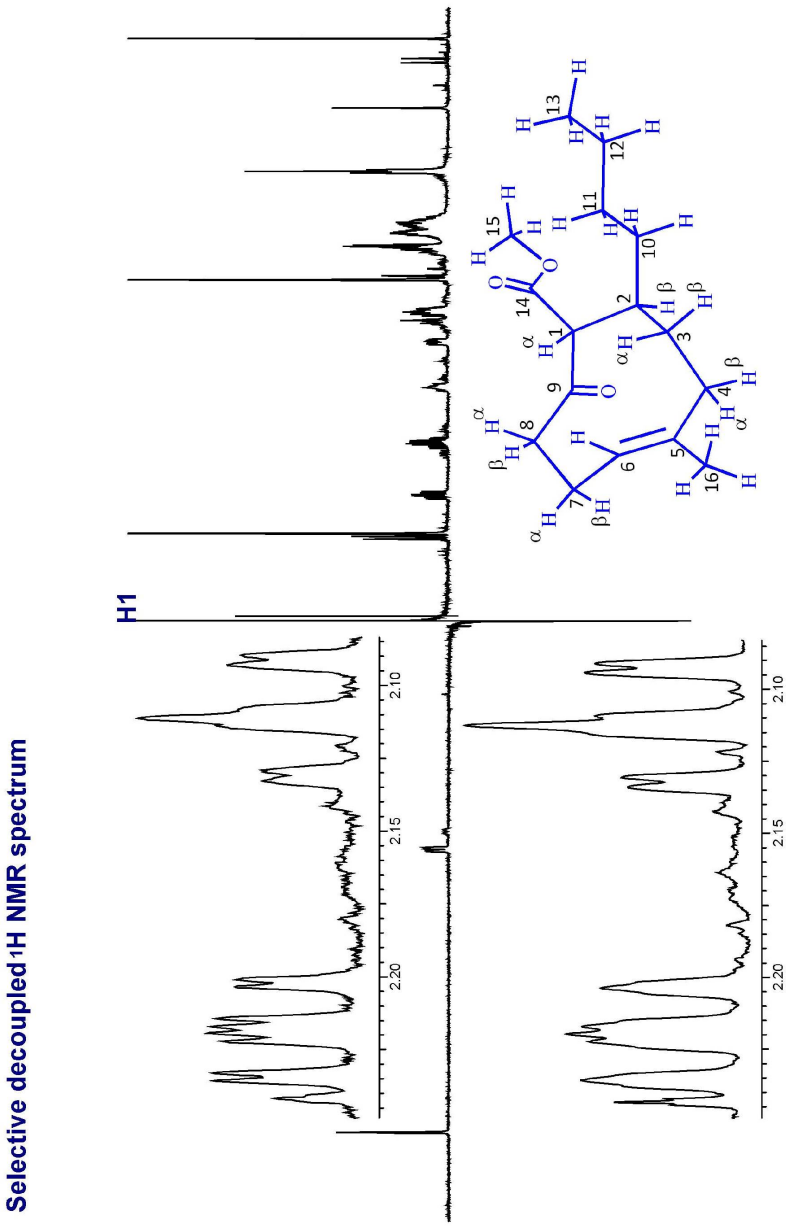
Selective decoupled 1H NMR spectrum
H1
2.10
2.15
2.20
2.10
2.15
2.20

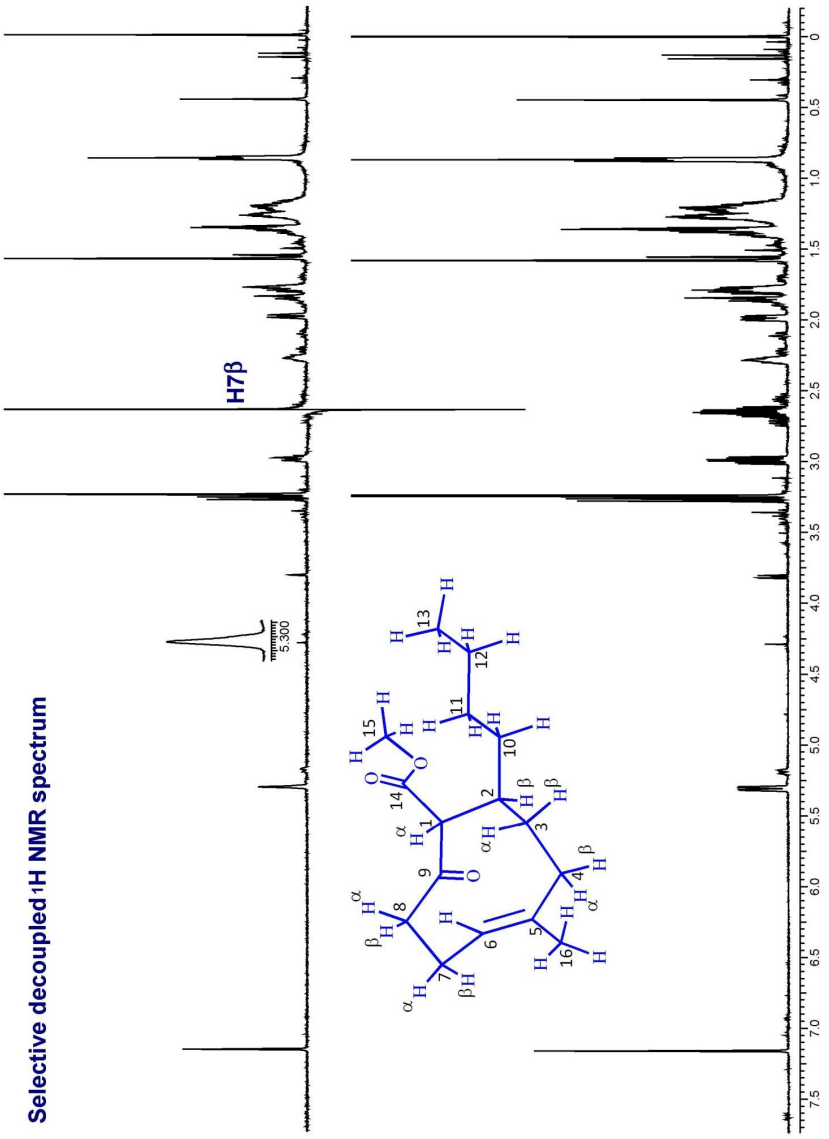
Selective decoupled ¹H NMR spectrum
H7β
5.300

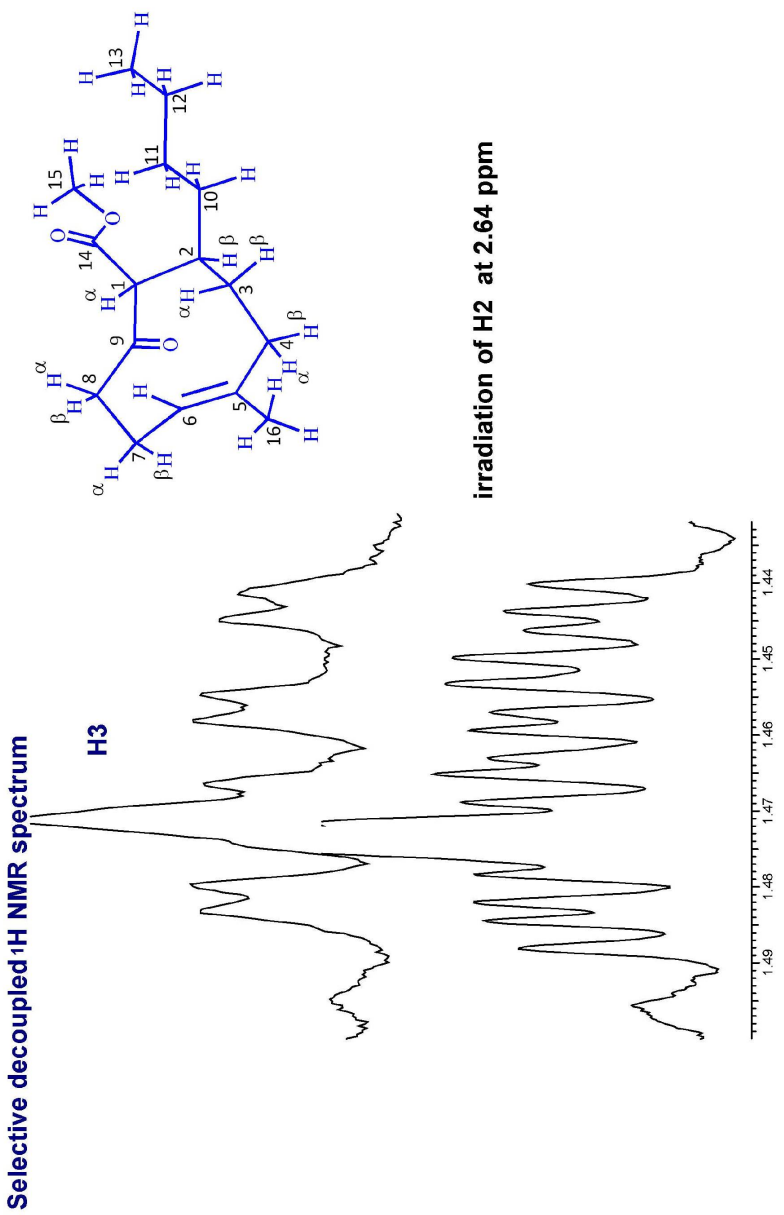
Selective decoupled ¹H NMR spectrum
H3
irradiation of H2 at 2.64 ppm
1.49
1.48
1.47
1.46
1.45
1.44

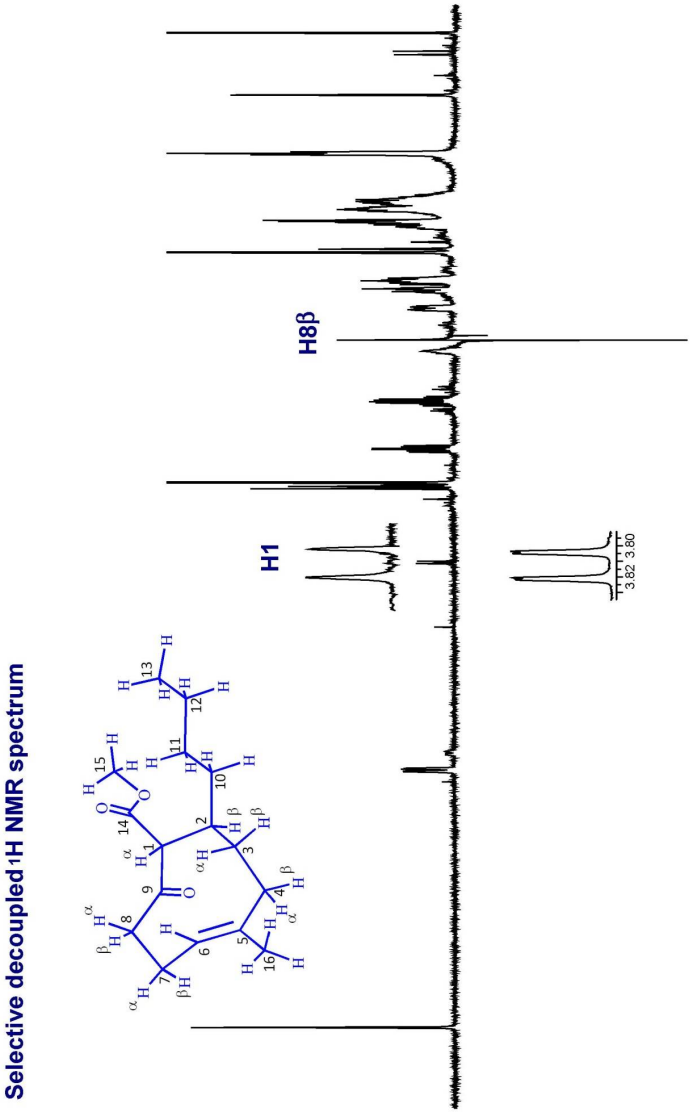
Selective decoupled ¹H NMR spectrum
H8β
H1
3.82 3.80

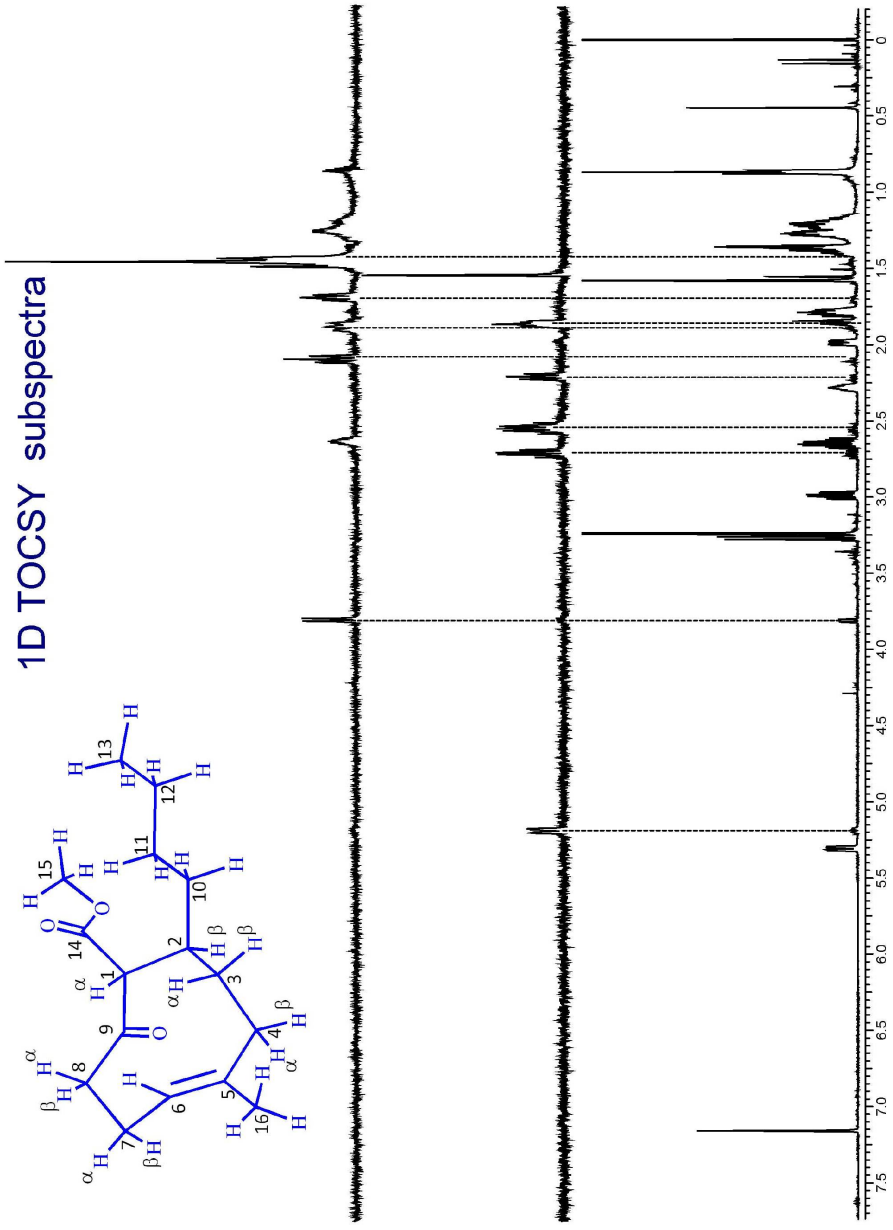
1D TOCSY subspectra

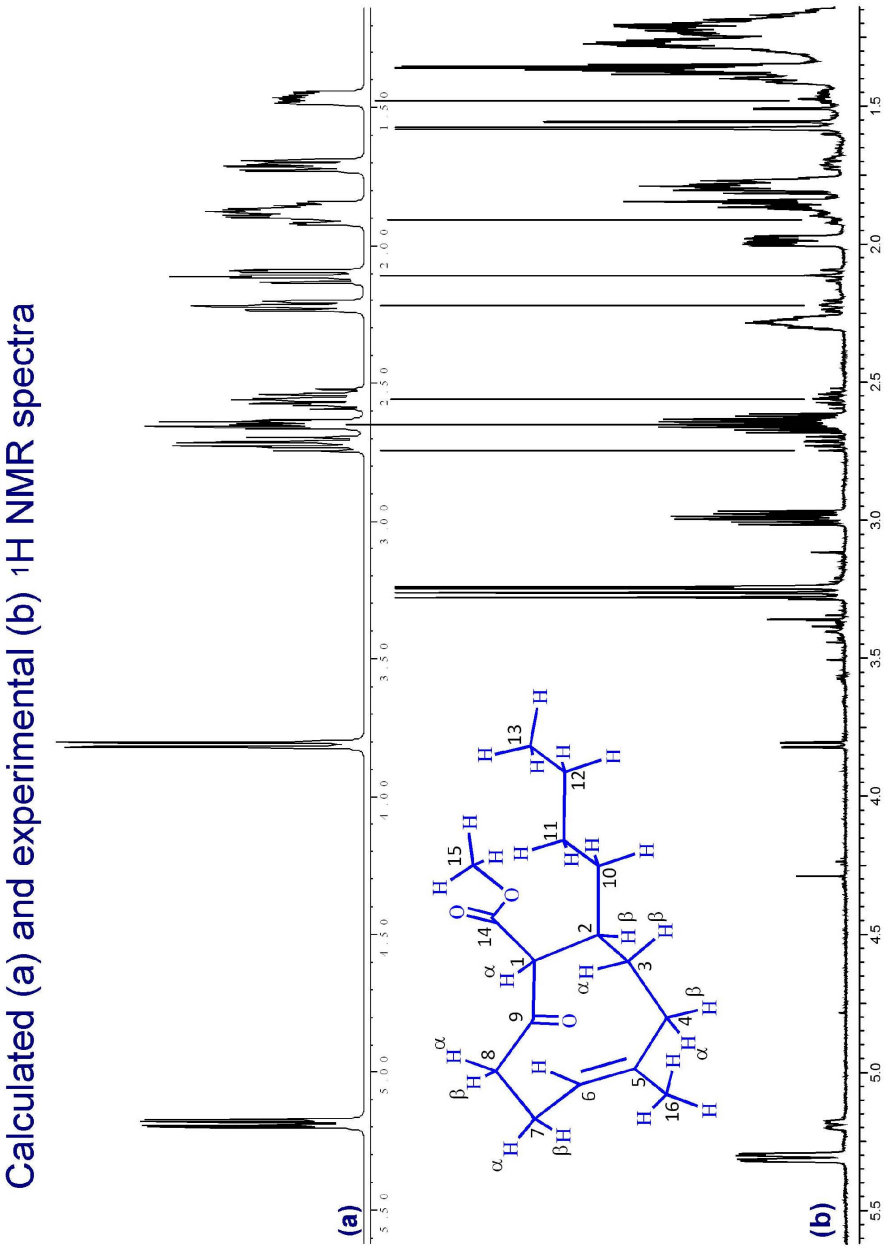
Calculated (a) and experimental (b) 1H NMR spectra
(a)
(b)

Calculated (a) and experimental (b) ^{1}H NMR spectra

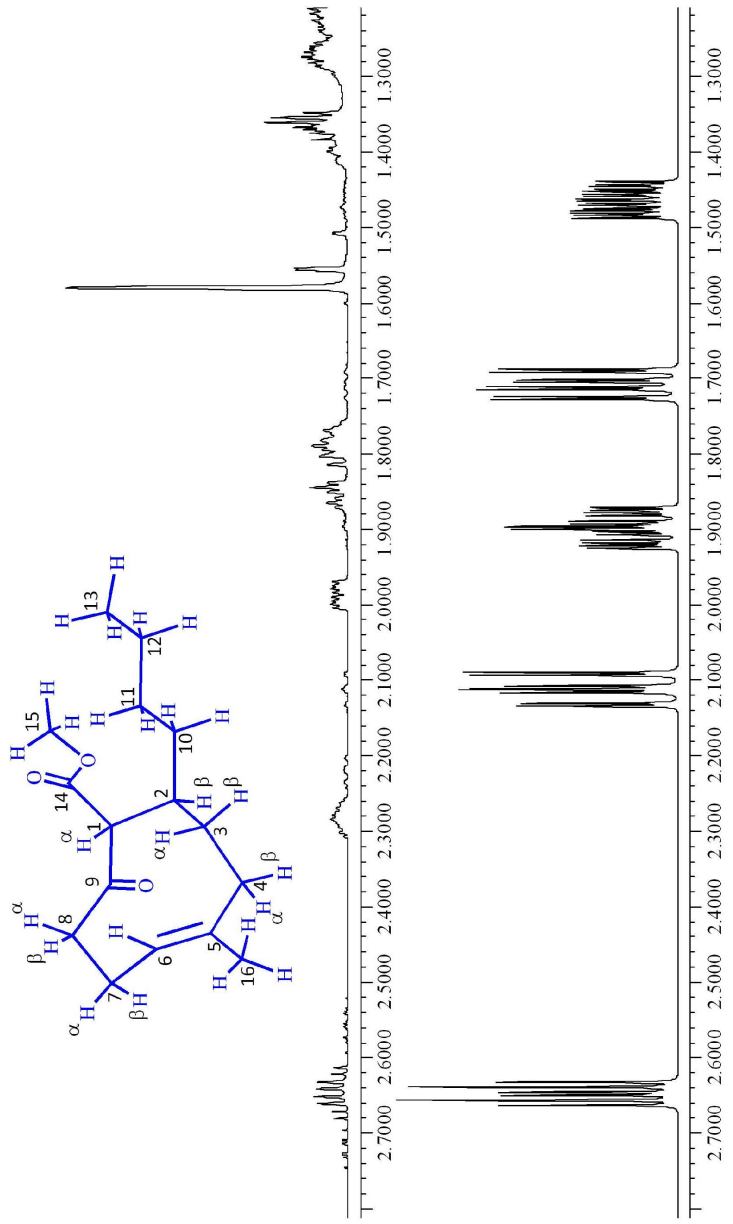

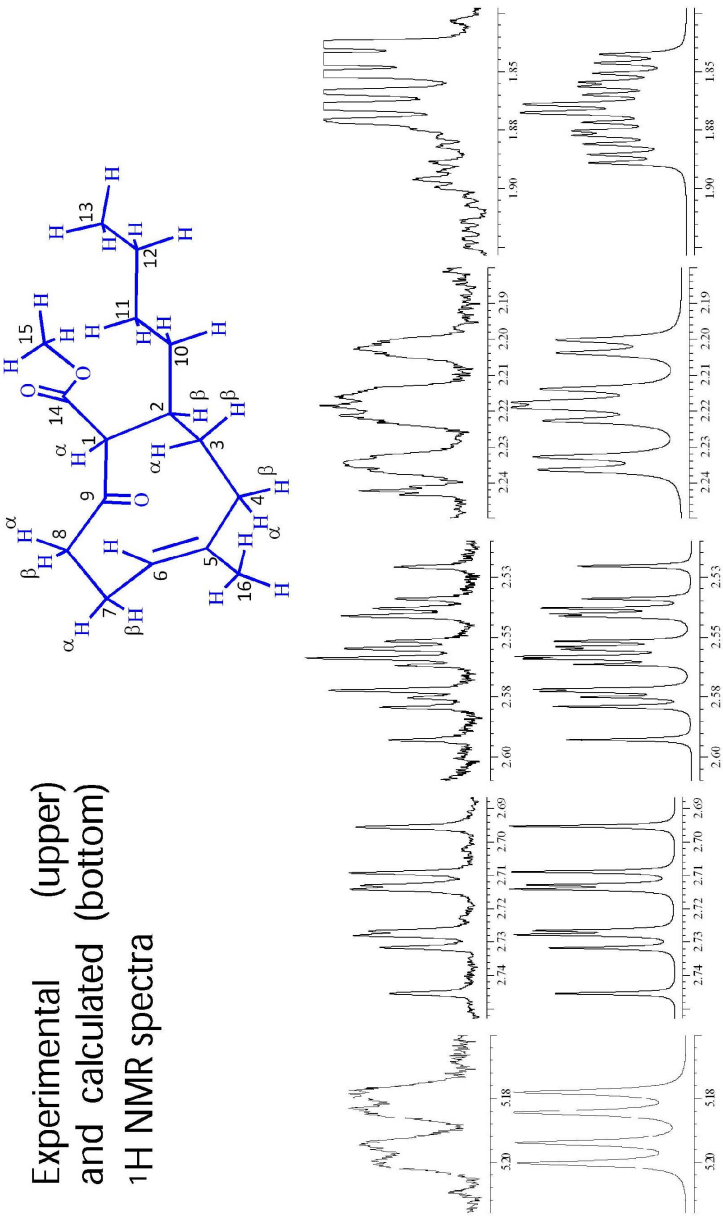
Experimental (upper)
and calculated (bottom)
1H NMR spectra

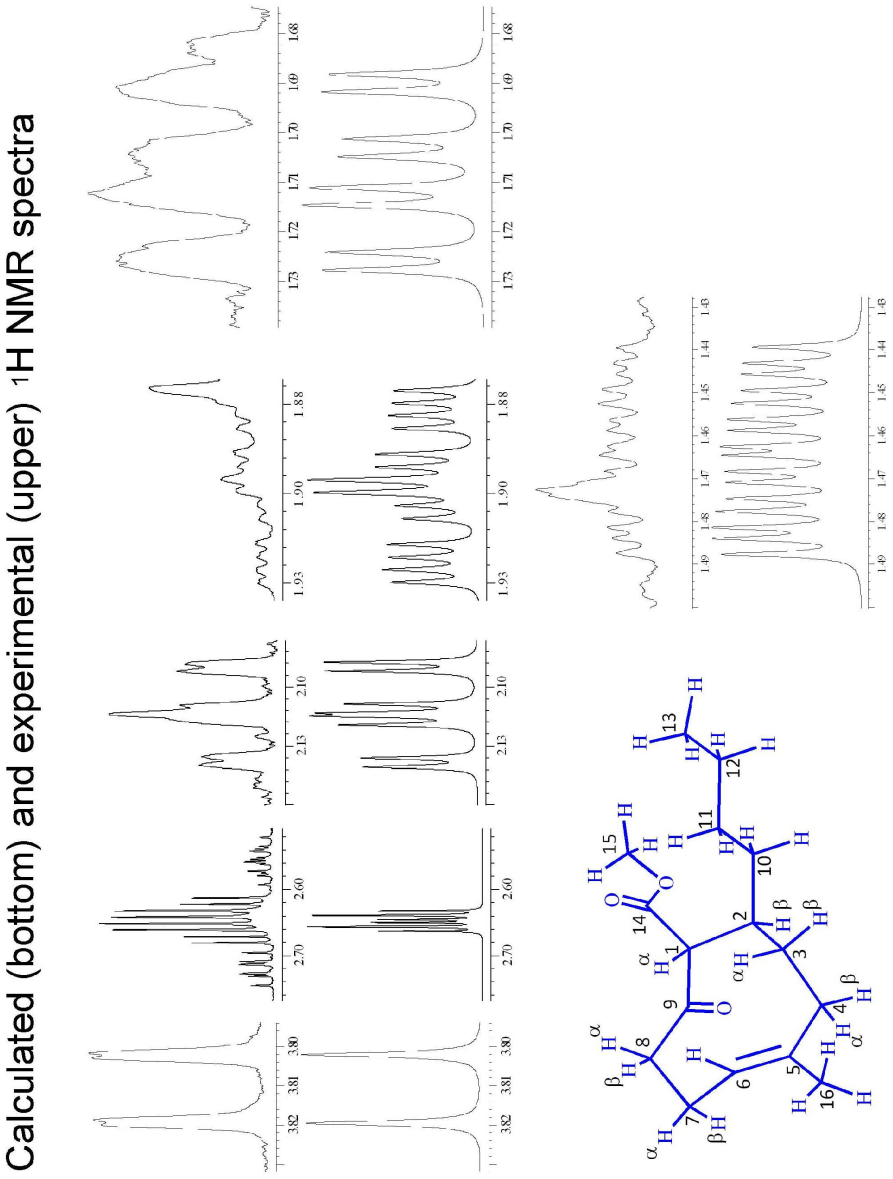
Calculated (bottom) and experimental (upper) ¹H NMR spectra

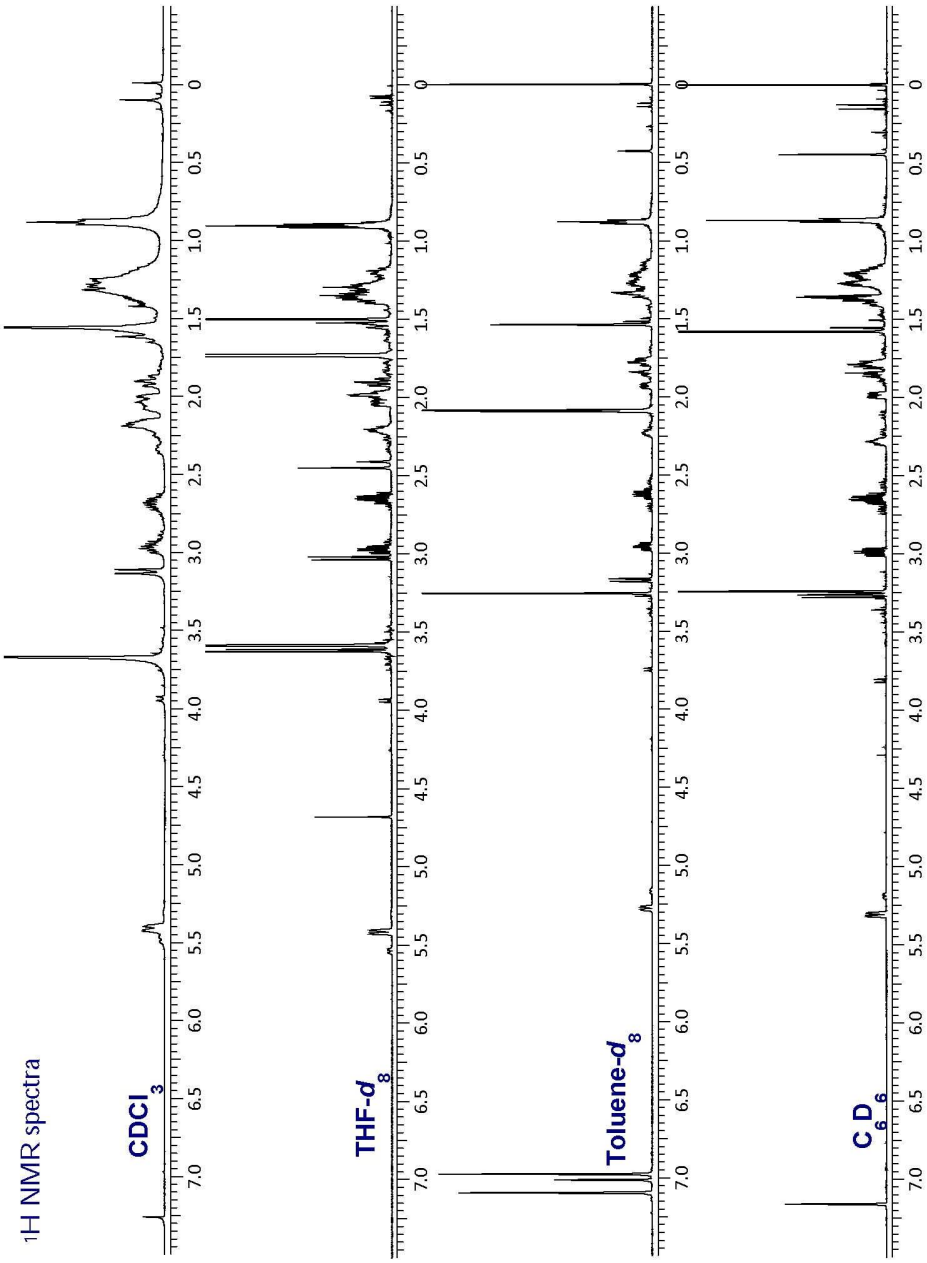
^{1}H NMR spectra
$CDCl_3$
$THF\text{-}d_8$
$Toluene\text{-}d_8$
C_6D_6

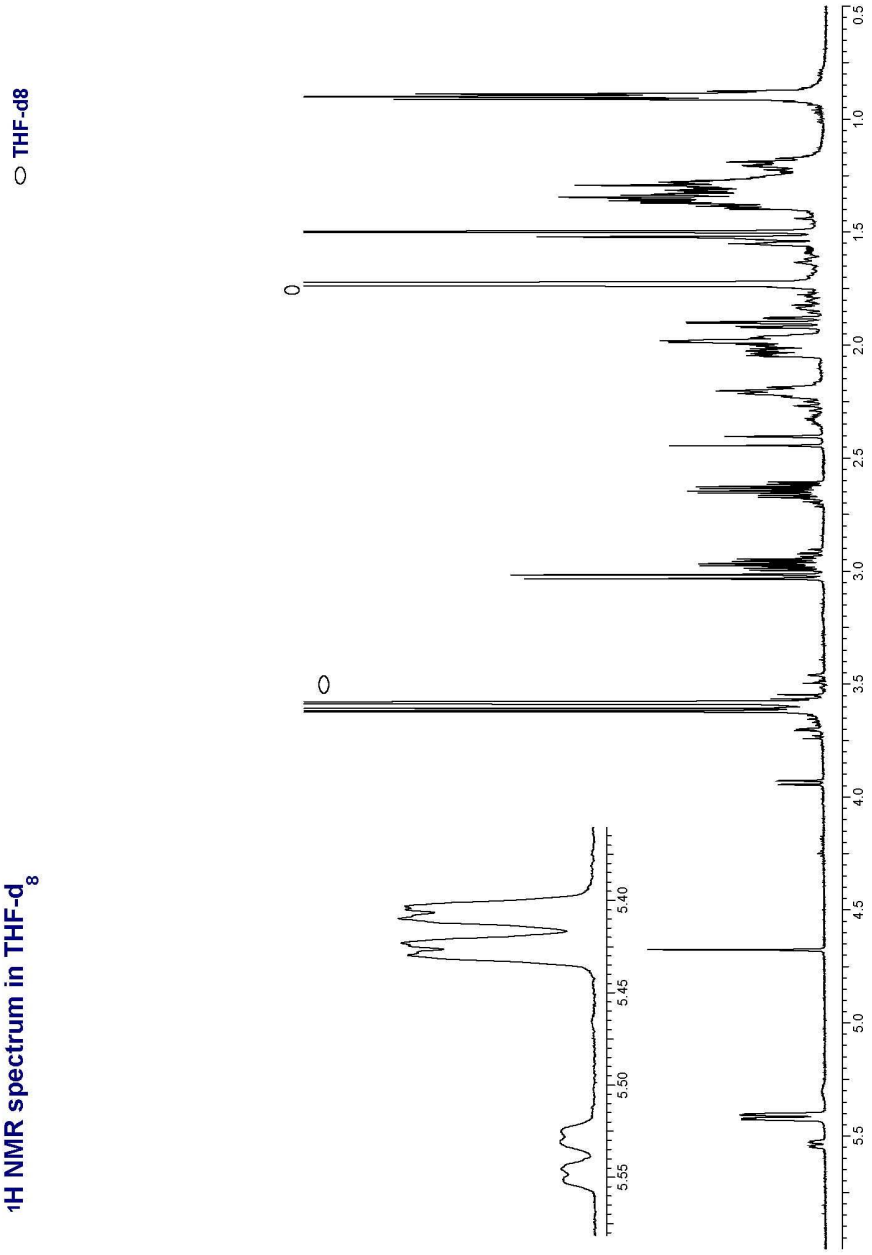
1H NMR spectrum in THF-d8
THF-d8
5.55
5.50
5.45
5.40
5.5
5.0
4.5
4.0
3.5
3.0
2.5
2.0
1.5
1.0
0.5

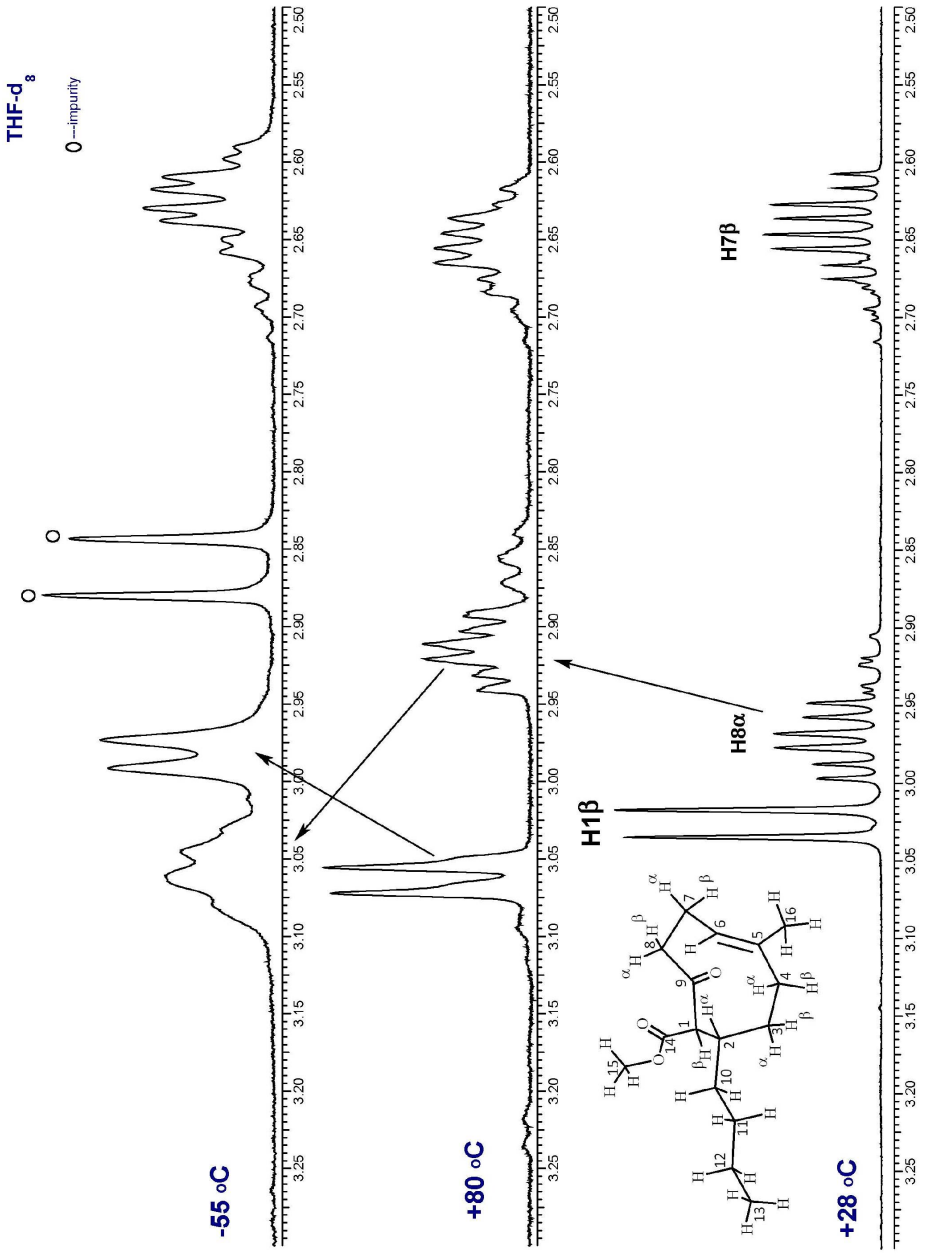
THF-d8
O---impurity
O
O
-55 oC
+80 oC
+28 oC
H1β
H8α
H7β

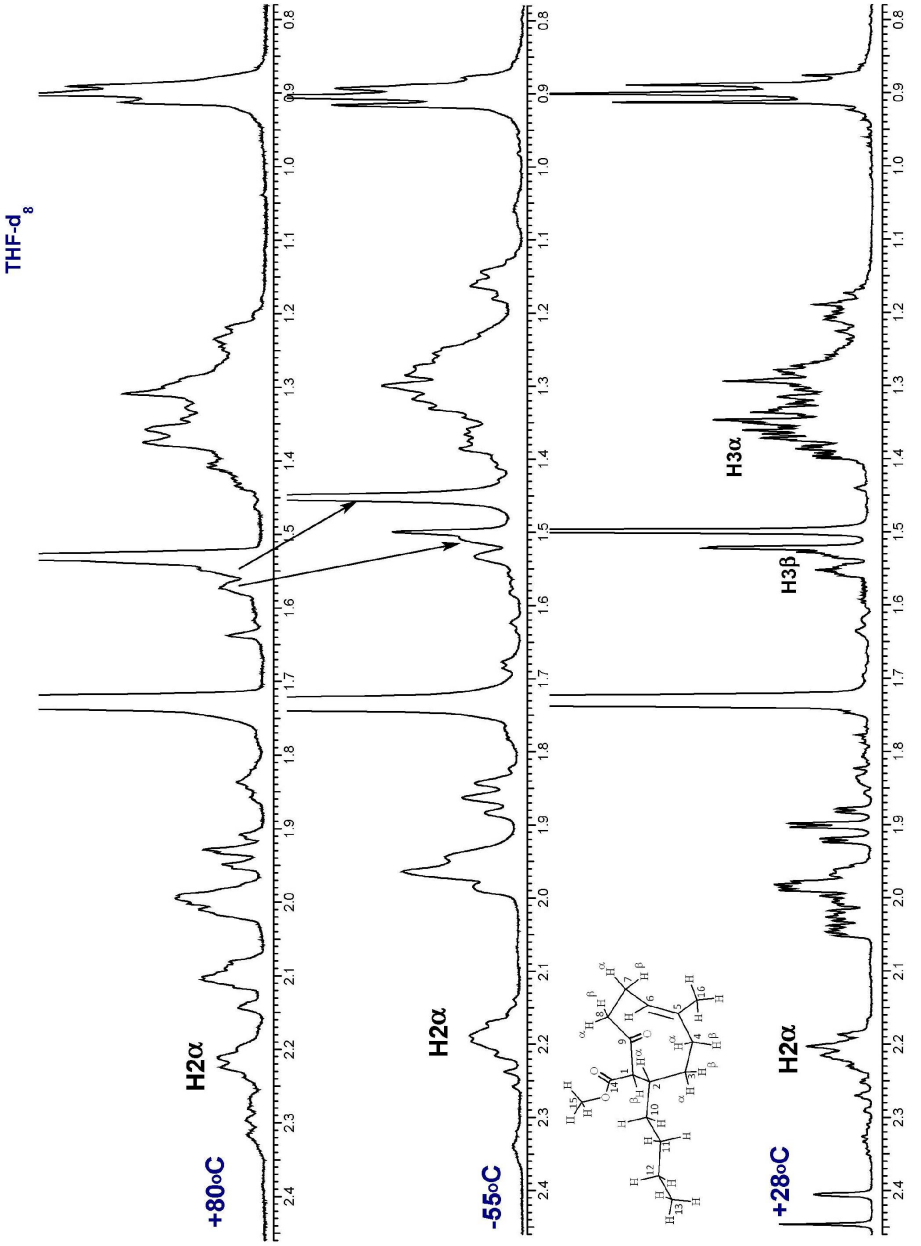
THF-d8
+80oC
H2α
-55oC
H2α
+28oC
H2α
H3β
H3α

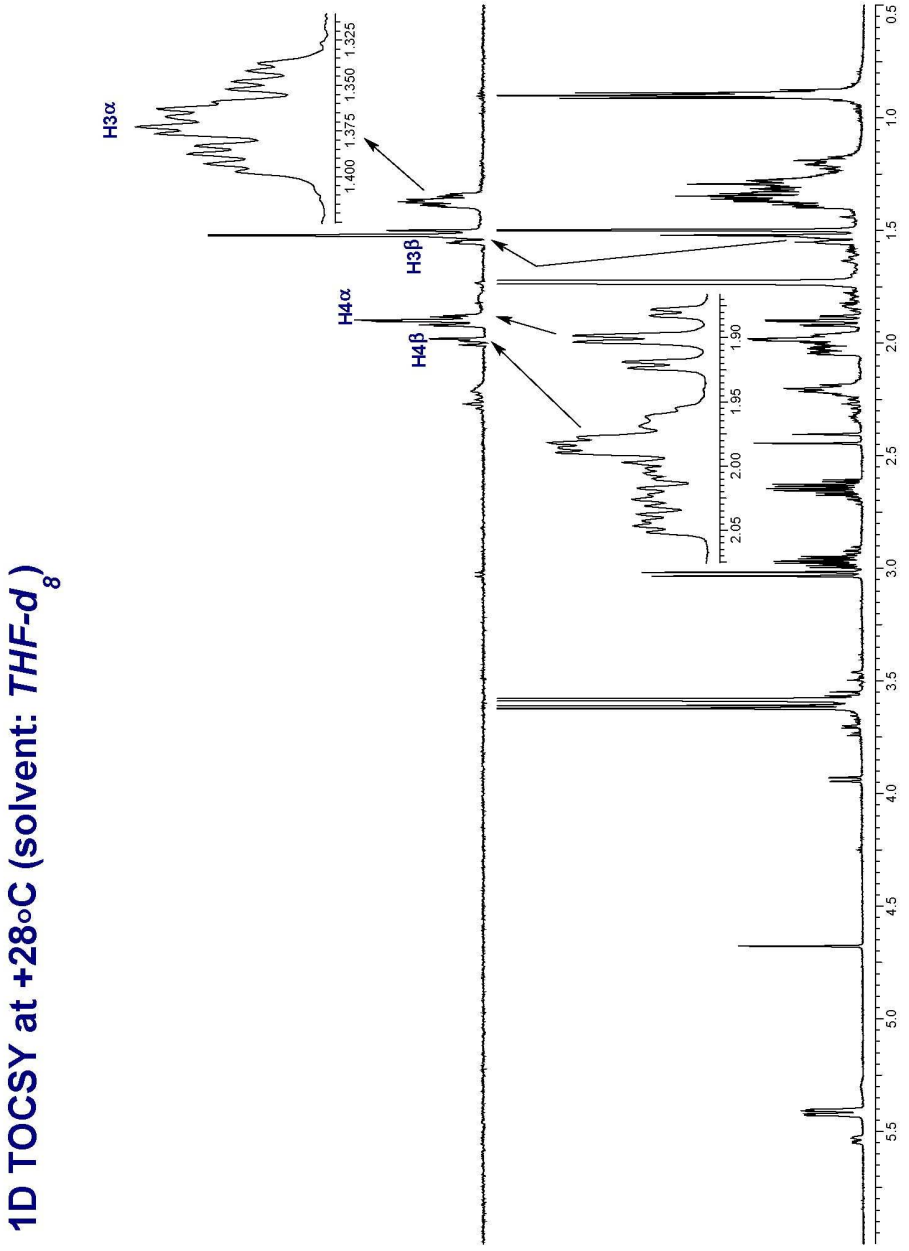
1D TOCSY at +28°C (solvent: THF-d8)
H3α
H4α
H4β
H3β

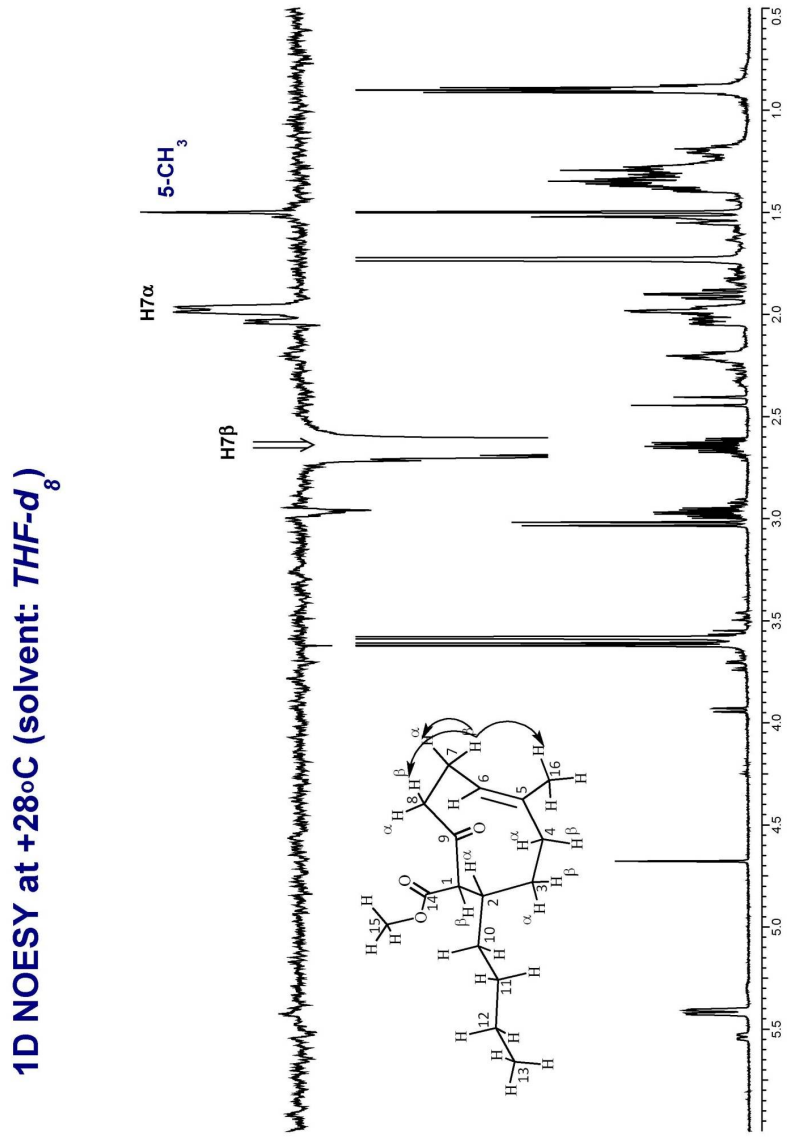
1D NOESY at +28oC (solvent: THF-d8)
H7α
5-CH3
H7β

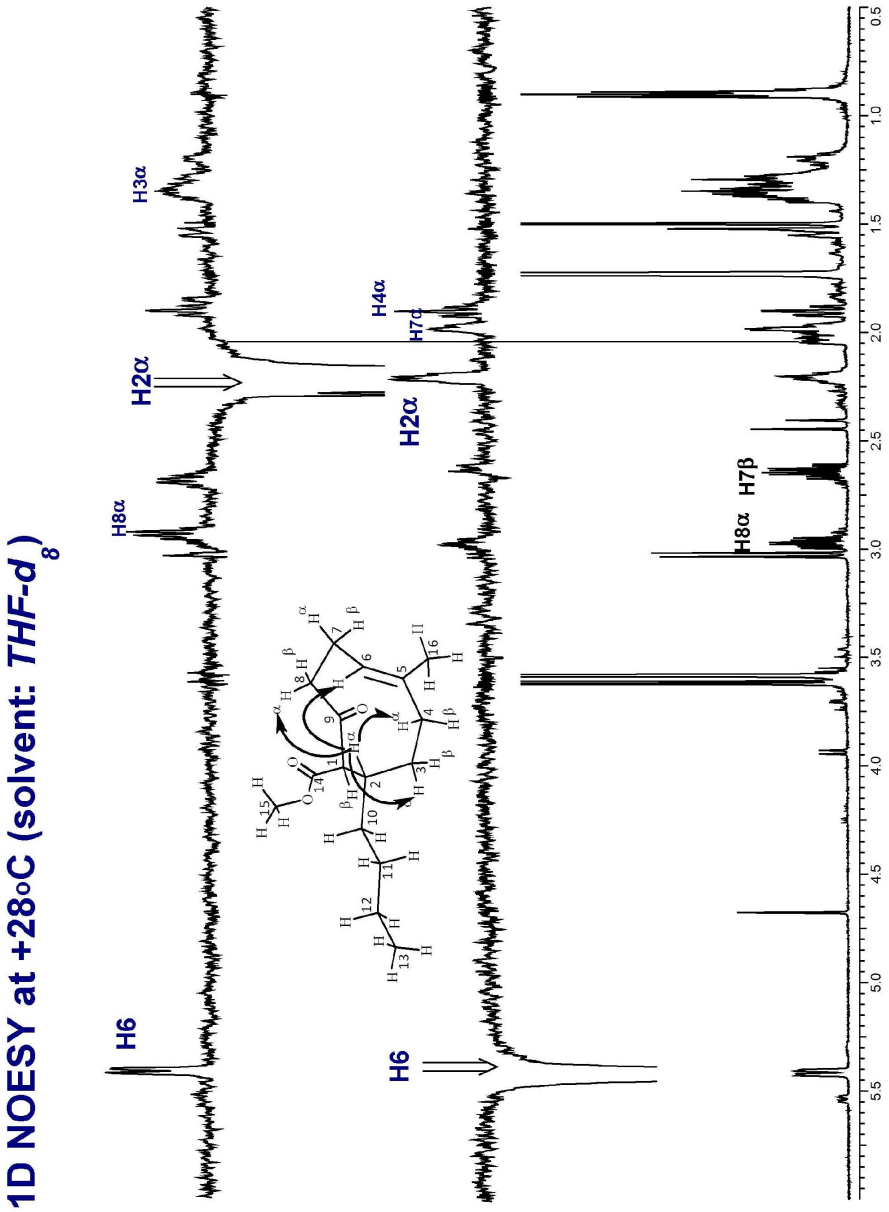
1D NOESY at +28oC (solvent: THF-d8)
H6
H8α
H2α
H3α
H4α
H7α
H2α
H6
H8α
H7β

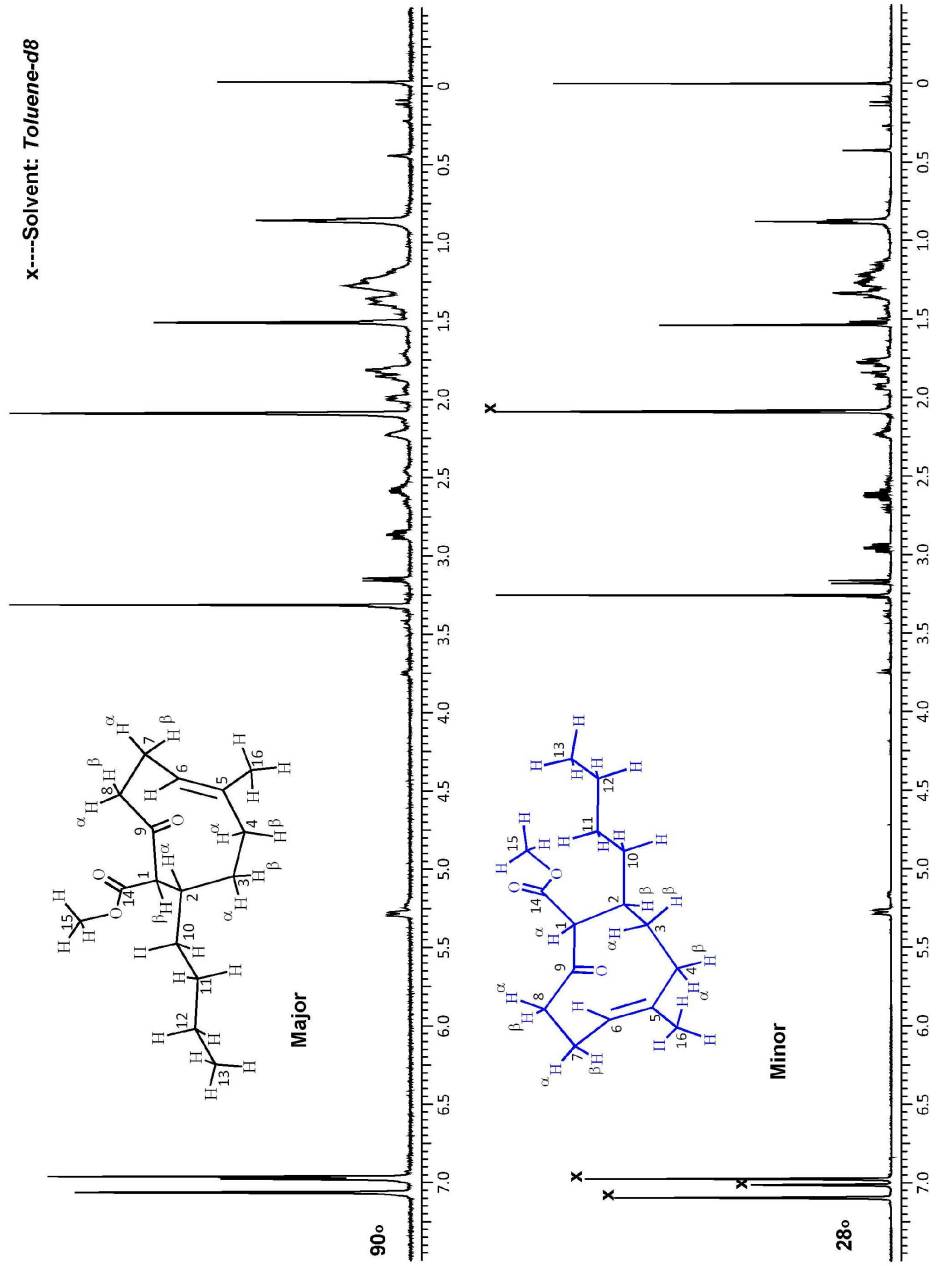
x---Solvent: Toluene-d8
90°
Major
28°
Minor
x
x
x

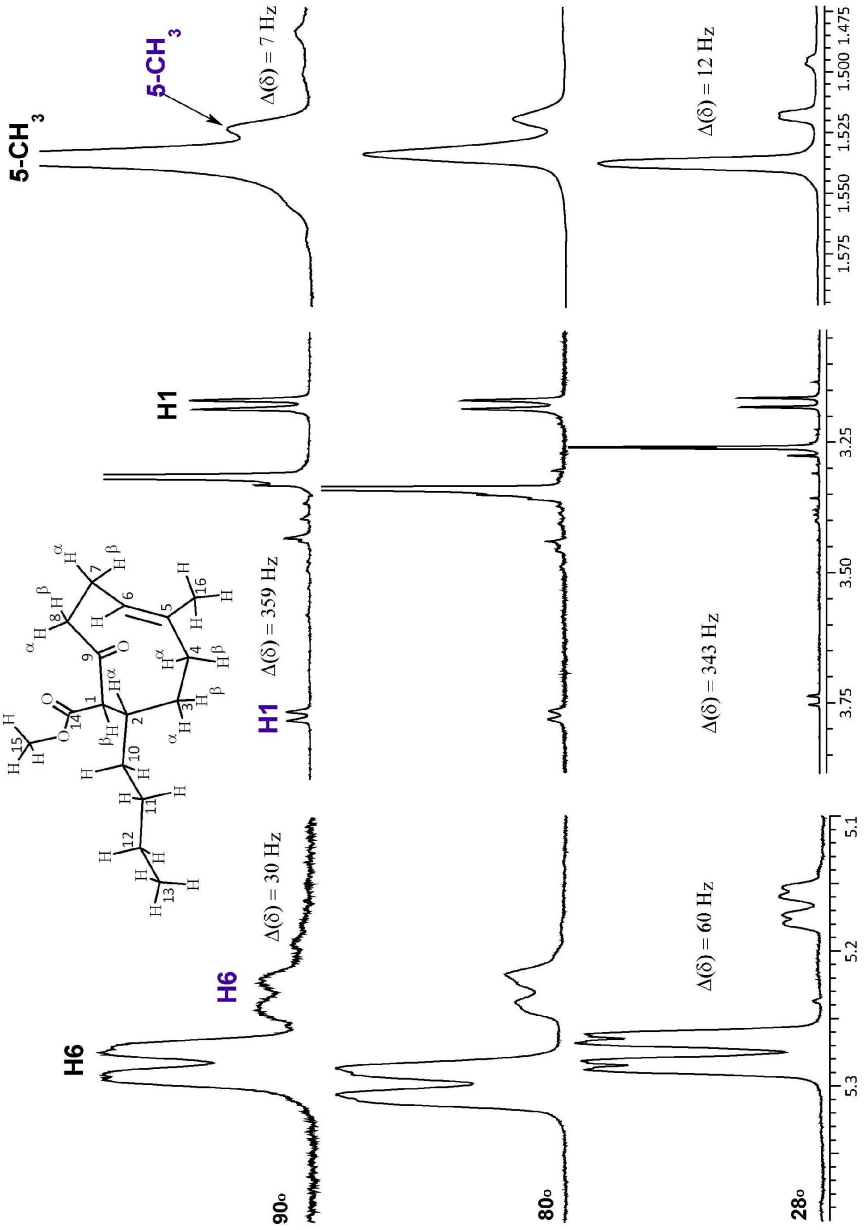
5-CH3
5-CH3
Δ(δ) = 7 Hz
H1
H1
Δ(δ) = 359 Hz
H6
H6
Δ(δ) = 30 Hz
90°
Δ(δ) = 343 Hz
80°
Δ(δ) = 60 Hz
Δ(δ) = 12 Hz
28°
1.575
1.550
1.525
1.500
1.475
3.75
3.50
3.25
5.3
5.2
5.1

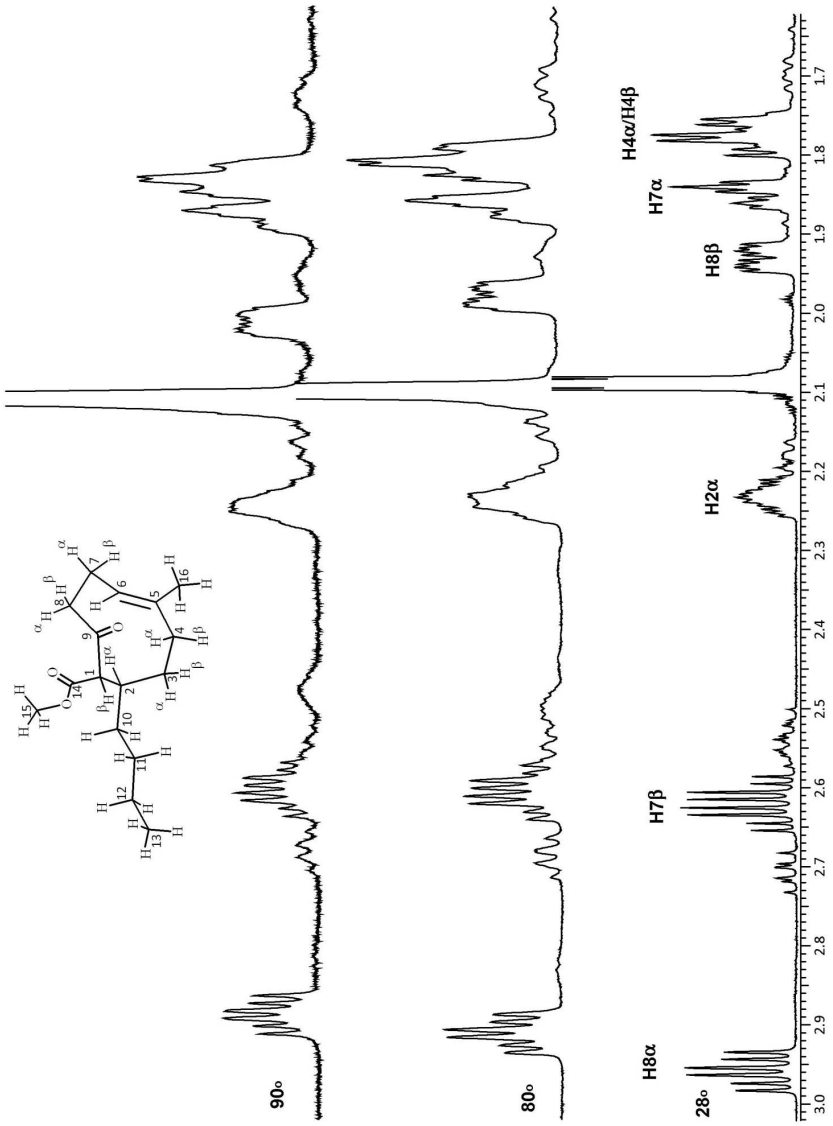
90
80
28
H8α
H7β
H2α
H8β
H7α
H4α/H4β
3.0
2.9
2.8
2.7
2.6
2.5
2.4
2.3
2.2
2.1
2.0
1.9
1.8
1.7

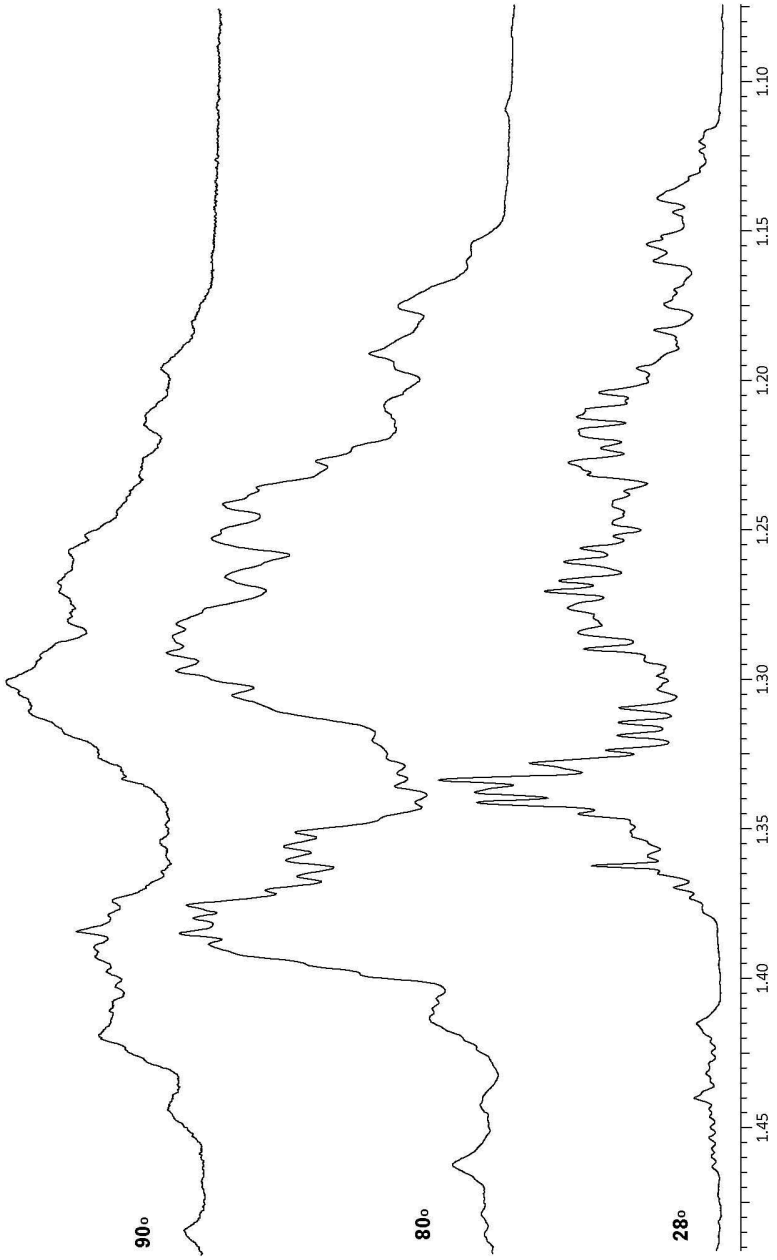
90°
80°
28°
1.10
1.15
1.20
1.25
1.30
1.35
1.40
1.45

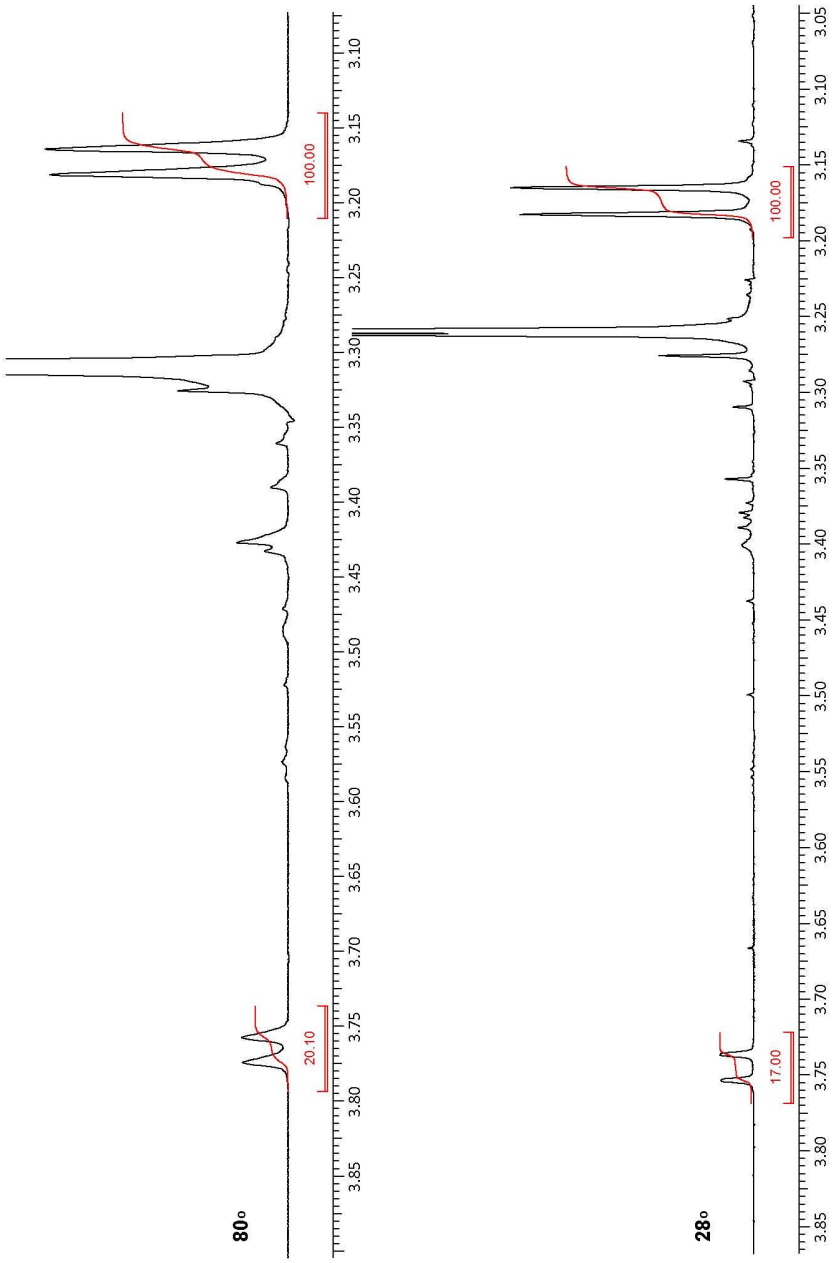
80o
20.10
100.00
28o
17.00
100.00
3.05
3.10
3.15
3.20
3.25
3.30
3.35
3.40
3.45
3.50
3.55
3.60
3.65
3.70
3.75
3.80
3.85

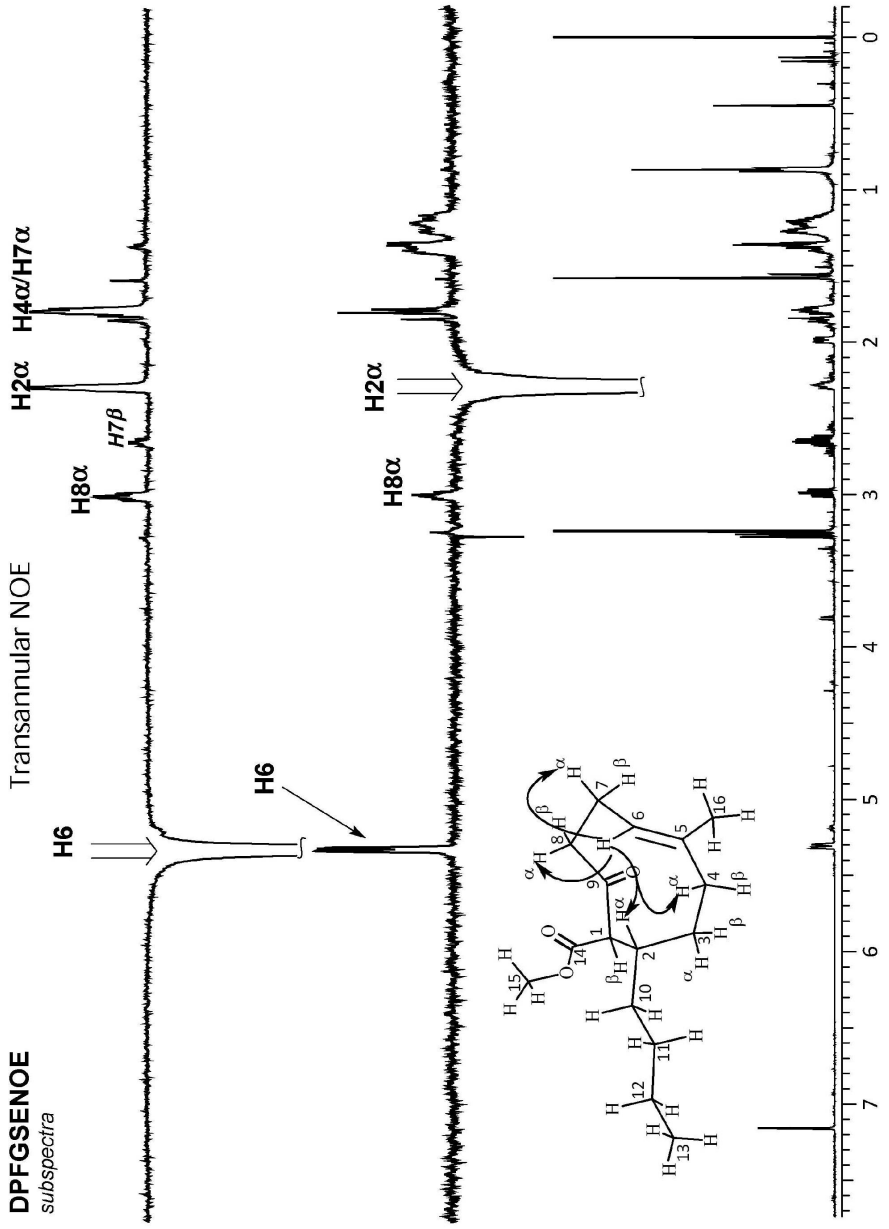
DPFGSENOE
subspectra
Transannular NOE
H6
H6
H8α
H7β
H2α
H4α/H7α
H8α
H2α

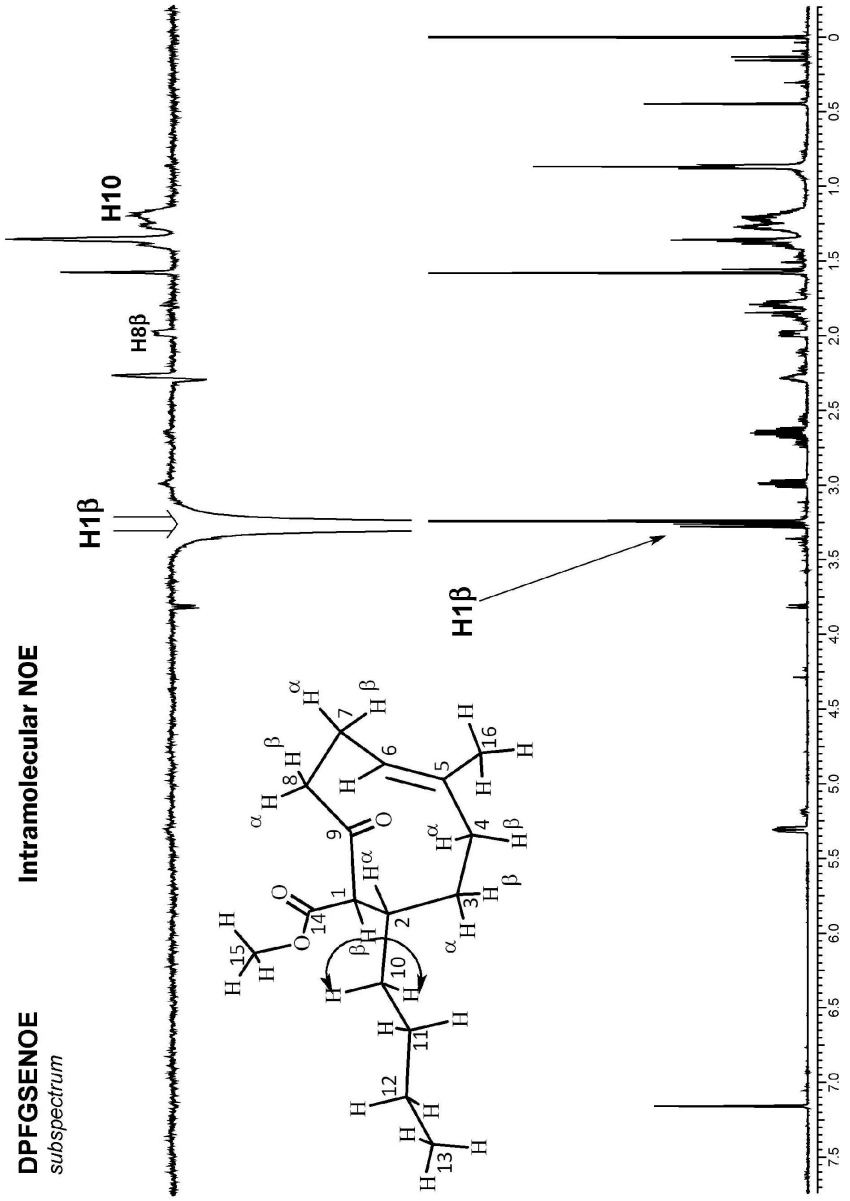
DPFGSENOE
subspectrum
Intramolecular NOE
H1β
H8β
H10
H1β

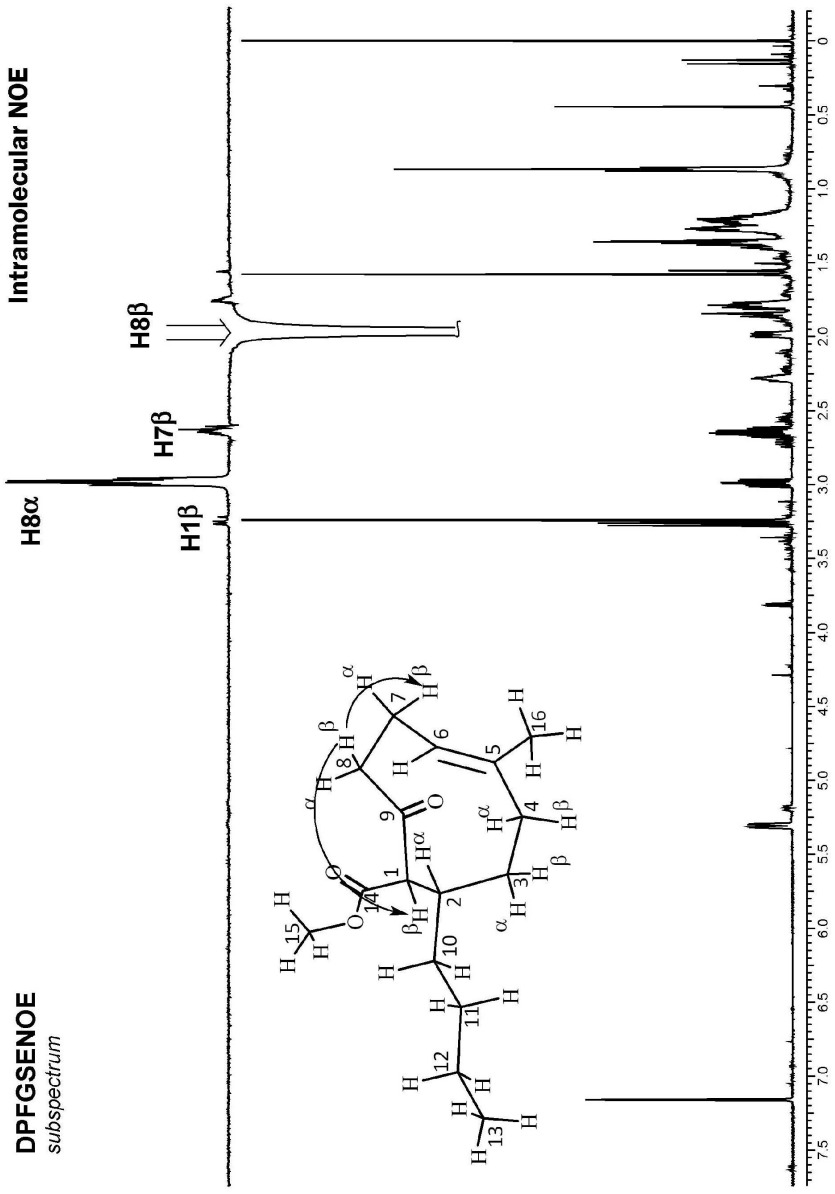
DPFGSENOE
subspectrum
Intramolecular NOE
H8α
H1β
H7β
H8β

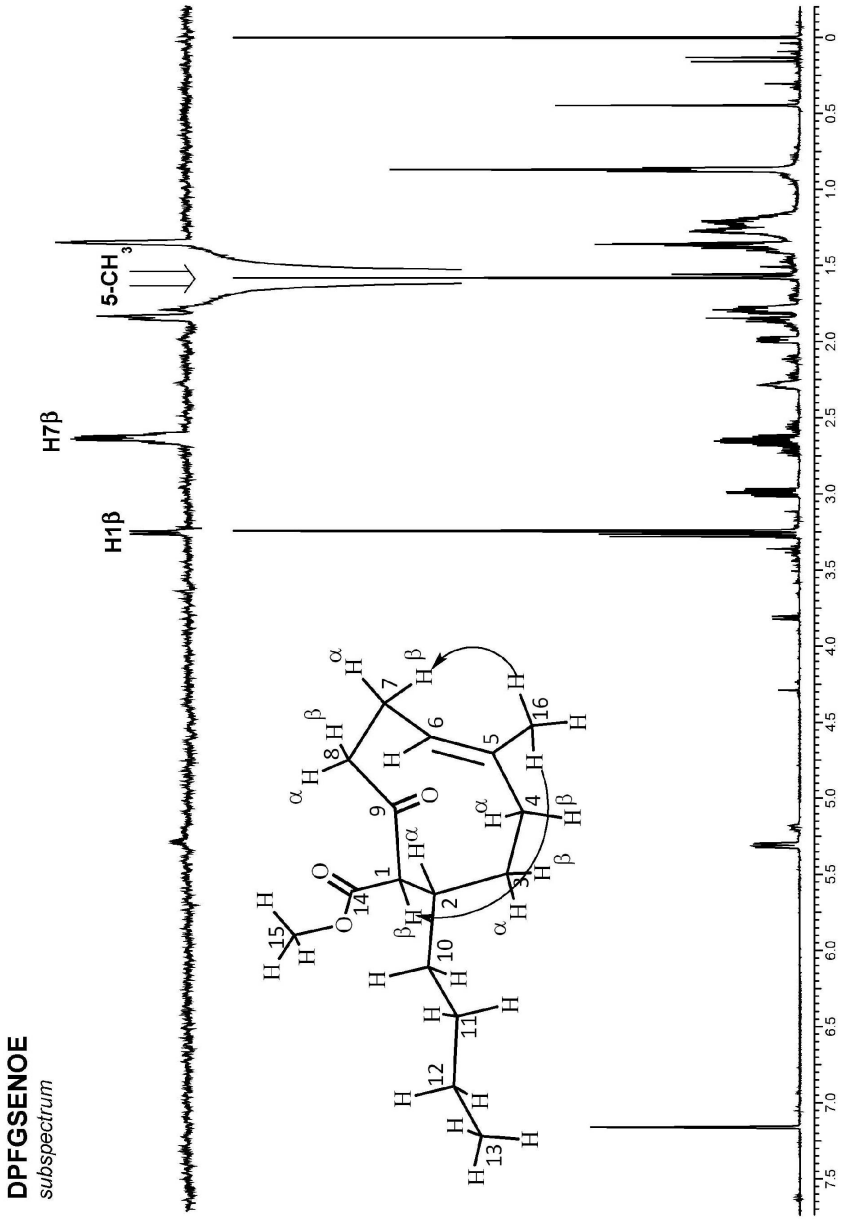
DPFGSENOE
subspectrum
H1β
H7β
5-CH3

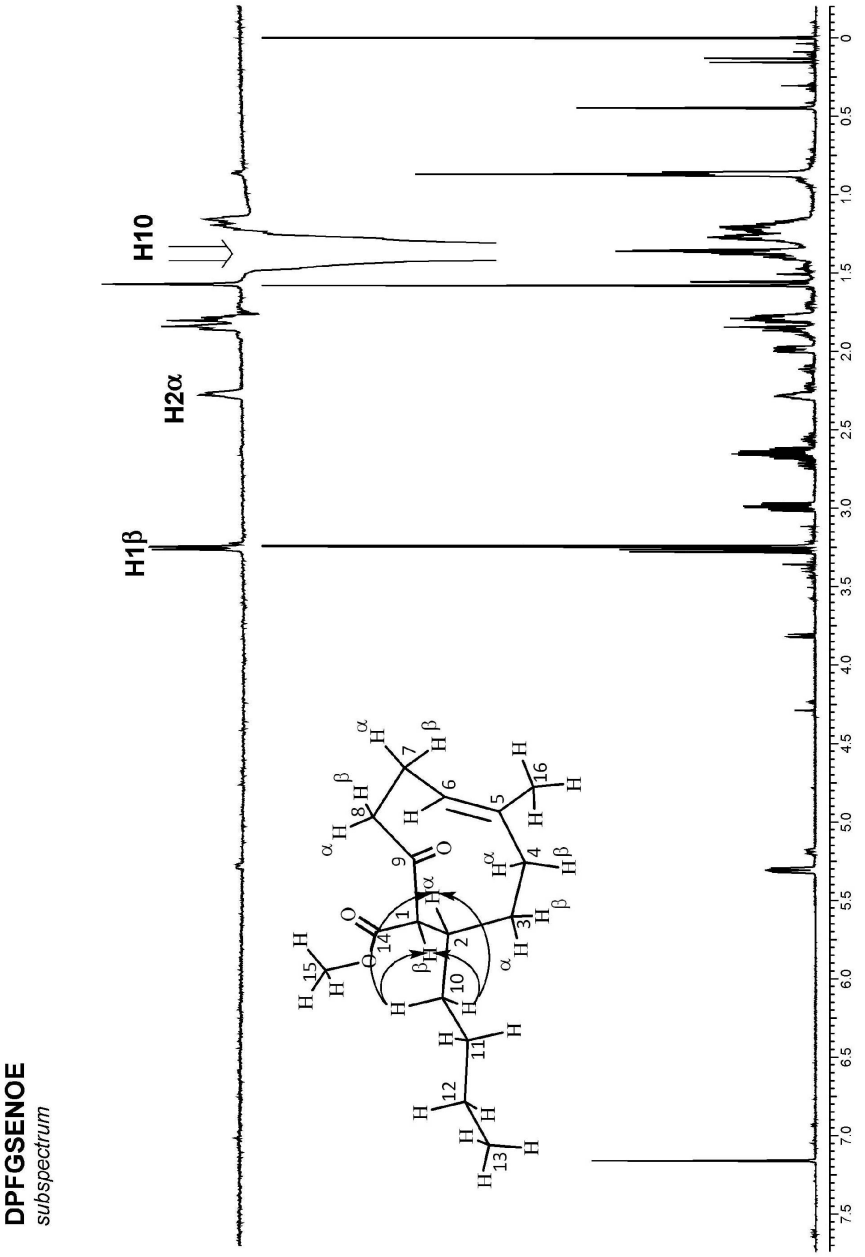
DPFGSENOE
subspectrum
H1β
H2α
H10

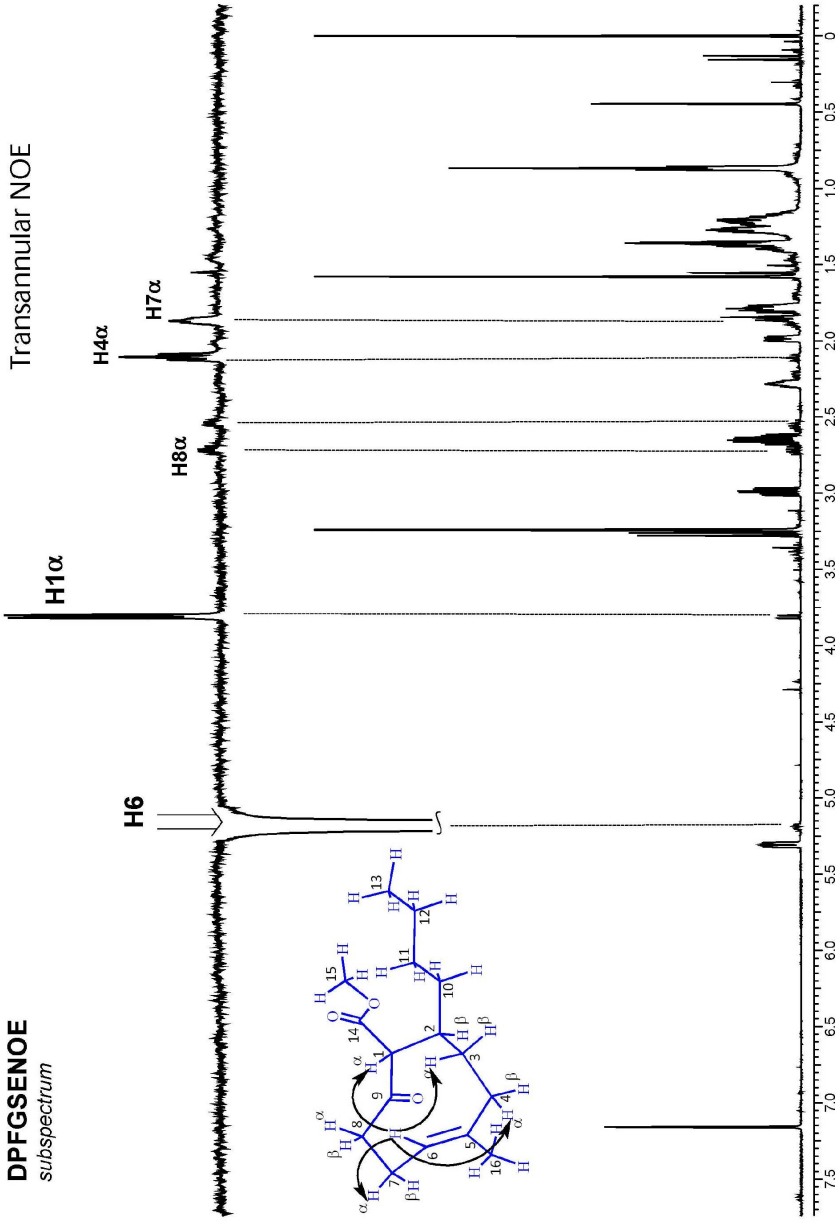
DPFGSENOE
subspectrum
Transannular NOE
H6
H1α
H8α
H4α
H7α

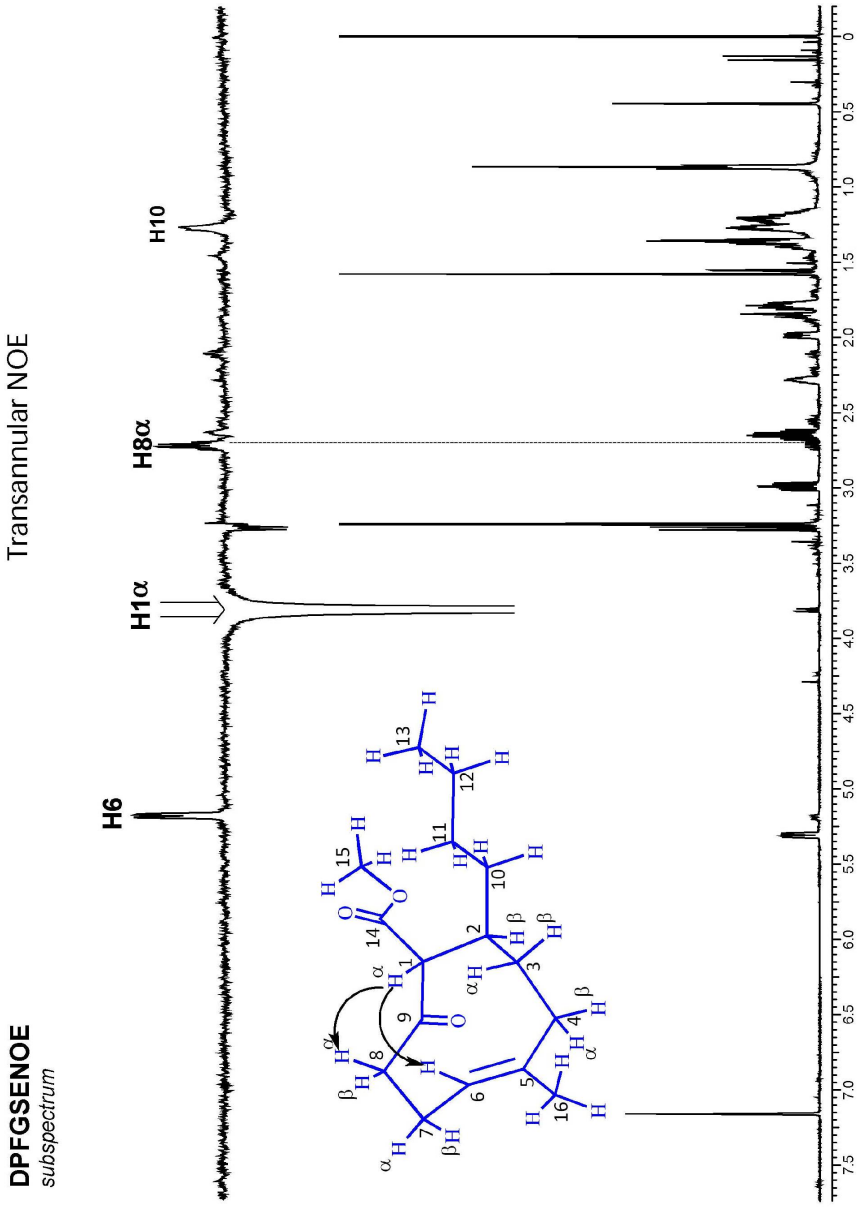
DPFGSENOE
subspectrum
Transannular NOE
H6
H1α
H8α
H10

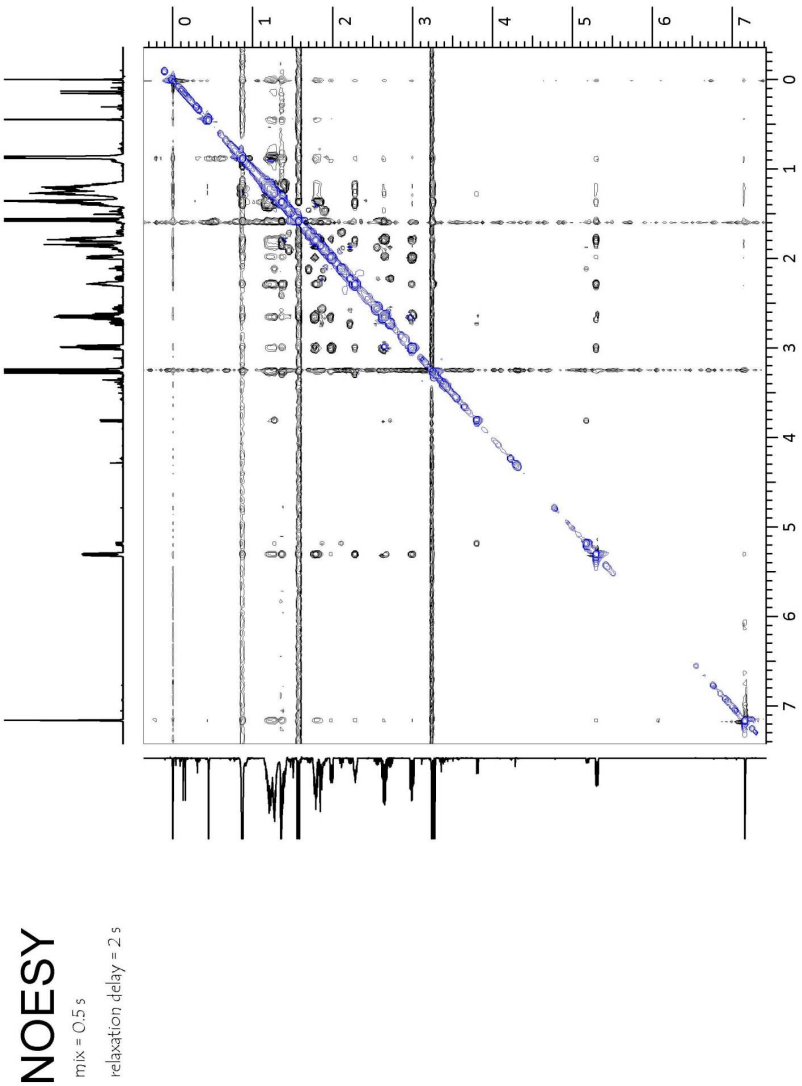
NOESY
mix = 0.5 s
relaxation delay = 2 s
0
1
2
3
4
5
6
7

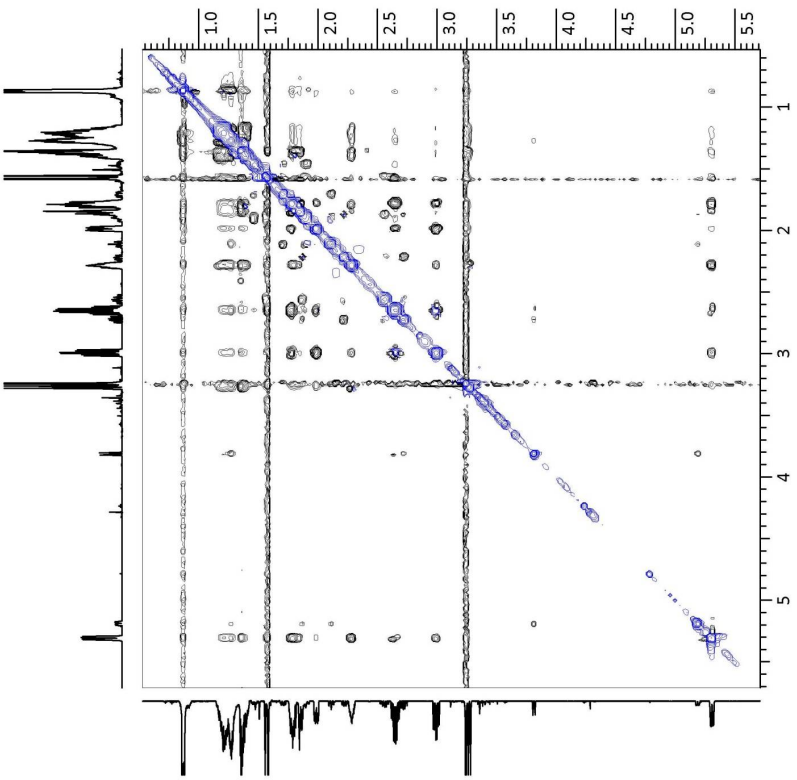

NOESY

expansion

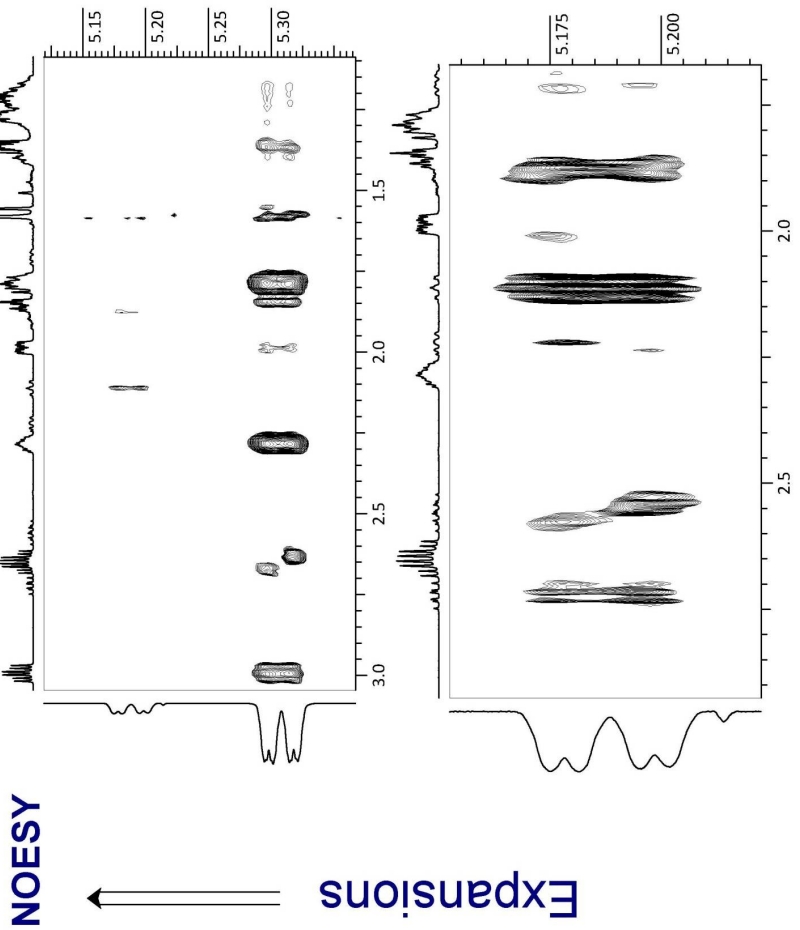
NOESY
Expansions
5.15
5.20
5.25
5.30
1.5
2.0
2.5
3.0
5.175
5.200
2.0
2.5

Protons	Distance / Å	
	Conformers	
	Major	Minor
H1-----H6	4.59	2.75
H2-----H6	2.21	3.91

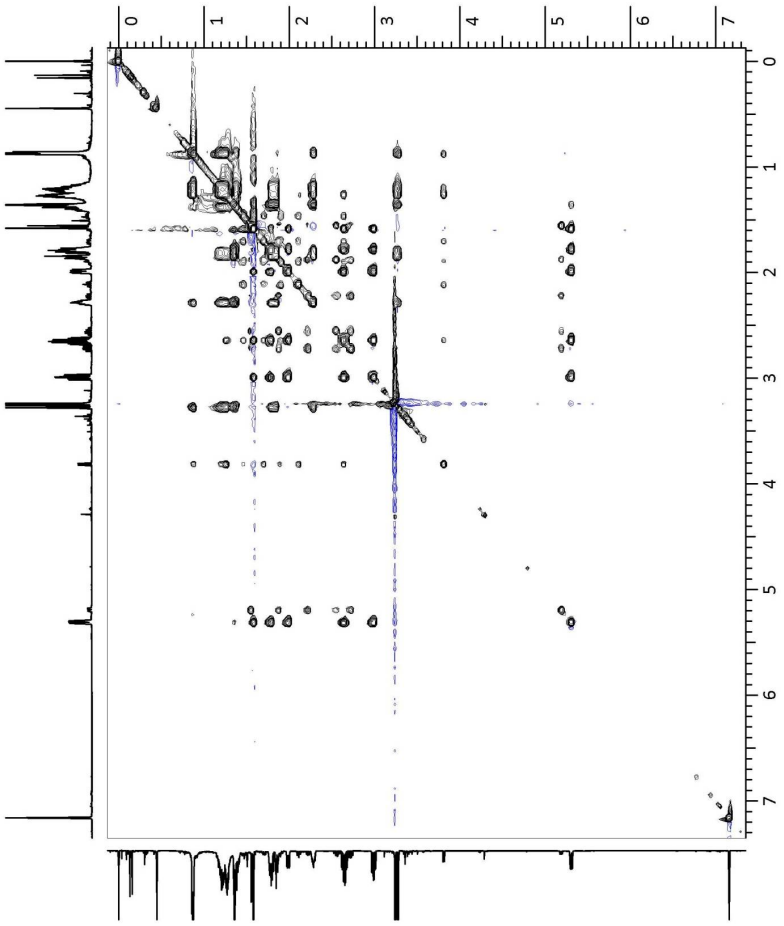
TOCSY
mix = 250 ms
0
1
2
3
4
5
6
7

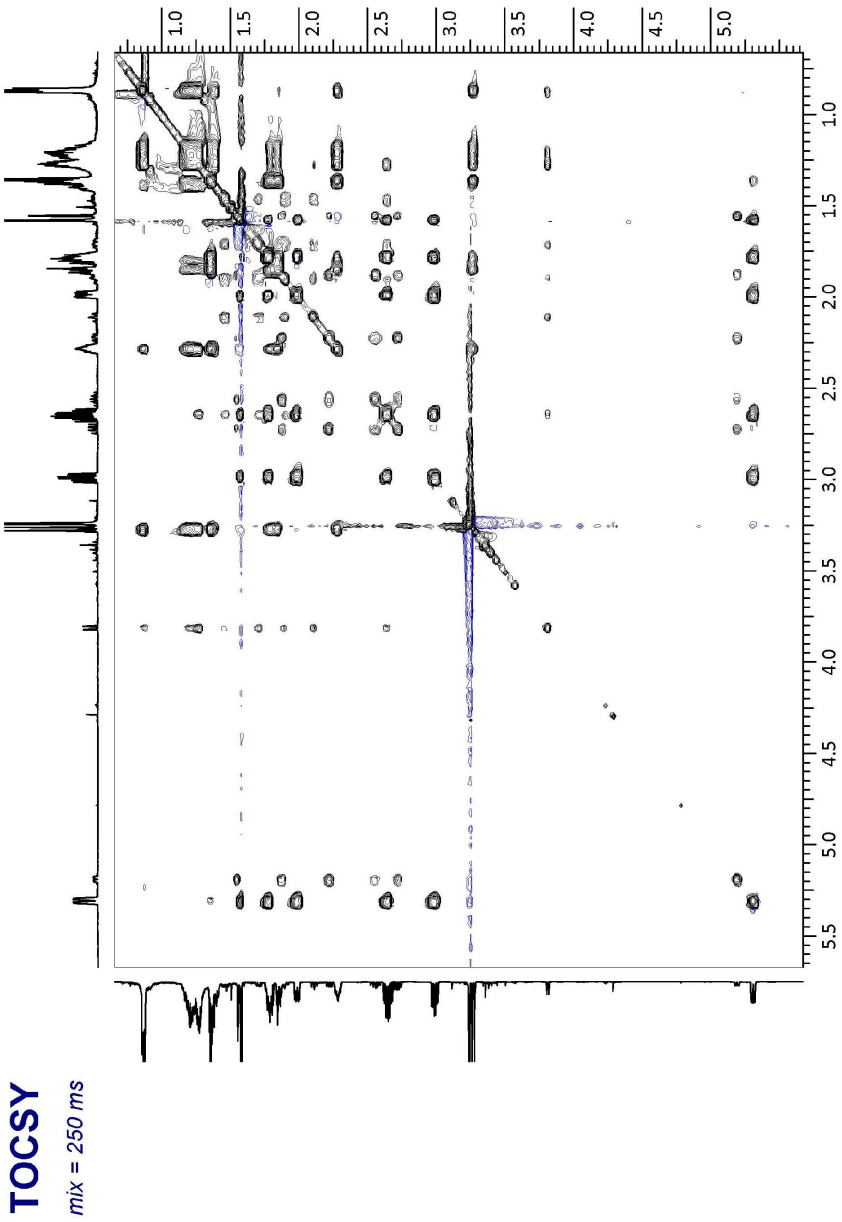
TOCSY
mix = 250 ms
1.0
1.5
2.0
2.5
3.0
3.5
4.0
4.5
5.0
5.5

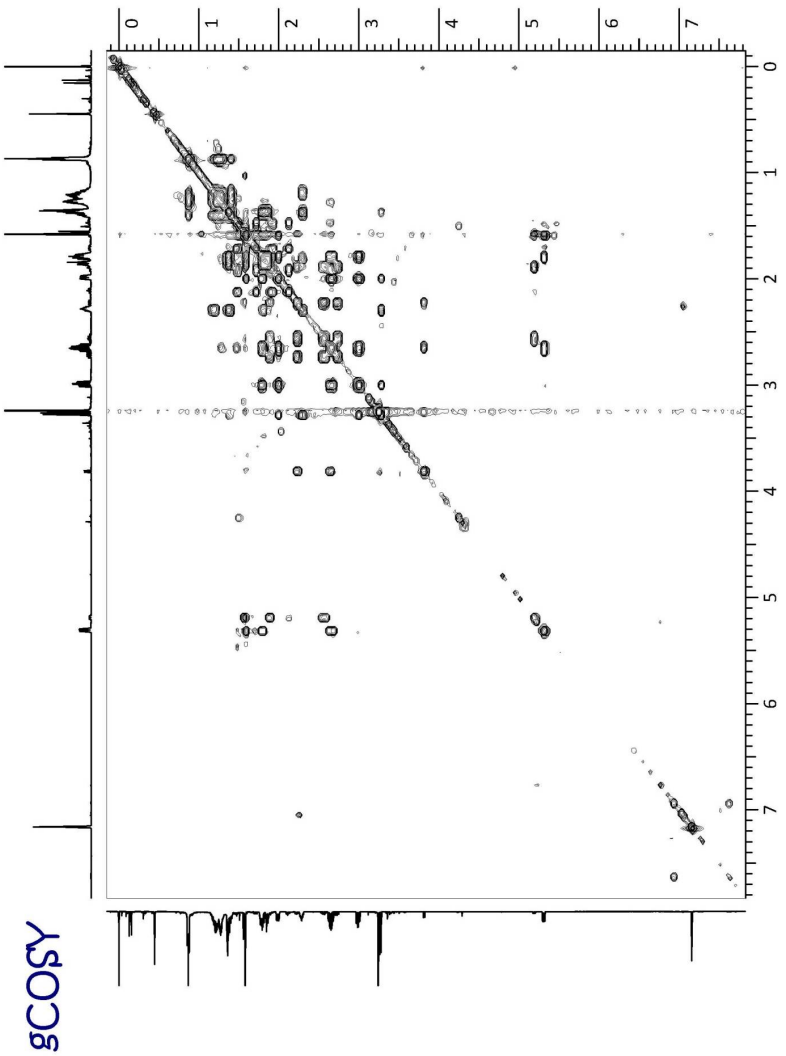
gCOSY
0
1
2
3
4
5
6
7

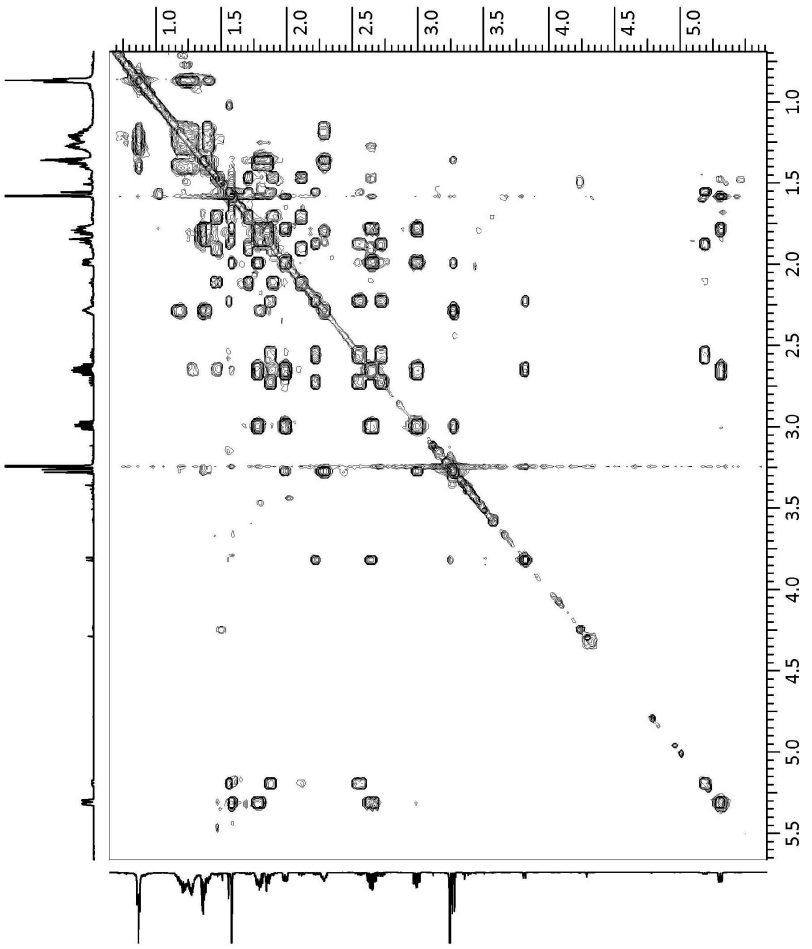

gCOSY

expansion

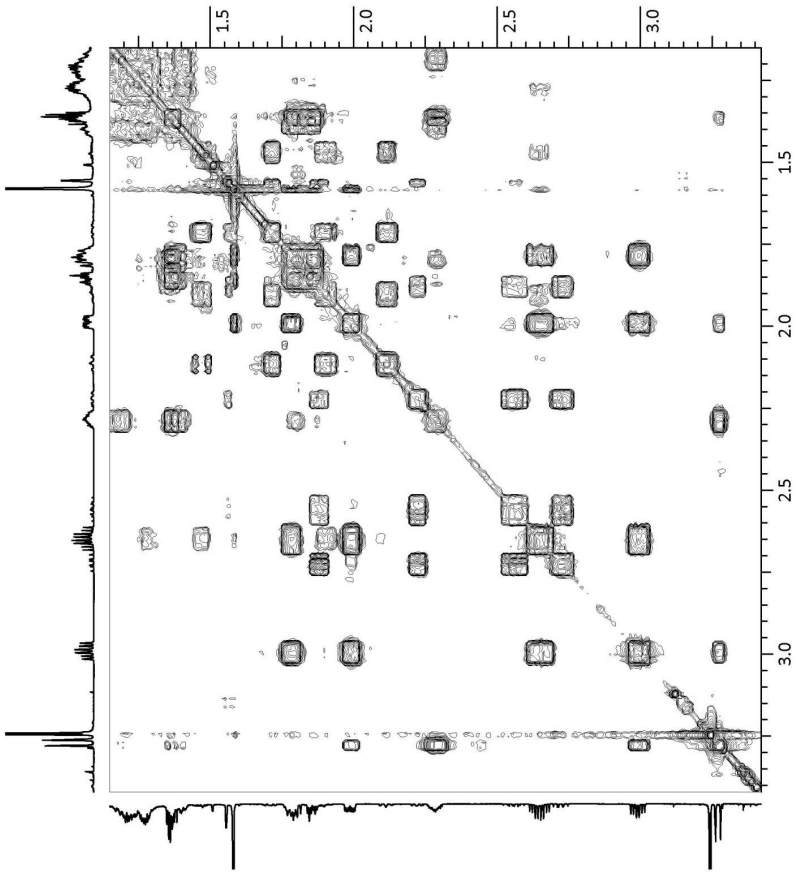

gCOSY

expansion

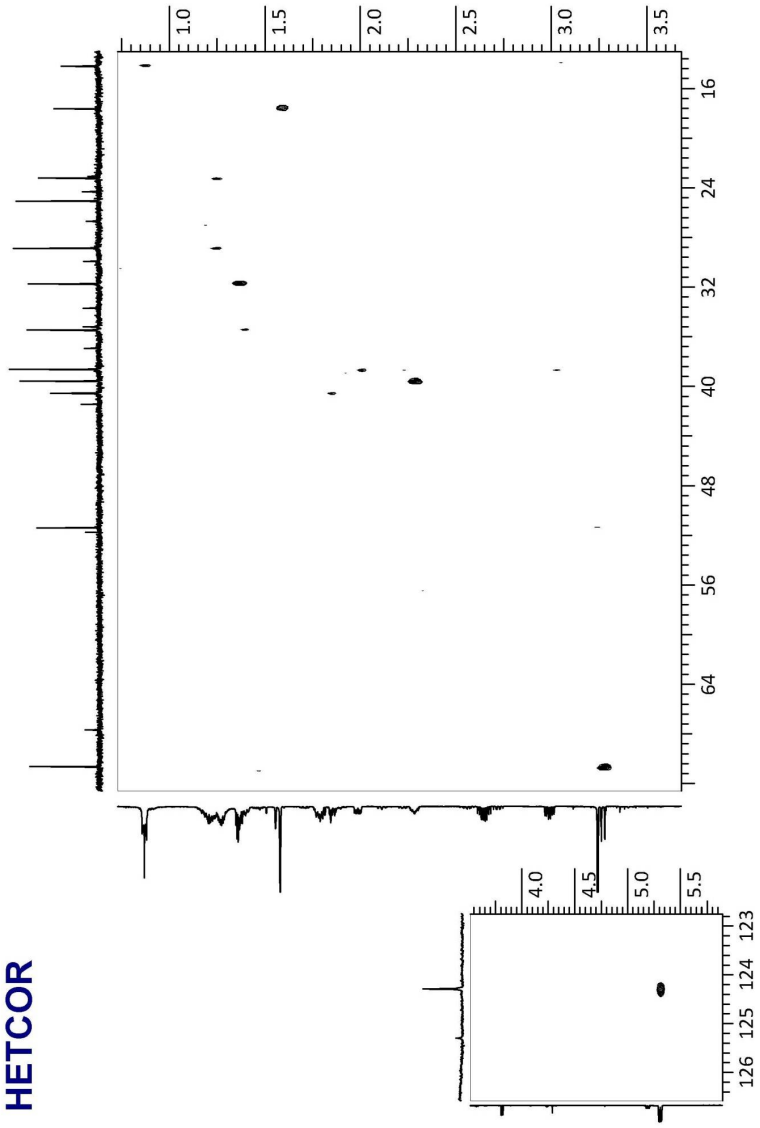
HETCOR
1.0
1.5
2.0
2.5
3.0
3.5
16
24
32
40
48
56
64
4.0
4.5
5.0
5.5
123
124
125
126

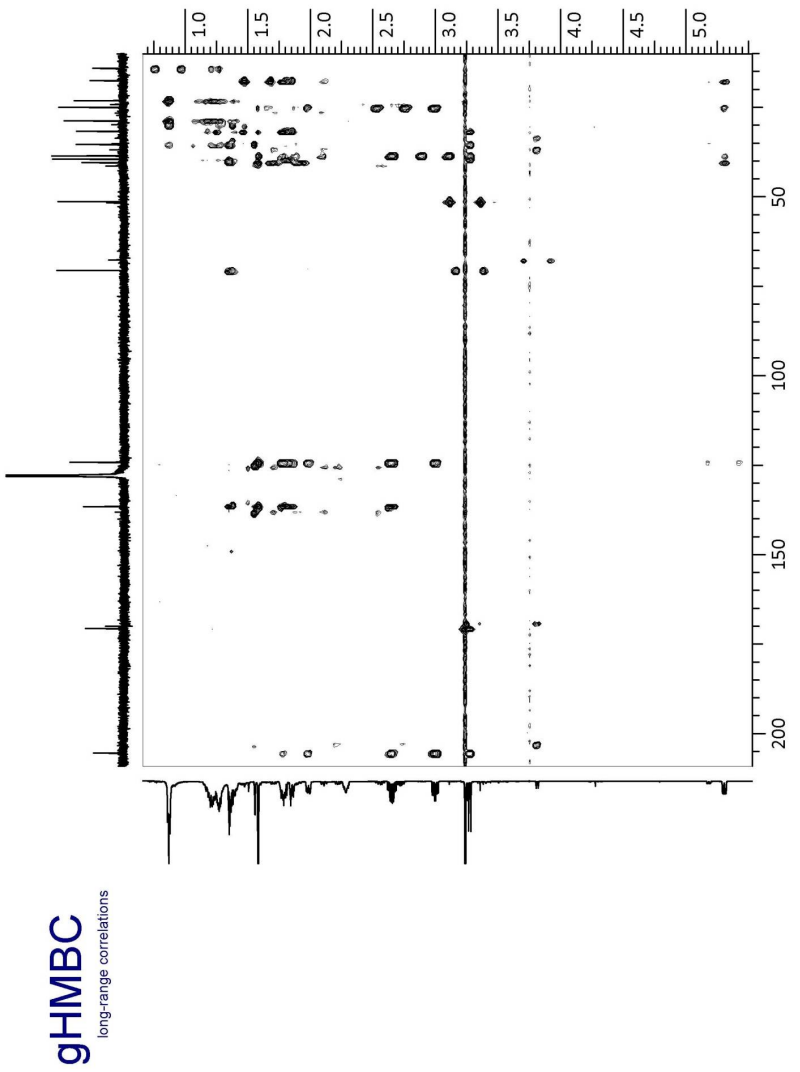
gHMBC
long-range correlations
1.0
1.5
2.0
2.5
3.0
3.5
4.0
4.5
5.0
50
100
150
200

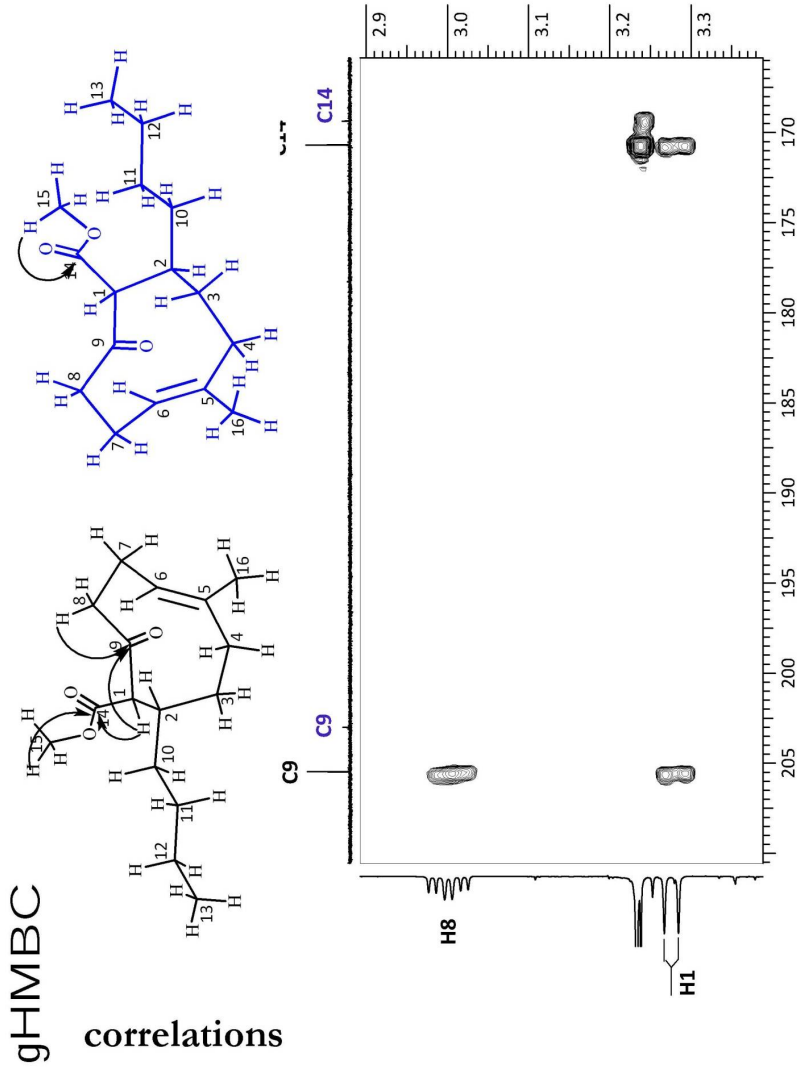
gHMBC
correlations
C14
C9
C9
H8
H1
2.9
3.0
3.1
3.2
3.3
170
175
180
185
190
195
200
205

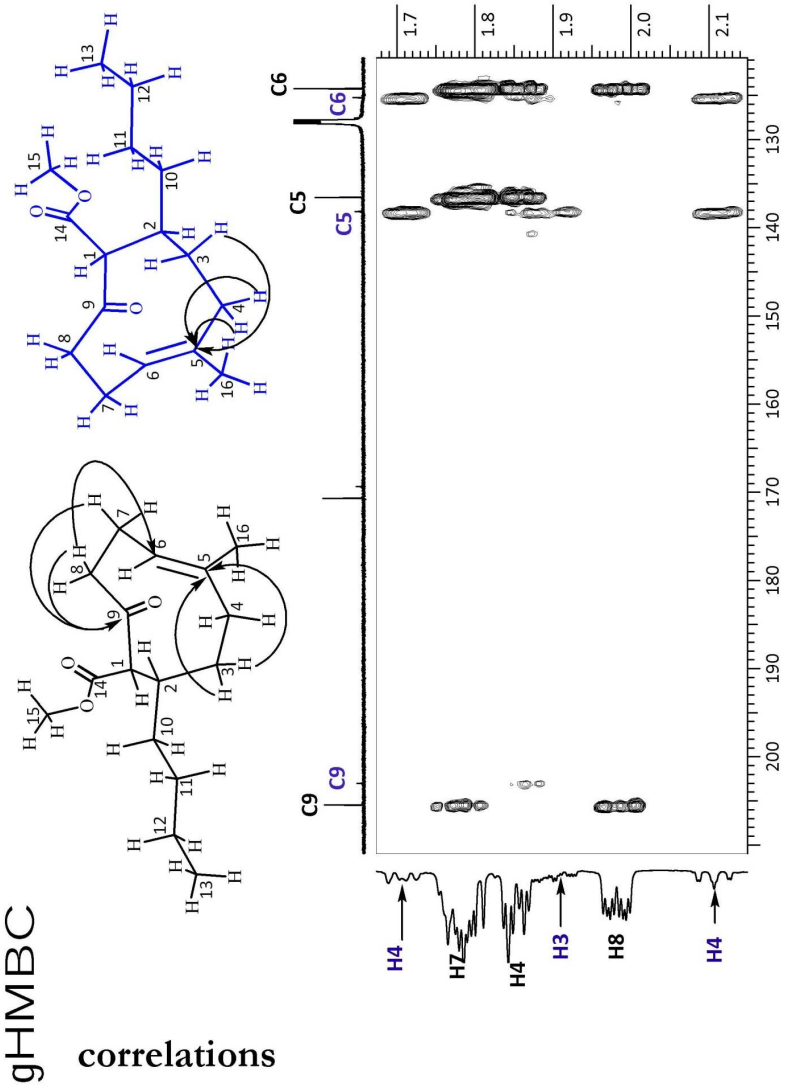
gHMBC
correlations
C6
C5
C9
H4
H7
H4
H3
H8
H4
1.7
1.8
1.9
2.0
2.1
130
140
150
160
170
180
190
200

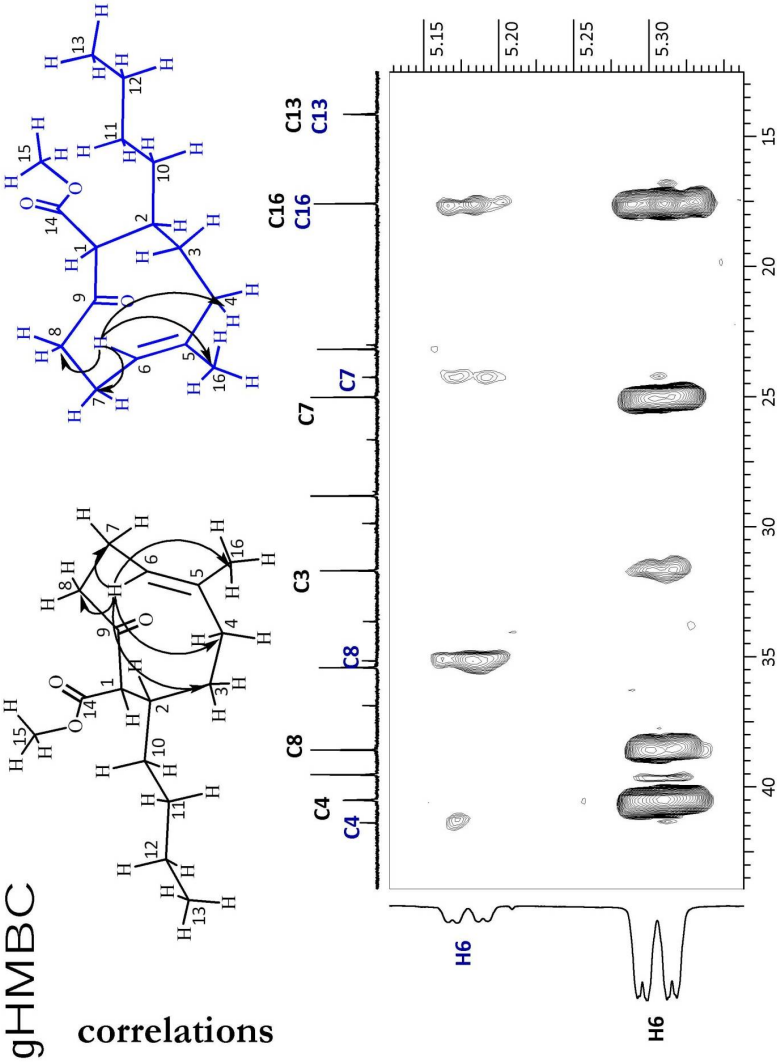
gHMBC
correlations
C13
C16
C7
C3
C8
C4
H6
5.15
5.20
5.25
5.30
15
20
25
30
35
40

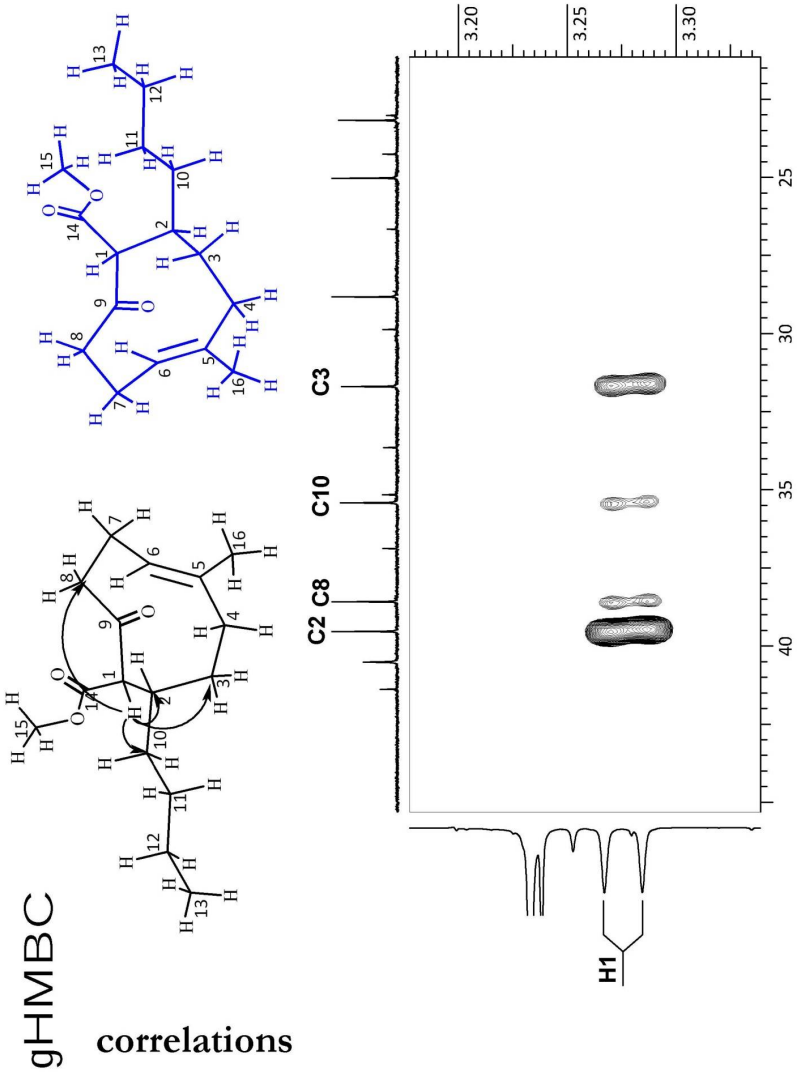
gHMBC
correlations
C2 C8
C10
C3
H1
3.20
3.25
3.30
25
30
35
40

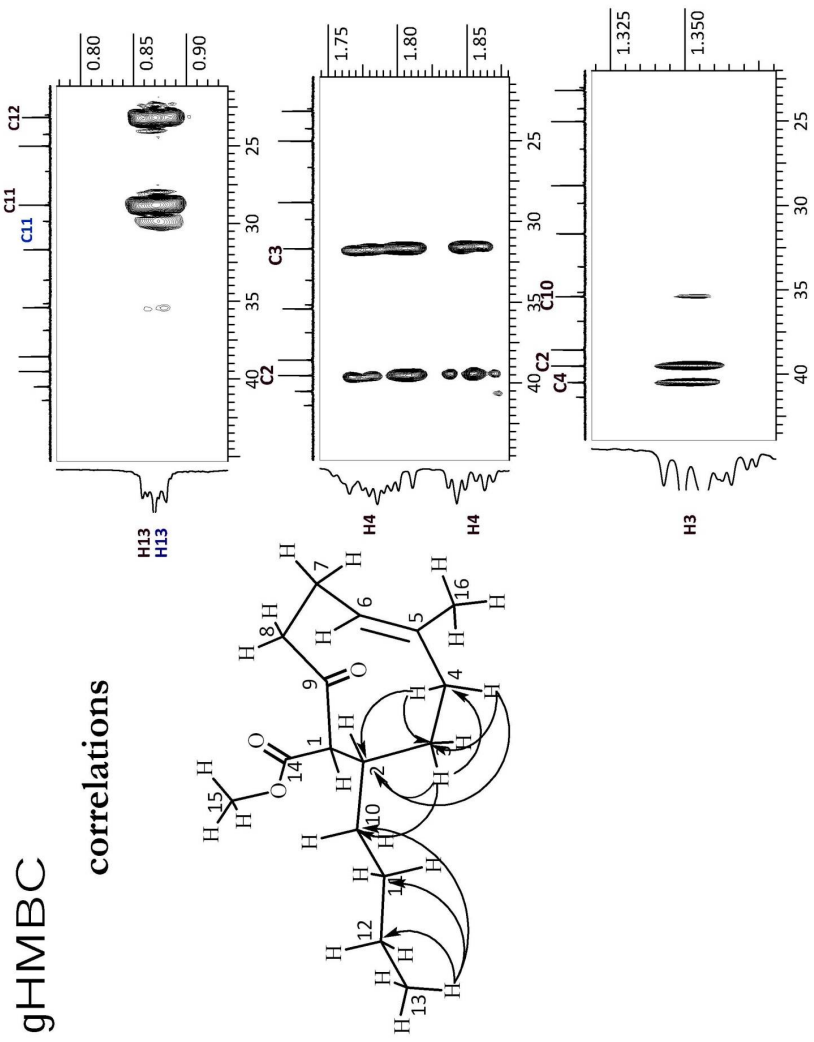
gHMBC
correlations
C12
C11
C11
C2
C3
C10
C2
C4
H13
H13
H4
H4
H3
0.80
0.85
0.90
1.75
1.80
1.85
1.325
1.350
25
30
35
40

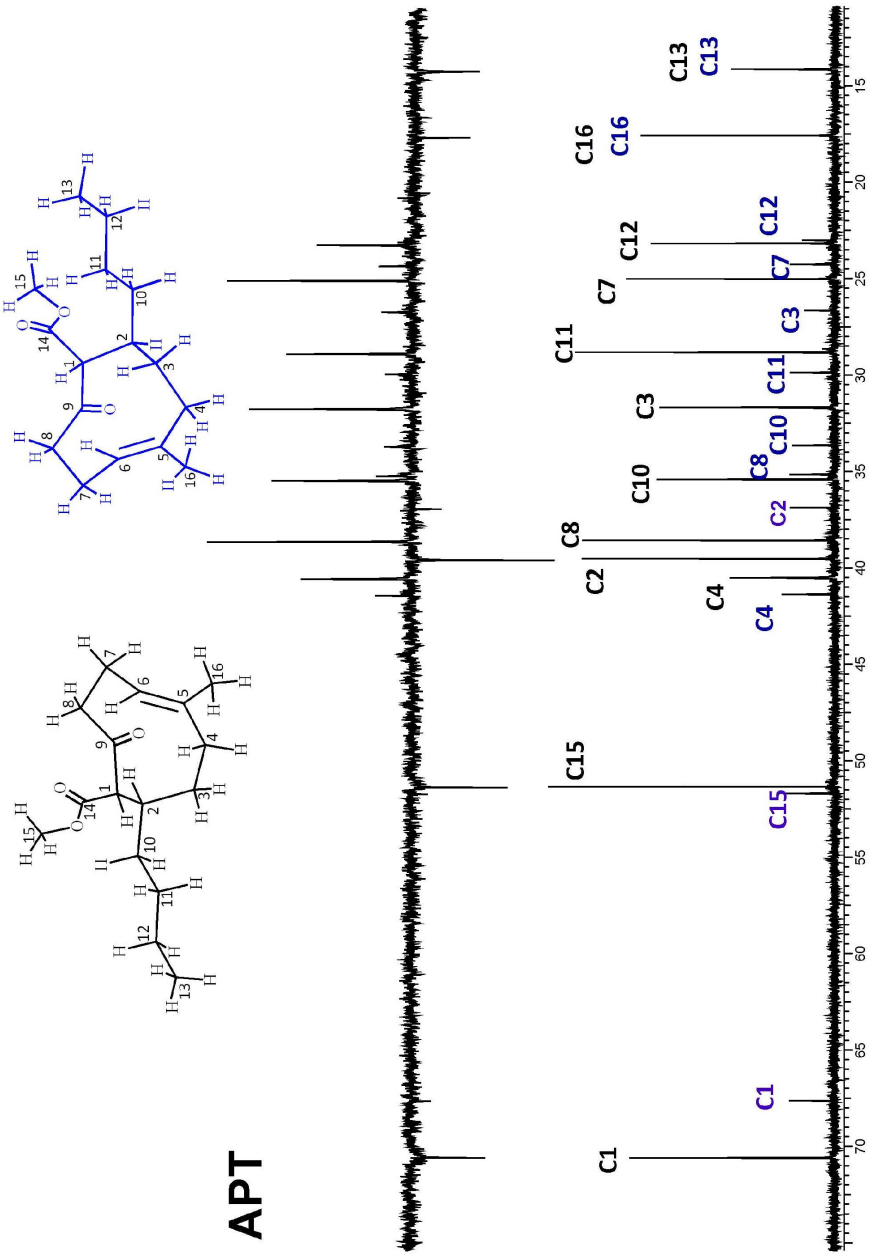
APT
C1
C15
C4
C2
C8
C10
C3
C11
C7
C12
C16
C13

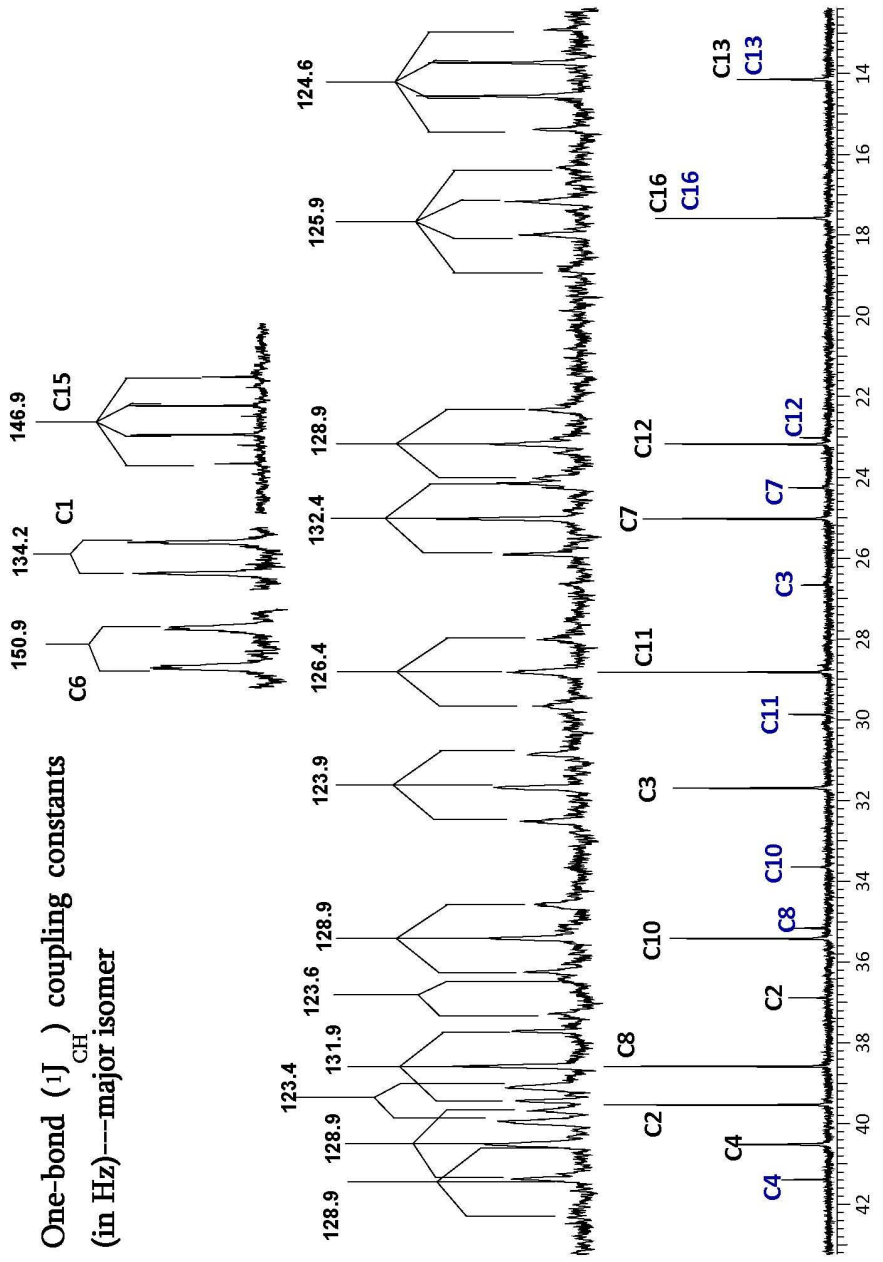
One-bond ($^1J_{CH}$) coupling constants
(in Hz)---major isomer
150.9
134.2
146.9
C6
C1
C15
123.4
131.9
123.6
128.9
128.9
128.9
123.9
126.4
132.4
128.9
124.6
125.9
C8
C2
C10
C3
C11
C7
C12
C16
C13
C4
C2
C8
C10
C11
C3
C7
C12
C16
C13
C4
42
40
38
36
34
32
30
28
26
24
22
20
18
16
14

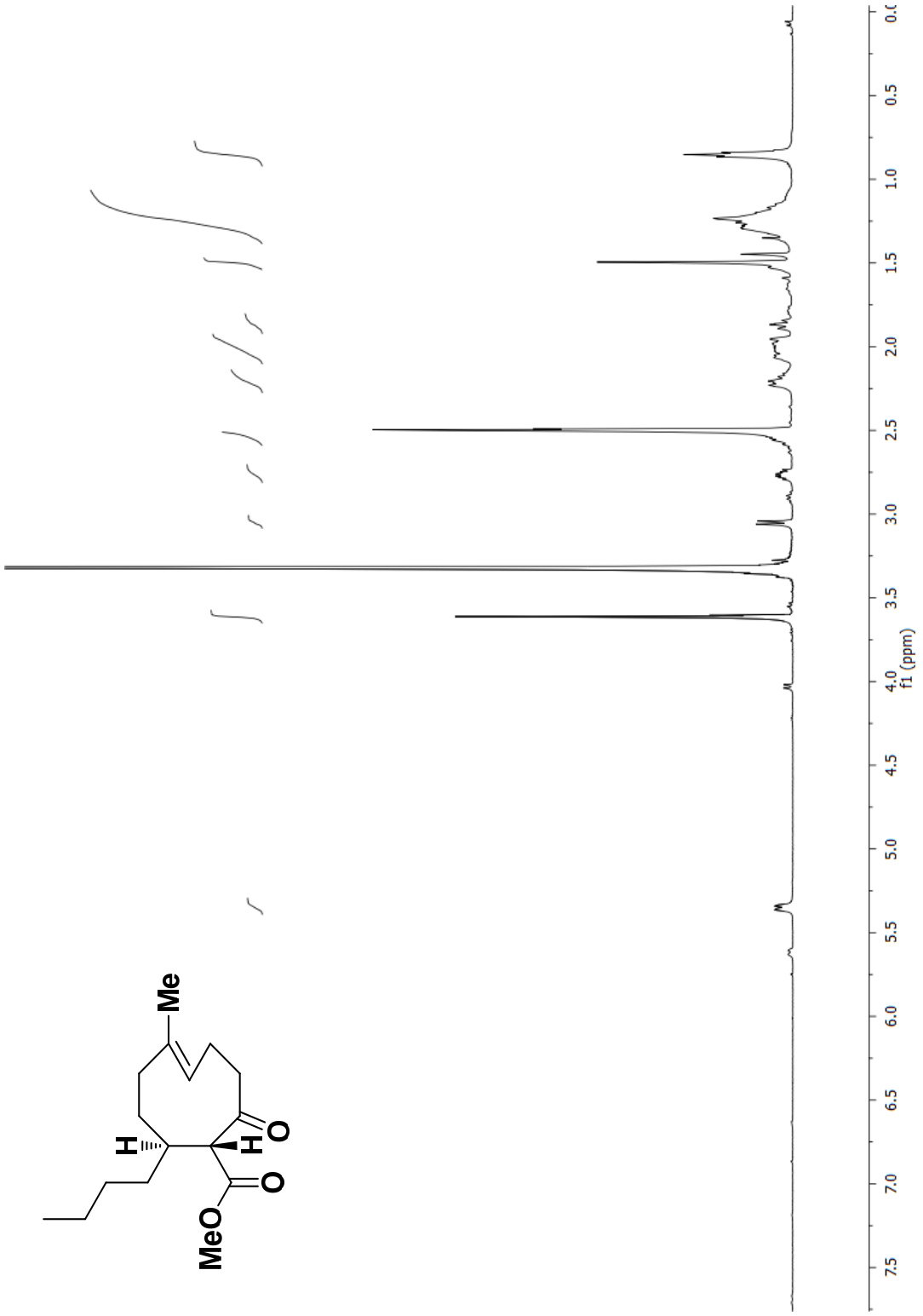
Me
H
H
O
O
MeO
f1 (ppm)

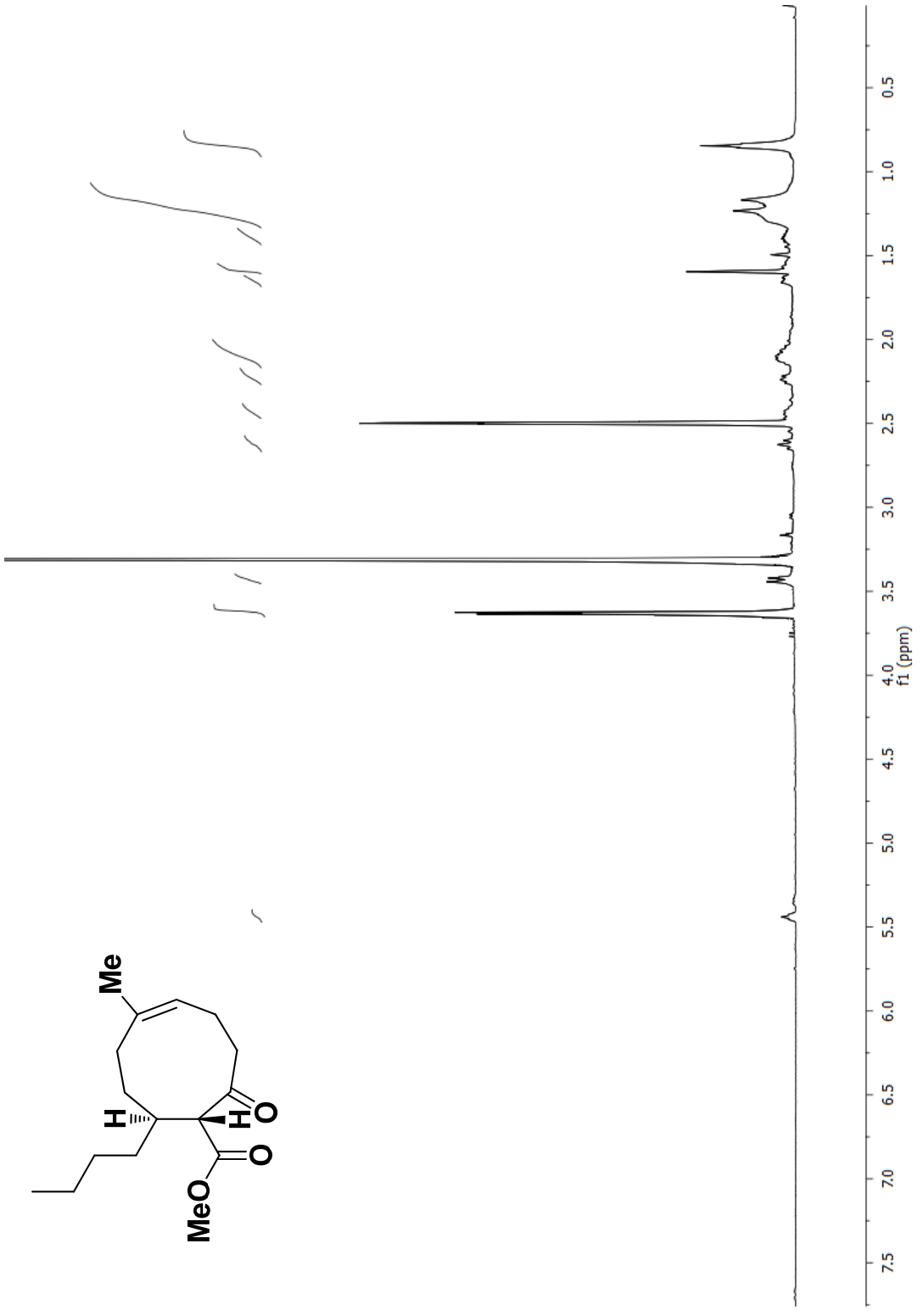
Me
H
H
O
O
MeO
7.5
7.0
6.5
6.0
5.5
5.0
4.5
4.0
3.5
3.0
2.5
2.0
1.5
1.0
0.5
f1 (ppm)

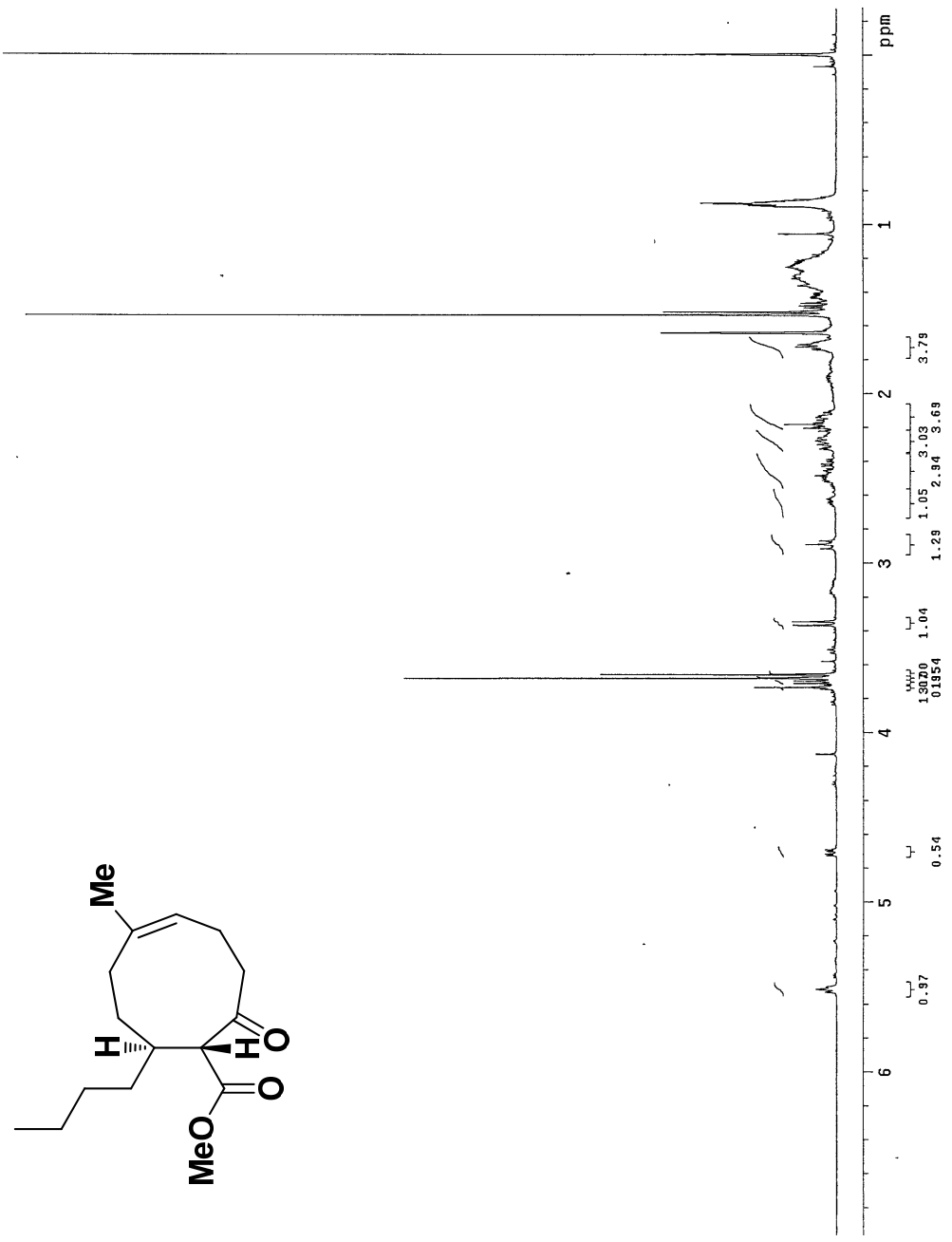
Me
H
H
O
O
MeO
ppm
1
2
3
4
5
6
0.97
0.54
13020
01954
1.04
1.29
1.05
3.03
2.94
3.69
3.79

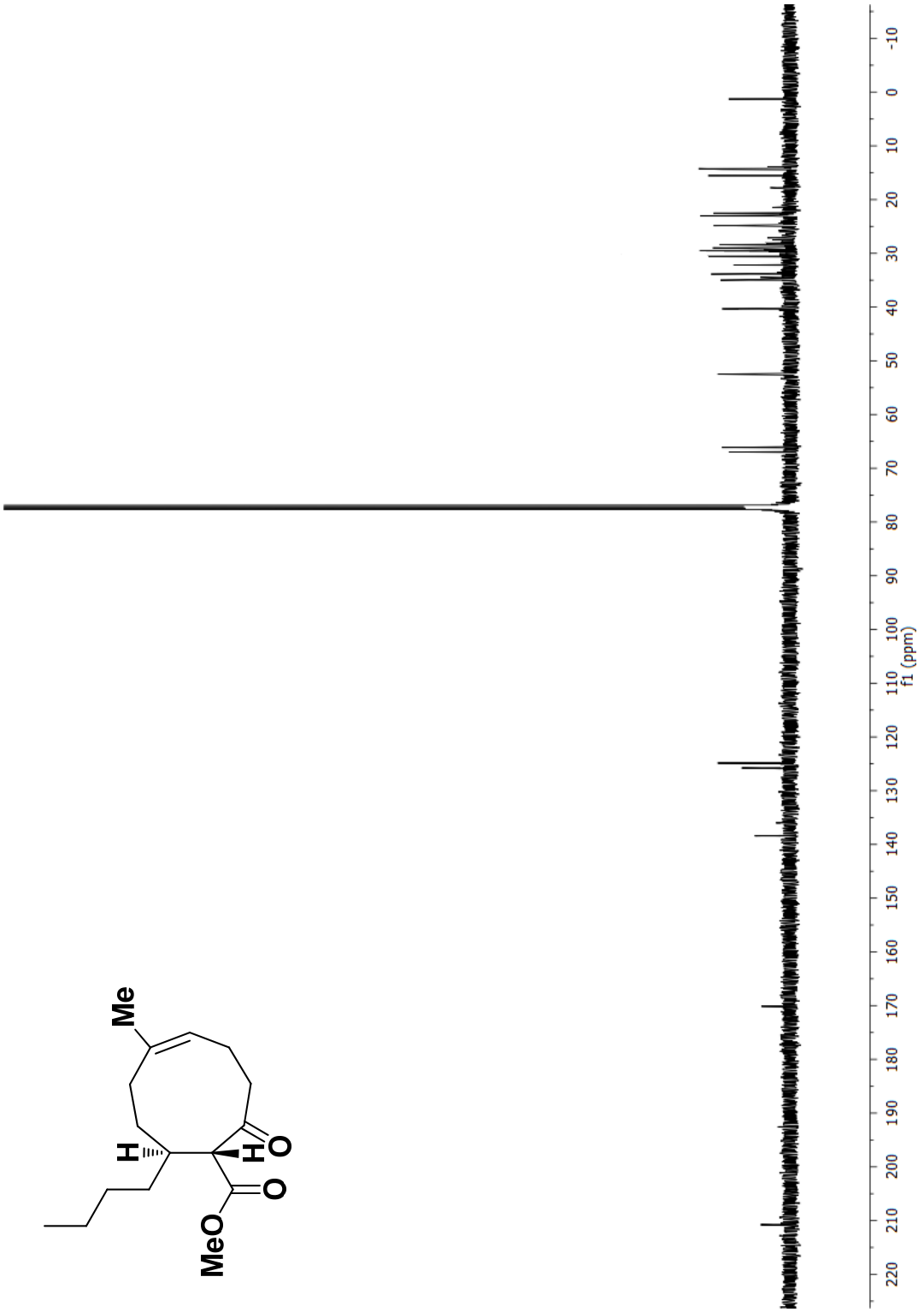
Me
H
H
O
O
MeO
f1 (ppm)

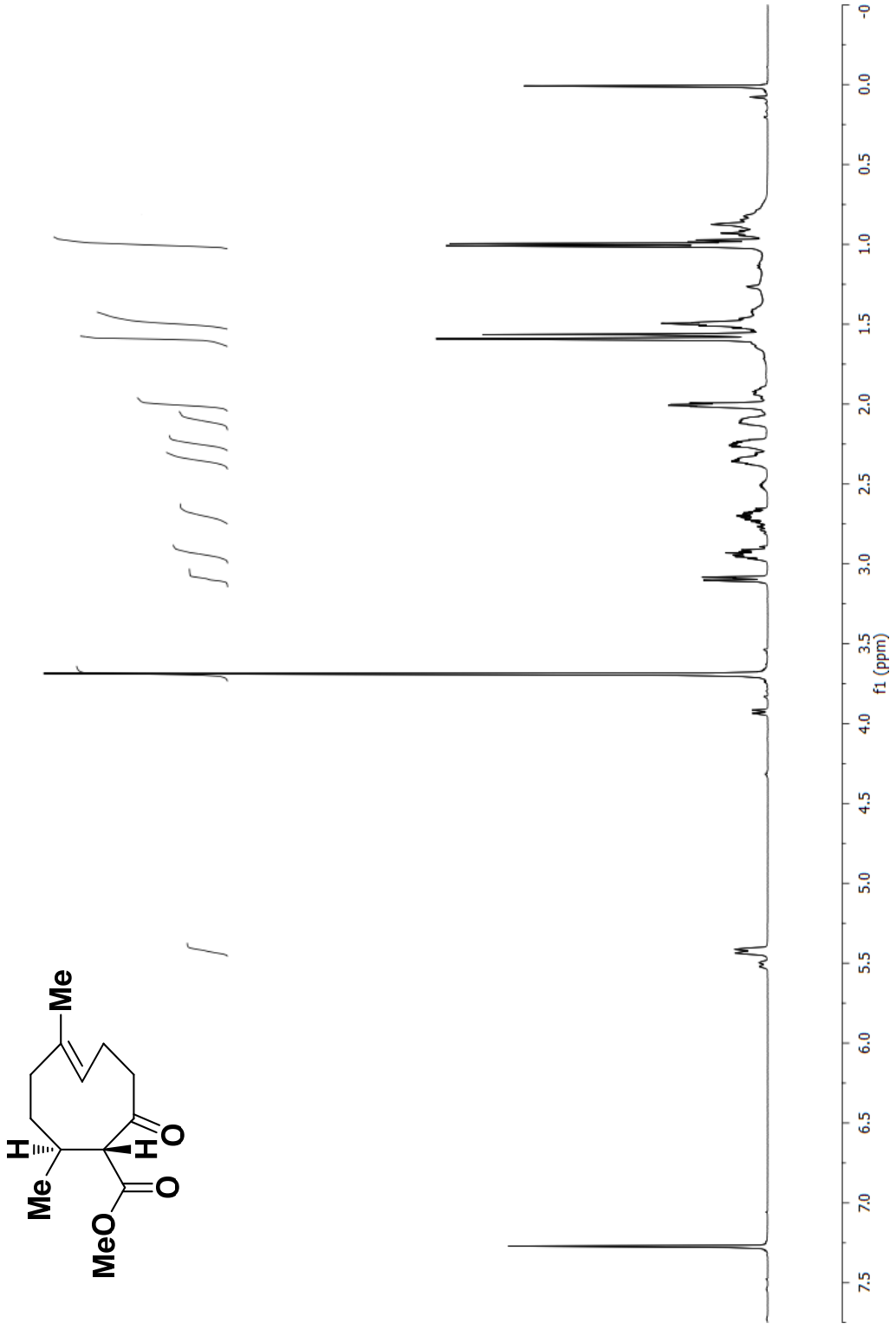
Me
H
Me
MeO
O
H
O
f1 (ppm)

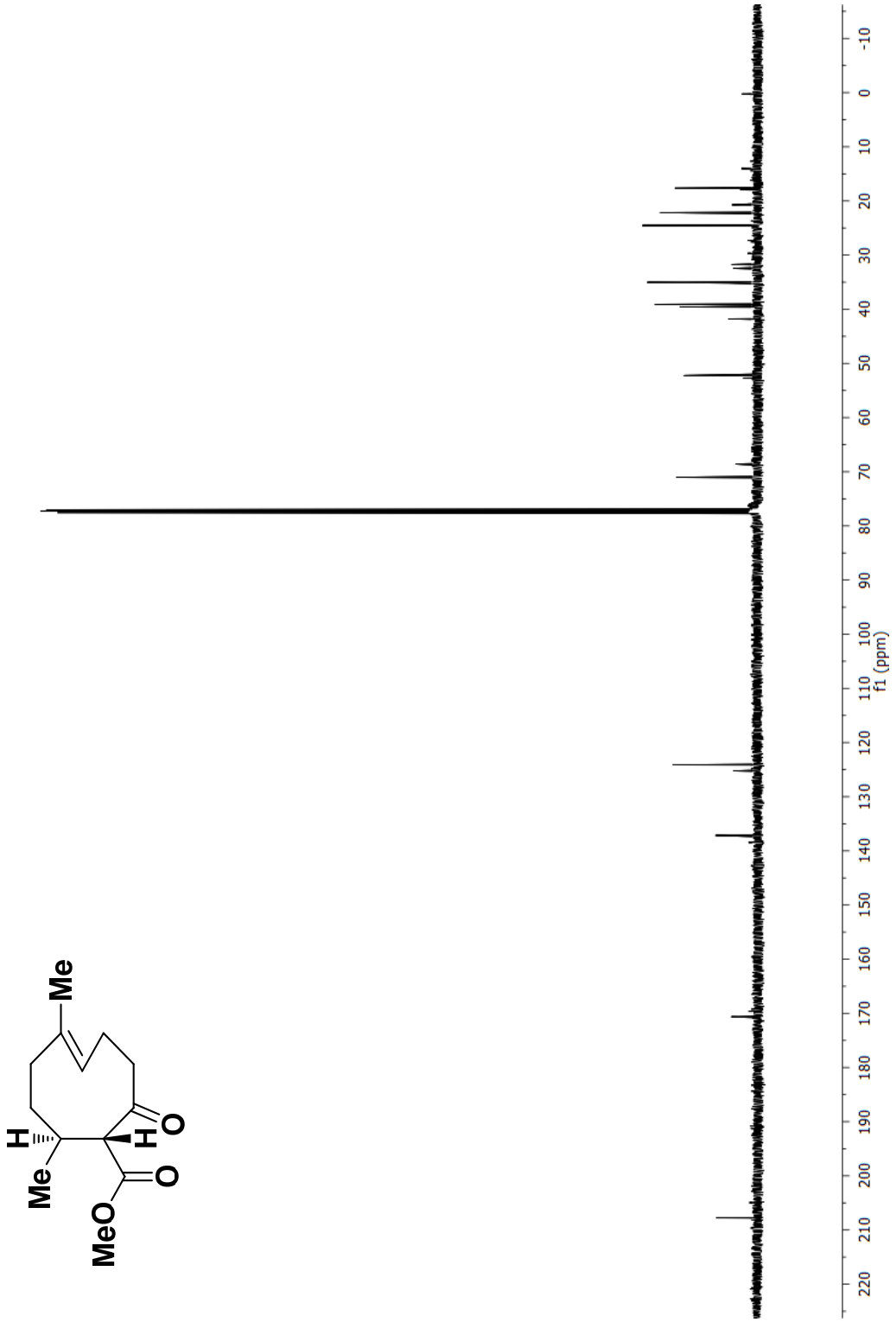
Me
H
Me
MeO
O
H
O
f1 (ppm)

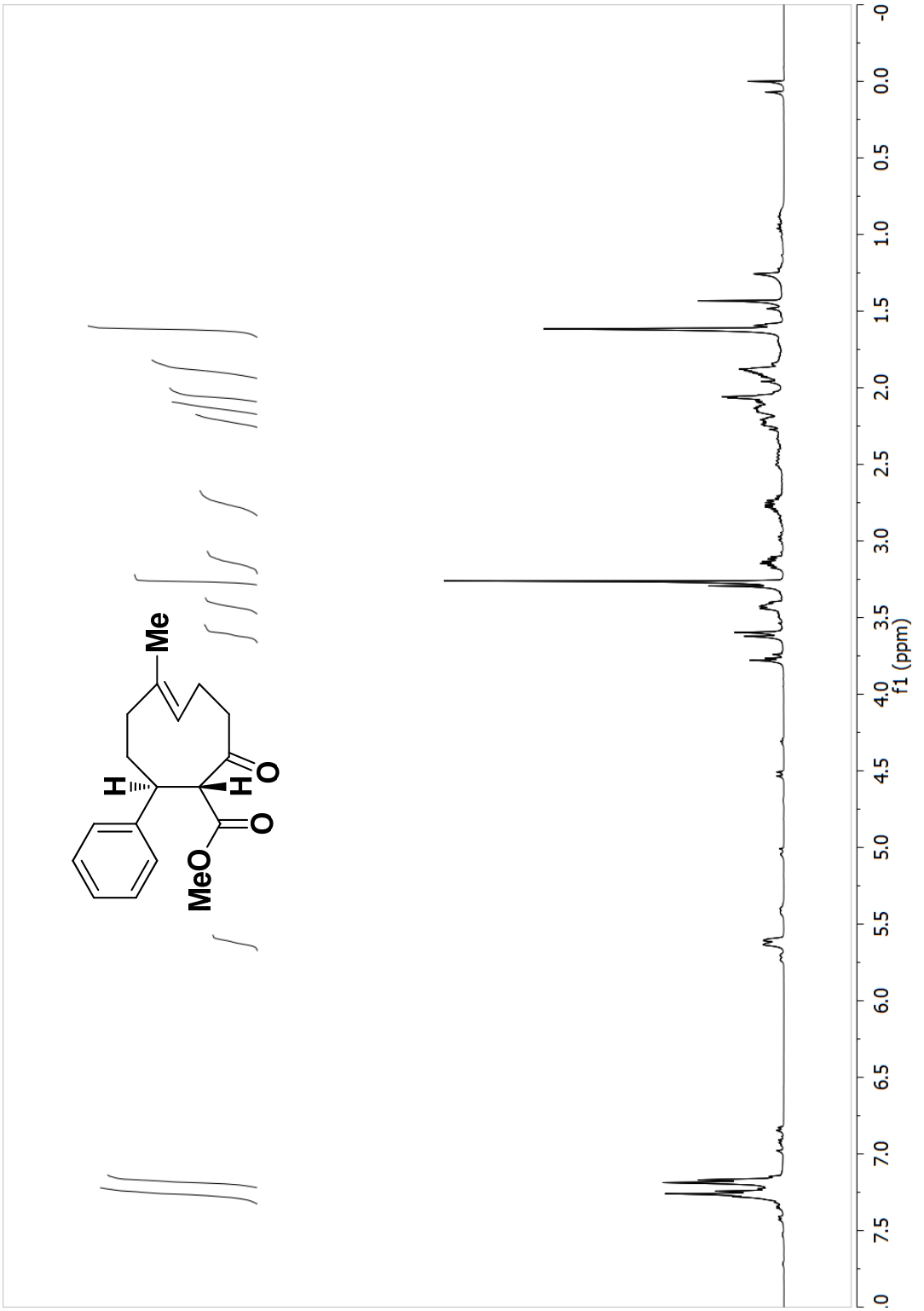
Me
H
H
O
O
MeO
f1 (ppm)

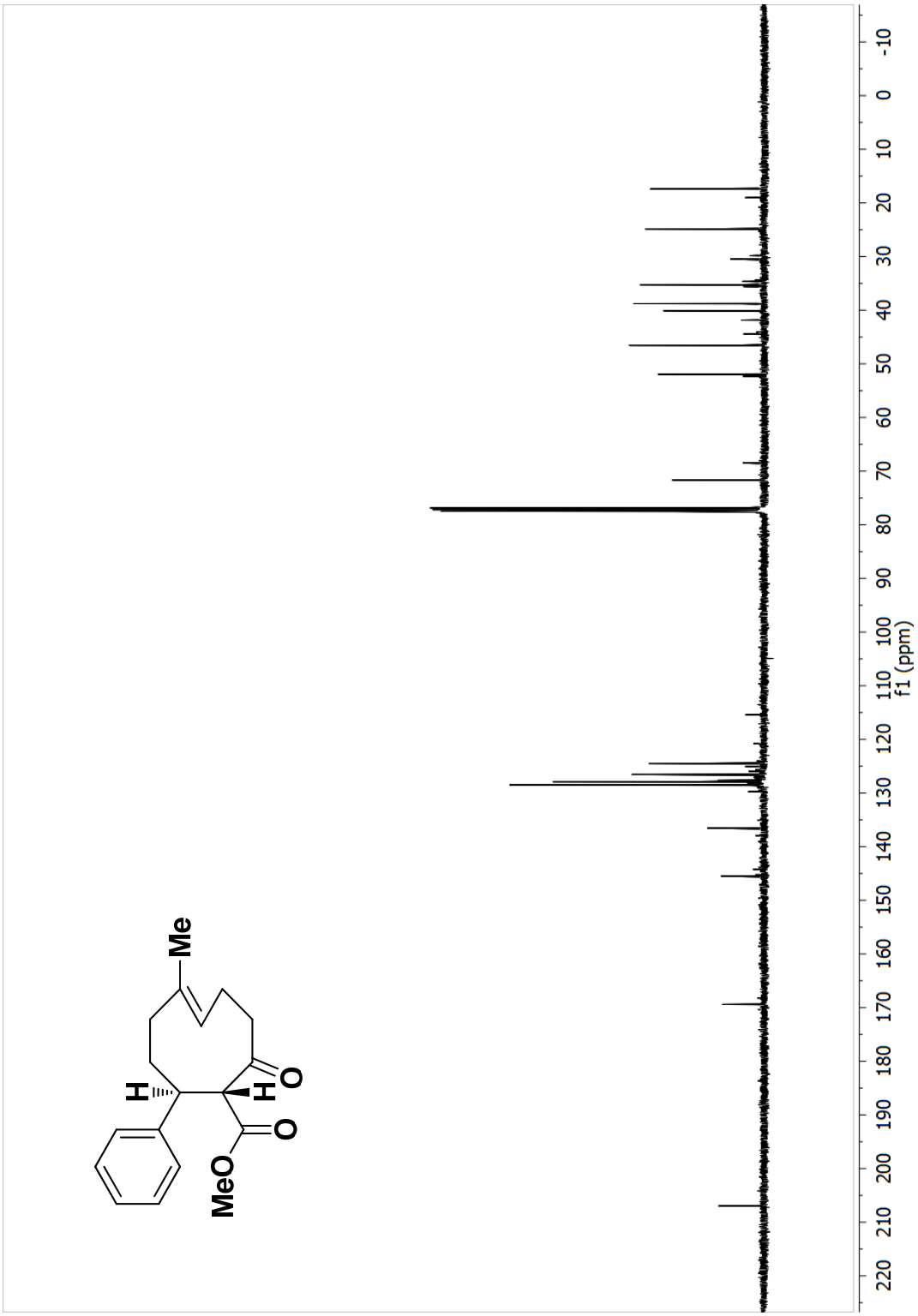
Me
H
H
O
O
MeO
-10
0
10
20
30
40
50
60
70
80
90
100
110
120
130
140
150
160
170
180
190
200
210
220
f1 (ppm)

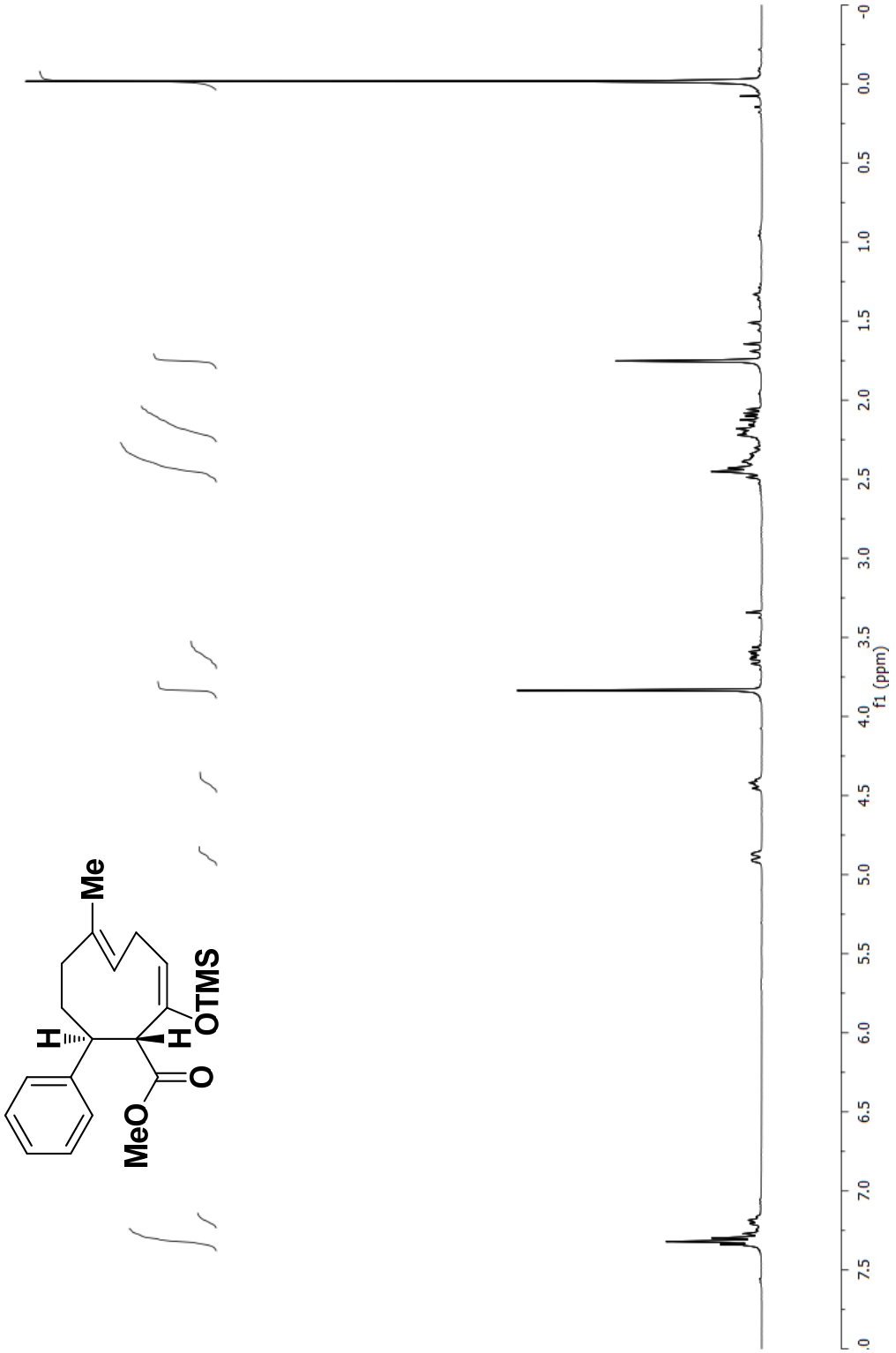
Me
H
H
OTMS
O
MeO
f1 (ppm)

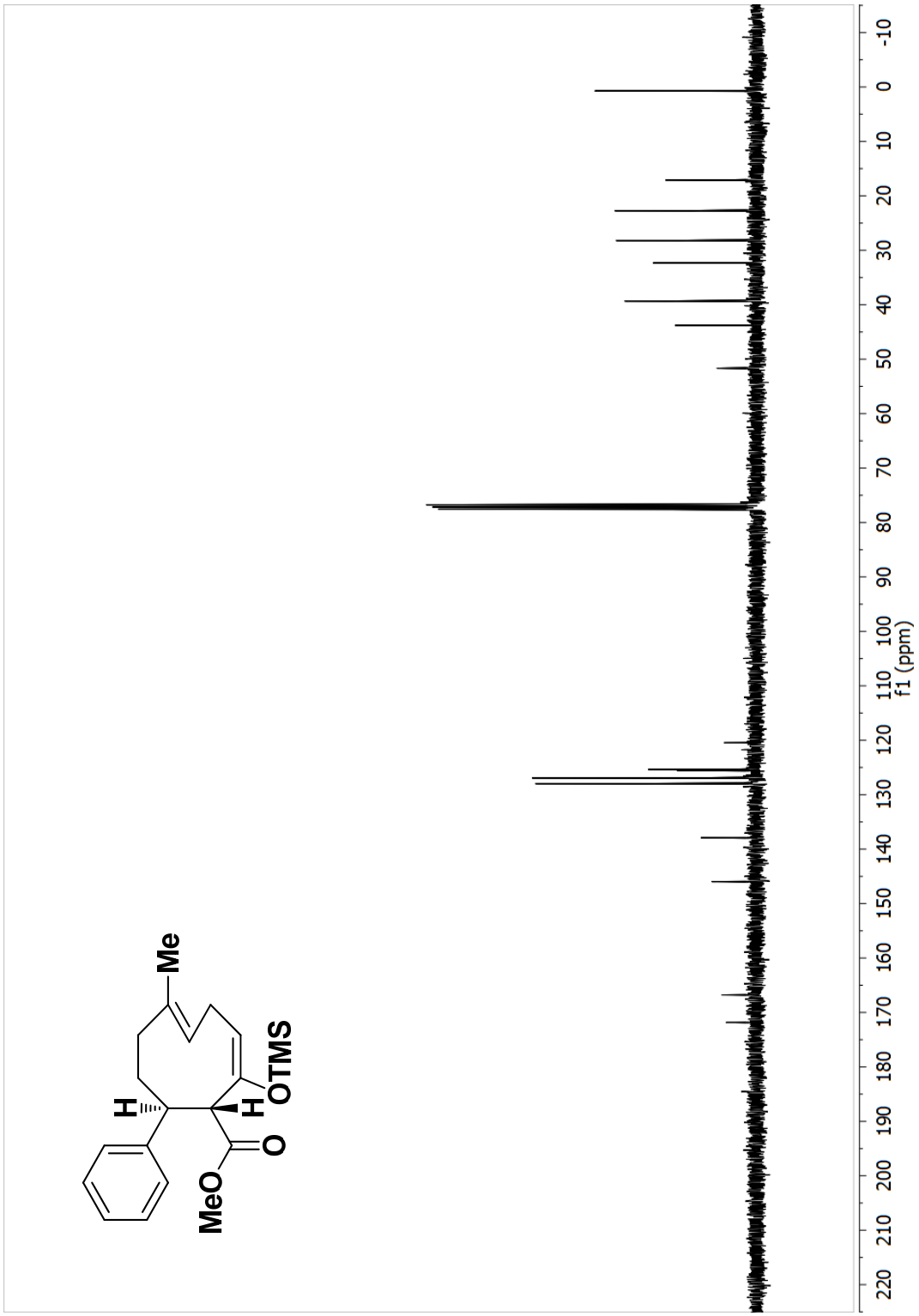
Me
H
H
OTMS
O
MeO
-10
0
10
20
30
40
50
60
70
80
90
100
110
120
130
140
150
160
170
180
190
200
210
220
f1 (ppm)

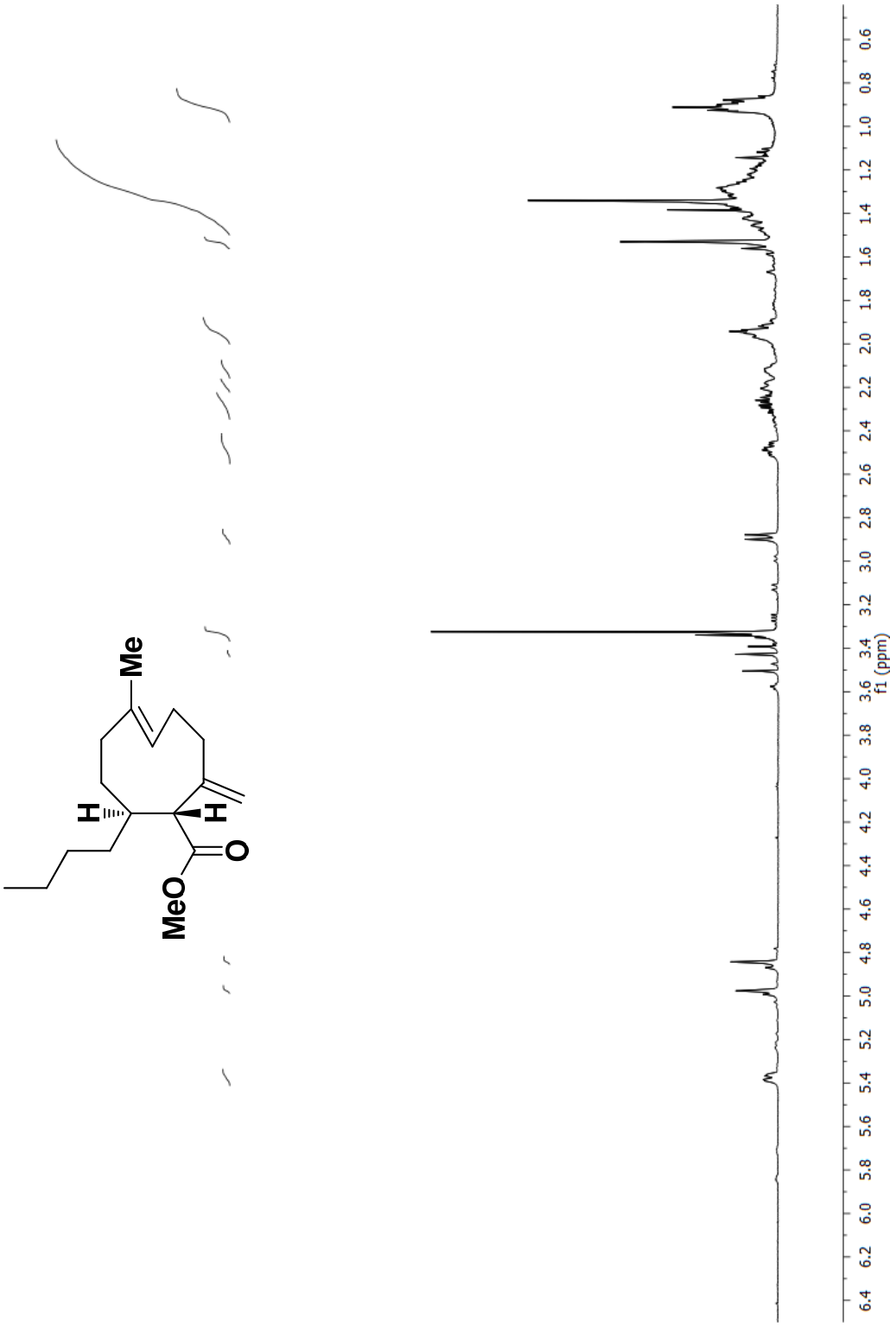
Me
H
H
O
MeO
6.4
6.2
6.0
5.8
5.6
5.4
5.2
5.0
4.8
4.6
4.4
4.2
4.0
3.8
3.6
3.4
3.2
3.0
2.8
2.6
2.4
2.2
2.0
1.8
1.6
1.4
1.2
1.0
0.8
0.6
f1 (ppm)

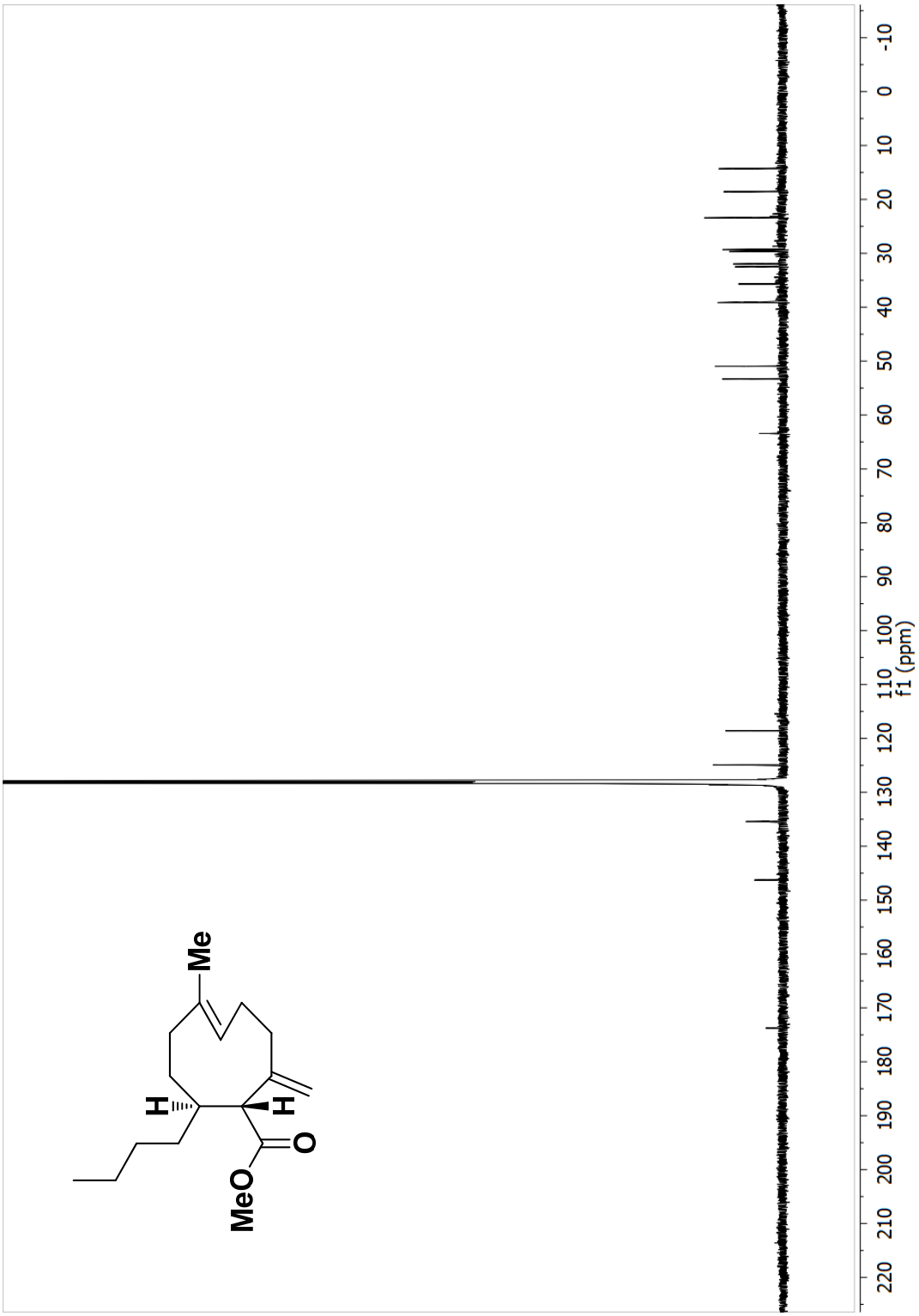
Me
H
H
O
MeO
220 210 200 190 180 170 160 150 140 130 120 110 100 90 80 70 60 50 40 30 20 10 0 -10
f1 (ppm)

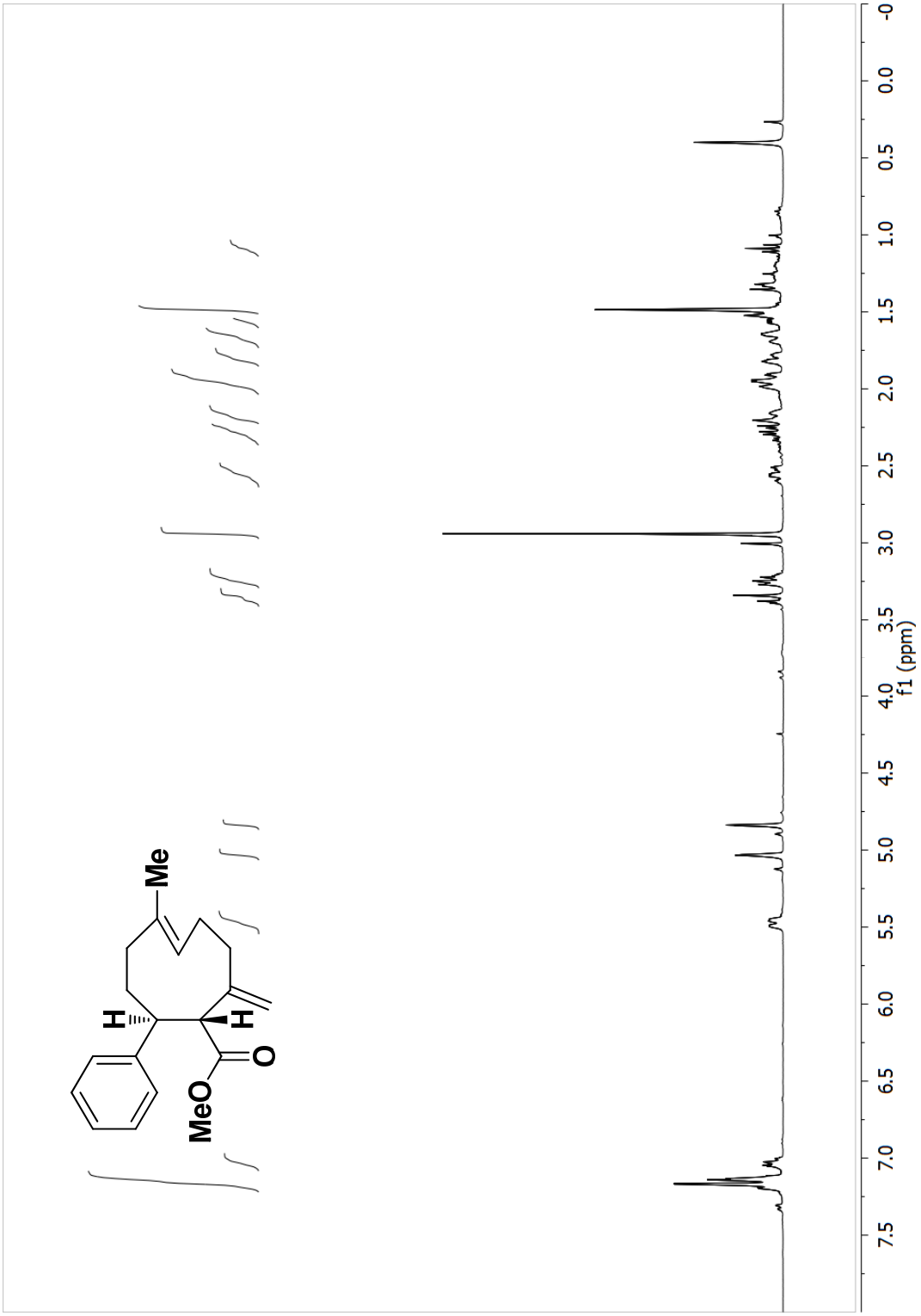
Me
H
H
O
MeO
7.5
7.0
6.5
6.0
5.5
5.0
4.5
4.0
3.5
3.0
2.5
2.0
1.5
1.0
0.5
0.0
-0
f1 (ppm)

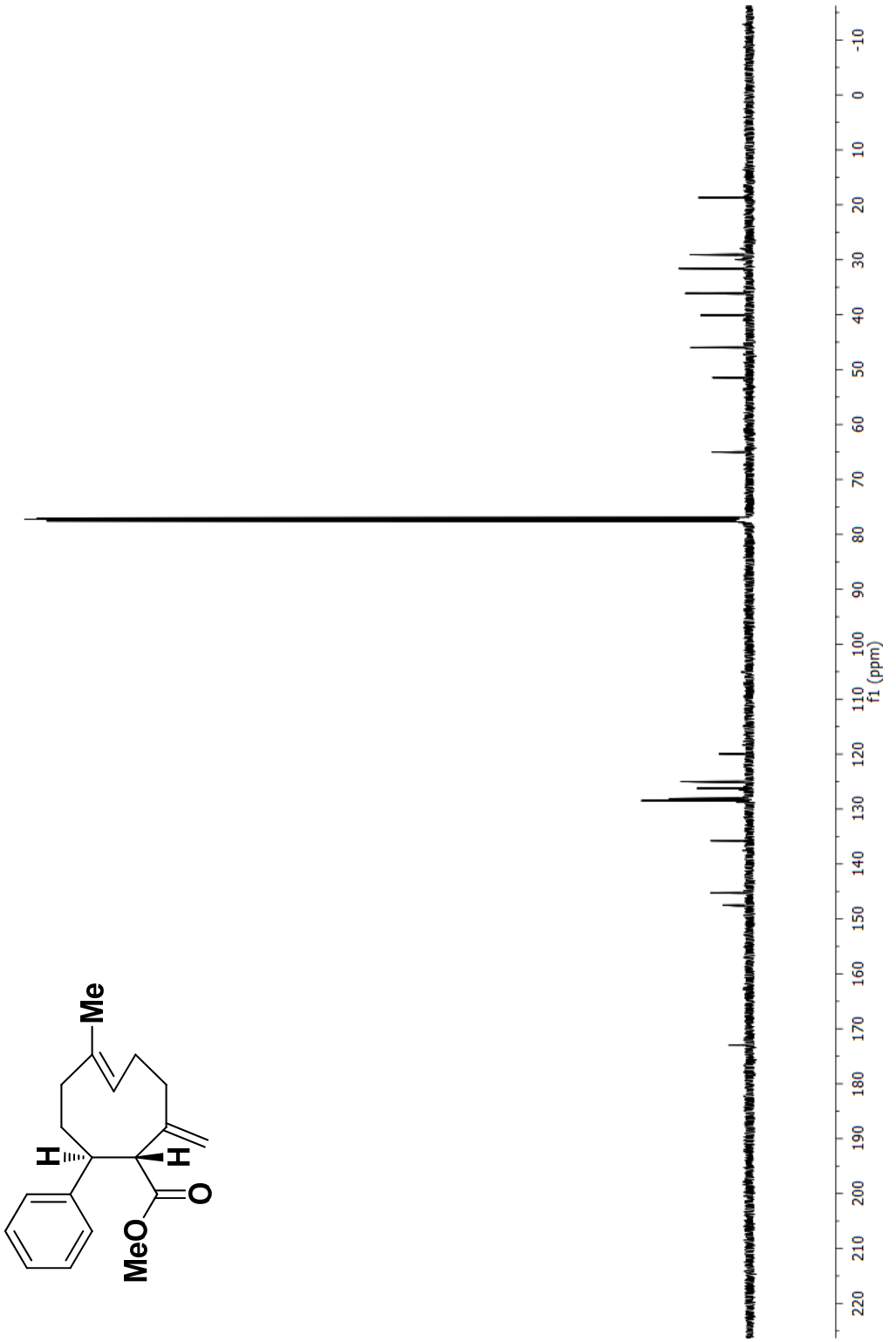
Me
H
H
O
MeO
f1 (ppm)

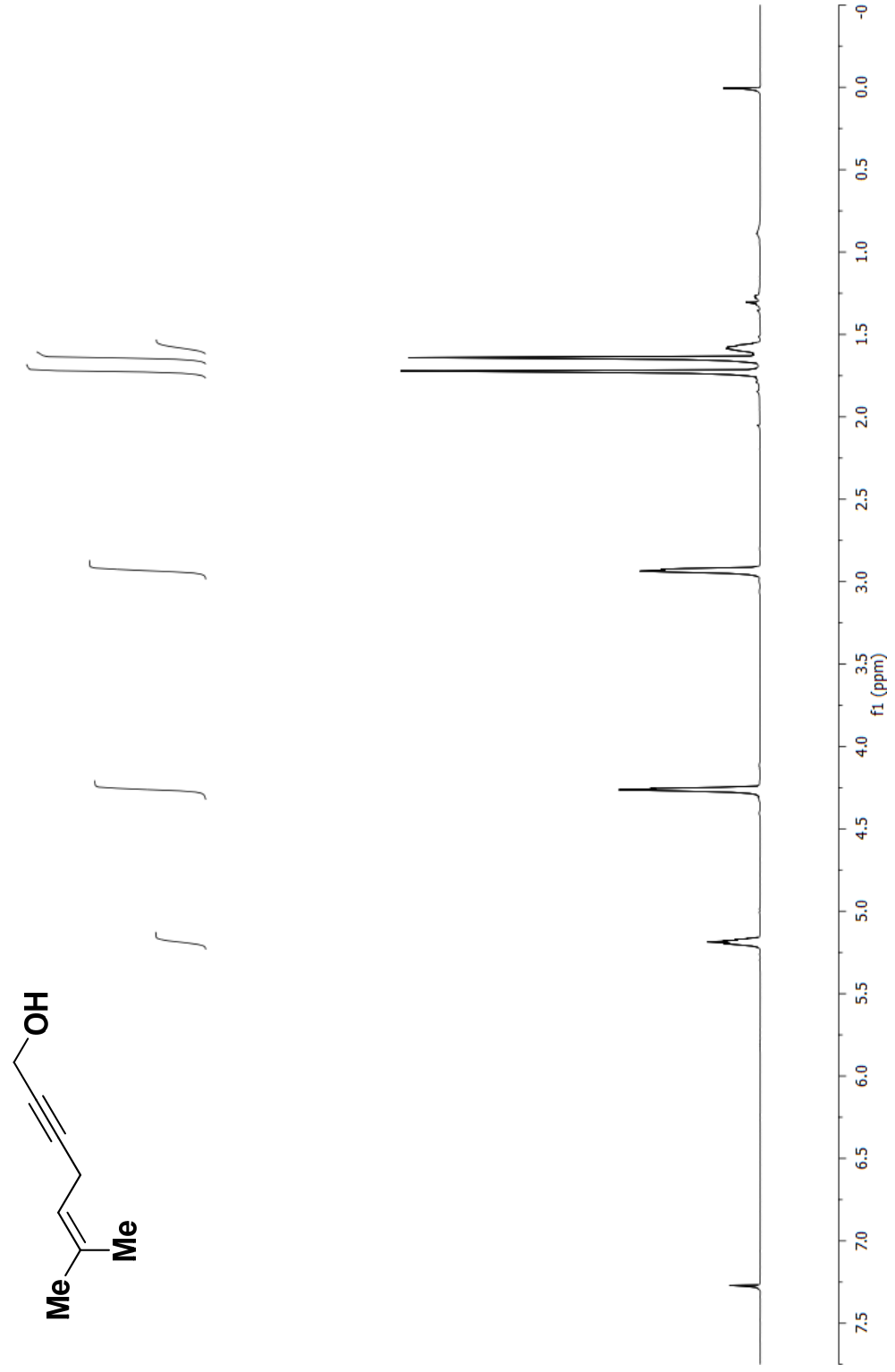
OH
Me
Me
f1 (ppm)

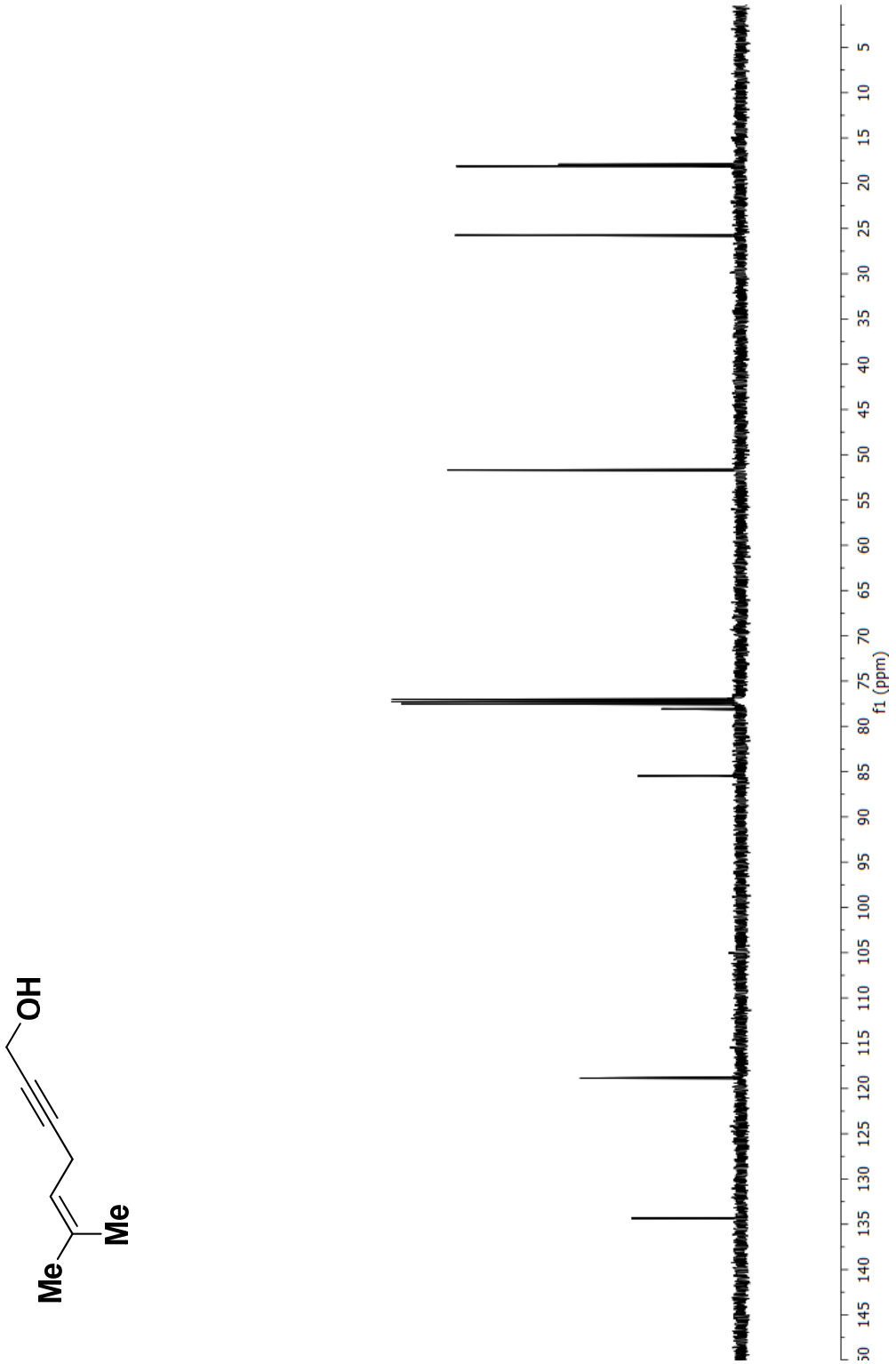
OH
Me
Me
f1 (ppm)

^{1}H NMR spectrum in $CDCl_3$

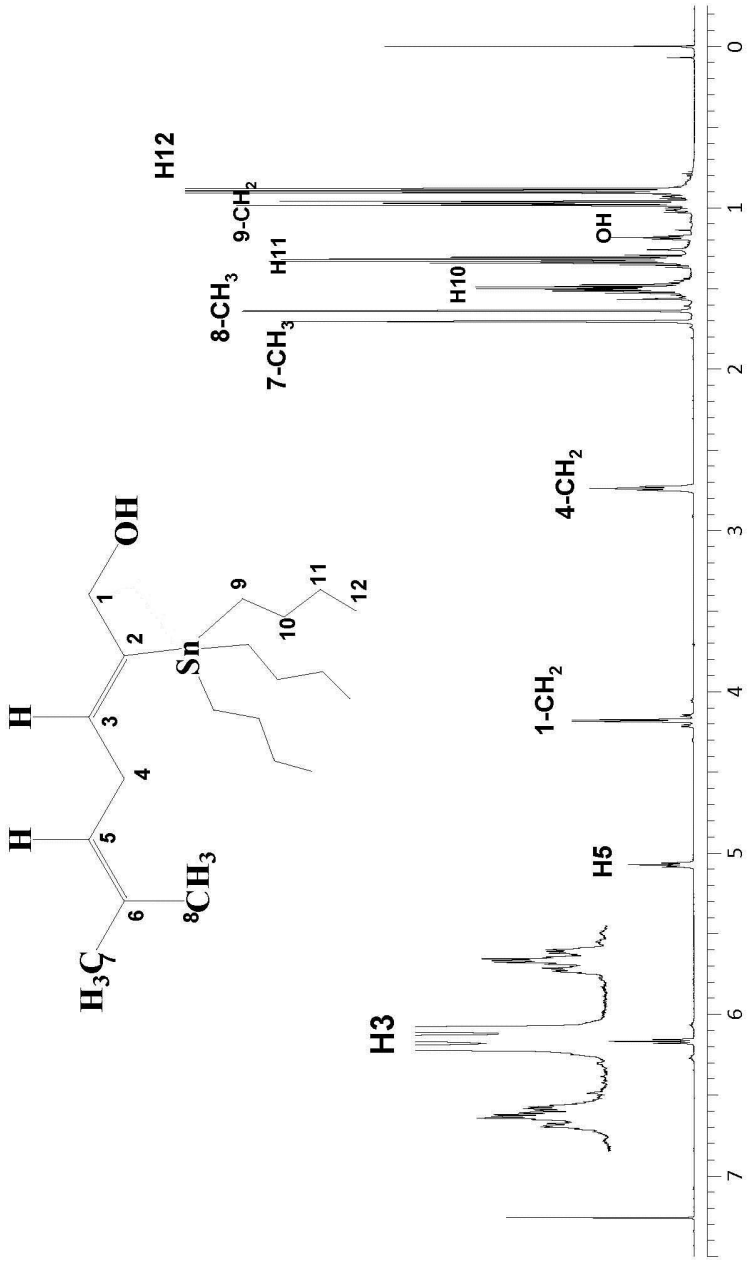

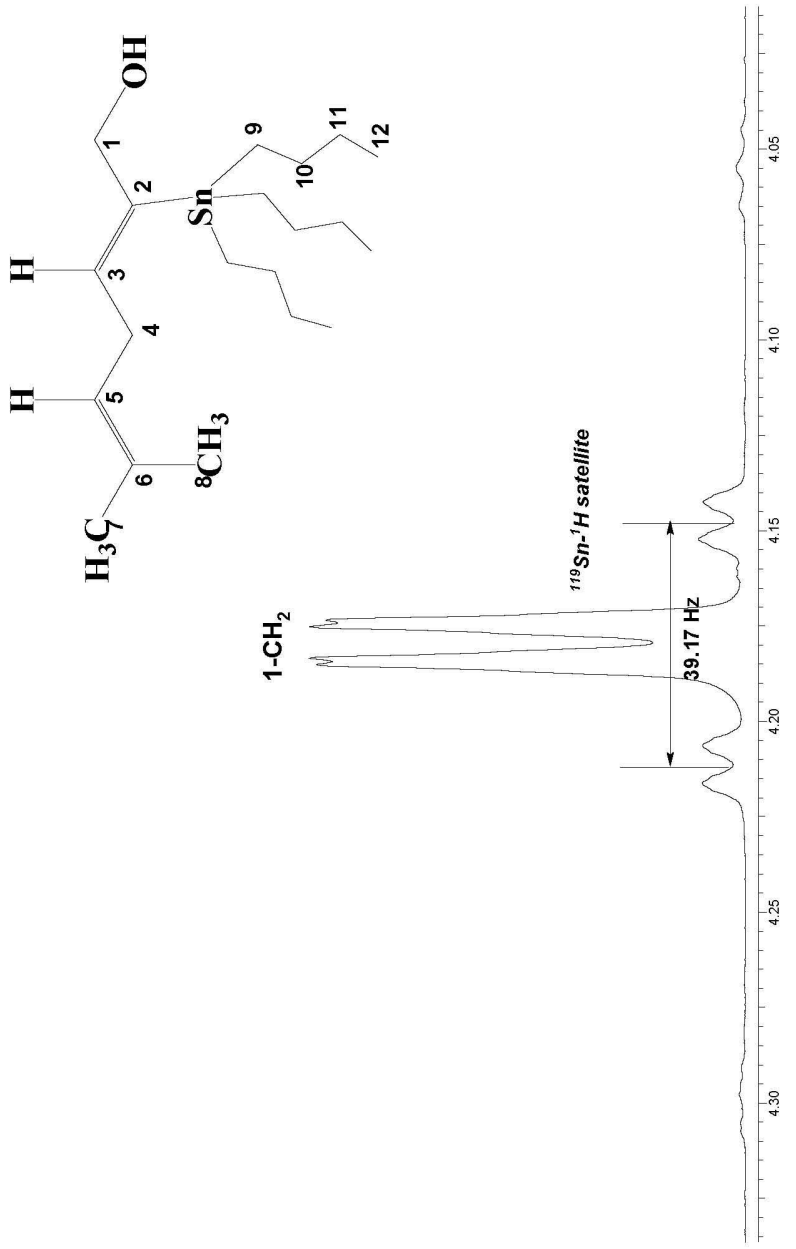
OH
1
2
Sn
9
10
11
12
H
3
4
H
5
6
$^{8}CH_3$
H_3C
7
1-CH_2
^{119}Sn-^{1}H satellite
39.17 Hz
4.05
4.10
4.15
4.20
4.25
4.30

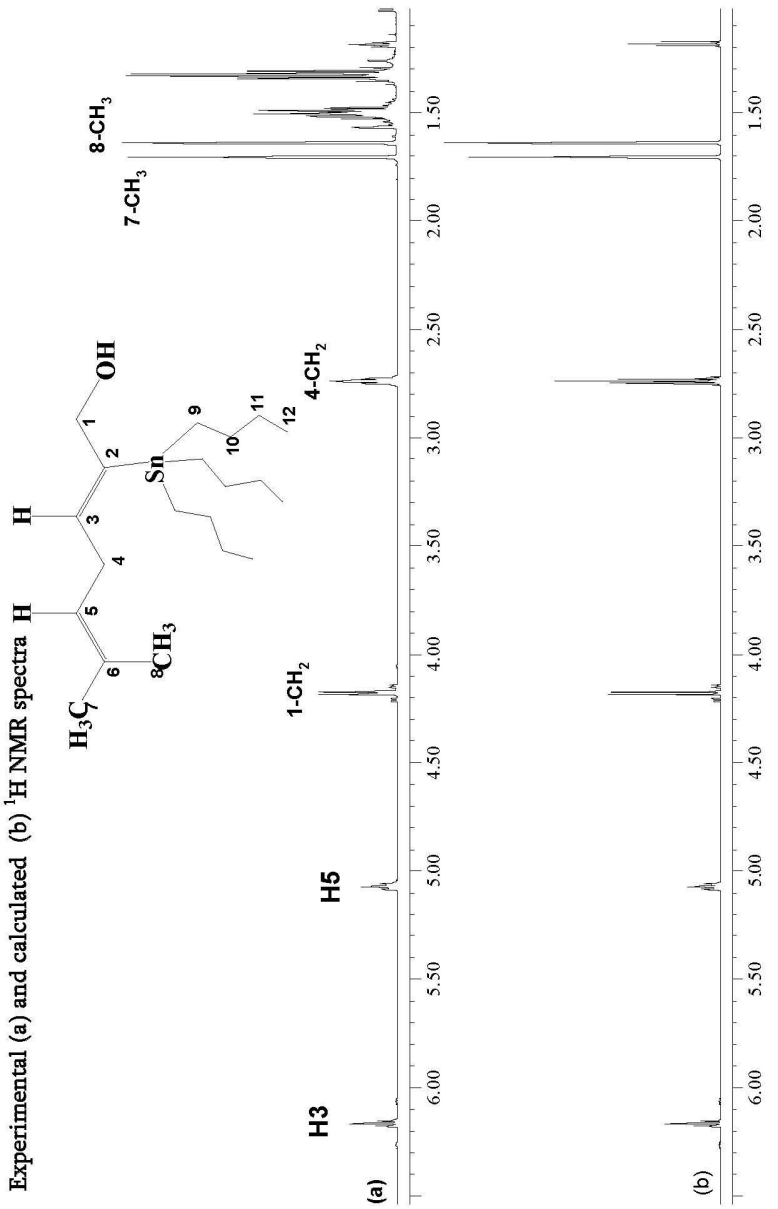
Experimental (a) and calculated (b) ^{1}H NMR spectra
H
H
OH
H_3C
$^8CH_3$
Sn
1
2
3
4
5
6
9
10
11
12
8-CH_3
7-CH_3
4-CH_2
1-CH_2
H5
H3
(a)
(b)
6.00
5.50
5.00
4.50
4.00
3.50
3.00
2.50
2.00
1.50

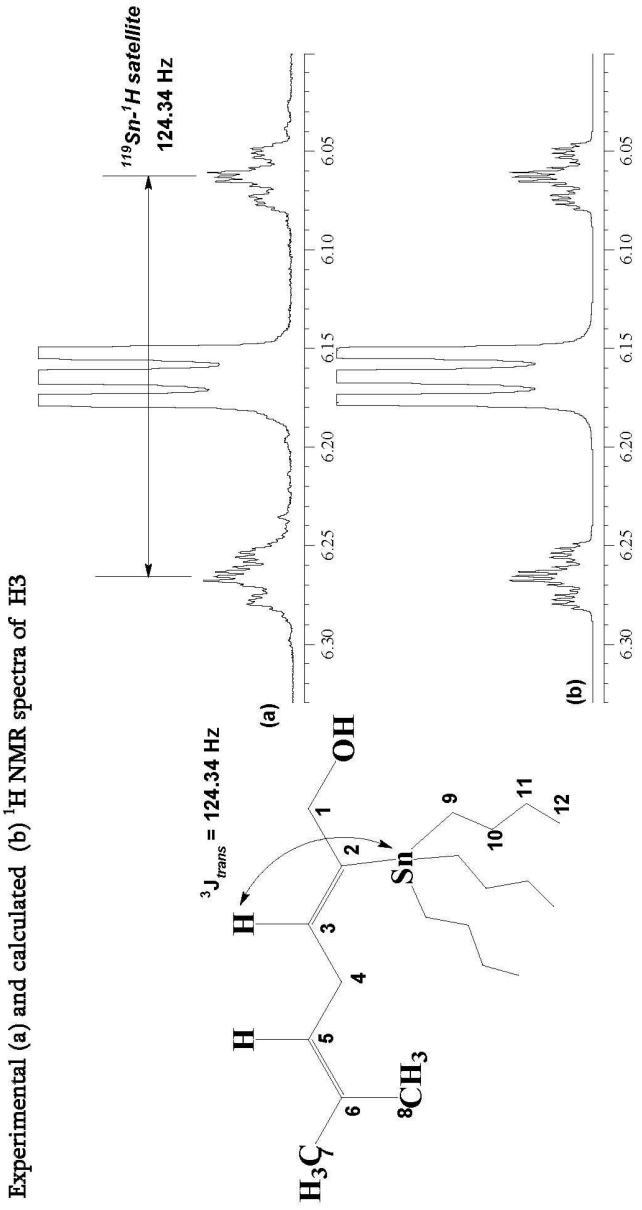
Experimental (a) and calculated (b) ^{1}H NMR spectra of H3
^{119}Sn-^{1}H satellite
124.34 Hz
(a)
(b)
6.30
6.25
6.20
6.15
6.10
6.05
$^3J_{trans}$ = 124.34 Hz
OH
H
H
Sn
H_3C
$^8CH_3$
1
2
3
4
5
6
9
10
11
12

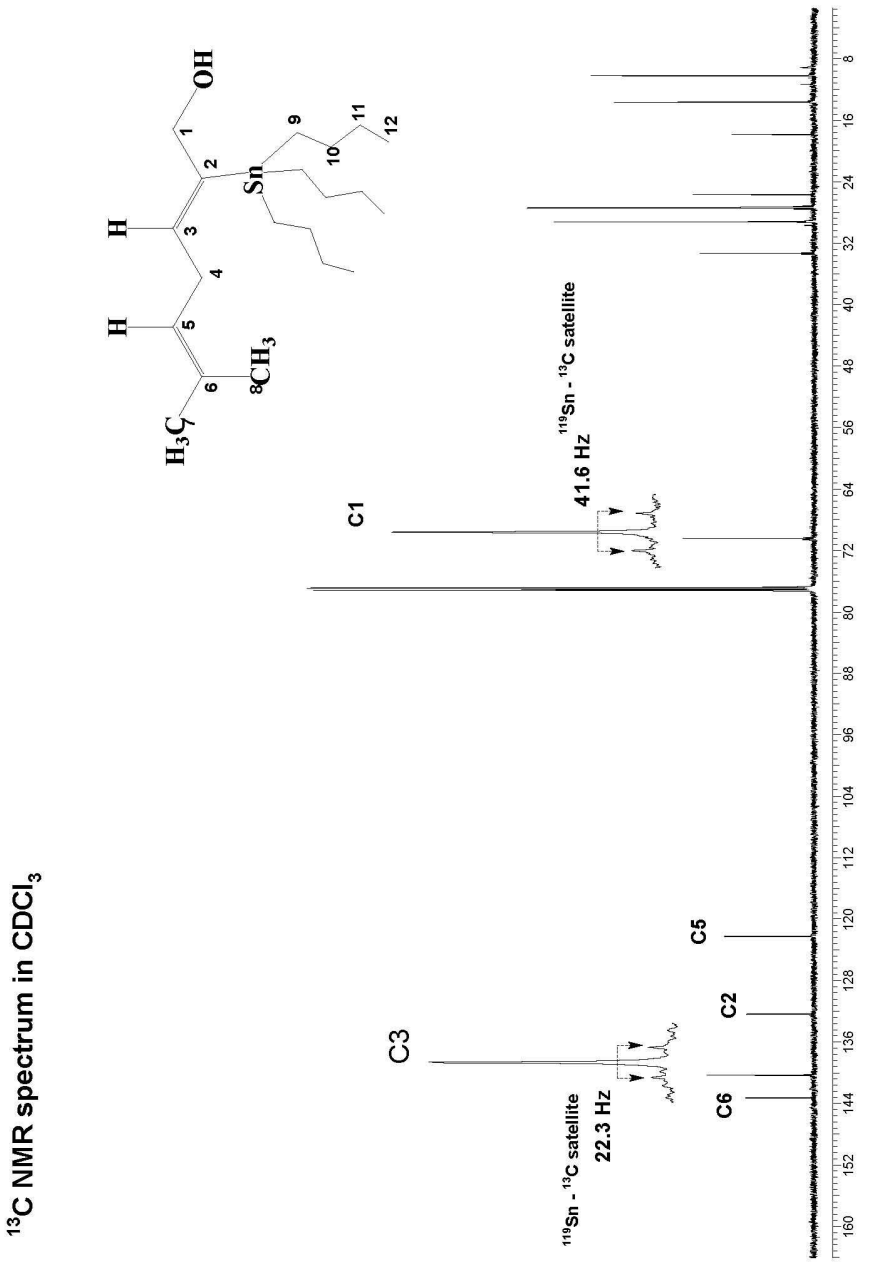
^{13}C NMR spectrum in $CDCl_3$
OH
H
H
Sn
H_3C
CH_3
C1
C2
C3
C5
C6
^{119}Sn - ^{13}C satellite
41.6 Hz
^{119}Sn - ^{13}C satellite
22.3 Hz

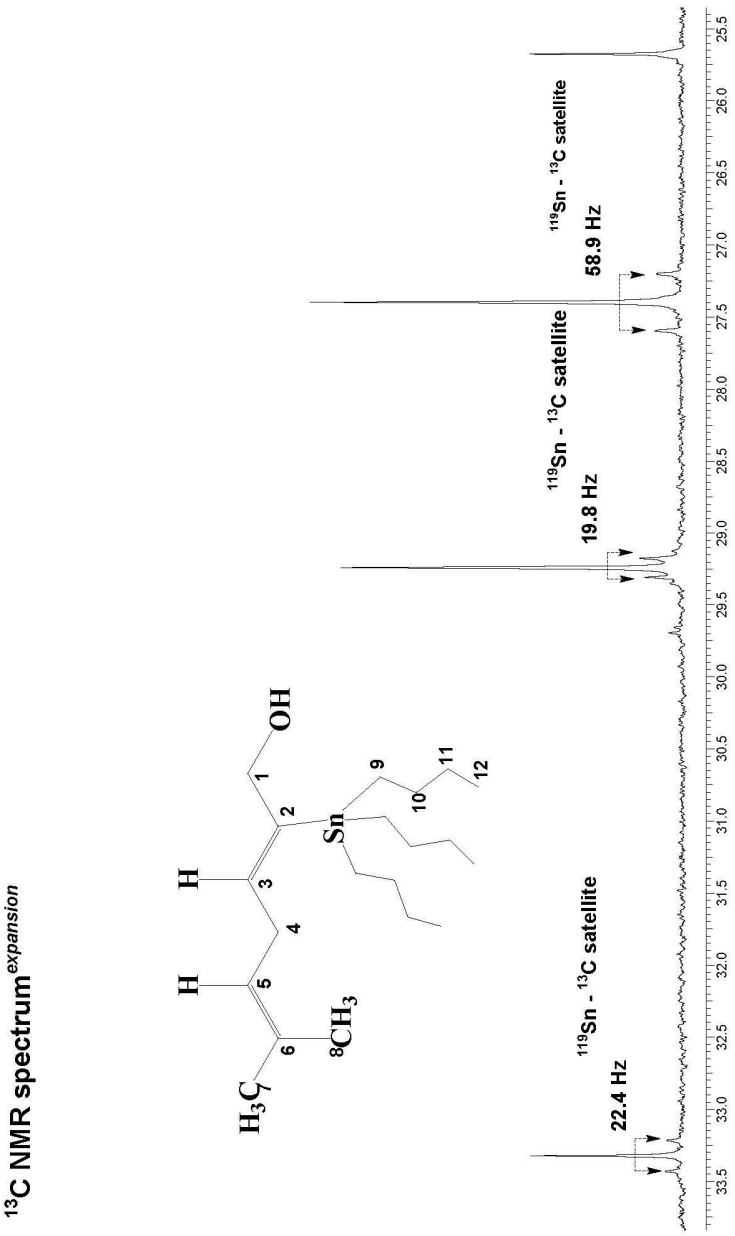
^{13}C NMR spectrum *expansion*
OH
H
H
Sn
H_3C
$^8CH_3$
1
2
3
4
5
6
9
10
11
12
^{119}Sn - ^{13}C satellite
22.4 Hz
^{119}Sn - ^{13}C satellite
19.8 Hz
^{119}Sn - ^{13}C satellite
58.9 Hz
33.5
33.0
32.5
32.0
31.5
31.0
30.5
30.0
29.5
29.0
28.5
28.0
27.5
27.0
26.5
26.0
25.5

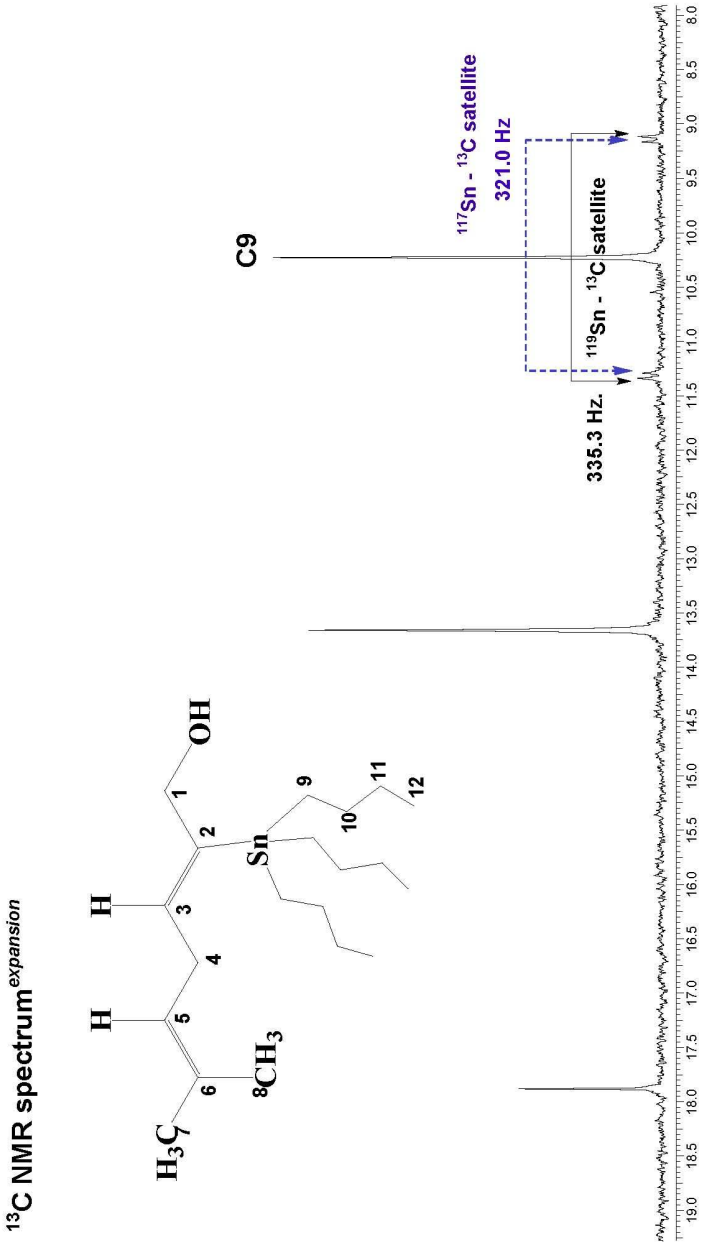
^{13}C NMR spectrum^{expansion}
C9
^{117}Sn - ^{13}C satellite
321.0 Hz
^{119}Sn - ^{13}C satellite
335.3 Hz.
OH
H
H
Sn
H_3C
$^{8}CH_3$
1
2
3
4
5
6
9
10
11
12

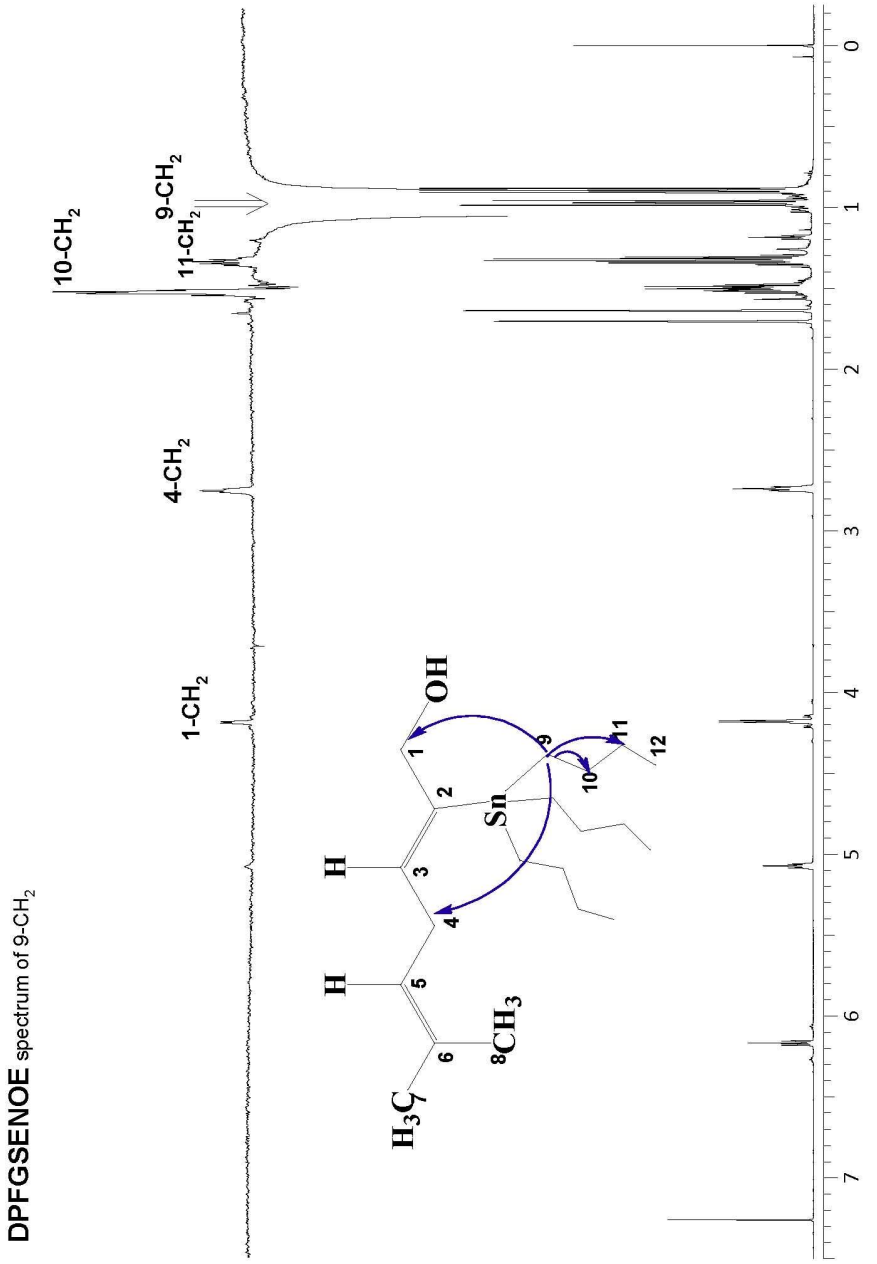
DPFGSENOE spectrum of 9-CH2
10-CH2
9-CH2
11-CH2
4-CH2
1-CH2
OH
H
H
H3C
8CH3
Sn
1
2
3
4
5
6
9
10
11
12
0
1
2
3
4
5
6
7

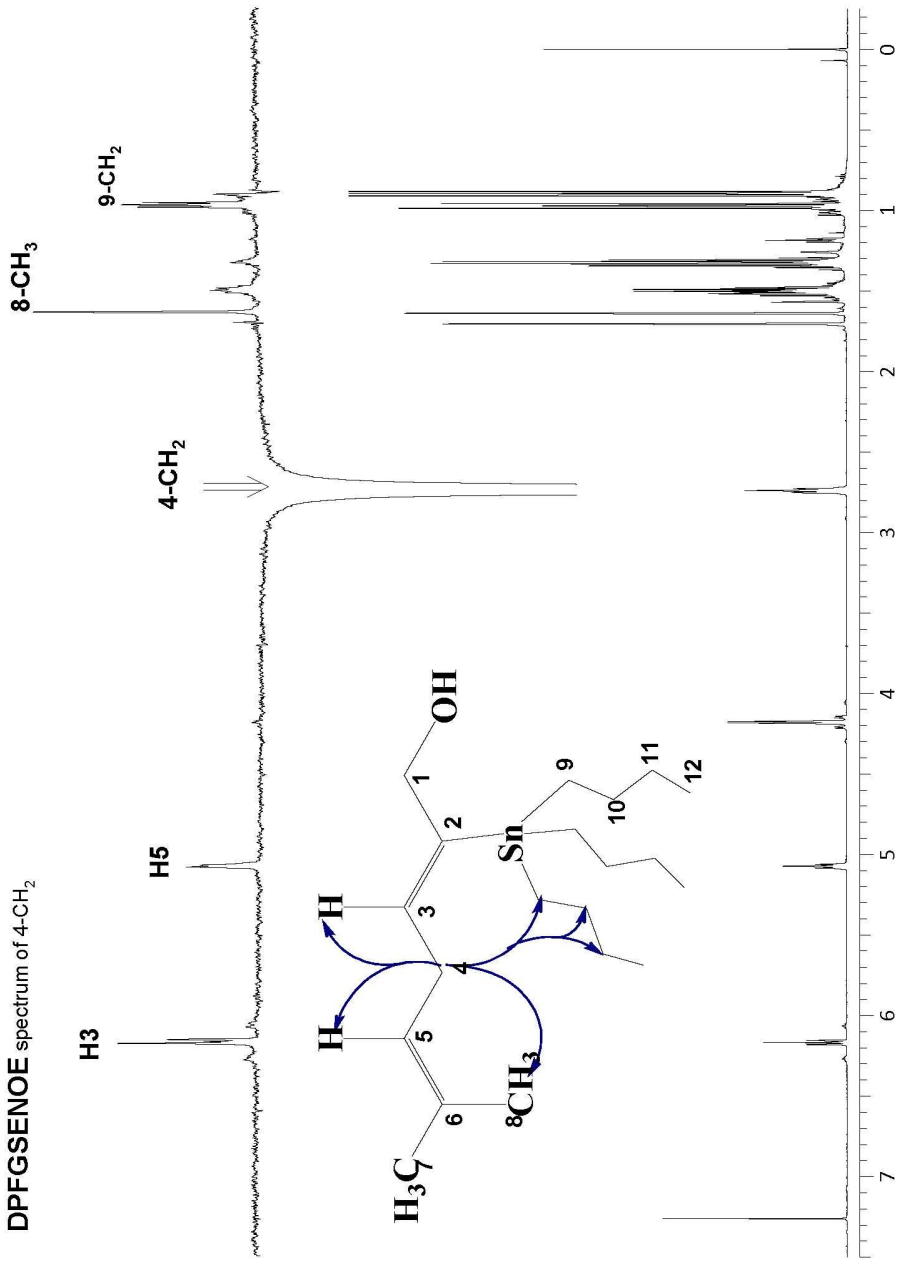
DPFGSENOE spectrum of 4-CH2
H3
H5
4-CH2
8-CH3
9-CH2
OH
Sn
H
H
H3C
8CH3
1
2
3
4
5
6
9
10
11
12
0
1
2
3
4
5
6
7

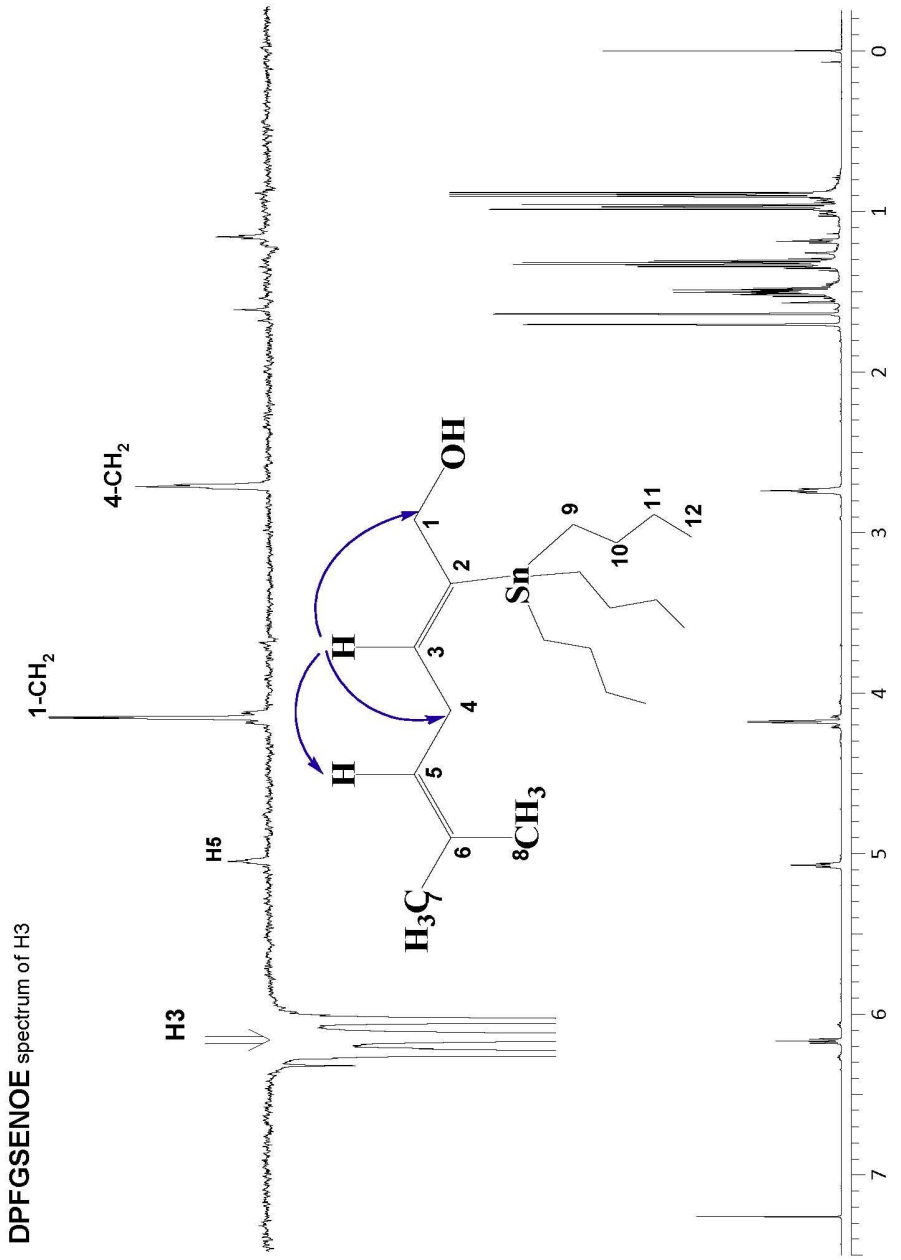
DPFGSENOE spectrum of H3
H3
H5
1-CH2
4-CH2
OH
Sn
H
H
H3C
8CH3
1
2
3
4
5
6
9
10
11
12
0
1
2
3
4
5
6
7

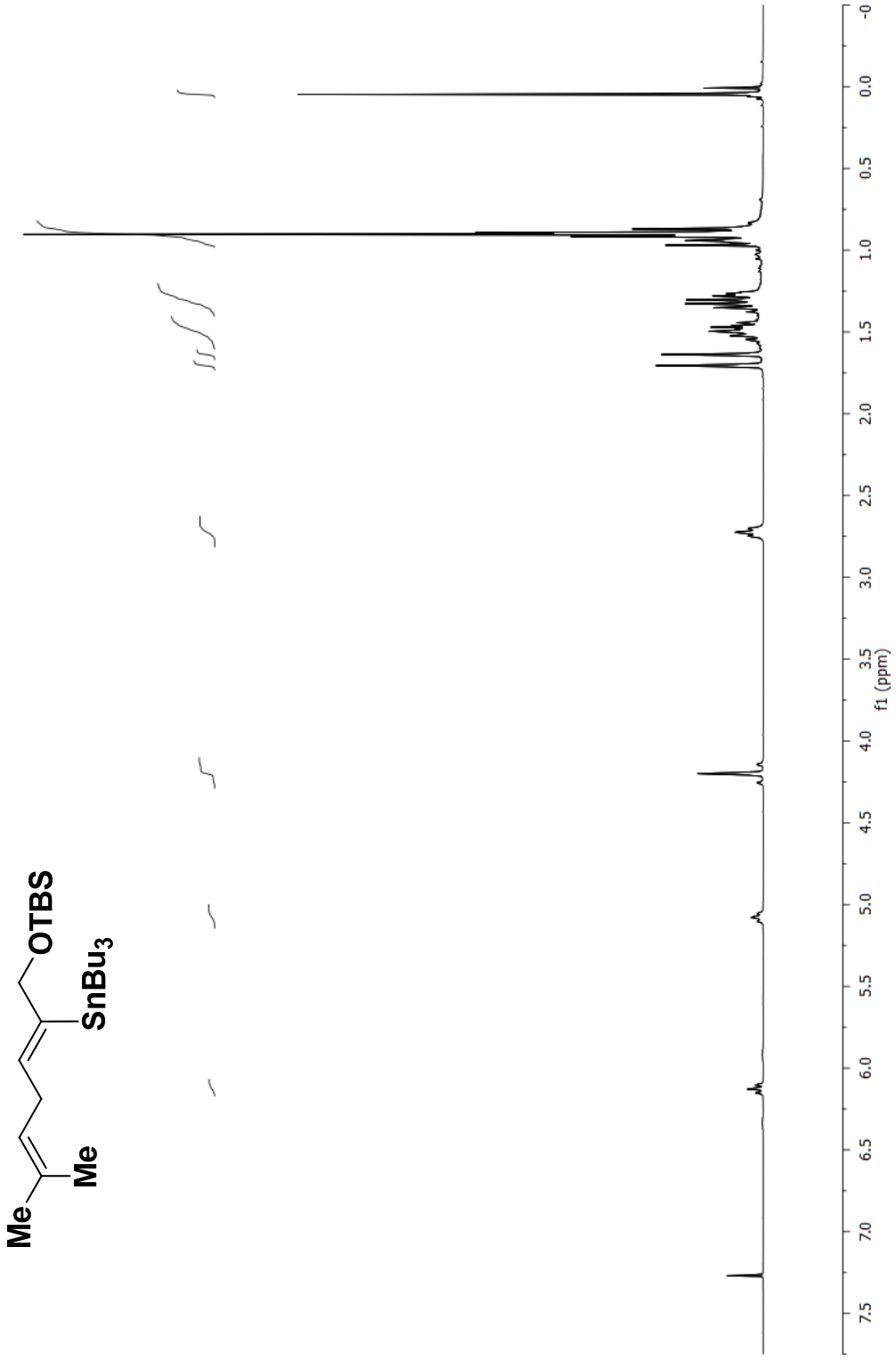
OTBS
SnBu3
Me
Me
f1 (ppm)

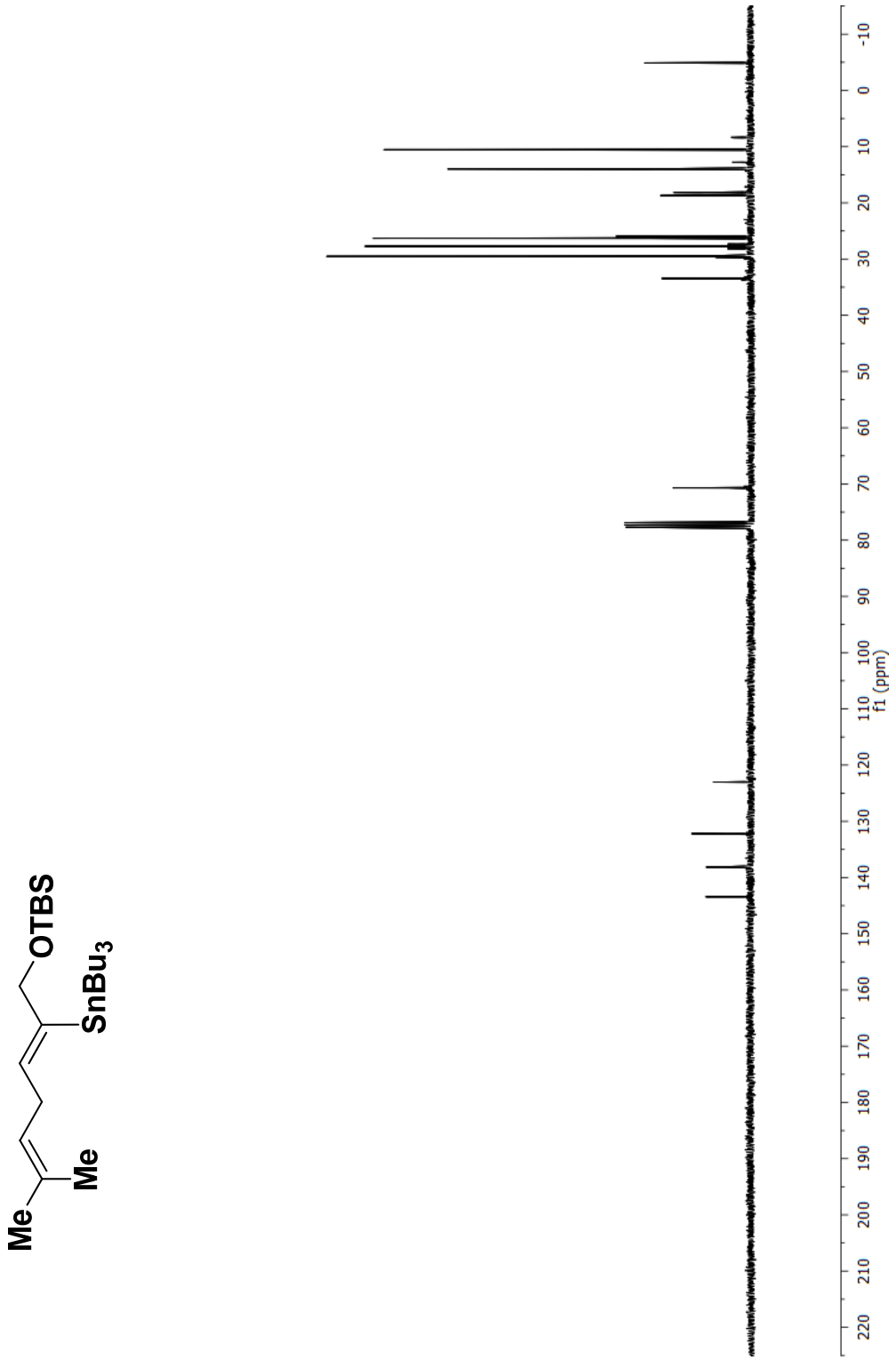
OTBS
SnBu3
Me
Me
f1 (ppm)

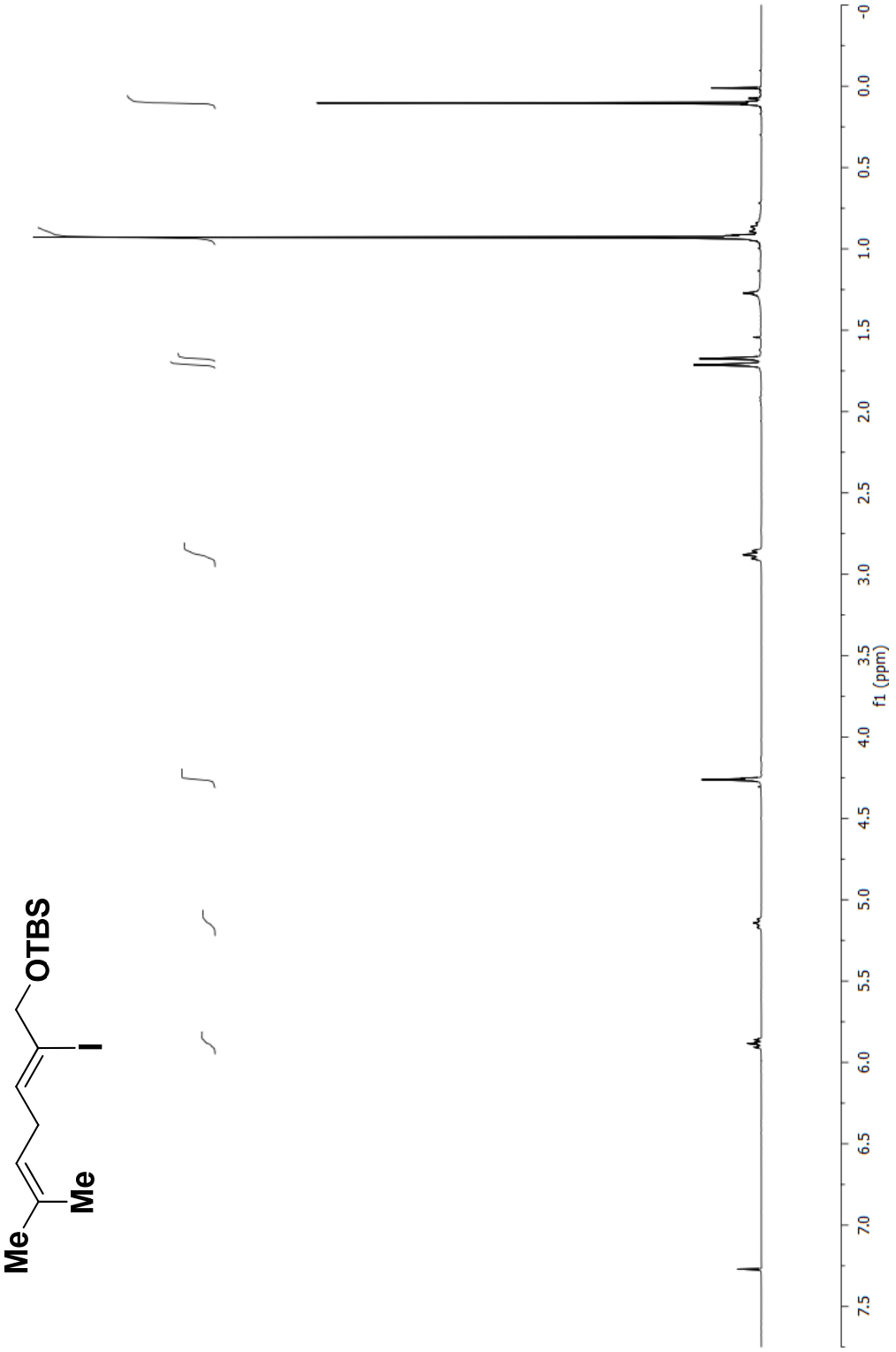
OTBS
I
Me
Me
f1 (ppm)

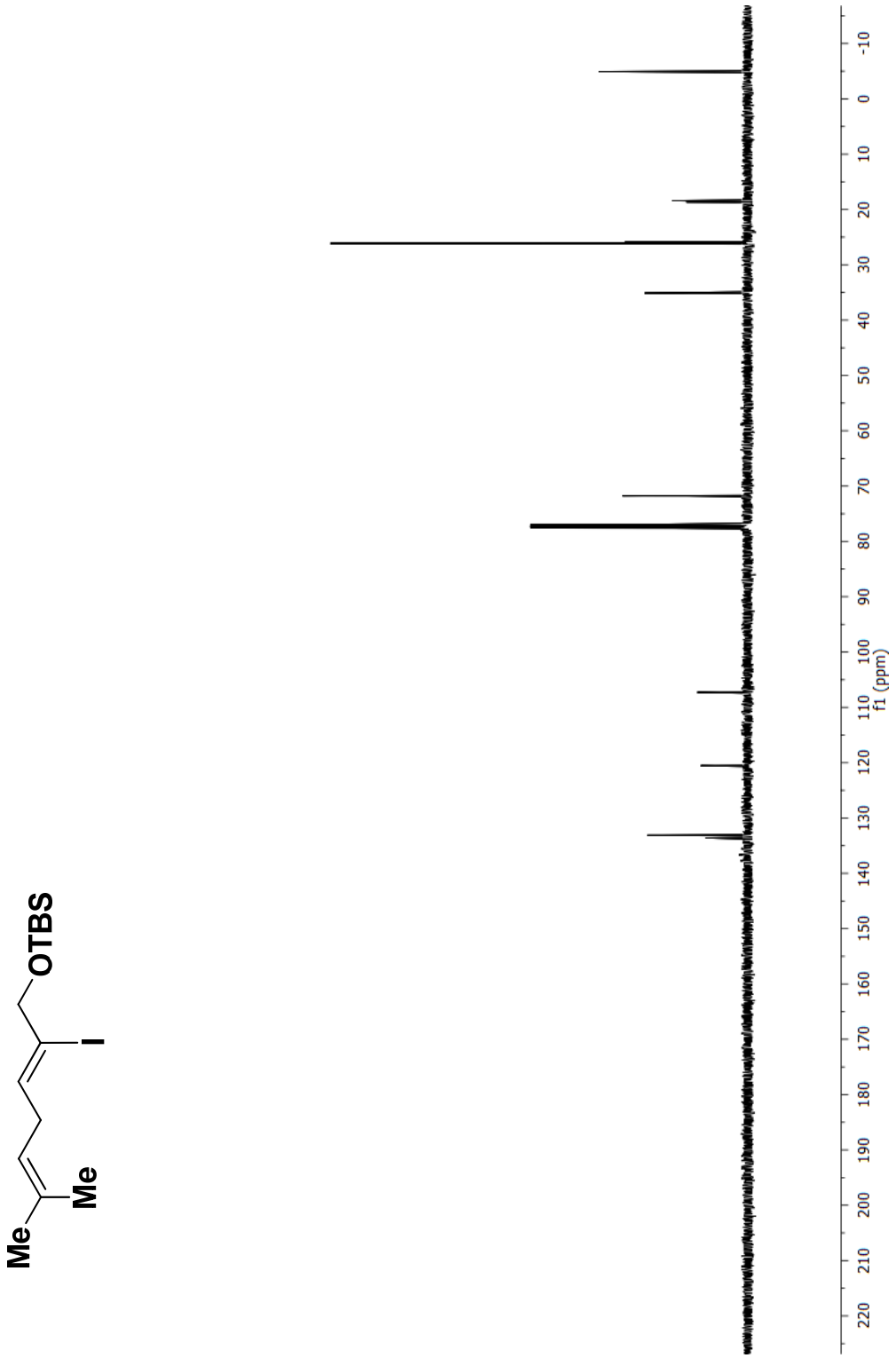
OTBS
I
Me
Me
f1 (ppm)

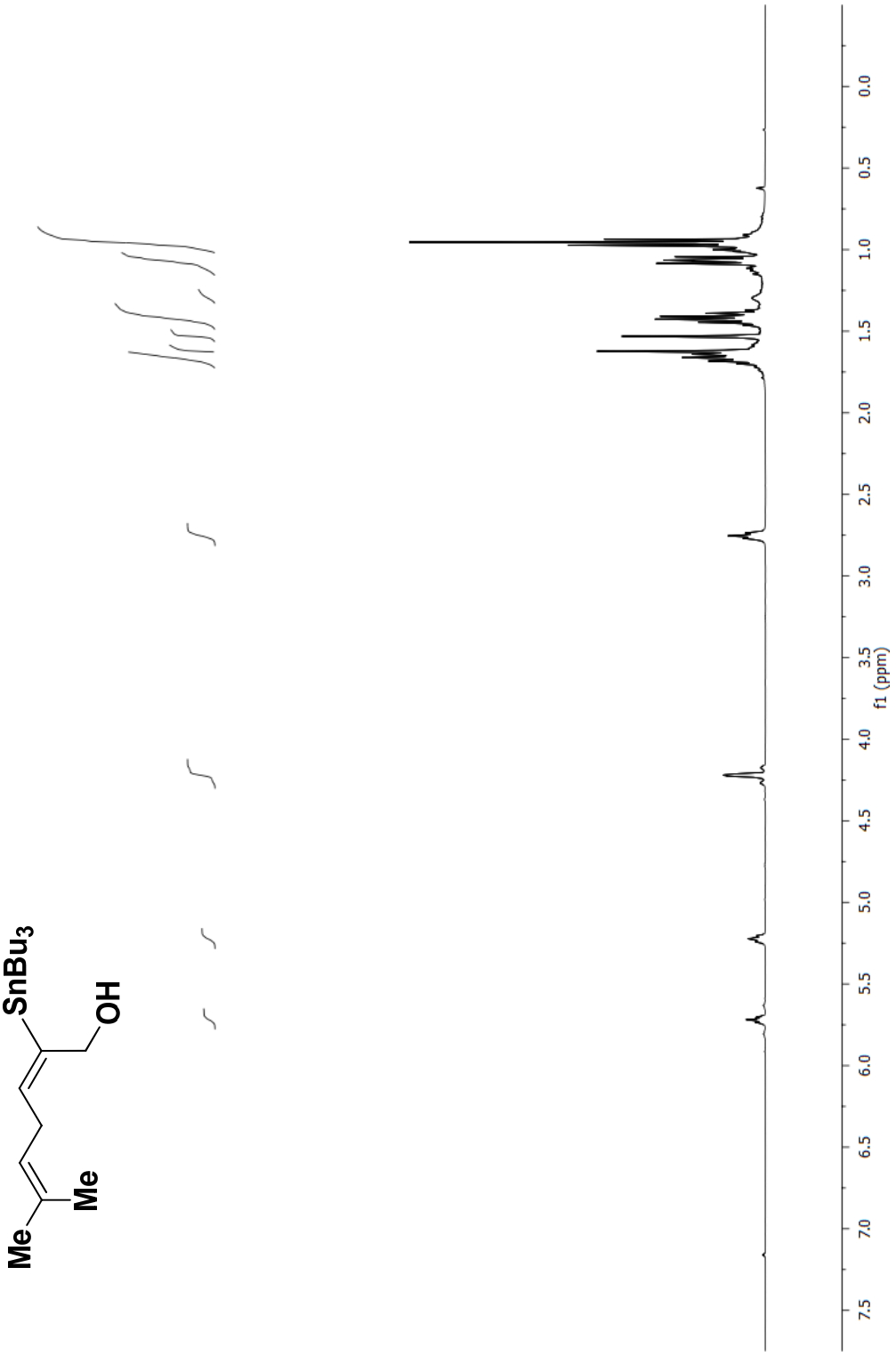
SnBu3
OH
Me
Me
f1 (ppm)

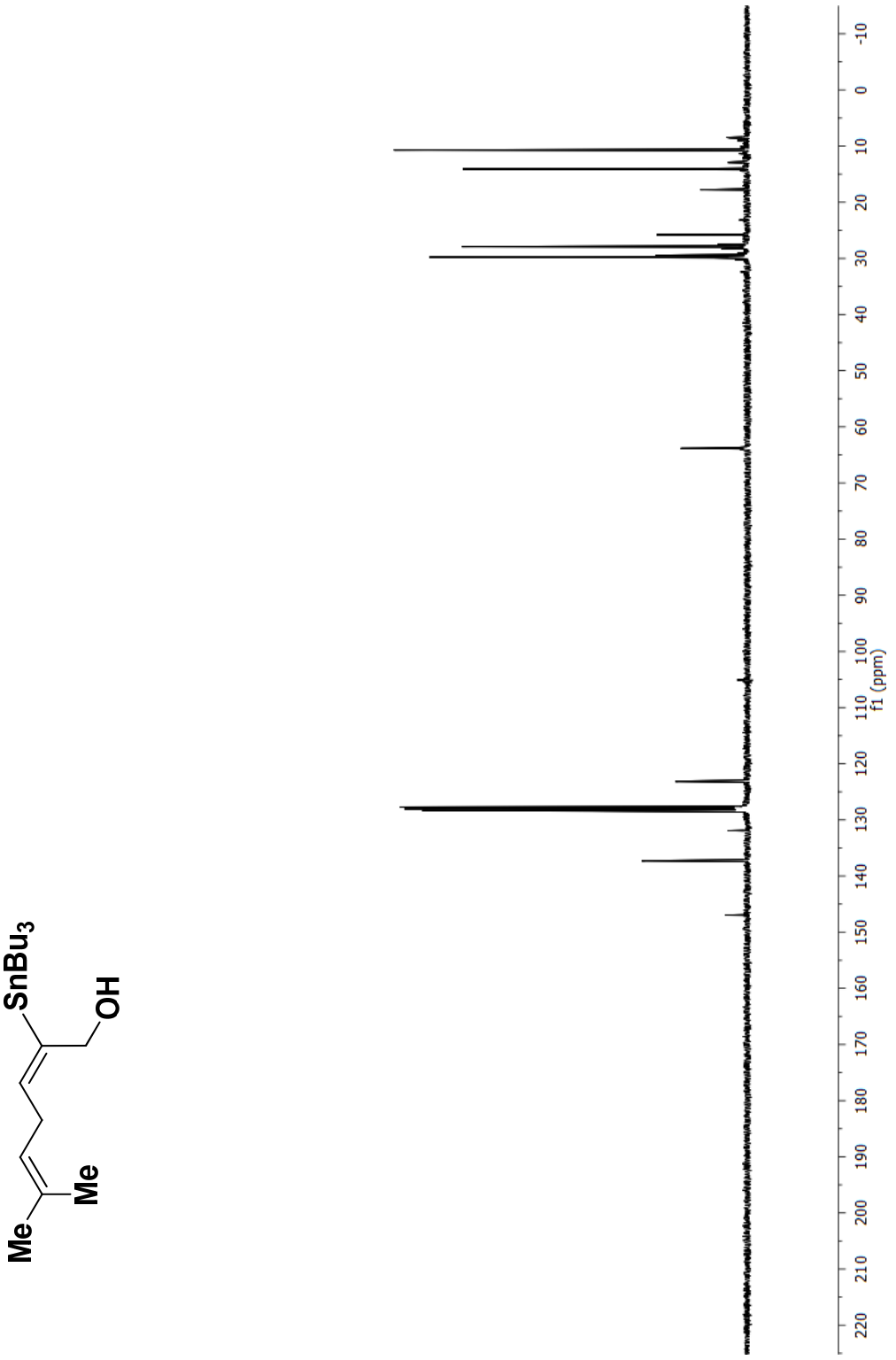
SnBu3
OH
Me
Me
f1 (ppm)

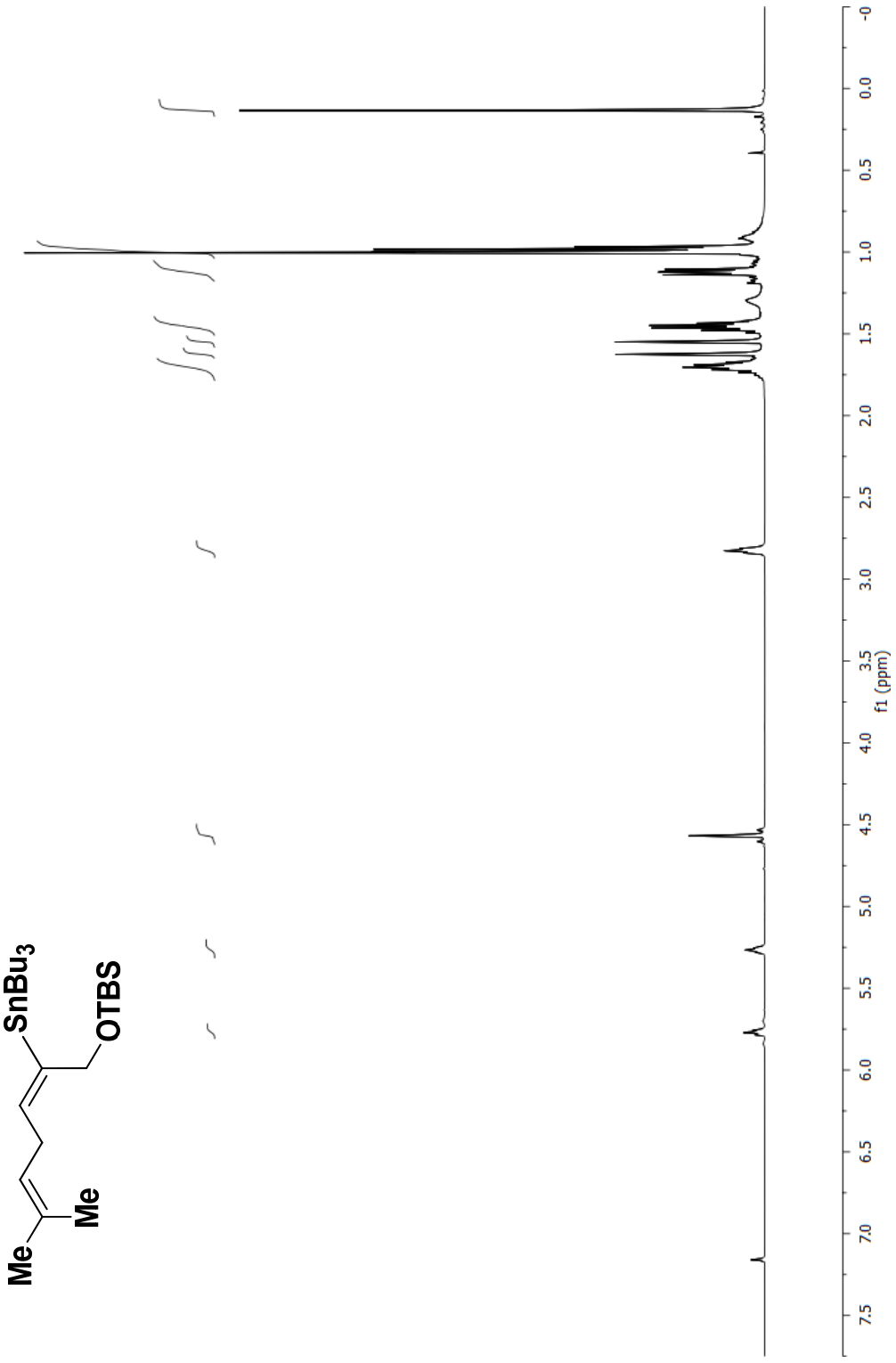
SnBu3
OTBS
Me
Me
f1 (ppm)

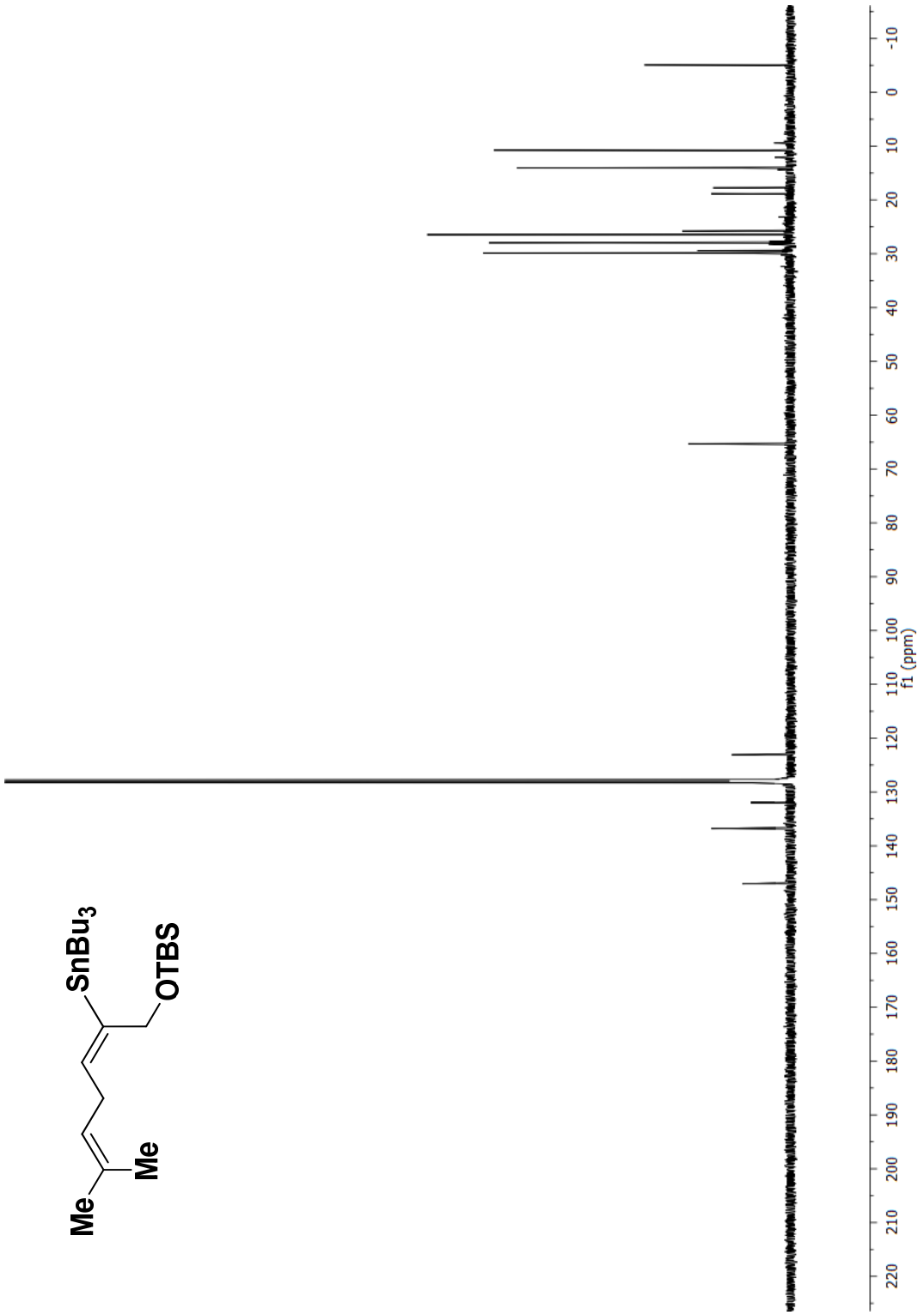
SnBu3
OTBS
Me
Me
f1 (ppm)

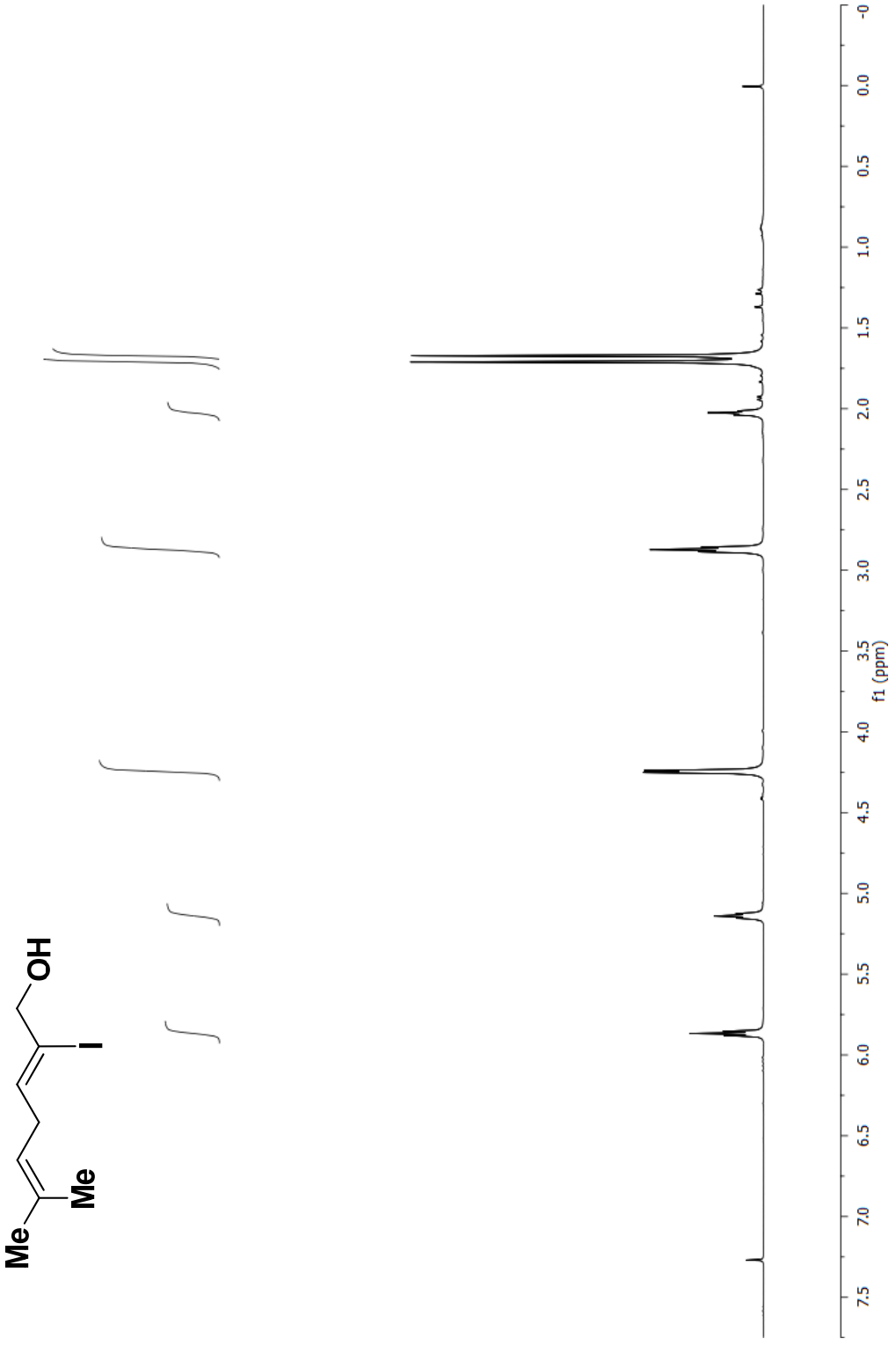
OH
I
Me
Me
f1 (ppm)

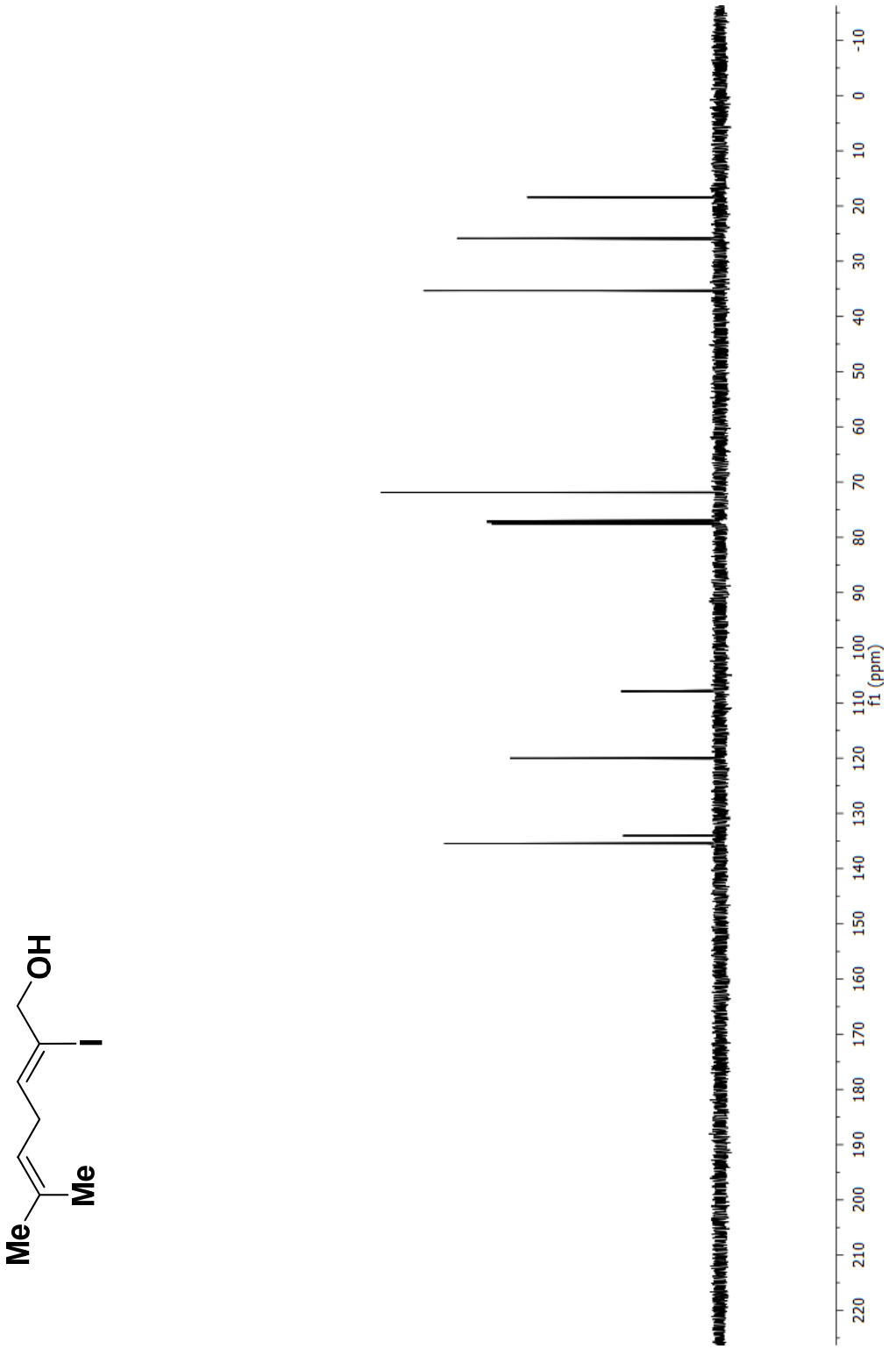
OH
I
Me
Me
f1 (ppm)

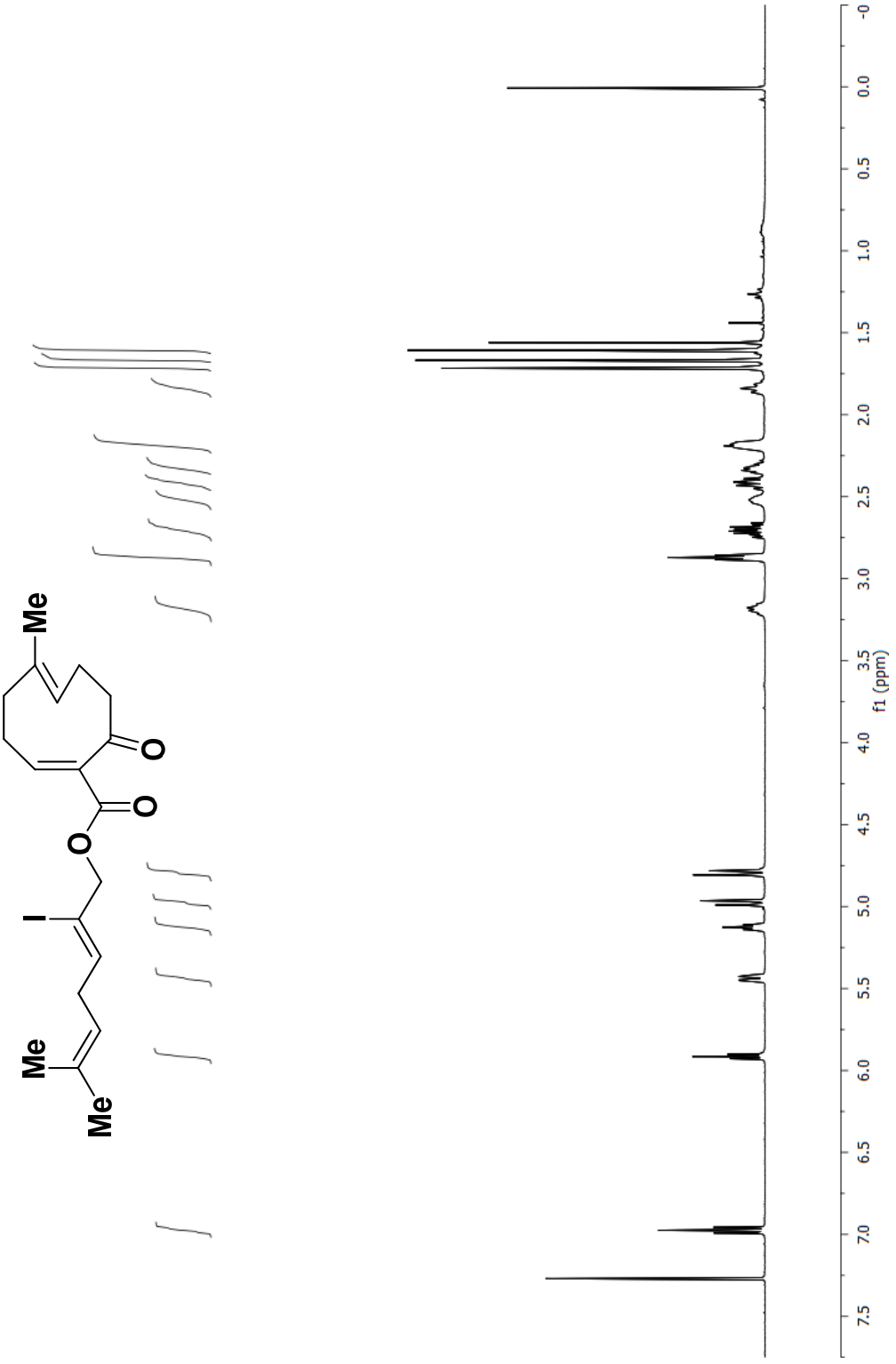
Me
O
O
O
I
Me
Me
f1 (ppm)

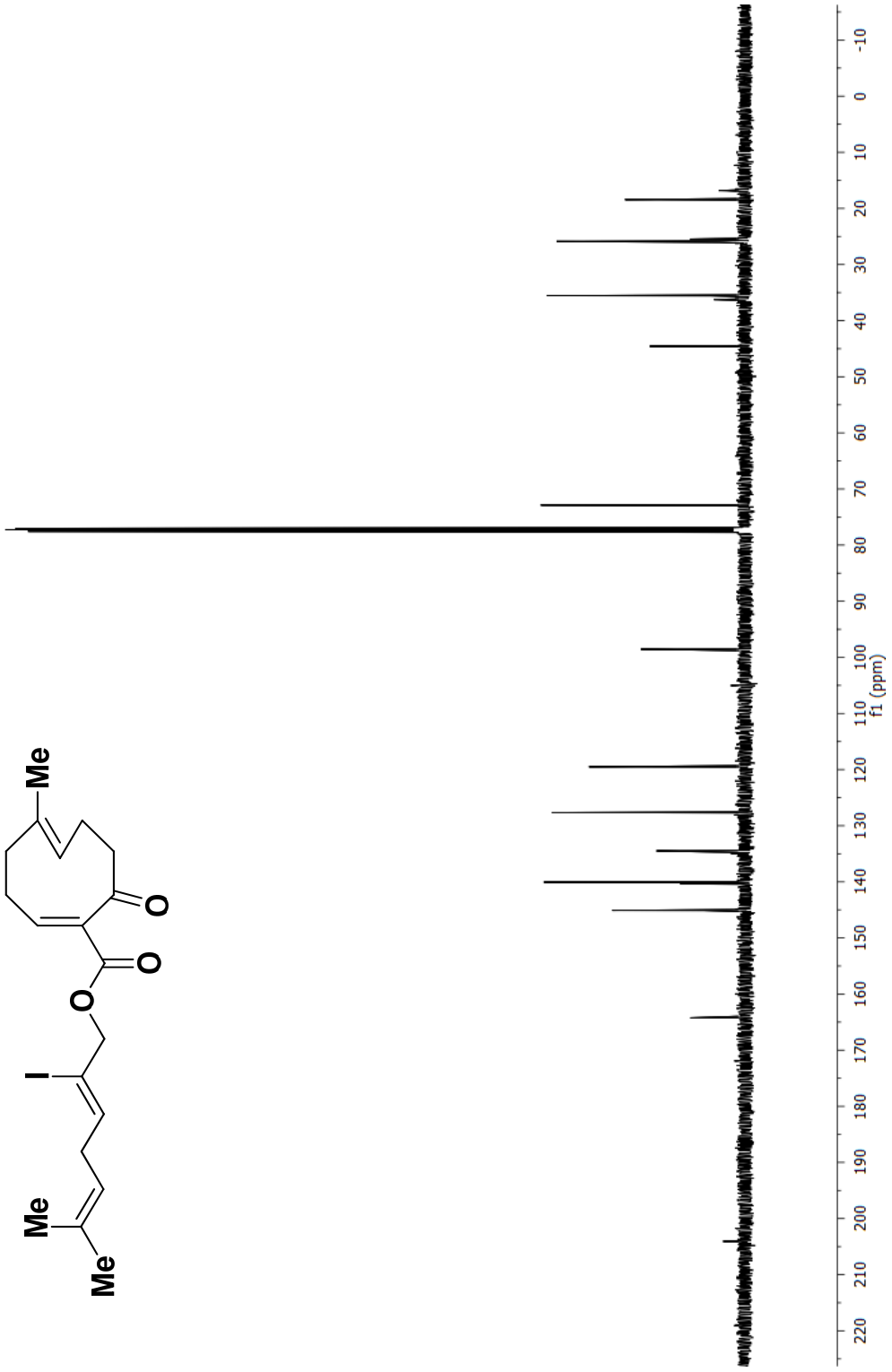
Me
O
O
O
I
Me
Me
-10
0
10
20
30
40
50
60
70
80
90
100
110
120
130
140
150
160
170
180
190
200
210
220
f1 (ppm)

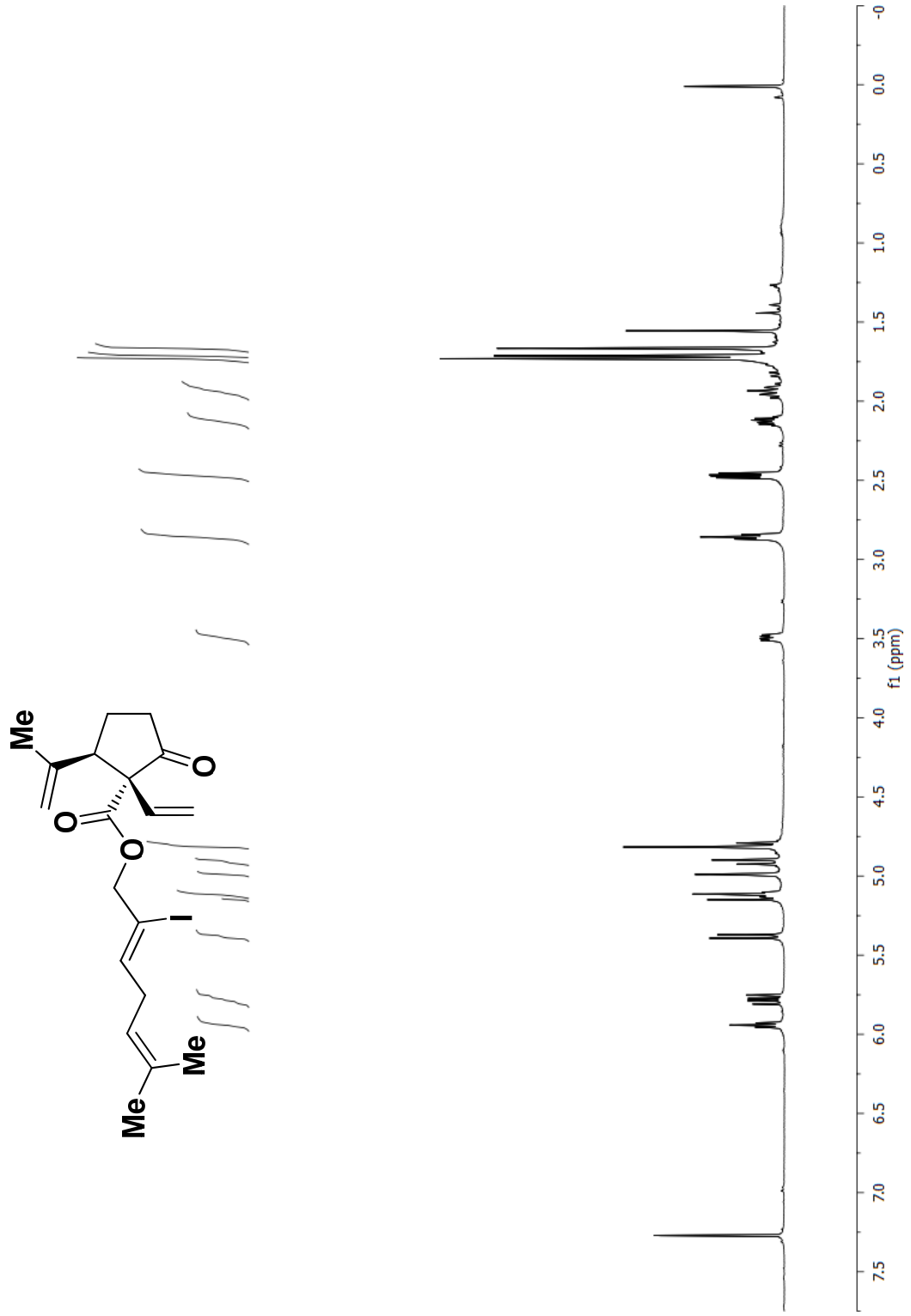
Me
O
O
O
I
Me
Me
f1 (ppm)

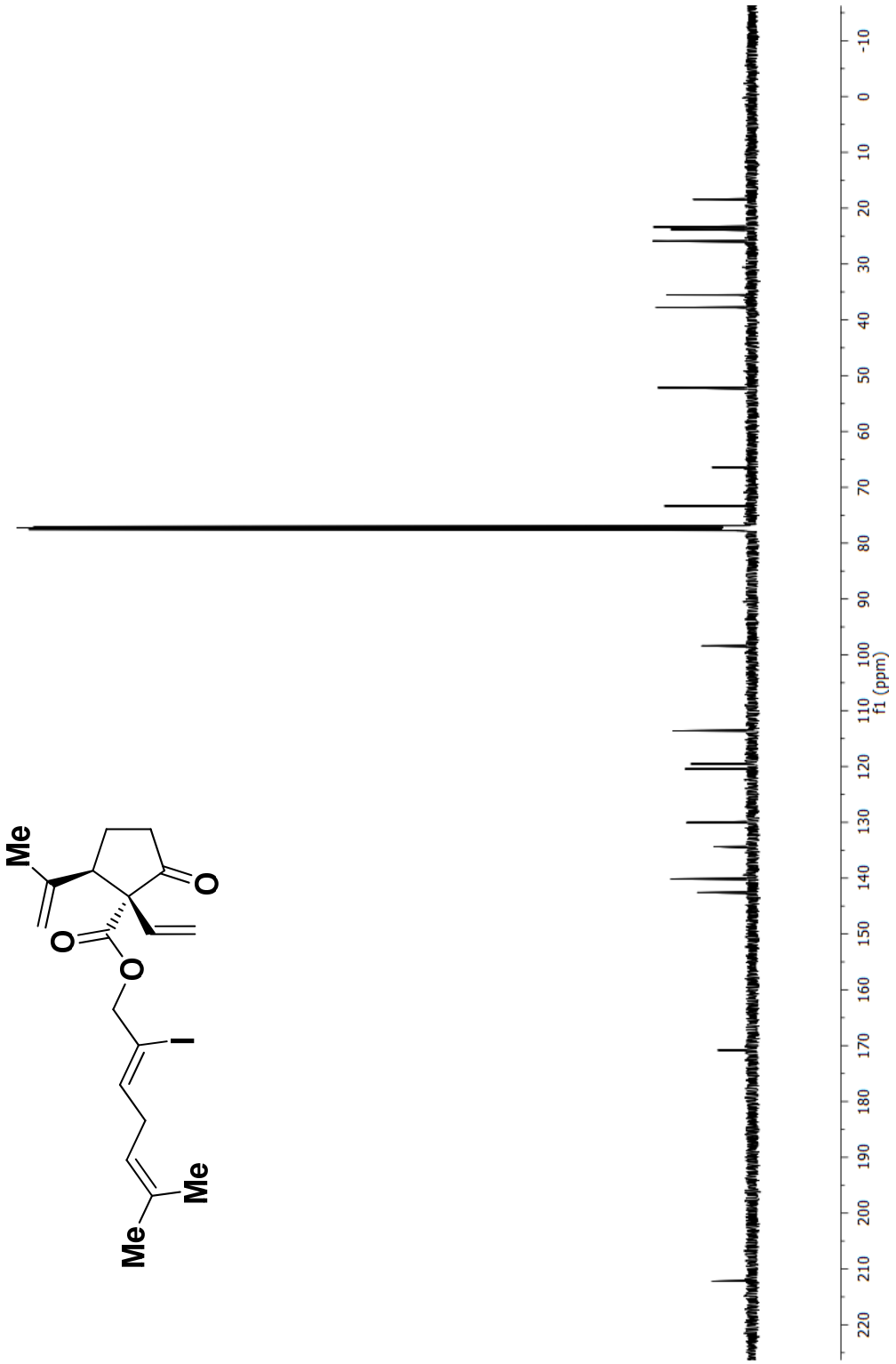
Me
O
O
O
I
Me
Me
f1 (ppm)

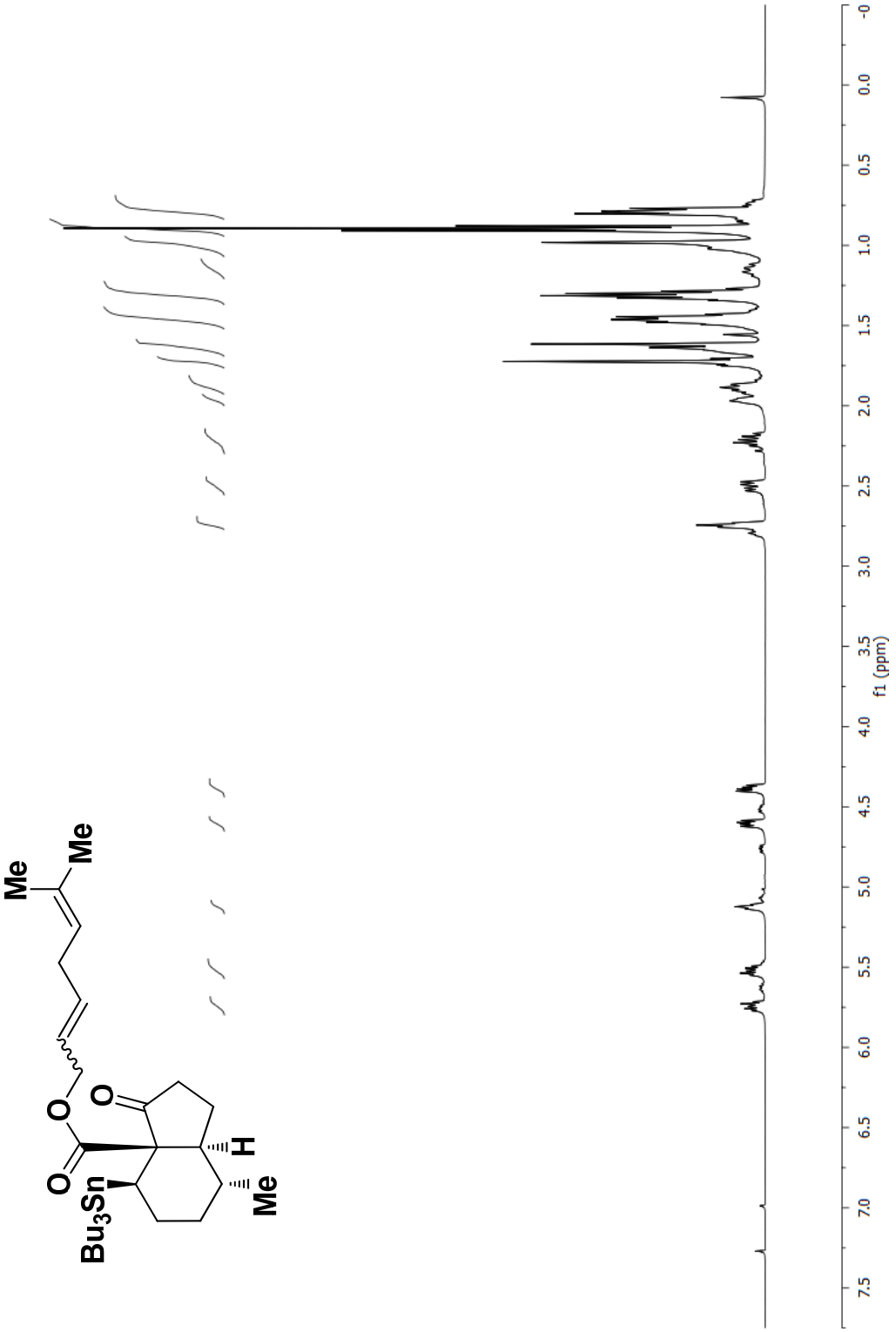
Me
Me
O
O
O
O
H
Me
Bu3Sn
7.5
7.0
6.5
6.0
5.5
5.0
4.5
4.0
3.5
3.0
2.5
2.0
1.5
1.0
0.5
0.0
-0
f1 (ppm)

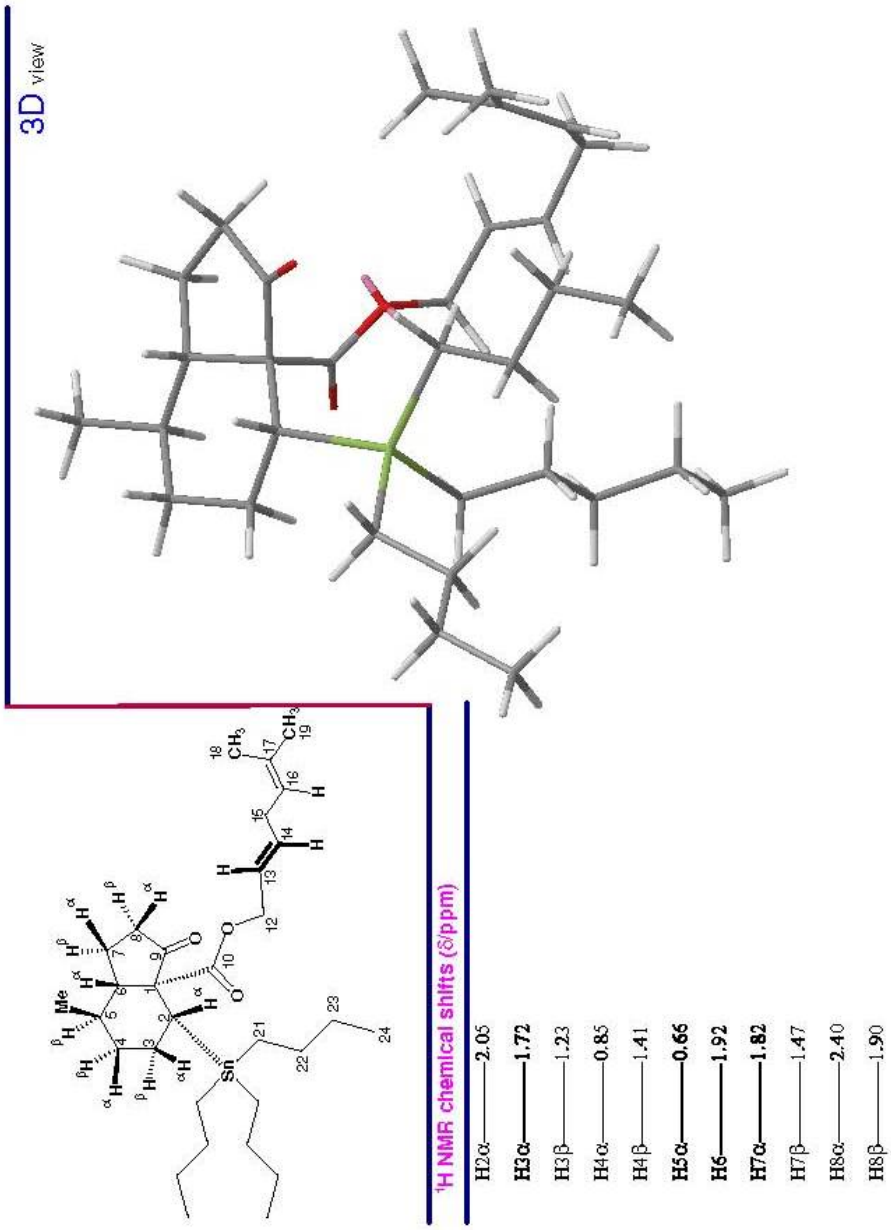
3D view
^{1}H NMR chemical shifts (δ/ppm)
H2α—2.05
H3α—1.72
H3β—1.23
H4α—0.85
H4β—1.41
H5α—0.66
H6—1.92
H7α—1.82
H7β—1.47
H8α—2.40
H8β—1.90

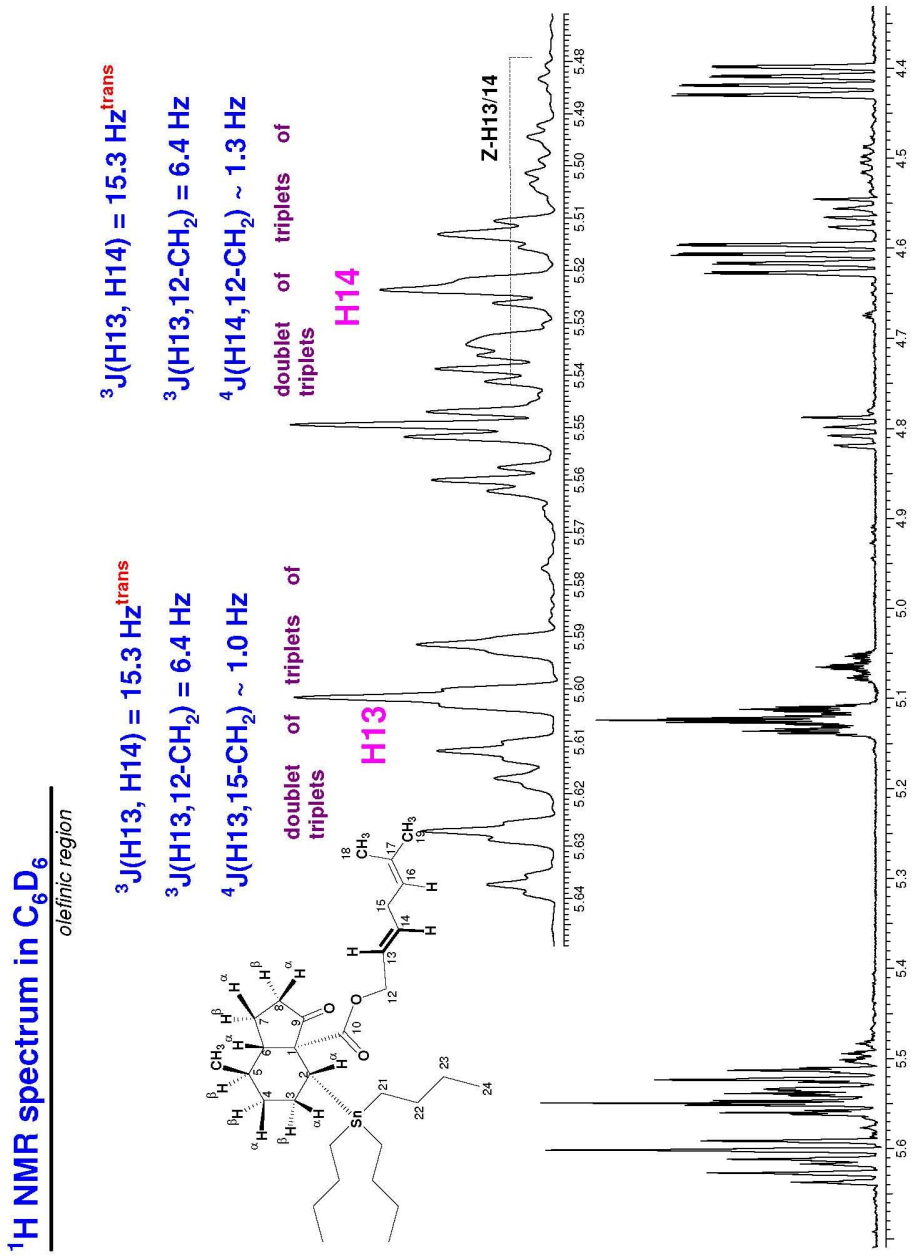
^{1}H NMR spectrum in C_6D_6
olefinic region
^{3}J(H13, H14) = 15.3 Hz^{trans}
^{3}J(H13,12-CH$_2$) = 6.4 Hz
^{4}J(H13,15-CH$_2$) ~ 1.0 Hz
doublet of triplets of triplets
H13
^{3}J(H13, H14) = 15.3 Hz^{trans}
^{3}J(H13,12-CH$_2$) = 6.4 Hz
^{4}J(H14,12-CH$_2$) ~ 1.3 Hz
doublet of triplets of triplets
H14
Z-H13/14

^{1}H NMR spectrum in C_6D_6

olefinic region

^3J(H16, 15-CH_2) = 7.2 Hz

^4J(H16, 18-CH_3) = 1.4 Hz

^4J(H16, 19-CH_3) = 1.4 Hz

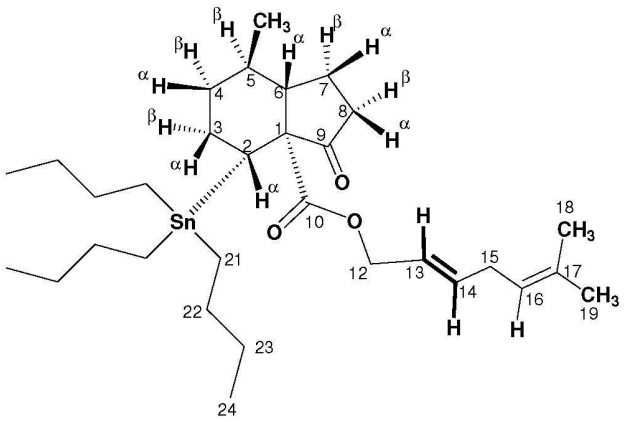

E---H16

tiplet of septets

Z---H16

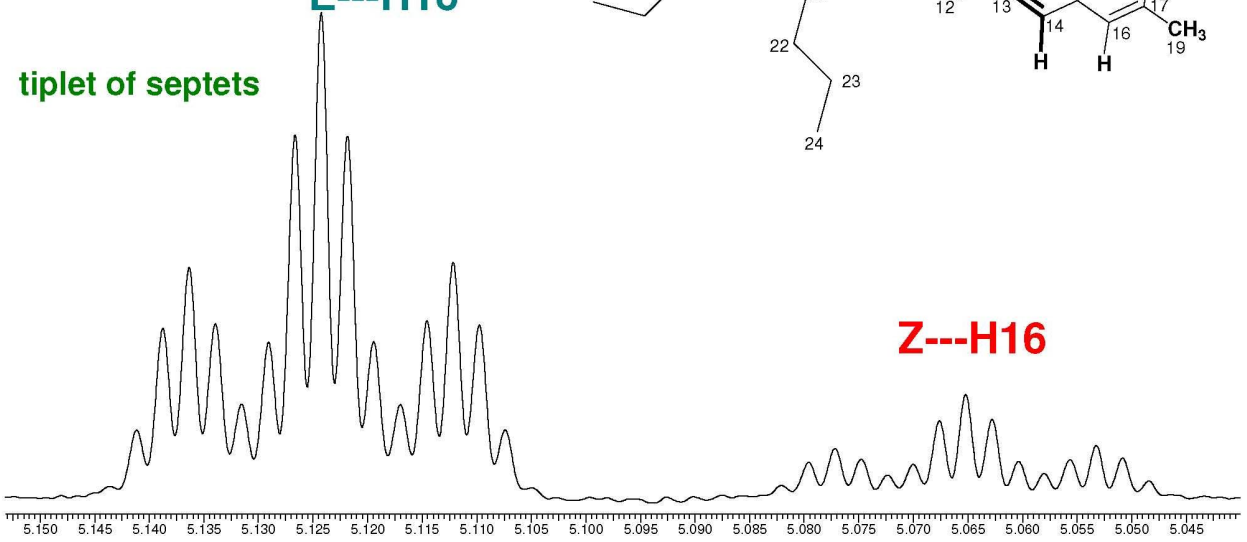

$^{2}J(H12^{A},H12^{B}) = 12.4$ Hz

$^{3}J(H12^{A},H13) = 6.4$ Hz

$^{4}J(H12^{A},H14) \sim 1.0$ Hz

$^{5}J(H12^{A},15\text{-}CH_2) \sim 1.0$ Hz

doublet of doublets of quartets

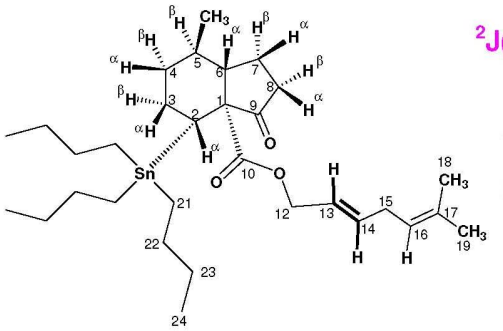

$^{2}J(H12^{B},H12^{B}) = 12.4$ Hz

$^{3}J(H12^{B},H13) = 6.4$ Hz

$^{4}J(H12^{B},H14) \sim 1.0$ Hz

$^{5}J(H12^{B},15\text{-}CH_2) \sim 1.0$ Hz

doublet of doublets of quartets

$H12^{A}$

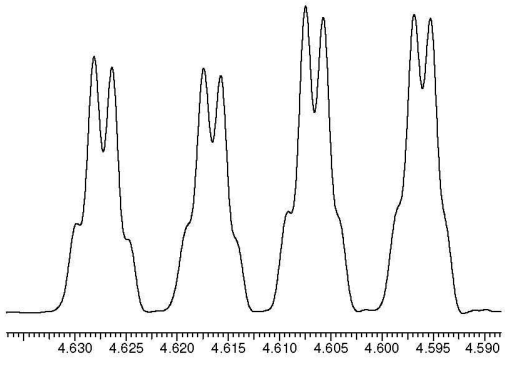

$H12^{B}$

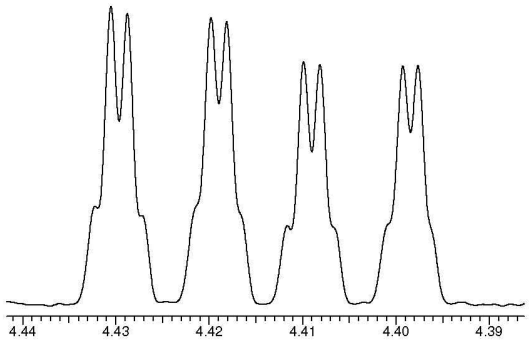

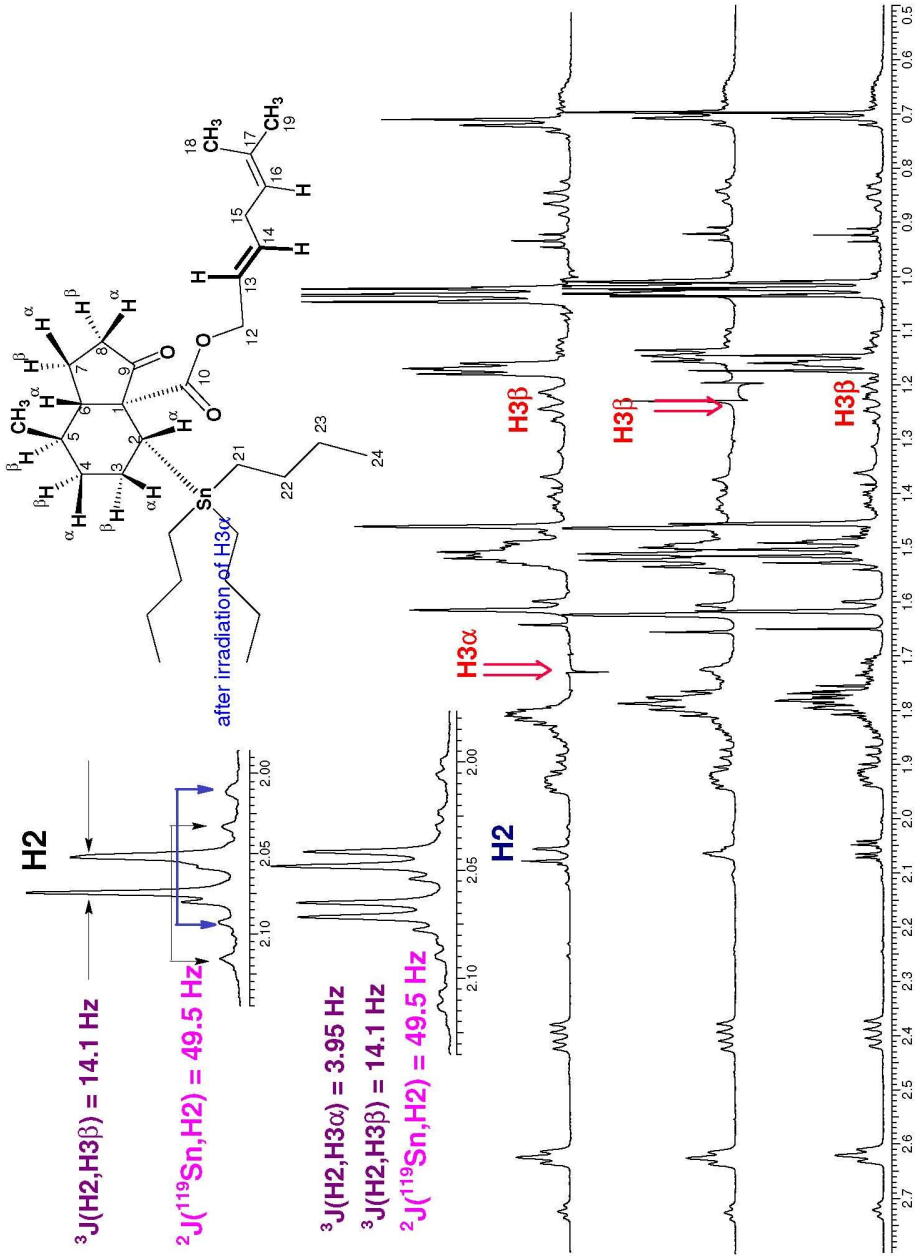
H2
^3J(H2,H3β) = 14.1 Hz
^2J(^{119}Sn,H2) = 49.5 Hz
after irradiation of H3α
^3J(H2,H3α) = 3.95 Hz
^3J(H2,H3β) = 14.1 Hz
^2J(^{119}Sn,H2) = 49.5 Hz
H3α
H3β
H3β
H3β
H2

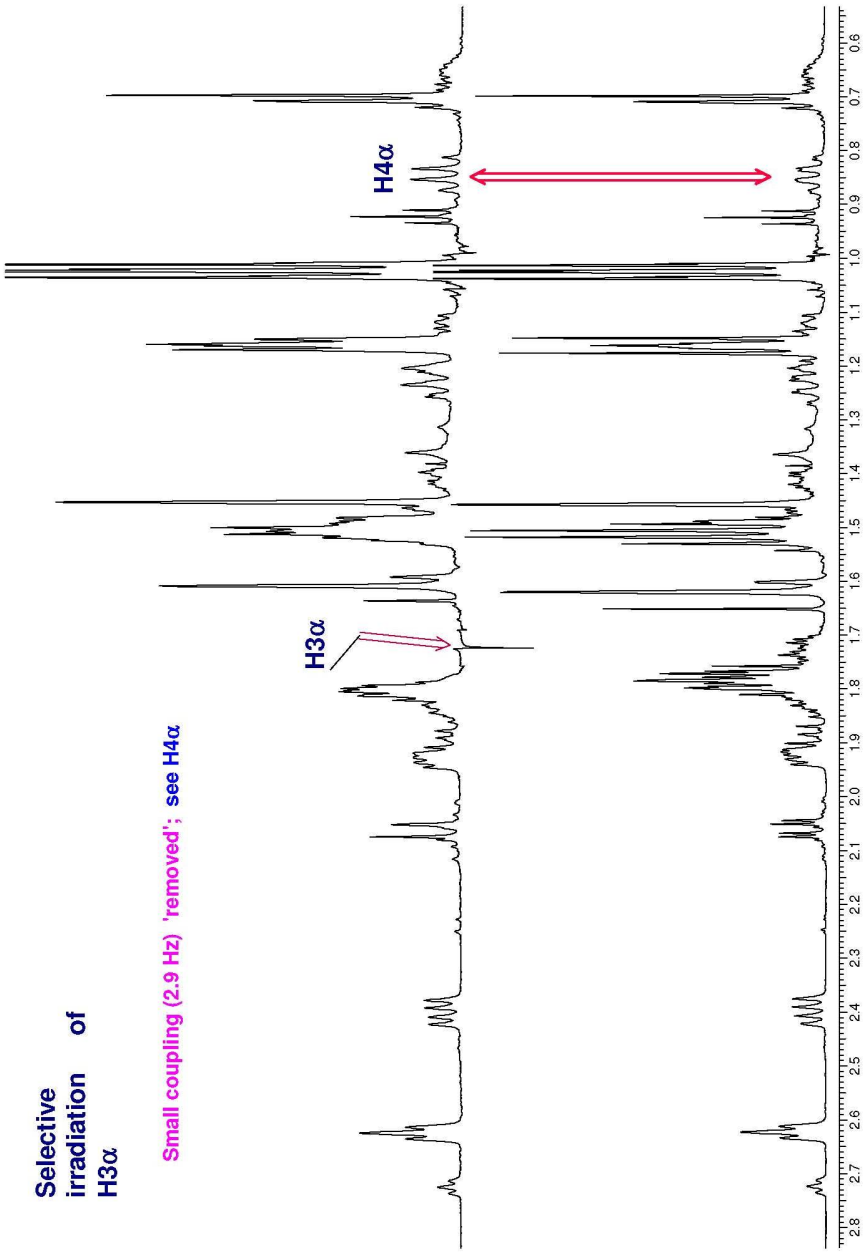
Selective irradiation of H3α
Small coupling (2.9 Hz) 'removed'; see H4α
H3α
H4α

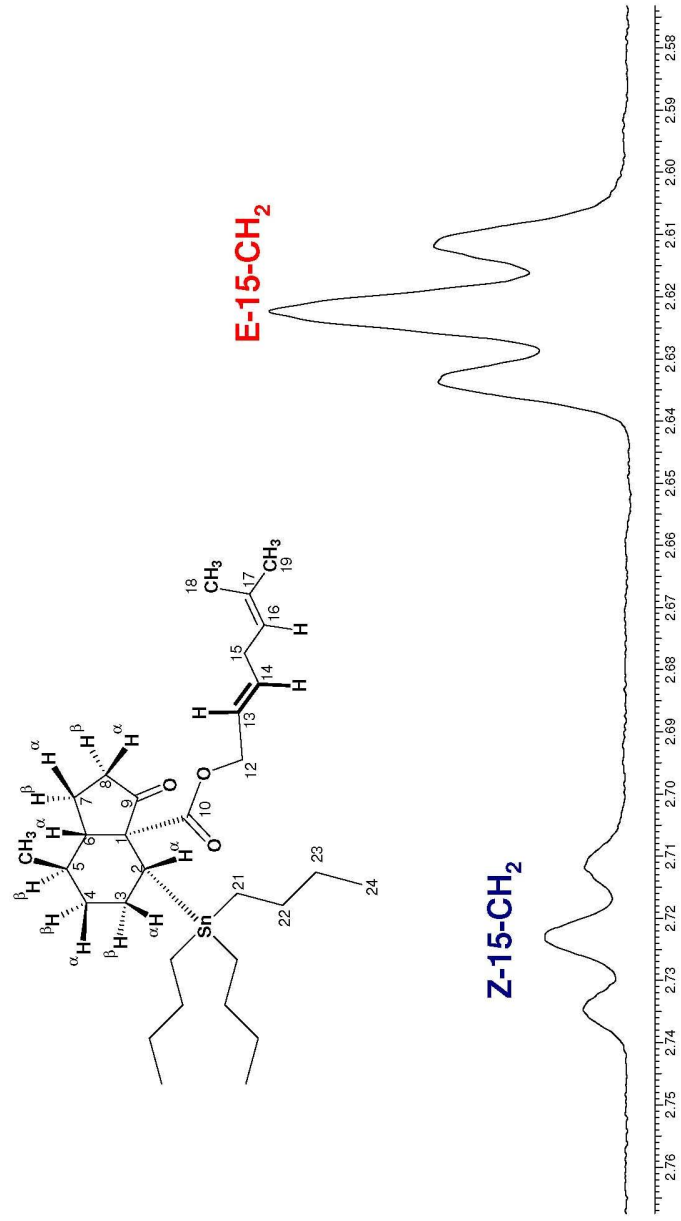
E-15-CH2
Z-15-CH2
2.76
2.75
2.74
2.73
2.72
2.71
2.70
2.69
2.68
2.67
2.66
2.65
2.64
2.63
2.62
2.61
2.60
2.59
2.58

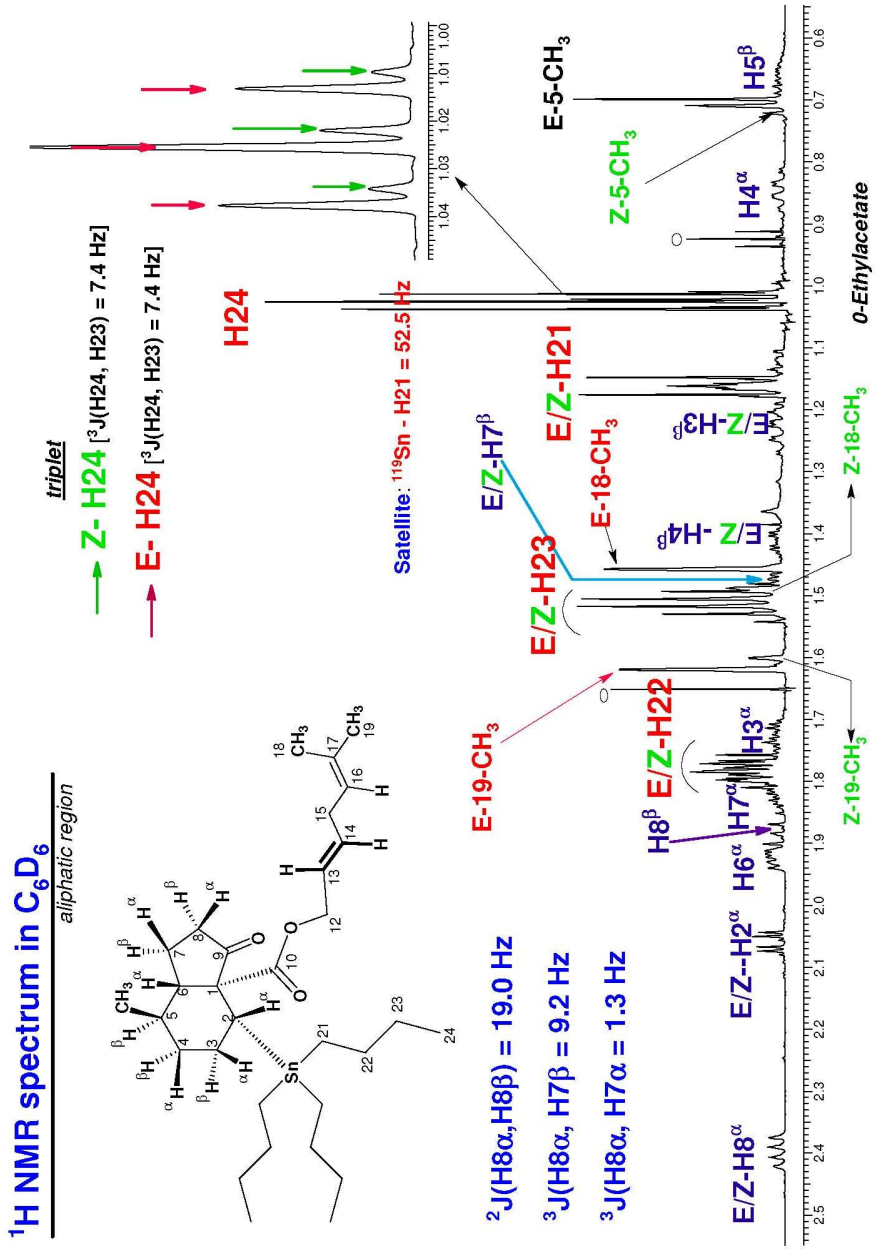
^{1}H NMR spectrum in C_6D_6
aliphatic region
triplet
Z- H24 [^{3}J(H24, H23) = 7.4 Hz]
E- H24 [^{3}J(H24, H23) = 7.4 Hz]
H24
Satellite: ^{119}Sn - H21 = 52.5 Hz
E-5-CH$_3$
Z-5-CH$_3$
H5$^\beta$
H4$^\alpha$
E/Z-H3$^\beta$
E/Z -H4$^\beta$
E-18-CH$_3$
E/Z-H21
E/Z-H23
E/Z-H7$^\beta$
E-19-CH$_3$
H8$^\beta$ E/Z-H22
H7$^\alpha$
H3$^\alpha$
H6$^\alpha$
E/Z--H2$^\alpha$
E/Z-H8$^\alpha$
Z-18-CH$_3$
Z-19-CH$_3$
0-Ethylacetate
^{2}J(H8α,H8β) = 19.0 Hz
^{3}J(H8α, H7β = 9.2 Hz
^{3}J(H8α, H7α = 1.3 Hz

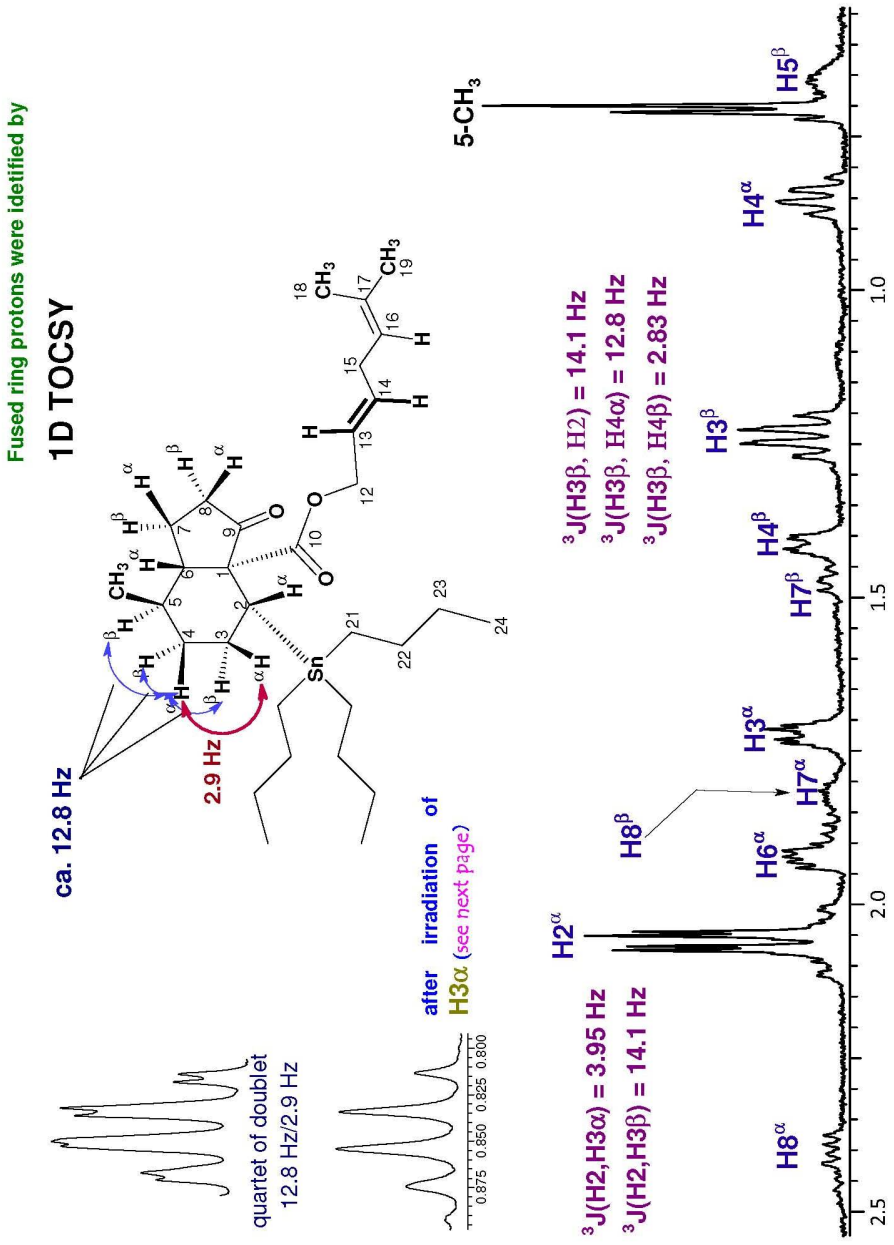
Fused ring protons were idetified by
1D TOCSY
ca. 12.8 Hz
2.9 Hz
quartet of doublet
12.8 Hz/2.9 Hz
after irradiation of
Hα (see next page)
0.875 0.850 0.825 0.800
5-CH3
H5β
H4α
H4β
H3β
H3α
H7β
H7α
H6α
H8β
H2α
H8α
3J(Hβ, H2) = 14.1 Hz
3J(Hβ, Hα) = 12.8 Hz
3J(Hβ, Hβ) = 2.83 Hz
3J(H2,Hα) = 3.95 Hz
3J(H2,Hβ) = 14.1 Hz
2.5
2.0
1.5
1.0

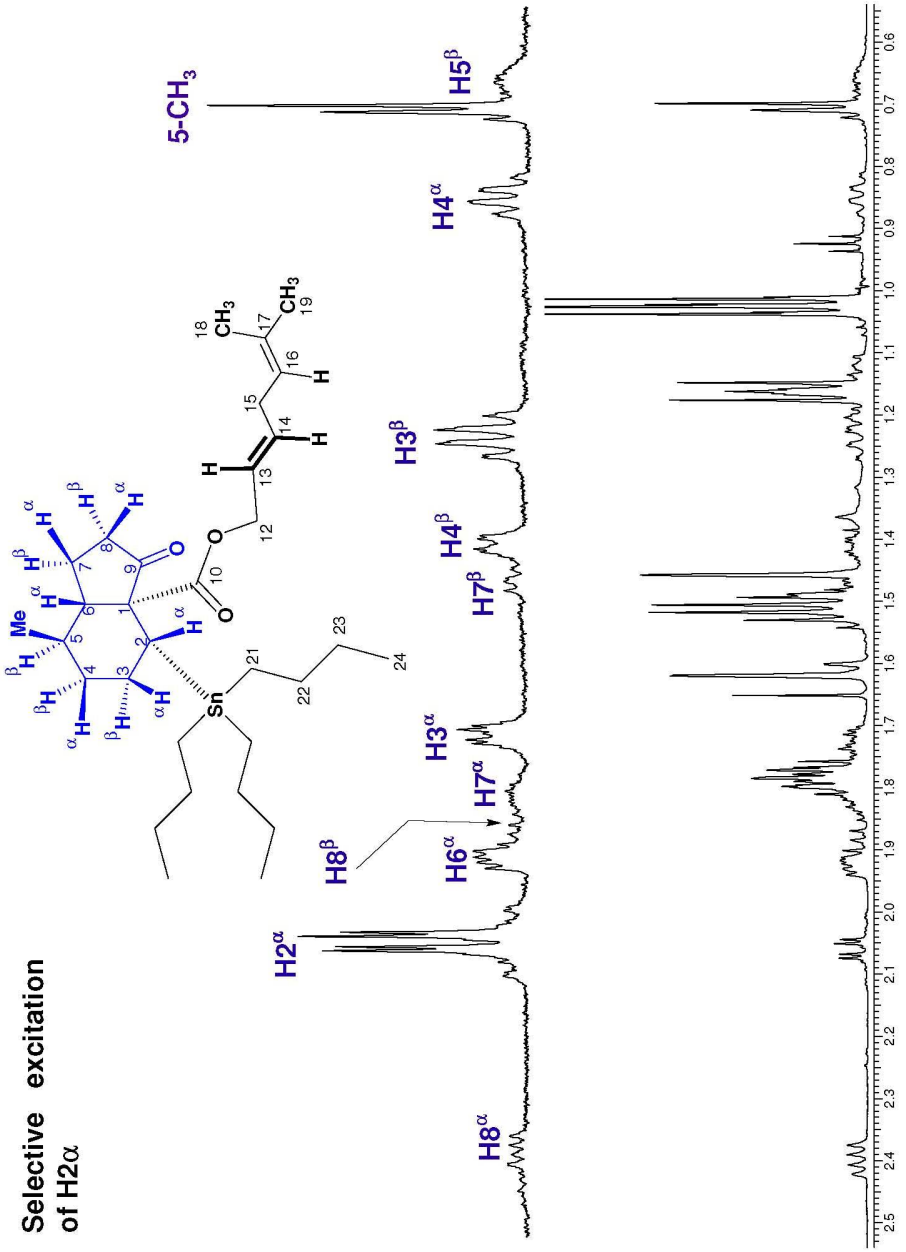
Selective excitation of H2α
H2α
H8β
H6α
H7α
H3α
H8α
H4β
H7β
H3β
H4α
H5β
5-CH3
Me
Sn

Why 5-CH_3 doublets in both $CDCL_3$ and C_6D_6 does not show a typical doublet splitting patterns with an equal intensity of each line of doublets?

AB_3 spin system

Chemical shift difference between 5-CH_3 and H5 are too small causing a 'roof' effcet.

Intensity distortion of doublet lines of 5-CH_3; outer lines (they are shown by red arrows) intesity less then inner line

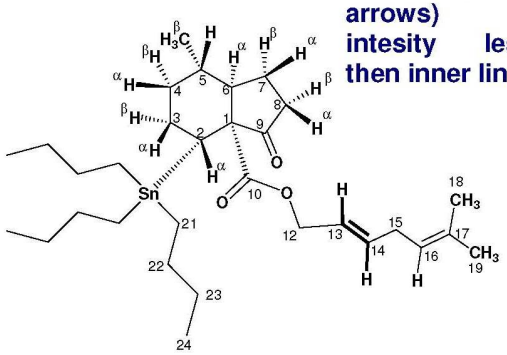

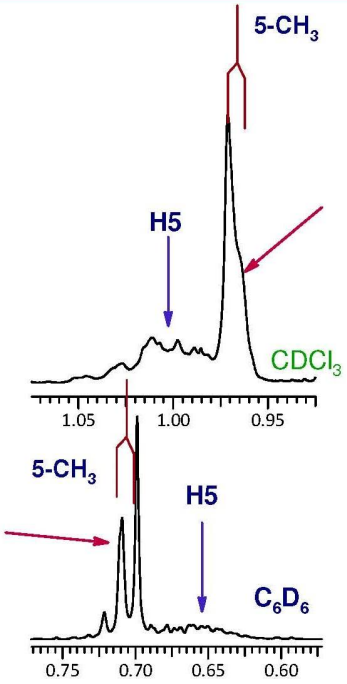

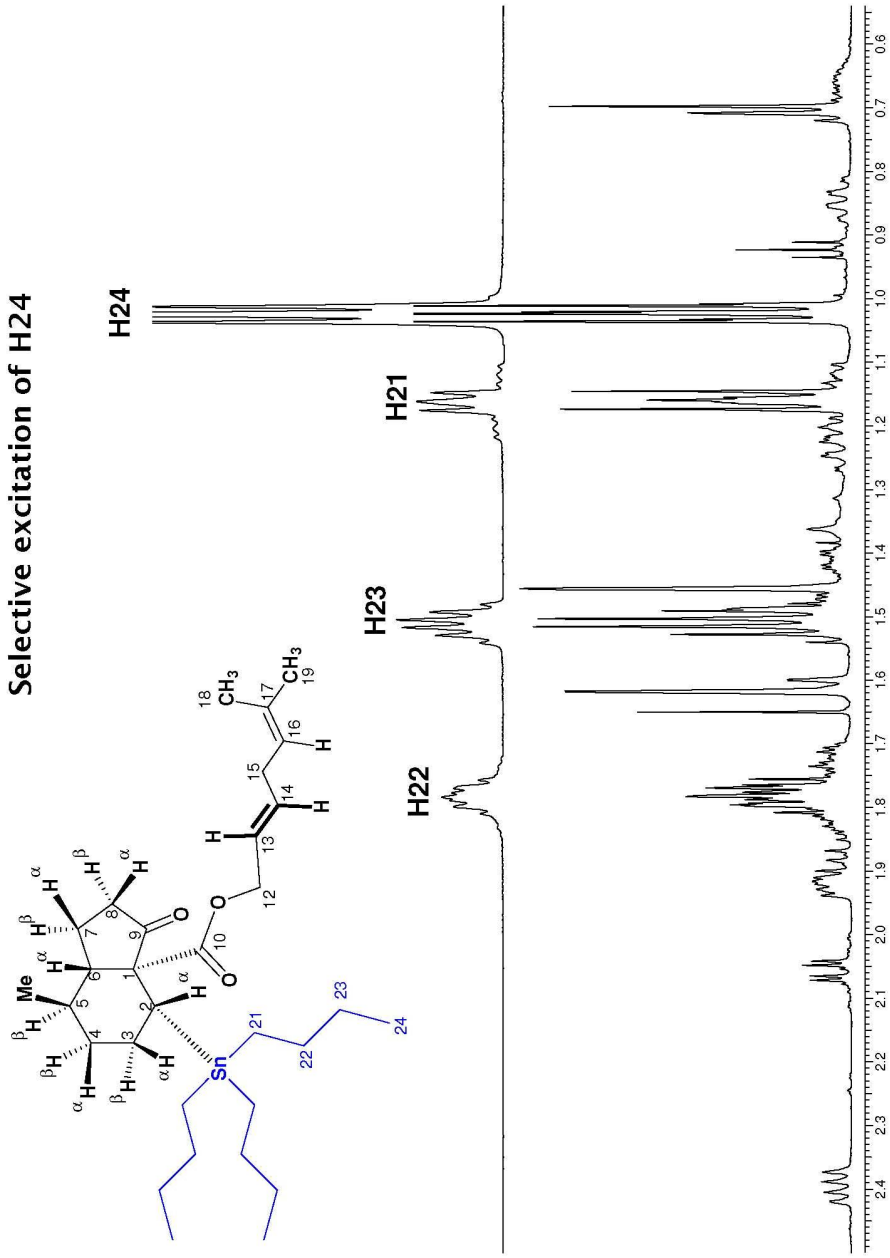
Selective excitation of H24
H24
H21
H23
H22
Me
Sn
CH3
CH3

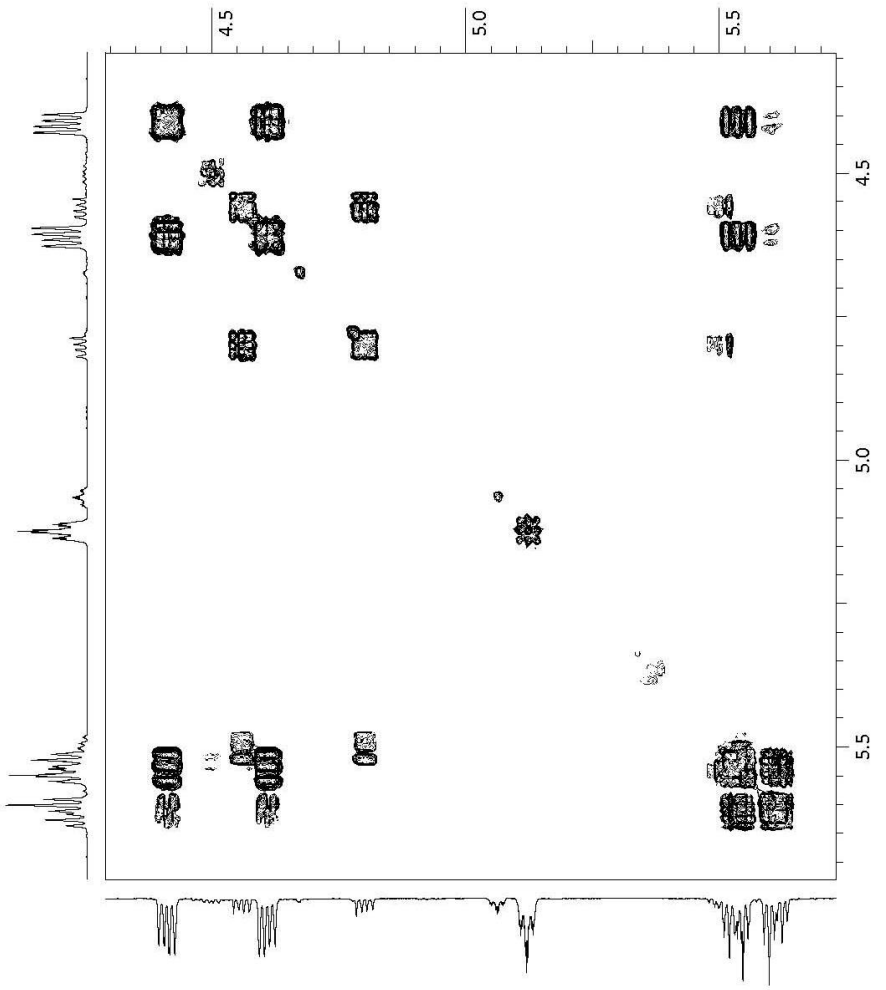

gCOSY

olefinic region

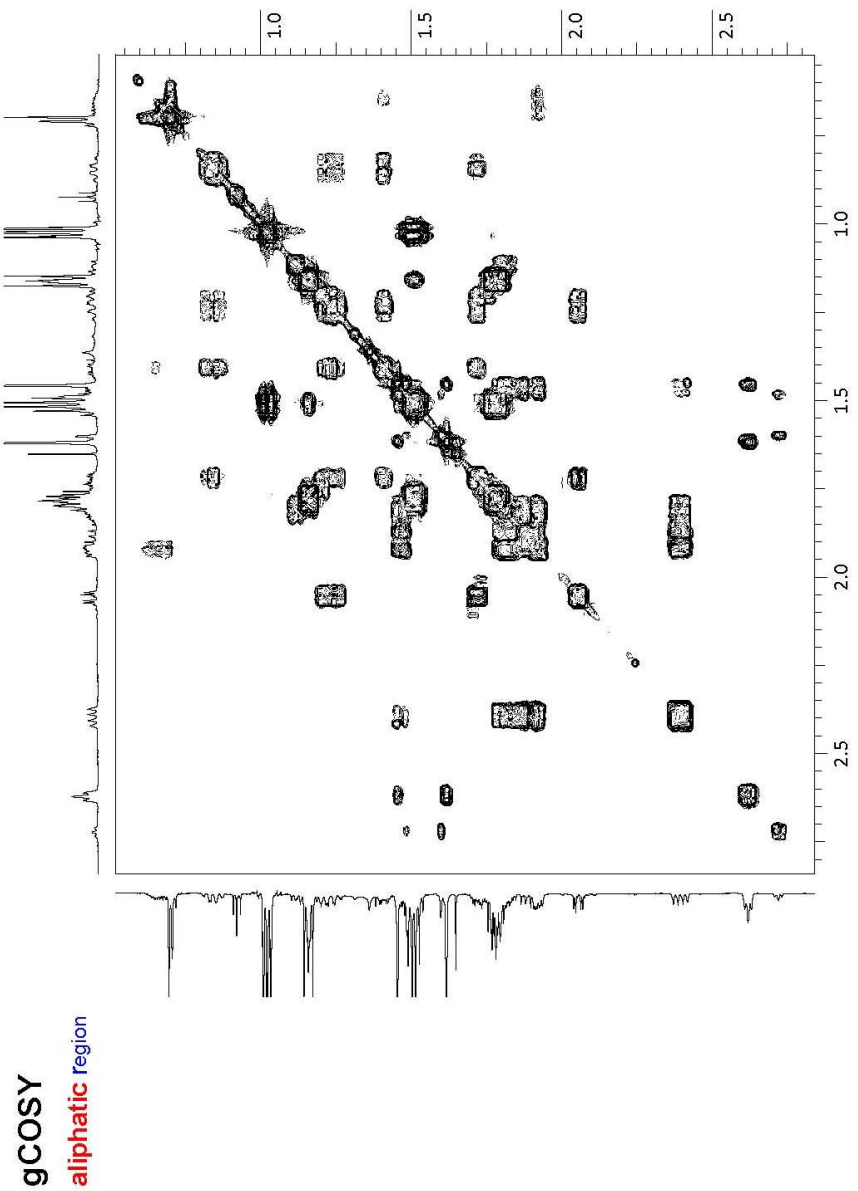
gCOSY
aliphatic region
1.0
1.5
2.0
2.5
1.0
1.5
2.0
2.5

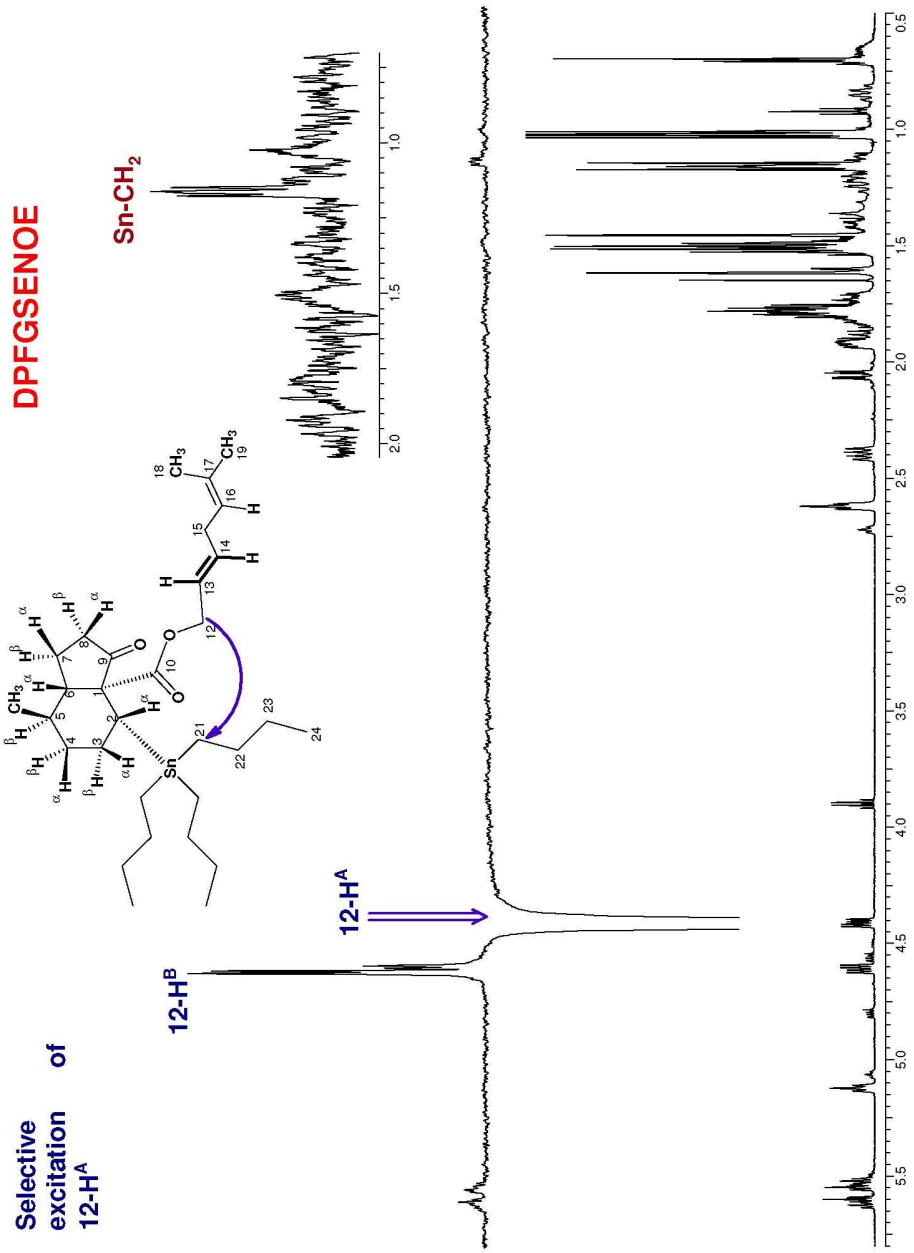
DPFGSENOE
Selective excitation of 12-H^A
12-H^B
12-H^A
Sn-CH2

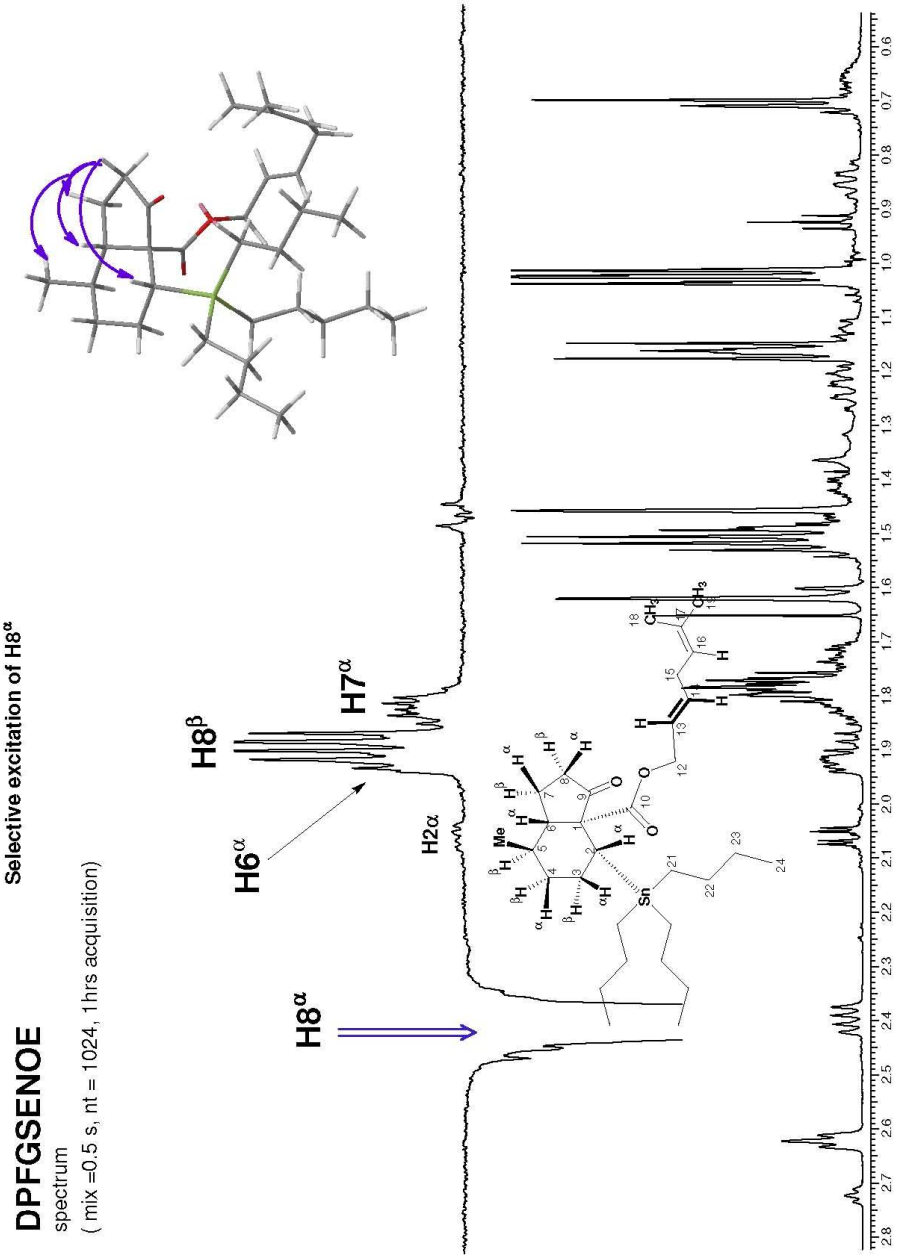
DPFGSENOE
spectrum
(mix =0.5 s, nt = 1024, 1hrs acquisition)
Selective excitation of H8α
H8α
H6α
H8β
H7α
H2α
Me
Sn

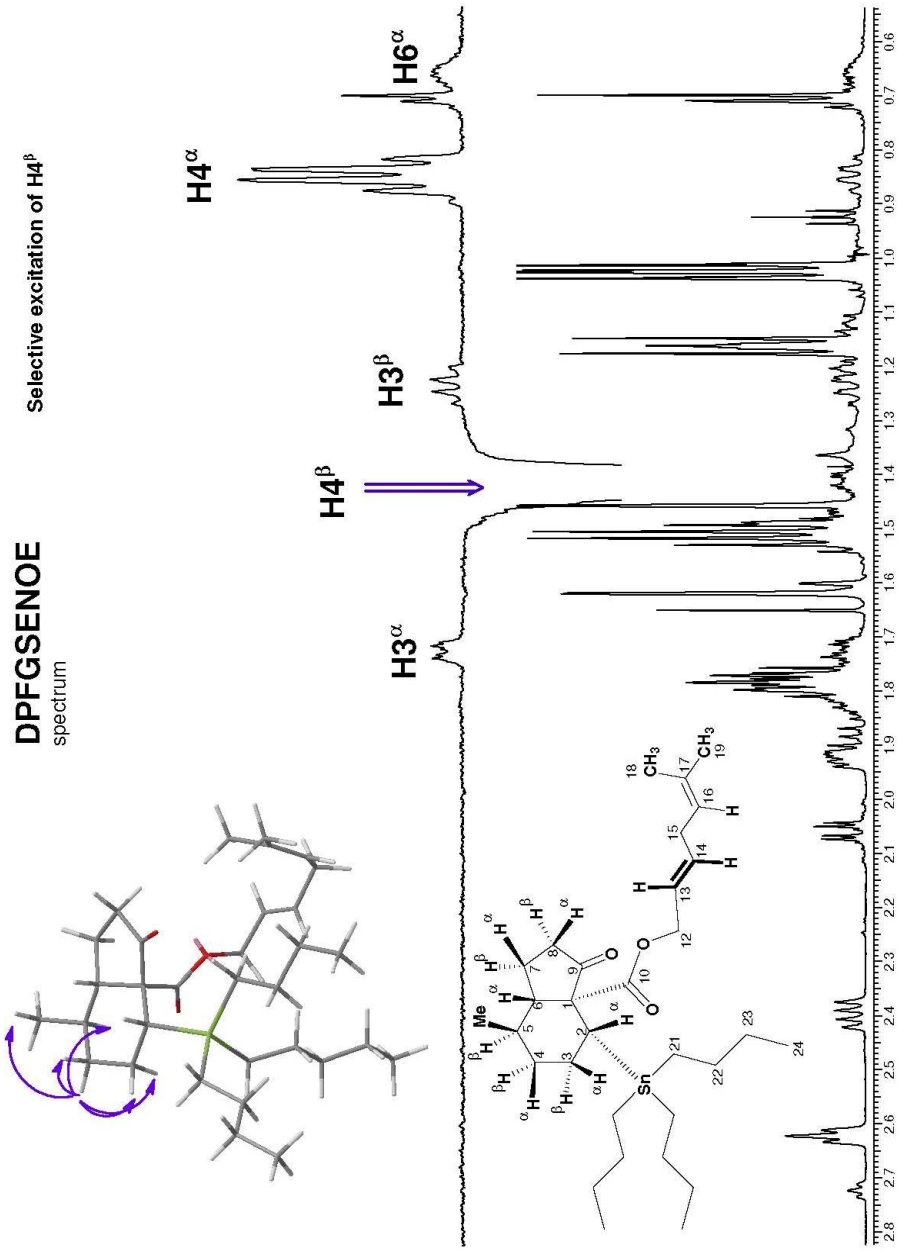
DPFGSENOE
spectrum
Selective excitation of H4β
H4α
H6α
H3β
H4β
H3α

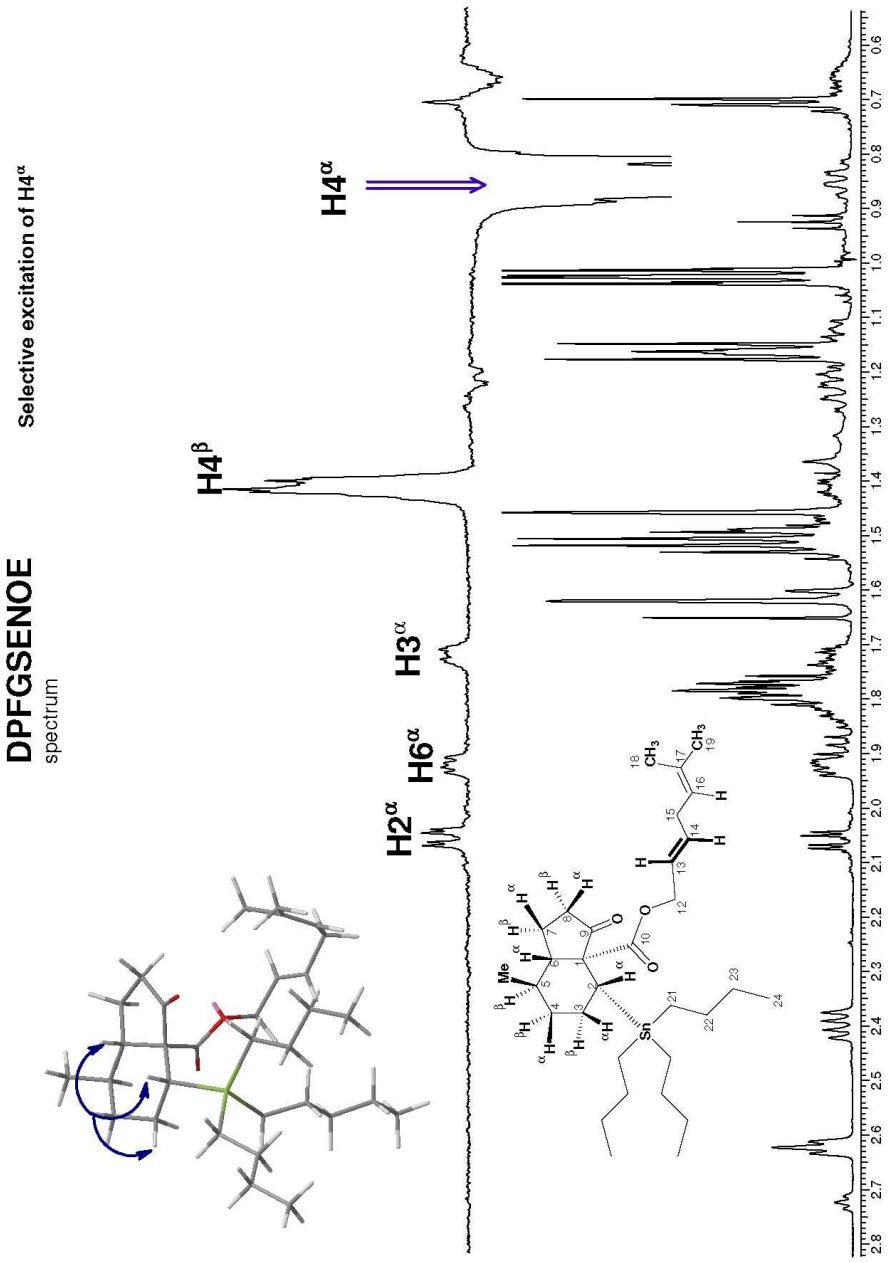
DPFGSENOE
spectrum
Selective excitation of H4α
H4β
H4α
H3α
H6α
H2α
Me
Sn
CH3
CH3

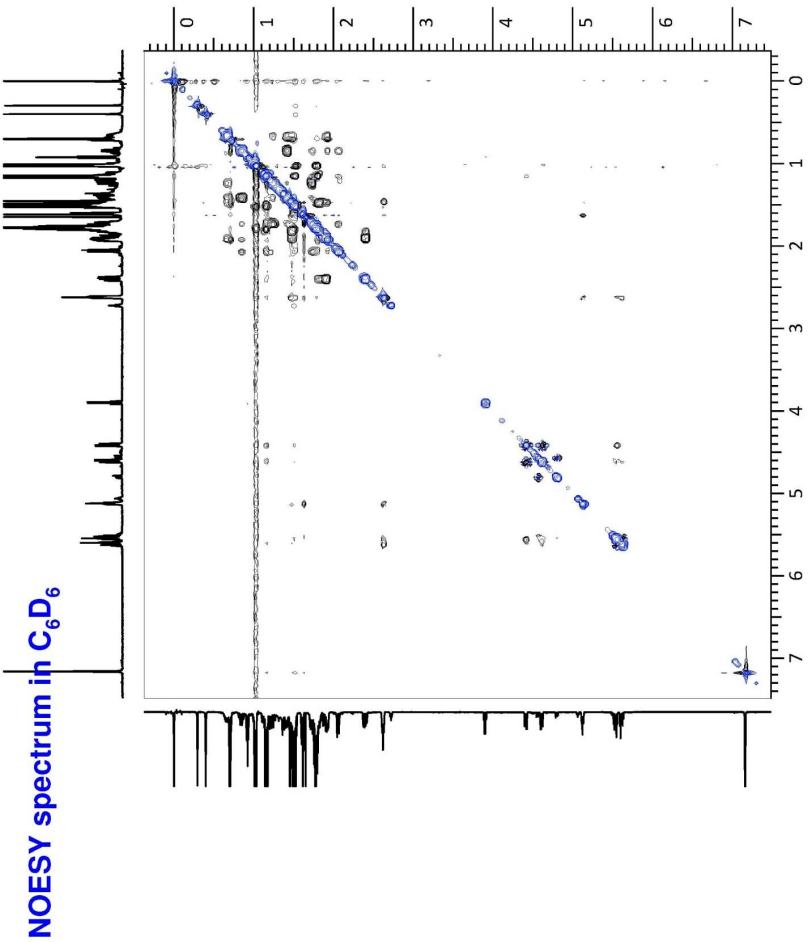
NOESY spectrum in C_6D_6
0
1
2
3
4
5
6
7

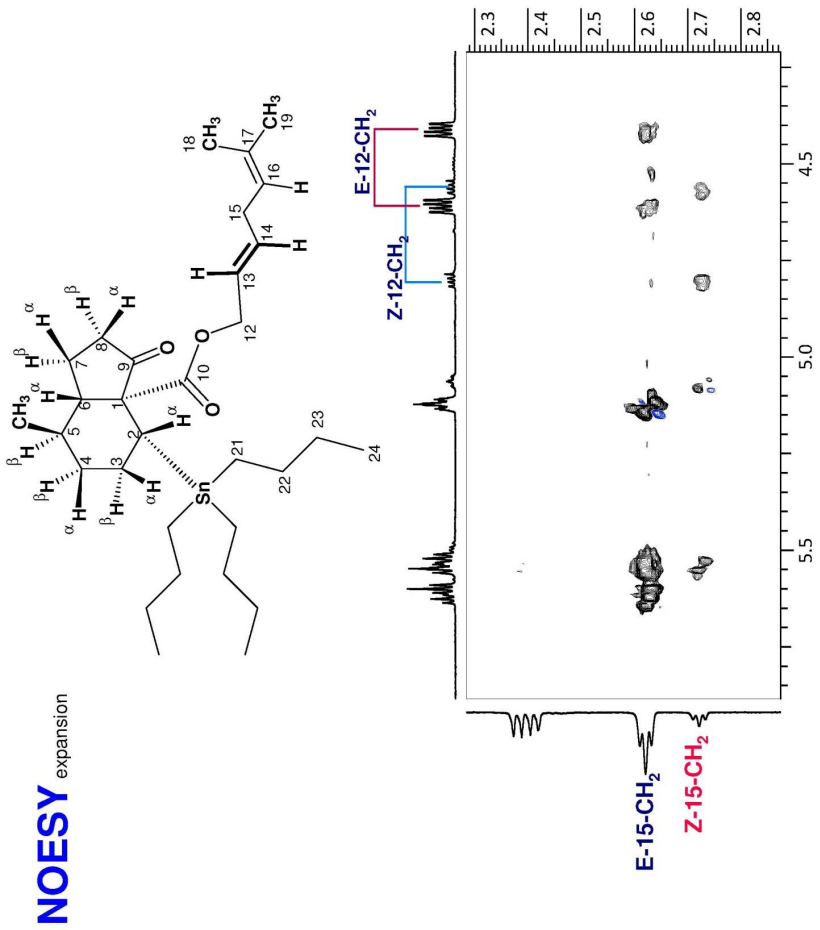
NOESY expansion
E-12-CH2
Z-12-CH2
E-15-CH2
Z-15-CH2
Sn
CH3
2.3
2.4
2.5
2.6
2.7
2.8
4.5
5.0
5.5

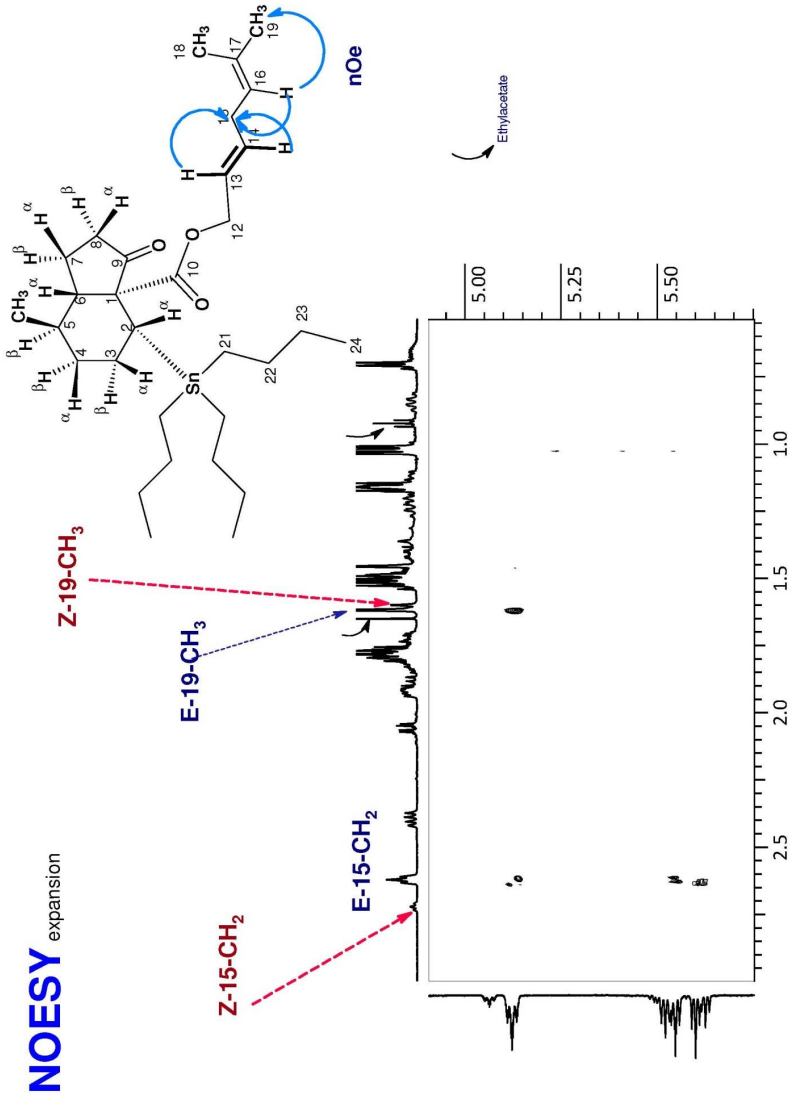
NOESY expansion
Z-19-CH3
E-19-CH3
E-15-CH2
Z-15-CH2
nOe
Ethylacetate
5.00
5.25
5.50
2.5
2.0
1.5
1.0

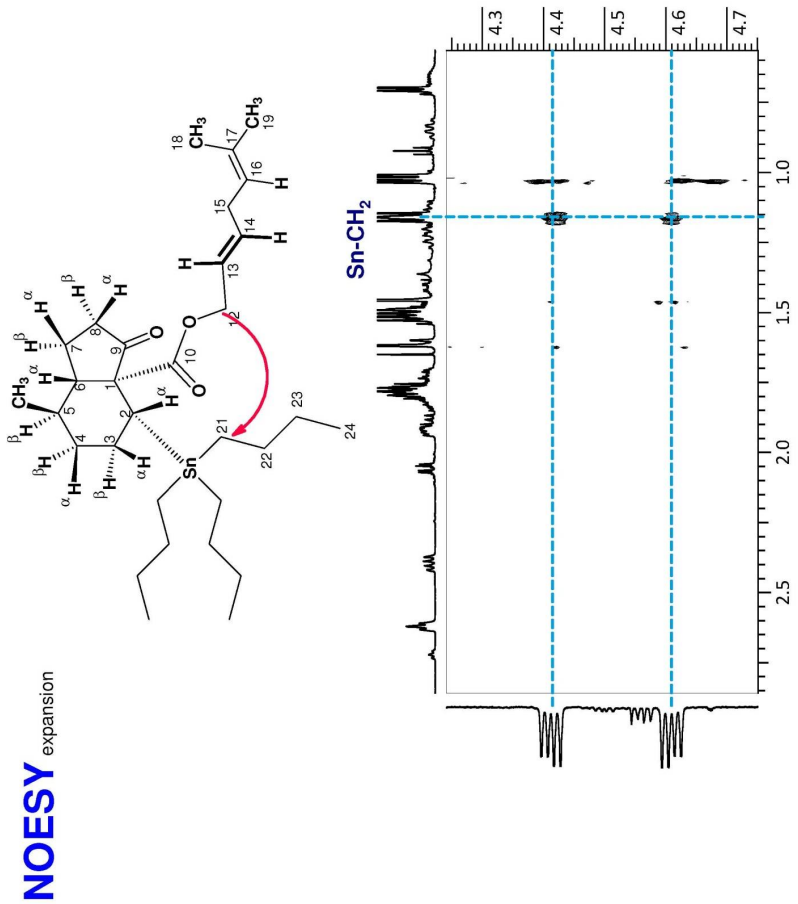
NOESY expansion
Sn-CH2
4.3
4.4
4.5
4.6
4.7
1.0
1.5
2.0
2.5

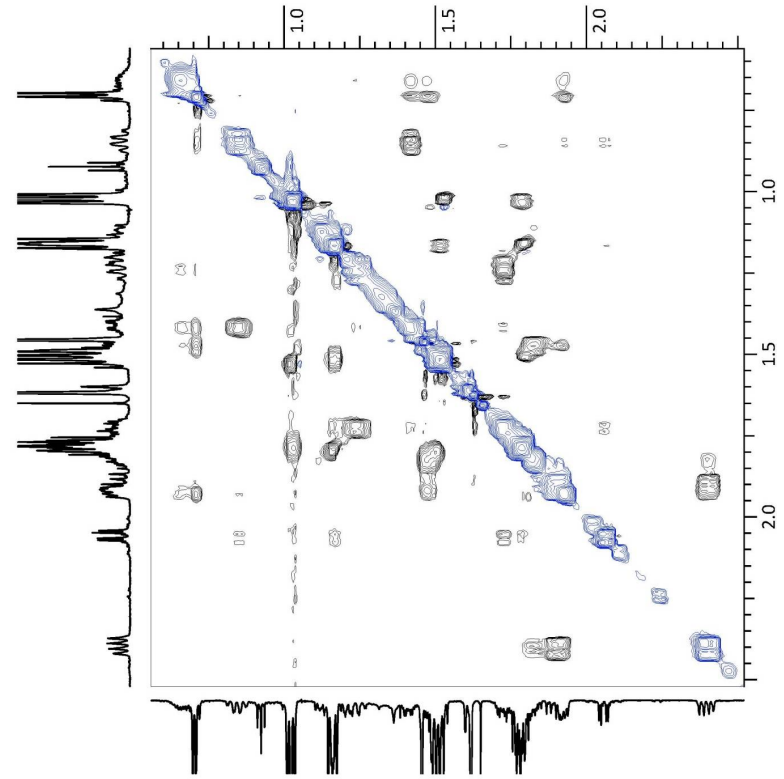

NOESY expansion

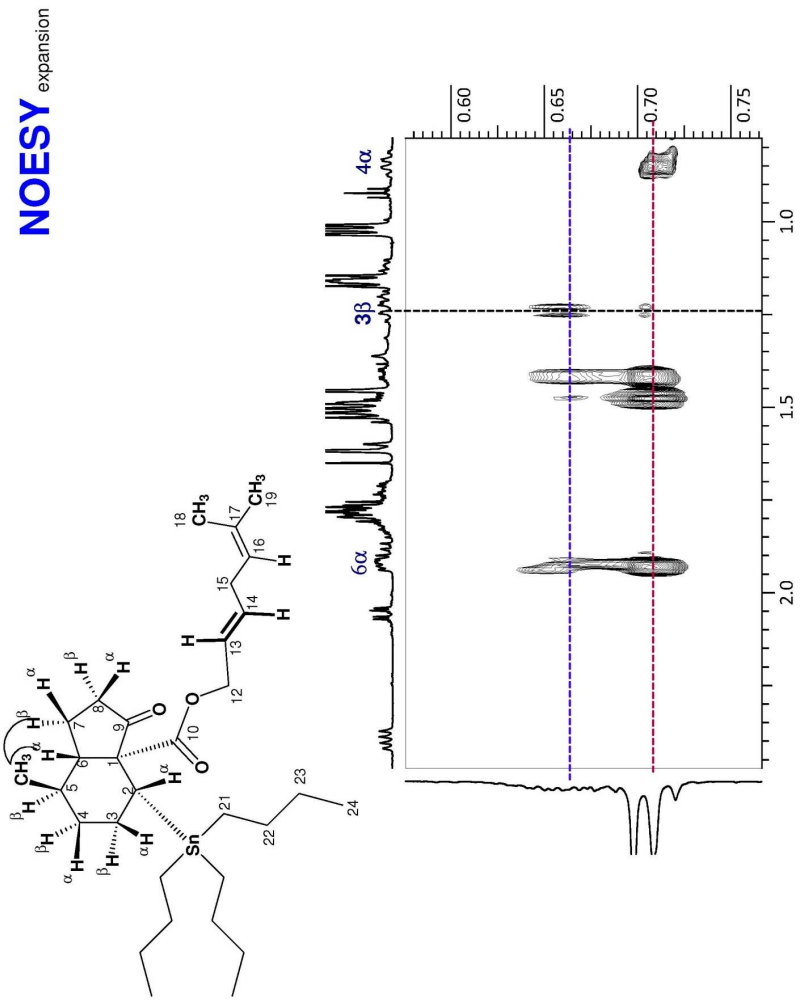
NOESY expansion
6α
3β
4α
0.60
0.65
0.70
0.75
2.0
1.5
1.0
Sn
O
CH3
CH3

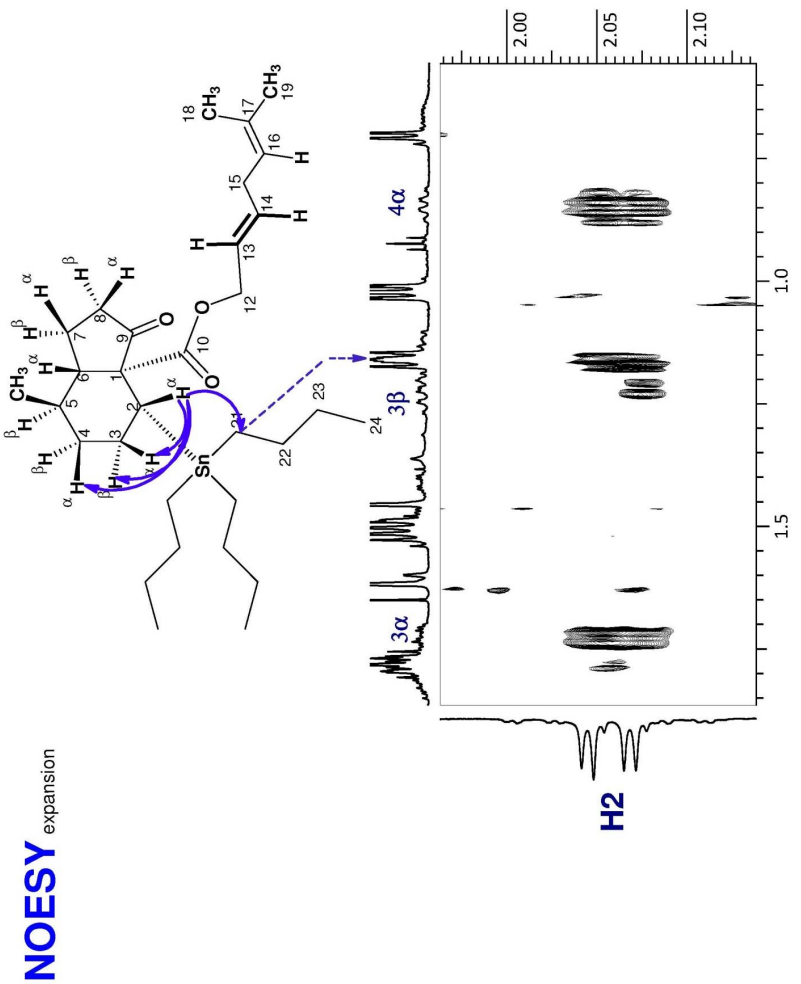
NOESY expansion
H2
3α
3β
4α
2.00
2.05
2.10
1.5
1.0
Sn

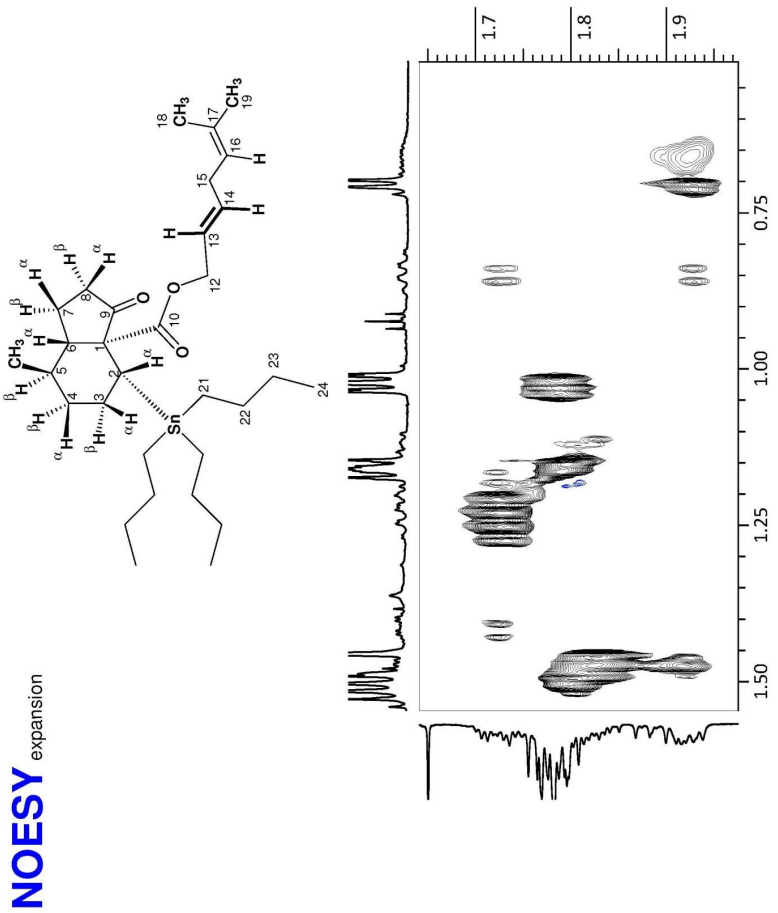
NOESY expansion
1.7
1.8
1.9
1.50
1.25
1.00
0.75

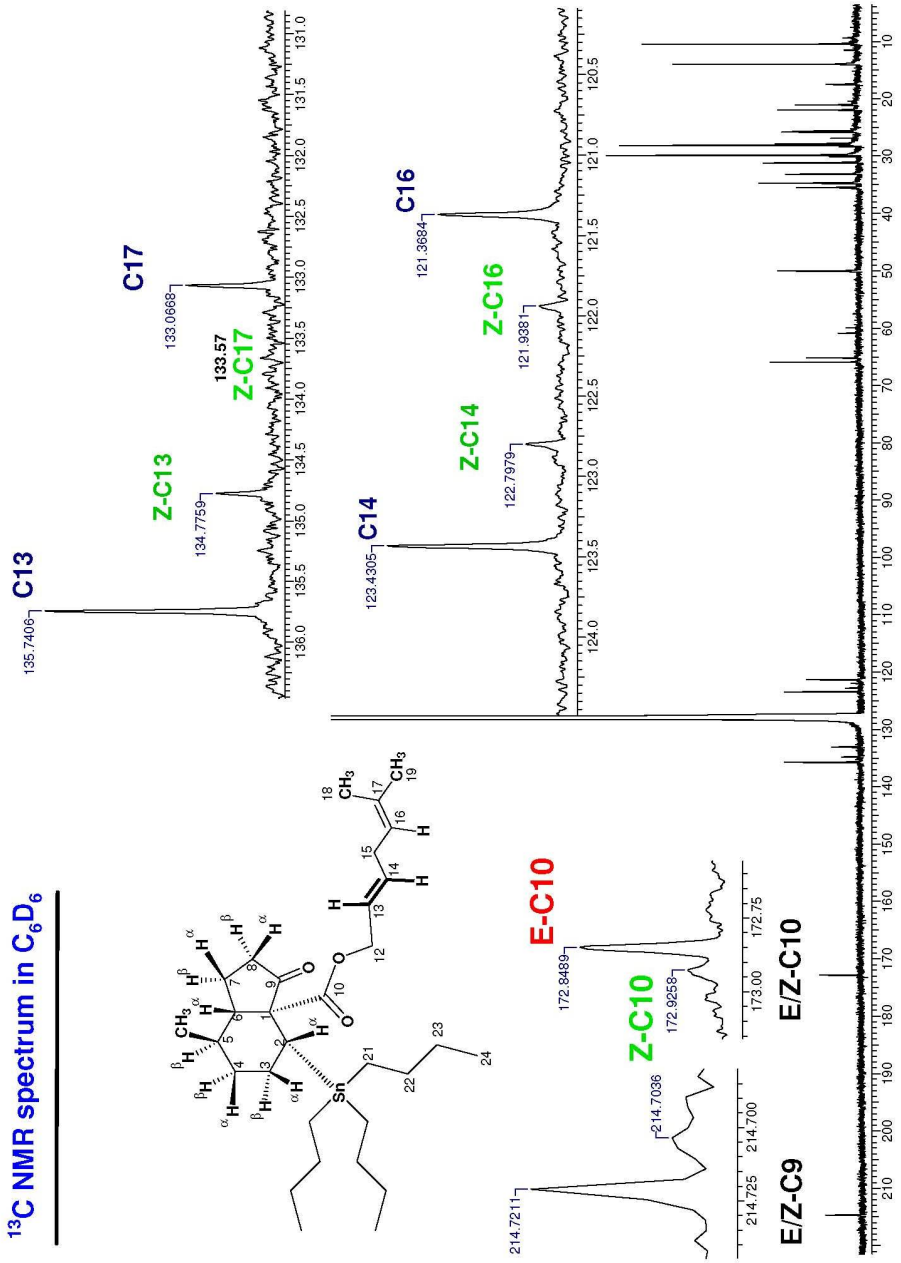
^{13}C NMR spectrum in C_6D_6
C13
135.7406
Z-C13
134.7759
C17
133.0668
133.57
Z-C17
C14
123.4305
Z-C14
122.7979
Z-C16
121.9381
C16
121.3684
E-C10
172.8489
Z-C10
172.9258
214.7211
214.7036
E/Z-C9
214.725
214.700
E/Z-C10
173.00
172.75

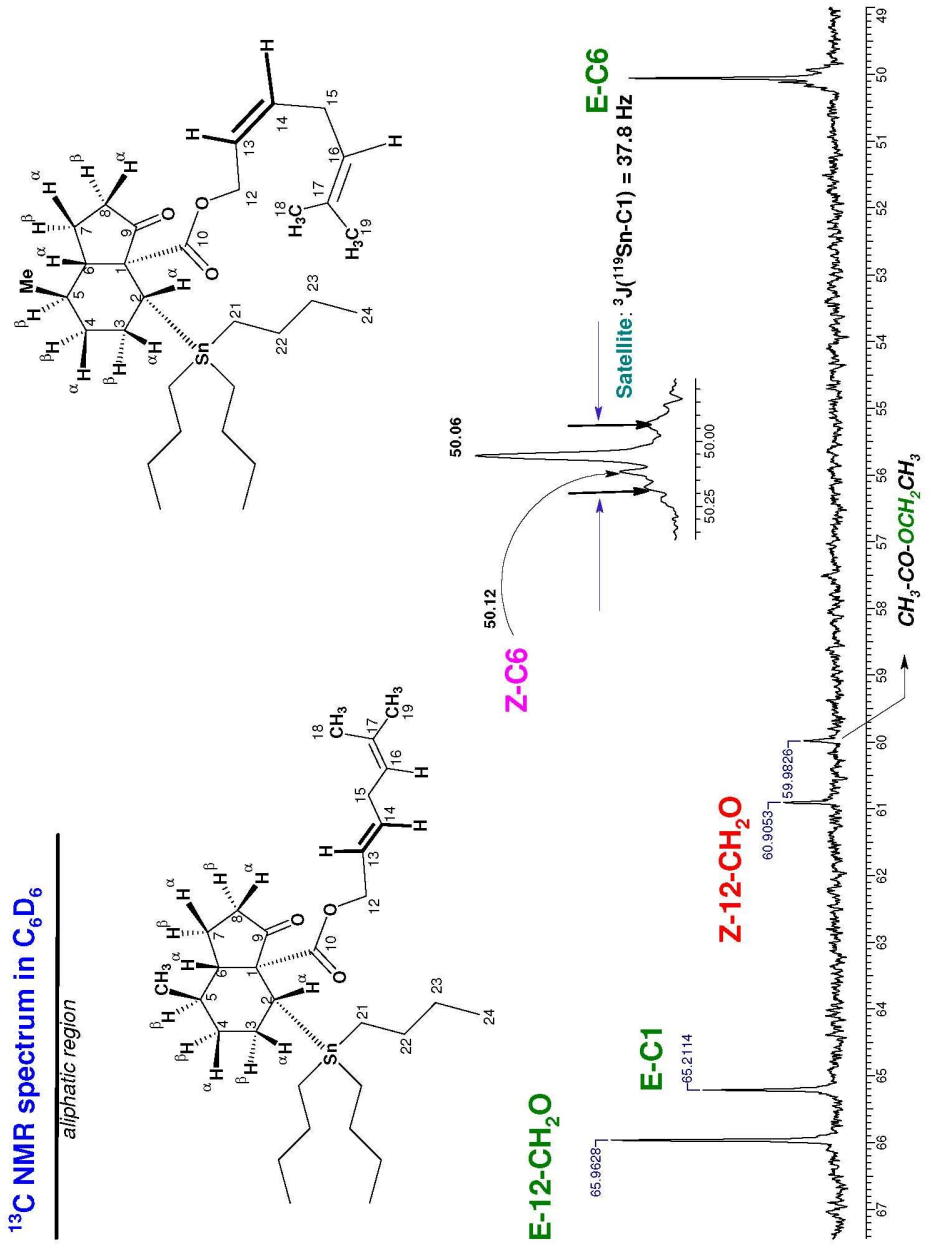
^{13}C NMR spectrum in C_6D_6
aliphatic region
E-12-CH_2O
E-C1
Z-12-CH_2O
Z-C6
E-C6
Satellite: $^3J(^{119}Sn\text{-}C1)$ = 37.8 Hz
65.9628
65.2114
60.9053
59.9826
50.06
50.12
50.25
50.00
CH_3-CO-OCH_2CH_3

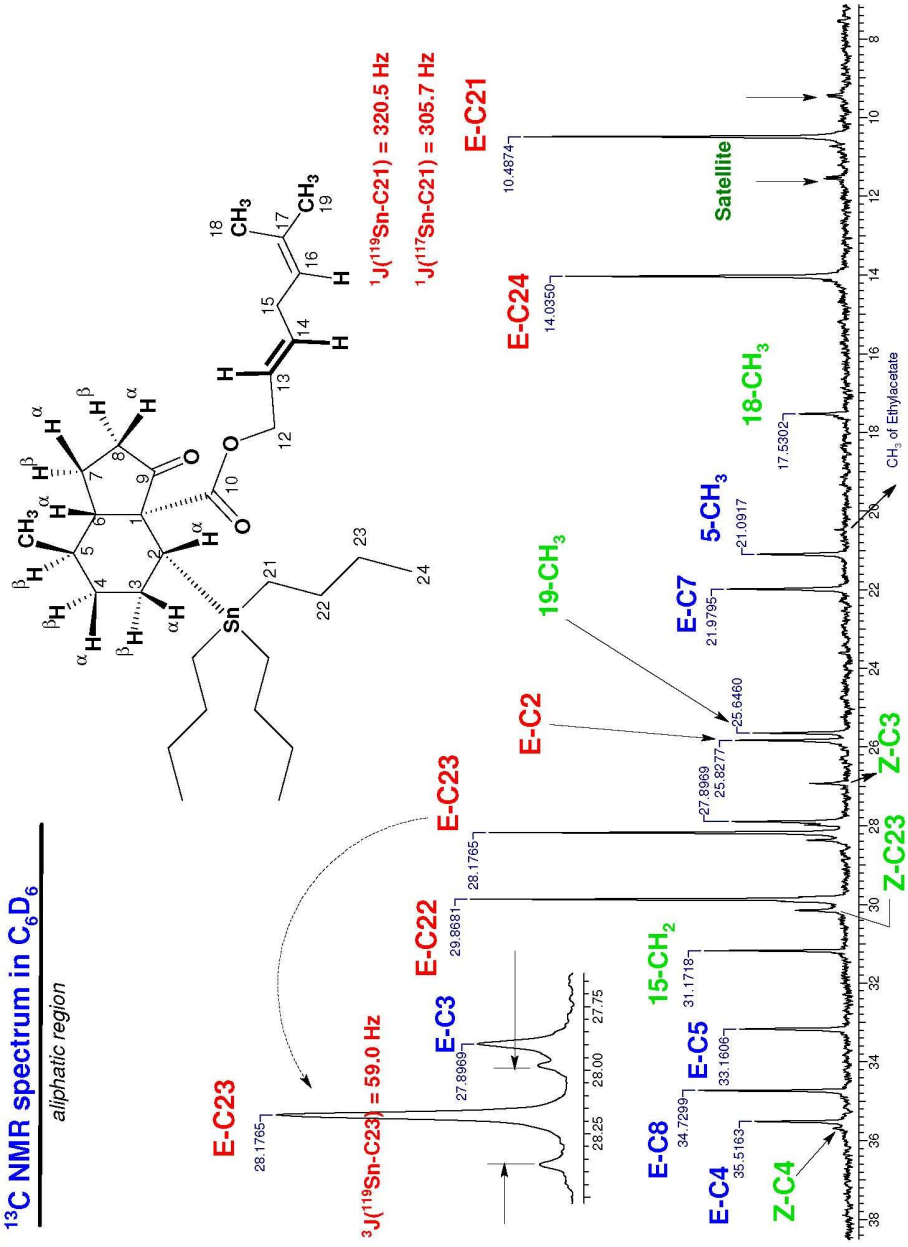
^{13}C NMR spectrum in C_6D_6
aliphatic region
$^1J(^{119}Sn-C21) = 320.5$ Hz
$^1J(^{117}Sn-C21) = 305.7$ Hz
$^3J(^{119}Sn-C23) = 59.0$ Hz
E-C23
E-C22
E-C3
E-C2
19-CH$_3$
E-C7
5-CH$_3$
18-CH$_3$
E-C21
E-C24
Satellite
15-CH$_2$
E-C8
E-C5
E-C4
Z-C4
Z-C23
Z-C3
CH$_3$ of Ethylacetate

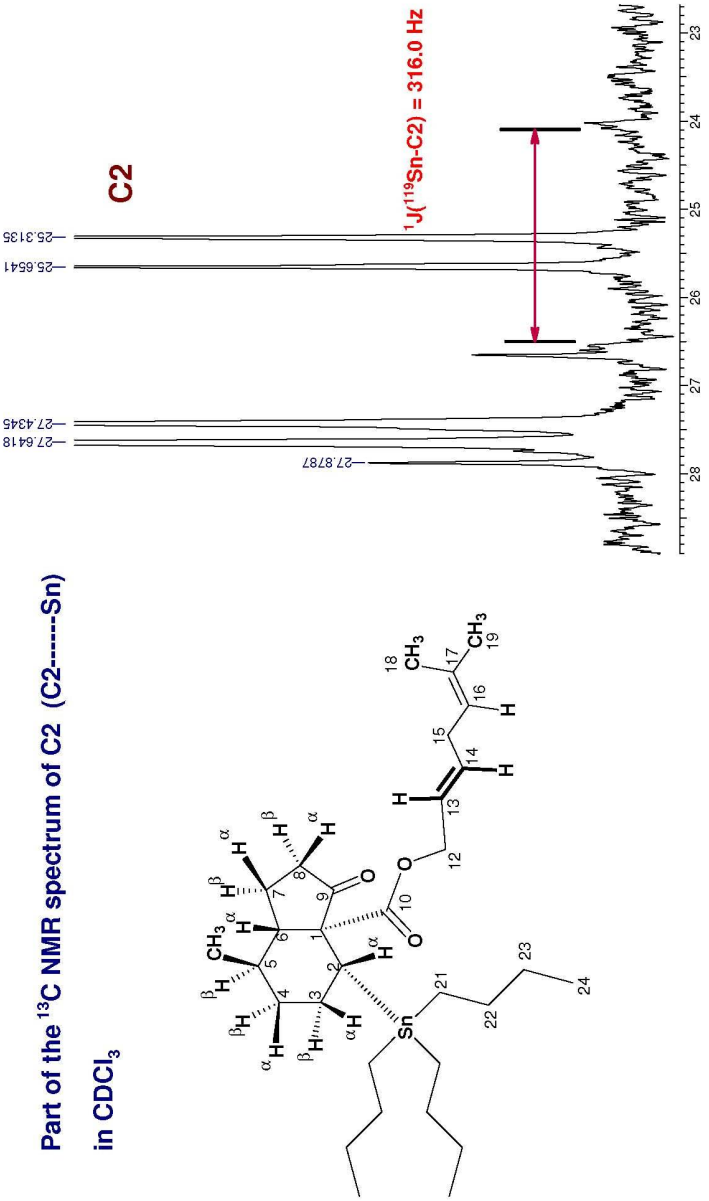
Part of the ^{13}C NMR spectrum of C2 (C2-----Sn)
in $CDCl_3$
C2
$^{1}J(^{119}Sn\text{-}C2) = 316.0$ Hz
25.3135
25.6541
27.4345
27.6418
27.8787
Sn
O
CH_3

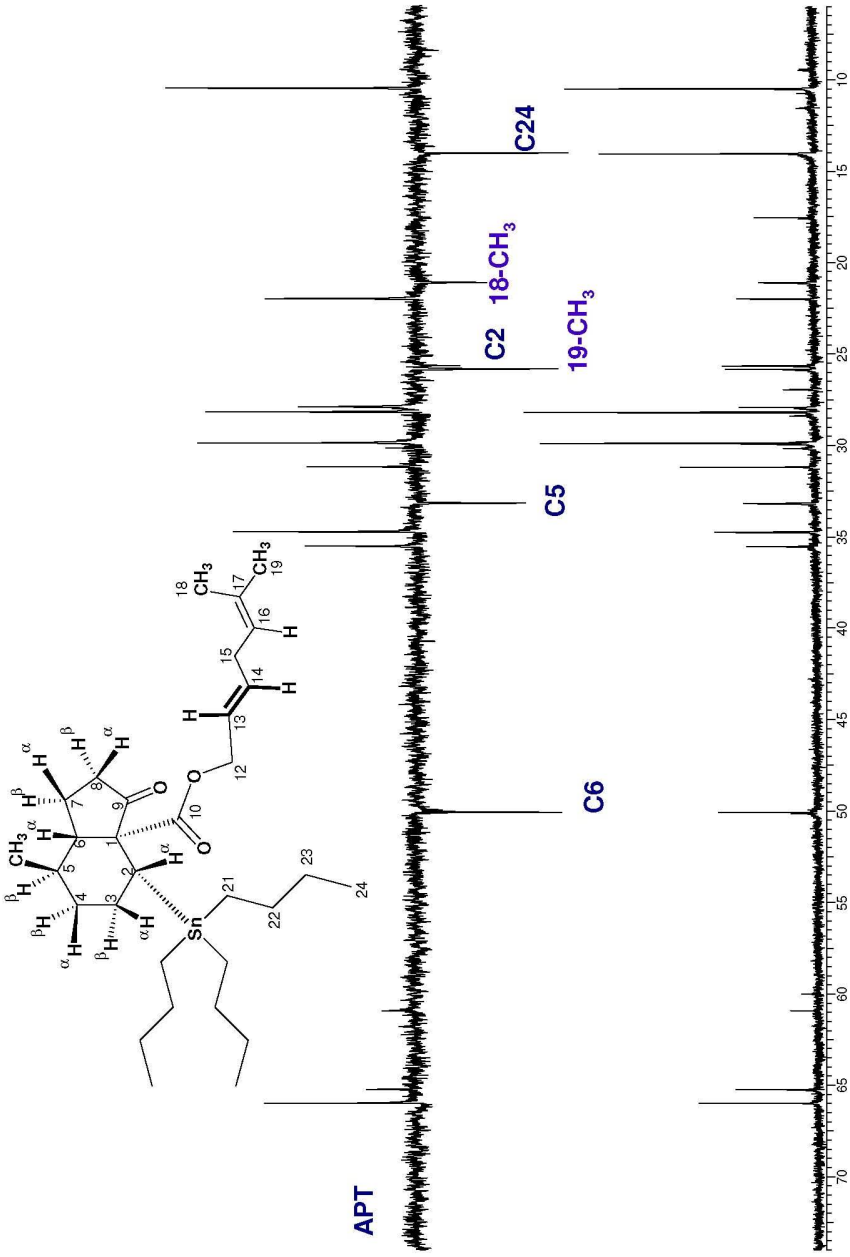
APT
C6
C5
C2
18-CH3
19-CH3
C24

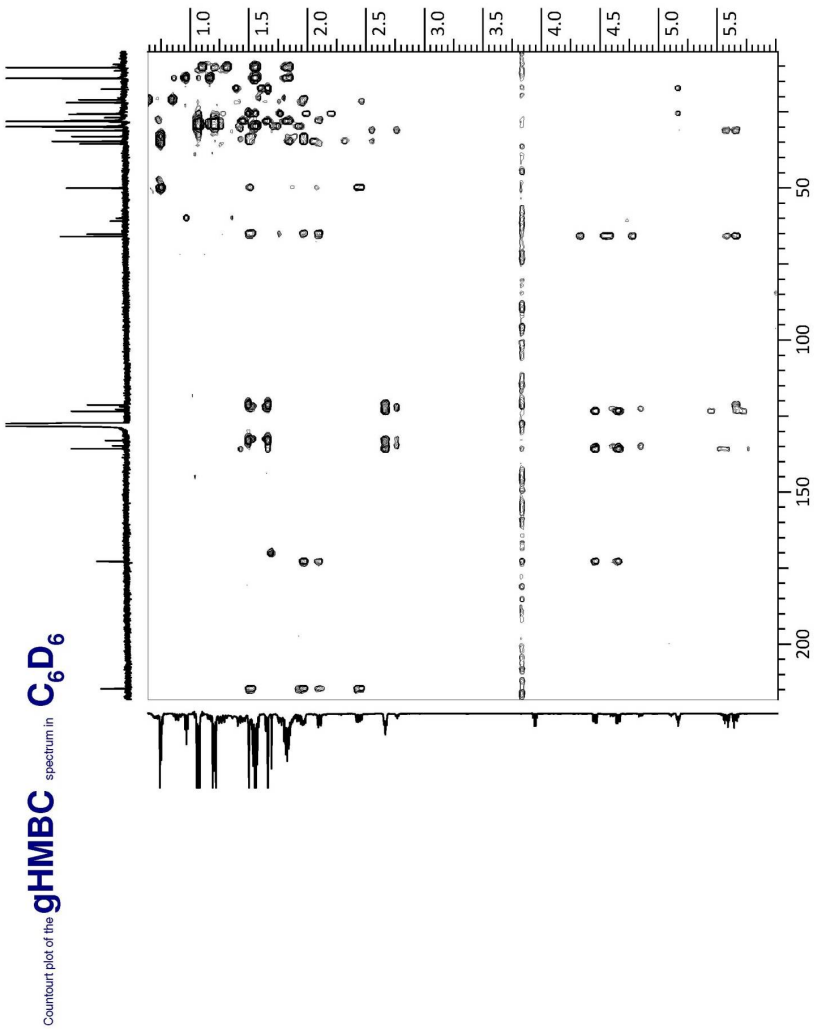
Countourt plot of the gHMBC spectrum in C6D6
1.0
1.5
2.0
2.5
3.0
3.5
4.0
4.5
5.0
5.5
50
100
150
200

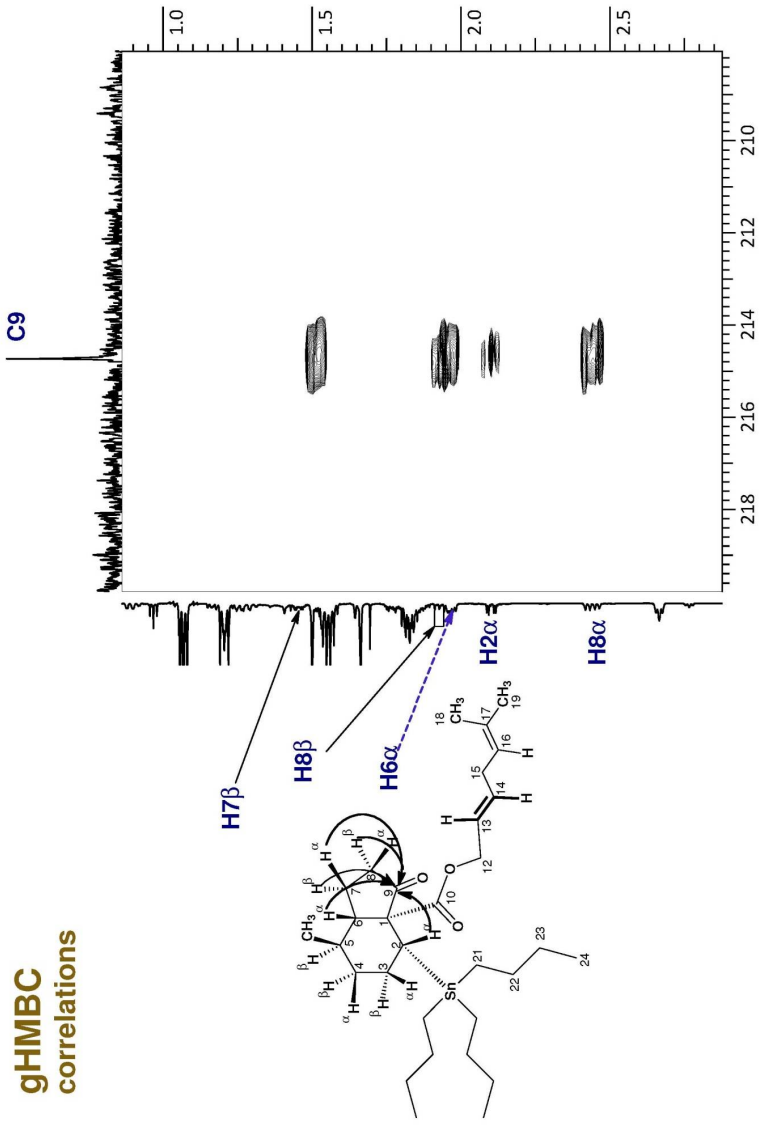
gHMBC
correlations
C9
H7β
H8β
H6α
H2α
H8α
1.0
1.5
2.0
2.5
210
212
214
216
218
Sn
O
CH3

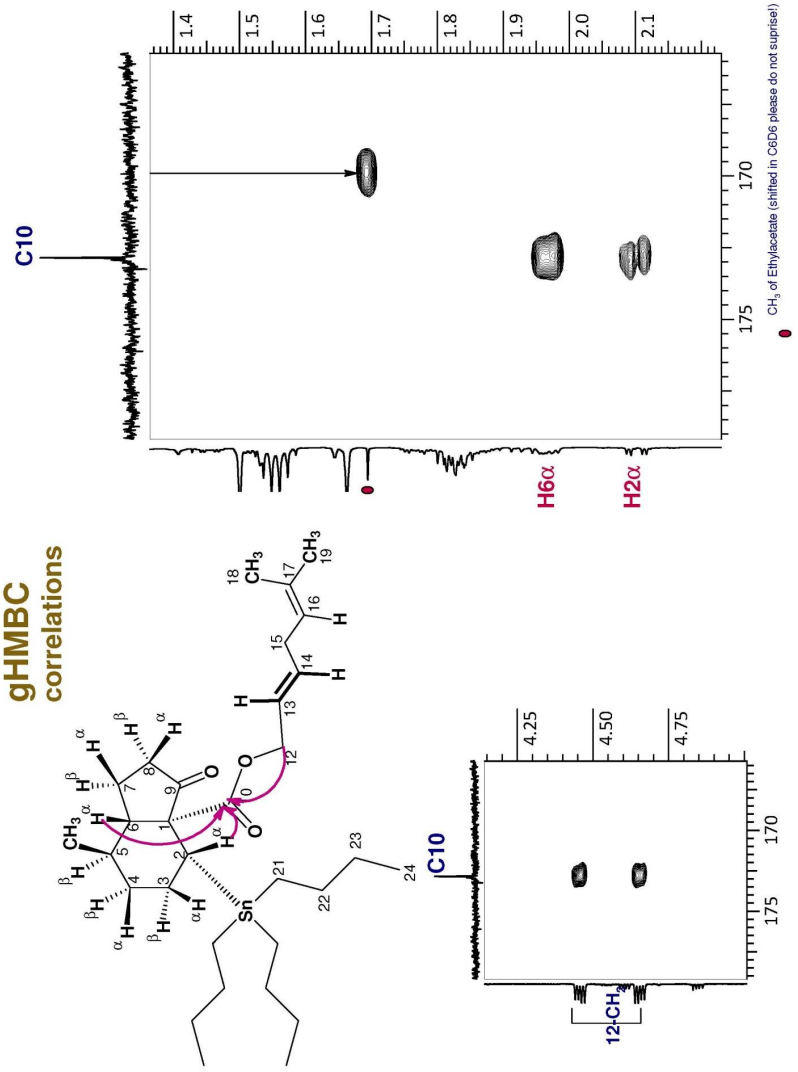
gHMBC
correlations
C10
H6α
H2α
CH3 of Ethylacetate (shifted in C6D6 please do not suprise!)
C10
12-CH2

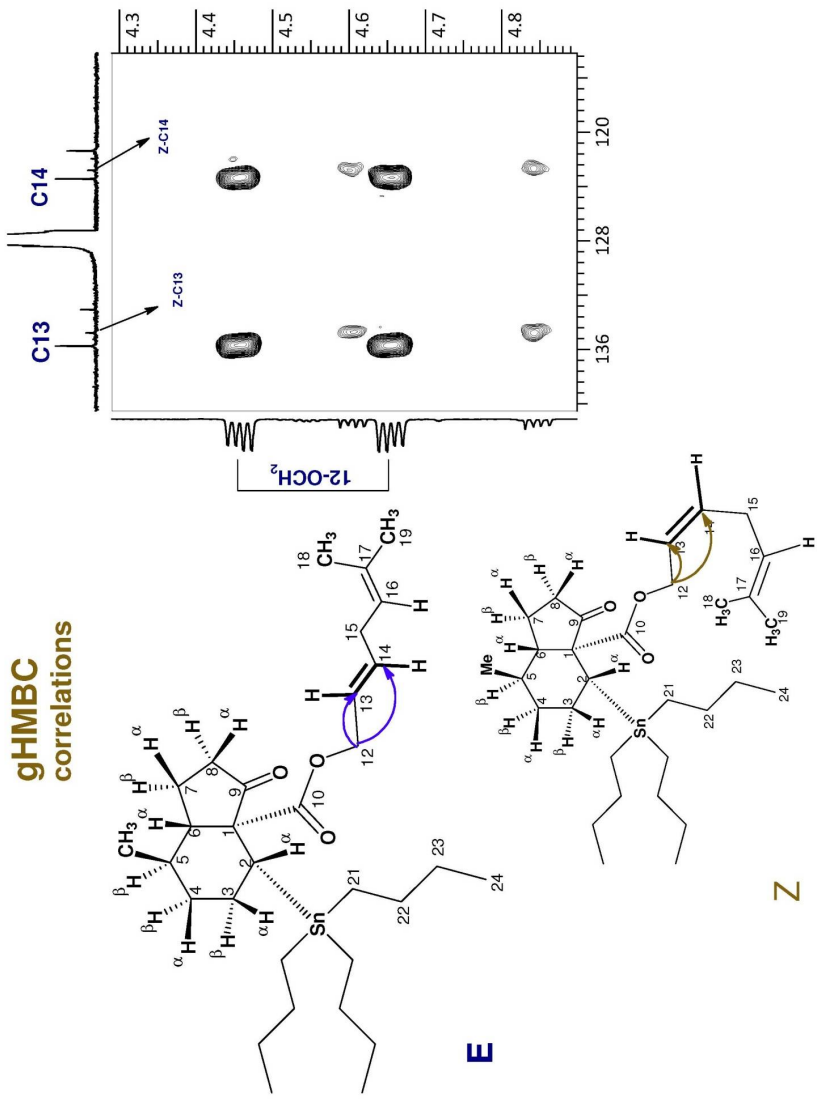
gHMBC
correlations
C14
C13
z-C14
z-C13
12-OCH2
4.3
4.4
4.5
4.6
4.7
4.8
120
128
136
E
Z

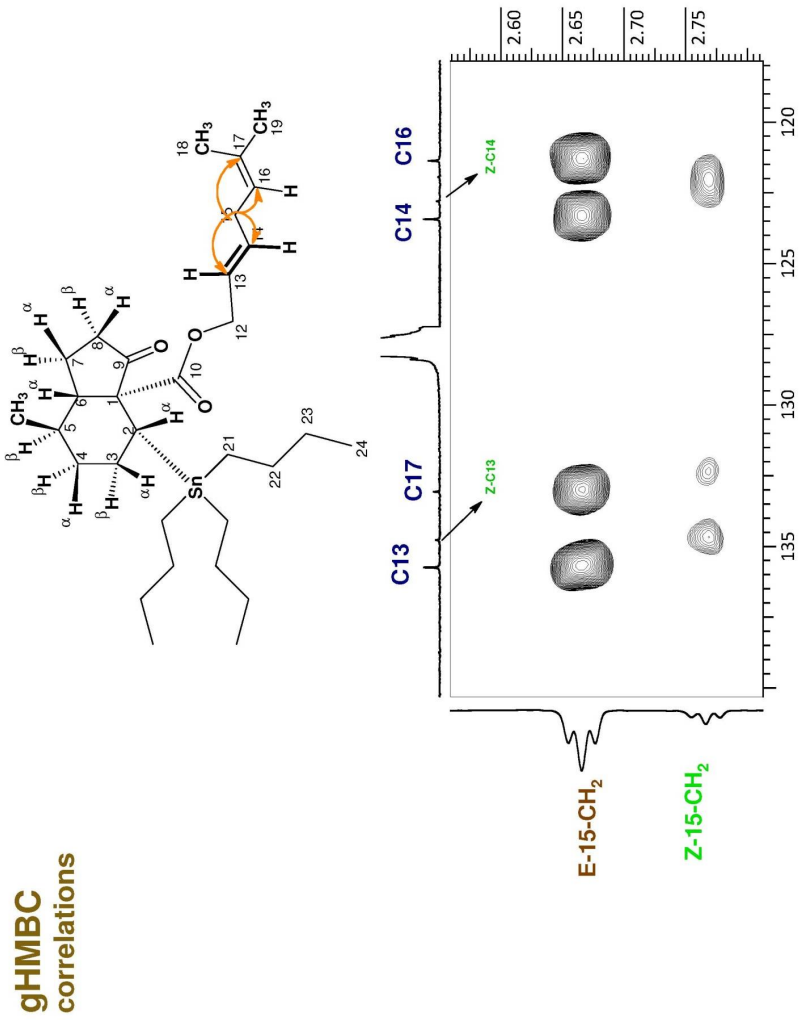
gHMBC
correlations
C13
C17
C14
C16
Z-C13
Z-C14
E-15-CH2
Z-15-CH2
2.60
2.65
2.70
2.75
120
125
130
135

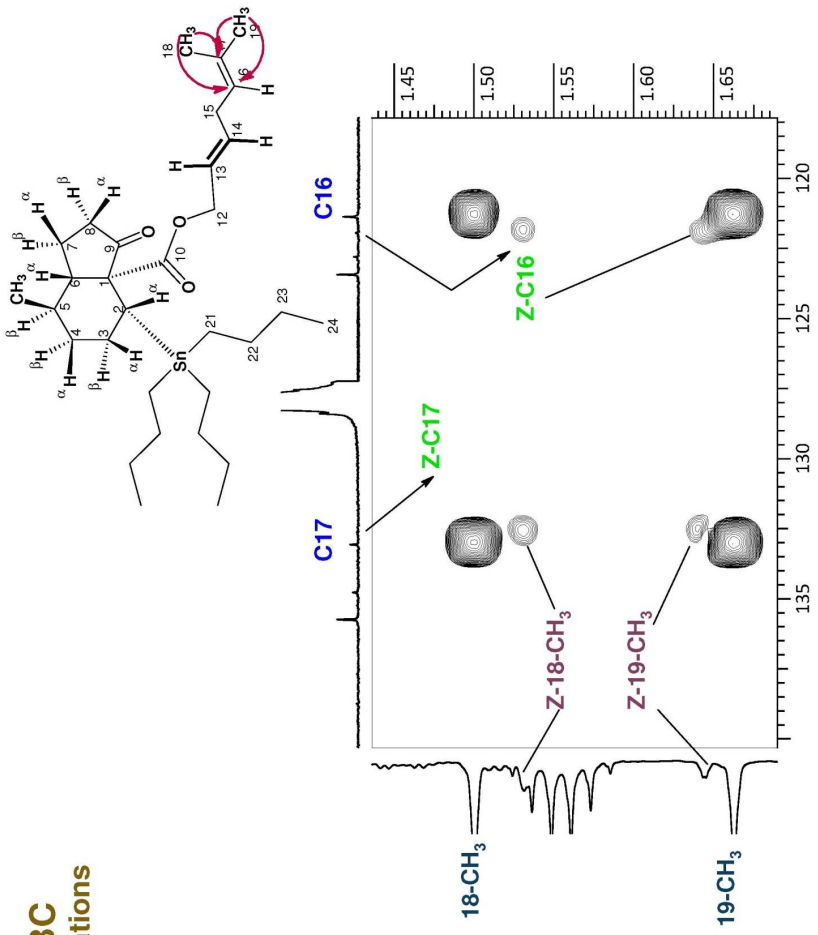
gHMBC
correlations
C16
C17
Z-C16
Z-C17
Z-18-CH3
Z-19-CH3
18-CH3
19-CH3
1.45
1.50
1.55
1.60
1.65
120
125
130
135

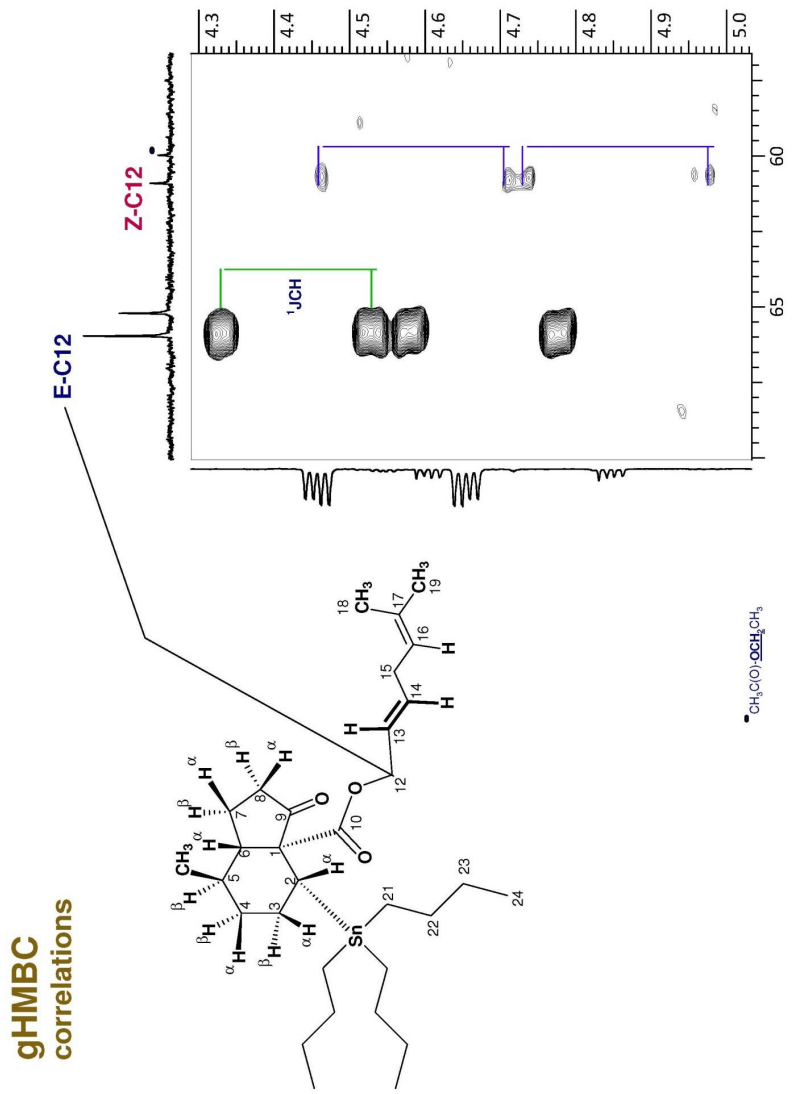
gHMBC
correlations
E-C12
Z-C12
^{1}JCH
4.3
4.4
4.5
4.6
4.7
4.8
4.9
5.0
60
65
Sn
O
CH$_3$
•CH$_3$C(O)-OCH$_2$CH$_3$

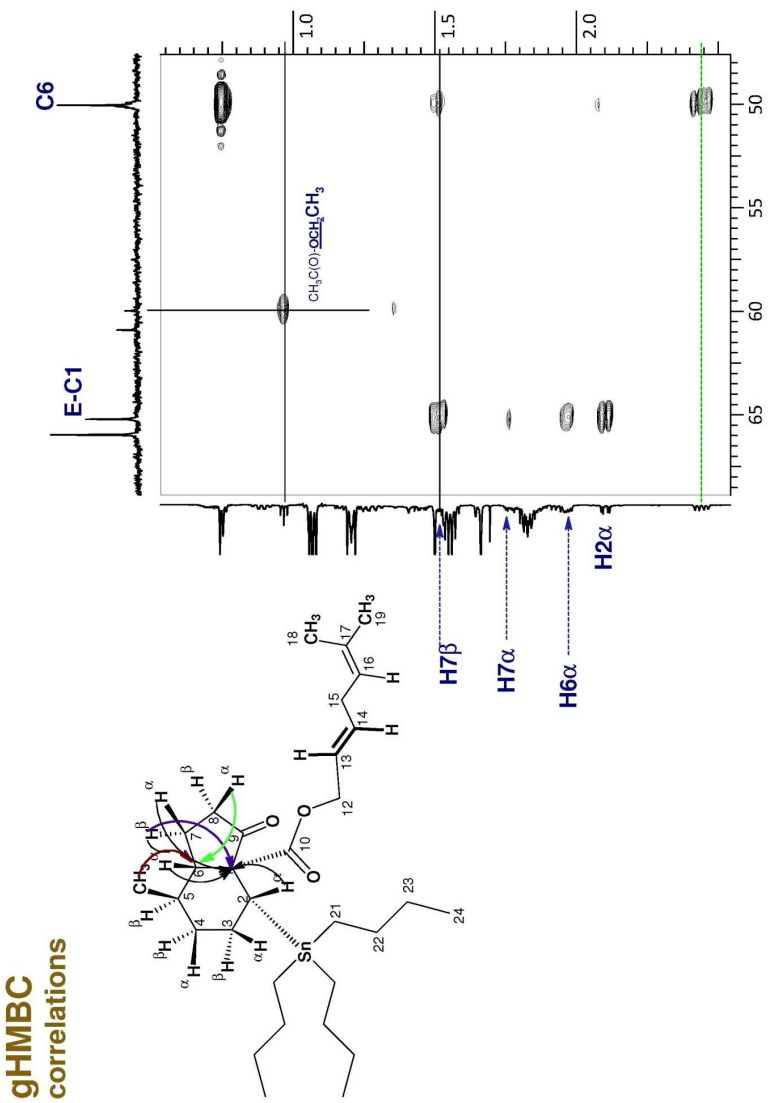
gHMBC
correlations
C6
E-C1
1.0
1.5
2.0
50
55
60
65
H7β
H7α
H6α
H2α
Sn

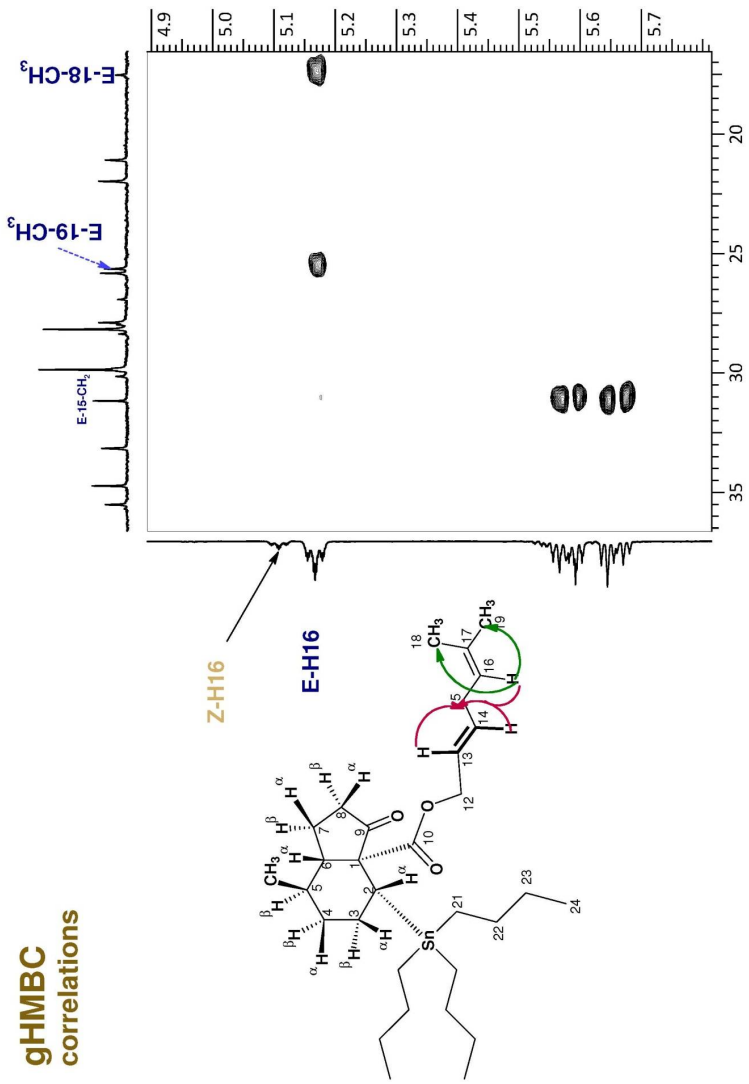
gHMBC
correlations
Z-H16
E-H16
E-18-CH3
E-19-CH3
E-15-CH2
4.9
5.0
5.1
5.2
5.3
5.4
5.5
5.6
5.7
20
25
30
35
Sn
O
CH3

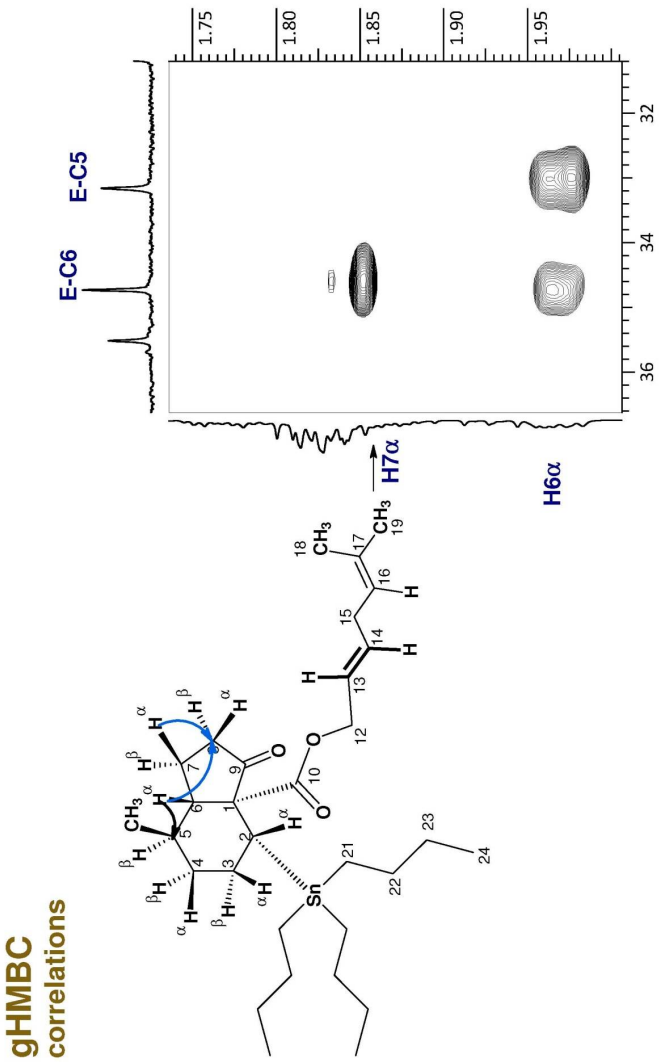
gHMBC
correlations
E-C6
E-C5
H7α
H6α
1.75
1.80
1.85
1.90
1.95
32
34
36
Sn
O
CH3

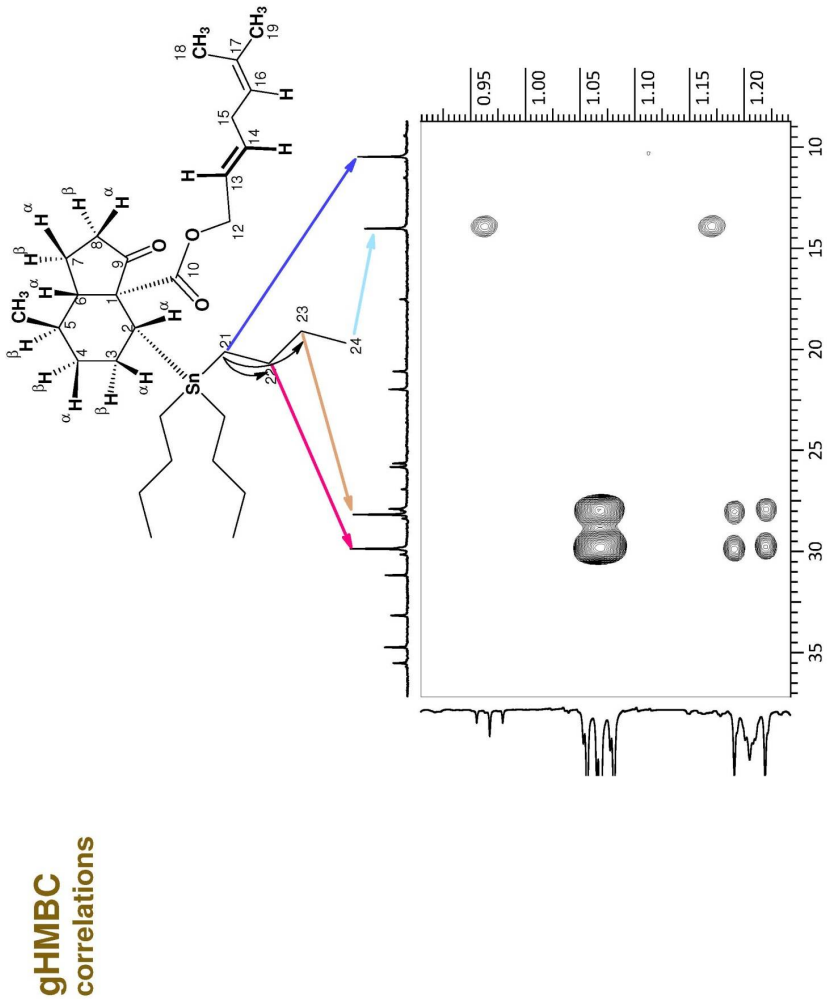
gHMBC
correlations
0.95
1.00
1.05
1.10
1.15
1.20
10
15
20
25
30
35

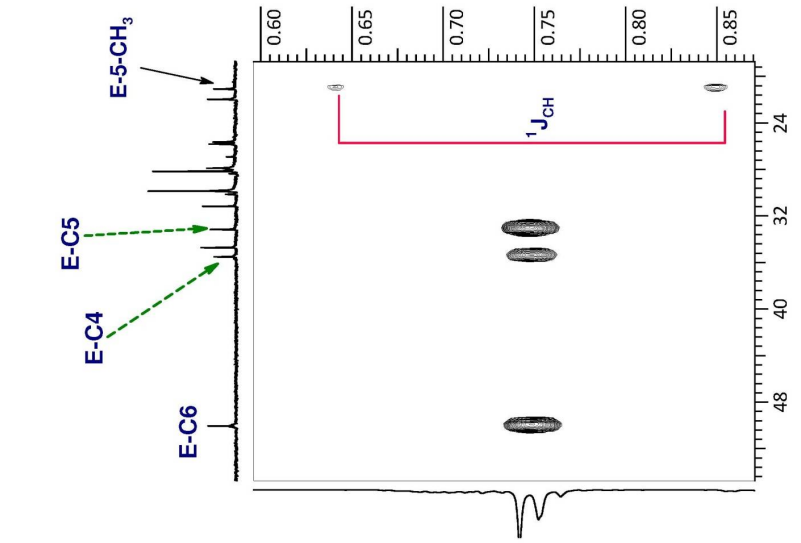

gHMBC
correlations

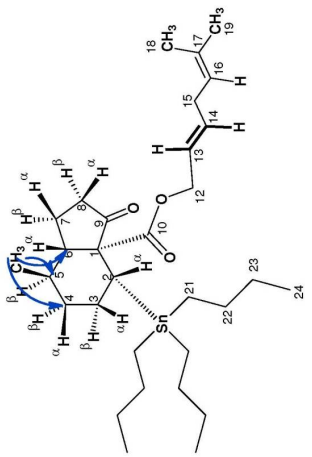

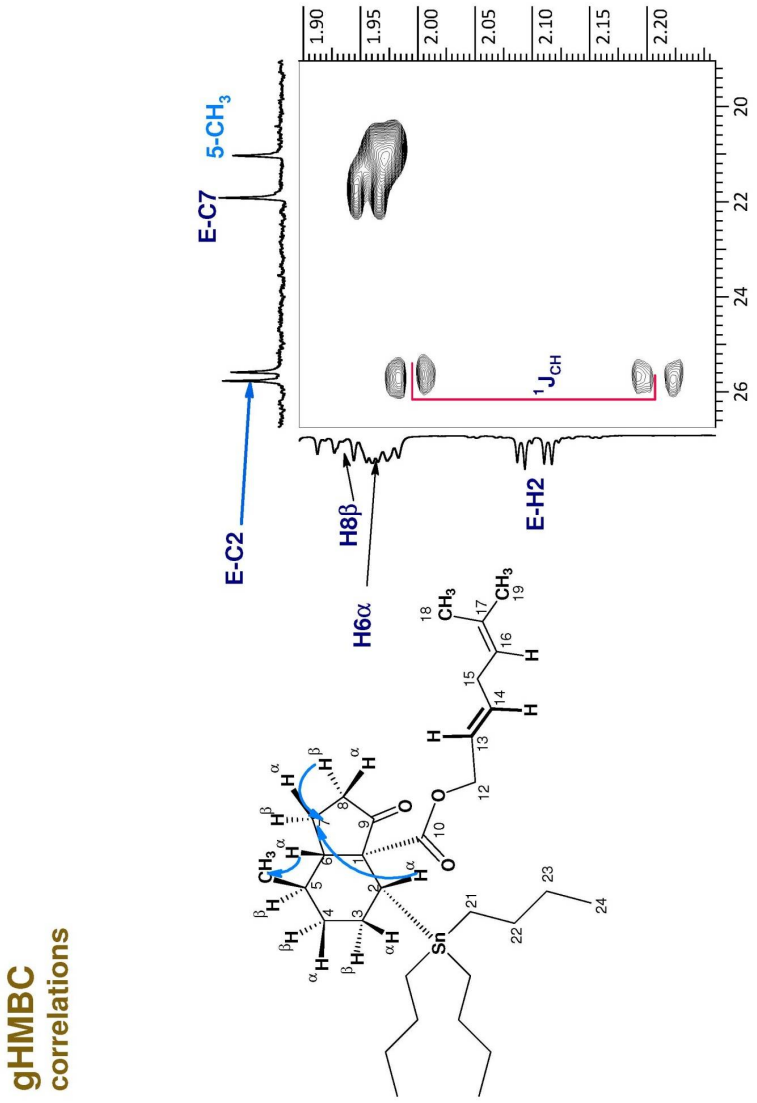
gHMBC
correlations
E-C2
E-C7
5-CH3
H8β
H6α
E-H2
1JCH
1.90
1.95
2.00
2.05
2.10
2.15
2.20
20
22
24
26
Sn

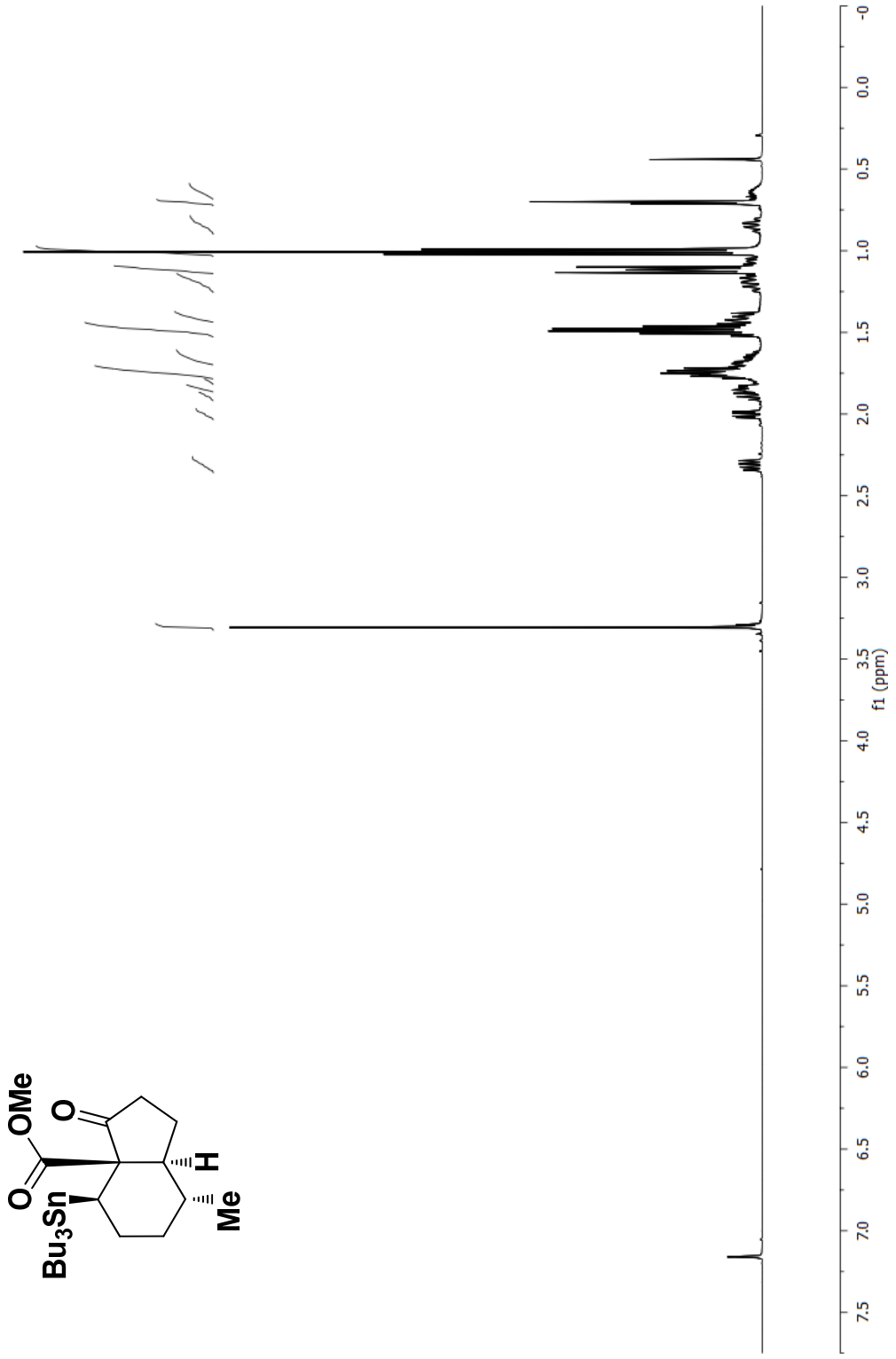
OMe
O
O
H
Bu3Sn
Me
f1 (ppm)

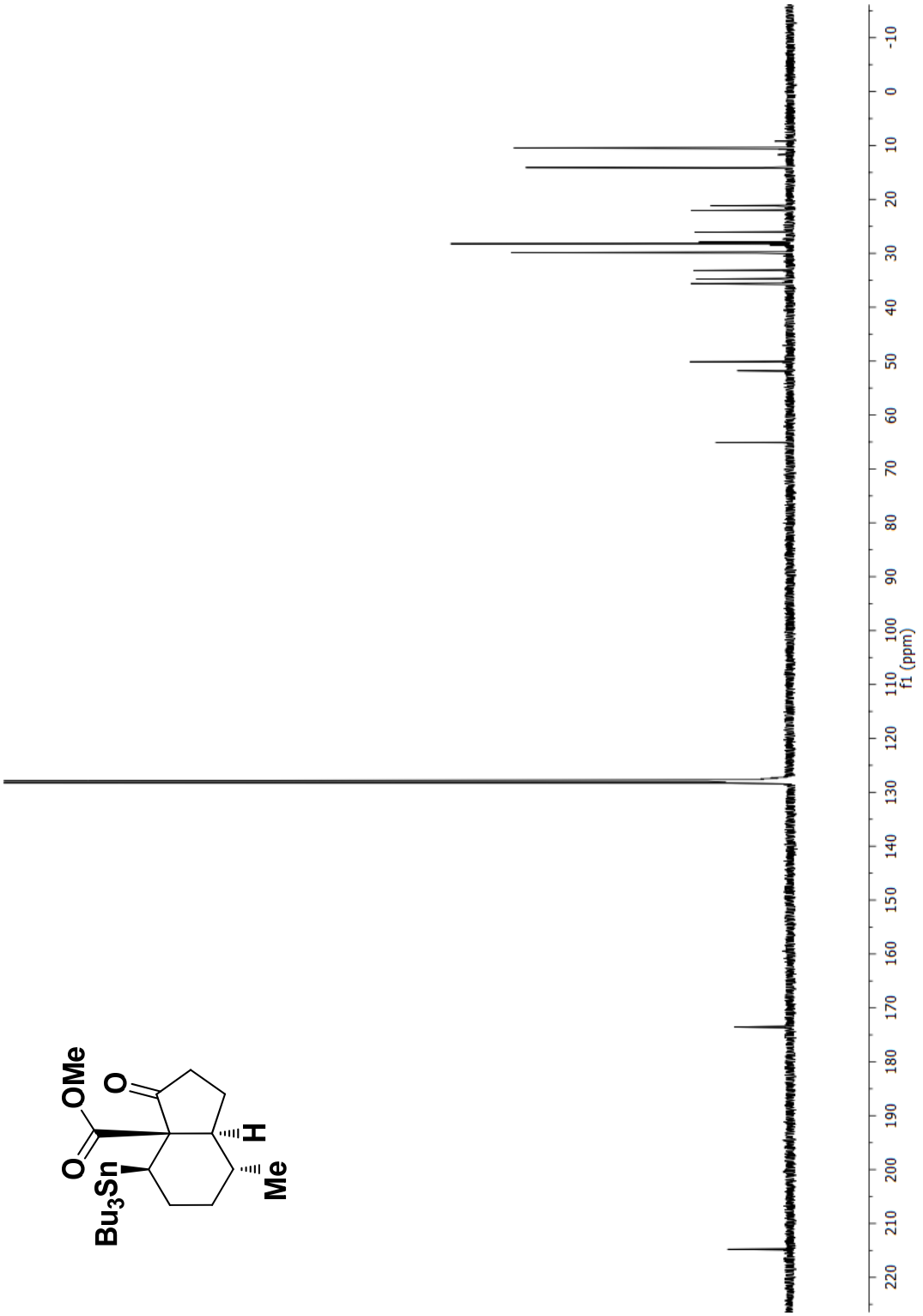
OMe
O
O
Bu3Sn
H
Me
f1 (ppm)

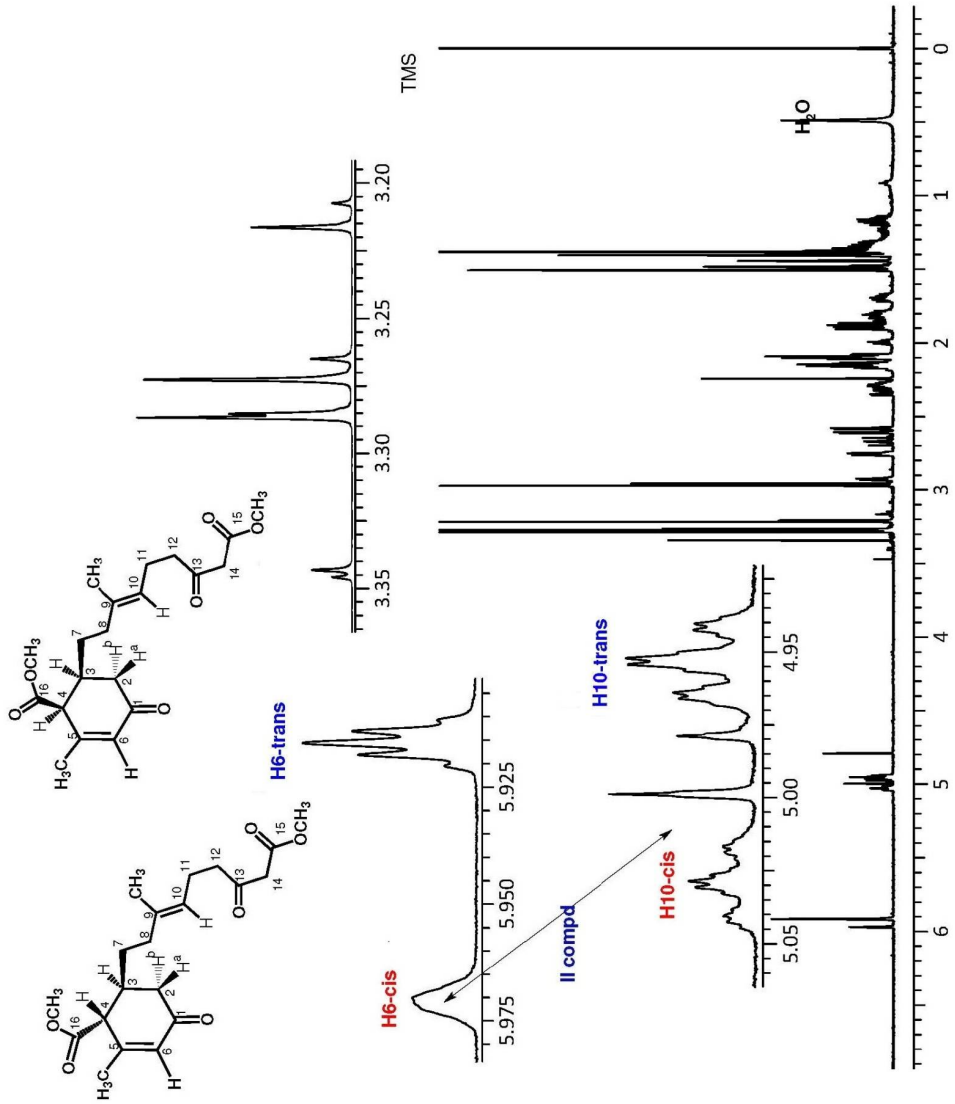
H6-trans
H6-cis
II compd
H10-trans
H10-cis
TMS
H2O
3.35
3.30
3.25
3.20
5.975
5.950
5.925
5.05
5.00
4.95
6
5
4
3
2
1
0

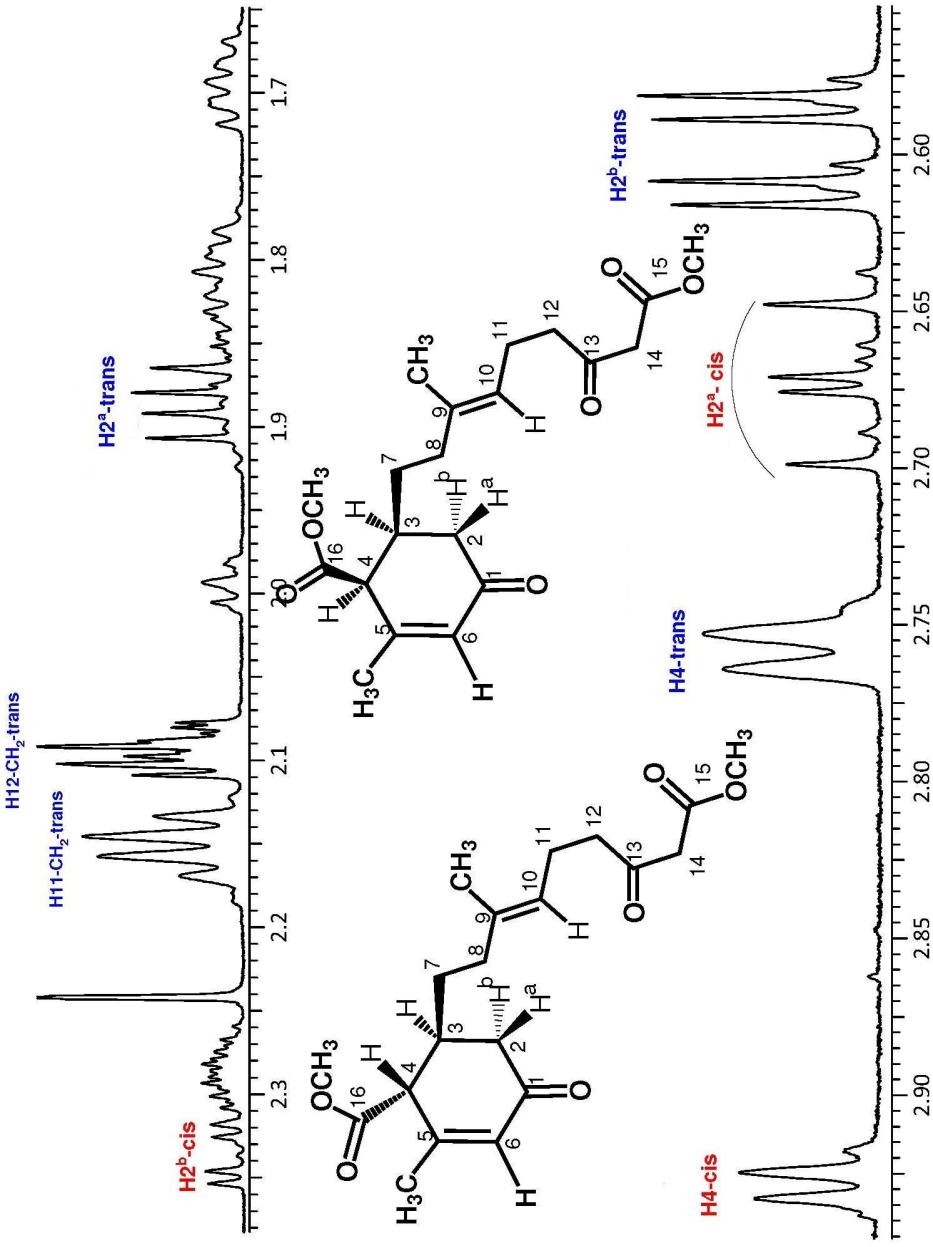
H12-CH2-trans
H11-CH2-trans
H2a-trans
H2b-cis
H2b-trans
H2a- cis
H4-trans
H4-cis
OCH3
CH3
H3C
1.7
1.8
1.9
2.1
2.2
2.3
2.60
2.65
2.70
2.75
2.80
2.85
2.90

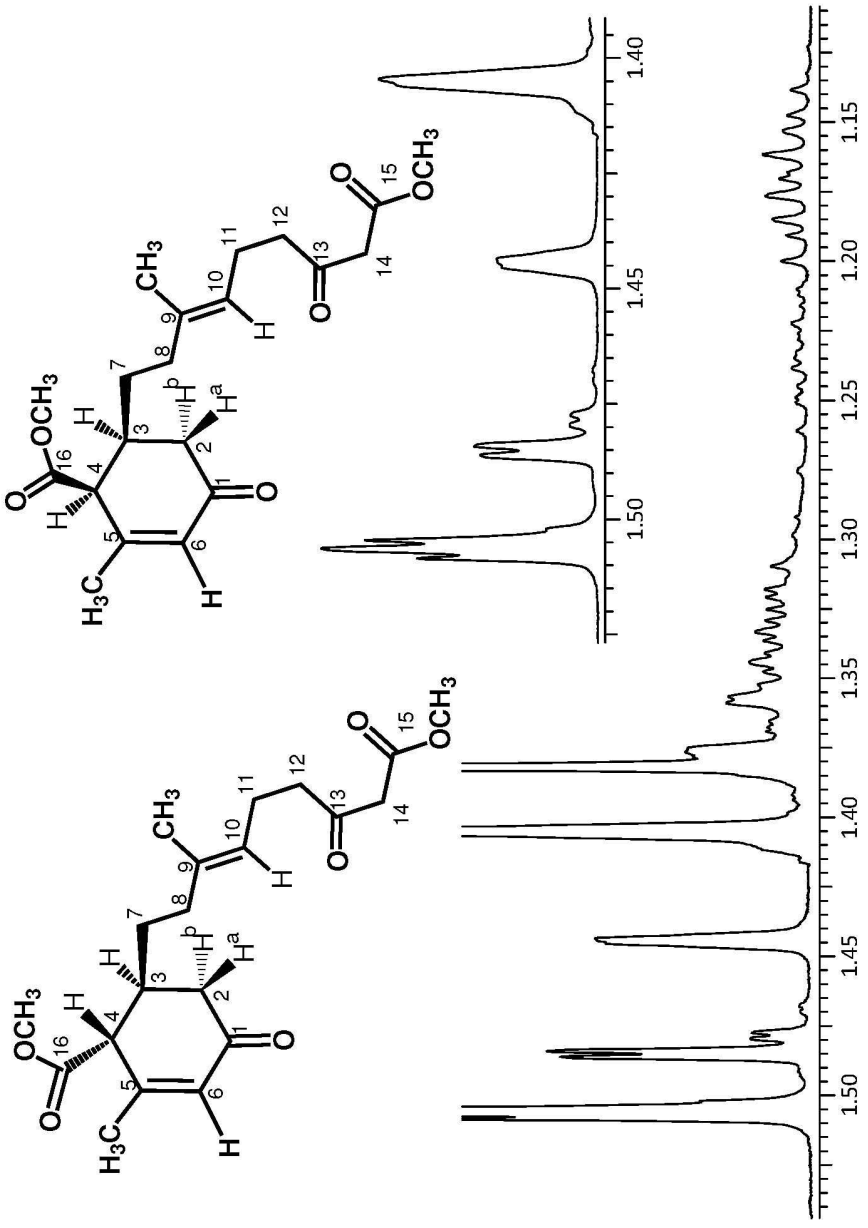
OCH3
O
H
4
16
5
H3C
6
H
3
7
2
Ha
Hb
1
O
8
9
CH3
10
H
11
12
13
O
14
15
O
OCH3
1.50
1.45
1.40
1.35
1.30
1.25
1.20
1.15

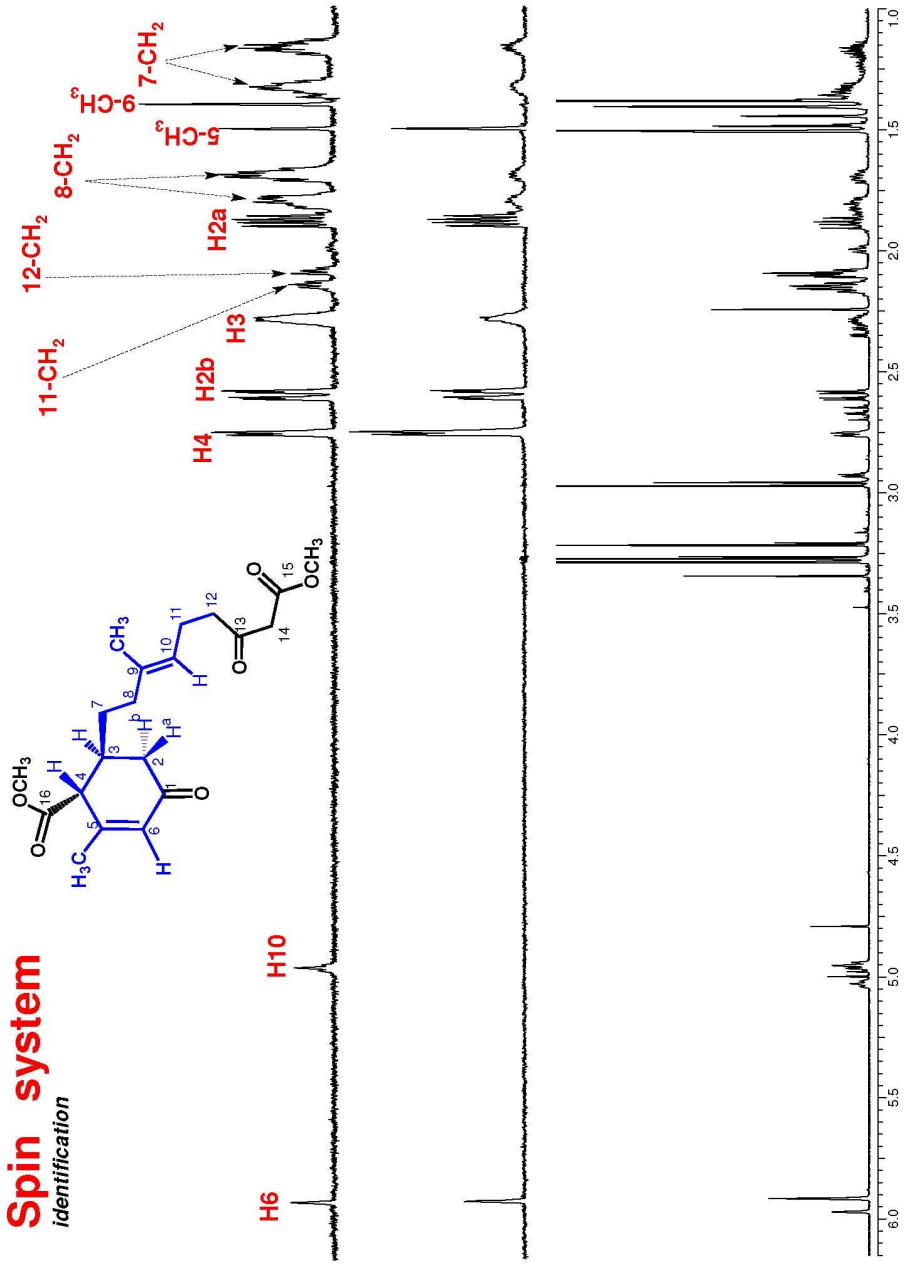
Spin system
identification
H6
H10
H4
H2b
H3
H2a
11-CH2
12-CH2
8-CH2
5-CH3
9-CH3
7-CH2
OCH3
CH3
H3C
6.0
5.5
5.0
4.5
4.0
3.5
3.0
2.5
2.0
1.5
1.0

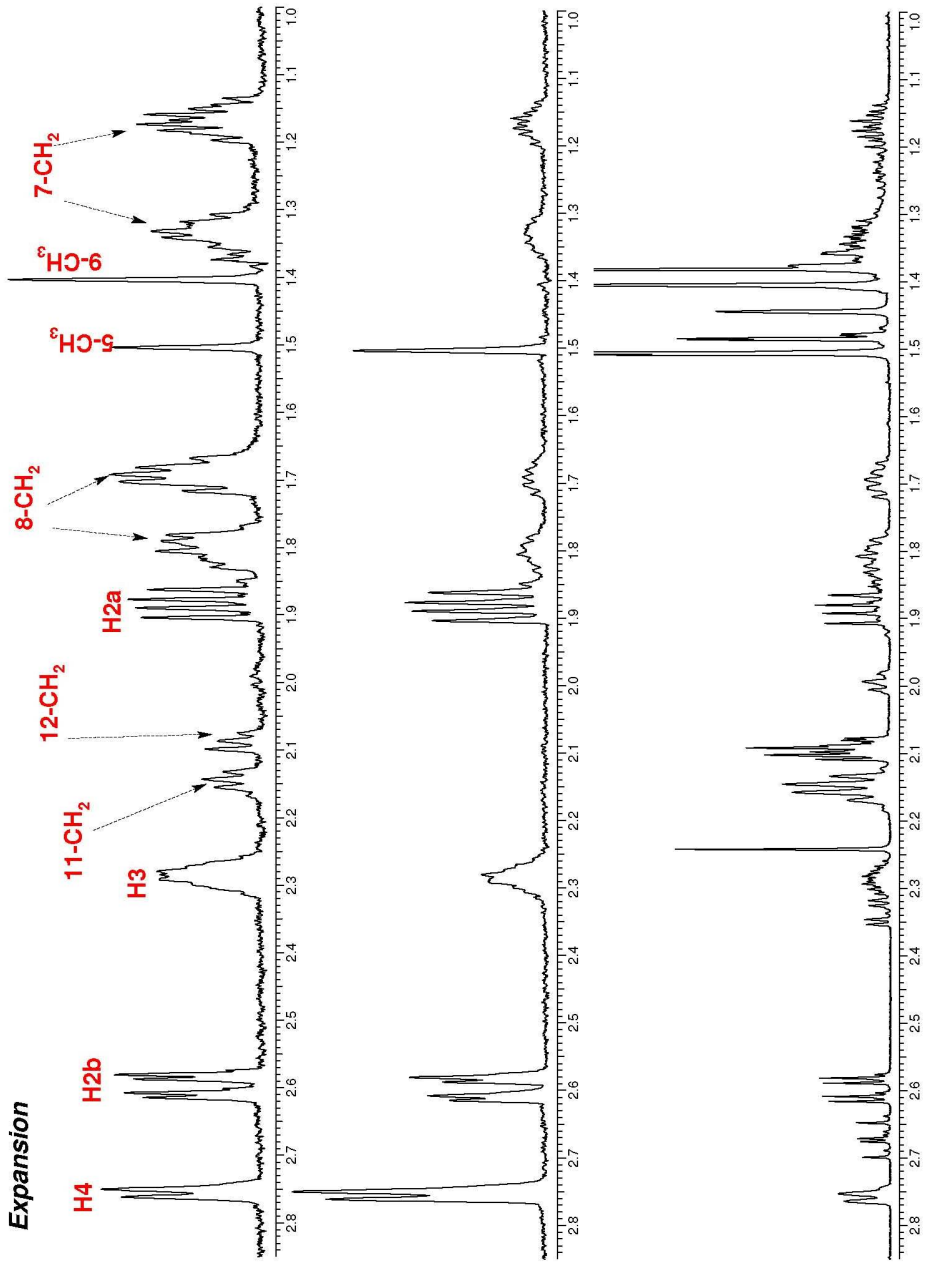
Expansion
H4
H2b
H3
11-CH2
12-CH2
H2a
8-CH2
5-CH3
9-CH3
7-CH2

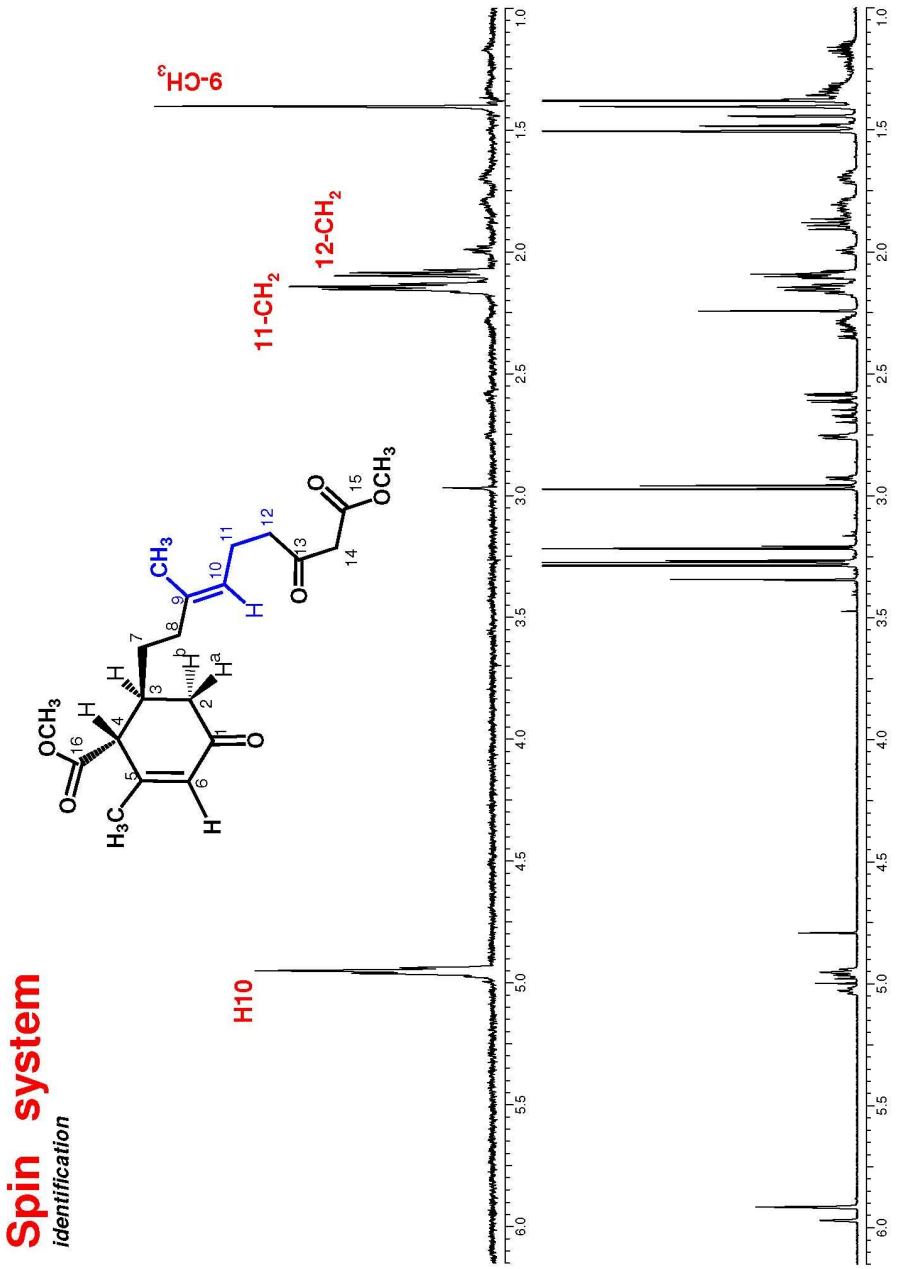
Spin system
identification
H10
11-CH2
12-CH2
9-CH3
OCH3
CH3
H3C
O
H
Ha
Hb

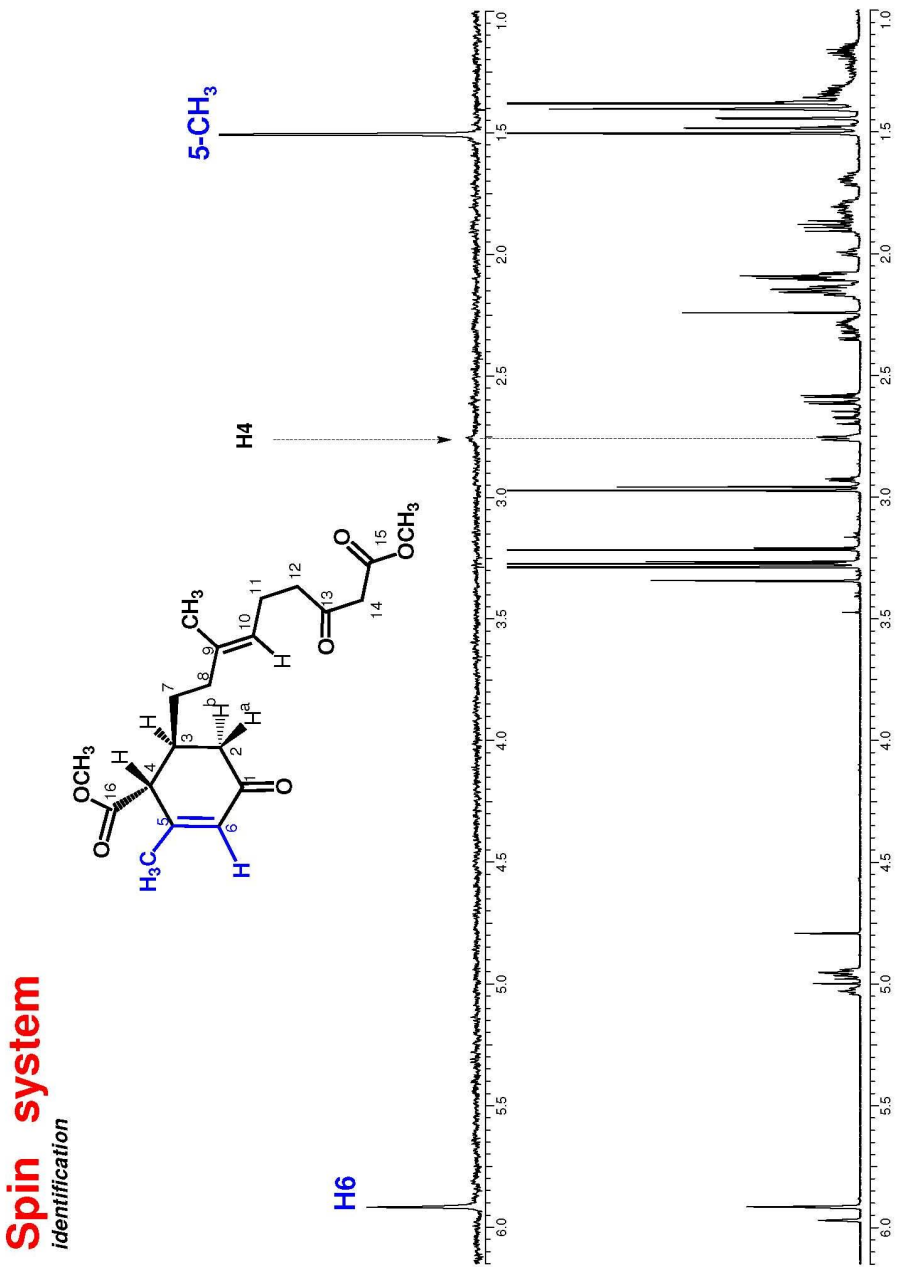
Spin system
identification
H6
H4
5-CH3
OCH3
CH3
H3C
O

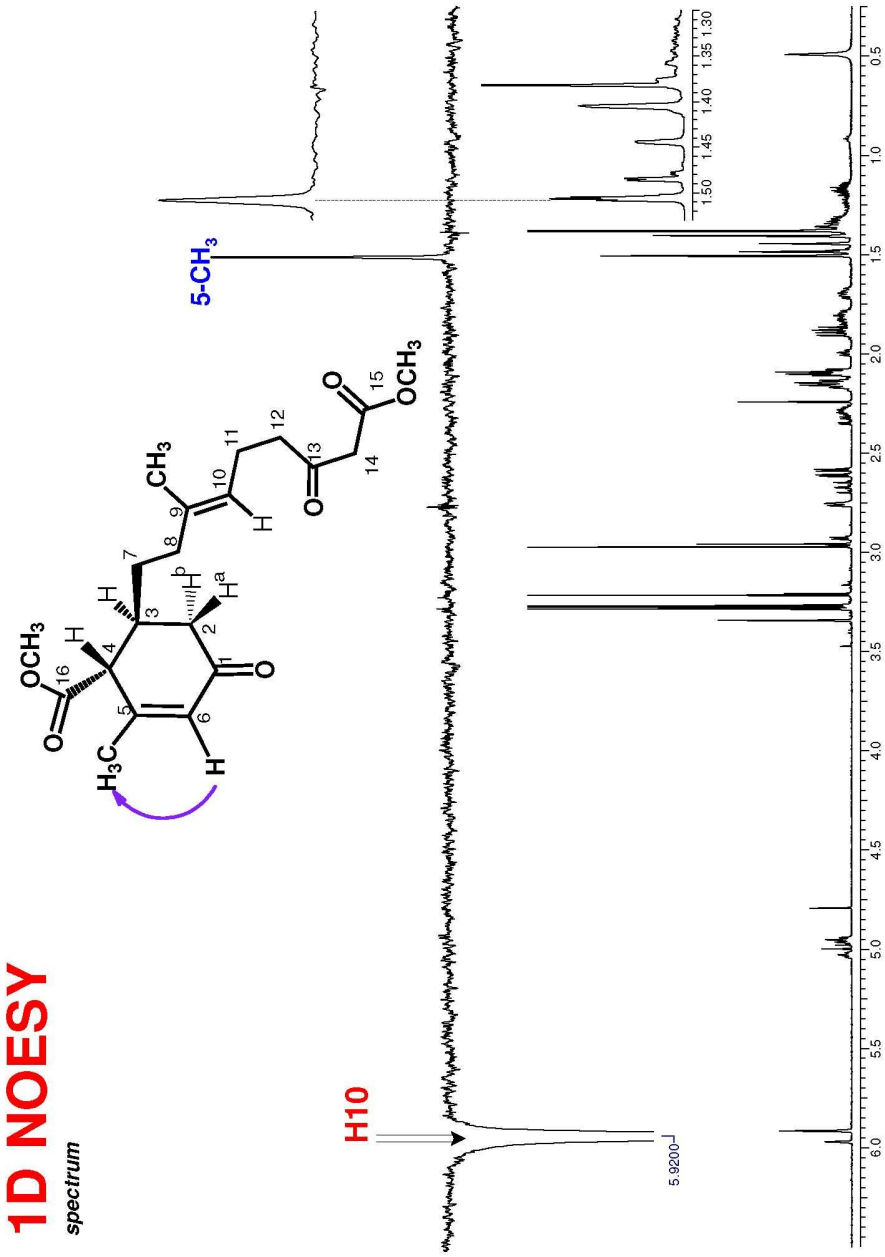
1D NOESY
spectrum
H10
5-CH3
5.9200

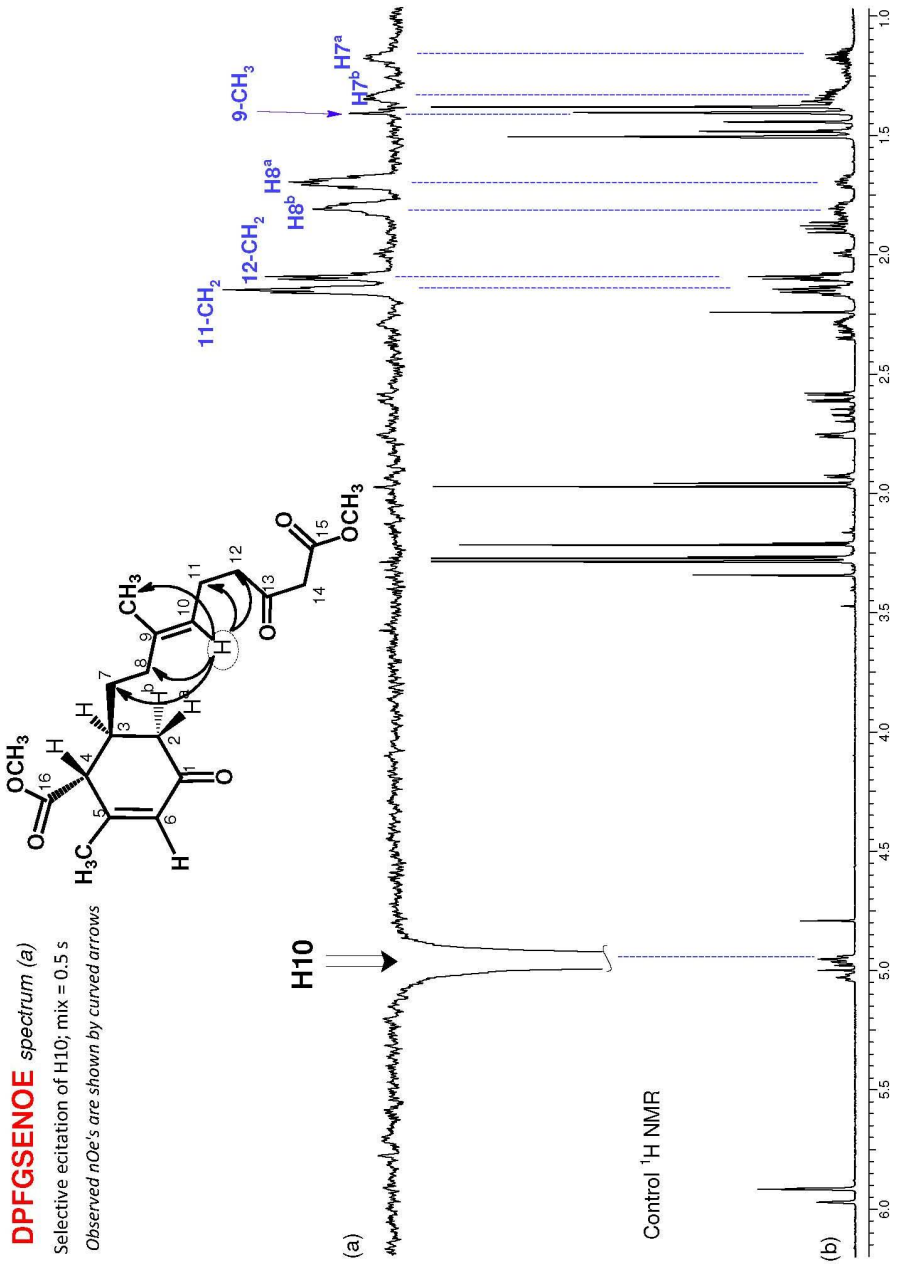
DPFGSENOE spectrum (a)
Selective ecitation of H10; mix = 0.5 s
Observed nOe's are shown by curved arrows
H10
11-CH2
12-CH2
H8a
H8b
9-CH3
H7b
H7a
(a)
Control 1H NMR
(b)

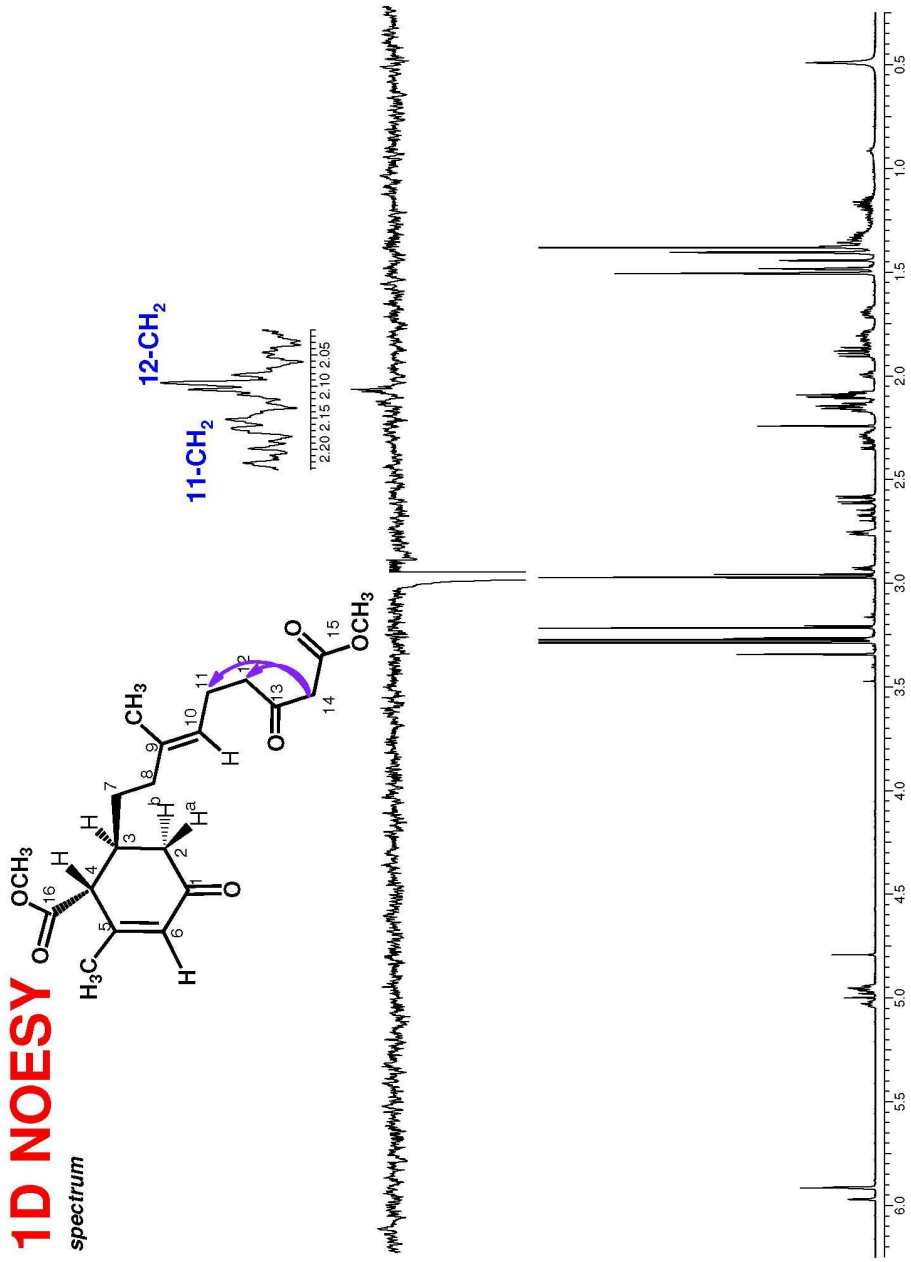
1D NOESY
spectrum
12-CH2
11-CH2
2.20 2.15 2.10 2.05
OCH3
CH3
OCH3
H3C
Ha
Hb

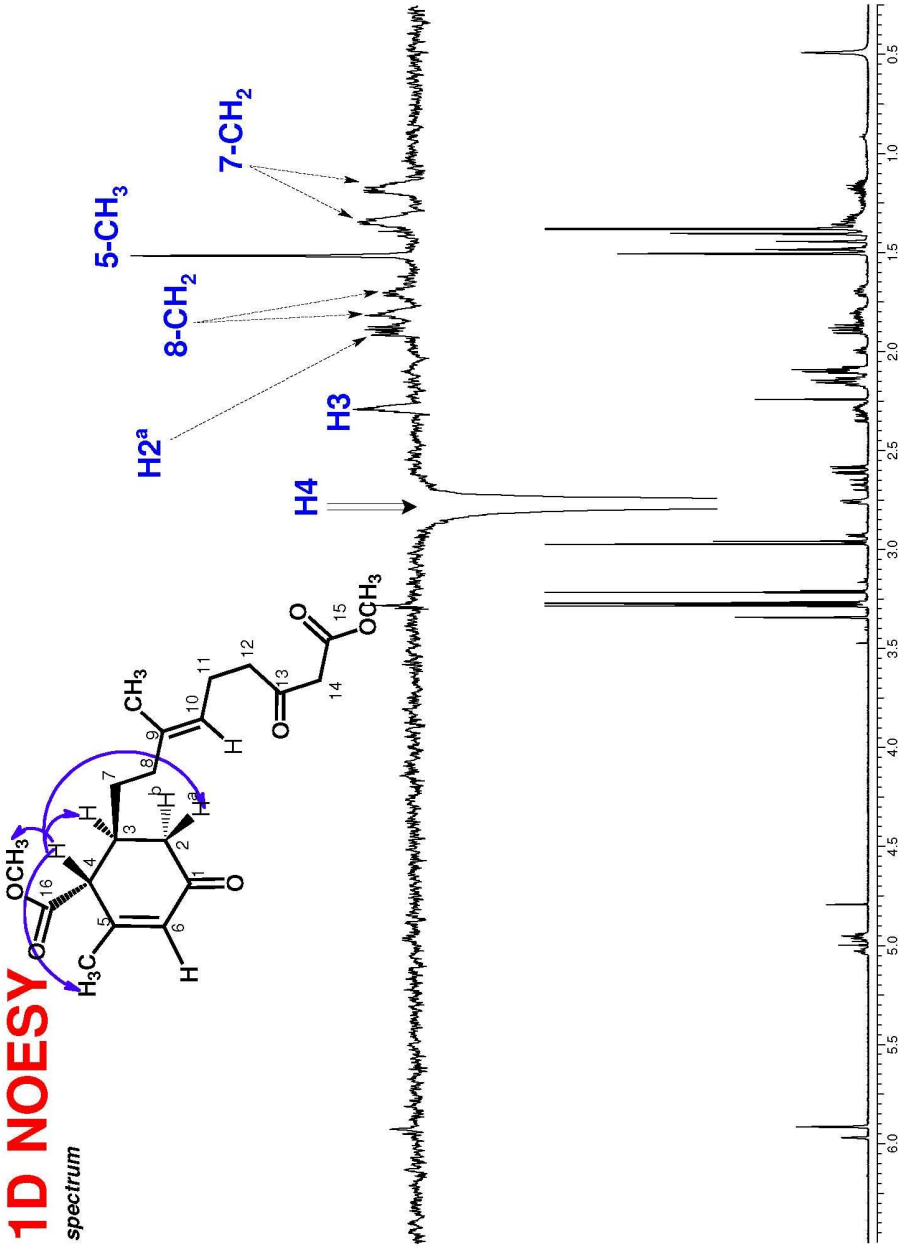
1D NOESY
spectrum
5-CH3
8-CH2
7-CH2
H2a
H3
H4
OCH3
CH3
H3C
O
H
Ha
Hb

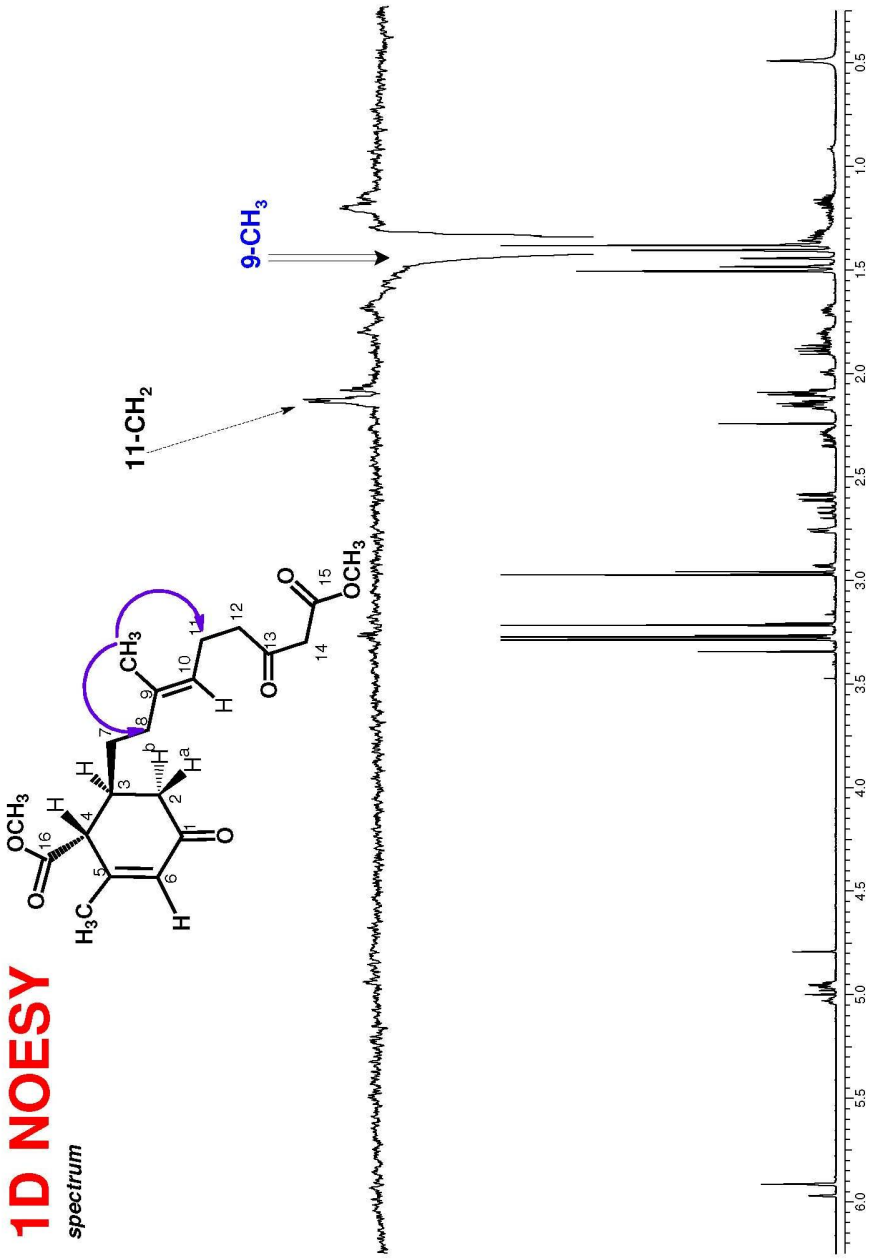
1D NOESY
spectrum
11-CH2
9-CH3
OCH3
CH3
H3C
OCH3
O
H
Ha
Hb

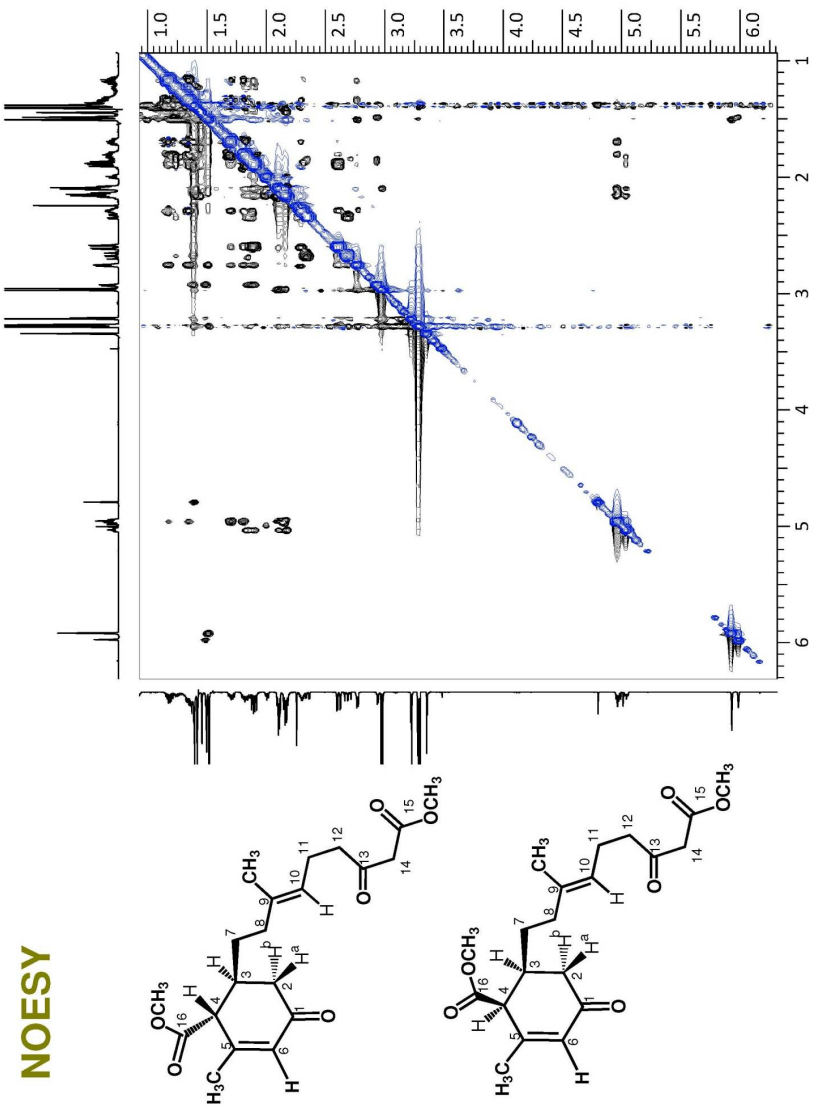
NOESY
1.0
1.5
2.0
2.5
3.0
3.5
4.0
4.5
5.0
5.5
6.0
1
2
3
4
5
6
OCH3
CH3
H3C
O

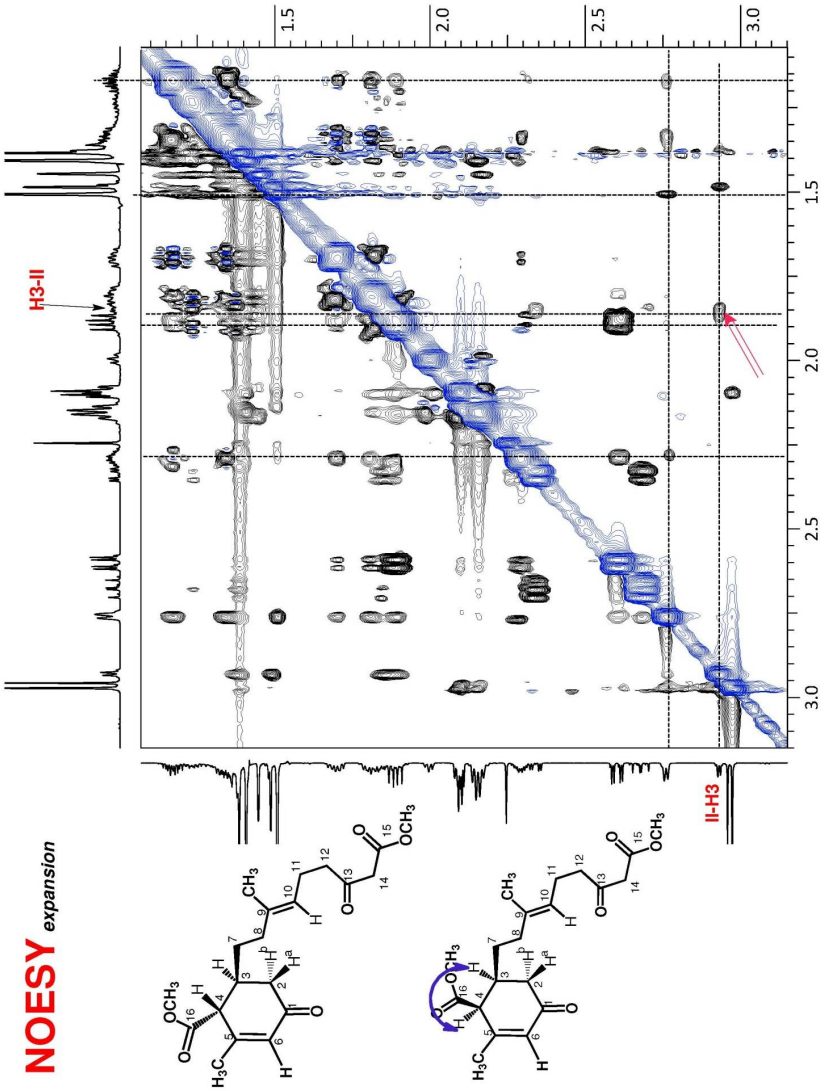
NOESY expansion
H3-II
II-H3
1.5
2.0
2.5
3.0
OCH3
CH3
H
Ha
Hb
O
H3C

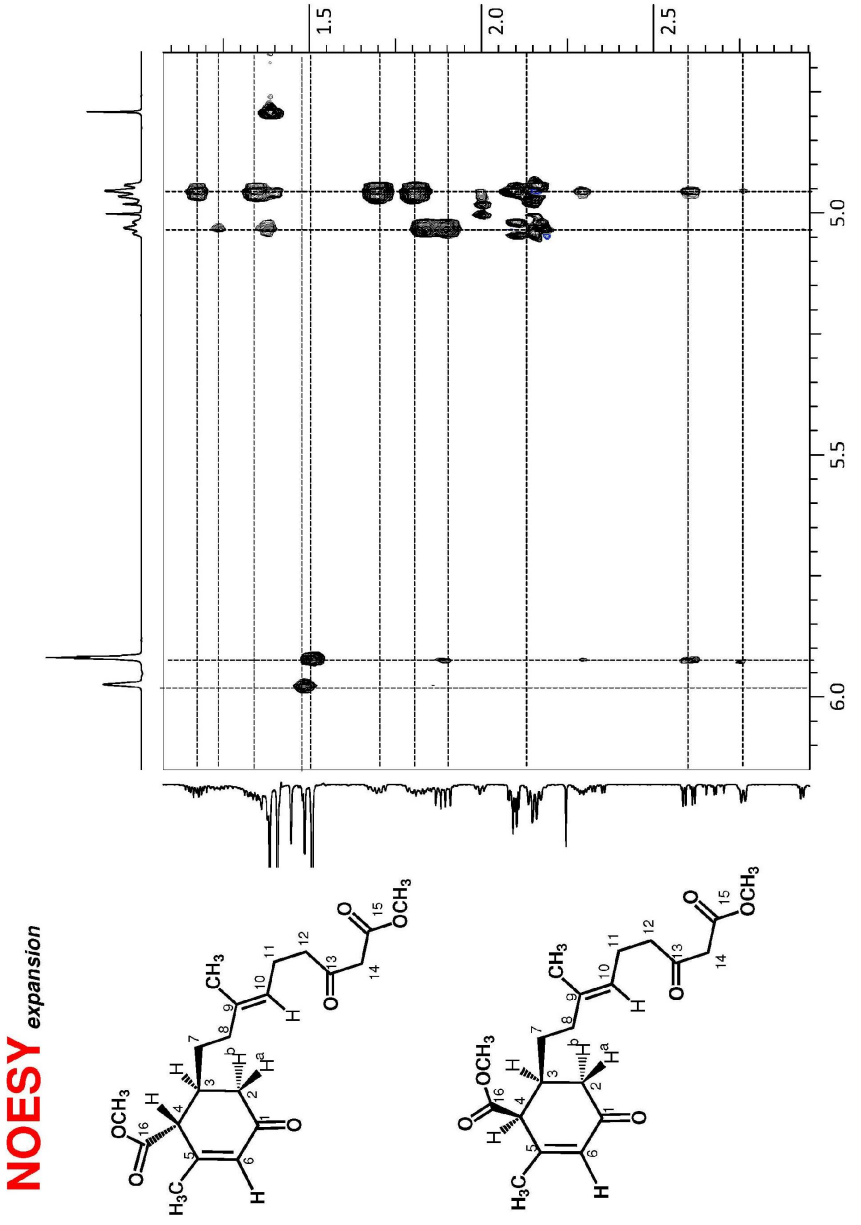
NOESY expansion
1.5
2.0
2.5
5.0
5.5
6.0
OCH3
CH3
H3C
H
O

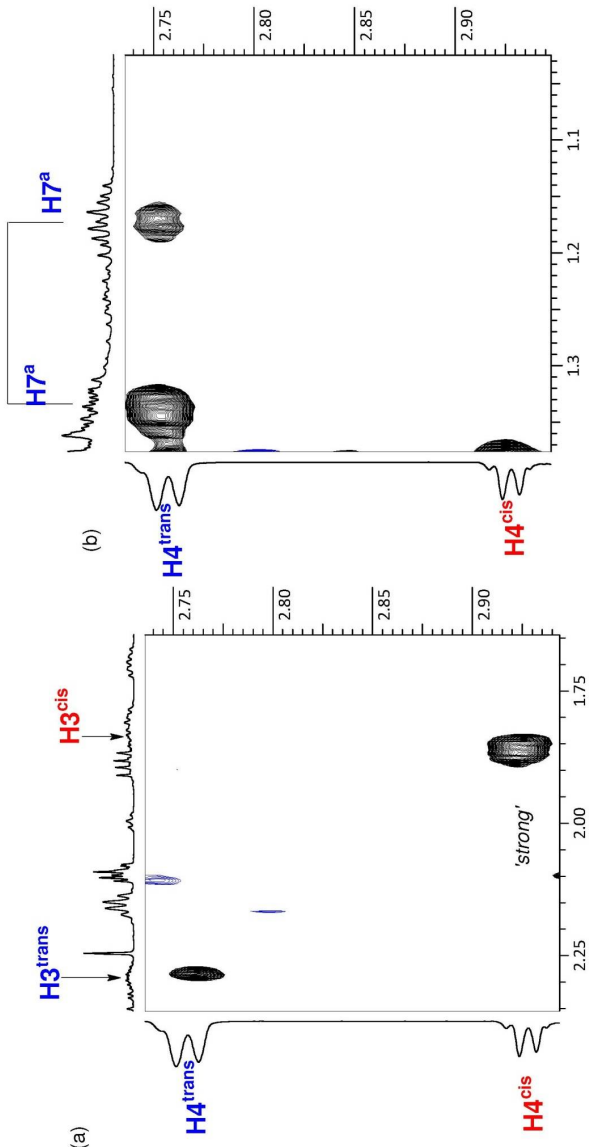

Expanded portions of the NOESY spectrum; *No nOe's were observed between H4-cis and 7-CH_2 protons confirming anti realtionship between them.*

Expanded portions of the NOESY spectrum; *No nOe was observed between H4-cis and H2^a -cis protons confirming anti realtionship between them.*

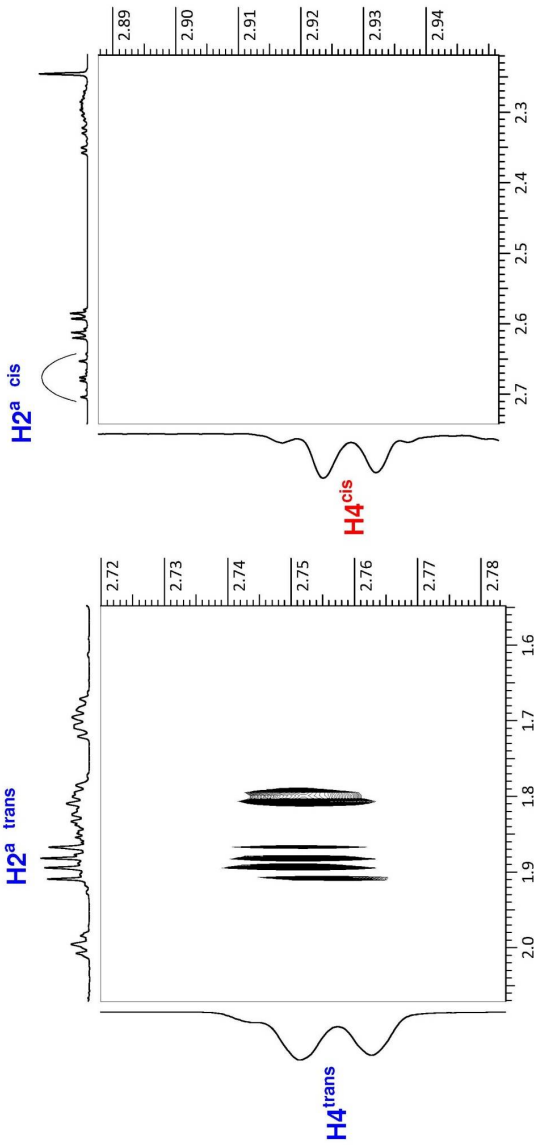

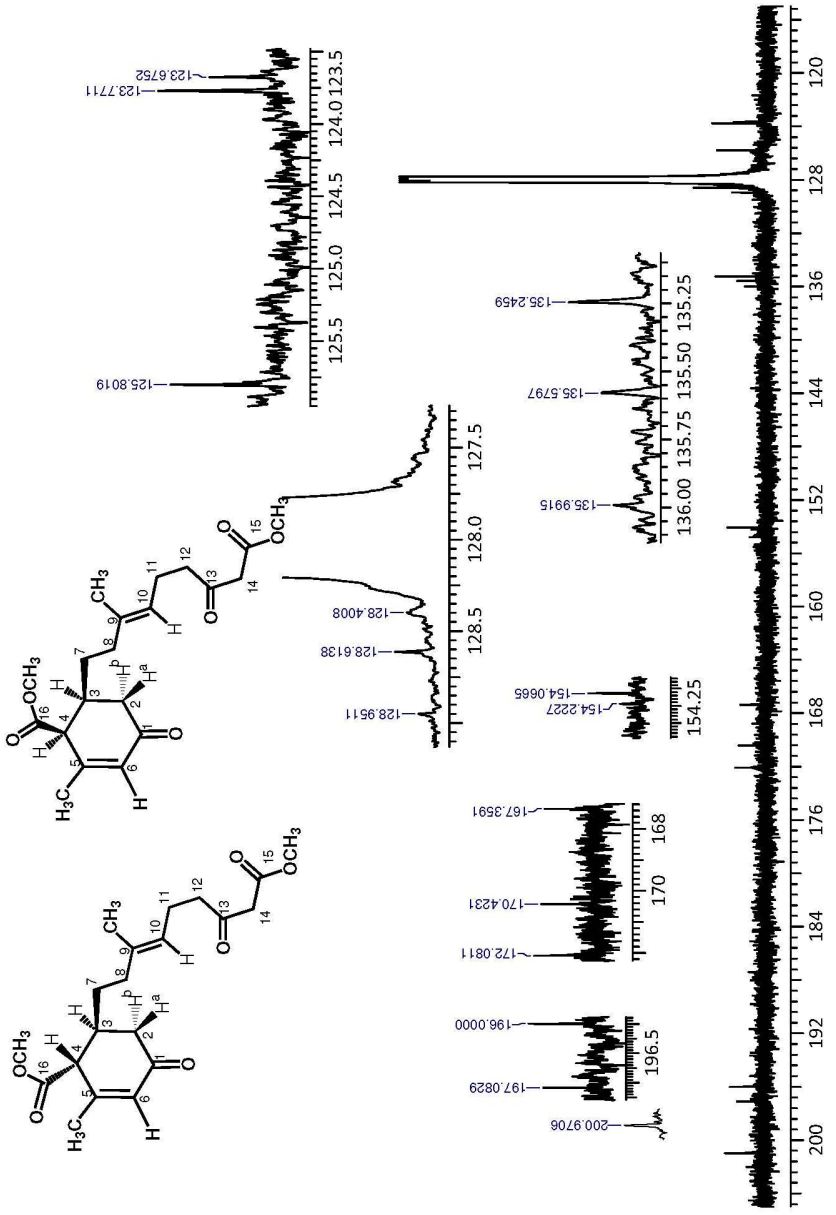
123.6752
123.7711
125.8019
128.4008
128.6138
128.9511
135.2459
135.5797
135.9915
154.0665
154.2227
167.3591
170.4231
172.0811
196.0000
197.0829
200.9706
OCH3
CH3
H3C
Ha
Hb

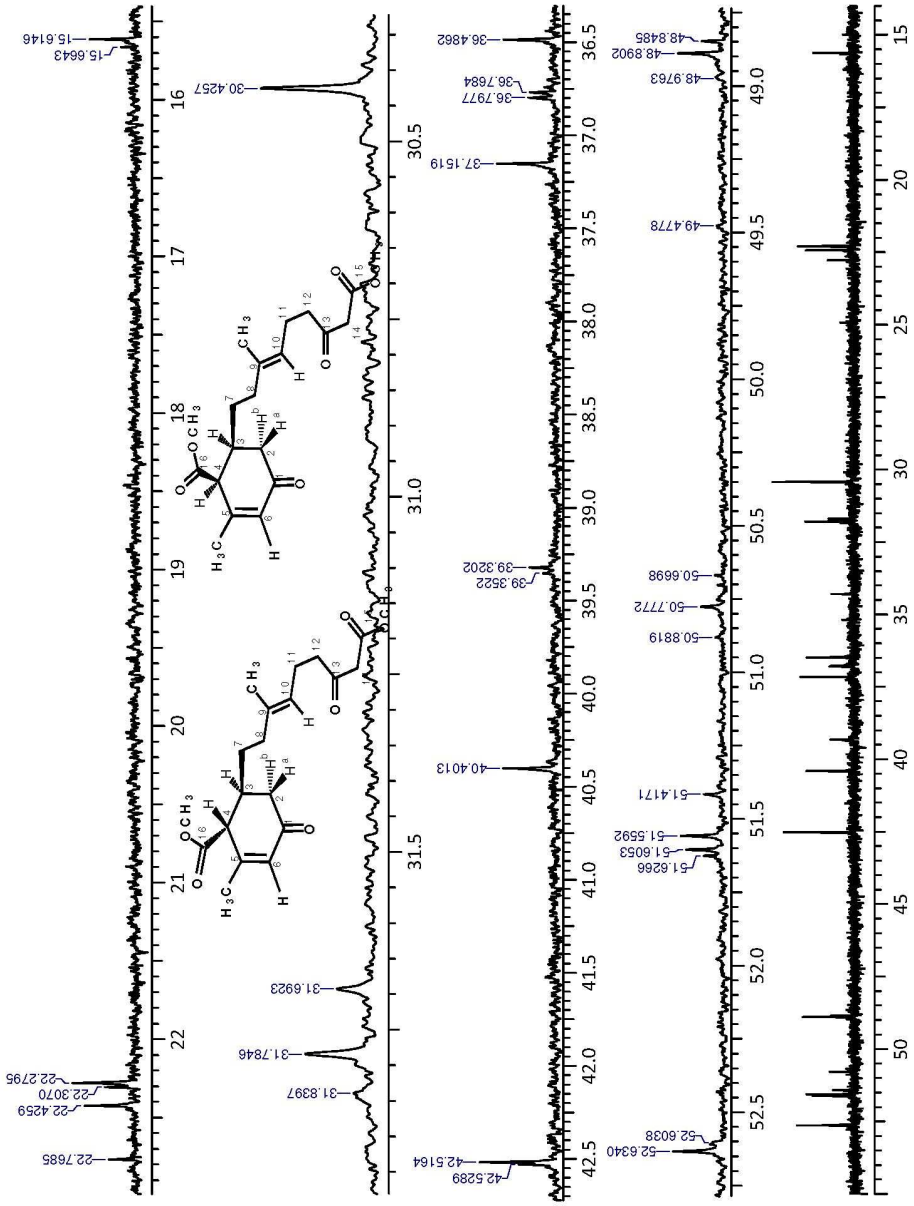
15.6146
15.6643
22.7685
22.2795
22.3070
22.4259
31.8397
31.7846
31.6923
30.4257
42.5289
42.5164
40.4013
39.3522
39.3202
37.1519
36.7977
36.7684
36.4862
52.6340
52.6038
51.6266
51.6053
51.5592
51.4171
50.8819
50.7772
50.6698
49.4778
48.9763
48.8902
48.8485

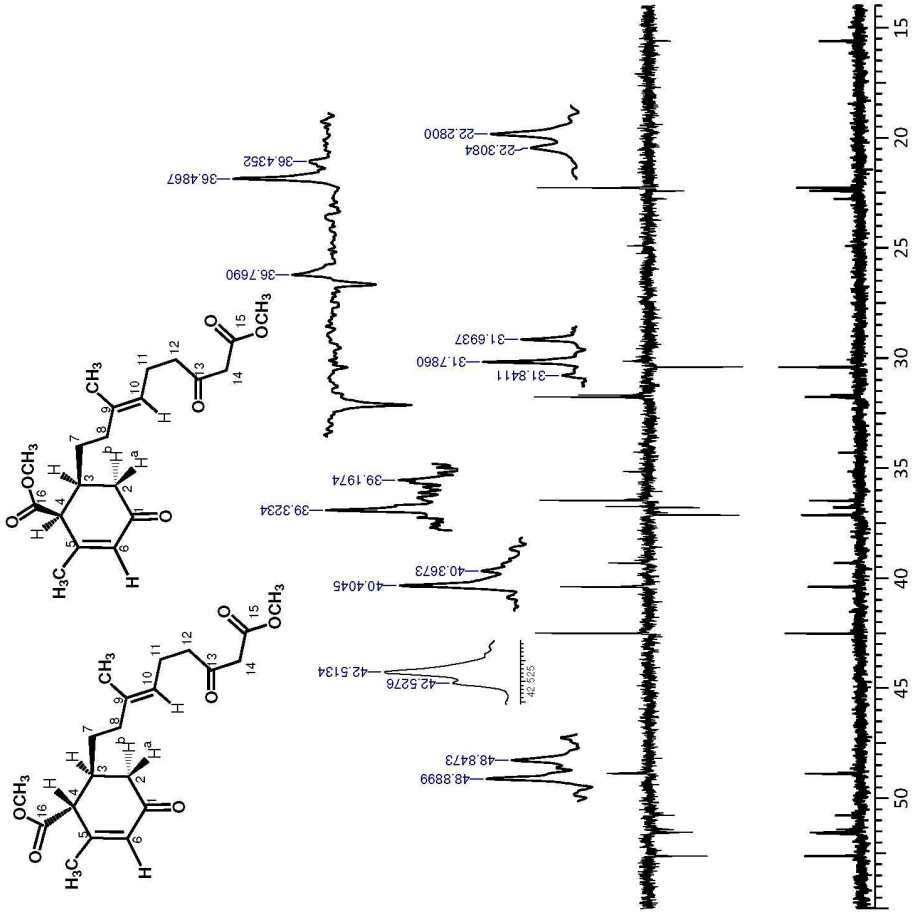
22.2800
22.3084
31.6937
31.7860
31.8411
36.4352
36.4867
36.7690
39.1974
39.3234
40.3673
40.4045
42.5134
42.5276
48.8473
48.8899
15
20
25
30
35
40
45
50

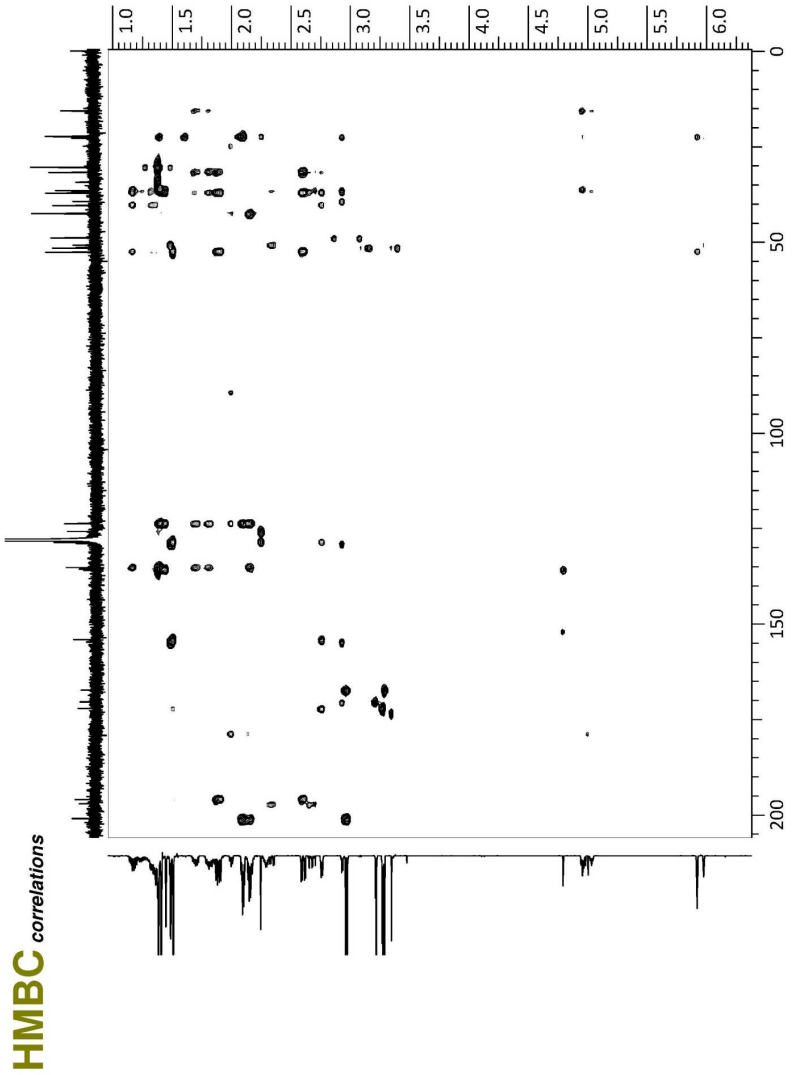
HMBC correlations
1.0
1.5
2.0
2.5
3.0
3.5
4.0
4.5
5.0
5.5
6.0
0
50
100
150
200

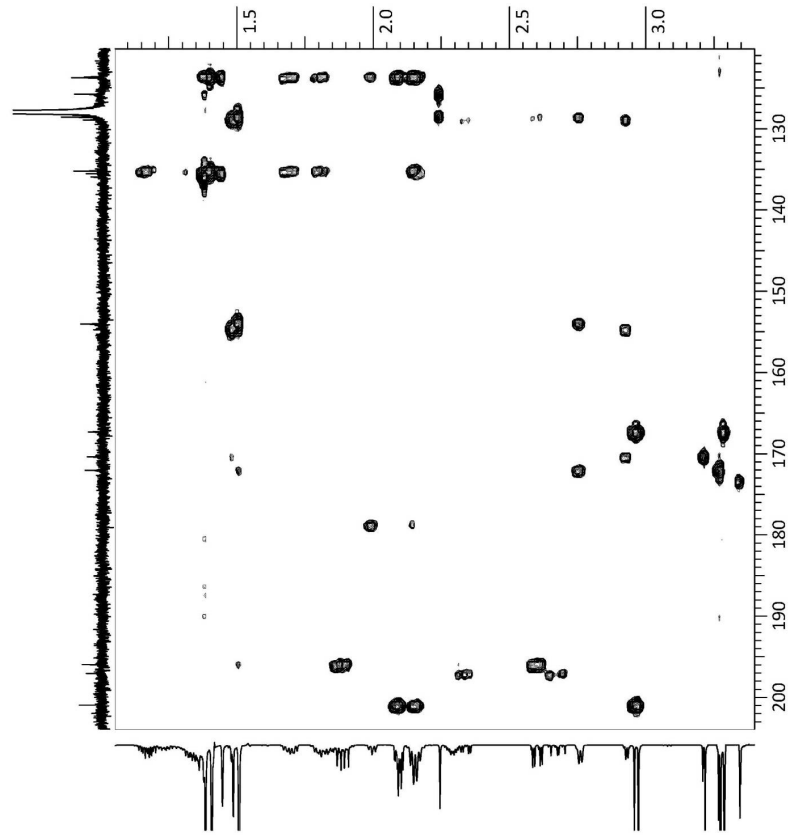

Selected HMBC *correlations*

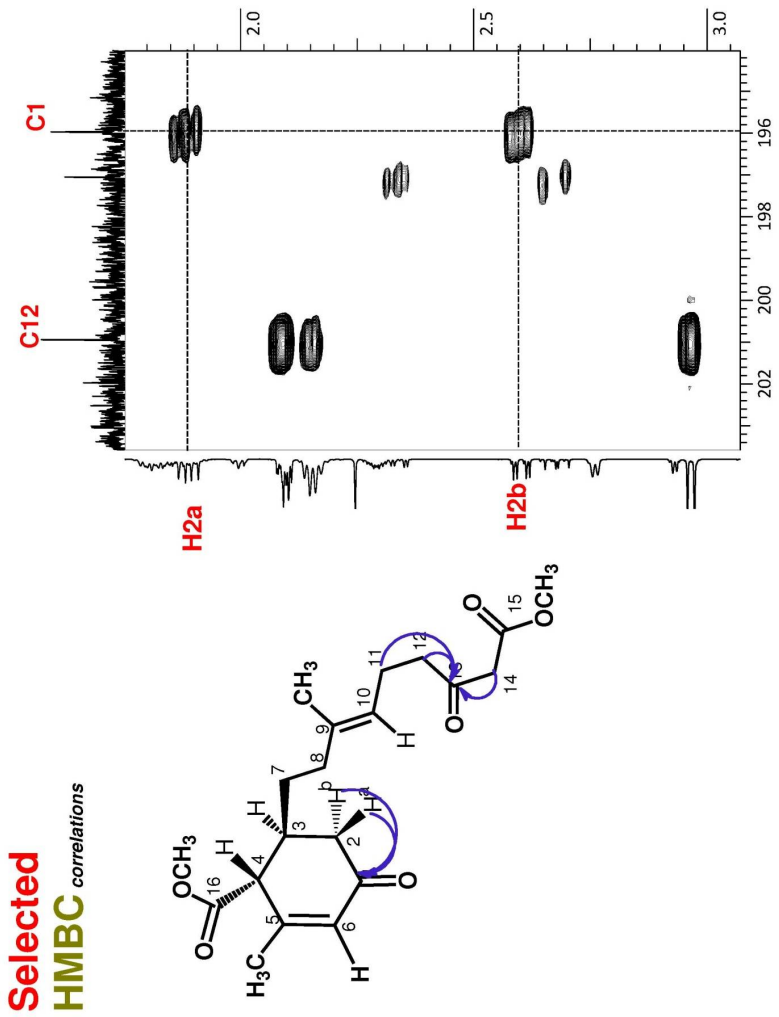
Selected
HMBC correlations
C1
C12
H2a
H2b
2.0
2.5
3.0
196
198
200
202
OCH3
CH3
H3C
O

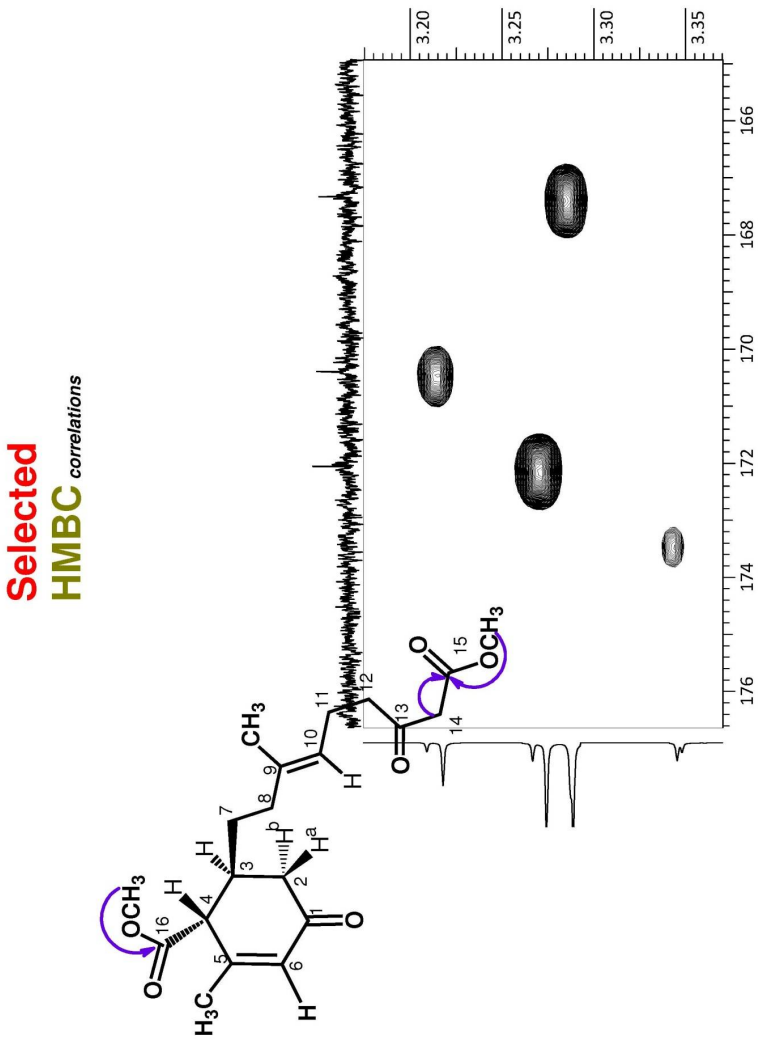
Selected
HMBC correlations
OCH3
H
H3C
H
H
Ha
Hb
CH3
H
O
O
OCH3
3.20
3.25
3.30
3.35
166
168
170
172
174
176

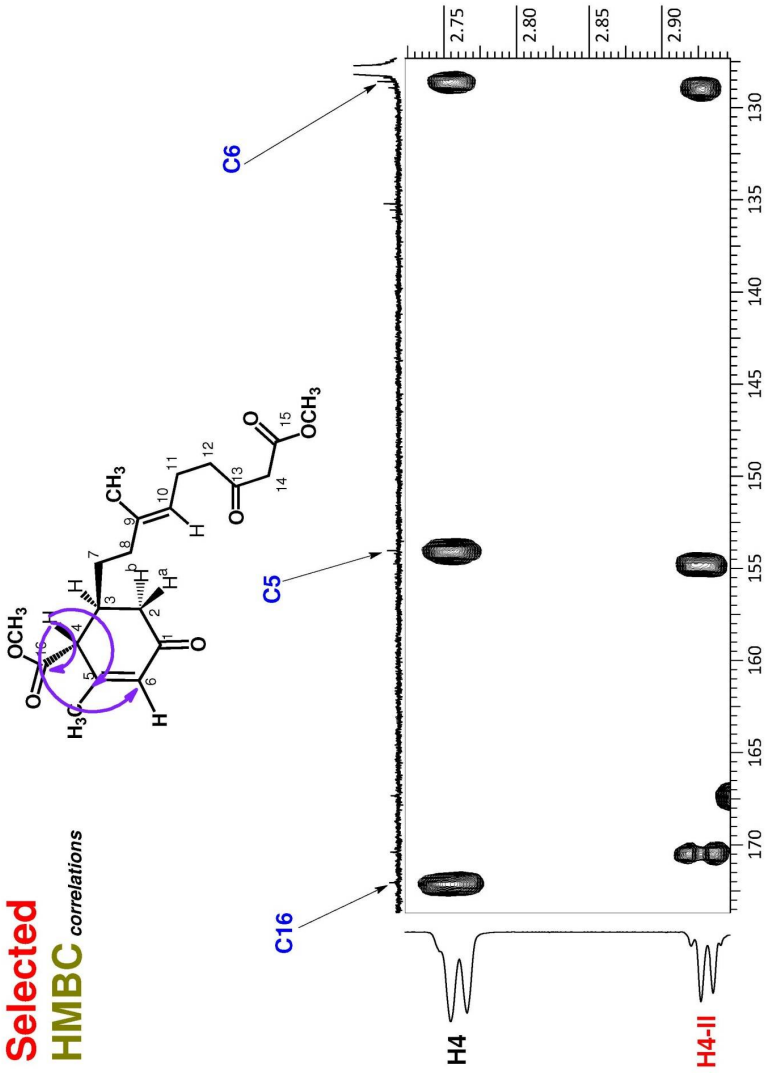
Selected
HMBC correlations
C6
C5
C16
H4
H4-II
2.75
2.80
2.85
2.90
130
135
140
145
150
155
160
165
170

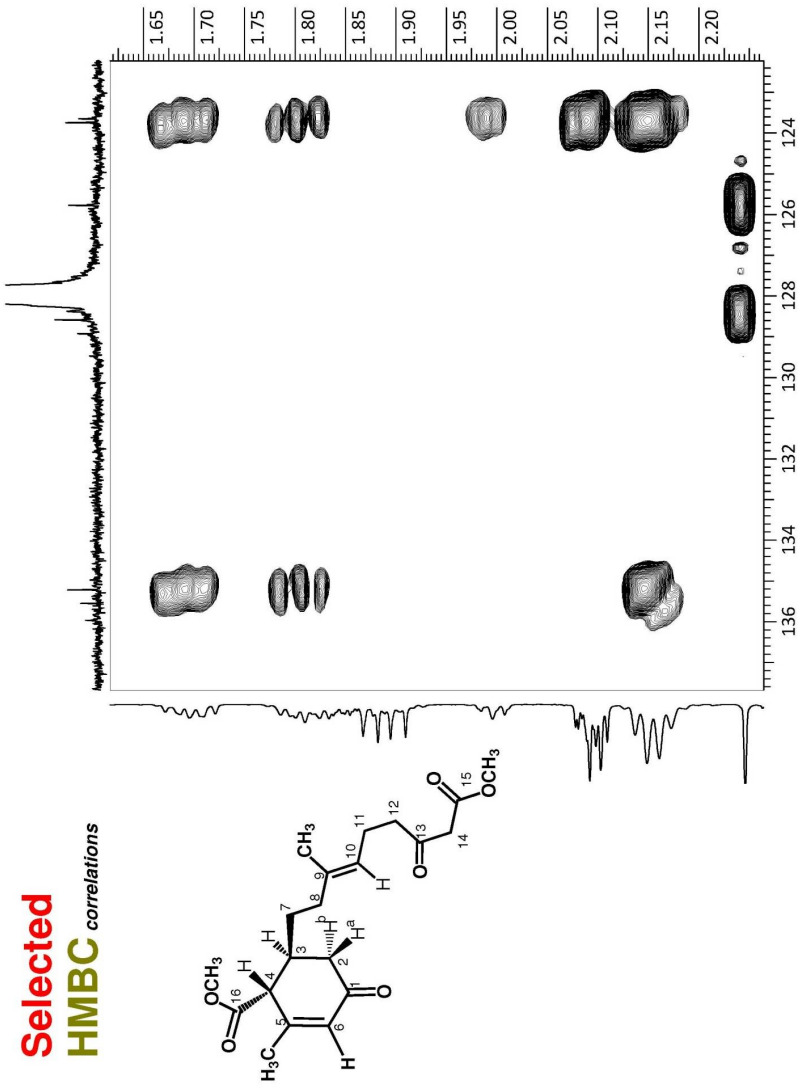
Selected
HMBC correlations
1.65
1.70
1.75
1.80
1.85
1.90
1.95
2.00
2.05
2.10
2.15
2.20
124
126
128
130
132
134
136
OCH3
O
H3C
CH3
OCH3
O

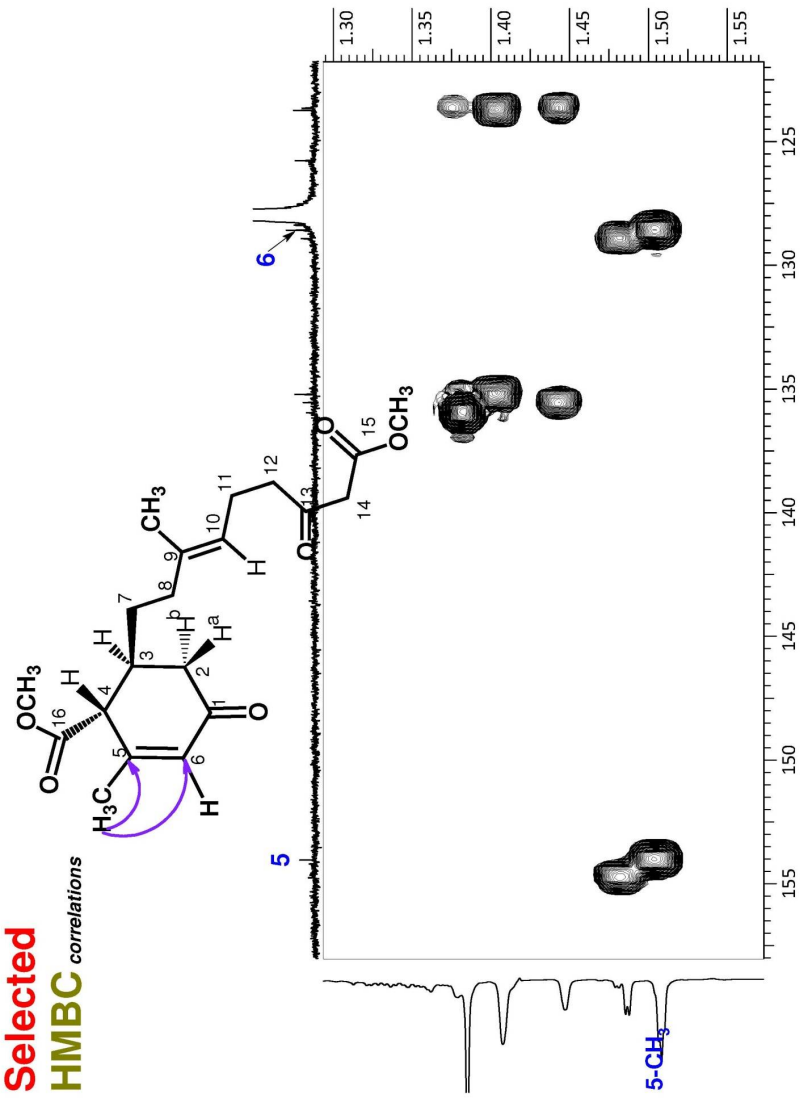
Selected
HMBC correlations
OCH3
O
H
H3C
CH3
OCH3
5
6
5-CH3
1.30
1.35
1.40
1.45
1.50
1.55
125
130
135
140
145
150
155

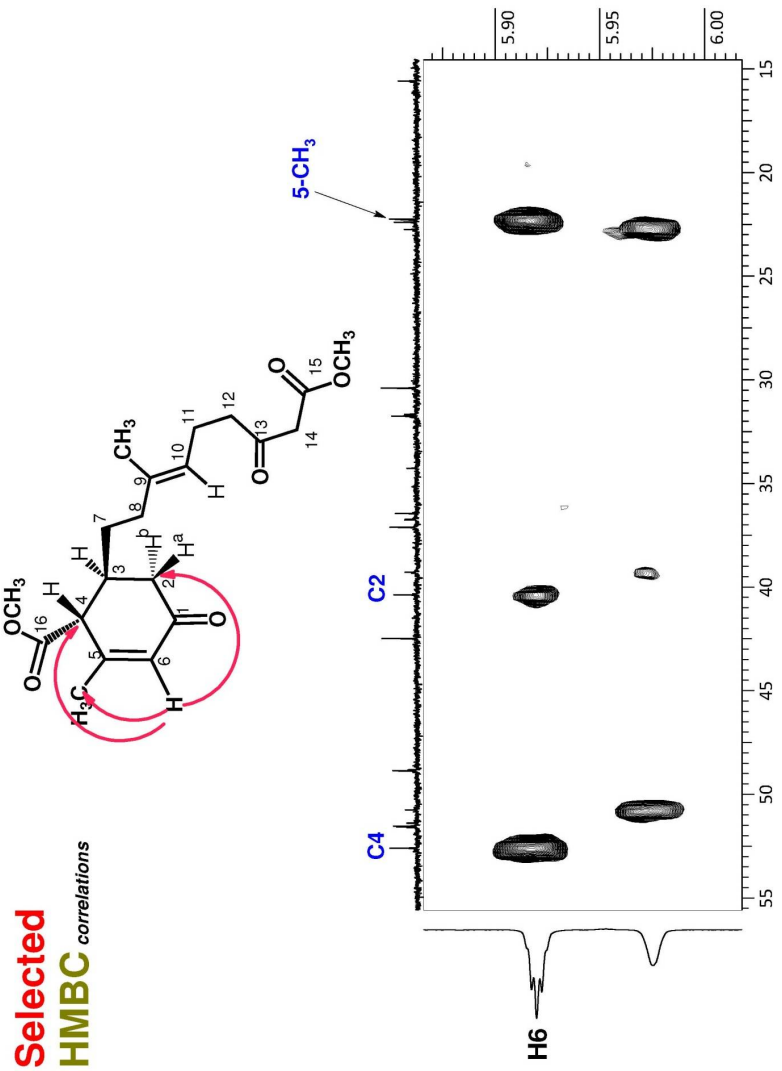
Selected
HMBC correlations
5-CH3
C2
C4
H6
5.90
5.95
6.00
15
20
25
30
35
40
45
50
55
OCH3
CH3
OCH3
H3C
O
H
Ha
Hb

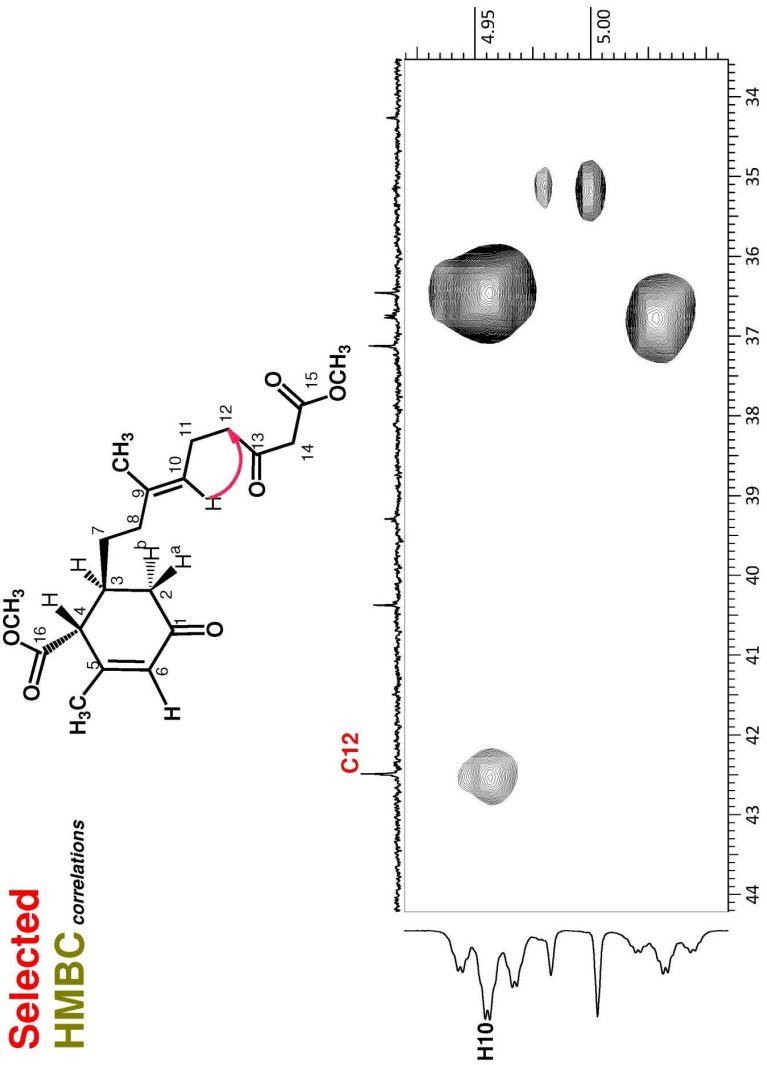
Selected
HMBC correlations
OCH3
O
16
H
4
5
H3C
H
6
1
O
3
H
7
2
Ha
b
8
9
CH3
10
11
12
H
13
O
14
15
O
OCH3
C12
H10
4.95
5.00
34
35
36
37
38
39
40
41
42
43
44

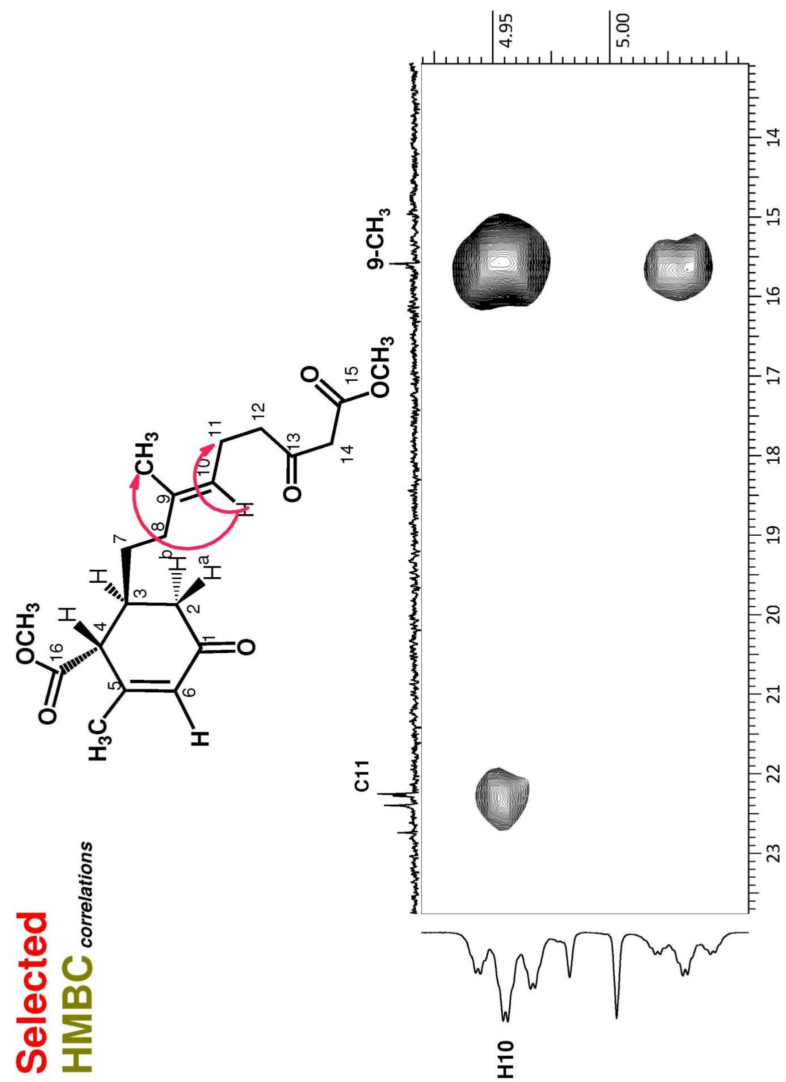
Selected
HMBC correlations
H10
C11
9-CH3
4.95
5.00
14
15
16
17
18
19
20
21
22
23

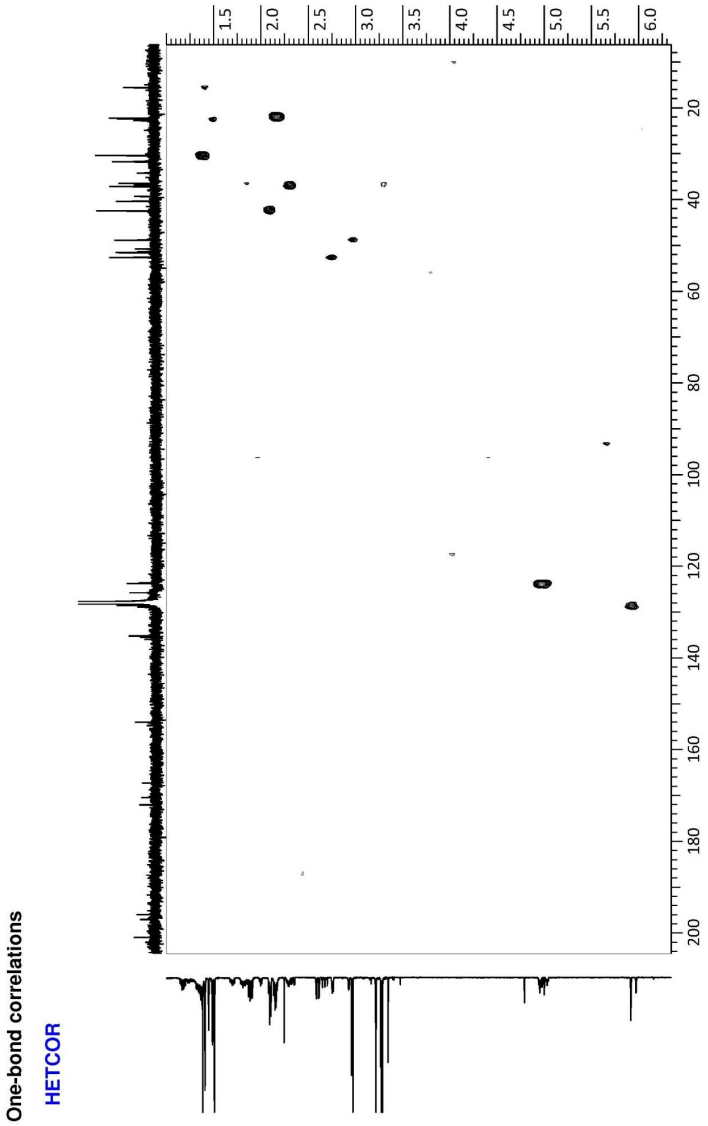
One-bond correlations
HETCOR
1.5
2.0
2.5
3.0
3.5
4.0
4.5
5.0
5.5
6.0
20
40
60
80
100
120
140
160
180
200

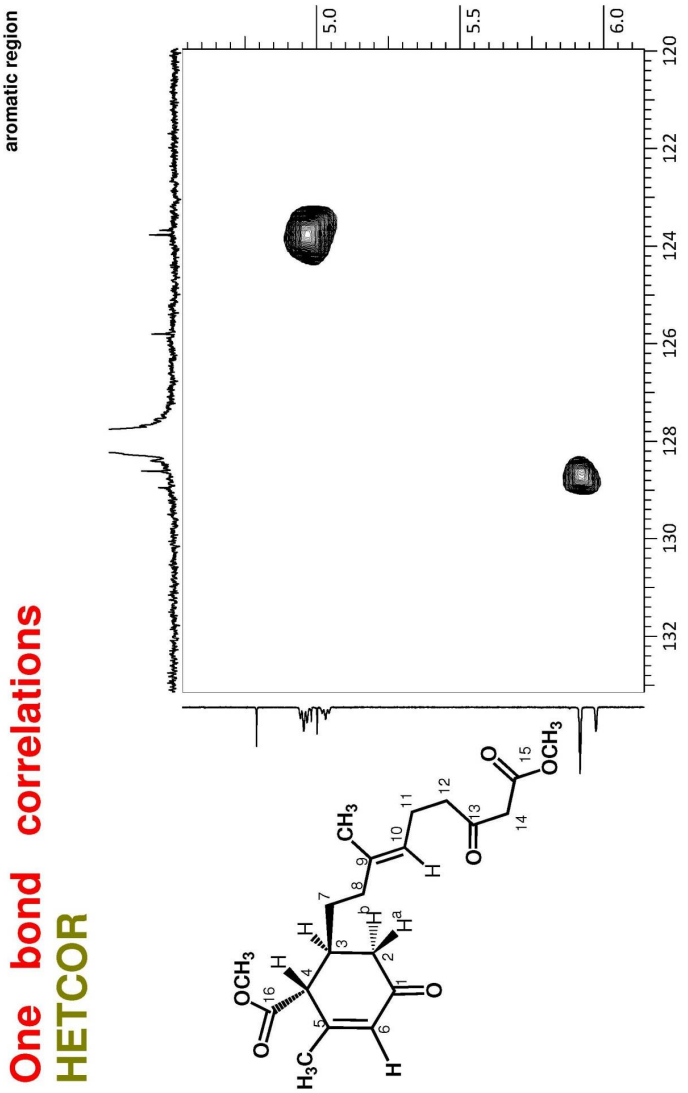
One bond correlations
HETCOR
aromatic region
5.0
5.5
6.0
120
122
124
126
128
130
132
OCH3
H3C
CH3
OCH3

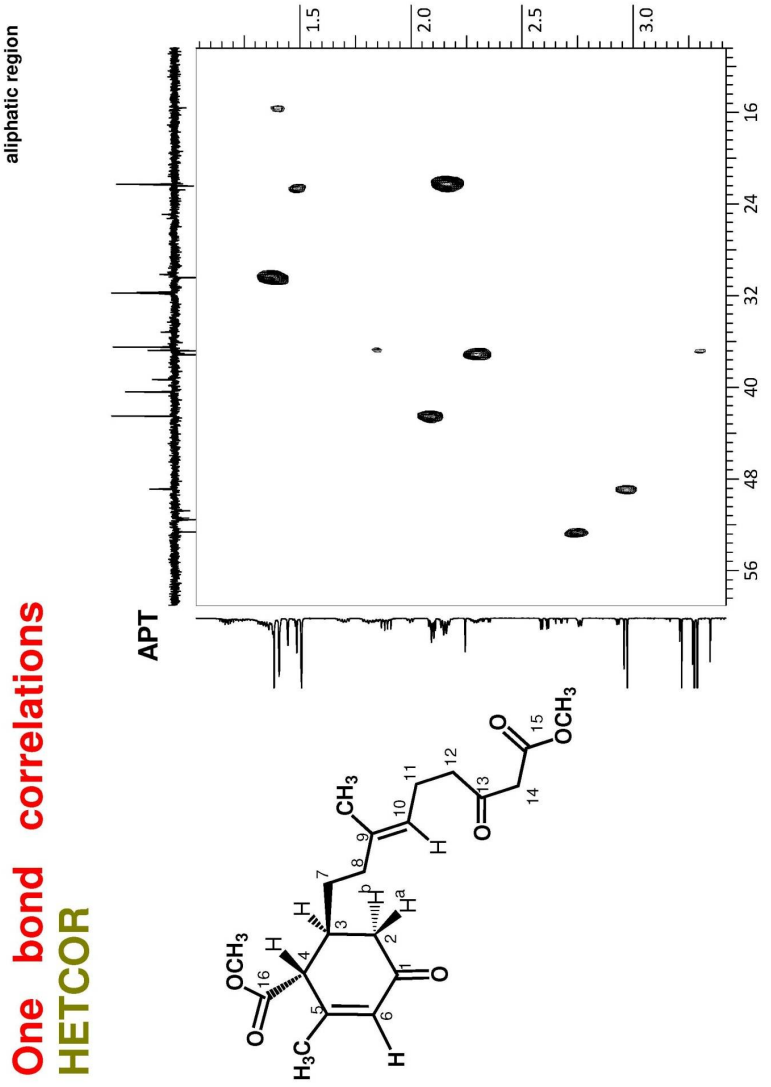
One bond correlations
HETCOR
aliphatic region
APT
1.5
2.0
2.5
3.0
16
24
32
40
48
56
OCH3
O
H
H3C
CH3
OCH3

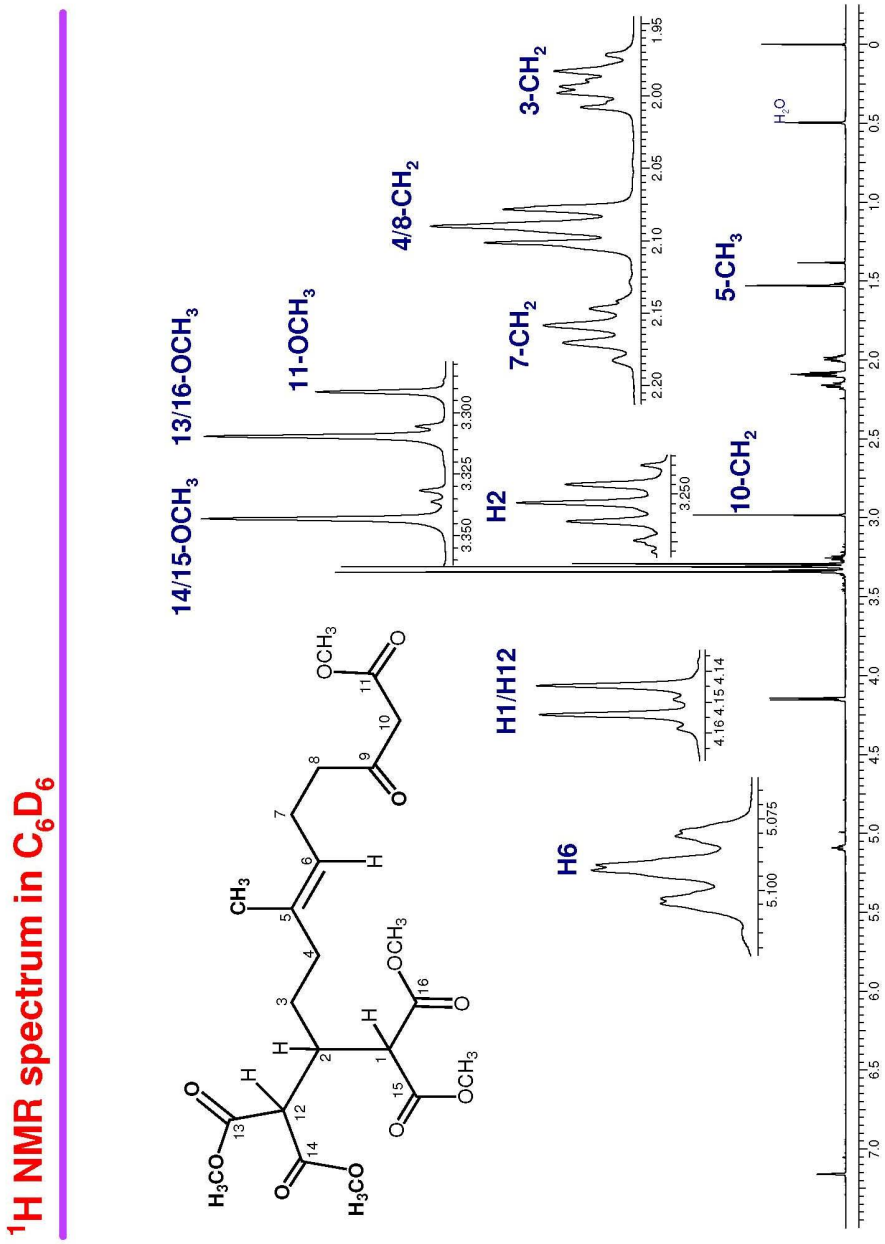
^{1}H NMR spectrum in C_6D_6
14/15-OCH$_3$
13/16-OCH$_3$
11-OCH$_3$
4/8-CH$_2$
3-CH$_2$
7-CH$_2$
H2
10-CH$_2$
5-CH$_3$
H1/H12
H6
H$_2$O
H$_3$CO
OCH$_3$
CH$_3$

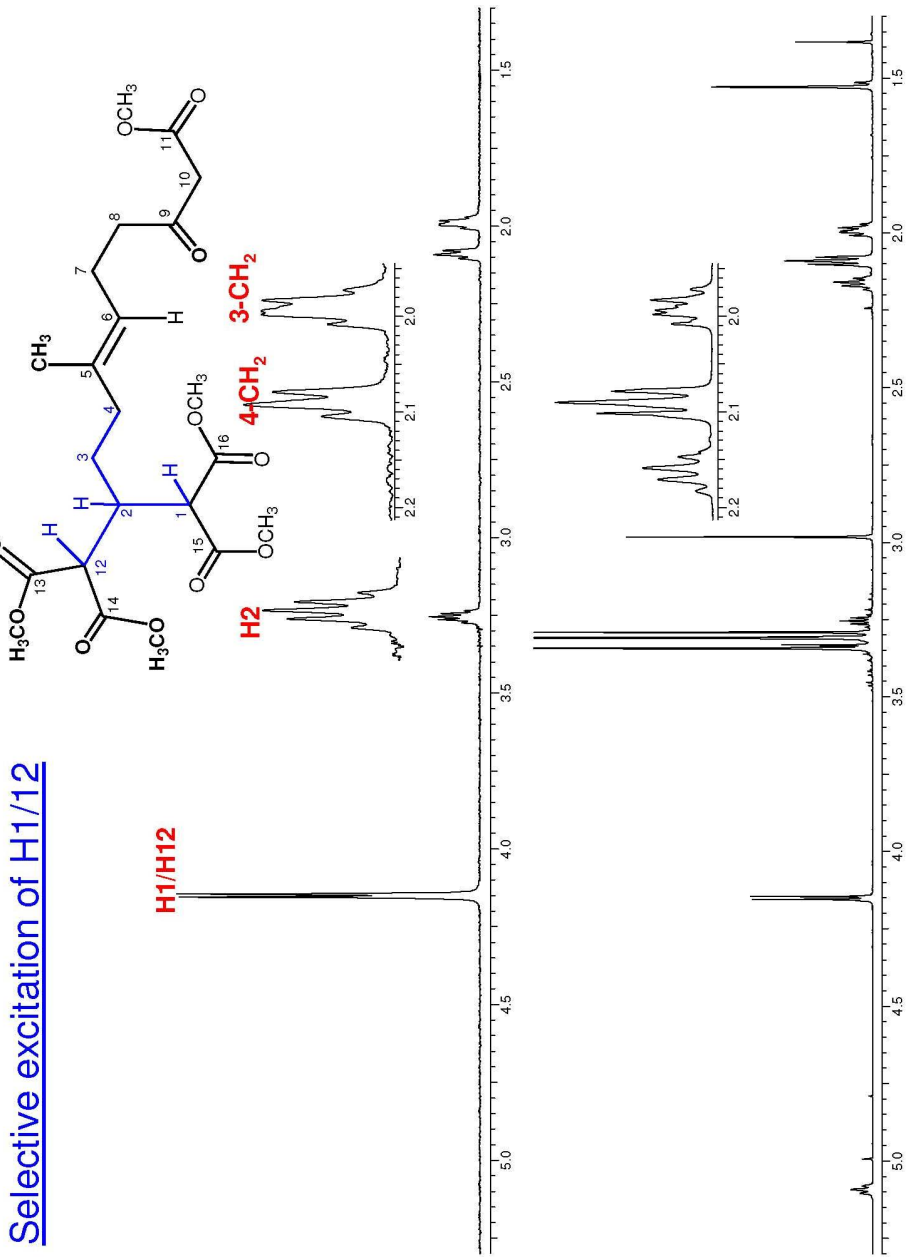
Selective excitation of H1/12
H1/H12
H2
4-CH2
3-CH2

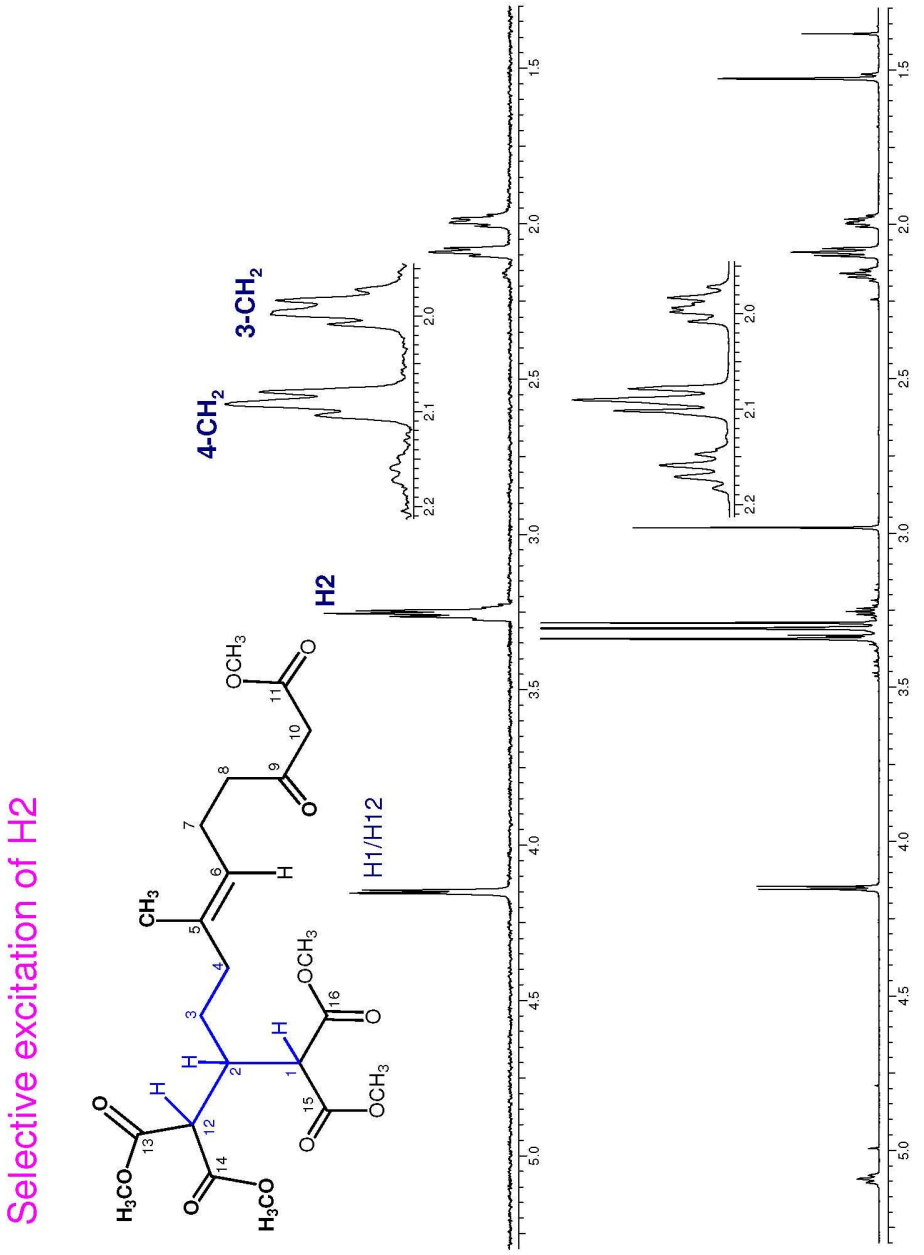
Selective excitation of H2
H2
H1/H12
4-CH2
3-CH2

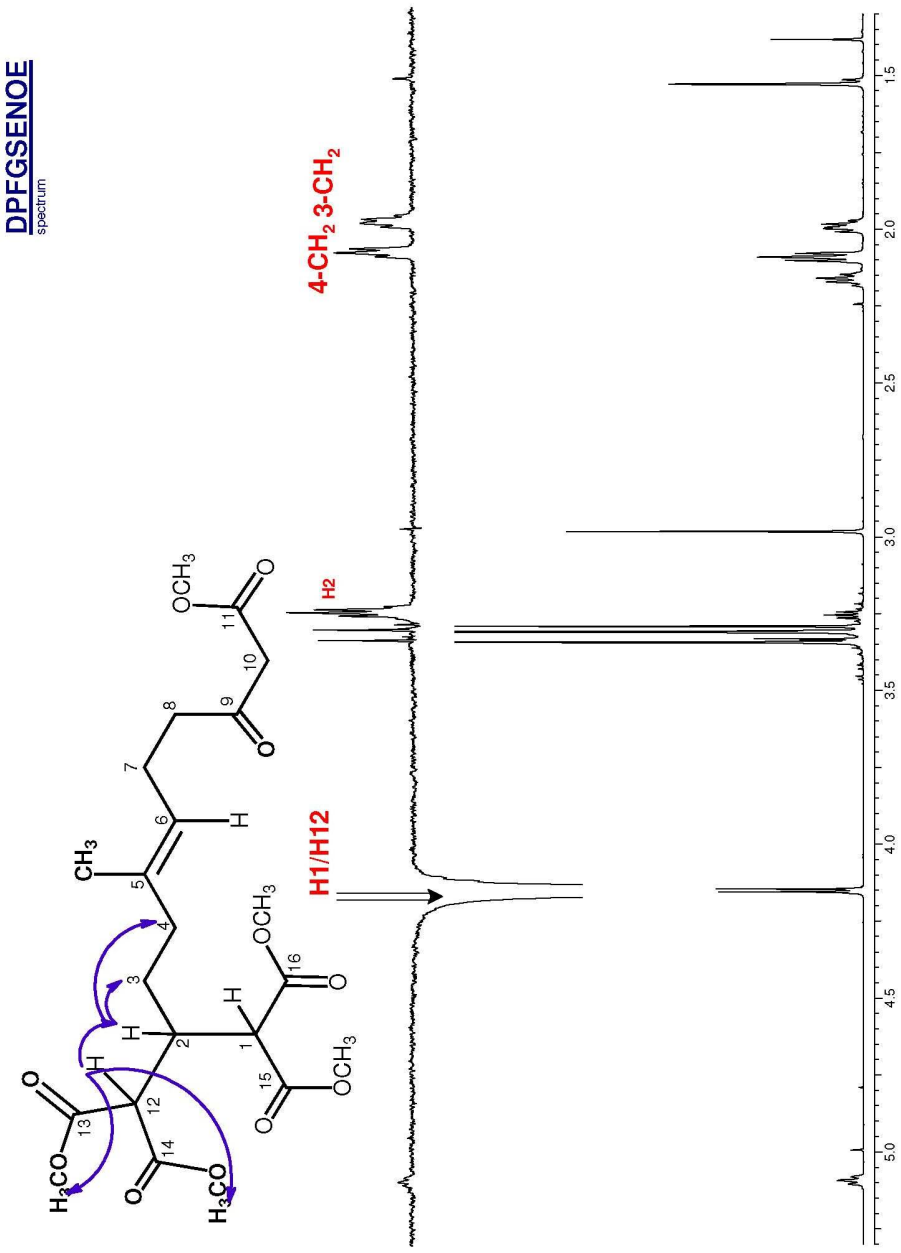
DPFGSENOE
spectrum
H1/H12
H2
4-CH2 3-CH2
CH3
OCH3
OCH3
OCH3
H3CO
H3CO
O
O
O
O
O
O
H
H
H
H
1
2
3
4
5
6
7
8
9
10
11
12
13
14
15
16
5.0
4.5
4.0
3.5
3.0
2.5
2.0
1.5

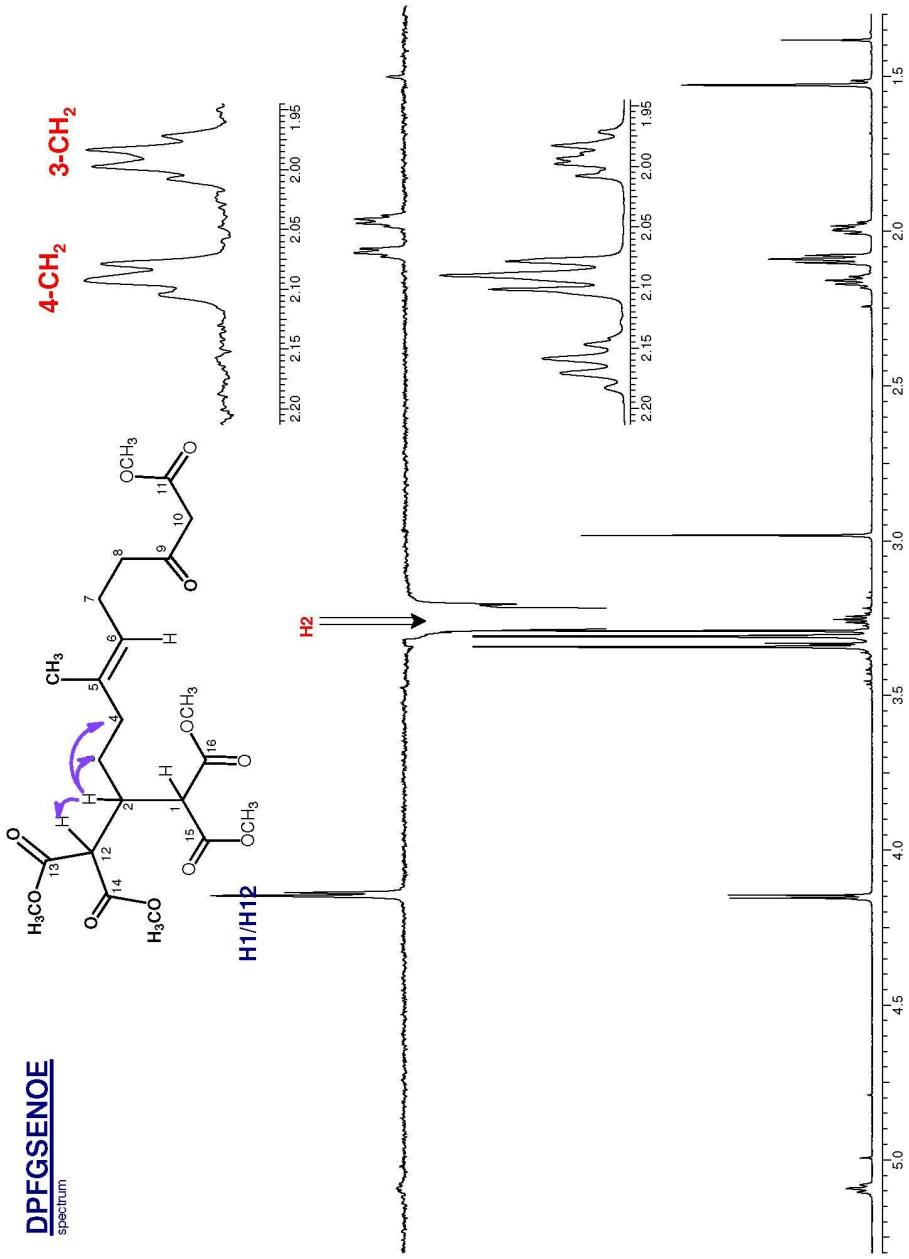
DPFGSENOE
spectrum
H1/H12
H2
4-CH2
3-CH2
H3CO
OCH3
CH3

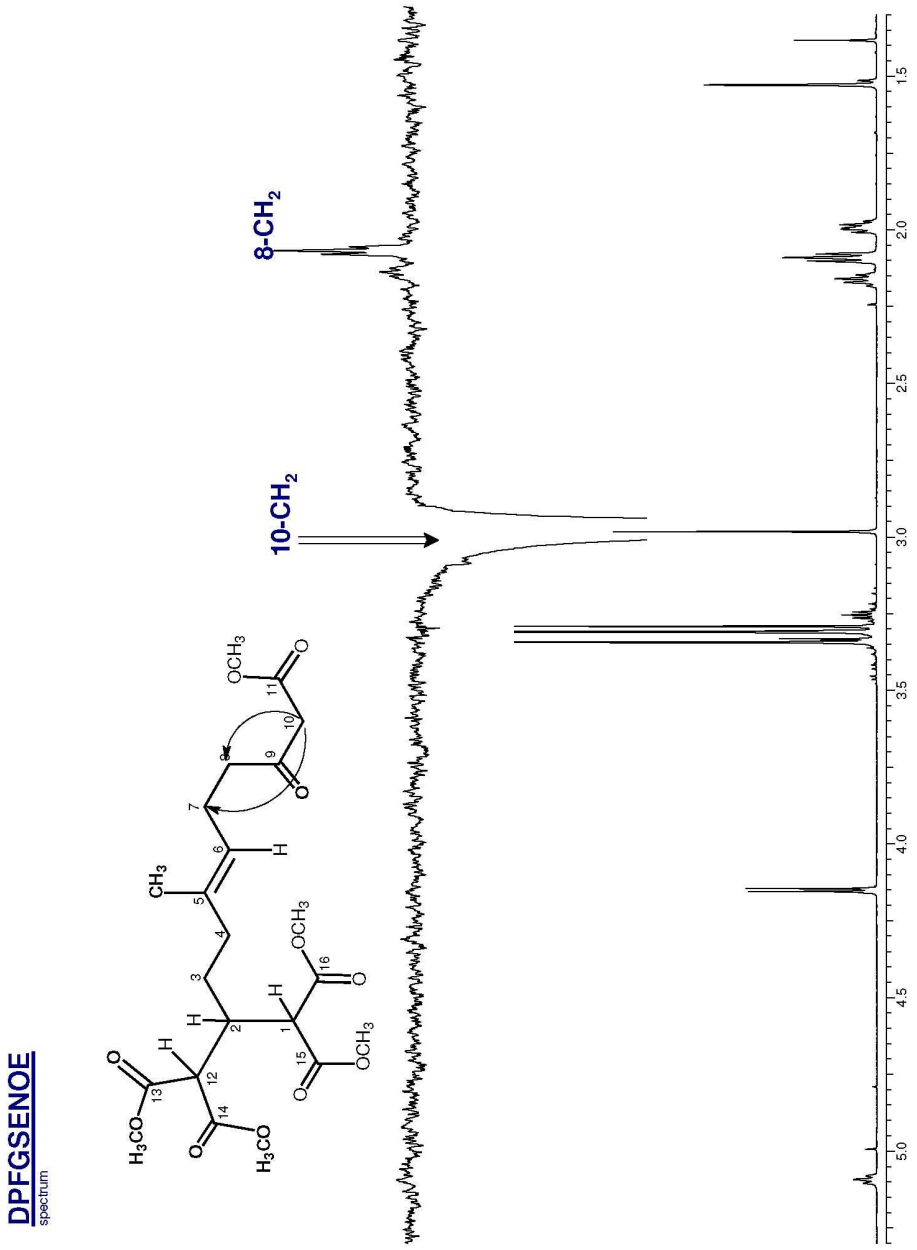
DPFGSENOE
spectrum
8-CH2
10-CH2
CH3
OCH3
OCH3
OCH3
H3CO
H3CO
H
H
H
H
O
O
O
O
O
O
O
O
1
2
3
4
5
6
7
8
9
10
11
12
13
14
15
16
5.0
4.5
4.0
3.5
3.0
2.5
2.0
1.5

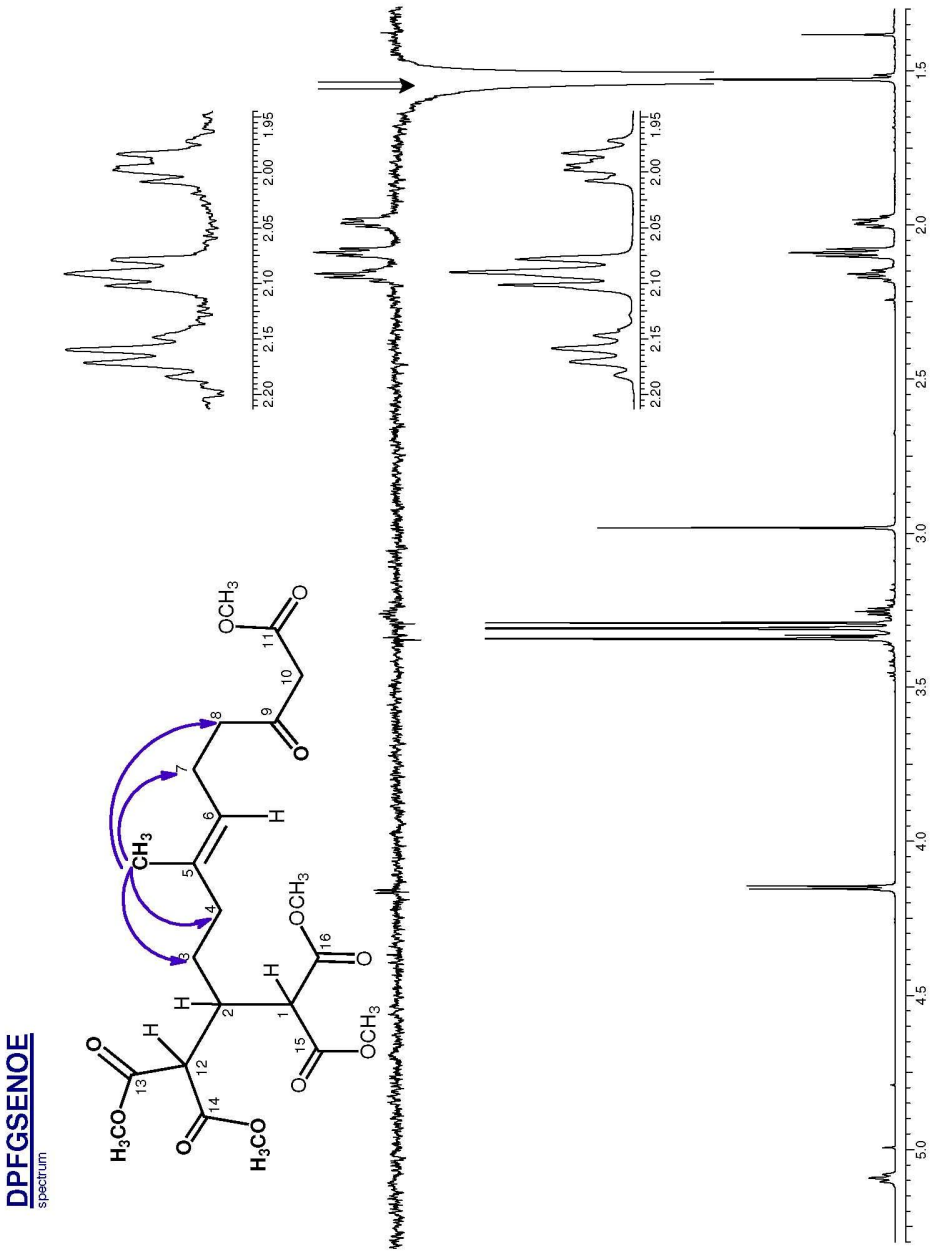
DPFGSENOE
spectrum
H3CO
H3CO
OCH3
OCH3
OCH3
CH3
H
H
H
1
2
3
4
5
6
7
8
9
10
11
12
13
14
15
16
5.0
4.5
4.0
3.5
3.0
2.5
2.0
1.5
2.20
2.15
2.10
2.05
2.00
1.95

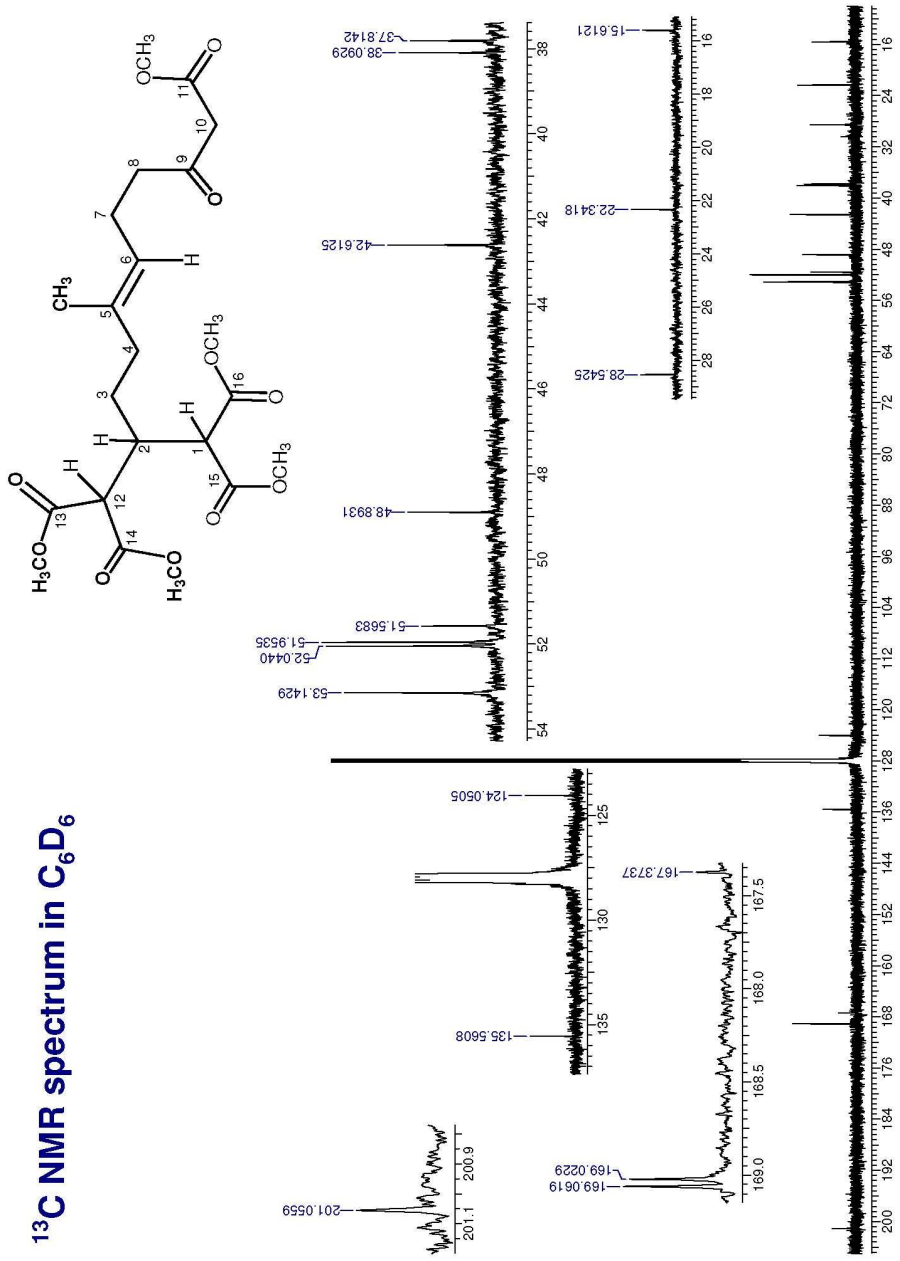
^{13}C NMR spectrum in C_6D_6
H_3CO
OCH_3
CH_3
H
O
1
2
3
4
5
6
7
8
9
10
11
12
13
14
15
16
37.8142
38.0929
42.6125
48.8931
51.5683
51.9535
52.0440
53.1429
15.6121
22.3418
28.5425
124.0505
135.5608
167.3737
169.0229
169.0619
201.0559

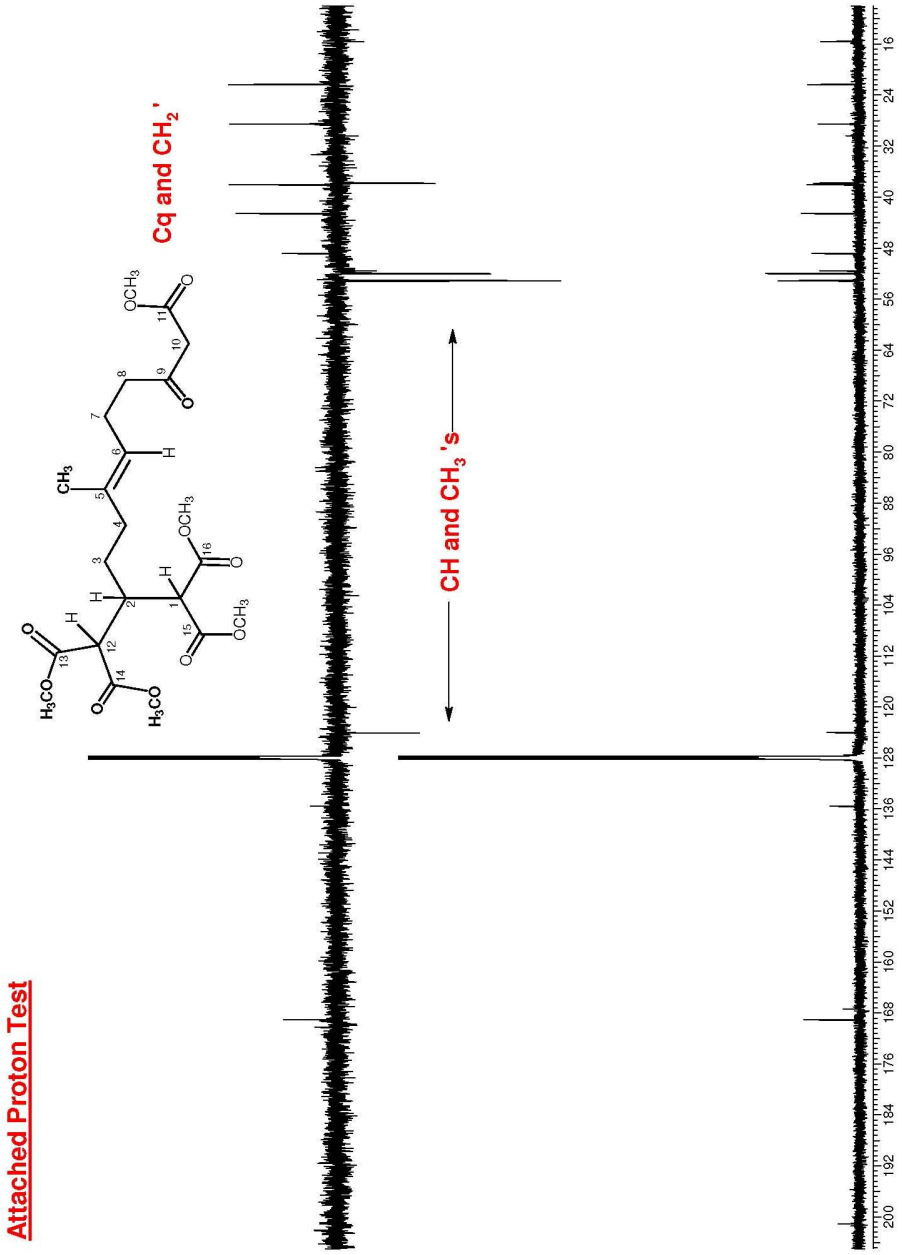
Attached Proton Test
Cq and CH2 '
CH and CH3 's

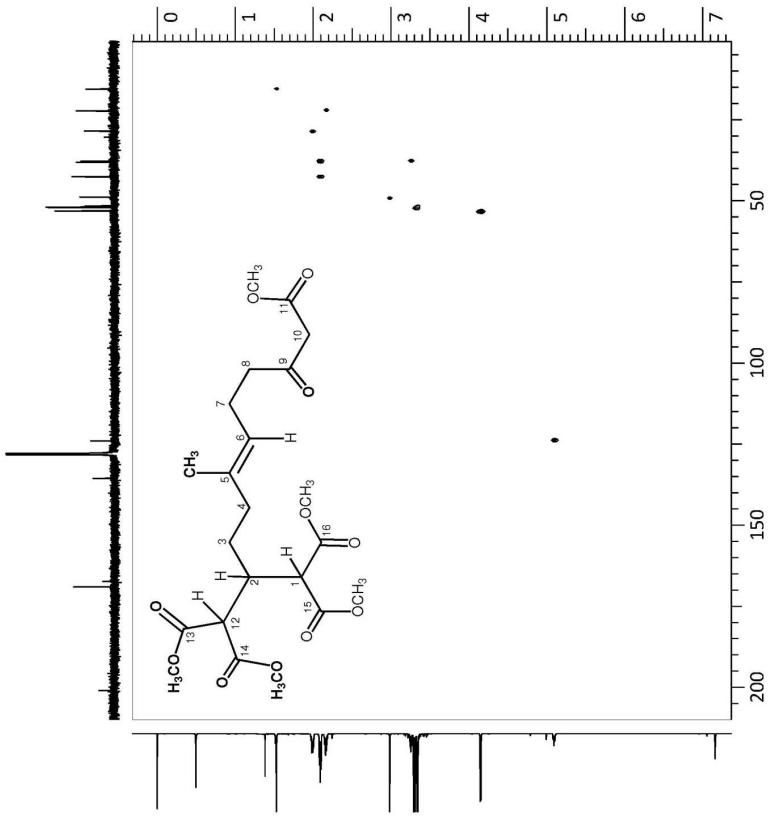

One-bond correlations

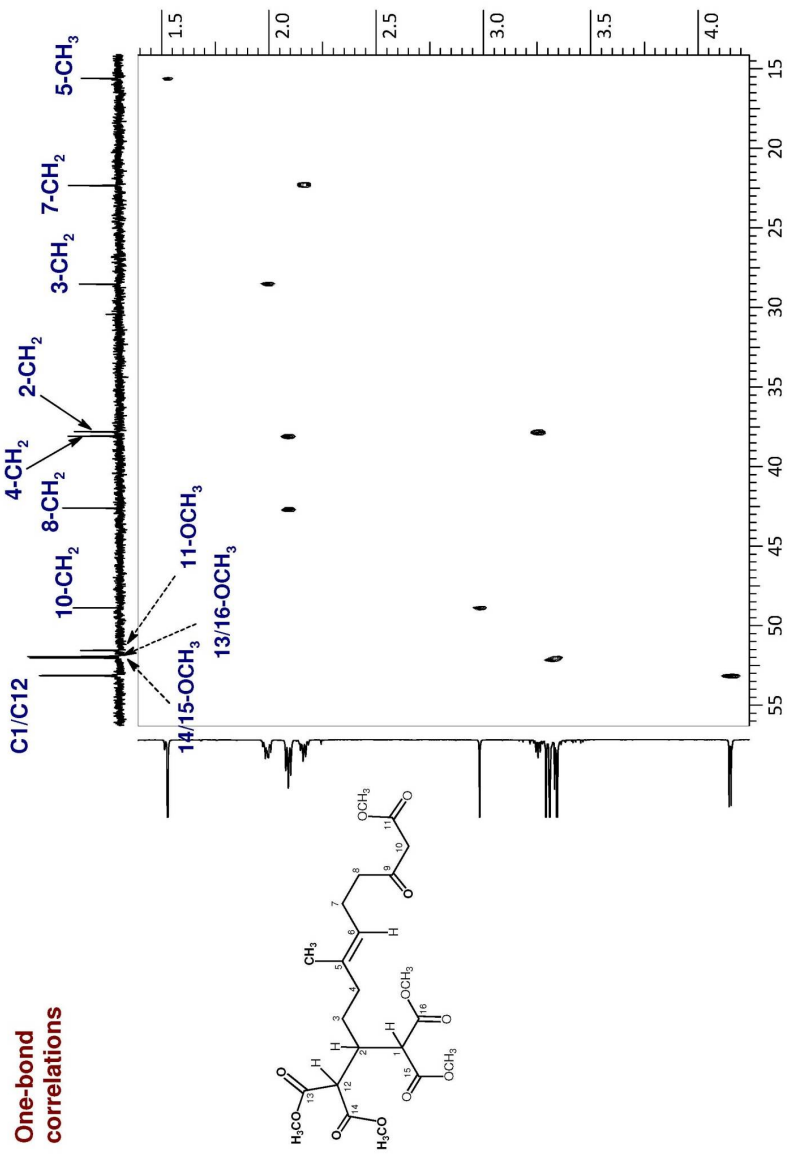
One-bond correlations
C1/C12
14/15-OCH3
10-CH2
8-CH2
4-CH2
2-CH2
3-CH2
7-CH2
5-CH3
11-OCH3
13/16-OCH3
1.5
2.0
2.5
3.0
3.5
4.0
15
20
25
30
35
40
45
50
55

Selected long-range HMBC correlations

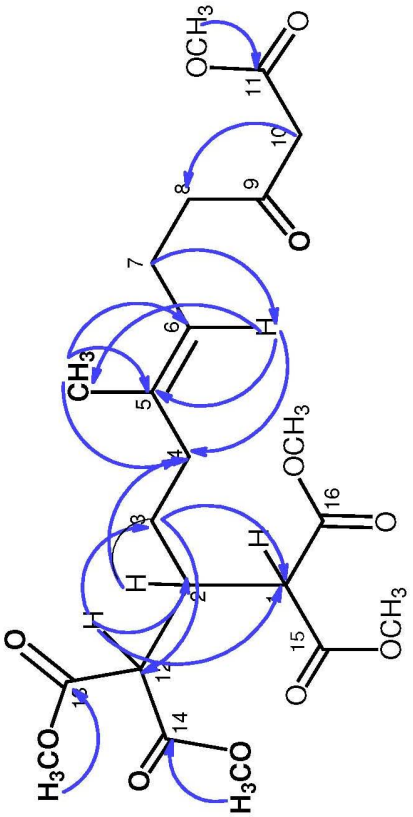

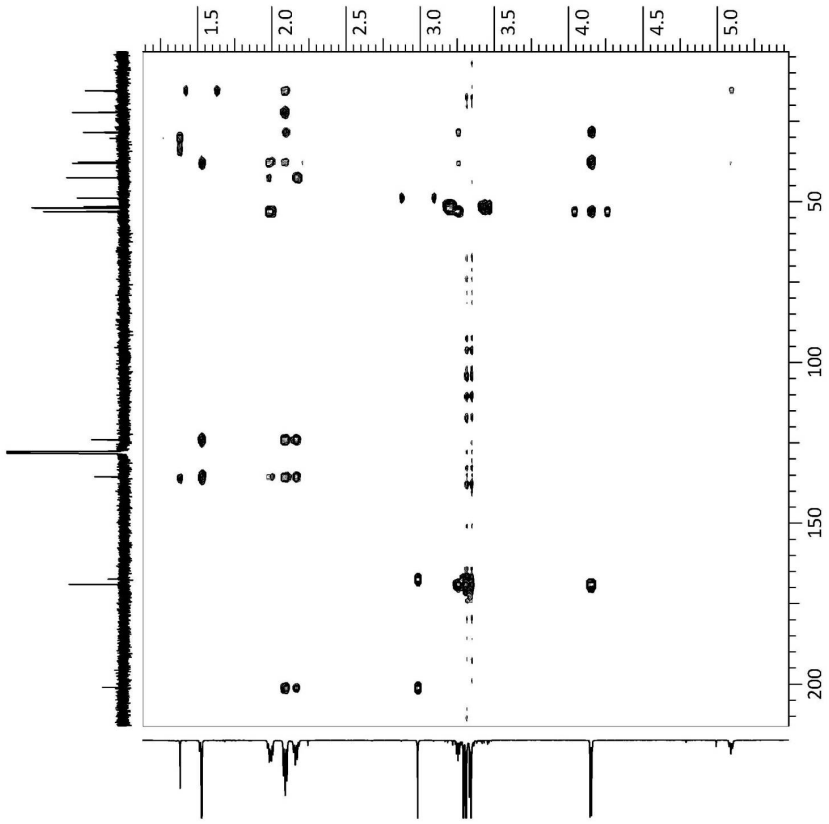

gHMBC
long-range correlations

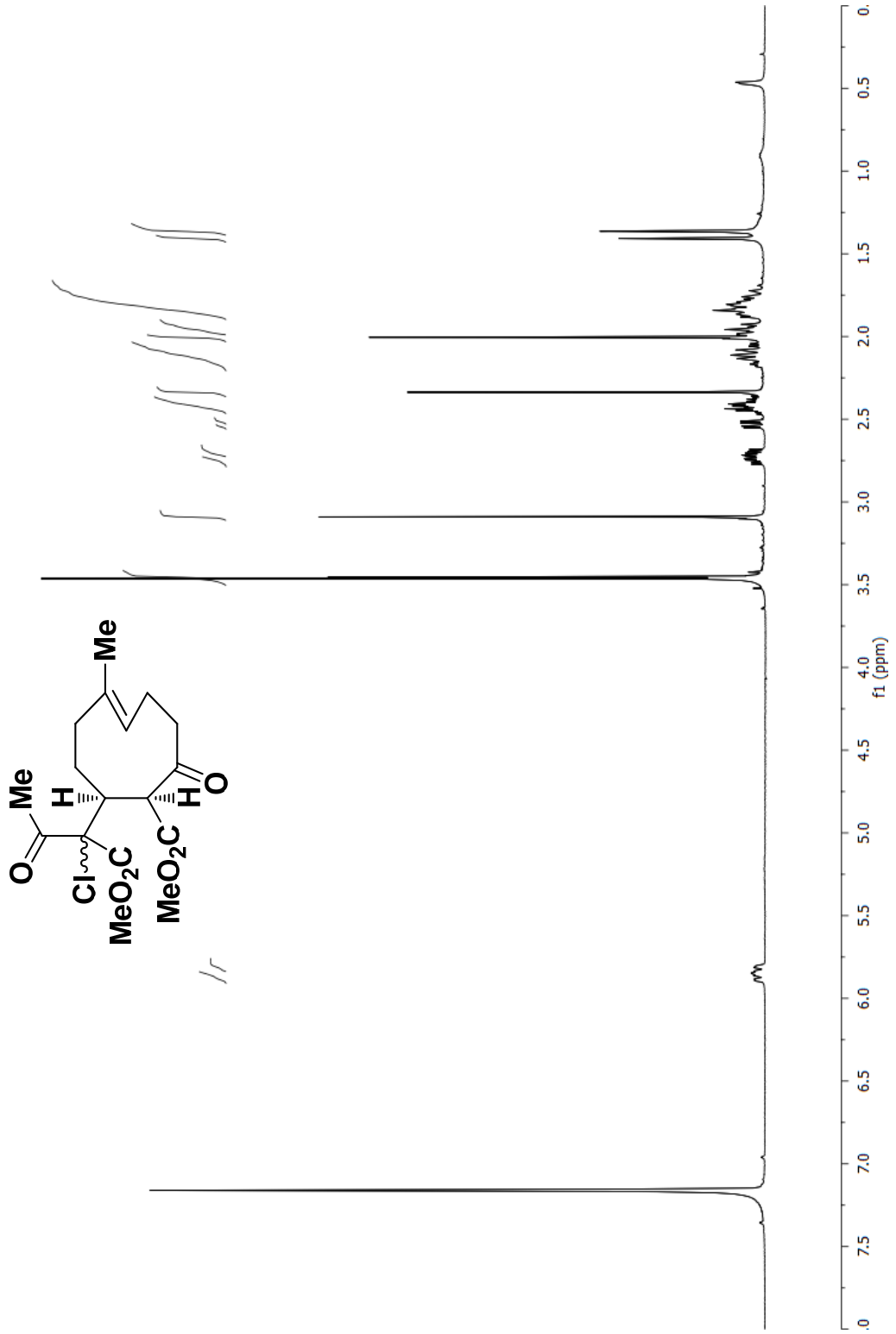
Me
H
O
Cl
MeO2C
MeO2C
H
O
Me
f1 (ppm)

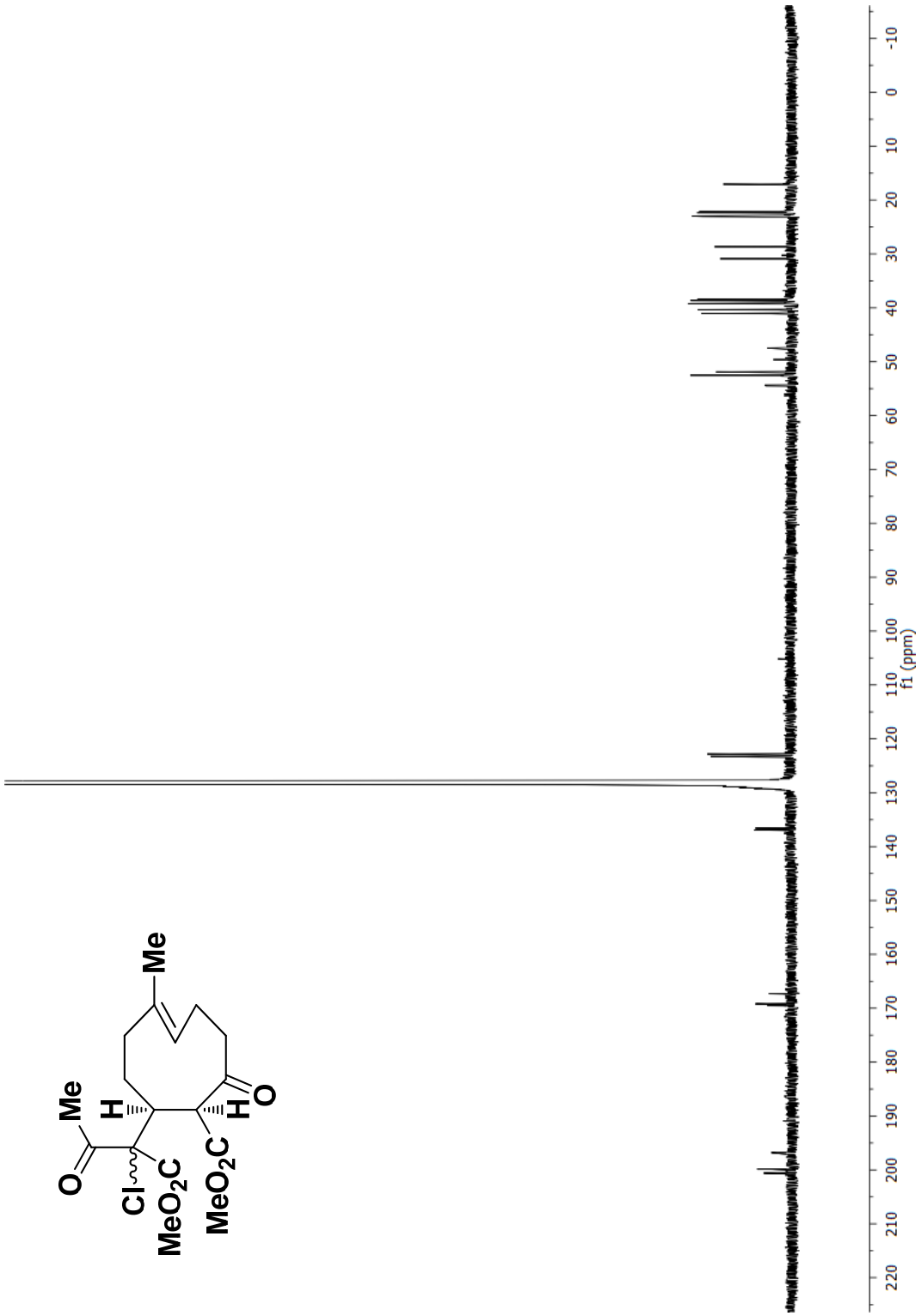
Me
H
O
Cl
MeO2C
MeO2C
H
O
Me
f1 (ppm)

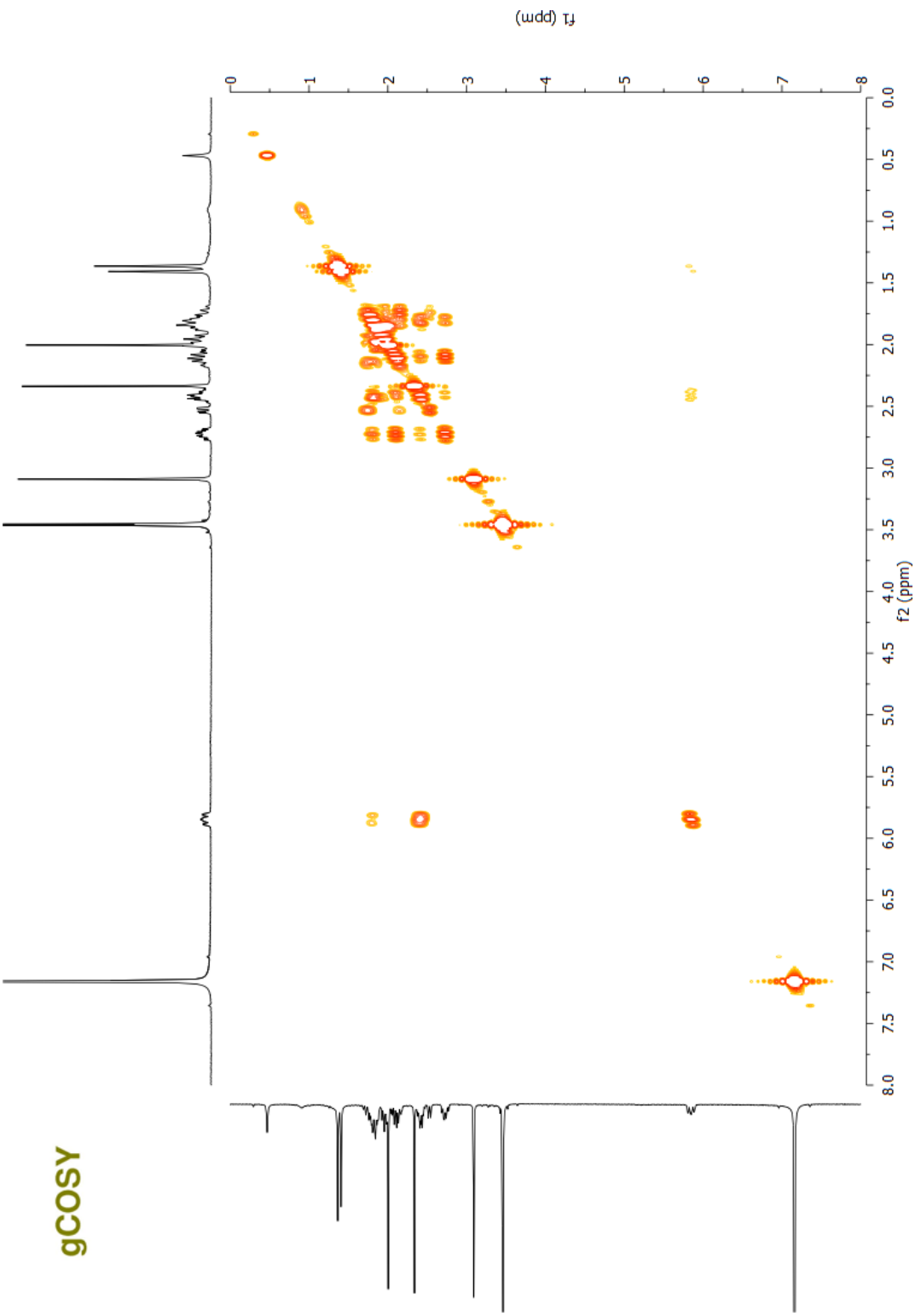
gCOSY
f1 (ppm)
f2 (ppm)

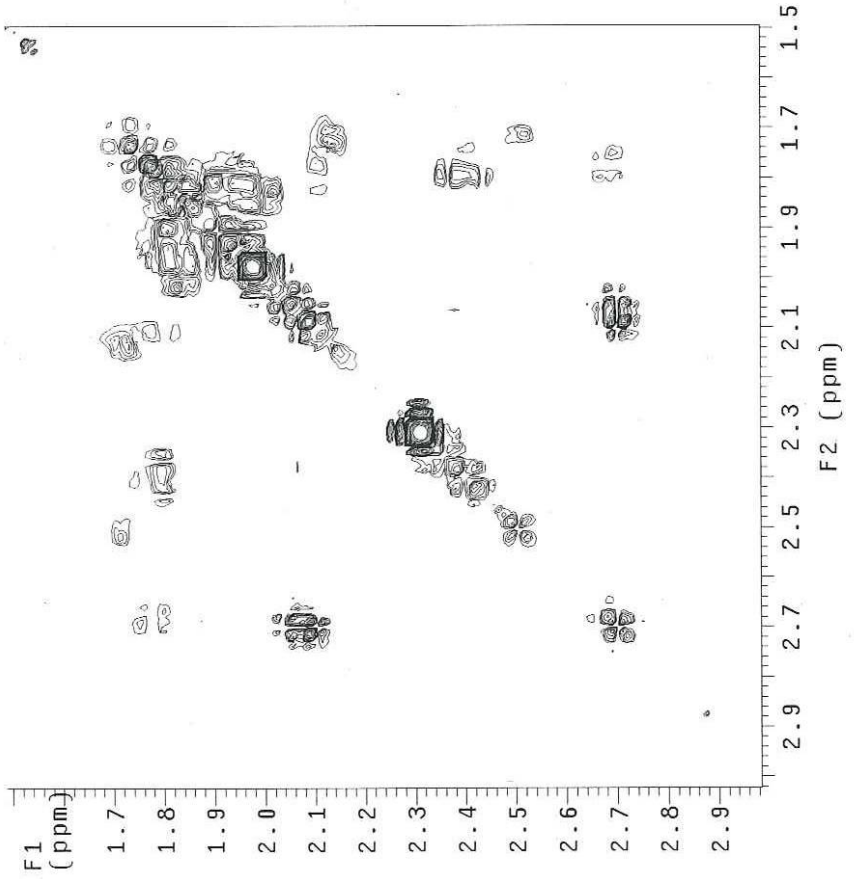

Std proton

File: xen035-chlorideadditionproductCOSYMurali

Pulse Sequence: gCOSY

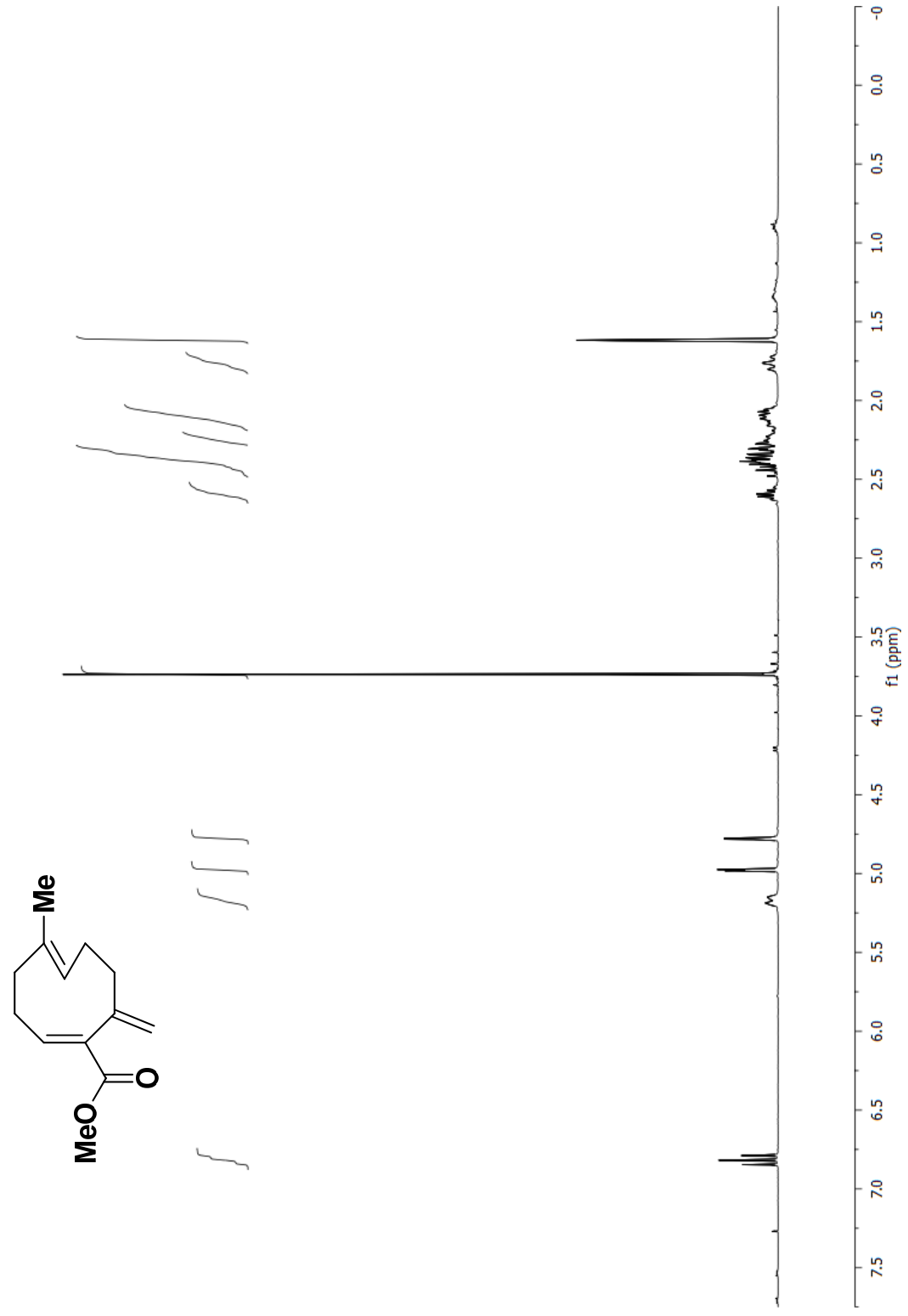
Me
MeO
O
f1 (ppm)

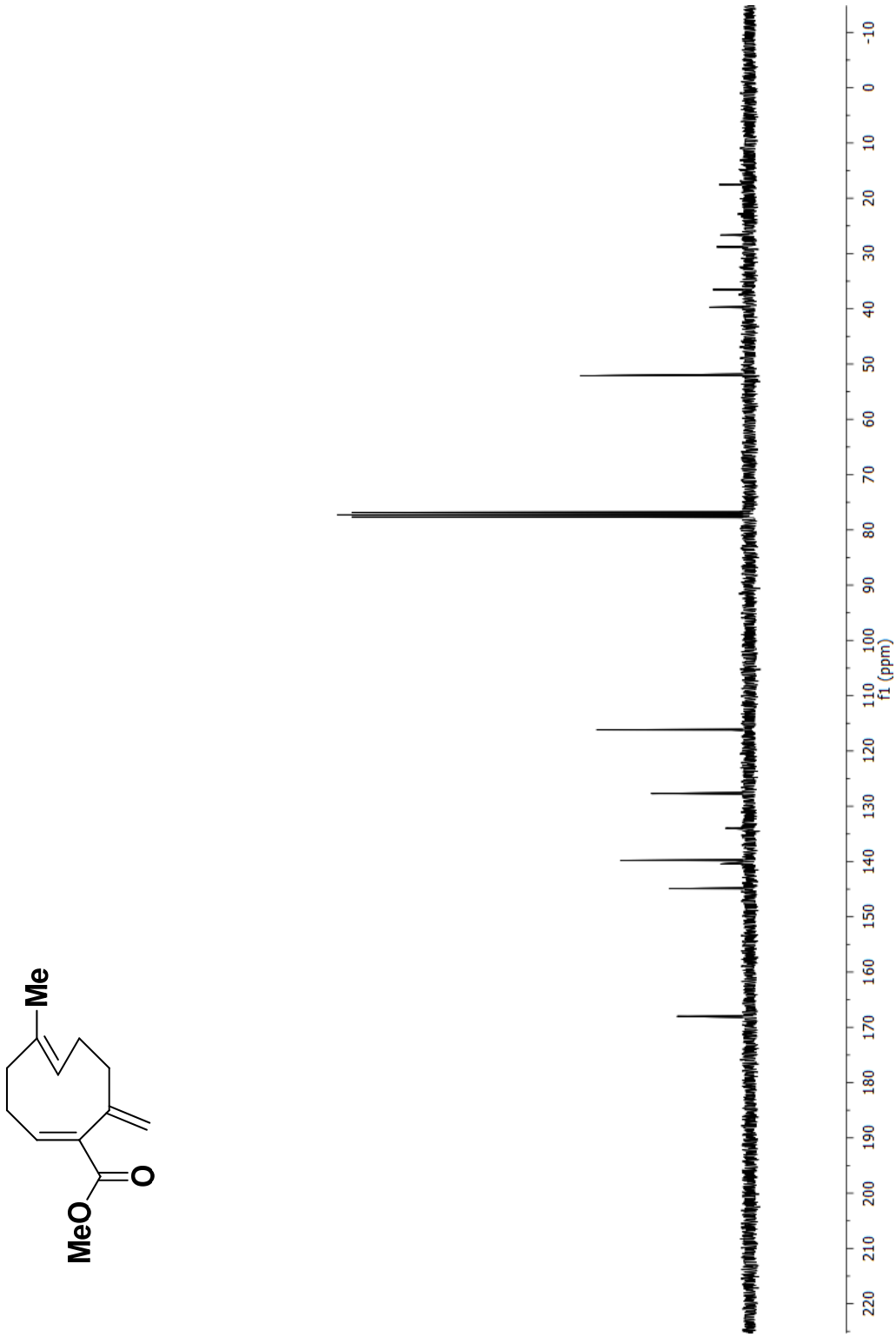
Me
MeO
O
f1 (ppm)
-10
0
10
20
30
40
50
60
70
80
90
100
110
120
130
140
150
160
170
180
190
200
210
220

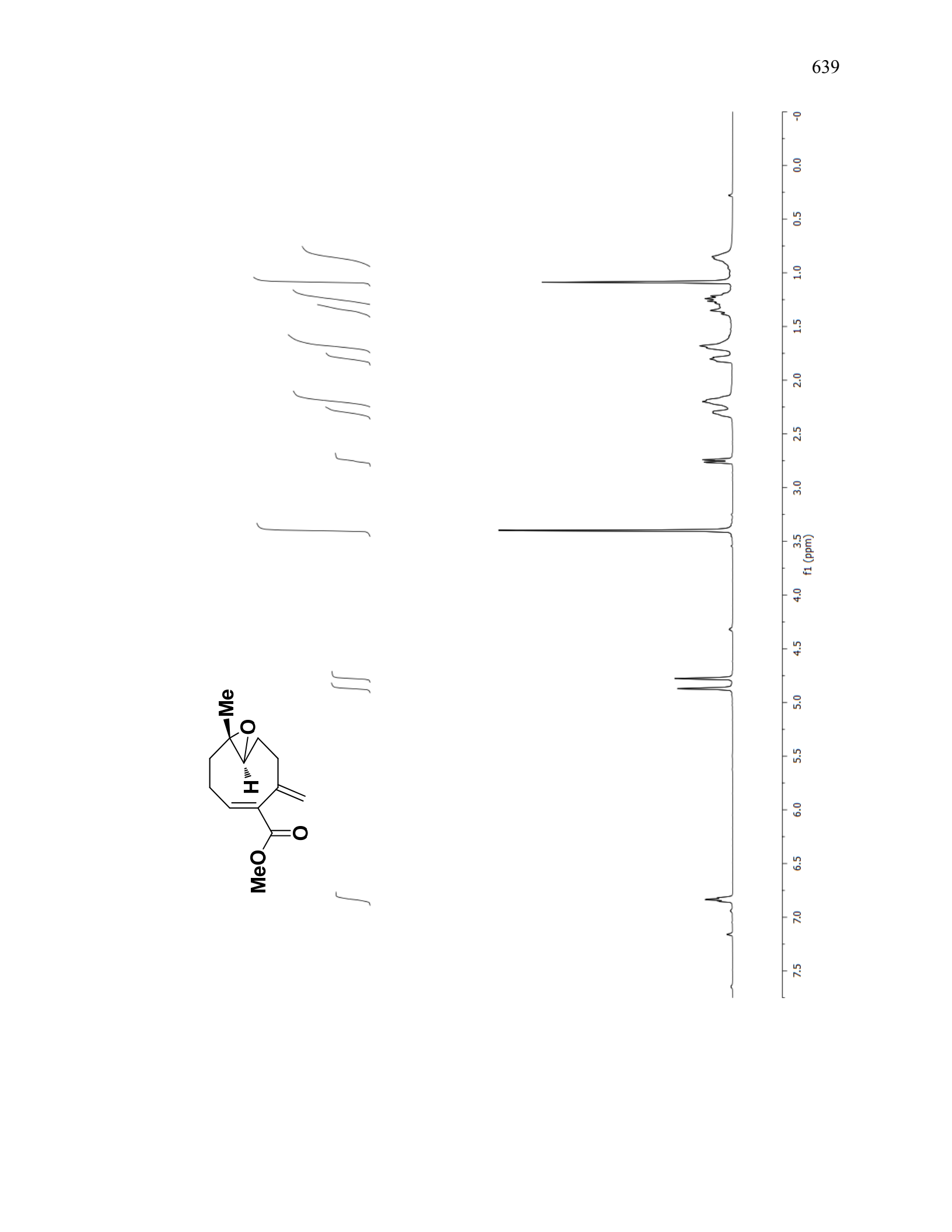
Me
O
H
O
MeO
f1 (ppm)

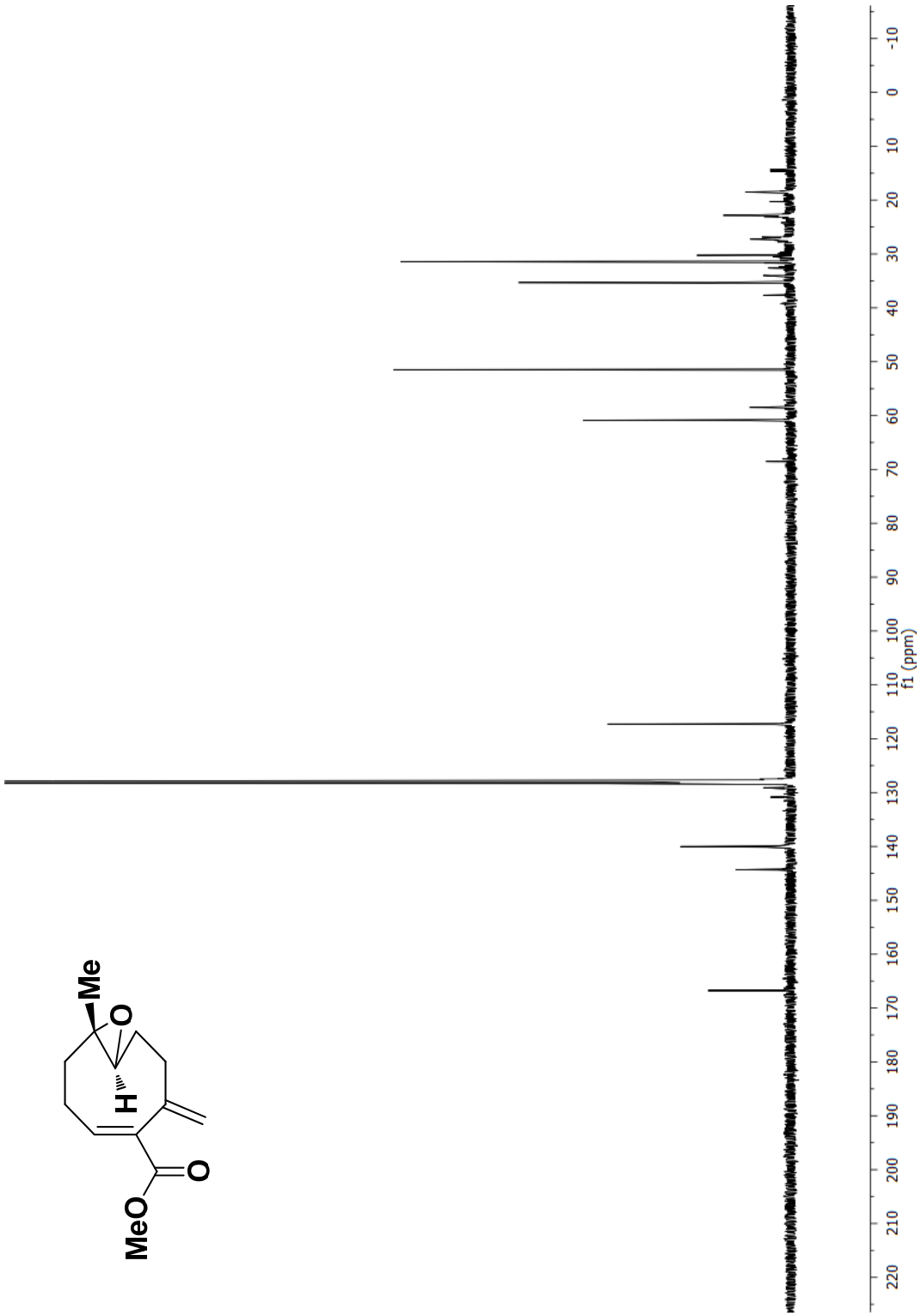
Me
O
H
O
MeO
f1 (ppm)

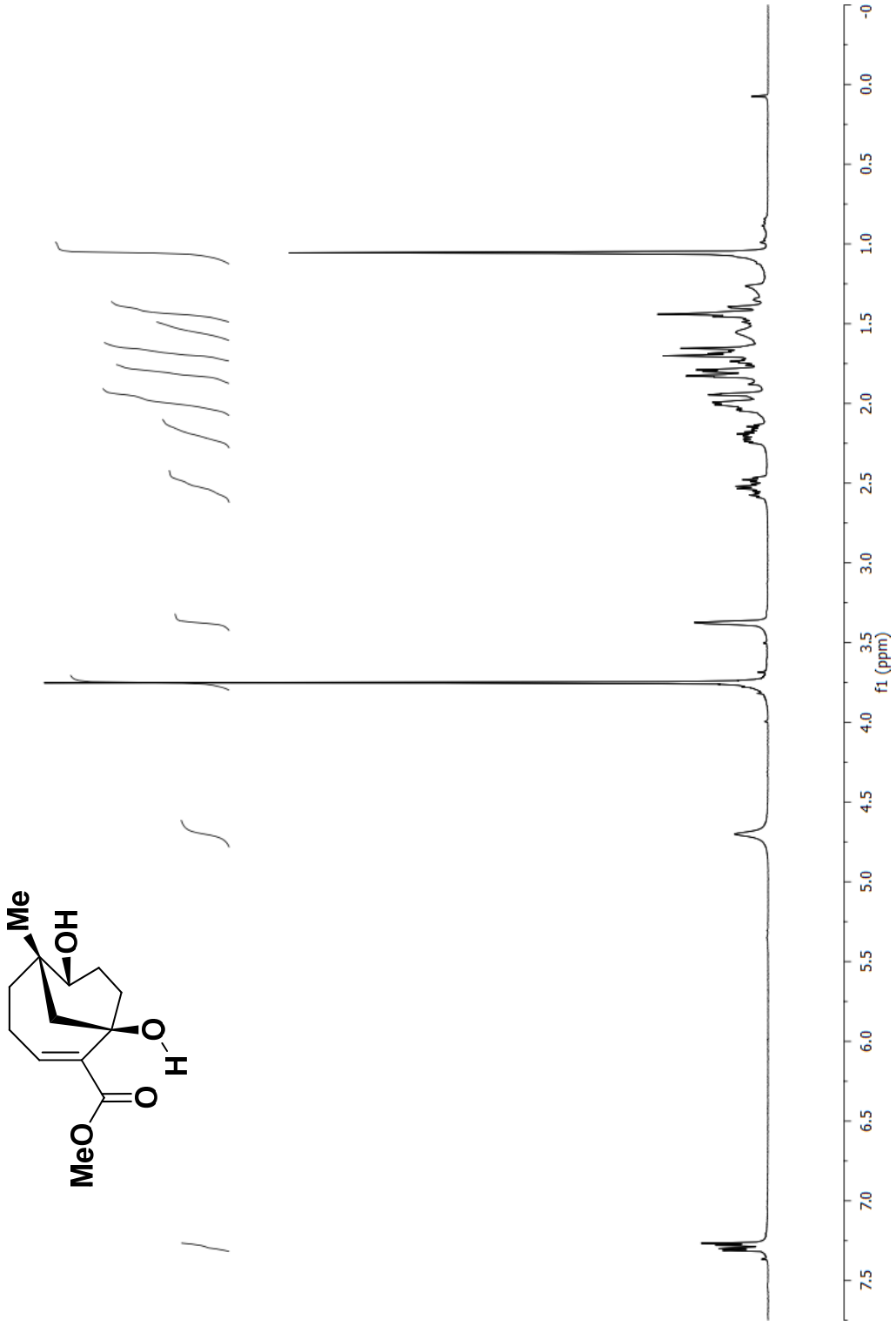
Me
OH
O
H
O
MeO
-0
0.0
0.5
1.0
1.5
2.0
2.5
3.0
3.5
4.0
4.5
5.0
5.5
6.0
6.5
7.0
7.5
f1 (ppm)

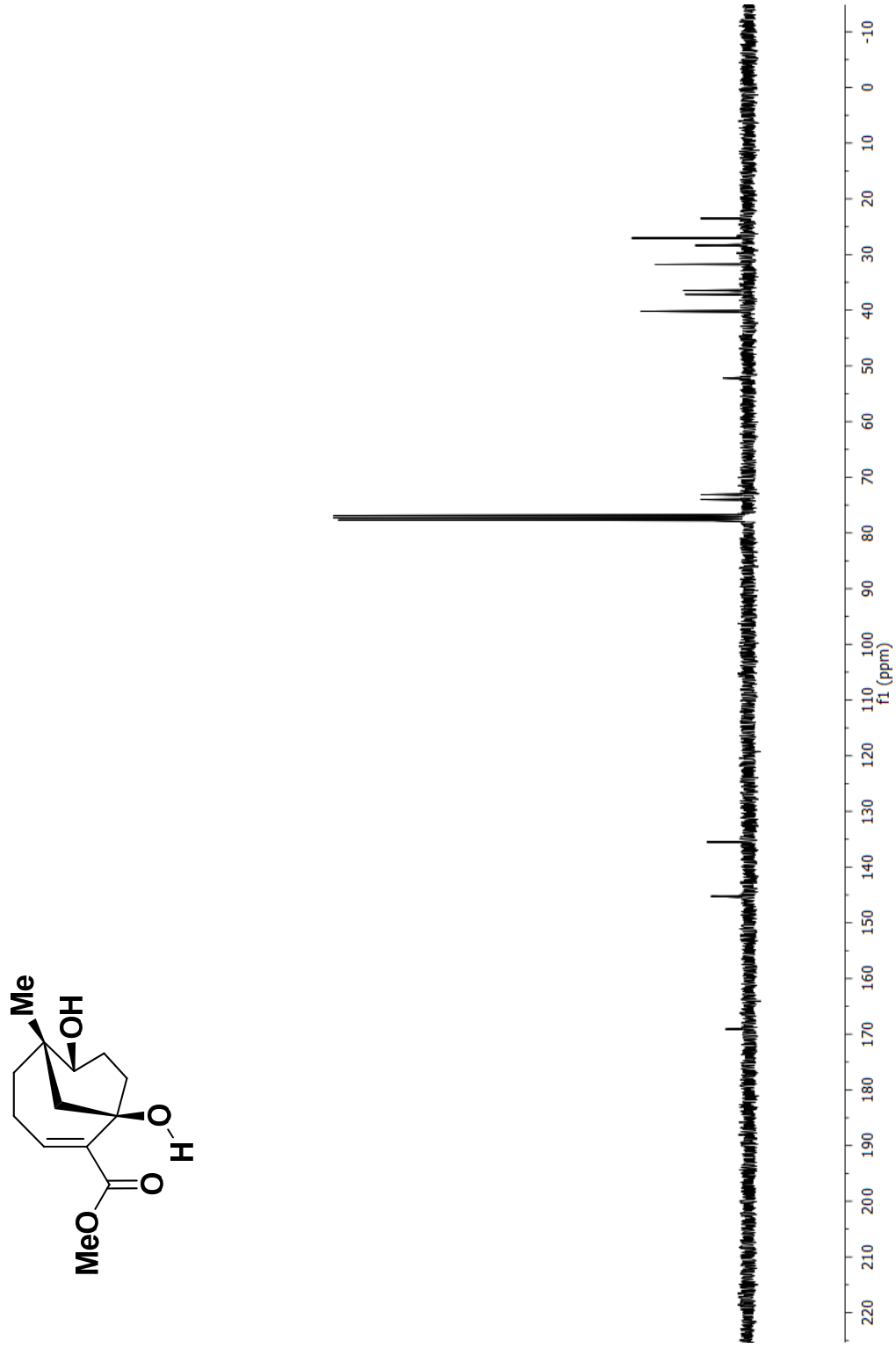
Me
OH
O
H
O
MeO
-10
0
10
20
30
40
50
60
70
80
90
100
110
120
130
140
150
160
170
180
190
200
210
220
f1 (ppm)

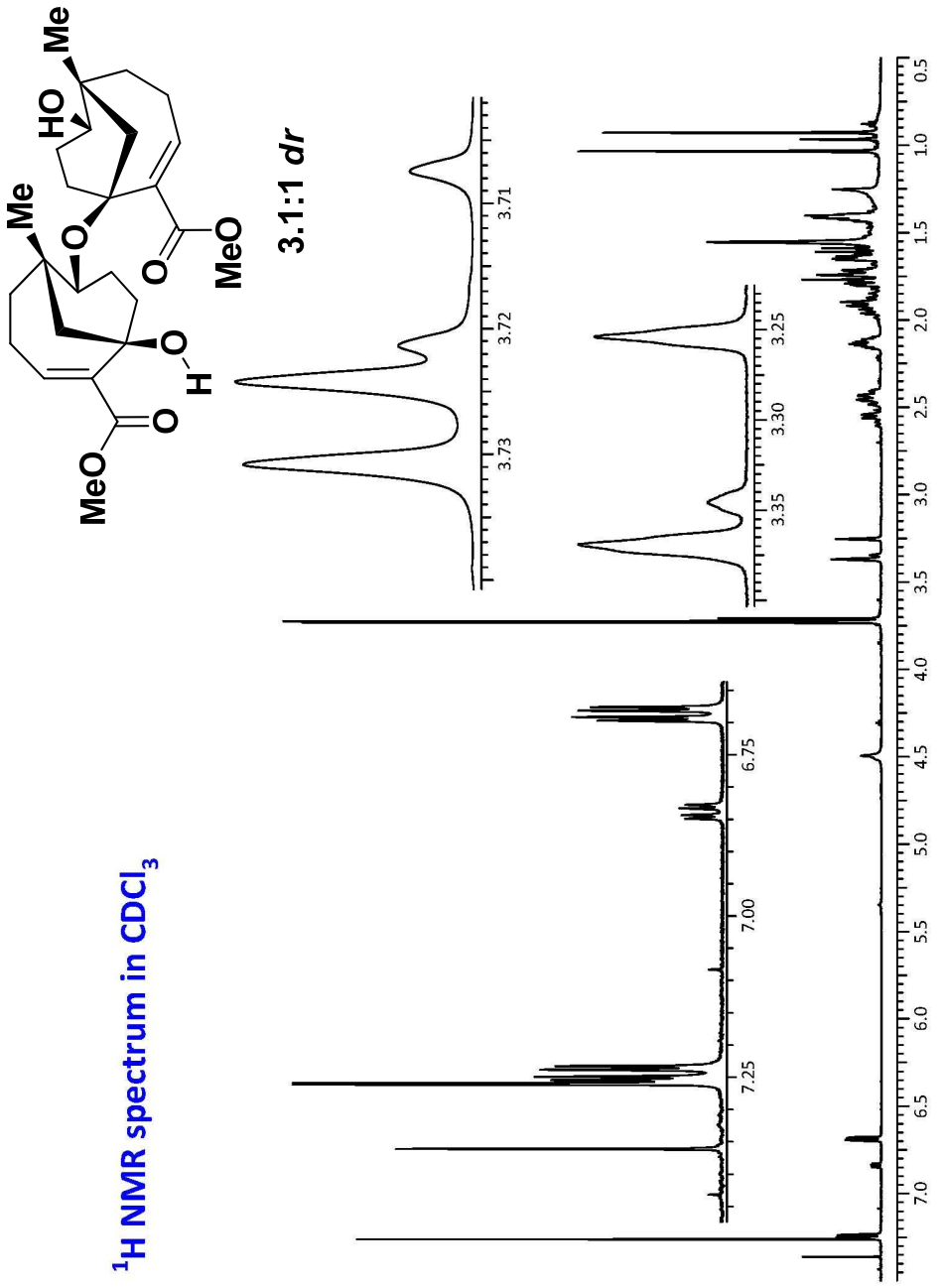
Me
HO
Me
O
O
MeO
O
O
H
MeO
3.1:1 dr
^{1}H NMR spectrum in CDCl$_3$
7.25
7.00
6.75
3.73
3.72
3.71
3.35
3.30
3.25
7.0
6.5
6.0
5.5
5.0
4.5
4.0
3.5
3.0
2.5
2.0
1.5
1.0
0.5

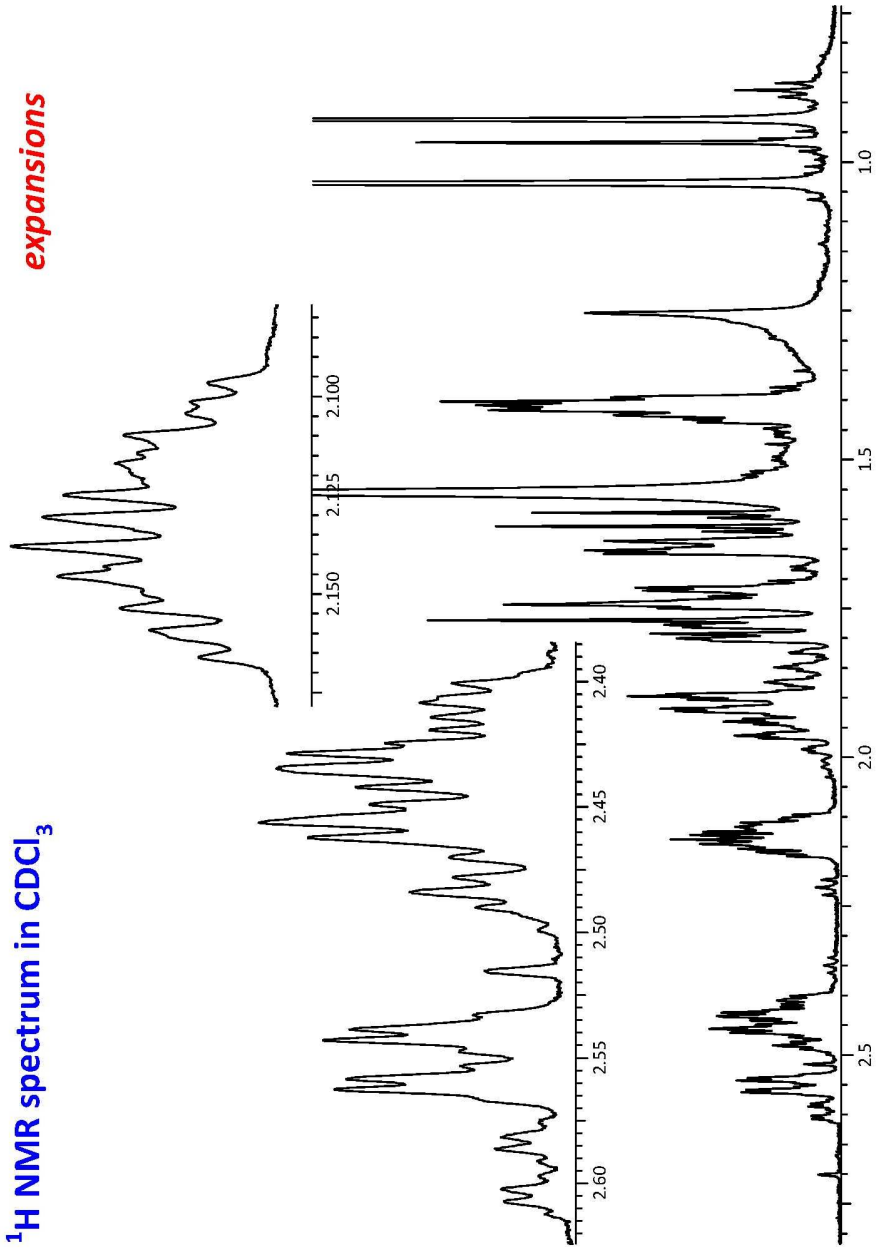
^{1}H NMR spectrum in $CDCl_3$
expansions
2.150
2.125
2.100
2.60
2.55
2.50
2.45
2.40
2.5
2.0
1.5
1.0

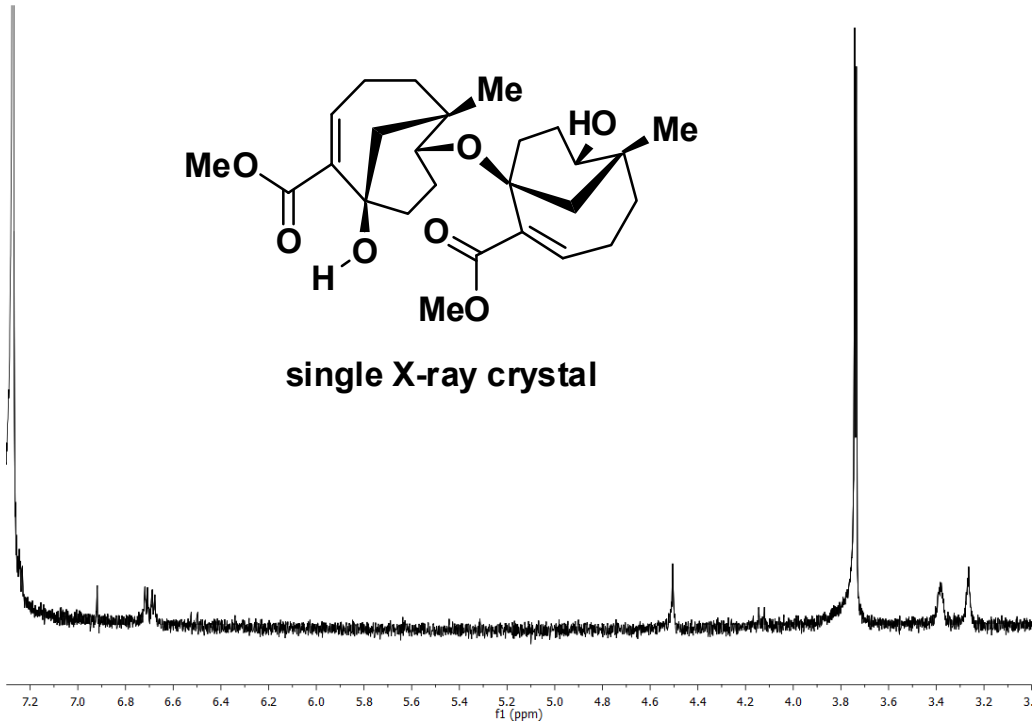
Me
HO
Me
MeO
O
O
O
H
O
MeO
single X-ray crystal
7.2 7.0 6.8 6.6 6.4 6.2 6.0 5.8 5.6 5.4 5.2 5.0 4.8 4.6 4.4 4.2 4.0 3.8 3.6 3.4 3.2
f1 (ppm)

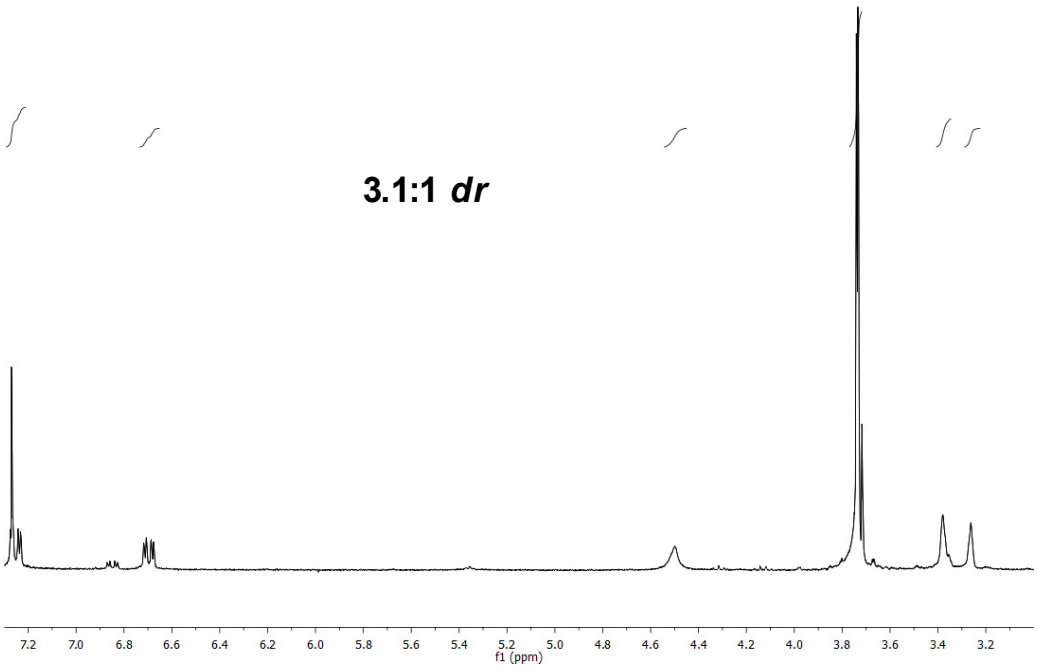
3.1:1 *dr*
7.2 7.0 6.8 6.6 6.4 6.2 6.0 5.8 5.6 5.4 5.2 5.0 4.8 4.6 4.4 4.2 4.0 3.8 3.6 3.4 3.2
f1 (ppm)

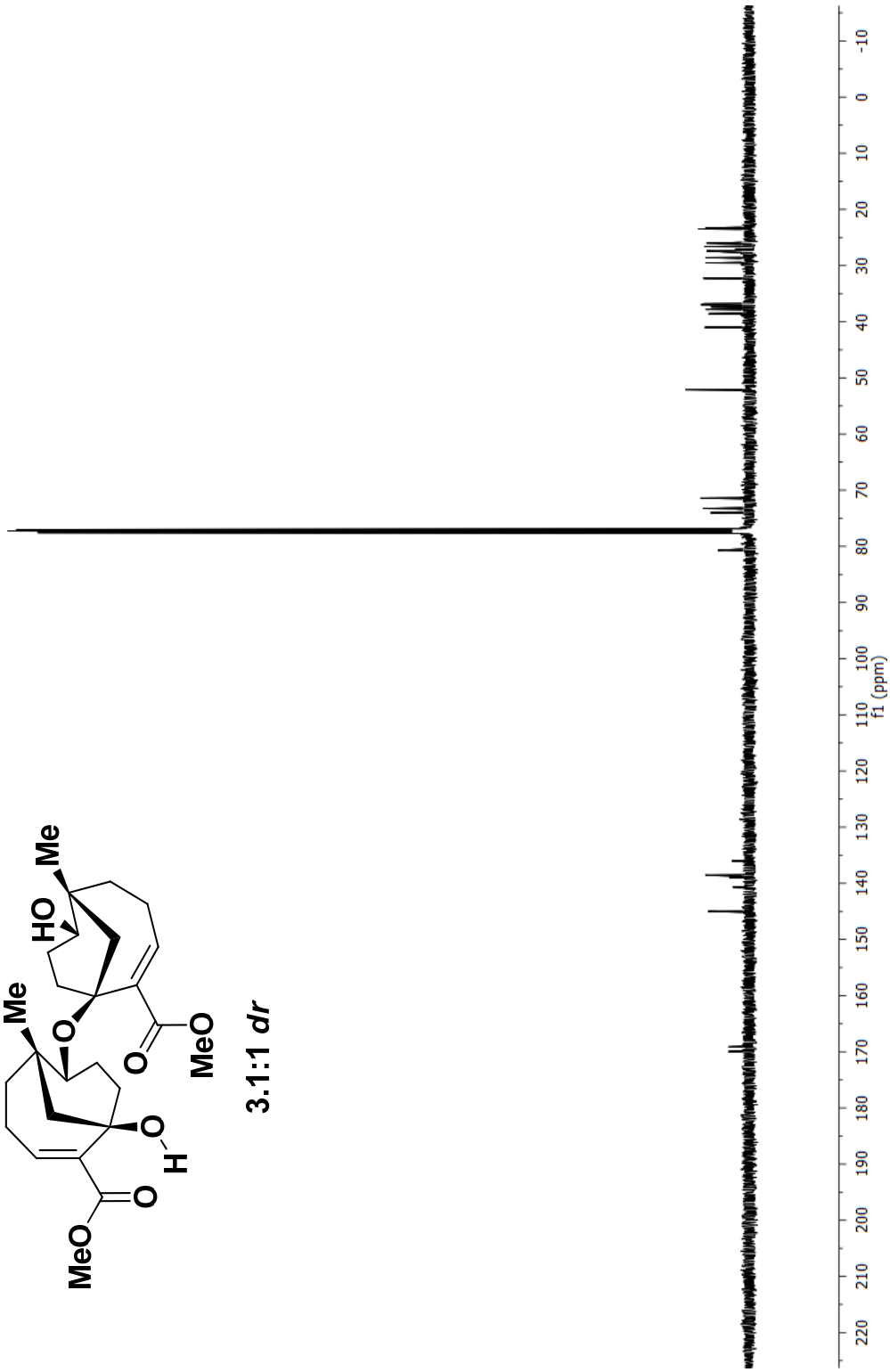
Me
HO
Me
O
O
MeO
O
H
MeO
3.1:1 dr
f1 (ppm)

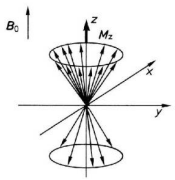

^{1}H NMR spectrum in C_6D_6

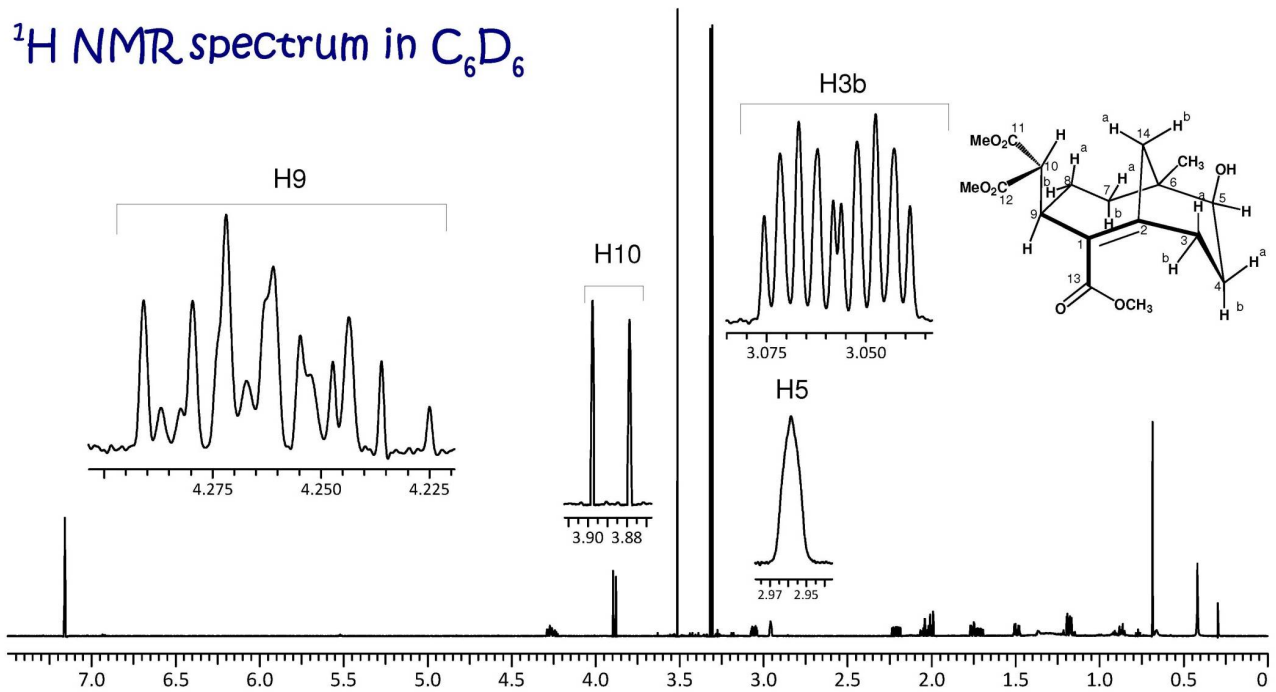

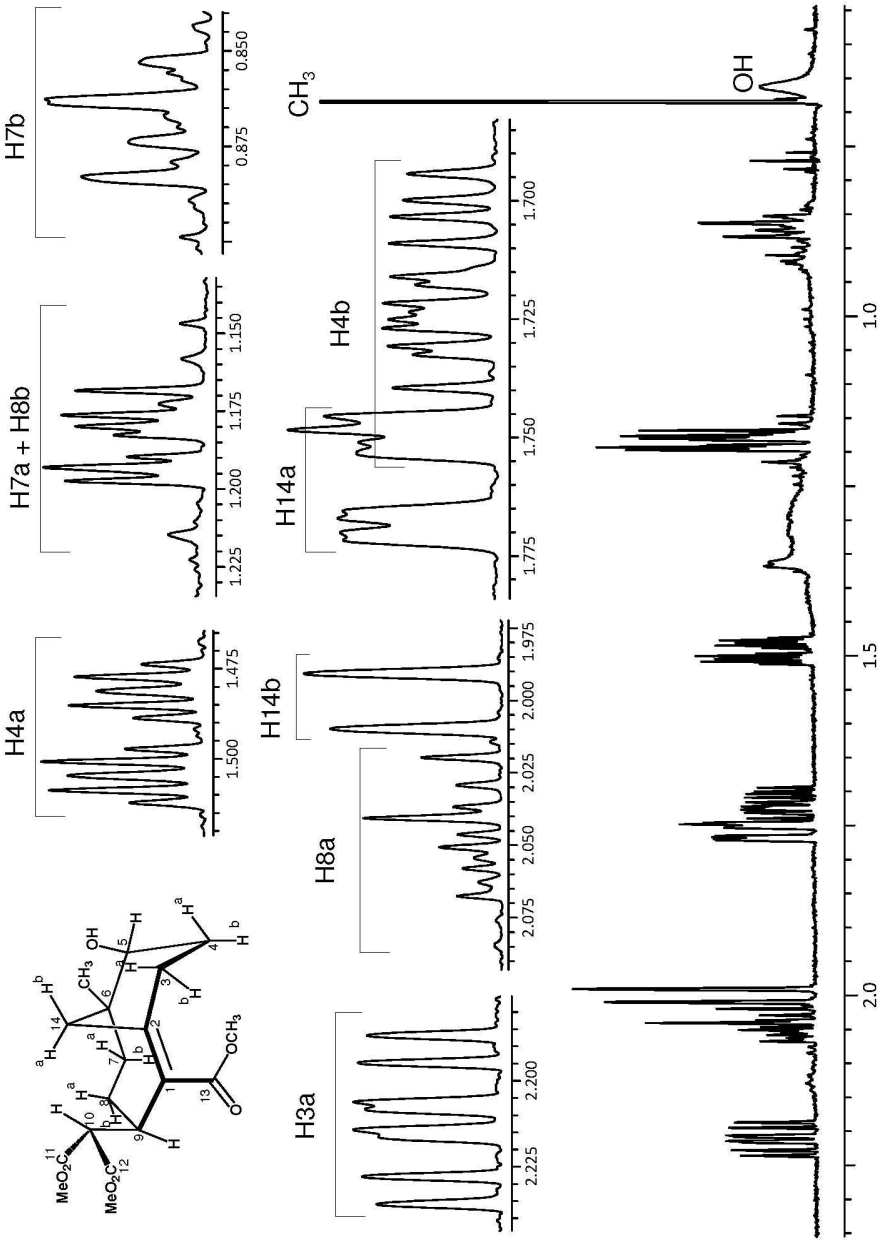
H7b
H7a + H8b
H4a
H14b
H14a
H4b
H8a
H3a
CH3
OH
2.0
1.5
1.0

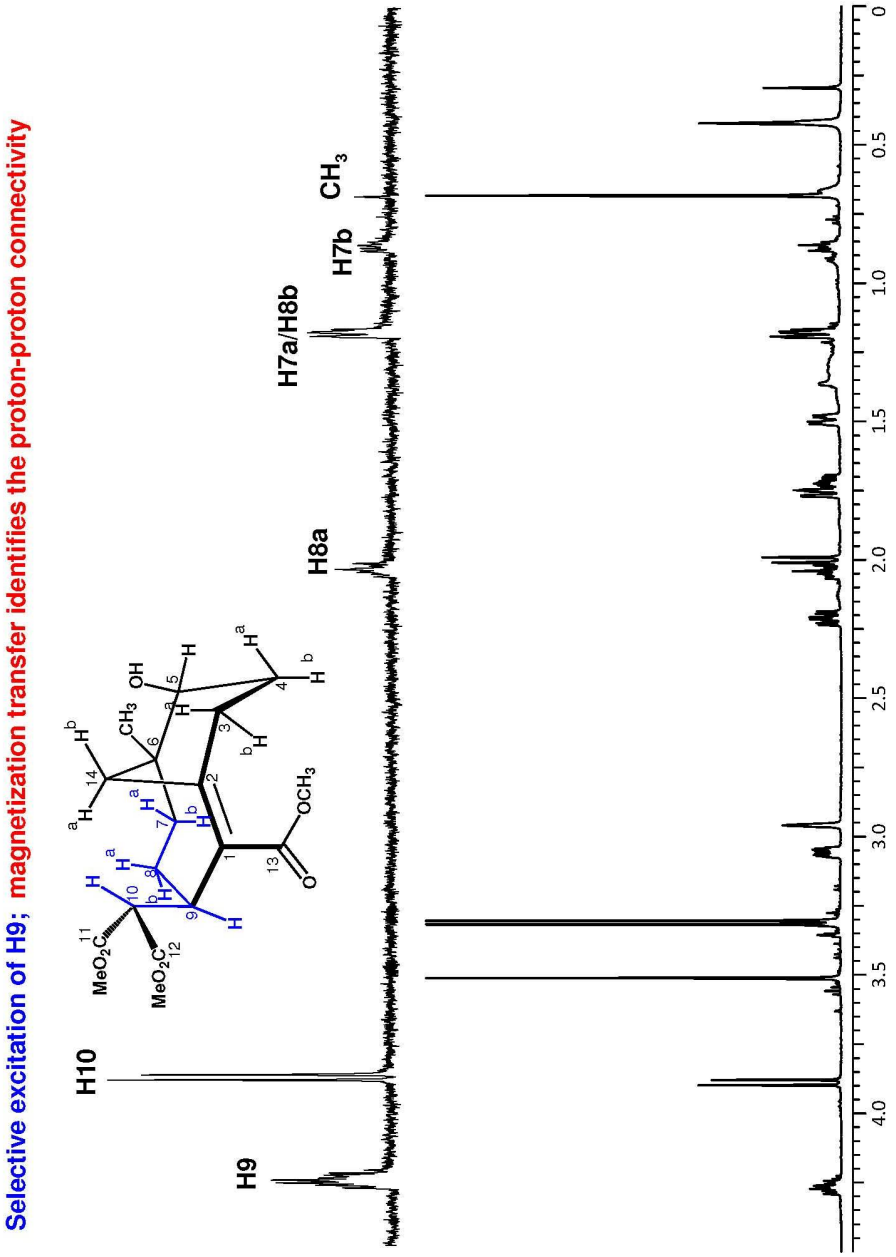
Selective excitation of H9; magnetization transfer identifies the proton-proton connectivity
H9
H10
H8a
H7a/H8b
H7b
CH3
4.0
3.5
3.0
2.5
2.0
1.5
1.0
0.5
0

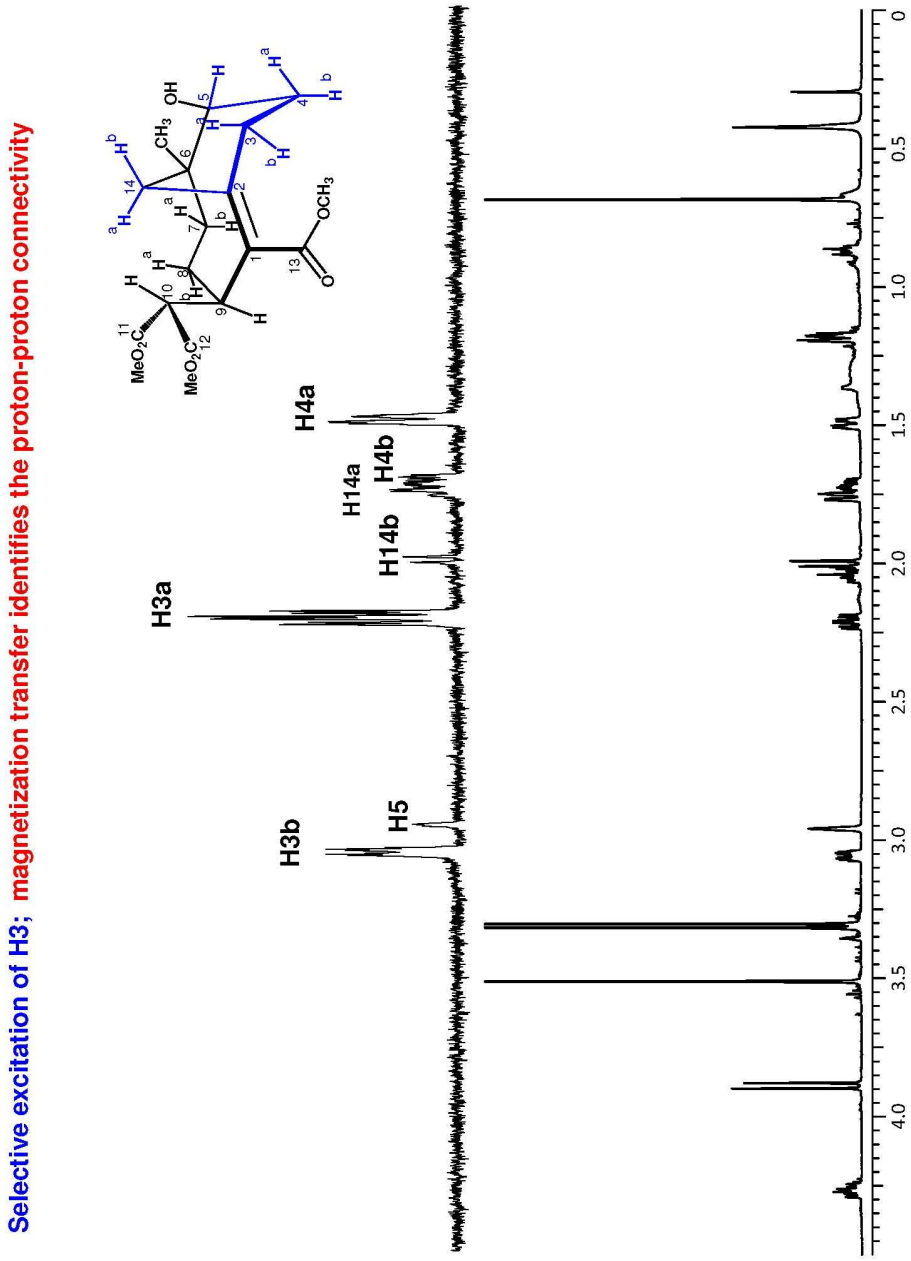
Selective excitation of H3; magnetization transfer identifies the proton-proton connectivity
H3a
H3b
H5
H14b
H14a
H4b
H4a
4.0
3.5
3.0
2.5
2.0
1.5
1.0
0.5
0

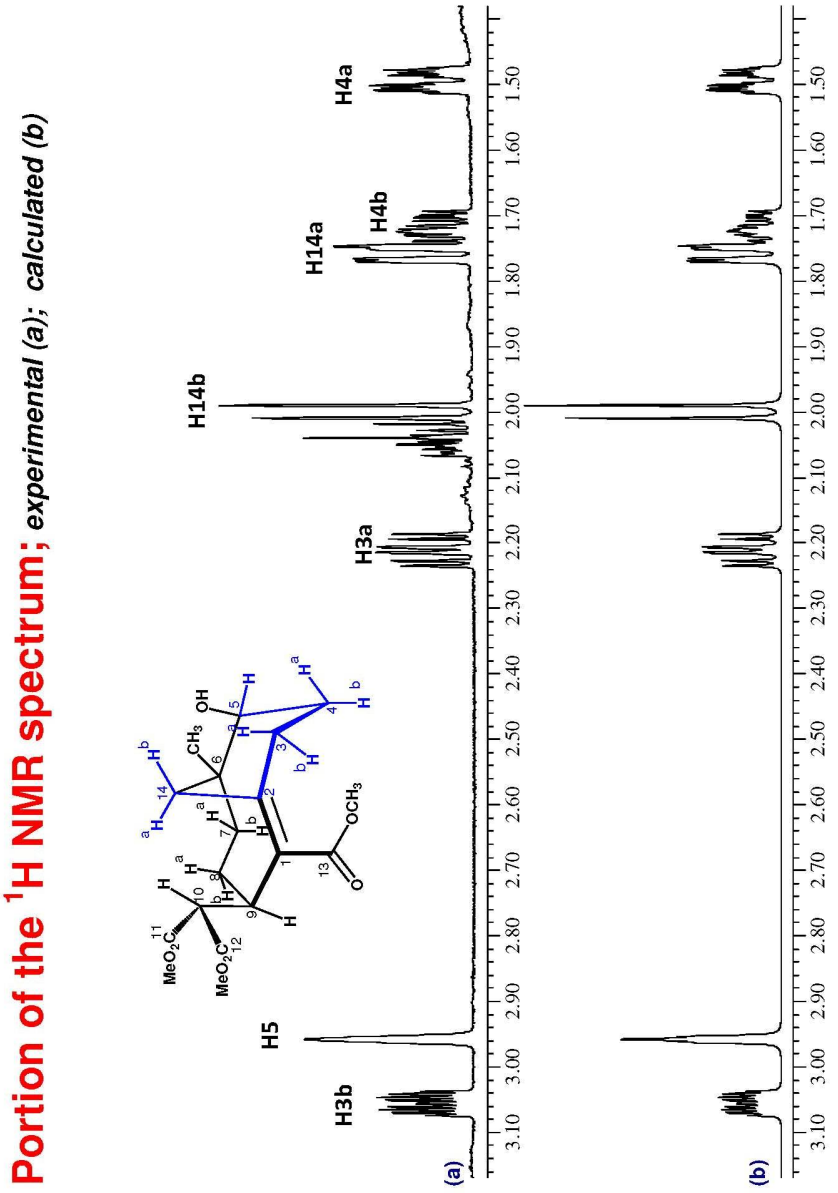
Portion of the ¹H NMR spectrum; experimental (a); calculated (b)
H3b
H5
H3a
H14b
H14a
H4b
H4a
(a)
(b)
3.10
3.00
2.90
2.80
2.70
2.60
2.50
2.40
2.30
2.20
2.10
2.00
1.90
1.80
1.70
1.60
1.50
MeO2C
MeO2C
CH3
OH
OCH3
O

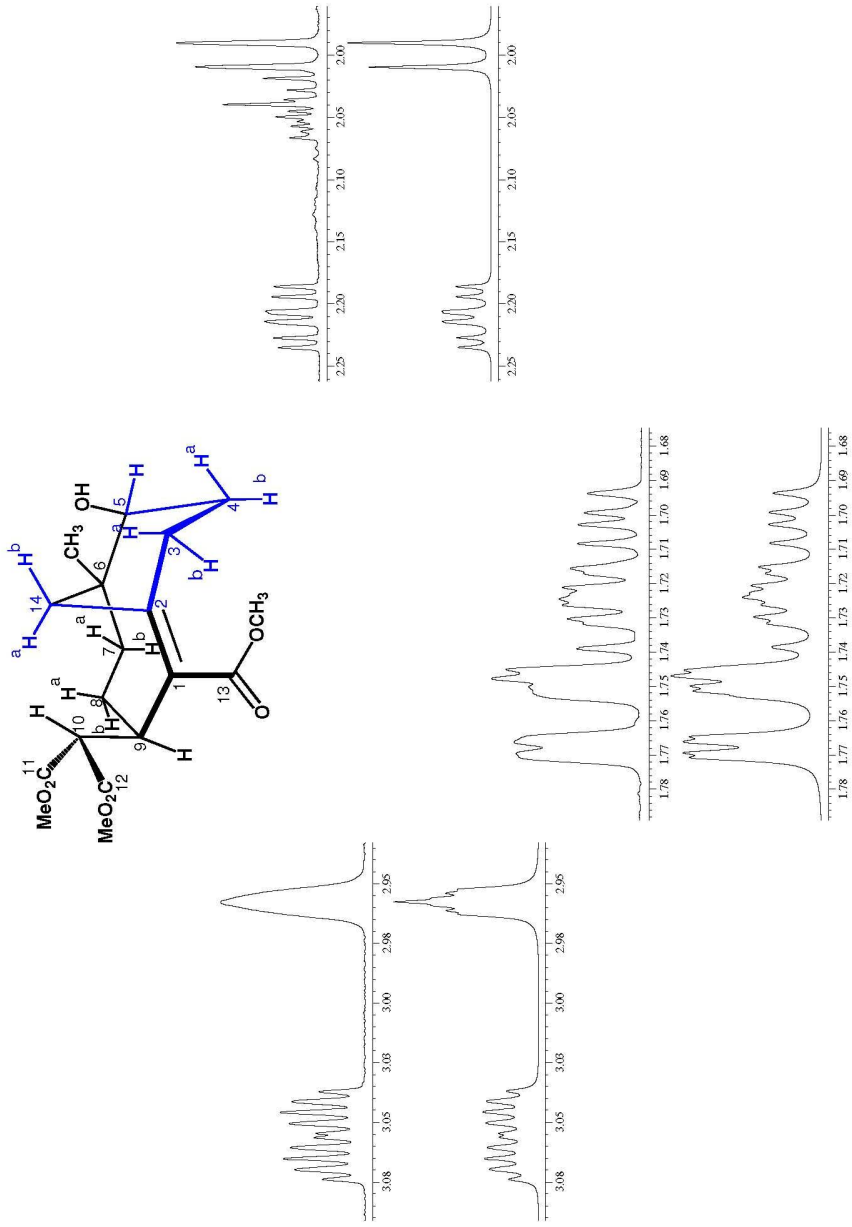
MeO2C
MeO2C
CH3
OH
OCH3
O
H
Ha
Hb

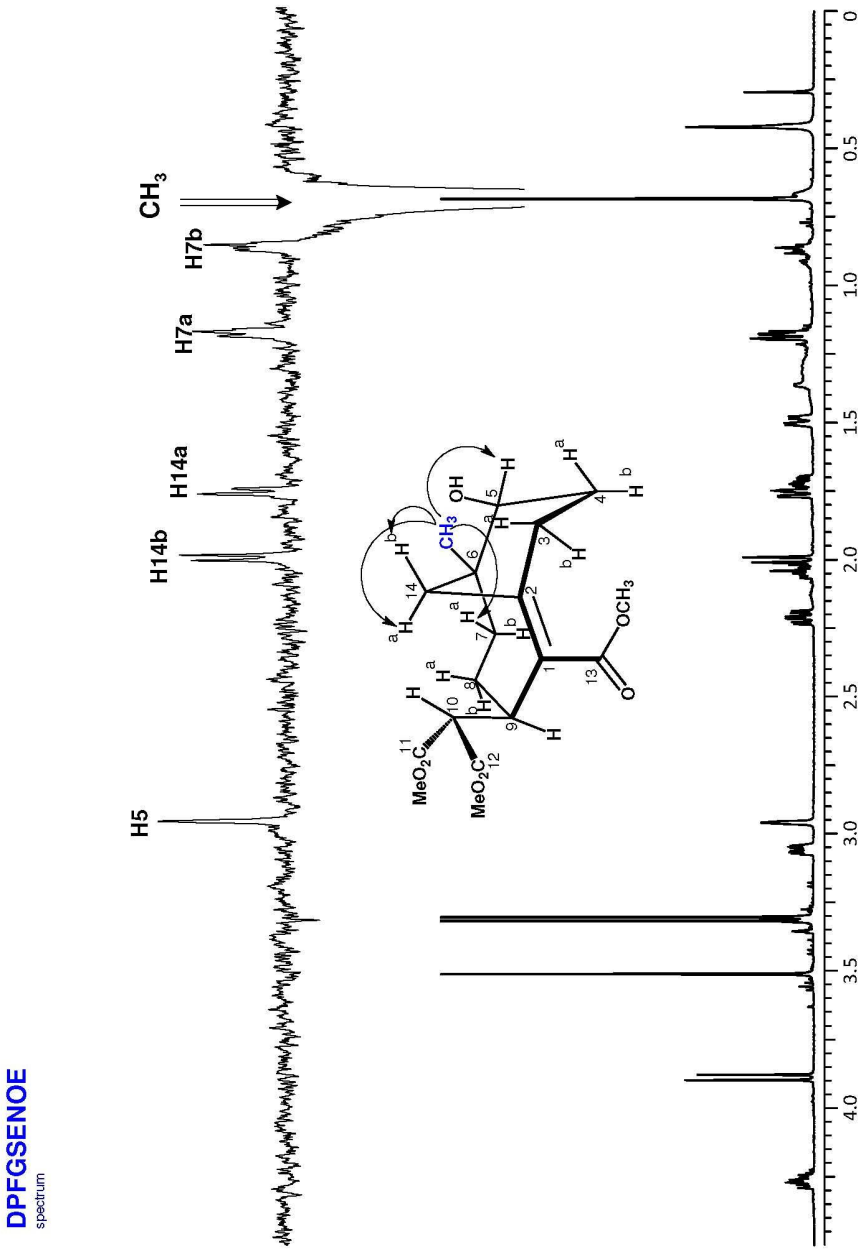
DPFGSENOE
spectrum
H5
H14b
H14a
H7a
H7b
CH3
MeO2C
MeO2C
OCH3
OH
CH3
4.0
3.5
3.0
2.5
2.0
1.5
1.0
0.5
0

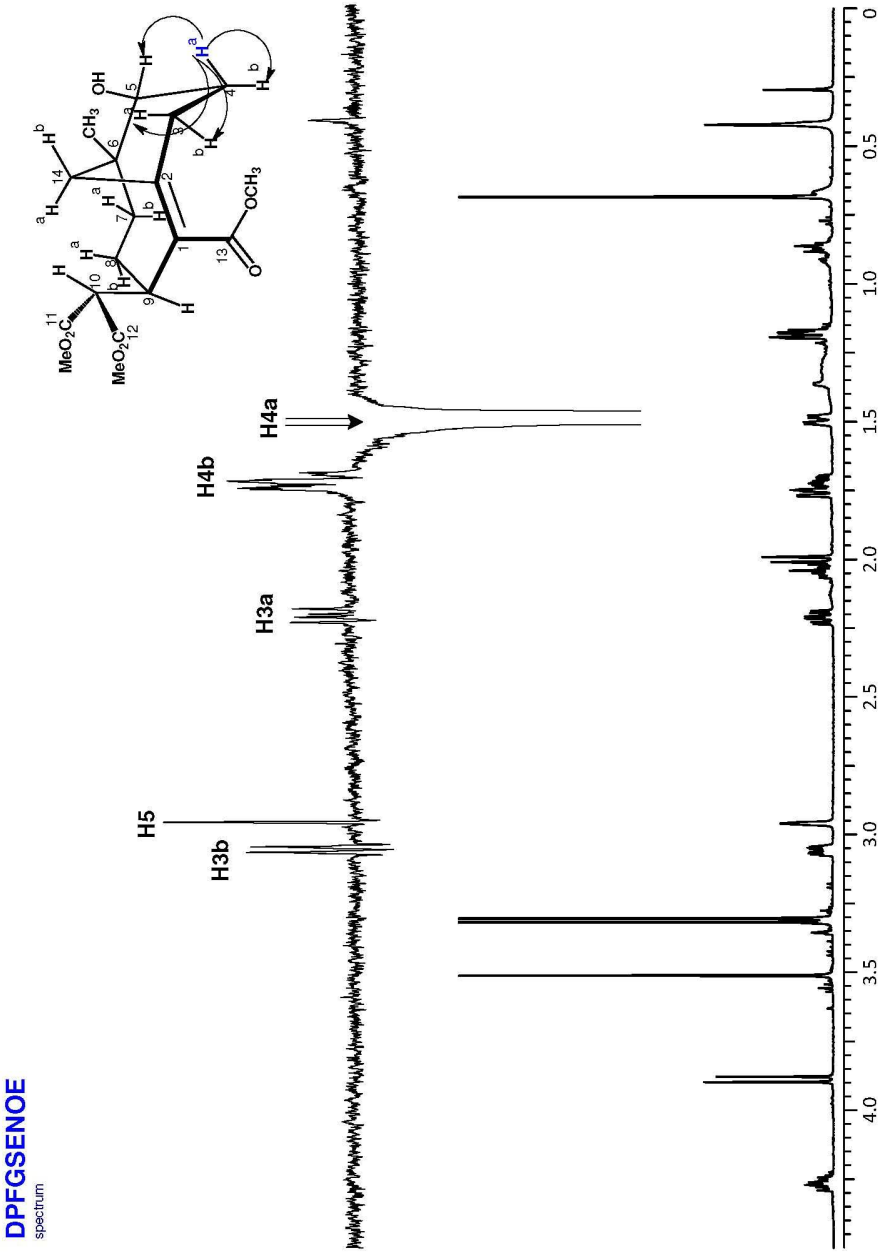
DPFGSENOE
spectrum
H5
H3b
H3a
H4b
H4a
4.0
3.5
3.0
2.5
2.0
1.5
1.0
0.5
0

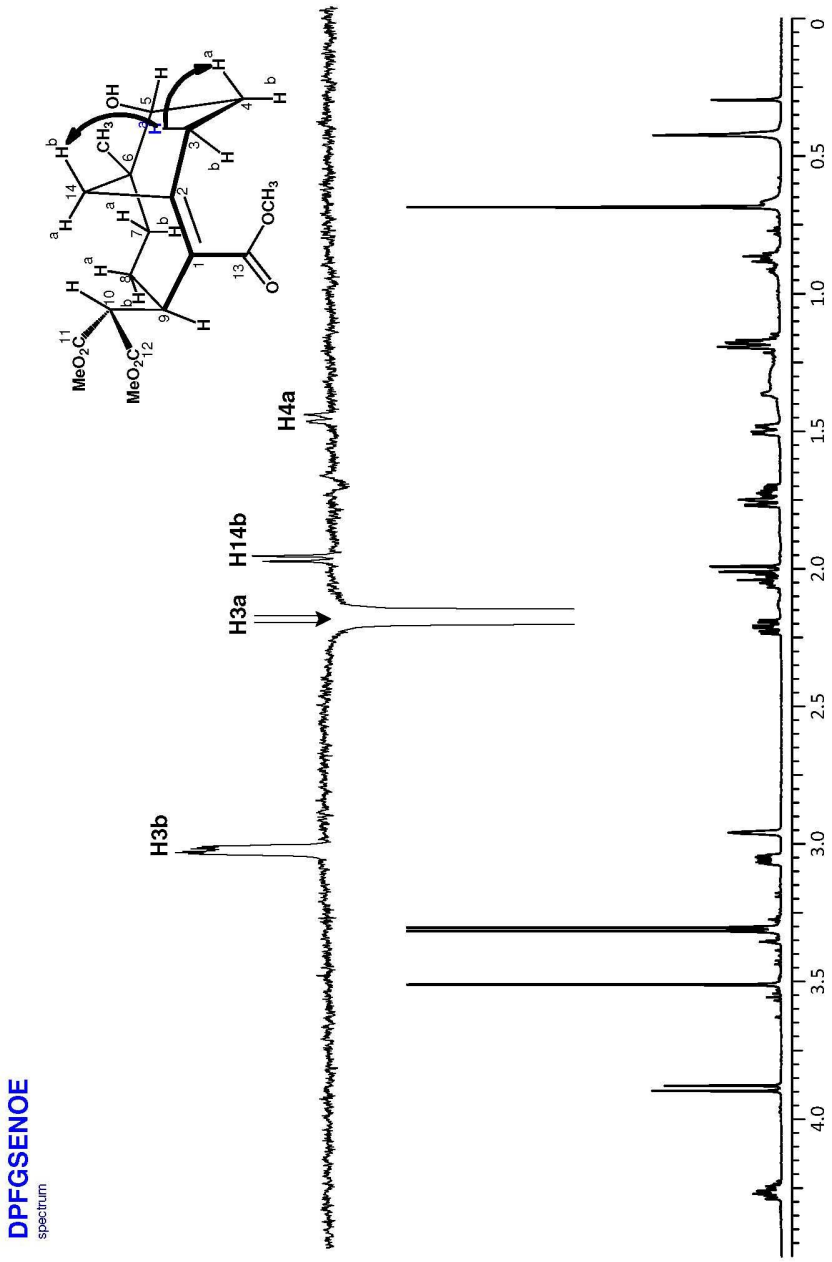
DPFGSENOE
spectrum
H3b
H3a
H14b
H4a
4.0
3.5
3.0
2.5
2.0
1.5
1.0
0.5
0

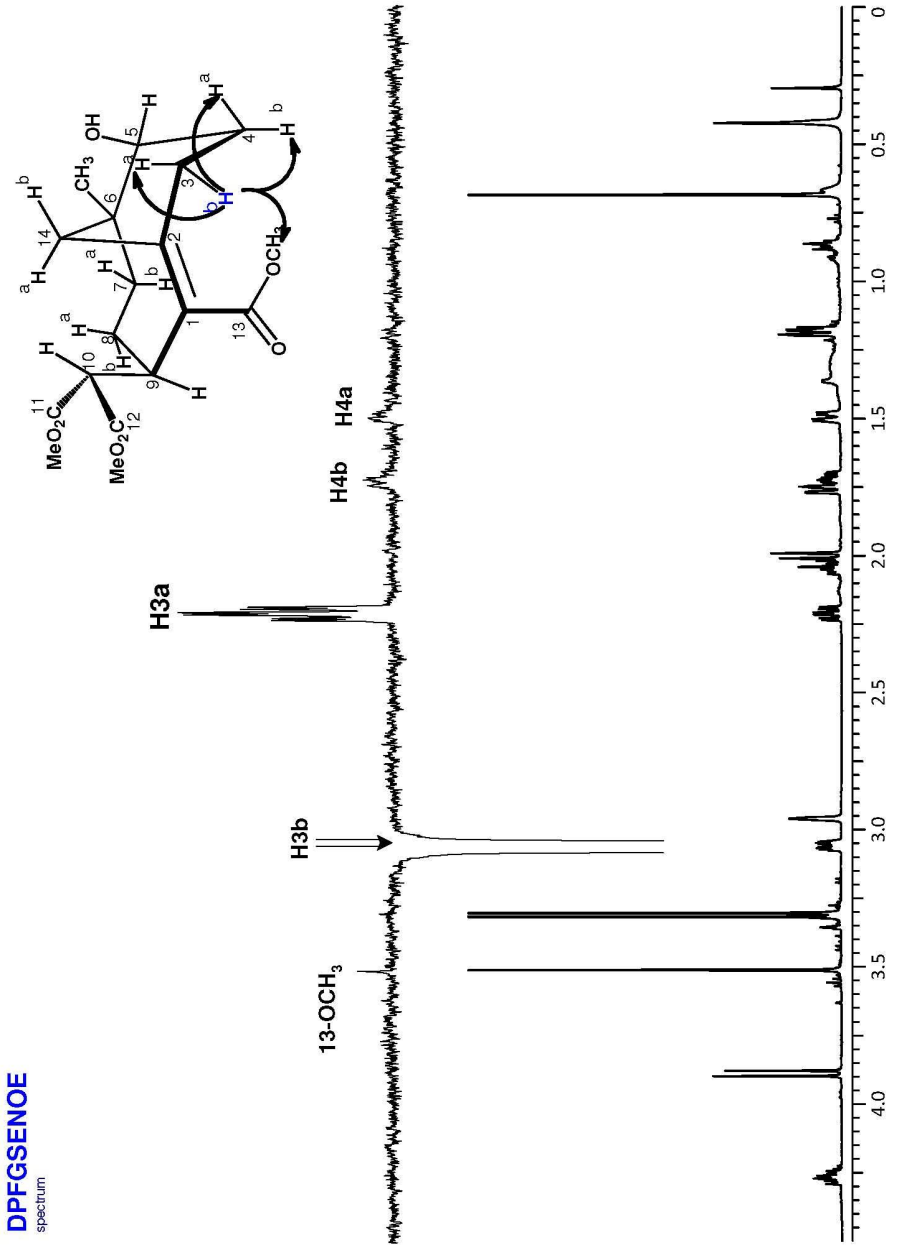
DPFGSENOE
spectrum
H3a
H3b
H4b
H4a
13-OCH3
MeO2C
MeO2C
CH3
OH
OCH3
4.0
3.5
3.0
2.5
2.0
1.5
1.0
0.5
0

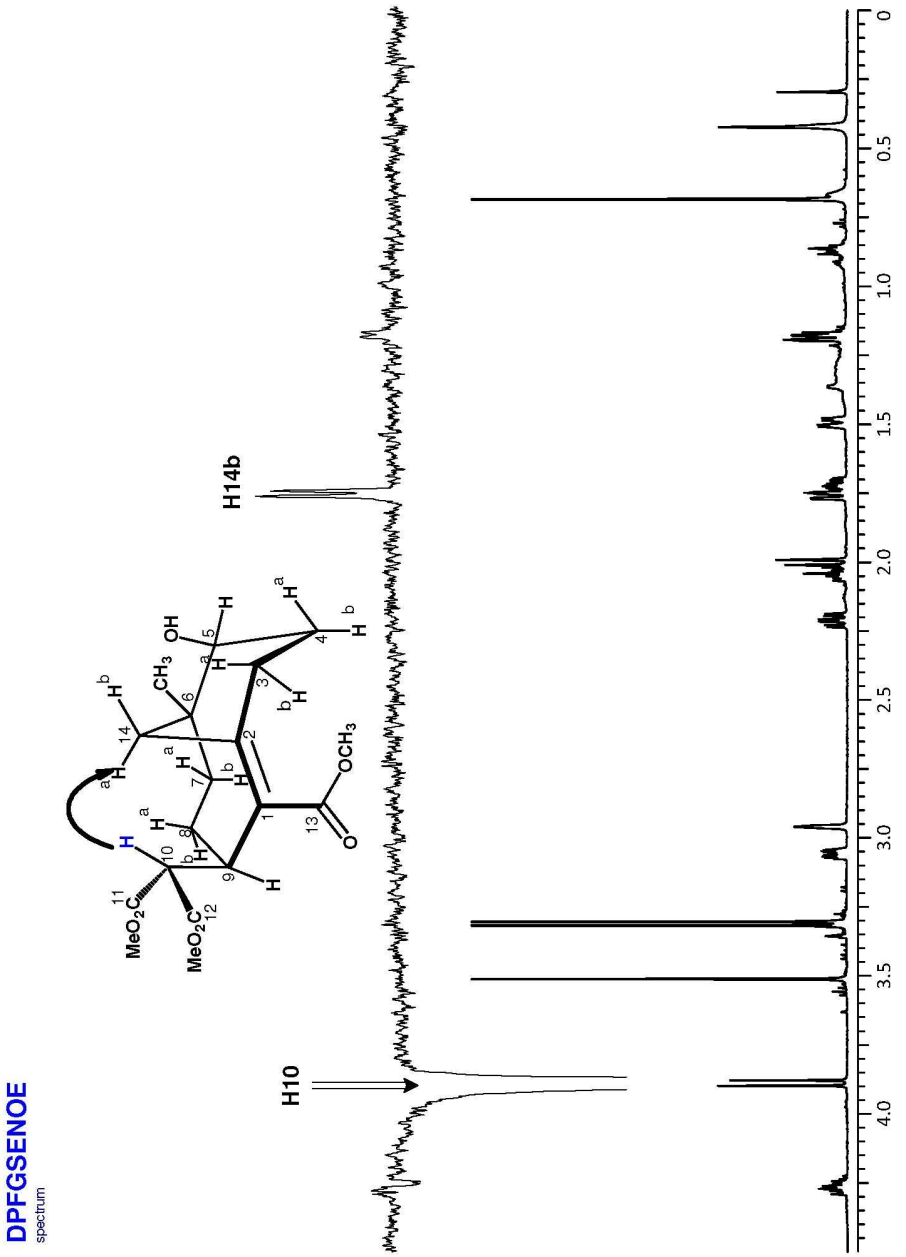
DPFGSENOE
spectrum
H10
H14b
OCH3
OH
CH3
MeO2C
MeO2C
4.0
3.5
3.0
2.5
2.0
1.5
1.0
0.5
0

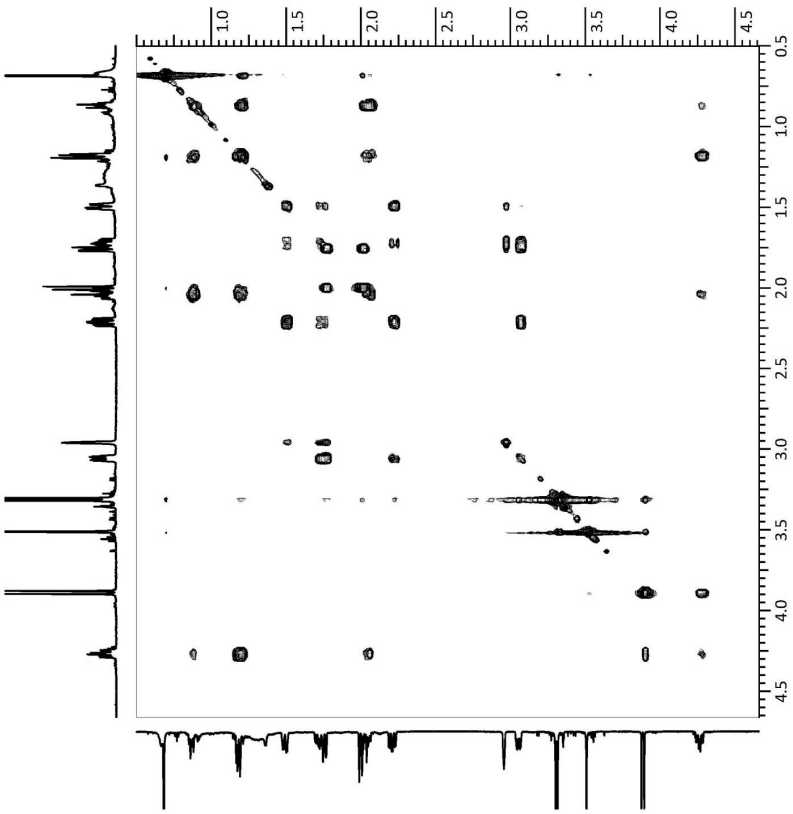
gCOSY
1.0
1.5
2.0
2.5
3.0
3.5
4.0
4.5
0.5

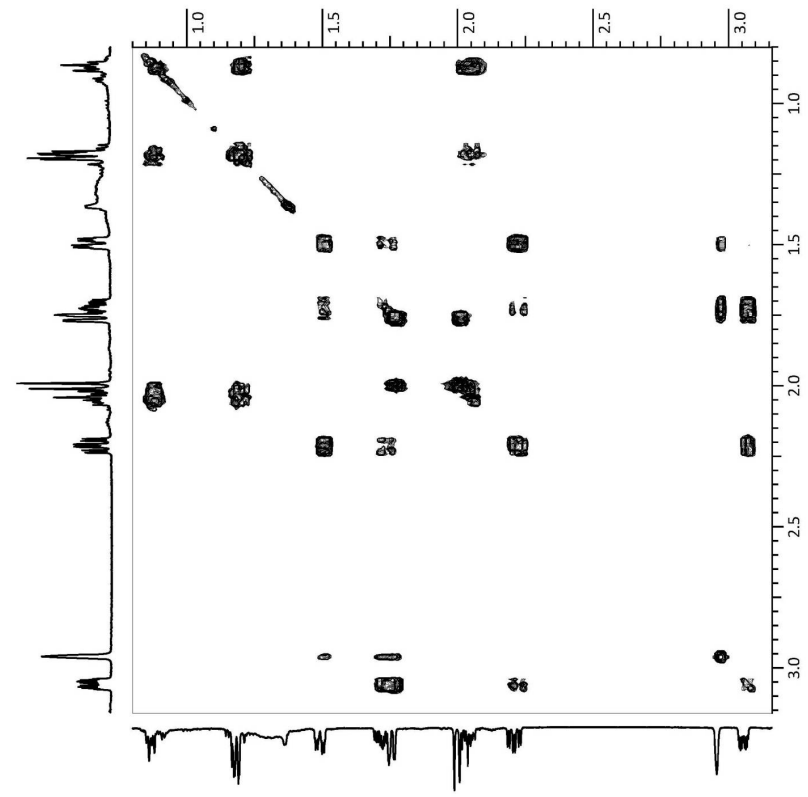

gCOSY *expansion*

^{13}C NMR spectrum in C6D$_6$

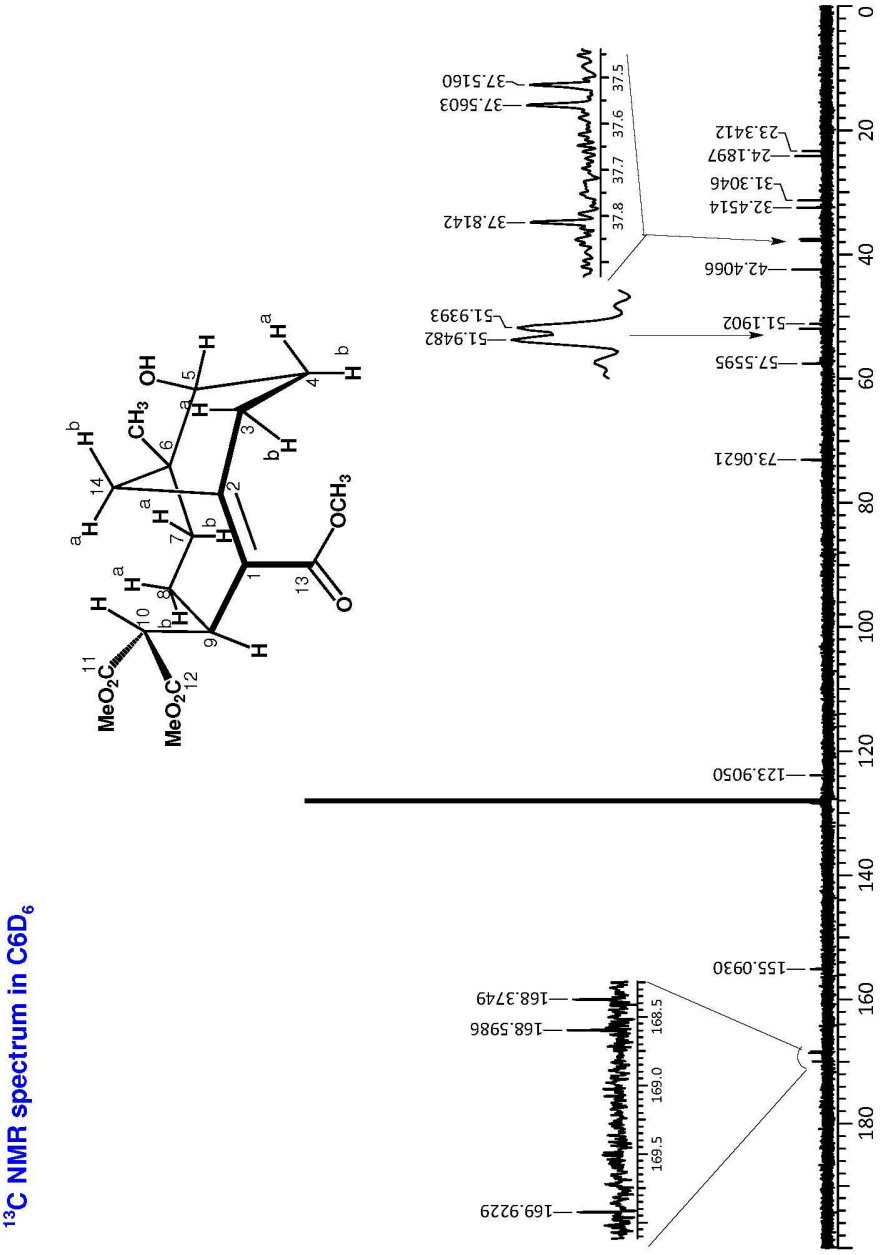

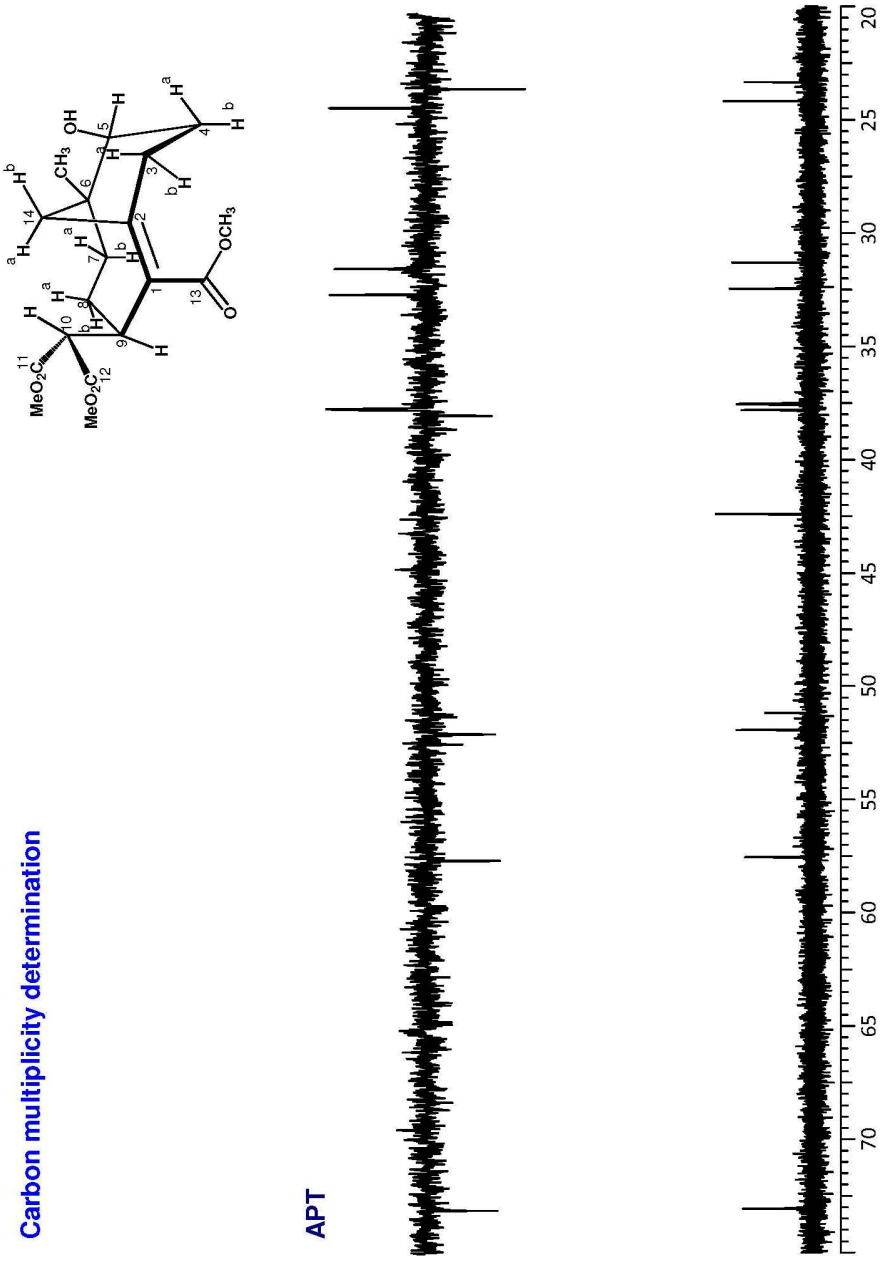
Carbon multiplicity determination
APT
MeO2C
MeO2C
CH3
OH
OCH3
O
70
65
60
55
50
45
40
35
30
25
20

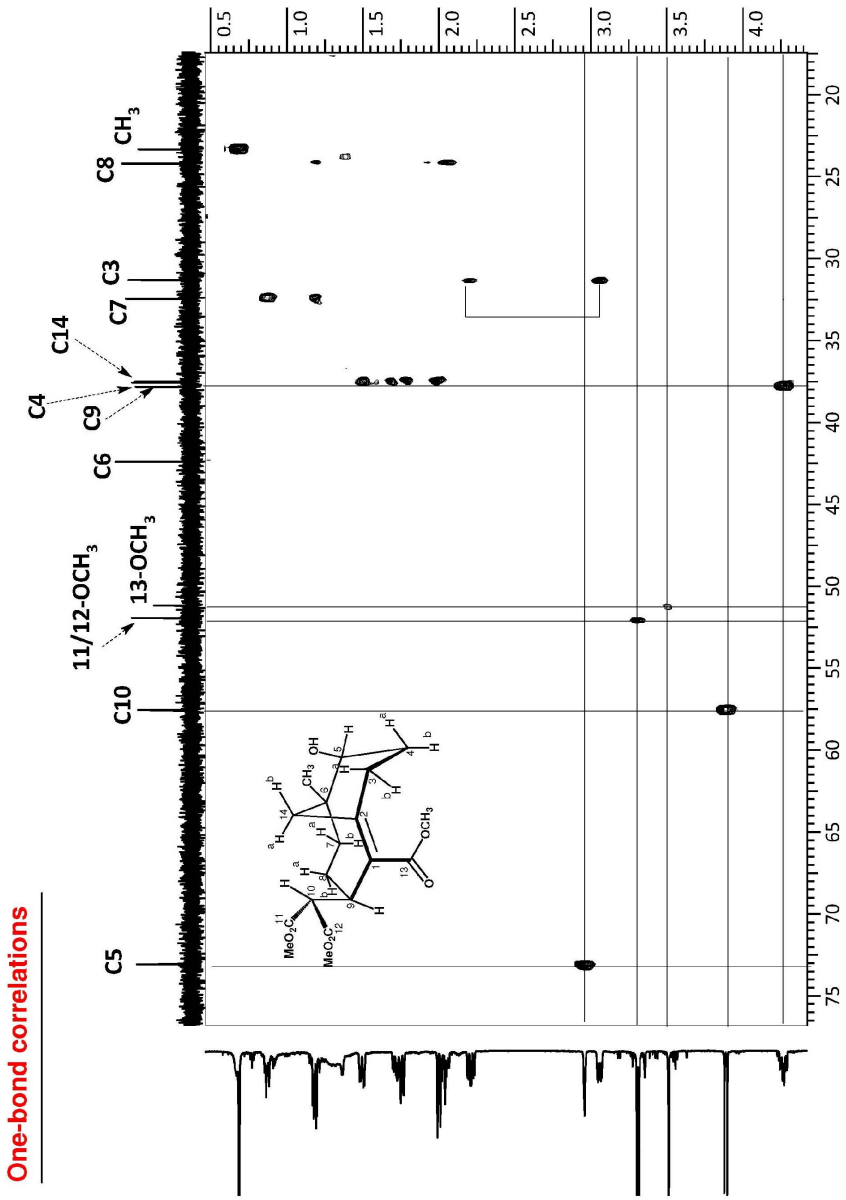
One-bond correlations
C5
C10
11/12-OCH3
13-OCH3
C6
C4
C14
C9
C7
C3
C8
CH3
0.5
1.0
1.5
2.0
2.5
3.0
3.5
4.0
20
25
30
35
40
45
50
55
60
65
70
75

Exapansion of the countour plot of the HETCOR spectrum (one bond correlations)

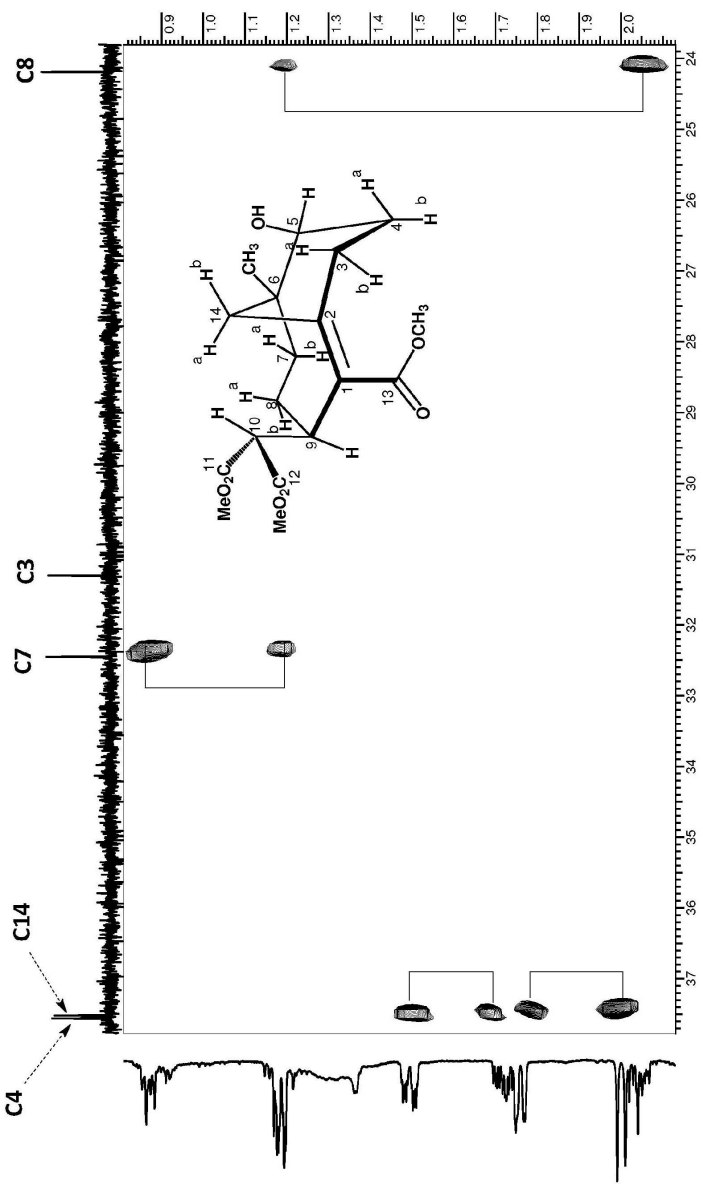

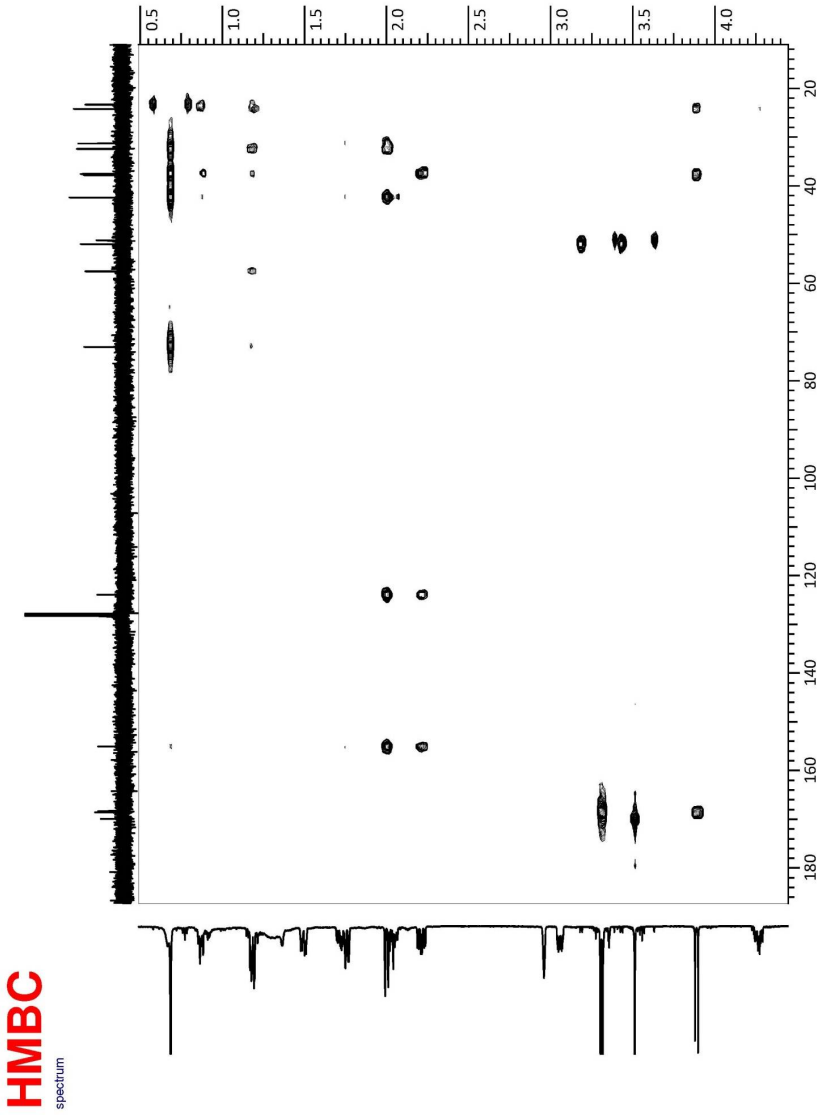
HMBC
spectrum
0.5
1.0
1.5
2.0
2.5
3.0
3.5
4.0
20
40
60
80
100
120
140
160
180

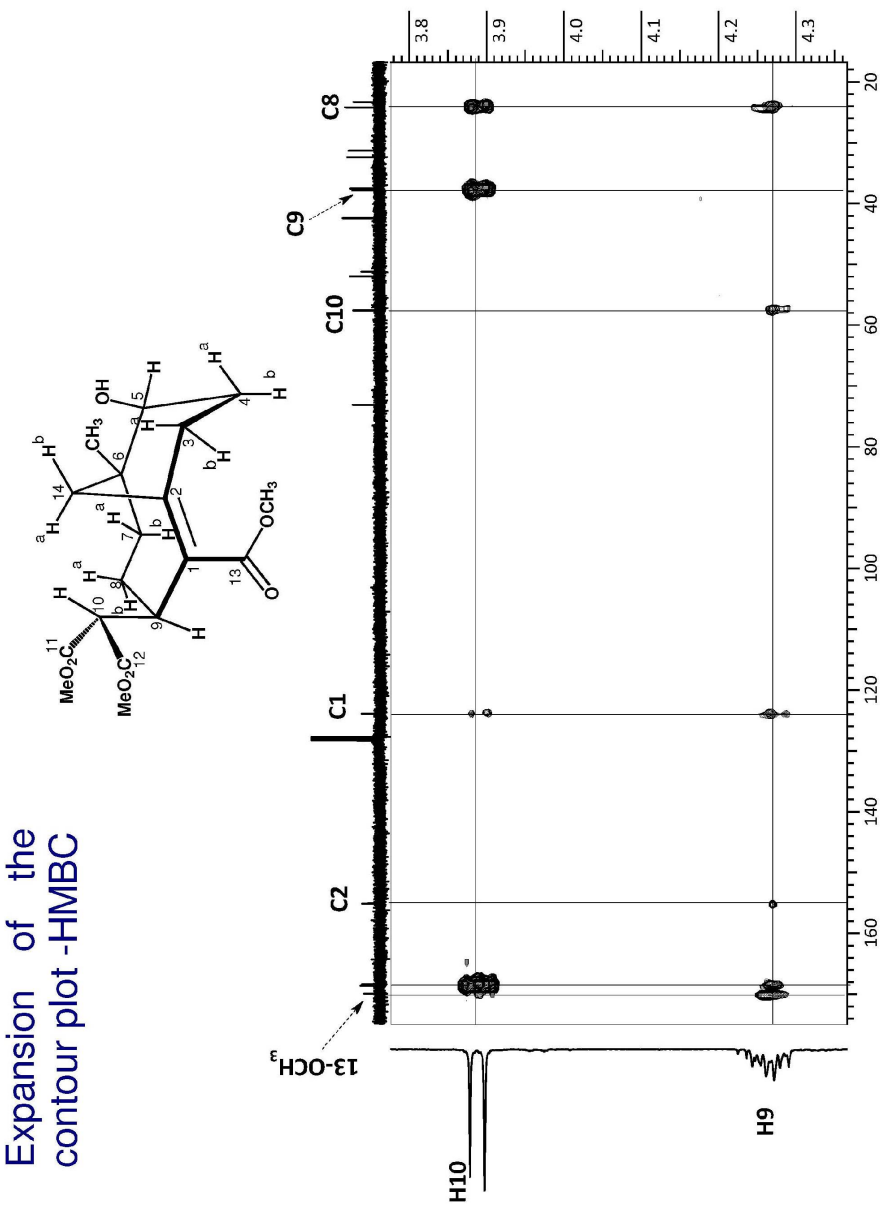
Expansion of the contour plot -HMBC
C8
C9
C10
C1
C2
13-OCH3
H10
H9
3.8
3.9
4.0
4.1
4.2
4.3
20
40
60
80
100
120
140
160
OH
CH3
OCH3
MeO2C
MeO2C
O

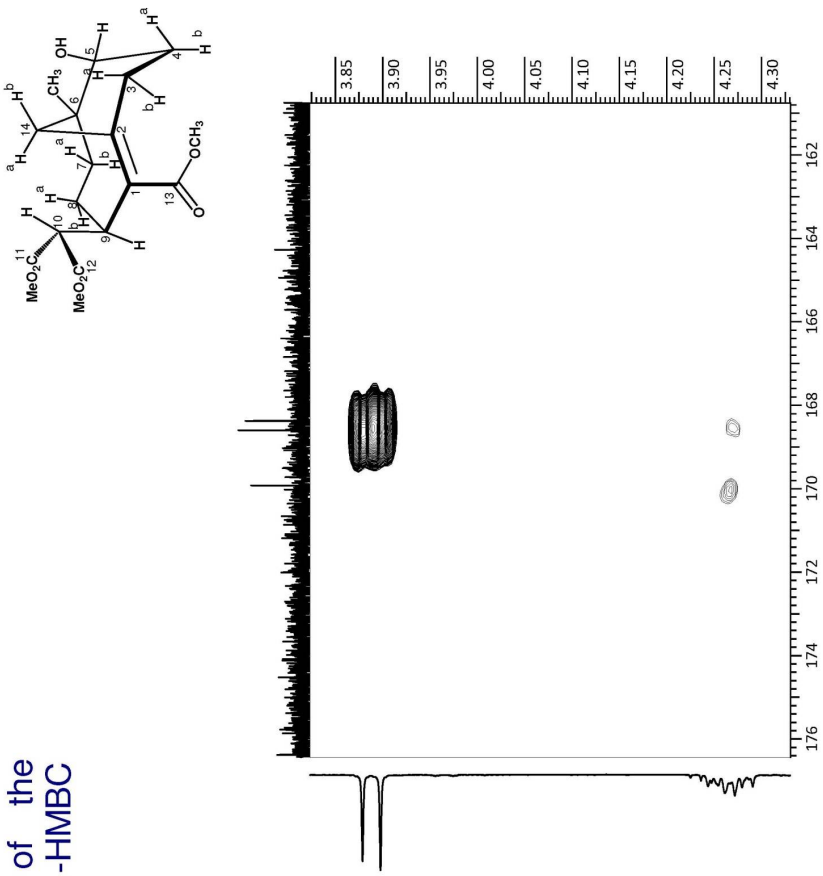

Expansion of the contour plot -HMBC

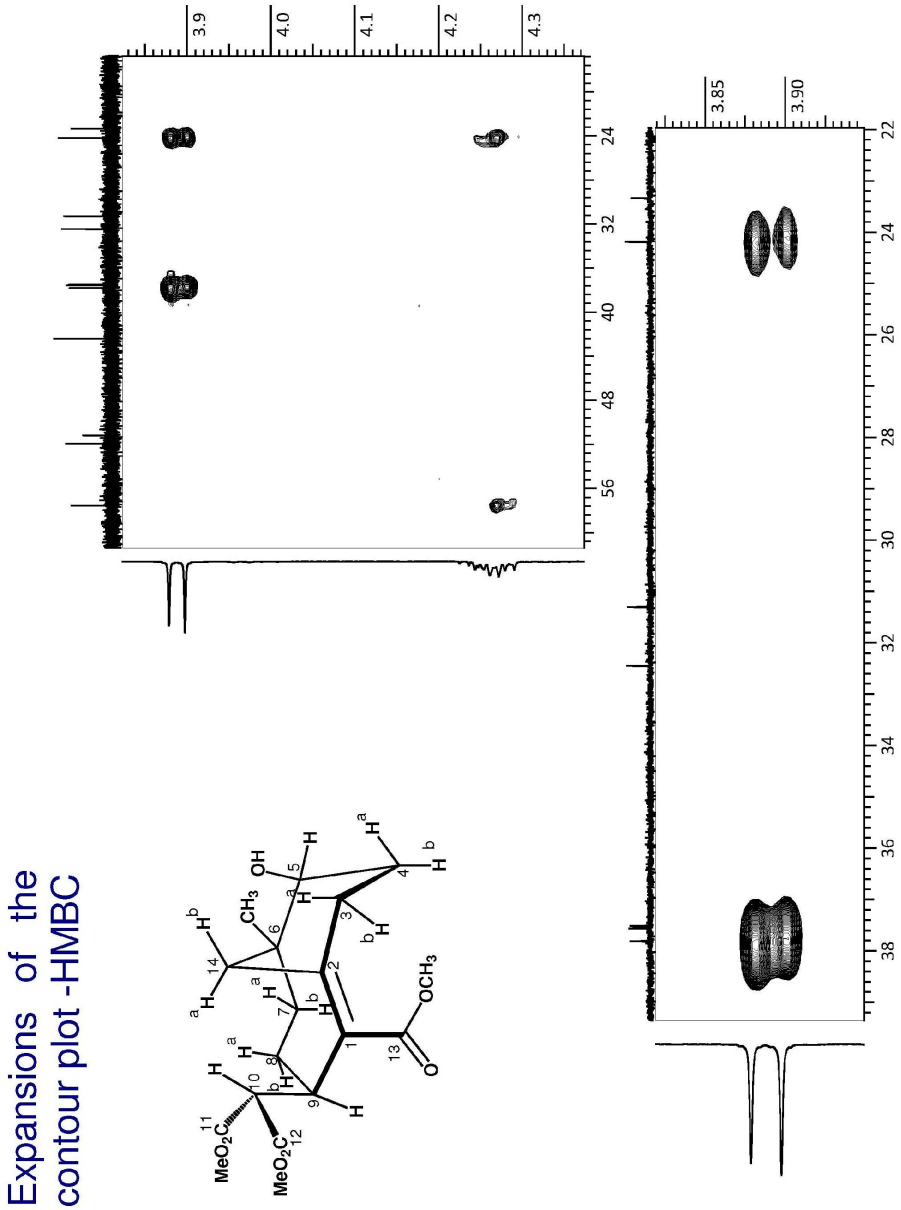
Expansions of the contour plot -HMBC
3.9
4.0
4.1
4.2
4.3
3.85
3.90
OCH3
CH3
OH
MeO2C
MeO2C

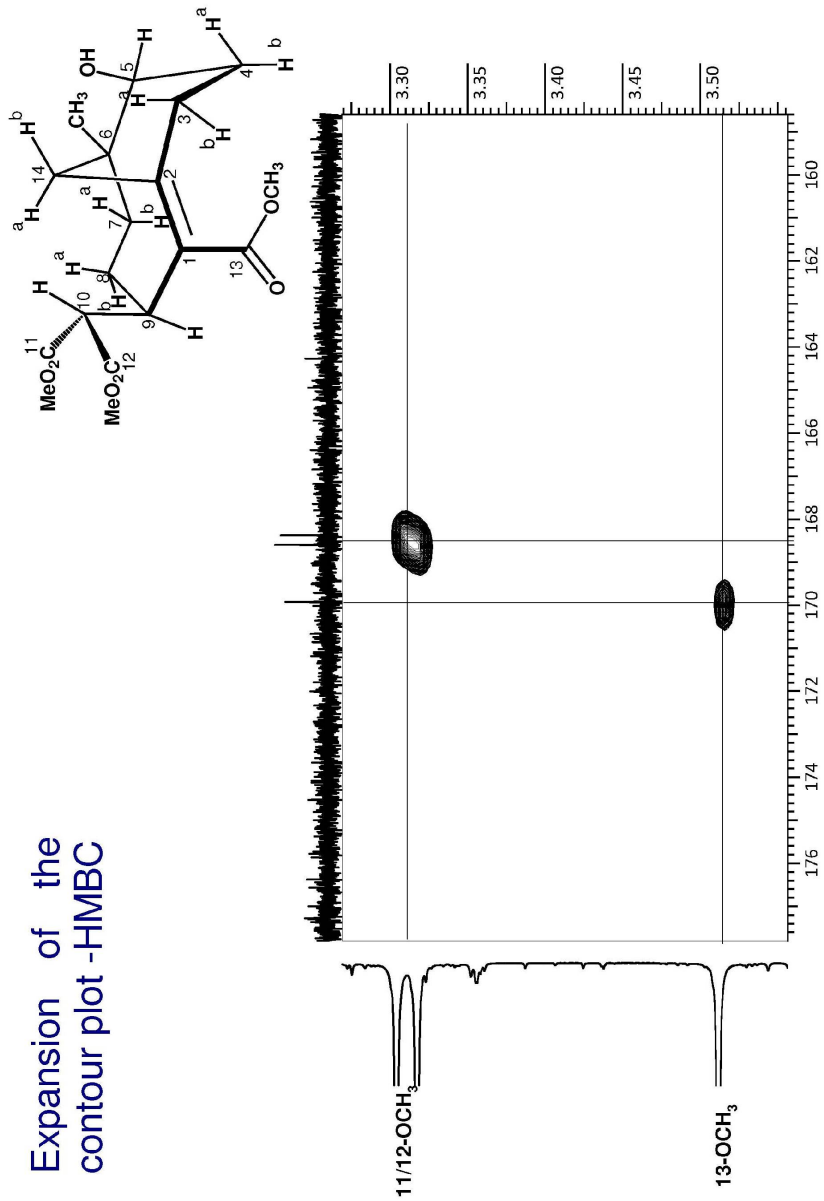
Expansion of the contour plot -HMBC
11/12-OCH3
13-OCH3
3.30
3.35
3.40
3.45
3.50
160
162
164
166
168
170
172
174
176
MeO2C
MeO2C
CH3
OH
OCH3
O

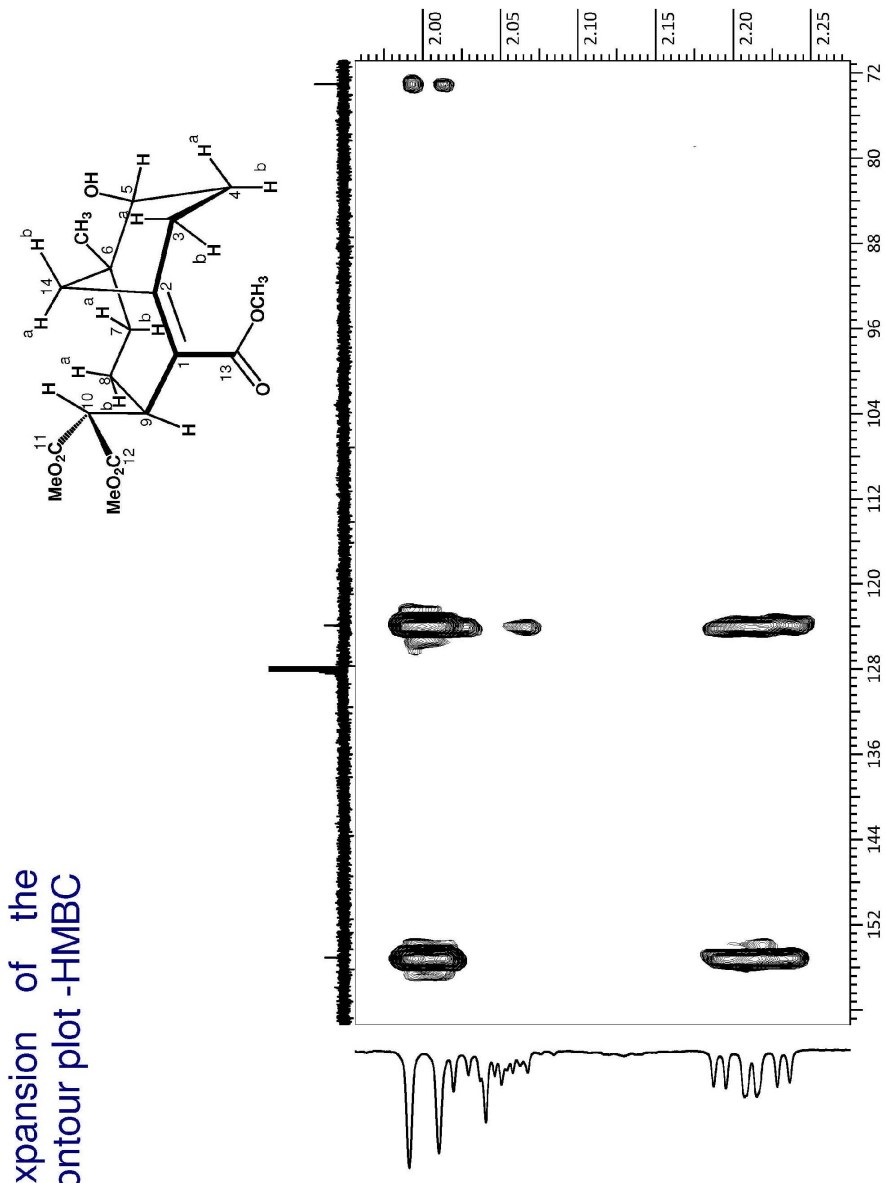
Expansion of the contour plot -HMBC
2.00
2.05
2.10
2.15
2.20
2.25
72
80
88
96
104
112
120
128
136
144
152
OCH3
OH
CH3
MeO2C
MeO2C

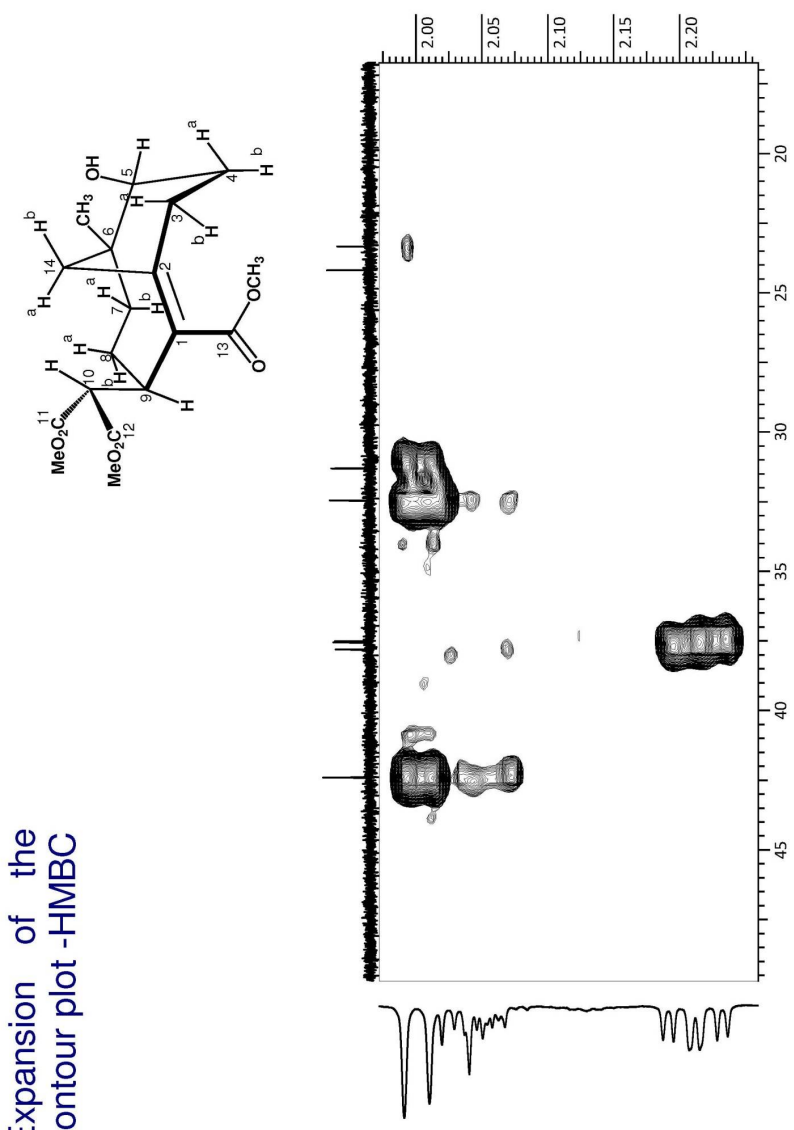
Expansion of the contour plot -HMBC
OCH3
OH
CH3
MeO2C
MeO2C
2.00
2.05
2.10
2.15
2.20
20
25
30
35
40
45

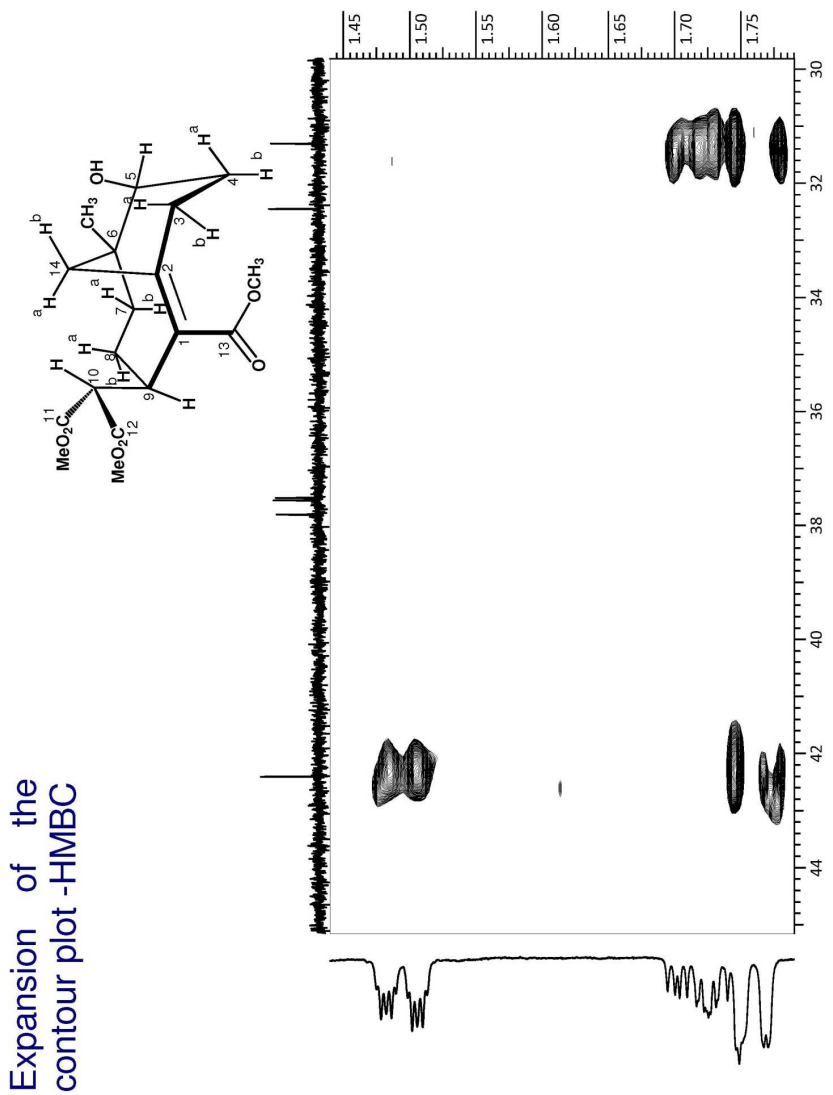
Expansion of the contour plot -HMBC
MeO2C
MeO2C
CH3
OH
OCH3
O
1.45
1.50
1.55
1.60
1.65
1.70
1.75
30
32
34
36
38
40
42
44

Expansion of the contour plot -HMBC

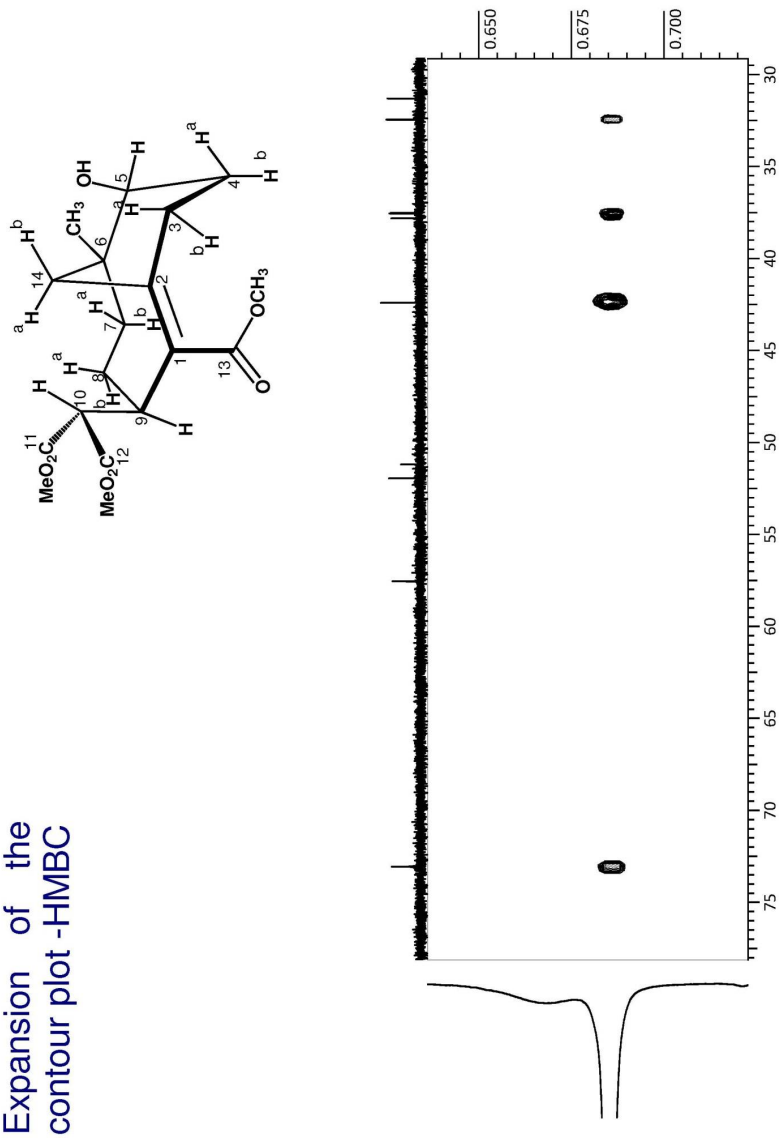

Expansion of the contour plot -HMBC

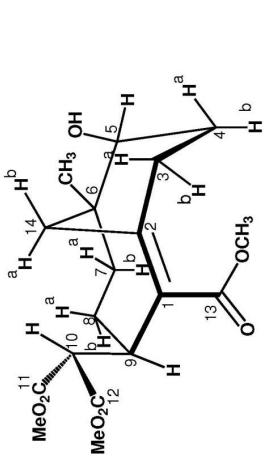

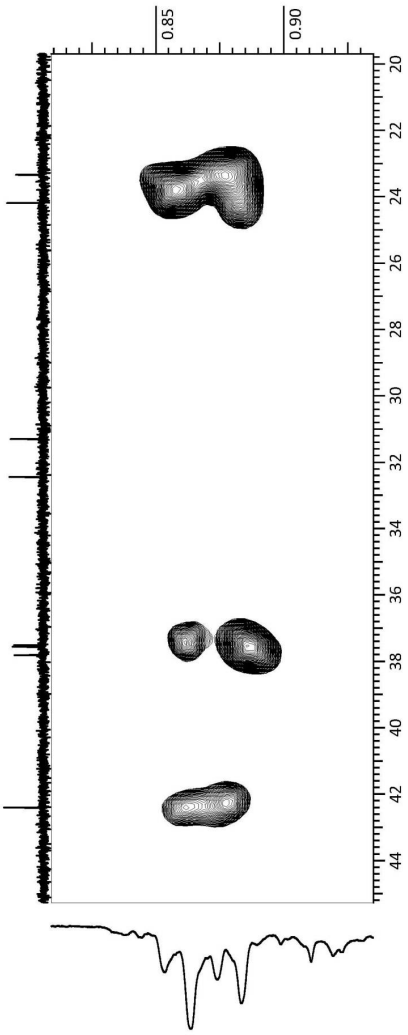

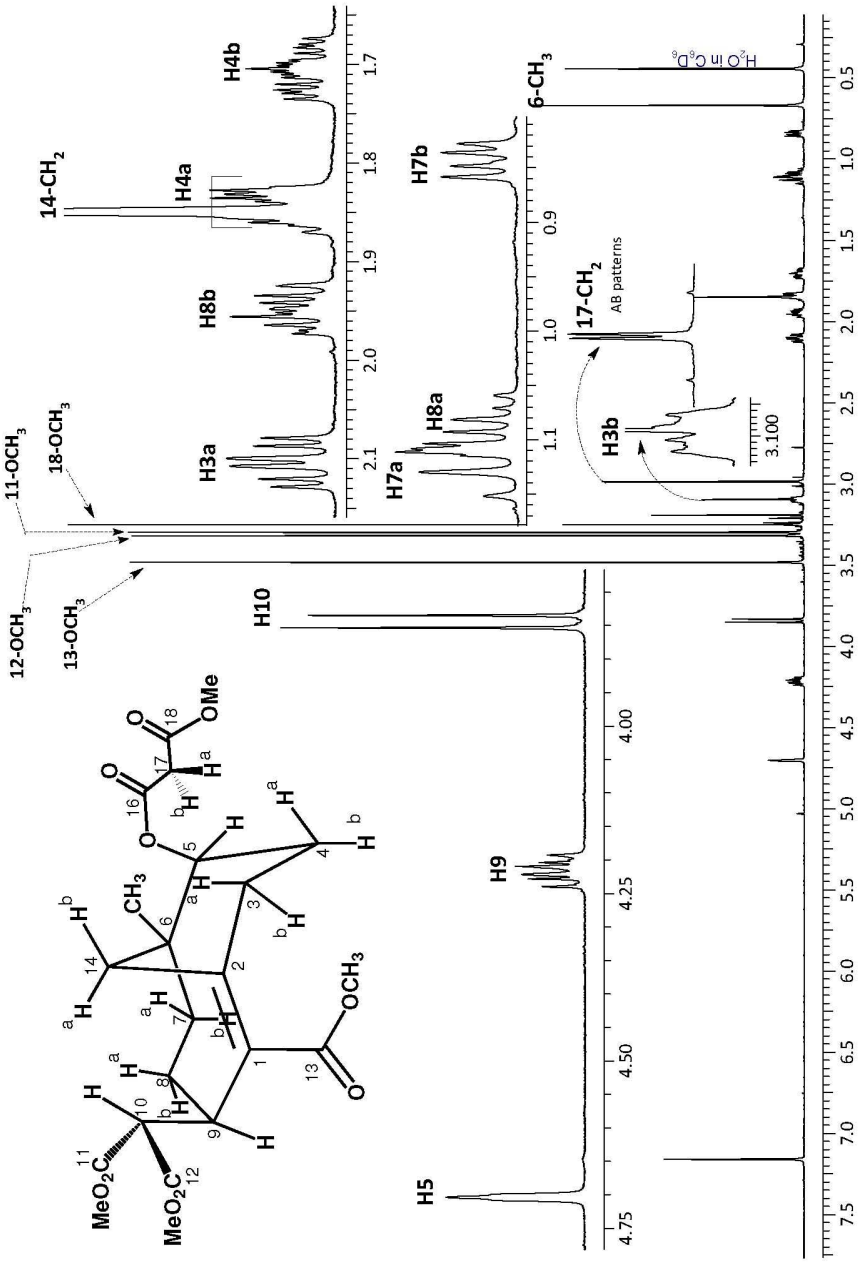
11-OCH3
18-OCH3
12-OCH3
13-OCH3
14-CH2
H4a
H4b
H8b
H3a
H7a
H8a
H7b
6-CH3
17-CH2
AB patterns
H3b
3.100
H10
H9
H5
H2O in C6D6
MeO2C
MeO2C
OMe
OCH3
CH3

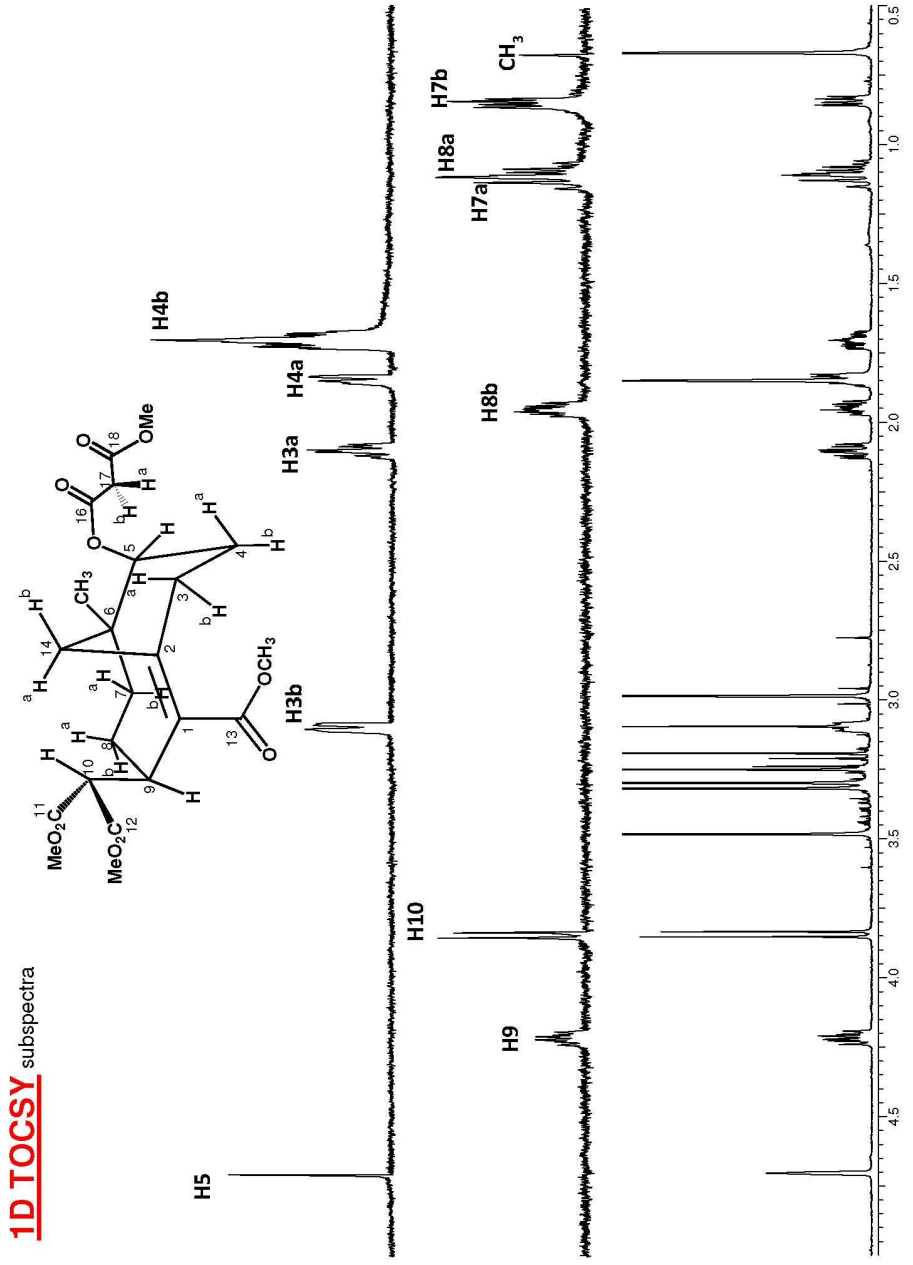
1D TOCSY subspectra
H5
H3b
H4a
H4b
H10
H9
H8b
H7a
H8a
H7b
CH3
4.5
4.0
3.5
3.0
2.5
2.0
1.5
1.0
0.5

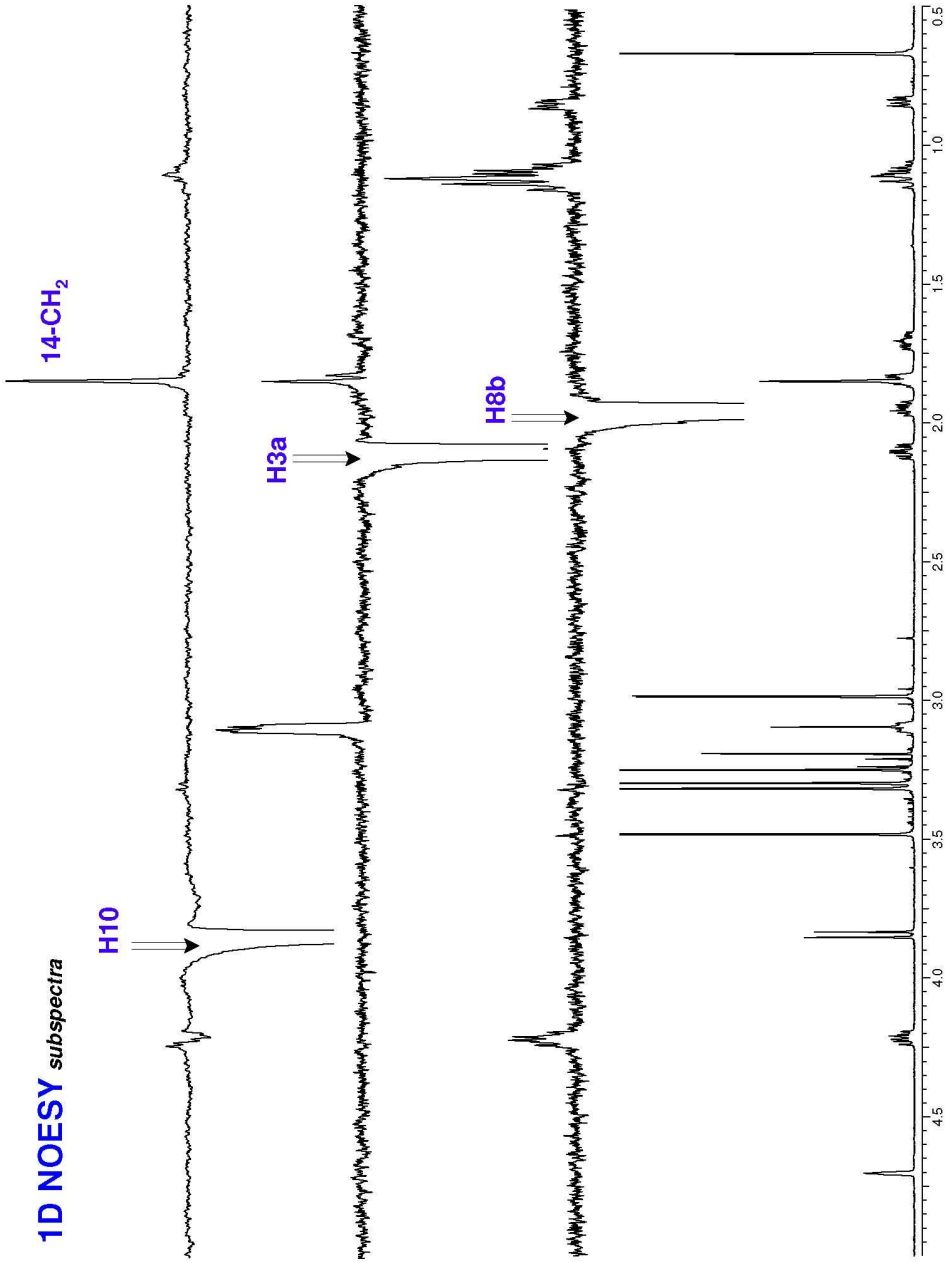
1D NOESY subspectra
H10
14-CH2
H3a
H8b
4.5
4.0
3.5
3.0
2.5
2.0
1.5
1.0
0.5

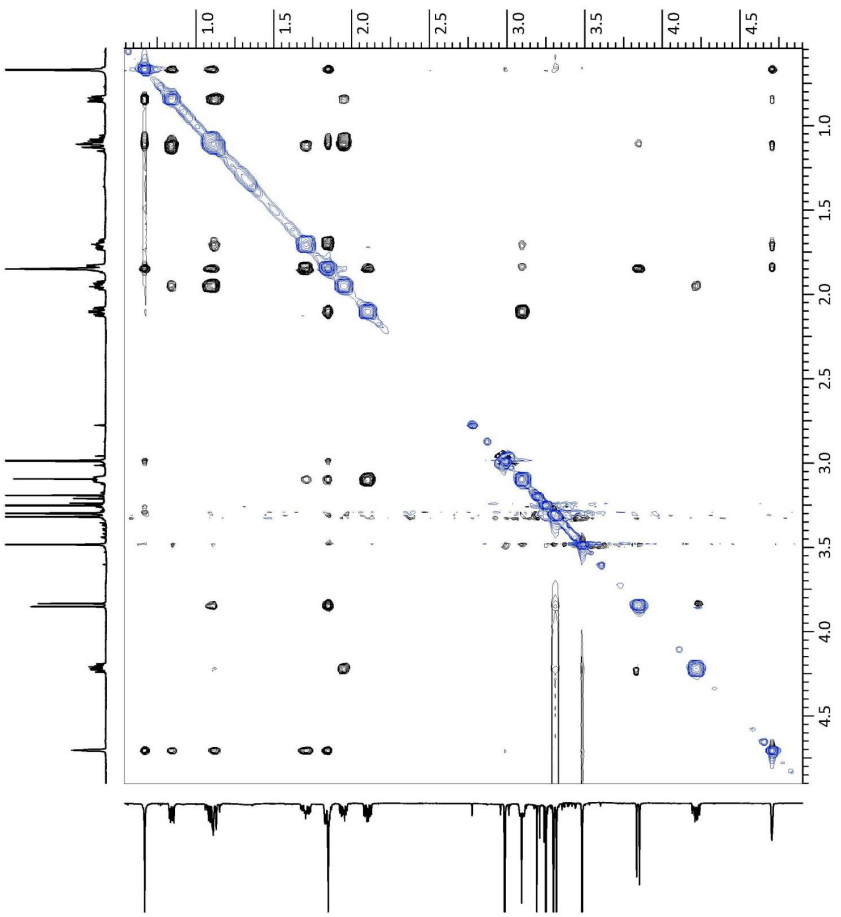

NOESY

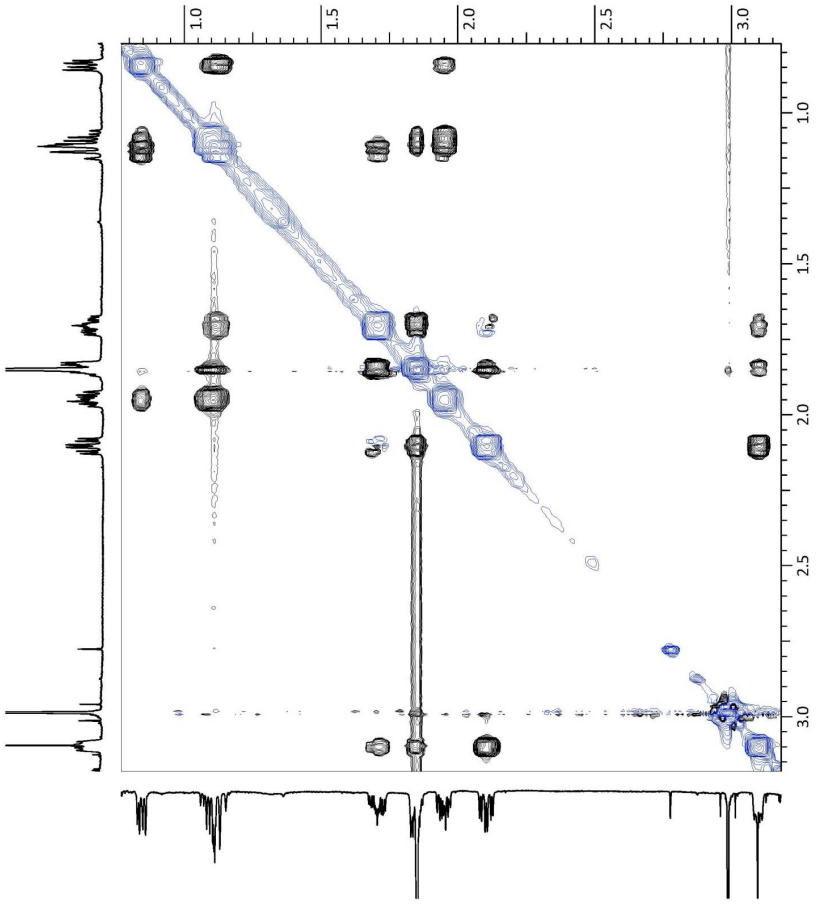

NOESY

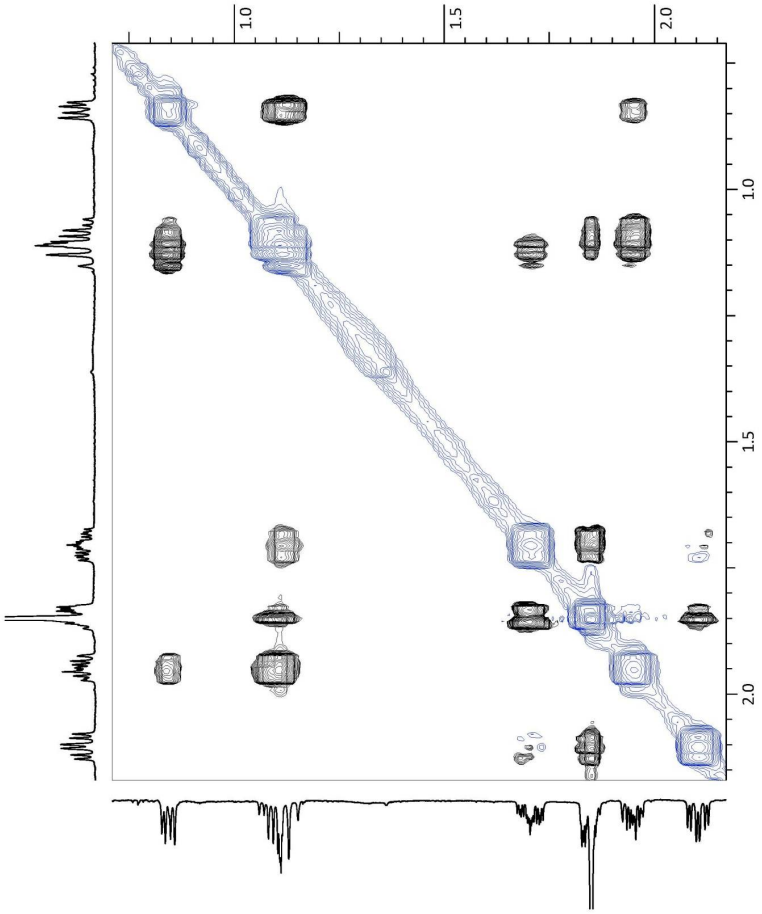

NOESY

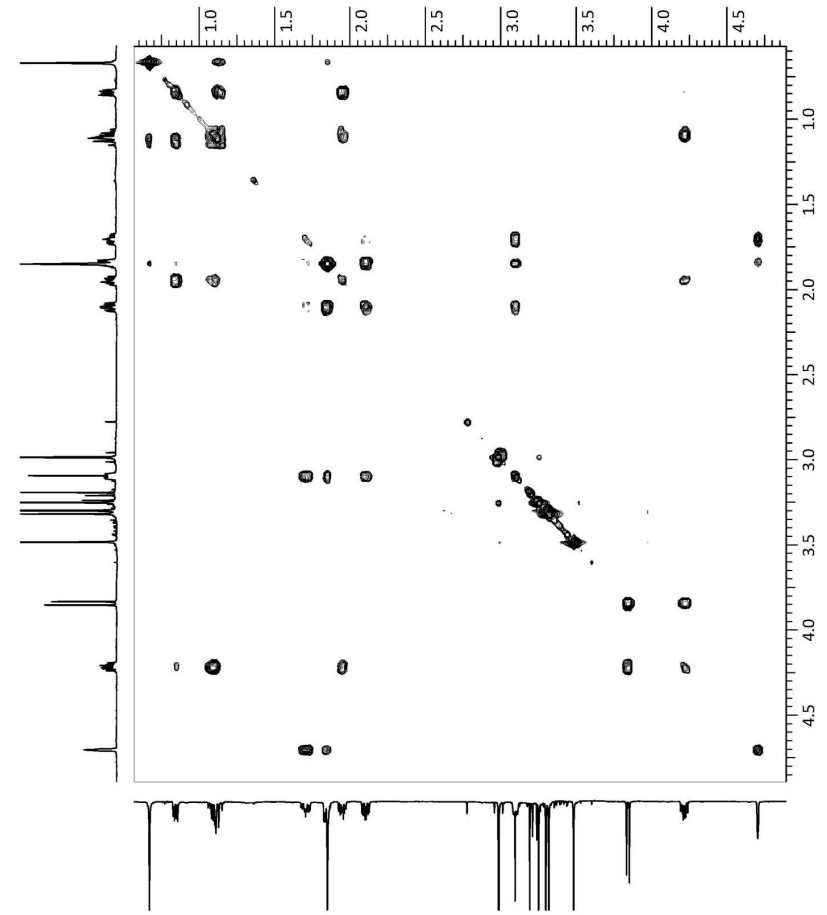

GCOSY

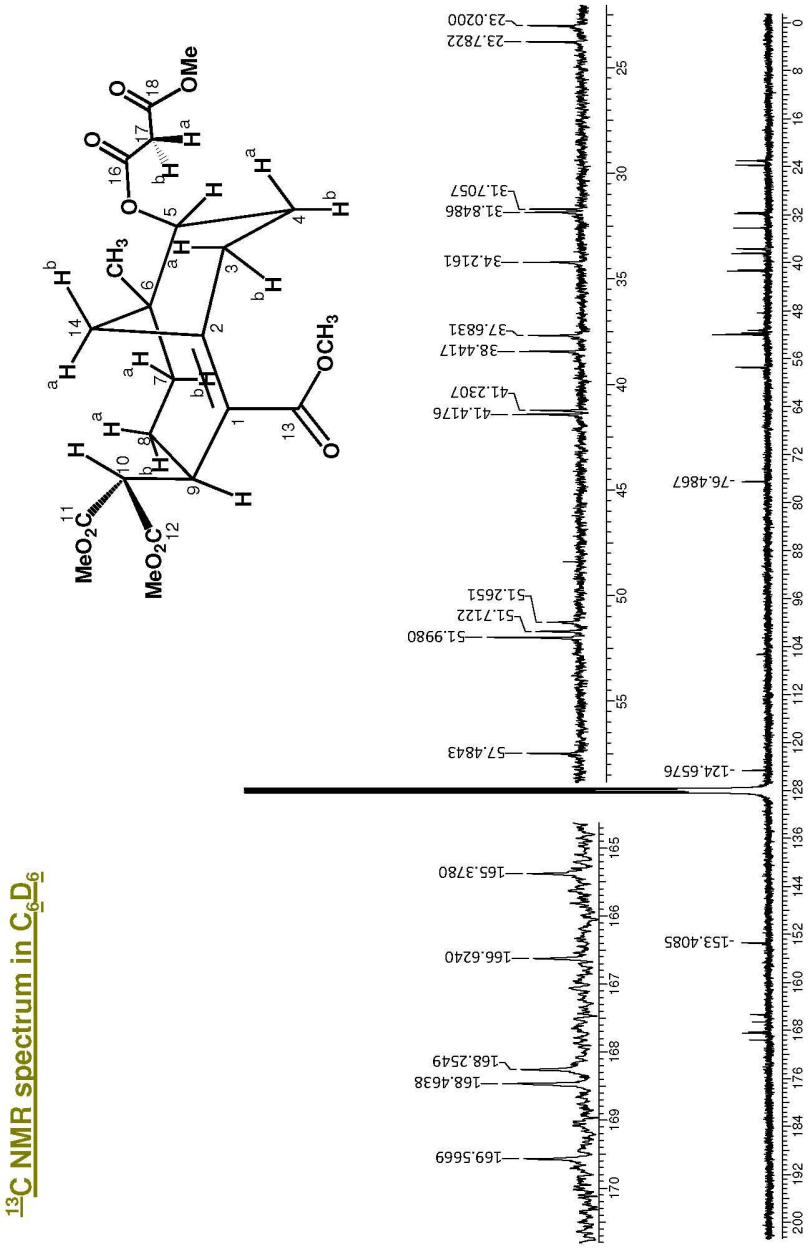
^{13}C NMR spectrum in C_6D_6
MeO2C
MeO2C
OCH3
CH3
OMe
23.0200
23.7822
31.7057
31.8486
34.2161
37.6831
38.4417
41.2307
41.4176
51.2651
51.7122
51.9980
57.4843
76.4867
124.6576
153.4085
165.3780
166.6240
168.2549
168.4638
169.5669

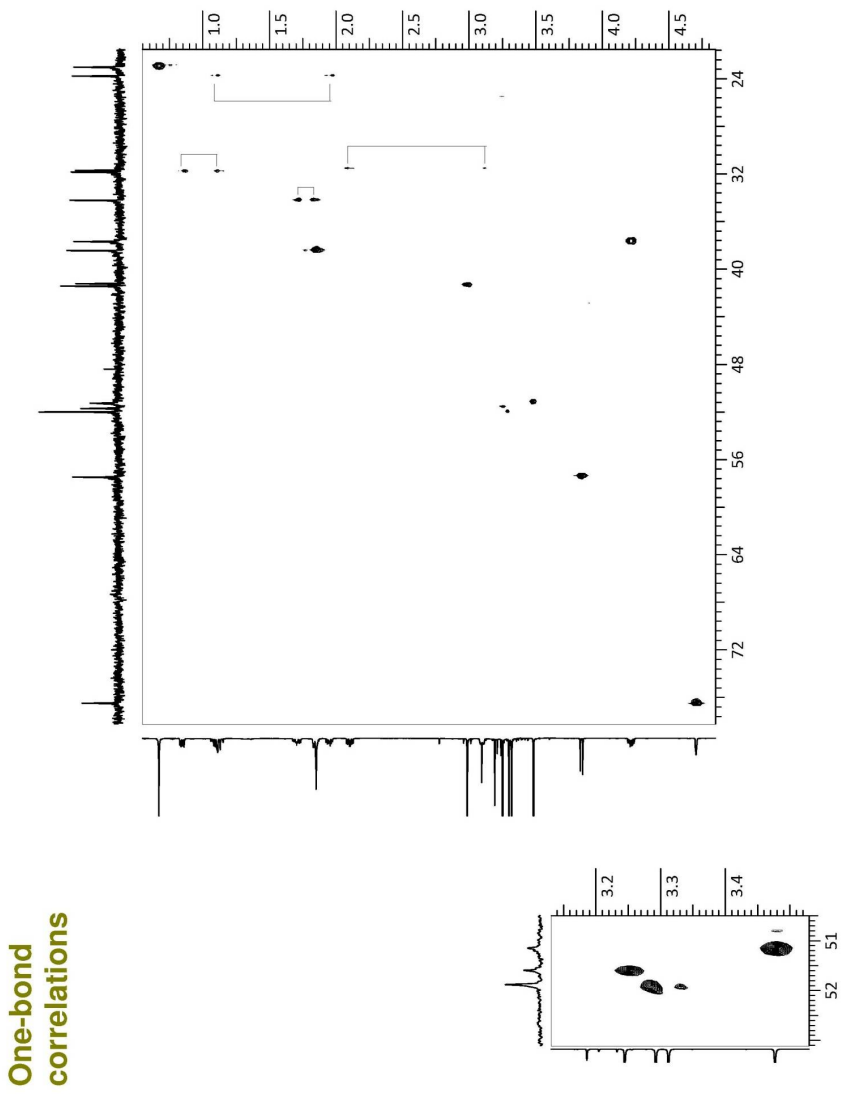
One-bond
correlations
1.0
1.5
2.0
2.5
3.0
3.5
4.0
4.5
24
32
40
48
56
64
72
3.2
3.3
3.4
51
52

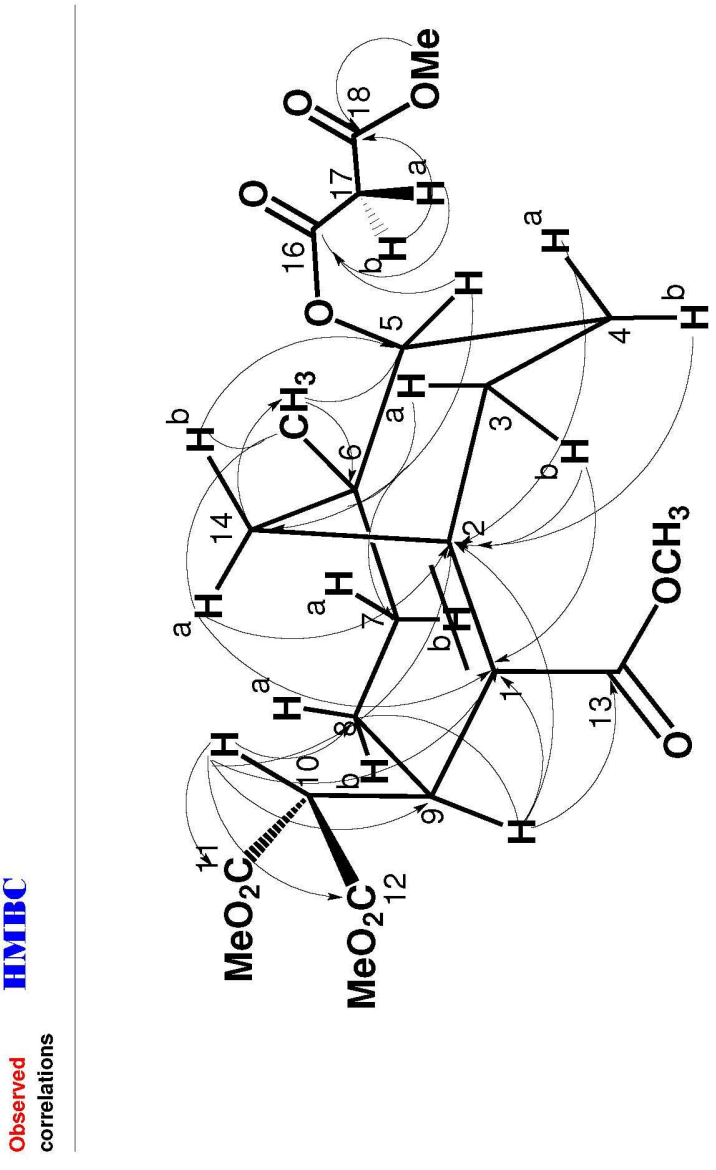
HMBC
Observed correlations
MeO2C
MeO2C
CH3
OCH3
OMe
O
H
a
b

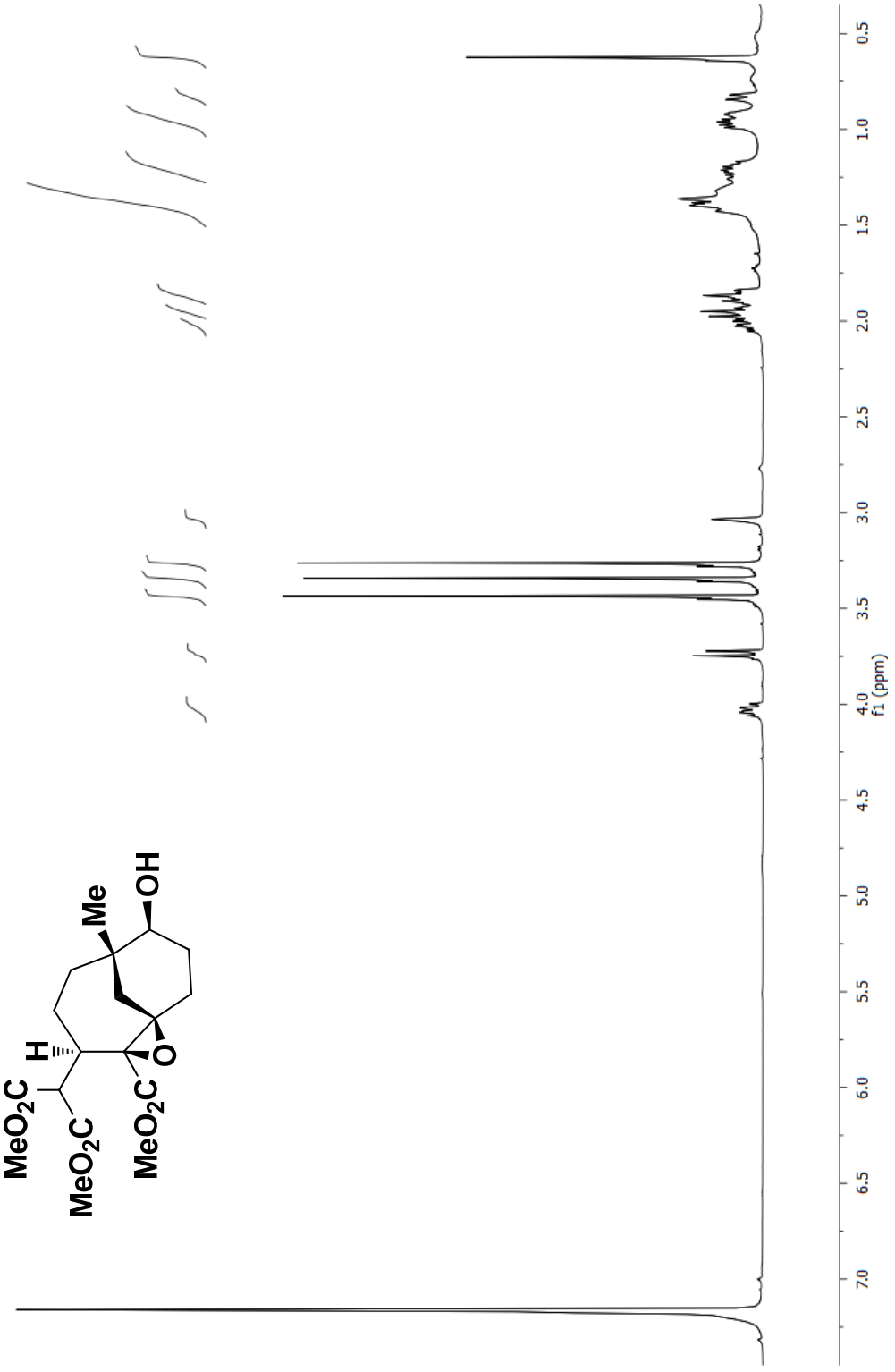
MeO2C
MeO2C
H
MeO2C
O
Me
OH
7.0
6.5
6.0
5.5
5.0
4.5
4.0
3.5
3.0
2.5
2.0
1.5
1.0
0.5
f1 (ppm)

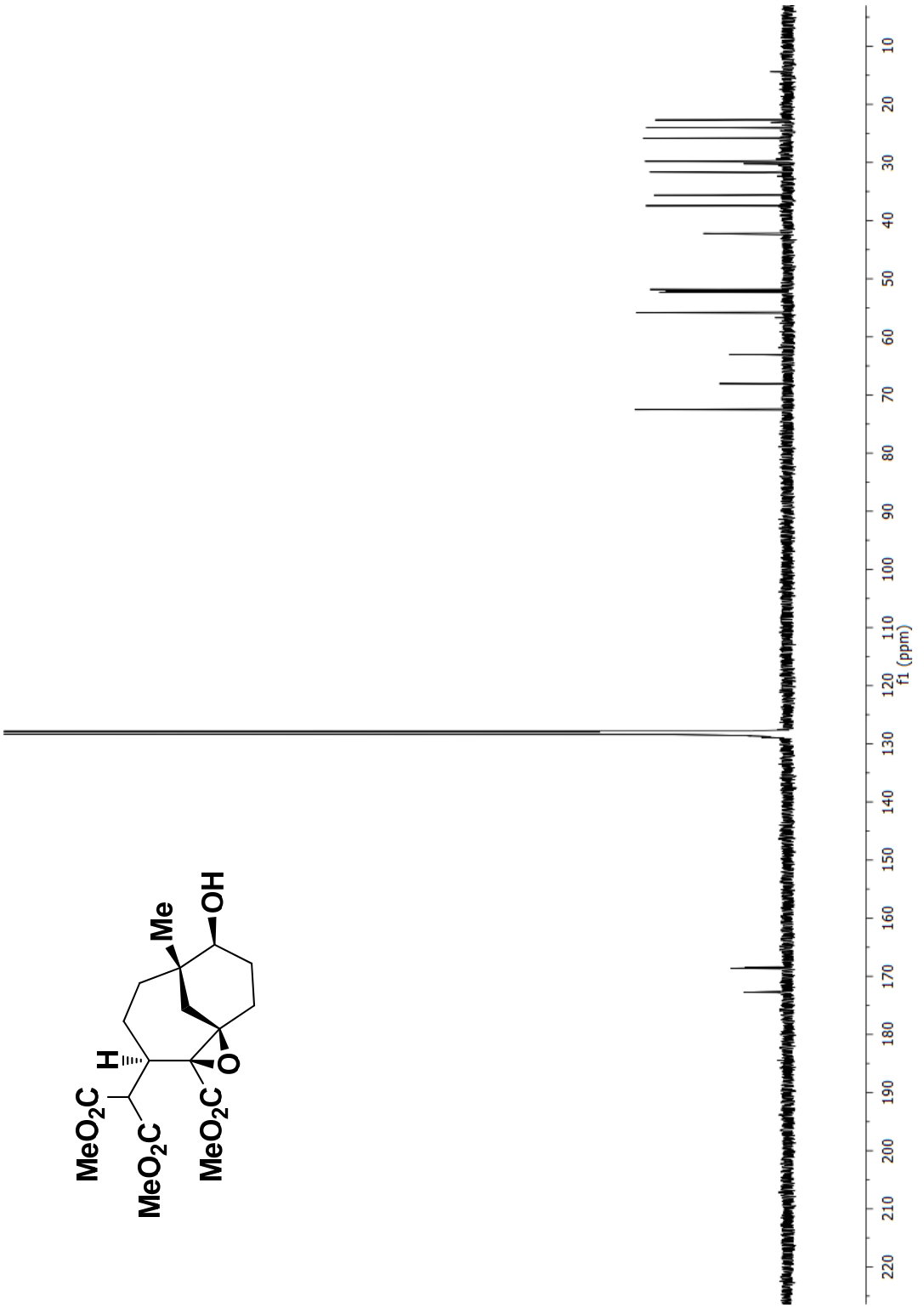
MeO2C
MeO2C
H
MeO2C
O
Me
OH
f1 (ppm)

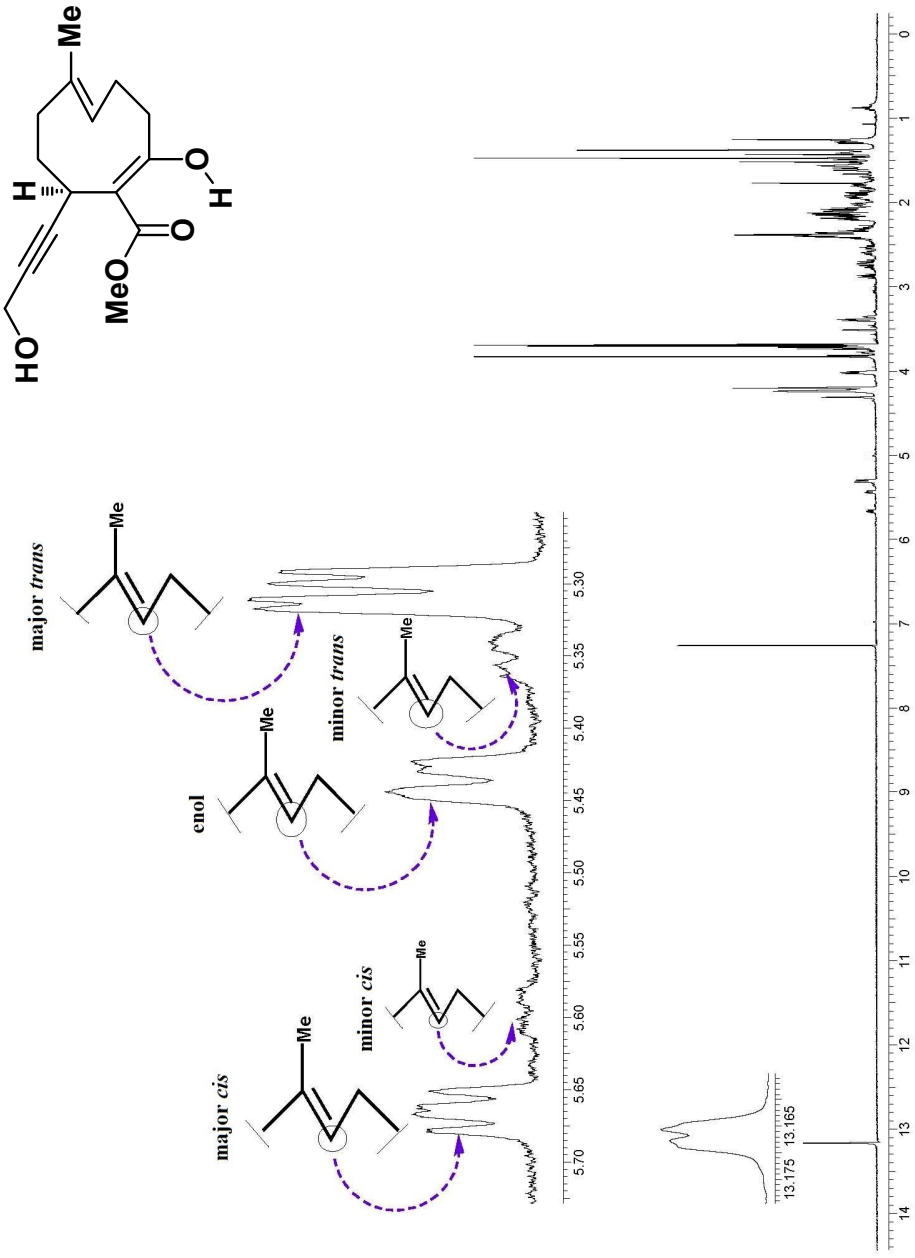
Me
H
O
H
MeO
O
HO
major trans
Me
enol
Me
minor trans
Me
major cis
Me
minor cis
Me
5.70
5.65
5.60
5.55
5.50
5.45
5.40
5.35
5.30
13.175
13.165
14
13
12
11
10
9
8
7
6
5
4
3
2
1
0

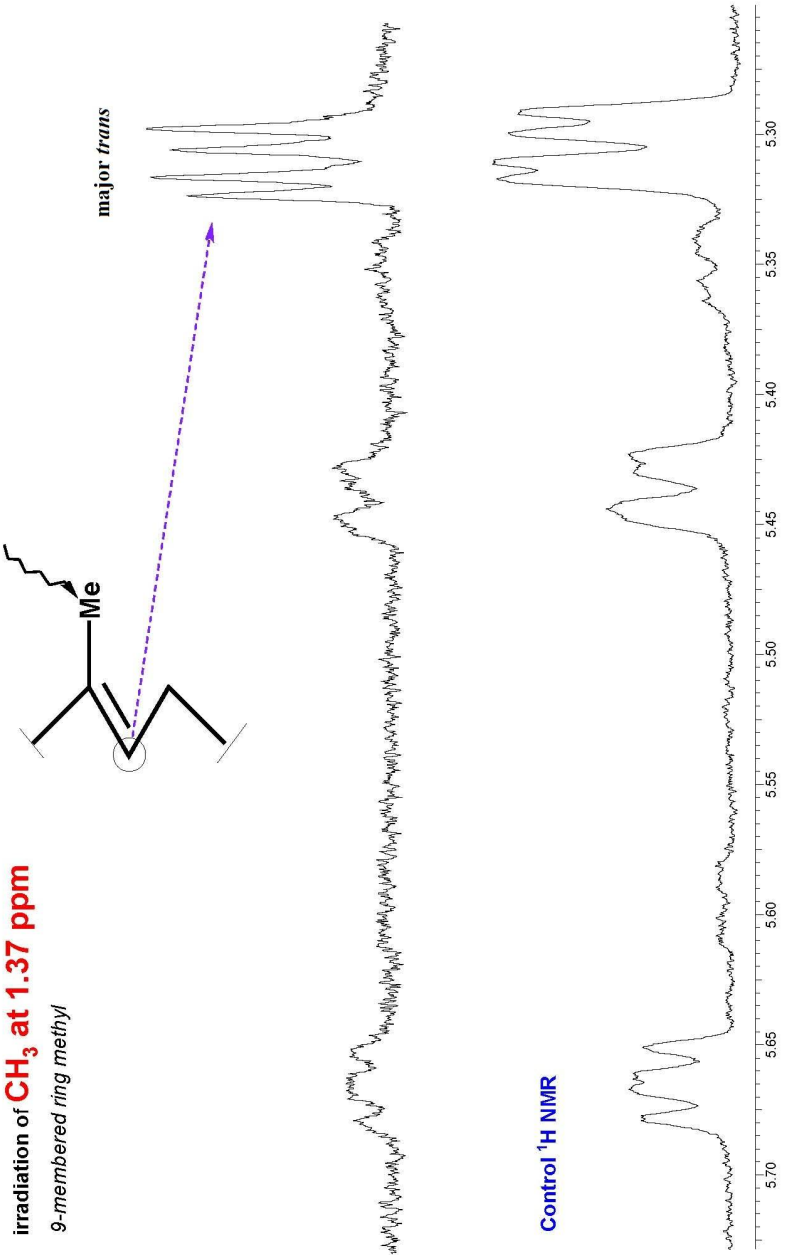
irradiation of CH_3 at 1.37 ppm
9-membered ring methyl
Me
major trans
Control ^{1}H NMR
5.70
5.65
5.60
5.55
5.50
5.45
5.40
5.35
5.30

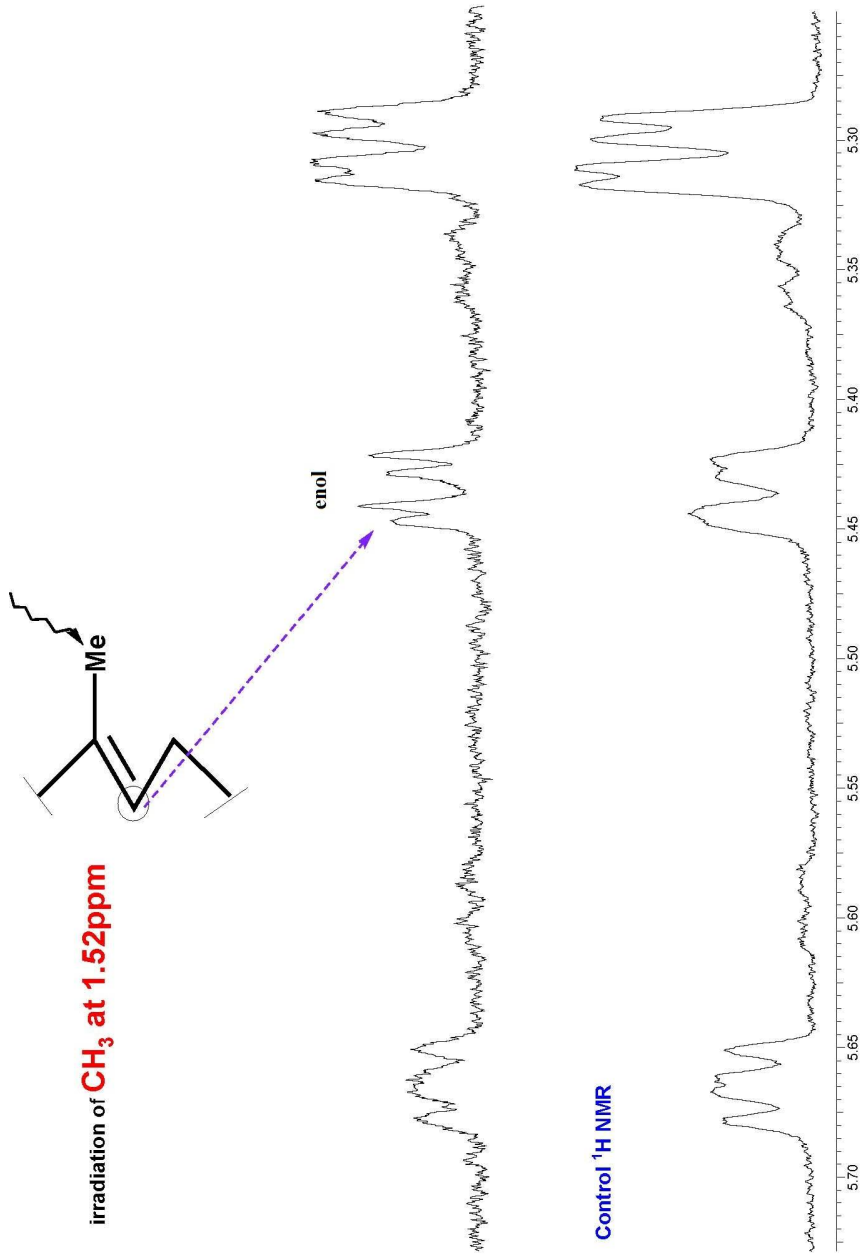
irradiation of CH3 at 1.52ppm
Me
enol
Control 1H NMR
5.70
5.65
5.60
5.55
5.50
5.45
5.40
5.35
5.30

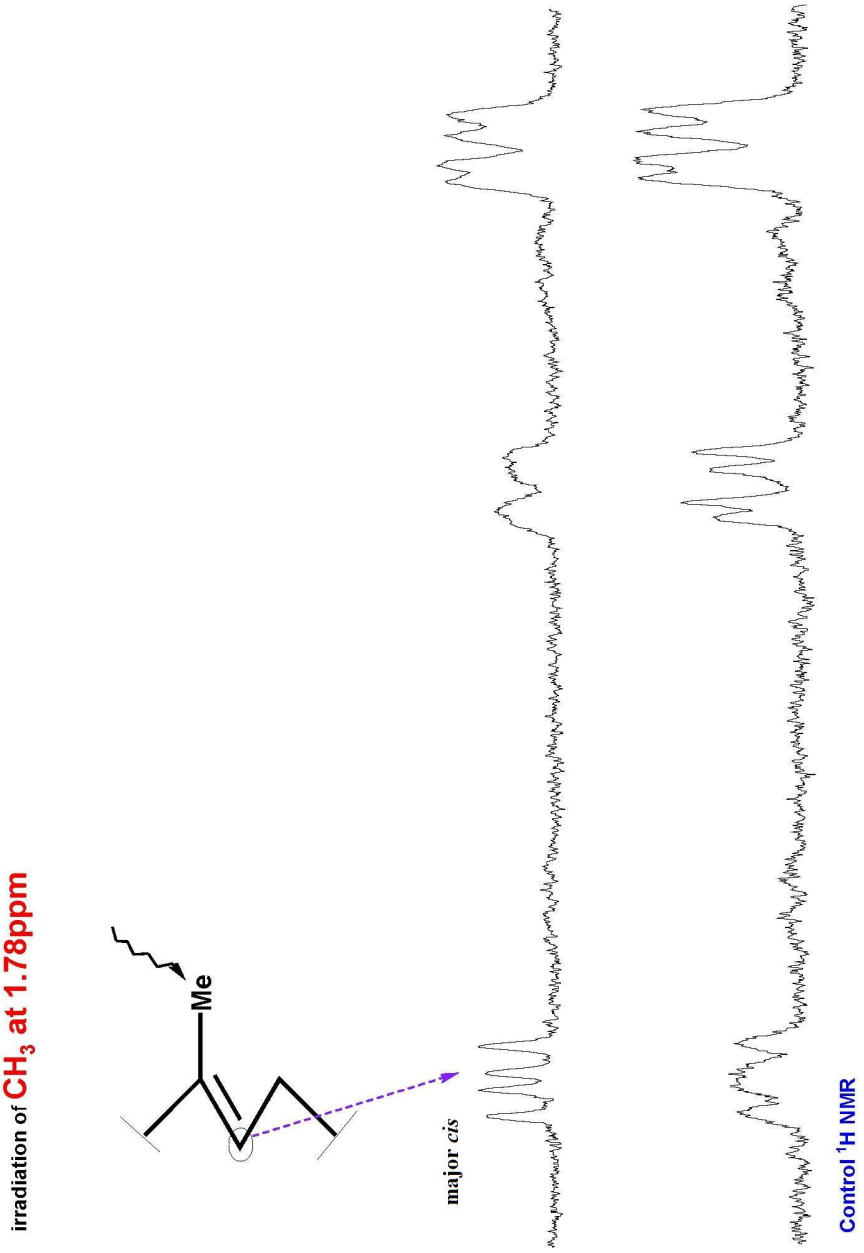
irradiation of CH3 at 1.78ppm
Me
major cis
Control 1H NMR

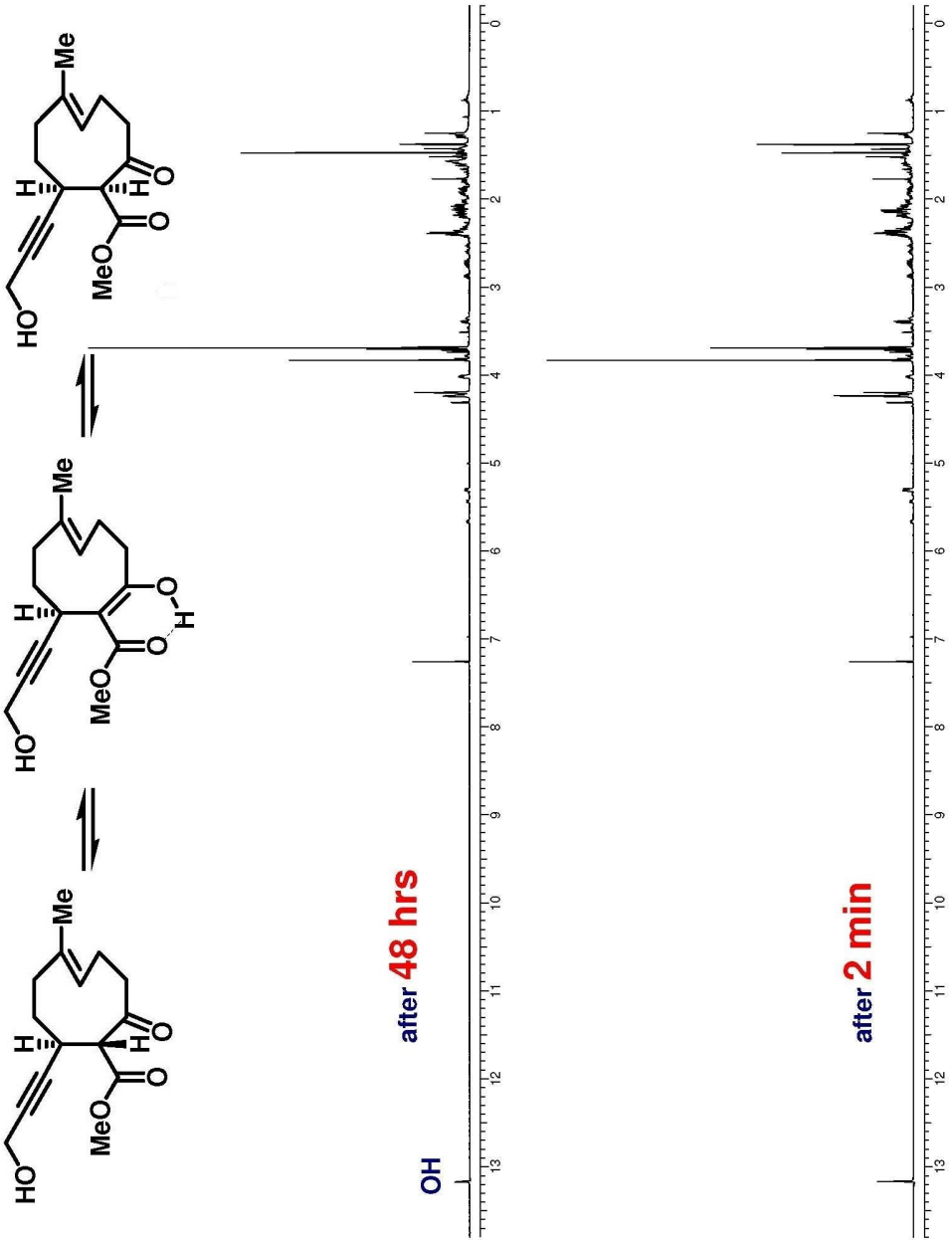
Me
H
O
H
O
MeO
HO
OH
after 48 hrs
after 2 min

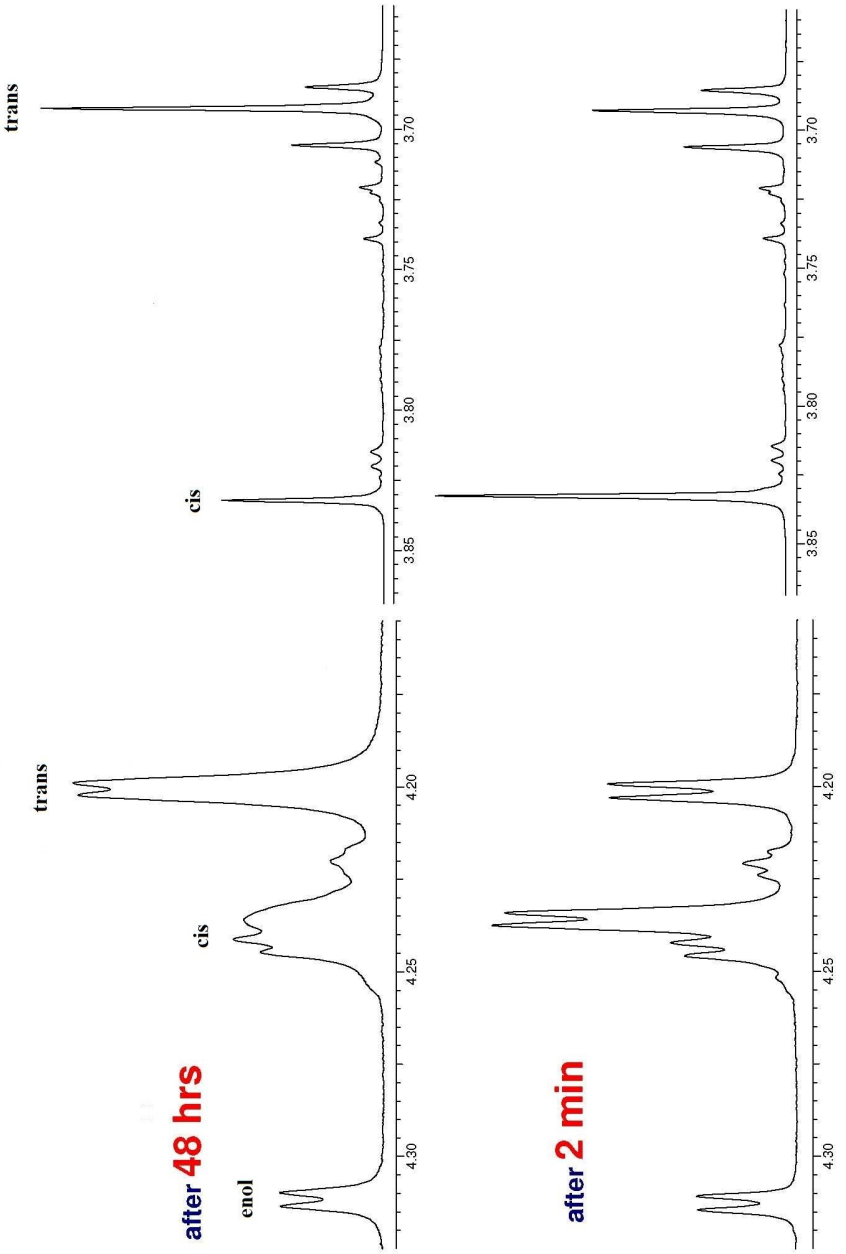
trans
cis
trans
cis
enol
after 48 hrs
after 2 min
3.70
3.75
3.80
3.85
4.20
4.25
4.30

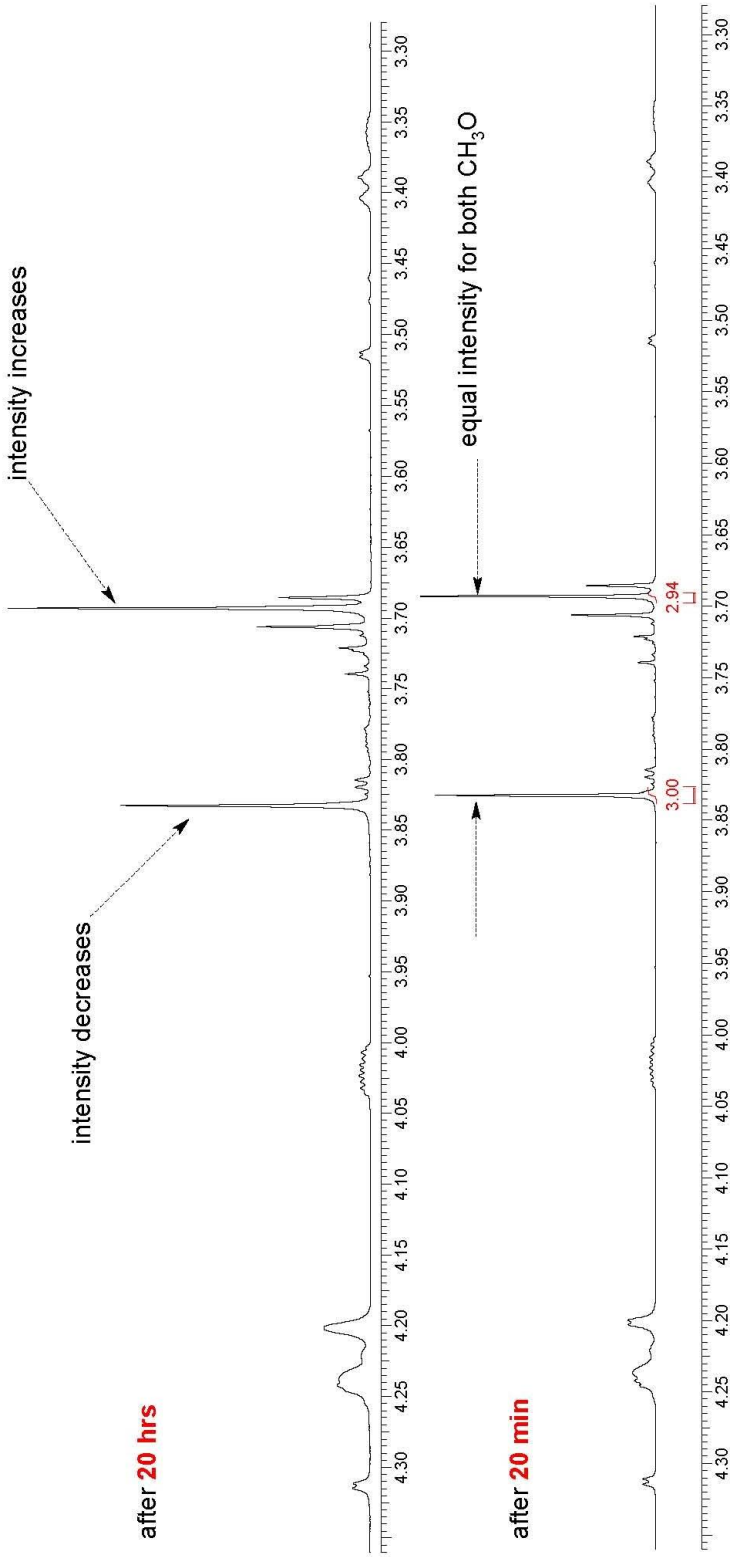
intensity increases
intensity decreases
after 20 hrs
equal intensity for both CH_3O
after 20 min
3.00
2.94

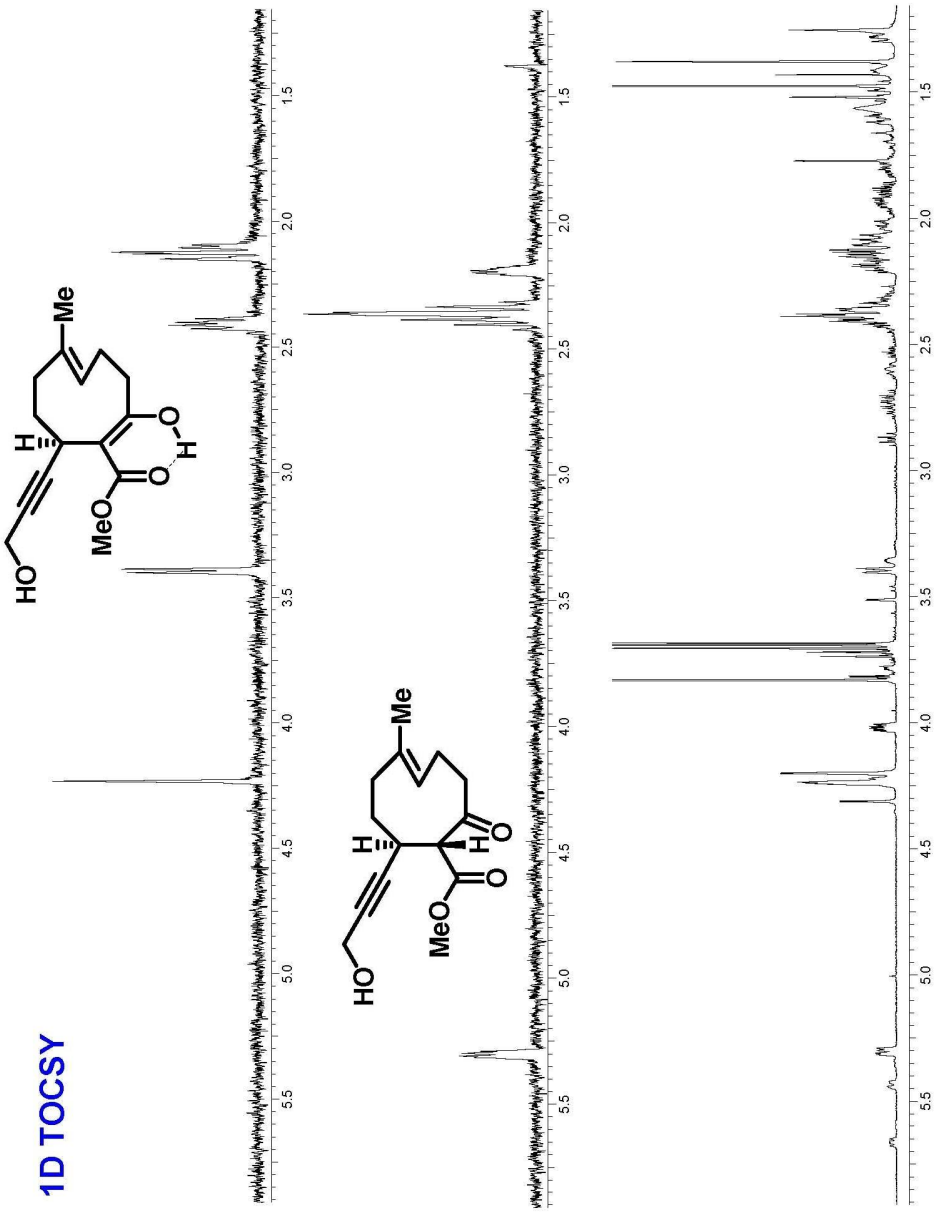
1D TOCSY
Me
H
HO
MeO
O
H
O
Me
H
HO
MeO
H
O
O
5.5
5.0
4.5
4.0
3.5
3.0
2.5
2.0
1.5

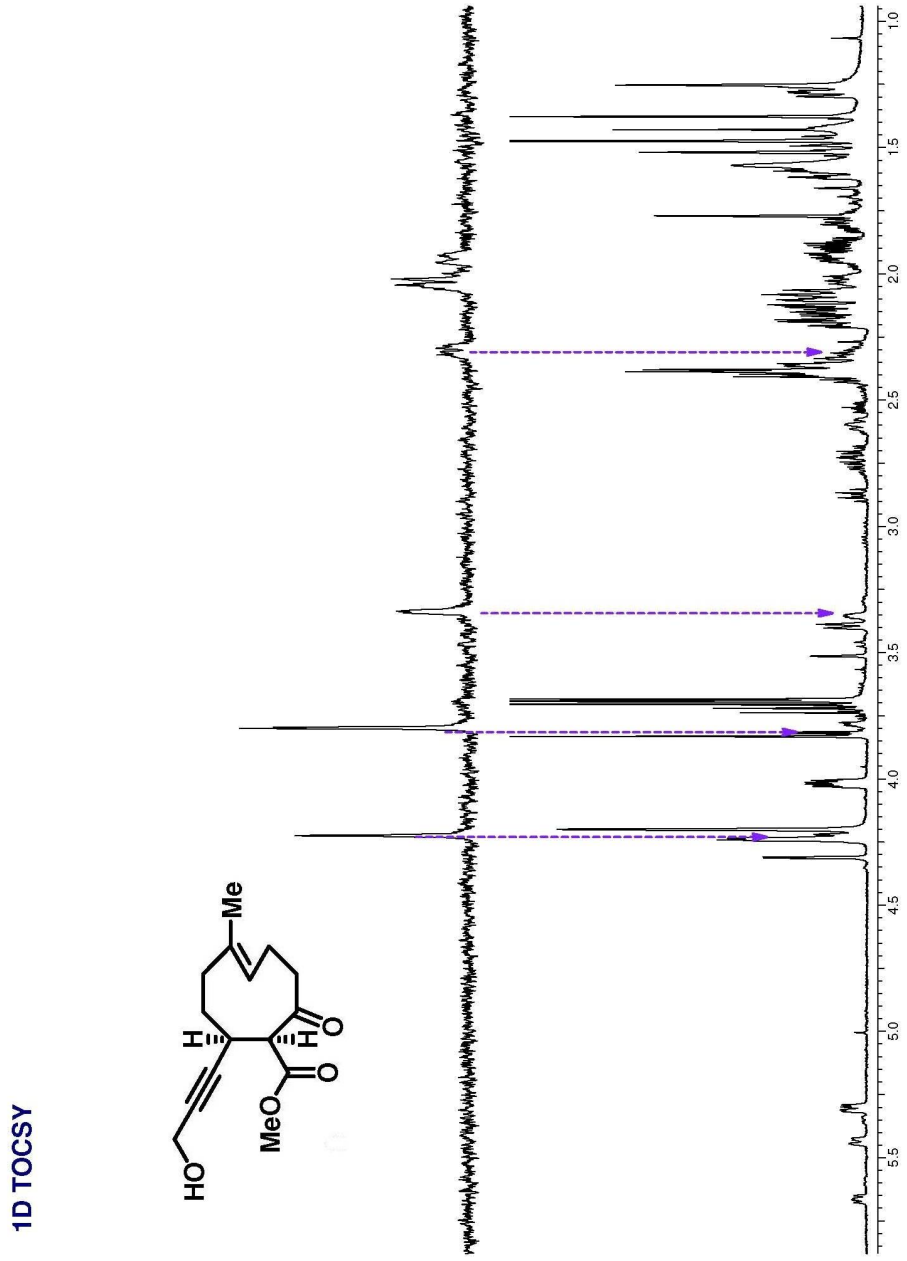
1D TOCSY
Me
H
O
H
O
MeO
HO
5.5
5.0
4.5
4.0
3.5
3.0
2.5
2.0
1.5
1.0

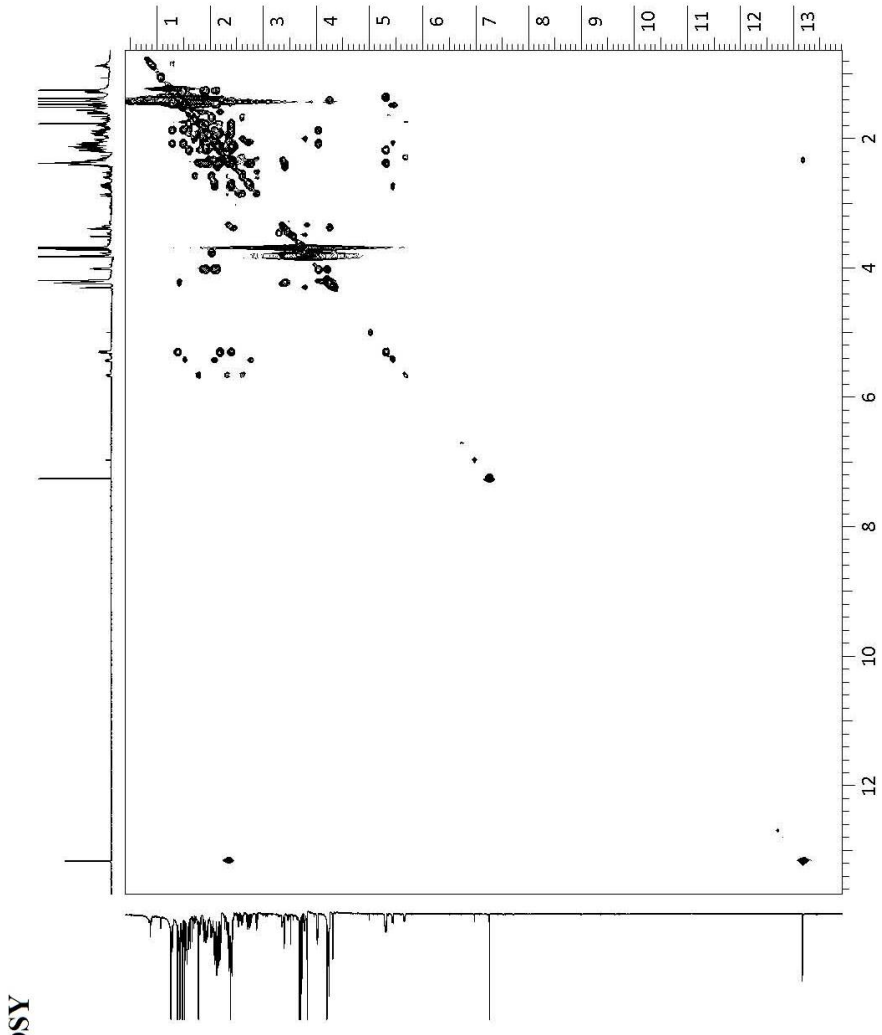

COSY

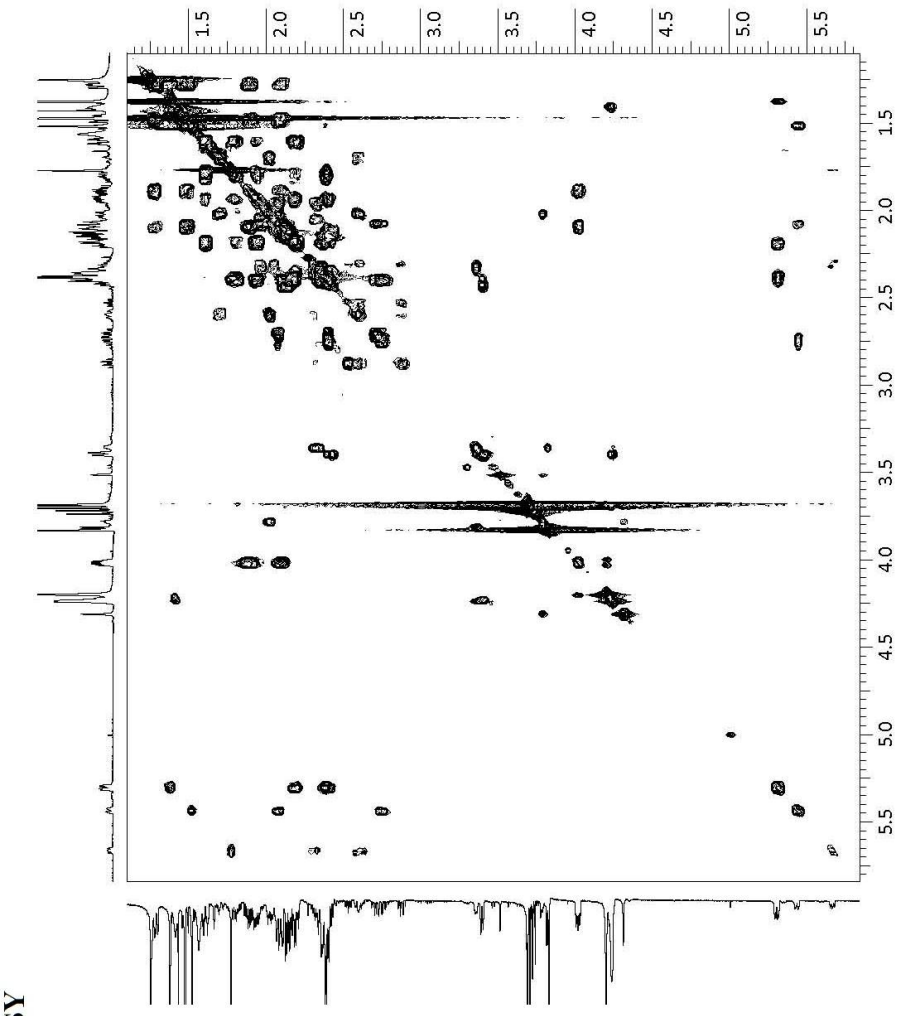

COSY

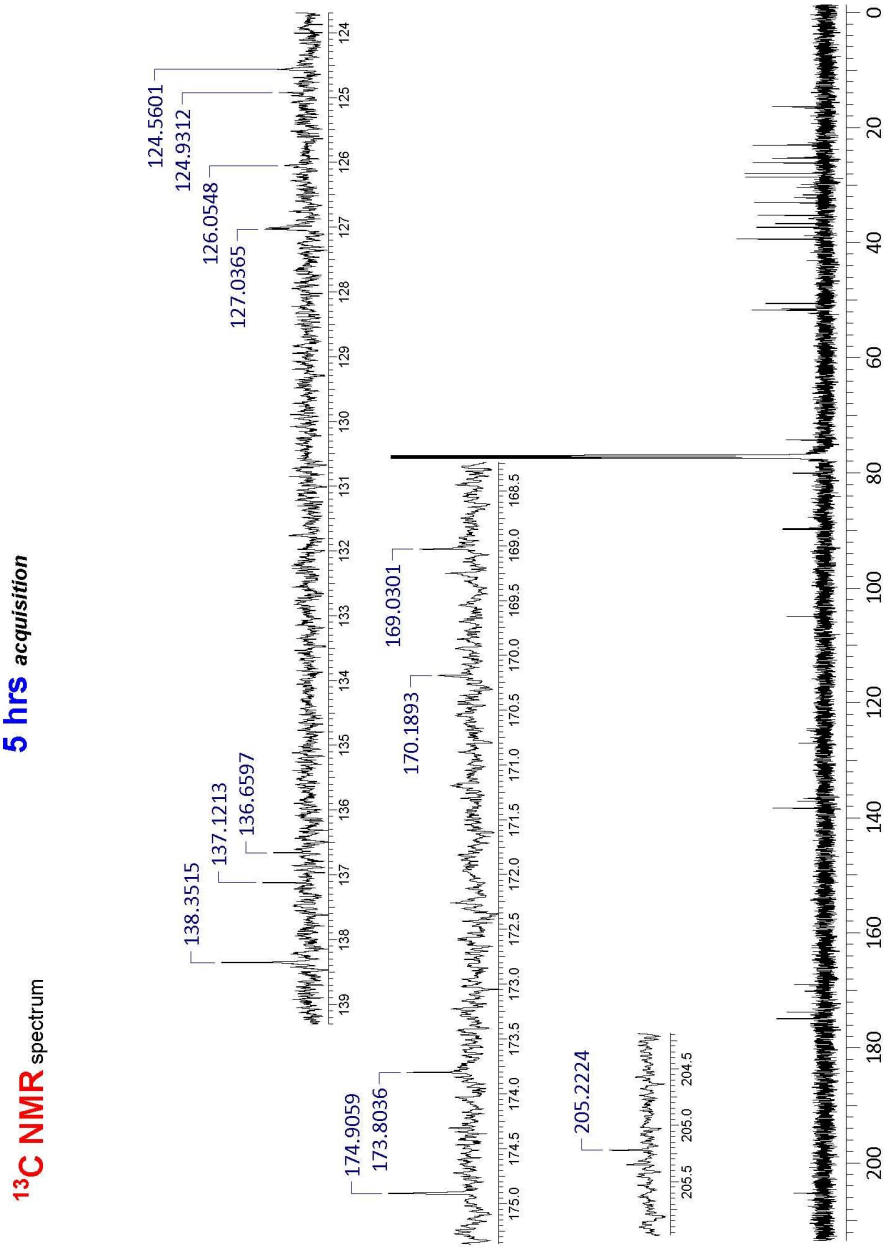
^{13}C NMR spectrum
5 hrs acquisition
124.5601
124.9312
126.0548
127.0365
138.3515
137.1213
136.6597
174.9059
173.8036
170.1893
169.0301
205.2224

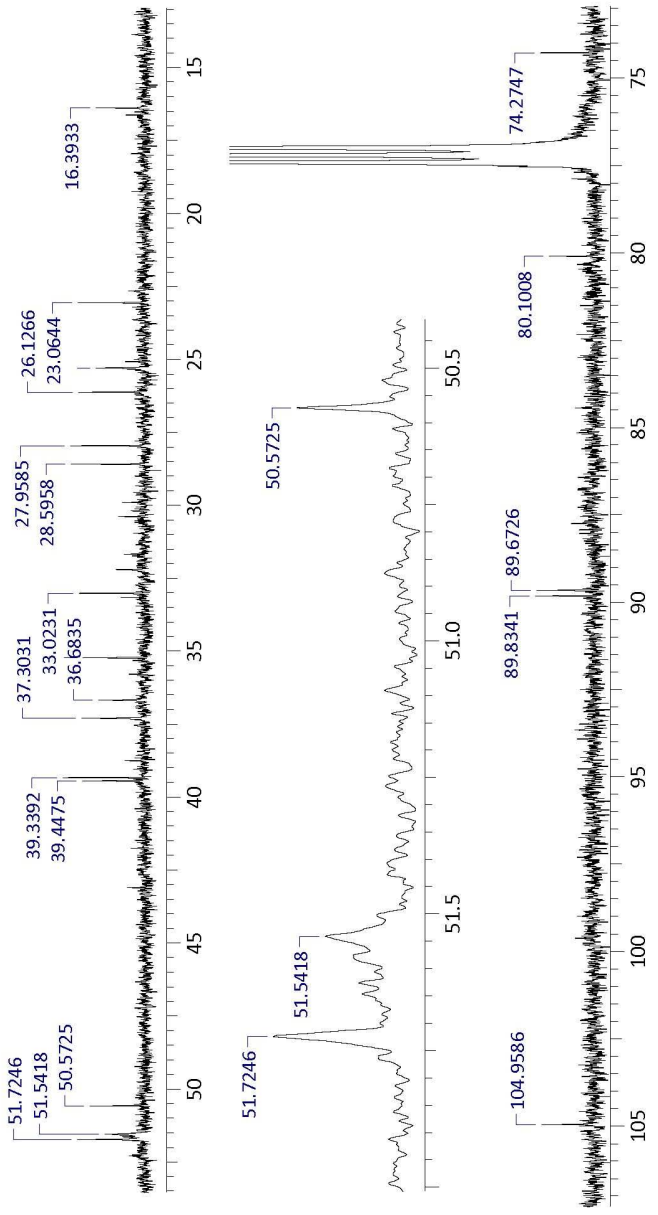
51.7246
51.5418
50.5725
39.3392
39.4475
37.3031
33.0231
36.6835
27.9585
28.5958
26.1266
23.0644
16.3933
74.2747
80.1008
89.6726
89.8341
104.9586
50.5725
51.5418
51.7246
50
45
40
35
30
25
20
15
105
100
95
90
85
80
75
51.5
51.0
50.5

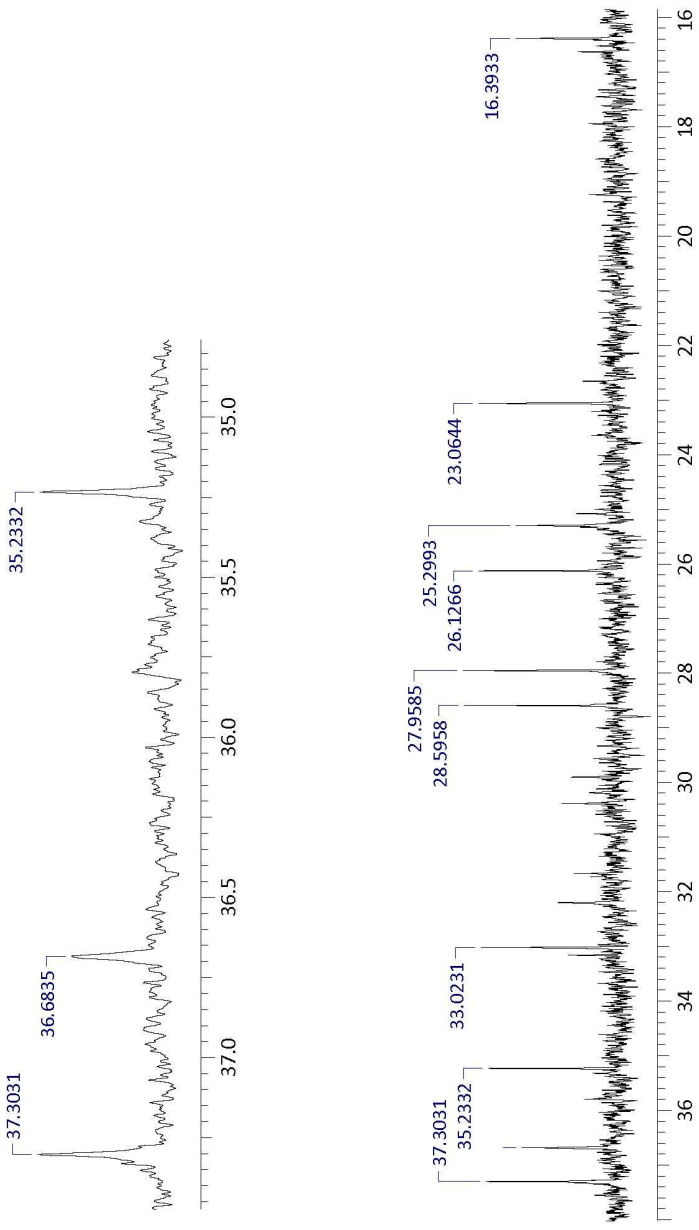
37.3031
36.6835
35.2332
37.0
36.5
36.0
35.5
35.0
37.3031
35.2332
33.0231
28.5958
27.9585
26.1266
25.2993
23.0644
16.3933
36
34
32
30
28
26
24
22
20
18
16

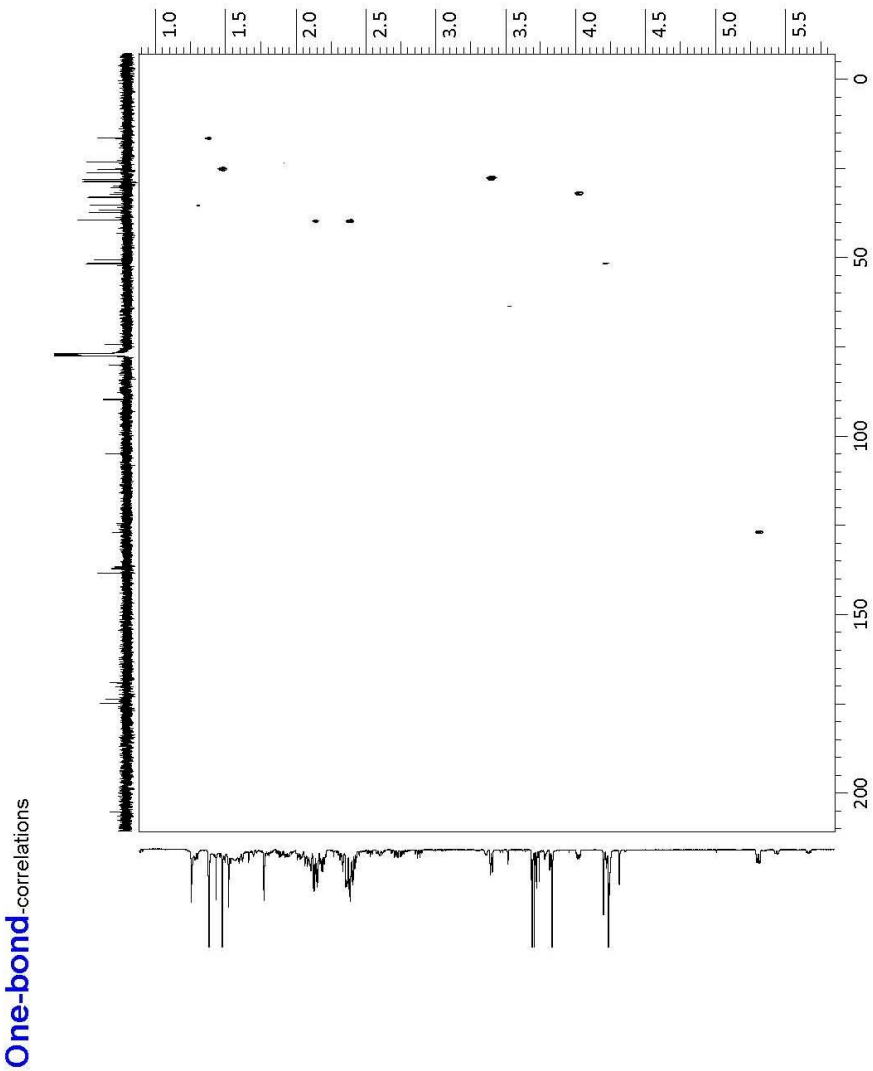
One-bond-correlations
1.0
1.5
2.0
2.5
3.0
3.5
4.0
4.5
5.0
5.5
0
50
100
150
200

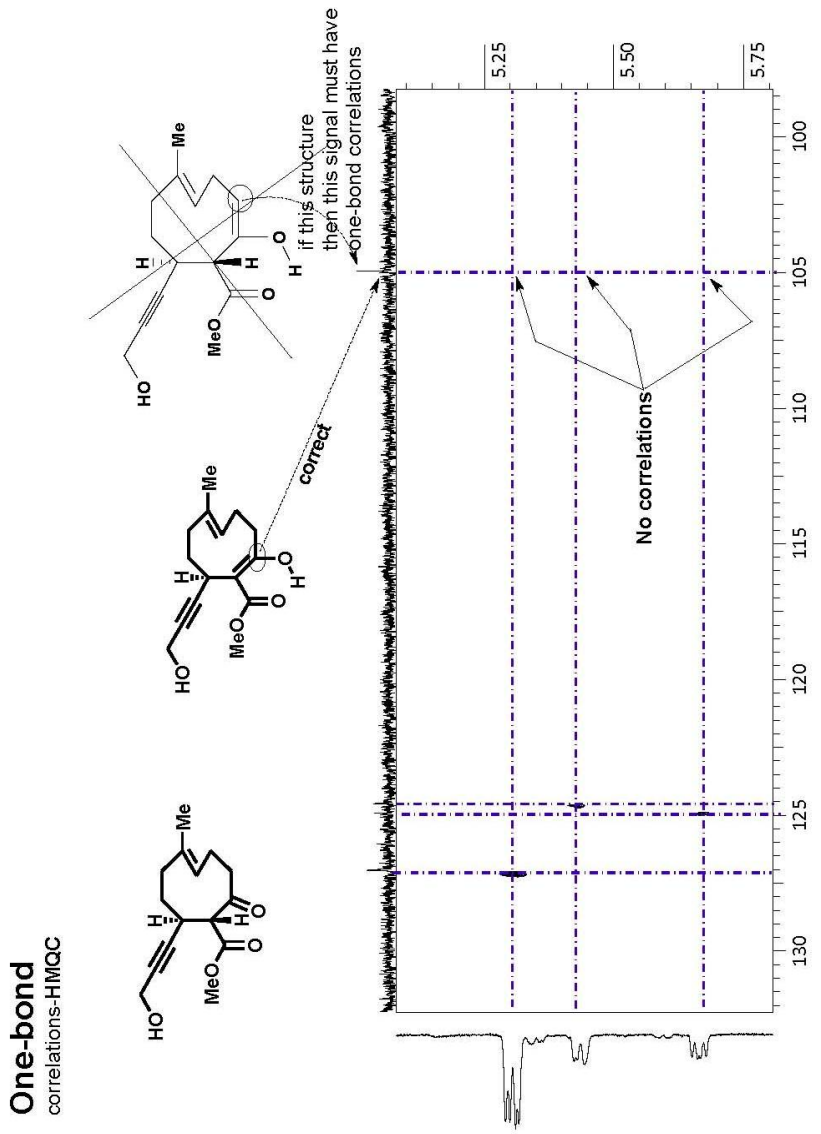
One-bond
correlations-HMQC
if this structure
then this signal must have
one-bond correlations
correct
No correlations
5.25
5.50
5.75
100
105
110
115
120
125
130
Me
MeO
HO

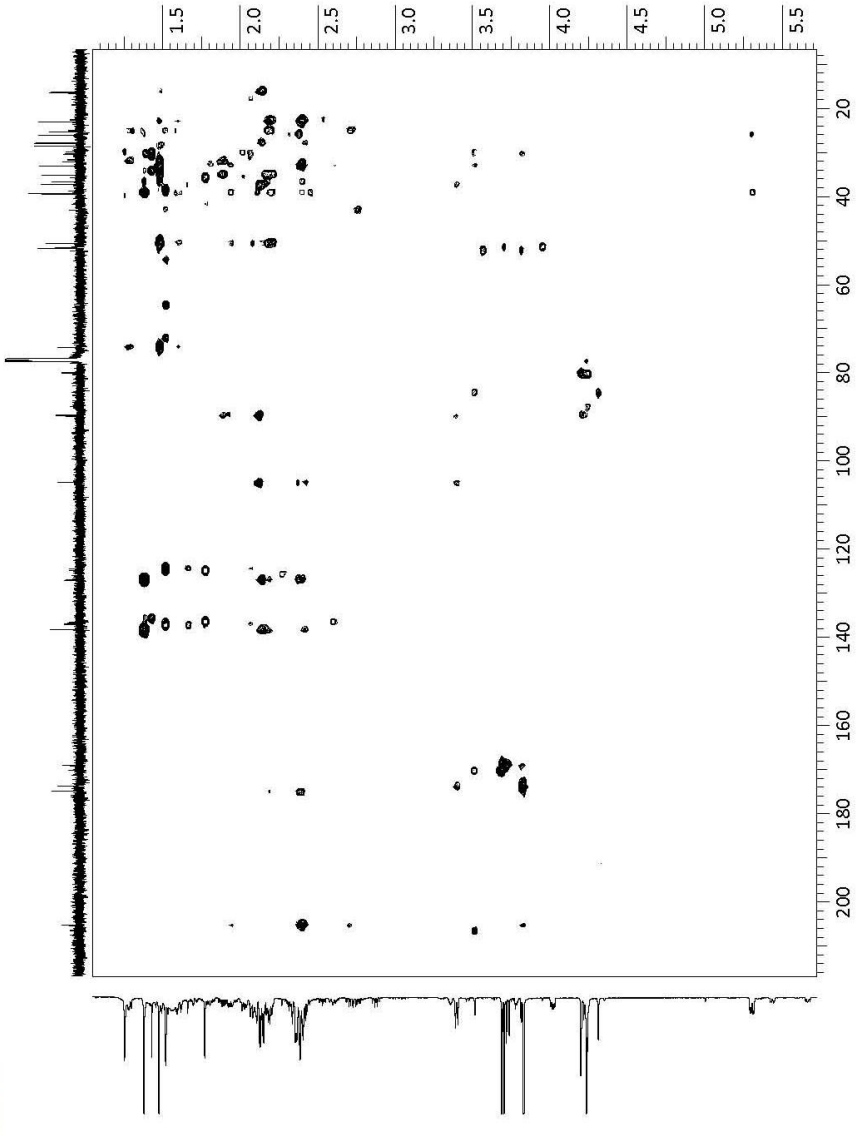

HMBC

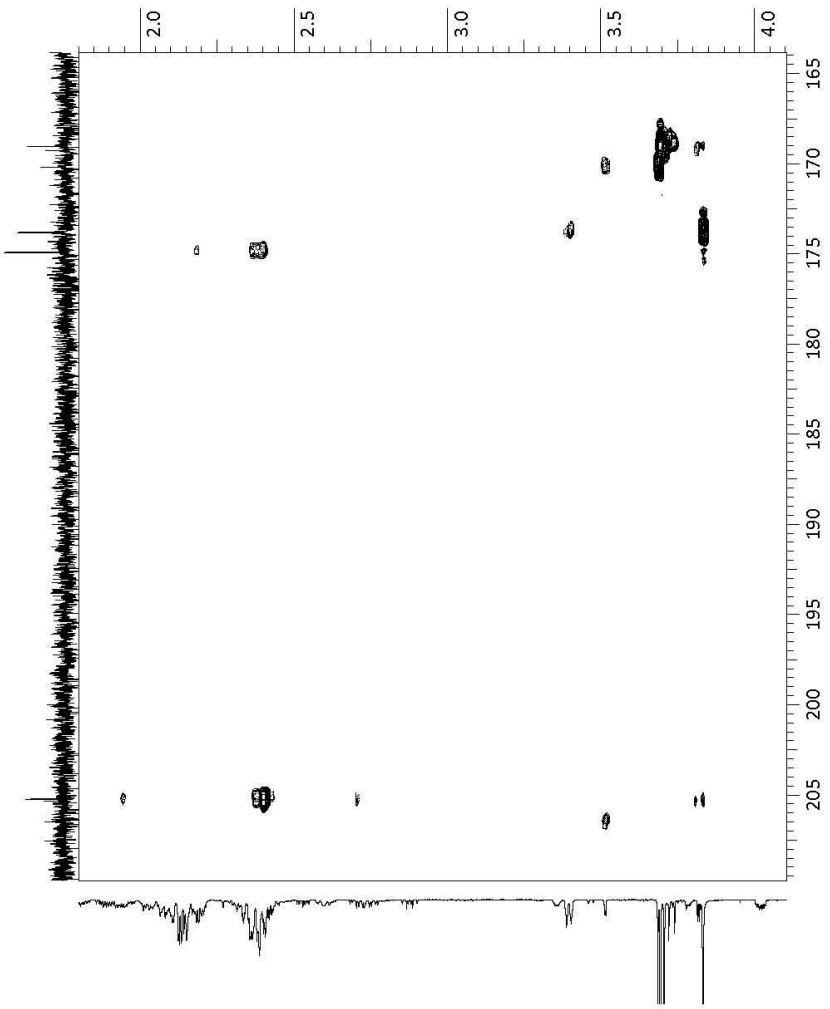

HMBC

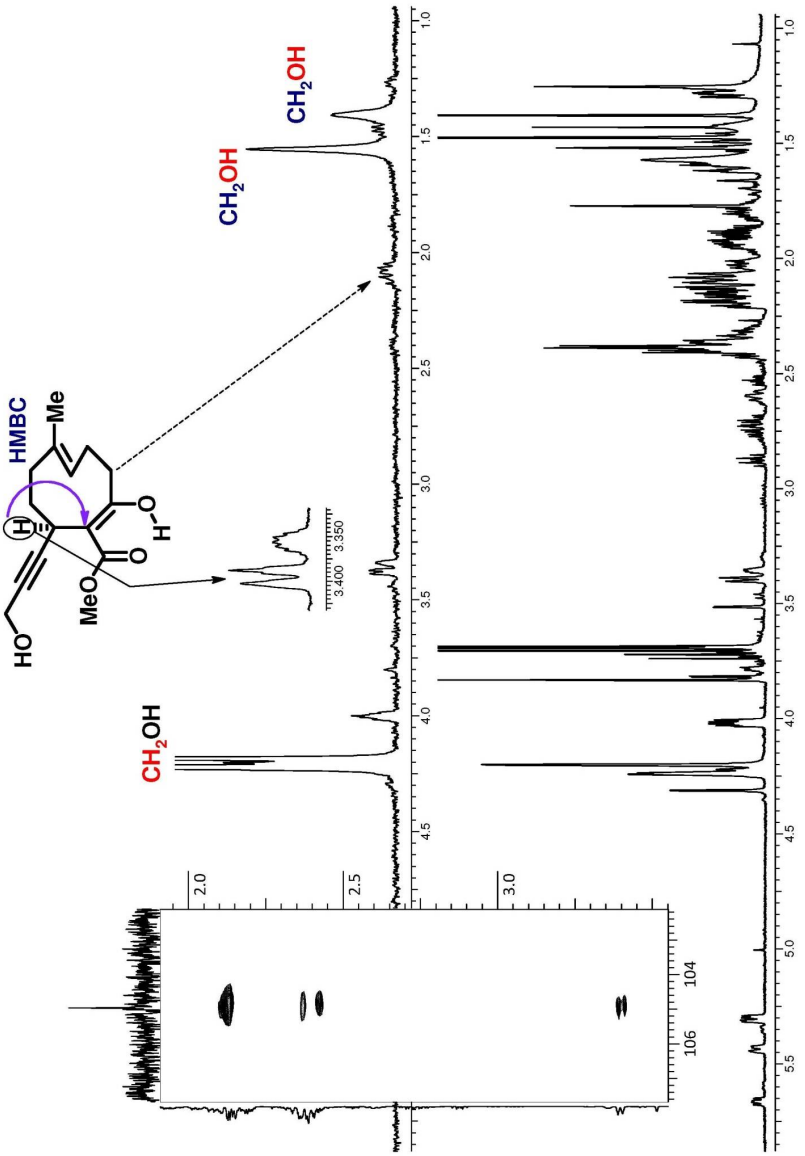
HMBC
Me
HO
MeO
O
H
CH2OH
CH2OH
CH2OH
3.400
3.350

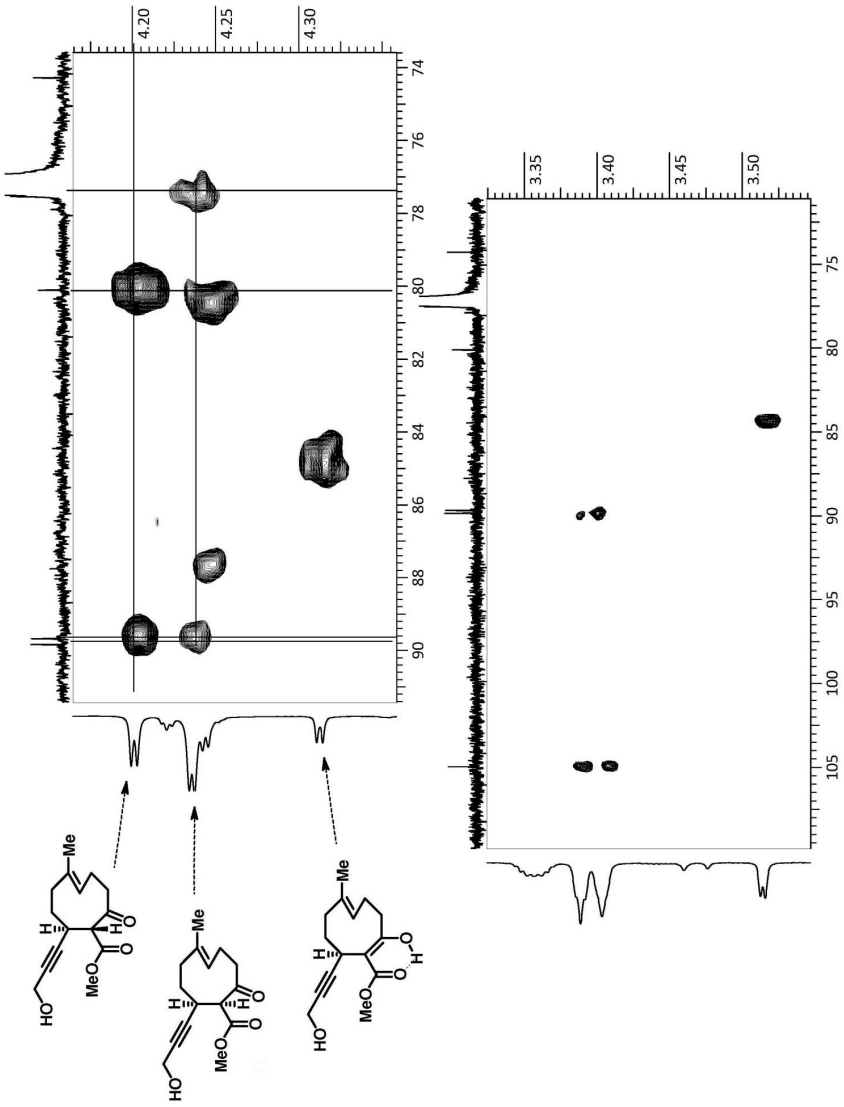
4.20
4.25
4.30
74
76
78
80
82
84
86
88
90
3.35
3.40
3.45
3.50
75
80
85
90
95
100
105
Me
H
O
H
MeO
O
HO
Me
H
O
H
MeO
O
HO
Me
H
O
H
MeO
O
HO

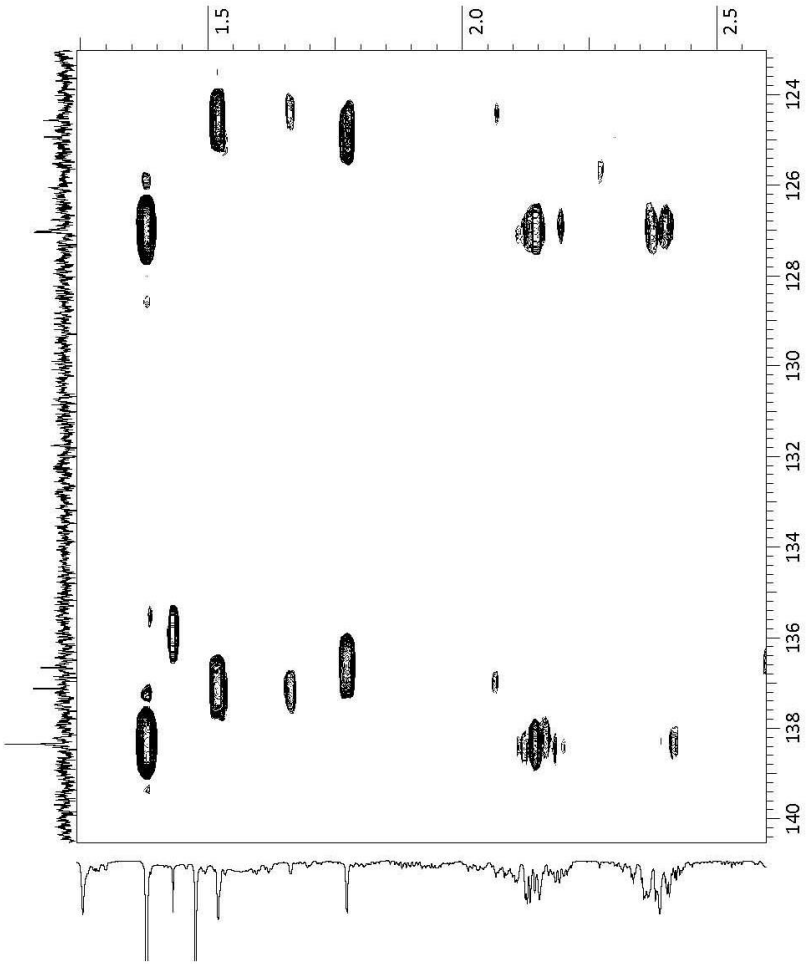

HMBC

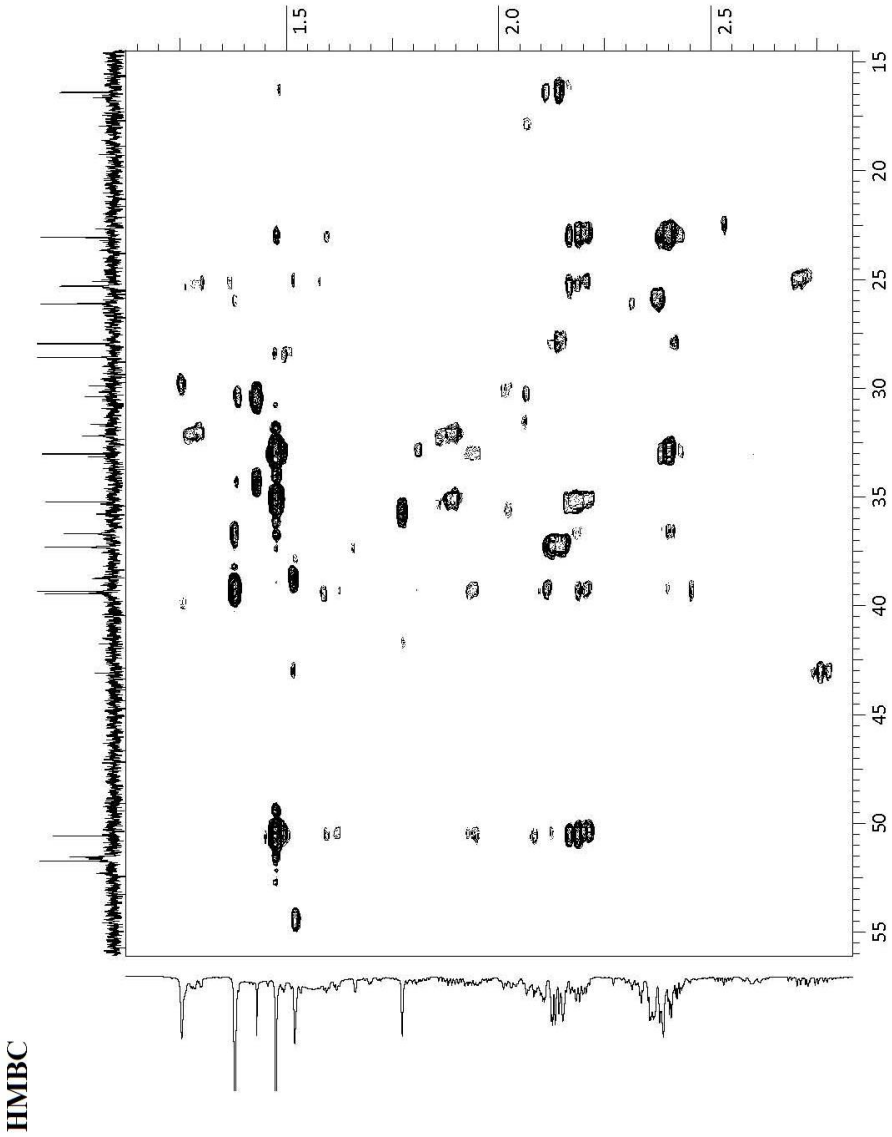

HMBC

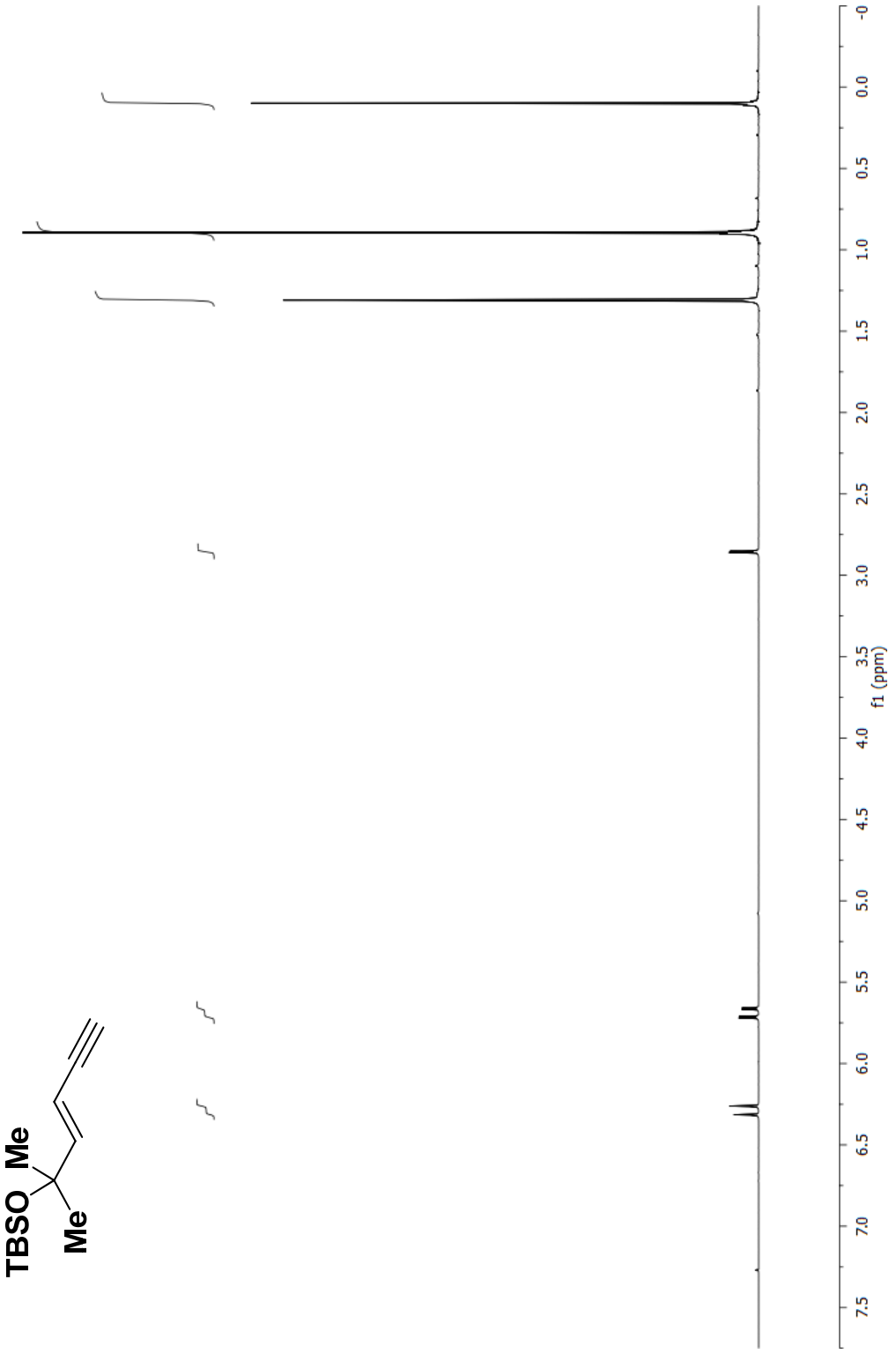
TBSO
Me
Me
f1 (ppm)

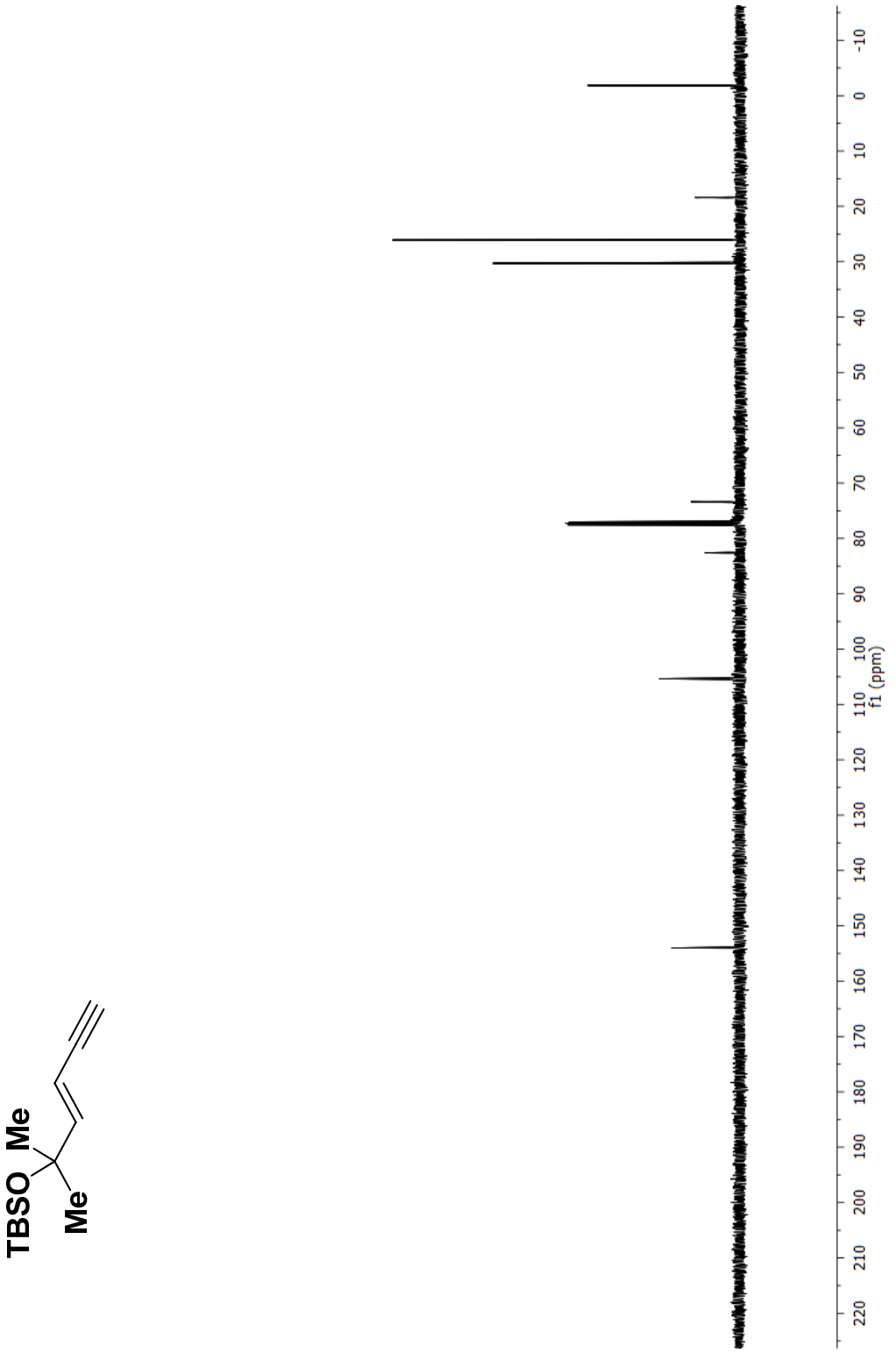
TBSO
Me
Me
f1 (ppm)

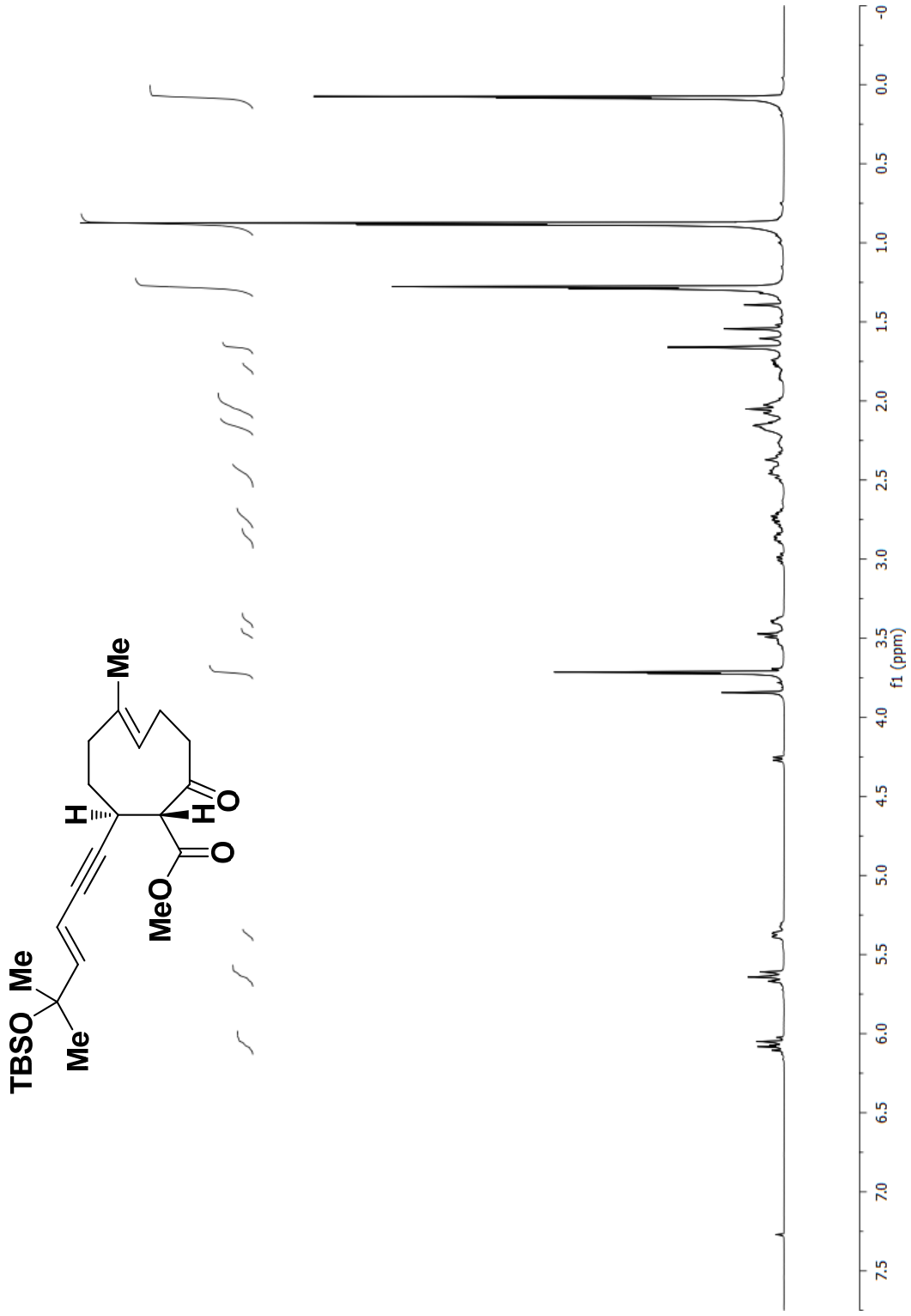
TBSO
Me
Me
H
MeO
O
O
H
Me
f1 (ppm)

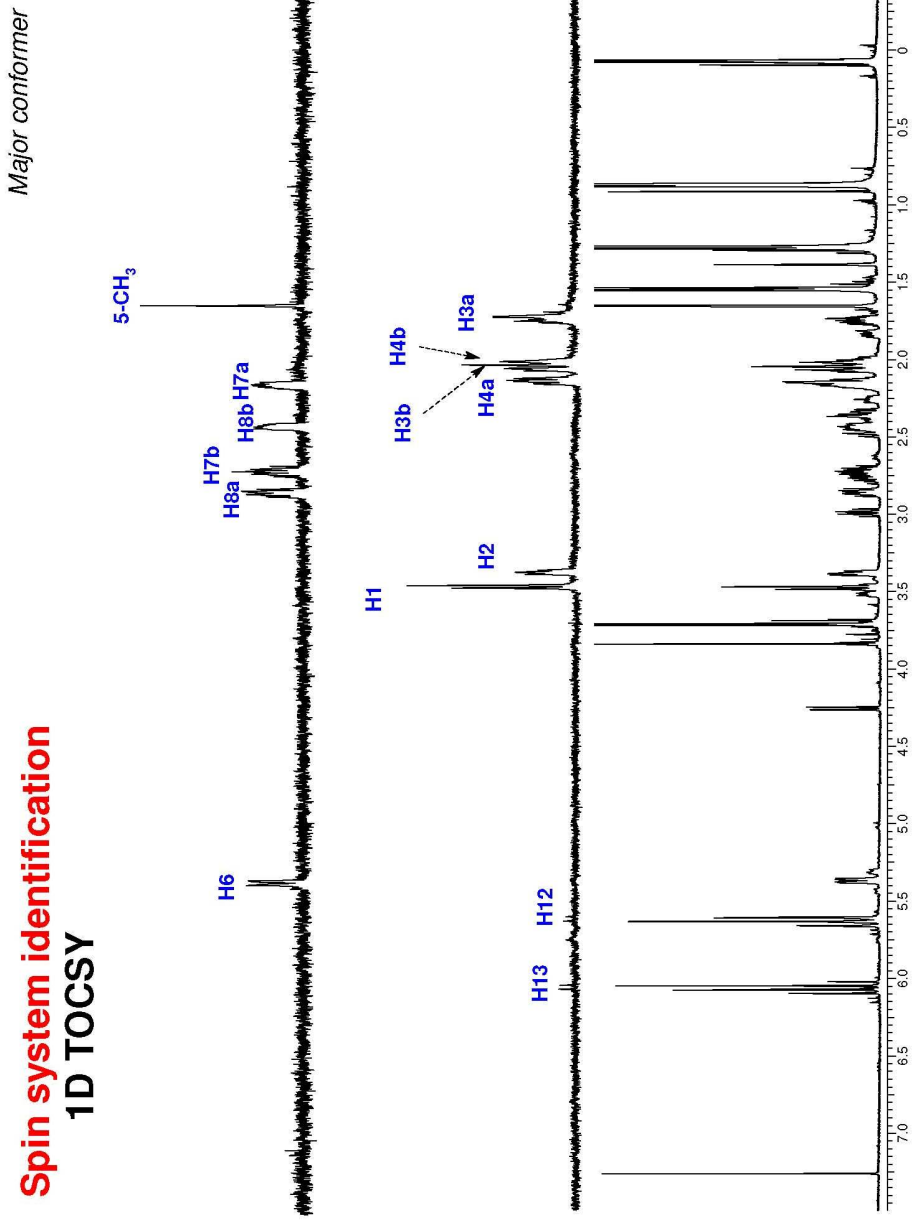
Spin system identification
1D TOCSY
Major conformer
5-CH3
H6
H8a
H7b
H8b
H7a
H1
H2
H13
H12
H3b
H4a
H4b
H3a

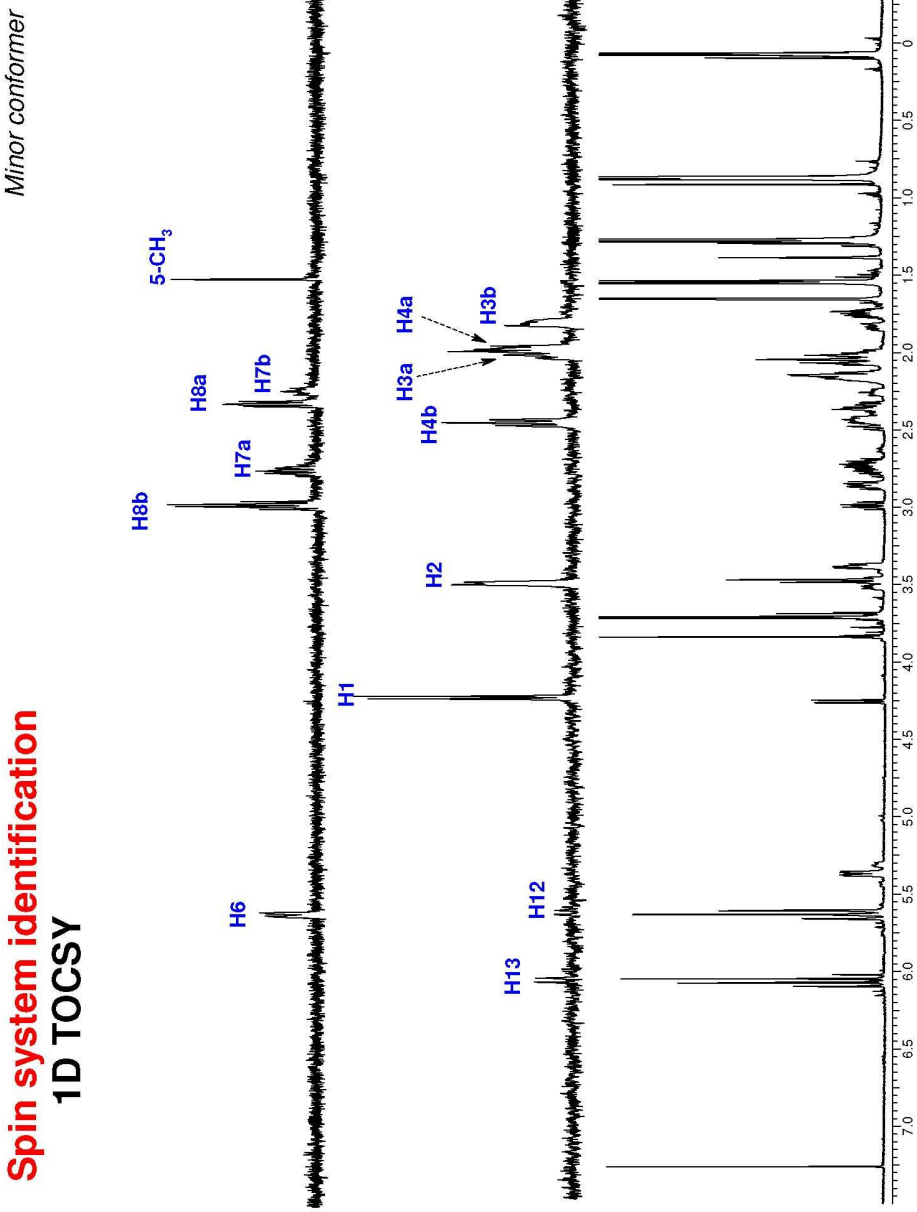
Spin system identification
1D TOCSY
Minor conformer
5-CH3
H8a
H7b
H8b
H7a
H6
H1
H4a
H3b
H3a
H4b
H2
H13
H12

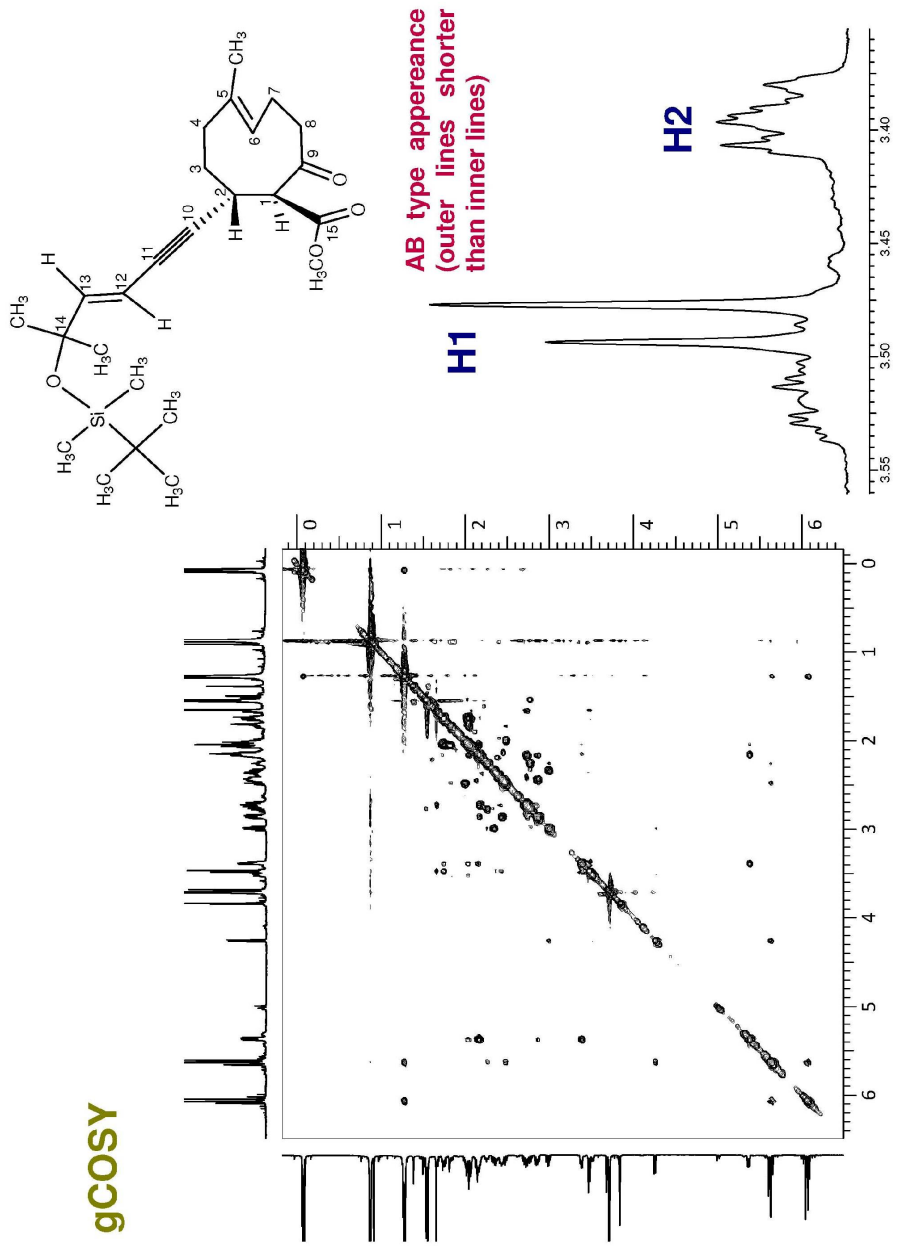
gCOSY
H1
H2
AB type appereance
(outer lines shorter
than inner lines)

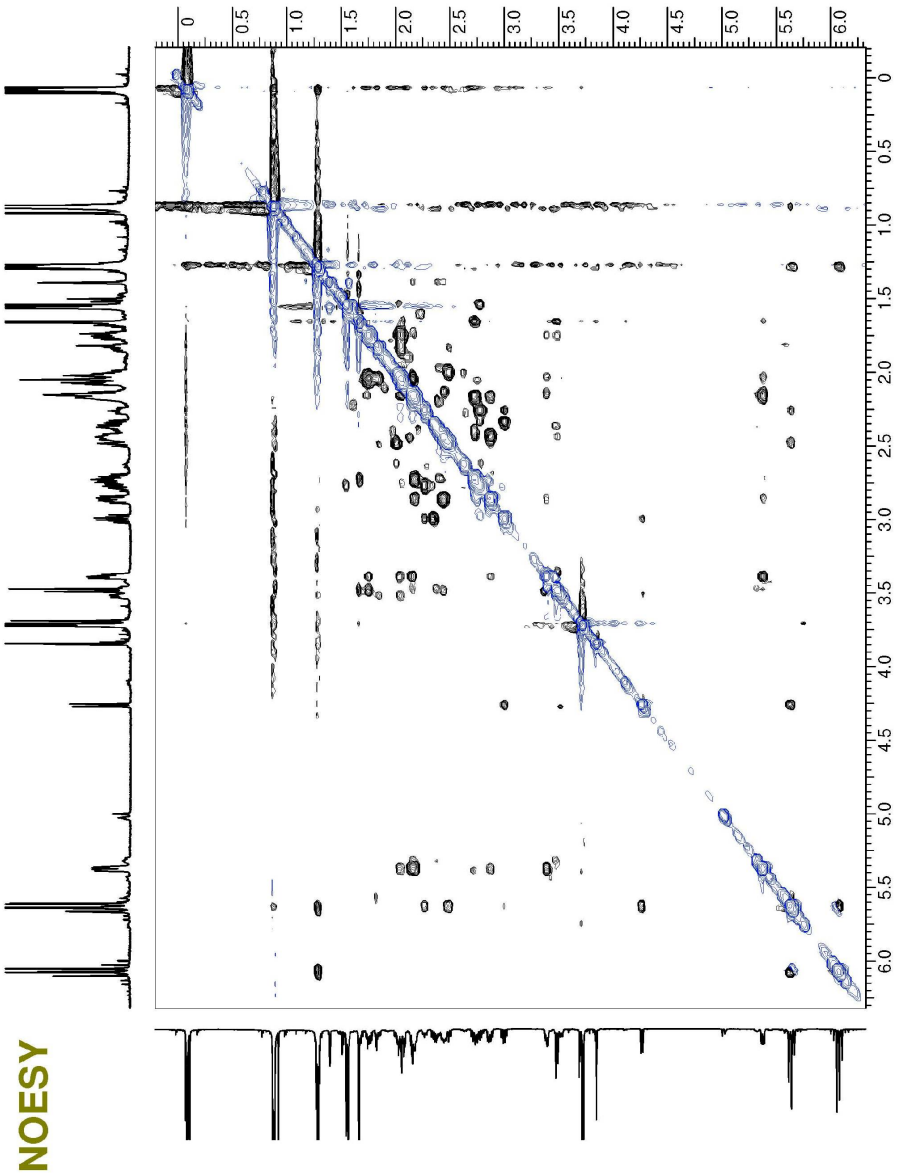
NOESY
0
0.5
1.0
1.5
2.0
2.5
3.0
3.5
4.0
4.5
5.0
5.5
6.0

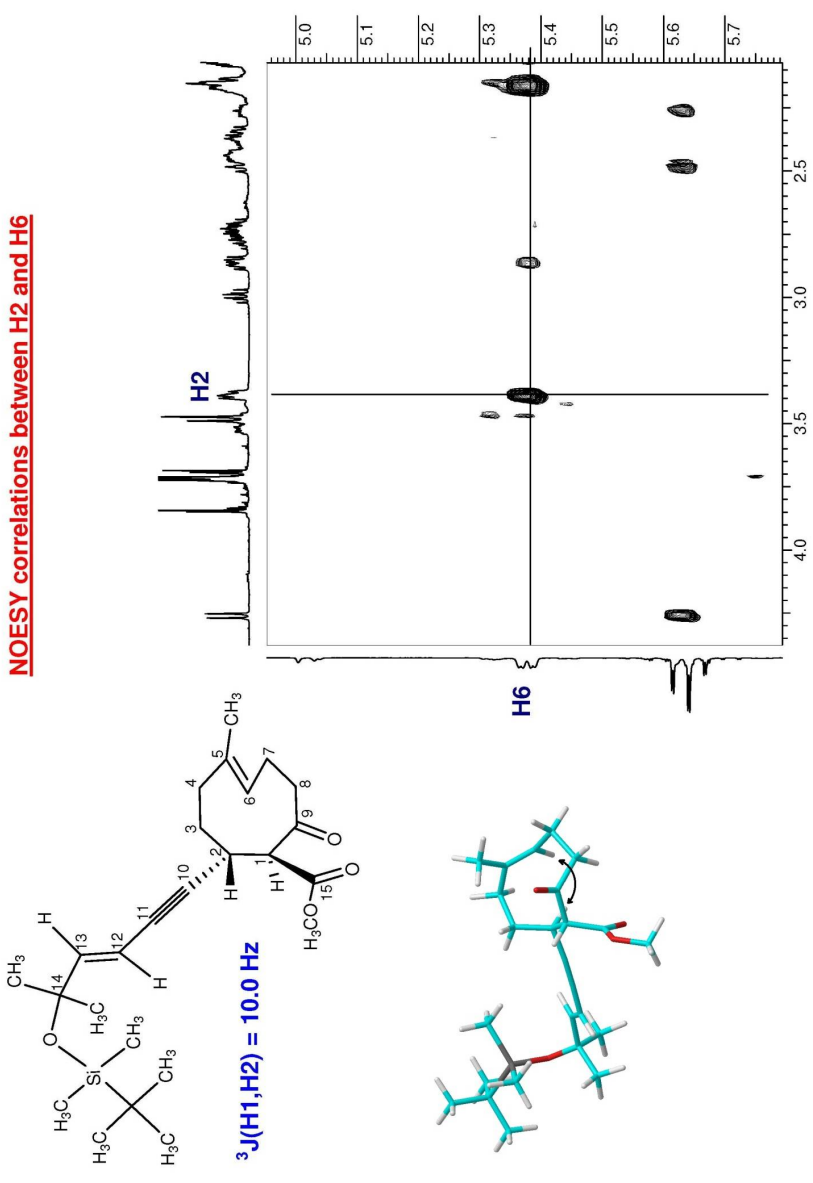
NOESY correlations between H2 and H6
H2
H6
5.0
5.1
5.2
5.3
5.4
5.5
5.6
5.7
4.0
3.5
3.0
2.5
^{3}J(H1,H2) = 10.0 Hz

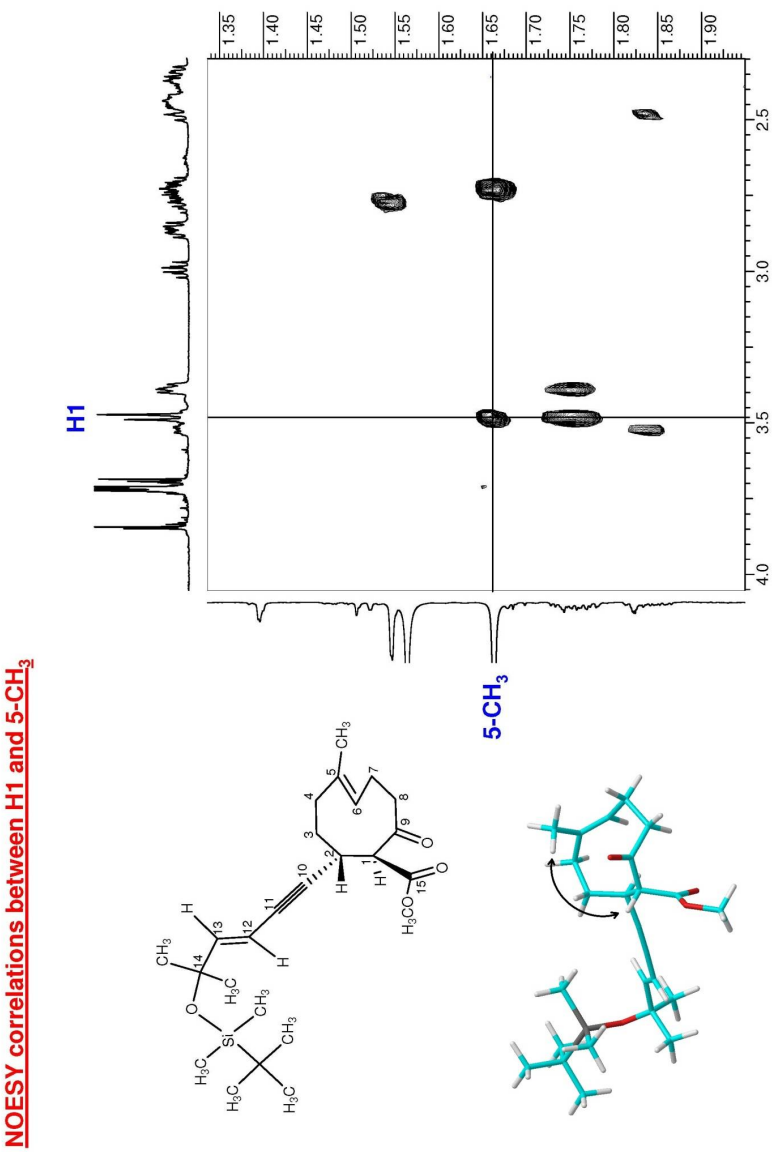
NOESY correlations between H1 and 5-CH3
H1
5-CH3
1.35
1.40
1.45
1.50
1.55
1.60
1.65
1.70
1.75
1.80
1.85
1.90
2.5
3.0
3.5
4.0
CH3
H
H
H
H3C
CH3
H3C
Si
CH3
H3C
CH3
O
H3CO
O
O

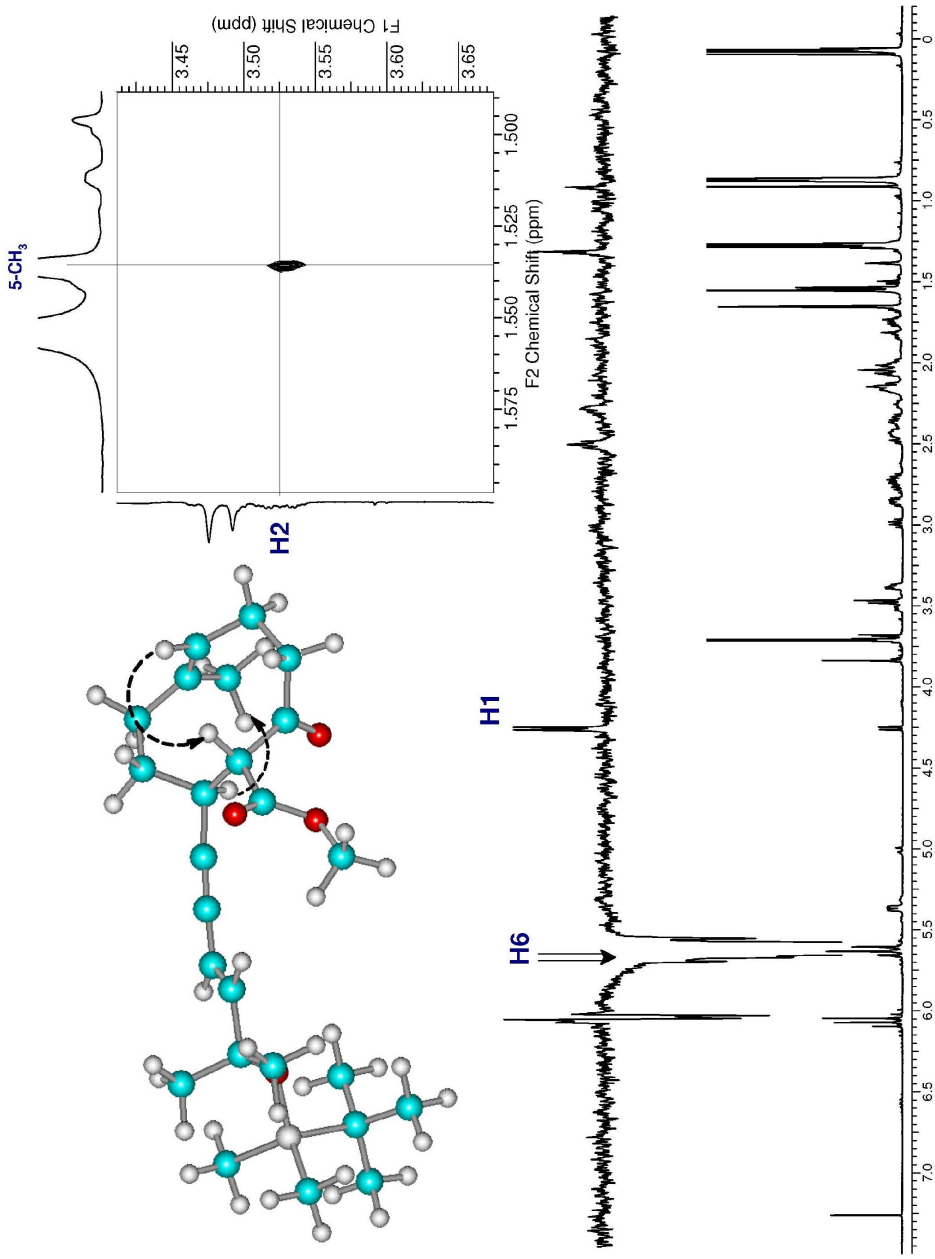
5-CH3
H2
H1
H6
F1 Chemical Shift (ppm)
F2 Chemical Shift (ppm)

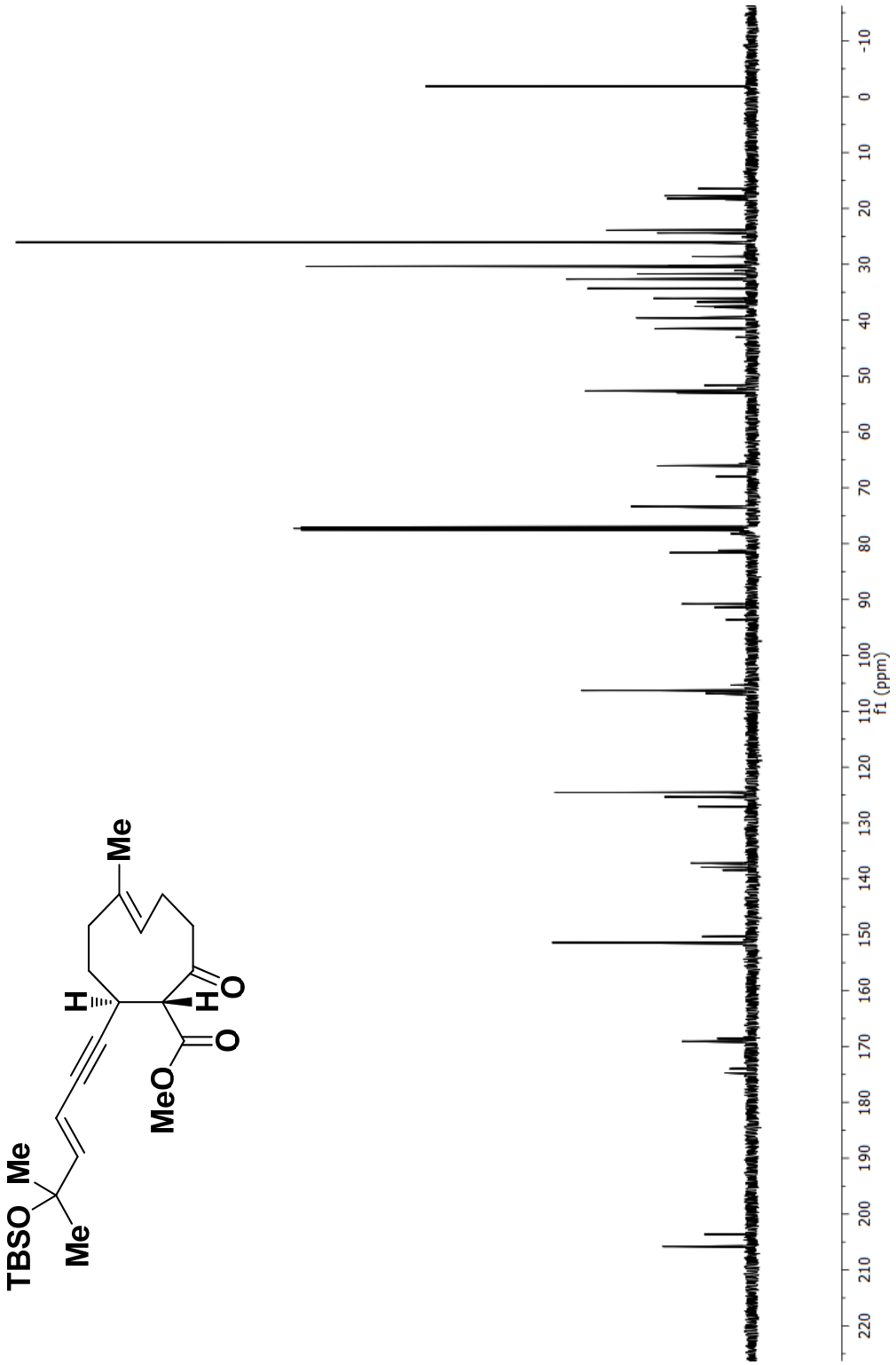
TBSO
Me
Me
MeO
O
O
H
H
Me
f1 (ppm)

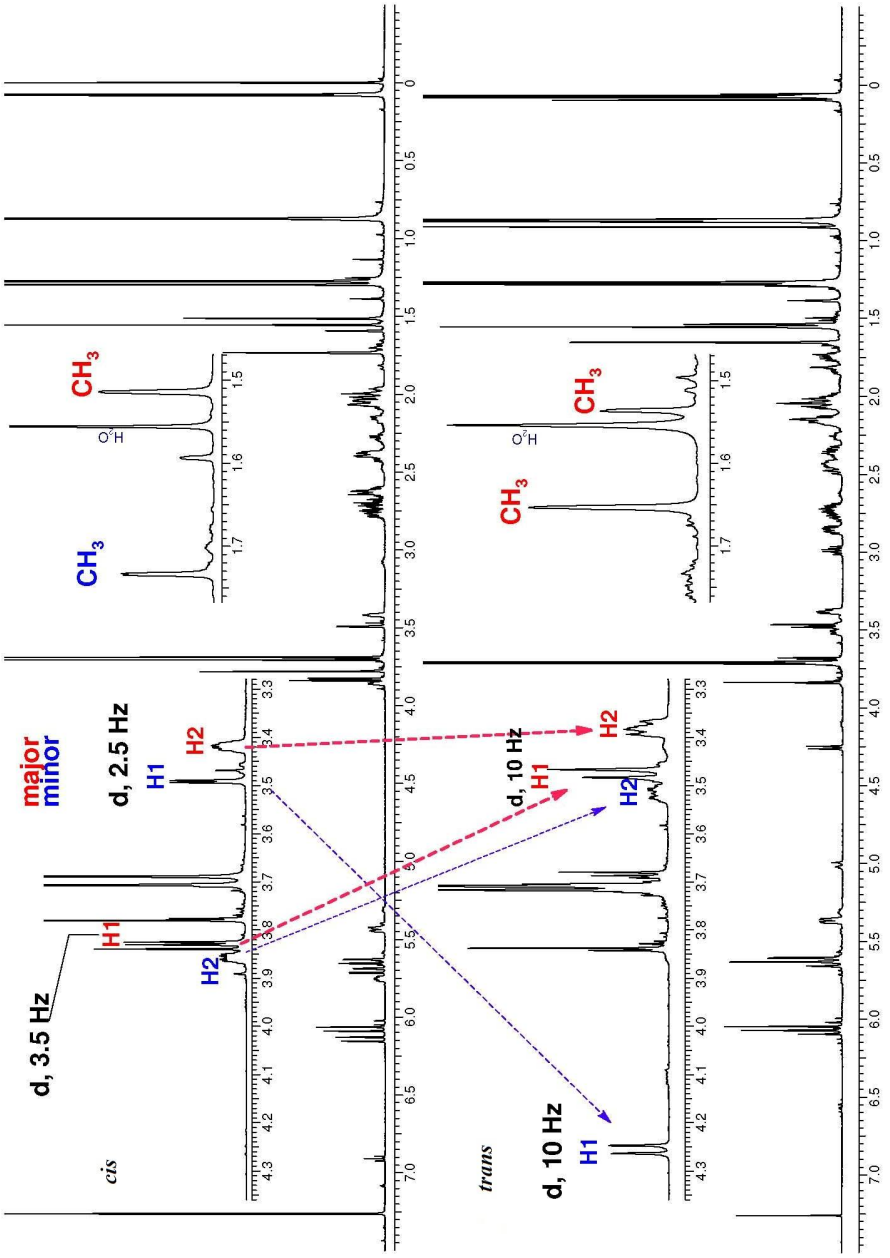
major
minor
d, 3.5 Hz
H1
H2
d, 2.5 Hz
H1
H2
CH3
CH3
O2H
cis
d, 10 Hz
H1
H2
d, 10 Hz
H1
H2
CH3
CH3
O2H
trans

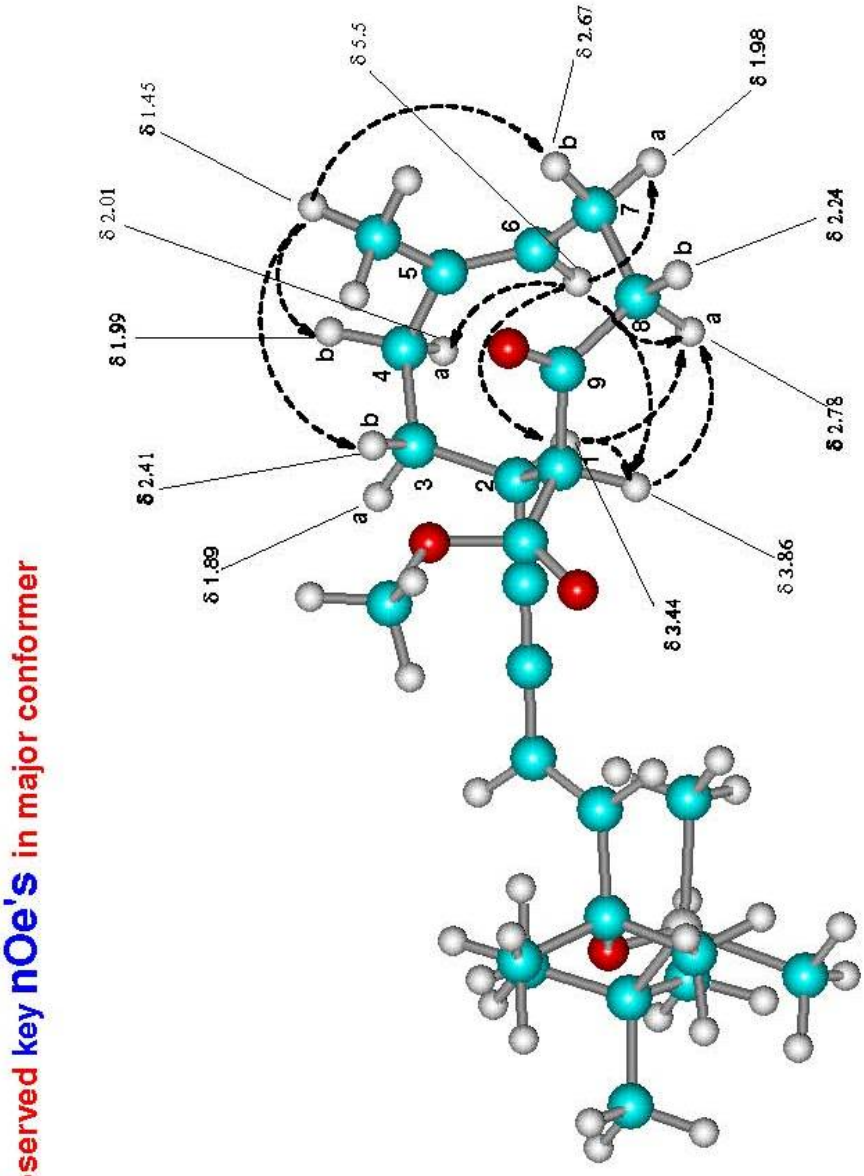
Observed key nOe's in major conformer
δ 1.45
δ 5.5
δ 2.67
δ 1.98
δ 2.01
δ 2.24
δ 1.99
δ 2.78
δ 2.41
δ 1.89
δ 3.86
δ 3.44

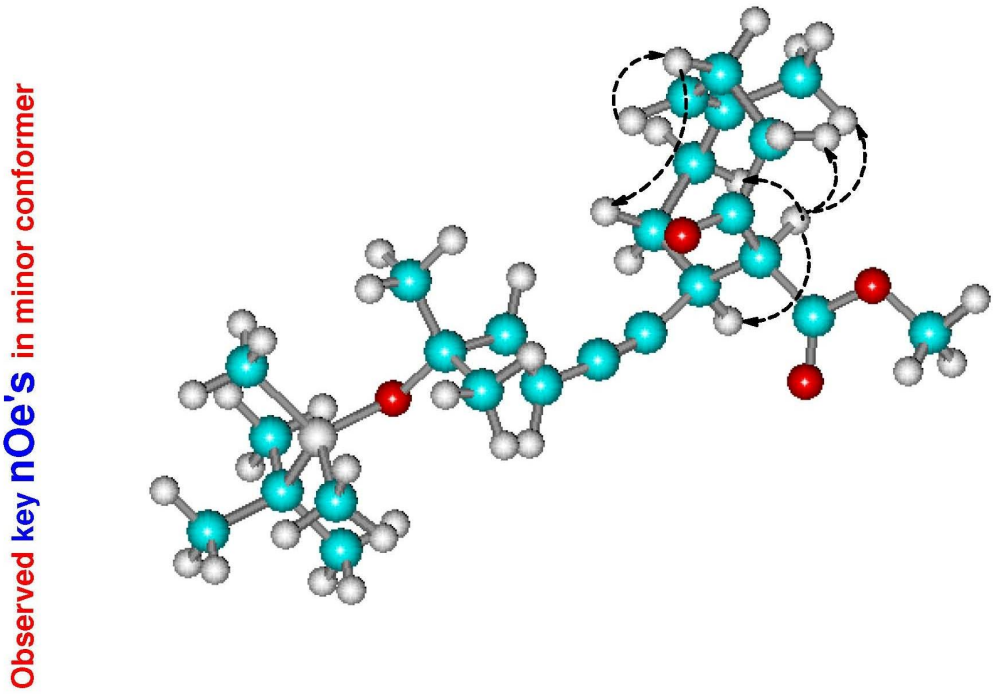
Observed key nOe's in minor conformer

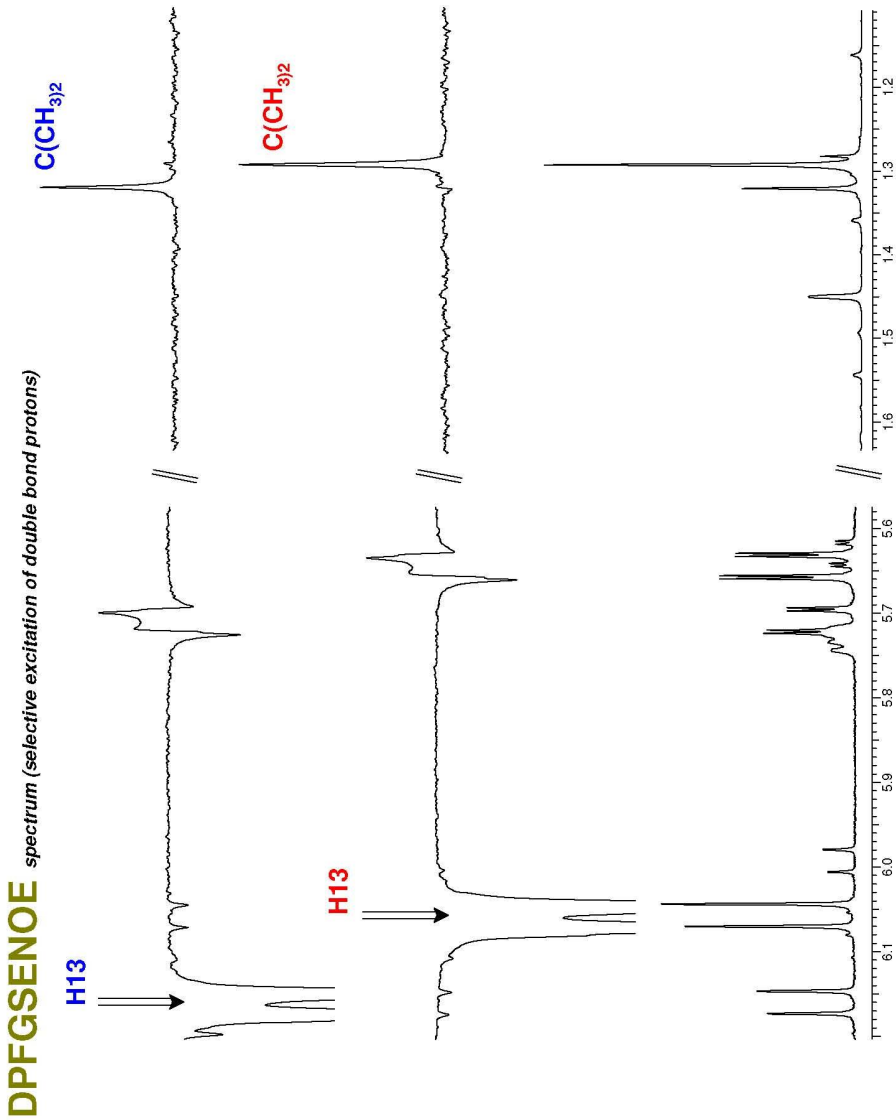
DPFGSENOE
spectrum (selective excitation of double bond protons)
H13
H13
C(CH3)2
C(CH3)2
6.1
6.0
5.9
5.8
5.7
5.6
1.6
1.5
1.4
1.3
1.2

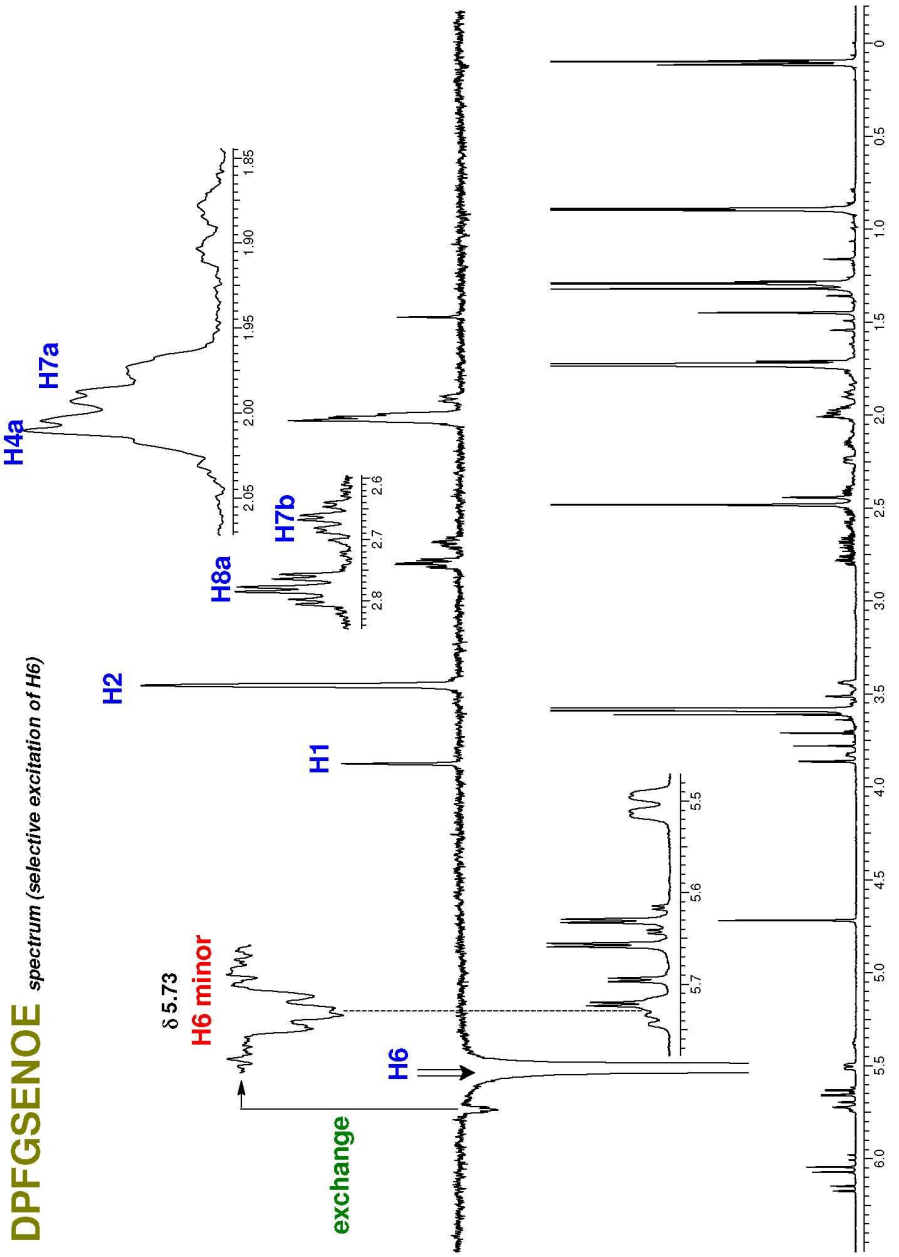
DPFGSENOE
spectrum (selective excitation of H6)
δ 5.73
H6 minor
exchange
H6
H1
H2
H8a
H7b
H4a
H7a

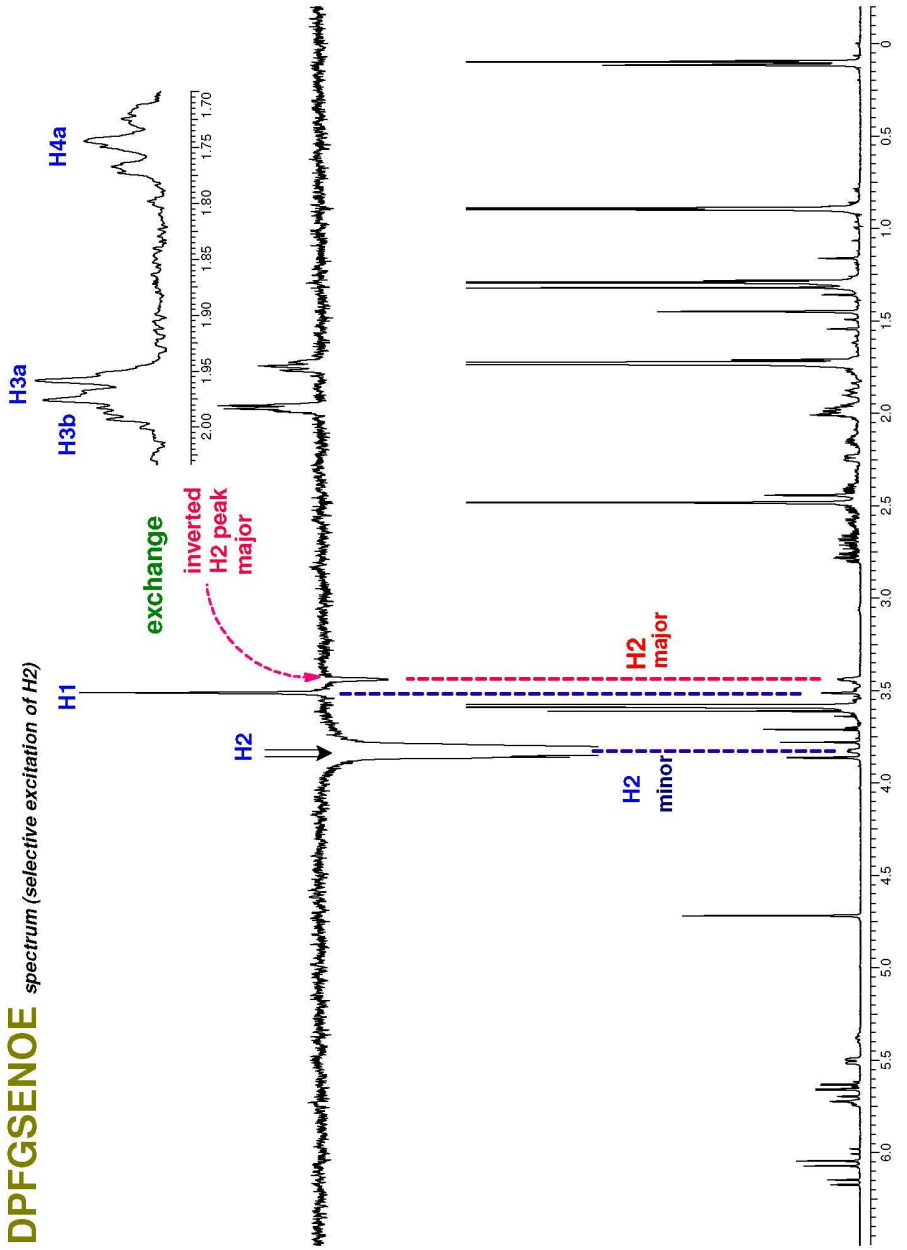
DPFGSENOE
spectrum (selective excitation of H2)
H1
H2
H3a
H3b
H4a
exchange
inverted
H2 peak
major
H2
major
H2
minor

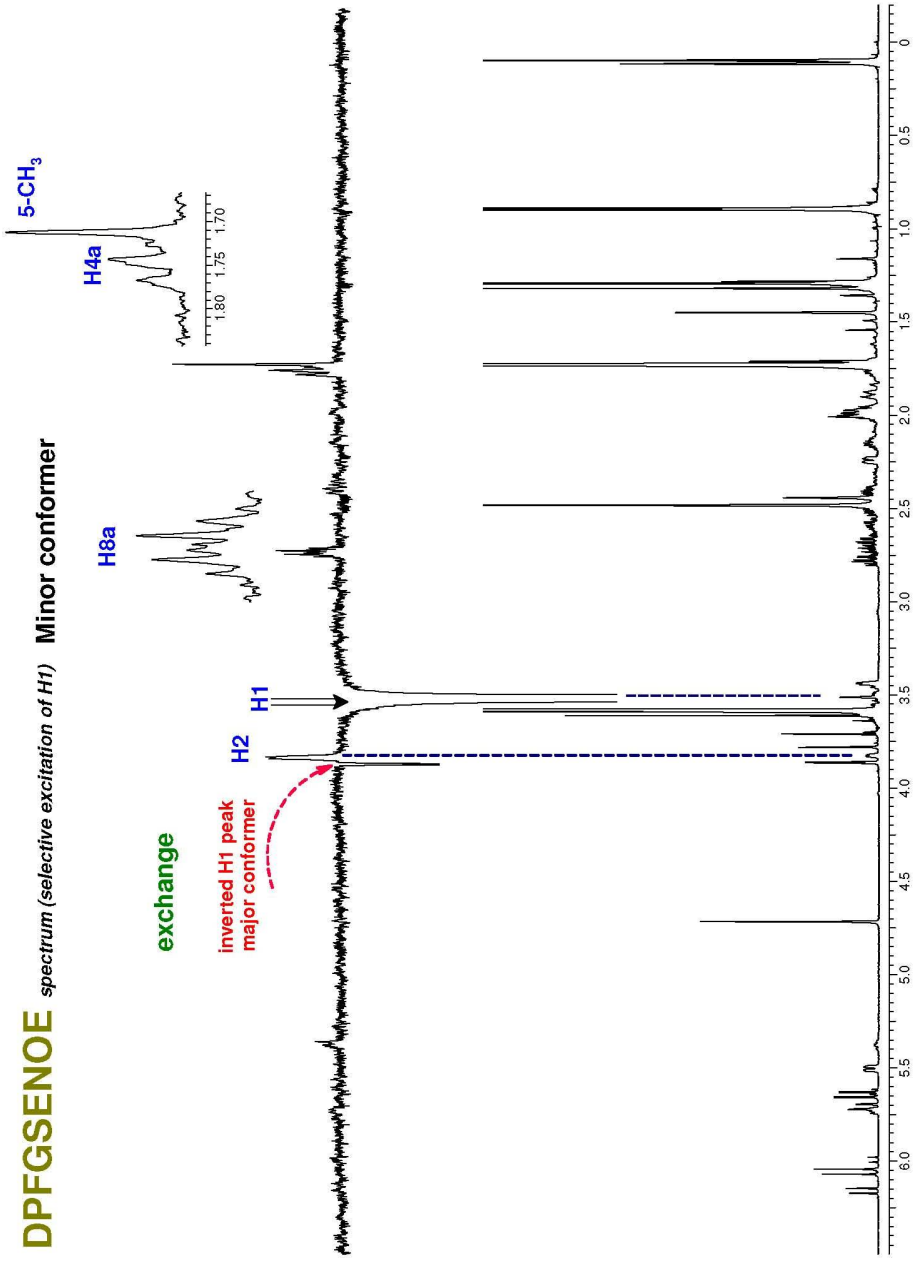
DPFGSENOE
spectrum (selective excitation of H1)
Minor conformer
5-CH3
H4a
H8a
H1
H2
exchange
inverted H1 peak
major conformer

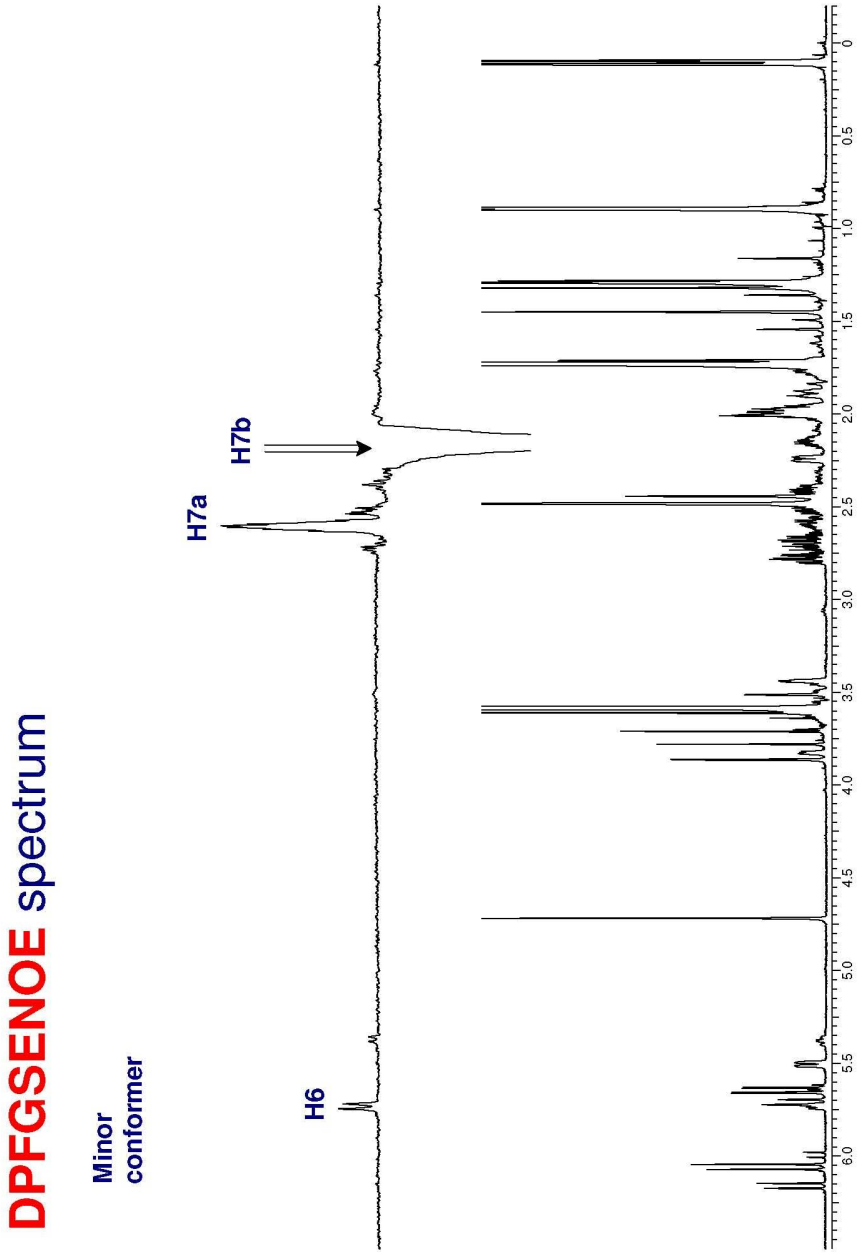
DPFGSENOE spectrum
Minor conformer
H6
H7a
H7b

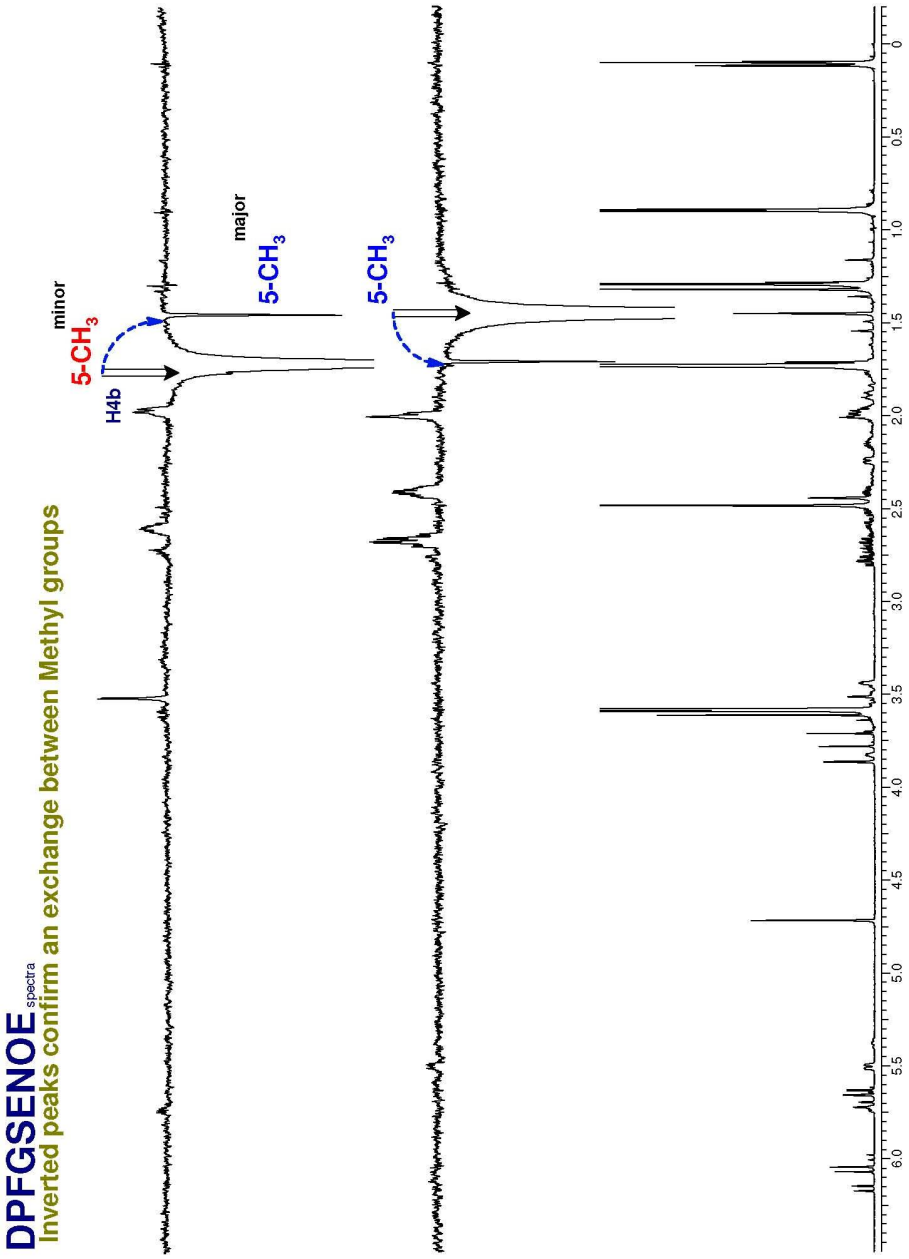
DPFGSENOE spectra
Inverted peaks confirm an exchange between Methyl groups
minor
5-CH3
H4b
major
5-CH3
5-CH3

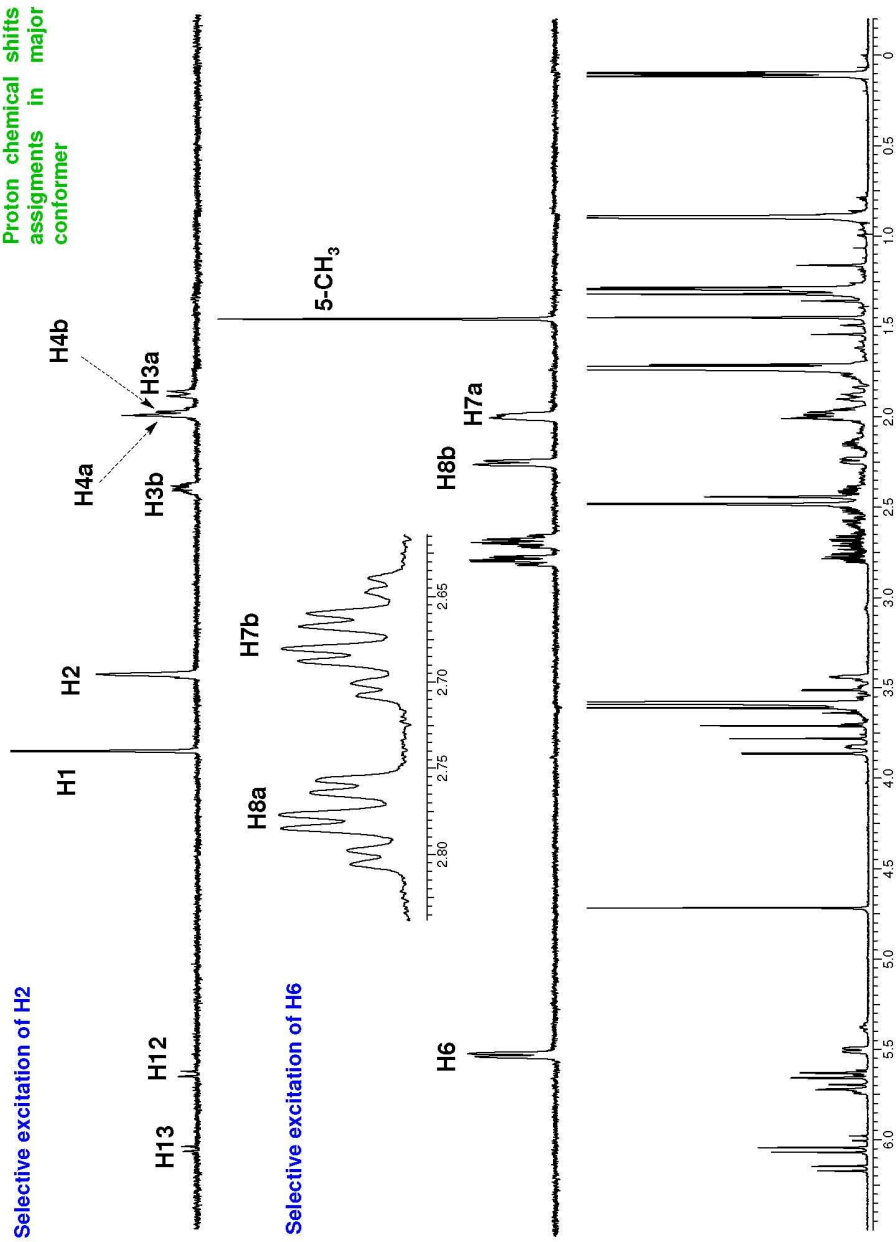
Proton chemical shifts assigments in major conformer
Selective excitation of H2
Selective excitation of H6
H1
H2
H4b
H4a
H3a
H3b
H12
H13
H7b
H8a
5-CH3
H8b
H7a
H6

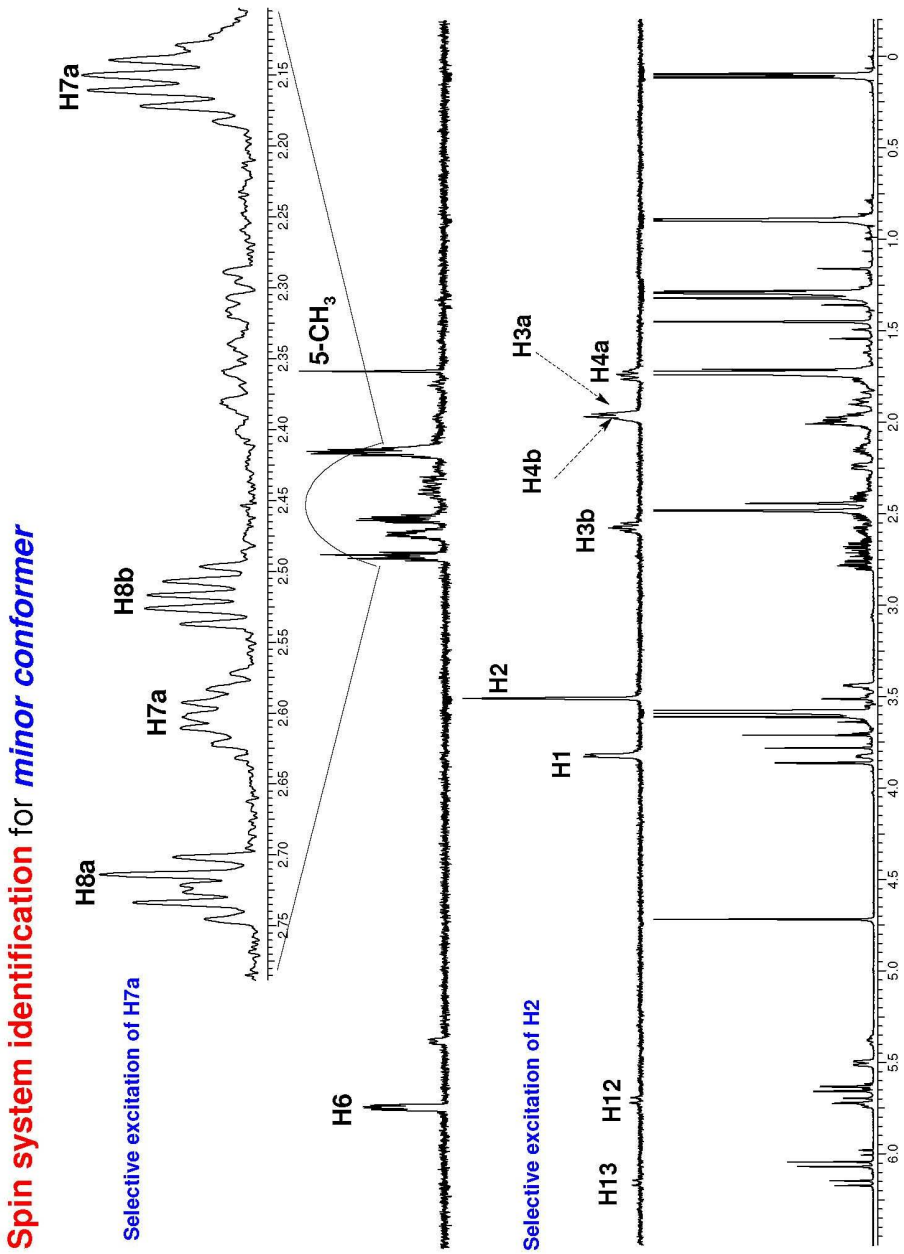
Spin system identification for minor conformer
Selective excitation of H7a
H8a
H7a
H8b
H7a
5-CH3
H6
Selective excitation of H2
H2
H1
H3a
H4a
H4b
H3b
H13
H12

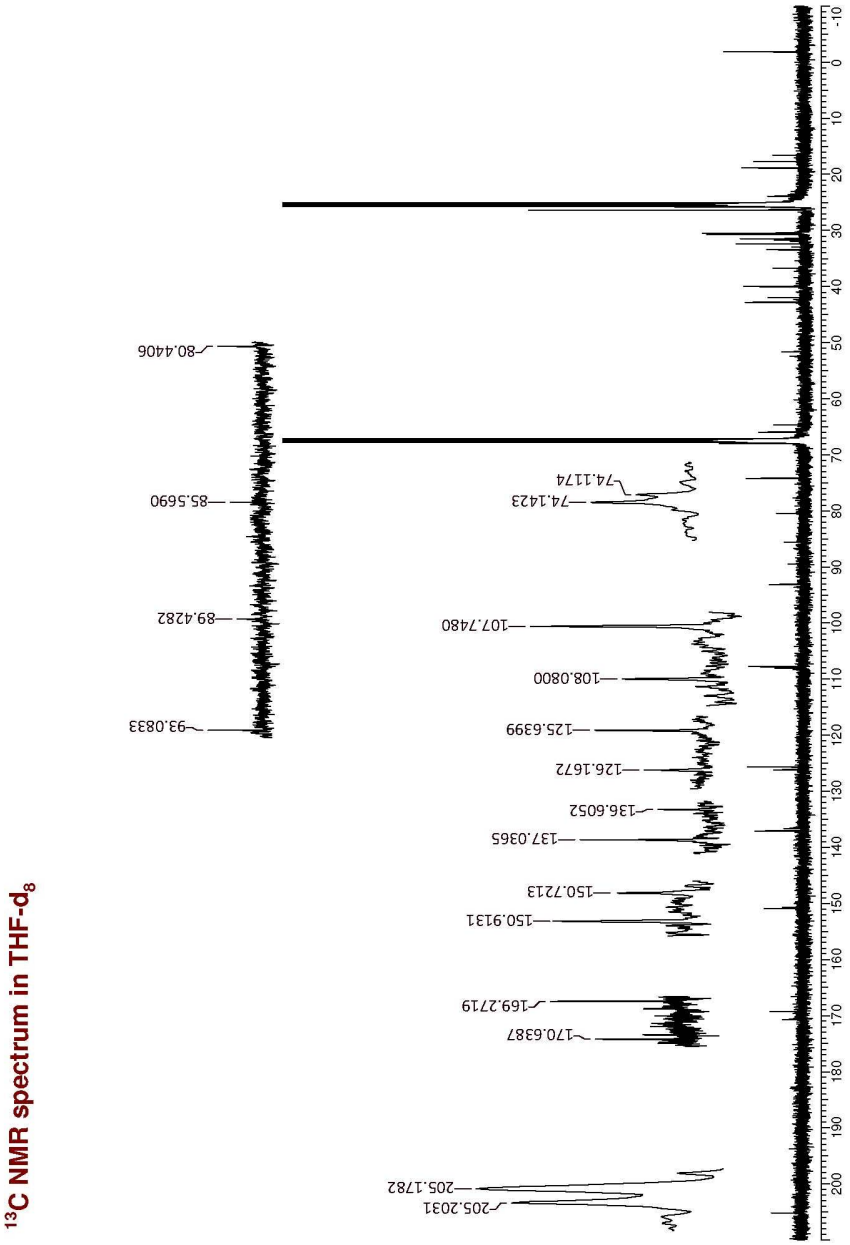
^{13}C NMR spectrum in THF-d$_8$
205.2031
205.1782
170.6387
169.2719
150.9131
150.7213
137.0365
136.6052
126.1672
125.6399
108.0800
107.7480
74.1423
74.1174
80.4406
85.5690
89.4282
93.0833

^{13}C NMR spectrum in THF-d_8

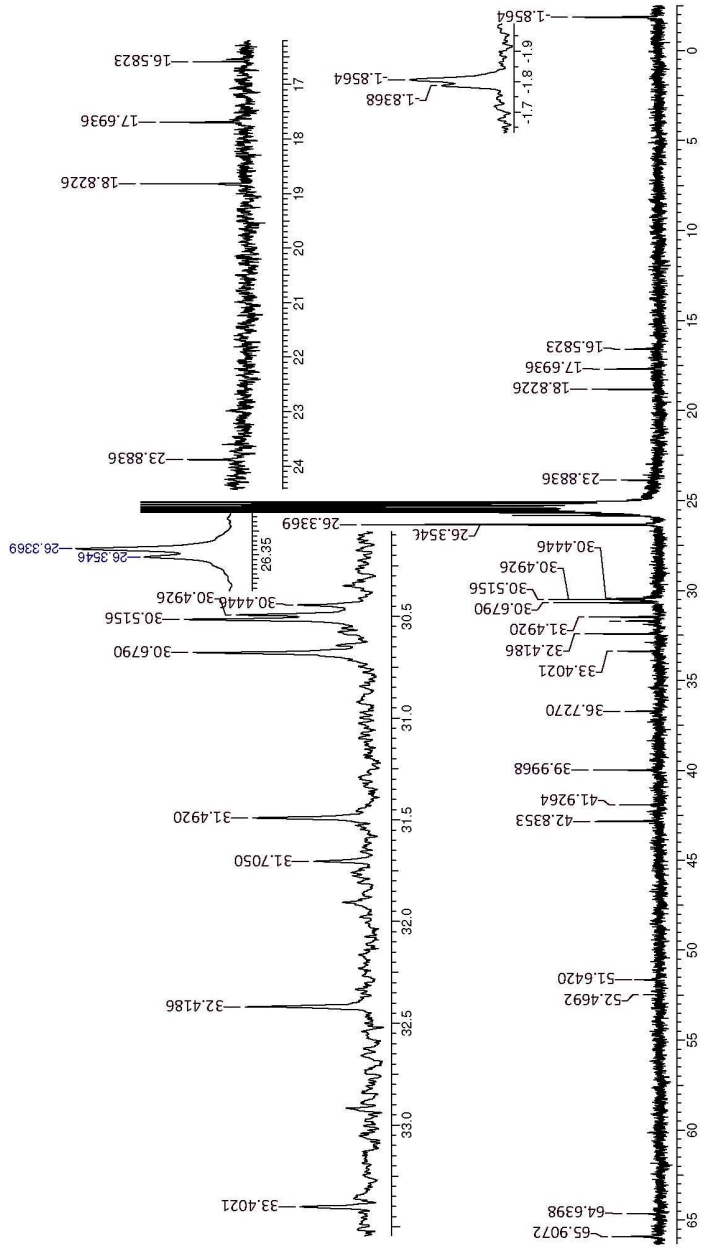

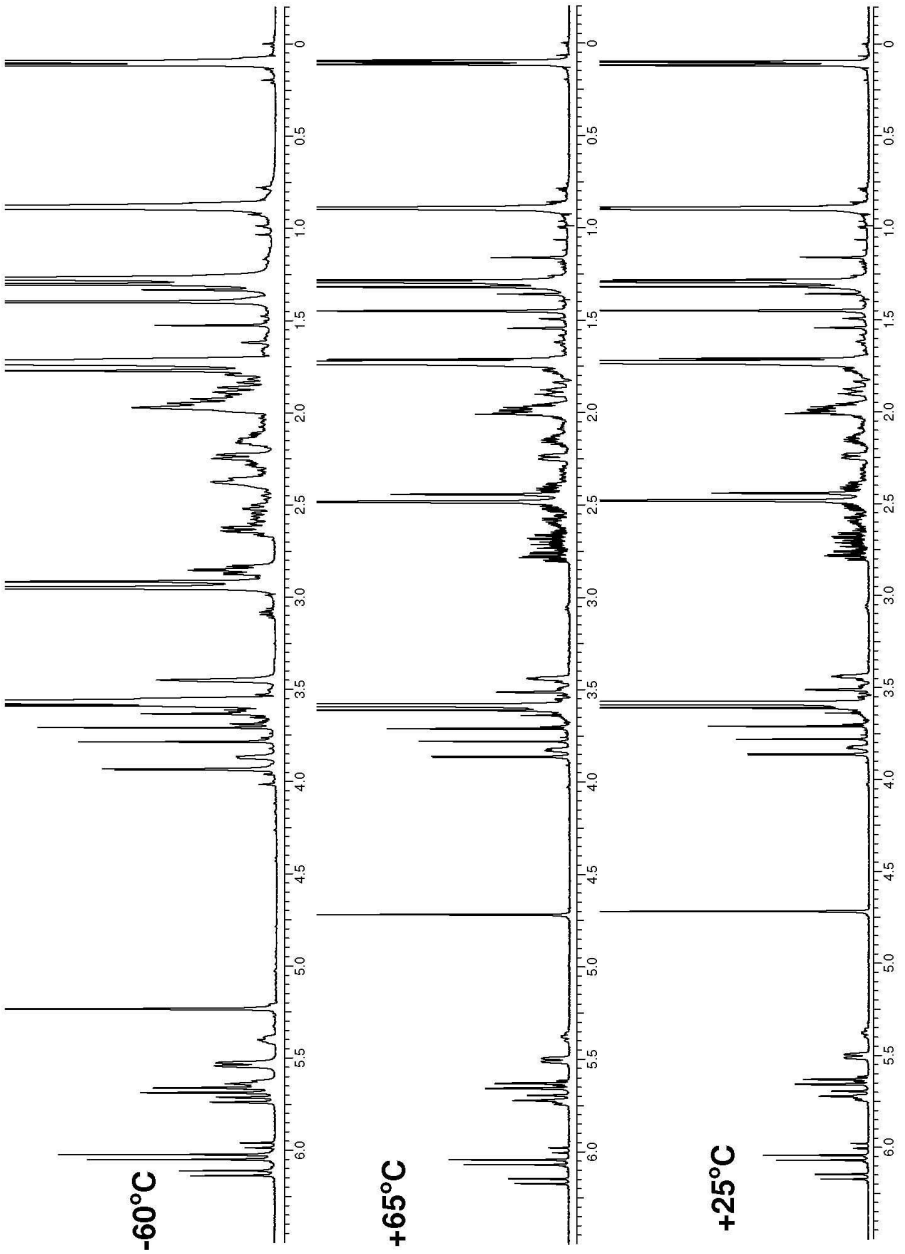
-60°C
+65°C
+25°C

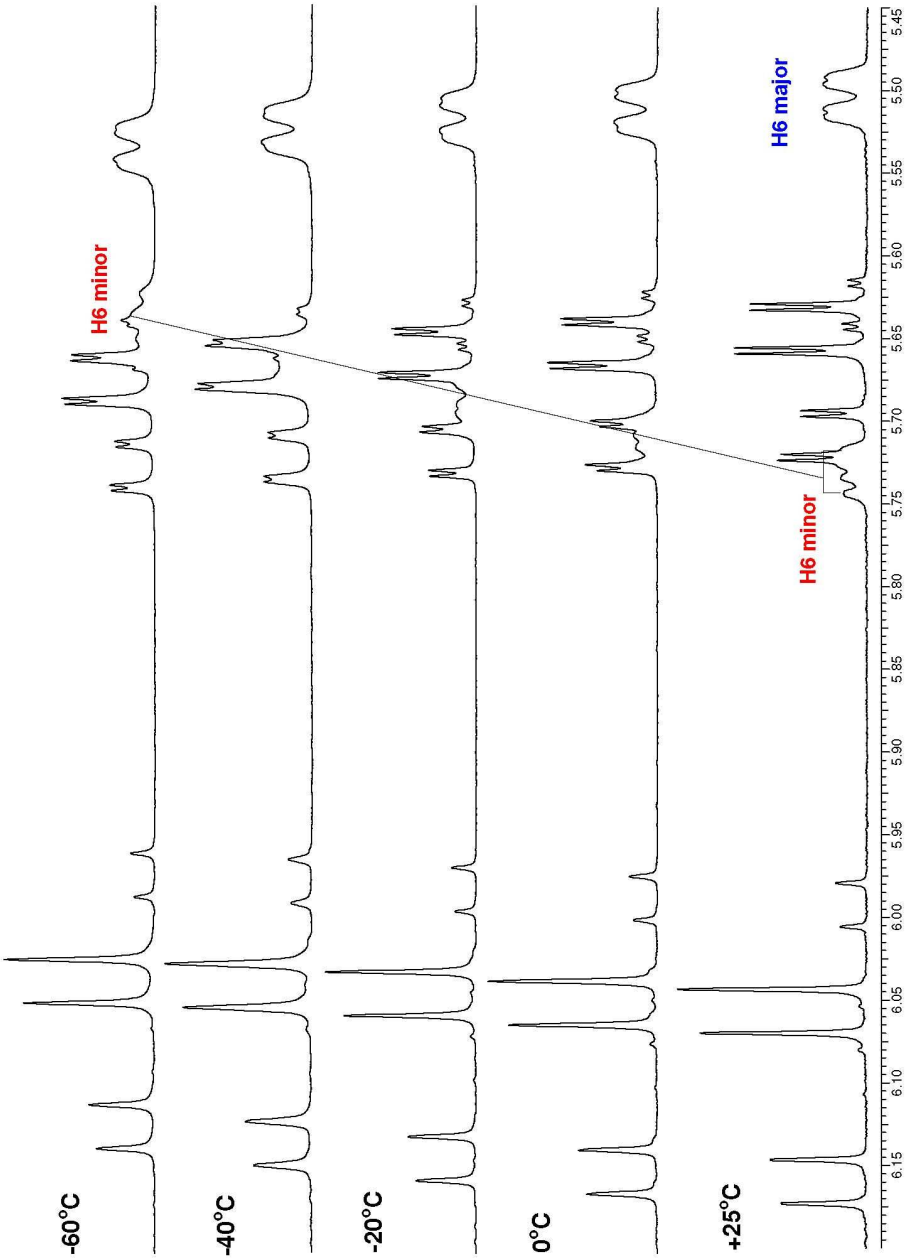
H6 minor
H6 major
H6 minor
-60°C
-40°C
-20°C
0°C
+25°C
6.15
6.10
6.05
6.00
5.95
5.90
5.85
5.80
5.75
5.70
5.65
5.60
5.55
5.50
5.45

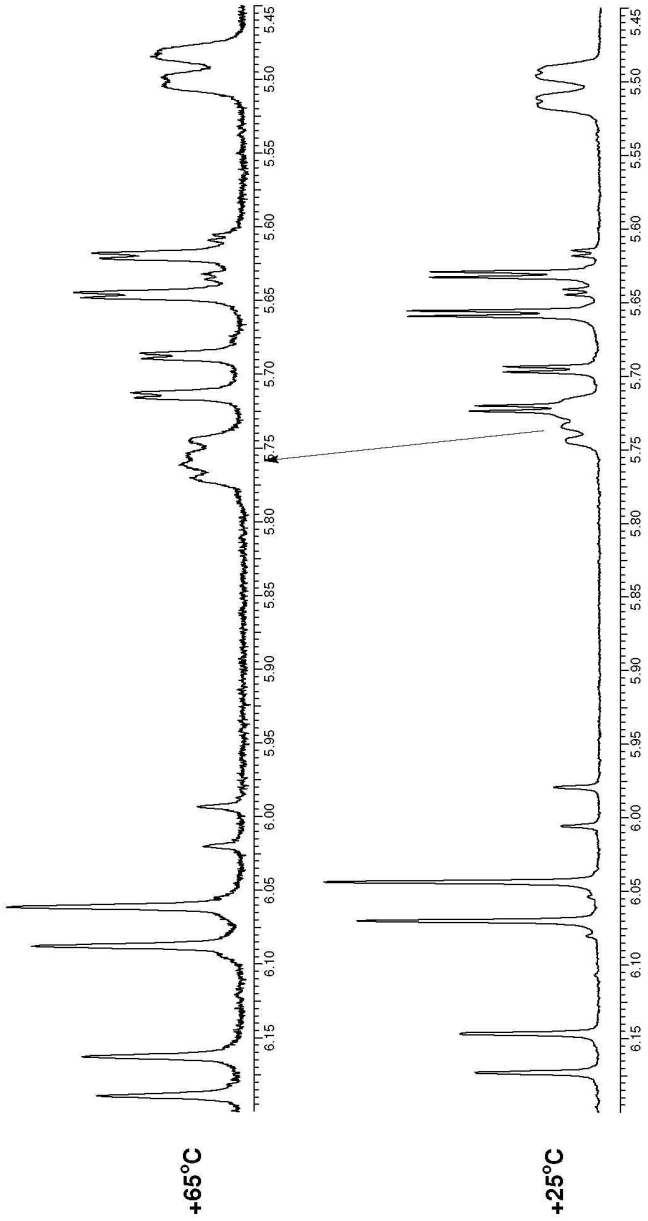
+65°C
+25°C
6.15
6.10
6.05
6.00
5.95
5.90
5.85
5.80
5.75
5.70
5.65
5.60
5.55
5.50
5.45

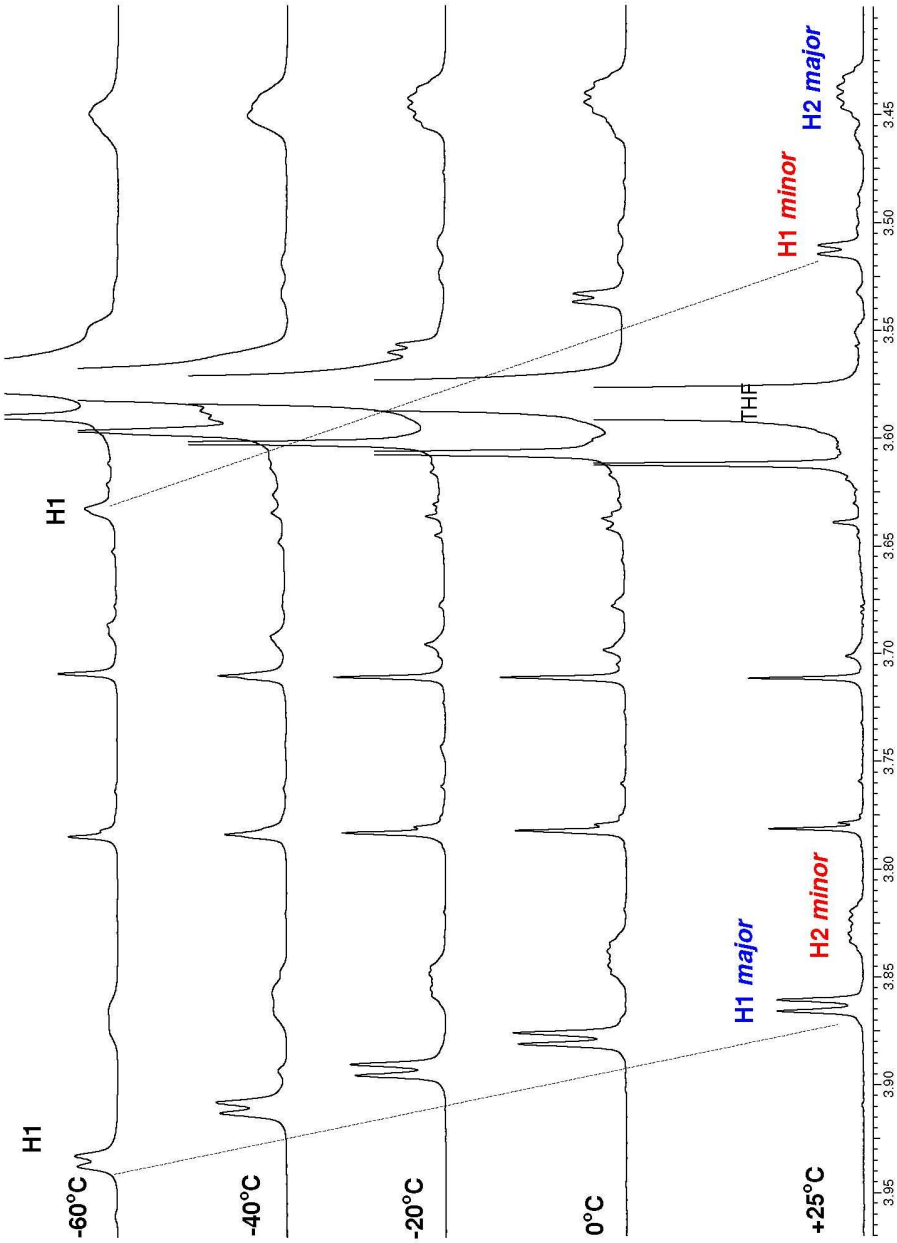
H1
-60°C
-40°C
-20°C
0°C
+25°C
H1
THF
H1 major
H2 minor
H1 minor
H2 major
3.95
3.90
3.85
3.80
3.75
3.70
3.65
3.60
3.55
3.50
3.45

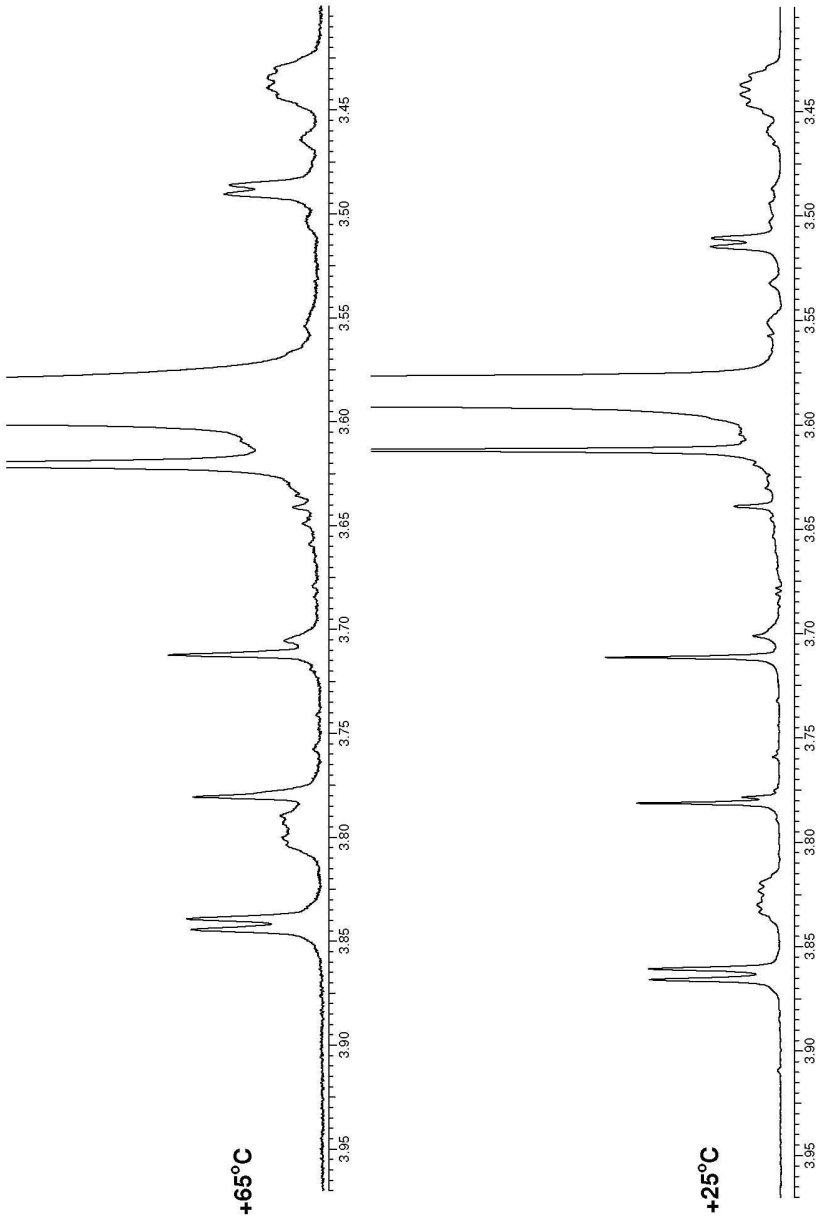
+65°C
+25°C
3.95
3.90
3.85
3.80
3.75
3.70
3.65
3.60
3.55
3.50
3.45

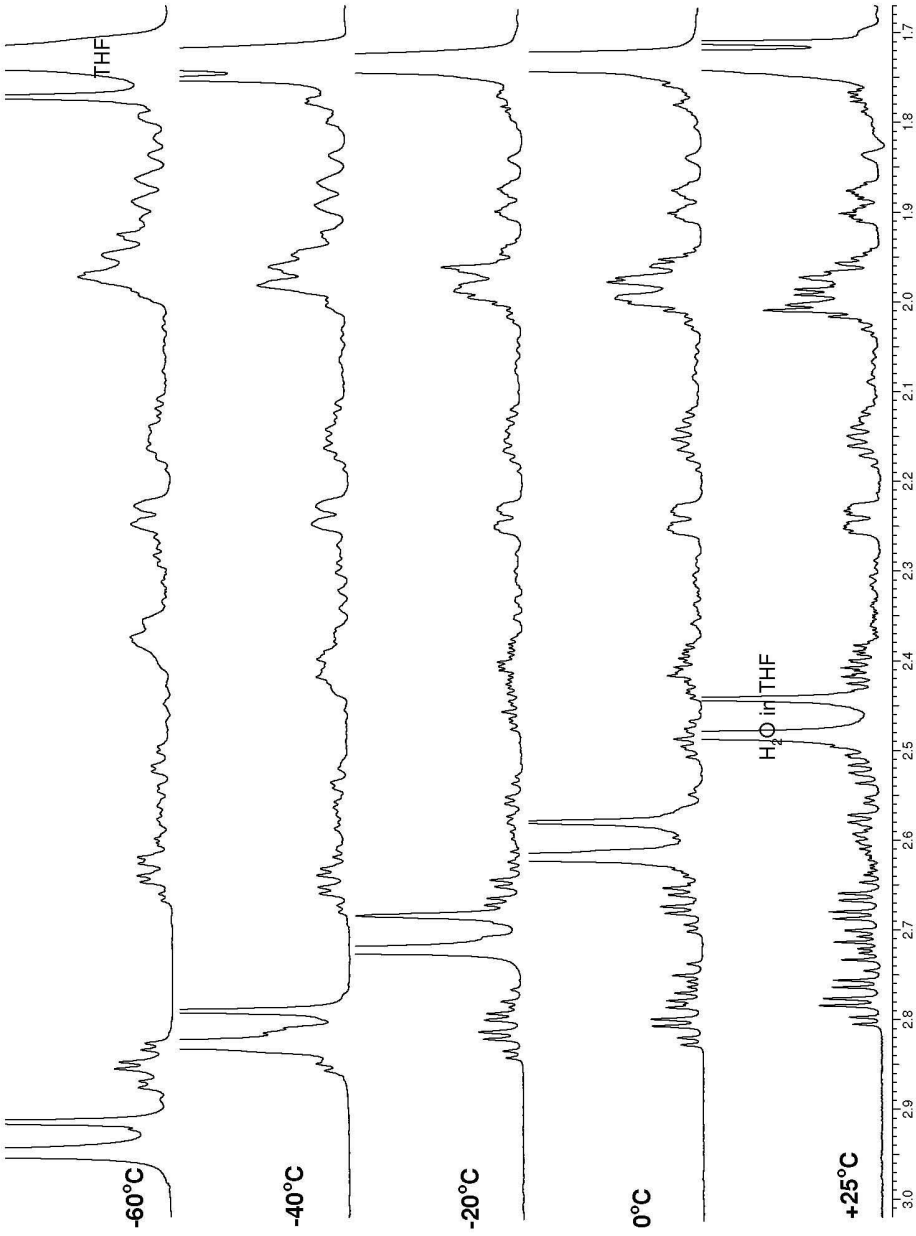
-60°C
-40°C
-20°C
0°C
+25°C
THF
H2O in THF
3.0
2.9
2.8
2.7
2.6
2.5
2.4
2.3
2.2
2.1
2.0
1.9
1.8
1.7

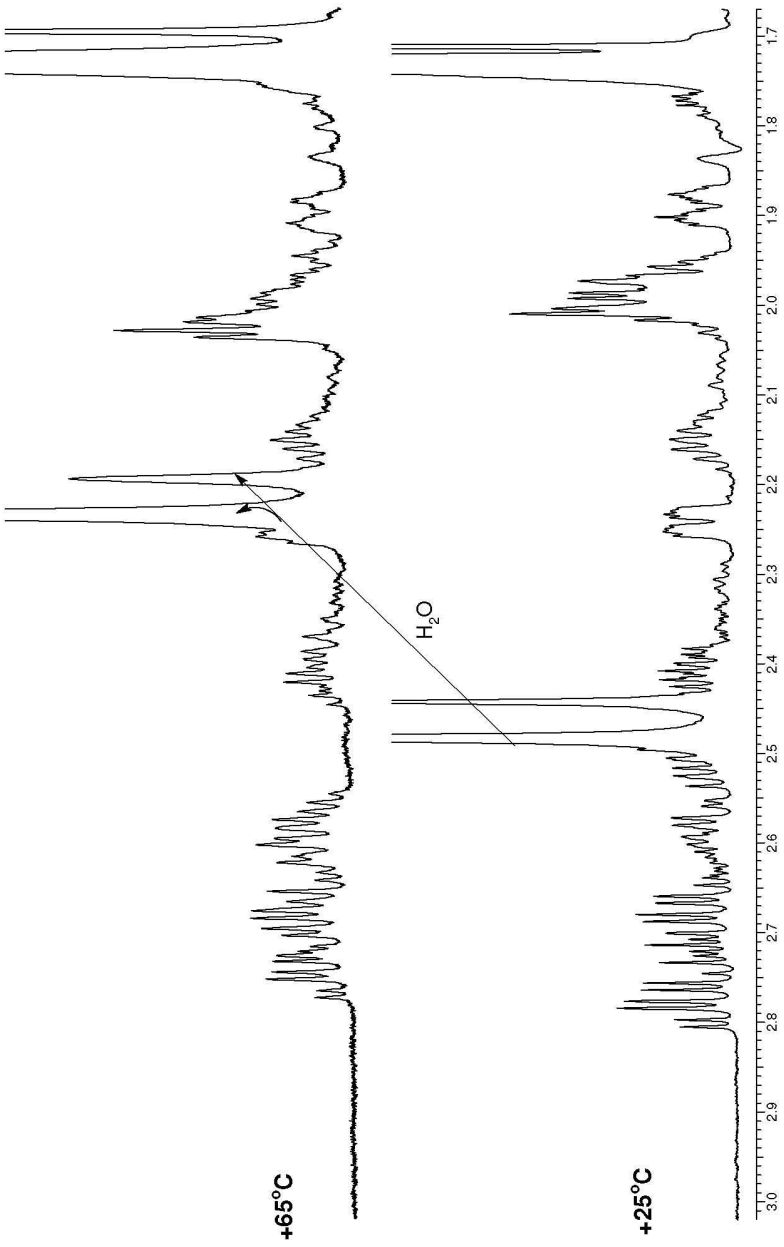
+65°C
H_2O
+25°C
3.0
2.9
2.8
2.7
2.6
2.5
2.4
2.3
2.2
2.1
2.0
1.9
1.8
1.7

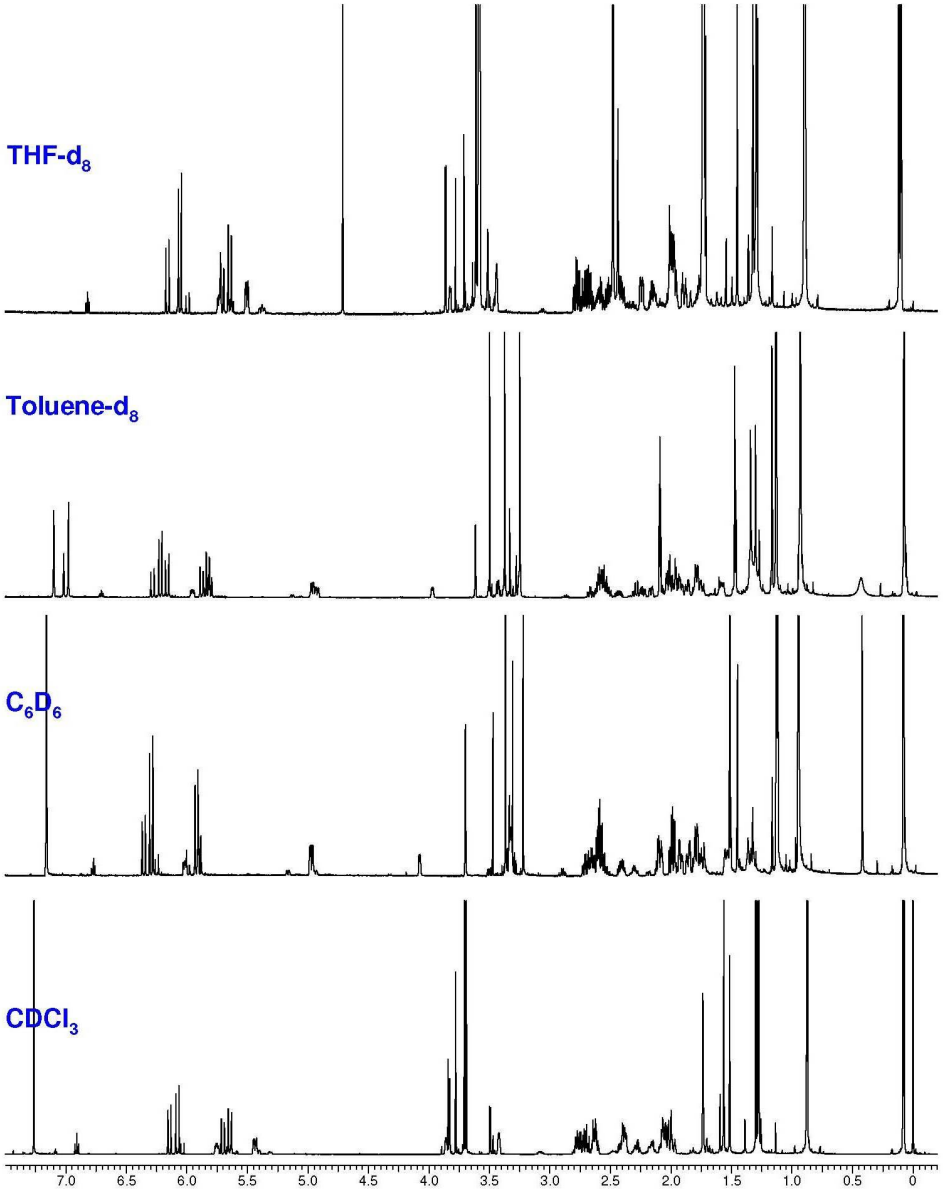
THF-d8
Toluene-d8
C6D6
CDCl3
7.0
6.5
6.0
5.5
5.0
4.5
4.0
3.5
3.0
2.5
2.0
1.5
1.0
0.5
0

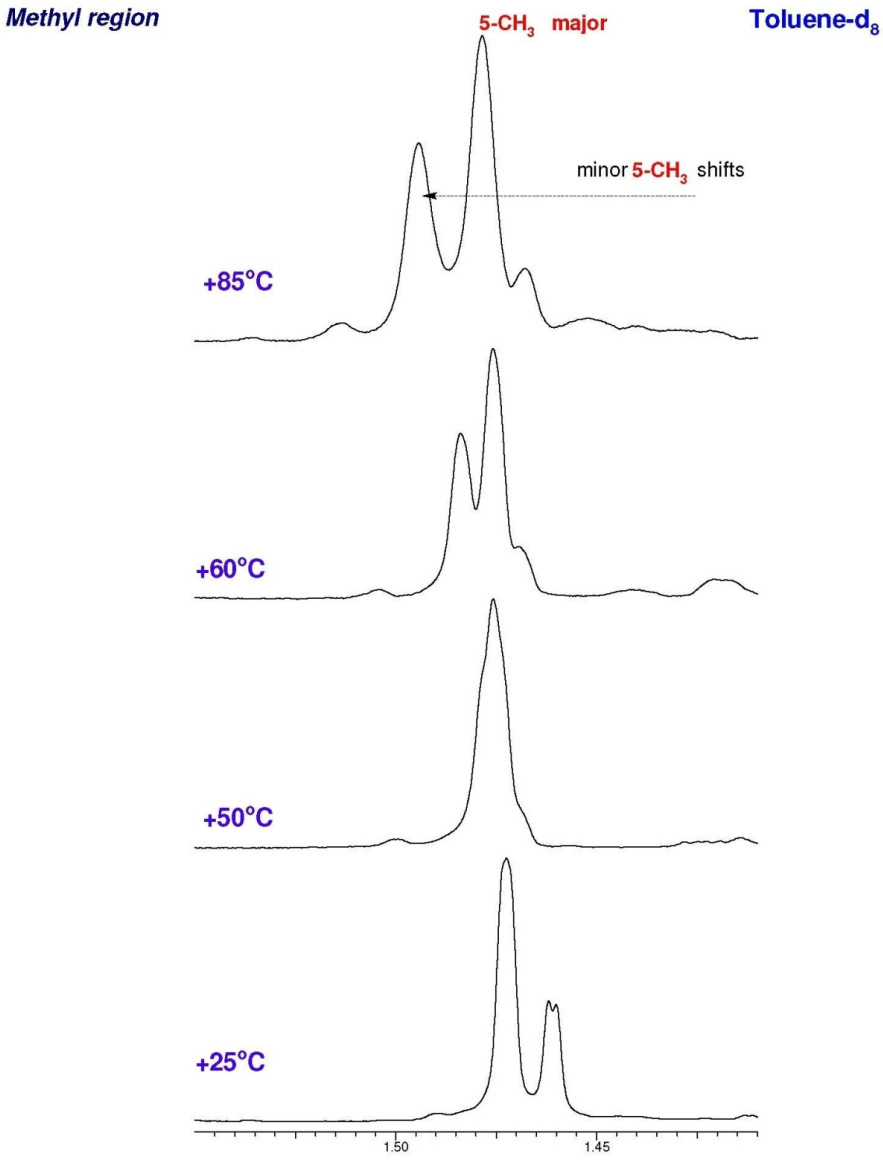
Methyl region
5-CH3 major
Toluene-d8
minor 5-CH3 shifts
+85°C
+60°C
+50°C
+25°C
1.50
1.45

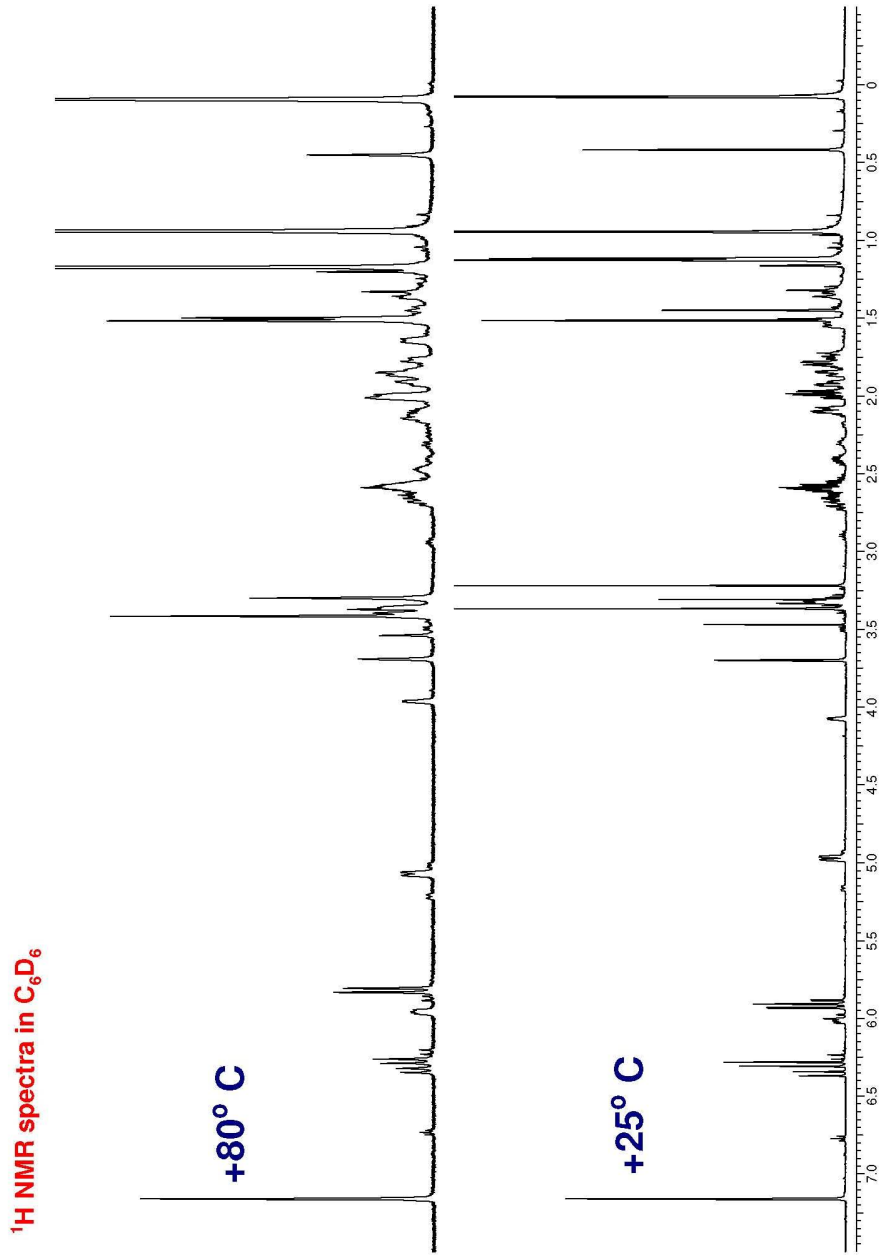
^{1}H NMR spectra in C_6D_6
+80° C
+25° C
7.0
6.5
6.0
5.5
5.0
4.5
4.0
3.5
3.0
2.5
2.0
1.5
1.0
0.5
0

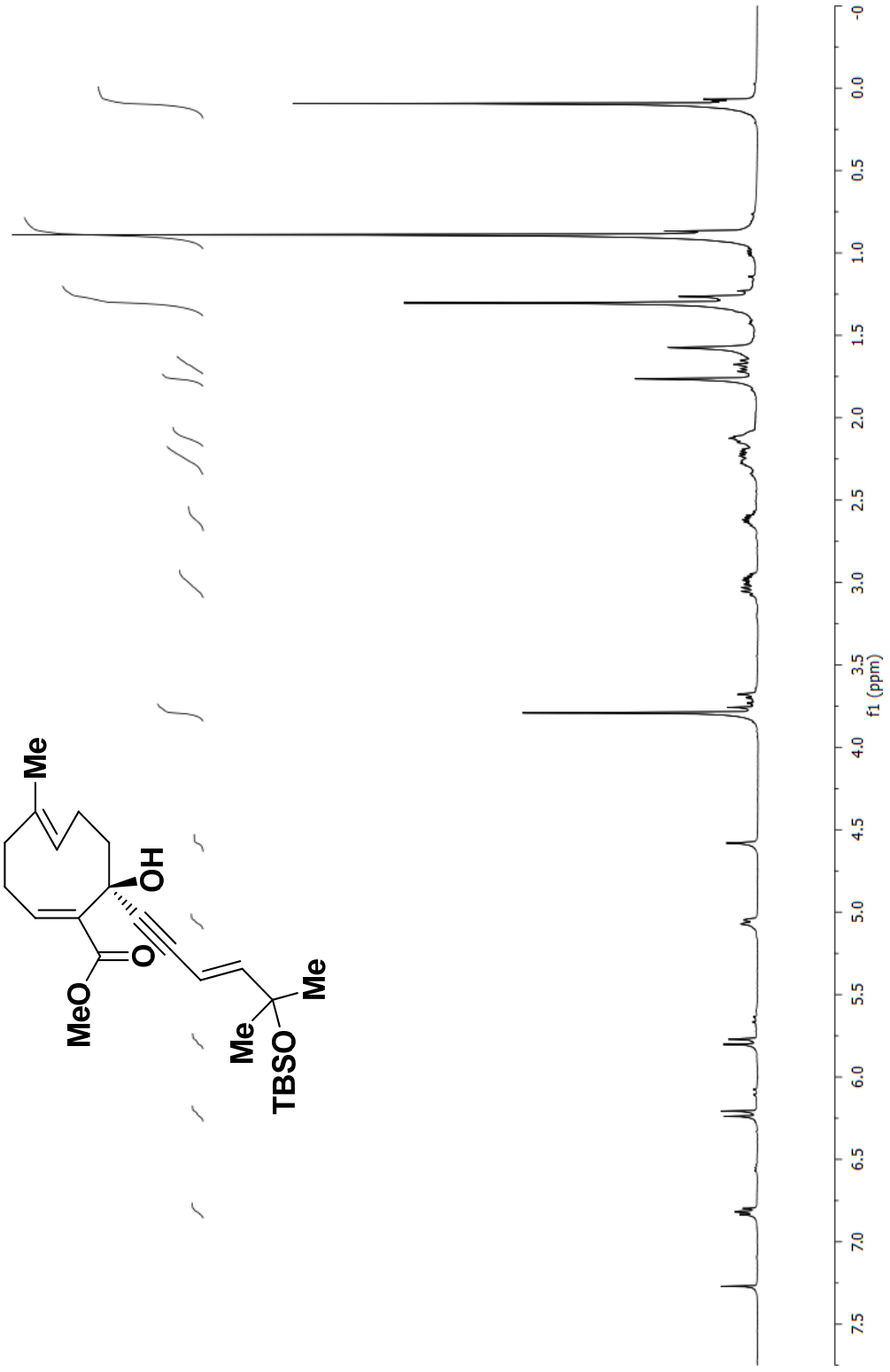
Me
OH
O
MeO
Me
TBSO
Me
7.5
7.0
6.5
6.0
5.5
5.0
4.5
4.0
3.5
3.0
2.5
2.0
1.5
1.0
0.5
0.0
-0
f1 (ppm)

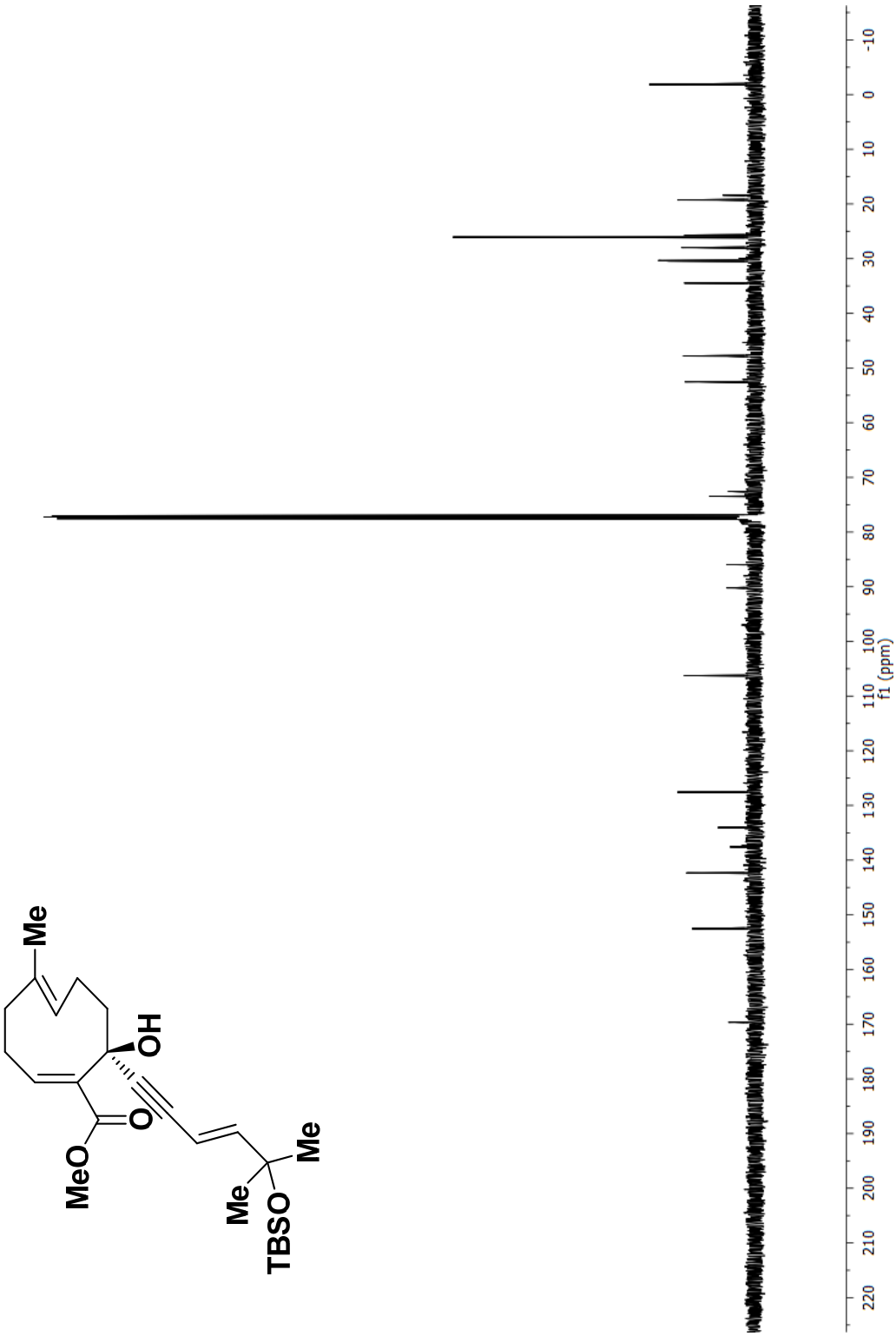
Me
OH
O
MeO
Me
TBSO
Me
f1 (ppm)
-10
0
10
20
30
40
50
60
70
80
90
100
110
120
130
140
150
160
170
180
190
200
210
220

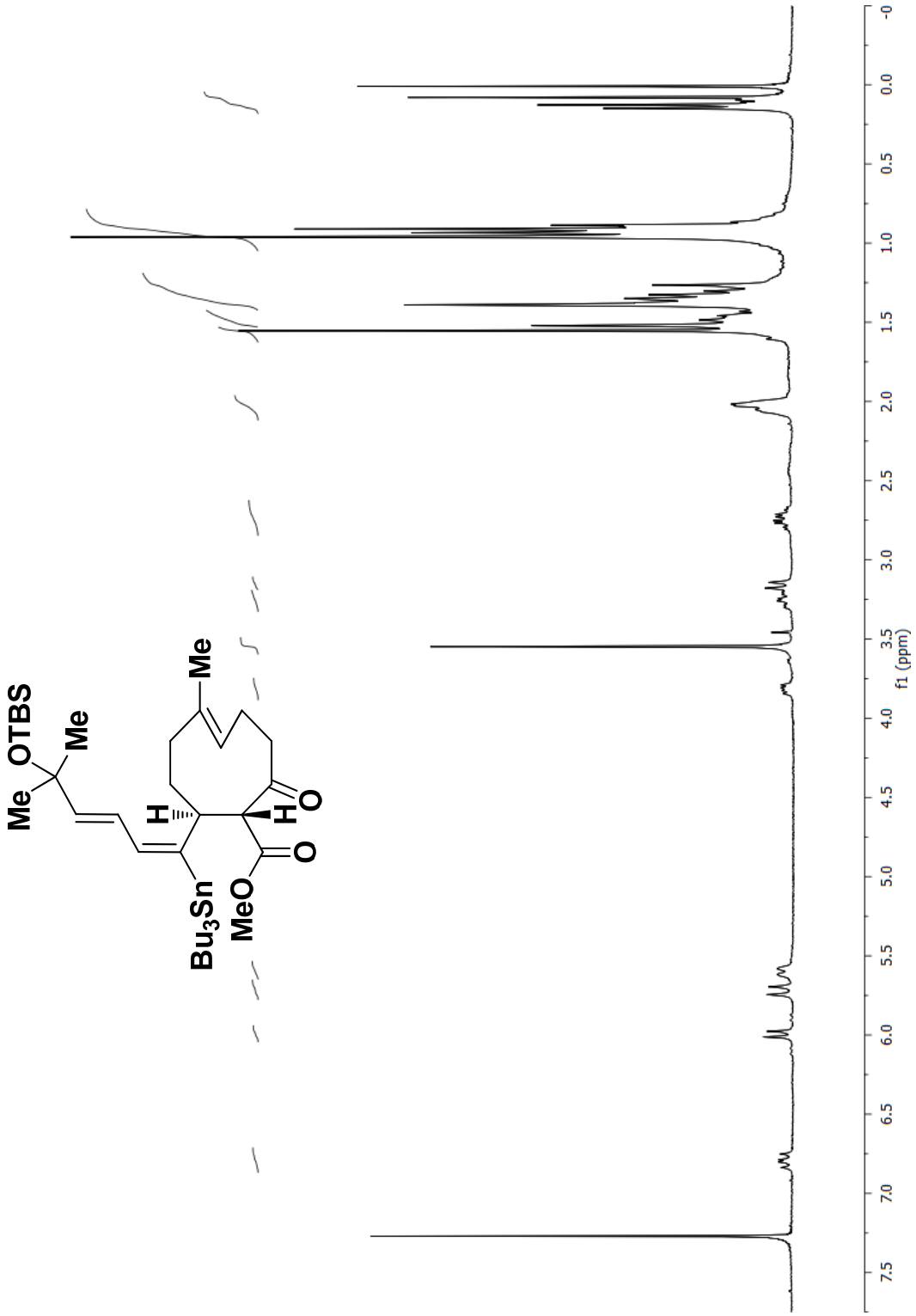
Me
OTBS
Me
H
Me
O
H
O
Bu3Sn
MeO
f1 (ppm)

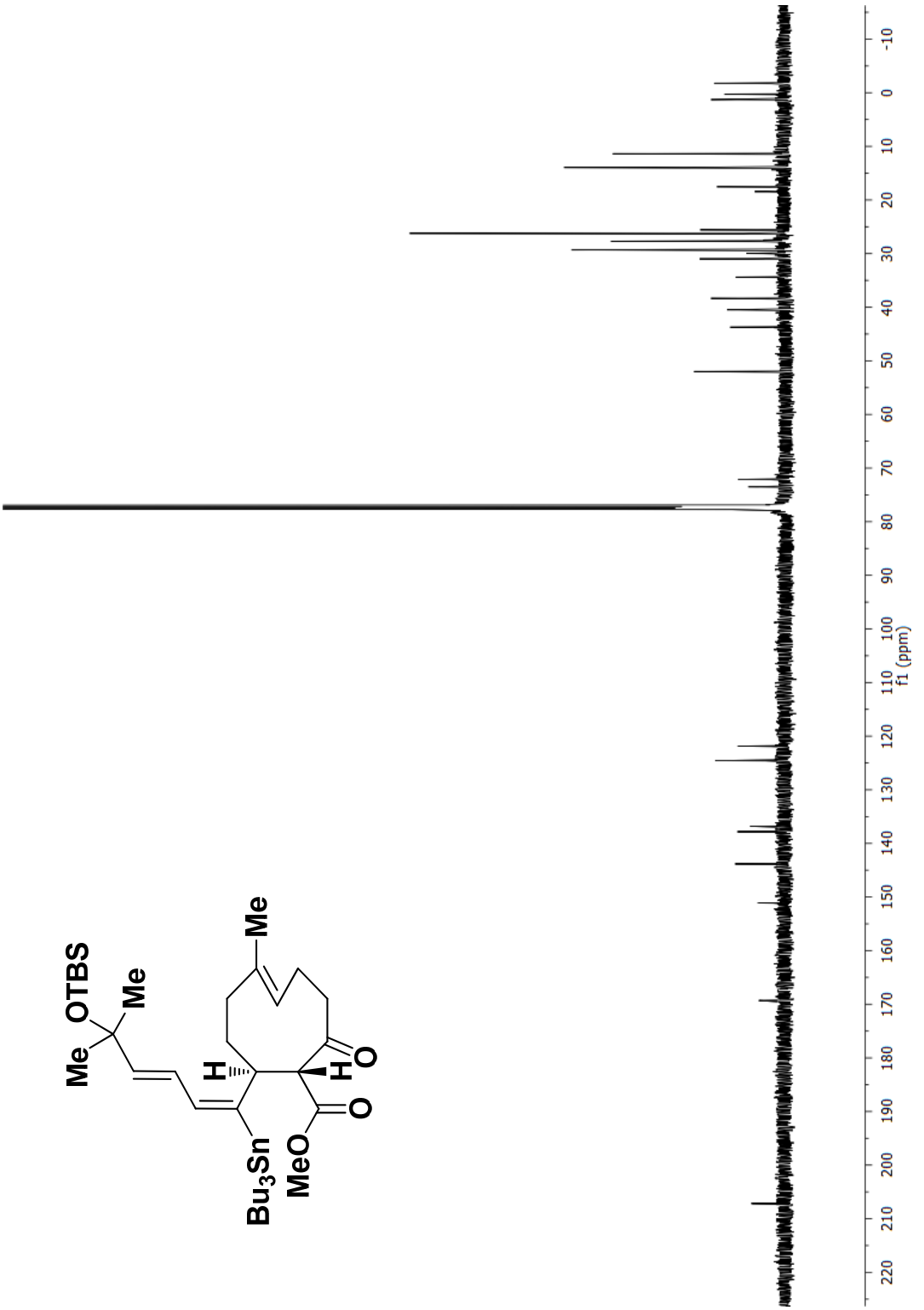
Me
OTBS
Me
H
Me
O
H
O
Bu3Sn
MeO
f1 (ppm)

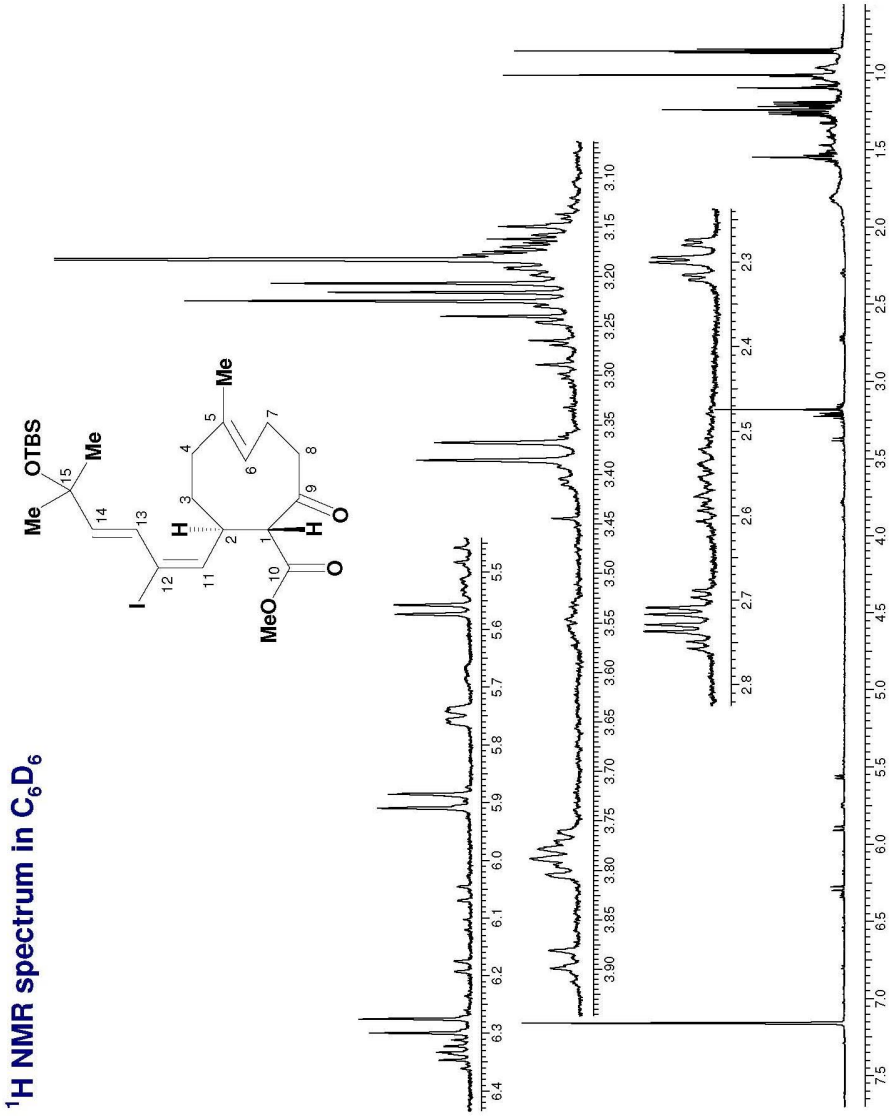
^{1}H NMR spectrum in C_6D_6
Me
OTBS
Me
I
H
H
Me
MeO
O
O

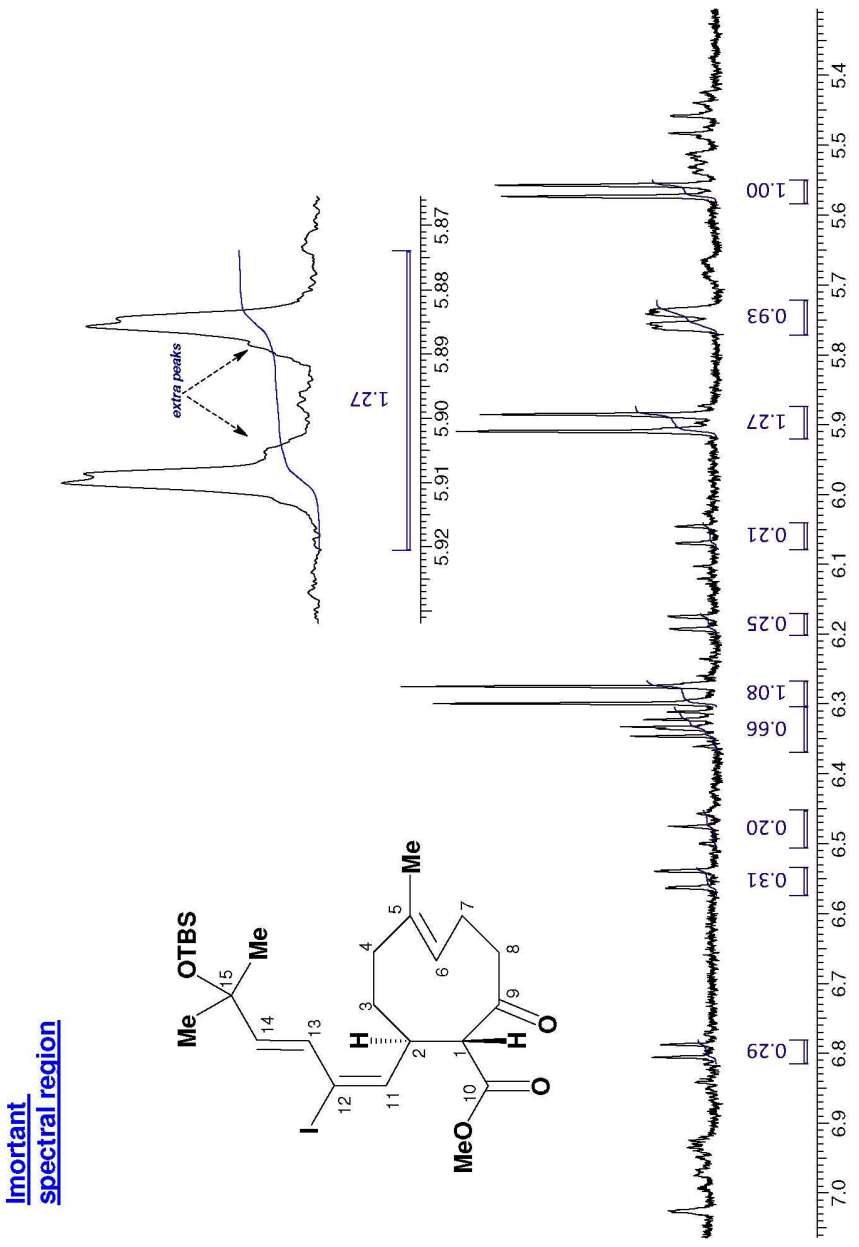
Imortant
spectral region
extra peaks
1.27
0.29
0.31
0.20
0.66
1.08
0.25
0.21
1.27
0.93
1.00
Me
OTBS
Me
H
H
O
O
MeO
I
Me

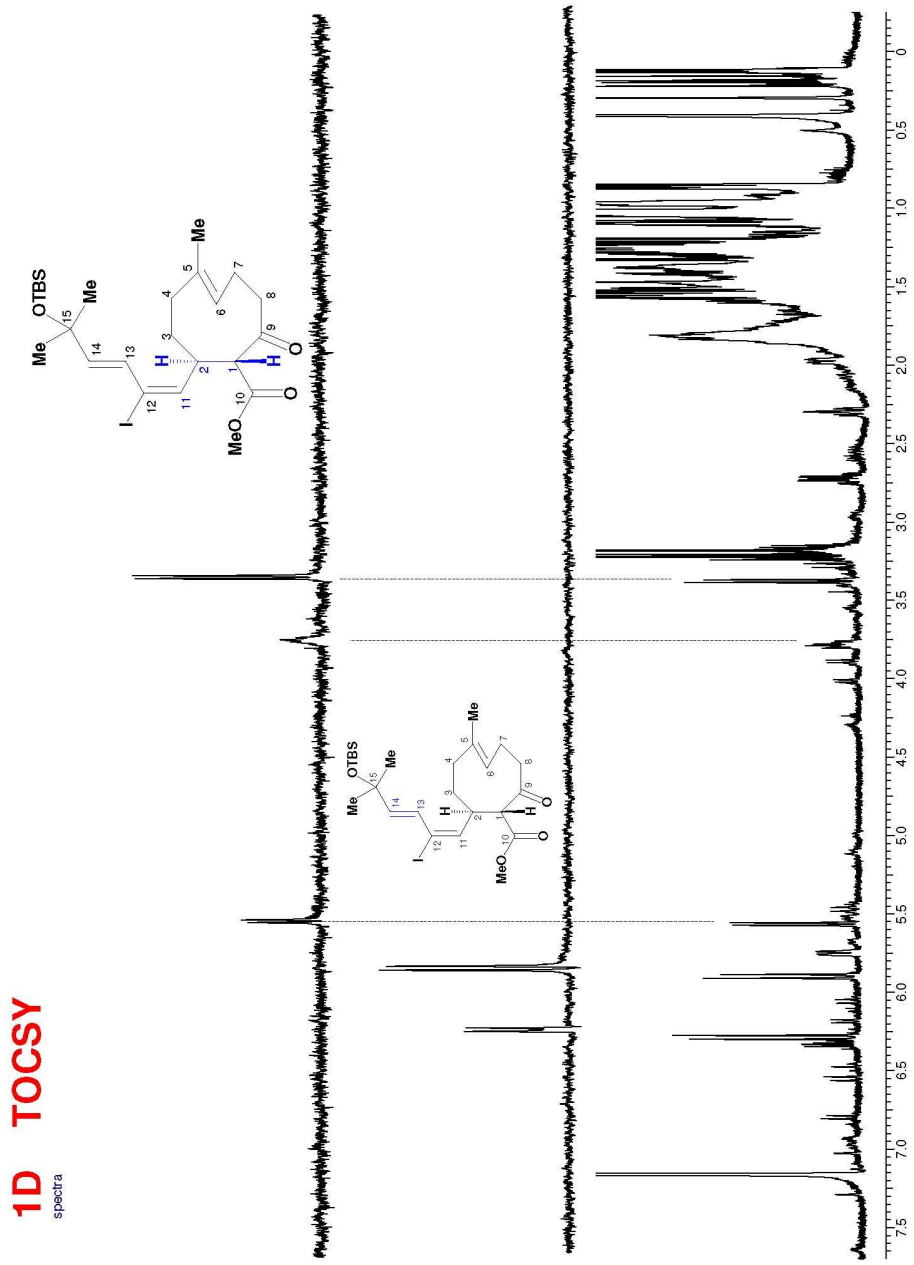
1D TOCSY
spectra
OTBS
Me
Me
I
MeO
H
H
O
O
Me
7.5
7.0
6.5
6.0
5.5
5.0
4.5
4.0
3.5
3.0
2.5
2.0
1.5
1.0
0.5
0

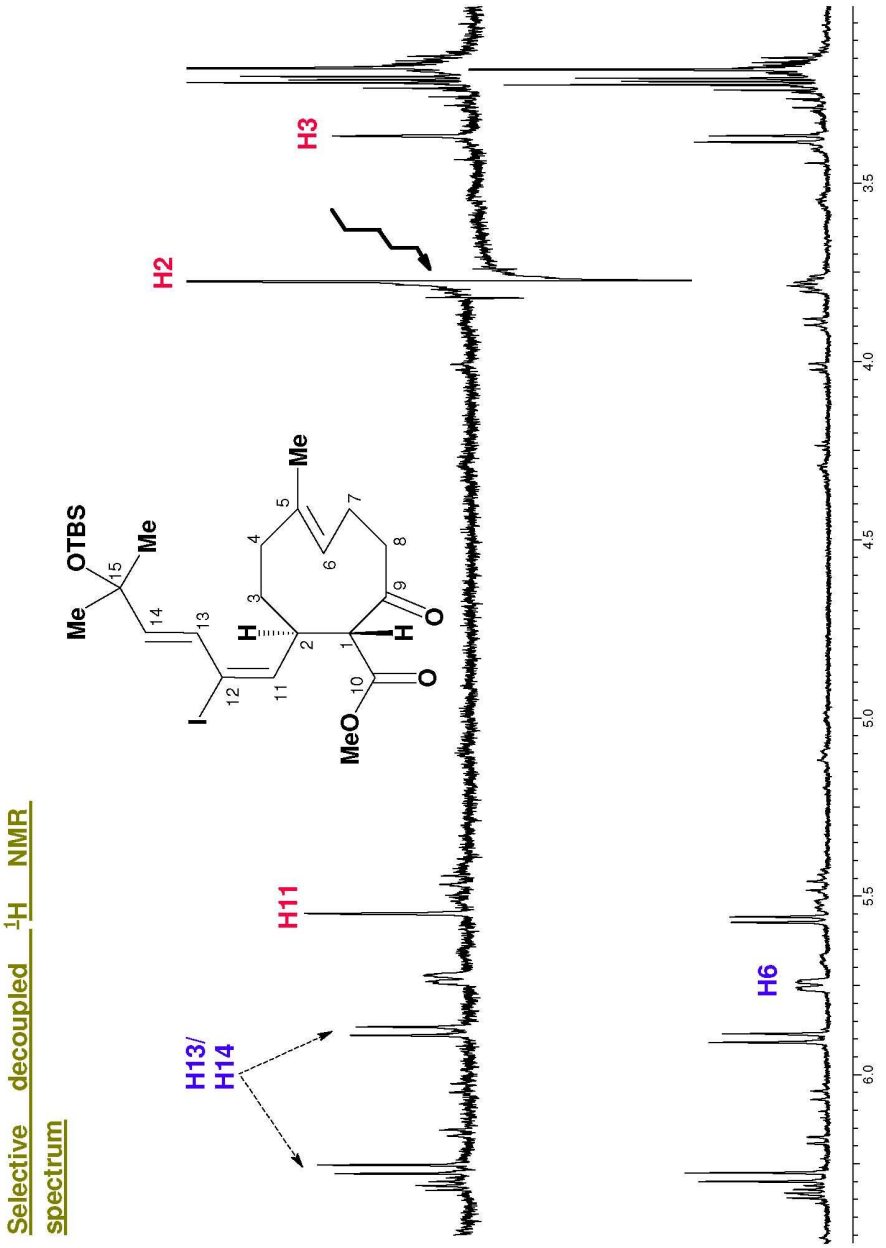
Selective decoupled ^{1}H NMR spectrum
H13/ H14
H11
H2
H3
H6
Me
OTBS
Me
I
H
H
MeO
O
O
6.0
5.5
5.0
4.5
4.0
3.5

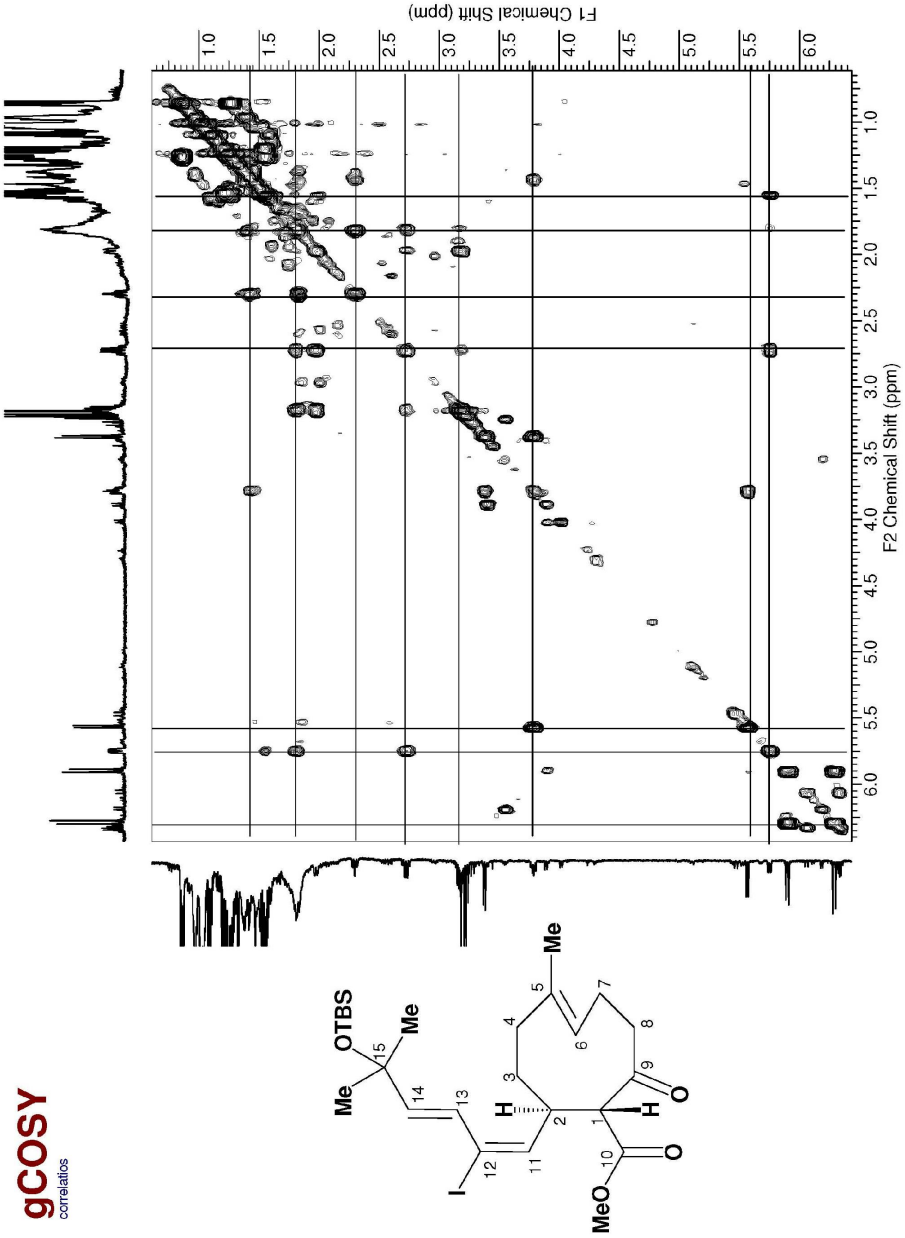
gCOSY
correlatios
F1 Chemical Shift (ppm)
F2 Chemical Shift (ppm)
1.0
1.5
2.0
2.5
3.0
3.5
4.0
4.5
5.0
5.5
6.0
OTBS
Me
Me
Me
H
H
O
O
I
MeO

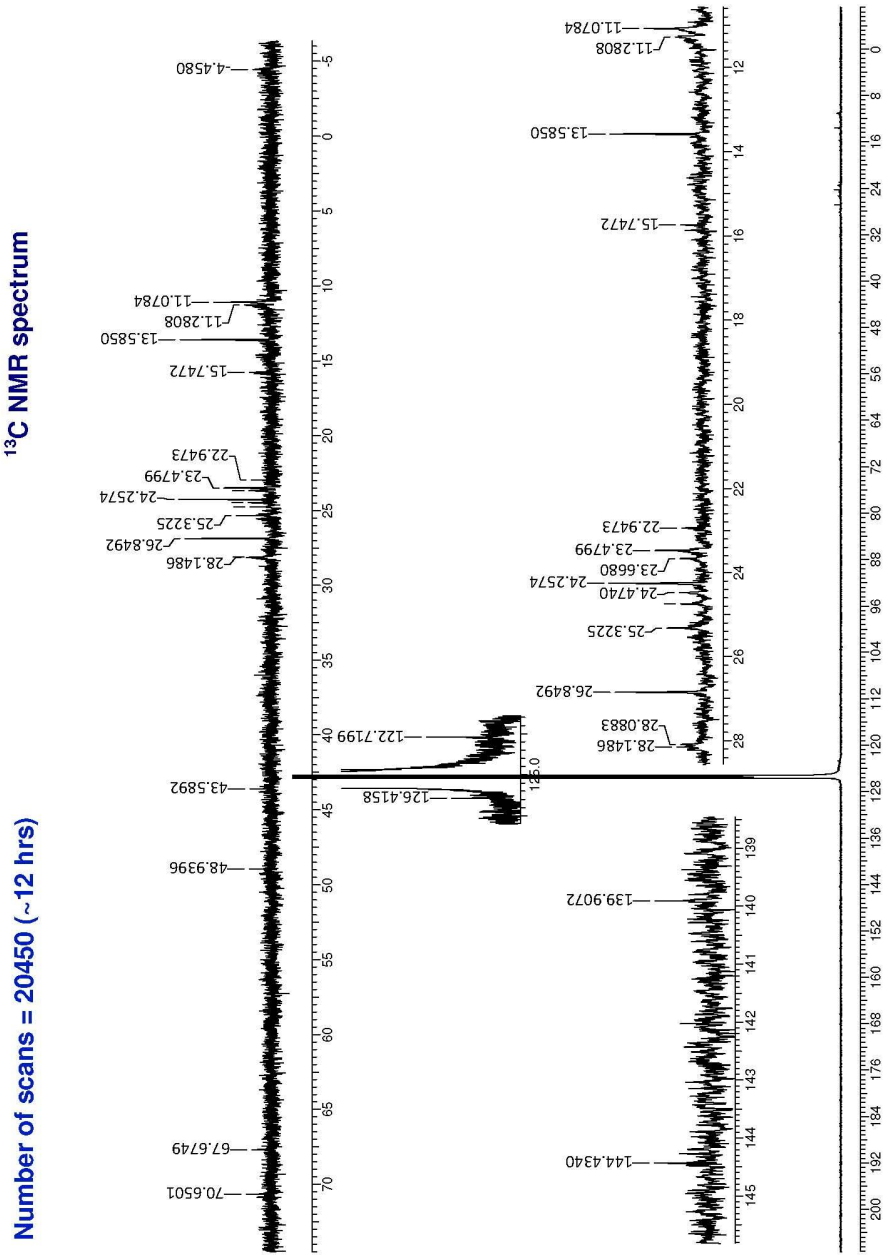
^{13}C NMR spectrum
Number of scans = 20450 (~12 hrs)
-4.4580
11.0784
11.2808
13.5850
15.7472
22.9473
23.4799
24.2574
25.3225
26.8492
28.1486
43.5892
48.9396
67.6749
70.6501
122.7199
126.4158
125.0
11.0784
11.2808
13.5850
15.7472
22.9473
23.4799
23.6680
24.2574
24.4740
25.3225
26.8492
28.0883
28.1486
139.9072
144.4340

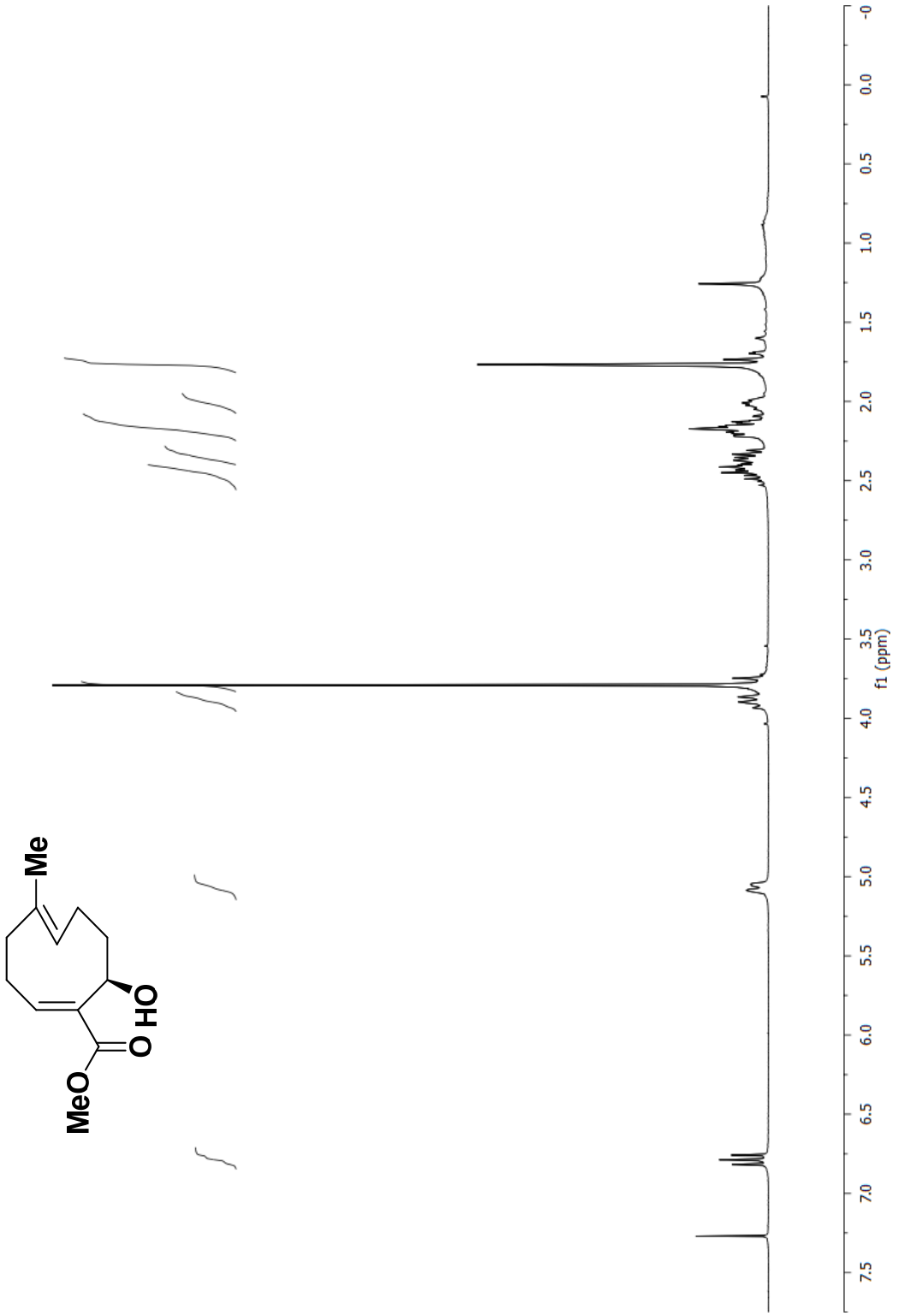
Me
HO
O
MeO
f1 (ppm)
-0
0.0
0.5
1.0
1.5
2.0
2.5
3.0
3.5
4.0
4.5
5.0
5.5
6.0
6.5
7.0
7.5

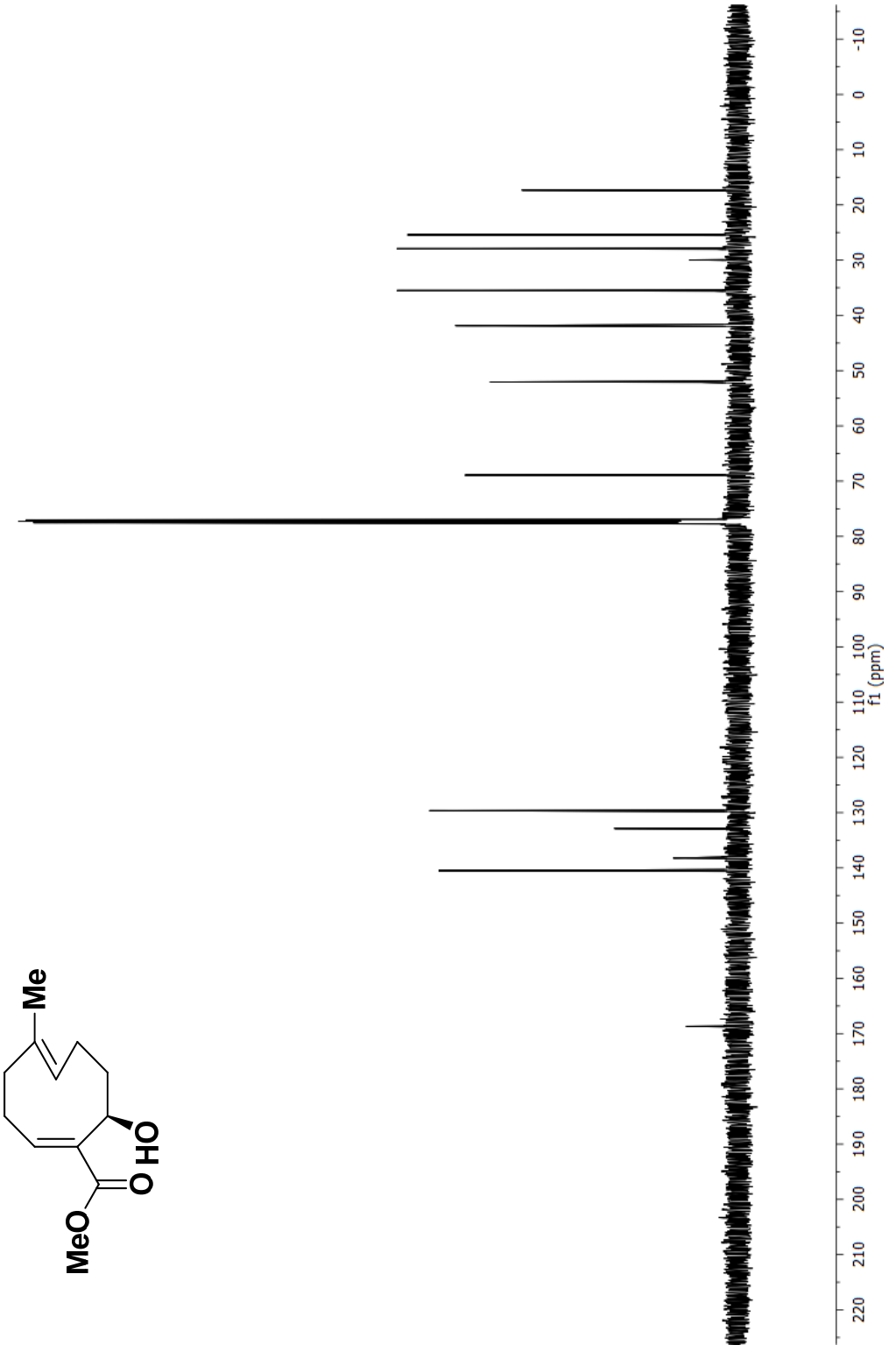
Me
HO
O
MeO
f1 (ppm)

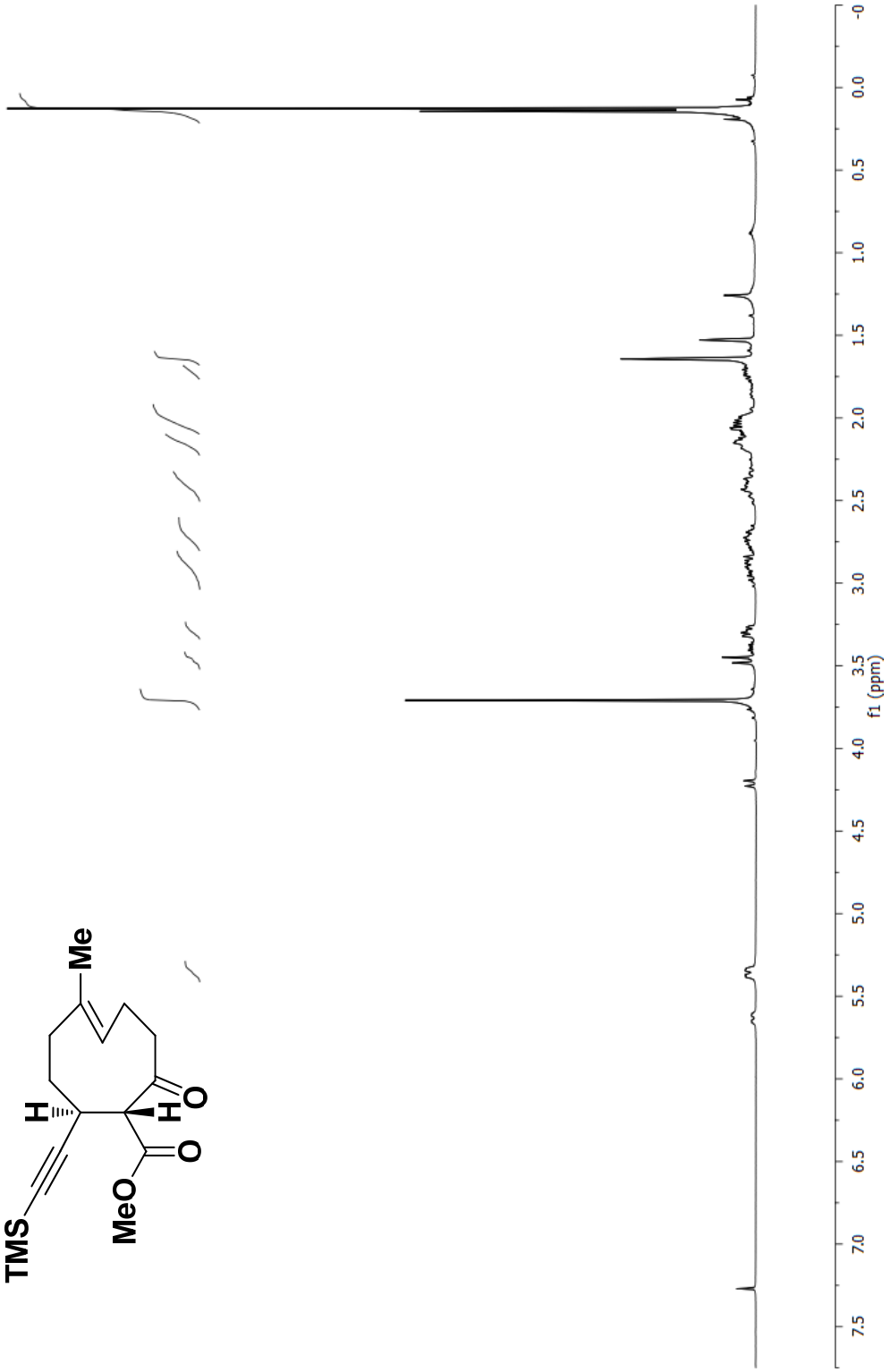
Me
H
H
O
O
MeO
TMS
f1 (ppm)

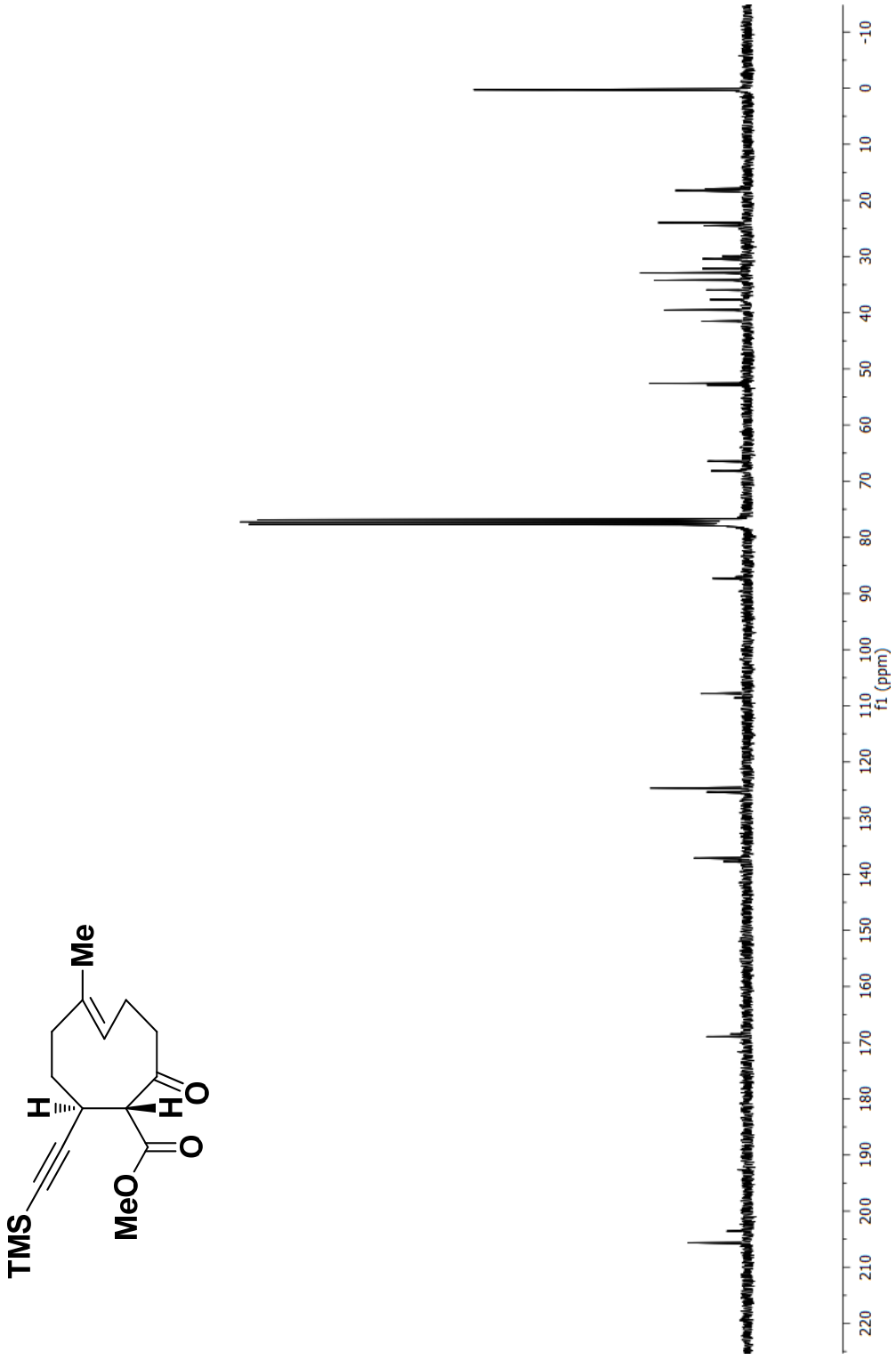
Me
H
H
O
O
MeO
TMS
f1 (ppm)

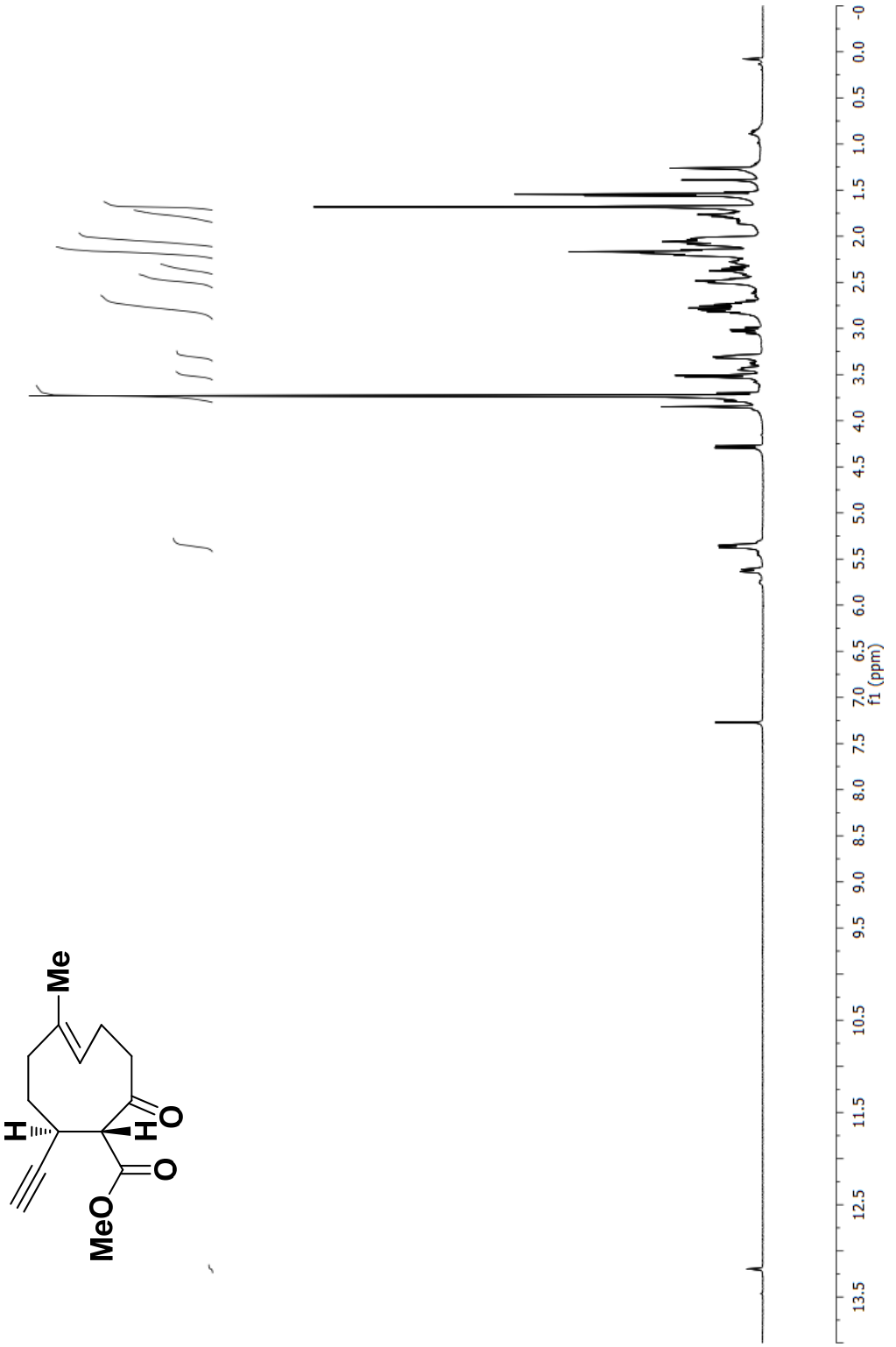
Me
H
H
O
O
MeO
13.5
12.5
11.5
10.5
9.5
9.0
8.5
8.0
7.5
7.0
6.5
6.0
5.5
5.0
4.5
4.0
3.5
3.0
2.5
2.0
1.5
1.0
0.5
0.0
-0
f1 (ppm)

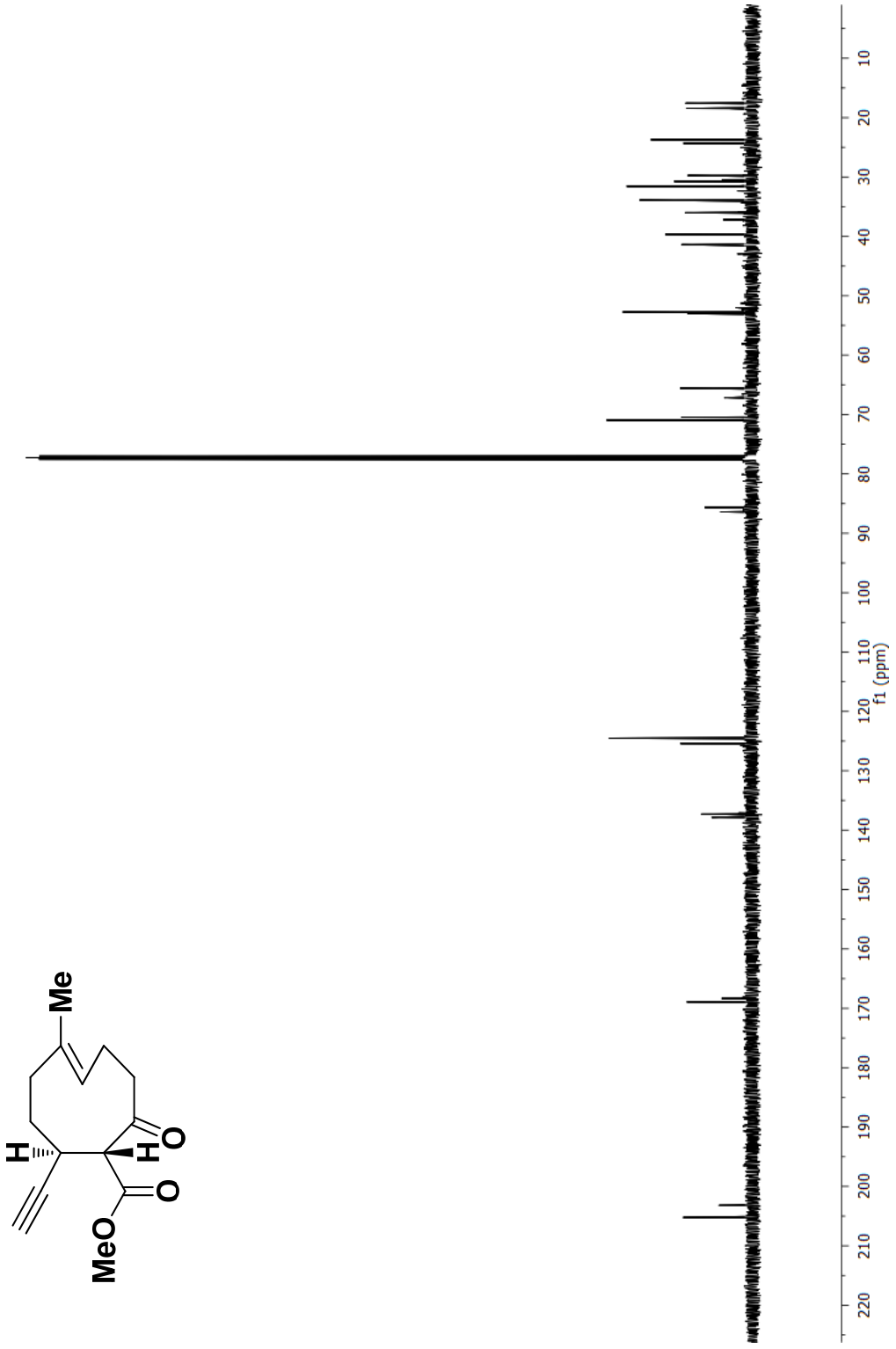
Me
H
H
O
O
MeO
f1 (ppm)

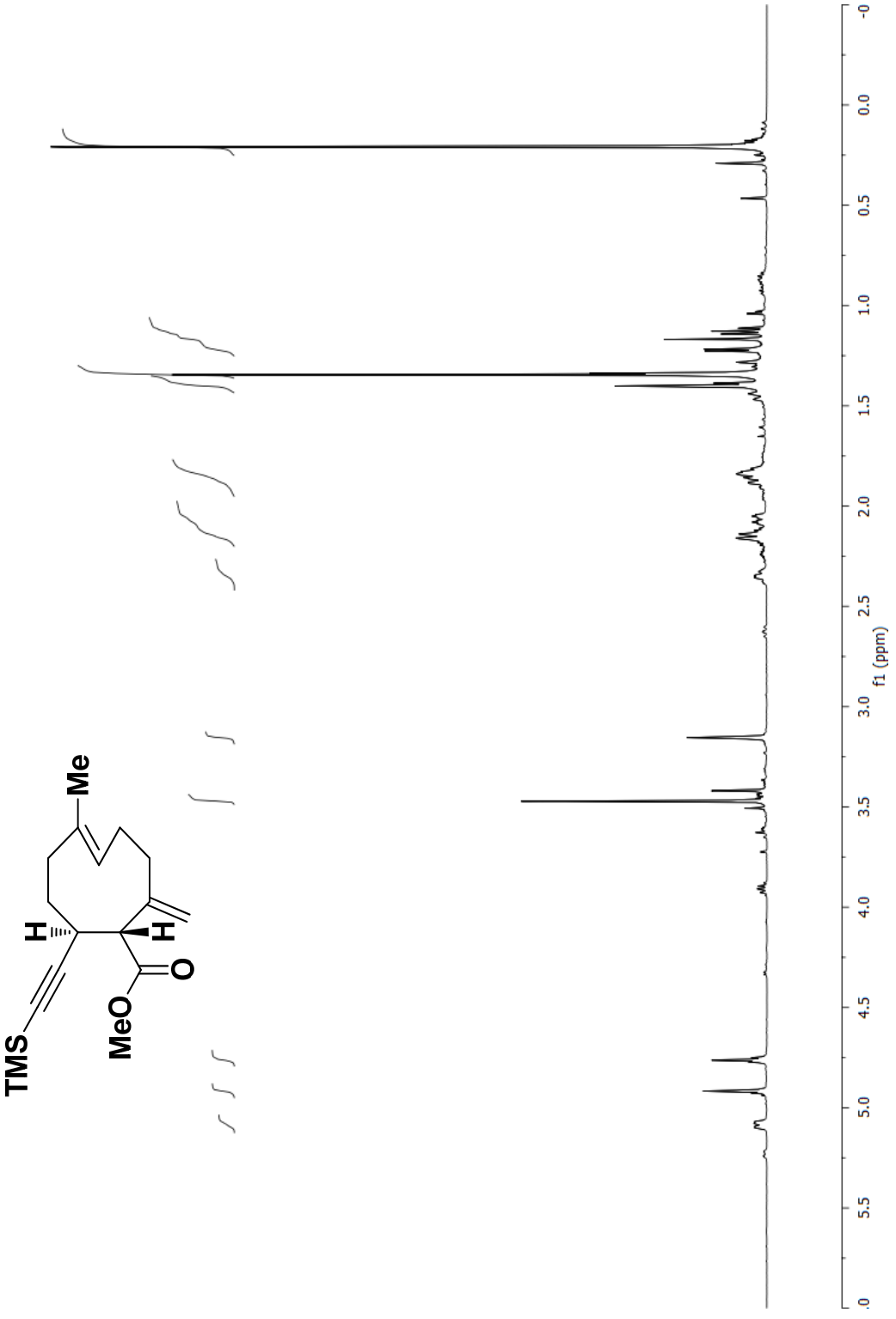
Me
H
H
O
MeO
TMS
f1 (ppm)
.0
5.5
5.0
4.5
4.0
3.5
3.0
2.5
2.0
1.5
1.0
0.5
0.0
-0

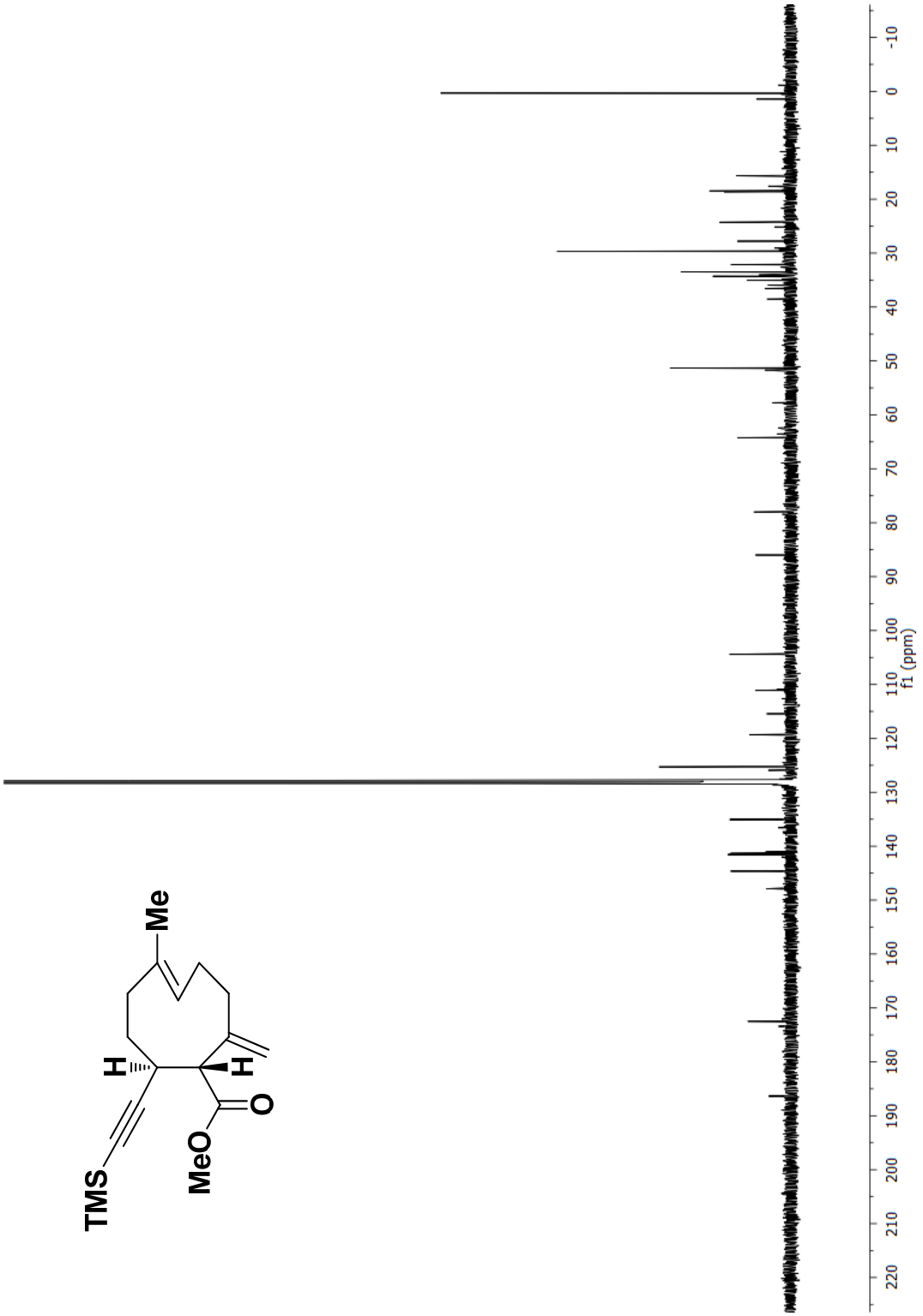
Me
H
H
O
MeO
TMS
f1 (ppm)

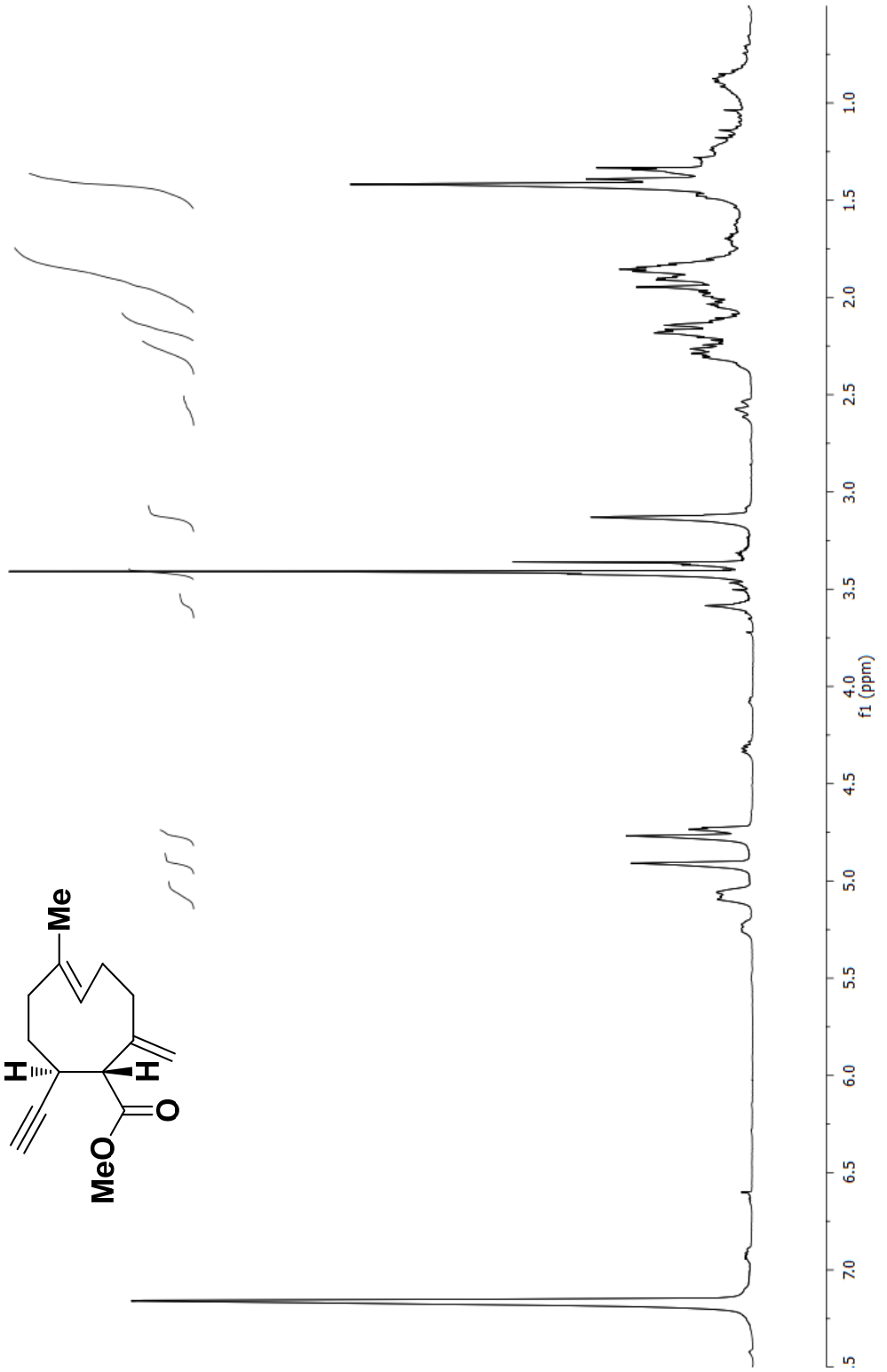
Me
H
H
O
MeO
7.0
6.5
6.0
5.5
5.0
4.5
4.0
3.5
3.0
2.5
2.0
1.5
1.0
.5
f1 (ppm)

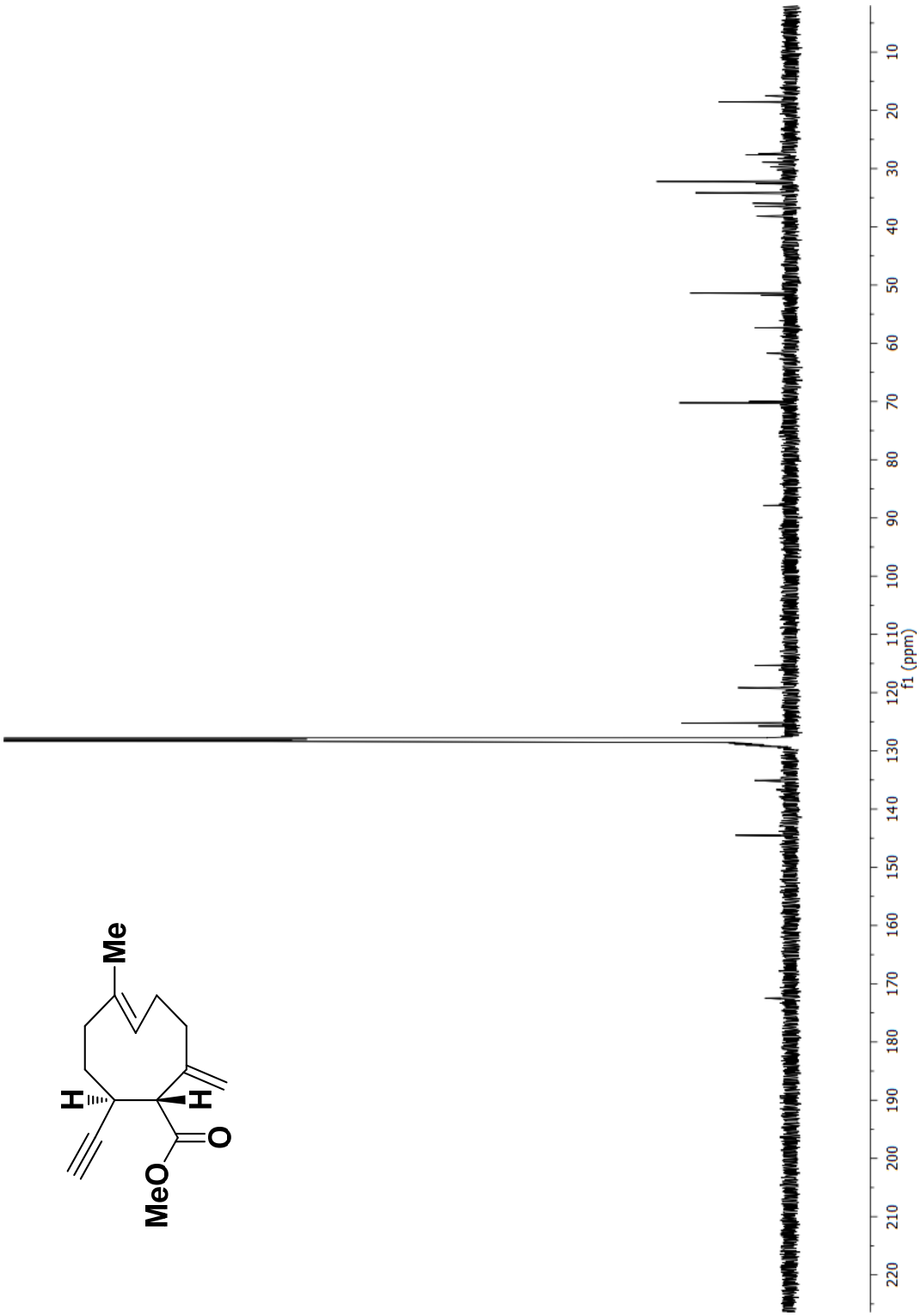
Me
H
H
O
MeO
f1 (ppm)

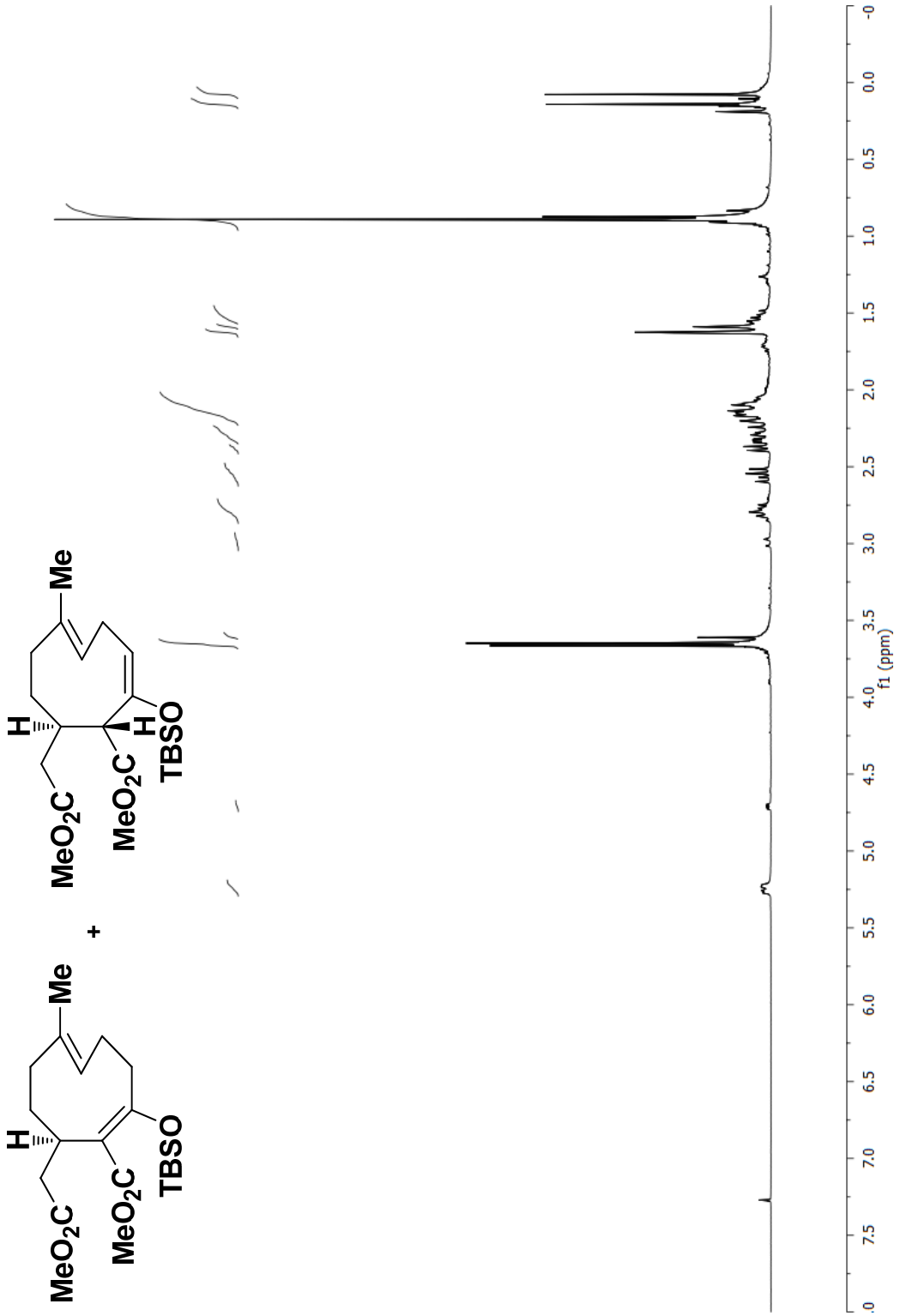
Me
H
MeO2C
MeO2C
H
TBSO
+
Me
H
MeO2C
MeO2C
TBSO
f1 (ppm)

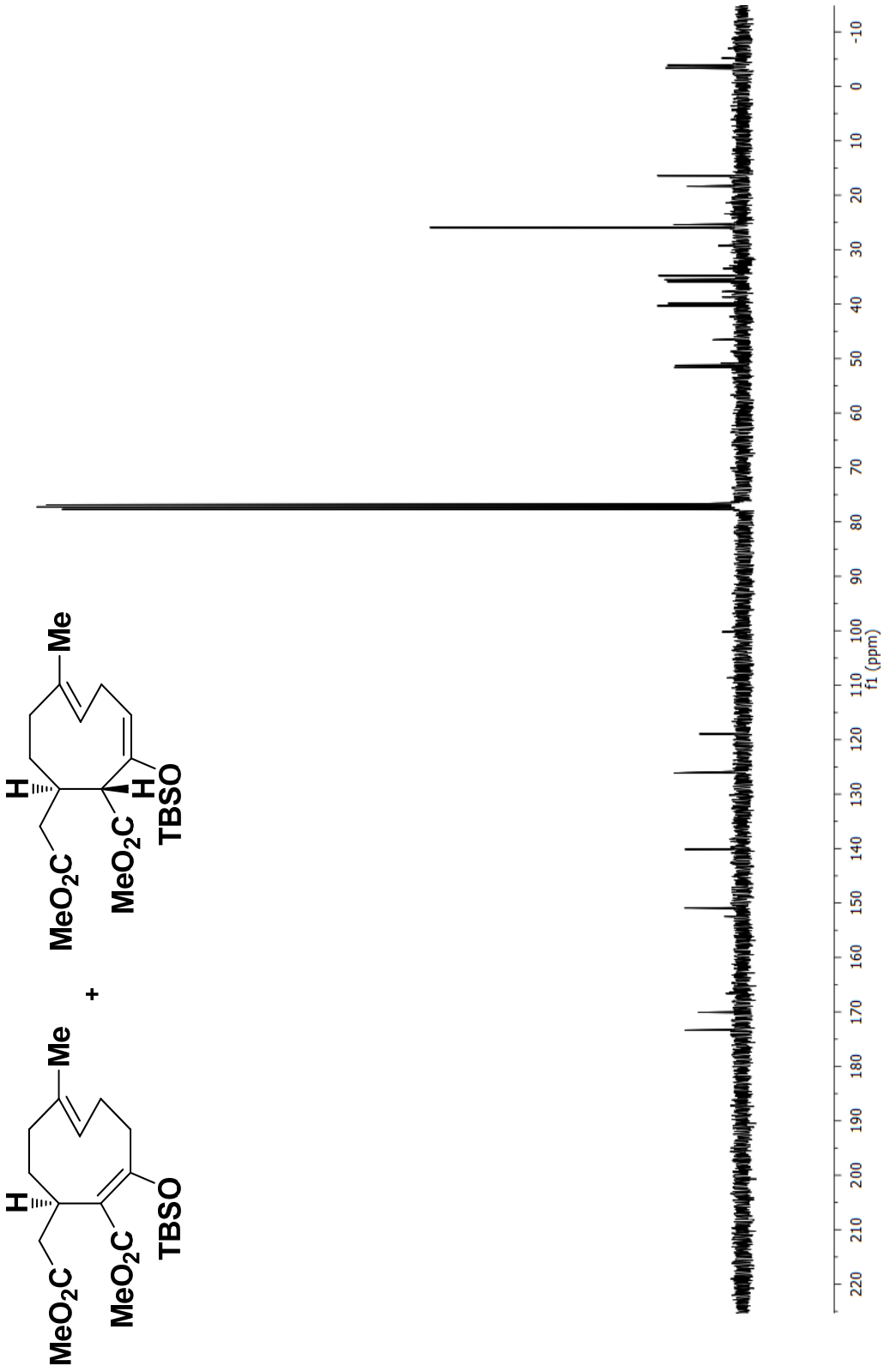
Me
H
MeO2C
MeO2C
H
TBSO
+
Me
H
MeO2C
MeO2C
TBSO
f1 (ppm)

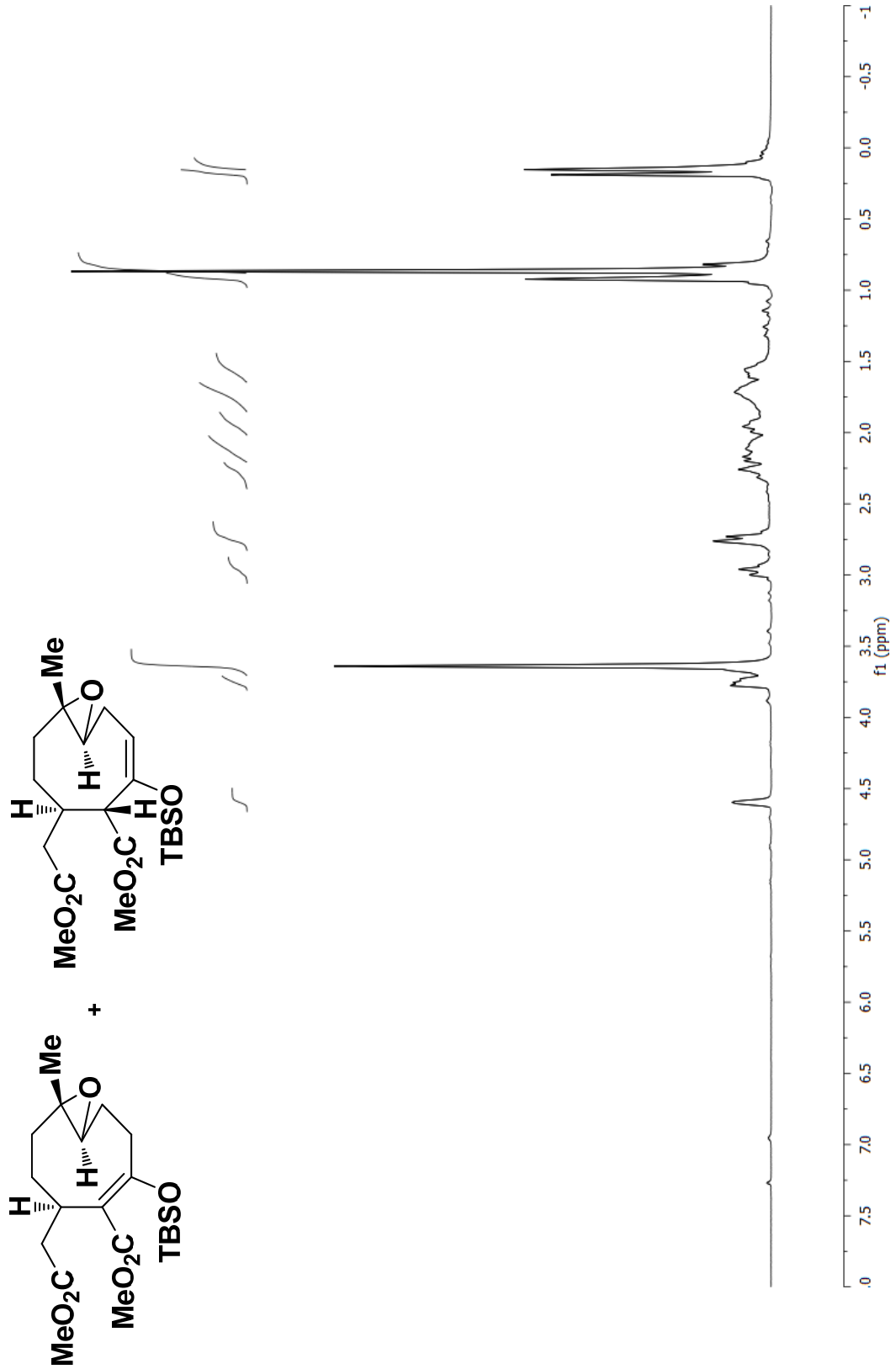
Me
O
H
H
MeO2C
MeO2C
H
TBSO
+
Me
O
H
H
MeO2C
MeO2C
TBSO
f1 (ppm)

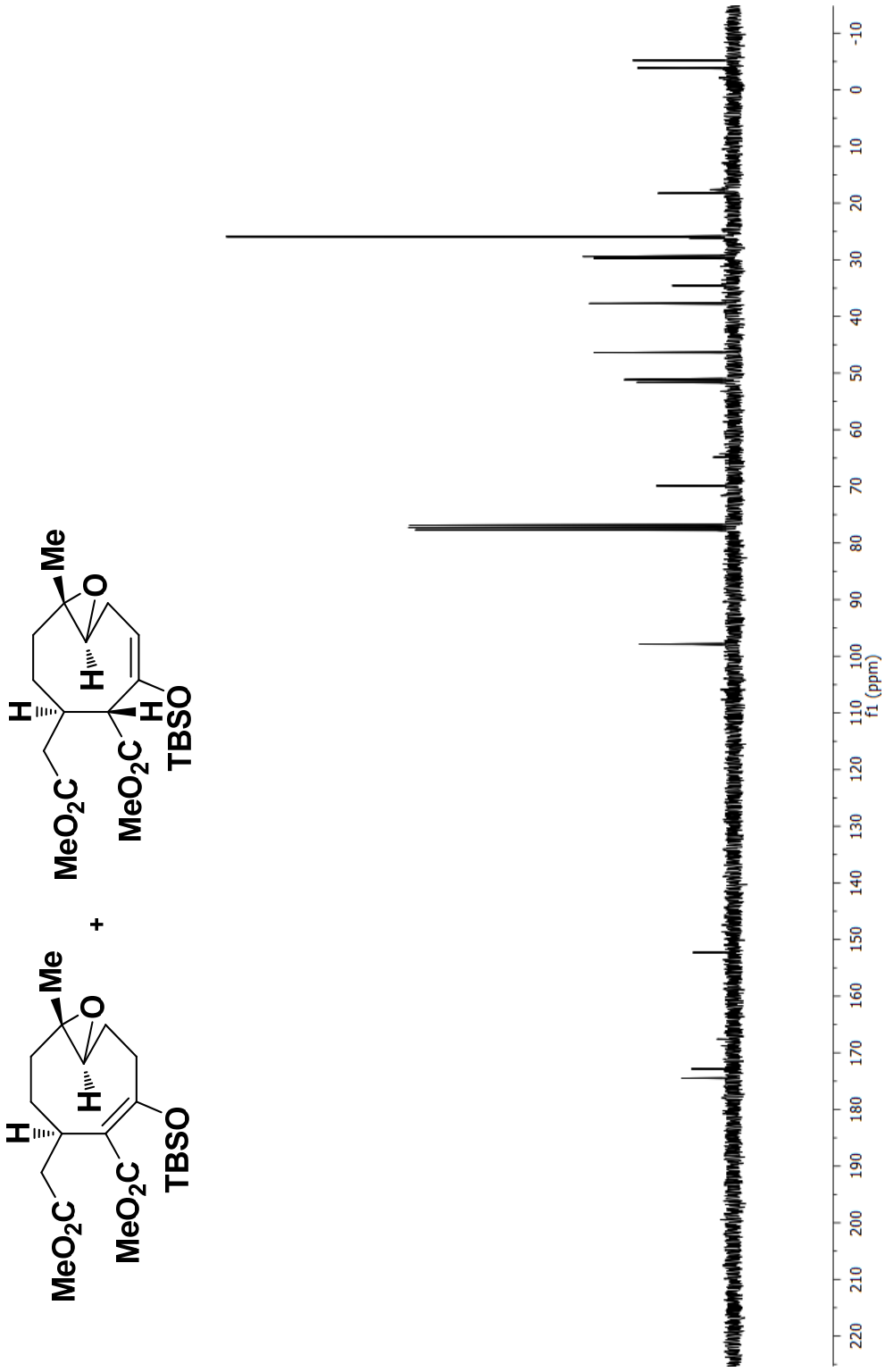
Me
O
H
H
MeO2C
MeO2C
H
TBSO
+
Me
O
H
H
MeO2C
MeO2C
TBSO
f1 (ppm)

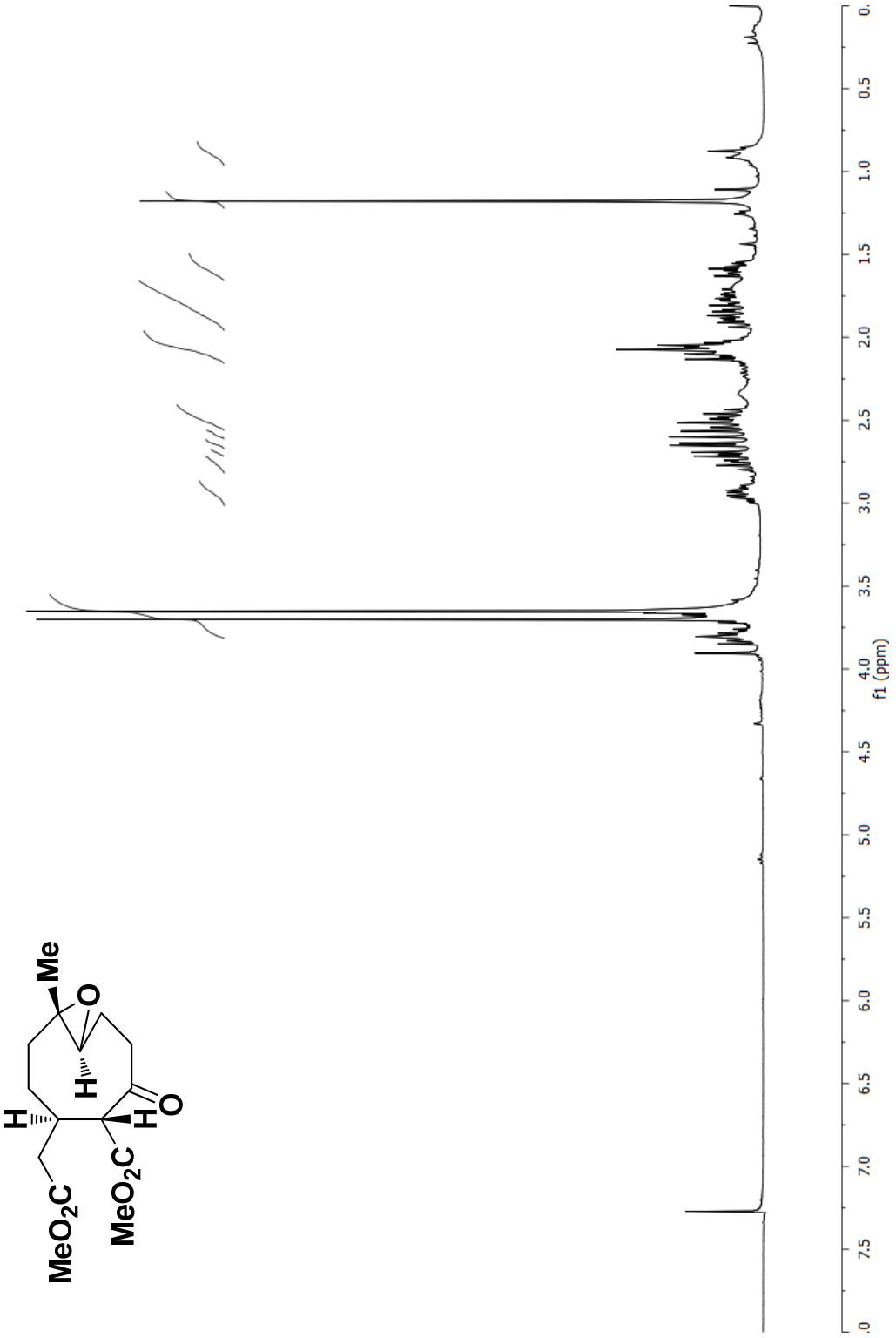
Me
O
H
H
O
H
MeO2C
MeO2C
7.5
7.0
6.5
6.0
5.5
5.0
4.5
4.0
3.5
3.0
2.5
2.0
1.5
1.0
0.5
f1 (ppm)

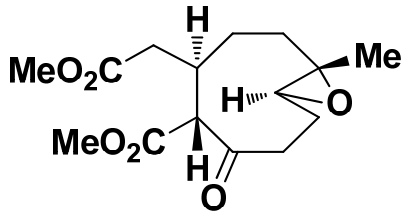
H
MeO2C
Me
H
O
MeO2C
H
O

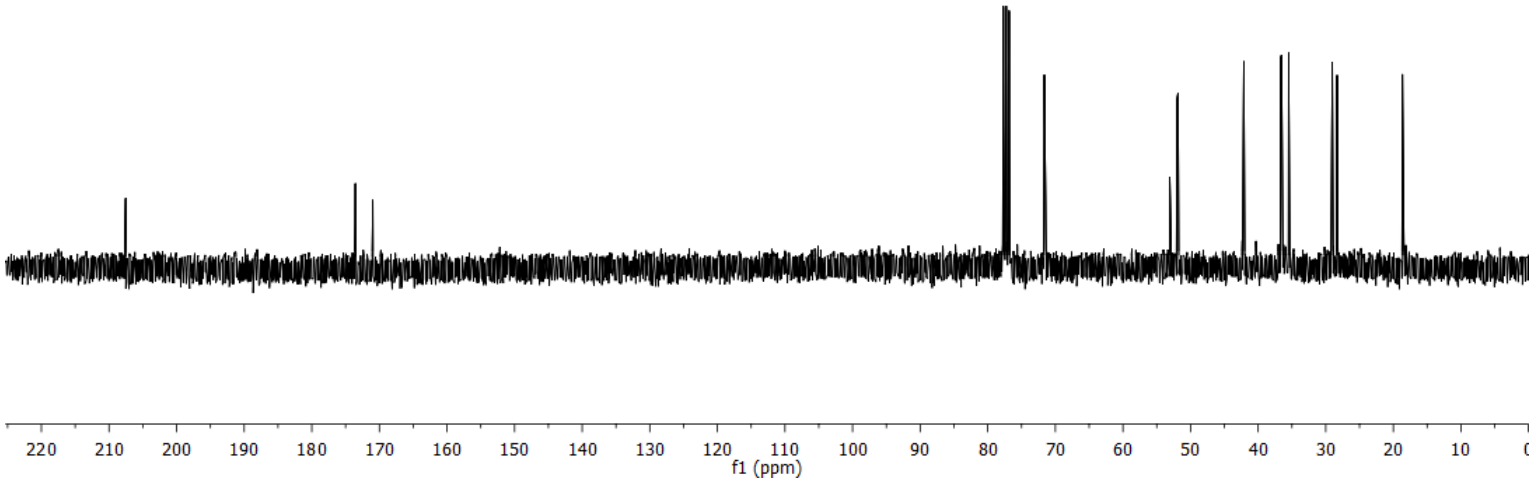
220
210
200
190
180
170
160
150
140
130
120
110
100
90
80
70
60
50
40
30
20
10
f1 (ppm)

Michael A. Drahl

EDUCATION

Ph.D. in Organic Chemistry — Rutgers University – New Brunswick, NJ
2013 — Advisor: Prof. Lawrence J. Williams

S.B. in Chemistry
A.S. in Business Administration — Elmira College – Elmira, NY
2008

PUBLICATIONS & PATENTS

Drahl, M. A.; Manpadi, M.; Williams, L. J. "C-C Fragmentation: Origins and Recent Applications." invited review for *Angew. Chem., Int. Ed.*, in press.

Williams, L. J.; Drahl, M. A.; Manpadi, M. Synthetic methods and intermediates for the preparation of xenicanes. U.S. Patent Application #13/215,931, filed August 23, 2011.

Xu, D.; Drahl, M. A.; Williams, L. J. "Toward an Integrated Route to the Vernonia Allenes and Related Sesquiterpenoids." *Beilstein J. Org. Chem.* **2011**, *7*, 937-943.

Drahl, M. A.; Akhmedov, N. G.; Williams, L. J. "Selective Conversion of an Enantioenriched Cyclononadienone to the Xeniolide, Xenibellol, and Florlide Cores: An Integrated Routing Strategy." *Tetrahedron Lett.* **2011**, *52* (2), 325-328.

Jung, J.; Solanki, A.; Memoli, K. A.; Kamei, K.-I.; Kim, H.; Drahl, M. A.; Williams, L. J.; Tseng, H.-R.; Lee, K.-B. "Selective Inhibition of Human Brain Tumor Cells through Multifunctional Quantum-Dot-Based siRNA Delivery." *Angew. Chem., Int. Ed.* **2010**, *49* (1), 103-107.

Mangion, I.; Strotman, N.; Drahl, M.; Imbriglio, J.; Guidry, E. "Dynamic Kinetic Asymmetric Allylation of Hydrazines and Hydroxylamines." *Org. Lett.* **2009**, *11* (15), 3258-3260.

Drahl, M. A.; Wang, H.; Manpadi, M.; Akhmedov, N. G.; Emge, T. J.; Williams, L. J. "Accessing Anticancer Structure Space: Total Synthesis of Xenicane Diterpenoids and Diverse Motifs." *Manuscript in preparation.*

Hu, G.; Drahl, M. A.; Williams, L. J. "Catalytic Stereoselective Allene Epoxidation." *Manuscript in preparation.*